

TURBULENT FLOW ENHANCEMENT BY POLYELECTROLYTE ADDITIVES:
MECHANISTIC IMPLICATIONS FOR DRAG REDUCTION

by

DAVID LEONARD WAGGER

B.S.Ch.E., U.C. Berkeley

(1985)

Submitted to the Department of Chemical Engineering in Partial
Fulfillment of the Requirements for the Degree of

DOCTOR OF PHILOSOPHY
in Chemical Engineering

at the

MASSACHUSETTS INSTITUTE OF TECHNOLOGY

February 1992

© Massachusetts Institute of Technology 1992
All rights reserved

Signature of Author.....
Department of Chemical Engineering
January 29, 1992

Certified by.....
Preetinder Singh Virk
Thesis Advisor

Accepted by.....
William M. Deen
Chairman, Committee on Graduate Students

MASSACHUSETTS INSTITUTE
OF TECHNOLOGY

FEB 13 1992

LIBRARIES

ARCHIVES

TURBULENT FLOW ENHANCEMENT BY POLYELECTROLYTE ADDITIVES:
MECHANISTIC IMPLICATIONS FOR DRAG REDUCTION

by

DAVID LEONARD WAGGER

Submitted to the Department of Chemical Engineering on January 29, 1992
in partial fulfillment of the requirements for the Degree of Doctor of Philosophy
in Chemical Engineering

ABSTRACT

The drag reduction phenomenon was experimentally studied in two pipes, of diameters 1.46 and 1.02 cm, using seven polyelectrolytic HPAM additives, with molecular weights from 1 to 20×10^6 g/mole and degree of backbone hydrolysis from 8 to 60%, at concentrations from 1 to 1000 wppm, in saline solutions containing from 0.3 to 0.00001 N NaCl.

Both laminar and turbulent flow behavior were greatly influenced by salinity-induced changes in the initial conformation of the HPAM additives. Initially collapsed, random-coiling conformations exhibited Newtonian laminar flow and Type-A turbulent drag reduction, while initially extended conformations exhibited shear-thinning in laminar flow and Type-B turbulent drag reduction. The gross-flow physics of Type-B drag reduction were delineated. A characteristic "ladder" structure prevailed, with polymeric regime segments that were roughly parallel to, but shifted upward from, the Prandtl-Karman line.

In the polymeric regime, both Type-A fan and Type-B ladder structures were essentially independent of pipe diameter, and were scaled by the wall shear stress. The wall shear stress also scaled degradation during drag reduction. New onset and slope increment correlations were presented for Type-A drag reduction by HPAM additives. In Type-B drag reduction, flow enhancement was found proportional to additive concentration, and the intrinsic slip, $\Sigma = S'/(c/M_w)$, varied roughly as the third power of backbone chain links N_{bb} . New intrinsic slip and retro-onset correlations were presented for Type-B drag reduction by HPAM additives. Analysis of Type-B literature revealed a wide range of additive efficacies, with specific slips S'/c from 0.0001 to 4. For the most effective additives, HPAM and asbestos fibers, the additive-pervaded volume fraction per unit flow enhancement, $X_v/S' \approx 3000$, implied that these additives align during drag reduction.

The slip ratio R_{sc} , which is the relative flow enhancement induced in Type-A and Type-B drag reduction at constant additive concentration, was found to be a universal function of the normalized turbulent flow strength ($Re_s \sqrt{f}/Re_s \sqrt{f^*}$). The extension of initially

collapsed, random-coiling, HPAM macromolecules by the turbulent flow field thus seems independent of additive parameters and absolute wall shear stress levels. Gross flow additive equivalence was detected at iso-slip points, where different polymer solutions induced equal flow enhancements. At numerous such points, the collapsed to extended slip ratio at constant concentration, R_{sc} , was essentially equal to the extended to collapsed concentration ratio at constant slip, R_{cs} . Thus, for fixed total additive concentration, the R_{sc} observed at any $Re_p\sqrt{f}$ simply represents the fraction of originally collapsed macromolecules that have become extended in the flow, and thence effective in drag reduction.

Thesis Supervisor: Dr. Preetinder Singh Virk
Title: Professor of Chemical Engineering

ACKNOWLEDGEMENTS

I would like to thank the Fannie & John Hertz Foundation for its generous support during a goodly portion of this thesis. Professor Preetinder Singh Virk, my thesis advisor, has my profound gratitude for his guidance and helpful suggestions throughout this work.

I further thank my fellow graduate students for their camaraderie and the many professors for enlightening me in subjects ranging from chemical engineering to international relations and political science, all of whom made MIT a much more enriching experience.

Outside of MIT, I thank RFB for providing some balance during my thesis work and my family for its moral support. Finally, many thanks go to the AAAS Science, Engineering, and Diplomacy Fellowship Program and USAID/R&D/EI for their flexibility in the completion of this work.

"Science increases our power in proportion as it lowers our pride."

Claude Bernard, 1928

"Wisdom entereth not into a malicious mind, and science without conscience is but the ruin of the soul."

François Rabelais, 1534

CONTENTS

SECTION	page
I SUMMARY	25
1.1 Objectives and Approach	25
1.2 Motivation	26
1.3 Background	27
1.3.1 Previous Work	27
1.3.2 HPAM Polymer Characterization	32
1.4 Experimental Apparatus	33
1.5 Results	34
1.5.1 Solvent Runs	34
1.5.2 Polymer-Solution Runs	36
1.5.3 Flow-Parameter Summary	45
1.6 Discussion	50
1.6.1 Influence of Pipe Diameter	50
1.6.2 Effect of Additive Conformation	53
1.6.3 Type-A Drag Reduction	55
1.6.4 Type-B Drag Reduction	59
1.6.5 Comparisons Between Types A and B of Drag Reduction	65
1.7 Modelling Types A and B of Drag Reduction	68
1.8 Conclusions	69

CONTENTS(continued)

SECTION	page
II INTRODUCTION	71
2.1 Objective and Motivation	71
2.2 Introduction	73
2.3 Drag-Reduction Literature Review.....	79
2.3.1 Gross Flow	79
2.3.1.1 The Effect of Pipe Diameter	92
2.3.1.2 Drag Reduction vs. Concentration	99
2.3.1.3 Drag Reduction vs. Downstream Distance from Injector	101
2.3.2 Mean-Velocity Profiles	103
2.3.3 Turbulence Structure I: Intensities and Stresses	116
2.3.4 Turbulence Structure II: Bursting and Spanwise Spacing	142
2.3.5 Summary of Literature	146
2.4 PAM and HPAM Polymers	150
2.4.1 Static and Dynamic Properties of PAM and HPAM	150
2.4.2 Theoretical Background	151
2.4.3 Empirical MHKS Relations	153
III EXPERIMENTAL APPARATUS	166
3.1 Gravity-Driven Flow System	166
3.2 Pump-Driven Flow System	170

CONTENTS(continued)

SECTION	page
3.3	System Modules175
3.4	Experimental Equipment191
3.5	Chemicals196
IV	PROCEDURES197
4.1	Polymer Master Batch Preparation197
4.1.1	Master Batch Preparation: Method #1197
4.1.2	Master Batch Preparation: Method #2201
4.2	Transducer Calibration204
4.3	Tank Calibration226
4.4	Pump Calibration227
4.5	Set-Up Procedure for the Gravity-Driven Flow System252
4.6	Experimental Run in the Gravity-Driven Flow System256
4.7	Set-Up Procedure for the Pump-Driven Flow System259
4.8	Experimental Run in the Pump-Driven Flow System266
4.9	Data Reduction270
V	RESULTS273
5.1	Solvent Runs273
5.2	Polymer-Solution Runs283
5.2.0	Turbulent-Flow Development in Polymer Solutions285
5.2.1	Introductory Examples: Representative Flow Trajectories289

CONTENTS(continued)

SECTION	page
5.2.2 Experimental Summary Tables	298
5.2.3 Detailed Descriptions	326
5.2.4 Comparative Descriptions for Similar Additives of Varying Backbone Charge	374
5.2.5 Comparative Descriptions for the Effect of Salinity	389
5.3 Turbulent-Flow Parameters	399
5.3.1 The Apparent Slip S'	400
5.3.2 The Slope Increment δ	412
5.3.3 The Onset Wall Shear Stress T_w^*	421
5.3.4 The Retro-Onset Wall Shear Stress $T_w^{\#}$	429
5.4 Laminar-Flow Parameters	431
VI DISCUSSION	442
6.1 Effect of Pipe Diameter	442
6.1.1 Additive Degradation	454
6.2 Effect of Macromolecular Conformation	455
6.3 Type-A Drag Reduction	463
6.3.1 Onset	464
6.3.2 Slope Increment	468
6.4 Type-B Drag Reduction	477
6.4.1 Flow Enhancement	477
6.4.2 Retro-Onset	489

CONTENTS(continued)

SECTION	page
6.5 Slip Ratios and Additive Equivalence	491
6.5.1 Slip Ratio at Constant Concentration	491
6.5.2 Additive Equivalence Between Types A and B Drag Reduction	497
6.5.2.1 Analysis of Isoslip Points and Additive Equivalences	499
6.5.2.2 Summary of Additive Equivalence and Isoslip Points	520
6.6 Comparison of Type-B Drag Reduction with Literature	525
6.6.1 Present and Literature Flow Enhancement Data	525
6.6.2 Present and Literature Retro-Onset Data	535
6.7 Modelling Types A and B of Drag Reduction	537
6.7.1 Modelling a Perfect Type-A Fan	538
6.7.2 Modelling a Perfect Type-B Ladder	541
VII CONCLUSIONS	544
VIII RECOMMENDATIONS	547
IX APPENDICES	548
A Linear Polymers: Theory and Experiment	549
B Equipment and Vendors	564
C Water and Mercury Manometers	568
D Manufacturers' Polymer Data	571
E Solvent Data Sets 1 - 5	572

CONTENTS(continued)

SECTION	page
F Polymer-Solution Data	601
G NOMENCLATURE	873
H REFERENCES	879
I BIOGRAPHICAL NOTE	886

ILLUSTRATIONS

FIGURE		page
2.3.1	Example of Type-A Behavior from Berman(1977)	83
2.3.2	Example of Quasi-Type-A Behavior from Berman(1977)	84
2.3.3	Example of Type-B Behavior from Berman et al.(1978)	85
2.3.4	Example of Type-B Behavior from Berman et al.(1978)	86
2.3.5	Effect of Tap-Water Differences from Kwack et al.(1981)	87
2.3.6	Effect of Mixing on Drag Reduction from Stenberg et al.(1977)	89
2.3.7	Drag Reduction by Cationic Soap Solutions from Elson & Garside(1983)	90
2.3.8	Effect of Pipe Diameter(Burger et al., 1980)	93
2.3.9	Effect of Pipe Diameter with 10 wppm PEO Powder (Sellin & Ollis, 1983)	94
2.3.10	Effect of Pipe Diameter with 10 wppm HPAM Powder (Sellin & Ollis, 1983)	95
2.3.11	Effect of Pipe Diameter with 10 wppm HPAM Emulsion (Sellin & Ollis, 1983)	96
2.3.12	Effect of Pipe Diameter(Interthal & Wilski, 1985)	98
2.3.13	Additive Flow-Enhancement Effectiveness	100
2.3.14	Axial Flow-Enhancement Development via Polymer Diffusion	102
2.3.15	Velocity Profiles from Asbestos-Fiber Solutions (Kale & Metzner, 1976)	106
2.3.16	Velocity Profiles from Fiber-Solution Injection (Sharma et al., 1979)	108

ILLUSTRATIONS(continued)

FIGURE	page
2.3.17	Velocity Profiles for PEO-Solution Injection (McComb & Rabie, 1982b)109
2.3.18	Velocity Profiles for Premixed HPAM Solutions in 44-mm Pipe (Bartels et al., 1984)110
2.3.19	Velocity Profiles for Premixed HPAM Solutions in 16-mm Pipe (Bartels et al., 1984)111
2.3.20	Velocity Profiles for HPAM-Solution Injection (Bewersdorff, 1984)113
2.3.21	Two-Fluid Profile from Bewersdorff(1984)114
2.3.22	Velocity Profiles for Fiber Solutions in Multipass System (McComb & Chan, 1985)115
2.3.23	Newtonian-Turbulence Data at $Re_s = 5 \times 10^4$ (Laufer, 1954)119
2.3.24	Newtonian-Turbulence Data at $Re_s = 5 \times 10^5$ (Laufer, 1954)120
2.3.25	Turbulent Normal Stresses and Kinetic Energy at $Re_s = 5 \times 10^4$ (Laufer, 1954)122
2.3.26	Turbulent Normal Stresses and Kinetic Energy at $Re_s = 5 \times 10^5$ (Laufer, 1954)123
2.3.27	Axial Turbulence-Intensity Profiles (McComb & Rabie, 1982b)125
2.3.28	Axial- and Radial-Intensity Profiles in 16-mm Pipe (Bartels et al., 1984)127
2.3.29	Reynolds-Stress Profile in 16-mm Pipe (Bartels et al., 1984)128
2.3.30	Turbulent Normal-Stress Ratios in 16-mm Pipe (Bartels et al., 1984)129

ILLUSTRATIONS(continued)

FIGURE	page
2.3.31	Axial Turbulence-Intensity Profiles in 44-mm Pipe (Bartels et al., 1984)131
2.3.32	Radial Turbulence-Intensity Profiles in 44-mm Pipe (Bartels et al., 1984)132
2.3.33	Axial Turbulence-Intensity Maxima from Various Studies133
2.3.34	Radial Turbulence-Intensity Maxima from Various Studies134
2.3.35	Reynolds-Stress Profiles in 44-mm Pipe (Bartels et al., 1984)136
2.3.36	Correlation-Coefficient Profiles in 44-mm Pipe (Bartels et al., 1984)137
2.3.37	Axial Turbulence-Intensity Profiles from Various Sources139
2.3.38	Axial Turbulence-Intensity Profiles from Various Sources140
2.3.39	Axial Turbulence-Intensity Profiles from a Fiber Solution (McComb & Chan, 1985)141
2.3.40	Normalized Azimuthal Spacings from Various Studies147
2.3.41	Normalized Time Between Bursts from Various Studies148
2.3.42	Time Between Bursts from Various Studies149
2.4.1	Intrinsic-Viscosity Correlations from Various Studies156
2.4.2	Intrinsic-Viscosity Correlation (Kulicke et al., 1982) and Data160
2.4.3	Radius-of-Gyration Correlation (Kulicke et al., 1982) and Data162

ILLUSTRATIONS(continued)

FIGURE	page
2.4.4	Effect of Salinity on the Intrinsic Viscosity for Additives C836A and P500165
3.1	Gravity-Driven Flow System167
3.2	Pump-Driven Flow System171
3.3.1	Test-Pipe Section Interface177
3.3.2	Moyno-Pump Schematic180
3.3.3	Pressure-Transducer Board183
3.3.4	Flow-Control Unit185
3.3.5	Timer and Flow-Diverter Unit187
3.3.6	Temperature-Probe Unit190
3.3.7	Flex Section190
3.4.2	Mass-Flow Meter Unit194
4.2.1	0.1-psid Pressure-Transducer Calibration207
4.2.2	1.0-psid Pressure-Transducer Calibration209
4.2.3	10-psid Pressure-Transducer Calibration213
4.3.1	Right-Tank Calibration228
4.3.2	Left-Tank Calibration231
4.4.1	Pump Calibration #1 with Distilled H ₂ O237
4.4.2	Pump Calibration #2 with Distilled H ₂ O241
4.4.3	Pump Calibration #3 with 50-wppm C832A245
4.4.4	Pump Calibration #4 with Distilled H ₂ O249

ILLUSTRATIONS(continued)

FIGURE		page
4.9	Data-Reduction Flow Diagram	271
5.1.1	Solvent Data Set 1	276
5.1.2	Solvent Data Set 2	277
5.1.3	Solvent Data Set 3	278
5.1.4	Solvent Data Set 4	279
5.1.5	Solvent Data Set 5	280
5.1.6	Solvent Data in the 1.458-cm Pipe Using Various Tap Pairs	281
5.1.7	Solvent Data in the 1.021-cm Pipe Using Various Tap Pairs	282
5.2.1	Experimental Grids	284
5.2.2	Axial Polymer Degradation in the 1.458-cm Pipe	286
5.2.3	Axial Polymer Degradation with Pass Number in the 1.021-cm Pipe	288
5.2.4	Representative Flow Trajectories #1	291
5.2.5	Representative Flow Trajectories #2	297
5.2.6	Cyanamid 832A in 0.3 N NaCl in the 1.458-cm Pipe	327
5.2.7	Cyanamid 832A in 0.0001 N NaCl in the 1.458-cm Pipe	331
5.2.8	Cyanamid 832A in 0.3 N NaCl in the 1.021-cm Pipe	336
5.2.9	Cyanamid 832A in 0.0001 N NaCl in the 1.021-cm Pipe	339
5.2.10	Betz 1120 in 0.3 N NaCl in the 1.458-cm Pipe	345
5.2.11	Betz 1120 in 0.0001 N NaCl in the 1.458-cm Pipe	348

ILLUSTRATIONS(continued)

FIGURE	page
5.2.12	Pusher 500-F in 0.3 and 0.0001 N NaCl in the 1.458-cm Pipe353
5.2.13	Pusher 500-F in 0.3 and 0.0001 N NaCl in the 1.021-cm Pipe358
5.2.14	ALCOMER 507 in 0.3 N NaCl in the 1.458-cm Pipe364
5.2.15	ALCOMER 507 in 0.0001 N NaCl in the 1.458-cm Pipe366
5.2.16	DSR 1438 in 0.3 N NaCl in the 1.458-cm Pipe369
5.2.17	DSR 1438 in 0.0001 N NaCl in the 1.458-cm Pipe371
5.2.18	Cyanamid 837A in 0.1 N NaCl in the 1.458-cm Pipe375
5.2.19	Cyanamid 836A in 0.1 N NaCl in the 1.458-cm Pipe376
5.2.20	Cyanamid 832A in 0.1 N NaCl in the 1.458-cm Pipe377
5.2.21	Cyanamid 837A in 0.001 N NaCl in the 1.458-cm Pipe378
5.2.22	Cyanamid 836A in 0.001 N NaCl in the 1.458-cm Pipe379
5.2.23	Cyanamid 832A in 0.001 N NaCl in the 1.458-cm Pipe380
5.2.24	Cyanamid 837A in 0.0003 N NaCl in the 1.458-cm Pipe383
5.2.25	Cyanamid 836A in 0.0003 N NaCl in the 1.458-cm Pipe384
5.2.26	Cyanamid 832A in 0.0003 N NaCl in the 1.458-cm Pipe385
5.2.27	Cyanamid 832A in 0.00001 N NaCl in the 1.458-cm Pipe386
5.2.28	30-wppm Pusher 500-F at Various Salinities390
5.2.29	20.6-wppm Cyanamid 836A at Various Salinities396
5.3.1	Apparent Slip S'_3 for Cyanamid 832A403

ILLUSTRATIONS(continued)

FIGURE	page
5.3.2	Apparent Slip S'_1 for Cyanamid 832A from Pump-Driven System in Both Pipes404
5.3.3	Apparent Slip S'_1 for Cyanamid 832A from Both System405
5.3.4	Apparent Slip S'_3 for Betz 1120406
5.3.5	Apparent Slip S'_3 for Pusher 500-F in Both Pipes407
5.3.6	Apparent Slip S'_1 for Pusher 500-F in Both Pipes408
5.3.7	Apparent Slip S'_3 for ALCOMER 507 and DSR 1438409
5.3.8	Apparent Slip S'_1 for Cyanamid 837A410
5.3.9	Apparent Slip S'_1 for Cyanamid 836A411
5.3.10	Slope Increment for Cyanamid 832A414
5.3.11	Slope Increment for Cyanamid 832A from the Pump-Driven System in Both Pipes415
5.3.12	Slope Increment for Betz 1120416
5.3.13	Slope Increment for Pusher 500-F from the Pump-Driven System in Both Pipes417
5.3.14	Slope Increment for ALCOMER 507 and DSR 1438418
5.3.15	Slope Increment for Cyanamid 837A419
5.3.16	Slope Increment for Cyanamid 836A420
5.3.17	Regressed Onset Wall Shear Stress for Cyanamid 832A423
5.3.18	Regressed Onset Wall Shear Stress for Betz 1120424
5.3.19	Regressed Onset Wall Shear Stress for Pusher 500-F425

ILLUSTRATIONS(continued)

FIGURE	page
5.3.20	Regressed Onset Wall Shear Stress for ALCOMER 507 and DSR 1438426
5.3.21	Regressed Onset Wall Shear Stress for Cyanamid 837A427
5.3.22	Regressed Onset Wall Shear Stress for Cyanamid 836A428
5.3.23	Retro-Onset Wall Shear Stress for All Additives430
5.4.1	Estimated Intrinsic Viscosity for Cyanamid 832A435
5.4.2	Estimated Intrinsic Viscosity for Betz 1120436
5.4.3	Estimated Intrinsic Viscosity for Pusher 500-F437
5.4.4	Estimated Intrinsic Viscosity for ALCOMER 507438
5.4.5	Estimated Intrinsic Viscosity for DSR 1438439
5.4.6	Estimated Intrinsic Viscosity for Cyanamid 837A440
5.4.7	Estimated Intrinsic Viscosity for Cyanamid 836A441
6.1.1	Superposition of P500 Data at High Salinity from Different Pipes, Before Transformation445
6.1.2	Superposition of P500 Data at High Salinity from Different Pipes, After Transformation446
6.1.3	Superposition of P500 Data at Low Salinity from Different Pipes, Before Transformation447
6.1.4	Superposition of P500 Data at Low Salinity from Different Pipes, After Transformation448
6.1.5	Superposition of C832A Data at High Salinity from Different Pipes, Before Transformation450
6.1.6	Superposition of C832A Data at High Salinity from Different Pipes, After Transformation451

ILLUSTRATIONS(continued)

FIGURE		page
6.1.7	Superposition of C832A Data at Low Salinity from Different Pipes, Before Transformation	452
6.1.8	Superposition of C832A Data at Low Salinity from Different Pipes, After Transformation	453
6.2.1	Observed Effects of Macromolecular Additive Conformation on Gross-Flow Behavior	456
6.2.2	The Progression of Turbulent Drag-Reduction Behavior from Type A to Type B, as Seen with HPAM Additives in Solutions of Decreasing Salinity	460
6.2.3	The Dependence of Turbulent Drag-Reduction Behavior on Salinity	462
6.3.1	Relation Between Macromolecular Coil Size and Onset	465
6.3.2	Onset Correlation for Collapsed HPAM Additives	467
6.3.3	Relation Between Macromolecular Coil Size and Slope Increment	469
6.3.4	Concentration Dependence of Slope Increment	470
6.3.5	Concentration Dependence of Specific Slope Increment	475
6.3.6	Intrinsic Slope Increment for HPAM Additives	476
6.4.1	Concentration Dependence of Apparent Slip S'_3	478
6.4.2	Concentration Dependence of Apparent Slip S'_1	479
6.4.3	Concentration Dependence of Apparent Slip, Effect of Pipe Diameter	481
6.4.4	Concentration Dependence of the Specific Slip S'_3/c	483

ILLUSTRATIONS(continued)

FIGURE	page
6.4.5	Concentration Dependence of the Specific Slip S'_1/c484
6.4.6	Intrinsic Slip for Extended HPAM Additives486
6.5.1	Dependence of Slip Ratio at Constant Concentration on Stress and Salinity492
6.5.2	Dependence of Slip Ratio at Constant Concentration on Stress494
6.5.3	Dependence of Slip Ratio at Constant Concentration on Normalized Stress496
6.5.4	Example of Additive Equivalence at an Isoslip Point498
6.5.5	Isoslip Points for Cyanamid 832A with $c = 5$ and 20 wppm in the 1.458-cm Pipe501
6.5.6	Isoslip Points for Cyanamid 832A with $c = 2$ and 10 wppm in the 1.458-cm Pipe504
6.5.7	Isoslip Points for Cyanamid 832A with $c = 5$ and 20 wppm in the 1.021-cm Pipe506
6.5.8	Isoslip Points for Cyanamid 832A with $c = 2$ and 10 wppm in the 1.021-cm Pipe509
6.5.9	Isoslip Points for Additive C832A with $c = 10$ and 20.7 wppm in the 1.458-cm Pipe511
6.5.10	Isoslip Points for Betz 1120 with $c = 5$ and 20 wppm513
6.5.11	Isoslip Points for Betz 1120 with $c = 2$ and 10 wppm515
6.5.12	Isoslip Points for Pusher 500-F in the 1.458-cm Pipe517
6.5.13	Isoslip Points for Pusher 500-F in the 1.021-cm Pipe519
6.5.14	Slip Ratio vs. Concentration Ratio Among Slip Triads521

ILLUSTRATIONS(continued)

FIGURE		page
6.6.1	Apparent Slips of HPAM Additives in Type-B Flow Enhancement	526
6.6.2	Intrinsic Slip for Extended HPAM Additives	528
6.6.3	Flow Enhancement by Various Additives in Type-B Drag Reduction	530
6.6.4	Retro-Onset Wall Shear Stress for HPAM Additives	536
6.7.1	Modelling for Type-A Fan for Betz 1120	540
6.7.2	Modelling for Type-B Ladder for Betz 1120	543

ILLUSTRATIONS(continued)

TABLE	page
1.3.1	Parameters in Drag-Reduction Experiments 28
1.3.2	Themes of Recent Drag Reduction Studies 30
1.3.3	Summary of MHKS Equations for Aqueous PAM Solutions 33
1.5.1	Solvent Data Set Parameters 36
1.5.2a	Experimental Conditions for B1120 Runs 47
1.5.2b	Turbulent Flow Parameters for B1120 Runs 48
1.5.2c	Laminar Flow Parameters for B1120 Runs 49
1.5.3	Inferred Polymer Characteristics 51
1.6.1	Onset Data for Type-A Drag Reduction by HPAM Additives 57
1.6.2	Specific and Intrinsic Slope Increment Data 59
1.6.3	Flow-Enhancement Data in Type-B Drag Reduction for Various Additives 62
2.1	Parameters in Drag-Reduction Experiments 77
2.3.1	Gross Flow Themes and Sources 91
2.3.2	Sources of Mean Flow Data 105
2.3.3	Sources of Turbulence Intensity I Data 124
2.3.4	Sources of Turbulence Structure II Data 143
2.4.1	Summary of MHKS Equations 155
2.4.2	Onset Data Shown in Figures 2.4.2 and 2.4.3 158
4.1.1	Polymer Characterization Data for Method #1 200

ILLUSTRATIONS(continued)

TABLES	page
4.1.2	Polymer Characterization Data for Method #2203
4.2	Transducer Calibration Constants215
5.1.1	Solvent Data Set Parameters274
5.2.1	Experimental Conditions for All Runs300
5.2.2	Turbulent-Flow Parameters310
5.2.3	Laminar-Flow Parameters319
5.3.3	Overall Average T_w^* for Each Polymer Additive422
5.4.1	Inferred Polymer Characteristics433
5.4.2	Macromolecular Expansion434
6.2	Inferred Polymer Characteristics458
6.3.1	Type-A Drag Reduction Onset Constants471
6.3.2	Specific and Intrinsic Slope Increment Data474
6.4	Specific and Intrinsic Slip Data488
6.5	Summary of Isoslip Points and Slip Triads522
6.6	Flow-Enhancement Data in Type-B Drag Reduction for Various Additives533

CHAPTER I

SUMMARY

1.1 Objectives and Approach

The thesis' objective was to examine the influence of macromolecular conformation on drag reduction in turbulent flow. This was achieved by exploring the drag reduction induced by dilute solutions of polyelectrolytic additives in both their collapsed and extended macromolecular conformations, as exhibited in solvents of high and low ionic strengths, respectively.

The experimental investigation comprised gross-flow, that is, pressure drop versus flow rate, measurements in two pipes, of diameters 1.021 and 1.458 cm, using aqueous solutions of seven partially hydrolyzed polyacrylamides(HPAM) at several salinities. The HPAM additives varied in molecular weights from 1×10^6 to 20×10^6 g/mole and had degrees of hydrolysis from 8 to 60%; they were employed at concentrations from 1 to 1000 wppm, in aqueous solutions with salinities from 0.00001 N to 0.3 N NaCl. Turbulent drag reductions induced by the additives varied from zero to the asymptotic maximum possible, about 80%.

1.2 Motivation

The present work was motivated by the observation (Virk, 1975a) of striking differences between the gross-flow drag-reduction behavior of collapsed and extended polyelectrolytes. On Prandtl-Karman (PK) coordinates, turbulent-flow trajectories for the collapsed polyelectrolytes, in common with other initially random-coiling macromolecules, were characterized by an abrupt onset of drag reduction, beyond which they departed upward from the Newtonian friction-factor relation, into a regime with drag reduction, with slopes significantly greater than Newtonian. In contrast, trajectories of extended polyelectrolytes, in common with those of fiber suspensions, exhibited no clear onset of drag reduction, but rather exhibited relatively constant drag reduction, with slopes roughly parallel to the Newtonian friction-factor relation. These two distinct types of flow trajectories, respectively named Type A and Type B, suggested that drag reduction was inherently dependent upon the conformation, that is, the actual shape, of the additive in solution, and the present work was undertaken to delineate this dependence. Polyelectrolyte additives were particularly suited to the present study because their static conformations could be altered greatly by changing solvent salinities while maintaining the identical backbone length, which is perhaps the single most important of the macromolecular parameters known to affect drag reduction. Finally, it was hoped that the systematic delineation of drag-reduction Types A and B, and the quantitative comparisons between them, might also provide fresh physical insights into the role of the additive in the mechanism of the phenomenon.

1.3 Background

Since Toms(1948) first observed the drag-reduction phenomenon, an extensive literature has accumulated on the subject, driven by industrial, military, and scientific interests.

Methods to reduce turbulent drag involve alteration of either the wetted surfaces or the flowing fluid. Surface modifications, while permanent, provide relatively little flow enhancement. Fluid modifications, by additives such as polymers, fibers, small solid particles, and air bubbles, can provide significant flow enhancement, polymeric additives having proven the most successful. For example, in the Trans-Alaskan pipeline from Prudhoe Bay to Valdez, part per million quantities of polyolefinic additives have been used for the last decade to increase oil throughput without the costly installation of additional pumping stations.

1.3.1 Previous Work

Drag reduction work prior to 1977 has been considered in several reviews, including Hoyt(1972), Lumley(1973), and Virk(1975b). The last-named reference provided a comprehensive review of polymer-induced drag reduction, with attention primarily on the behavior of homogeneous solutions of linear, random-coiling polymers, such as polyethylene oxide(PEO) in turbulent pipe flows. Table 1.3.1 illustrates the numerous experimental variables that exist for drag reduction, as well as provides references for those who have investigated these experimental aspects.

Table 1.3.1
Parameters in Drag-Reduction Experiments

PARAMETER				
Additive Type	flow cross-section(Del Villar et al., 1984)			
	smooth vs. rough surface(Virk, 1971a)			
	polymers	molecular weight M_w (Gramain & Borreill, 1978)		
		backbone structure (Ting, 1982)		
		side groups (McCormick et al., 1990a)		
		conformation	coiled vs. uncoiled (Parker & Hedley, 1972)	
			preextended vs. collapsed (Virk, 1975a)	
		flexibility vs. rigidity (Rocheffort & Middleman, 1984)		
		rheology	elasticity(relaxation) (Bewersdorff & Berman, 1988)	
			viscosity (Pinho & Whitelaw, 1990)	
		behavior in solvent	homogeneous dispersal (Oliver & Bakhtiyarov, 1983)	
			heterogenous dispersal	aggregates (Dunlop & Cox, 1977)
	micelles (Ohlendorf et al., 1988)			
networks (Inge et al., 1979)				
fibers and fibers/polymers (McComb & Chan, 1981)				
gas bubbles (Madavan et al., 1985)				

PARAMETER		
Solvent Type	highly vs. poorly dispersing (good solvent vs. Θ solvent) (Zakin & Hunston, 1980)	
	high vs. low pH (White & Gordon, 1975)	
	high vs. low ionic strength (Banijamali et al., 1974)	
Flow Conditions	transition vs. full turbulence (Ogawa & Kuroda, 1986)	
	single vs. multiple pass (Kowalik et al., 1987)	
Method of additive introduction	premixed solution (Kulicke et al., 1989)	
	flow injection	centerline ($y^+ = R^+$) (Hoyt & Sellin, 1988)
		near wall ($y^+ \approx 20$) (Frings, 1988)
		wall ($y^+ = 0$) (Wells & Spanger, 1967)

Table 1.3.2
Themes of Recent Drag Reduction Studies

A. Gross Flow	
1. Effect of Polymer Structure	
Berman(1977)	●Type-A behavior with PEO, PAM.
Berman et al.(1978)	●Type-B behavior with DNA, Collagen.
2. Importance of Polymer Solution Preparation Methods	
Stenberg et al.(1977)	●For same polymer, DR depended on mixing methods.
Kwack et al.(1980)	●For same PEO polymer and pipe, 3 labs obtained widely different DR levels.
3. Effect of Pipe Diameter	
Burger et al.(1980)	●10 wppm CDR additive(olefinic) in Crude Oil in pipes, 26 mm < D < 1194 mm.
Sellins & Ollis(1983)	●10 wppm HPAM and 10 wppm PEO in H ₂ O in pipes with 2 mm < D < 50 mm.
Interthal & Wilski(1985)	●30 wppm HPAM in river water in pipes with 3 mm < D < 750 mm.
4. Effect of Additive Concentration	
Gramain & Borreill (1978)	●Polystyrene/Toluene; 6.25 wppm < c < 500 wppm, Re = 2×10 ⁴ .
Oliver & Bakhtiyarov (1983)	●Extremely dilute HPAM; 0.02 wppm < c < 0.5 wppm, Re = 15.5×10 ³ .
5. Drag Reduction vs. Downstream Distance: Polymer Diffusion	
Frings(1984)	●Annularly injected HPAM @ 80 < y ⁺ < 93, C _p = 0.2%, <C> = 50 wppm, Re = 3×10 ⁴ .

B. Mean and Turbulent Flow Structure	
1. Injected Additive	
McComb & Rabie(1982a, b)	<ul style="list-style-type: none"> ●Centerline and wall injection of PEO, $C_p = 0.3\%$, $\langle C \rangle = 10.8$ wppm in 0.2% aqueous NaCl, $Re = 4 \times 10^4$, $D = 26$ mm. ●Coordinated measurements of DR vs x/D; polymer and salt diffusion; mean-velocity profiles; axial turbulent intensity profiles; turbulent shear stress; and axial auto-correlation data.
Bewersdorff(1984)	<ul style="list-style-type: none"> ●Centerline injection of HPAM; $C_p = 0.5\%$; $\langle C \rangle = 20$ wppm; $Re = 4 \times 10^4$, 6×10^4 and 8×10^4. ●Axial DR vs x/D; mean velocity and turbulent intensity profiles.
Willmarth et al.(1987)	<ul style="list-style-type: none"> ●Noted "stress deficit" during DR, with turbulent shear stress from measured $\langle uv \rangle$ correlation significantly less than estimated from the wall shear stress and mean-velocity profile.
2. Premixed Additive	
Bartels et al.(1984)	<ul style="list-style-type: none"> ●$50 < c < 320$ wppm HPAM solutions; $Re = 2 \times 10^4$ in pipes of ID = 16 and 44 mm. ●Mean velocity; turbulent intensity; and shear stress profiles.
McComb & Chan(1985)	<ul style="list-style-type: none"> ●300 wppm asbestos fiber and some fiber/HPAM mixtures in pipe flow, single and multiple passes. ●Mean velocity; axial and azimuthal turbulent intensity profiles at $15 \times 10^3 \leq Re \leq 50 \times 10^3$.
Oldaker & Tiederman(1977)	<ul style="list-style-type: none"> ●HPAM in a 2D channel, $D_b = 45.45$ mm, $Re < 23000$. ●Streak dyeing; spacing, z^+, from streak pictures.

Table 1.3.2 encapsulates some themes examined in recent studies of drag reduction, after 1977.

No systematic study of Type B drag reduction has yet been reported in the literature.

1.3.2 HPAM Polymer Characterization

The synthetic HPAM additives used in the present work were characterized by means of intrinsic viscosity-molecular weight relationships reported in the literature, summarized in Table 1.3.3. The correlation of Kulicke et al.(1982) best approximated the data in Table 1.3.3 over the range of present interest, $10^5 < M_w < 10^8$ g/mole, and also well represented the independently gathered data of Clarke(1970) and McCormick et al.(1990). The final equation was:

$$[\eta] = 1.00 \times 10^{-2} M_w^{0.755} \quad (2.4-10)$$

An experimental R_G - M_w relation derived from the same data was:

$$R_G \equiv \langle R^2 \rangle_w^{1/2} = 1.5 \times 10^{-2} M_w^{0.59} \quad (2.4-11)$$

When used with the Flory-Fox equation, the above two correlations result in a reasonable value of the universal constant $\Phi = 2.96 \times 10^{23}$ mole⁻¹, showing that they are self-consistent.

Table 1.3.3
Summary of MHKS Equations for Aqueous P_{AM} Solutions

Source	$[\eta] = K'M_w^a$		Experimental Conditions	M _w Range
	K'	a		(10 ⁶ g/mole)
	(cm ³ /g)			
Scholtan(1954)	6.31×10^{-3}	0.80	H ₂ O, 25°C	< 5.0
American Cyanamid Co.(1955)	3.73×10^{-2}	0.66	1.0N NaNO ₃ , 30°C	?
Collinson et al.(1956)	6.8×10^{-2}	0.66	H ₂ O, 25°C(?)	?
Klein & Conrad (1978, 1980)	4.9×10^{-3}	0.80	H ₂ O, 25°C	0.5-5.5
Klein & Conrad (1978, 1980)	7.19×10^{-3}	0.77	0.5 N NaCl, 25°C	0.5-5.5
Munk et al.(1980)	3.09×10^{-2}	0.67	H ₂ O, 20°C	< 3.0
Munk et al.(1980)	3.02×10^{-2}	0.68	0.2 N NaCl, 20°C	< 3.0
Munk et al.(1980)	2.88×10^{-2}	0.69	1.0 N NaCl, 20°C	< 3.0
Kulicke et al.(1982)	1.00×10^{-2}	0.755	H ₂ O, 20°C	0.038-9.0
Kulicke et al.(1982)	7.90×10^{-2}	0.5	Θ solvent, 25°C	0.5-6.0

1.4 Experimental Apparatus

The majority of experimental measurements were made using the pump-driven flow system, shown schematically in Figure 3.2, in plan view. The large diameter test-pipe shown consisted of four sections of tubing, each with a pressure-tap, cut from a single length of ¾"-OD, 0.574"-ID, 316-stainless-steel tubing. A small diameter test-pipe was also used, made from four sections cut from a single length of ½"-OD, 0.402"-

ID, low carbon, stainless-steel, microsmooth tubing. The pressure drop between any pair of taps could be measured by any one of the 0.1, 1.0, and 10 psid pressure transducers mounted on the PT board. The flow system was fed from two elevated 55-gallon, stainless-steel tanks, used for mixing, heating, and holding experimental solutions. An electronically-controlled positive-displacement Moyno 3L4-SSQ-AAA pump provided flow rates between 3.2 and 19.2 gpm. The pump discharge connected to the test pipe through a 2" flexible stainless-steel hose, a reducer, a 1" union cross, and an entrance ball valve. Three 2"-OD \times $\frac{1}{8}$ "-cell \times 3"-long pieces of honeycomb were inserted into the flexible hose to calm the flow. A pump-bypass loop, from the pump suction to the cross downstream of the pump, permitted gravity-driven flow through the test pipe, with the pump off and valves B2 and B3 open. The apparatus described was capable of measuring both flow rates and pressure drops to within about $\pm 1\%$ of their absolute values over their respective ranges.

1.5 Results

The experimental results are presented in three sections, dealing respectively with solvent runs, polymer-solution runs, and flow parameters extracted from the data.

1.5.1 Solvent Runs

Numerous solvent runs were conducted before and after polymer-solution runs. Fully-developed, Newtonian, Poiseuille flow(L) and turbulent flow(N) in smooth pipes

respectively obey the equations:

$$\frac{1}{\sqrt{f}} = \frac{Re_s \sqrt{f}}{16} \quad (2.3-1)$$

$$\frac{1}{\sqrt{f}} = A_n \log(Re_s \sqrt{f}) - B_n \quad (5.1-1)$$

where f is the Fanning friction factor, Re is the Reynolds Number, and subscript s implies the use of solvent physical properties. In Equation 5.1-1, the universal Prandtl-Karman(PK) relation results when $(A_n, B_n) = (4, 0.4)$. Solvent runs have been arranged in five sets, shown in Table 1.5.1.

In Figure 5.1.2, solvent data set 2, for the 1.021-cm pipe, is plotted in semilogarithmic PK coordinates, the ordinate and abscissa of which are $1/\sqrt{f}$ and $Re_s \sqrt{f}$, respectively. The lowest flow rate, with $Re_s \sqrt{f} \approx 40 (Re_s \approx 100)$, is in the laminar regime L. As $Re_s \sqrt{f}$ increases, the data follow L until $Re_s \sqrt{f} \approx 180 (Re_s \approx 2000)$. Here, the flow begins a transition to turbulence, the data dropping from L towards the turbulent PK line. At $Re_s \sqrt{f} \approx 400 (Re_s \approx 4000)$, the flow has become fully turbulent; thereafter the data continue along PK up to the highest flow rate, which corresponds to $Re_s \sqrt{f} \approx 10000 (Re_s = 160000)$. It is evident that the Newtonian laminar and turbulent flow relations were both closely obeyed.

Figure 5.1.7 is a PK plot of solvent data obtained in the turbulent regime using various pressure tap pairs in the 1.021-cm pipe. A solid line, 1.00PK, and two dotted lines, 1.01PK and 0.99PK, have been drawn into the figure, the latter two representing respectively $\pm 1\%$ deviations from the PK relation. Comparison between the results for

Table 1.5.1
Solvent Data Set Parameters

Solvent Set Number	System	Pipe ID	Pipe Aspect Ratio	Number of runs	Turbulent Flow Parameters	
		(cm)	L/D		A _n	B _n
1	Pump	1.458	183.0	33	4.0	0.4
2	Pump	1.021	203.2	11	4.0	0.4
3	Gravity	1.458	209.8	9	4.0	0.4
4	Gravity	1.458	209.8	10	2.98	-2.00
5	Gravity	1.458	209.8	7	3.54	-0.79

all pressure tap pairs shows that the differences between tap pairs were insignificant relative to the inherent data scatter, which is approximately $\pm 1\%$ around the PK correlation. It is evident that fully-developed turbulent flow in a smooth pipe was achieved with the solvent.

1.5.2 Polymer-Solution Runs

Polymer-solution results are grouped in three sets: (1) the high molecular-weight polymer additives C832A and B1120 in the pump-driven system; (2) the low molecular-weight polymer additives P500, A507, and D1438 in the pump-driven system; and (3) the high molecular-weight polymer additives C837A, C836A, and C832A in the gravity-driven system. Additives C832A and P500 in sets 1 and 2, respectively, were each studied separately in two pipes of inner diameters 1.458 and 1.021 cm, to infer the effect of flow scale.

Figure 5.2.1 illustrates the experimental grids executed. For each polymer, a logarithmic series of polymer concentrations was used, and each polymer concentration was studied at both high and low salinities. The columns in Figure 5.2.1 reflect the actual experimental procedure in that a polymer solution of given concentration, once made up, was used for the entire [NaCl] range to be studied; this revealed the effect of salinity-induced conformational changes while maintaining both the additive amount and its molecular-weight distribution constant.

Gross Flow Physics: Introduction. Aspects of the observed polymer-solution flow behavior are introduced in Figure 5.2.4, a PK plot of experiments in the pump-driven system using 10-wppm solutions of additive B1120, an HPAM of high molecular-weight and high backbone charge, in, respectively, 0.3(▼) and 0.0001(▼) N NaCl.

In this figure, lines L and N respectively represent Newtonian laminar and turbulent flows, whereas the line M represents the maximum drag reduction(MDR) asymptote(Virk et al., 1970):

$$\frac{1}{\sqrt{f}} = 19.0 \log(Re_s \sqrt{f}) - 32.4 \quad (2.3-7)$$

Lines N and M envelop the region of turbulent drag reduction, called the "polymeric regime" because, within it, the extent of drag reduction depends on additive parameters.

Consider first the data at high salinity(▼), which typify results obtained with initially-collapsed conformations of HPAM additives. At low $Re_s \sqrt{f} < 150$, the polymer-solution data closely follow Poiseuille's law L. At $Re_s \sqrt{f} \approx 150$, the data deviate downward from L and then drop toward N, which is reached at $Re_s \sqrt{f} \approx 350$. The laminar-to-turbulent transition observed here is similar to that seen with solvent in

Figure 5.1.2. For $350 < Re_s \sqrt{f} < 500$, the polymer-solution data follow the solvent turbulent-flow line N. Then at $Re_s \sqrt{f} \approx 500$ the data abruptly lift up from N at the "onset" point, hereafter denoted by an asterisk, which marks the onset of flow enhancement; i.e., for any fixed $Re_s \sqrt{f} > Re_s \sqrt{f}^*$, $1/\sqrt{f_p} > 1/\sqrt{f_n}$. For $Re_s \sqrt{f} > 500$ the data exhibit flow enhancement, rising into the polymeric regime along a near-linear segment P, with slope and intercept $(A_p, B_p) = (17.2, 36.1)$ for $500 < Re_s \sqrt{f} < 3500$. At the highest $Re_s \sqrt{f} \approx 4000$ the data depart slightly downward from the line segment, possibly because of polymer degradation within the test pipe. The flow enhancements achieved are measured by the apparent slip, $S' = (1/\sqrt{f_p} - 1/\sqrt{f_n})$ at fixed $Re_s \sqrt{f}$. At $Re_s \sqrt{f} = 1000$, $1/\sqrt{f_p} = 15.6$, $1/\sqrt{f_n} = 11.6$, and $S' = 4.0$, corresponding to fractional flow enhancement $S_f = S'/(1/\sqrt{f_n}) = 0.34$ relative to solvent; at $Re_s \sqrt{f} = 3000$, $S' = 10.2$ and $S_f = 0.76$.

The flow trajectory observed for 10 wppm of B1120 in 0.3 N NaCl thus contains three segments: laminar flow, L; turbulent flow without drag reduction, N; and turbulent flow with drag reduction, P; a distinct onset of drag reduction separates the N and P segments. Such LNP trajectories are commonly exhibited by solutions of random-coiling macromolecules and are termed "Type A" drag-reduction behavior. The polymeric-regime segment P observed during Type-A drag reduction can be quantitatively characterized by the onset wall shear stress, T_w^* , which is related to $Re_s \sqrt{f}^*$, and the slope increment $\delta = A_p - A_n$. In this example, $Re_s \sqrt{f}^* = 450$, $T_w^* = 4.1$ dyne/cm², and $\delta = 17.2 - 4.0 = 13.2$.

Consider next the low salinity data(∇), which typify results obtained with initially extended conformations of HPAM additives. For $60 < Re_s \sqrt{f} < 400$ the data are

displaced rightwards from Poiseuille's law L , to higher $Re_p\sqrt{f}$ at fixed $1/\sqrt{f}$; this "viscosity shift", reflects the relative viscosity η_r of the polymer solution. Note that in this region of low $Re_p\sqrt{f}$, the polymer-solution is drag-enhancing, its data being displaced downwards from L . For $60 < Re_p\sqrt{f} < 400$, the data follow a Poiseuille-like path, but as $Re_p\sqrt{f}$ increases, the viscosity shift decreases, corresponding to shear-thinning behavior with power law index $n' = 0.81$. The data pass through the Newtonian turbulent-flow baseline N , at $Re_s\sqrt{f} \approx 220$, and enter the polymeric regime without exhibiting the laminar-to-turbulent transition observed in the 0.3-N data. For $400 < Re_p\sqrt{f} < 1500$, the data ascend toward, and lie nearly parallel to, the MDR asymptote M . At $Re_p\sqrt{f} \approx 1500$, they depart downwards from M into the polymeric regime at a "retro-onset" point, denoted by an octathorpe($\#$). The retro-onset point separates the region of asymptotic maximum drag reduction, which is independent of additive properties, from the polymeric regime, within which drag reduction is dependent on additive properties; in this sense, retro-onset is the converse of onset, which separates Newtonian flow, with no drag reduction, from the polymeric regime. For $1500 < Re_p\sqrt{f} < 3400$, the data continue into the polymeric regime along a near-linear segment P with slope and intercept $(A_p, B_p) = (8.0, -1.2)$. At the highest $Re_p\sqrt{f} \approx 4000$, the data descend slightly from segment P , possibly because of polymer degradation within the test pipe. The following flow enhancements are observed: At $Re_p\sqrt{f} = 1000$, $1/\sqrt{f_p} = 1/\sqrt{f_m} = 24.6$, corresponding to $S' = 13.0$ and $S_p = 1.1$; and at $Re_p\sqrt{f} = 3000$, $S' = 14.7$, and $S_p = 1.09$.

The trajectory observed for 10 wppm of B1120 in 0.0001 N NaCl thus has three segments: drag-enhanced laminar flow with relative viscosity $\eta_r > 1$ and shear-thinning;

maximum drag reduction along the MDR asymptote, M ; and turbulent drag reduction, P , with a retro-onset that separates the M and P segments. Such LMP trajectories have been previously observed with solutions of extended macromolecules and constitute "Type B" drag-reduction behavior. A feature of Type-B behavior is that the polymeric-regime segment P is almost parallel to N .

Comparisons between the two sets of data in Figure 5.2.4 reveal the influence of additive conformation. In laminar flow for $Re_i\sqrt{f} < 200$, both conformations enhance drag relative to solvent, the extended conformation more so than the collapsed conformation. In turbulent flow, however, for $Re_i\sqrt{f} > 400$, the extended conformation reduces drag relative to solvent more than does the collapsed conformation. It is instructive to follow S'_A/S'_B , the ratio of the flow enhancement induced by the collapsed conformation during its Type-A behavior to that induced by the expanded conformation exhibiting Type-B behavior. For $Re_i\sqrt{f} < Re_i\sqrt{f}^*$, $S'_A/S'_B = 0$, the collapsed conformation providing no flow enhancement before onset, while the extended conformation does. For $Re_i\sqrt{f} \geq Re_i\sqrt{f}^*$, S'_A/S'_B increases with increasing $Re_i\sqrt{f}$, approaching unity at higher $Re_i\sqrt{f}$; also, after onset, S'_A increases faster than does S'_B with increasing $Re_i\sqrt{f}$, because the Type-A P segment has a steeper slope than the Type-B P segment. In this example, at $Re_i\sqrt{f} = 500, 1000, \text{ and } 3000$, $S'_A/S'_B = 0, 0.31, \text{ and } 0.69$, respectively.

A second illustration of polymer-solution flow behavior is given in Figure 5.2.5, a PK plot of experiments in the gravity-driven system using 20.6-wppm solutions of additive C836A, an HPAM of high molecular-weight and moderate backbone charge, at two salinities, respectively, 0.1(♦) and 0.001(◇) N NaCl.

The data at high salinity, for an initially-collapsed conformation of C836A, exhibit an LNP trajectory typical of Type-A behavior. Parameters of the polymeric-regime segment P are: $Re_3\sqrt{f}^* \approx 770$ and $T_w^* \approx 13.7$ dyne/cm², slope increment $\delta = 15.1$; also, at $Re_3\sqrt{f} = 1000$, $S' = 1.4$, with $S_p = 0.12$. These data exhibit some curvature in the vicinity of the onset point. Thus, as indicated in the figure, the visually determined onset point, $Re_3\sqrt{f}^* \approx 660$, where the data first depart significantly from N, does not coincide with the regressed onset point, $Re_3\sqrt{f}^* \approx 770$, where the linear segment P, extrapolated backward, intersects N.

Data at low salinity illustrate the behavior of an initially expanded conformation of the C836A macromolecule. At low flowrates, $80 < Re_3\sqrt{f} < 300$, the data follow a laminar path that is almost parallel to, but shifted rightward from, Poiseuille's law L, corresponding to relative viscosity $\eta_r = 1.8$, with slight shear thinning, $n' = 0.91$. Between $350 < Re_3\sqrt{f} < 550$, the polymer solution undergoes a laminar-to-turbulent transition, the data abruptly shifting horizontally rightward from their laminar-flow path to a turbulent flow segment P that lies in the polymeric regime. The observed transition is noteworthy because the polymer-solution exhibits drag reduction immediately upon attaining turbulent flow. For $550 < Re_3\sqrt{f} < 1100$, the polymer-solution data rise into the polymeric regime along a linear segment P, of slope and intercept $(A_p, B_p) = (19.8, 38.9)$, with slope increment $\delta = 15.8$. At $Re_3\sqrt{f} = 1000$, $S' = 9.0$ and $S_p = 0.79$. The flow trajectory has two distinct segments: drag-enhanced laminar flow, with relative viscosity $\eta_r \approx 1.8$, amidst slight shear thinning, and drag-reduced turbulent-flow along a linear polymeric-regime segment P. This LP trajectory evidently differs from both the LNP and LMP types of trajectories seen in earlier examples, lacking a central turbulent-

flow segment along either N or M, and displaying neither onset nor retro-onset. The behavior of 20.6-wppm C836A in 0.001 N NaCl is classified Type A, not Type B, because the polymeric-regime segment possesses a slope similar to, not much shallower than, that of the 20.6-wppm C836A in 0.1 N NaCl, which was clearly Type-A.

Figure 5.2.5 shows that, relative to the collapsed conformation, the expanded conformation of C836A causes greater drag in laminar flow, but yet induces the greater drag reduction in turbulent flow. Despite differences in their drag reduction extents, both conformations of C836A exhibit the Type-A behavior associated with random-coiling macromolecules.

Gross Flow Physics: Details. Detailed results for additive B1120 at $1 \leq c$, wppm ≤ 100 in 0.3 N and 0.0001 N NaCl, respectively, are presented in Figures 5.2.10 and 5.2.11.

In Figure 5.2.10, at high salinity, for the initially-collapsed conformation of B1120, the flow trajectories observed at all concentrations are akin to the Type-A trajectory earlier described for $c = 10$ wppm B1120 in 0.3 N NaCl (Figure 5.2.4), with the following elaboration. LNP trajectories are exhibited by $c = 1, 2, 5, 10$ and 20 wppm; however, $c = 50$ and 100 wppm trace LPM trajectories, the data remaining above N after transition, and attaining the MDR asymptote at the highest $Re_\nu \sqrt{f}$. Laminar-flow paths for $c \leq 20$ wppm are virtually indistinguishable from the solvent line L and both 50 and 100 wppm solutions also exhibit Newtonian viscosities, even though they show $\eta_r > 1$. In turbulent flow, the P segments for $1 \leq c \leq 20$ wppm have slopes, and slope increments, that increase with increasing concentration, $\delta = 0.9, 3.7, 8.4, 13.2,$ and 18.0 , respectively, the corresponding $Re_\nu \sqrt{f}^* \approx 960, 580, 640, 510,$ and

480. These five segments appear to radiate from a narrow band on the turbulent baseline N, forming a Type-A "fan" characteristic of drag reduction by solutions of random-coiling additives.

Figure 5.2.11 shows data at low salinity, for the initially-extended conformation of B1120. The flow trajectories observed here are related to the Type-B trajectory earlier described for $c = 10$ wppm B1120 in 0.0001 N NaCl. For $c = 1$ and 2 wppm the trajectories are respectively LNP and LP; for $c = 5$ and 10 wppm both LMP; and for $c = 20, 50,$ and 100 wppm all LM. In laminar flow, these solutions exhibit high relative viscosities, with shear-thinning. In turbulent flow, the polymeric-regime segments P are approximately parallel to, but displaced upwards from, the turbulent baseline N; thus, for $c = 1, 2, 5,$ and 10 wppm, the respective P segment slopes are $A_p = 4.0, 7.4, 5.3,$ and 8.0, with flow enhancements $S' = 1.0, 4.4, 9.5,$ and 14.7 at $Re_p\sqrt{f} \approx 3000$. The resulting polymeric-regime structure resembles a "ladder", the rungs of which are the ascending parallel linear P segments; this Type-B "ladder" is characteristic of drag reduction by solutions of extended additives.

Figure 5.3.4 summarizes turbulent flow enhancements S' obtained at $Re_p\sqrt{f} \approx 1000$ (○ ●) and 3000 (△ ▲) in the Type-A fan (open points) and Type-B ladder (closed points) respectively exhibited by the collapsed and extended conformations of B1120. At $Re_p\sqrt{f} \approx 1000$ for $c = 1, 2, 5,$ and 10 wppm, $S'_A = 0.3, 0.5, 1.1,$ and 4.0, whereas $S'_B = 0.5, 3.0, 8.8,$ and 13.0; thus, $S'_A/S'_B = (0.52, 0.15, 0.12,$ and 0.31), respectively. At $Re_p\sqrt{f} \approx 3000$, $S'_A = 0.45, 2.7, 5.3,$ and 10.2, $S'_B = 1.0, 4.4, 9.5,$ and 14.7, and $S'_A/S'_B = 0.47, 0.61, 0.56,$ and 0.69. The preceding show that, for fixed $Re_p\sqrt{f}$ and c , $S'_A < S'_B$, always. At any fixed c , S'_A/S'_B increases toward unity as $Re_p\sqrt{f}$

is increased, with S'_A increasing strongly but S'_B only weakly. This suggests that, as $Re_c\sqrt{f}$ increases, initially collapsed macromolecules are progressively stretched toward their extended conformations. Further, at both the chosen $Re_c\sqrt{f}$, S'_B increases roughly tenfold over the tenfold range of c from 1 to 10 wppm, suggesting an approximately linear relationship between S'_B and c at low concentrations. At the highest concentrations, 50 and 100 wppm, it is found that $S'_A = S'_B = S'_M$, the asymptotic maximum drag reduction being attained at both $Re_c\sqrt{f}$, independent of additive parameters.

Detailed results for additive D1438, an HPAM of low molecular weight and moderate backbone charge, at $30 \leq c$, wppm ≤ 1000 in 0.3 N and 0.0001 N NaCl, respectively, are presented in Figures 5.2.16 and 5.2.17.

In Figure 5.2.16, at high salinity, for the initially-collapsed conformation of D1438, all solutions display LNP trajectories. Relative viscosities in laminar flow are small, $\eta_r < 1.5$, with Newtonian behavior. The observed laminar-to-turbulent transitions are all akin to those seen in normal Newtonian flows. In turbulent flow with drag reduction, for all c , from 30 to 997 wppm, P segments rise from onset points in the vicinity of $Re_c\sqrt{f}^* \approx 1500$, with increasing respective slope increments δ , from 1.4 to 11.4, forming a Type-A fan.

In Figure 5.2.17, at low salinity, for the initially-expanded conformation of D1438, all solutions display LNP trajectories. In laminar flow, the relative viscosities increase greatly as concentration increases, upto $\eta_r \approx 5$, but the behavior remains Newtonian, with no shear thinning. Evidently, the lowered salinity increases the size of the macromolecular coils but does not distort their shape enough to allow significant

orientation in laminar flow. The observed laminar-to-turbulent transitions are all Newtonian in nature. In turbulent flow, all solutions possess N segments, without drag reduction. For c from 30 to 300 wppm, onsets occur in a narrow band, $Re_p\sqrt{f^*} \approx 1200$, and beyond onset, P segment slope increments increase with increasing concentration, with δ from 1.7 to 9.3, describing an imperfect Type-A fan.

Both collapsed and expanded conformations of D1438 exhibit Type-A drag reduction behavior, the fan for the expanded conformation showing onset at lower $Re_p\sqrt{f^*}$ than that for the collapsed conformation. These results suggest that even the expanded conformation of D1438 retains random-coiling character.

1.5.3 Flow-Parameter Summary

Experimental conditions, turbulent-flow parameters, and laminar-flow parameters for all 122 runs made are summarized in Tables 5.2.1, 5.2.2, and 5.2.3, respectively, from which abbreviated Tables 1.5.2a, 1.5.2b, and 1.5.2c for additive B1120 are taken.

Table 1.5.2a summarizes the experimental conditions in seven columns: Entry; Run; Concentration, c ; Salinity, [NaCl]; Solvent Turbulent Baseline Constants, A_n and B_n ; and Temperature Range. Table 1.5.2b summarizes the turbulent-flow parameters extracted from each run and contains eight columns: Entry; Polymeric-Regime Constants, A_p and B_p ; Apparent Slips, S'_1 and S'_3 ; Slope Increment δ ; Onset & Retro-Onset Wall Shear Stresses, T_w^* and $T_w^\#$. Table 1.5.2c summarizes the laminar-flow parameters extracted from each run and contains five columns: Entry; Arithmetic-Mean and Geometric-Mean Estimated Intrinsic Viscosities, η_{sp}/c^a and η_{sp}/c^g , and Pseudo-Power-Law

Coefficient and Exponent, K' and n' . The Entry columns common to each of Tables 1.5.2a, 1.5.2b, and 1.5.3c link their rows.

Polymer Characterization from Laminar Flow Parameters. Figure 5.4.3 is a representative double-logarithmic plot of the estimated intrinsic viscosity η_{sp}/c versus concentration c , for additive P500, obtained from the present experimental laminar flow parameters. Data for η_{sp}/c at high salinity, $[\text{NaCl}] \geq 0.01 \text{ N}$, and high polymer concentration, $c \geq 30 \text{ wppm}$, were averaged, to obtain the estimated intrinsic viscosity of P500 in its collapsed conformation, as quoted in the figure. Data for η_{sp}/c at low salinity, $[\text{NaCl}] \leq 0.001 \text{ N}$, were separately averaged, to obtain the estimated intrinsic viscosity of P500 in its extended conformation, along with the ratio of extended to

Table 1.5.2a
Experimental Conditions for B1120 Runs

Entry	Run	Concentration	Salinity	Solvent Turbulent Baseline Constants		Temperature Range (°C - °C)
		c	[NaCl]	A _n	B _n	
		(wppm)	(N)			
Betz 1120 = B1120; Pump-Driven System; Pipe ID = 1.458 cm						
27	B1P01496	1.00	1.00 × 10 ⁻⁴	4	0.4	25.05-25.5
28	B2P01494	2.02	1.00 × 10 ⁻⁴	4	0.4	24.4-25.1
29	B5P01490	5.07	1.00 × 10 ⁻⁴	4	0.4	24.4-25.05
30	B1P11486	9.96	1.00 × 10 ⁻⁴	4	0.4	24.0-24.9
31	B2P11483	20.0	1.00 × 10 ⁻⁴	4	0.4	23.5-24.7
32	B5P11480	49.9	1.00 × 10 ⁻⁴	4	0.4	23.9-25.2
33	B1P21477	100	1.00 × 10 ⁻⁴	4	0.4	24.4-24.9
34	B1P03197	1.00	3.00 × 10 ⁻¹	4	0.4	24.5-25.1
35	B2P03195	2.02	3.00 × 10 ⁻¹	4	0.4	24.2-25.1
36	B5P03191	5.07	3.00 × 10 ⁻¹	4	0.4	24.6-25.3
37	B1P13187	9.96	3.01 × 10 ⁻¹	4	0.4	24.1-25.1
38	B2P13184	20.0	3.00 × 10 ⁻¹	4	0.4	23.8-25.2
39	B5P13181	49.9	3.00 × 10 ⁻¹	4	0.4	23.7-24.9
40	B1P23178	100	3.00 × 10 ⁻¹	4	0.4	24.3-25.1

Table 1.5.2b
Turbulent Flow Parameters for B1120 Runs

Entry	Polymeric-Regime Constants		Apparent Slips ^a		Slope Increment	Onset & Retro-Onset Wall Shear Stresses ^b	
	A _p	B _p	S' ₁	S' ₃	δ	T _w [*]	T _w [#]
						(dyne/cm ²)	
Betz 1120 = B1120; Pump-Driven System; Pipe ID = 1.458 cm							
27	4.01	-0.57	0.5	1.0	~0	3.3(3.8?)	
28	7.43	7.69	3.0	4.4	3.43		
29	5.29	-4.76	8.8	9.5	1.29		
30	7.98	-1.18	13.0	14.7	3.98		23.4(38)
31			11.8	18.2			MDR
32			10.8	19.1			MDR
33			9.7	18.6			MDR
34	4.92	3.14	0.3	0.5	0.92	17.8(22?)	
35	7.70	10.6	0.5	2.7	3.70	6.5(13.5)	
36	12.4	23.9	1.3	5.4	8.40	7.4(6.1)	
37	17.2	36.1	4.0	10.2	13.2	5.1(4.1)	
38	22.0	48.8	5.6	14.5	18.0		
39			11.0	19.0			MDR
40			11.2	18.6			MDR
<p>(a) S'₁ and S'₃ denote S' evaluated at Re_v√f = 1000 and 3000, respectively. (b) () = visual value. † = before onset; ‡ = highest Re_v√f < 1000.</p>							

Table 1.5.2c
Laminar Flow Parameters for B1120 Runs

Entry	Arithmetic- and Geometric-Mean Estimated Intrinsic Viscosities		Pseudo-Power-Law Coefficient and Exponent	
	η_{sp}/c^a	η_{sp}/c^g	K'	n'
	(cm ³ /g)		(s ^{n'} · dyne/cm ²)	
Betz 1120 = B1120; Pump-Driven System; Pipe ID = 1.458 cm				
27	26869	24388	0.0090	1.006
28	84479	80687	0.0119	0.956
29	123199	113391	0.0210	0.861
30	113990	109283	0.0300	0.814
31	54709	52839	0.0296	0.847
32	116809	109491	0.2150	0.543
33	111709	104565	0.4176	0.490
34	0	0	0.0090	1.007
35	0	0	0.0093	0.997
36	7703	7689	0.0097	0.998
37	3658	3585	0.0096	1.002
38	2470	2357	0.0098	1.002
39	3398	3373	0.0109	1.004
40	4001	3993	0.0131	1.000
Superscripts: a = arithmetic mean; g = geometric mean.				

collapsed intrinsic viscosities, termed the coil expansion factor α^3 , the cube of the linear expansion factor α .

Table 1.5.3 lists the intrinsic viscosities, η_{sp}/c , estimated at high salinity for each HPAM additive. These were used, with equations 2.4-10 and 2.4-11 from the literature, to infer the molecular weight and rms radius of gyration of each additive, and thence the associated number of backbone chain links and contour lengths quoted in the table. Additional information is also provided about the present HPAM additives, including manufacturers' estimates of their molecular weights and extents of backbone hydrolysis, estimated intrinsic viscosities derived in the present work at low salinities, and apparent coil expansion factors.

1.6 Discussion

The present experimental results are discussed in five sections, concerning the influence of pipe diameter, the effect of additive conformation, the analysis of each of Type-A and Type-B drag reduction, and comparisons between them.

1.6.1 Influence of Pipe Diameter

The influence of pipe diameter upon both Types A and B of turbulent drag reduction was sought from the experiments with additives P500 and C832A in each of the 1.458- and 1.021-cm pipes.

Table 1.5.3
Inferred Polymer Characteristics†

Polymer	Manufacturer's Data‡		Estimated Intrinsic Viscosity at High Salinity	Parameters Inferred from Equations 2.4-10 and 2.4-11	
	Molecular Weight	Degree of Hydrolysis		Molecular Weight	Radius of Gyration
	$M_w \times 10^{-6}$		η_{sp}/c	$M_w \times 10^{-6}$	R_G
	(g/mole)	(%)	(cm ³ /g)	(g/mole)	(nm)
C832A	14 - 17	50(?)	3000±600	18.0±5.0	280±50
B1120	8 - 10	High(?)	3300±800	20.1±6.4	300±60
P500	2 - 3	30	1850±500	9.5±3.5	190±40
A507	1 - 2	60	340±80	1.0±0.3	50±10
D1438	2 - 4	10	440±150	1.4±0.6	60±20
C837A	14 - 17	8(?)	2700±900	15.7±6.7	260±70
C836A	14 - 17	15(?)	2700±1450	15.5±11.0	260±110
Polymer	Number of Backbone Chain Links	Contour Length	Estimated Intrinsic Viscosity at Low Salinity	Coil Expansion Ratio	Linear Expansion Factor
	$N_{bb} \times 10^{-5}$	L_c	η_{sp}/c	α^3	α
		(μm)	(cm ³ /g)		
C832A	5.0±1.4	64±18	97000±2000	32.4	3.2
B1120	5.6±1.8	71±23	97000±3000	29.6	3.1
P500	2.7±1.0	34±12	72000±2000	38.7	3.4
A507	0.3±0.1	3.6±1.1	7000±500	20.3	2.7
D1438	0.4±0.2	5.0±2.2	5800±400	13.0	2.4
C837A	4.4±1.9	56±24	31000±2000	11.4	2.2
C836A	4.4±3.1	55±39	48000±4000	17.9	2.6

† ± values are average standard errors.
‡ The accuracy of manufacturers' data is unknown.

Figure 6.1.1 shows the direct superposition, on PK coordinates, of all the original data for additive P500 at high salinity in the 1.458- and 1.021-cm pipes. In the polymeric-regime, at every concentration, the data in the 1.021-cm pipe lie systematically somewhat higher than the corresponding data in the 1.458-cm pipe. Figure 6.1.2 shows the same results after a transformation wherein the original 1.458-cm data are left intact while the 1.021-cm pipe data are translated rightward and upward, along line N, by an abscissa factor of $1.458/1.021$, the pipe-diameter ratio. All of the transformed 1.021-cm pipe polymeric-regime data are simultaneously superimposed upon the corresponding data in the 1.458-cm pipe. The transformation described above also serves to superimpose all the data for P500 at low salinity in both pipes, as shown by Figures 6.1.3 and 6.1.4. This remarkable coincidence of the entire Type-A fan and Type-B ladder structures in both pipes suggests that, in the polymeric regime, both types of drag reduction are independent of pipe diameter and are scaled by the wall shear stress. Theoretically, this result implies that drag reduction in the polymeric regime is relatively unaffected by the large scales of turbulence, imposed by the pipe diameter, and is instead controlled by the finer wall-turbulence scales related to the wall shear stress.

Polymeric-regime data for additive C832A at both high and low salinities in both the 1.458- and 1.021-cm pipes, Figures 6.1.5 - 6.1.8, are also found to scale with wall shear stress rather than pipe diameter, reinforcing the results shown for additive P500.

Additive Degradation. The aforementioned superposition of polymeric regimes further succeeds in superposing the degradation-induced maxima and downward departures from P segments observed in both pipes at the highest $Re_w\sqrt{f}$. Thus the wall shear stress also appears to scale polymer degradation during drag reduction. Perusal

of Figures 6.1.2 and 6.1.4 shows that for additive P500 at both high and low salinities, degradation becomes significant beyond a characteristic "falloff" wall shear stress, $T_w^* \approx 690 \text{ dynes/cm}^2$, corresponding to $Re_p \sqrt{f^*} \approx 6000$ in the 1.458-cm pipe. Note also that the Type-A fans in Figure 6.1.2 exhibit onset at $Re_p \sqrt{f^*} \approx 700$, where $T_w^* \approx 9.5 \text{ dynes/cm}^2$. For P500, a 70 fold range of wall shear stress thus separates onset from the degradation falloff; this is the region within which its initially-collapsed conformation can effectively reduce turbulent drag. The C832A data exhibited degradation falloffs at $T_w^* \approx 170 \text{ dynes/cm}^2$, corresponding to $Re_p \sqrt{f^*} \approx 3000$ in the 1.458 cm pipe, and Type-A onsets at $Re_p \sqrt{f^*} \approx 550$, where $T_w^* \approx 5.7 \text{ dynes/cm}^2$; in this case only a 30-fold range of wall shear stress separated onset from the degradation falloff. Lastly, the molecular weights of additives P500 and C832A are in the ratio $9.5/18 \approx 0.5$ while their falloff shear stresses are in the ratio $690/170 \approx 4$; this provides the following dimensional inverse-square relation for degradation of HPAM additives in the present pipes:

$$T_w^* \approx 5.9 \times 10^{16} M_w^{-2} \quad (6.1-2)$$

with T_w^* and M_w in dyne/cm^2 and g/mole , respectively.

1.6.2 Effect of Additive Conformation

The effects of macromolecular additive conformation on gross flow physics are summarized in the central kernel of Figure 6.2.1. Observations with any additive and salinity fell into one of three sets: (i), laminar flow that was Newtonian with relative viscosities near unity, and turbulent flow with Type-A drag reduction; (ii), laminar flow

that was Newtonian but with relative viscosities appreciably greater than unity, and turbulent flow with Type-A drag reduction; and (iii), laminar flow with shear-thinning and relative viscosities greatly in excess of unity, and turbulent flow with Type-B drag reduction. The preceding are associated with each of three initial conformations of the additive: (i) collapsed random-coil, (ii) expanded random-coil, and (iii) the extended macromolecule. The observed examples actually used to derive the above classification are given in the bottom row of Figure 6.2.1. Comparisons between these and the HPAM characterization data in Table 1.5.3 show that, while Type-A drag reduction behavior is achieved by the initially-collapsed conformations of all additives, Type-B drag reduction behavior, associated with the initially-extended macromolecular conformation, is only accessible to additives of the highest molecular weight and backbone charge. The lowest molecular weight additives, D1438 and A507, each with $M_w \approx 1 \times 10^6$ g/mole, did not exhibit Type-B behavior, despite the latter possessing a highly charged backbone, with nominal degree of hydrolysis $\approx 60\%$. The highest molecular weight additives, B1120 and C832A, with $M_w \approx 20 \times 10^6$ g/mole, and high backbone charge $\approx 50\%$, both exhibited Type-B drag reduction. However, P500, with $M_w \approx 10 \times 10^6$ g/mole, and backbone charge $\approx 30\%$ achieved Type-B behavior, whereas C837A and C836A, with $M_w \approx 16 \times 10^6$ g/mole, and backbone charges ≈ 8 and 15% , did not. These data suggest that, at any given molecular weight, a threshold backbone charge must be exceeded to induce Type-B behavior; for our $M_w \times 10^{-6} \approx 1, 10, 16,$ and 20 , these threshold charges are, respectively, $>60\%$, $<30\%$, $>15\%$, and $<50\%$.

Figure 6.2.3 details the dependence of turbulent drag reduction behavior on salinity as actually observed with the present HPAM additives. In the columns of the

figure, each of the two broad categories, the Type-A fan and the Type-B ladder, are amplified into their perfect, observed, and imperfect counterparts, respectively representing their idealized, typical, and distorted (but still recognizable) forms. Thus the perfect Type-A fan emanates from a single onset point on N, with P segments radiating into the polymeric regime, their slope increments increasing as the square-root of additive concentration. The perfect Type-B ladder has P segments that come off M at retro-onset points and lie parallel to N, but shifted upwards therefrom, by amounts that are proportional to additive concentration. The rows in the figure represent the HPAM additives studied, with the salinities exhibiting a given behavior noted in the appropriate column. All the kinds of turbulent flow behavior listed, except the perfect Type-A fan, were observed, the widest range with additive C832A.

1.6.3 Type-A Drag Reduction

Type-A drag reduction has been known for long, and here the focus is exclusively on the present new results for HPAM additives in their variously random-coiling conformations. A Type-A fan is defined by the wall shear stress at its onset point, and by the slope increments of the P segments emanating therefrom; we consider the dependence of these parameters on molecular properties.

Onset. Figure 6.3.1 illustrates a direct relationship between macromolecular coil size and onset for 20.6-wppm solutions of additive C836A at salinities from 0.1 to 0.0003 N. The onset $Re_c\sqrt{f^*}$, obtained from the intersection of the observed P segments with the solvent line N, decreases monotonically as the intrinsic viscosity η_{sp}/c increases, the

conformational expansion here induced by decreasing salinity.

More generally, the onset wall shear stress T_w^* is found to correlate inversely with the rms radius of gyration R_G of the additive. All the present onset data are presented in this standard form in Table 1.6.1. Part A of the table contains the more reliable data, using average values of T_w^* from the Type-A fans observed at high salinity and R_G data from Table 1.5.3; part B of the table contains individual values of T_w^* at various salinities, with R_G estimated from the corresponding η_{sp}/c via coil expansion factors.

Figure 6.3.2 is an onset correlation for collapsed HPAM additives, displaying the data in Table 1.6.1 on doubly logarithmic coordinates of T_w^* vs R_G . The solid line of slope -2 drawn through the experimental data represents the equation:

$$T_w^* = 5.79 \times 10^5 R_G^{-2} \quad (6.3-5)$$

where T_w^* and R_G are in dyne/cm² and nm, respectively. The proportionality constant in equation 6.3-5 corresponds to a nondimensional "length-based" onset constant $\Omega_L = R_G u_* / \nu_s = 8.3 \times 10^{-3}$, which is of the same order as that, $\Omega_L = (8.2 \pm 0.4) \times 10^{-3}$, previously quoted for PAM additives in the literature (Virk, 1975b).

Slope Increments. Figure 6.3.3 illustrates a direct relationship between macromolecular coil size and slope increment for 20.6-wppm solutions of additive C836A at salinities from 0.1 to 0.0003 N. The slope increment remains essentially constant, $\delta = 15.3 \pm 0.7$, over a 25-fold range of the intrinsic viscosity η_{sp}/c , which increases from 2500 to 70000 cm³/g with decreasing salinity. Thus, in Type-A drag reduction, the slope increment is essentially independent of coil size, in contrast to the onset wall shear stress, which decreases markedly with increasing coil size.

Table 1.6.1
Onset Data for Type-A Drag Reduction by HPAM Additives†

HPAM	Concentration Range	Salinity	Estimated Intrinsic Viscosity	Radius of Gyration	Onset Wall Shear Stress ¹	Length-Based Onset Constant
	c		[NaCl]		η_{sp}/c	T_w^*
	(wppm)	(N)	(cm ³ /g)	(nm)	(cm ³ /g)	
Part A: Average Values						
C832A ²	20-100	0.3	3000	280±50	7.7±2.2	8.5±2.7
B1120	10-100	0.3	3300	300±60	6.4±1.2	8.3±2.4
P500 ²	30-100	0.3	1850	190±40	9.5±4.6	6.5±3.1
A507	300-1000	0.3	340	50±10	50.4±20.1	4.0±1.5
D1438	100-1000	0.3	440	60±20	41.0±19.2	4.4±2.2
C837A	50	0.1	2700	260±70	13.7±7.9	10.8±5.9
C836A	20	0.1	2700	260±110	15.2±4.6	11.2±6.5
Part B: Other Individual Values						
C836A ³	20.6	0.0003	69170	715	0.77(190)	7.1
C836A ³	20.6	0.001	36330	580	1.6(270)	8.3
C836A	20.6	0.01	8190	350	5.8(510)	9.4
C836A ⁴	20.6	0.1	2820	250	10.8(690)	9.0
C836A ⁴	20.6	0.1	2560	240	13.7(770)	9.8
P500	30	0.01	8480	300	2.9	5.8
P500 ⁴	30	0.3	1630	170	8.4	5.4
A507	30-300	0.0001	7000	135	23.7 ⁵	8.6
A507 ⁴	30-300	0.3	330	49	45.6	4.0

HPAM	Concentration Range	Salinity	Estimated Intrinsic Viscosity	Radius of Gyration	Onset Wall Shear Stress ¹	Length-Based Onset Constant
	c		[NaCl]		η_{sp}/c	T_w^*
	(wppm)	(N)	(cm ³ /g)	(nm)	(cm ³ /g)	
D1438	30-300	0.0001	5800	140	30	10.1
D1438 ⁴	30-300	0.3	440	60	46.5	4.4

†All solvent physical properties are evaluated at 25°C.

1 Values in parentheses are the corresponding $Re_s\sqrt{f^*}$.

2 Data are included from both pipes.

3 T_w^* and $Re_s\sqrt{f^*}$ are virtual values regressed via (A_p , B_p) data.

4 Data are incorporated into Part-A averages.

5 T_w^* average value is visual.

More generally, the slope increment is found to increase with the square root of additive concentration; this leads to a specific slope increment, δ/\sqrt{c} , and thence an intrinsic slope increment $\Pi = \delta/\sqrt{(c/M_w)}$. For many polymer-solvent systems, the molecular quantity Π is found to correlate with the 3/2 power of the number of backbone chain links, N_{bb} , their proportionality constant being called the slope modulus, κ . The present slope increment data are presented in this standard form in Table 1.6.2, using average values of δ/\sqrt{c} from the Type-A fans observed at high salinity and N_{bb} data from Table 1.5.3.

Figure 6.3.6 shows intrinsic slope increments for collapsed HPAM additives, displaying the data from Table 1.6.2 on doubly logarithmic coordinates of Π vs N_{bb} . The solid line of slope 3/2 drawn through the experimental data represents the equation:

Table 1.6.2
Specific and Intrinsic Slope Increment Data

Polymer	Molecular Weight	Number of Backbone Chain Links	Average Specific Slope Increment	Average Intrinsic Slope Increment	Slope Modulus†
	$M_w \times 10^{-6}$	$N_{bb} \times 10^{-5}$	$\delta V/c$	$\Pi \times 10^{-3}$	$\kappa \times 10^6$
	(g/mole)				
C832A	18.0±5.0	5.0±1.4	4.1±0.7	17.2±5.3	47.9
B1120	20.1±6.4	5.7±1.8	3.6±0.6	16.2±5.4	38.3
P500	9.5±3.5	2.7±1.0	2.3±0.2	7.0±2.0	51.1
A507	1.0±0.3	0.3±0.1	0.16±0.02	0.16±0.04	42.8
D1438	1.4±0.6	0.4±0.2	0.29±0.05	0.35±0.14	56.4
C837A	15.7±6.7	4.4±1.9	2.8±0.6	1.1±0.5	38.1
C836A	15.5±11.0	4.4±3.1	2.5±0.6	9.9±5.9	34.4

† Slope moduli are averages; uncertainties in N_{bb} cause very large uncertainties in the slope moduli.

$$\Pi = 43.5 \times 10^{-6} N_{bb}^{3/2} \quad (6.3-7)$$

The slope modulus, $\kappa = 43.5 \times 10^6$ found from equation 6.3-7 is of the same order as that, $\kappa = (80 \pm 20) \times 10^6$ previously quoted for PAM additives in the literature (Virk, 1975b).

1.6.4 Type-B Drag Reduction

Type-B drag reduction has hitherto been little studied. Here we focus mainly on our new results for HPAM additives in their extended conformations, and also attempt

to discuss (the few) other data available in the literature. A Type-B ladder is primarily defined by the flow enhancements induced by its P segment rungs at a known, high, $Re_p\sqrt{f}$; and secondarily by the wall shear stresses at its retro-onset points, where the rungs intersect the MDR asymptote. The dependence of both these parameters on the molecular properties of the additive are considered.

Flow Enhancement. The present results, §1.5.2, indicates that in Type-B drag reduction, the nondimensional flow enhancement or apparent slip, S' , is only weakly dependent on flow parameters, such as $Re_p\sqrt{f}$ and pipe diameter, but is strongly dependent on additive parameters, such as concentration and molecular weight.

Figure 6.6.1 depicts the flow enhancement by six HPAM additives, including both the present data for additives C832A, B1120, and P500, as well as literature data from three sources (Clarke, 1970; Oliver & Bakhtiyarov, 1983; Interthal & Wilski, 1985). With all polymers, an approximately linear relationship between S' and c is observed at all $c < 50$ wppm (the highest concentrations, $c > 50$ wppm, attain the MDR asymptote, so $S' = S_M$, independent of c). We can now define the specific slip, S'/c , characteristic of additive efficacy in Type-B drag reduction, and also the intrinsic slip $\Sigma = S'/(c/M_w)$, a measure of flow enhancement per molecule. Since the intrinsic slip Σ is a molecular quantity, one might expect it to depend upon a molecular attribute of the additive, of which N_{bb} , the number of backbone chain links, is the most basic.

Figure 6.6.3 shows the intrinsic slip for extended HPAM additives on doubly logarithmic coordinates of Σ vs N_{bb} . It is found that Σ increases roughly as N_{bb}^3 along the solid line shown in the figure, which represents the approximate relation:

$$\Sigma = 2.21 \times 10^{-10} N_{bb}^3 \quad (6.6-2)$$

The proportionality constant between Σ and N_{bb}^3 is termed the "slip modulus", λ , with average value 2.2×10^{-10} g/mole/wppm; slip moduli for individual entries are shown in the legend of Figure 6.6.2.

Type-B flow enhancement data from the present work and all available literature are summarized in Table 1.6.3, which provides both additive characterization information as well as specific and intrinsic slip data.

Figure 6.6.3 depicts the flow enhancement by various additives in Type-B drag reduction, showing all entries from Table 1.6.3; these include the six HPAM additives shown in Figure 6.6.2, as well as additional results for xanthan gum (Rochefort & Middleman, 1985), asbestos fibers (Sharma et al., 1979; McComb & Chan, 1985), nylon fibers (Bobkowicz & Gauvin, 1965) and paper fibers (Lee & Duffy, 1976). All the additional data also show apparent slips roughly proportional to additive concentration.

Table 1.6.3
Flow-Enhancement Data in Type-B Drag Reduction for Various Additives

Additive†	Molecular Weight	Number of Backbone Chain Links	Contour Length	Pipe Diameter
	$M_w \times 10^{-6}$	$N_{bb} \times 10^{-5}$	$L_c \times 10^3$	D
	(g/mole)		(cm)	(cm)
HPAM Additives				
C832A	18.0±5.0	5.0±1.4	6.4±1.8	1.021, 1.458
B1120	20.1±6.4	5.7±1.8	7.1±2.3	1.458
P500	9.5±3.5	2.7±1.0	3.4±1.2	1.021, 1.458
AP30 ¹	9.2	2.6	3.2	1.03
MagE10 ²	23	6.5	8.1	0.597
HSB125 ³	16.5	4.6	5.8	1.4
Xanthan ⁴	2.0?	0.02?	0.25?	0.238
Slip Data				
Stress Level of Data	Specific Slip	Intrinsic Slip	Volume Fraction Per wppm	Volume Fraction Per Unit Slip
$Re\sqrt{f}$	S'/c	$\Sigma \times 10^{-6}$	X_v/c	X_v/S'
	(wppm ⁻¹)	(g/mole/wppm)	(wppm ⁻¹)	
3000	1.87	33.6±9.4	4500	2410
3000	1.62	32.5±10.4	5640	3490
3000	0.58	5.45±2.02	1250	2180
3000	0.31	2.85	7380	1800
1600	4.1	94.3	3800	4180
3000	0.91	15.0	1180	3812
450	0.067	0.134?	2.5?	40?

Additive†	Fiber Diameter	Aspect Ratio	Fiber Length	Pipe Diameter
	$d_f \times 10^3$	l_f/d_f	l_f	D
	(cm)		(cm)	(cm)
Fiber Additives				
Asbestos ⁵	0.003	40000	0.14	1.9
Asbestos ⁶	0.005	28000	0.14	1.95
Paper ⁷	3.0	90	0.27	10.0
Nylon ⁸	2.0	51	0.10	4.98
Stress Level of Data				
Stress Level of Data	Specific Slip	Intrinsic Slip	Volume Fraction Per wppm	Volume Fraction Per Unit Slip
$Re\sqrt{f}$	S'/c	$\Sigma \times 10^{-6}$	X_v/c	X_v/S'
	(wppm ⁻¹)	(g/mole/wppm)	(wppm ⁻¹)	
1600	0.03	n/a	420	13900
1300	0.041	n/a	205	4980
3000	0.0015	n/a	0.006	4.1
5800	0.00021	n/a	0.0015	7.1
<p>† Note the wrap-around nature of this table in both the HPAM- and Fiber-Additive sections.</p> <p>1 — Clarke(1970); 2 — Oliver & Bakhtiyarov(1983); 3 — Interthal & Wilski (1985); 4 — Rochefort & Middleman(1984); 5 — Sharma et al.(1979); 6 — McComb & Chan(1985); 7 — Bobkowicz & Gauvin(1965); 8 — Lee & Duffy (1976).</p> <p>n/a = not applicable</p>				

The specific slips seen in the figure span nearly five orders of magnitude, from $S'/c = 0.00016$ for nylon fibers to $S'/c \approx 4.1$ for the highest molecular weight HPAM. To help interpret this wide variation in additive efficacy, the last two columns of Table 1.6.3 respectively list the additive-pervaded volume fraction per unit concentration, X_v/c , derived from either the macromolecular contour length L_c or the fiber length l_f and aspect ratio l_f/d_f , and then the additive-pervaded volume fraction required to induce unit slip, X_v/S' . For the most effective additives, HPAMs and asbestos fibers, $X_v/S' \approx 3000$, implying, since X_v cannot physically exceed unity, that these additives must be significantly aligned during drag reduction.

Retro-Onset. From the geometry of a perfect Type-B ladder, the rung for concentration c , with flow enhancement S' , should exhibit retro-onset at $\log Re_s \sqrt{f}^\# = \log Re_s \sqrt{f}^\#_o + S'/15$, where $\log Re_s \sqrt{f}^\#_o$ refers to the intersection of the MDR asymptote M with the Prandtl-Karman line N . Since $Re_s \sqrt{f}$ is formed with T_w , and S' is proportional to polymer concentration, we should expect a linear relationship between $\log T_w^\#$ and c .

Figure 6.6.4 presents a retro-onset correlation for extended HPAM additives, using coordinates of $\log T_w^\#$ vs c . The present data for additives C832A and B1120 in the 1.458-cm pipe are fitted by the line:

$$\log T_w^\# = -0.436 + 0.134c \quad (5.3-1)$$

with $T_w^\#$ and c in dyne/cm² and wppm, respectively. The ordinal intercept $T_w^\#_o = 0.37$ dyne/cm² is close to the value $T_w^\#_o = 0.35$ dyne/cm² at the intersection of $N(c = 0)$ with M ; the slope of the line corresponds to an apparent $S'/c = 1$, somewhat lower than the

observed $S'/c \approx 1.7$ for these additives. The same form of correlation also applies to the data for P500, after adjustment for its lower S'/c and different pipe diameter. Retro-onset results from the literature are also accommodated by the correlation.

1.6.5 Comparisons Between Type-A and Type-B Drag Reduction

Relative Flow Enhancements. Data calculated from the flow trajectories of 30-wppm P500 solutions at salinities of 0.3, 0.01, 0.001, and 0.0001 N in the 1.021-cm pipe are presented in Figure 6.5.1, as a plot of the "slip ratio", $S'_{[N]}/S'_{0.0001}$, vs $Re_p\sqrt{f}$. The ordinate is the ratio of S' induced at any salinity relative to the S' induced by the lowest salinity, that is, by the most extended initial conformation of the additive, at the same $Re_p\sqrt{f}$. For the initially collapsed conformation, at the highest salinity of 0.3 N NaCl, the slip ratio increases monotonically from near zero at $Re_p\sqrt{f} \approx 500$ to almost unity at $Re_p\sqrt{f} \approx 5000$; this physically reflects the progressive extension of the initially collapsed macromolecular conformation with increasing turbulent flow strength. For the next lower salinity of 0.01 N, the slip ratio is ≈ 0.6 at $Re_p\sqrt{f} \approx 500$ and then increases monotonically to unity at $Re_p\sqrt{f} \approx 5000$. Finally, at salinity 0.001 N, the slip ratio is essentially unity over the entire range of $Re_p\sqrt{f}$ from 500 to 5000. These results suggest that the extended conformations of the additive induce drag reduction, and thence the more closely an initial conformation resembles the active extended form, the more effective it is in drag reduction. For additives that exhibit Type-A behavior at high salinity and Type-B behavior at low salinity, we can define the special slip ratio, $R_{sc} = [S'_A/S'_B]_c$, that is, the ratio of Type-A to Type-B flow enhancements at fixed

concentration and $Re_s\sqrt{f}$. Since $S'_A = 0$ for $Re_s\sqrt{f} < Re_s\sqrt{f}^*$, and $S'_A < S'_B$, always, we expect $0 \leq R_{sc} \leq 1$ for $(Re_s\sqrt{f}/Re_s\sqrt{f}^*) \geq 1$.

Figure 6.5.3 is a semilogarithmic plot of the slip ratio R_{sc} versus the normalized turbulent flow strength $(Re_s\sqrt{f}/Re_s\sqrt{f}^*)$ for 10 pairs of Type-A and Type-B data exhibited by two concentrations each of three HPAM additives in two pipes. The data scatter around a single, universal, curve that rises monotonically, but with decreasing slope, from $R_{sc} = 0$ at $(Re_s\sqrt{f}/Re_s\sqrt{f}^*) = 1$ to $R_{sc} = 0.8$ at $(Re_s\sqrt{f}/Re_s\sqrt{f}^*) = 10$, being well represented by the equation:

$$R_{sc} = 1 - \left[\frac{Re_s\sqrt{f}}{Re_s\sqrt{f}^*} \right]^{-2/3} \quad (6.5-2)$$

Equation 6.5-2 physically represents the extension of initially collapsed, random-coiling, HPAM macromolecules towards their fully extended conformations by the turbulent flow field. It is interesting that this process seems relatively independent of additive parameters and absolute wall shear stress levels.

Additive Equivalence and Isoslip Points. Figure 6.5.4 is a PK plot of data obtained with additive C832A in the 1.458 cm pipe, specifically showing results for three solutions, namely 5.6-wppm in 0.00001 N NaCl(\square , abbr 5.6B), 20.9-wppm in 0.00001 N NaCl(\diamond , abbr 20.9B), and 20.7-wppm in 0.1 N NaCl(\blacklozenge , abbr 20.7A). The former two trajectories are part of a Type-B ladder, while the third belongs to a Type-A fan. It is seen that trajectory 20.7A intersects 5.6B at coordinates $(Re_s\sqrt{f}, 1/\sqrt{f}) = (975, 15.2)$. This is termed an "isoslip" point, since both solutions here exhibit the identical flow enhancement, $S' = 3.6$. At this isoslip point, 20.7 wppm of the initially collapsed

conformation and 5.6 wppm of the extended conformation are evidently equivalent in the ability to reduce drag. The term "additive equivalence" is used to describe such a case, where two different additive solutions cause the same drag reduction. Continuing, at the isoslip $Re_s\sqrt{f} = 975$, the trajectory 20.9B exhibits $S' = 12.7$, generating a "slip triad" (20.9B, 20.7A, 5.6B) with associated $S'(12.7, 3.6, 3.6)$. Within this triad, the collapsed to extended slip ratio at constant concentration is $R_{sc} = 3.6/12.7 = 0.28$, while the extended to collapsed concentration ratio at constant slip is $R_{cs} = 5.6/20.9 = 0.27$. The essential equality between R_{sc} and R_{cs} is striking, and warrants elaboration.

Figure 6.5.10 presents data for additive B1120 in the 1.458 cm pipe, showing five additional isoslip points, where the trajectory 5A intersects the trajectories 1B and 2B, and where 20A intersects 2B, 5B, and 10B.

A total of 42 isoslip points, along with their associated slip triads, were identified in the present data for additives C832A, B1120, and P500. Figure 6.5.14 is a plot of the slip ratio R_{sc} versus the concentration ratio R_{cs} among all slip triads. It is evident that $R_{sc} = R_{cs}$, reinforcing the earlier observation in Figure 6.5.4. This result offers a noteworthy physical insight. Namely, that for fixed total additive concentration, the collapsed to extended slip ratio R_{sc} observed at any $Re_s\sqrt{f}$ simply represents the fraction of originally collapsed macromolecules that have become extended in the flow, and thence effective in drag reduction. Further, if the extended additive states are the active species responsible for drag reduction, then Type-B behavior should emerge as the fundamental feature of the phenomenon, with the better known Type-A behavior viewed as a special case wherein the initially randomly-coiled and ineffective macromolecules are extended, and hence activated, by the turbulent flow field.

1.7 Modelling Types A and B Drag Reduction

From the correlations in §1.6.3 and §1.6.4, perfect Type-A fans and perfect Type-B ladders, respectively, may be qualitatively modelled.

In modelling a perfect Type-A fan, equation 2.4-11 provides an estimated rms radius of gyration R_G from molecular weight. Equation 6.3-5 is then used to calculate the onset wall shear stress, T_w^* , and thus $Re_s\sqrt{f^*}$, from the estimated R_G . Next, equation 6.3-7 yields the specific slope increment δ/\sqrt{c} , and thus δ , with $N_{bb} = M_w/m$. For any concentration c , the polymeric-regime segment P is given by

$$\frac{1}{\sqrt{f_p}} = 4.0 \log(Re_s\sqrt{f}) - 0.4 + \sqrt{c} \left[\frac{\delta}{\sqrt{c}} \right] \log \left[\frac{Re_s\sqrt{f}}{Re_s\sqrt{f^*}} \right] \quad (6.7-1)$$

Equation 6.7-1 is subject to lower and upper bounds on $Re_s\sqrt{f}$: The former is $Re_s\sqrt{f^*}$; the latter, degradation-falloff $Re_s\sqrt{f^{\wedge}}$, via equation 6.1-2.

In modelling a perfect Type-B ladder, equation 6.6-2 gives the intrinsic slip Σ , and thus S'/c , from molecular weight and mass per backbone chain link. For any concentration c , the corresponding ladder rung is described by equation 6.4-7:

$$\frac{1}{\sqrt{f_p}} = 4.0 \log Re_s\sqrt{f} - 0.4 + c \left[\frac{S'}{c} \right] \quad (6.4-7)$$

The valid range of $Re_s\sqrt{f}$ in equation 6.4-7 is bounded below by $Re_s\sqrt{f^{\#}}$, via equation 6.4-8, and above by $Re_s\sqrt{f^{\wedge}}$, via equation 6.1-2.

These models agree best with B1120 data at intermediate $5 < c < 10$ wppm.

1.8 Conclusions

1. The drag reduction phenomenon was experimentally studied in two pipes, of diameters 1.46 and 1.02 cm, using seven polyelectrolytic HPAM additives, with molecular weights from 1 to 20×10^6 g/mole and degree of backbone hydrolysis from 8 to 60%, at concentrations from 1 to 1000 wppm, in saline solutions containing from 0.3 to 0.00001 N NaCl.

2. Both laminar and turbulent flow behavior were greatly influenced by salinity-induced changes in the initial conformation of the HPAM additives. Initially collapsed, random-coiling conformations exhibited Newtonian laminar flow and Type-A turbulent drag reduction, while initially extended conformations exhibited shear-thinning in laminar flow and Type-B turbulent drag reduction.

3. The gross-flow physics of Type-B drag reduction were delineated. A characteristic "ladder" structure prevailed, with polymeric regime segments that were roughly parallel to, but shifted upward from, the Prandtl-Karman line and intersected the maximum drag reduction asymptote at retro-onset points.

4. In the polymeric regime, both Type-A fan and Type-B ladder structures were essentially independent of pipe diameter, and were scaled by the wall shear stress. Thus both types of drag reduction are insensitive to the large turbulence scales imposed by pipe diameter, and are controlled instead by the finer wall-turbulence scales associated with the wall shear stress. The wall shear stress also scaled incipient degradation during drag reduction.

5. New correlations were presented for Type-A drag reduction by HPAM additives, as follows:

$$\text{(Onset Correlation)} \quad T_w^* = 5.79 \times 10^5 R_G^{-2} \quad (6.3-5)$$

$$\text{(Slope-Increment Correlation)} \quad \Pi = 43.5 \times 10^{-6} N_{bb}^{3/2} \quad (6.3-7)$$

6. In Type-B drag reduction it was found that the flow enhancement S' was proportional to additive concentration, and that the intrinsic slip, $\Sigma = S'/(c/M_w)$, varied roughly as the third power of backbone chain links N_{bb} . New correlations were presented for Type-B drag reduction by HPAM additives:

$$\text{(Intrinsic-Slip Correlation)} \quad \Sigma = 2.21 \times 10^{-10} N_{bb}^3 \quad (6.6-2)$$

$$\text{(Retro-Onset Correlation)} \quad \log T_w^* = -0.436 + 0.134c \quad (5.3-1)$$

7. Analysis of available literature for Type-B drag reduction by polyelectrolytic and fiber additives revealed a wide range of additive efficacies, with specific slips S'/c from 0.0001 to 4. For the most effective additives, HPAM and asbestos fibers, the additive-pervaded volume fraction per unit flow enhancement, $X_v/S' \approx 3000$, implied that these additives align during drag reduction.

8. The slip ratio R_{sc} , which is the relative flow enhancement induced in Type-A and Type-B drag reduction at constant additive concentration, was found to be a universal function of the normalized turbulent flow strength ($Re_s\sqrt{f}/Re_s\sqrt{f^*}$), as follows:

$$R_{sc} = 1 - \left[\frac{Re_s\sqrt{f}}{Re_s\sqrt{f^*}} \right]^{-2/3} \quad (6.5-2)$$

The extension of initially collapsed, random-coiling, HPAM macromolecules by the turbulent flow field thus seems independent of additive parameters and absolute wall shear stress levels.

9. Gross flow additive equivalence was detected at iso-slip points, where different polymer solutions induced equal flow enhancements. At numerous such points, the collapsed to extended slip ratio at constant concentration, R_{xc} , was essentially equal to the extended to collapsed concentration ratio at constant slip, R_{cs} . Thus, for fixed total additive concentration, the collapsed to extended slip ratio R_{xc} observed at any $Re_s\sqrt{f}$ simply represents the fraction of originally collapsed macromolecules that have become extended in the flow, and thence effective in drag reduction.

10. If extended additive states are the active species responsible for drag reduction, as appears likely, then Type-B behavior should underlie the basic mechanism of additive-turbulence interaction.

CHAPTER II

INTRODUCTION

This chapter sets forth the objective of, and the motivation behind, the present work. A brief background is given of the drag-reduction phenomenon, followed by a review of pertinent previous drag-reduction literature, and a summary of macromolecular characterization data for the polyelectrolyte additives used in this work.

2.1 Objective and Motivation

The thesis' objective was to examine the influence of macromolecular conformation on drag reduction in turbulent flow. This was achieved by exploring the drag reduction induced by dilute solutions of polyelectrolytic additives in both their collapsed and expanded macromolecular conformations, as exhibited in solvents of high and low ionic strengths, respectively.

The experimental investigation comprised gross-flow, that is, pressure drop versus flow rate, measurements in two pipes, using aqueous solutions of seven partially hydrolyzed polyacrylamide, HPAM, additives at several salinities. The following ranges of flow and additive parameters were: pipes of inner diameter and length-to-diameter ratios, $(D, L/D) = (1.021 \text{ cm}, 203)$ and $(1.458 \text{ cm}, 183)$; laminar- and turbulent-flow regimes with Reynolds numbers from 1×10^2 to 2×10^5 ; and wall shear stresses from 1×10^{-2} to 1×10^3 dyne/cm². The HPAM additives used varied in molecular weights from

1×10^6 to 20×10^6 g/mol and had degrees of hydrolysis from 8 to 60%; they were employed at concentrations from 1 to 1000 weight-parts per million, in aqueous solutions with salinities from 0.00001 N to 0.3 N NaCl. Turbulent drag reductions induced by the additives varied from zero to the asymptotic maximum possible.

The present work was motivated by the observation (Virk 1975a) of striking differences between the gross-flow drag-reduction behavior of collapsed and extended polyelectrolytes. On Prandtl-Karman (PK) coordinates, turbulent-flow trajectories for the collapsed polyelectrolytes, in common with other initially random-coiling macromolecules, were characterized by an abrupt onset of drag reduction, beyond which they departed upward from the Newtonian friction-factor relation, into a regime with drag reduction, with slopes significantly greater than Newtonian. In contrast, trajectories of extended polyelectrolytes, in common with those of fiber suspensions, exhibited no clear onset of drag reduction, but rather exhibited relatively constant drag reduction, with slopes roughly parallel to the Newtonian friction-factor relation. These two distinct types of flow trajectories, respectively named Type A and Type B, suggested that drag reduction was inherently dependent upon the conformation, that is, the actual shape, of the additive in solution, and the present work was an undertaking to delineate this dependence. Polyelectrolyte additives were particularly suited to the present study because their static conformations could be altered greatly by changing solvent salinities while maintaining the identical backbone length, which is perhaps the single most important of the macromolecular parameters known to affect drag reduction. Finally, it was hoped that the systematic delineation of drag-reduction Types A and B, and the quantitative comparisons between them, might also provide fresh physical insights into

the role of the additive in the mechanism of the phenomenon.

2.2 Introduction

After Toms(1948) observed and reported the drag-reduction phenomenon, later to be called the "Toms Effect", engineers have sought to take advantage of it in real world applications.

From the beginning, most drag reduction research has been driven by industrial and military interests. For various additives, percent drag reduction achieved, degradation resistance, and ease of application were investigated. Correlations were sought for design and scale-up, and to increase the efficiency, of flow systems. The friction reduction at constant flow rates, that is, at a constant Reynolds number Re , was of particular interest, as a %DR was defined as the difference in pressure drop between solvent-flow and polymer-solution flow, respectively, at the same volumetric flow rate Q (or $\langle \bar{U} \rangle$), expressed as a percentage of the solvent flow pressure drop:

$$\%DR = \frac{\Delta P_n - \Delta P_p}{\Delta P_n} \quad (2.2-1)$$

where the subscripts p and n denote polymer and solvent(Newtonian) conditions, respectively. From equations defining the Fanning friction factor f and representing a force balance on a length of pipe $D \times L$, respectively,

$$f \equiv \frac{2T_w}{\rho \langle U \rangle^2} \quad (2.2-2)$$

$$T_w = \frac{D}{4} \left[\frac{-\Delta P}{L} \right] \quad (2.2-3)$$

the percent drag reduction can be rewritten:

$$\%DR = 1 - \frac{f_p}{f_n} \quad (2.2-4)$$

The features of the mean and turbulent velocity fields were also uncovered and quantified. Standard double-logarithmic friction-factor plots of f vs. Re soon gave way to semilogarithmic Prandtl-Karman(PK) plots of $1/\sqrt{f}$ vs. $Re_s\sqrt{f}$ because drag-reduction data in PK coordinates invariably follow straight lines and are easier to interpret. In PK coordinates, the ordinate and abscissa, respectively, are:

$$\frac{1}{\sqrt{f}} = \frac{\langle U \rangle}{\sqrt{2}u_\tau} \quad (2.2-5)$$

$$Re_s\sqrt{f} = \frac{\sqrt{2}Du_\tau}{\nu_s} = 2\sqrt{2} \left[\frac{Ru_\tau}{\nu_s} \right] = 2\sqrt{2}R^+ \quad (2.2-6)$$

where the subscript s refers to solvent and the friction velocity $u_\tau \equiv (T_w/\rho)^{1/2}$. In these coordinates, the apparent slip S' provides a measure of flow enhancement:

$$S' \equiv \left[\frac{1}{\sqrt{f_p}} - \frac{1}{\sqrt{f_n}} \right]_{u_\tau} = \left[\frac{1}{\sqrt{f_p}} - \frac{1}{\sqrt{f_n}} \right]_{Re_s\sqrt{f}} \quad (2.2-7)$$

The apparent slip S' represents the upward shift from the PK law and provides a more intuitive measure of drag reduction than does percent drag reduction. The advantage of this method is that S' can be mathematically related to the mean velocity profile; thus,

reporting S' indicates something about flow structure. In the literature review that follows, S' was found to correlate the various facets of drag reduction better than does %DR.

Methods that have been employed to reduce turbulent drag involve alteration either the wetted surfaces or the flowing fluid. Contoured surfaces, while offering a permanent solution for reducing drag, provide relatively little flow enhancement and, thus, are the least used. Adding small amounts of various substances to the fluid, in concentrations on the order of tens of weight-parts per million, has been the easiest and most popular method to reduce drag. Additives, in order of decreasing popularity, include polymers, fibers, small particles, and bubbles. The latter two are difficult to apply.

In systems which have a fixed configuration(i.e. have permanent pumps and ducts) additives can be especially advantageous with the improved performance and lower pumping costs offsetting the cost. For example, in the Alaskan oil pipeline at Prudhoe Bay, drag-reducing additives increase the throughput without the costly installation of additional pumping stations. Ideally, the additive should not degrade. However, in closed-looped systems, additive degradation is a real problem and limits the extent and duration of drag reduction. In open systems, such as pipelines, firehoses, drains and sewers, and hulls of water vessels, additives are continuously lost; thus, to be effective, additives must be easy to apply, inexpensive, and durable.

After Toms' discovery, most of the research has focussed on drag reduction in turbulent pipe flow by dilute solutions of long-chained polymers (macromolecules) dissolved in a Newtonian solvent. From this basic framework the variety of experiments

conducted is immense, as illustrated by Table 2.1.

The experiments in this project are limited to smooth circular-pipe geometries, polymeric additives, good solvents with varying ionic strengths, fully developed turbulent flow in a single-pass system, and premixed homogeneous solutions. The molecular weight M_w and conformation are the independent polymer-additive variables of interest.

Table 2.1
Parameters in Drag-Reduction Experiments

PARAMETER				
	flow cross-section(Del Villar et al., 1984)			
	smooth vs. rough surface(Virk, 1971a)			
Additive Type	polymers	molecular weight M_w (Gramain & Borreill, 1978)		
		backbone structure (Ting, 1982)		
		side groups (McCormick et al., 1990a)		
		conformation	coiled vs. uncoiled (Parker & Hedley, 1972)	
			preextended vs. collapsed (Virk, 1975a)	
		flexibility vs. rigidity (Rocheffort & Middleman, 1984)		
		rheology	elasticity(relaxation) (Bewersdorff & Berman, 1988)	
			viscosity (Pinho & Whitelaw, 1990)	
		behavior in solvent	homogeneous dispersal (Oliver & Bakhtiyarov, 1983)	
			heterogenous dispersal	aggregates (Dunlop & Cox, 1977)
	micelles (Ohlendorf et al., 1988)			
	networks (Inge et al., 1979)			
	fibers and fibers/polymers (McComb & Chan, 1981)			
gas bubbles (Madavan et al., 1985)				

PARAMETER		
Solvent Type	highly vs. poorly dispersing (good solvent vs. Θ solvent) (Zakin & Hunston, 1980)	
	high vs. low pH (White & Gordon, 1975)	
	high vs. low ionic strength (Banijamali et al., 1974)	
Flow Conditions	transition vs. full turbulence (Ogawa & Kuroda, 1986)	
	single vs. multiple pass (Kowalik et al., 1987)	
Method of additive introduction	premixed solution (Kulicke et al., 1989)	
	flow injection	centerline ($y^+ = R^+$) (Hoyt & Sellin, 1988)
		near wall ($y^+ \approx 20$) (Frings, 1988)
		wall ($y^+ = 0$) (Wells & Spanger, 1967)

2.3 Drag-Reduction Literature Review

In "Drag Reduction Fundamentals", Virk(1975b) provided a comprehensive review of polymer-induced drag reduction, with attention primarily on the behavior of homogeneous solutions of linear, random-coiling polymers, such as polyethylene oxide(PEO). The review also delineated three echelons of flow structure during drag reduction — gross flow, mean flow, and turbulence structure — which will be used to describe the latest literature developments.

2.3.1 Gross Flow

In pipe flows, when $Re_c < 2000$, the friction factor data follow Poiseuille's law for laminar flow(L):

$$\frac{1}{\sqrt{f}} = \frac{Re_c \sqrt{f}}{16} \quad (2.3-1)$$

for both solvent and polymer solution flows. For $Re_c > 2000$, both solvent and polymer flows exhibit intermittency or transition. For $Re_c > 4000$, both flows, in general, obey the PK equation(N):

$$\frac{1}{\sqrt{f}} = 4.0 \log(Re_c \sqrt{f}) - 0.4 \quad (2.3-2)$$

which is the universal Prandtl-Karman correlation for Newtonian fully turbulent flow. The polymer flow continues to adhere to N until onset occurs. Onset describes a sudden

divergence from N of the polymer solution's friction-factor trajectory into the "polymeric" regime with drag reduction. Onset is characterized by the onset friction velocity, u_r^* , or, equivalently, the onset wall shear stress, T_w^* . According to the time-based onset hypothesis, onset occurs when the polymer relaxation time, λ_p , and the critical wall flow time, $[(u_r^*)^2/\nu_s]^{-1}$, are of equal magnitude, that is, $\lambda_p(u_r^*)^2/\nu_s \approx 1$. From theoretical polymer mechanics, which predicts that $\lambda_p \propto M[\eta] \propto R_G^3$, and the onset criterion, a time-based onset relation arises:

$$\Omega_T = R_G^3 T_w^* \quad (2.3-3)$$

On the other hand, the length-based onset hypothesis asserts that at onset that the product of the characteristic polymer length, R_G , and the inverse turbulent length scale u_r^*/ν_s (or wavenumber W^*) is constant:

$$\Omega_L = \frac{R_G u_r^*}{\nu_s} = R_G W^* \quad (2.3-4)$$

After onset, the slope increment δ , the difference between the polymeric-regime slope and the N slope both in PK coordinates, depends empirically on the molecular weight M_w and \sqrt{c} :

$$\Pi = \delta \left[\frac{M}{c} \right]^{1/2} \quad (2.3-5)$$

Because data suggest that $\Pi = \kappa N_{bb}^{3/2}$, another relationship for δ arises:

$$\delta = \frac{\kappa N_{bb}^{3/2} c^{1/2}}{M^{1/2}} \quad (2.3-6)$$

where κ is the slope modulus and N_{bb} is the number of backbone links. As c , hence δ ,

factor relation, into a regime with drag reduction, with slopes significantly greater than Newtonian. This was termed Type-A behavior. In contrast, trajectories of solutions of extended polyelectrolytes, in common with fiber suspensions, exhibited no clear onset of drag reduction, but rather exhibited relatively constant drag reduction, with slopes roughly parallel to the Newtonian friction-factor relation. This was termed Type-B behavior.

Examples of Type-A and Type-B behavior can be seen in subsequent literature. Figures 2.3.1 and 2.3.2 from Berman(1977) show typical Type-A behavior for PEO, a random coiling polymer, and the quasi-Type-A behavior of Separan NP-10, a collapsed polyelectrolyte in this instance. Berman et al.(1978) studied DNA and collagen solutions, and these stiff additives exhibited "Type-B" behavior, as seen in Figures 2.3.3 and 2.3.4. No onset was observed. Their "Type-B" behavior likely resulted from the extension of collagen and DNA additives in solution, respectively.

Kwack et al.(1981) compared three nominally identical drag reduction experiments, a 70 wppm PEO/tap water solution flowing in a 1-cm \times 1-cm duct, from three different laboratories. These data are presented in Figure 2.3.5. Different onset points and levels of drag reduction were obtained in each laboratory despite the nominal similarity of their polymer solutions. Profound differences existed in the ionic character of the tap water used in two of the three experiments, and the widely differing results were attributed to the pH and electrolyte content of the tap water. Even though the tap water likely played a role neither the polymer polydispersity nor the method of preparation of the PEO solutions, which can cause the observed large differences, were examined. Stenberg et al.(1977) noted great differences in the drag-reducing ability of

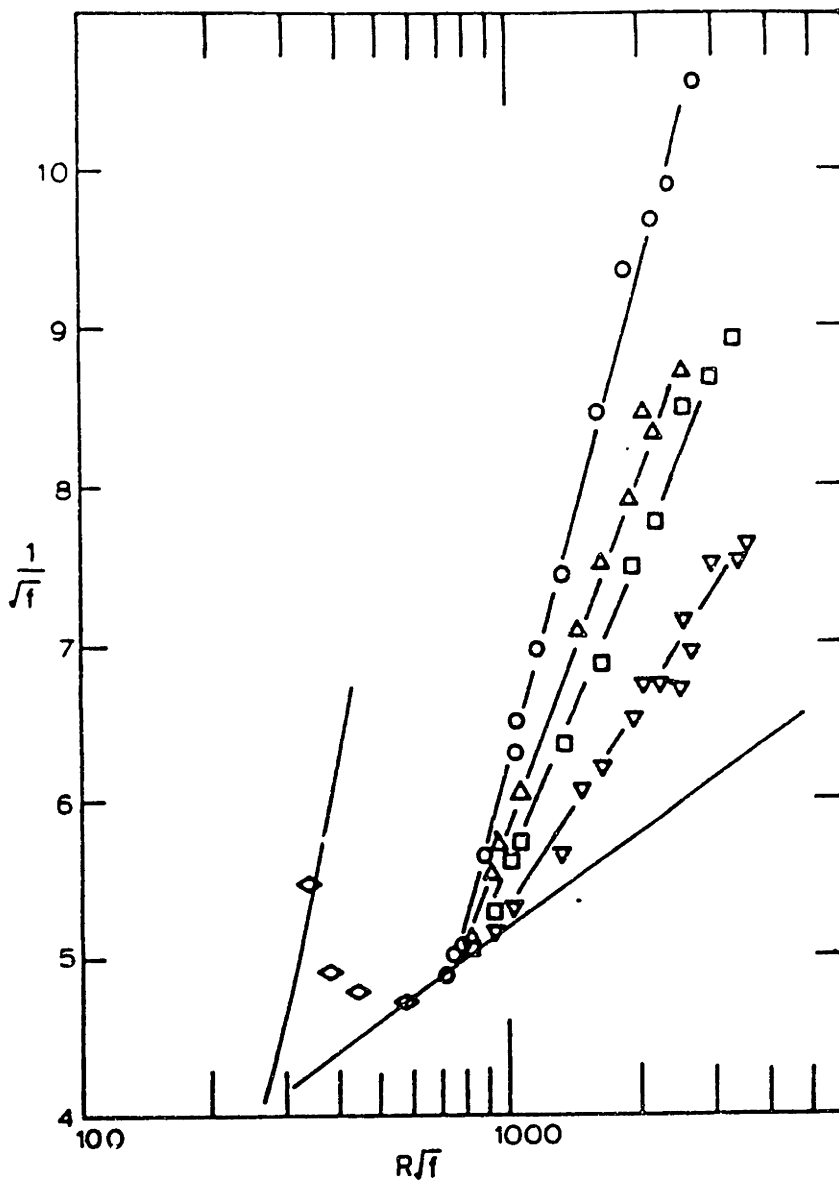


FIG. 2. Concentration dependence of drag reduction for Polyox WSR 205 in a 0.554 cm diam tube. Concentrations are 10 ppm, ∇ ; 20, \square ; 30, Δ ; and 50, \circ . The symbol \diamond illustrates points representative of all concentrations.

Figure 2.3.1: Example of Type-A Behavior from Berman(1977)

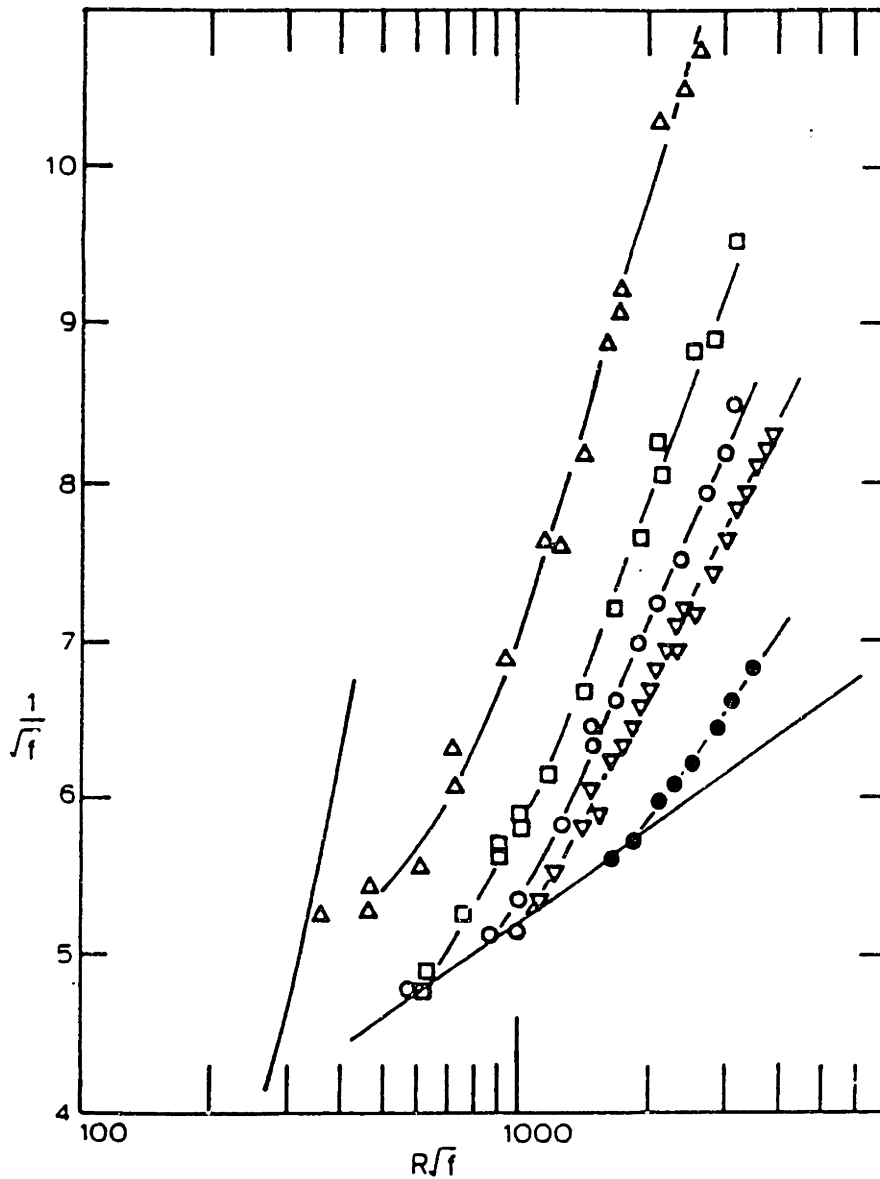


FIG. 3. Concentration dependence of drag reduction for Separan NP-10 dissolved in tap water in a 0.554 cm diam tube. Concentrations are 20 ppm, \circ ; 50, ∇ ; 100, \circ ; 200, \square ; and 400, \triangle .

Figure 2.3.2: Example of Quasi-Type-A Behavior from Berman(1977)

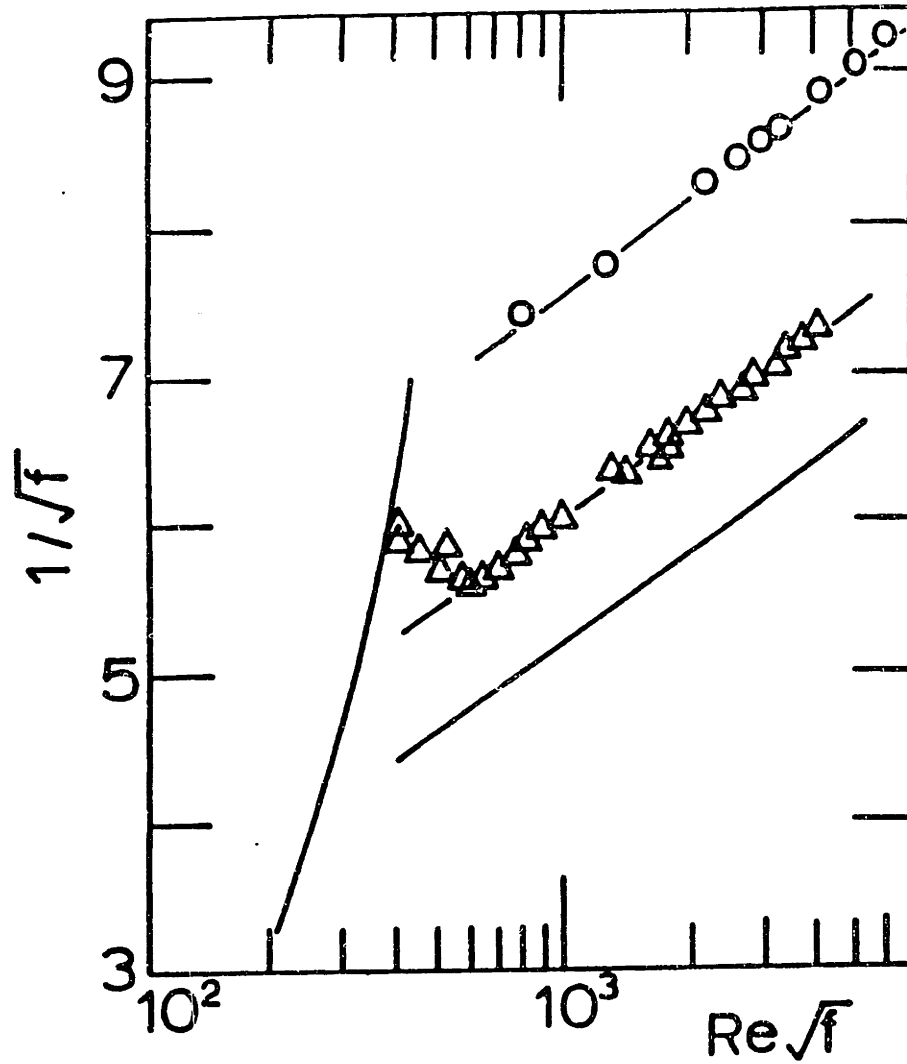


Fig. 3. Drag reduction trajectories for 50 ppm solution of DNA in 5.54 mm tube Δ and 14.94 mm tube \circ .

Figure 2.3.3: Example of Type-B Behavior from Berman et al.(1978)

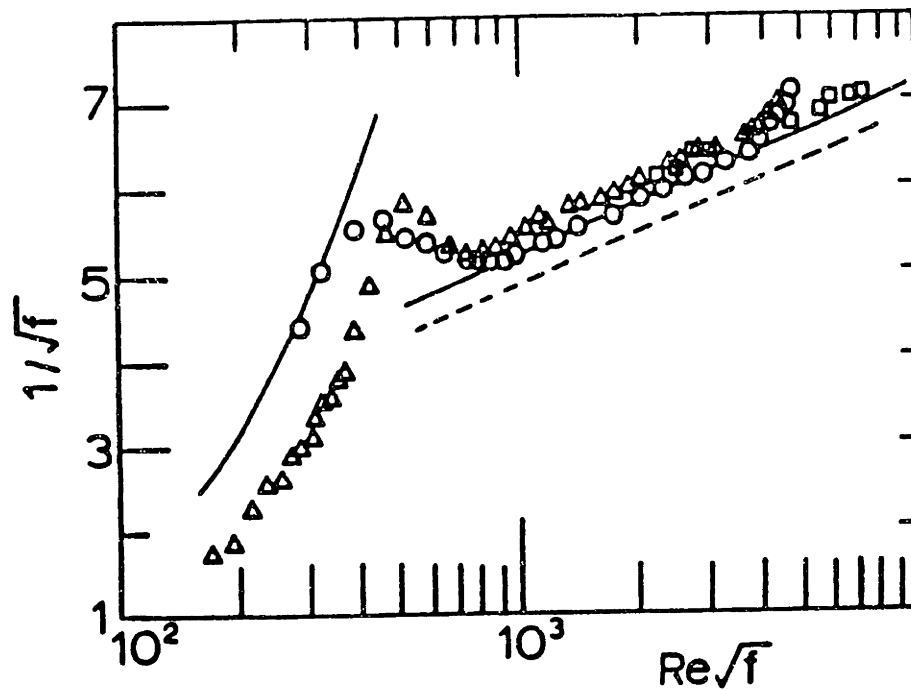


Fig. 4. Drag reduction of 200 ppm collagen in 0.01 M acetic acid. Data corresponding to the list in Table I are for run 1, Δ ; runs 2 and 3, \square ; and run 4, \circ . The points are based on the viscosity of the solvent. The dashed line represents Newtonian turbulent flow at the viscosity of the solution for run 1 points.

Figure 2.3.4: Example of Type-B Behavior from Berman et al.(1978)

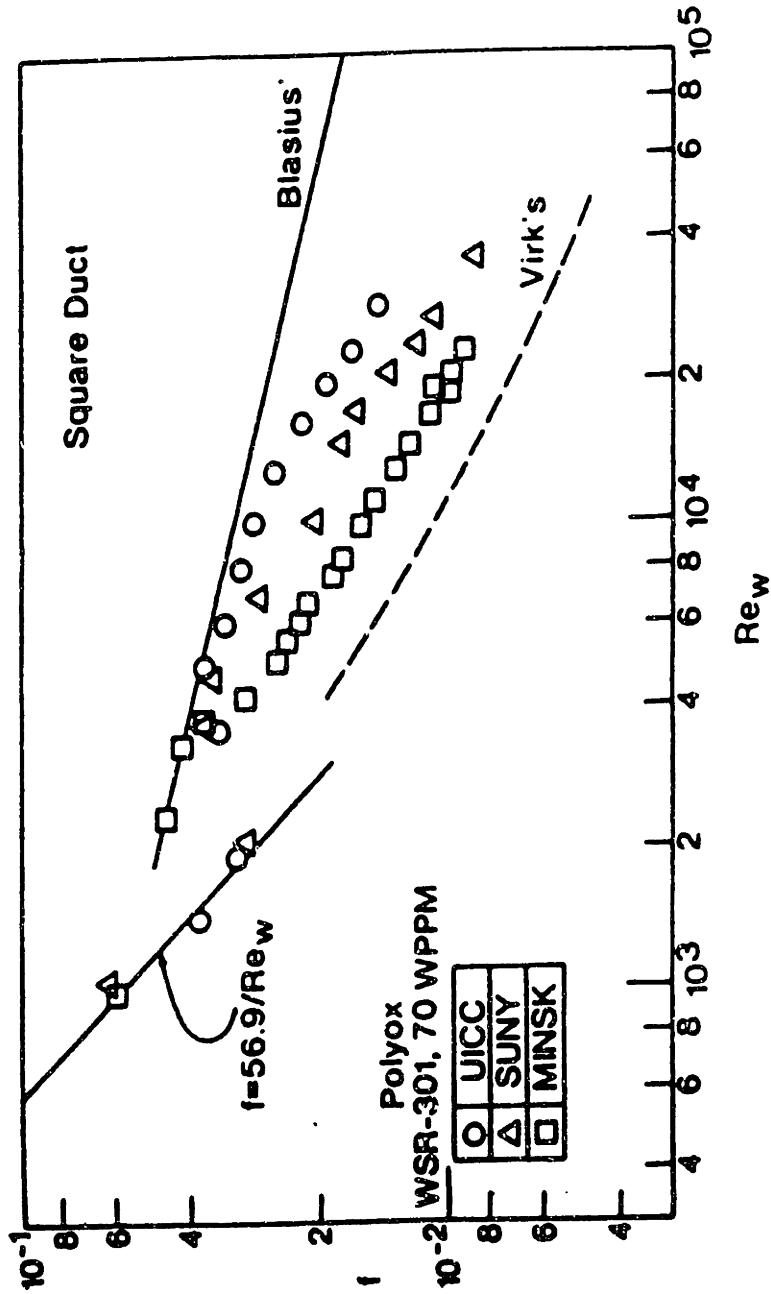


Fig. 4. Friction factor vs. Reynolds number for 70 wppm Polyox solution in 1 cm X 1 cm square duct.

Figure 2.3.5: Effect of Tap-Water Differences from Kwack et al.(1981)

PEO as a function of the mixing rate during solution preparation. These differences are displayed in Figure 2.3.6. Moderate mixing resulted in lower drag than did no mixing and high speed mixing. Apparently, mixing greatly influences the molecular state and often permits supramolecular structures to exist throughout an otherwise homogeneous fluid. These structures were deemed responsible for the flow enhancements observed. Figures 2.3.5 and 2.3.6 emphasize how truly precarious drag reduction comparisons are and how careful delineation of all experimental procedures, no matter how seemingly trivial, is required to avoid discrepancies.

Other additives, such as fibers, surfactants, and micellar solutions, also have been reported to cause drag reduction. Elson & Garside(1983) investigated the drag reducing behavior of cationic soap solutions and found that the friction factor data followed M closely even at low Reynolds numbers, as shown in Figure 2.3.7. Unlike Type-A additives, there was no onset. The solutions exhibited what Virk(1975a) called "retro-onset", meaning that drag reduction starts along the M and then reverts to the polymeric regime. Interestingly, there was also an "offset" point (for lack of a better symmetric term) at which the flow reverted all the way back to the N line of no drag reduction. Disruption of the micellar structures by too great a shear stress was thought to explain these observations.

Table 2.3.1 outlines additional gross-flow themes investigated by various authors, giving some important experimental parameters; these merit further discussion.

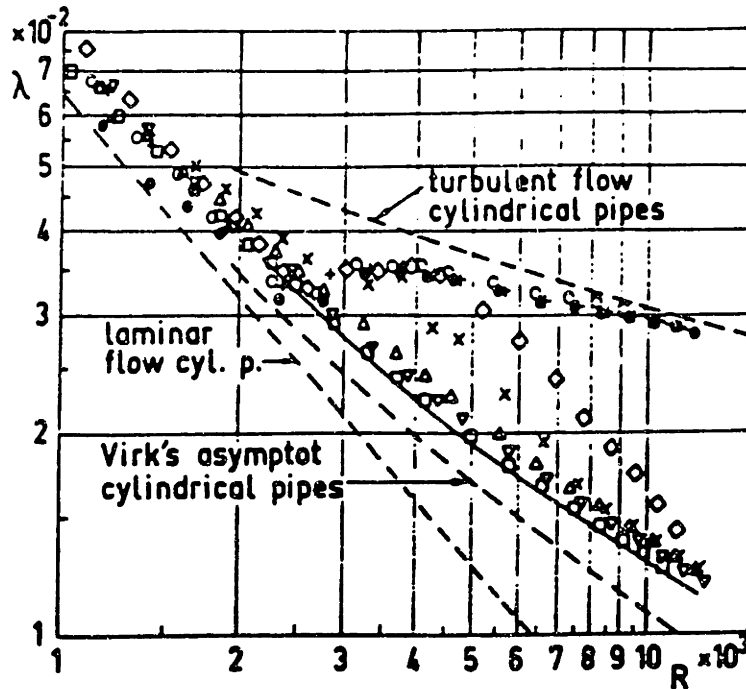


FIG. 3. Flow experiments with water and water plus 50 ppm additive of Polyox WSR 301 maintained by injection of 1% parent suspension. ○ water; mixer not in operation. ● water; mixer working at 20 r/sec. + water; mixer working at 40 r/sec. △ water + 50 ppm additive; mixer not in operation. ◻ water + 50 ppm additive; mixer working at 10 r/sec. ▽ water + 50 ppm additive; mixer working at 20 r/sec. × water + 50 ppm additive; mixer working at 30 r/sec. ◊ water + 50 ppm additive; mixer working at 40 r/sec.

Figure 2.3.6: Effect of Mixing on Drag Reduction from Stenberg et al.(1977)

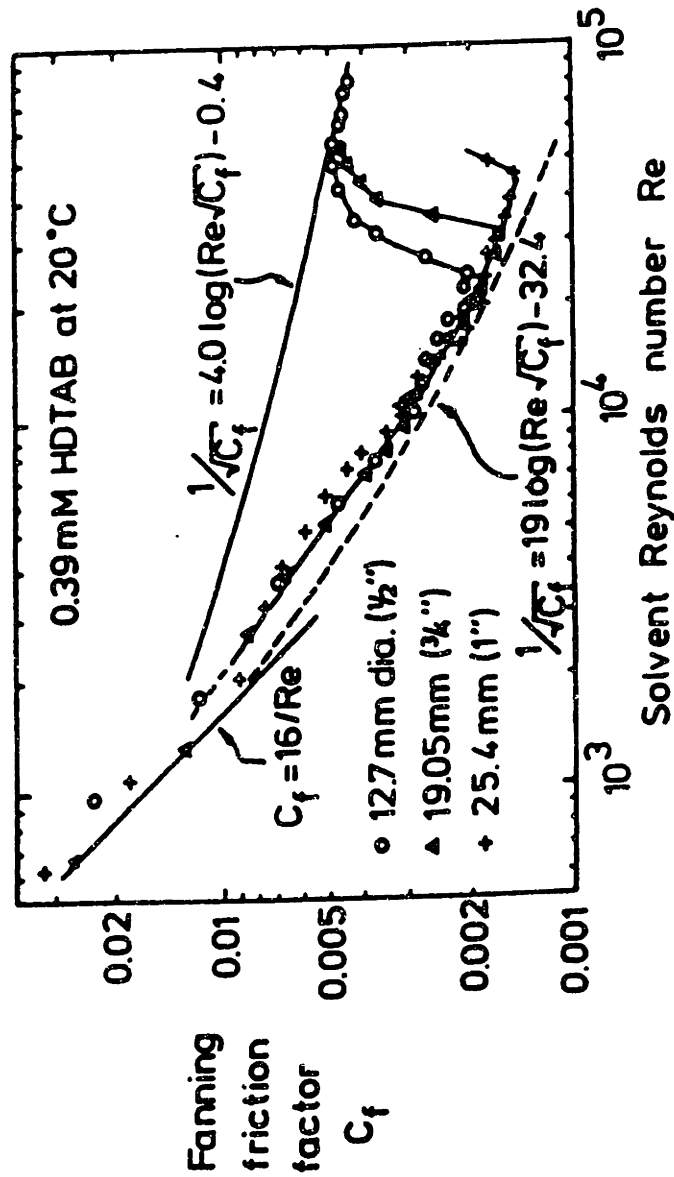


Fig. 2. Effect of pipe diameter on friction factors of equimolar 0.39 mM HDTAB, 1-naphthol solutions. The accepted Newtonian laminar and turbulent lines are illustrated as is Virk's [6] maximum drag-reduction asymptote (---).

Figure 2.3.7: Drag Reduction by Cationic Soap Solutions from Elson & Garside(1983)

Table 2.3.1
Gross Flow Themes and Sources

I. Order of Magnitude Effect of Pipe Diameter	
Burger et al.(1980)	10 wppm CDR additive(olefinic) in Crude Oil in pipes, 26 mm < D < 1194 mm
Sellins & Ollis(1983)	10 wppm HPAM and 10 wppm PEO in H ₂ O in pipes with 2 mm < D < 50 mm
Interthal & Wilski(1985)	30 wppm HPAM in river water in pipes with 3 mm < D < 750 mm
II. Drag Reduction versus Concentration	
Sharma et al.(1979)	Wall and centerline injection of fiber and fiber/HCMC solutions in H ₂ O pipeflow; 21 wppm < [fiber] < 64 wppm and 250 wppm HPMC; $2 \times 10^4 < Re < 6 \times 10^4$
Gramain & Borreill(1978)	Polystyrene/Toluene; 6.25 wppm < c < 500 wppm; $Re = 2 \times 10^4$
Oliver & Bakhtiyarov(1983)	Extremely dilute HPAM; 0.02 wppm < c < 0.5 wppm; $Re = 15.5 \times 10^3$
Interthal & Wilski(1985)	HPAM/H ₂ O; 2.5 wppm < c < 30 wppm; $Re = 1 \times 10^4$ and 2×10^4
III. Drag Reduction vs. Downstream Distance: Polymer Diffusion	
Frings(1984)	Annularly injected HPAM @ $80 < y^+ < 93$; $C_p = 0.2\%$; $\langle C \rangle = 50$ wppm; $Re = 3 \times 10^4$
McComb & Rabie(1982a)	Centerline PEO injection; $C_p = 0.3\%$; $\langle C \rangle = 10.8$ wppm in 0.2% aqueous NaCl; $Re = 4.5 \times 10^4$
Bewersdorff(1984)	Centerline HPAM; $C_p = 0.5\%$; $\langle C \rangle = 20$ wppm; $Re = 4 \times 10^4, 6 \times 10^4$ and 8×10^4

2.3.1.1 The Effect of Pipe Diameter

Since most practical applications for drag reduction involve pipelines, much research has gone toward scale-up methods for industrial use. Typically, higher levels of drag reduction are reported in small pipes than in larger pipes, with scale-up not straightforward.

In the first group of studies, gross flow data from three investigations are compared. Burger et al.(1980) studied scale-up methods from drag reduction under lab conditions to that under conditions at Prudhoe Bay. Pipe diameters ranged from 26.64 to 1194 millimeters in single pass systems, both in the lab and field. A plot of %DR vs. ν_t/u_r , the turbulent length scale, from experiments in pipes of different diameters gave distinct lines for each pipe diameter at all solution concentrations; a similar plot of %DR vs. ν_t/u_r^2 , the turbulent time scale, yielded a single for all pipe diameters at low concentrations, with distinct lines for each diameter becoming more apparent at higher concentrations. A viscoelasticity-based correlation, which had two flow parameters and one polymer-solvent parameter but no explicit pipe-diameter dependence, gave good agreement with measured quantities. Converting their data for 10 wppm CDR in crude oil into PK coordinates, as shown in Figure 2.3.8, reveals no diameter effect since all the data scattered about the line for which $S' \approx 2$.

Sellin & Ollis(1983) studied the effect of diameter on drag reduction in an attempt to derive a universal scaling law. They investigated the drag-reducing characteristics of 10 wppm solutions of PEO, HPAM(Magnifloc-1011® in coarse-powder form), and HPAM (Alcomer 110-L® in an oil-based emulsion) in pipes ranging from 2 to 50

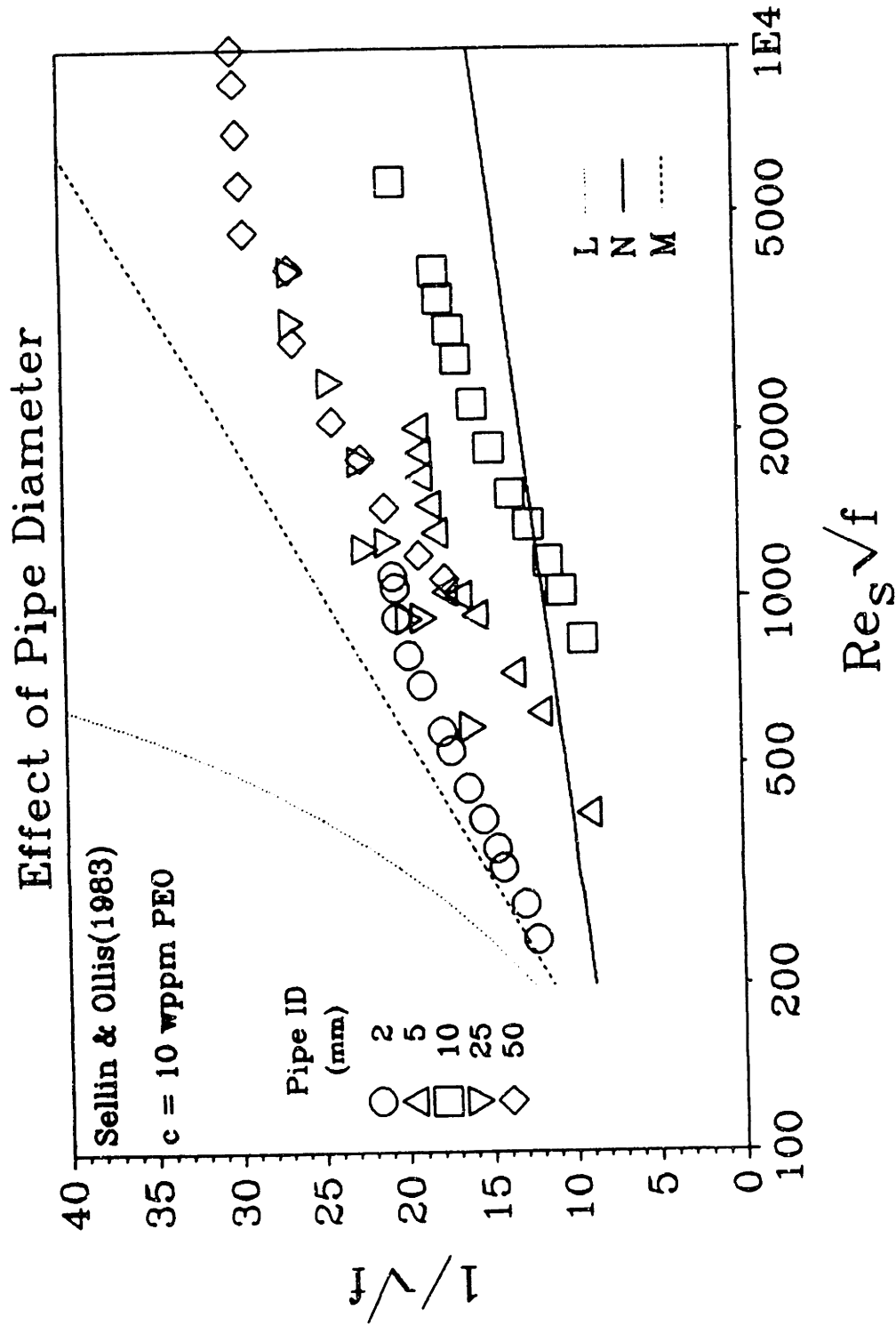


Figure 2.3.9: Effect of Pipe Diameter with 10 wppm PEO Powder(Sellin & Ollis, 1983)

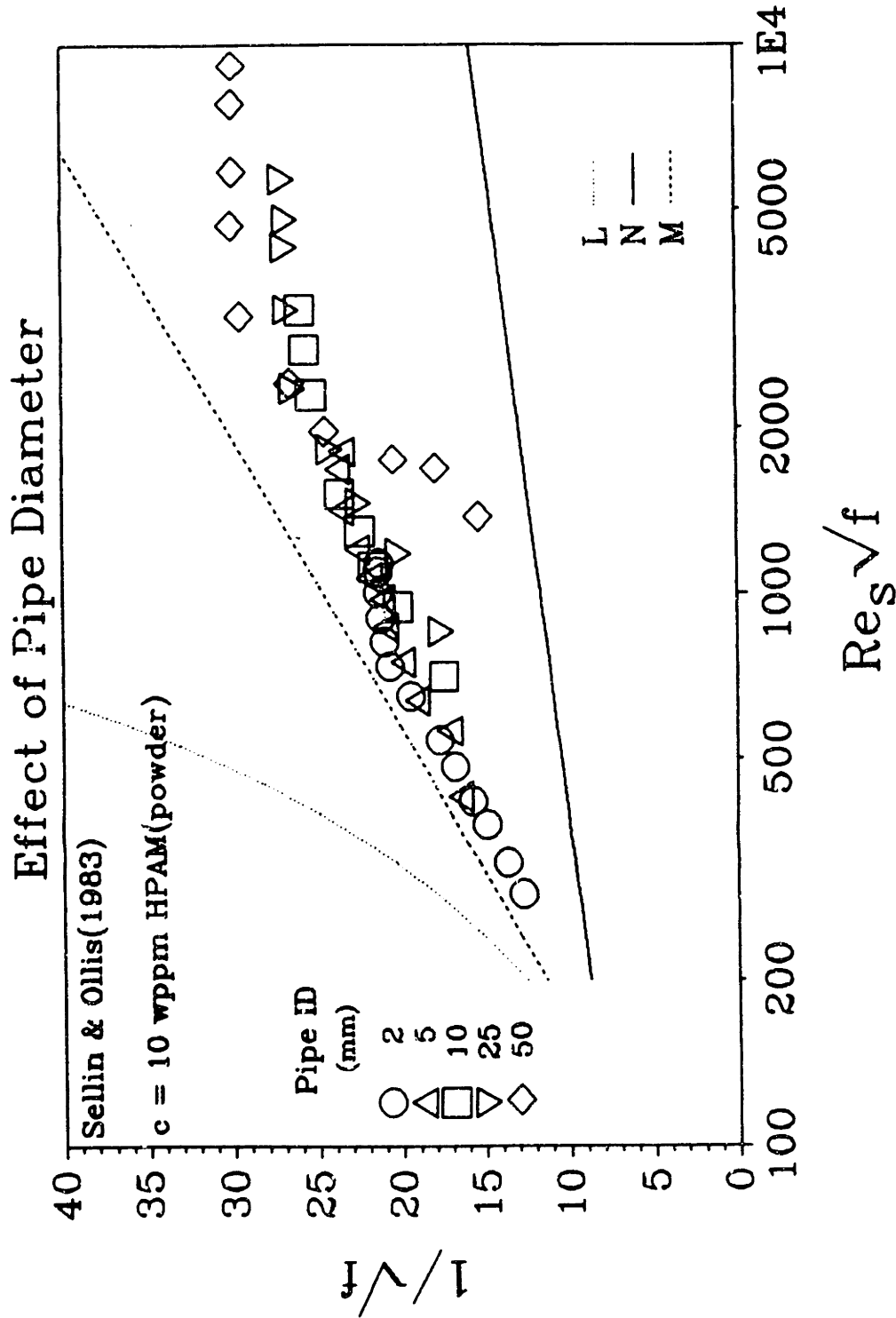


Figure 2.3.10: Effect of Pipe Diameter with 10 wppm HPAM Powder(Sellin & Ollis, 1983)

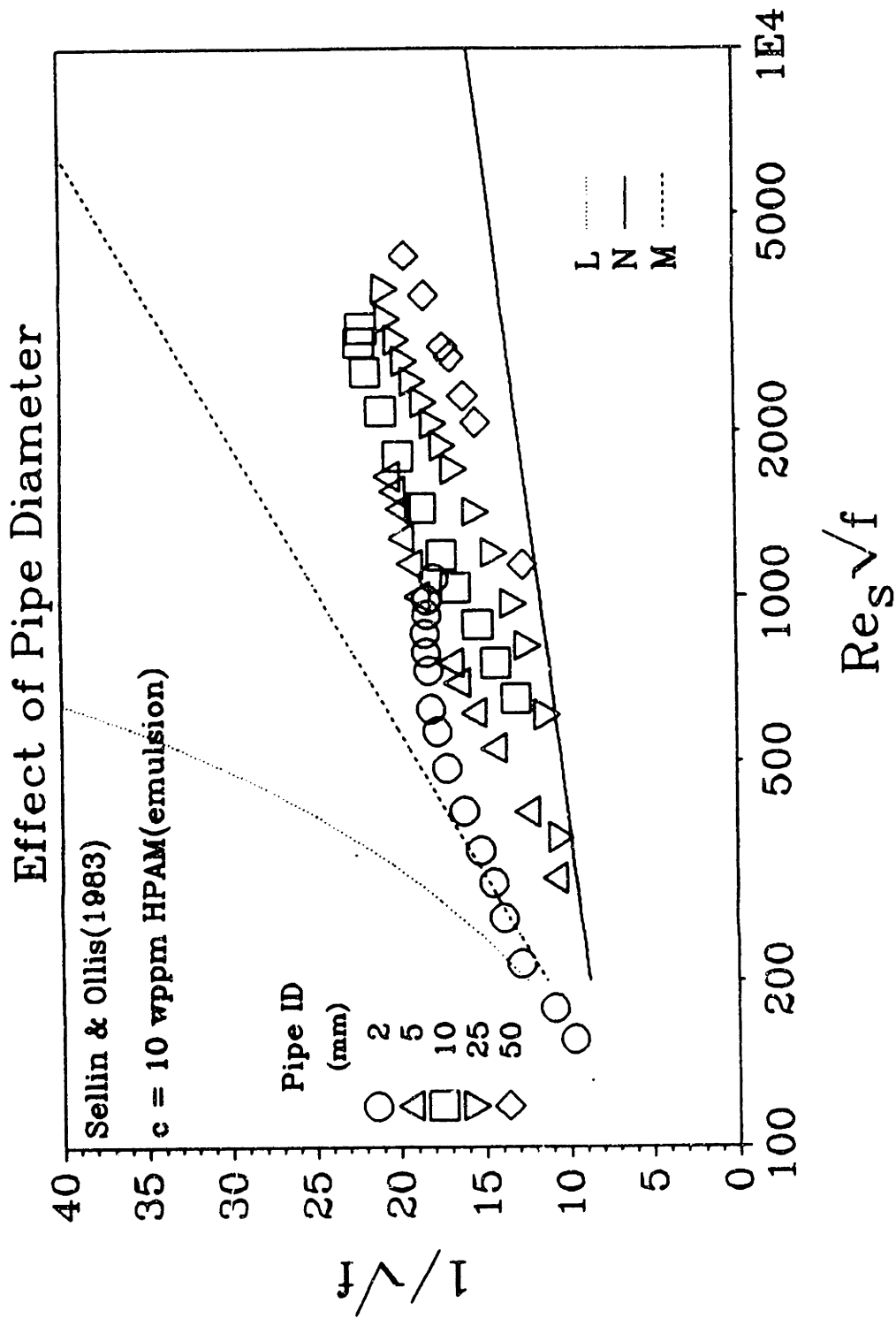


Figure 2.3.11: Effect of Pipe Diameter with 10 wppm HPAM Emulsion(Sellin & Ollis, 1983)

millimeters in diameter. Figures 2.3.9, 2.3.10, and 2.3.11 show the gross flow data for these three solutions, respectively. The PEO data were split into two groups: the 2, 5, and 10 mm pipes and the 25 and 50 mm pipes. In either set, effectiveness grew with decreasing diameter, but there were inexplicable inconsistencies between sets, with the 2 and 25 mm pipes, the smallest in each set, showing similar results. The HPAM-powder solutions exhibited flow enhancement near M at low $Re_s\sqrt{f}$ for all but the largest pipe size. In the largest pipe, $Re_s\sqrt{f} \approx 1100$ was required to reach significant flow enhancement, but its data then rapidly joined those for all other pipes by $Re_s\sqrt{f} \approx 3000$. The data revealed no clear dependence on pipe diameter. The HPAM-emulsion solution exhibited increasing drag reduction with decreasing pipe size at a given $Re_s\sqrt{f}$; however, scale-up was hampered because the $Re_s\sqrt{f}$ range that exhibited significant drag reduction for each pipe was different.

An important point is that the two HPAM solutions, while both 30% hydrolysed, differed in their premixed form, powder vs. emulsion, and in their preparation. The differences in form and preparation likely accounted for the great differences in flow behavior. Such a lack of additive reproducibility makes scale-up difficult.

Interthal & Wilski(1985) investigated drag reduction in industrial pipelines, several thousand meters in length, using 30-wppm solutions of HPAM. Their data, which have been transformed into PK coordinates, are given in Figure 2.3.12 and exhibited similar differences between small pipes and large pipes. In their smallest four laboratory pipes, with tap-water solvent, all data were either on or close to M . In the four largest pipes, with river-water solvent, the real industrial set-up consisted of large winding kilometer-long pipes, which exhibited about only half the flow enhancement seen in the

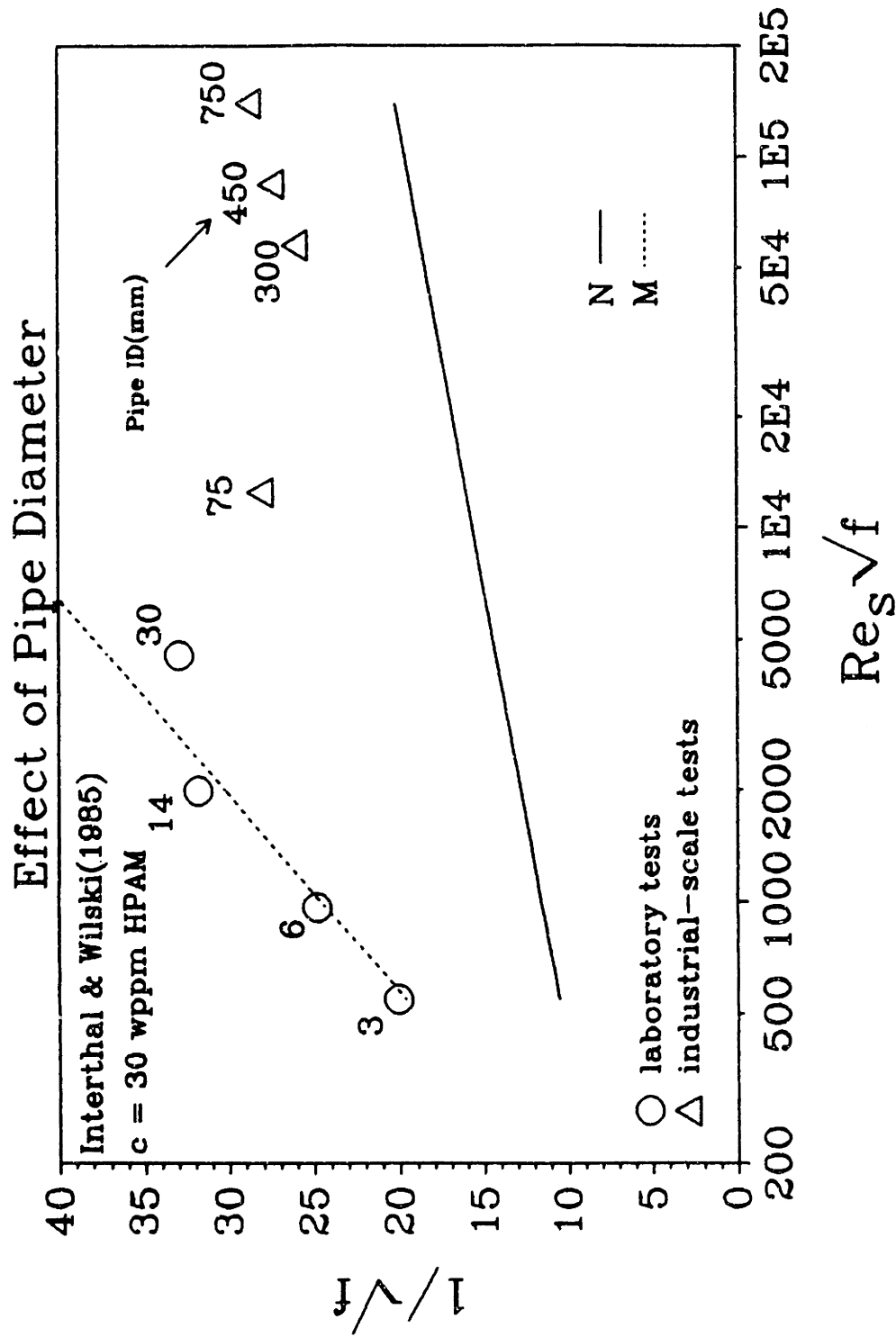


Figure 2.3.12: Effect of Pipe Diameter(Interthal & Wilski, 1985)



The Libraries
Massachusetts Institute of Technology
Cambridge, Massachusetts 02139

Institute Archives and Special Collections
Room 14N-118
(617) 253-5688

This is the most complete text of the
thesis available. The following page(s)
were not included in the copy of the
thesis deposited in the Institute Archives
by the author:

81/93

smaller pipes. Thus, the drag-reducing effectiveness of HPAM in the field could not be well estimated from the lab data.

What these three papers emphasize is that the scaling of drag reduction is difficult at best. One must ensure reproducibility at every phase of solution preparation, from polymer polydispersities to solvent properties, and operate the experiment at low drag reduction where the MDR asymptote does not interfere with the sought-after diameter effect.

2.3.1.2 Drag Reduction vs. Concentration

The efficiency of several different additive-solvent pairs introduced into the turbulent flow in various ways is compared in Figure 2.3.13 on log-log coordinates of flow enhancement S' vs. additive concentration c , in wppm.

Data derived from Sharma et al.(1979) show the differences between wall and centerline injection of fibers and fiber suspensions at fixed $Re = 2 \times 10^4$ in a 19-mm pipe. Wall injection was generally more efficient than centerline injection, giving about twice the flow enhancement at fixed (final) concentration.

Data are also shown for polystyrene in toluene at $Re_s = 2 \times 10^4$ (Gramain & Borreill, 1978) and for aqueous HPAM at $Re_s = 1 \times 10^4$ and 1×10^5 in a 14-mm pipe and at $Re_s \approx 2.0 \times 10^4$ in a 5.97-mm pipe(Oliver & Bakhtiyarov, 1983). Evidently, HPAM in water was more effective than polystyrene in toluene which was, in turn, more effective than the asbestos fiber suspensions. Quantitatively, Oliver & Bakhtiyarov's (1983) data for the extremely dilute solution show their HPAM additive to provide

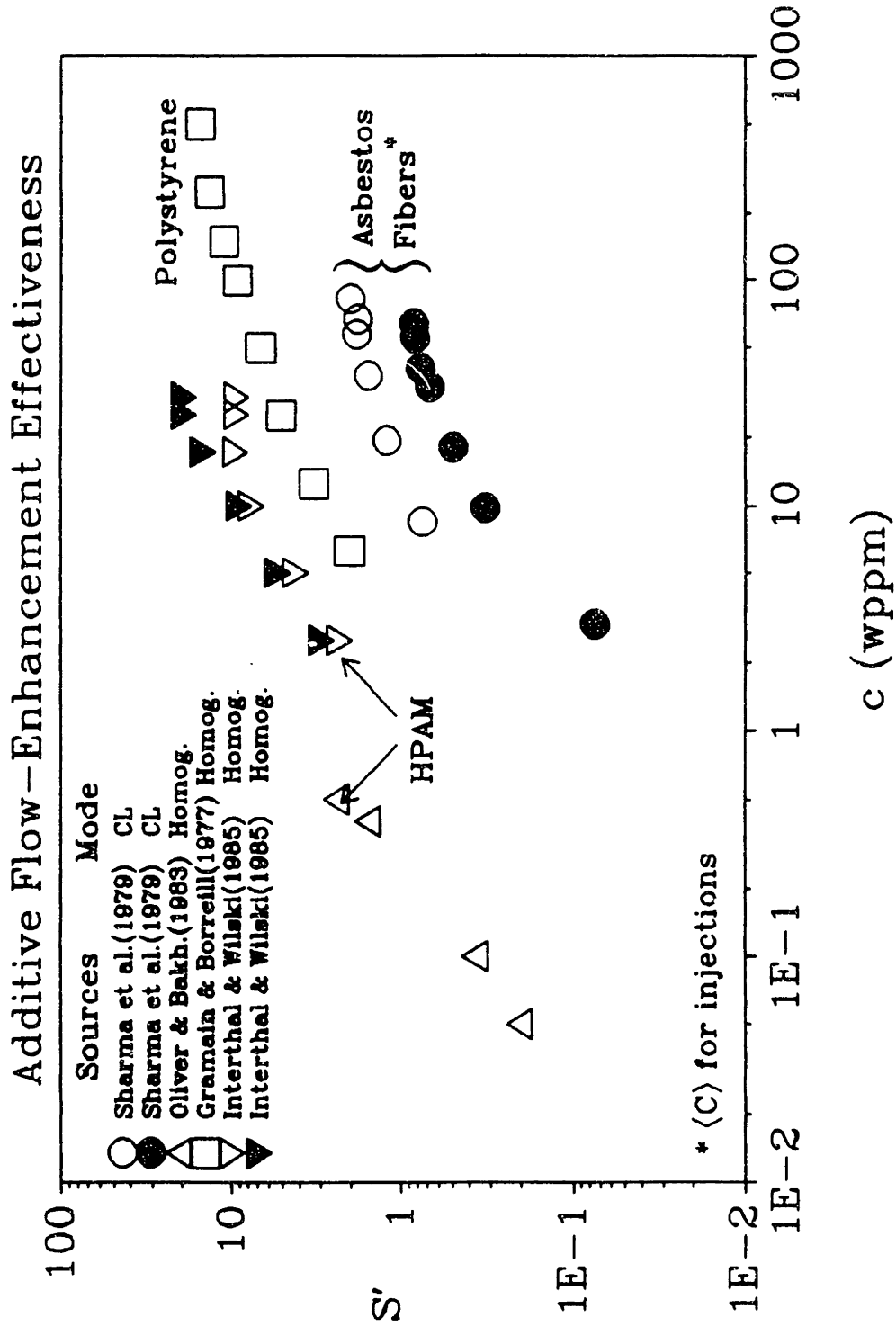


Figure 2.3.13: Additive Flow-Enhancement Effectiveness

$S' \approx 0.4$ at $c \approx 0.1$ wppm, whereas Sharma's(1979) data for asbestos fibers show $S' \approx 1$ at $c \approx 10$ to 50 wppm; thus, the HPAM polymer was about 2 to 3 orders of magnitude more effective than the asbestos fibers on a weight basis.

2.3.1.3 Drag Reduction vs. Downstream Distance from Injector

Polymer diffusion can be measured by the increase in flow enhancement S' as a function of downstream x/D during an injection experiment. Figure 2.3.14 presents data from the three authors listed in Table 2.3.1. Annular injection data from Frings(1984, 1988) show a much sharper initial rise in S' than other centerline-injection data even though Frings' data were taken at the lowest Re . This is likely due to polymer being injected directly into the buffer layer, the radial location where drag reduction is believed to originate. Thus, little diffusion was required before the onset of drag reduction. The characteristic development length, the x/D where the initial gradient in S' vs. x/D intercepts the asymptotic S' value, for the annular injection was ~ 60 while that for all centerline-injection data was ~ 120 . The characteristic development lengths derived from the data of McComb & Rabie(1982a) and Bewersdorff(1984) agreed well, despite the great variation in Re and drag reduction. This suggests that polymer diffusion in the core does not depend significantly on the flow strength.

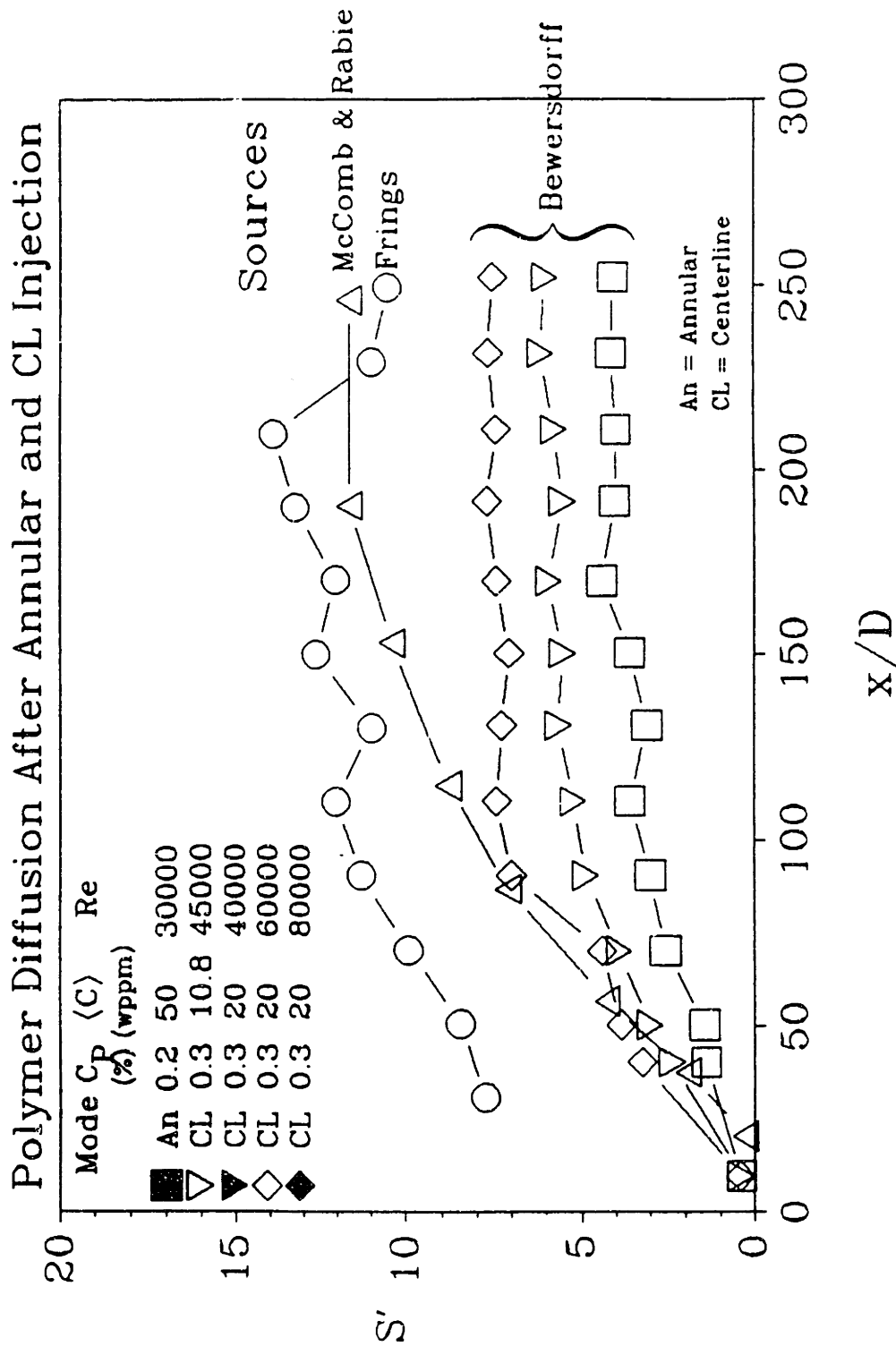


Figure 2.3.14: Axial Flow-Enhancement Development via Polymer Diffusion

2.3.2 Mean-Velocity Profiles

Starting with the Navier-Stokes equations and employing scaling arguments, the following mean velocity profiles for turbulent pipe flows of Newtonian fluids can be derived:

$$\text{(viscous sublayer)} \quad U^* = y^* \quad 1 < y^* < 5 \quad (2.3-9)$$

$$\text{(buffer layer)} \quad U^* = 10 \tan^{-1} \left[\frac{y^*}{10} \right] + 1.2, \quad 5 < y^* < 30 \quad (2.3-10)$$

OR

$$\text{(buffer layer)} \quad U^* = 5 \ln(y^*) - 3.05, \quad 5 < y^* < 30 \quad (2.3-11)$$

$$\text{(log layer)} \quad U^* = 2.5 \ln(y^*) + 5.5, \quad 30 < y^* < R^* \quad (2.3-12)$$

Of the two buffer layer equations, the lower is a simple fit to the zone boundaries whereas the upper is based on the physics of the buffer layer, where most of the turbulent production occurs. This zone is of great import and interest in the study of drag reduction. Drag-reducing additives tend to thicken the buffer layer into what Virk called the "elastic layer"; the elastic layer separates the viscous sublayer from the Newtonian core and gives rise to an "effective slip". Thus, the intercept of the log layer equation becomes greater than 5.5 while the slope remains the same. The log layer extends from the outer edge(nearer the wall) of the buffer layer to the pipe axis or core. The constant slope 2.5 is the inverse of the Newtonian Von Karman constant $\kappa_n \approx 0.4$.

Virk(1971a) collected much data on mean flow and proposed a three zone "elastic sublayer model"(ESM) for the mean velocity profile of drag-reducing flow. These three

equation comprise the ESM model:

$$(viscous\ sublayer) \quad U^* = y^* \quad y^* < y^*_v \quad (2.3-13)$$

$$(elastic\ sublayer) \quad U^* = 11.7 \ln(y^*) - 17.0 \quad y^*_v < y^* < y^*_e \quad (2.3-14)$$

$$(Newtonian\ plug) \quad U^* = 2.5 \ln(y^*) + 5.5 + 9.2 \ln \left[\frac{y^*_e}{y^*_v} \right] \quad y^*_e < y^* < R^* \quad (2.3-15)$$

where the $9.2 \ln(y^*_e/y^*_v)$ term is also known as ΔB .

Implicitly, the scheme requires that an M profile exists in the elastic sublayer for even the smallest amount of drag reduction. As the polymer concentration increases, the drag reduction increases, and with it the thickness of the elastic layer. The M profile of slope 11.7, extends over a larger portion of the pipe in real and reduced distances with increasing drag reduction. Low radial momentum transport in the elastic layer is a feature associated with drag reduction and is indicated by a reduced Von Karman constant $\kappa_m = 1/11.7 \approx 0.085$. At the outer edge of the elastic layer, the profile slope changes to the Newtonian value with larger $\kappa_n \approx 0.4$; however, the intercept value in the Newtonian plug is much greater than the Newtonian value, 5.5. The difference between this value and 5.5 is known as the "effective slip" or ΔB . Since the ESM was proposed, much mean flow data has been generated to verify it. The following table summarizes some of the major contributions.

Table 2.3.2
Sources of Mean Flow Data

Investigators	Experimental Conditions
Kale & Metzner(1976)	<ul style="list-style-type: none"> ● Homogeneous fiber and fiber/HPAM solutions; [fiber] = 1000 wppm and 2000 wppm; c = 150 wppm.
Sharma et al.(1979)	<ul style="list-style-type: none"> ● Injected 0.3-% fiber solutions into H₂O and 250-wppm polymer solution; $1 \times 10^4 < Re < 1 \times 10^5$. ● Wall and centerline injection; [fiber] < 71 wppm; $2 \times 10^4 < Re < 4 \times 10^4$.
McComb & Rabie(1982b)	<ul style="list-style-type: none"> ● Centerline PEO injection into H₂O; $\langle C \rangle < 20$ wppm; $Re = 3.5 \times 10^4$.
Bartels et al.(1984)	<ul style="list-style-type: none"> ● Homogeneous HPAM solutions; c < 320 wppm; $Re = 2 \times 10^4$.
Bewersdorff(1984)	<ul style="list-style-type: none"> ● Homogeneous 20-wppm and 50-wppm PAM solutions and centerline-injected PAM with $0.1\% < C_p < 1.0\%$ into H₂O; $Re < 8 \times 10^4$.
McComb & Chan(1985)	<ul style="list-style-type: none"> ● Homogeneous 300-wppm fiber and 300/150- wppm fiber/PAM solutions; $1.4 \times 10^4 < Re < 5.3 \times 10^4$.

Figure 2.3.15 displays velocity profiles from Kale & Metzner(1976) of concentrated fiber and fiber-HPAM solutions at high Re. These profiles were consistent with the Newtonian-plug equation 2.3-15, showing "effective slip". The addition of polymer to the fiber solution results in greater ΔB . The 1000-wppm asbestos-fiber solution had an upshift per wppm $\Delta B/c = 0.007$. Adding 150 wppm PAA to that fiber solution resulted $\Delta B/c = 0.02$. Clearly, HPAM is a much more effective additive than asbestos fiber.

Sharma et al.(1979) injected fibers into turbulent pipe flows of water and HPMC solutions. Injections were made into the centerlines and at the wall. The resulting average

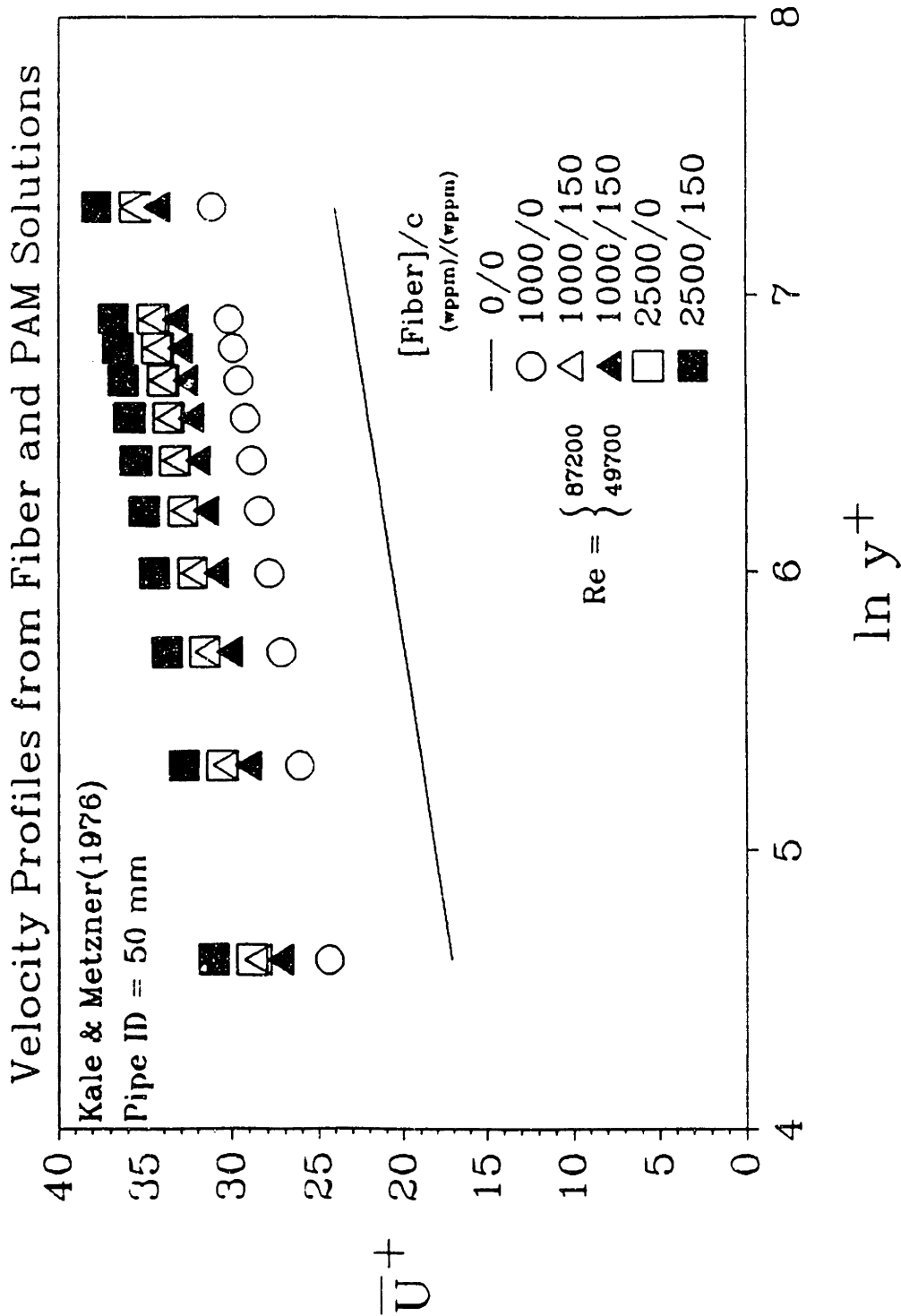


Figure 2.3.15: Velocity Profiles from Asbestos-Fiber Solutions(Kale & Metzner, 1976)

concentrations $\langle C \rangle$ were nearly two orders of magnitude lower than those of Kale & Metzner(1976). The behavior of mixed solutions, fiber and HPMC, is depicted in Figure 2.3.16 for both wall and CL injections, with the former more effective than the latter. Although still well below M , these profiles show that the presence of polymer increases ΔB for the same fiber concentration; however, $\Delta B/c$ is less for the mixed than for the fiber-only case. In these data, the fibers are more efficient than polymer, contrary to the results of Kale & Metzner(1976).

McComb & Rabie(1982b) injected PEO solutions into the centerline of a water pipe flow and measured the profiles at successive distances down the pipe, x/D , in order to observe the development of drag reduction in an already turbulent Newtonian flow. Figure 2.3.17 exhibits how the profile lifts off the Newtonian line. The profiles show that the three-zone model does not quite hold in that the profile slope in the elastic layer is somewhat less than M but greater than Newtonian; however, the core profile seems nearly parallel to the Newtonian line. In successive profiles, the growth of the elastic layer is clear. As the polymer diffuses into the elastic layer with downstream distance, $8 \leq x/D \leq 214$, the thickening layer in the region $30 < y^+ < 100$ gives rise to a velocity profile in the core that lies increasingly closer to M , with the flow enhancement S' rising from ~ 0 to 10.8 Only when the elastic layer is saturated and its extent restricted by pipe geometry rather than polymer availability, does the profile approach that of maximum drag reduction.

Bartels et al.(1984) investigated pipe flows of premixed HPAM solutions. Their results, shown in Figure 2.3.18, concur with those of McComb & Rabie(1982b) and display the similar differences among profiles of increasing polymer concentration at

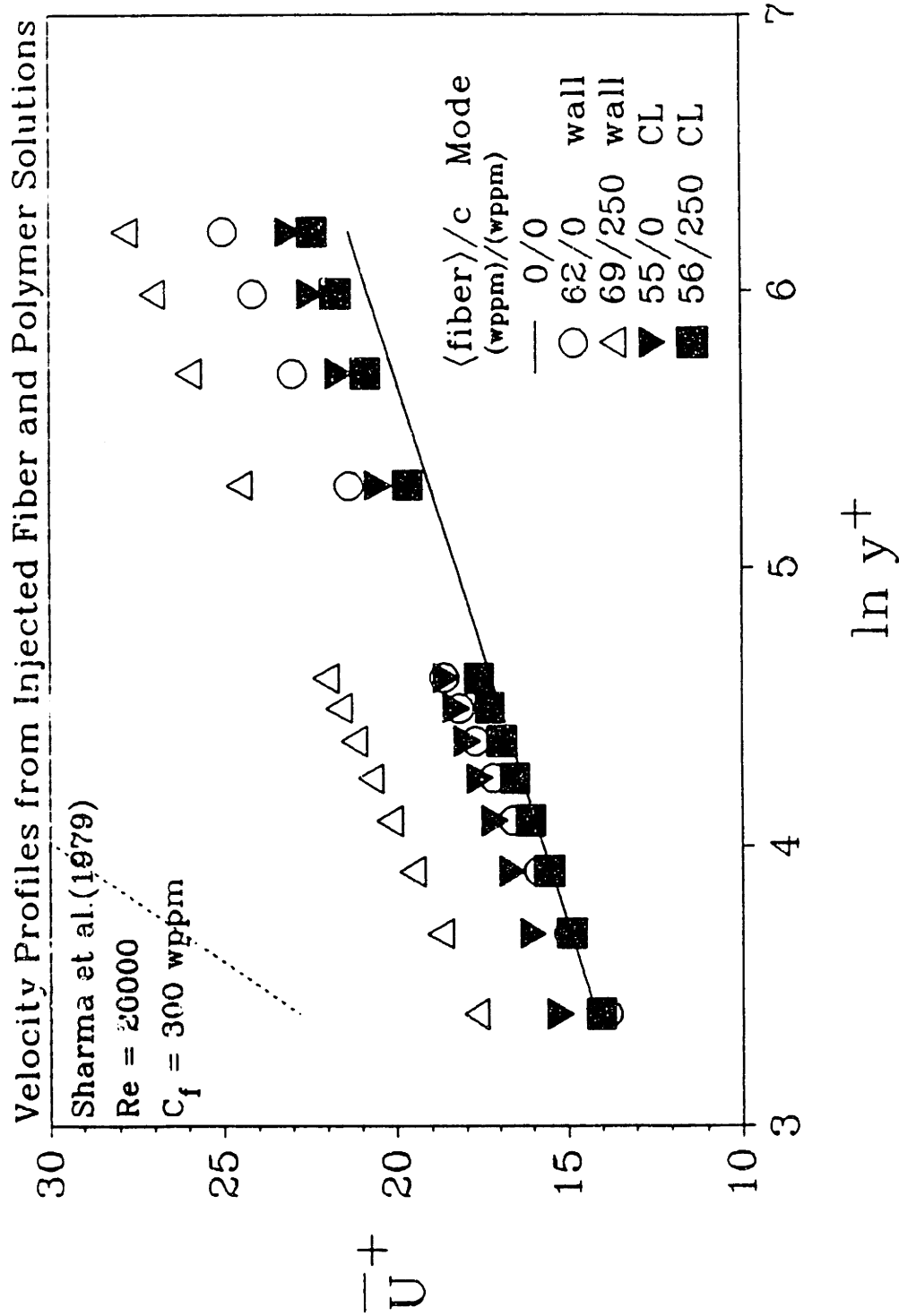


Figure 2.3.16: Velocity Profiles from Fiber-Solution Injection (Sharma et al., 1979)

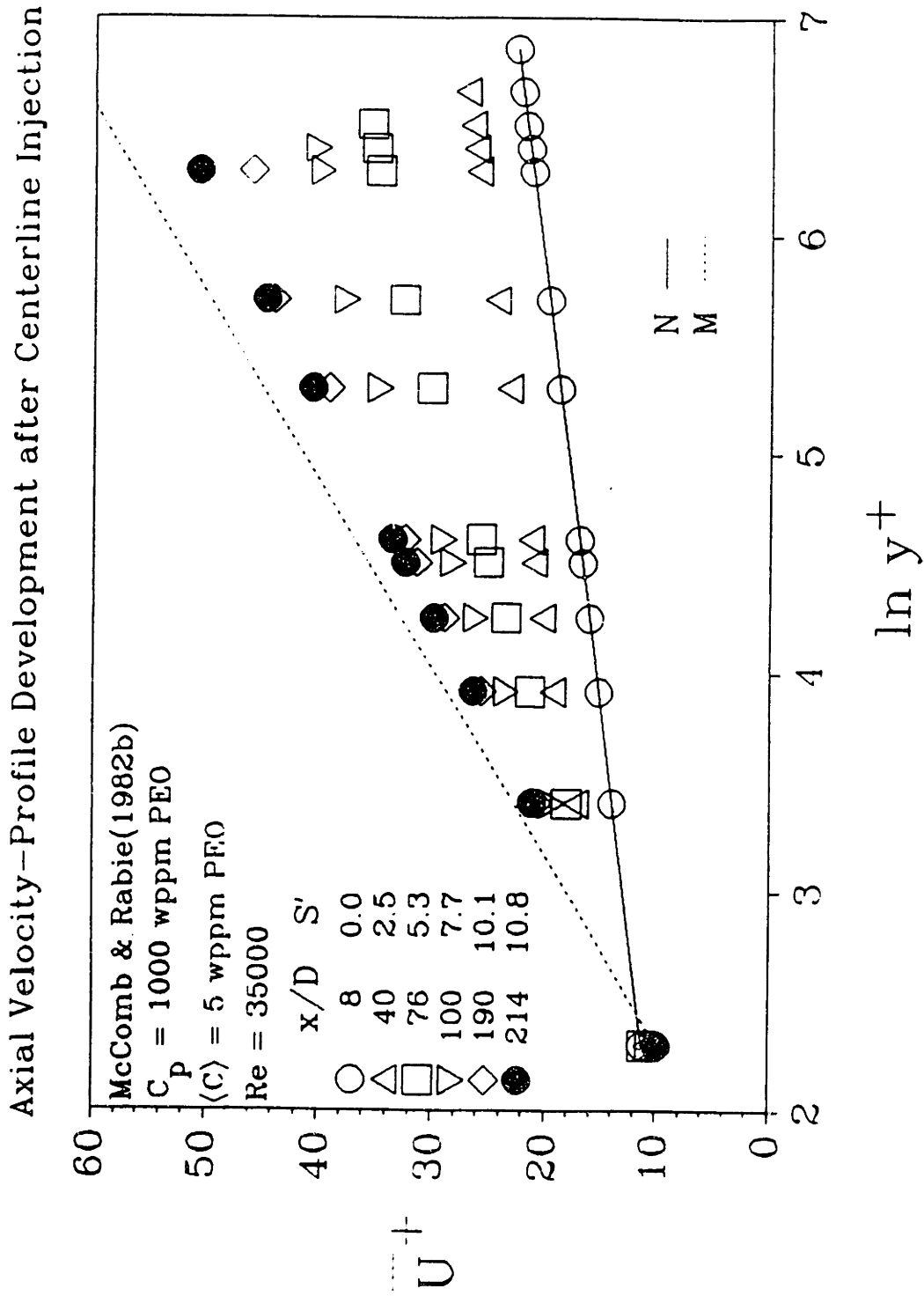


Figure 2.3.17: Velocity Profiles from PEO-Solution Injection(McComb & Rabie, 1982b)

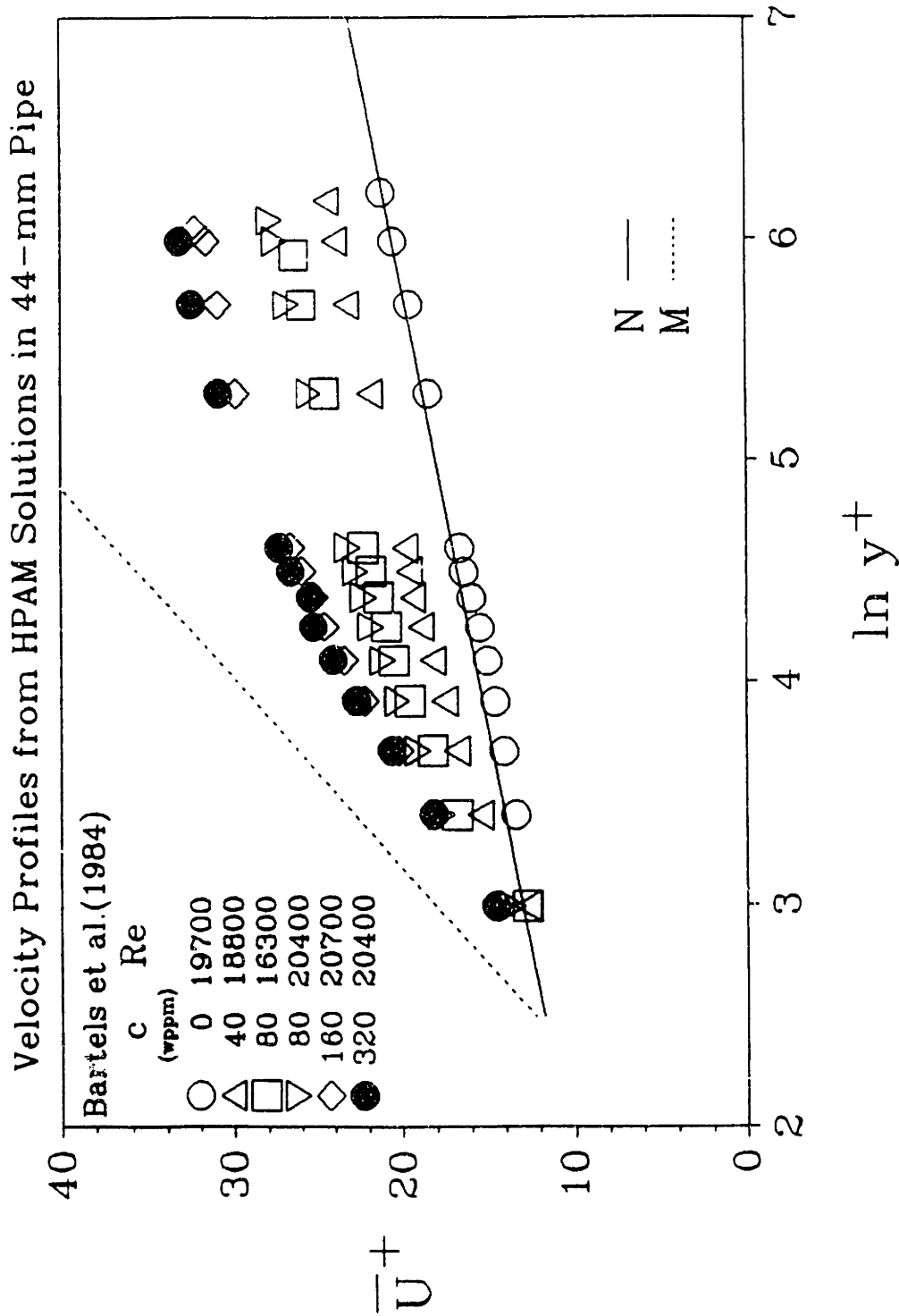


Figure 2.3.18: Velocity Profiles from Premixed HPAM Solutions in 44-mm Pipe (Bartels et al., 1984)

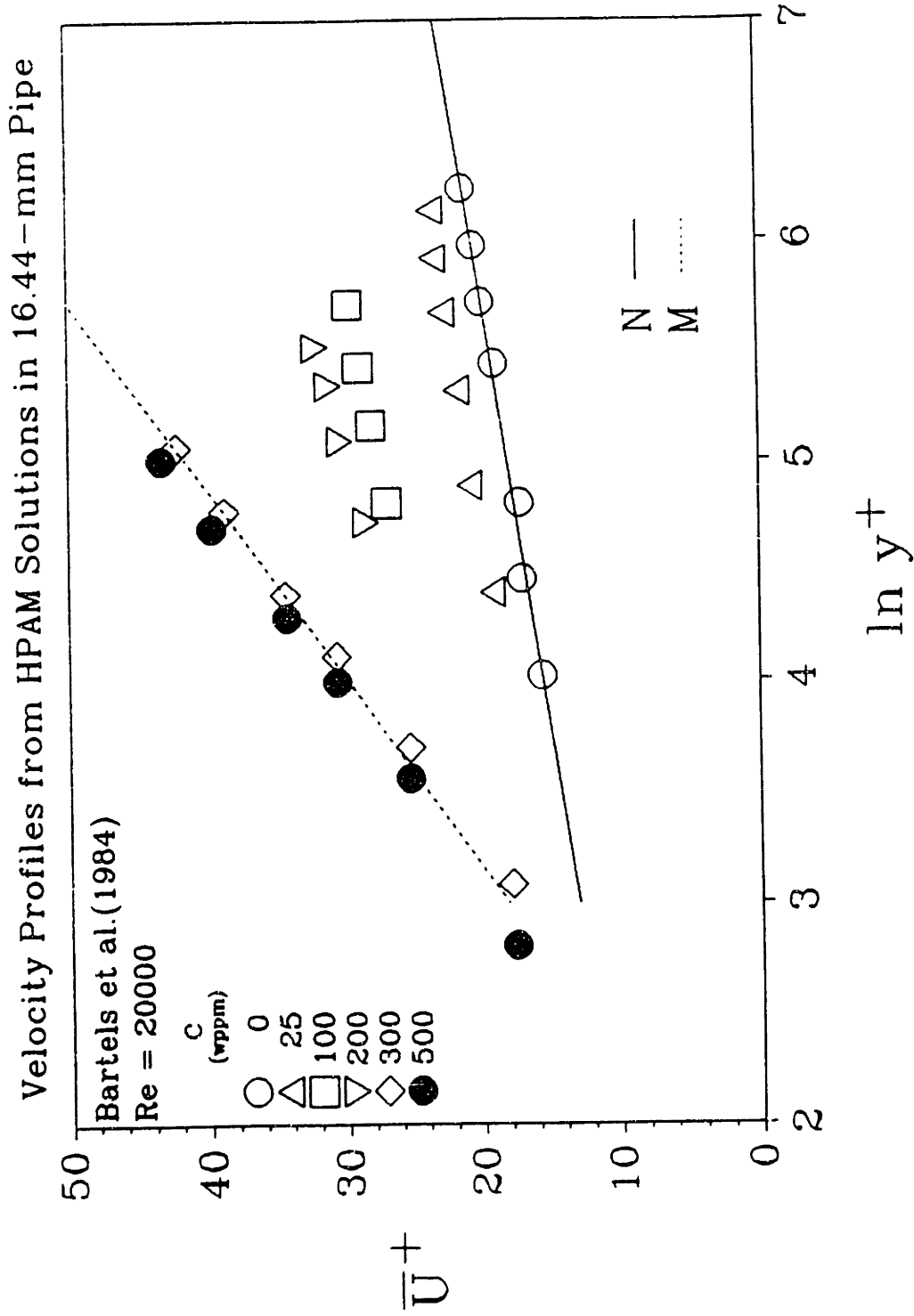


Figure 2.3.19: Velocity Profiles from Premixed HPAM Solutions in 16-mm Pipe (Bartels et al., 1984)

nearly identical conditions in a 44-mm pipe. Figure 2.3.19 exhibits the same trend in a 16-mm pipe, wherein several of the higher concentrations achieve maximum drag reduction.

Bewersdorff(1984) injected very concentrated HPAM solutions into the centerline of turbulent pipe flow, so concentrated in fact that the polymer threads remained intact as a single thick undulating cord along the centerline. Figure 2.3.20 shows that at a fixed Re , or a near-constant R^+ , the less concentrated injections gave greater ΔB even though the final average concentration $\langle C \rangle = 20$ wppm for each C_p . Again this indicates the importance of polymer diffusion from the central cord that forms when concentrations are as high as 10000 wppm. Polymer diffusion may account for this strange trend. Figure 2.3.21, taken from Bewersdorff(1984), demonstrates the interesting development of the velocity profile under his conditions. The profile looks as if it were representing two fluids. From the wall, the flow is Newtonian perhaps because the polymer has not diffused to that region. At some point, $y^+ > 50$, where the profile diverges from the water line, it behaves similarly to the profiles from McComb & Rabie(1982b) and Bartels et al.(1984). At greater y^+ from the divergence, a small region shows a profile of slope about half that of M and greater than that of N. Towards the core, the profile flattens and become nearly parallel to the Newtonian line. Bewersdorff & Berman(1988) observed similar "bifurcating" velocity profiles using surfactant solutions. No completely satisfactory explanation has yet been offered for these curious observations.

McComb & Chan(1985) measured profiles in pipe flows of fiber and fiber-PAA solutions at various Re . Figure 2.3.22 shows that in their flow loop at $Re = 1.4 \times 10^4$, a 300-wppm fiber solution exceeded M on its first two passes. Subsequent passes

Velocity Profiles from Centerline—Injected HPAM Solutions into Water

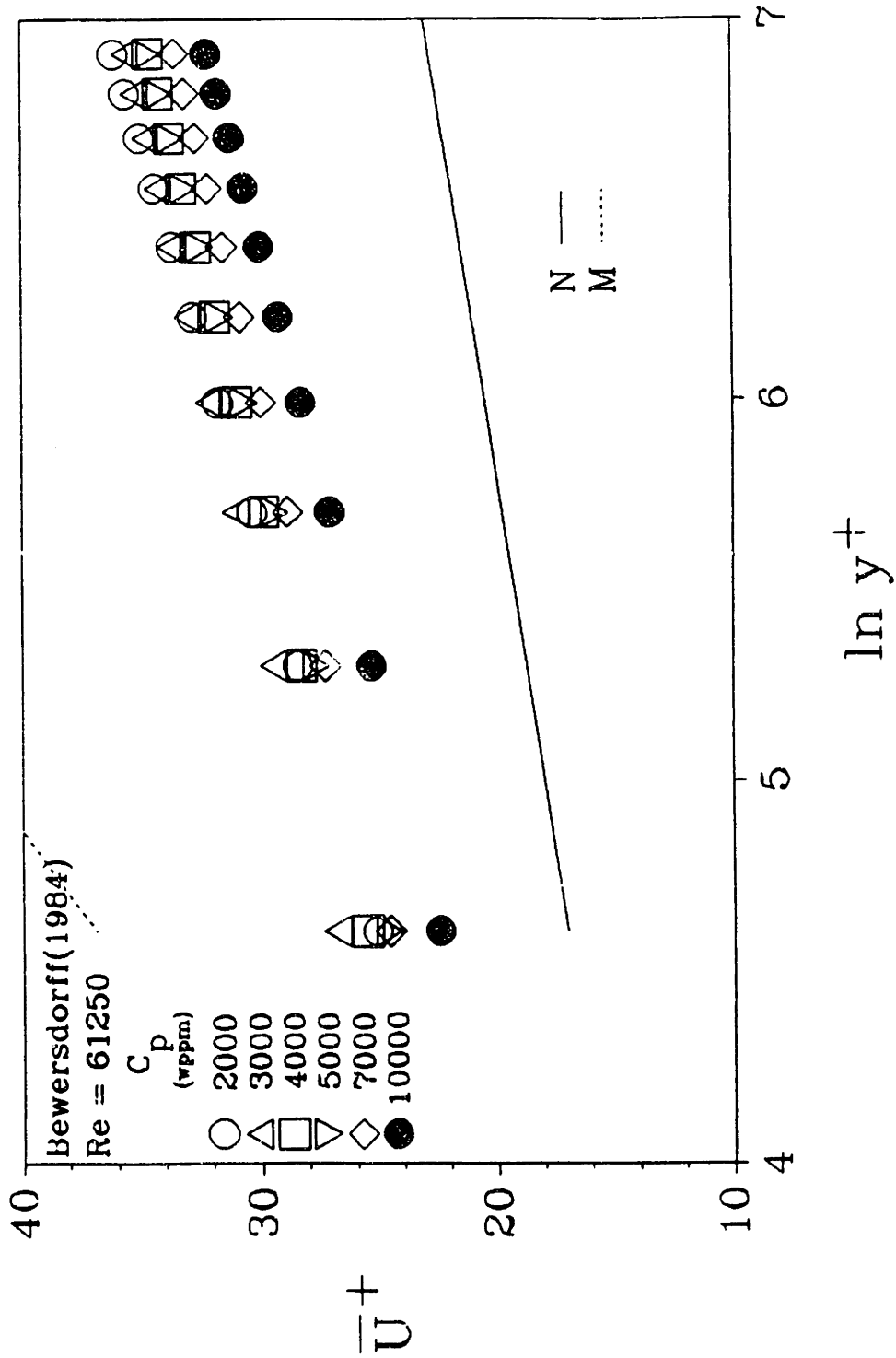


Figure 2.3.20: Velocity Profiles from HPAM-Solution Injection(Bewersdorff, 1984)

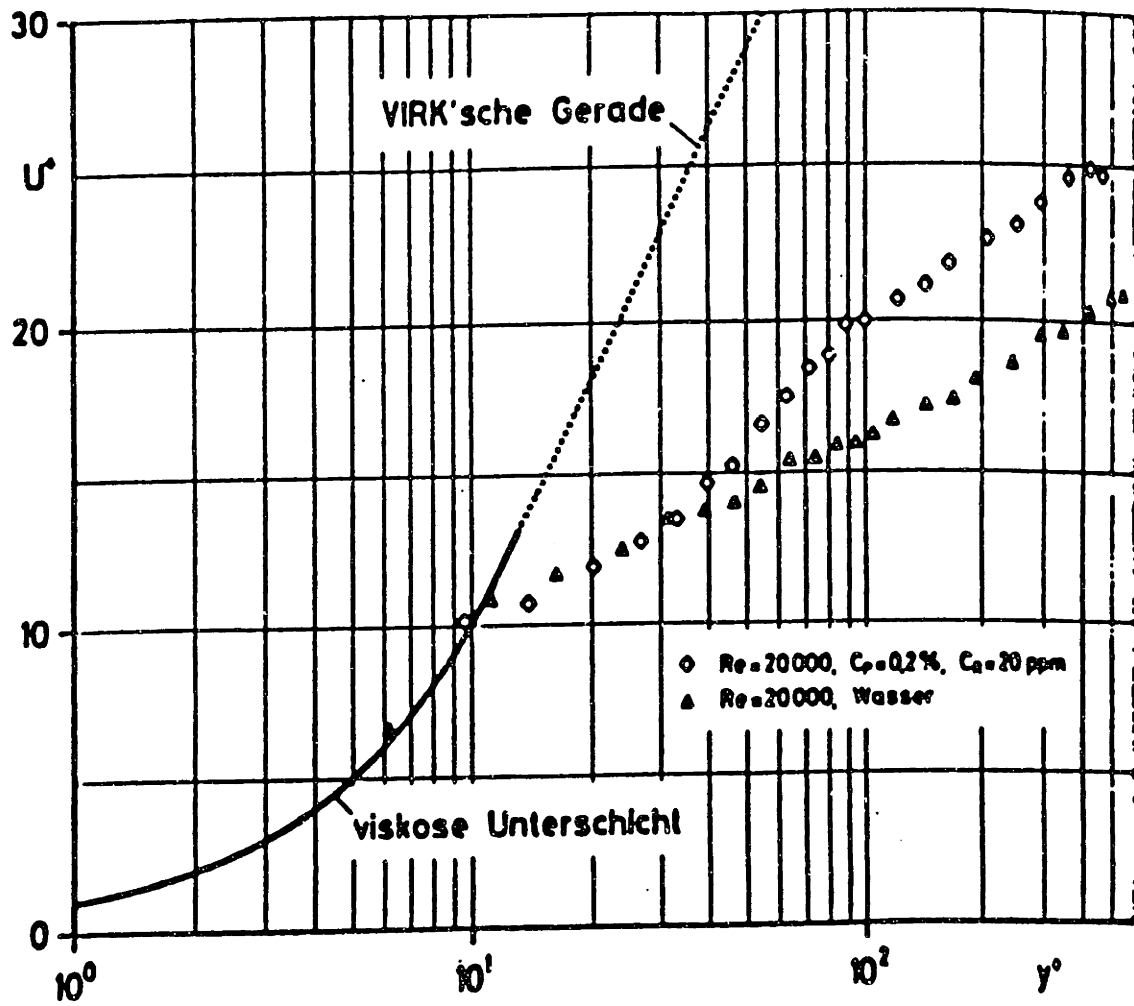


Abb. 16. Geschwindigkeitsprofil bei Injektion von Polymeren ($Re = 20000$)

Figure 2.3.21: Two-Fluid Profile from Bewersdorff(1984)

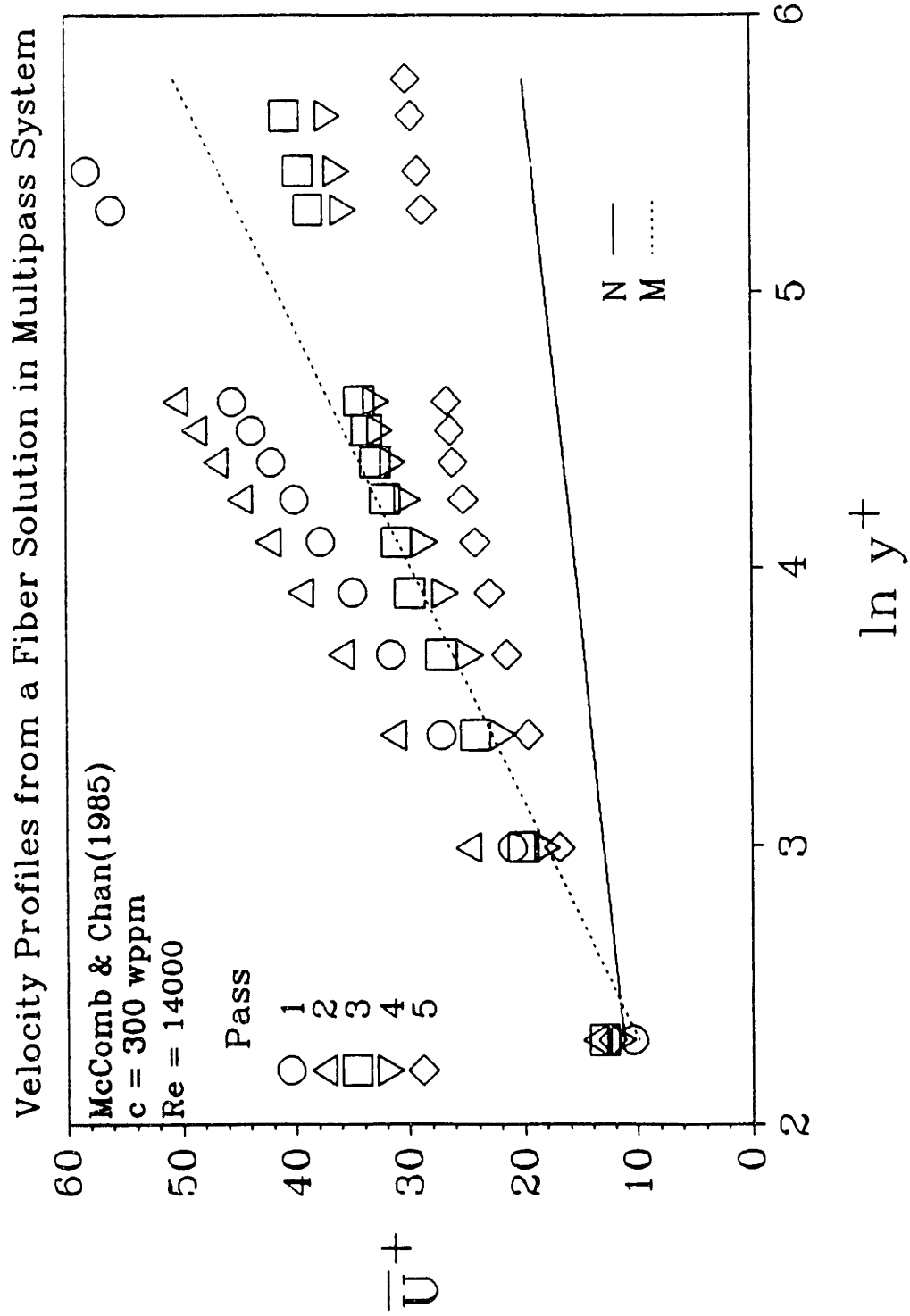


Figure 2.3.22: Velocity Profiles from Fiber Solutions in Multipass System(McComb & Chan, 1985)

behaved similarly to polymer flows. Since the MDR asymptote was first discovered, no data exist which exceed M (in either mean or gross flow) after entering the fully turbulent envelope between N and M . The profiles from passes 1 and 2 likely did not become fully developed. Thus, the authors called them "fiber-like" suggesting that fiber agglomeration rather than the individual fibers themselves may account for this behavior. Similar experiments were performed at $Re = 3.2 \times 10^4$ and 5.3×10^4 . The profile trend for successive passes at these Re concurred with the earlier findings of McComb & Rabie (1982b) and Bartels et al. (1984), and showed no unusual features, only the usual effect of degradation as the drag reduction decreased with increasing number of passes.

2.3.3 Turbulence Structure I: Intensities and Stresses

An understanding of Newtonian turbulence structure is required to appreciate how additives alter the turbulent-flow structure.

In pipe flow, laminar flow prevails for $Re_s < 2100$. When $2100 < Re_s < 4000$, a transition region occurs with zones of intermittent turbulence which arise from certain points along the pipe. With increasing Re_s , these zones pervade all space, leading to fully-developed turbulence when $Re > 4000$.

In a fully-turbulent pipe flow, pairs of counter-rotating rolls, also called streamwise vortices, exist near walls with a mean azimuthal spacing $z^+ \approx 100$. Their axes are separated by $\sim 50 z^+$ units, and the average axial length of a single roll is $\sim 1000 z^+$ units. Vortex pairs "pump" low speed fluid from the wall region and create low speed zones between the axes. This gives rise to the so called streaky structure. In

the low speed zones, shear instabilities intermittently occur which are involved in a ring-vortex mechanism and which commence events called "bursts".

Lift-up, oscillation, and break-up events characterize bursts. The bursting process disrupt the rolls' identities every ~ 1000 units such that zones of high and low velocities appear to be randomly distributed in space and time. Fluid elements in the viscous sublayer are lifted into the buffer layer. Lift-up is associated with the ring-vortex mechanism, but the exact relationship is unclear. In the low speed zones, inflectional instabilities in the mean velocity profile initiate oscillations which amplify as they are advected downstream. After travelling some characteristic lengths, these oscillations break-up, and the process begins anew. Associated with "bursts" are "ejections" which occur twice as frequently on average but with less strength. What starts the ejection process is unclear, but lift-up appears to be related. Low momentum fluid elements leave the wall area and act as sinks in higher momentum regions; thus, the Reynolds stress $\langle uv \rangle$ associated with ejection is positive. The frequency of bursts and ejections correlate with the wall shear stress and fluid viscosity. The ejection process ends via the sweep. Sweeps also contribute a positive Reynolds stress, but in the opposite sense. Fluid elements from the higher-momentum outer flow move wallward, create high shear layers with the low-speed fluid, and initiate instabilities. The lateral extent of a sweep is ~ 80 units, while its velocity is about 75 percent of the maximum mean velocity. A newer flow structure, designated "pocket" by Falco(1977), is similar to a sweep, only penetrating more deeply into the near-wall region. They are ~ 100 by ~ 100 units in the lateral and axial directions. Again, the causes of pocket formation are unknown.

Visual and tracer studies have identified structures and described their

characteristics, but they can not attribute causality among these events. Constant formation and destruction of these structures randomly in space and time do not permit one to ascribe a "beginning" and an "end". Studying the transition to turbulence might permit causality among these structures to be established. Visual and tracer studies may be less important than reliable mean flow and velocity fluctuation data in that the latter may yield better, less-subjective data than the former. More in-depth discussions of classical turbulence may be found in Monin & Yaglom(1971), Hinze(1975), and Schlichting(1979) and of flow structure in Laufer(1954), Kline et al.(1967), Lumley(1973), and Blackwelder & Kaplan(1976). Laufer(1954) presented the first detailed measurements of turbulence fluctuations. The intensities and Reynolds stresses, u'^{+} , v'^{+} , and, w'^{+} and $-\langle uv \rangle^{++}$, were carefully determined for air flow in a nominal 10-inch pipe(9.72 inches ID) at $Re = 5 \times 10^4$ and 5×10^5 . Skewness and flatness, the third and fourth moments of the velocity fluctuations, respectively, as well as production, dissipation, and one-dimensional energy spectra were calculated. Since intensities and Reynolds stresses are easier to obtain and usually provide more mechanistic insight than the skewness, flatness, production, dissipation, and one-dimensional energy spectrum, the latter five quantities have not been widely measured. The intensities u'^{+} , v'^{+} , and, w'^{+} and Reynolds stress $-\langle uv \rangle^{++}$, and correlation coefficient C_{uv} at $Re_s = 5 \times 10^4$ and 5×10^5 are presented in Figures 2.3.23 and 2.3.24. To measure turbulence stretchiness and isotropy, an analogy with shear-free polymer flows can be used in which the Reynolds-stress tensor components $-\rho \langle u_i u_j \rangle$ replace the stress-tensor components τ_{ij} ; thus, first and second turbulence normal-stress ratios and kinetic energy can be defined:

Turbulence-Intensity, Reynolds-Stress, & Correlation-Coefficient Profiles

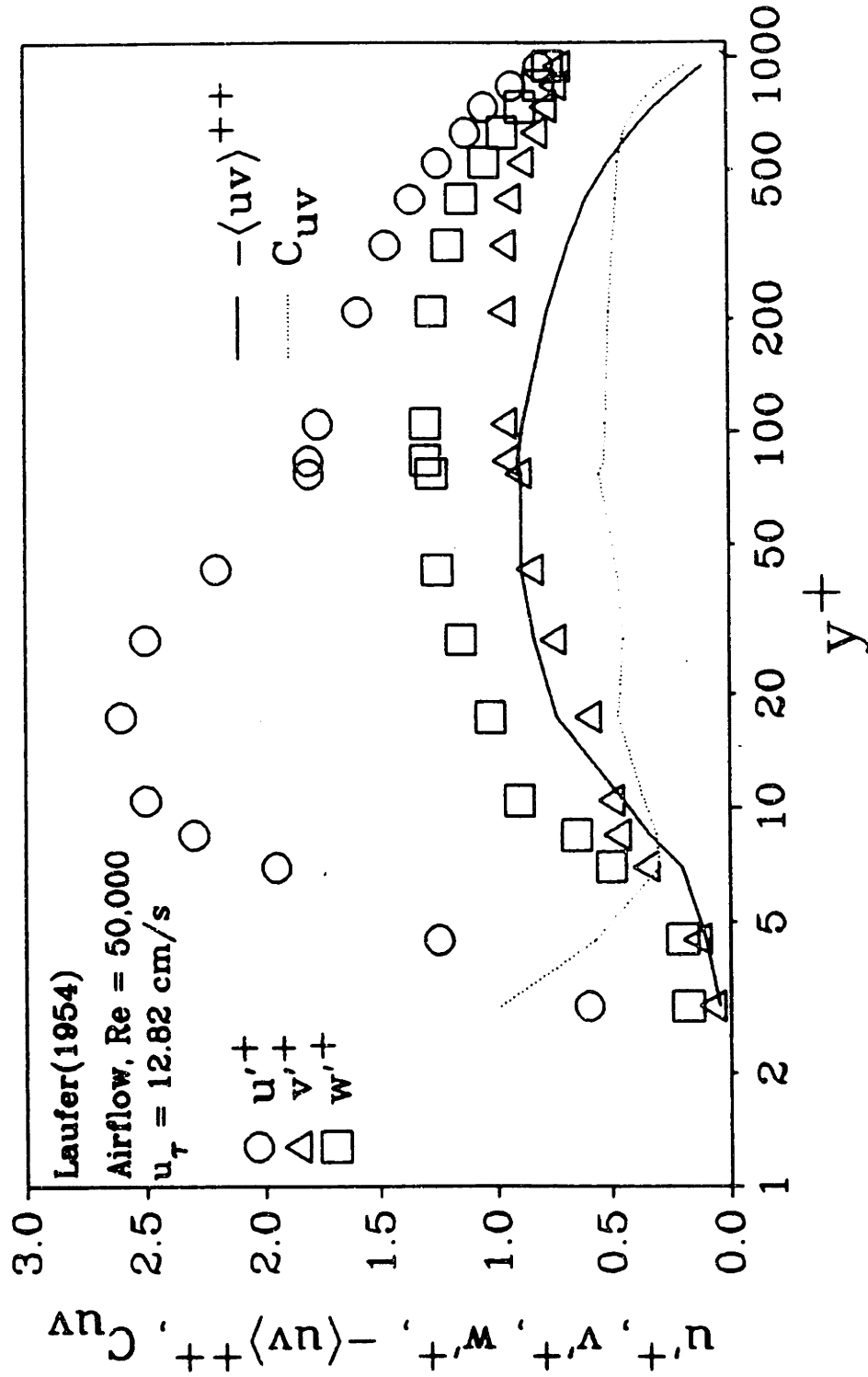


Figure 2.3.23: Newtonian-Turbulence Data at $Re_s = 5 \times 10^4$ (Laufer, 1954)

Turbulence-Intensity, Reynolds-Stress, & Correlation-Coefficient Profiles

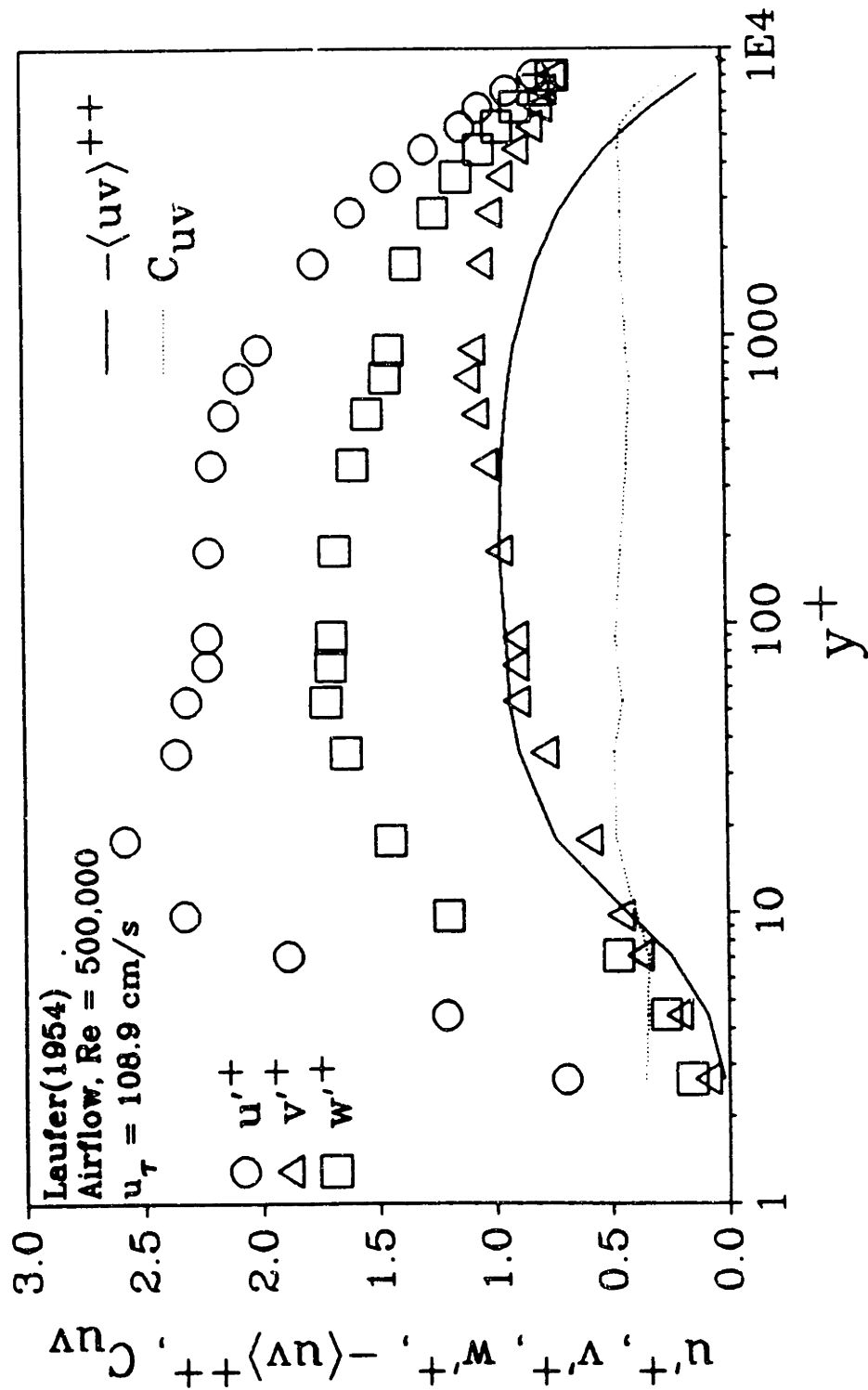


Figure 2.3.24: Newtonian-Turbulence Data at $Re_s = 5 \times 10^5$ (Laufer, 1954)

$$N_{11} = \frac{\langle uu \rangle - \langle vv \rangle}{\langle uv \rangle} \quad (2.3-16)$$

$$N_{22} = \frac{\langle vv \rangle - \langle ww \rangle}{\langle uv \rangle} \quad (2.3-17)$$

$$q^{++} = \frac{(u^2 + v^2 + w^2)}{2u^2} = \frac{1}{2} (u'^+)^2 + \frac{1}{2} (v'^+)^2 + \frac{1}{2} (w'^+)^2 \quad (2.3-18)$$

From Laufer's data, N_{11} , N_{22} , and q^{++} can be calculated; their profiles for $Re = 5 \times 10^4$ and 5×10^5 are shown in Figures 2.3.25 and 2.3.26, respectively. To date, the analogy between fluid rheology and turbulence has not been used to characterize either Newtonian or non-Newtonian turbulence. These data are still the most extensive turbulence measurements for Newtonian turbulence and offer the best estimates for N_{11} , N_{22} , and q^{++} for Newtonian fluids. Differences in N_{11} , N_{22} , and q^{++} between Newtonian and drag-reducing flows may offer insight into the kinematic aspects of turbulence structure during drag reduction.

Virk(1975b) characterized the normalized axial intensity, u'^+ , profiles for Newtonian and drag-reducing flows as similar. The latter has a greater u'^+ at every y^+ . The axial intensity u'^+_{\max} occurs at y^+_{\max} , in the buffer-elastic sublayer. Both values are greater than those for Newtonian profiles. Both profiles have an equal initial slope which extend to the coordinates $(y^+_{\max}, u'^+_{\max})$ and then drop off sharply. At the centerline, both u'^+ are equal. For the radial intensity v'^+ , the relative trend is reversed with the Newtonian always slightly larger at every y^+ ; the Newtonian v'^+ profile has a shallow maximum in the log layer. The drag-reducing v'^+ profile shows no local maximum and just increases from the wall to the core where its value equals that for the Newtonian

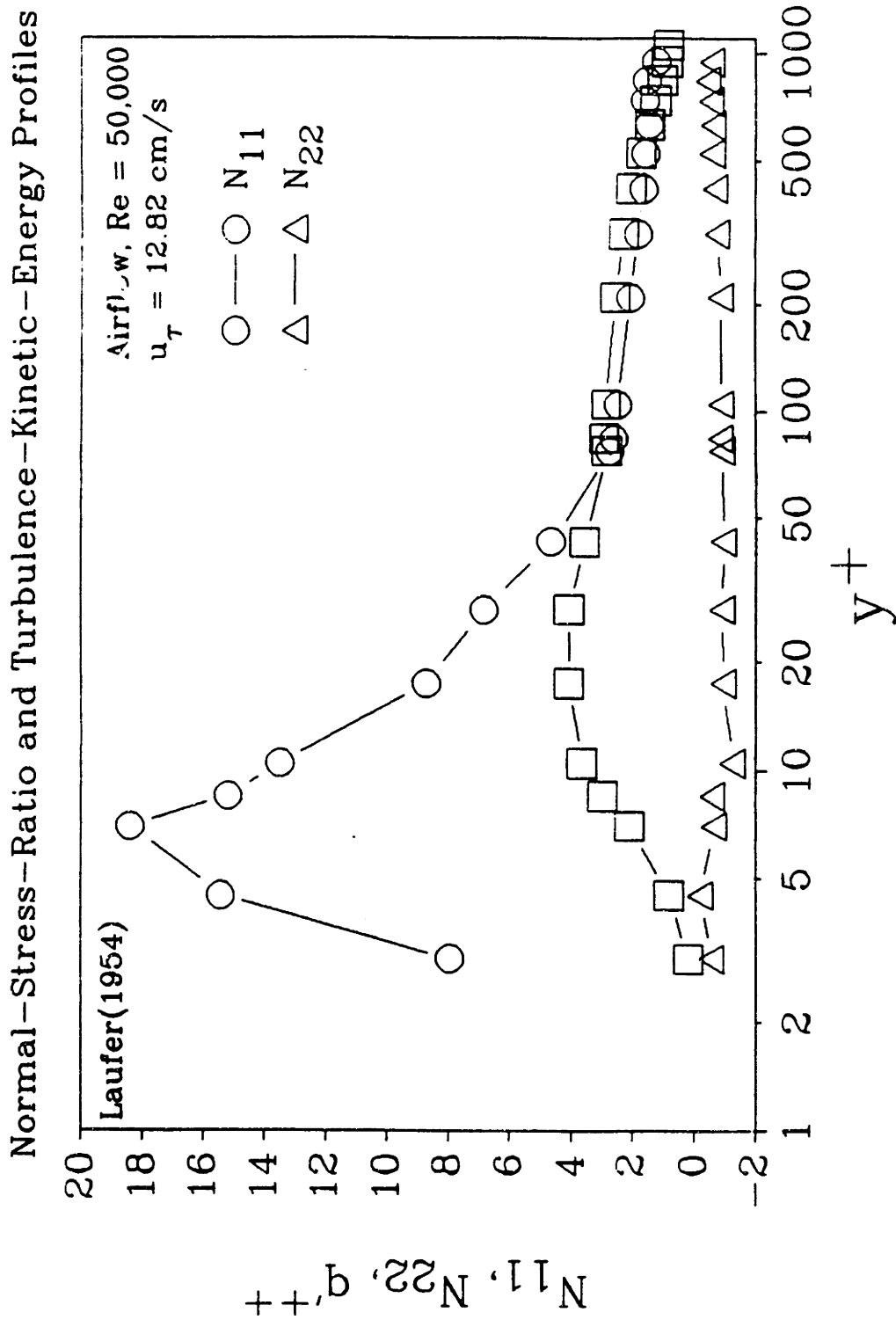


Figure 2.3.25: Turbulent Normal Stresses and Kinetic Energy at $Re_s = 5 \times 10^4$ (Laufer, 1954)

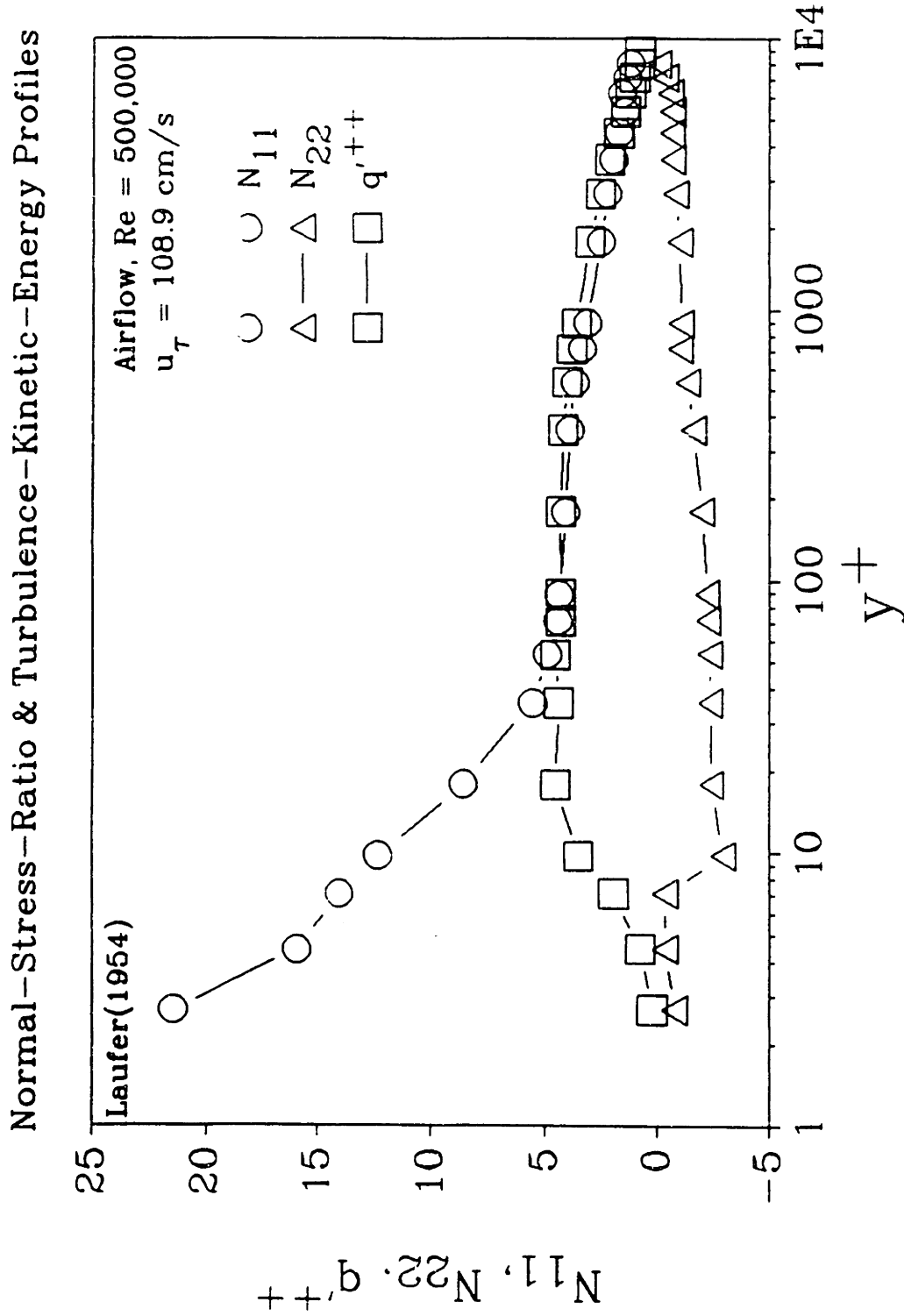


Figure 2.3.26: Turbulent Normal Stresses and Kinetic Energy at $Re_s = 5 \times 10^5$ (Laufer, 1954)

case. Trends for the Reynolds stress, $-\langle uv \rangle^{++}$, and the correlation coefficient, $C_{uv} = -\langle uv \rangle^{++}/(u'^{++}v'^{++})$, follow those for v'^{++} . The following table summarizes some recent turbulence-intensity measurements during drag reduction.

Table 2.3.3
Sources of Turbulence Intensity I Data

Investigators	Experimental Conditions
McComb & Rabie(1982b)	<ul style="list-style-type: none"> ●CL and wall PEO injection into H₂O pipe flow. ●u'^{++}, $-\langle uv \rangle^{++}$ vs. y^+ at single C_p and $\langle C \rangle$.
Bartels et al.(1984)	<ul style="list-style-type: none"> ●homogeneous HPAM solution in pipes of ID = 16 mm and 44 mm. ●u'^{++}, v'^{++}, w'^{++}, $-\langle uv \rangle^{++}$ vs. y/R at several c.(Note: u'^{++}, v'^{++}, and w'^{++} were not obtained simultaneously, and $-\langle uv \rangle^{++}$ was inferred from \bar{U}^+ vs. y^+ and the N-S equations.)
Bewersdorff(1984)	<ul style="list-style-type: none"> ●CL HPAM injection in H₂O pipe flow at several Re and $\langle C \rangle$. ●u'^{++}, v'^{++}, $-\langle uv \rangle^{++}$ vs. y/R.
McComb & Chan(1985)	<ul style="list-style-type: none"> ●homogeneous fiber and fiber/HPAM solutions in pipe flow. ●u'^{++} and w' vs. y/R at several Re and c.

McComb & Rabie(1982b) performed drag reduction experiments by injecting a PEO solution into the centerline and near-wall region of fully developed turbulent pipe flow. Figure 2.3.27 shows their measurements of u'^{++} for CL injection with $C_p = 0.1\%$, which yielded $\langle C \rangle = 5$ wppm. The graphs show that u'^{++} generally increases, the location of u'^{++}_{\max} moves away from the wall, as drag-reduction increases. The region of the profile where u'^{++} exceeds solvent can be associated with the elastic sublayer.

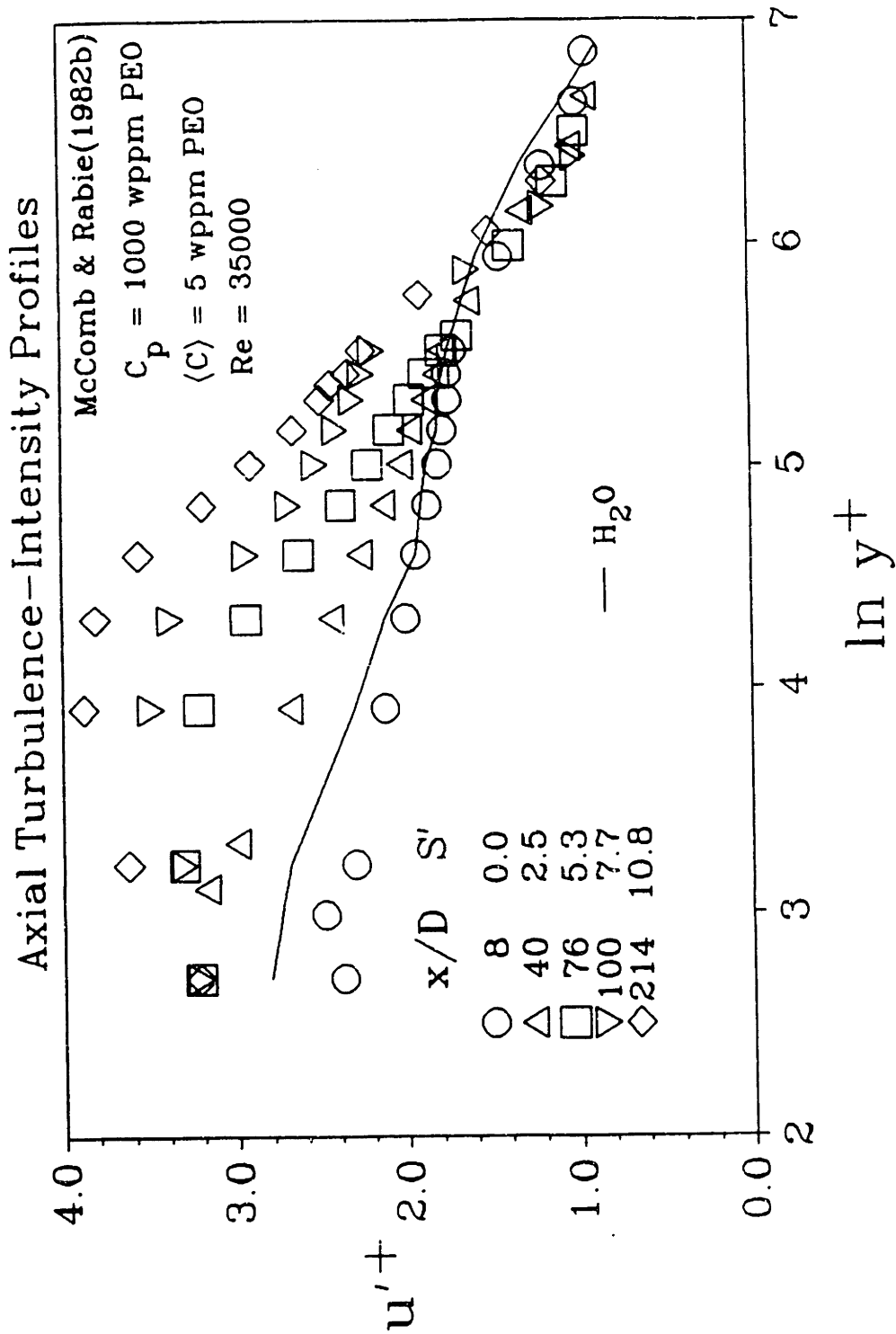


Figure 2.3.27: Axial Turbulence-Intensity Profiles(McComb & Rabie, 1982b)

Bartels et al.(1984) examined the intensity structure of HPAM-solution flows in 16.44- and 44-mm pipes. In the smaller pipe, u'^+ , v'^+ , and w'^+ were measured; however, all three were not thoroughly measured for all concentrations. Figures 2.3.28, 2.3.29, and 2.3.30 show data for u'^+ & v'^+ , $-\langle uv \rangle^{++}$ & C_{uv} , and N_{11} & N_{22} , respectively, from flows with $c = 0, 200, \text{ and } 300$ wppm in a 16.44-mm pipe. Unfortunately, u'^+ , v'^+ , and w'^+ were not measured in the same flow for a given concentration, rather they were taken at nearly the same $S'(\%DR)$ at a given concentration. Thus, the conclusions drawn from these data may not be exactly correct and must be considered tentative since the intensities seem sensitive to S' . In Figure 2.3.28, the concentration dependence for u'^+ and v'^+ are $u'^+(200) \approx u'^+(300) > u'^+(0)$ and $v'^+(200) \approx v'^+(300) < v'^+(0)$. Near the wall, u'^+ levels were raised, and v'^+ levels were lowered relative to solvent. In the core, the u'^+ level for polymer-solution flows was ~ 0.81 , slightly larger than Laufer's(1954) value of 0.76, while the v'^+ core value was ~ 0.63 , less than the 0.72 from Laufer(1954). The profiles for $-\langle uv \rangle^{++}$ and C_{uv} , displayed in Figure 2.3.29, confirm Virk's observation(1975b) that these trends should follow that of v'^+ ; however, the C_{uv} values are elevated relative to earlier results. This may arise because the u'^+ and v'^+ were not determined under identical conditions and because $-\langle uv \rangle^{++}$ was derived from mean velocity profiles. The first and second normal-stress ratios, N_{11} and N_{22} , are given in Figure 2.3.30. Their patterns should follow those of u'^+ and v'^+ , respectively. The N_{11} and N_{22} values observed in solvent are below those of Laufer(1954), but both quantities increase dramatically during drag reduction. Figures 2.3.31 and 2.3.32 show u'^+ and v'^+ profiles in the 44-mm pipe(Bartels et al., 1984); they monotonically increased and decreased, respectively, with

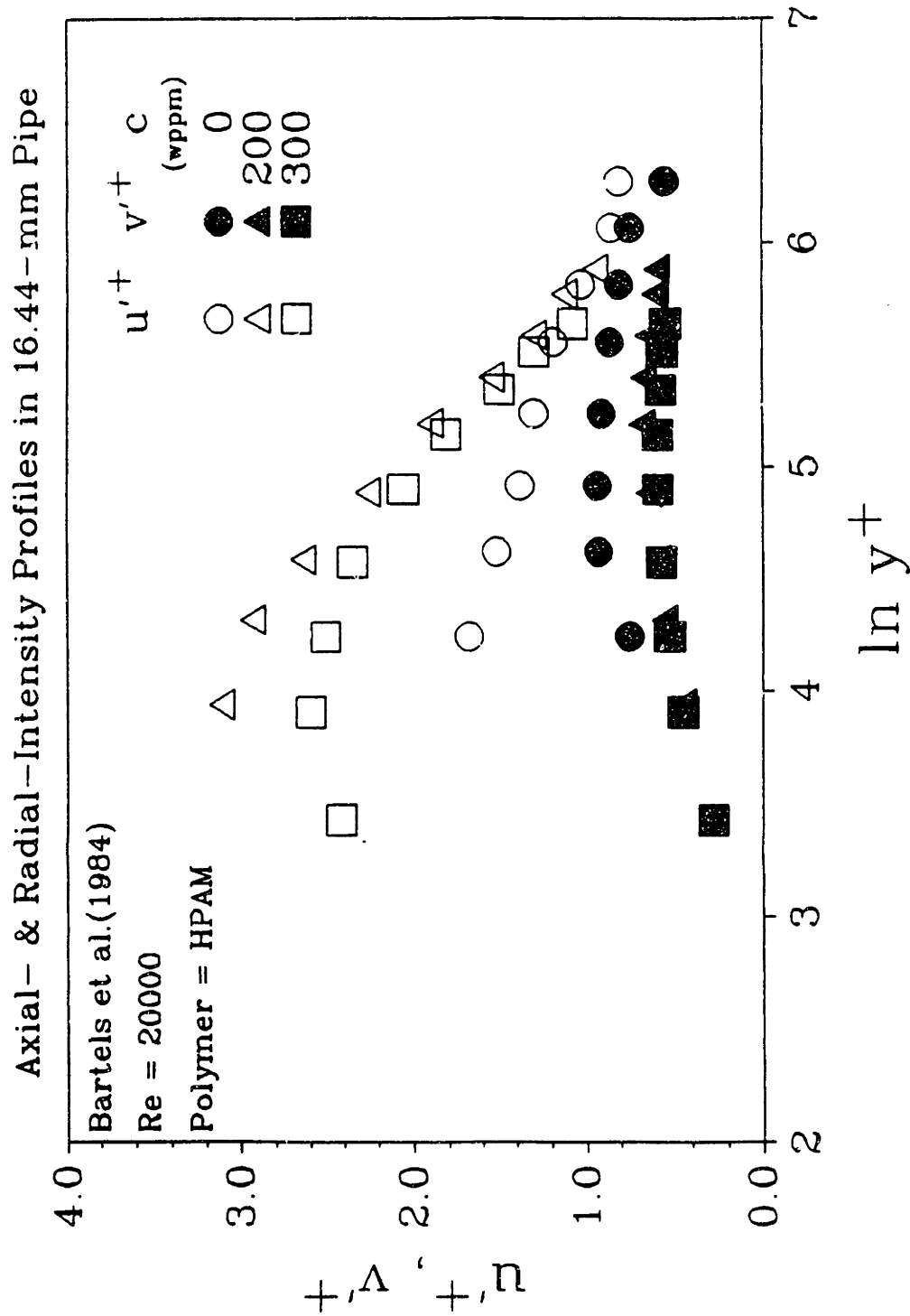


Figure 2.3.28: Axial- and Radial-Intensity Profiles in 16-mm Pipe(Bartels et al., 1984)

Reynolds-Stress & Correlation - Coefficient Profiles in 16.44-mm Pipe

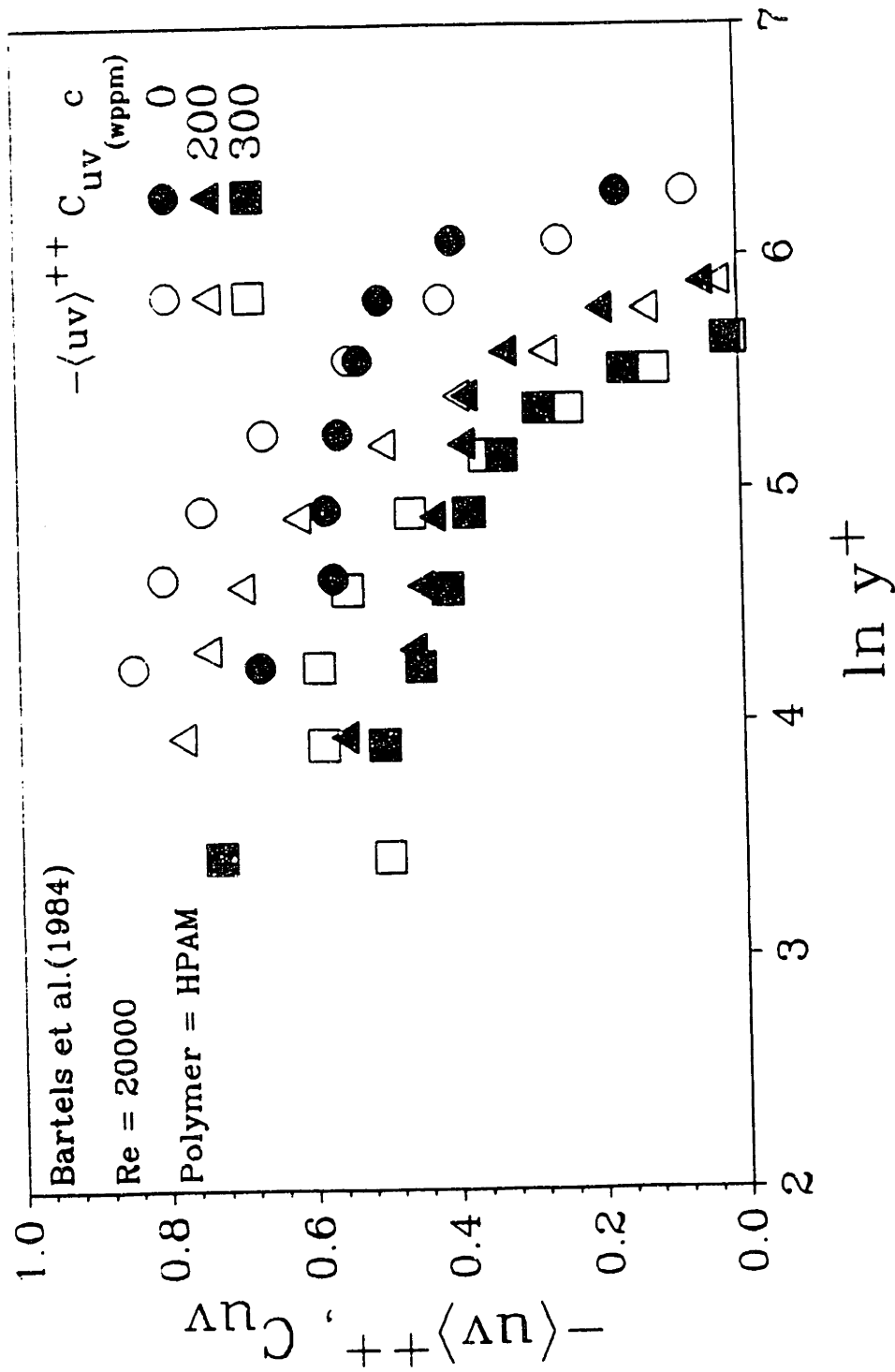


Figure 2.3.29: Reynolds-Stress Profile in 16-mm Pipe (Bartels et al., 1984)

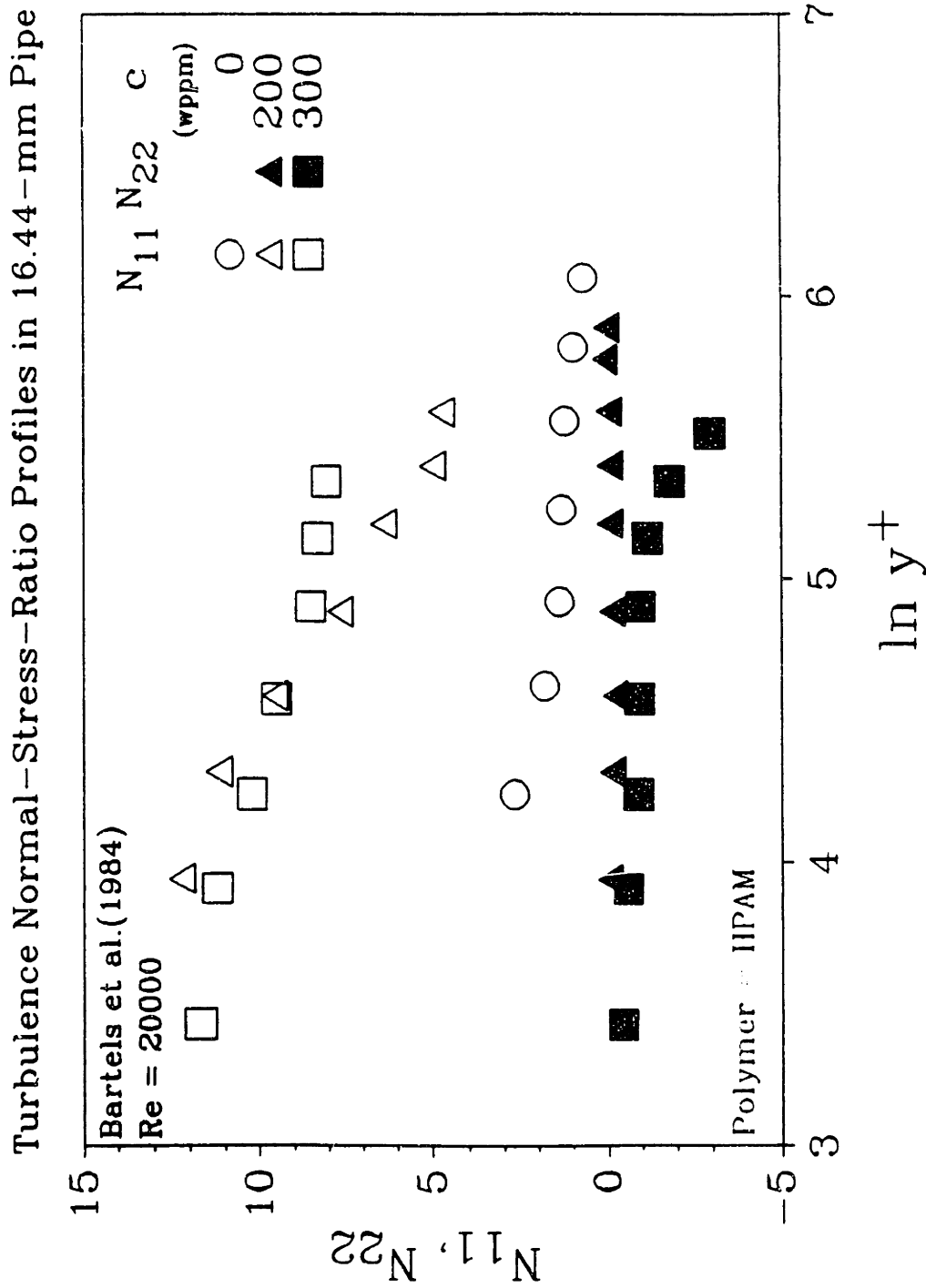


Figure 2.3.30: Turbulence Normal-Stress Ratios in 16-mm Pipe (Bartels et al., 1984)

increasing S' . The u'^+_{\max} and v'^+_{\max} values also displayed the same trends, with their loci moving coreward as S' increased. However, these maximum-intensity loci never extended much beyond $y^+ = 30$, and did not move with elastic-sublayer thickening, as seen in the corresponding mean profiles. In this respect, the present data differ from those of McComb & Rabie(1982b). However, the u'^+_{\max} values as a function of S' coincide with those from Laufer(1954)(solvent) and McComb & Rabie(1982b)(polymer solution). The data for Newtonian and homogeneous-polymer solutions(open symbols) are compared in Figure 2.3.33; the best-fit line has an intercept and slope of ~ 2.74 and ~ 0.113 , respectively. A similar plot of v'^+_{\max} vs. S' appears in Figure 2.3.34, and v'^+_{\max} decreases linearly with S' with an intercept and slope of ~ 0.99 and ~ -0.041 , respectively. Coincidentally, the ratios of the respective u'^+_{\max} and v'^+_{\max} intercepts, $2.74/0.99 = 2.75$, has the same magnitude as the ratio of the respective slopes, $0.11/-0.041 = -2.76$. This suggests powerful similarities in the scaling of axial and radial turbulence intensities, regardless of the level of drag reduction. A new picture of the elastic layer emerges from the u'^+ and v'^+ profiles. The y^+ range bounded by the loci of u'^+_{\max} and v'^+_{\max} defines the most-active portion of the elastic layer. Based on this observation, an alternative definition for the elastic layer might be the region bounded by the y^+ where the wallward maximum in u'^+ occurs to the y^+ where the peak in v'^+ occurs. Some of the v'^+ profiles show that v'^+_{\max} occurs at the centerline; that is, the elastic layer has penetrated to the core, implying that M has been reached. Figures 2.3.35 and 2.3.36 respectively show profiles of $-\langle uv \rangle^{++}$ and C_{uv} vs. $\ln y^+$. Both quantities have been derived from mean-flow and turbulence-intensity data of Barteis et al.(1984). It can be seen that the profiles of $-\langle uv \rangle^{++}$, and especially C_{uv} , during drag

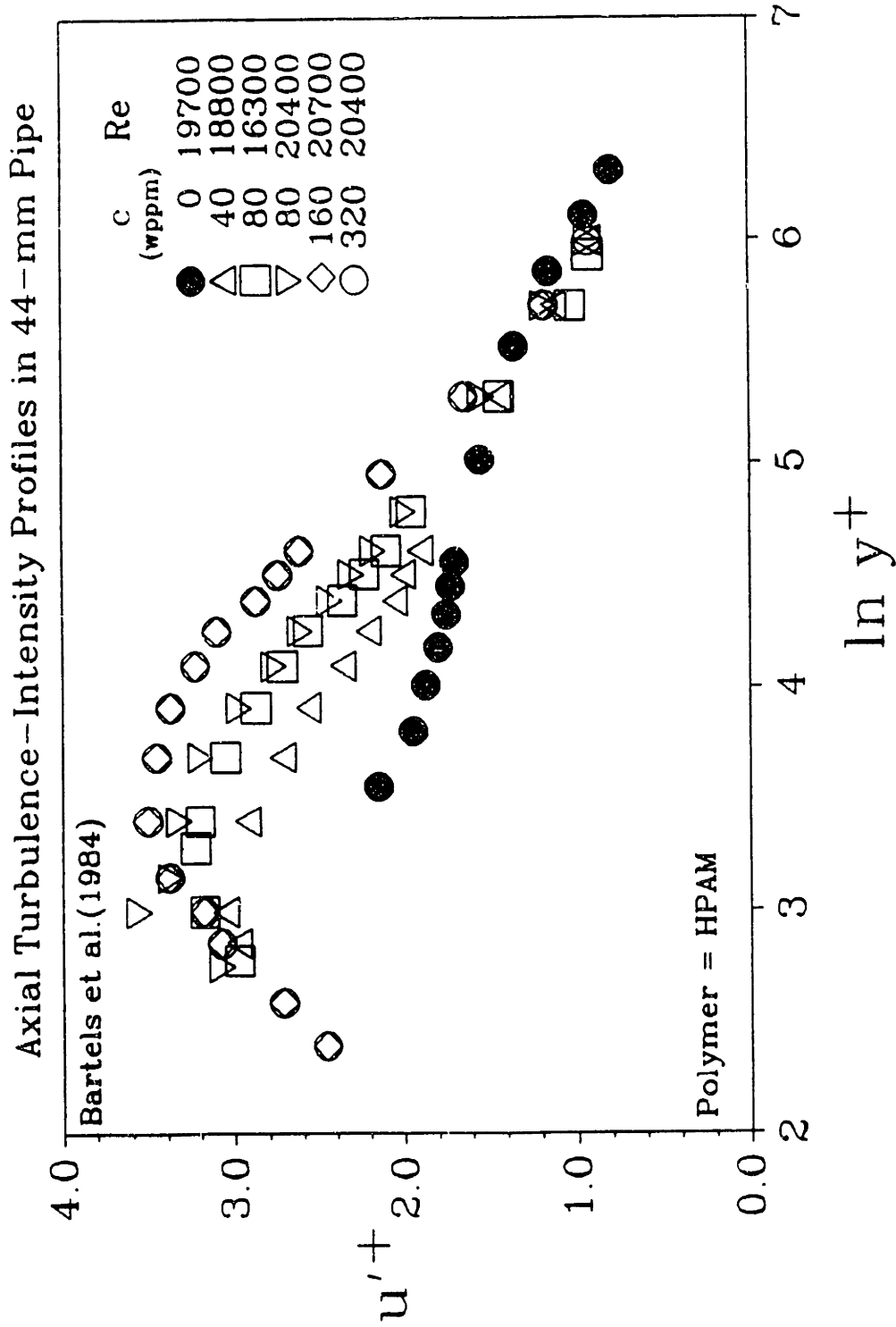


Figure 2.3.31: Axial Turbulence-Intensity Profiles in 44-mm Pipe(Bartels et al., 1984)

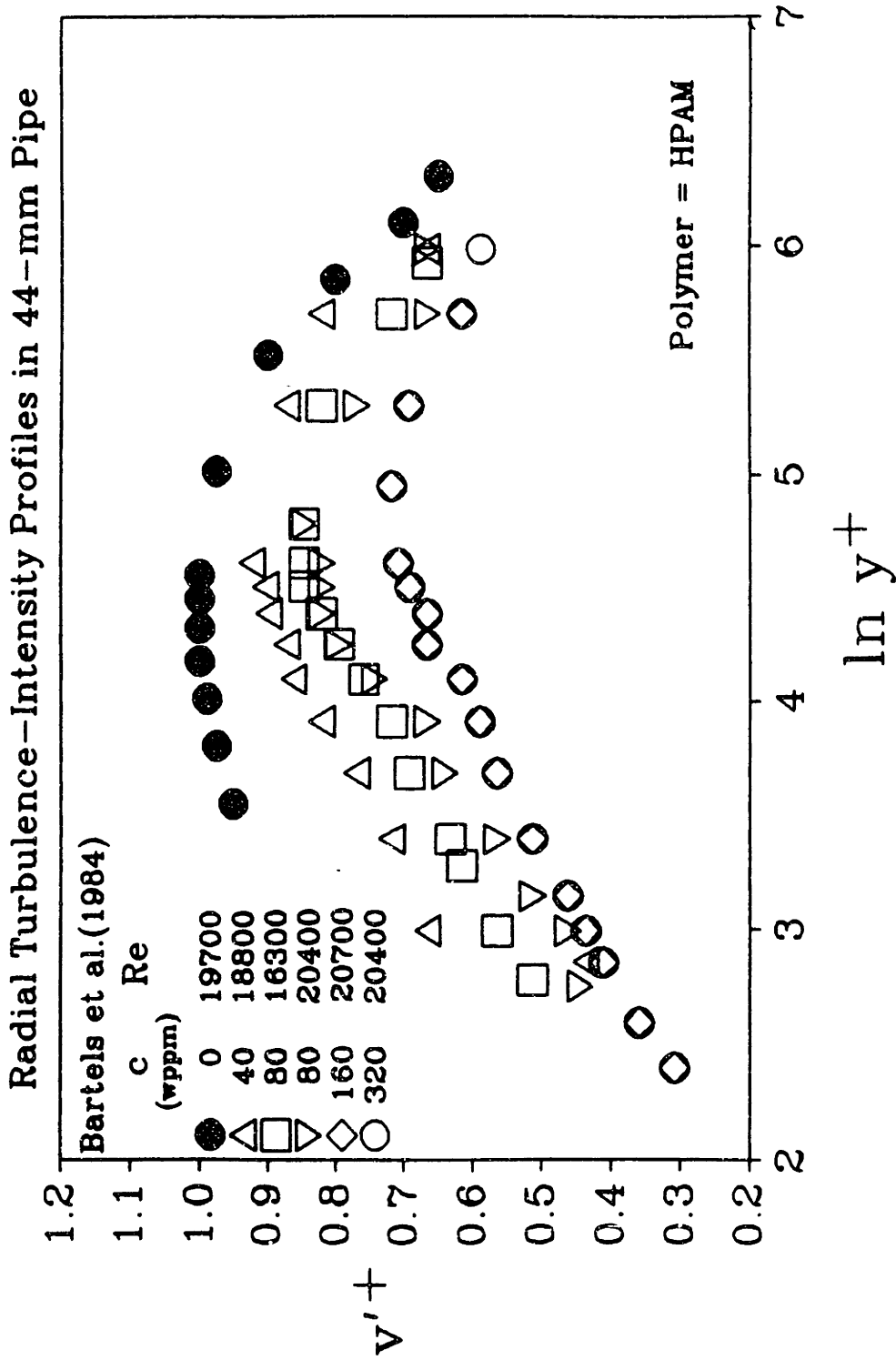


Figure 2.3.32: Radial Turbulence-Intensity Profiles in 44-mm Pipe (Bartels et al., 1984)

Dependence of Axial Turbulence-Intensity Maxima on Flow Enhancement

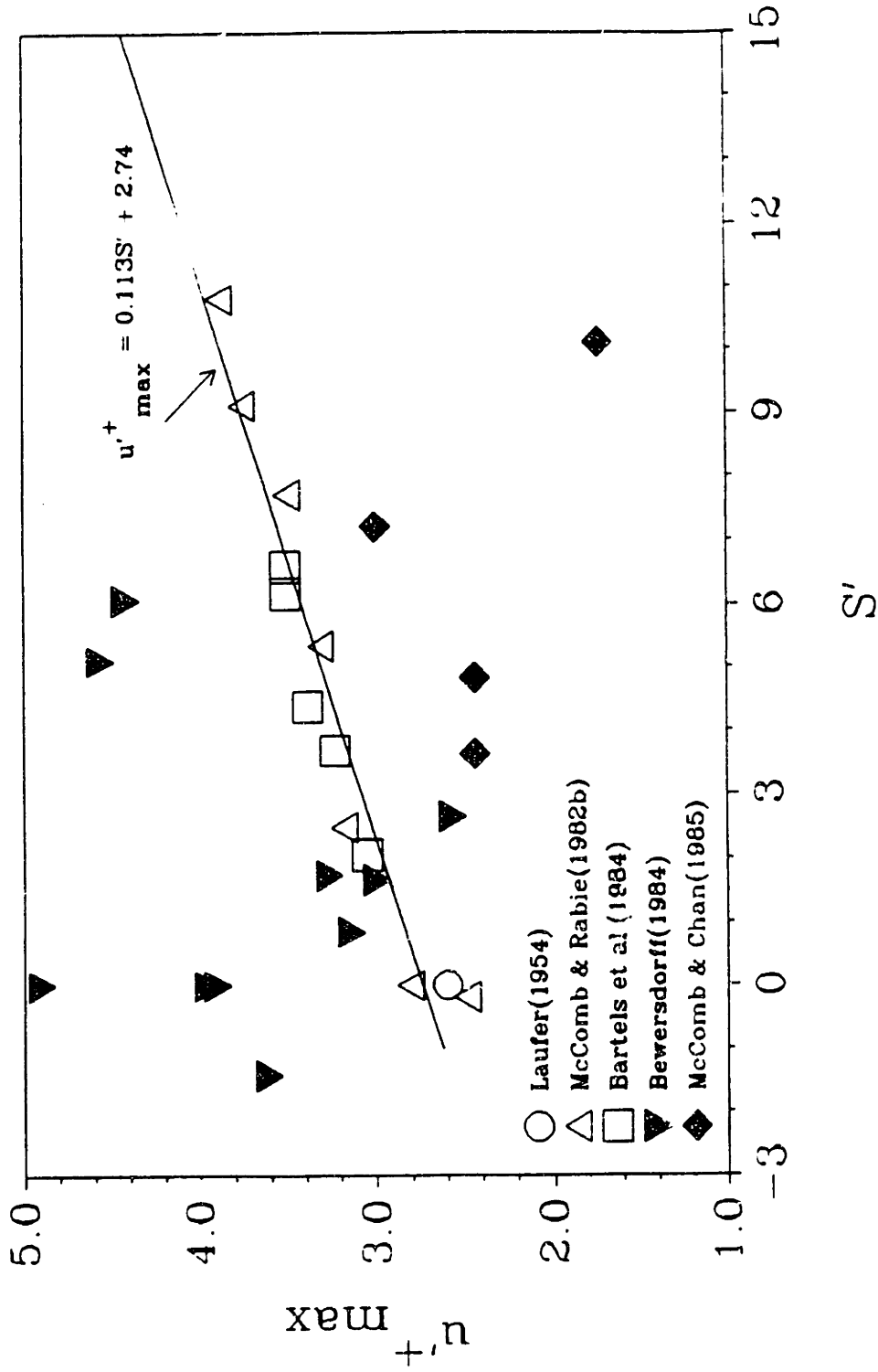


Figure 2.3.33: Axial Turbulence-Intensity Maxima from Various Studies

Dependence of Radial Turbulence-Intensity Maxima on Flr w Enhancement

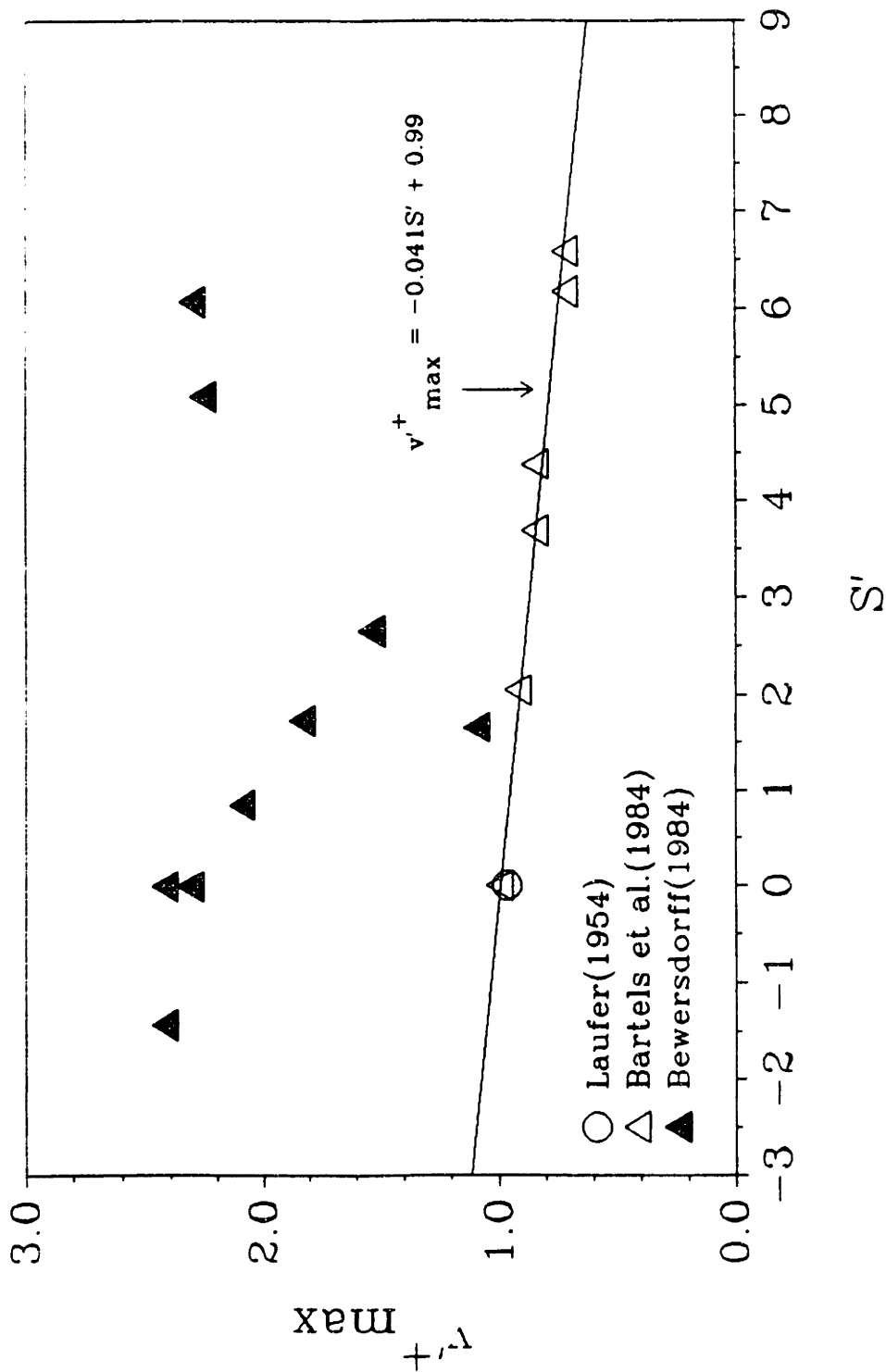


Figure 2.3.34: Radial Turbulence-Intensity Maxima from Various Studies

reduction are lower than Newtonian profiles. Also, the maxima of both $-\langle uv \rangle^{++}$ and C_{uv} appear to lie in the elastic sublayer region defined by the axial and radial turbulence-intensity maxima. In these examples of both Newtonian and homogeneous polymer-solution flows, the total stress T_w near and at the core was equal to $-\rho \langle uv \rangle^{++}$ and governed by the dimensionless equation derivable from Navier-Stokes:

$$-\langle uv \rangle^{++} = 1 - \frac{y^*}{R^*} - \frac{dU^*}{dy^*} \quad (2.3-19)$$

More recently, Willmarth et al.(1987), Bewersdorff & Berman(1988) and Usui et al.(1988) observed a "stress deficit" in polymer-thread-injection experiments. The first group noted that $-\langle uv \rangle^{++}$ calculated via equation 2.3-19 was about 1.5 times the measured value across the pipe diameter. Attributing the deficit to a varying local viscosity, the second group introduced an "elastic modulus" term G into equation 2.3-19 and then lumped G into an effective viscosity to get a new governing equation:

$$-\langle uv \rangle^{++} = 1 - \frac{y^*}{R^*} - \frac{dU^*}{dy^*} - G = 1 - \frac{y^*}{R^*} - \frac{\nu_{eff}}{\nu_s} \left[\frac{dU^*}{dy^*} \right] \quad (2.3-20)$$

Via this equation "bifurcated" mean-velocity profiles were shifted onto M ; thus, what the effective-viscosity function must have been was inferred. Despite this rheological manipulation, it was concluded that the drag-reduction mechanism does not depend on rheology. The third group hypothesized that a third, viscoelastic momentum-transfer mechanism might exist in polymer-injection experiments.

Bewersdorff(1984) took extensive \bar{U}^+ , u'^+ , and v'^+ data for centerline injection of HPAM solutions into turbulent pipe flows of water. These u'^+ and v'^+ data are

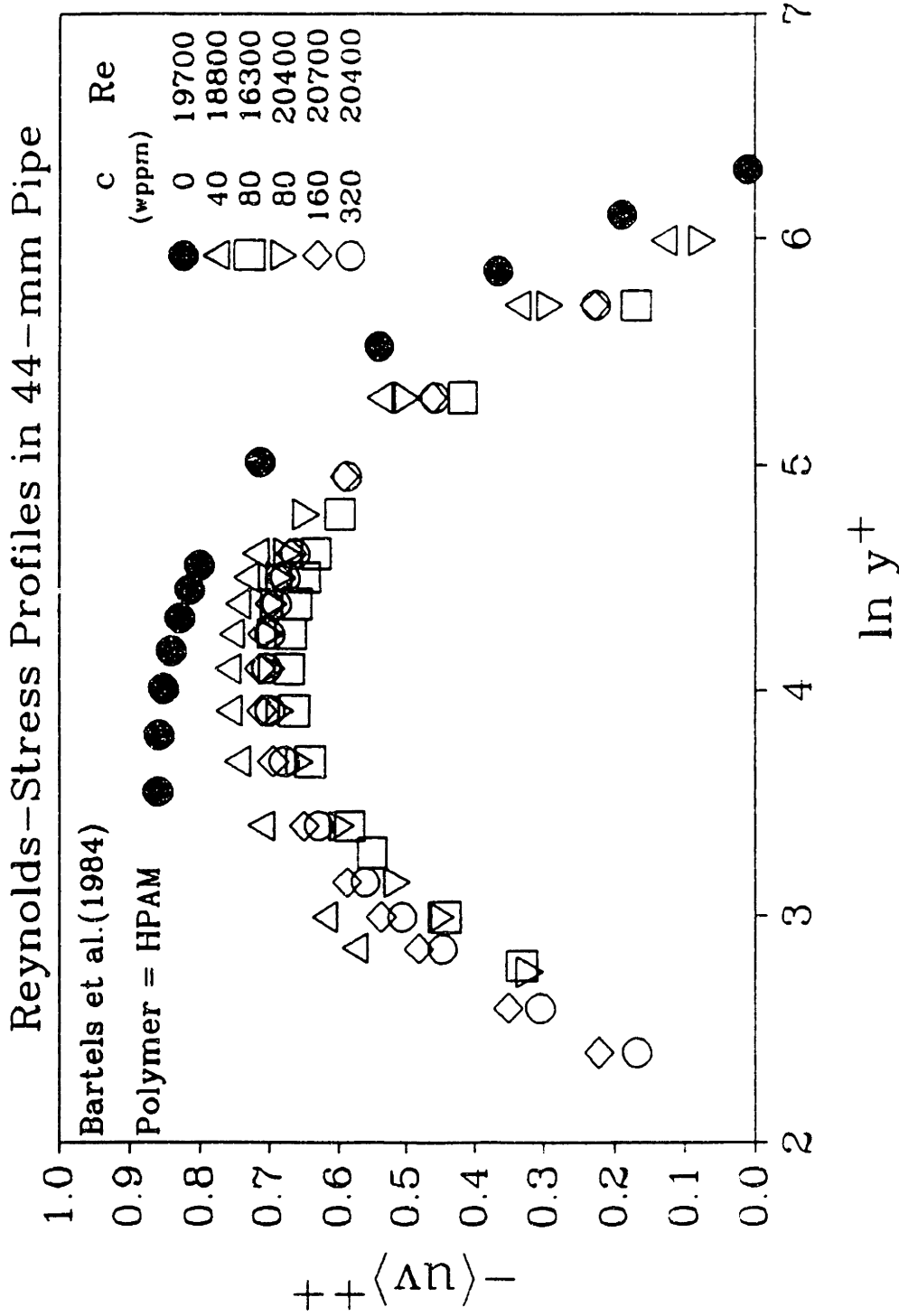


Figure 2.3.35: Reynolds-Stress Profiles in 44-mm Pipe (Bartels et al., 1984)

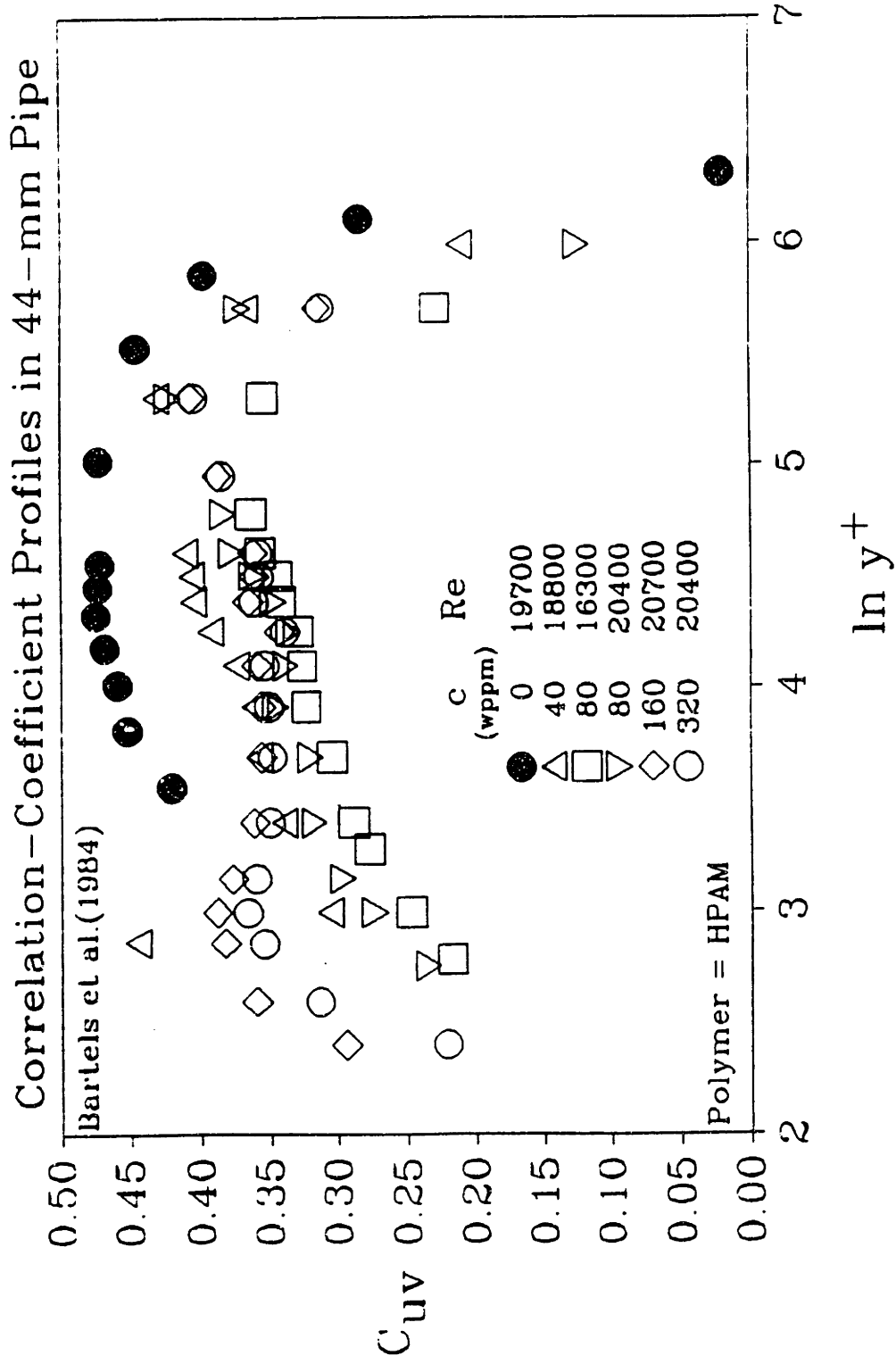


Figure 2.3.36: Correlation-Coefficient Profiles in 44-mm Pipe(Bartels et al., 1984)

anomalous when compared with the data of other investigators, as shown respectively in Figures 2.3.37 and 2.3.38, which compare some of his intensity data with those of others at similar conditions. In both figures, the data from Laufer(1954), Bartels et al.(1984), and McComb & Rabie(1982b) have a great degree of similarity over a range of R^+ while Bewersdorff's data differ markedly. An essential experimental difference between Bewersdorff and the others lies in that the injected polymer formed a large thread which remained intact down the centerline under flow conditions, possibly forming another phase in the flow that affected the LDA measurements of the turbulence intensities.

McComb & Chan(1985) investigated flows of asbestos-fiber suspensions at various Re and measured u'^+ (and a few w'). At $Re = 32000$, the u'^+ trends for 300-wppm fiber-suspension flows coincided with those reported by others. Figure 2.3.39 shows how the u'^+ profile changed with the number of passes. In the first pass, unusual "fiber-like" behavior was observed, as indicated by a suppressed u'^+ profile.

In summary, profiles of u'^+ , v'^+ , $-\langle uv \rangle'^+$, and C_{uv} have provided a wealth of information about the inner structure of both Newtonian and non-Newtonian turbulent flow. Turbulence normal-stress ratios N_{11} and N_{22} derived from intensity measurements also offer valuable insights into drag reduction. Intensity maxima correlate well with S' at low drag reduction. Better measurement of u'^+ and v'^+ , especially at MDR, are necessary to characterize and to understand how flow-enhancing additives alter flow structure.

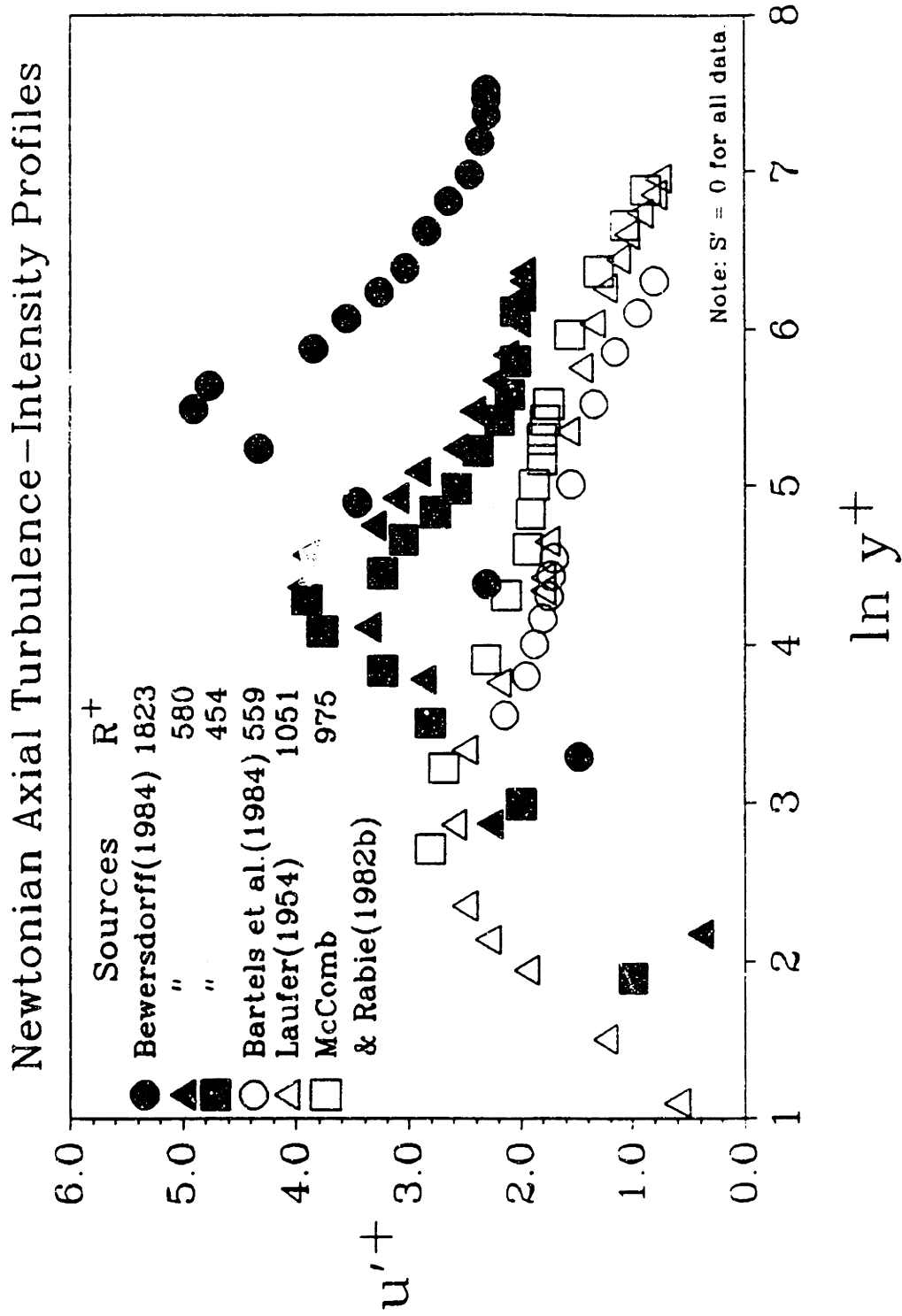


Figure 2.3.37: Axial Turbulence-Intensity Profiles from Various Sources

Axial Turbulence-Intensity Profiles at Comparable Flow Enhancement

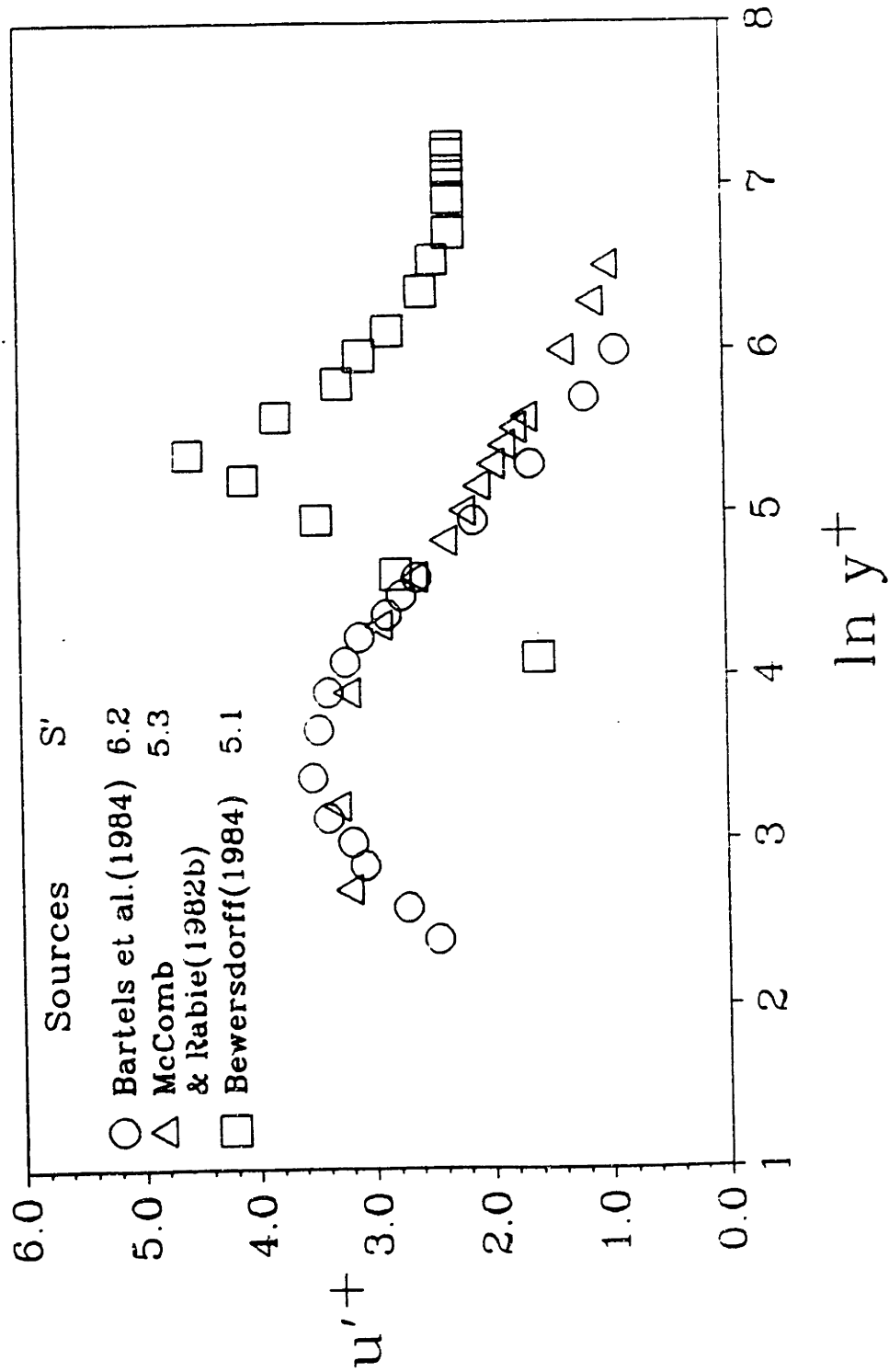


Figure 2.3.38: Axial Turbulence-Intensity Profiles from Various Sources

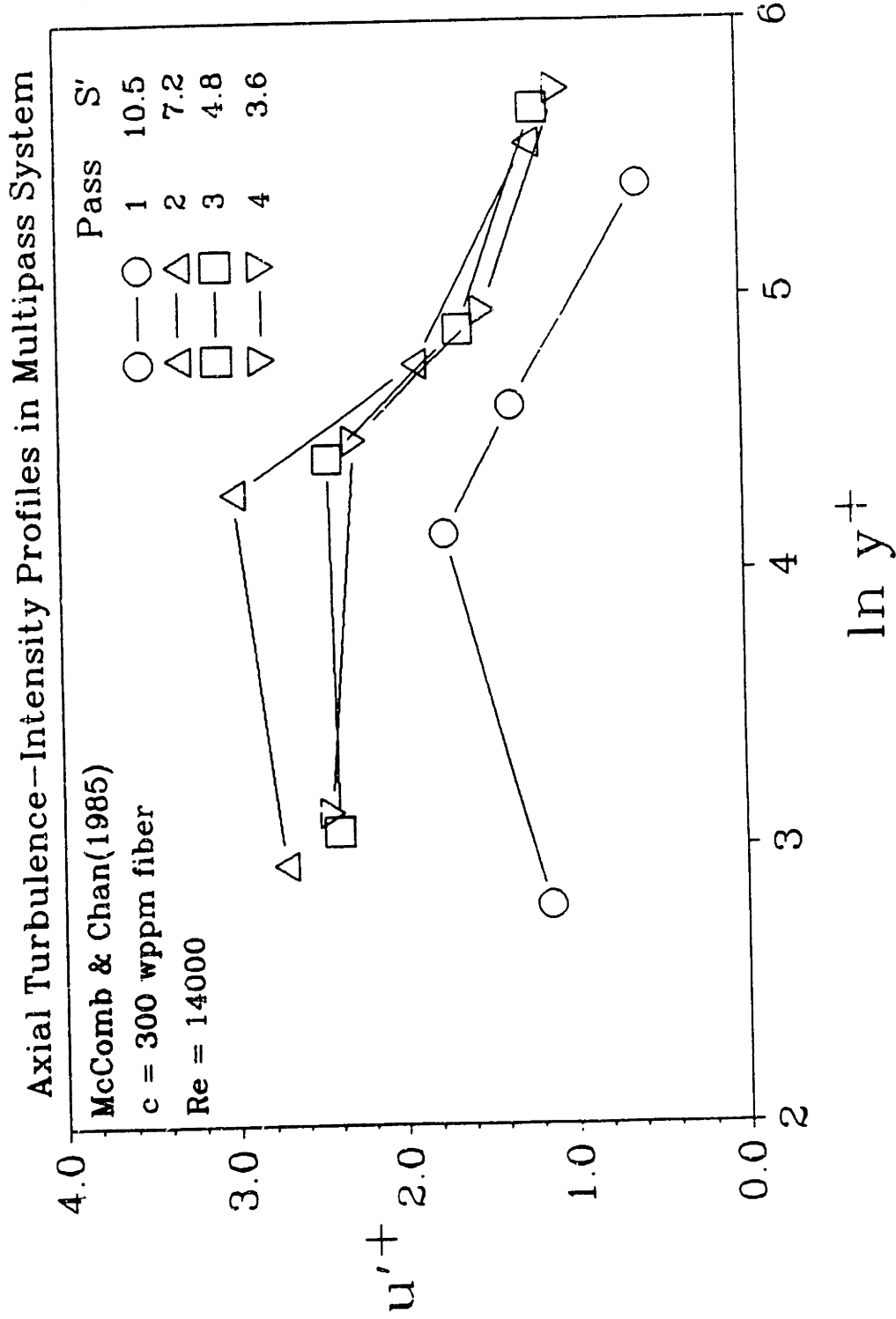


Figure 2.3.39: Axial Turbulence-Intensity Profiles from a Fiber Solution(McComb & Chan, 1985)

2.3.4 Turbulence Structure II: Bursting and Spanwise Spacing

Either time- or ensemble-averaged velocity(or pressure) fluctuations provide information about the structure of turbulent flow. Characteristic lengths and times can be inferred from spatial and temporal auto-correlations. Among the first researchers to record and to calculate these scales were Kline et al.(1967). Visual dye-tracer and hydrogen-bubble experiments on turbulent water (Newtonian)flows yielded average azimuthal spacings, bursting times, and streak lifetimes under various flow conditions. It was shown the low-speed(low-momentum) streaks begin to oscillate at $8 < y^+ < 12$, to amplify as they moved coreward, and then to break-up at $y^+ < 30$. This break-up and ejection process was considered a major mode of energy transfer from the boundary region to the outer flow.

Virk(1975b) collected data from various authors on azimuthal spacings, z^+ , and the time between bursts, T_{bb+} . Azimuthal spacings in drag-reducing flows, when normalized by the Newtonian $z_{n+} \approx 100$, depended exponentially on the apparent slip S' :

$$\ln \left[\frac{z_p^+}{z_n^+} \right] = 0.156 S' \quad (2.3-21)$$

where p and n denote polymer and Newtonian, respectively. Because spatial turbulence structure depended on S' , temporal turbulence structure, characterized by T_{bb+} , was likely to follow similar trends, but not enough data were available then.

Investigators have since measured z^+ and T_{bb+} for both Newtonian and non-

Newtonian flows. Determining z^+ has depended mostly on subjective examinations of video recordings of tracer experiments; thus, there have been discrepancies among researchers who use different criteria in their analyses. On the other hand, T_{bb}^+ may be derived more objectively from auto-correlations; however, even here some subjectivity results from cut-off criteria and threshold levels. Also, measuring T_{bb}^+ from video recordings by combining streak frequency per unit width, F^+ , and z^+ has been attempted but seems prone to even greater uncertainty. The following table lists the major contributions to z^+ and T_{bb}^+ information.

Table 2.3.4
Sources of Turbulence Structure II Data

Investigators	Experimental Conditions
Donohue et al.(1972)	<ul style="list-style-type: none"> ●streak dyeing, H₂ bubble tracing. ●z^+ and F^+ from streak pictures. ●$T_{bb}^+ = (z^+F^+)^{-1}$. ●$Re < 22800$. ●PEO-FRA ●2D channel, $D_h = 74.4$ mm.
Eckelman et al.(1972)	<ul style="list-style-type: none"> ●mass transfer probes to detect S_x and S_z. ●z^+ derived from $\langle S_x \rangle$, S_x wavelength, and viscosity. ●pipe ID = 25 mm.
Achia & Thompson(1977)	<ul style="list-style-type: none"> ●interferometric methods. ●z^+ and F^+ from $R_c(z)$. ●$R_c(z)$ from video frames. ●$T_{bb}^+ = (z^+F^+)^{-1}$. ●$Re < 11000$. ●HPAM(Separan AP30). ●pipe with flat wall, ID = 26.3 mm.

Investigators	Experimental Conditions
Mizushina & Usui(1977)	<ul style="list-style-type: none"> ● Laser-Doppler Anemometry(LDA). ● T_{bb}^+ from rerises in $R_c(t)$. ● $Re < 40000$. ● PEO(Alcox E-160). ● T_{bb} assumed constant for $10 < y^+ < 100$. ● pipe ID = 25.3 mm.
Oldaker & Tiederman(1977)	<ul style="list-style-type: none"> ● streak dying. ● z^+ from streak pictures. ● stringent z^+ criteria: 3σ test & valid $z^+ \geq x^+/4$ with no minimum. ● z^+ assumed constant for $y^+ < 8$. ● $Re < 50000$. ● HPAM(Separan AP273). ● 2D channel, $D_h = 71.7$ mm.
McComb & Rabie(1982b)	<ul style="list-style-type: none"> ● LDA. ● T_{bb}^+ from $R_c(t)$. ● $Re = 35000$. ● PEO(WSR-301). ● pipe ID = 26 mm.
Usui et al.(1984)	<ul style="list-style-type: none"> ● LDA. ● T_{bb}^+ from short-sampled $R_c(t)$. ● $Re < 10000$. ● PEO(WSR-301). ● pipe ID = 25.4 mm.
Tiederman et al.(1985)	<ul style="list-style-type: none"> ● streak dying. ● z^+ from streak pictures. ● stringent z^+ criteria: 3σ test & valid $z^+ \geq x^+/4$ with no minimum. ● $Re < 23000$. ● HPAM(Separan AP273). ● 2D channel, $D_h = 45.45$ mm.

Of these authors only Eckelman et al.(1972), Oldaker & Tiederman(1977), Achia & Thompson(1977), Donohue et al.(1982), and Tiederman et al.(1985) measured z^+ for both Newtonian and drag-reducing flows. All authors agree that $z_n^+ = 100 \pm 20$. Such consistency arises from the universal structure of Newtonian turbulent flow. Recently,

Lyons et al.(1988) calculated via a model relating z^+ to a mechanical-energy balance that turbulence production and dissipation are balanced when $z^+ \approx 93$ and that this balance was sensitive to relatively small perturbations about $z^+ \approx 100$.

Because viscous- and elastic-sublayer thickening are associated with drag reduction, changes in z^+ are not a priori predictable. Equation 2.3-21 implies that the real physical extent, z , increases since S' measures the differences between drag-reduced and Newtonian flow at the same u_r . If the fluid viscosity remains the same(only small viscosity increases occur at low c), then z^+ will represent the azimuthal extent of the vortex rolls, an important feature of the turbulence structure.

Eckelman et al.(1972) probably had the best technique, associating z^+ with the velocity gradient S_z and its wavelength in the azimuthal direction. In Figure 2.3.40, their z^+ data aligned with equation 2.3-21 at the highest S' . At lower S' , z^+ data from Donohue et al.(1972), Achia & Thompson(1977), and Tiederman et al.(1985) scattered about the correlation. Data from Oldaker & Tiederman(1977) straddled the line with high and low z^+ at low and high S' , respectively. Their method of confining the streak dying region to $y^+ < 8$ may account for their wide scatter.

The time between bursts T_{bb}^+ was measured by Donohue et al.(1972), Achia & Thompson(1977), Mizushima & Usui(1977), McComb & Rabie (1982b), and Usui et al. (1984). These data are shown in Figures 2.3.41 and 2.3.42. The former shows the normalized time T_{bb}^+/T_{bbn}^+ versus S' , whereas the latter shows the absolute T_{bb}^+ versus S' . Agreement among investigators is hampered by their use of different sampling methods. The data of McComb & Rabie(1982b) obeyed accord well with the spanwise-spacing relation, equation 2.3-21, suggesting that both the spacing and frequency scales

with elastic-sublayer thickness. The data of Mizushima et al.(1977) and those of Usui et al.(1984) also show that T_{bb}^+/T_{bbn}^+ increases with S' , but at a smaller rate than equation 2.3-21. Donohue et al.(1972) and Achia & Thompson(1977) both derived T_{bb}^+ by combining z^+ with the reduced bursting frequency per unit width F^+ . Inconsistencies between the established F^+ and z^+ may account for the apparent decrease of T_{bb}^+ from T_{bbn}^+ at a given R^+ . New approaches that can cleanly separate the additive and turbulent contributions to the changes in T_{bb}^+ with S' and R^+ are required.

2.3.5 Summary of Literature

A comprehensive review of drag-reduction literature since 1975 has been presented. Gross flow, mean-velocity profiles, and turbulence-flow-structure data have all been separately considered and analyzed. The elastic sublayer model(ESM), with parameter "apparent slip", S' , shows promise in unifying and correlating aspects of the mean-flow and turbulence structure during drag reduction. From close examination of the limited reliable u'^+ , v'^+ , and $-\langle uv \rangle^{++}$ data, a relationship between S' and each of u'^+_{max} and v'^+_{max} was inferred. The mean spacing z^+ , and time between bursts T_{bb}^+ still comprise the least consistent aspects of drag-reduction data, being widely scattered. However, it is exciting to note that the relationship found between u'^+_{max} and S' agrees in form with the earlier empirical dependence of azimuthal streak spacings. The physics of the inner flow also support some connection between these different forms of turbulence-structure data, and further attempts to link them are warranted.

Normalized Azimuthal Spacings at Several S' from Various Sources

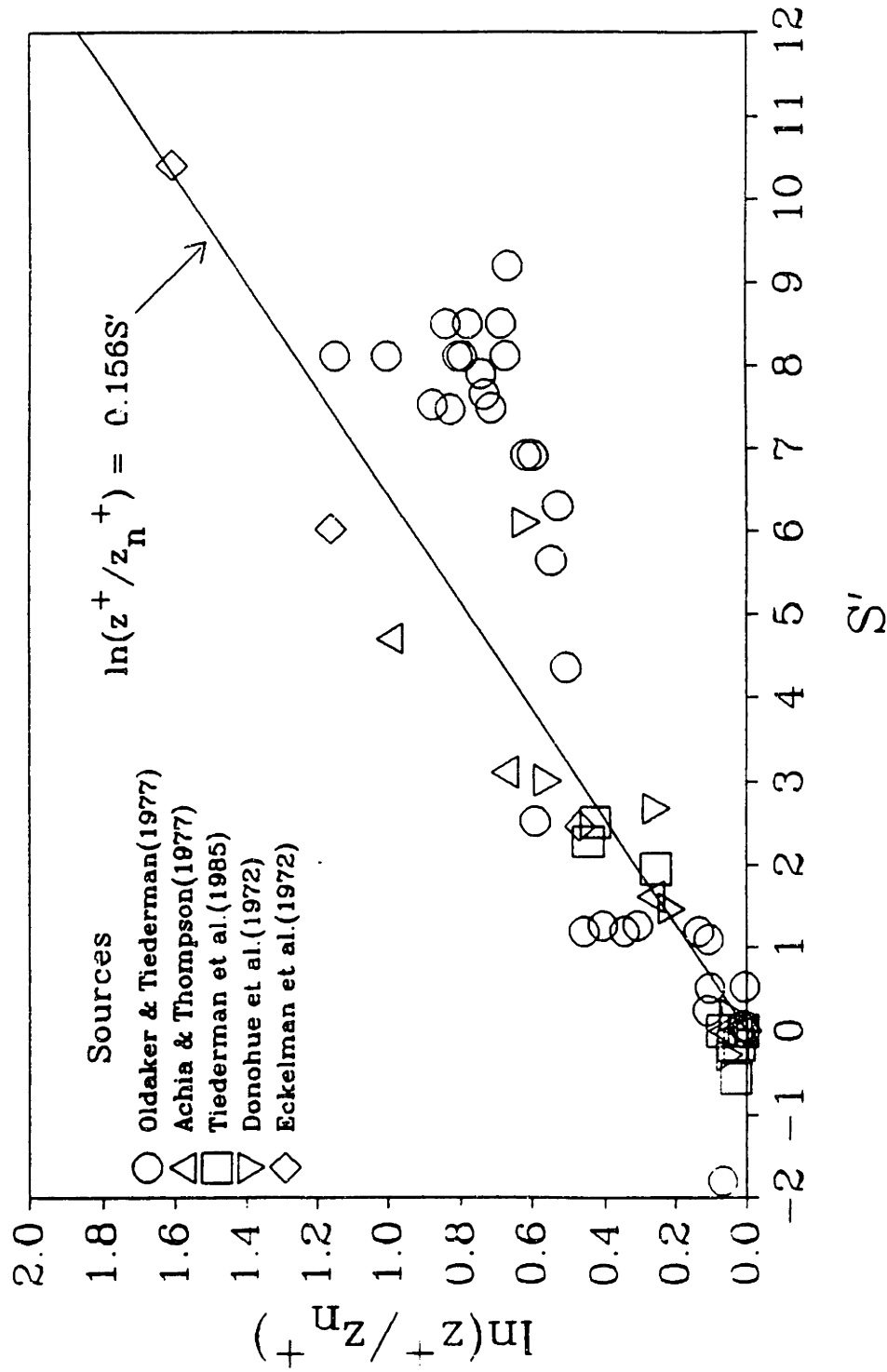


Figure 2.3.40: Normalized Azimuthal Spacings from Various Studies

Normalized Time Between Bursts at Several S' from Various Sources

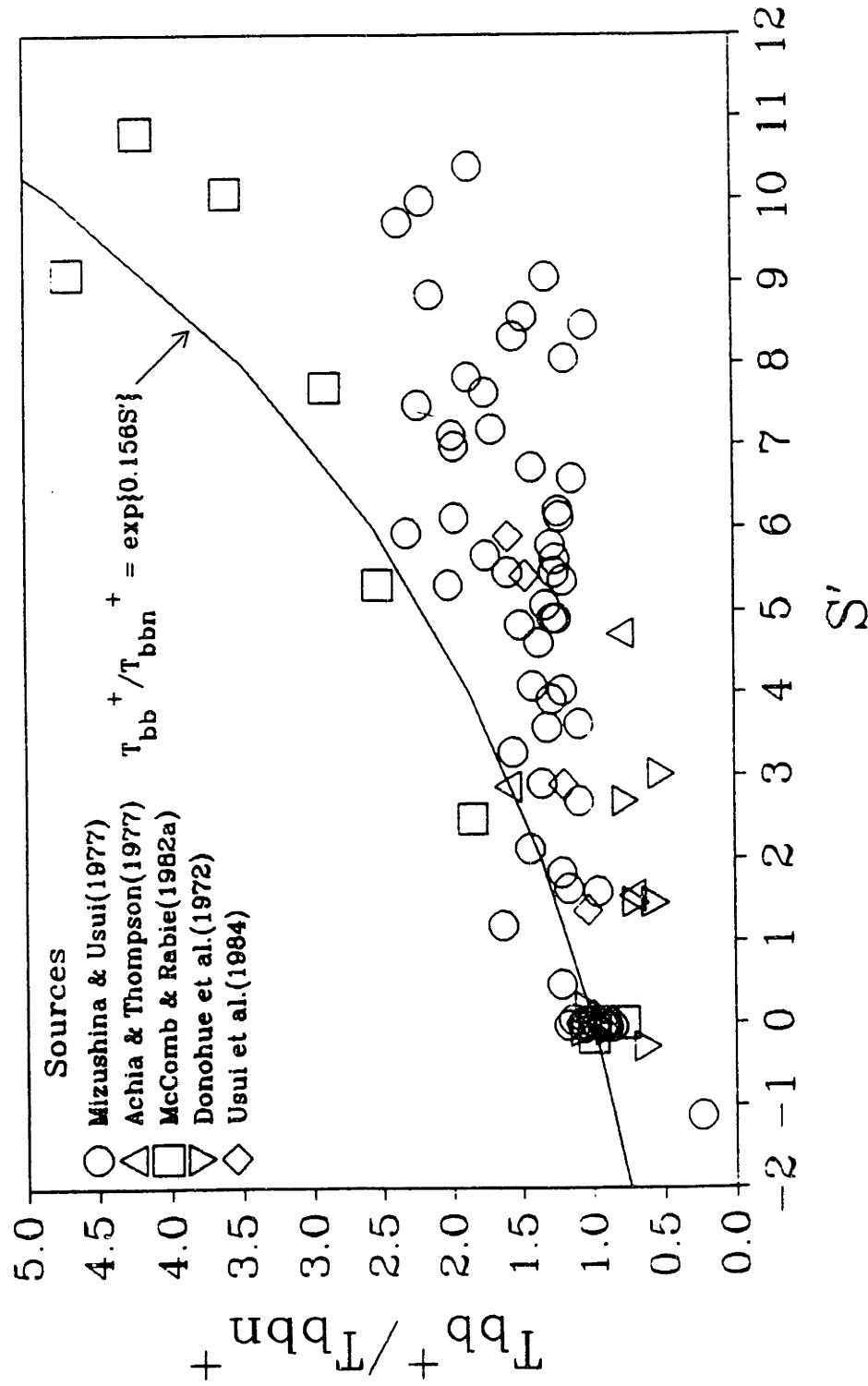


Figure 2.3.41: Normalized Time Between Bursts from Various Studies

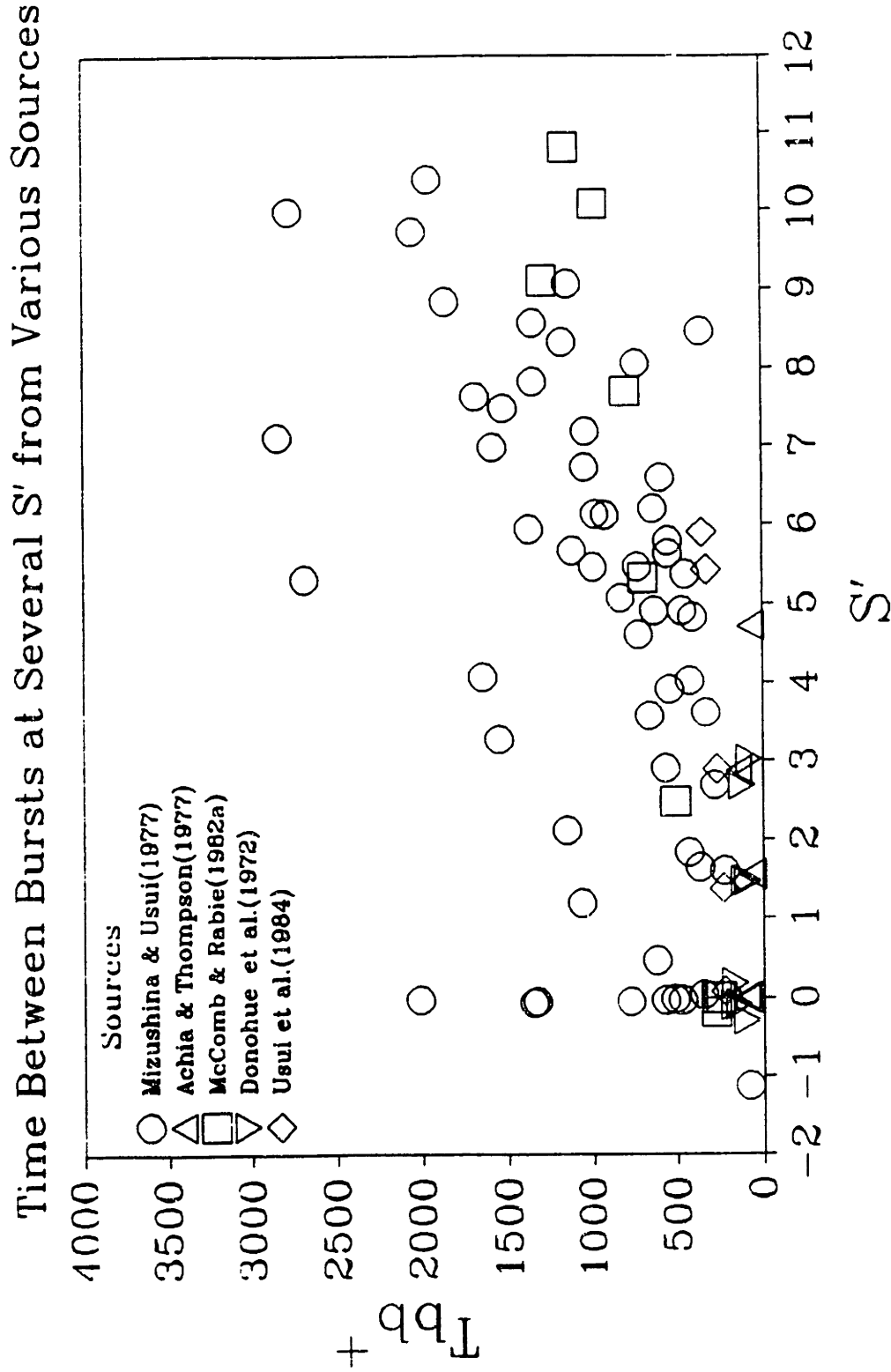


Figure 2.3.42: Time Between Bursts from Various Studies

2.4 PAM and HPAM Polymers

High-molecular-weight polymers are widely used in industry as flocculants, coagulants, clarifiers, and flow enhancers. Synthetic polyacrylamides(PAM) are popular drag-reduction additives, on account of their effectiveness and resistance to mechanical degradation. Hydrolyzing the acrylamide residues to sodium acrylate or acrylic acid makes the resulting HPAM more hydrophilic and drastically changes its static and dynamic properties. PAM and its derivative polymers have been studied widely, with an extensive literature. Some fundamental theoretical equations and empirical correlations required in the present work are presented in this section.

An overview of the theoretical and experimental literature for PAM characterization is provided in Appendix A.

2.4.1 Static and Dynamic Properties of PAM and HPAM

In this section, several Mark-Houwink-Kuhn-Sakurada(MHKS) equations are presented for aqueous PAM solutions under various conditions and summarized in Table 2.4.1. These equations are plotted at various M_w values in Figure 2.4.1. Figure 2.4.2 presents the best MHKS equation and includes some independent data that are unrelated to the equation's development. A correlation for the radius of gyration, $R_G \equiv \langle R^2 \rangle^{1/2}$, also has been developed and is shown in Figure 2.4.3 with some independently obtained data. Before the necessary MHKS equations for PAM and HPAM are given, the theory and assumptions underlying the MHKS equations are briefly reviewed.

2.4.2 Theoretical Background

In a dilute polymer solution, the average conformation of individual polymer chains determines its transport properties, of which $[\eta]$ is the most important here. Each chain, described as either random-flight or random-coiling, is modelled as an ensemble of unconnected segments which behaves statistically as if the segments were linearly connected; the solution is considered an ensemble of identical, noninteracting polymer chains, that is, monodisperse. How each chain distributes itself in space can be calculated given some simplifying assumptions: infinitely thin, noninteracting bonds; equal bond lengths; freely rotating bonds; short-range intramolecular forces only; perfect chain solvation; homogeneity; and isotropy. The radius of gyration, R_G , can be calculated given the bond length, ℓ , and the number of bonds, N :

$$R_G \equiv \langle R^2 \rangle^{1/2} = \ell \left(\frac{N}{6} \right)^{1/2} \quad (2.4-1)$$

Despite idealizations, it qualitatively characterizes real chains. Under more realistic assumptions, how a real chain deviates from ideality can be determined from the temperature, the length or M of the chain, and some thermodynamic properties. This deviation is characterized by the linear-expansion factor:

$$\alpha \equiv \frac{R_G}{R_{G_0}} \quad (2.4-2)$$

in which the 0 subscript indicates random-flight conditions.

If a laminar flow field is imposed on this dilute solution, the frictional properties

of the solution can be derived for any polymer and solvent. The intrinsic viscosity, $[\eta]$, was defined to quantify the polymer contribution to the solution viscosity:

$$[\eta] = \lim_{c \rightarrow 0} \frac{\eta_{sp}}{c} = \lim_{c \rightarrow 0} \frac{\eta_r - 1}{c} = \lim_{c \rightarrow 0} \frac{\eta - \eta_s}{c\eta_s} \quad (2.4-3)$$

in which the subscript s indicates solvent. It was later observed that for "random-flight" polymers, the slope of the η_{sp}/c curve varied with $[\eta]^2$, yielding the Huggins' equation:

$$\frac{\eta_{sp}}{c} = [\eta] + k'[\eta]^2c, \quad (2.4-4)$$

in which the Huggins' coefficient k' varies with M_w and is typically between 0.35 and 0.40, although experimental values widely vary. Its physical significance has yet to be elucidated.

Theories of intrinsic viscosity have successfully derived an equation that correlates $[\eta]$, R_G , and M for polymers that exhibit some random-coiling behavior. The Flory-Fox equation followed from these theories:

$$[\eta] = \frac{\Phi \langle h^2 \rangle^{3/2}}{M} = \frac{6^{3/2} \Phi R_G^3}{M} \quad (2.4-5)$$

in which the universal constant Φ ranges between 1.5×10^{23} and 3.0×10^{23} mole⁻¹ both theoretically and experimentally, depending respectively upon the model and the experimental method used. The "best" value for Φ is 2.5×10^{23} mole⁻¹; however, to account for good solvents being used instead of ideal Θ solvents, to which the Flory-Fox equation applies, a coefficient of 0.8 is introduced. It follows that $\Phi' \equiv 0.8\Phi = 2.0 \times 10^{23}$ mole⁻¹, which is used here.

To account for real-chain deviations from ideal random-flight behavior, the Flory-

Fox equation can be modified to include the linear-expansion factor, $\alpha \equiv R_G/R_{G0}$:

$$[\eta] = \phi^{3/2} \Phi' \left[\frac{\langle R^2 \rangle_0}{M} \right]^{3/2} M^{1/2} \alpha^3 = KM^{1/2} \alpha^3 \quad (2.4-6)$$

in which $\langle R^2 \rangle_0/M$ is constant, in theory. For $\alpha = 1$, Θ conditions obtain, and $[\eta]_0 = KM^{1/2}$, which has been experimentally verified. Since experiments also indicate that $\alpha^3 \propto \log M$, the intrinsic viscosity can be expressed in terms of M :

$$[\eta] = K'M^a \quad (2.4-7)$$

If the polymer in solution is polydisperse, this equation can be transformed theoretically to incorporate polydispersity:

$$[\eta] = K'M_v^a \quad (2.4-8)$$

in which K' is some constant and M_v is the viscosity-averaged molecular weight. Because M_w , the weight-averaged molecular weight, and M_v do not differ too much; M_w may be substituted into the above equation. Thus, the empirical MHKS equation,

$$[\eta] = K'M_w^a \quad (2.4-9)$$

also can be defended theoretically in its application to polymer-solvent systems, if the polymer behaves somewhat like a random-coil.

2.4.3 Empirical MHKS Relations

Over the past 40 years, the properties of PAM have been exhaustively investigated. The following reviews chronologically the most widely cited relations and

sources, which are listed in Table 2.4.1.

Scholtan(1954) polymerized acrylamide(AM) and performed ultracentrifugation on seven PAM fractions in aqueous solution. For PAM of $M_w \leq 5 \times 10^6$ g/mole in solution at 25°C, the MHKS parameters, K' and a , were 6.31×10^{-3} cm³/g and 0.80, respectively. (According to convention, K' assumes the dimensions of $[\eta]$ while a is considered a pure number.) American Cyanamid Co.(1955) published a MHKS correlation for high-molecular-weight PAM in 1.0 N aqueous NaNO₃ at 30°C; K' and a were given as 3.73×10^{-2} cm³/g and 0.66, respectively. Collinson et al.(1956) polymerized AM in aqueous solution by radical initiation and measured the viscosities of unfractionated PAM in aqueous solution at 25°C(?). From chemical-kinetics calculations, K' and a were determined to be 6.8×10^{-2} cm³/g and 0.66 ± 0.05 , respectively, with M_n replacing M_w in the MHKS relationship. Klein & Conrad(1978, 1980) investigated PAM with $M_w \leq 5.5 \times 10^6$ g/mole via light-scattering and viscometry. For solvents of water and 0.5-N aqueous NaCl at 25°C, K' and a were 4.9×10^{-3} cm³/g & 0.8 and 7.19×10^{-3} cm³/g & 0.77, respectively. Munk et al.(1980) synthesized PAM of $M_w \leq 3 \times 10^6$ g/mole by radical initiation and measured intrinsic viscosities. For solvents of water, 0.2-N aqueous NaCl, and 1.0-N aqueous NaCl at 20°C, K' and a were 3.09×10^{-2} cm³/g and 0.67, 3.02×10^{-2} cm³/g and 0.68, and 2.88×10^{-2} cm³/g and 0.69, respectively. In a survey of PAM, Kulicke et al.(1982) investigated polymerization, dilute-solution characterization and properties, and solution rheology. For aqueous solutions of PAM with $3.8 \times 10^4 \leq M_w \leq 9 \times 10^6$ g/mole at 25°C, K' and a were 1.00×10^{-2} cm³/g and 0.755, respectively; for PAM with $5 \times 10^6 \leq M_w \leq 6 \times 10^6$ g/mole in a Θ solvent at 25°C, K' and a were 7.90×10^{-2} cm³/g and 0.50, respectively.

Table 2.4.1
Summary of MHKS Equations

Source	$[\eta] = K' M_w^a$		Experimental Conditions	M_w Range
	K'	a		(10 ⁶ g/mole)
	(cm ³ /g)			
Scholtan(1954)	6.31×10^{-3}	0.80	H ₂ O, 25°C	< 5.0
American Cyanamid Co.(1955)	3.73×10^{-2}	0.66	1.0N NaNO ₃ , 30°C	?
Collinson et al.(1956)	6.8×10^{-2}	0.66	H ₂ O, 25°C(?)	?
Klein & Conrad (1978, 1980)	4.9×10^{-3}	0.80	H ₂ O, 25°C	0.5-5.5
Klein & Conrad (1978, 1980)	7.19×10^{-3}	0.77	0.5 N NaCl, 25°C	0.5-5.5
Munk et al.(1980)	3.09×10^{-2}	0.67	H ₂ O, 20°C	< 3.0
Munk et al.(1980)	3.02×10^{-2}	0.68	0.2 N NaCl, 20°C	< 3.0
Munk et al.(1980)	2.88×10^{-2}	0.69	1.0 N NaCl, 20°C	< 3.0
Kulicke et al.(1982)	1.00×10^{-2}	0.755	H ₂ O, 20°C	0.038-9.0
Kulicke et al.(1982)	7.90×10^{-2}	0.5	Θ solvent, 25°C	0.5-6.0

Intrinsic Viscosity Correlations for PAM

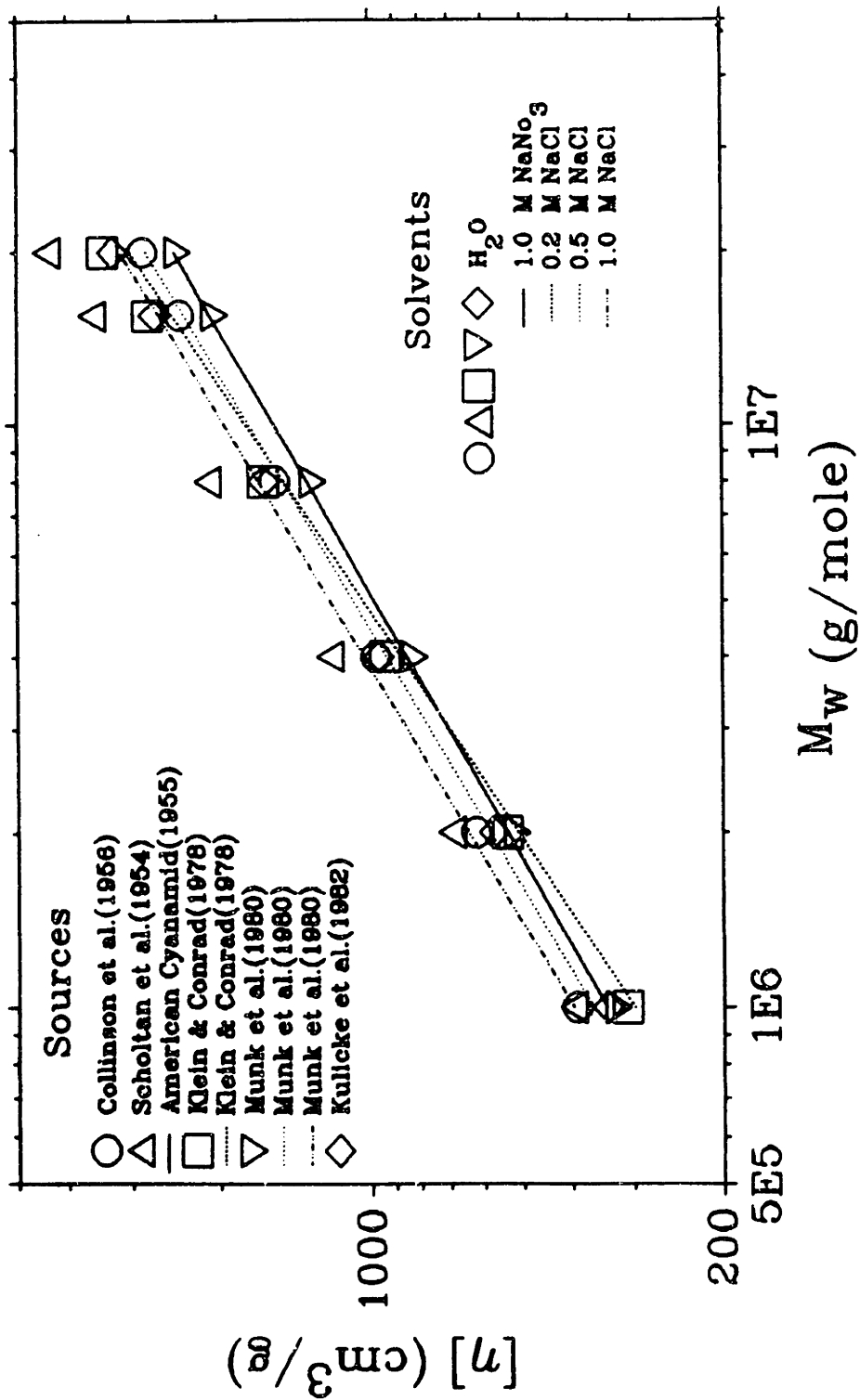


Figure 2.4.1: Intrinsic-Viscosity Correlations for HPAM from Various Studies

Because it best approximates these literature correlations, especially in the range of present interest, $M_w > 1 \times 10^6$ g/mole, the correlation from Kulicke et al.(1982),

$$[\eta] = 1.00 \times 10^{-2} M_w^{0.755} \quad (2.4-10)$$

is used to interpret the laminar-flow data. Figure 2.4.2 shows this correlation and the data from which it was ultimately derived. The closed symbols represents independently gathered data from Clarke(1970) and McCormick et al.(1990). These data match the correlation quite well. If the independent data are included in the regression, the coefficient and exponent become $8.1 \times 10^{-3} \text{ cm}^3/\text{g}$ and 0.769, respectively; these two sets of parameters yield intrinsic viscosities that differ by less than five percent in the range $1.0 \times 10^5 \text{ g/mole} < M_w < 1.0 \times 10^8 \text{ g/mole}$. Table 2.4.2 provides the dependent and independent data shown in Figure 2.4.2. When M_w , $[\eta]$, and R_G are available, Φ has been calculated via the Flory-Fox equation to show how well it is obeyed. That Φ fluctuates about a value $\sim 2.0 \times 10^{23} \text{ mole}^{-1}$ indicates that the Flory-Fox equation holds for PAM in water and HPAM in brine.

Table 2.4.2
Data Shown in Figures 2.4.2 and 2.4.3

Source	M_w	$[\eta]$	R_G	Φ
	(g/mole)	(cm ³ /g)	(nm)	(10 ²³ /mole)
Klein & Conrad (1978)	490000	183	29.6	2.35
	550000	209	39.2	1.30
	770000	263	32.0	4.20
	1050000	246	49.2	1.48
	1100000	345	50.1	2.05
	1250000	412	55.3	2.07
	2020000	606	71.7	2.26
	2660000	740	88.3	1.94
	2860000	738	84.2	2.41
	5510000	1360	131.8	2.23
Kulicke et al(1982)	813000	331	48.2	1.64
	4240000	950	110.7	2.02
	4314000	1109	134.4	1.34
	4950000	1067	129.6	1.65
	5044000	1400	145.5	1.56
	5050000	1500	143.9	1.73
	7560000	1458	163.6	1.71
Clarke(1970)	7800000	1490	170.0	1.61
	9200000	1640	193.7	1.41

Source	M_w	$[\eta]$	R_G	Φ
	(g/mole)	(cm ³ /g)	(nm)	(10 ²³ /mole)
McCormick et al.(1990)	3900000	840	--	--
	6000000	930	--	--
	6900000	1600	--	--
	7500000	1800	--	--
	24000000	3400	--	--
	25000000	5200	--	--
	28000000	4700	--	--
Muller et al.(1979)	3700000	--	133.6	--
	3800000	--	113.8	--
	3800000	--	124.9	--
	4000000	--	118.6	--
	4400000	--	131.2	--

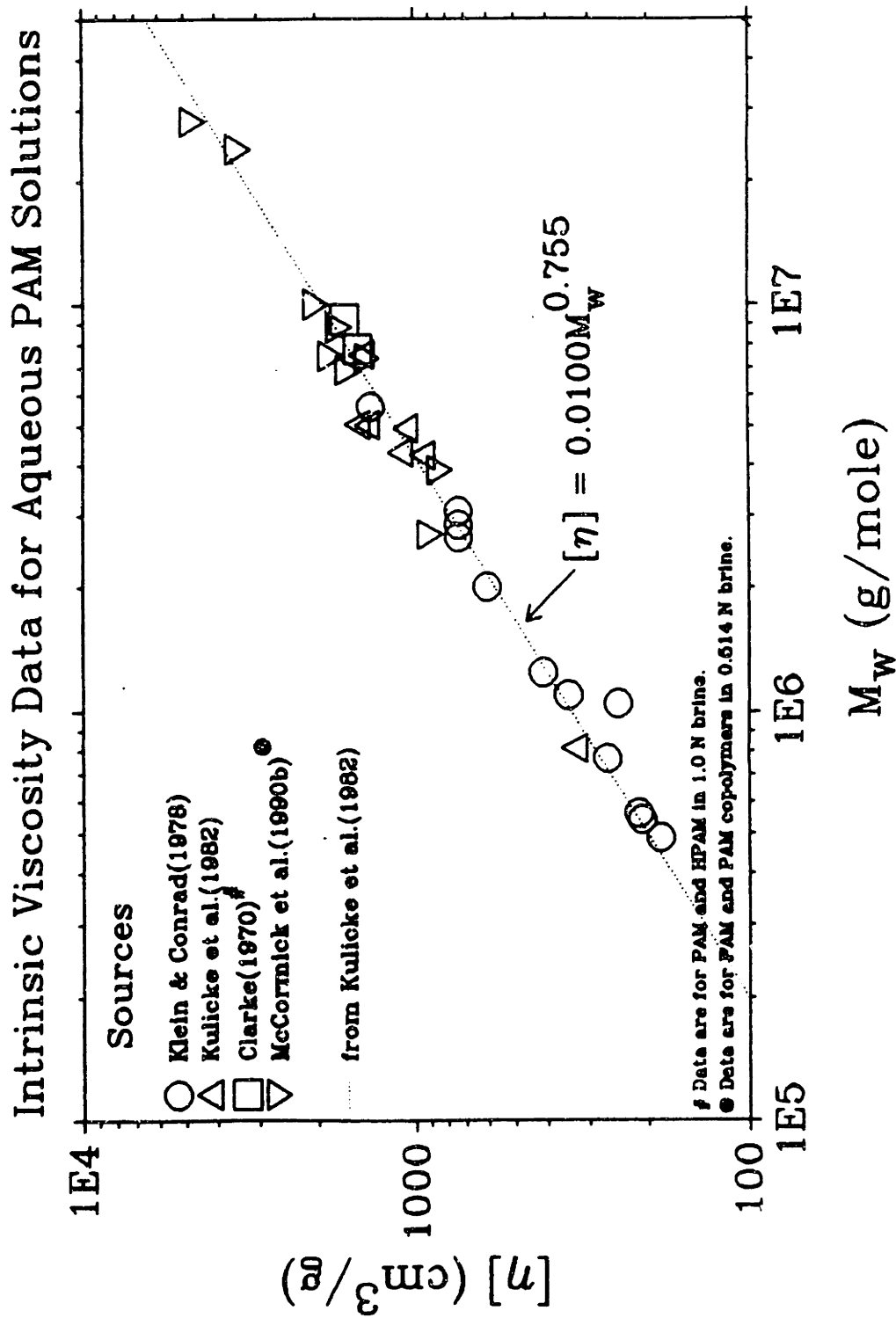


Figure 2.4.2: Intrinsic-Viscosity Correlation for PAM(Kulicke et al., 1982) and Data

In addition to $[\eta]$ - M_w correlations, cross-correlations for polymer-coil size have also been determined. Klein & Conrad(1978, 1980) developed a $\langle h^2 \rangle_z^{1/2}$ - M_w correlation with analogous K' and a of 4.9×10^{-2} nm and 0.59, respectively. Kulicke et al(1982) developed a $\langle h^2 \rangle_w^{1/2}$ - M_w correlation using their own data and those from Klein & Conrad(1978, 1980). The $\langle R^2 \rangle_z^{1/2}$ and $\langle h^2 \rangle_z^{1/2}$ data obtained from light scattering were converted to $\langle R^2 \rangle_w^{1/2}$ (or R_G) and $\langle h^2 \rangle_w^{1/2}$ via assumptions about polydispersity.(See Kulicke et al.(1982)) The resulting $\langle h^2 \rangle_w^{1/2}$ - M_w correlation had analogous K' and a of 3.9×10^{-2} nm and 0.59, respectively. Via the same correction technique, a R_G - M_w correlation emerges:

$$R_G = \langle R^2 \rangle_w^{1/2} = 1.5 \times 10^{-2} M_w^{0.59} \quad (2.4-11)$$

in which R_G is in nm. Figure 2.4.3 shows this cross-correlation and the data from which it was ultimately derived. The closed symbols represent independently gathered data from Clarke(1970) and Muller et al.(1979). The independent data agree well with the cross-correlation; thus, this equation is used in interpreting the laminar-flow data. If these data are included in the regression, the resulting coefficient and exponent are 1.2×10^{-2} nm and 0.60, respectively. In the range $1.0 \times 10^5 < M_w < 1.0 \times 10^8$ g/mole, the two sets of parameters estimate radii of gyration that differ by about five percent. Table 2.4.2 lists the data shown in Figure 2.4.3.

To check the consistency of the MHKS correlation and the R_G - M_w correlation, the MHKS correlation can be inserted into the Flory-Fox equation to yield another R_G - M_w correlation; theoretically, the original and the derived correlations should be identical. It follows that the exponent in the R_G - M_w cross-correlation must be $(a+1)/3$. In addition,

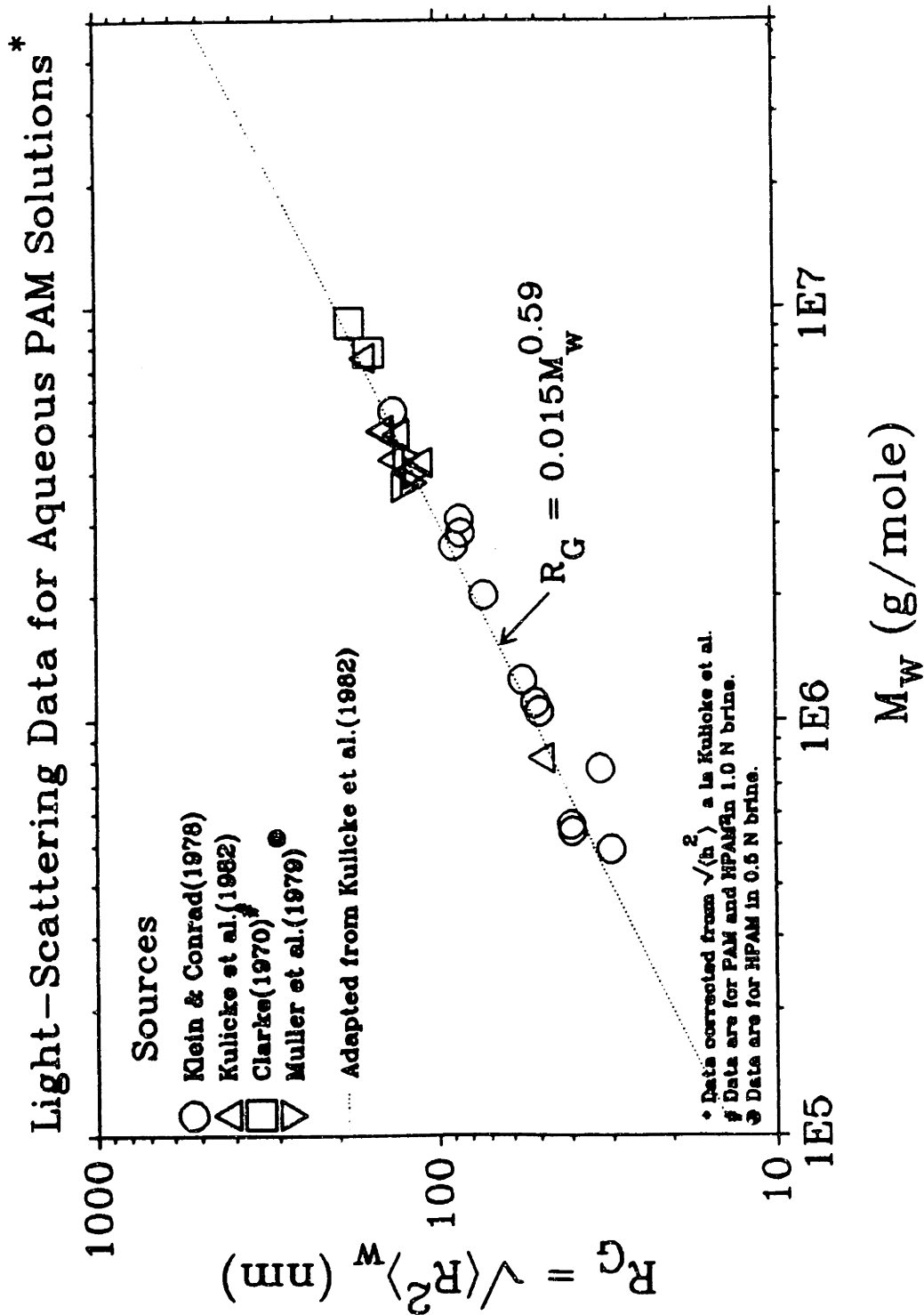


Figure 2.4.3: Radius-of-Gyration Correlation for PAM(Kulicke et al., 1982) and Data

by matching coefficients, Φ can be calculated. From the correlations shown in Figures 2.4.2 and 2.4.3, the exponents of the original and derived correlations are 0.59 and 0.585, respectively; the calculated Φ is 2.02×10^{23} mole⁻¹. (If the two correlations that include the independent data are used with the Flory-Fox equation, the original and derived exponents are 0.60 and 0.59, respectively, and the calculated Φ is 2.96×10^{23} mole⁻¹.) That the exponents match, with Φ having a very reasonable values, provides a high degree of confidence in using the two correlations, equations 2.4-10 and 2.4-11, in interpreting the laminar-flow data.

It must be remembered that these correlations apply to PAM solutions in which the macromolecules are somewhat random-coiling, i.e. not very aspherical. Thus, HPAM solutions must contain enough counterions(i.e. salt) to collapse the macromolecules through the mutual screening of backbone charges. Because HPAM solutions with small counterion concentrations contain mostly expanded macromolecules, neither the Flory-Fox nor the MHKS equation obtains. Experimentally for such solutions, $[\eta]$ depends not only on M_w , but also on c and $[\text{NaCl}]$. Equations reflecting these dependencies differ markedly from MHKS-type equations. Under certain conditions, two general equations describe intrinsic-viscosity data for expanded macromolecules:

$$\frac{\eta_{sp}}{c} = \frac{A}{1 + Bc^{1/2}} \quad (2.4-12)$$

$$[\eta] = [\eta]_{\infty} + k_{\infty}[\text{salt}]^{-1/2} \quad (2.4-13)$$

the coefficients of which depend on both polymer-solvent pair and temperature. Equation 2.4-14 has some basis on excluded-volume theory, but available data do not bear out its

universality. Several arguments against equation 2.4-13 have been made (Bohdanecký & Kovář, 1982), such as negative extrapolated values of $[\eta]_{s\infty}$ and applicability only at intermediate salinities.

A more recent experiment using aqueous solutions of HPAM suggests that $[\eta]$ is quadratic in $[\text{NaCl}]^{-1/2}$ (Tam & Tiu, 1989) with the following relationship

$$[\eta] = [\eta]_0 + 760[\text{NaCl}]^{-1/2} + 48[\text{NaCl}]^{-1} \quad (2.4-14)$$

in which $[\eta]$ and $[\text{NaCl}]$ are in cm^3/g and N , respectively. In Figure 2.4.4 η_{sp}/c is plotted against $[\text{NaCl}]^{-1/2}$ for additives C836A and P500. The solid line represents the best-fit line according to equation 2.4-13, with $[\eta]_{s\infty} \approx 2700 \pm 4100 \text{ cm}^3/\text{g}$ and $k_{s\infty} \approx 730 \pm 50 \text{ N}^{1/2} \cdot \text{cm}^3/\text{g}$. While a linear relationship is apparent, the large uncertainty in $[\eta]_{s\infty}$ demonstrates the limited usefulness of equation 2.4-13. The dotted and dashed lines in Figure 2.4.4 represent the values predicted by equation 2.4-14 for additives C836A and P500, respectively, for which $M_w \approx 15.5 \times 10^6$ and $9.5 \times 10^6 \text{ g/mole}$ and $[\eta]_0 \approx 310$ and $240 \text{ cm}^3/\text{g}$, the latter estimated by the last equation in Table 2.4.1 from Kulicke et al. (1982). Equation 2.4-14 not only overpredicts the intrinsic viscosity, but its quadratic form does not obtain for the C836A and P500 data. An equation that correctly predict the behavior of a wide range of polyelectrolytes has yet to be found.

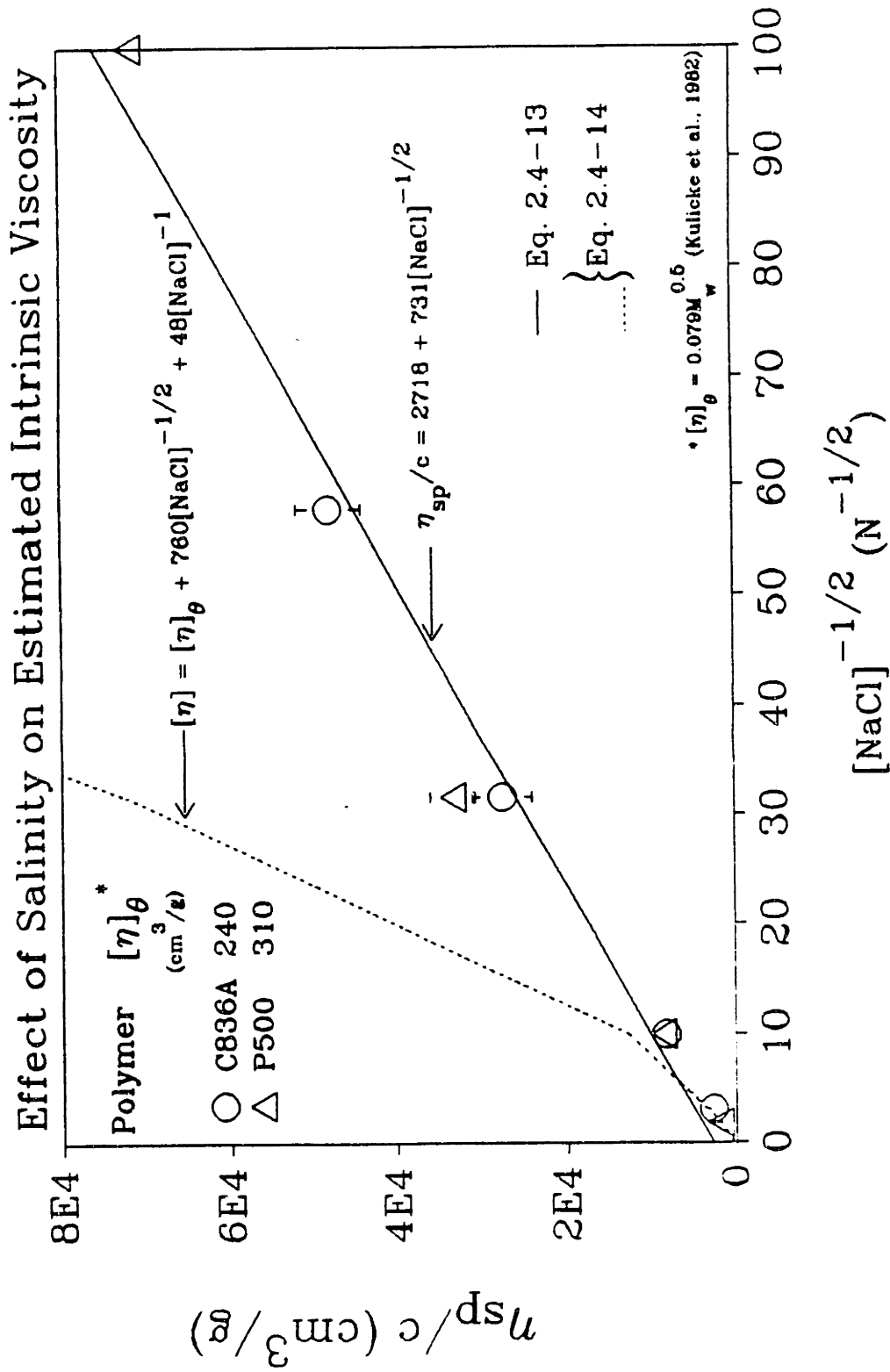


Figure 2.4.4: Effect of Salinity on Estimated Intrinsic Viscosity for Additives C836A and P500

CHAPTER III

EXPERIMENTAL APPARATUS

This chapter provides detailed descriptions of the experimental equipment and apparatus. Items include the gravity-driven and pump-driven flow systems, system modules, individual pieces of equipment, and chemicals. Table B3.0 in Appendix B contains a list of equipment and vendors.

3.1 Gravity-Driven Flow System

Figure 3.1 shows a schematic of the gravity-driven flow system. The test-pipe section included four lengths of tubing, each with a pressure-tap hole for measuring the pressure gradient. The four lengths were cut from a single length of 0.574"-ID(1.458-cm-ID), 316-stainless-steel tubing. Bored-through, $\frac{3}{8}$ ", stainless-steel unions held together and aligned adjacent lengths. A bored-through, $\frac{3}{8}$ ", stainless-steel, union tee fitted over each 0.025"-ID tap hole; its branch run received the pressure tap line from the pressure-transducer(PT) board. The 0.1- and 1.0-psid PTs mounted on the PT board and measured the pressure drop between any two of the four tap holes. Four ball valves connected to the tap holes via pressure-tap lines and could be adjusted to access any tap-hole pair. The flow was moderated by the flow-control unit. The flow-control unit contained a $\frac{3}{8}$ ", stainless-steel, ball valve and a $\frac{3}{8}$ ", stainless-steel, 10-turn, needle valve in parallel. Downstream of the flow-control unit, a mass-flow meter measured and displayed the flow

Gravity-Driven Flow System

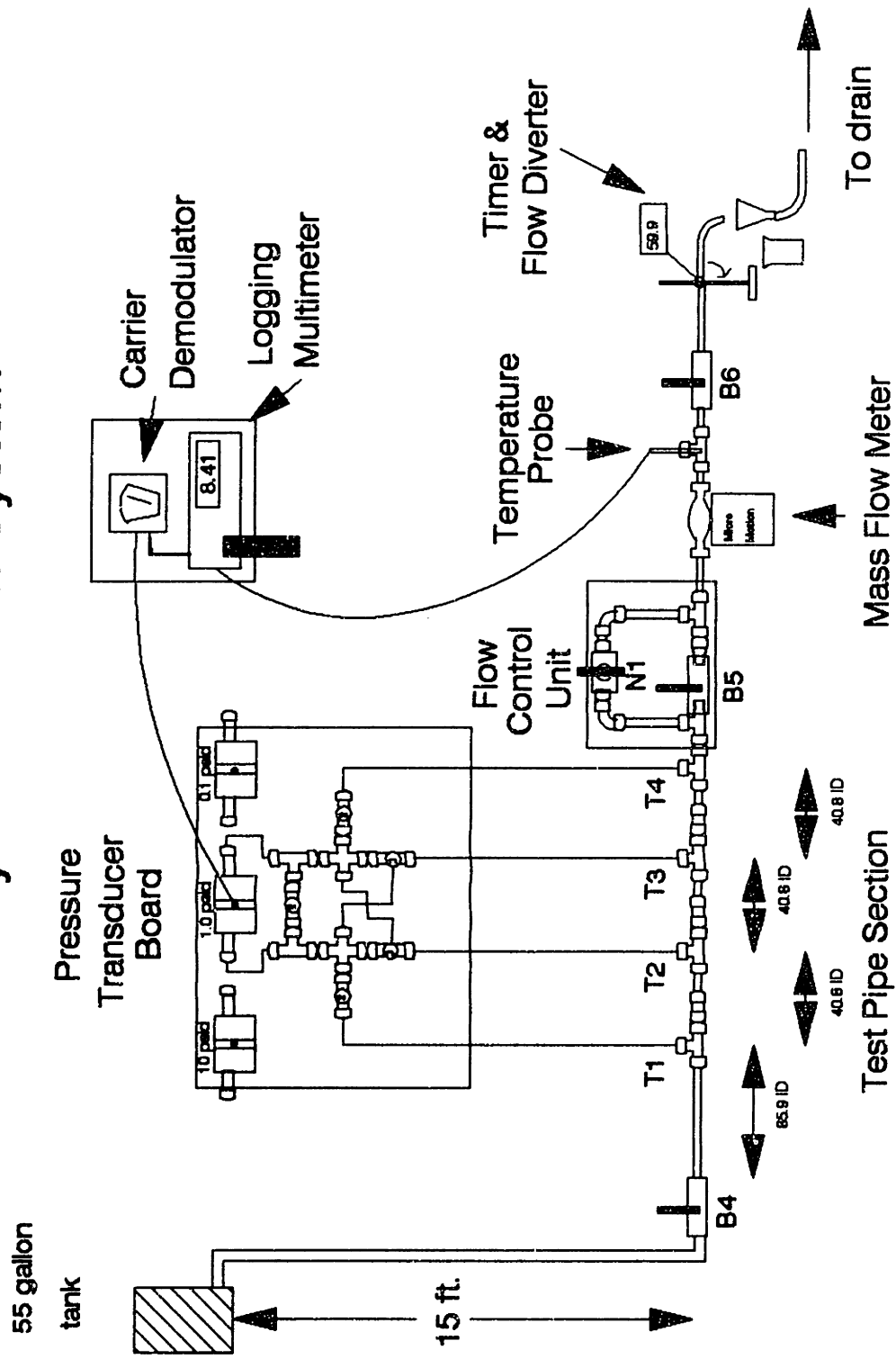


Figure 3.1: Gravity-Driven Flow System

rate. Further downstream, the temperature-probe unit, via its 5k- Ω thermistor, measured the temperature of the exiting flow. After the probe, a $\frac{3}{4}$ " stainless-steel ball valve was used to start and to stop the flow. At the system's end, a timer and flow diverter alternately measured the flow rate for low rates and discharged the effluent to the drain. A HP-3467A Logging Multimeter monitored, displayed, and printed out the PTs' output voltage; it also converted the thermistor's resistance output to temperature and displayed it.

At the most upstream position, a single 55-gallon stainless-steel tank was used for mixing and holding the experimental solutions. The tank was located on a second-floor balcony about 15' above the first-floor laboratory space. A 1" flexible tube delivered distilled water up to the tank from the distilled-water spigot on the first-floor laboratory space. The tank had an old 2" stainless-steel ball valve attached to its nipple. A 2" PVC elbow with a 2"-to-1" PVC reducer followed the valve. A 1 $\frac{1}{4}$ " flexible tube connected the PVC reducer to a $\frac{3}{4}$ " stainless-steel male tube adapter on the front end of the FNPT-ended, $\frac{3}{4}$ " stainless-steel ball valve(B4) that preceded the test-pipe section.

A long stretch of a unistrut double channel(P1001C) supported valve B4, the test-pipe section, the PT board, and the flow-control unit. Several floor-anchored posts upheld the P1001C. Valve B4 mounted flat onto an 9" \times 12" \times $\frac{1}{8}$ " aluminum plate that mounted vertically onto the side of the P1001C. This suspended the test pipe just above the P1001C and maintained it level as determined by a bubble level. A $\frac{3}{4}$ " stainless-steel male connector joined the back of valve B4 to the entry length of the test-pipe section. The next three segments of this section followed along the surface of the P1001C until

the ending length reached the flow-control unit. A bored-through $\frac{3}{4}$ " stainless-steel union sealed adjacent lengths together. A bored-through $\frac{3}{4}$ " stainless-steel union tee provided a seal over each tap hole and connected the tap hole hydraulically to its pressure-tap line. Four tap lines fed into the four ball valves on the PT board. The board bolted onto the side of the P1001C, adjacent to the middle lengths of the test-pipe section. The ending length inserted directly into the flow-control unit. A short length of $\frac{3}{4}$ " stainless-steel tubing and a $\frac{3}{4}$ "-port-to- $\frac{3}{8}$ "-NPT stainless-steel male connector in series joined the flow-control unit to the mass-flow meter. Another short length of $\frac{3}{4}$ " stainless-steel tubing connected the mass-flow meter to the temperature probe. A short length of $\frac{3}{4}$ " stainless-steel tubing and a $\frac{3}{4}$ " stainless-steel male connector followed the temperature probe and led to the FNPT-ended $\frac{3}{4}$ " stainless-steel rear ball valve(B6).

A $\frac{3}{4}$ " stainless-steel male tube adapter installed into the back of valve B6. Beyond this two flow configurations were used. At high flow rates when the mass-flow meter operated alone, one end of a 1" flexible tube was clamped to the tube adapter by a wormhose clamp. The other end went into the drain. At flow rates which required the timer and flow diverter, the $\frac{3}{4}$ "-port-to- $\frac{1}{2}$ "-stub reducer of the flow diverter was attached to the tube adapter. The end of the 1" flexible tube that had been clamped onto the tube adapter was placed over the tip of the flow diverter's funnel. The other end remained in the drain.

3.2 Pump-Driven Flow System

Figure 3.2 provides a plan view of the pump-driven flow system. The test-pipe section included four lengths of tubing, each with a pressure-tap hole for measuring the pressure drop. These four lengths were cut from a single length of $\frac{3}{4}$ "-OD, 0.574"-ID(1.458-cm-ID), 316-stainless-steel tubing. In later experiments, four lengths cut from a single length of $\frac{1}{2}$ "-OD, 0.402"-ID(1.021-cm-ID), low carbon, stainless-steel, microsmooth tubing were used in this section. Bored-through, $\frac{3}{4}$ "($\frac{1}{2}$ "), stainless-steel unions held together and aligned adjacent lengths. On each length a bored-through, $\frac{3}{4}$ "($\frac{1}{2}$ "), stainless-steel, union tee fitted over the 0.025"-ID tap hole; its branch run received the pressure-tap line from the PT board. The 0.1-, 1.0-, and 10-psid PTs mounted on the PT board and measured the pressure drop between any two of the four tap holes. Four ball valves connected to the tap holes via pressure-tap lines and could be adjusted to access any pair of taps. A positive-displacement Moyno 3L4-SSQ-AAA pump provided flow rates between 3.2 gpm(0.2 l/s) and 19.2 gpm(1.2 l/s). A pump-bypass loop emerged from the pump's suction housing and connected to the 1" union cross downstream; it permitted gravity-driven flow when valves B2 and B3 were open. The gravity-driven flow was moderated by the flow-control unit. The flow-control unit contained a $\frac{3}{4}$ ", stainless-steel, ball valve and a $\frac{3}{4}$ ", stainless-steel, 10-turn, needle valve in parallel. Further downstream, the temperature-probe unit, via its 5k- Ω thermistor, measured the effluent temperature. After the probe, a $\frac{3}{4}$ ", stainless-steel, ball valve was used to start and to stop the flow. At the system's end, a timer and flow diverter alternately measured the flow rate for low rates and discharged the effluent to

Pump-Driven Flow System

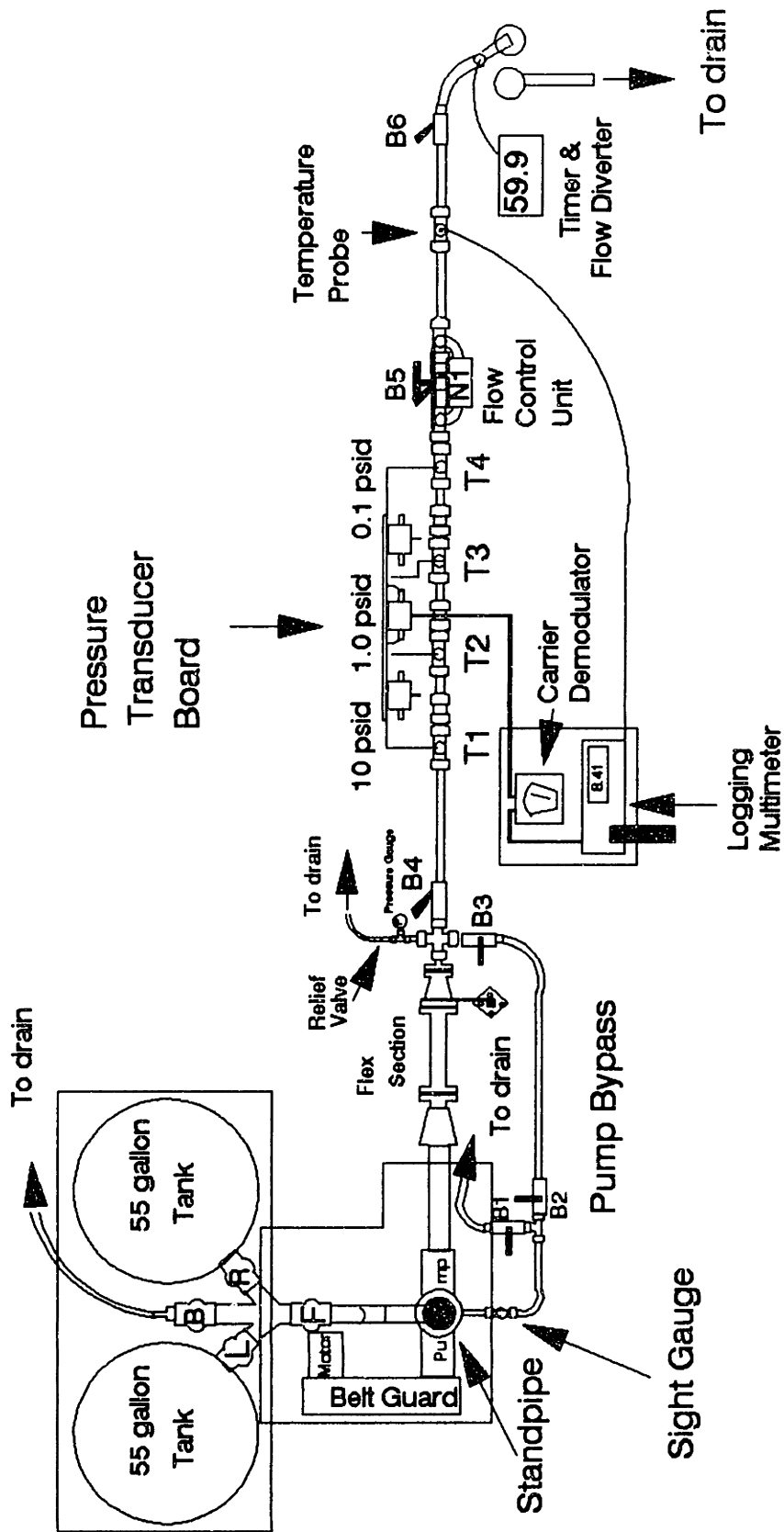


Figure 3.2: Pump-Driven Flow System

the drain. A HP-3467A LoggingMultimeter monitored, displayed, and printed out the PTs' output voltage; it also converted the thermistor's resistance output to temperature and displayed it.

At the most upstream position, two 55-gallon, stainless-steel tanks were used for mixing, heating, and holding experimental solutions. These tanks were elevated atop a reinforced unistrut frame about five feet above the laboratory floor. A hose connected to a distilled-water spigot provided the large volumes(up to 380 liters) necessary for most runs. A Model-10 Lightnin mixer that clamped onto the rim of either tank mixed the solutions, and a drum heater around each tank warmed the solutions before use. A FNPT-ended, 2", ball valve attached directly onto the 2" MNPT nipple of each tank. Valves L and R on the left and right tanks were stainless steel and PVC, respectively. A schedule-80, MNPT-ended, 2", PVC double nipple joined each ball valve with a schedule-80, 2", PVC ring flange. The ring valves provided convenient removal of both tanks from the system. From either ring flange, another schedule-80, MNPT-ended, 2", PVC double nipple connected indirectly to a 2" PVC double wye via a FNPT-to-socket, 2", PVC adapter. Socket-ended, 2", PVC ball valves F and B attached onto both the front and the back socket of the double wye, respectively, via a short length of schedule-40, 2" PVC pipe. Attached to valve B, a schedule-40, 2" × 1¼" spigot-to-female-bushing connected to an adjustable wrench, 1¼" adapter. Clamped onto this adapter, a long 1¼" flexible tube led to and emptied into the drain. Via a short length of schedule-40, 2", PVC pipe, valve F connected to a schedule-40, 2", PVC elbow that pointed downwards. From the elbow, another short length of pipe led into a vertical length of 3"-OD, 2½"-ID flexible tubing. The lower end of the flexible tubing attached onto

another identical elbow via a short pipe length. From the elbow, another pipe length led into a schedule-40, 2½" × 2", PVC bushing which in turn connected to the branch run of a 2½" PVC socket tee. In the upper run of the tee, an eight-foot length of schedule-40, 2½", PVC pipe served as a stand pipe. From the lower run, a length of 2½" pipe inserted into a 2½" PVC socket flange that directly bolted onto the suction end of the Moyno pump.

Two separate flow paths emerged from the pump and then rejoined downstream at the 1" stainless-steel union cross. One path flowed through the pump discharge; the other bypassed the pump elements and flowed through the suction-housing drain plug.

A 2" flange assembly screwed directly into the pump discharge. The 2" flange assembly consisted of a 2" length of 2" stainless-steel pipe with one MNPT end welded onto a 2" stainless-steel neck-weld flange. With an intervening silicone gasket, the flange assembly bolted onto the "flex section." The flex section consisted of a flange-ended 2" flexible stainless-steel hose with a 16" total length. Three 2"-OD × ⅛"-cell × 3"-long pieces of honeycomb were inserted into the flexible hose to calm the flow. With another intervening silicone gasket, the flex section bolted onto a 2"-to-1" reducer assembly. The 2"-to-1" reducer assembly consisted of a 2" stainless-steel flange, a 2"-to-1" stainless-steel concentric reducer, and a 1" stainless-steel flange. These were welded together serially. Due to intervening equipment and the long distance from pump discharge to the test-pipe section, the reducer assembly required support. A thin rectangular metal plate with a large U-shape cut into it attached both onto the 2" flange of the reducer assembly and onto a floor-anchored post. A 1" flange assembly bolted onto the reducer assembly with an intervening silicone gasket. The 1" flange assembly consisted of a 2" length of

1" stainless-steel pipe with one MNPT end welded to a 1" stainless-steel flange. A 1" stainless-steel female tube adapter connected the flange unit to the 1" stainless-steel union cross.

In the second flow path, a ½" stainless-steel male elbow fit into the suction-housing drain plug so that the elbow pointed away from the tanks and 90° from the pump discharge direction. The elbow connected to the run of a ½" stainless-steel union tee via a length of ½" stainless-steel tubing. Nylon ferrules were used with all stainless-steel fittings for easy maintenance. Pointing upwards, the branch run of the tee held an eight-foot length of ½" clear rigid PVC tubing. This length consisted of two-foot and six-foot lengths sealed together by a ½" brass union and served as a sight gauge of the tanks' fluid levels. The other tee run held a long length of ½" stainless-steel tubing that bent 90° in the pump-discharge direction. A ½"-port-to-1"-stub stainless-steel reducer joined the ½" stainless-steel tubing to the run of a 1" stainless-steel union tee. From the branch run of the tee, a 1" stainless-steel male tube adapter inserted into a FNPT-ended 1" stainless-steel ball valve(B1). Another 1" stainless-steel male tube adapter installed into the back of valve B1. Clamped into the adapter, a long 1¼" flexible tube led to and emptied into the drain. The following pieces linked in series the other run end of the tee with an arm of the 1" union cross: a 1" stainless-steel male tube adapter; a FNPT-ended 1" stainless-steel ball valve(B2); a second 1" stainless-steel male tube adapter; a length of 1¼" flexible tubing; a third 1" stainless-steel male tube adapter; another FNPT-ended 1" stainless-steel ball valve (B3); and a fourth 1", stainless-steel male tube adapter.

The two remaining arms of the 1" stainless-steel union cross led to the drain as an overpressure release and to the test-pipe section. The relief arm opposed the bypass

arm. A 1"-stub-to-½"-port stainless-steel reducer and a ½" stainless-steel port connector joined the relief arm to a ½" stainless-steel female branch tee. A ½"-to-¼" stainless-steel reducing bushing connected a 0-160-psig pressure gauge(P) to the female branch run. The tee run joined to a 100-psig spring-loaded relief valve(SS-CH-S8-100) via a ½" stainless-steel port connector. Another ½" stainless-steel port connector inserted into the other end of the relief valve. Clamped onto the port connector by a wormhose clamp, a long ½" flexible tube led to and emptied into the drain.

Inserted into the union arm opposite the pump-discharge arm, a 1"-stub-to-¾"-NPT male tube adapter installed directly into the FNPT-ended ¾" stainless-steel ball valve(B4) preceding the test-pipe section. The test-pipe sections with the ¾" and ½" stainless-steel tubing and fittings and the two flow configurations used beyond B6 were the same as those in the Gravity-Driven flow system.

3.3 System Modules

(1) Test-Pipe Sections

In the first, larger test-pipe section, the pipe was a 316-stainless-steel, seamless tube with a ¾" OD and a nominal 0.584" ID. Measurements of the inner diameter with a dial caliper indicated that the real pipe ID was 0.574 inch(1.458 cm). This accorded with the hydraulic diameter(D_h) determined from subsequent solvent run data.

Cut from a single length of tubing, the test-pipe section consisted of an entry length, two middle lengths, and an ending length. For the gravity-driven flow system,

they had lengths of $49 \frac{5}{16}$ " , $23 \frac{3}{8}$ " , $23 \frac{3}{8}$ " , and $24 \frac{3}{8}$ " , respectively; these corresponded to 85.9 ID, 40.7 ID, 40.7 ID, and 42.5 ID, respectively. For the pump-driven flow system, the entry section was shortened to $33 \frac{15}{16}$ " (59.1 ID) to accommodate the pump.

For the entry length, a 0.025" ID pressure-tap hole was located $2 \frac{19}{32}$ " from the downstream end. For the middle lengths and ending length, the 0.025" ID pressure-tap holes were drilled at locations $2 \frac{9}{16}$ " and $3 \frac{9}{16}$ " from the downstream end, respectively. This allowed the ending length to insert directly into the flow-control unit. The sequential intertap distances were $23 \frac{13}{32}$ " (41.4 ID), $23 \frac{3}{8}$ " (40.7 ID), and $23 \frac{3}{8}$ " (40.7 ID). Care was taken to drill all tap holes with their axes normal the tube axis. The inner surface of each length was manually smoothed with a gun barrel cleaning brush and fine sandpaper. Providing a more uniform polish, a milling machine rotated the tube while a brush and sandpaper, with some lubricating oil, were moved back and forth inside the tube. Next, a manually-rotated, 0.025" drill bit (size 72) was moved in and out of each tap hole to ensure that the tap hole was perfectly circular and unobstructed. The spot where the tap hole penetrated the inner tube wall was sanded with a jeweler's file to remove burrs and debris. Inside the tube, each tap hole was virtually invisible.

Figure 3.3.1 depicts the test-pipe section junction. Where the faces of adjacent lengths met, a $\frac{3}{4}$ " bored-through stainless-steel union held the two ends and matched the two abutting faces almost seamlessly. Fitted with nylon ferrules, the tightened union nuts gripped the tubes, both creating a fluid-tight seal and permitting disassembly and reassembly without causing damage. With its branch run centered over each tap hole, a $\frac{3}{4}$ " bored-through stainless-steel union tee created a fluid-tight volume above the hole

Test-Pipe Section Interface

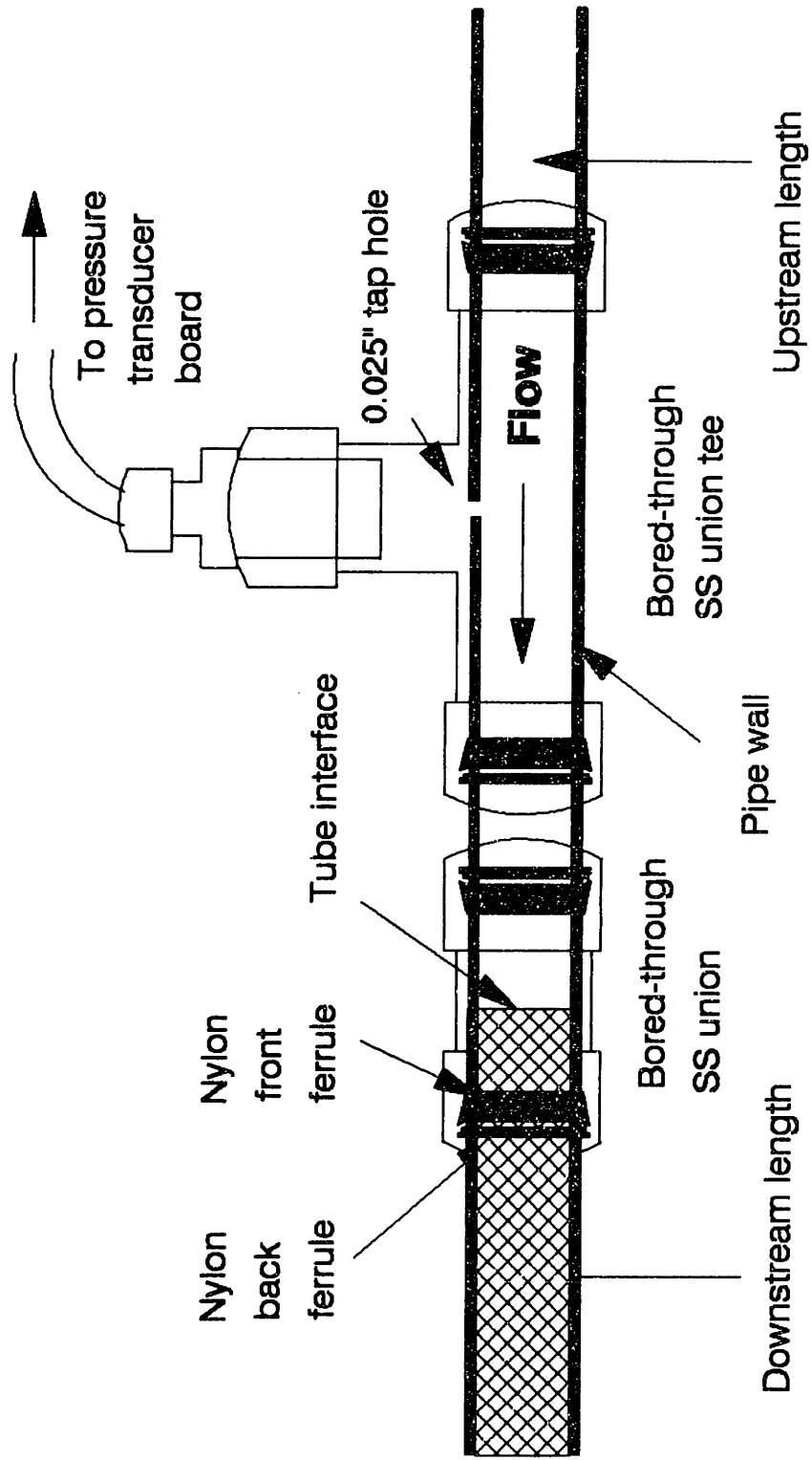


Figure 3.3.1: Test-Pipe Section Interface

with its tightened nuts and nylon ferrules providing seals. Its branch run served as the port for the pressure-tap line leading to the PT board. Placed into each branch run, a $\frac{3}{8}$ "-stub-to- $\frac{1}{4}$ "-port reducer accommodated the $\frac{1}{4}$ " OD pressure tap line. The entire test-pipe section rested atop a stretch of P1001C about a foot above the floor.

In the second, smaller test-pipe section, the pipe was a low-carbon, 316-stainless-steel, seamless tube with a $\frac{1}{2}$ " OD and with an electro-polished ID of 0.402 ± 0.000005 inch (1.021 cm). Dial caliper measurements of the ID and flow data accorded with the given ID value.

Cut from a single length of tubing, the test-pipe section had an entry length, two middle lengths, an ending length. They had lengths of $33 \frac{53}{64}$ ", $15 \frac{5}{8}$ ", $15 \frac{39}{64}$ ", and $16 \frac{5}{8}$ ", respectively; these corresponded to 84.1 ID, 38.9 ID, 38.8 ID, and 41.4 ID, respectively. For the entry and middle lengths, a 0.025"-ID, pressure-tap hole was drilled at a location approximately $2 \frac{3}{4}$ " from the downstream end. The 0.025"-ID, pressure-tap hole in the ending length was drilled at a location approximately $3 \frac{3}{4}$ " from the downstream end. This allowed the ending length to insert directly into the flow-control unit via a $\frac{3}{8}$ "-stub-to- $\frac{1}{2}$ "-port reducer. The four tap-hole-to-end distances were 2.743", 2.747", 2.741", and 3.746", respectively, as measured with a dial caliper. The sequential intertap distances were 15.62"(38.86 ID), 15.62"(38.84 ID), and 15.62"(38.86 ID). Care was taken to drill these holes with their axes normal to the tube axis. Next, a manually-rotated, 0.025" drill bit (size 72) was moved in and out of each tap hole to ensure that the tap hole was perfectly circular and unobstructed. Then the spot where the tap hole penetrated the inner tube wall was sanded delicately with a jeweler's file to remove burrs and debris. Inside the tube, each tap hole was virtually invisible. The ends

of these lengths, where the saw blade had passed, required polishing. To polish the inner ends, a 0.40" OD metal rod and very fine sandpaper, with some lubricating oil, were moved back and forth inside the tube while it was rotated on a milling machine.

Just as with the $\frac{3}{4}$ " tubing, $\frac{1}{2}$ " bored-through stainless-steel unions with nylon ferrules sealed the faces between adjacent lengths of the smaller tubing. Similarly, $\frac{1}{2}$ " bored-through stainless-steel union tees provided fluid-tight volumes above the tape holes; their ports accommodated the pressure-tap lines that lead to the PT board with $\frac{1}{2}$ "-stub-to- $\frac{1}{4}$ "-port reducers. The entire test-pipe section rested upon a stretch of P1001C about a foot above the floor.

(2) The Pump Unit

The following components comprised the pump unit: an L-shaped steel base; a Moyno 3L4-SSQ-AAA Pump; timing belts, pulleys, and belt guard; and a Reliance 2-Hp TEFC-XE motor controlled remotely by a T. B. Woods 2-Hp variable-frequency E-trAC AC Inverter.

Figure 3.3.2 presents the vendor-supplied pump-unit schematic. An L-shape steel base served as both a platform and an anchor for the motor, the timing belts, pulleys, and belt guard, and the pump. While the base height was about three inches, its edges bent downwards and met the floor. Around its periphery about a three-inch-wide strip of metal pressed flush against the floor. The base bolted directly onto the laboratory floor via the bolt holes in the strip around the base periphery.

The pump was designed to operate between 100 rpm and 940 rpm. Its discharge

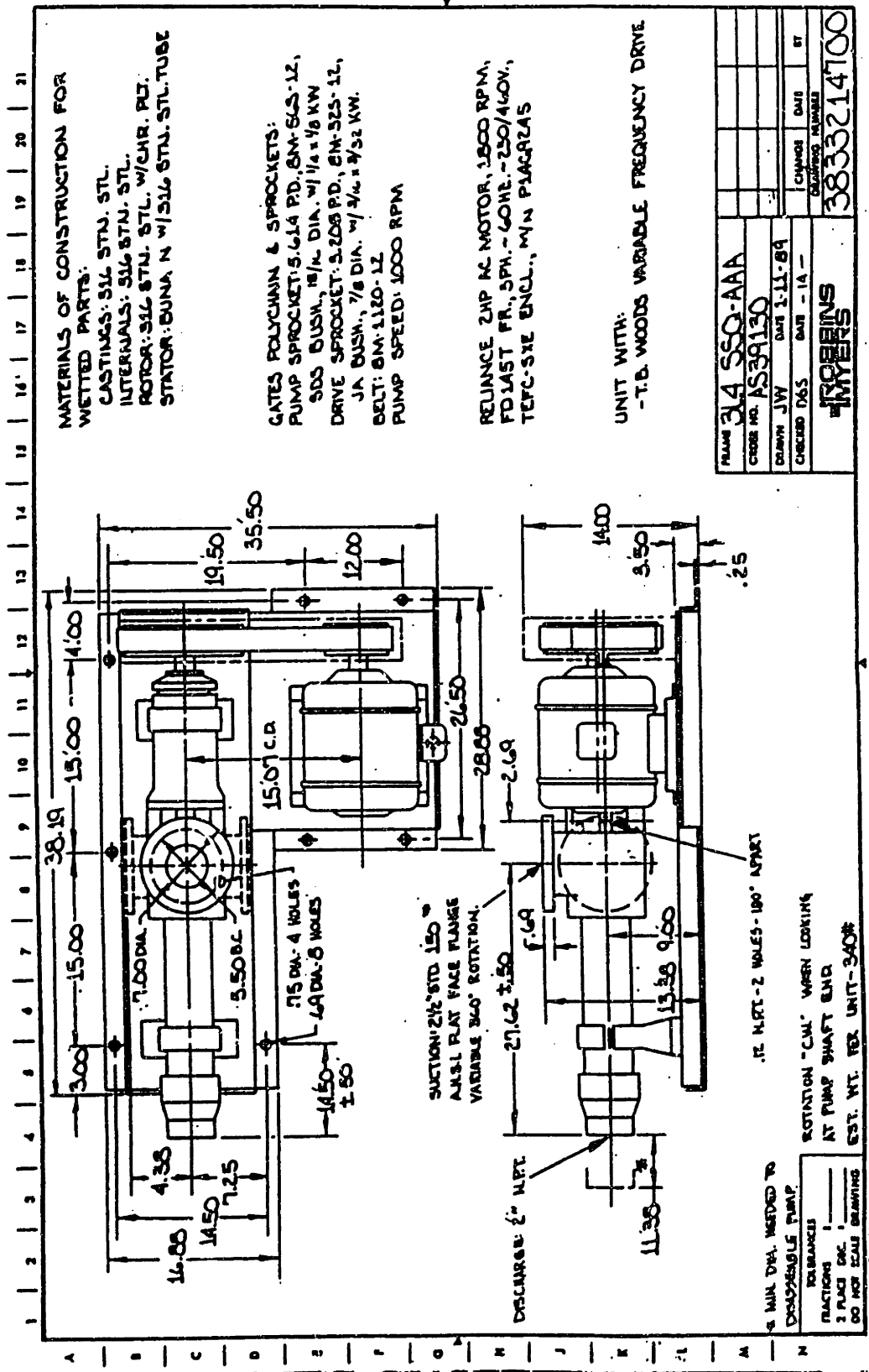


Figure 3.3.2: Moyno-Pump Schematic

pressure range was rated from 10 psig to 100 psig, and its designated capacity was rated from 2 gpm(0.13 l/s) to 17 gpm(1.07 l/s). The pumping capacity actually realized was 3.2 gpm(0.2 l/s) to 19.2 gpm(1.21 l/s). The pump had size-4 pumping elements and originally three stages. Because the 2-Hp motor could not turn over the 3L4 rotor frame, a 2L4 rotor frame was used while the 3L4 stator frame remained. The SSQ designation indicated that the body casting and all wetted internal parts were 316 stainless steel and that the stator material was Buna "N" 100, 700 Durometer. The AAA designation identified the sealing, internal, and rotor variations as braided teflon & graphite packing, standard plated shaft, and standard size with chrome plating, respectively. The discharge end came fitted with a 2" NPT female thread; the suction end came fitted with a 2½" flange. The timing belt provided the mechanical connection between the pump's rear pulley and the drive pulley of the Reliance 2-Hp TEFC-XE motor. The removable belt guard covered both pulleys and the timing belt, protecting them from being accidentally contacted. The Reliance, 2-Hp, TEFC-XE, Model- P14G9245 motor had a 145T frame and was placed atop the base parallel to and opposite from the pump. The three-phase motor was designed to operate 230 VAC, 60 Hz current. Its rated speed was 1800 rpm.

A T. B. Woods 2-Hp variable-frequency E-trAC AC Inverter, Model- AFC2002-0B2, controlled the Reliance motor remotely. The drive unit was located above and near the test-pipe section, where other instruments were located. A long, well-protected, well-insulated conduit housed the wires electrically connecting the inverter and the motor. The inverter provided adjustable frequencies and constant torque to the motor. The inverter delivered up to 2-Hp to the motor. The CPU was the "brain" of the inverter and consisted of a 16-bit microprocessor and a custom Large Scale Integrated(LSI)

circuit. The inverter was programmable via a soft-touch membrane keypad on the front panel. Eight snap-dome switches, a four-digit, seven-segment, LED display, and a 10-segment LED bargraph comprised the keypad.

(3) Pressure-Transducer Board

The pressure-transducer (PT) board shown in Figure 3.3.3 supported the three PTs, the valves, fittings, and tubing that hydraulically connected the PTs to the pressure-tap lines. A 14" × 19" × 1/8" aluminum plate bolted onto two foot-long pieces of unistrut channel. These two channels bolted upright onto the P1001C at their lower ends. The board stood in front of and adjacent to the test-pipe section. As seen from behind the board, the 10-psid, 1.0-psid, and 0.1-psid PTs mounted from left to right across the top of the aluminum plate at 5 1/2" intervals. The pressure equalizing (PE) valve was a 1/4" brass 2-way ball valve and was located about two inches below the 1.0-psid PT. To either end of the PE valve connected the branch run of a 1/4" brass union tee via a 1/4" brass port connector. From the top run of each of these two tees emerged a short length of 1/8" flexible tubing with a 1/8" nut and 1/8" nylon ferrules on its free end. Each 1/8" nut attached directly onto a PT arm, connecting the PT and the board. To the bottom run of each tee attached a 1/4" brass union cross via a 1/4" brass port connector. A 1/4" brass 2-way ball valve connected to the outer arm of each cross. On the left cross, nearer the 10-psid PT, the 2-way ball valve received the tap line from tap 1 (T1). On the right cross, nearer the 0.1-psid PT, the 2-way ball valve received the tap line from T4. A 1/4" brass 3-way ball valve connected to the lower arm of each cross. On the left cross, a 3-way

Pressure-Transducer Board

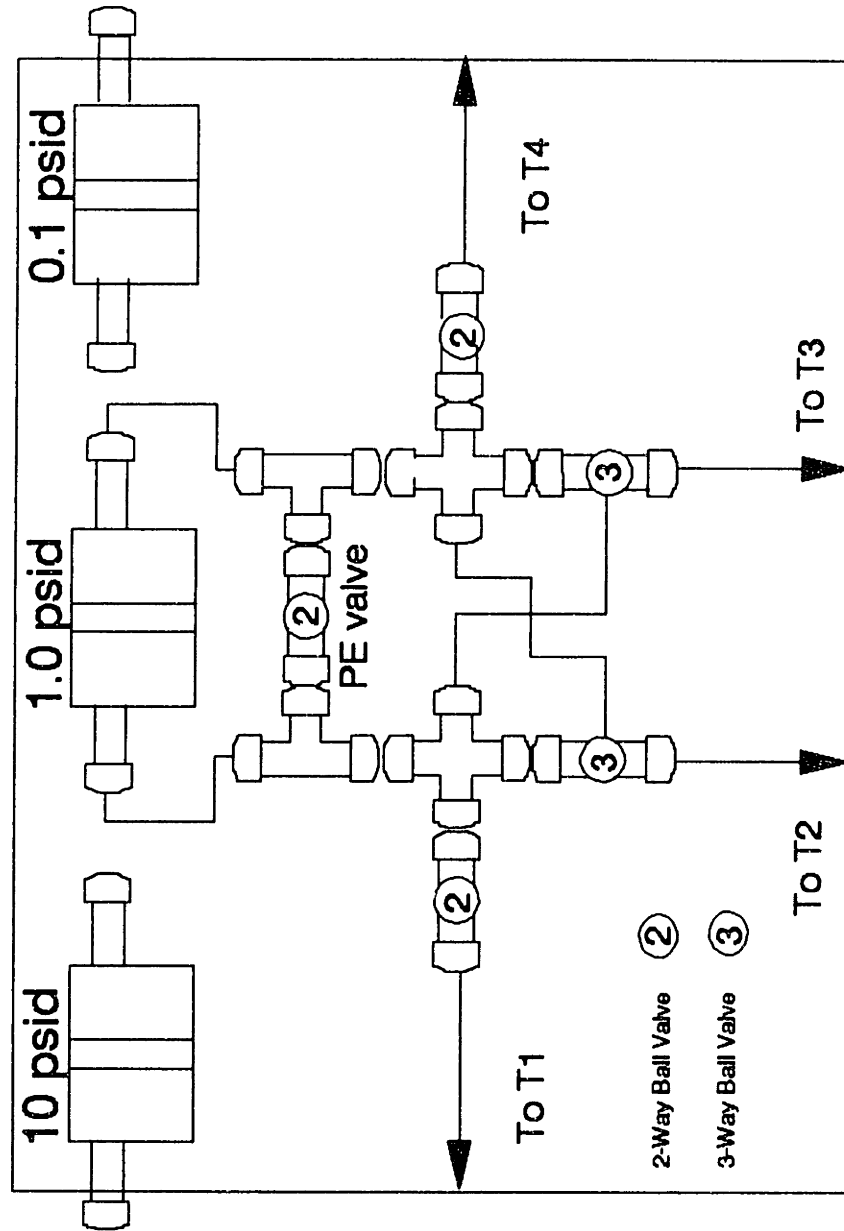


Figure 3.3.3: Pressure-Transducer Board

ball valve received the tap line from T2 on its lower run. Out of the right arm of the left cross, a ¼" flexible tube plugged into the left arm of the right cross. On the right cross, the 3-way ball valve received the tap line from T3 on its lower run. Out of the left arm of the right cross a, ¼" flexible tube plugged into the right arm of the left cross.

With the PE valve closed, the pressure drop across any tap pair could be determined by the proper positioning of the four valves. To test the integrity of the board, the two open valves, the others already closed, were suddenly closed while measuring the pressure drop. The pressure drop reading remained constant for several minutes, indicating that the board had no pressure leaks.

(4) Flow-Control Unit

A 10" × 12" × ⅛" aluminum plate served as the platform for the flow-control unit. A schematic is presented in Figure 3.3.4. Two 9/16" holes were drilled along the bottom plate to fasten the plate to the P1001C that supported this part of the flow system. Just above these bolt holes smaller holes were made to install a ¾" stainless-steel ball valve(B5) with ¾" female NPT fittings. About 6" higher on the plate, a large hole was cut from the plate to accommodate a ¾" stainless-steel 10-turn needle valve(N1) with ¾" port fittings. A ¾" stainless-steel male run tee installed directly into the upstream female fitting of the ball valve. The most downstream end of the test-pipe section entered directly into this tee. A ¾" stainless-steel male connector fit into the valve's downstream female fitting. Via a ¾" stainless-steel port connector, the ¾" stainless-steel male connector joined to a ¾" stainless-steel union tee, through which fluid exited the flow-

Flow-Control Unit

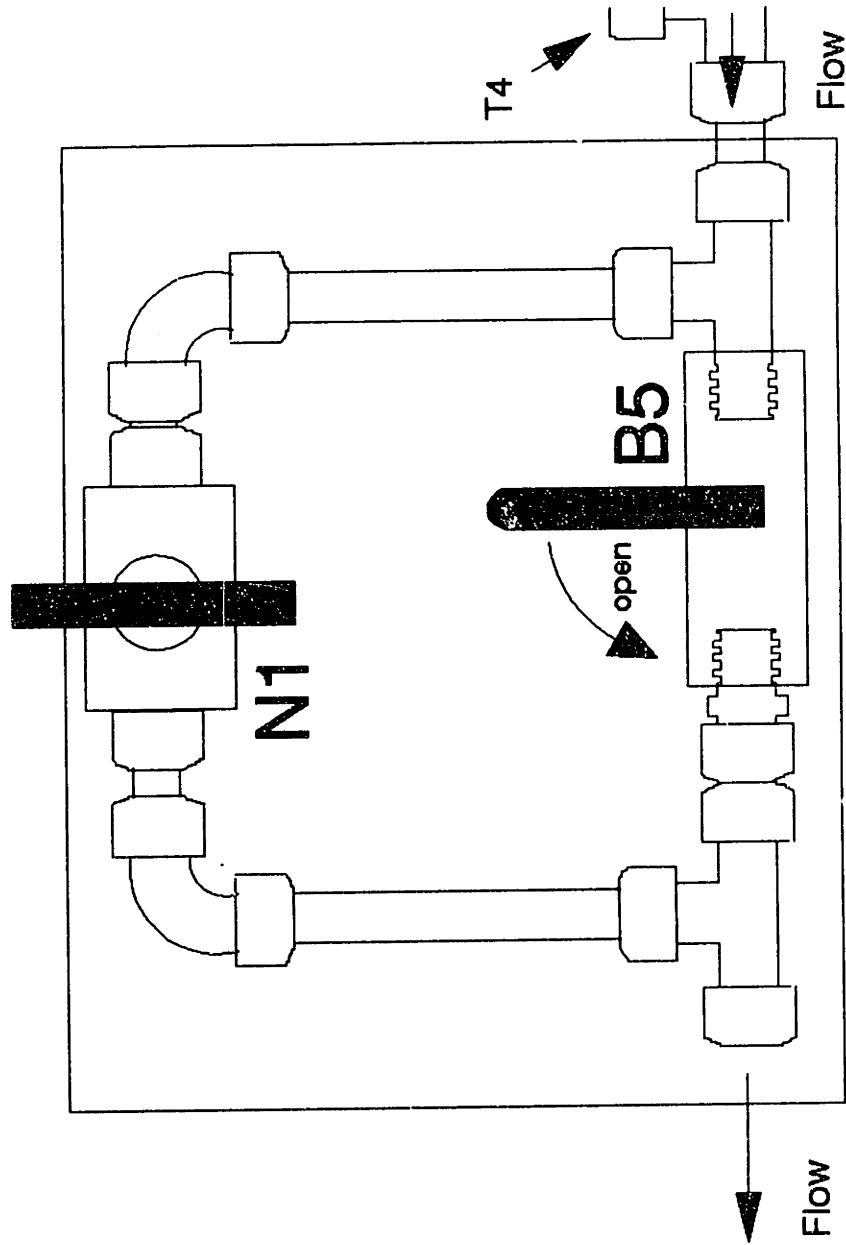


Figure 3.3.4: Flow-Control Unit

control unit. The needle-valve bypass loop began from the male branch run of the upstream tee. An extra length of $\frac{3}{4}$ " stainless-steel tubing, a $\frac{3}{4}$ " stainless-steel elbow, and a very short piece of $\frac{3}{4}$ " stainless-steel tubing in series linked the male branch run with the upstream end of the needle valve. The same arrangement in reverse order connected the downstream end of the needle valve with the branch run of the downstream tee. The plate bolted directly onto the P1001C, just downstream of the test-pipe section.

(5) The Timer and Flow-Diverter Unit

Under gravity-driven flow conditions, this unit measured the time interval that elapsed while collecting a volume of system effluent. Its main components were an electronic timer, a switch box, a ring-stand-mounted rotating arm with snap switch, and a ring-stand-mounted funnel as shown in Figure 3.3.5. A large vessel received the diverted flow for later volumetric measurement.

A DX100 Solid State Time/Count Totalizer measured the elapsed time and provided a visual reading on a $4\frac{1}{2}$ -digit, $\frac{1}{2}$ "-high, LCD display. It required 120 VAC, 60 Hz current. Proper wiring was necessary to activate the 1999.9-second timing range and to create a remote reset switch. A $2\frac{1}{4}$ " \times $2\frac{1}{4}$ " \times 5" aluminum switch box housed the reset switch. On the box, red and green lights signaled the open and closed condition, respectively, of the timing circuit. Mounted near the pivoting arm, a snap switch toggled the timing circuit as the arm's trip screw would either press or release the snap switch.

A straight length of $\frac{1}{2}$ " copper tubing with a gentle 90°-bend at the discharge end comprised the pivoting arm. The copper tube's straight end fit tightly into and passed

Timer and Flow-Diverter Unit

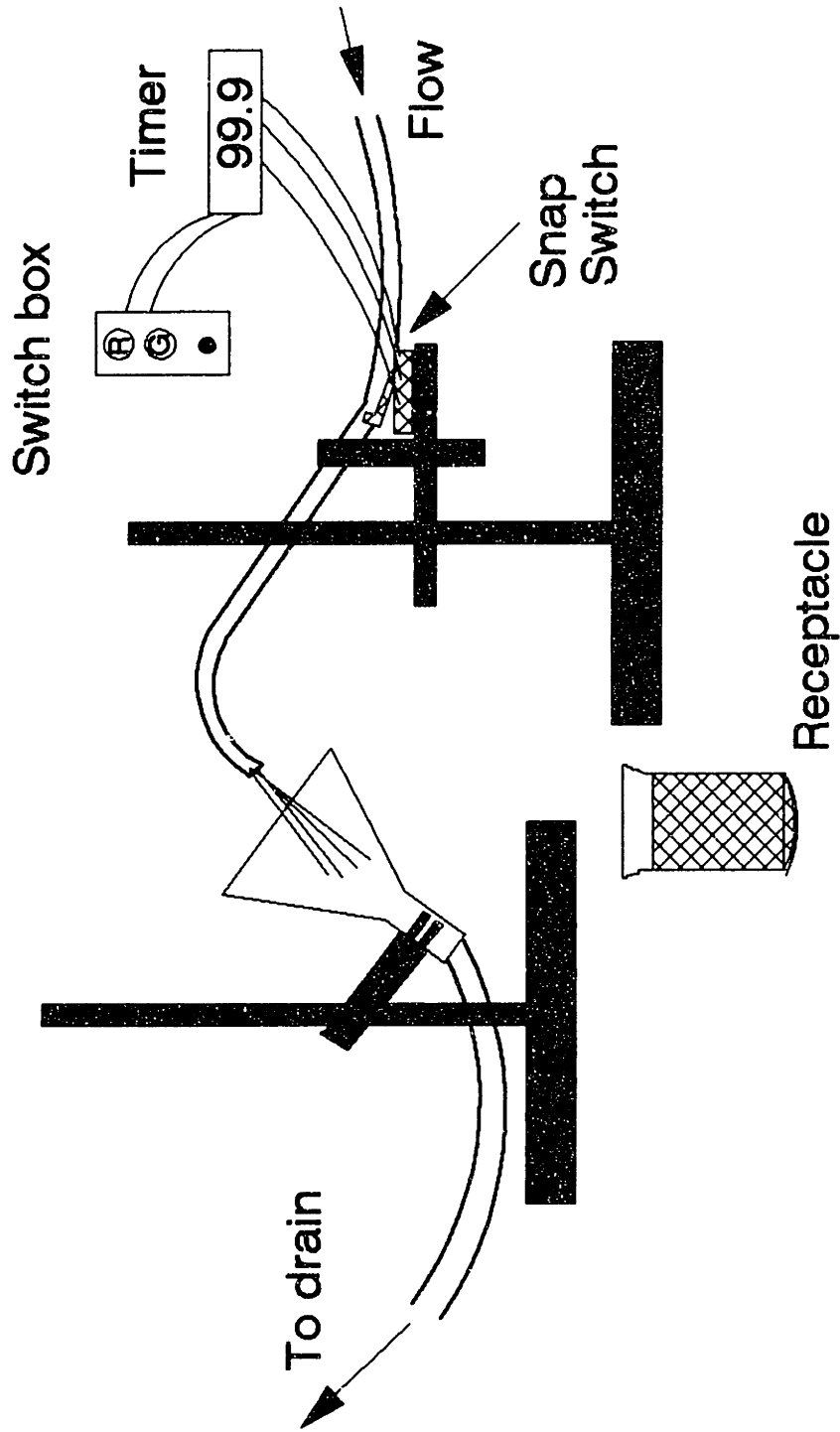


Figure 3.3.5: Timer and Flow-Diverter Unit

through a bored-through rod-end connector. One end of a 1/2" flexible tube attached onto the copper tube by a wormhose clamp; its other end attached onto a 1/2"-stub-to-3/4"-port reducer. This reducer joined onto the 3/4" stainless-steel male tube adapter on the rear valve(B6). The other hole of the bored-through rod-end connector was perpendicular to the first hole and loosely held an aluminum rod to permit rotation of the arm about the rod. This aluminum rod fit tightly into another bored-through rod-end connector, which held a second aluminum rod perpendicularly. The snap switch attached to the second rod by a screw. A ring stand supported this second aluminum rod at one end via a regular clamp holder.

A ring-stand-mounted funnel received the undiverted flow from the arm's bent discharge end. Gripping the ring stand, a regular holder clamped onto a three-prong clamp. This three-prong clamp gripped the large powder funnel just below its cone. One end of a long 1" flexible tube fitted over the funnel's tip while its other end went into the drain.

(6) Temperature-Probe Unit

The temperature probe measured the temperature of the fluid leaving the system. A 3/4" stainless-steel union tee, a 5k Ω thermistor in a 1/8" stainless-steel casing, a 3/4"-tube-to-1/2"-NPT female tube adapter, and a 1/2"-NPT-to-1/8"-port male connector comprised the unit, as shown in Figure 3.3.6. Long wires connected the thermistor's two wire leads to the input terminals of the HP-3467A, which was internally configured to calculate the temperature in °C from the thermistor resistance. The thermistor had an

accuracy of 0.1 °C.

(7) Flexible-Pipe Section

The "flex section" consisted of a 2", braided, flexible, stainless-steel, metal-hose assembly with coupled 2" stainless-steel fixed flanges. Three pieces of honeycomb were placed inside as shown in Figure 3.3.7. The hose's corrugated inner surface had 30 "convolutions" per foot. Without the honeycomb, the extreme roughness caused a large pressure gradient along the section. The pressure drop could be calculated from the equation

$$\Delta P = \frac{NCV^2R_o}{9256} \quad (3.1-1)$$

The equation variables are: the pressure drop ΔP in psid/ft, the number of convolutions per foot N , the loss coefficient $C = 0.05514$, the velocity V in ft/s, and the Reynolds number R_o . At the maximum flow rate, $Q_{\max} = 19.2$ gpm, $\Delta P/L = 23.6$ -psid/ft, and $\Delta P = 23.6$ psid.

To calm the flow, three pieces of Spiral Wrap Tricomb Honeycomb were inserted into the flexible hose. That the presence of honeycomb was vital can not be overemphasized. Installing the three pieces erased flow artifacts created by the pump and corrugated inner-surface of the flexible pipe. Each 3"-long, 2"-OD cylindrical piece was a tightly-rolled sheet of ¼"-cell honeycomb encased in a stainless-steel sleeve. In each cell, which was closer to ⅛" in size, $Re_{\max} = 2120$ with $T_w = 13.6$ dyne/cm². This compared to $Re_{\max} = 33900$ with $T_w = 67800$ dyne/cm² in the empty hose.

Temperature-Probe Unit

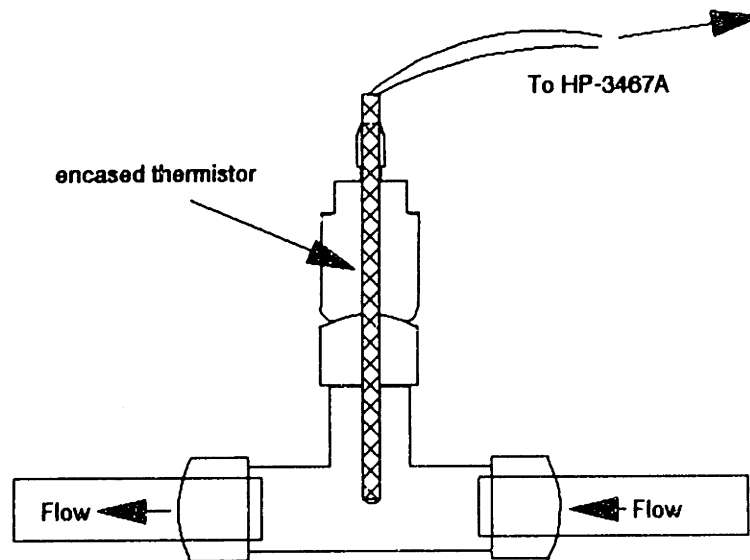


Figure 3.3.6: Temperature-Probe Unit

Flex Section

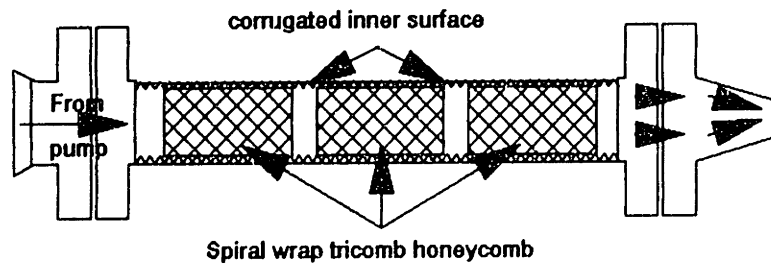


Figure 3.3.7: Flex Section

3.4 Experimental Equipment

(1) Pressure Transducers and Carrier Demodulator

Three differential pressure transducers(PT) with range maxima of 0.1-psid, 1.0-psid and 10-psid were used to measure the pressure drop in the test-pipe section. All were Model CJ3D Differential Pressure Transducers made by C. J. Enterprises. They operated on the variable reluctance principle. Their VDC output was linear with imposed pressure differential to within $\pm 0.5\%$ of full scale. Hysteresis was 0.5% of full scale(FS), and overpressure was 200% of range with less than 0.5% FS zero shift. Their stainless-steel diaphragms and pressure cavities resisted corrosion from brine. Stainless-steel $\frac{1}{2}$ " fittings, called arms, screwed into the pressure ports of the PTs and accepted the two small tubes from the PT board. The maximum temperature errors were 3% FS for ranges above 1.0-psid and 5% FS for ranges below 0.1-psid.

A Model CJCD-4111M Carrier Demodulator was used to convert reluctance output from the PT to an electric DC signal. The demodulator operated on unregulated 115 VAC, 60 Hz current and provided FS output of ± 10 VDC. In practice, however, the FS scale output was about ± 13.5 VDC, depending upon the PT in use. Its maximum output could be adjusted from ± 1 VDC to ± 10 VDC by setting the span dial(S) between zero and ten. Its zero level could be adjusted up to $\pm 75\%$ FS by setting a zero dial(Z) between zero and ten. Its linearity and drift varied less than $\pm 0.5\%$ FS. Its temperature error was less than 0.017% FS per $^{\circ}\text{C}$.

(2) Mass-Flow Meter Unit

In the gravity-driven flow system at high flow rates, the mass-flow meter measured and displayed the flow rate in ml/s and the cumulative fluid volume in liters. Three major components comprised this unit: a Model D40 S-SS Mass-flow Element(MFE), a Model DUL115-AF Remote Electronics Unit(REU), and a Model FMS-3 Flow Monitoring System(FMS).

Externally, the MFE consisted of a $8\frac{3}{4}$ " \times $7\frac{1}{2}$ " \times $2\frac{1}{4}$ " hermetically-sealed, stainless-steel, sensor housing and a 7" stainless-steel cylinder having tapered ends with $\frac{3}{8}$ " NPT male fittings. The housing encased two parallel U-tubes, two position detectors, a temperature sensor, and a drive coil. The drive coil received signals from the REU, processed the input, and vibrated the tubes accordingly. The flow entered one end of the cylinder, flowed through both vibrating U-tubes, and emerged from the cylinder's other end as a single stream.

The MFE measured from 12 ml/s(0.19 gpm) to 900 ml/s(14.3 gpm) with a $\pm 0.22\%$ error at full scale. While the MFE provided non-invasive measurements, it incurred a large ΔP penalty. In the gravity-driven flow system, at $Q_{\max} \approx 250$ ml/s(3.96 gpm), the $\Delta P_{\text{MFE}} \approx 4.4$ psid, or about 70% of the available pressure head! In the pump-driven flow system, at $Q_{\max} \approx 1210$ ml/s(19.2 gpm), the ΔP_{MFE} would have been about 95 psid and would have consumed almost all of the pump's rated discharge pressure! Operating the pump at moderate Q with the MFE on-line caused vibrational feedback between the pump and MFE. The resultant surging flow and large ΔP penalty made using the MFE in the pump-driven flow system unfeasible.

A teflon cable electrically connected the MFE to the REU. The REU required 115 VAC and operated in the 0 - 900 Hz frequency and 4 to 20 mA ranges. Its five basic components were drive, signal, isolation, analog, and frequency boards. Measuring the coriolis force generated in the vibrating tubes, the REU calculated the mass flow rate. The output from the REU were sent, via two wires, to the FMS-3. On the back of its 5.66" × 5.66" × 6.50" housing, a junction box received the power cable and wires from the REU. The front panel contained a two-digit LED mode display, a six-digit LED setup/rate display, an eight-digit LED totalizer display, and a six-key, membrane, function panel. The FMS-3 was programmable and could display flow rates and volumes in various common units.

As shown in Figure 3.4.2, a unistrut frame held the three components in close proximity. Separated by 22½", two floor-anchored, five-foot-high posts supported three cross beams. From lowest beam, two short arms held the MFE level with the test-pipe section, at a height just enough for the sensor housing to hang down without touching the floor. Between the two upper beams, the FMS-3 and REU mounted onto a 12¼" × 19" × ¼" aluminum plate that spanned the beams. The FMS-3 inserted into a square hole cut into the upper half of the plate so that its front panel was flush with the plate. Just beneath, the REU mounted horizontally across the lower half of the plate.

(3) Water and Mercury Manometers

The 0.1-psid and 1.0-psid PTs were calibrated with a water-filled manometer constructed from two glass tubes, a meter stick, two ring stands, a small separation

Mass-Flow Meter Unit

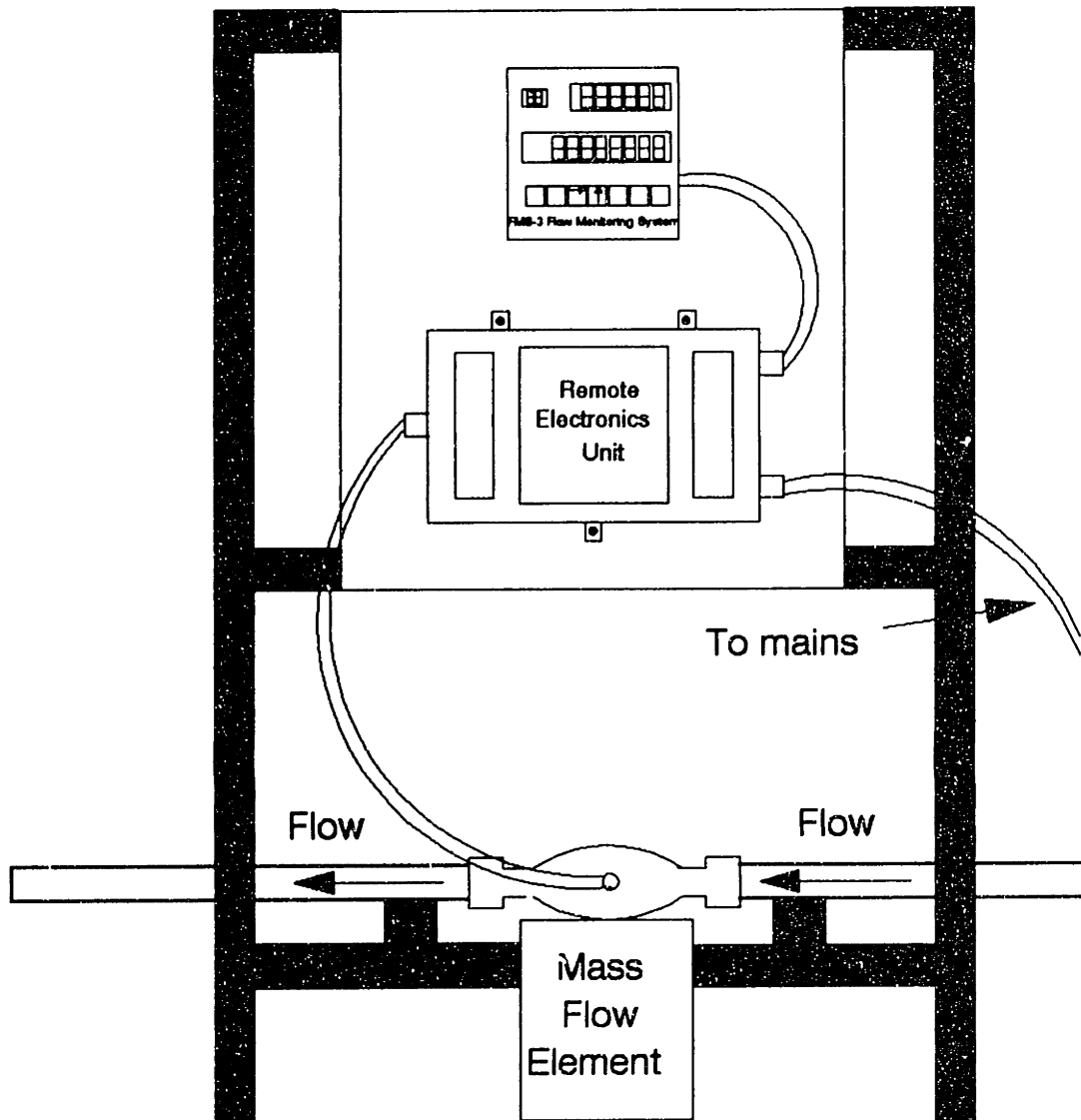


Figure 3.4.2: Mass-Flow Meter Unit

funnel, tubing, valves, and fittings. The 10-psid PT was calibrated with a mercury-filled manometer comprised of a U-tube with meter stick, mercury, a ring stand, a compressed air cylinder with regulating valve, a mercury trap, tubing, valves, and fittings. More detailed descriptions and Figures C3.4.3a and C3.4.3b are provided in §C3.4 in Appendix C.

(4) Digital Multimeters

A Hewlett-Packard Model 3467A Logging Multimeter displayed and printed the output signals from the carrier demodulator and the temperature probe. The HP-3467A had four channels, a 4½-digit LED readout, and a 4-function printing multimeter. The four-channel scanner read sequentially from all four channels and sent sequentially the input to the logging multimeter. The four functions were DC volts, AC volts, ohms, and temperature. The thermal printer created a hardcopy of the channel data and elapsed time with up to 16 characters per line and could be initiated manually or by a timer. A monolithic, 8-bit, parallel microprocessor and a Motorola MC6802 MPU with a 6k-byte ROM Operating System controlled the display, the printing, the internal data transfers, and the mathematical operations. The HP-3467A had accuracies of $\pm(0.03\%$ of the VDC input + 1 count) and $\pm 0.3^{\circ}\text{C}$.

During the experimental runs, a HP-3467A received input from the carrier demodulator and the temperature probe. It displayed the output voltage from the carrier demodulator on its LED readout in real time. Scanning these data every four seconds, it printed the results on thermal paper. The HP-3467A also measured the resistance in

the temperature probe's $5k\Omega$ thermistor and converted it internally into a temperature reading in $^{\circ}\text{C}$.

In calibrating the 0.1- to 1.0-psid PTs, the HP-3467A provided visual readings from the carrier demodulator output. A small Hewlett-Packard 34702A Digital Multimeter displayed the output during the calibration of the 10-psid PT only.

3.5 Chemicals

The flow-enhancement additives were commercial polymers obtained directly from the manufacturer as one pound samples. The precise chemical composition, weight- or number-averaged molecular weight, polydispersity, and backbone charge were not known. Table D3.5 in Appendix D reports the best available data. Most of the polymers were polyacrylamide-based. Usually, "pure" polyacrylamide was partially hydrolyzed to create sodium acrylate or acrylic acid residues randomly along the backbone; however, some samples were co-polymers of polyacrylamide and sodium acrylate.

To alter the equilibrium conformation of polyelectrolytes in solution, pure NaCl crystals (Mallinckrodt and Fisher), having less than 0.0001% impurities, were added to experimental solutions. Besides their affect on polyelectrolytic polymers, aqueous Na^+ and Cl^- ions, even at 0.00001 N concentrations, overwhelmed the ions contributed by aqueous H_2CO_3 , arising from the small solubility of CO_2 in water. A 5% solution of NaCl at 25°C had a pH of 6.9, nearly neutral.

CHAPTER IV

PROCEDURES

This chapter describes in detail the various procedures performed in the course of this thesis work. The procedures are presented in the following order: polymer preparation, system calibrations, experimental technique, and data reduction.

4.1 Polymer Master Batch Preparation

Two related methods were used in this thesis. The first requires a vacuum oven while the second does not; both yielded reproducible, consistent results.

4.1.1 Master Batch Preparation: Method #1

1.1) A five-liter, baffled, stainless-steel vessel was filled with about four liters of distilled water.

2.1) The mixer speed was initially set at 400 rpm to ensure rapid polymer dispersal without degradation.

3.1) About 15 grams of polymer were slowly added into the churning water.

4.1) The mixer speed was maintained for another 10 minutes after the polymer had been added completely.

5.1) The speed was lowered to about 200 rpm for about three hours. Polymer networks and lumps were broken up manually with a stirring rod or spatula.

6.1) The speed was further reduced to about 120 rpm for another three hours.

7.1) The mixer was stopped, the impeller was removed, and the vessel was covered with Saran Wrap™.

8.1) After a day or two, the master batch was decanted successively into four or five clean, one-quart, suitably labelled, glass jars with screw lids.

9.1) For each jar at least three aluminum weighing boats were labelled for use in determining the average weight concentration of the polymer solution in each jar. To reduce the chances of contamination by foreign matter, the boats always were placed on clean tissue, except when in the oven, and were handled only with forceps.

10.1) An empty boat was weighed on an analytical balance and then filled with about 15 grams of fluid. It was immediately weighed and placed in the vacuum oven.

11.1) The samples were desiccated in the vacuum oven at about 60°C and 40

mm Hg absolute for at least 10 hours.

12.1) After desiccation, the oven was turned off and left to cool to ambient temperature.

13.1) The polymer-residue encrusted boats were weighed. The average weight concentration, c , as well as the standard deviation, σ_c , for the fluid in each jar was determined from these data. Table 4.1.1 lists c and σ_c for all the polymer characterizations performed by Method #1.

Table 4.1.1
Polymer Characterization Data for Method #1

Date	Polymer	c	σ_c	σ_c/c
		(wppm)	(wppm)	(%)
12/20/88	C832A	2449.9	24.3	0.99
12/20/88	C832A	2579.0	35.8	1.39
12/20/88	C832A	2656.8	25.5	0.96
12/20/88	C832A	2840.7	81.0	2.85
01/28/89	C837A	2679.6	27.2	1.02
01/28/89	C837A	2706.3	14.5	0.54
01/28/89	C837A	2773.6	40.6	1.46
01/28/89	C837A	2768.7	43.9	1.59
01/28/89	C837A	2996.6	23.5	0.78
02/25/89	C836A	2766.1	28.0	1.01
02/25/89	C836A	2765.2	36.4	1.32
02/25/89	C836A	2835.6	53.8	1.90
02/25/89	C836A	2918.2	58.5	2.00
05/01/90	C832A	2730.0	25.6	0.94
05/01/90	C832A	2692.0	38.3	1.42
05/01/90	C832A	2742.1	50.0	1.82
05/01/90	C832A	2714.9	27.2	1.00
05/01/90 ^(a)	C832A	2739.3	58.2	2.12

(a) The oven became unreliable soon after. Method #2 was adopted for the remainder of the investigation.

4.1.2 Master Batch Preparation: Method #2

1.2) From the polymer solution concentration desired in an experiment and the solvent volume, the mass of polymer required was calculated.

2.2) A baffled five-liter stainless-steel vessel was filled with about four liters of distilled water. When the stainless-steel vessel was in use, a one-gallon glass jar filled with about three liters of distilled water was used.

3.2) An empty boat was weighed on an analytical balance. The required amount of polymer was put into the boat, which was reweighed. For maximum precision the boats were handled only with forceps.

4.2) With the impeller going at about 400 rpm, the polymer was added slowly into the water. Special care was taken to prevent water from splashing onto the boat.

5.2) The empty boat was weighed on the analytical balance. The solvent volume for the experimental run was adjusted for any difference between the calculated required polymer mass and actual polymer mass in the vessel.

6.2) A wash bottle containing distilled water was used to remove undissolved polymer stuck to various surfaces.

7.2) The mixer speed was maintained at 400 rpm for another 10 minutes after the polymer had been added completely.

8.2) The speed was lowered to about 200 rpm for about three hours and then further reduced to about 120 rpm for another three hours. To facilitate thorough mixing, from time to time the impeller speed was increased, and more distilled water was added.

9.2) After the mixing, the impeller was lifted out of the solution, while remaining suspended above it, and its shaft and blades were rinsed thoroughly free of polymer, the washings falling back into the vessel. Thus, all the polymer added remained in the vessel.

10.2) The vessel was covered immediately with Saran Wrap™.

11.2) This solution was used within two days.

Table 4.1.2 lists the following data for solutions prepared by Method #2 from each experimental run: the mass of polymer deposited into the left and right tanks, the total fluid volume in both tanks, and the best c for the solution in each tank.

Table 4.1.2
Polymer Characterization Data for Method #2

Run(s)	Polymer Mass Per Tank		Solvent Volume Per Tank		C _{Left}	C _{Right}
	Left	Right	Left	Right		
	(g)	(g)	(ml)	(ml)	(wppm)	
Q2P11456/3157	3.5996	3.6145	180526	181158	20.00	20.01
B1P21477/3178	17.66	17.68	177000	177400	100.1	99.95
B5P11480/3181	8.94	9.06	179474	182211	49.96	49.87
B2P11483/3184	3.5902	3.5971	179895	180316	20.02	20.01
B1P11486/3187	1.8027	1.8029	181368	181579	9.969	9.958
B5P01401(a)		1.7810		178632		5.00
A1P21403/3104	17.68	17.70	177400	177600	99.95	99.95
A3P21406/3107	53.35	53.82	178632	179895	299.5	300.0
A3P11409/3110	5.13	5.29	171474	177200	30.01	29.94
A1P31412/3113	166.31	169.59	166667	170000	999.8	999.6
D1P21415/3116	17.45	17.63	175400	177000	99.77	99.89
D3P11418/3119	5.15	5.13	172316	171474	29.97	30.00
D3P21421/3122	53.48	53.55	179053	179053	299.5	299.9
D1P31424/3125	141.33 ^(b)	139.41	141789	140600	1000.	993.5
U1P21427/3128	17.57	17.67	176200	177200	100.0	100.0
V1P21431/3132	17.58	17.60	176000	176400	100.2	100.1
V1P11434/3135	1.7791	1.7869	177400	179895	10.06	9.962
V3P11437/3138	5.3630	5.3685	179474	179474	29.97	30.00
Y1P01443/3144	0.1690	0.1831	169556	183684	1.000	1.000
Y2P01446/3147	0.3430	0.3538	172105	177400	1.999	2.000
Y5P01449/3150	0.8825	0.9141	177000	183263	5.001	5.003
Y1P11452/3153	1.8010	1.7798	180737	178421	9.994	10.00
Y1P11455/3156	3.5879	3.5968	179895	180316	20.00	20.01

Run(s)	Polymer Mass Per Tank		Solvent Volume Per Tank		C _{Left}	C _{Right}
	Left	Right	Left	Right		
	(g)	(g)	(ml)	(ml)	(wppm)	
Y1P1DEGL		1.7935		179895		10.00
Y1P1DEGH		1.8173		182211		9.83
Y5P11459/3160	8.9988	9.0056	180526	180526	49.99	50.03
W1P11462/3163	1.8069	1.8035	181158	180947	10.00	9.997
W3P11465/3166	5.4151	5.3992	180947	180526	30.01	30.00
W3P11468/3169	17.9968	18.0025	180737	180526	99.56	100.0
W3P11371/1272	5.3817	5.3960	179895	180316	30.00	30.01
(a) This tank was split in subsequently. (b) Maximum amount due to small losses.						

4.2 Transducer Calibration

The 0.1- and 1.0-psid differential pressure transducers (PTs) were calibrated with a water-filled manometer; the 10-psid differential PT was calibrated with a mercury-filled manometer.

The calibration procedure for the 0.1- and 1.0-psid transducers was:

1.1) The PTs were connected to the water-filled manometer via the long 1/8" flexible vincon tubes with 1/8", stainless-steel nuts and nylon ferrules. The bleed screws were opened to fill the diaphragm chamber entirely with fluid and to remove trapped gas.

2.1) The electrical connections between the PT and carrier demodulator and between the carrier demodulator and HP-3467A Logging Multimeter were made.

3.1) Before turning on the demodulator, the span(S) and zero(Z) dials were set at the values to be used during the experiment. The span setting changed very little except after the PT was repaired; the zero setting invariably required adjustment.

4.1) The arms of the manometer were hydraulically isolated by closing the stopcock. The initial water column heights, which were arbitrary but approximately equal, and PT output, which was close to zero volts, were recorded.

5.1) The water reservoir was lowered incrementally down the ring stand by adjusting the clamp supporting the reservoir. After the reservoir had been in place for 30 seconds, the water-column heights and output voltage were recorded. This greatly reduced, but did not eliminate, the problem of voltage drift. As seen in Figures 4.2.1 and 4.2.2, data taken as the pressure differential was increased did not exactly coincide with those taken when the pressure differential was decreased. This constituted voltage drift. Still, precise calibration constants were obtained. As seen from the r^2 column in Table 4.2, the square of the correlation coefficient for each calibration was better than 0.999, indicating high linearity.

6.1) When either the PT output topped -10 volts or the imposed pressure differential exceeded -0.1 or -1.0 psid, the reservoir was no longer lowered. It was then

incrementally raised stopping at levels between those during lowering. In Figures 4.2.1 and 4.2.2 the alternating "up"(\square) and "down"($+$) symbols illustrate intermeshing h_i and h_r columns. Experimental liquid-column heights are listed in the data sheets corresponding to each figure.

7.1) Linear regression of these data provided the calibration constant in volt/psid, equal to the slope of the best-fit line of the output voltage versus differential pressure data. Figures 4.2.1 and 4.2.2 illustrate the regression of DP vs. V data; these data are listed in the DP and D < V > columns in the corresponding data sheet.

0.1 PSID Transd. Calibration: TRNSD158

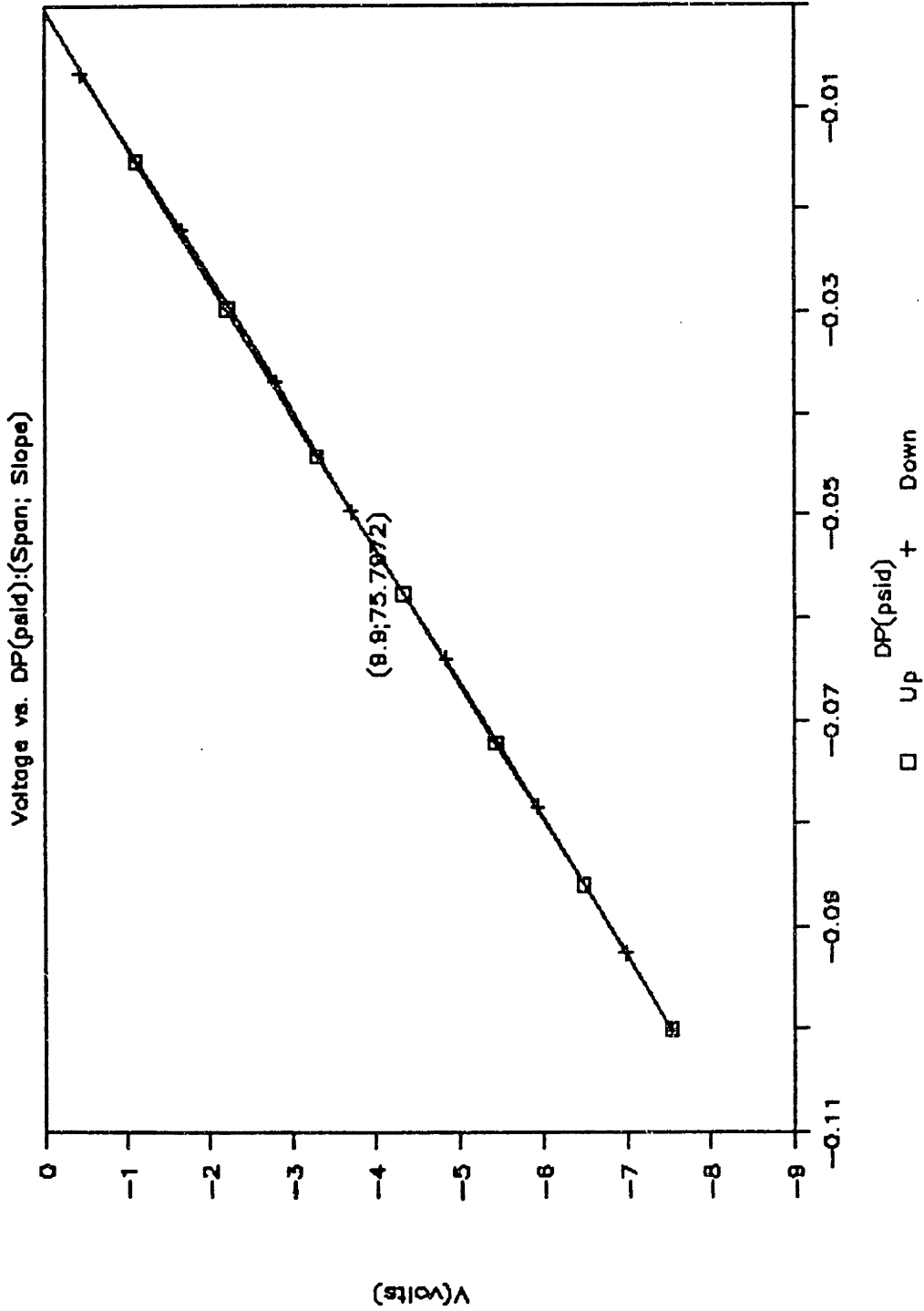


Figure 4.2.1: 0.1-psid Pressure-Transducer Calibration

TRNSD158 Pressure Transducer Calibrations 5/15/90 16:06

0.1 PSID S = 9.9 Z = 7.45 t(deg C) = 23.8

	hl(mm)	hr(mm)	V)low	V)high	Dh	DP(psid)	D<V>
	471	471	0.027	0.028	0	0	0.0275
	471	460.2	-1.111	-1.11	-10.8	-0.01531	-1.1105
	471	450	-2.206	-2.205	-21	-0.02978	-2.2055
	471	439.8	-3.307	-3.306	-31.2	-0.04424	-3.3065
(9.9;75.7	470.9	430.2	-4.339	-4.338	-40.7	-0.05771	-4.3385
	470.9	420	-5.421	-5.42	-50.9	-0.07218	-5.4205
	470.9	410.3	-6.473	-6.472	-60.6	-0.08593	-6.4725
	470.9	400.3	-7.536	-7.535	-70.6	-0.10012	-7.5355
	470.9	405.6	-6.974	-6.973	-65.3	-0.09260	-6.9735
	470.9	415.6	-5.922	-5.921	-55.3	-0.07842	-5.9215
	470.9	425.8	-4.832	-4.831	-45.1	-0.06395	-4.8315
	470.9	435.9	-3.713	-3.712	-35	-0.04963	-3.7125
	470.9	444.9	-2.784	-2.783	-26	-0.03687	-2.7835
	470.9	455.3	-1.669	-1.668	-15.6	-0.02212	-1.6685
	470.9	466.2	-0.428	-0.427	-4.7	-0.00666	-0.4275

Data Sheet for Figure 4.2.1

1 PSID Transducer Calibration:TRNSD160

Voltage vs. DP(paid):(Span; Slope)

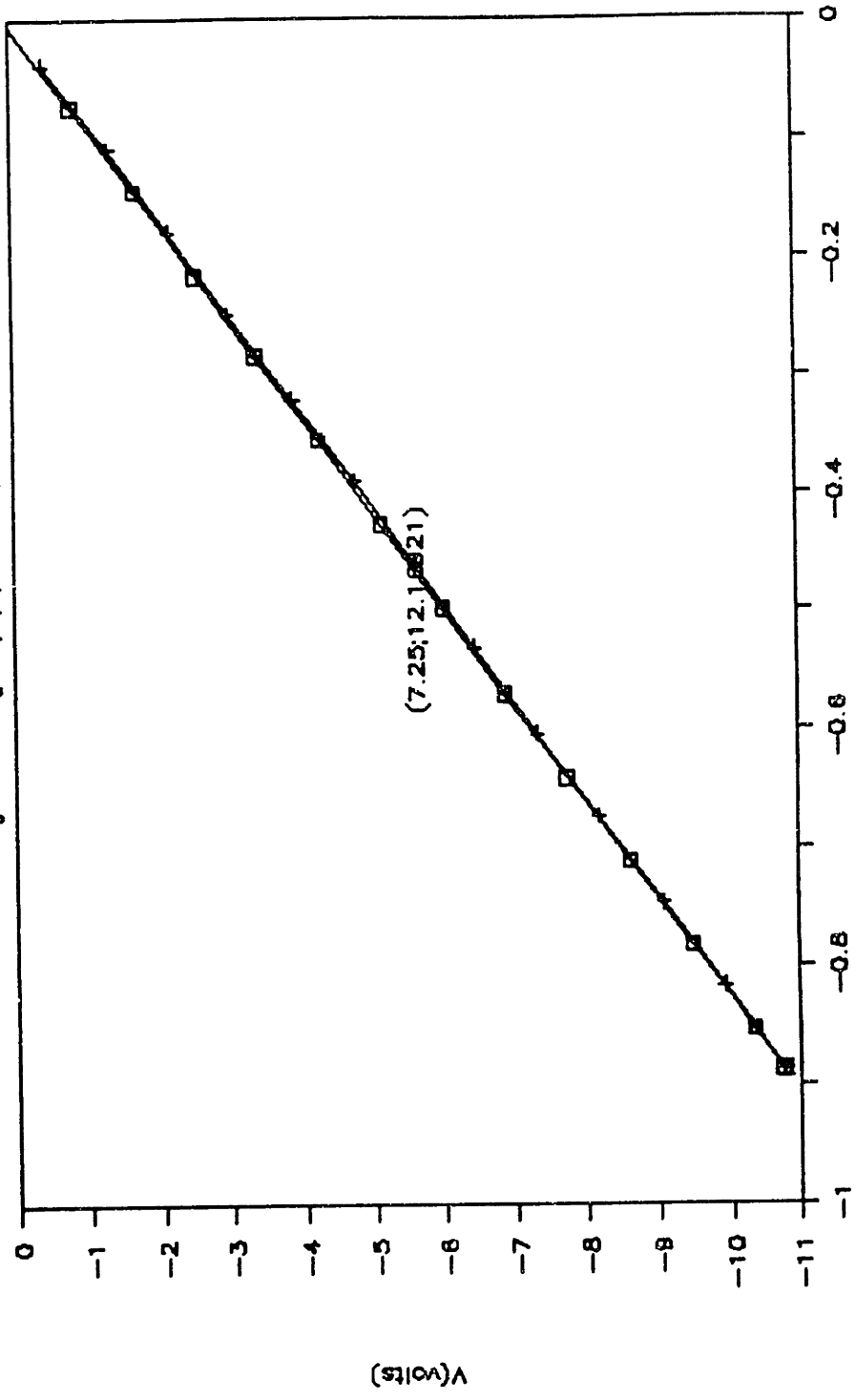


Figure 4.2.2: 1.0-psid Pressure-Transducer Calibration

TRNSD160 Pressure Transducer Calibrations 5/20/90 15:44

1.0 PSID S = 7.25 Z = 8.25 t(deg C)= 23.1

	hl(mm)	hr(mm)	V)low	V)high	Dh	DP(psid)	D<V>
	702	702.3	0.07	0.071	0	0	0.0705
	701.9	650.1	-0.842	-0.841	-52.1	-0.07389	-0.8415
	701.9	600.1	-1.701	-1.7	-102.1	-0.14481	-1.7005
	701.9	549.9	-2.564	-2.563	-152.3	-0.21602	-2.5635
	701.9	501.5	-3.4	-3.399	-200.7	-0.28467	-3.3995
	701.9	451.5	-4.267	-4.266	-250.7	-0.35559	-4.2665
	701.9	400.8	-5.14	-5.139	-301.4	-0.42750	-5.1395
	701.8	350.3	-6.013	-6.012	-351.8	-0.49898	-6.0125
(7.25;12.	701.7	299.4	-6.897	-6.896	-402.6	-0.57104	-6.8965
	701.7	250	-7.753	-7.754	-452	-0.64111	-7.7535
	701.7	200.3	-8.615	-8.614	-501.7	-0.71160	-8.6145
	701.7	150.4	-9.47	-9.469	-551.6	-0.78238	-9.4695
	701.7	100.3	-10.337	-10.336	-601.7	-0.85344	-10.3365
	701.7	76.9	-10.755	-10.754	-625.1	-0.88663	-10.7545
	701.7	126.7	-9.905	-9.904	-575.3	-0.81599	-9.9045
	701.7	175.8	-9.069	-9.068	-526.2	-0.74635	-9.0685
	701.7	226.8	-8.197	-8.196	-475.2	-0.67401	-8.1965
	701.7	276.2	-7.349	-7.348	-425.8	-0.60394	-7.3485
	701.7	327.3	-6.47	-6.469	-374.7	-0.53147	-6.4695
	701.7	376.2	-5.636	-5.635	-325.8	-0.46211	-5.6355
	701.7	426.2	-4.773	-4.772	-275.8	-0.39119	-4.7725
	701.7	476.1	-3.911	-3.91	-225.9	-0.32041	-3.9105
	701.8	526.6	-3.028	-3.027	-175.5	-0.24892	-3.0275
	701.8	576	-2.184	-2.183	-126.1	-0.17885	-2.1835
	701.8	625	-1.339	-1.338	-77.1	-0.10935	-1.3385
	701.8	675.8	-0.448	-0.449	-26.3	-0.03730	-0.4485

Data Sheet for Figure 4.2.2

8.1) Due to its extreme sensitivity, the 0.1-psid PT was calibrated before and after each experiment. The calibration constant of the 1.0-psid PT was fairly stable ($\pm 2\%$) over a month, but weekly calibrations were done. Table 4.2 provides the calibration histories for these PTs.

In calibrating the 10-psid PT, the general procedure was:

1.2) One PT arm was connected first to the compressed air supply via the long $\frac{1}{8}$ " , flexible vincon tube with a $\frac{1}{8}$ " , stainless-steel nut and nylon ferrules; the other arm was exposed to the atmosphere.

2.2) The electrical connections between the PT and carrier demodulator and between carrier demodulator and HP-34702A multimeter were made.

3.2) Before turning on the demodulator, the span(S) and zero(Z) dials were set at the values to be used during the experiment. The span setting changed very little except after the PT was repaired; the zero setting invariably required adjustment.

4.2) After the initial height and voltage data were recorded, the pressure release valve was **SLOWLY** opened, forcing the mercury from the right arm into the left arm of the glass U-tube. Then the pressure release valve was closed, trapping the compressed air and keeping the mercury elevated. After the mercury levels had been stable for about 30 seconds, the height and voltage data were recorded. This greatly reduced, but did not

eliminate, the problem of voltage drift. As seen in Figure 4.2.3, data taken as the pressure differential was increased did not coincide with those taken as the pressure differential was decreased. This constituted voltage drift. Still, a precise calibration constant was obtained. In the r^2 column of Table 4.2, high precision and linearity are indicated by $r^2 \geq 0.999$.

5.2) When the imposed pressure differential reached 10 psid, the pressure was released incrementally, stopping at levels between those during the pressure increase. The alternating "up"(\square) and "down"($+$) symbols in Figure 4.2.3 illustrate intermeshing h_i and h_r columns. Experimental liquid-column heights are listed in the data sheet corresponding to Figure 4.2.3.

6.2) Linear regression of these data provided the calibration constant in volt/psid equal to the slope of the best-fit line of the output voltage versus differential pressure data. Figure 4.2.3 illustrates the regression of the DP vs. V data; these data are listed in the DP and $D < V >$ columns in the corresponding data sheet.

7.2) The calibration constant of the 10-psid PT was fairly stable($\pm 2\%$) over months. Monthly calibrations were done, unless a solvent run indicated that the calibration constant had changed. Table 4.2 also provides the calibration history of the 10-psid PT.

10 PSID Transducer Calib.: TRNSD171

Voltage vs. DP(paid):(Span; Slope)

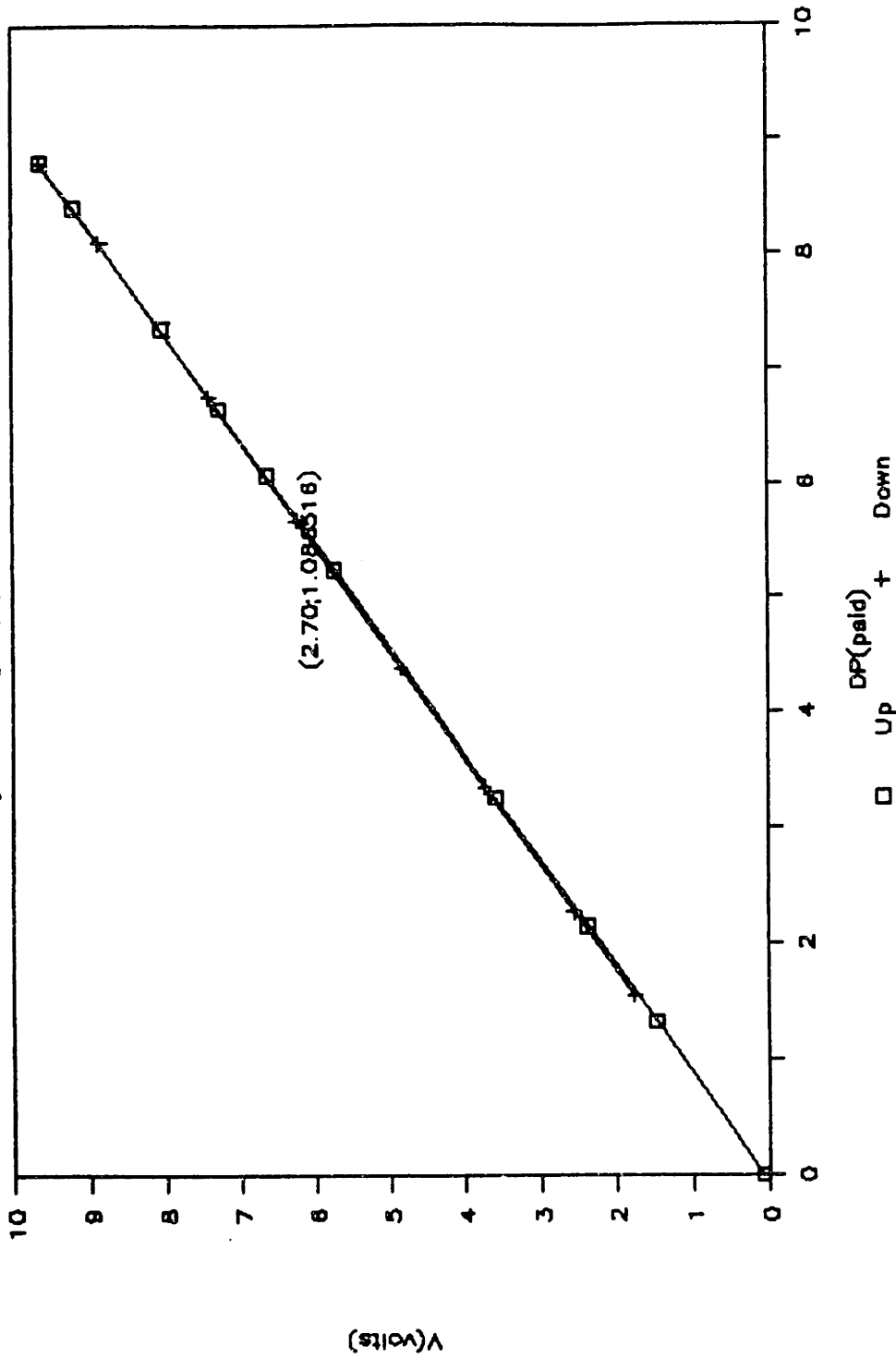


Figure 4.2.3: 10-psid Pressure-Transducer Calibration

TRNSD171 Pressure Transducer Calibrations 7/6/90 10:50

10 PSID S = 2.70 Z = 2.7 t(deg C)= 24

	hl(mm)	hr(mm)	V)low	V)high	Dh	DP(psid)	D<V>
	333.2	333.2	0.0912	0.0913	0	0	0.09125
	359.8	291	1.4809	1.481	68.8	1.329364	1.48095
	376	264.7	2.3824	2.3825	111.3	2.150556	2.38245
	398	229.2	3.566	3.5661	168.8	3.261580	3.56605
(2.70;1.0	437.3	166	5.7217	5.7218	271.3	5.242102	5.72175
	453.9	139.9	6.6269	6.627	314	6.067158	6.62695
	465.3	121.2	7.2705	7.2706	344.1	6.648755	7.27055
	479.2	99	8.0378	8.0379	380.2	7.346285	8.03785
	500.5	65.4	9.1899	9.19	435.1	8.407071	9.18995
	508.3	53.1	9.6307	9.6308	455.2	8.795447	9.63075
	494.2	75.1	8.86	8.8601	419.1	8.097917	8.86005
	467.3	118.1	7.3946	7.3947	349.2	6.747298	7.39465
	446	152.4	6.2362	6.2363	293.6	5.672986	6.23625
	420.4	193.3	4.8347	4.8348	227.1	4.388062	4.83475
	400	226.3	3.7057	3.7058	173.7	3.356259	3.70575
	378.2	260.6	2.5623	2.5624	117.6	2.272286	2.56235
	364.2	283.5	1.7709	1.771	80.7	1.559298	1.77095
	349.9	307	0.9881	0.9882	42.9	0.828920	0.98815
	333.3	333.2	0.0889	0.089	0.1	0.001932	0.08895

Data Sheet for Figure 4.2.3

Table 4.2
Transducer Calibration Constants

Date	File	Trans- ducer	Span	Zero	K	r ²
					(V/psid)	
10/11/88	TRNSD001	0.1	7.93	7.17	48.86	0.99996
10/11/88	TRNSD001	0.1	9.94	7.18	72.81	0.999964
10/20/88	TRNSD002	0.1	9.94	7.26	72.62	0.9997
10/20/88	TRNSD002	0.1	7.93	7.26	49.058	0.999755
11/09/88	TRNSD006	0.1	9.94	7.14	68.526	0.999963
11/09/88	TRNSD006	0.1	10.05	7.19	70.314	0.999971
11/20/88	TRNSD009	0.1	10.15	7.21	66.5048	0.999978
12/10/88	TRNSD013	0.1	10.05	6.88	57.79140	0.999885
12/15/88	TRNSD014	0.1	10.05	7.21	61.46408	0.999702
12/17/88	TRNSD016	0.1	10.05	6.72	60.9112	0.99996
01/08/89	TRNSD018	0.1	10.05	6.43	60.22719	0.999991
01/13/89	TRNSD022	0.1	10.05	7.23	81.30932	0.999908
01/13/89	TRNSD022	0.1	5.11	7.23	38.12897	0.999927
01/17/89	TRNSD023	0.1	10.05	7.27	83.35598	0.999972
01/17/89	TRNSD025	0.1	10.05	7.27	83.83672	0.99998
01/22/89	TRNSD028	0.1	10.05	7.27	82.21182	0.999716
01/24/89	TRNSD030	0.1	8.00	4.90	75.0614	0.999655
01/29/89	TRNSD032	0.1	10.05	7.27	83.22382	0.999979
01/29/89	TRNSD033	0.1	8.00	4.90	84.19413	0.999796
02/06/89	TRNSD036	0.1	8.00	4.90	85.14261	0.999836
03/03/89	TRNSD041	0.1	10.05	4.92	73.79766	0.999995
03/07/89	TRNSD042	0.1	10.05	4.92	73.94846	0.999821
04/06/89	TRNSD045	0.1	10.05	4.60	84.25618	0.999894
04/12/89	TRNSD047	0.1	10.05	4.60	84.25618	0.999866

Date	File	Trans- ducer	Span	Zero	K	r ²
					(V/psid)	
05/01/89	TRNSD048	0.1	10.05	4.96	81.83694	0.9997
05/10/89	TRNSD051	0.1	10.05	4.90	81.72632	0.999798
08/09/89	TRNSD053	0.1	10.05	5.00	58.47773	0.999475
08/09/89	TRNSD053	0.1	7.18	5.00	33.51341	0.999743
08/18/89	TRNSD056	0.1	10.05	7.12	76.63642	0.999722
08/21/89	TRNSD058	0.1	10.05	7.11	76.20957	0.999657
08/23/89	TRNSD060	0.1	10.05	7.00	76.31588	0.99978
08/28/89	TRNSD064	0.1	10.05	6.97	76.40294	0.999769
09/10/89	TRNSD067 ^(a)	0.1	10.05	6.62	79.56422	0.999579
09/11/89	TRNSD068	0.1	10.05	3.44	98.07934	0.999797
09/11/89	TRNSD069	0.1	10.05	3.44	98.28819	0.999816
09/22/89	TRNSD074	0.1	10.05	4.11	98.41659	0.999867
09/27/89	TRNSD076	0.1	10.05	4.22	96.3605	0.999828
10/02/89	TRNSD079	0.1	10.05	4.40	95.11395	0.999795
10/07/89	TRNSD082 ^(b)	0.1	7.85	3.58	102.07	0.994751
10/10/89	TRNSD084	0.1	10.05	6.10	97.17752	0.999887
10/12/89	TRNSD087	0.1	10.05	5.50	113.1092	0.999739
10/13/89	TRNSD089	0.1	10.05	7.60	79.99924	0.999754
10/13/89	TRNSD089	0.1	10.05	6.85	82.88132	0.999775
10/14/89	TRNSD089 ^(b)	0.1	10.05	7.60	83.53885	0.999750
10/15/89	TRNSD090	0.1	10.05	7.10	78.83565	0.999657
10/18/89	TRNSD092	0.1	10.05	7.35	78.37642	0.999870
10/23/89	TRNSD096	0.1	10.05	7.75	90.88766	0.999892
10/25/89	TRNSD097	0.1	10.05	7.67	76.32052	0.999733
10/25/89	TRNSD097	0.1	10.05	7.60	74.01564	0.999740
10/28/89	TRNSD099	0.1	10.05	7.72	76.42426	0.999631

Date	File	Trans-ducer	Span	Zero	K	r ²
					(V/psid)	
10/30/89	TRNSD099	0.1	10.05	7.50	73.36316	0.999938
11/13/89	TRNSD102	0.1	10.06	7.80	69.8097	0.999681
11/11/89	TRNSD102	0.1	10.05	7.75	68.28726	0.999676
11/15/89	TRNSD105	0.1	10.05	7.90	70.83384	0.999759
11/14/89	TRNSD105	0.1	10.05	7.85	69.9713	0.999589
11/15/89	TRNSD105	0.1	10.05	7.90	70.40149	0.999771
11/19/89	TRNSD107 ^(a)	0.1	10.05	5.60	88.37565	0.999818
11/21/89	TRNSD108 ^(b)	0.1	10.05	7.80	126.1543	0.999309
11/22/89	TRNSD108	0.1	8.80	7.80	99.68092	0.999525
11/22/89	TRNSD108	0.1	8.80	7.85	98.61889	0.999552
11/27/89	TRNSD109	0.1	8.80	8.85	98.01992	0.999139
12/04/89	TRNSD112 ^(b)	0.1	9.60	8.25	95.66494	0.999769
12/05/89	TRNSD114	0.1	9.60	8.1	98.39966	0.999811
12/05/89	TRNSD114	0.1	9.60	8.15	98.9334	0.999867
12/09/89	TRNSD115 ^(a)	0.1	8.50	5.90	99.02889	0.998326
12/18/89	TRNSD117	0.1	8.50	9.10	98.57166	0.999764
12/21/89	TRNSD121	0.1	8.50	9.15	98.39153	0.999834
12/25/89	TRNSD122	0.1	8.50	9.70	96.43758	0.999839
12/30/89	TRNSD125	0.1	8.50	9.95	95.03889	0.999882
01/03/90	TRNSD126	0.1	9.90	9.97	80.83505	0.999749
01/02/90	TRNSD126	0.1	9.90	7.50	97.48596	0.999732
01/19/90	TRNSD128	0.1	9.90	6.80	72.74352	0.999782
02/01/90	TRNSD130	0.1	9.90	6.65	77.51999	0.999822
02/04/90	TRNSD131	0.1	9.90	6.65	78.59397	0.999862
02/06/90	TRNSD132	0.1	9.90	6.60	78.75403	0.999859
02/07/90	TRNSD132	0.1	9.90	6.60	79.34951	0.999905

Date	File	Transducer	Span	Zero	K	r ²
					(V/psid)	
02/08/90	TRNSD133	0.1	9.90	6.80	79.81819	0.999638
02/12/90	TRNSD133	0.1	9.90	6.80	78.02002	0.999865
02/22/90	TRNSD136	0.1	9.90	7.10	80.03842	0.999805
03/19/90	TRNSD139	0.1	9.90	7.35	78.17769	0.999862
04/04/90	TRNSD142	0.1	9.90	7.25	76.80585	0.99994
04/12/90	TRNSD143	0.1	9.90	7.40	76.33338	0.999787
04/11/90	TRNSD143	0.1	9.90	7.40	77.98275	0.999863
04/17/90	TRNSD145	0.1	9.90	7.35	75.55558	0.999887
04/19/90	TRNSD145	0.1	9.90	7.45	74.23541	0.999871
04/23/90	TRNSD147	0.1	9.90	7.55	75.54508	0.999912
04/26/90	TRNSD149	0.1	9.90	7.60	75.75206	0.999897
05/01/90	TRNSD153	0.1	9.90	7.60	76.04142	0.99992
05/07/90	TRNSD155	0.1	9.90	7.65	74.66555	0.999841
05/09/90	TRNSD157	0.1	9.90	7.40	76.33526	0.999923
05/15/90	TRNSD158	0.1	9.90	7.45	75.79972	0.999938
05/20/90	TRNSD161	0.1	9.90	7.45	75.61796	0.999999
06/13/90	TRNSD163	0.1	9.90	7.45	78.07879	0.999866
06/25/90	TRNSD166	0.1	9.90	7.35	78.98393	0.999872
07/02/90	TRNSD169	0.1	9.90	7.20	79.06431	0.999813
07/20/90	TRNSD174	0.1	9.90	7.10	81.57181	0.999992
07/23/90	TRNSD175	0.1	9.90	7.05	82.0894	0.999819
07/30/90	TRNSD177	0.1	9.90	7.05	79.63686	0.999827
08/01/90	TRNSD179	0.1	9.90	7.00	78.70749	0.999981
08/03/90	TRNSD179	0.1	9.90	6.90	79.55358	0.999926
08/08/90	TRNSD181	0.1	9.90	6.85	80.93545	0.999843
08/12/90	TRNSD183	0.1	9.90	6.90	79.89031	0.99983

Date	File	Trans- ducer	Span	Zero	K	r ²
					(V/psid)	
08/14/90	TRNSD185	0.1	9.90	6.90	79.71477	0.999923
08/24/90	TRNSD187	0.1	9.90	6.85	80.1597	0.999985
08/30/90	TRNSD188	0.1	9.90	6.85	79.692	0.999934
08/30/90	TRNSD189	0.1	9.90	6.85	79.79777	0.999987
09/07/90	TRNSD191	0.1	9.90	6.85	79.42137	0.999919
09/15/90	TRNSD194	0.1	9.90	6.85	80.92975	0.999897
09/22/90	TRNSD195	0.1	9.90	6.85	80.63355	0.999897
09/21/90	TRNSD195	0.1	9.90	6.80	78.34361	0.999901
09/26/90	TRNSD196	0.1	9.90	6.90	78.91503	0.999932
09/26/90	TRNSD196	0.1	9.90	6.90	78.67313	0.999749
10/04/90	TRNSD197	0.1	9.90	6.85	79.72605	0.999553
10/25/90	TRNSD199	0.1	9.90	6.90	79.91174	0.999878
10/29/90	TRNSD201	0.1	9.90	6.90	79.89385	0.99989
10/31/90	TRNSD203	0.1	9.90	6.90	81.82122	0.999938
11/04/90	TRNSD205	0.1	9.90	6.90	83.13996	0.999877
11/07/90	TRNSD207	0.1	9.90	6.90	82.43988	0.999914
11/14/90	TRNSD212	0.1	9.90	6.90	82.65572	0.999909
11/15/90	TRNSD212	0.1	9.90	6.90	81.50076	0.999815
11/21/90	TRNSD216	0.1	9.90	6.90	84.29793	0.99993
11/24/90	TRNSD218	0.1	9.90	6.80	82.65316	0.999866
11/28/90	TRNSD219	0.1	9.90	6.95	82.54038	0.999952
11/28/90	TRNSD219	0.1	9.90	6.85	83.38349	0.999919
12/04/90	TRNSD222	0.1	9.90	6.90	84.98972	0.999985
12/04/90	TRNSD222	0.1	9.90	6.90	83.99103	0.999895
12/11/90	TRNSD224	0.1	9.90	6.85	83.85071	0.999913
12/11/90	TRNSD224	0.1	9.90	6.90	84.78139	0.999902

Date	File	Transducer	Span	Zero	K	r ²
					(V/psid)	
12/22/90	TRNSD225	0.1	9.90	6.95	84.54326	0.999904
12/22/90	TRNSD225	0.1	9.90	6.95	82.58022	0.999924
12/25/90	TRNSD226	0.1	9.90	6.95	82.52987	0.99995
12/25/90	TRNSD226	0.1	9.90	6.90	82.56793	0.999962
10/11/88	TRNSD001	1.0	8.00	5.27	9.52	0.99993
10/11/88	TRNSD001	1.0	5.00	5.28	6.49	0.99996
10/20/88	TRNSD002	1.0	8.00	5.30	9.492	0.999879
10/20/88	TRNSD002	1.0	8.00	5.33	6.446	0.999983
10/24/88	TRNSD003	1.0	8.00	5.20	9.5358	0.999981
11/10/88	TRNSD007	1.0	8.00	5.17	9.4525	0.999999
11/15/88	TRNSD008	1.0	8.00	5.14	9.44895	0.999998
12/10/88	TRNSD012	1.0	8.00	5.14	9.251516	0.999976
12/15/88	TRNSD015	1.0	8.00	5.05	9.5666	0.999985
12/19/88	TRNSD017	1.0	8.00	5.05	9.637244	0.999997
01/13/89	TRNSD020	1.0	8.00	5.14	9.407184	0.999949
01/13/89	TRNSD021	1.0	8.00	4.94	9.581598	0.999997
01/17/89	TRNSD024	1.0	8.00	4.90	9.4676	0.999959
01/20/89	TRNSD026	1.0	8.00	4.90	9.481430	0.999963
01/22/89	TRNSD027	1.0	8.00	4.90	9.3928	0.999968
01/24/89	TRNSD031	1.0	10.05	7.27	9.4644	0.999975
02/02/89	TRNSD034	1.0	8.00	4.90	9.402316	0.999904
02/02/89	TRNSD035	1.0	10.05	7.27	9.483509	0.999995
02/06/89	TRNSD036	1.0	10.05	4.90	9.525949	0.999966
02/12/89	TRNSD037	1.0	10.05	4.90	14.25395	0.999999
02/19/89	TRNSD038	1.0	10.05	4.92	14.2489	0.99998

Date	File	Trans- ducer	Span	Zero	K	r ²
					(V/psid)	
02/19/89	TRNSD039	1.0	10.05	4.82	14.28768	0.999935
02/26/89	TRNSD040	1.0	10.05	4.90	14.23522	0.999951
03/07/89	TRNSD043	1.0	10.05	4.90	14.25176	0.999998
04/06/89	TRNSD044	1.0	10.05	4.86	13.87506	0.999973
04/12/89	TRNSD046	1.0	10.05	4.70	13.97521	0.99999
05/01/89	TRNSD049	1.0	10.05	4.43	14.08113	0.999994
05/10/89	TRNSD050	1.0	10.05	4.40	14.213	0.99994
08/08/89	TRNSD052	1.0	10.05	4.00	13.93282	0.999949
08/15/89	TRNSD054	1.0	10.05	4.11	13.94509	0.999953
08/17/89	TRNSD055	1.0	10.05	4.11	14.12357	0.999994
08/18/89	TRNSD057	1.0	10.05	4.11	13.9635	0.999991
08/23/89	TRNSD059	1.0	10.05	4.12	13.9196	0.999986
08/28/89	TRNSD063	1.0	10.05	4.10	13.92606	0.999981
09/06/89	TRNSD065	1.0	10.05	4.31	13.556	0.99955
09/09/89	TRNSD066	1.0	10.05	4.95	17.35183	0.999821
09/11/89	TRNSD070	1.0	10.05	5.04	17.50439	0.999969
09/22/89	TRNSD073	1.0	10.05	5.04	17.71172	0.999896
09/27/89	TRNSD075	1.0	10.05	5.31	17.65151	0.999944
10/02/89	TRNSD078	1.0	10.05	5.34	17.83705	0.999975
10/07/89	TRNSD081	1.0	7.25	5.36	10.19435	0.999977
10/08/89	TRNSD083	1.0	7.25	5.43	10.12039	0.999910
10/12/89	TRNSD086	1.0	7.25	6.10	10.1462	0.999946
10/15/89	TRNSD091	1.0	7.25	6.25	10.08697	0.999983
10/15/89	TRNSD091	1.0	7.50	6.10	10.53907	0.999952
10/18/89	TRNSD093	1.0	7.25	5.50	10.10833	0.999868
10/26/89	TRNSD098	1.0	7.25	5.90	10.09309	0.999979

Date	File	Transducer	Span	Zero	K	r ²
					(V/psid)	
10/25/89	TRNSD098	1.0	7.25	5.95	10.08204	0.99998
10/29/89	TRNSD100	1.0	7.25	5.90	11.85022	0.999875
10/30/89	TRNSD100	1.0	7.25	6.25	11.88974	0.999905
11/11/89	TRNSD103	1.0	7.25	6.60	11.85364	0.999785
11/15/89	TRNSD106	1.0	7.25	6.65	11.86867	0.999767
11/27/89	TRNSD110	1.0	7.25	6.90	11.89484	0.999853
12/03/89	TRNSD111	1.0	7.25	7.05	11.92289	0.999745
12/18/89	TRNSD118	1.0	7.25	7.25	12.0867	0.999685
12/21/89	TRNSD120	1.0	7.25	7.25	12.09851	0.999997
12/25/89	TRNSD123	1.0	7.25	7.30	12.073	0.999534
12/29/89	TRNSD124	1.0	7.25	7.35	12.10268	0.999595
01/19/90	TRNSD129	1.0	7.25	7.55	12.19997	0.999982
02/08/90	TRNSD134	1.0	7.25	7.60	12.31038	0.999729
02/22/90	TRNSD135	1.0	7.25	7.75	12.28248	0.999996
03/19/90	TRNSD140	1.0	7.25	7.85	12.19433	0.999676
04/12/90	TRNSD144	1.0	7.25	7.90	12.26293	0.999771
04/19/90	TRNSD146	1.0	7.25	7.95	11.68401	0.999755
04/23/90	TRNSD148	1.0	7.25	8.00	11.76185	0.999752
04/27/90	TRNSD150	1.0	7.25	8.00	11.93037	0.999991
05/01/90	TRNSD152	1.0	7.25	8.10	11.96208	0.99976
05/09/90	TRNSD156	1.0	7.25	8.15	12.03909	0.999862
05/15/90	TRNSD159	1.0	7.25	8.15	12.09069	0.999878
05/20/90	TRNSD160	1.0	7.25	8.25	12.16921	0.999915
06/13/90	TRNSD164	1.0	7.25	8.75	12.37189	0.99993
06/25/90	TRNSD167	1.0	7.25	8.90	12.48441	0.999996
07/02/90	TRNSD170	1.0	7.25	8.90	12.40044	0.999814

Date	File	Transducer	Span	Zero	K	r ²
					(V/psid)	
07/13/90	TRNSD173	1.0	7.25	8.95	12.56699	0.999868
07/24/90	TRNSD176	1.0	7.25	9.05	12.79437	0.999918
07/30/90	TRNSD178	1.0	7.25	9.05	12.56946	0.999776
08/08/90	TRNSD180	1.0	7.25	9.10	12.75206	0.999865
08/12/90	TRNSD184	1.0	7.25	9.05	12.77237	0.999981
08/17/90	TRNSD186	1.0	7.25	9.05	12.75147	0.999971
08/30/90	TRNSD190	1.0	7.25	9.05	12.8687	0.999953
09/07/90	TRNSD192	1.0	7.25	9.10	12.85295	0.999965
10/26/90	TRNSD200	1.0	7.25	9.00	13.29777	0.999983
10/29/90	TRNSD202	1.0	7.25	9.05	13.19632	0.999965
11/07/90	TRNSD206	1.0	7.25	9.25	13.45545	0.999951
11/14/90	TRNSD211	1.0	7.25	9.10	13.4881	0.999965
11/21/90	TRNSD217	1.0	7.25	9.30	13.84841	0.99998
11/28/90	TRNSD220	1.0	7.25	9.20	13.79691	0.999907
08/24/89	TRNSD061	10.0	10.05	3.39	0.208574	0.995124
08/24/89	TRNSD061	10.0	10.05	3.33	0.221723	0.999274
08/25/89	TRNSD062	10.0	10.05	3.41	0.20675	0.991471
09/14/89	TRNSD071	10.0	2.70	2.93	1.071034	0.999752
09/14/89	TRNSD071	10.0	10.05	2.91	3.075481	0.999612
09/19/89	TRNSD072	10.0	2.70	2.80	1.080677	0.999891
09/29/89	TRNSD077	10.0	2.70	2.80	1.06711	0.999957
10/02/89	TRNSD080	10.0	2.70	2.90	1.078322	0.999957
10/10/89	TRNSD085	10.0	2.70	2.65	1.069926	0.999522
10/12/89	TRNSD088	10.0	2.70	2.80	1.071837	0.999862
10/22/89	TRNSD094	10.0	2.70	2.70	1.078165	0.999749

Date	File	Trans- ducer	Span	Zero	K	r ²
					(V/psid)	
10/22/89	TRNSD095	10.0	2.70	2.70	1.072608	0.999758
10/29/89	TRNSD101	10.0	2.70	2.70	1.06504	0.9998
11/11/89	TRNSD104	10.0	2.70	2.70	1.076613	0.999836
12/04/89	TRNSD113	10.0	2.70	2.70	1.076645	0.99972
12/10/89	TRNSD116	10.0	2.70	2.70	1.086647	0.999218
02/25/90	TRNSD137	10.0	2.70	2.70	1.106182	0.999535
03/07/90	TRNSD138	10.0	2.70	2.70	1.088082	0.999898
03/31/90	TRNSD141	10.0	2.70	2.70	1.088684	0.999949
04/03/90	TRNSD141	10.0	2.70	2.70	1.089026	0.999935
04/29/90	TRNSD151	10.0	2.70	2.70	1.097177	0.999867
05/01/90	TRNSD151	10.0	2.70	2.70	1.094631	0.999926
05/06/90	TRNSD154	10.0	2.70	2.70	1.083886	0.999928
05/21/90	TRNSD162	10.0	2.70	2.70	1.088055	0.999956
06/17/90	TRNSD165	10.0	2.70	2.70	1.091023	0.999942
06/25/90	TRNSD168	10.0	2.70	2.70	1.085095	0.999975
07/06/90	TRNSD171	10.0	2.70	2.70	1.086052	0.999958
07/12/90	TRNSD172	10.0	2.70	2.70	1.08859	0.999774
08/09/90	TRNSD182	10.0	2.70	2.70	1.077888	0.999967
09/09/90	TRNSD193	10.0	2.70	2.70	1.085877	0.99987
10/24/90	TRNSD198	10.0	2.70	2.70	1.078748	0.999649
10/31/90	TRNSD204	10.0	2.70	2.70	1.098348	0.999936
11/14/90	TRNSD210	10.0	2.70	2.85	1.440286	0.999657
11/18/90	TRNSD214	10.0	2.70	2.70	1.445043	0.999911
11/19/90	TRNSD215	10.0	2.70	2.70	1.450513	0.999794
11/19/90	TRNSD215 ^(a)	10.0	1.00	5.75	1.180945	0.999615
11/30/90	TRNSD221	10.0	1.00	5.00	1.186618	0.999721

Date	File	Trans- ducer	Span	Zero	K	r ²
					(V/psid)	
12/10/90	TRNSD223	10.0	1.00	4.60	1.161491	0.999775
(a) Its diaphragm was removed, cleaned, and reinstalled. (b) A new diaphragm was installed.						

4.3 Tank Calibration

While the 55-gallon tanks used in the experimental apparatus were apparently cylindrical, their bottoms bowed upwards. The height difference between the axis and the edge of the bottom was about two inches. Assuming a cylindrical shape of volume $\pi/4 \times (\text{tank diameter})^2 \times (\text{tank height})$ overestimated the volume by about five percent and, thus, underestimated the polymer and salt concentrations by about five percent. This underestimation can be seen from the apparent-tank-diameter data in Figures 4.3.1 and 4.3.2.

During the initial polymer runs in the gravity-driven flow system, this problem was not recognized; the reported concentrations were retroactively corrected.

In the pump-driven flow system, both the left and right tanks were calibrated as follows:

- 1) When the tank was completely empty, a metal yardstick was clamped in an upright position against the inside wall of the empty tank. The yardstick's position became permanent for all subsequent fluid measurements in that tank.

- 2) Into this initially empty, isolated tank, distilled water was added in 2000 ml increments. The liquid level was read from the yardstick. The incremental volume, cumulative volume, and height were recorded.

- 3) Step 2 was repeated. When the cumulative volume reached 50000 ml, the

increments increased to 4000 ml.

- 4) When the tank was nearly full, the calibration stopped.
- 5) The cumulative volume and fluid level data were tabulated; this "look-up" table was used in the experiments to convert measured heights into volumes by linear interpolation. Figures 4.3.1 and 4.3.2 show the height-versus-volume data for the right and left tanks, respectively; the corresponding data sheets are also presented.

4.4 Pump Calibration

- 1) Initially, the left tank was completely empty. Valves L and B were closed. The right tank was filled to about 90% capacity with the distilled-water hose. The hose's valve was closed, and the hose set aside. The metal yardstick was clamped against the wall inside the tank at its proper position to indicate the fluid level.

- 2) The system as shown in Figure 3.2 was altered by closing valves B2 and B3 and removing the tubing between them. The 1 ¼" flexible vincon tubing connected onto valve B was detached and was clamped onto valve B3; the last few feet of its other end was put inside the left tank on the bottom. To prevent the tubing from slipping out of the tank when the pump operated, two C clamps were used to hold the tubing against the tank's inner rim.

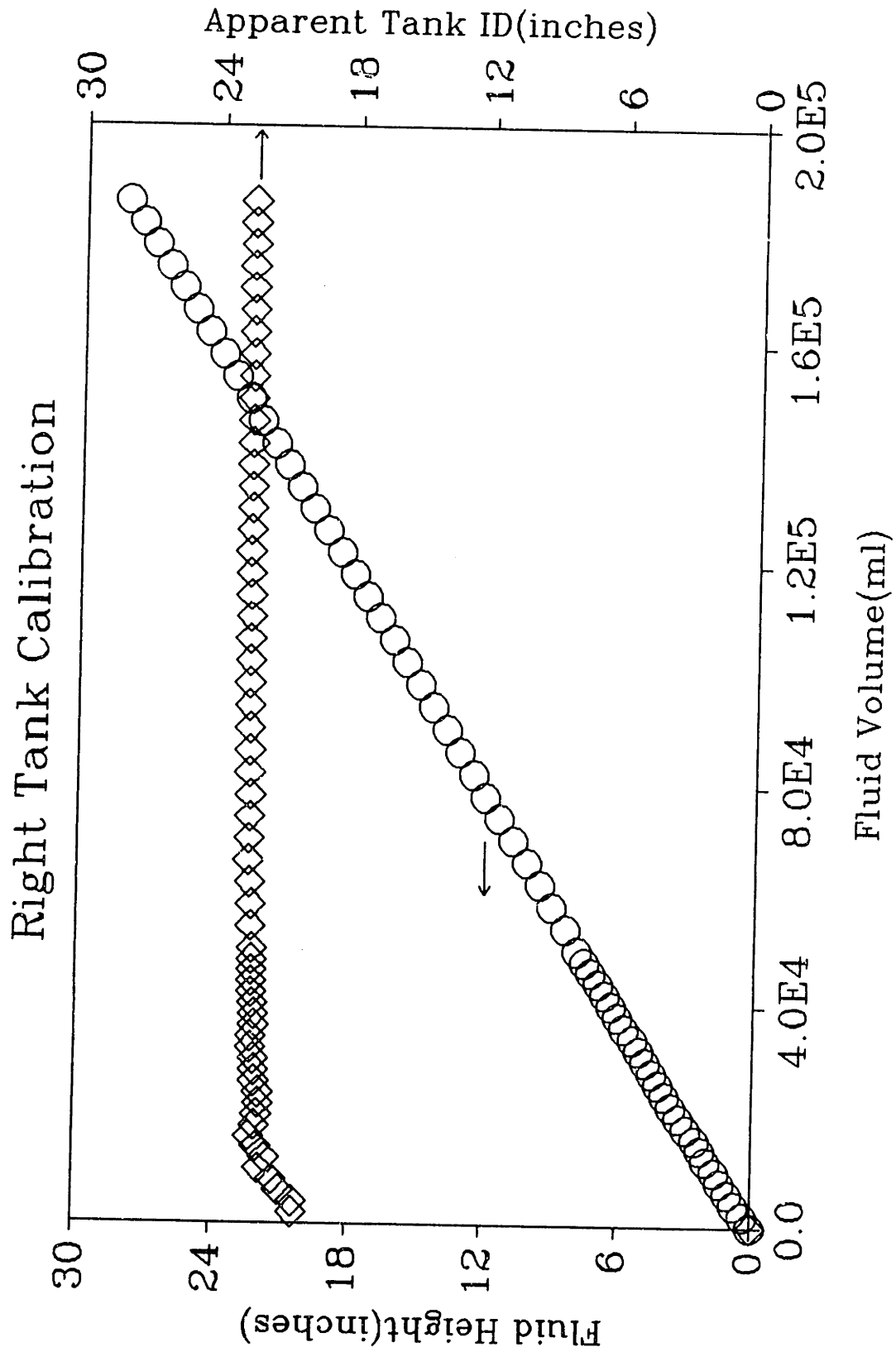


Figure 4.3.1: Right-Tank Calibration

Right Tank Calibration 9/23/89 13:05

Total Volume (gal)	Total Volume (cu. in.)	Height (inches)	Height Deltas (inches)	Corrected Height (inches)	Apparent ID) tank (inches)	Corrected Apparent ID) tank (inches)	
0	0	0		0			
2000	122.0474	0.375		0.375	20.34089	20.34089	
4000	244.0949	0.75		0.75	20.34089	20.34089	
6000	366.1424	1.0625		1.0625	20.93149	20.93149	
8000	488.1899	1.375		1.375	21.24673	21.24673	
10000	610.2374	1.625		1.625	21.85186	21.85186	
12000	732.2849	2		2	21.57661	21.57661	
14000	854.3324	2.25		2.25	21.97308	21.97308	
16000	976.3799	2.5		2.5	22.28518	22.28518	
18000	1098.427	2.875		2.875	22.04131	22.04131	
20000	1220.474	3.1875	0.03125	3.21875	22.06534	21.95782	
22000	1342.522	3.5625		3.5625	21.89021	21.89021	
24000	1464.569	3.875		3.875	21.92233	21.92233	
26000	1586.617	4.125		4.125	22.11549	22.11549	
28000	1708.664	4.4375		4.4375	22.12749	22.12749	
30000	1830.712	4.75		4.75	22.13789	22.13789	
32000	1952.759	5		5	22.28518	22.28518	
34000	2074.807	5.3125		5.3125	22.28518	22.28518	
36000	2196.854	5.6875		5.6875	22.16224	22.16224	
38000	2318.902	6		6	22.16866	22.16866	
40000	2440.949	6.25	0.03125	6.28125	22.28518	22.22961	
42000	2562.997	6.5625		6.5625	22.28518	22.28518	
44000	2685.044	6.875		6.875	22.28518	22.28518	
46000	2807.092	7.1875		7.1875	22.28518	22.28518	
48000	2929.139	7.5		7.5	22.28518	22.28518	
50000	3051.187	7.8125		7.8125	22.28518	22.28518	
54000	3295.282	8.375		8.375	22.36829	22.36829	
58000	3539.377	9		9	22.36253	22.36253	
62000	3783.472	9.5625		9.5625	22.43055	22.43055	
66000	4027.567	10.125		10.125	22.49084	22.49084	
70000	4271.662	10.75		10.75	22.47894	22.47894	
74000	4515.757	11.375		11.375	22.46833	22.46833	
78000	4759.852	12		12	22.45883	22.45883	
82000	5003.947	12.5625		12.5625	22.50611	22.50611	
86000	5248.041	13.1875		13.1875	22.49569	22.49569	
90000	5492.136	13.8125	-0.03125	13.78125	22.48621	22.51172	
94000	5736.231	14.375		14.375	22.52642	22.52642	
98000	5980.326	15	-0.03125	14.96875	22.51642	22.53994	
22.76056	102000	6224.421	15.625	-0.03125	15.59375	22.50721	22.52978
	106000	6468.516	16.1875		16.1875	22.54216	22.54216
	110000	6712.611	16.8125		16.8125	22.53266	22.53266
	114000	6956.706	17.375	0.03125	17.40625	22.56436	22.54407
	118000	7200.801	18	-0.03125	17.96875	22.55473	22.57436
	122000	7444.896	18.5625		18.5625	22.58371	22.58371
	126000	7688.991	19.1875		19.1875	22.57404	22.57404

Data Sheet 1 for Figure 4.3.1

Right Tank Calibration Summary Sheet

130000	7933.086	19.9125		19.8125	22.56499	22.56499
134000	8177.181	20.375	0.03125	20.40625	22.59109	22.57377
138000	8421.276	21	-0.03125	20.96875	22.58205	22.59889
142000	8665.371	21.5625	0.03125	21.59375	22.60626	22.58987
146000	8909.466	22.1875		22.1875	22.59728	22.59728
150000	9153.561	22.75		22.75	22.61983	22.61983
154000	9397.656	23.375		23.375	22.61094	22.61094
158000	9641.751	24	-0.03125	23.96875	22.60252	22.61727
162000	9885.846	24.5625		24.5625	22.62329	22.62329
166000	10129.94	25.1875		25.1875	22.61496	22.61496
170000	10374.03	25.75		25.75	22.63448	22.63448
174000	10618.13	26.375	-0.03125	26.34375	22.62627	22.63970
178000	10862.22	26.9375	0.03125	26.96875	22.64469	22.63155
182000	11106.32	27.5625		27.5625	22.63660	22.63660
186000	11350.41	28.125	0.03125	28.15625	22.65403	22.64144
190000	11594.51	28.75		28.75	22.64607	22.64607

Volume vs. Hc
Regression Output: 22.27760

Constant	-112.315
Std Err of Y Est	10.28576
R Squared	0.999988
No. of Observations	45
Degrees of Freedom	43

X Coefficient(s)	406.8703
Std Err of Coef.	0.208219

ID) tank = 22.76056

Data Sheet 2 for Figure 4.3.1

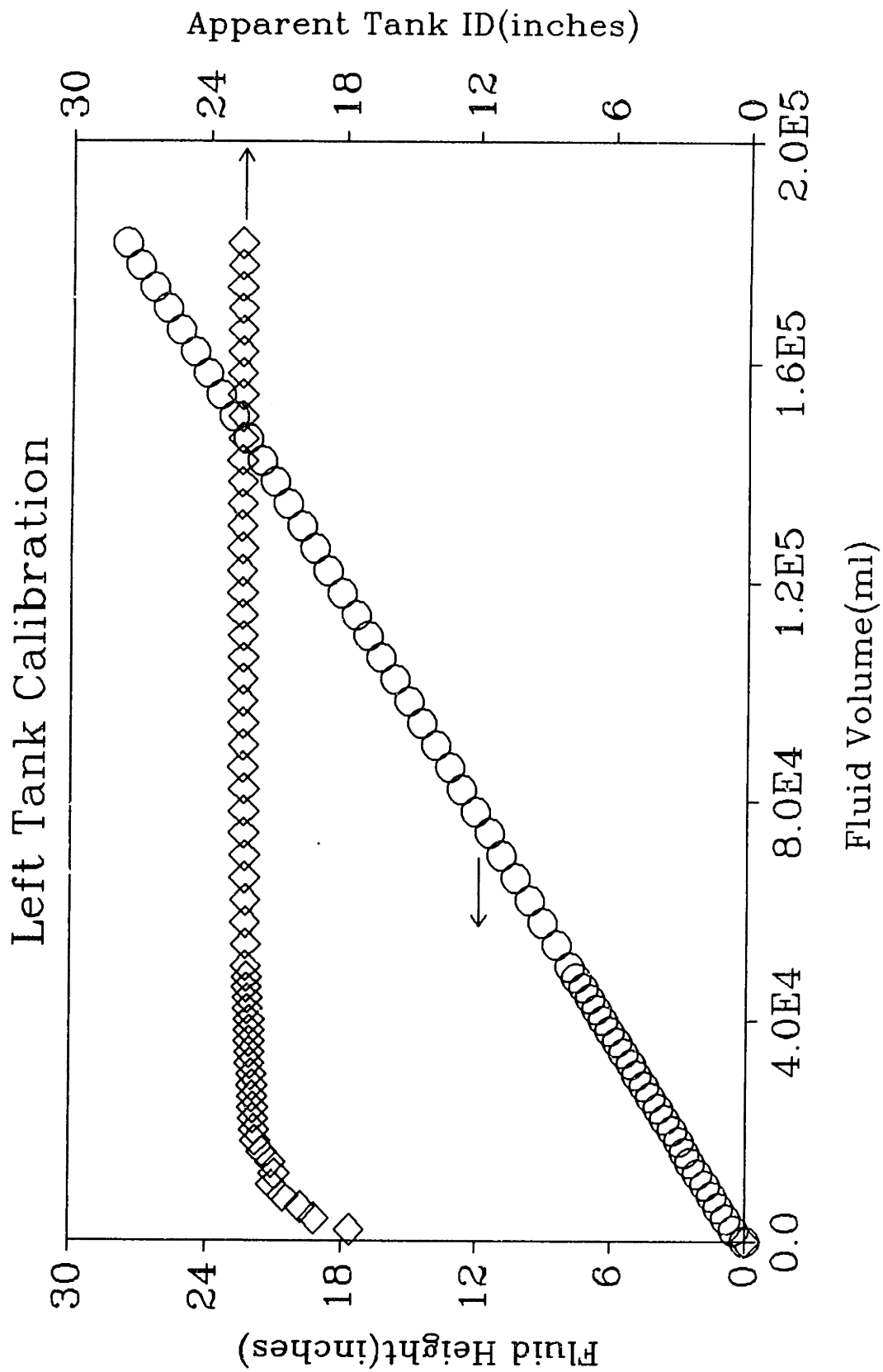


Figure 4.3.2: Left-Tank Calibration

Left Tank Calibration 9/24/89 10:55

Total Volume (gal)	Total Volume (cu. in.)	Height (inches)	Height Deltas (inches)	Corrected Height (inches)	Apparent ID(tank) (inches)	Corrected Apparent ID(tank) (inches)	
0	0	0		0			
2000	122.0474	0.5		0.5	17.61121	17.61121	
4000	244.0949	0.875	-0.03125	0.84375	18.82959	19.17573	
6000	366.1424	1.1875		1.1875	19.79752	19.79752	
8000	488.1899	1.5	-0.03125	1.46875	20.34089	20.35647	
10000	610.2374	1.75		1.75	21.05590	21.05590	
12000	732.2849	2.125		2.125	20.93149	20.93149	
14000	854.3324	2.4375		2.4375	21.10990	21.10990	
16000	976.3799	2.6875		2.6875	21.49271	21.49271	
18000	1098.427	2.9375		2.9375	21.80525	21.80525	
20000	1220.474	3.25		3.25	21.85186	21.85186	
22000	1342.522	3.5625		3.5625	21.89021	21.89021	
24000	1464.569	3.875		3.875	21.92233	21.92233	
26000	1586.617	4.1875		4.1875	21.94961	21.94961	
28000	1708.664	4.5		4.5	21.97308	21.97308	
30000	1830.712	4.8125		4.8125	21.99348	21.99348	
32000	1952.759	5.125	-0.03125	5.09375	22.01138	22.07889	
34000	2074.807	5.4375	-0.03125	5.40625	22.02721	22.09086	
36000	2196.854	5.6875	0.03125	5.71875	22.16224	22.10153	
38000	2318.902	6	0.03125	6.03125	22.16866	22.11108	
40000	2440.949	6.3125	0.03125	6.34375	22.17444	22.11969	
42000	2562.997	6.625		6.625	22.17968	22.17968	
44000	2685.044	6.9375		6.9375	22.18444	22.18444	
46000	2807.092	7.25	-0.03125	7.21875	22.18879	22.23683	
48000	2929.139	7.5	0.03125	7.53125	22.28518	22.23884	
50000	3051.187	7.8125		7.8125	22.28518	22.28518	
54000	3295.282	8.4375		8.4375	22.28518	22.28518	
58000	3539.377	9	0.03125	9.03125	22.36253	22.32375	
62000	3783.472	9.625	0.03125	9.65625	22.35751	22.32126	
66000	4027.567	10.25		10.25	22.35311	22.35311	
70000	4271.662	10.875		10.875	22.34921	22.34921	
74000	4515.757	11.4375		11.4375	22.40678	22.40678	
78000	4759.852	12.0625		12.0625	22.40050	22.40050	
82000	5003.947	12.6875		12.6875	22.39483	22.39483	
86000	5248.041	13.25		13.25	22.44251	22.44251	
90000	5492.136	13.875		13.875	22.43544	22.43544	
94000	5736.231	14.5	-0.03125	14.46875	22.42899	22.45323	
98000	5980.326	15.0625		15.0625	22.46960	22.46960	
22.68871	102000	6224.421	15.6875	15.6875	22.46228	22.46228	
	106000	6468.516	16.3125	16.3125	22.45552	22.45552	
	110000	6712.611	16.875	0.03125	16.90625	22.49084	22.47002
	114000	6956.706	17.5	-0.03125	17.46875	22.48353	22.50366
	118000	7200.801	18.125	-0.03125	18.09375	22.47672	22.49615
	122000	7444.896	18.6875		18.6875	22.50795	22.50795
	126000	7688.991	19.3125		19.3125	22.50078	22.50078

Data Sheet 1 for Figure 4.3.2

170000	7933.086	19.875		19.875	22.52944	22.52944
174000	8177.181	20.5		20.5	22.52207	22.52207
178000	8421.276	21.0625	0.03125	21.09375	22.54848	22.53175
142000	8665.371	21.6875		21.6875	22.54097	22.54097
146000	8909.466	22.3125		22.3125	22.53381	22.53381
150000	9153.561	22.9375		22.9375	22.52707	22.52707
154000	9397.656	23.5		23.5	22.55065	22.55065
158000	9641.751	24.125	-0.03125	24.09375	22.54382	22.55845
162000	9885.846	24.6875		24.6875	22.56587	22.56587
166000	10129.94	25.3125		25.3125	22.55898	22.55898
170000	10374.03	25.875		25.875	22.57968	22.57968
174000	10618.13	26.5	-0.03125	26.46875	22.57277	22.58611
178000	10862.22	27.0625	0.03125	27.09375	22.59226	22.57922
182000	11106.32	27.6875		27.6875	22.58538	22.58538
186000	11350.41	28.3125		28.3125	22.57879	22.57879

Volume vs. Hc

22.05260

Regression Output:

Constant	-107.291
Std Err of Y Est	18.27117
R Squared	0.999972
No. of Observations	60
Degrees of Freedom	58

X Coefficient(s)	404.3054
Std Err of Coef.	0.276862

ID) tank= 22.68871

Data Sheet 2 for Figure 4.3.2

- 3) Valve B4 was closed, and the power switch for the E-trAC inverter was engaged.
- 4) Via the inverter keypad, the pump speed was set to the maximum 60 Hz. Valve B3 was fully open to provide the least back pressure, indicated by the pressure gauge(P). A hand-held stopwatch was set to zero.
- 5) The pump was started.
- 6) As the dropping fluid level in the right tank(feed tank) was observed, starting and stopping levels for measuring the elapsed time were chosen arbitrarily, but quickly; a five-inch drop was chosen to give about a 30-second elapsed-time interval at the highest flow rate.
- 7) Before the pump was stopped, the back pressure was read from gauge P. The starting and stopping heights, the elapsed time, and the back pressure were recorded.
- 8) The stopwatch was reset. Valve B3 was slightly closed to make the back pressure about 20 psig. Subsequent back pressures at a given flow rate were 40 psig, 60 psig and 80 psig. After the 80 psig run, the flow rate was lowered by 10 Hz on the keypad, and valve B3 was opened fully again. The lowest flow rate was 20 Hz.
- 9) Steps 5 through 8 were repeated. When the right tank(feed tank) was

nearly empty, the pump was run until the fluid level could be seen in the 3" OD clear tubing between the 2" PVC elbows.

10) Valve R was closed, and valve L was opened. The tubing and clamps were removed from the left tank(the new feed tank) and set up on the right tank(now empty). The calibration could now continue.

11) Step 9 was repeated.

12) When the last data point, 20 Hz at 80 psig, was taken, the flow system was returned to its normal operating configuration as depicted in Figure 3.2.

13) The height interval data were converted to volume from the tank calibration data. From the volume change and the elapsed time, the flow rate at a given pump speed and back pressure was calculated. The relationship between flow rate and speed was linear.

Figures 4.4.1 - 4.4.4 present data from four pump calibrations. Figure 4.4.1 presents the results from the first pump calibration. Water-flow-rate data in l/s are plotted against the pump-frequency setting in Hz. The different symbols indicate the applied back pressure; the dotted line represents the regression used to calculate flow rates in subsequent experiments. Figure 4.4.2 presents results from the second pump calibration; this verified the first pump calibration after questionable turbulent polymer-solution data were obtained. Figure 4.4.3 presents results from the third pump calibration. Using a 50-

wppm solution of C832A eliminated shear-thinning effects as causing the questionable data. Among the three calibrations, the average calibration constant $\langle q \rangle$ and its standard deviation σ_q were 0.020242 and 0.000030 1/s/Hz, respectively, for which $\sigma_q/\langle q \rangle$ was 0.15 percent. After the third calibration, the absence of honeycomb was related to the turbulent-flow data problems.

Figure 4.4.4 presents results from the fourth pump calibration. This calibration differed from the previous three in that the flow passed through the test-pipe section rather than being rerouted through valve B3. With the small tube comprising the test-pipe section, the back pressure at top pump speed with valve B4 fully open was ~ 80 psid. With the large tube under the same conditions, the back pressure never got exceeded ~ 20 psid. The calibration constant was 0.019693 1/s/Hz, lower than before by about three percent.

Because high back pressures were unavoidable, instead of dismantling the pump-bypass loop, a long piece of 1" flexible tubing was clamped onto valve B6. The last few feet of its other end was put inside the left tank on the bottom. The tube was clamped as described in Step 2. Valve B3 remained closed, and valve B4 was left fully opened, allowing the back pressure to be what it may. The other aspects of calibration were identical to those previously described.

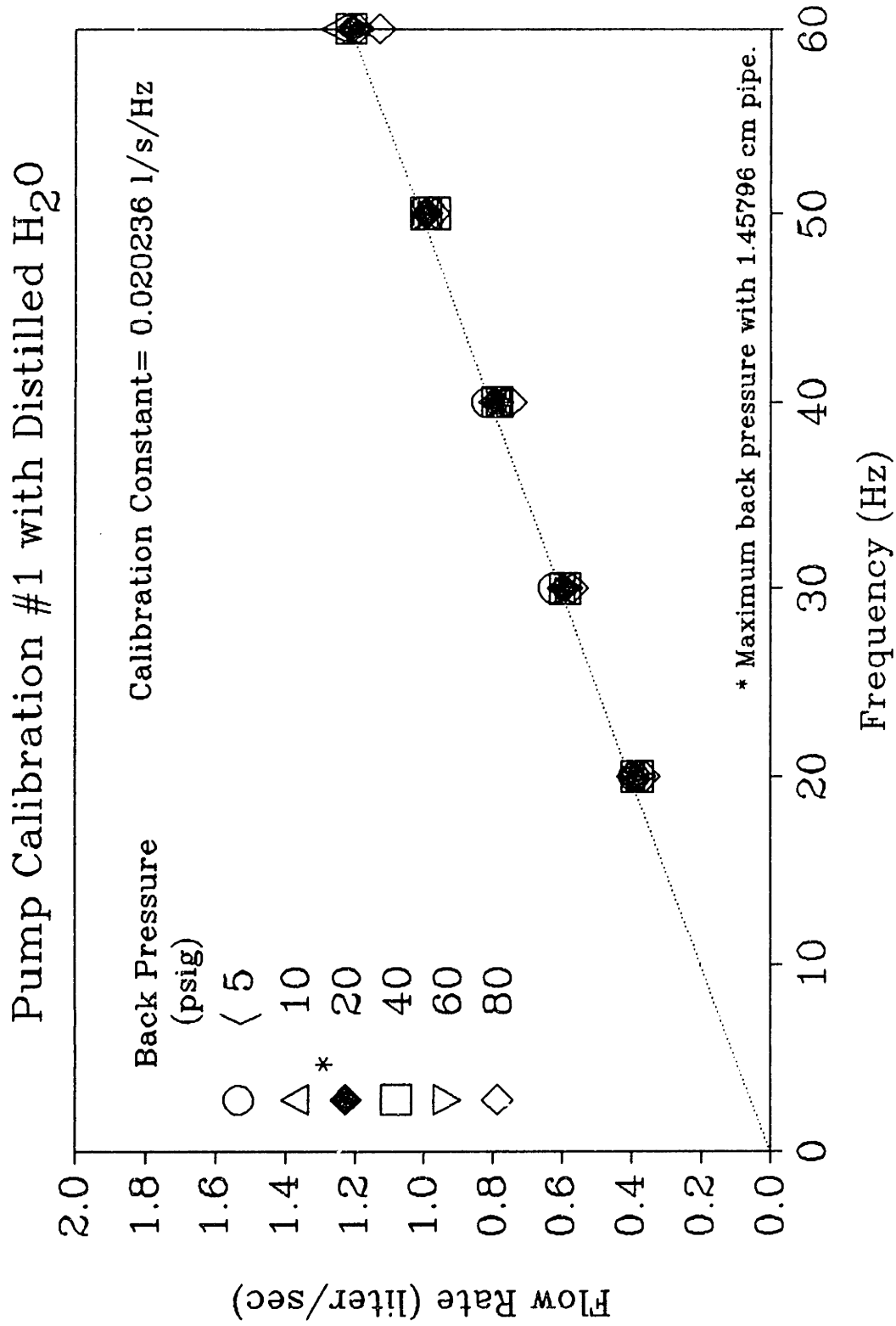


Figure 4.4.1: Pump Calibration #1 with Distilled H₂O

Flow System Calibration 9/27/89 & 9/28/89
14:55 11:09

H)left begin	H)left end	H)right begin	H)right end	DF (psid)	Freq. (Hz)	tf - to (sec)
20	15.0625			10	60	35.8
12	5.875			20	60	35.5
		23	18	40	60	27.5
		14.5	10.5	60	60	22.7
		7	4	90	60	17.5
23	18			80	60	27.7
12.875	7.875			100	60	33.9
		24	19	10	50	33.4
		16	11	20	50	33.3
		6.5	3.5	40	50	20.5
24	19			40	50	33.5
16	11			60	50	33.3
9	4			80	50	27.2
		24	19	5	40	40.7
		16	11	10	40	41.9
22	17			15	40	41.5
14	9			20	40	41.5
		23.5	18.5	40	40	42.1
		16.5	11.5	60	40	42.5
		9	4.5	80	40	39.5
23.5	19.5			5	30	42.7
17.5	13.5			10	30	44.1
11.5	7.5			20	30	44.7
		24	20	40	30	45.5
		18	14	60	30	46.1
		12	8	80	30	46.7
		7	4	5	20	50.3
23.5	20.5			10	20	49.7
19	16			20	20	50.5
14.5	11.5			40	20	51.7
10	7			60	20	53.9
5.5	3.5			80	20	35.9

Data Sheet 1 for Figure 4.4.1.

begin V)left (ml)	end V)left (ml)	begin V)right (ml)	end V)right (ml)	Flow Rate (l/s)	Flow Rate (gpm)
130631.5	98000			1.259906	19.96992
77600	37000			1.211940	19.20964
		151600	118210.5	1.214162	19.24487
		94842.10	68400	1.185744	18.79443
		44800	25000	1.131428	17.93350
150444.4	117400			1.192940	18.90848
93333.33	50400			0.971484	15.39834
		158210.5	124800	1.000315	15.85531
		104736.8	71600	0.995100	15.77266
		41555.55	21636.36	0.971667	15.40125
157368.4	124000			0.996072	15.78806
104000	70888.88			0.994327	15.76041
51200	24800			0.970588	15.38413
		158210.5	124800	0.820897	13.01148
		104736.8	71600	0.790855	12.53531
144000	110666.6			0.803212	12.73118
90842.10	57800			0.796195	12.61995
		154842.1	121578.9	0.790098	12.52332
		108000	74800	0.781176	12.38189
		58000	28400	0.749367	11.87771
154000	127333.3			0.624512	9.898718
114200	87600			0.603174	9.560512
74400	47777.77			0.595575	9.440063
		158210.5	131263.1	0.592249	9.387351
		118210.5	91473.68	0.579974	9.192789
		78000	51333.33	0.571020	9.050862
		44800	25000	0.393638	6.239292
154000	134000			0.402414	6.378399
124000	104000			0.396039	6.277355
94210.52	74400			0.383182	6.073563
64315.78	44444.44			0.368670	5.843548
34600	21600			0.362116	5.739671

Data Sheet 2 for Figure 4.4.1.

Freq. (Hz)	Flow Rate (l/s)	Flow Rate vs. Freq. (l/s) (Hz)
40	0.820897	
30	0.624512	
20	0.393638	
60	1.259906	
50	1.000315	
40	0.790855	
40	0.803212	
30	0.603174	
20	0.402414	
60	1.211940	
50	0.995100	
40	0.796195	
30	0.595575	
20	0.396039	
60	1.214162	
50	0.971667	
50	0.996072	
40	0.790098	
30	0.592249	
20	0.383182	
60	1.185744	
50	0.994327	
40	0.791176	
30	0.579974	
20	0.368670	
60	1.131428	
60	1.192940	
50	0.970588	
40	0.749367	
30	0.571020	
20	0.362116	

Regression Output:	
Constant	-0.01820
Std Err of Y Est	0.023612
R Squared	0.993462
No. of Observations	31
Degrees of Freedom	29
X Coefficient(s)	0.020236
Std Err of Coef.	0.000304

Data Sheet 3 for Figure 4.4.1.

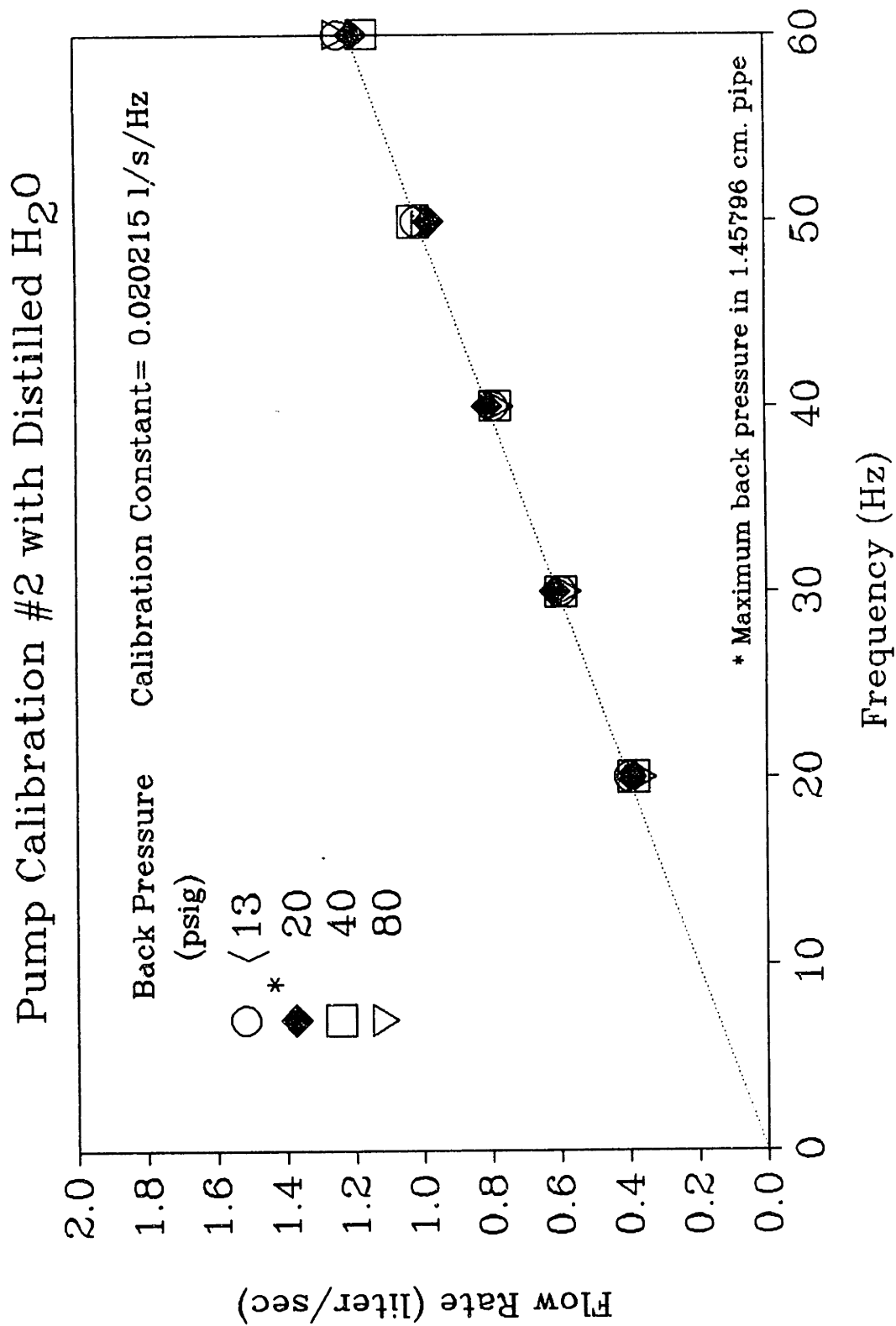


Figure 4.4.2: Pump Calibration #2 with Distilled H₂O

Flow System Calibration 10/22/89
14:09

H)left begin	H)left end	H)right begin	H)right end	DP (psid)	Freq. (Hz)	tf - to (sec)
		26	21	12.5	60	26.97
		16.5	11.5	20	60	27.7
		8.5	3.5	40	60	28.4
25	20			80	60	26.75
18	13			6	50	32.7
10.5	5.5			20	50	33.77
		25.5	20.5	40	50	32.64
		18	13	80	50	33.84
		11.5	6.5	5	40	41.97
25	20			20	40	41.04
18	13			40	40	42.28
10.5	5.5			80	40	42.72
		26	21	5	30	56.2
		19	14	20	30	54.14
		12.5	7.5	40	30	56.2
26	21			80	30	57.99
20	16			5	20	66.97
14	11			20	20	50.66
10	7			40	20	51.44
6	3			80	20	53.86

Data Sheet 1 for Figure 4.4.2.

begin V)left (ml)	end V)left (ml)	begin V)right (ml)	end V)right (ml)	Flow Rate (l/s)	Flow Rate (gpm)
		171684.2	138200	1.241535	19.67873
		108000	74800	1.198555	18.99749
		54800	21636.36	1.167733	18.50895
164000	130800			1.241121	19.67217
117400	84222.22			1.014610	16.08191
67600	34600			0.977198	15.48891
		168000	134666.6	1.021241	16.18701
		118210.5	84800	0.987308	15.64916
		74800	41555.55	0.792100	12.55504
164000	130800			0.808966	12.82238
117400	84222.22			0.784715	12.43799
67600	34600			0.772471	12.24392
		171684.2	138200	0.595804	9.443693
		124800	91473.68	0.615558	9.756794
		81555.55	48000	0.597073	9.463814
170842.1	137368.4			0.577232	9.149313
130800	104000			0.400179	6.342969
90842.10	70888.88			0.393865	6.242892
64315.78	44444.44			0.386301	6.123002
37800	18400			0.360193	5.709176

Data Sheet 2 for Figure 4.4.2.

Freq. (Hz)	Flow Rate (l/s)	Flow Rate vs. Freq. (l/s) (Hz)
60	1.241535	
60	1.241121	
60	1.198555	
60	1.167733	
50	1.021241	
50	1.014610	
50	0.987308	
50	0.977198	
40	0.808966	
40	0.792100	
40	0.784715	
40	0.772471	
30	0.615558	
30	0.597073	
30	0.595804	
30	0.577232	
20	0.400179	
20	0.393865	
20	0.386301	
20	0.360193	

Regression Output:	
Constant	-0.01237
Std Err of Y Est	0.019074
R Squared	0.995568
No. of Observations	18
Degrees of Freedom	16
X Coefficient(s)	0.020215
Std Err of Coef.	0.000337

Data Sheet 3 for Figure 4.4.2.

Pump Calibration #3 with 50 wppm C832A

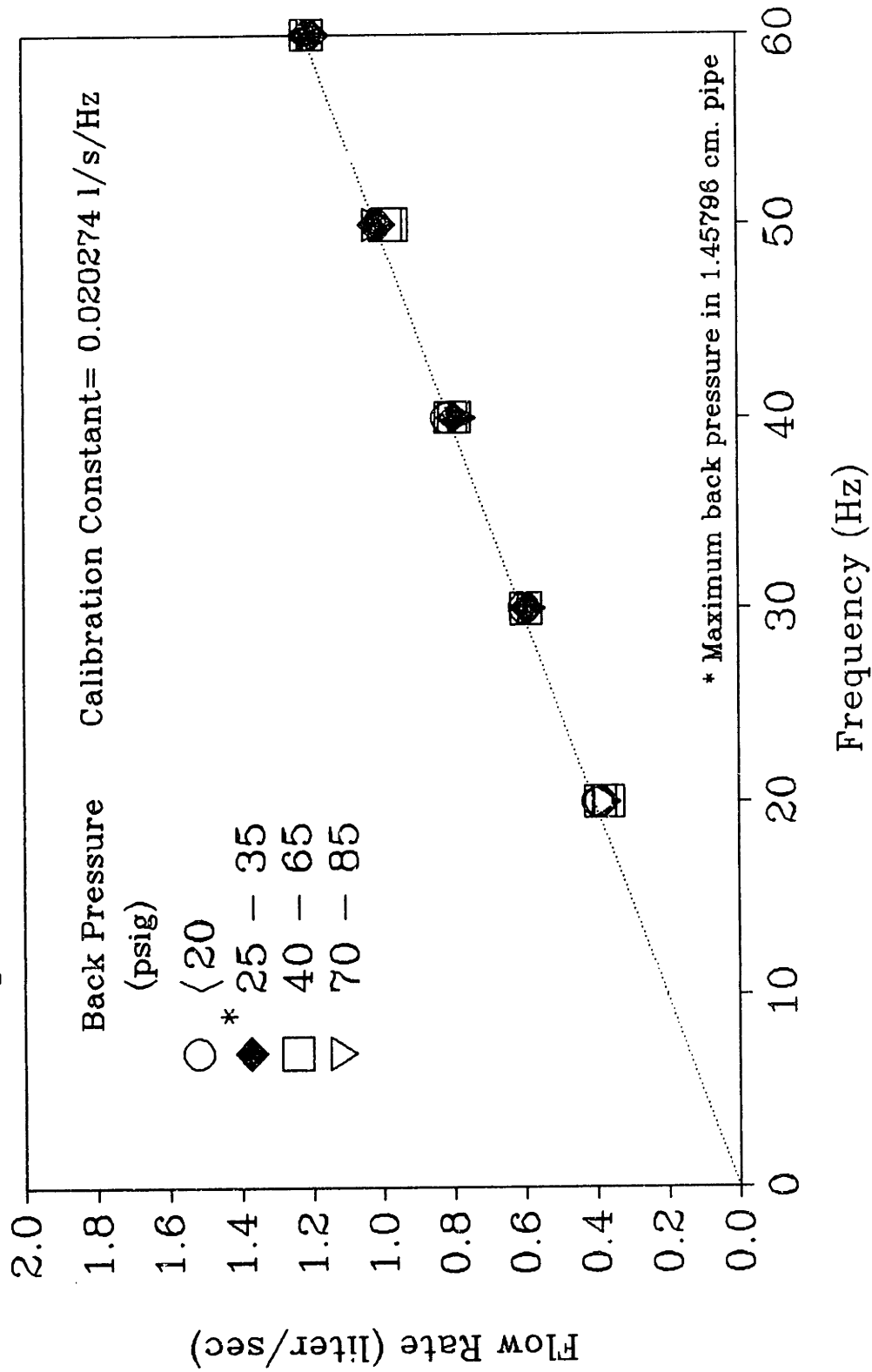


Figure 4.4.3: Pump Calibration #3 with 50-wppm C832A

Flow System Calibration 1/6/90
 With 50 ppm CS22A in 1E-4M NaCl

H)left begin	H)left end	H)right begin	H)right end	DP (psid)	Freq. (Hz)	tf - to (sec)
				30	60	
				30	60	
		17.5	12.5	30	60	27.3
		10.5	5.5	35	60	28.1
				55	60	
22.375	17.5			55	60	26.7
15	10			85	60	27.9
8	3			28	50	32.7
				38	50	
		22.5	17.5	32	50	32.9
		15.5	10.5	47	50	34.1
		8	3	65	50	33.1
				80	50	
22	17			75	50	32.9
15	10			17.5	40	40.7
8.5	3.5			25	40	41.1
				40	40	
		22.5	17.5	50	40	41.7
		16	11	55	40	41.7
		9.5	4.5	80	40	42.9
				10	30	
22	17			12	30	55.5
15	10			27	30	55.9
8.5	3.5			40	30	55.1
				65	30	
		22.5	17.5	70	30	57.9
				7.5	20	83.5
		16	11	15	20	84.9
		10	5	40.	20	
23	18			40	20	85.1
17	12			65	20	90.3
9	4			85	20	89.5

Data Sheet 1 for Figure 4.4.3.

Temp	begin V)left (ml)	end V)left (ml)	begin V)right (ml)	end V)right (ml)	Flow Rate (l/s)	Flow Rate (gpm)
23.6						
23.6						
23.6			114666.6	81555.55	1.212861	19.22424
23.6			68400	35000	1.188612	18.83988
23.5						
23.6	146400	114222.2			1.205160	19.10217
23.6	97578.94	64315.78			1.192227	18.89719
23.5	51200	18400			1.003058	15.89879
23.5						
23.6			148222.2	114666.6	1.019925	16.16615
23.6			101400	68400	0.967741	15.33902
23.6			51333.33	18727.27	0.985077	15.61379
23.5						
23.6	144000	110666.6			1.013171	16.05909
23.5	97578.94	64315.78			0.817276	12.95409
23.5	54421.05	21600			0.798565	12.65752
23.4						
23.5			148222.2	114666.6	0.804689	12.75458
23.5			104736.8	71600	0.794648	12.59543
23.5			61555.55	28400	0.772856	12.25002
23.1						
23.4	144000	110666.6			0.600600	9.519713
23.4	97578.94	64315.78			0.595047	9.431695
23.4	54421.05	21600			0.595663	9.441457
23.4						
23.4			148222.2	114666.6	0.579543	9.185948
			104736.8	71600	0.396848	6.290175
			65111.11	32000	0.390001	6.181644
	150444.4	117400			0.388301	6.154701
	110666.6	77600			0.366186	5.804178
	57789.47	24800			0.368597	5.842389

Data Sheet 2 for Figure 4.4.3.

Freq. (Hz)	Flow Rate (l/s)	Flow Rate vs. Freq. (l/s) (Hz)
60	1.212861	
60	1.205160	
60	1.192227	
60	1.188612	
50	1.003058	
50	1.019925	
50	0.967741	
50	0.985077	
50	1.013171	
40	0.817276	
40	0.798565	
40	0.804689	
40	0.794648	
40	0.772856	
30	0.600600	
30	0.595047	
30	0.579543	
30	0.595663	
20	0.396848	
20	0.390001	
20	0.388301	
20	0.366186	
20	0.368597	

Regression Output:	
Constant	-0.01679
Std Err of Y Est	0.014472
R Squared	0.997386
No. of Observations	21
Degrees of Freedom	19
X Coefficient(s)	0.020274
Std Err of Coef.	0.000238

Data Sheet 3 for Figure 4.4.3.

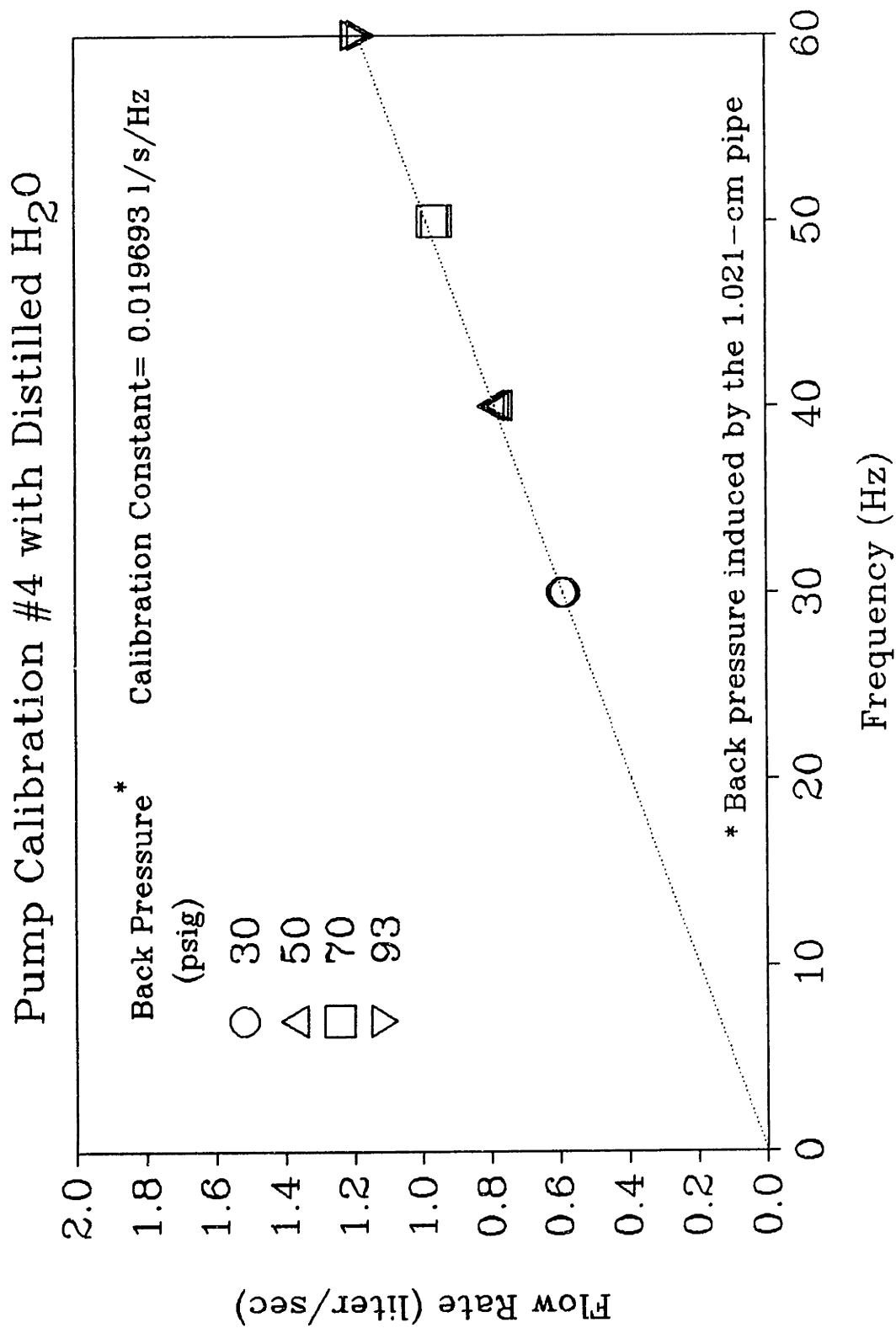


Figure 4.4.4: Pump Calibration #4 with Distilled H₂O

Flow System Calibration 11/2/90
9:43 - 10:55

H)left begin	H)left end	H)right begin	H)right end	DP (psid)	Freq. (Hz)	tf - to (sec)
		24	18	93	60	34.1
		16.5	10.5	70	50	40.9
25	19			50	40	50.2
17.5	12.5			32	30	56.3
		25.5	19.5	93	60	33.8
		17.5	11.5	70	50	41.3
		10	5	50	40	42.7
25	20			30	30	56.5
18	12			93	60	33.4
10	4			70	50	41.4
		24	18	50	40	51.7
		16	11	30	30	56.7
		10	4	50	40	51.1

Regression Outputs:

Constant	-0.00618	93	60
Std Err of Y Est	0.012658	93	60
R Squared	0.997023	70	50
No. of Observations	13	70	50
Degrees of Freedom	11	70	50
		50	40
X Coefficient(s)	0.019688	50	40
Std Err of Coef.	0.000324	50	40
		50	40
		32	30
		30	30
		30	30

Regression Outputs:

Constant	-0.00651	60
Std Err of Y Est	0.013326	50
R Squared	0.998171	40
No. of Observations	4	30
Degrees of Freedom	2	
X Coefficient(s)	0.019693	
Std Err of Coef.	0.000595	

Data Sheet 1 for Figure 4.4.4.

begin V)left (ml)	end V)left (ml)	begin V)right (ml)	end V)right (ml)	Flow Rate (l/s)	Flow Rate (gpm)
		158210.5	118210.5	1.173020	18.59275
		108000	68400	0.968215	15.34652
164000	124000			0.796812	12.62973
114200	80800			0.593250	9.403211
		168222.2	128000	1.190006	18.86198
		114666.6	74800	0.965294	15.30023
		65111.11	32000	0.775435	12.29090
164000	130800			0.587610	9.313818
117400	77600			1.191616	18.88751
64315.78	24800			0.954487	15.12893
		158210.5	118210.5	0.773694	12.26330
		104736.8	71600	0.584424	9.263309
		65111.11	25000	0.784953	12.44176

1.173020	60	1.173020
1.190006	50	0.968215
1.191616	40	0.796812
0.968215	30	0.593250
0.965294	60	1.190006
0.954487	50	0.965294
0.796812	40	0.775435
0.775435	30	0.587610
0.773694	60	1.191616
0.784953	50	0.954487
0.593250	40	0.773694
0.584424	30	0.584424
0.587610	40	0.784953

1.184881
0.962665
0.782724
0.588428

Data Sheet 2 for Figure 4.4.4.

4.5 Set-Up Procedure for the Gravity-Driven Flow System

In this description of the procedure, it is assumed that both the 0.1- and 1.0-psid PTs had been calibrated recently, that the Micro Motion mass-flow meter was in working order, and that the system had been adequately flushed with distilled water. Figure 3.1 shows a schematic of the gravity-driven flow system.

- 1) The mass-flow meter was turned on, and valve B6 was opened to flush out any air inside the flow meter. The FMS-3 was checked to make certain that it was displaying the flow rate in ml/s and the cumulative fluid volume in liters. Valve B6 was closed again.

- 2) All the valves on the PT board were shut. The ends of the two small connecting tubes from the board were placed in a beaker. Each valve was opened individually to release trapped air in the board and in the pressure-tap lines. The valves were shut again, and the two small tubes were attached to the arms of the 1.0-psid PT. The valves corresponding to the desired pair of taps were opened. The PE valve was opened to remove any pressure differentials across the transducer. The PT bleed screws were opened to release any trapped air and then were closed. The PT cable was connected to the carrier demodulator. The span and zero dials on the demodulator were set to their appropriate values. The HP-3467A Logging Multimeter and the carrier demodulator then were turned on. The FMS-3 was reset. If the multimeter was not displaying a near zero voltage from the carrier demodulator, the zero setting was changed. If that seemed

insufficient, the PT bleed screws were reopened. If the problem still persisted, then the tap lines were degassed again.

3) With valve B6 closed and valves B5 and N1 open, the tank was filled to near capacity. The water level was not so high as to cause spillage over the sides when the mixer operated. The height was measured, and the volume was calculated.

4) Given the volume of distilled water in the tank, the master batch concentration, and the target salt and polymer concentrations, the required masses of salt and of master batch were calculated.

5) A clean, small plastic boat was weighed. On an analytical balance, the boat was filled with the required amount of salt. The salt-laden boat was reweighed and then carried to the tank. Forceps were used to handle the boat. The boat was inverted above the tank, dumping the salt into the fluid. The now-empty boat was reweighed. The actual amount of added salt was calculated.

6) In adding the master batch, a beaker with a pouring lip was placed on a top-loading balance and weighed. Master batch from its jar was poured into the beaker. A small glass stirring rod was used to control and to guide the fluid because of its viscoelastic properties. Because the fluid tended to stick to the walls of the beaker, more master batch than that calculated was poured into the beaker. The fluid-filled beaker was reweighed and was carried over to the tank. The fluid was added by inverting the beaker

over the tank. The beaker was held above the tank until the last diaphanous streamers of fluid between the beaker and water surface had broken. The beaker was reweighed. The actual amount of master batch added was calculated. If the beaker had to be used again, this procedure was repeated. In this instance, because the walls of the beaker were already wetted, no "stickage" compensation was necessary.

7) Clamped to the side of the tank, the stirrer was positioned so that its impeller blades were well under water. The stirrer was turned to the lowest speed setting and was left running for at least one hour. The actual time depended upon the target polymer concentration. During this time, the actual salt and polymer concentrations were determined.

8) After the mixing period, the stirrer was stopped. The first part of the experiment then was performed.

9) After the first part was finished, the height of fluid in the tank was measured, and the remaining volume was calculated. Given the target salt concentration for the next part, the required amount of additional salt was calculated. Depending upon the required mass of salt, either a large plastic boat or an empty plastic salt bottle was weighed on a top-loading balance, filled with salt, and reweighed. Due to the larger salt masses involved, no special handling was needed. After the salt was added to the fluid, the fluid was stirred for another hour to dissolve the salt crystals completely and to allow solution equilibration. The new salt concentration was determined.

10) After the mixing period, the stirrer was turned off. The valves on the PT board were shut, and the carrier demodulator was turned off. The two small connecting tubes from the PT board were removed from the 0.1-psid PT and attached to the 1.0-psid PT. The cable belonging to the 0.1-psid PT was removed from the carrier demodulator and that belonging to the 1.0-psid PT was inserted. The span and zero dials were set to the appropriate values, and the carrier demodulator was turned on again. Two valves on the PT board were opened. The bleed screws of the 1.0-psid PT were opened to flush out any trapped air and then were closed.

11) The second part of the experiment was performed.

12) After the second part had ended, steps 9 and 10 were repeated. Then the third and final part of the experiment was performed.

13) After the experiment was finally over, step 10 was repeated. To remove any residual salt and polymer from the system, the system was flushed with distilled water by simultaneously filling the tank and keeping valve B6 open. At some point valve B5 was closed to flush fluid from the needle-valve bypass. During this flushing period, the 1.0-psid PT measured the pressure drop, and the mass-flow meter displayed the flow rate. When the pressure drop and the flow rate reached higher and lower constant values, respectively, the flushing could be stopped as very little drag reduction remained. During this time, both PTs were flushed with water from the water manometer to remove any polymer or salt that might have entered into the diaphragm chambers. After the

system and the PTs were flushed, the water supply valve and valve B6 were closed. The carrier demodulator, logging multimeter, and the mass-flow meter were shut off. Valves B5 and N1 were left fully open.

4.6 Experimental Run in the Gravity-Driven Flow System

1) After the set-up was complete and when the solution was fully mixed, the flow-totalizer display on the FMS-3 was set to zero. Valves B4, B5, and N1, as shown in Figure 3.1, were fully open.

2) The initial "zero voltage" of the 1.0-psid PT was recorded. The HP-3467A printer was started, and valve B6 was opened.

3) When the flow reached steady state, the flow rate displayed by the FMS-3 was recorded. Valve B6 was closed after about six liters had passed, as indicated by the flow totalizer. This corresponded to about six printed output scans per data point, the usual minimum.

4) The HP-3467A printer was stopped, the PT data channel was disengaged, and the temperature-probe data channel was engaged. The temperature was recorded, and then the data channels were switched back. The final "zero voltage" PT output was recorded. The paper in the printer was advanced to leave a blank between data points.

5) The flow-control valves were adjusted for the next data point. As long as the mass-flow meter measured the flow, steps 2 through 4 were repeated. For the next two data points, valve B5 was half-open and fully closed with N1 fully open. With valve B6 closed, valve N1 was closed gradually before each data point. With the 1.0-psid PT on line, the usual turn sequence was 3, 6, and 7.

6) At turn 7, the flow rate was ~ 40 ml/s; this corresponded to $Re_s \approx 3600$, at the high end of the transitional flow regime. At this point, the 0.1-psid PT replaced the 1.0-psid PT and resumed sensing the pressure drop.

7) The long 1" flexible vincon tube on the back end of valve B6 was removed and was attached to the tip of the funnel in the flow-diverter unit. The $\frac{3}{8}$ "-port-to- $\frac{1}{2}$ "-stub reducer attached to the pivoting arm was connected to the end of valve B6. Before proceeding, the locations of the ring-stand-mounted pivoting arm and funnel were adjusted to the proper positions; when the arm just crossed over to the receptacle from the funnel, the timer just began to count. On the switch box, the green light illuminated just as the red light went dark. Then the timer was reset to zero via the reset button on the switch box. Valve N1 was not adjusted.

8) The initial "zero voltage" of the 0.1-psid PT was recorded. The HP-3467A printer was started, and valve B6 was opened.

9) After steady state, the arm of the flow diverter was moved over the

receptacle, starting the timer. The arm was moved back to the funnel after either 30 seconds had elapsed or ~ 1000 ml of solution had been collected, whichever took longer. During this time, the flow rate displayed by the FMS-3 was recorded. After the arm was moved back, valve B6 was closed. The elapsed time was recorded, and then the timer was reset.

10) Step 4 was repeated.

11) The volume of fluid collected in the receptacle was determined by pouring the fluid into graduated cylinders. The solution was discarded down the sink drain.

12) Steps 8 through 11 were repeated. Both the mass-flow meter and the timer-and-flow-diverter unit measured the flow rate independently. The subsequent N1 turn sequence was $7\frac{1}{2}$, 8, $8\frac{1}{2}$, $8\frac{3}{4}$, 9, $9\frac{1}{4}$, and $9\frac{1}{2}$ turns. Below a flow rate of ~ 13 ml/s, the mass flow meter could not measure, and its display went dark. After $9\frac{1}{2}$ turns, at a flow rate of ~ 10 ml/s, valve N1 was closed just enough to halve the PT output from the previous data point. This diminution continued until the flow was slow small that the flow diverter actually impeded the flow. This point usually ended this part of the experiment, but more data points could be taken at higher flow rates if so desired.

13) After the set-up for the next part, the procedure began again at step 1. If the last part had been completed, the system was washed out as described in step 13 in §4.5.

4.7 Set-Up Procedure for the Pump-Driven Flow System

In this description of the procedure, it is assumed that the 0.1-, 1.0-, and 10-psid PTs had been calibrated recently and that the system had been adequately flushed with distilled water. Figure 3.2 shows a schematic of the pump-driven flow system.

1) Valve B was closed, and valve B3 was opened to permit gravity-driven flow through the system. The rest is the same as Step 1 in §4.5 but with no FMS-3.

2) The E-trAC inverter was switched on. Via the keypad, the pump speed was set to the value that caused the PT to give full-scale output under Newtonian flow conditions for a given tap pair. The PE valve was closed. The pump was started, and the PT output was monitored visually for about a minute. This ensured both a clean system and properly operating PT as well as warmed up the pump. Then the pump was stopped.

From this point the set-up procedure for filling the tanks and for preparing the solutions diverged due to the two different methods used to make the master batch; the procedures converge after step 10.

3.1) Under method #1, the tanks were filled to near capacity via the distilled-water hose. Valves L and R were shut. The water levels were measured in both tanks with a metal yardstick. From the "look-up" tables the volumes in both tanks were interpolated.

4.1) Step 4 in §4.5 was done for each tank.

5.1) Step 5 in §4.5 was done for each tank.

6.1) Step 6 in §4.5 was done for each tank.

7.1) Clamped to the side of one tank, the stirrer was positioned with its impeller blades well under water; it operated at its lowest speed for about 15 minutes. To guard against degradation, the stirrer was stopped whenever a large vortex formed. Over about 90 minutes, the stirrer alternated between the tanks at about 15 minute intervals.

8.1) Because the desired solution temperature was 25°C, heating was generally required, but this was not always the case. The ambient laboratory temperature ranged between 18°C and 26°C, depending mostly upon laboratory ventilation. Also, the temperature of the distilled water coming from the spigot reached temperatures as high as 29°C; thus, the amount of warming varied widely. A 0°C-to-30°C thermometer was used to monitor the solution temperature in both tanks about every five minutes. As needed, a drum heater on either tank warmed the solution at a low heating rate. The warming continued intermittently until the solution temperature reached about 25°C.

9.1) During the mixing and heating period, valves B and B3 were opened to remove most of the hold-up fluid between the tanks and the pump's suction flange. When

the hold-up fluid had been drained away, these two valves were closed.

3.2) Under method #2, the tanks were filled to heights of about 24 inches, corresponding to volumes of ~ 160,000 ml per tank, via the distilled-water hose. Valves L and R were closed.

4.2) Given the amount of polymer in the master batch vessel and the target salt and polymer concentrations, the required mass of salt and volume of distilled water were calculated for each tank. The tank volumes were converted to heights from the "look-up" tables.

5.2) See Step 5.1.

6.2) Due to the elevated tanks and cumbersome mixing vessels, a ladder was used when adding master batch to the tanks. The metal yardstick was placed inside the tank at its proper position and was clamped in an upright position against the wall to provide continuous height readings. One of the master batch vessels was uncovered and was placed on the bucket rack of the ladder. A wash bottle filled with distilled water also was placed on the bucket rack. A master batch vessel was held above its corresponding tank and then tipped to empty its contents into the tank. When almost all the master batch had been decanted, the vessel was returned slowly to its upright position to break the last diaphanous streamers of fluid between the vessel and the water surface. The wash bottle washed any master batch drops that stuck on the vessel lip back into the vessel. The

inner surfaces of the vessel were rinsed free of master batch fluid, which collected in the bottom of the vessel. After the vessel was filled partially with distilled water, it was moved in a gyrating manner to cause the liquid inside to swirl over the interior surface. This action removed master batch fluid that adhered to the interior surface. Care was taken not to lose any fluid inadvertently. After this swirling, the vessel was filled to near capacity with more distilled water, and then its contents were emptied into the tank. The rinsing, gyrating, filling, and emptying steps were repeated until the fluid height in the tank reached the target height.

7.2) Clamped to the side of one tank, the stirrer was positioned with its impeller blades well under water; it operated at its lowest speed for about 15 minutes. As the fluid was mixed, the yardstick was unclamped from the tank wall and held upright in the swirling liquid to wash away any master batch fluid stuck onto it. When no master batch fluid remained on the yardstick and when the solution seemed fairly homogeneous, the yardstick was removed. After the yardstick was rinsed with distilled water and dried, it was clamped to the inner wall of the other tank at the permanent position.

8.2) Step 6.2 was repeated for the other tank. During this time, the stirrer was mixing the solution in the other tank. To guard against degradation, the stirrer was stopped whenever a large vortex formed. The other solution was simultaneously mixed and warmed up to the desired 25°C. Heating was generally required, but this was not always the case. The rest is the same as Step 8.1.

9.2) When the master batch fluid had been transferred entirely into the second tank, step 7.2 was done for the second tank. The solution in the second tank also was warmed as described in step 8.2. Over about 90 minutes, the stirrer alternated between the tanks at about 15 minute intervals, and solution temperature in both were monitored about every five minutes.

10) After the warming and mixing period ended, the heaters and stirrer having been stopped, the system was ready for the first half of the experiment to commence.

11) After the first part was finished, valves L and R were shut. The height of fluid in both tanks were measured, and the remaining volumes were determined. Given the target salt concentration for the next part, the required amount of additional salt was calculated. A top-loading scale capable of weighing more than 3000 g was required. A empty large plastic bottle was weighed, filled with salt, and reweighed. With such large salt masses no special handling was needed. After its contents were dumped into the tank, the empty bottle was reweighed.

12) When ~2000 g NaCl was added to each solution, the salt did not easily dissolve, rather it remained mostly as crystals on the bottom of the tank. Instead of clamping the stirrer to the tank as before, the stirrer was held manually during mixing. For at least five minutes, the stirrer was moved to apply direct agitation to the "salt drifts" on the tank bottom. Only when the "salt drifts" had disappeared did the mixing stop. Each solution was treated in this way. During this step, that the stirring became

markedly easier as the salt dissolved evidenced the profound affect of salt on the polyelectrolyte solution. The solutions sat for about an hour to dissolve completely the salt crystals and to allow solution equilibration. The new salt concentrations were determined.

13) The temperature of the solutions were monitored with a 0°C-to-30°C thermometer during the equilibration period. After initial temperature readings, the drum heaters were used judiciously to warm the solutions back to about 25°C. Because the 10-psid PT was used at the end of the first half and at the start of the second half, switching PTs and degassing the lines were generally unnecessary.

14) Valves B and B3 were opened to release any fluid held up between the tanks and the pump's suction flange. These valves were closed when the hold-up fluid had been drained.

15) After the warming period with the heaters shut off, the second half of the experiment was performed.

16) The experiment usually ended with the 10-psid PT on line. If this was not the case, the carrier demodulator was turned off, and the cable of the on-line PT was removed from the carrier demodulator. Step 1 was done, but using the 10-psid PT instead. The valves on the PT board were adjusted to access the desired tap pair. The PE valve was closed, readying the PT for pressure drop measurements.

17) Valve B6 was closed, and the valve B3 was opened. Valves B5 and N1 were opened fully, if they were not already. The nozzle of the distilled-water hose was opened, and the hose was clamped to the inside of the right tank. The distilled-water valve was opened, filling the tanks. When the water could be seen filling the 3"-OD clear tube, valve B6 was opened to permit gravity-driven flow through the system. As the residual salt and polymer was washed from the system, the pressure drop noticeably increased. At some point the valve B5 was closed to flush the needle-valve bypass. Valve B5 was reopened. When the pump bypass seemed relatively free of polymer and salt, valve B3 was closed.

18) While the tanks were being filled, the pump was started and jogged up to maximum speed via the "shift" and "▲" keys. Again, as the salt and polymer were removed from the system, the pressure drop would rise towards its Newtonian value. The water level was watched constantly to avoid running the pump "on empty," a certain way to damage it. The pump was stopped often to allow the tanks to refill. The pump was operated a few more times to ensure that most of the salt and polymer had been removed. The distilled water valve was closed, the pump was stopped, and the power to the E-trAC inverter was cut. It often required several days to purge the system completely.

19) The valves on the PT board were closed. The two connecting tubes from the PT board were removed from the 10-psid PT, and the ends were placed in a beaker. The carrier demodulator and logging multimeter were shut off. Finally, the 0.1-, 1.0-,

and 10-psid PTs were flushed with water from the water manometer to remove any polymer or salt that might have entered into their diaphragm chambers.

4.8 Experimental Run in the Pump-Driven Flow System

1) After the set-up was complete and when the solution was fully mixed, valves L and R, as shown in Figure 3.2, were opened to fill the volume between the tanks and the pump's suction flange with solution.

2) With the 1.0-psid PT on line, valve B3 was opened to allow gravity-driven flow through the pump bypass. As the new solution displaced the old, the PT output dropped and took time to reach steady state. At this point valve B3 was closed. Valves B5 and N1 were fully open.

3) The initial pump speed was set on the keypad of the E-trAC inverter. This setting was 15 Hz, corresponding to that speed at which the 1.0-psid PT gave full-scale output. The initial "zero voltage" of the PT was recorded.

4) The HP-3467A printer was started, and the pump was started.

5) Due to the "old" hold-up in the pump, the PT output dropped and took more time to reach steady state. After steady state, the pump continued running at this speed until four scans had been printed out, the usual minimum.

6) After an initial setting of 15 Hz, the pump was jogged up to a higher speed via the "shift" and "▲" keys on the inverter. This higher speed depended upon the level of drag reduction, i.e. how much the pressure drop had fallen from the Newtonian value at this same flow rate. For example, if the initial output was 6 V and the transducer's full-scale output was 10 V, the next setting would be that which gave an 8 V output. After at least four scans, the pump speed was increased to that at which the PT output was full-scale. After four scans, the pump setting was reduced to 10 Hz, after which the pump was stopped.

7) See Step 4 in §4.6.

8) With the pump idle, valve B3 was opened, temporarily permitting gravity-driven flow. Valve B6 was closed quickly after. The rest is the same as Step 7 in §4.6.

9) At this point, if the tap pair needed changing, then the PE valve was opened, the appropriate valves on the PT board were adjusted, and the PE valve was closed.

10) The initial "zero voltage" was recorded. The printer was started, and valve B6 was opened. After steady state, the arm of the flow diverter was moved over the receptacle, starting the timer. After 15 seconds the arm was moved back to the funnel. At lower flow rates, at least 1000 ml was collected, unless the elapsed time exceeded 150 seconds. Valve B6 was closed. The elapsed time was recorded, and then the timer was

reset.

11) Step 7 was repeated.

12) See Step 11 in §4.6.

13) Valve B5 was closed. For the subsequent data points, valve N1, a 10-turn valve, was closed gradually at each data point. With the 1.0-psid PT on line, the usual turn sequence was 3, 6, 7, and 8. Steps 10 through 12 were repeated.

14) At this point, the 0.1-psid PT replaced the 1.0-psid PT and resumed sensing the pressure drop.

15) The subsequent turn sequence for valve N1 was 8, 8½, 8¾, 9, 9¼, and 9½ turns. After 9½ turns, at a flow rate of ~ 10 ml/s, valve N1 was closed just enough to halve the PT output from the previous data point. This diminution continued until the flow was slow small that the flow diverter actually impeded the flow. At this point valve N1 was opened sequentially to record more data points. This turn sequence was 7, 6, 3, and 0. Steps 10 through 12 were repeated for all these turn settings.

16) After valve N1 was fully open, the 10-psid PT replaced the 0.1-psid PT. Valve B5 was opened. The flow diverter was disengaged from valve B6. The tube end was removed from the funnel and clamped onto valve B6.

17) Valve B3 was closed, and valve B6 was opened. The pump speed was set at 60 Hz.

18) The initial "zero voltage" of the PT was recorded. The printer was started, and then the pump was started. After an initial setting of 60 Hz, the pump was jogged down to the next setting via the "shift" and "▼" keys on the inverter. The subsequent settings were 50, 40, 30, 20, 15, and 10 Hz, after which the pump was stopped. (Note: Jogging the pump and stopping on a targeted setting with 0.01 Hz precision required considerable practice. Because conserving solution was most important, the actual pump settings only approximated the settings given here. For example, an acceptable sequence was 60.00, 49.00, 41.00, 31.00, 22.00, 15.00, and 9.00 Hz.)

19) The first part ended, and the second part was set up.

20) After the set-up for the second half, the procedures for this part were nearly identical. The order of PT use was 10, 1.0, and 0.1 psid rather than 1.0, 0.1, and 10 psid. Steps 3 and 6 differed slightly. With the 1.0-psid PT on line, the initial pump speed was that which gave near full-scale output under experimental conditions. Subsequently, the pump would be jogged down to 10 Hz in regular increments.

4.9 Data Reduction

Figure 4.9 presents a flow-chart diagram for reducing the data. The data recorded in the laboratory notebook and that printed out on thermal paper were entered into a LOTUS-123™ spreadsheet. It contained all the calibration constants, intertap distances, and physical properties of H₂O and aqueous salt solutions to convert the flow rate, pressure drop, and temperature data into derived variables that could be analyzed. The final derived variables were T_w in dyne/cm², Q in cm³/s, $Re_s\sqrt{f}$, and $1/\sqrt{f}$.

The PT output, a sequence of voltage readings, was corrected by the initial and final "zero" readings to obtain the corrected output. The pressure drop in psid between the tap pair, ΔP , was calculated by dividing the corrected output by the appropriate PT constant. The wall shear stress in dyne/cm², T_w , was calculated by multiplying ΔP by the quantity $D/4L$, where D and L are the pipe ID and intertap distance, respectively. The flow data, both pump- and gravity-driven, were converted to give Q in ml/s. If the pump frequency in Hz was given, it was simply multiplied by the pump calibration constant and by 1000; if the data were the sample volume and time in ml and seconds, respectively, Q was calculated by dividing the time into the volume. The average velocity $\langle U \rangle$ in cm/s was calculated from $4Q/\pi D^2$, the flow rate in cm³/s divided by the pipe cross-sectional area in cm². From the temperature in °C and the salt concentration of the experimental solution, the density ρ , viscosity η , and the kinematic viscosity ν of the solvent were determined (CRC Handbook of Chemistry and Physics; Chemical Engineers' Handbook). Multiplying D and $\langle U \rangle$ together and dividing that by ν gave Re_s , the solvent-based Reynolds number. The friction velocity $u\tau$ in cm/s equalled $\sqrt{(T_w/\rho)}$. The

Data-Reduction Flow Diagram

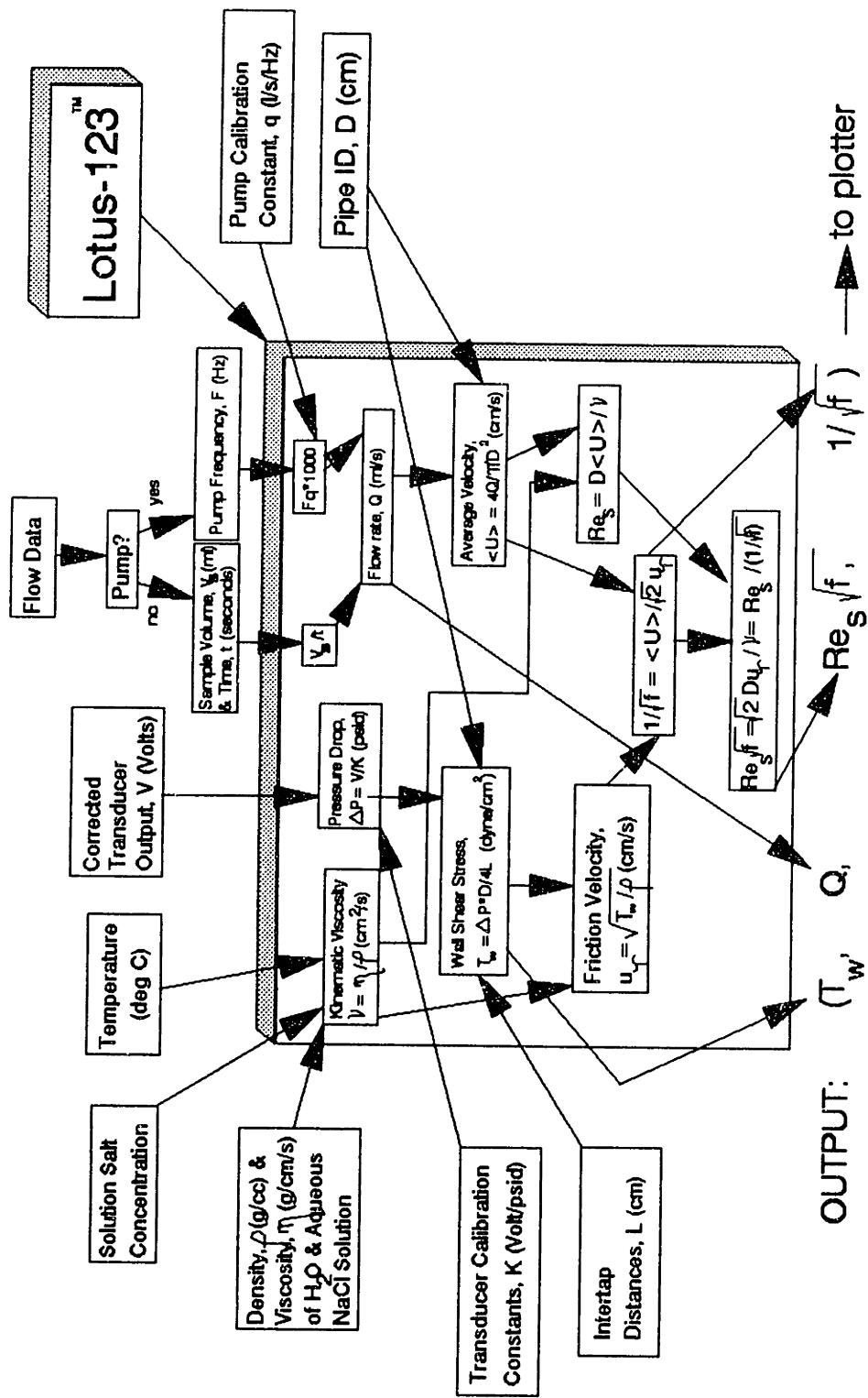


Figure 4.9: Data-Reduction Flow Diagram

ordinate of a Prandtl-Karman plot, $1/\sqrt{f}$, was derived by dividing $\langle U \rangle$ by $\sqrt{2}u_\tau$; its abscissa, $Re_\tau\sqrt{f}$ (actually $\log_{10}Re_\tau\sqrt{f}$), was derived by dividing Re_τ by $1/\sqrt{f}$. The four final derived variables were used in plots to display the experimental trends. Further analysis is given in the Discussion in Chapter VI.

CHAPTER V

RESULTS

Drag-reduction experiments were conducted with saline solutions of seven polyelectrolytic hydrolyzed-polyacrylamide(HPAM) additives, ranging in molecular weight from 1×10^6 to 20×10^6 g/mole, in two pipes of inner diameters 1.458 and 1.021 cm.

The experimental results are presented in three sections, dealing respectively with solvent runs, polymer-solution runs, and flow parameters extracted from the data.

5.1 Solvent Runs

Numerous solvent runs were conducted before and after polymer-solution runs. Adherence of the solvent to Poiseuille flow(L) and Newtonian turbulent flow(N) ensured that the system was free of flow artifacts and contained no residual polymer. For pipe flow, the general equations for the Newtonian baselines L and N are, respectively:

$$\frac{1}{\sqrt{f}} = \frac{Re_s \sqrt{f}}{16} \quad (2.3-1)$$

$$\frac{1}{\sqrt{f}} = A_n \log(Re_s \sqrt{f}) - B_n \quad (5.1-1)$$

where f is the Fanning friction factor, Re is the Reynolds Number, and subscript s

implies the use of solvent physical properties. In Equation 5.1-1, the universal Prandtl-Karman(PK) correlation for turbulent pipe flow results when $(A_n, B_n) = (4, 0.4)$, equation 2.3-2. (A minus sign is put before B_n to render it positive in most cases.)

Solvent runs have been arranged in five sets as shown in Table 5.1.1, which cites the number of runs and the average turbulent flow parameters. Solvent runs in the 1.458- and 1.021-cm pipes were respectively designated S00000??? and T00000??? with the last three places(???) as follows: Data Set #1 contained runs 243, 245, 248, 251, 252, 255, 258, 261, 264, 267, 270, 272, 276, 279, 282, 285, 288, 293, 298, 300, 302, 305, 308, 311, 314, 317, 320, 323, 326, 329, 333, 336, and 339 taken in the pump-driven system with the 1.458-cm pipe. Data Set #2 contained runs 341, 342, 345, 348, 351, 354, 358, 361, 364, 367, and 370 taken in the pump-driven system with the 1.021-cm pipe. Data Sets #3, #4, and #5 were taken in the gravity-driven system with the 1.458-cm pipe and consisted of the following runs: 011 - 013, 016, 022, 025, 034, 038, and 042; 065-069, 072, 077, 081, and 085; and 089, 093, 100, 116, 117, 125, and 131.

Table 5.1.1
Solvent Data Set Parameters

Solvent Data Set Number	System	Pipe ID	Pipe Aspect Ratio	Number of runs	Turbulent Flow Parameters	
		(cm)	L/D		A_n	B_n
1	Pump	1.458	183.0	33	4.0	0.4
2	Pump	1.021	203.2	11	4.0	0.4
3	Gravity	1.458	209.8	9	4.0	0.4
4	Gravity	1.458	209.8	10	2.98	-2.00
5	Gravity	1.458	209.8	7	3.54	-0.79

In Figure 5.1.1, solvent data set 1 is plotted in semilogarithmic PK coordinates, the ordinate and abscissa of which are $1/\sqrt{f}$ and $Re_s\sqrt{f}$, respectively. At the lowest flow rate, $Re_s\sqrt{f} \approx 40$, which corresponds to $Re_s \approx 100$ in the laminar flow regime L. As $Re_s\sqrt{f}$ increases, the data follow L until $Re_s\sqrt{f} \approx 180$ ($Re_s \approx 2000$). Here, the flow begins a transition to turbulence. The data drop down from L towards the PK baseline. At $Re_s\sqrt{f} \approx 400$ ($Re_s \approx 4000$), the flow has become fully turbulent; thereafter the data continue along PK up to the highest flow rate, which corresponds to $Re_s\sqrt{f} \approx 9000$ ($Re_s = 140000$).

Figures 5.1.2 - 5.1.5 contain the four composite PK plots corresponding to solvent data sets 2 - 5 and demonstrate how well L and PK were established in these cases.

Figures 5.1.6 and 5.1.7 present additional PK plots of solvent data in the turbulent regime using various different pairs of pressure taps in each of the 1.458- and 1.021-cm pipes, respectively. In both figures, a solid line, 1.00PK, and two dotted lines, 1.01PK and 0.99PK, have been drawn in, the latter two representing respectively $\pm 1\%$ deviations from the PK correlation. Comparison between the results for all pressure tap pairs shows that the differences between tap pairs were insignificant relative to the inherent data scatter, which is approximately $\pm 1\%$ around the PK correlation. These figures show that fully-developed turbulent flow in smooth pipes was achieved with the solvent.

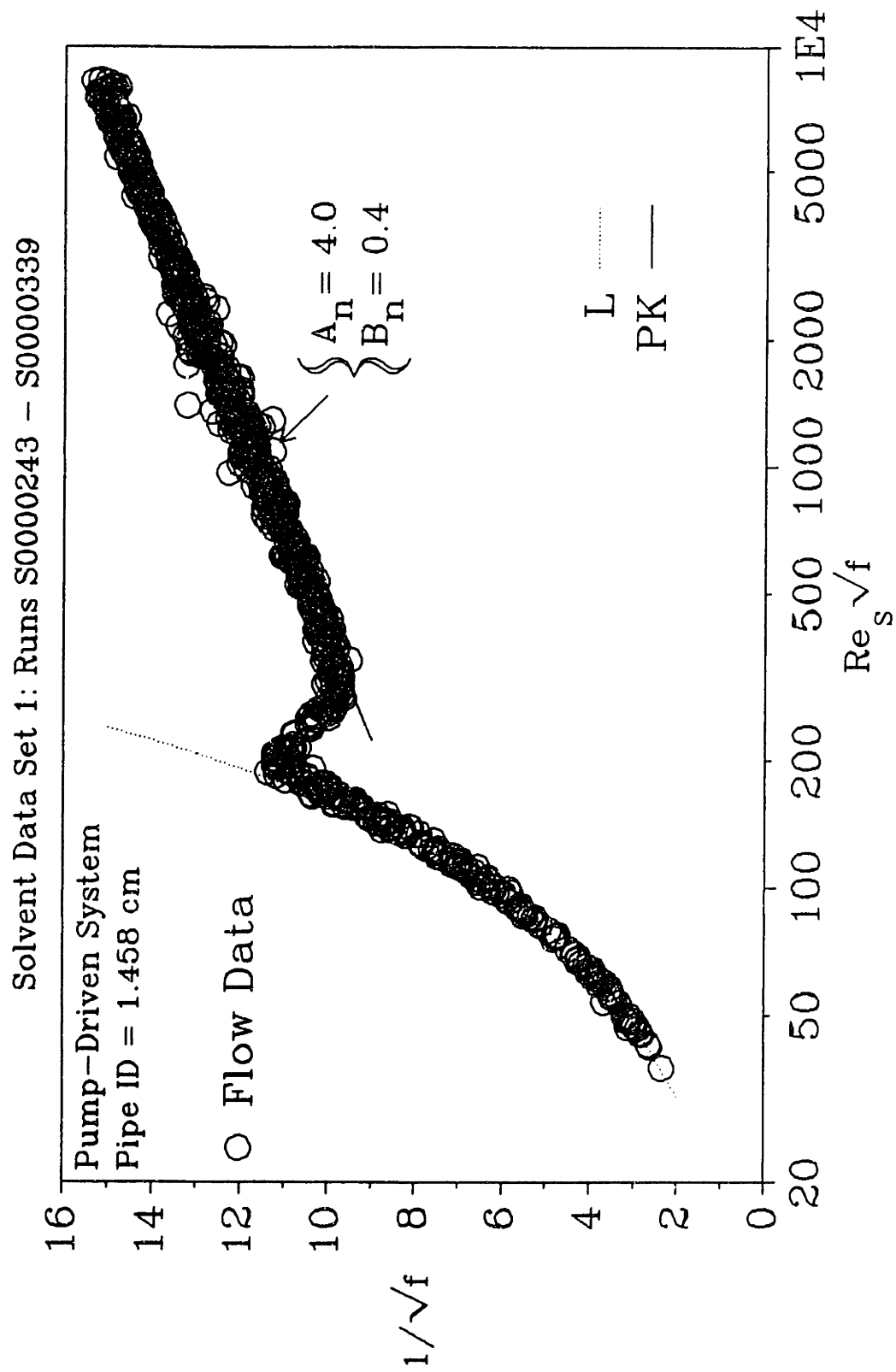


Figure 5.1.1: Solvent Data Set 1, Runs S0000243 - S0000339

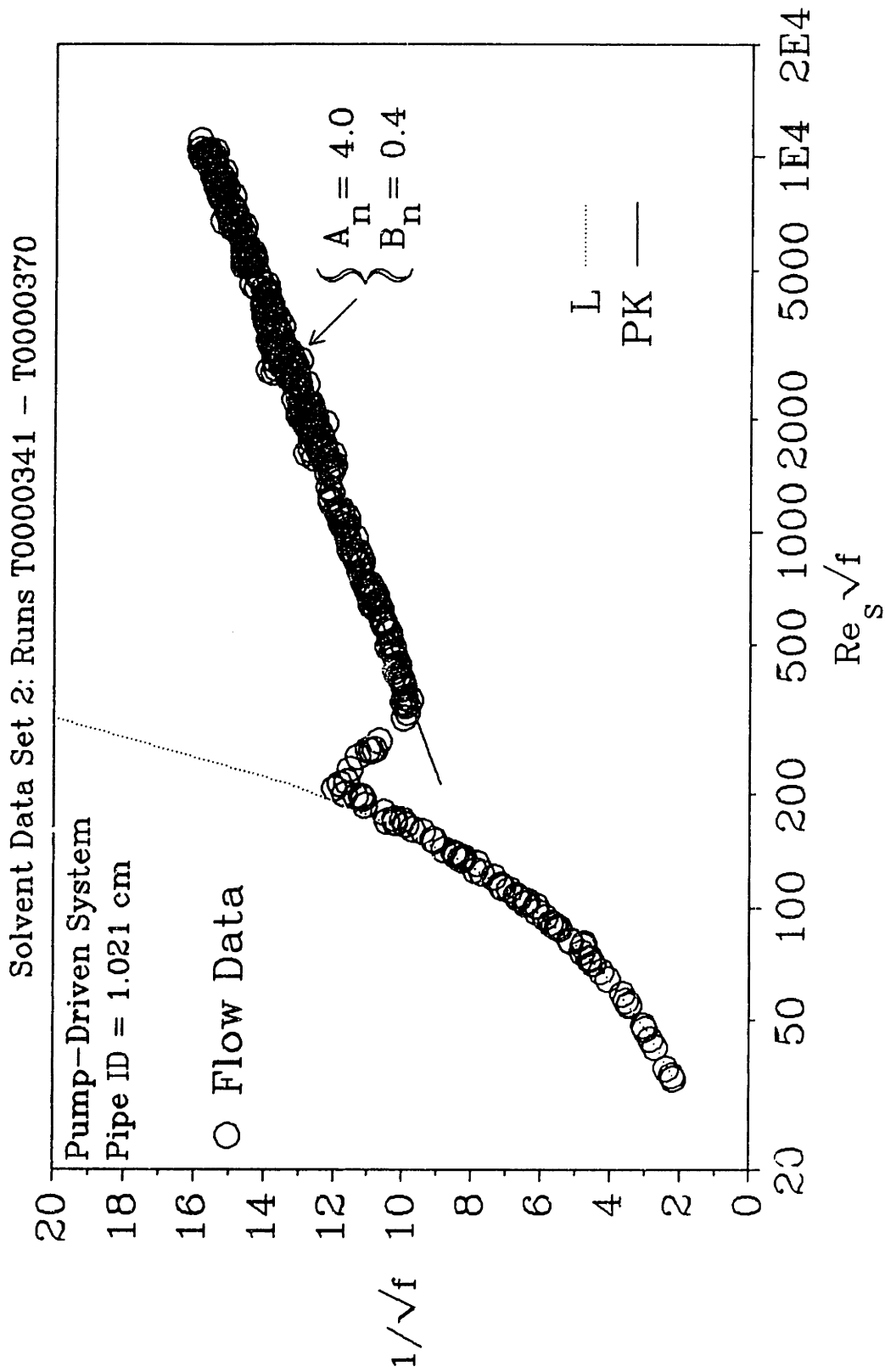


Figure 5.1.2: Solvent Data Set 2, Runs T0000341 - T0000370

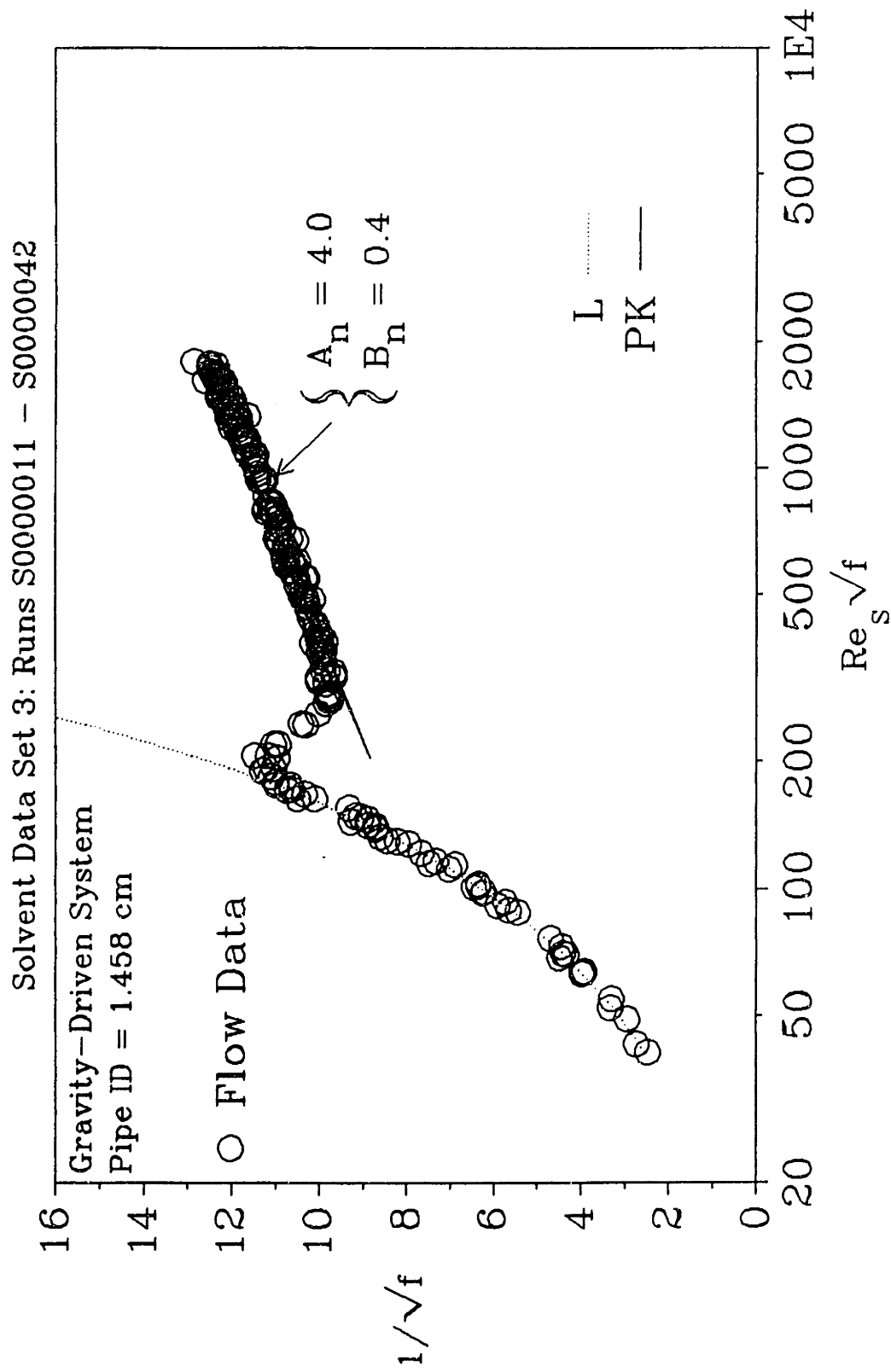


Figure 5.1.3: Solvent Data Set 3, Runs S0000011 - S0000042

Solvent Data Set 4: Runs S0000065 - S0000085

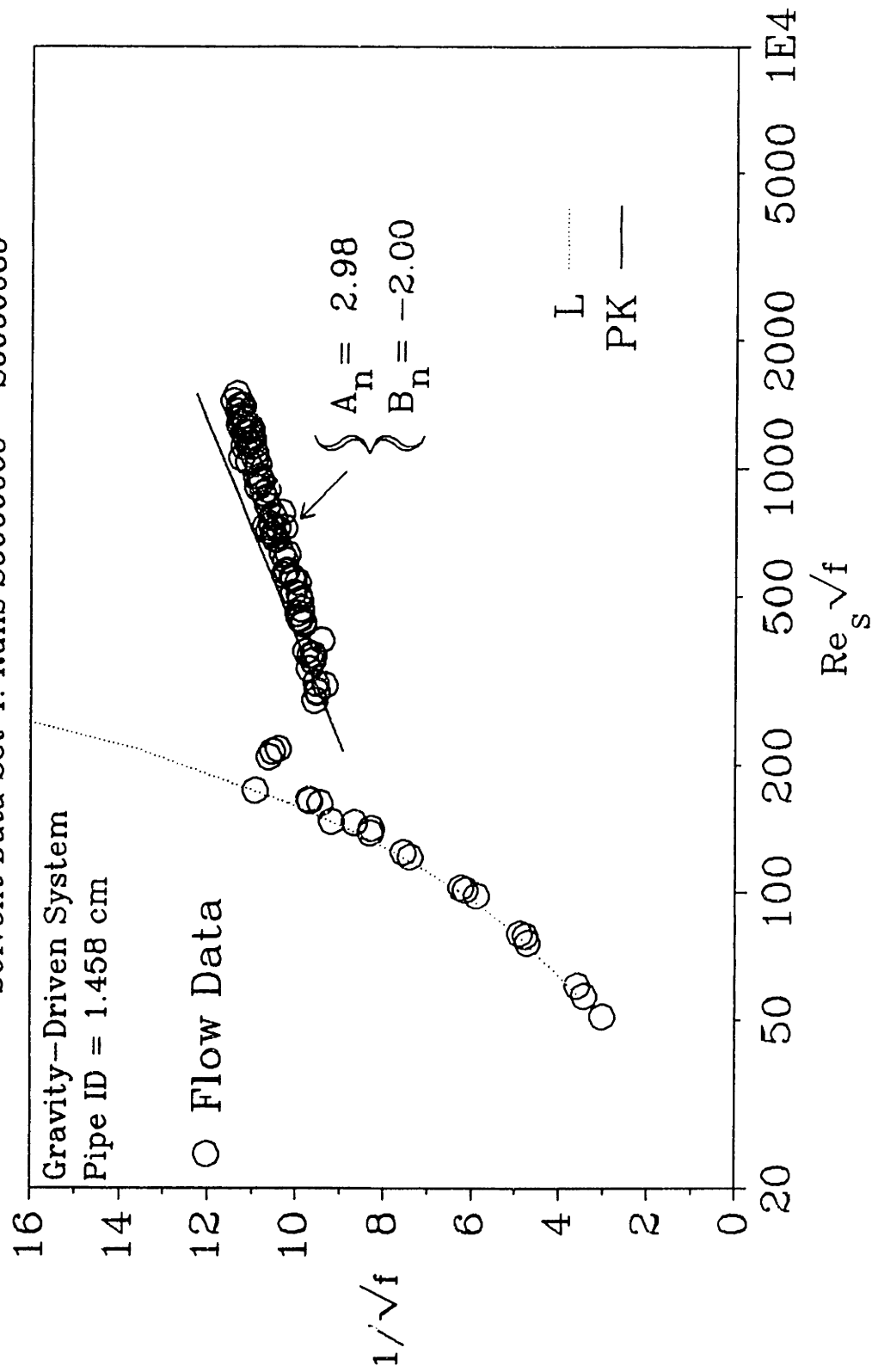


Figure 5.1.4: Solvent Data Set 4, Runs S0000065 - S0000085

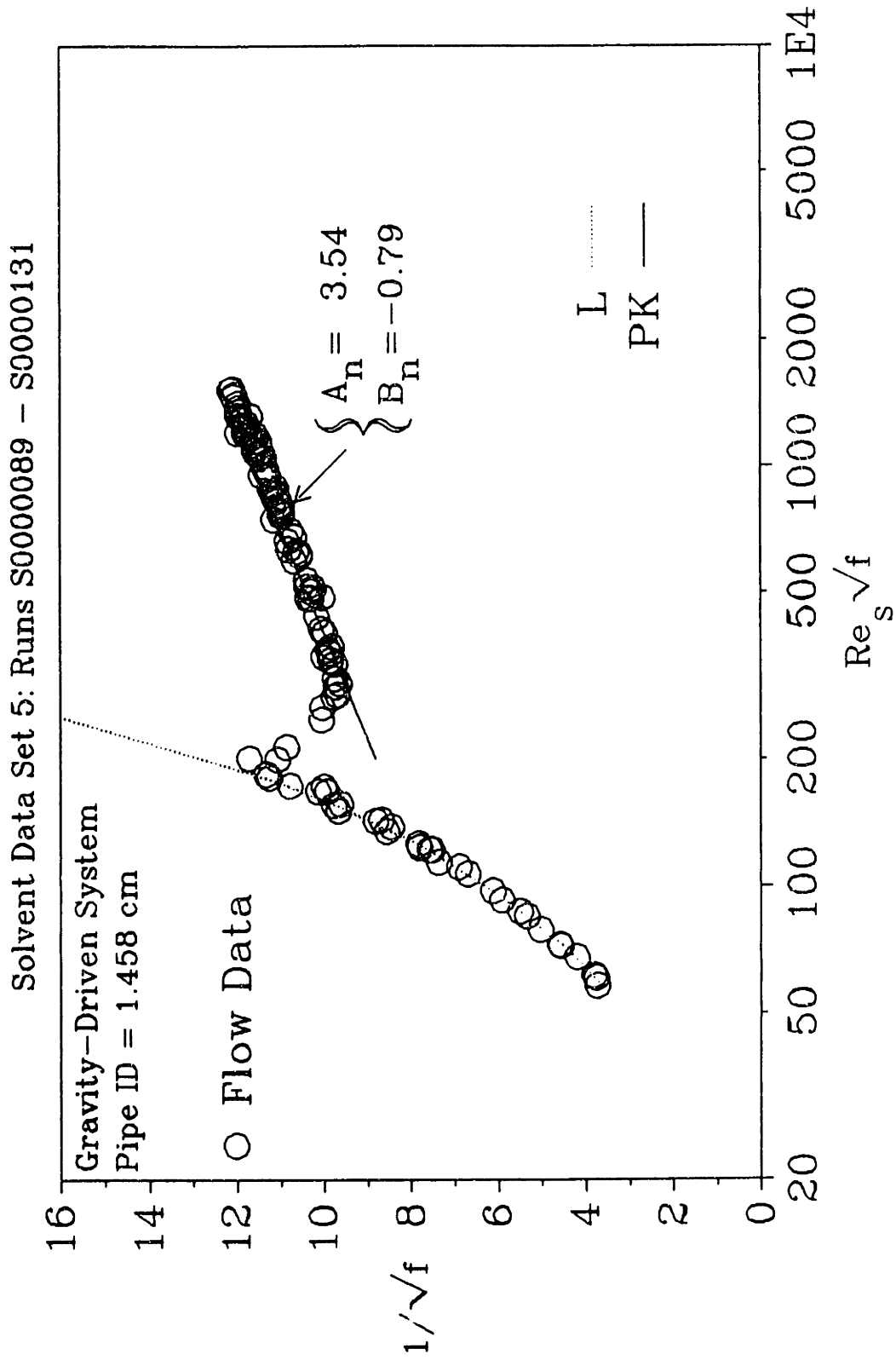


Figure 5.1.5: Solvent Data Set 5, Runs S0000089 - S0000131

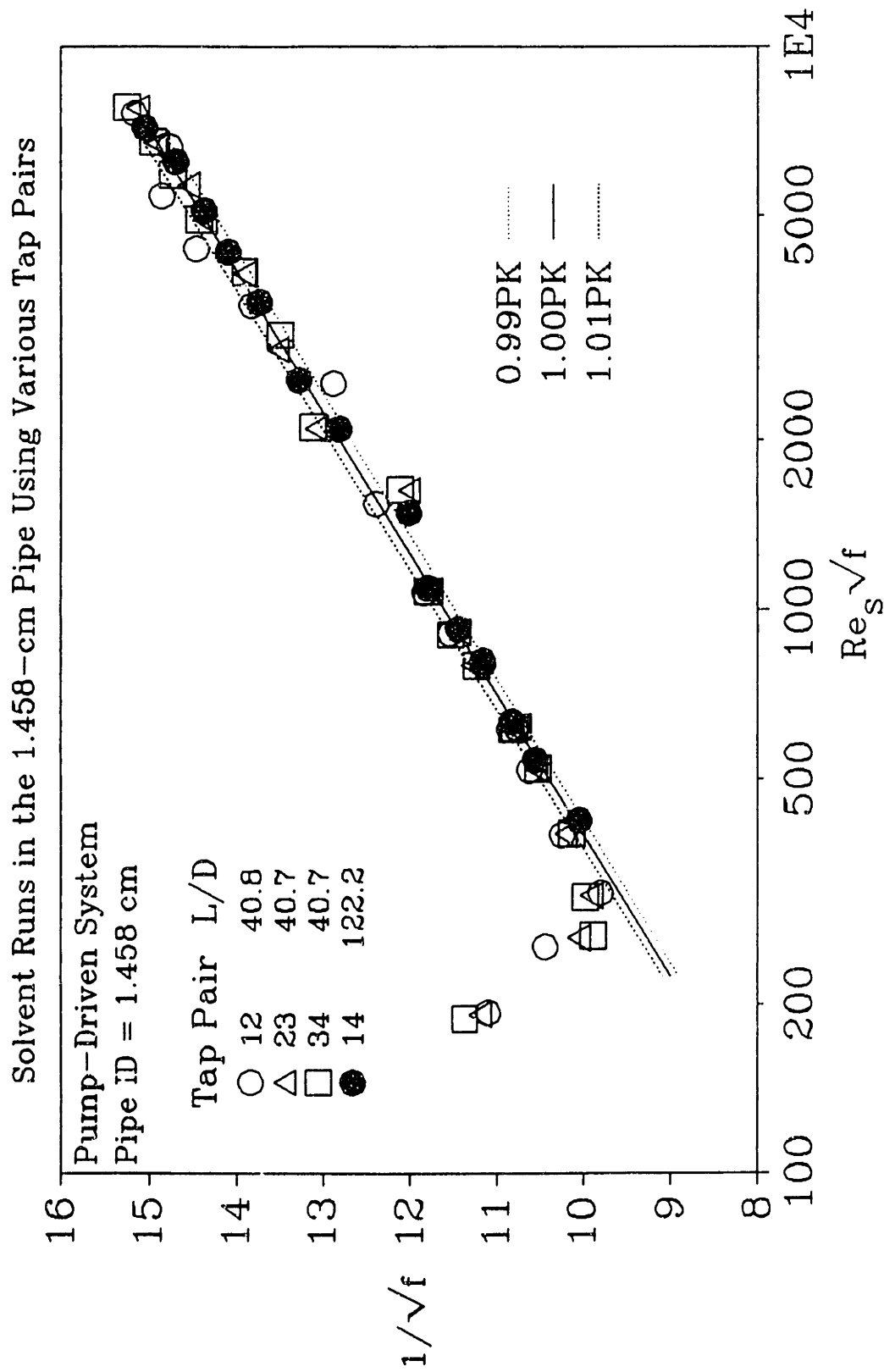


Figure 5.1.6: Solvent Runs in the 1.458-cm Pipe Using Various Tap Pairs

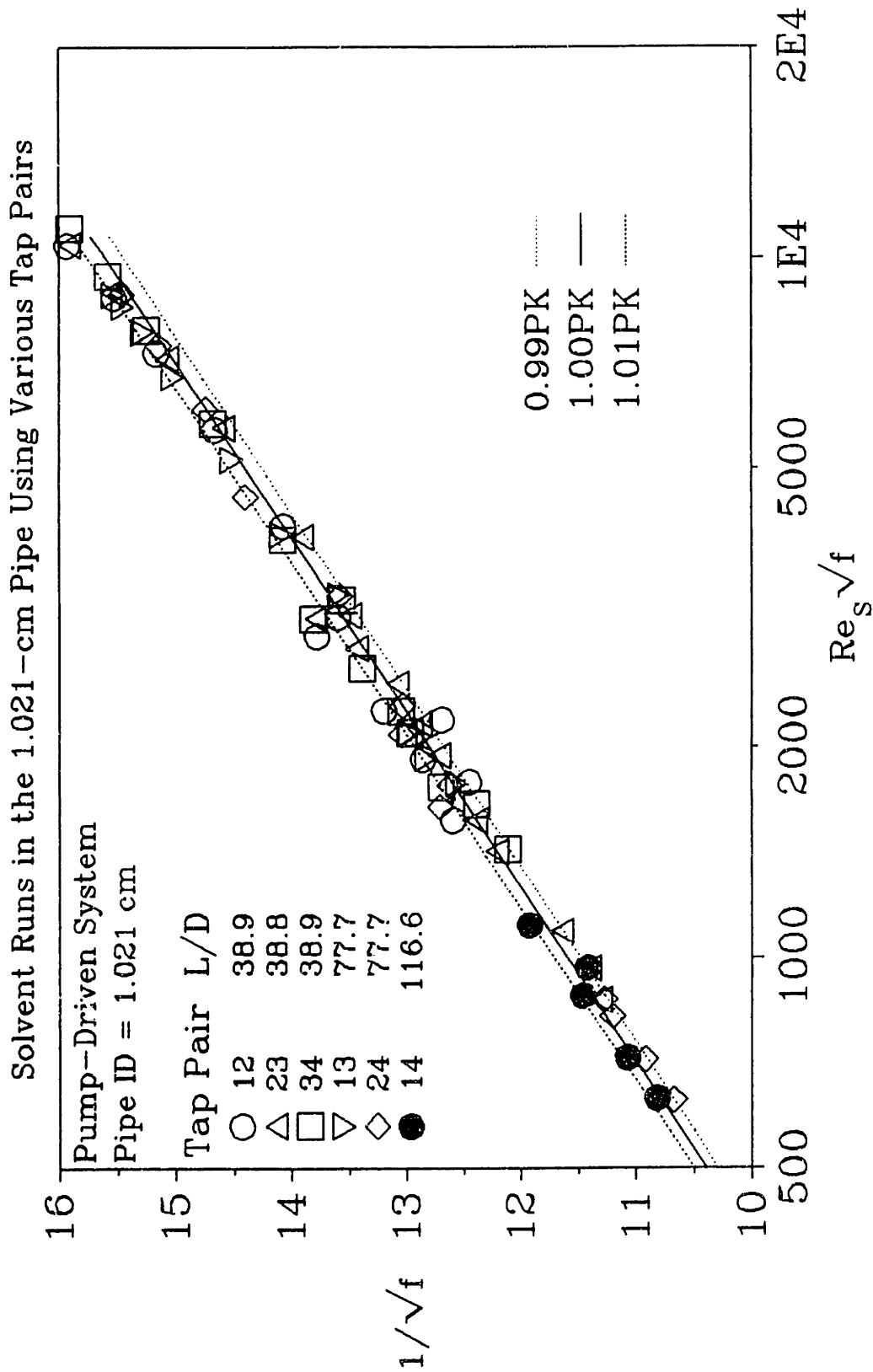


Figure 5.1.7: Solvent Runs in the 1.021-cm Pipe Using Various Tap Pairs

5.2 Polymer-Solution Runs

Polymer-solution results are presented in three sets: (1) the high molecular-weight polymer additives C832A and B1120 in the pump-driven system; (2) the low molecular-weight polymer additives P500, A507, and D1438 in the pump-driven system; and (3) the high molecular-weight polymer additives C837A, C836A, and C832A in the gravity-driven system. The first two sets sought the influence of additive molecular weight and conformation on flow enhancement, while the third set qualitatively explored how the backbone charge of a high molecular-weight polymer additive affected flow enhancement. Additives C832A and P500 in sets 1 and 2, respectively, were each studied separately in two pipes of inner diameters 1.458 and 1.021 cm to infer the effect of flow scale.

Figure 5.2.1 shows the actual experimental grids executed. For high molecular-weight polymers, a logarithmic series of polymer concentrations $c = (1, 2, 5, 10, \dots)$ wppm was used. For low molecular-weight polymers, the logarithmic series used was $(10, 30, 100, \dots)$ wppm. In the pump-driven system, each polymer concentration was studied at two salinities, $[\text{NaCl}] = 1.0 \times 10^{-4}$ and 3×10^{-1} N. In the gravity-driven system, each polymer concentration was studied at three salinities, $[\text{NaCl}] = 3.0 \times 10^{-4}$, 1.0×10^{-3} , and 1.0×10^{-1} N. The columns in Figure 5.2.1 reflect the actual experimental procedure. Each polymer solution was used for the entire $[\text{NaCl}]$ range studied to reveal the effect of salinity-induced conformational changes while maintaining both the additive amount and molecular-weight distribution constant.

Experimental Grids

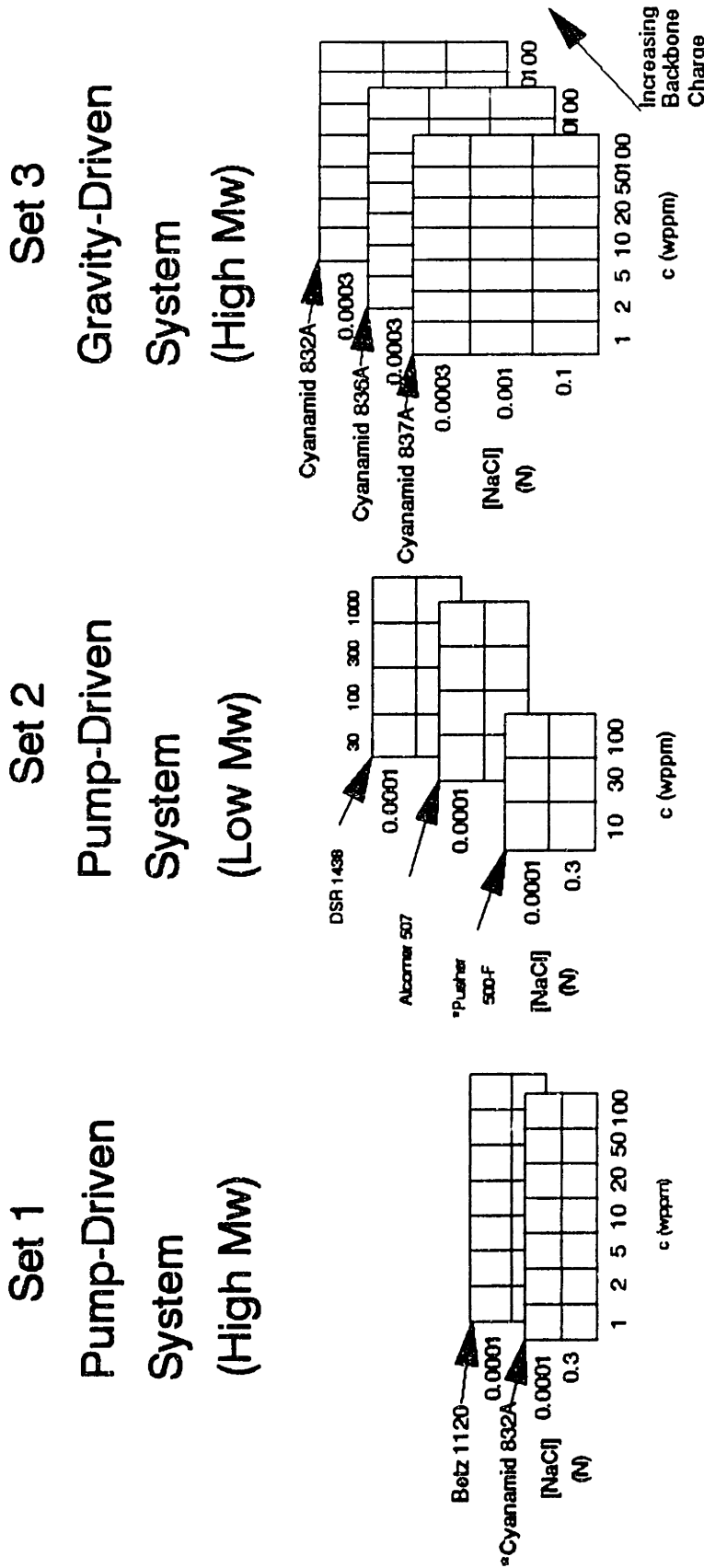


Figure 5.2.1: Experimental Grids

5.2.0 Turbulent-Flow Development in Polymer Solutions

Variations in the pressure drop at a constant flow rate measured by different pairs of pressure taps indicate simultaneously the inherent scatter among the polymer-solution data and the severity of axial polymer degradation. Even though separating the two phenomena may not be possible, measuring such variations provides some estimate of the uncertainty in the data from polymer-solution experiments.

Figure 5.2.2 shows the variations in data measured by tap pairs 12, 23, and 34 in the pump-driven system using the 1.458-cm pipe for turbulent flows of a solution having 5-wppm B1120 and 0.0001 N NaCl. The line M, provided for reference, represents the MDR asymptote. In PK coordinates, a variation in the measured pressure drop at a constant flow rate shifts both the abscissa $Re_s\sqrt{f}$ and the ordinate $1/\sqrt{f}$.

At the highest $Re_s\sqrt{f} \approx 5500$, tap pairs 12, 34, and 23 respectively measure increasing pressure drops at a constant flow rate, as indicated by increasing $Re_s\sqrt{f}$ and decreasing $1/\sqrt{f}$ in Figure 5.2.2, with the data from all taps lying within one ordinate unit. Because axial polymer degradation alone should cause tap pairs 12, 23, and 34 to measure increasing pressure drops, the observed differences among taps probably reflect the inherent data uncertainty. As $Re_s\sqrt{f}$ decreases, the average $1/\sqrt{f}$ of the data increases slightly, reaches a plateau for $4400 > Re_s\sqrt{f} > 3000$, and then declines roughly linearly. The plateau region strongly suggests that polymer degradation within the pipe becomes important at $Re_s\sqrt{f} > 4000$. At lower $Re_s\sqrt{f} \approx 2000$, the inherent data scatter remains about one unit of $1/\sqrt{f}$.

In experiments using the 1.458-cm pipe, the pressure drop was measured by tap

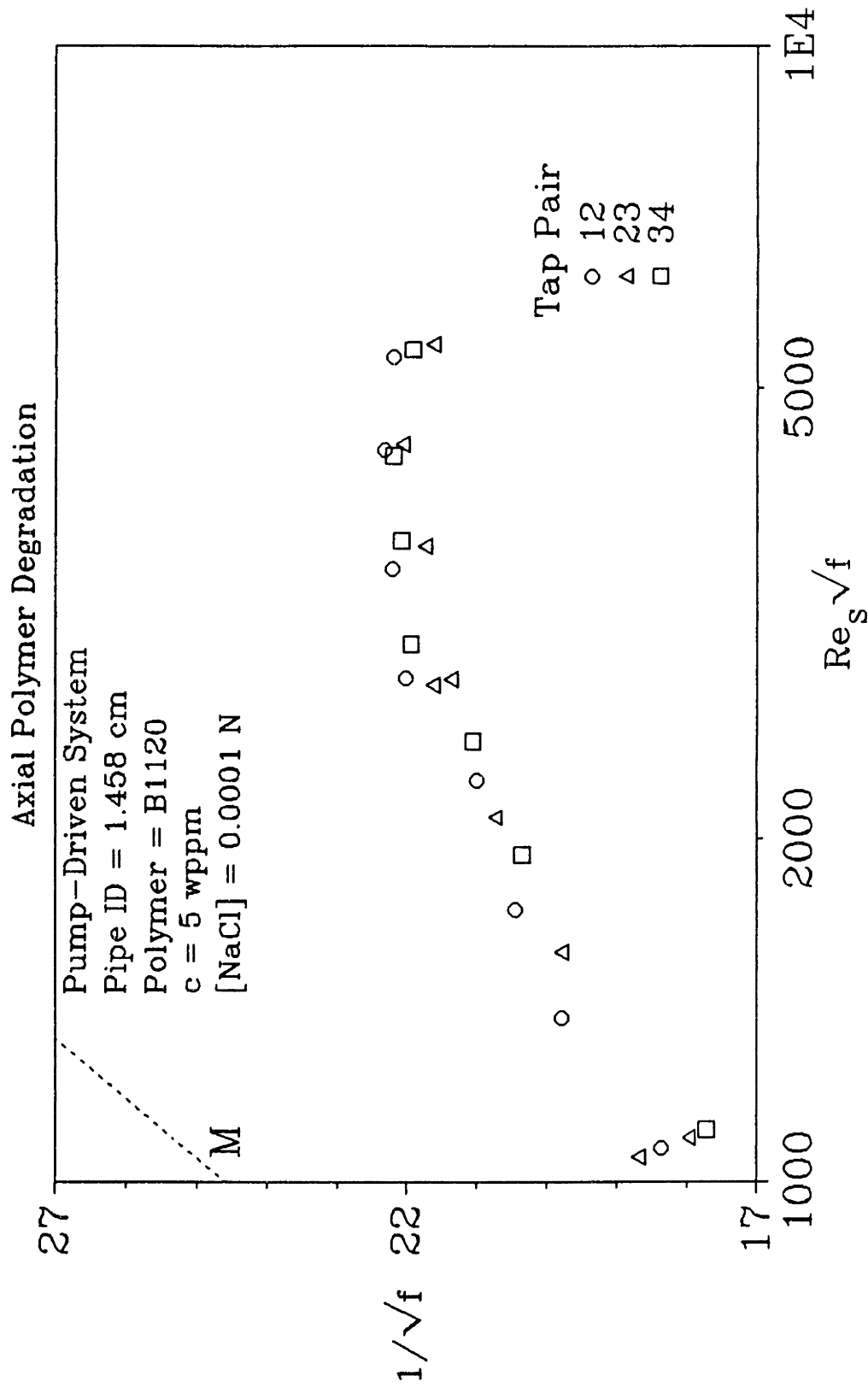


Figure 5.2.2: Axial Polymer Degradation in the 1.458-cm Pipe

pair 14, which provided the largest transducer signal. The experimental reported data, thus, reflect an average pressure drop across tap pairs 12, 23, and 34.

Figure 5.2.3 presents data measured by tap pairs 12, 23, and 34 for turbulent flows of a 10-wppm solution of C832A in 0.0001 N NaCl over five passes through the pump-driven system using the 1.021-cm pipe. The line M represents the MDR asymptote, which offers some perspective.

At the highest $Re_p\sqrt{f} \approx 7000$ in pass 1, tap pairs 12, 23, and 34 measure increasingly higher pressure drops, respectively, with the data from all taps lying within one ordinate unit. As $Re_p\sqrt{f}$ decreases, the average $1/\sqrt{f}$ increases and reaches a plateau at $Re_p\sqrt{f} \approx 3000$. The spread among the data measured by the tap pairs at the same flow rate also increases with decreasing $Re_p\sqrt{f}$, but remains within about one unit of $1/\sqrt{f}$. There is no entirely consistent pattern of tap measurements, but the $1/\sqrt{f}$ from pair 12 is always slightly greater than $1/\sqrt{f}$ from either 23 or 34, suggestive of polymer degradation in axial flow through the pipe.

In pass 2, the absolute levels of drag reduction are much lower than in pass 1, showing that the ancillary equipment needed to recycle the fluid degraded the polymer solution much more than a single pass through the system. At the highest $Re_p\sqrt{f} \approx 7300$, tap pairs 12, 23, and 34 respectively measure increasingly larger pressure drops. The data-scatter among them, $\sim 1/2$ unit of $1/\sqrt{f}$, is less than that in the first pass. As $Re_p\sqrt{f}$ decreases, the data measured by all tap pairs increase, peak at $Re_p\sqrt{f} \approx 5500$, and then decline down to $Re_p\sqrt{f} \approx 2500$. This observation likely reflects polymer degradation. Furthermore, not only does the scatter decrease among the data measured by the tap pairs at a constant flow rate, but the order in which they measure increasing pressure drops

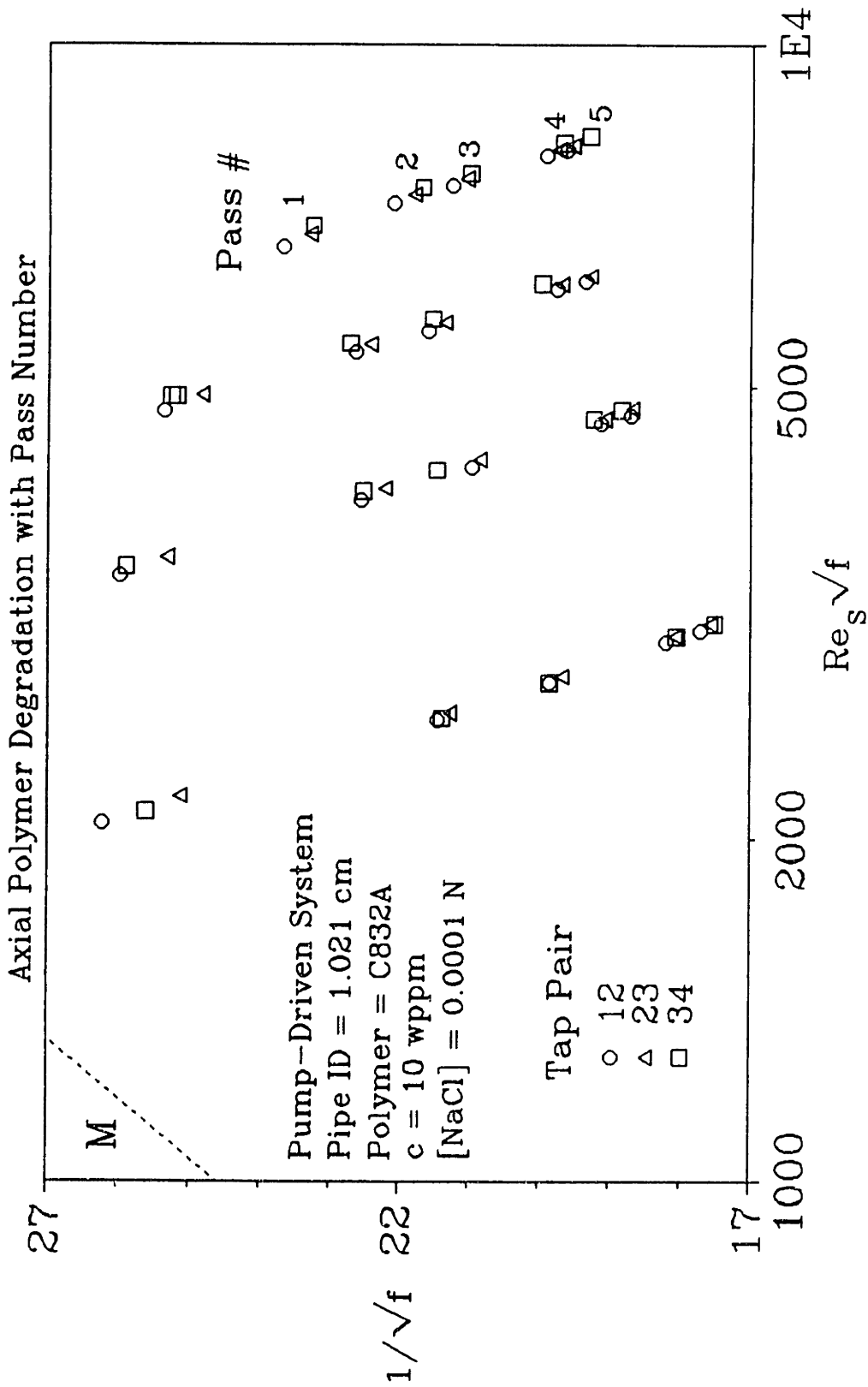


Figure 5.2.3: Axial Polymer Degradation with Pass Number in the 1.021-cm Pipe

appears more random. Thus, polymer degradation has a relatively less profound effect in pass 2 than in pass 1.

In passes 3, 4, and 5, the absolute drag-reduction levels fall further with each pass. The data-scatter appears to diminish, the tap-pair order becomes less regular, and the peak in the average $1/\sqrt{f}$ shifts to higher $Re_p\sqrt{f}$.

In experiments using the 1.021-cm pipe, tap pair 12 was used to measure the pressure drop at these high flow rates. Using tap pair 13, 24, or 14 would have saturated and very likely damaged the carrier demodulator needed to process the pressure-transducer signal. Tap pair 14 was used when the flow was gravity driven; at such lower stresses, polymer degradation was likely not a problem, especially in laminar flow. As seen in Figure 5.2.3, tap pair 12 consistently measures the lowest pressure drop in turbulent flows of fresh polymer solutions and probably provides the data least affected by polymer degradation.

5.2.1 Introductory Examples: Representative Flow Trajectories

Aspects of polymer-solution flow behavior are introduced in Figure 5.2.4, a PK plot of experiments in the pump-driven system using two 10-wppm solutions of additive B1120 in, respectively, 0.3(▼) and 0.0001(▼) N NaCl.

In this figure, lines L and N represent respectively the Newtonian laminar-flow and turbulent-flow baselines, equations 2.3-1 and 5.1-1, whereas the line M represents the empirically established maximum drag reducing(MDR) asymptote(Virk et al., 1970):

$$\frac{1}{\sqrt{f}} = 19.0 \log (Re_s \sqrt{f}) - 32.4 \quad (2.3-7)$$

Lines N and M envelop the region of turbulent drag reduction; this region is called the "polymeric regime" because within it the extent of drag reduction depends on additive parameters.

Consider first the data at high salinity, 0.3 N NaCl (\blacktriangledown), which typify results obtained with initially collapsed conformations of HPAM additives. At low $Re_s \sqrt{f} < 150$, the polymer-solution data closely follow Poiseuille's law L. At $Re_s \sqrt{f} \approx 150$, the data deviate downward from L and then drop toward N, which is reached at $Re_s \sqrt{f} \approx 350$. The laminar-to-turbulent transition observed here is similar to that observed in solvent runs, such as those in Figure 5.1.1, described earlier. For $350 < Re_s \sqrt{f} < 500$, the polymer-solution data follow the Newtonian turbulent-flow line N. Then at $Re_s \sqrt{f} \approx 500$ the data abruptly lift up from N at the "onset" point, denoted by an asterisk and so named because it marks the onset of flow enhancement; i.e., for any fixed $Re_s \sqrt{f} > Re_s \sqrt{f}^*$, $1/\sqrt{f_p} > 1/\sqrt{f_n}$. For $Re_s \sqrt{f} > 500$ the data exhibit flow enhancement rising into the polymeric regime along a near-linear segment P with slope and intercept $(A_p, B_p) = (17.2, 36.1)$ for $500 < Re_s \sqrt{f} < 3500$. At the highest $Re_s \sqrt{f} \approx 4000$ the data depart slightly downward from the line segment, possibly because of polymer degradation within the test pipe as seen in Figure 5.2.3. The flow enhancements achieved are also of interest, as measured by the apparent slip $S' = (1/\sqrt{f_p} - 1/\sqrt{f_n})$ at fixed $Re_s \sqrt{f}$. In Figure 5.2.4, at $Re_s \sqrt{f} = 1000$, $1/\sqrt{f_p} = 15.6$, $1/\sqrt{f_n} = 11.6$, and $S' = 4.0$, corresponding to fractional flow enhancement $S_p = 0.34$ relative to the solvent. At $Re_s \sqrt{f} = 3000$, $1/\sqrt{f_p} = 23.7$, $1/\sqrt{f_n} = 13.5$, and $S' = 10.2$ and $S_p = S'/(1/\sqrt{f_n}) = 0.76$ relative to the

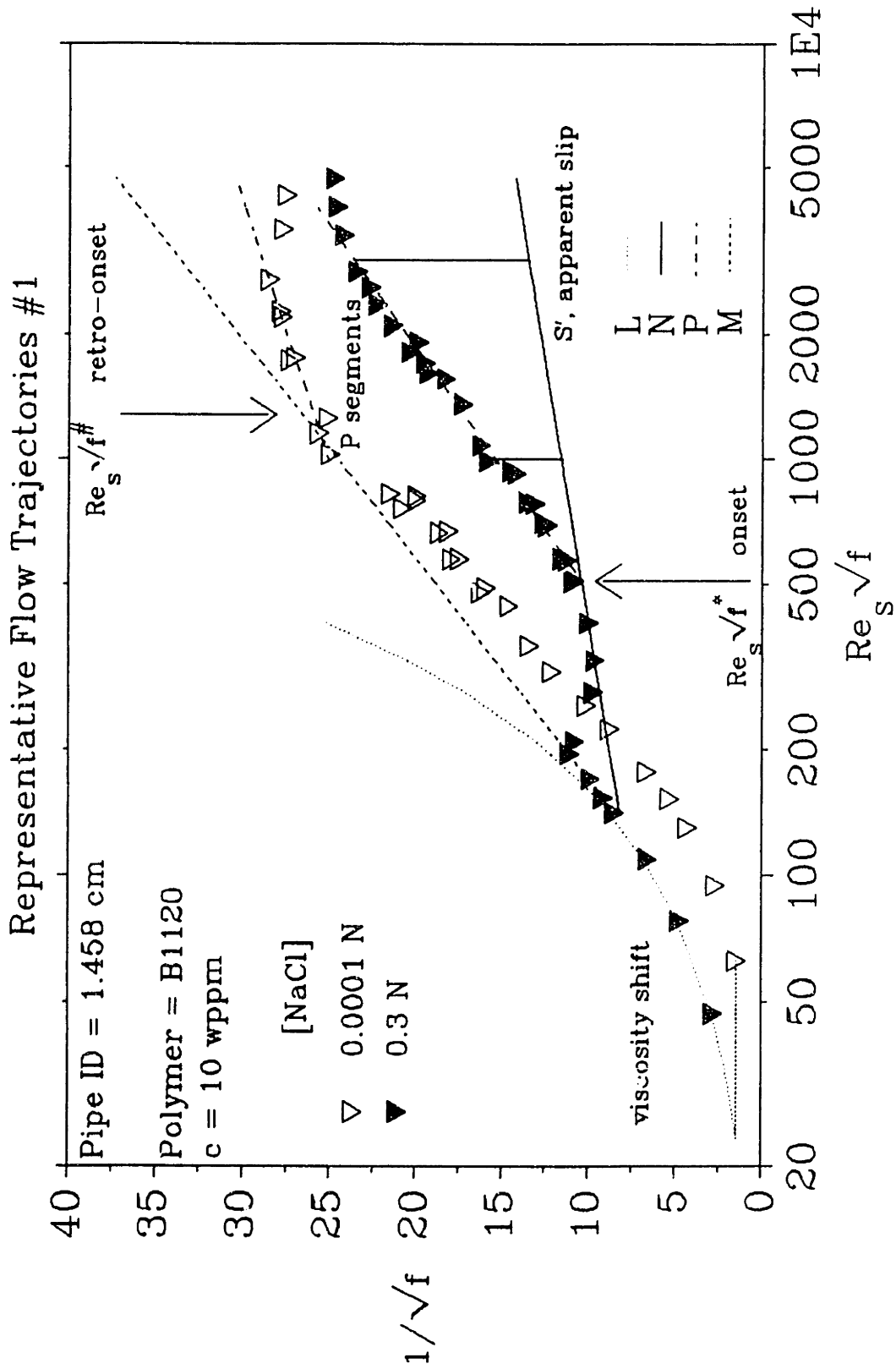


Figure 5.2.4: Representative Flow Trajectories #1

solvent. Note that S' increases from 4.0 to 10.2 as $Re_p\sqrt{f}$ increases from 1000 to 3000, respectively.

The flow trajectory observed for 10 wppm of B1120 in 0.3 N NaCl in Figure 5.2.2 thus contains three segments: laminar flow, L; turbulent flow without drag reduction, N; and turbulent flow with drag reduction, P, with a distinct onset of drag reduction that separates the N and P segments. Such LNP trajectories are commonly exhibited by solutions of random-coiling macromolecules and are termed "Type A" drag-reduction behavior. The polymeric-regime segment P observed during Type-A drag reduction can be quantitatively characterized by the onset wall shear stress, T_w^* , which is related to $Re_p\sqrt{f^*}$, and the slope increment $\delta = A_p - A_n$. In this example, $Re_p\sqrt{f^*} = 450$, $T_w^* = 4.1$ dyne/cm², and $\delta = 17.2 - 4.0 = 13.2$.

Next consider the second set of data in Figure 5.2.4 at low salinity, 0.0001 N NaCl(∇), which is representative of results obtained with initially extended conformations of HPAM additives. For $60 < Re_p\sqrt{f} < 400$ the data are displaced rightwards from Poiseuille's law L, to higher $Re_p\sqrt{f}$ at fixed $1/\sqrt{f}$; this displacement, labelled "viscosity shift" in Figure 5.2.4, reflects the relative viscosity η_r of the polymer solution. Note that in this region of low $Re_p\sqrt{f}$, the data being displaced downwards from L to lower $1/\sqrt{f}$, the polymer-solution is drag-enhancing. For $60 < Re_p\sqrt{f} < 400$, the data follow a Poiseuille-like path, but as $Re_p\sqrt{f}$ increases, the viscosity shift decreases, indicating shear-thinning behavior. The data pass through the Newtonian turbulent-flow baseline N, at $Re_s\sqrt{f} \approx 220$, and enter the polymeric regime without exhibiting the laminar-to-turbulent transition observed in the 0.3-N data. For $400 < Re_p\sqrt{f} < 1500$, the data ascend toward, and lie nearly parallel to, the maximum drag-reducing(MDR) asymptote M. At $Re_p\sqrt{f} \approx$

1500, the data depart downwards from M into the polymeric regime at a "retro-onset" point, denoted by an octathorpe(#). The retro-onset point separates the region of asymptotic maximum drag reduction, which is independent of additive properties, from the polymeric regime, within which drag reduction is dependent on additive properties; in this sense, retro-onset is the converse of onset, which separates Newtonian flow, with no drag reduction, from the polymeric regime. For $1500 < Re_s\sqrt{f} < 3400$, the data continue into the polymeric regime along a near-linear segment P with slope and intercept $(A_p, B_p) = (8.0, -1.2)$. At the highest $Re_s\sqrt{f} \approx 4000$, the data descend slightly from segment P, possibly because of polymer degradation within the test pipe. The following flow enhancements are observed: At $Re_s\sqrt{f} = 1000$, $1/\sqrt{f_p} = 1/\sqrt{f_m} = 24.6$, $1/\sqrt{f_n} = 11.6$, and $S' = 13.0$, corresponding to $S_p = 1.1$, the maximum achievable at $Re_s\sqrt{f} = 1000$; and at $Re_s\sqrt{f} = 3000$, $1/\sqrt{f_p} = 28.2$, $1/\sqrt{f_n} = 13.5$, and $S' = 14.7$, corresponding to a fractional flow enhancement $S_p = S'/(1/\sqrt{f_n}) = 1.09$ relative to the solvent.

The flow trajectory observed for 10 wppm of B1120 in 0.0001 N NaCl in Figure 5.2.4 thus has three parts: drag-enhanced laminar flow with a relative viscosity $\eta_r > 1$; maximum drag reduction along the MDR asymptote, M; and turbulent drag reduction, P, with a retro-onset that separates the M and P segments. Such LMP trajectories have been previously observed with solutions of extended macromolecules and constitute "Type B" drag-reduction behavior. Note the important feature of Type-B behavior: that the polymeric-regime segment P is almost parallel to N.

Finally, it is interesting to compare the two sets of data in Figure 5.2.4 to infer the effects of additive conformation. In laminar flow for $Re_s\sqrt{f} < 200$, the expanded conformation, in 0.0001 N NaCl, enhances drag relative to solvent more than does the

collapsed conformation, the former showing higher $1/\sqrt{f}$ than the latter by ~ 3.5 units. In turbulent flow, however, for $Re_s\sqrt{f} > 400$, the expanded conformation reduces drag relative to solvent more than does the collapsed conformation, the former always attaining higher $1/\sqrt{f}$ than the latter. Thus, the ratio of S' of the Type-A collapsed conformation to that of the Type-B expanded conformation, S'_A/S'_B increases with increasing $Re_s\sqrt{f}$. For $Re_s\sqrt{f} < Re_s\sqrt{f^*}$, $S'_A/S'_B = 0$, the collapsed conformation providing no flow enhancement before onset, at which $Re_s\sqrt{f^*}$ the extended conformation does. For $Re_s\sqrt{f} \geq Re_s\sqrt{f^*}$, S'_A/S'_B increases with increasing $Re_s\sqrt{f}$, approaching unity at higher $Re_s\sqrt{f}$; after onset, S'_A increases faster than does S'_B with increasing $Re_s\sqrt{f}$ because the Type-A P segment has a steeper slope than does the Type-B P segment. In this example, at $Re_s\sqrt{f} = 500, 1000, \text{ and } 3000$, $S'_A/S'_B = 0, 0.31, \text{ and } 0.69$, respectively.

A second illustration of polymer-solution flow behavior is given in Figure 5.2.5, a PK plot of experiments in the gravity-driven system using 20.6-wppm solutions of additive C836A, an HPAM of high molecular-weight and moderate backbone charge, at two salinities, 0.1(♦) and 0.001(◇) N NaCl, respectively.

Lines L, N, and M respectively represent Poiseuille's law for laminar flow, the Newtonian turbulent-flow baseline, and the MDR asymptote, the latter two envelop the polymeric regime P.

Data at high salinity, 0.1 N NaCl(♦), exemplify results obtained with an initially collapsed conformation of the C836A additive. At low $Re_s\sqrt{f} < 150$, the polymer-solution data closely follow L. At $Re_s\sqrt{f} \approx 180$, the data depart downward from L and then drop toward N, which is reached at $Re_s\sqrt{f} \approx 350$. This laminar-to-turbulent

transition is much like that seen with solvent alone in Figure 5.1.1. For $350 < Re_s\sqrt{f} < 600$, the polymer-solution data adhere closely to N, exhibiting no drag reduction. At $Re_s\sqrt{f} \approx 700$, the data rise weakly from N at an "onset" point, indicated on the figure, beyond which $1/\sqrt{f_p} > 1/\sqrt{f_n}$. For $700 < Re_s\sqrt{f} < 900$, the polymer-solution data initially ascend into the polymeric regime along a shallow knee that shortly joins a well-developed linear segment P, of slope and intercept $(A_p, B_p) = (18.6, 42.8)$ for $900 < Re_s\sqrt{f} < 1400$. As shown in Figure 5.2.5, the visually determined onset point, $Re_s\sqrt{f} \approx 660$, where the data along N first appear to depart significantly from N, does not necessarily coincide with the regressed onset point, $Re_s\sqrt{f}^* \approx 770$, where the linear segment P, extrapolated backward, would intersect the baseline N. At $Re_s\sqrt{f} = 1000$, the apparent slip $S' = (12.9 - 11.5) = 1.4$, corresponding to a fractional flow enhancement $S_F = 0.12$ relative to the solvent.

The preceding flow trajectory comprises three distinct segments, namely: laminar flow, L; turbulent-flow without drag reduction, N; and turbulent flow with drag reduction, P, with an onset point separating the N and P segments. This LNP trajectory exemplifies the Type-A drag-reduction flow behavior typically exhibited by solutions of random-coiling macromolecules. Characteristic parameters of the polymeric-regime segment P are: $T_w^* \approx 13.7$ dyne/cm² and $Re_s\sqrt{f}^* \approx 770$, and the slope increment $\delta = 15.1$.

Data at low salinity, 0.001 N NaCl(\diamond), in Figure 5.2.5 illustrate the behavior of an initially expanded conformation of the C836A macromolecule. At low flowrates, $80 < Re_s\sqrt{f} < 350$, the data follow a laminar path that is almost both parallel to, but shifted rightwards from, Poiseuille's law L. The displacement between L and the

laminar-flow data at constant $1/\sqrt{f}$, called "viscosity shift" in Figure 5.2.5, reflects the relative viscosity η_r of the polymer solution, which is thus seen to exhibit shear thinning. The polymer-solution evidently enhances drag in laminar flow, its data lying below L, with η_r decreasing from 1.9 at $Re_s\sqrt{f} = 80$ to 1.5 at $Re_s\sqrt{f} = 350$. Between $350 < Re_s\sqrt{f} < 550$, the polymer solution undergoes a laminar-to-turbulent transition, the data abruptly shifting horizontally rightward from their laminar-flow path to a turbulent flow segment P that lies in the polymeric regime. The observed transition is noteworthy because the polymer-solution exhibits drag reduction immediately upon attaining turbulent flow. For $550 < Re_s\sqrt{f} < 1100$, the polymer-solution data rise into the polymeric regime along a linear segment P, of slope and intercept $(A_p, B_p) = (19.8, 38.9)$. At $Re_s\sqrt{f} = 1000$, the apparent slip $S' = 20.5 - 11.5 = 9.0$ and fractional flow enhancement $S_p = 0.79$ relative to the solvent.

The flow trajectory observed for 20.6 wppm of C836A in 0.001 N NaCl has two distinct segments: drag-enhanced laminar flow, with relative viscosity $\eta_r \approx 1.7$, amidst some shear thinning, and drag-reduced turbulent-flow along a linear polymeric-regime segment P. This LP trajectory evidently differs from both the LNP and LMP types of trajectories seen in earlier examples, lacking a central turbulent-flow segment along either N or M, and displaying neither onset nor retro-onset. This observed behavior is classified Type A, not Type B, because the polymeric-regime segment possesses a slope similar to, not much shallower than, that of the 20.6-wppm C836A in 0.1 N NaCl, which clearly exhibited Type-A behavior.

Finally, comparing the two sets of data in Figure 5.2.5, it is seen that, relative to the collapsed conformation, the expanded conformation of C836A causes greater drag

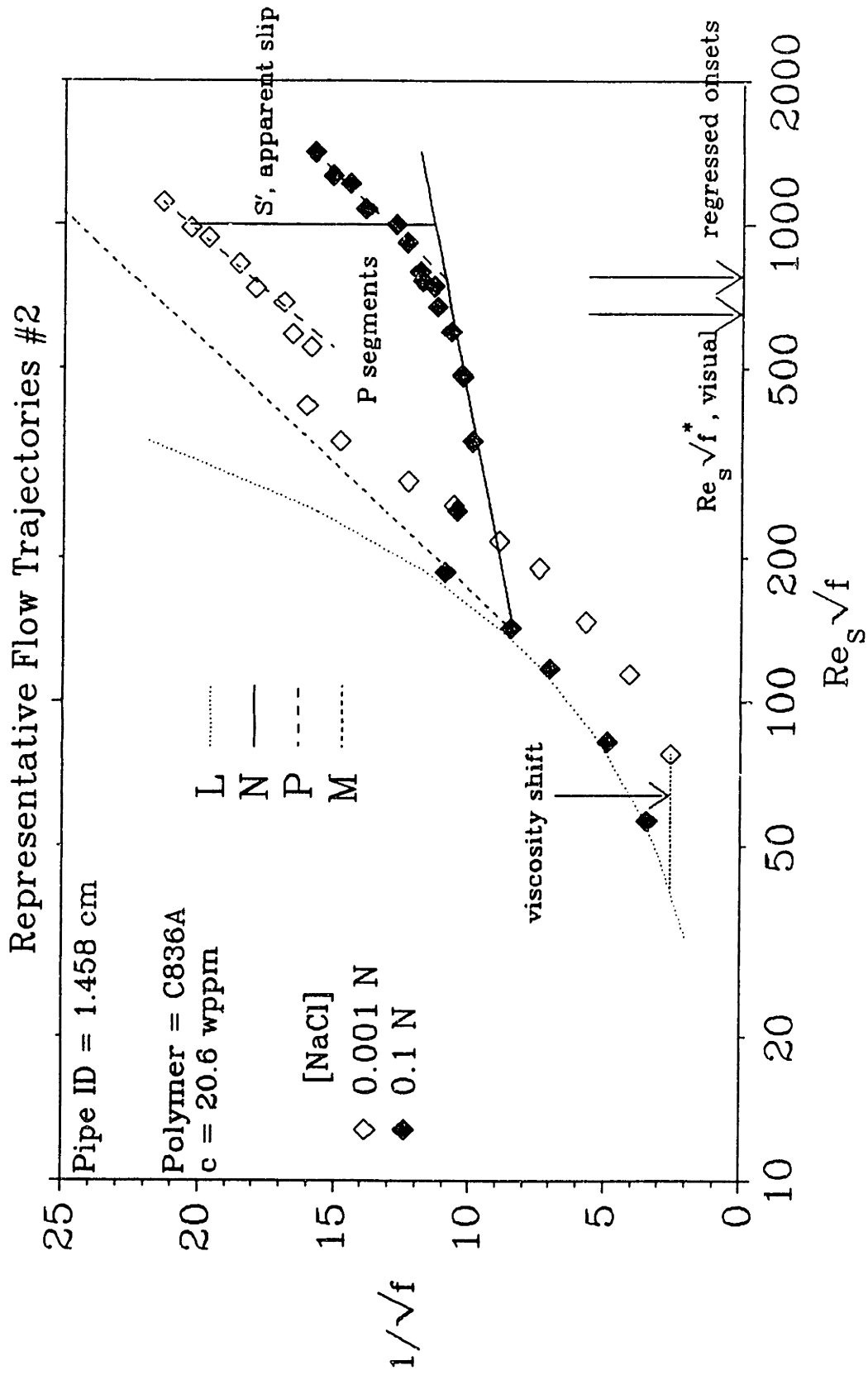


Figure 5.2.5: Representative Flow Trajectories #2

in laminar flow, but yet induces the greater drag reduction in turbulent flow. Despite differences in drag reduction extents, both conformations of C836A exhibit the Type-A drag-reduction behavior associated with random-coiling linear macromolecules.

5.2.2 Experimental Summary Tables

Experimental conditions, turbulent-flow parameters, and laminar-flow parameters for all runs are given in Tables 5.2.1, 5.2.2, and 5.2.3, respectively.

Table 5.2.1 summarizes the experimental conditions in seven columns: Entry; Run; Concentration, c ; Salinity, [NaCl]; Solvent; Turbulent Baseline Constants, A_n and B_n ; and Temperature Range. The Entry column provides an identifying number for each run and serves to link Table 5.2.1 with subsequent Tables 5.2.2 and 5.2.3. The Run column shows the label assigned to each run. The label itself contains experimental information about the polymer additive, the additive concentration, and the salinity used in the run. For example, runs Q1P01465 and Q1P03166 were executed from the same experimental batch of polymer solution. The Q identifies the polymer as Cynamid 832A in the pump-driven system. (In the gravity-driven system, all labels begin with P even though additives C837A, C836A, and C832A were used.) The sequence 1P0 indicates that the polymer concentration in wppm is 1 times ten to the Power of 0, $c \approx 1$ wppm. The next pairs of digits 14 and 31 indicate salinities of 1×10^{-4} and 3×10^{-1} N, respectively. The last pairs of digits 65 and 66 merely maintain the ordering among all solvent and polymer runs; these digits ranged between 00 and 99. In addition, for run dyads in the pump-driven system and run triads in the gravity-driven system, a single

computer file contained all the experimental and reduced data and had the same label as the run using the lowest salinity. Hence, computer file Q1P01465.wk1(A Lotus-123™ Spreadsheet; see Figure 4.9 in Chapter IV) contained data for runs Q1P01465 and Q1P03166. In the third column, the polymer-solution concentration in weight parts per million(wppm) is given for each run. This was calculated by dividing the mass of polymer contained in a tankful of solution by the sum of the solvent, polymer, and salt masses composing the solution and multiplying by 1×10^6 to get wppm units. The fourth column [NaCl] gives the saline normality(N) for each run. The normality was calculated by dividing the number of equivalents of NaCl in a tankful of solution by the total solution volume. The fifth and sixth columns provide, respectively, the slope A_n and intercept B_n of the best-fit baseline through the solvent data set associated with each experimental run. Constants A_n and B_n were determined by a least-squares regression of $1/\sqrt{f}$ vs. $\log Re_s \sqrt{f}$ to fit equation 5.1-1. The seventh column contains the minimum and maximum solution temperatures, in °C, measured during a run; however, solution temperature was recorded for every data point within each run to ensure accurate calculations of solvent physical properties.

Table 5.2.1
Experimental Conditions for All Runs

Entry	Run	Concentration	Salinity	Solvent Turbulent Baseline Constants		Temperature Range (°C - °C)
		c	[NaCl]	A _n	B _n	
		(wppm)	(N)			
Cyanamid 832A = C832A; Pump-Driven System; Pipe ID = 1.458 cm						
1	Q1P01465	1.01	1.00 × 10 ⁻⁴	4	0.4	24.2-25.15
2	Q2P01462	2.02	1.00 × 10 ⁻⁴	4	0.4	24.8-26.1
3	Q5P01459	4.99	1.00 × 10 ⁻⁴	4	0.4	24.3-25.0
4	Q1P11453	9.97	1.00 × 10 ⁻⁴	4	0.4	23.8-24.8
5	Q2P11456	20.0	1.00 × 10 ⁻⁴	4	0.4	24.1-25.1
6	Q5P11449	50.0	1.00 × 10 ⁻⁴	4	0.4	23.8-25.1
7	Q1P21446	100	1.00 × 10 ⁻⁴	4	0.4	23.9-25.1
8	Q1P03166	1.01	3.00 × 10 ⁻¹	4	0.4	24.5-25.3
9	Q2P03163	2.02	3.00 × 10 ⁻¹	4	0.4	24.0-25.3
10	Q5P03160	4.99	3.00 × 10 ⁻¹	4	0.4	24.1-24.8
11	Q1P13154	9.97	3.00 × 10 ⁻¹	4	0.4	24.1-24.9
12	Q2P13157	20.0	3.00 × 10 ⁻¹	4	0.4	23.9-24.9
13	Q5P13150	50.0	3.00 × 10 ⁻¹	4	0.4	24.0-25.5
14	Q1P23147	100	3.00 × 10 ⁻¹	4	0.4	24.0-24.9
Cyanamid 832A = C832A; Pump-Driven System; Pipe ID = 1.021 cm						
15	Y1P01443	1.00	1.00 × 10 ⁻⁴	4	0.4	23.6-24.9
16	Y2P01446	2.00	1.00 × 10 ⁻⁴	4	0.4	23.1-25.2
17	Y5P01449	5.00	1.00 × 10 ⁻⁴	4	0.4	23.0-25.0

Entry	Run	Concentration	Salinity	Solvent Turbulent Baseline Constants		Temperature Range (°C - °C)
		c	[NaCl]	A _n	B _n	
		(wppm)	(N)			
18	Y1P11452	10.0	1.00×10 ⁻⁴	4	0.4	22.5-24.9
19	Y2P11455	20.0	1.00×10 ⁻⁴	4	0.4	23.4-24.9
20	Y5P11459	50.0	1.00×10 ⁻⁴	4	0.4	23.5-25.1
21	Y1P03144	1.00	3.00×10 ⁻¹	4	0.4	23.9-24.9
22	Y2P03147	2.00	3.00×10 ⁻¹	4	0.4	23.3-25.0
23	Y5P01450	5.00	3.00×10 ⁻¹	4	0.4	22.7-24.9
24	Y1P13153	10.0	3.00×10 ⁻¹	4	0.4	22.5-25.1
25	Y2P13156	20.0	3.00×10 ⁻¹	4	0.4	24.05-25.9
26	Y5P13160	50.0	3.00×10 ⁻¹	4	0.4	22.9-25.1
Betz 1120 = B1120; Pump-Driven System; Pipe ID = 1.458 cm						
27	B1P01496	1.00	1.00×10 ⁻⁴	4	0.4	25.05-25.5
28	B2P01494	2.02	1.00×10 ⁻⁴	4	0.4	24.4-25.1
29	B5P01490	5.07	1.00×10 ⁻⁴	4	0.4	24.4-25.05
30	B1P11486	9.96	1.00×10 ⁻⁴	4	0.4	24.0-24.9
31	B2P11483	20.0	1.00×10 ⁻⁴	4	0.4	23.5-24.7
32	B5P11480	49.9	1.00×10 ⁻⁴	4	0.4	23.9-25.2
33	B1P21477	100	1.00×10 ⁻⁴	4	0.4	24.4-24.9
34	B1P03197	1.00	3.00×10 ⁻¹	4	0.4	24.5-25.1
35	B2P03195	2.02	3.00×10 ⁻¹	4	0.4	24.2-25.1
36	B5P03191	5.07	3.00×10 ⁻¹	4	0.4	24.6-25.3
37	B1P13187	9.96	3.01×10 ⁻¹	4	0.4	24.1-25.1

Entry	Run	Concentration	Salinity	Solvent Turbulent Baseline Constants		Temperature Range (°C - °C)
		c	[NaCl]	A _n	B _n	
		(wtppm)	(N)			
38	B2P13184	20.0	3.00×10^{-1}	4	0.4	23.8-25.2
39	B5P13181	49.9	3.00×10^{-1}	4	0.4	23.7-24.9
40	B1P23178	100	3.00×10^{-1}	4	0.4	24.3-25.1
Pusher 500-F = P500; Pump-Driven System; Pipe ID = 1.458 cm						
41	V1P11434	10.0	1.00×10^{-4}	4	0.4	24.0-24.9
42	V3P11437	30.0	1.00×10^{-4}	4	0.4	23.2-25.0
43	V1P21431	100	1.00×10^{-4}	4	0.4	23.8-25.0
44	V1P13135	10.0	3.00×10^{-1}	4	0.4	24.2-25.3
45	V3P13138	30.0	3.01×10^{-1}	4	0.4	23.4-25.2
46	V1P23132	100	3.00×10^{-1}	4	0.4	23.7-25.2
Pusher 500-F = P500; Pump-Driven System; Pipe ID = 1.021 cm						
47	W1P11462	10.0	1.00×10^{-4}	4	0.4	23.9-25.0
48	W3P11465	30.0	1.00×10^{-4}	4	0.4	24.0-25.2
49	W1P21468	99.8	1.00×10^{-4}	4	0.4	23.4-25.0
50	W3P11371	30.0	1.00×10^{-3}	4	0.4	23.75-25.15
51	W3P11272	30.0	1.00×10^{-2}	4	0.4	24.0-25.4
52	W1P13163	10.0	3.00×10^{-1}	4	0.4	24.55-25.4
53	W3P13166	30.0	3.00×10^{-1}	4	0.4	23.7-25.2

Entry	Run	Concentration	Salinity	Solvent Turbulent Baseline Constants		Temperature Range (°C - °C)
		c	[NaCl]	A _n	B _n	
		(wppm)	(N)			
54	W1P23169	99.8	3.00×10^{-1}	4	0.4	23.8-25.4
Alcomer 507 = A507; Pump-Driven System; Pipe ID = 1.458 cm						
55	A3P11409	30	1.00×10^{-4}	4	0.4	23.7-24.8
56	A1P21403	99.9	1.00×10^{-4}	4	0.4	22.6-24.8
57	A3P21406	300	1.00×10^{-4}	4	0.4	22.9-24.7
58	A1P31412	1000	1.00×10^{-4}	4	0.4	23.1-24.9
59	A3P13110	30.0	3.00×10^{-1}	4	0.4	23.5-25.2
60	A1P23104	99.9	3.00×10^{-1}	4	0.4	23.2-24.8
61	A3P23107	300	3.00×10^{-1}	4	0.4	23.5-24.9
62	A1P33113	1000	3.00×10^{-1}	4	0.4	23.55-25.05
DSR 1438 = D1438; Pump-Driven System; Pipe ID = 1.458 cm						
63	D3P11418	30	1.00×10^{-4}	4	0.4	23.2-25.0
64	D1P21415	99.8	1.00×10^{-4}	4	0.4	23.6-24.9
65	D3P21421	300	1.00×10^{-4}	4	0.4	22.8-25.1
66	D1P31424	997	1.00×10^{-4}	4	0.4	23.3-24.9
67	D3P13119	30.0	3.00×10^{-1}	4	0.4	23.4-24.9
68	D1P23116	99.8	3.00×10^{-1}	4	0.4	24.25-25.7
69	D3P23122	300	3.00×10^{-1}	4	0.4	23.6-25.5
70	D1P33125	997	3.00×10^{-1}	4	0.4	23.4-25.2

Entry	Run	Concentration	Salinity	Solvent Turbulent Baseline Constants		Temperature Range (°C - °C)
		c	[NaCl]	A _n	B _n	
		(wppm)	(N)			
Cyanamid 837A = C837A; Gravity System; Pipe ID = 1.458 cm						
71	P1P03478	1.03	3.08×10^{-4}	2.98	-2.00	21.9-22.05
72	P2P03497	2.09	3.09×10^{-4}	3.54	-0.79	20.45-20.65
73	P5P03486	5.16	3.09×10^{-4}	2.98	-2.00	21.2-21.4
74	P1P13490	10.3	3.09×10^{-4}	3.54	-0.79	20.65-20.85
75	P2P13494	20.8	3.12×10^{-4}	3.54	-0.79	21.8-22.0
76	P5P13401	52.0	3.12×10^{-4}	3.54	-0.79	23.8-24.1
77	P1P01379	1.03	1.04×10^{-3}	2.98	-2.00	21.7-21.85
78	P2P01398	2.09	1.03×10^{-3}	3.54	-0.79	20.35-20.65
79	P5P01387	5.16	1.04×10^{-3}	2.98	-2.00	21.2-21.4
80	P1P11391	10.3	1.04×10^{-3}	3.54	-0.79	20.45-20.65
81	P1P01180	1.03	1.04×10^{-1}	2.98	-2.00	21.4-21.65
82	P2P01199	2.09	1.05×10^{-1}	3.54	-0.79	20.2-20.55
83	P5P01188	5.16	1.04×10^{-1}	2.98	-2.00	21.2-21.6
84	P1P11192	10.3	1.03×10^{-1}	3.54	-0.79	20.2-20.55
85	P2P11195	20.8	1.05×10^{-1}	3.54	-0.79	21.8-22.0
86	P5P11102	52.0	1.07×10^{-1}	3.54	-0.79	23.75-24.0
Cyanamid 836A = C836A; Gravity System; Pipe ID = 1.458 cm						
87	P1P03404	1.03	3.09×10^{-4}	3.54	-0.79	21.2-21.65
88	P2P03407	2.07	3.09×10^{-4}	3.54	-0.79	20.8-21.4

Entry	Run	Concentration	Salinity	Solvent Turbulent Baseline Constants		Temperature Range (°C - °C)
		c	[NaCl]	A _n	B _n	
		(wppm)	(N)			
89	P5P03410	5.16	3.09×10^{-4}	3.54	-0.79	20.1-20.35
90	P1P13413	10.3	3.09×10^{-4}	3.54	-0.79	21.0-21.45
91	P2P13426	20.6	3.09×10^{-4}	3.54	-0.79	21.5-21.6
92	P1P01305	1.03	1.04×10^{-3}	3.54	-0.79	21.1-21.5
93	P2P01308	2.07	1.04×10^{-3}	3.54	-0.79	20.9-21.45
94	P5P01311	5.16	1.04×10^{-3}	3.54	-0.79	20.0-20.3
95	P1P11314	10.3	1.04×10^{-3}	3.54	-0.79	21.0-21.45
96	P2P11327	20.6	1.04×10^{-3}	3.54	-0.79	21.4-21.4
97	P2P11229	20.6	1.03×10^{-2}	3.54	-0.79	21.2-21.2
98	P1P11106	1.03	1.06×10^{-1}	3.54	-0.79	21.0-21.5
99	P2P01109	2.07	1.05×10^{-1}	3.54	-0.79	20.9-21.4
100	P5P01112	5.16	1.06×10^{-1}	3.54	-0.79	19.9-20.25
101	P1P11115	10.3	1.05×10^{-1}	3.54	-0.79	20.7-21.1
102	P2P11128	20.6	1.06×10^{-1}	3.54	-0.79	20.9-21.0
103	P2P11130	20.6	1.04×10^{-1}	3.54	-0.79	20.95-21.05
Cyanamid 832A = C832A; Gravity System; Pipe ID = 1.458 cm						
104	P1P01556	1.04	1.00×10^{-5}	2.98	-2.00	20.8-20.8
105	P2P01570	2.09	1.00×10^{-5}	2.98	-2.00	19.9-20.25
106	P5P01573	5.63	1.00×10^{-5}	2.98	-2.00	20.4-20.9
107	P1P11574	10.2	1.00×10^{-5}	2.98	-2.00	21.1-21.3

Entry	Run	Concentration	Salinity	Solvent Turbulent Baseline Constants		Temperature Range (°C - °C)
		c	[NaCl]	A _n	B _n	
		(wppm)	(N)			
108	P2P11575	20.9	1.00×10^{-5}	2.98	-2.00	21.2-21.45
109	P1P03443	1.03	3.08×10^{-4}	4	0.4	20.2-22.1
110	P2P03445	2.06	3.08×10^{-4}	4	0.4	21.9-22.0
111	P5P03448	5.57	3.08×10^{-4}	4	0.4	21.4-21.5
112	P1P13451	10.0	3.08×10^{-4}	4	0.4	20.0-20.0
113	P2P13457	20.7	3.09×10^{-4}	4	0.4	20.4-20.5
114	P1P01344	1.03	1.03×10^{-3}	4	0.4	20.0-20.15
115	P2P01346	2.06	1.03×10^{-3}	4	0.4	21.65-21.7
116	P5P01349	5.57	1.03×10^{-3}	4	0.4	21.1-21.1
117	P1P11352	10.0	1.01×10^{-3}	4	0.4	19.7-19.7
118	P2P11358	20.7	1.03×10^{-3}	4	0.4	20.4-20.6
119	P2P01147	2.06	1.05×10^{-1}	4	0.4	21.2-21.3
120	P5P01150	5.57	1.04×10^{-1}	4	0.4	20.6-20.7
121	P1P11153	10.0	1.05×10^{-1}	4	0.4	19.4-19.5
122	P2P11159	20.7	1.05×10^{-1}	4	0.4	20.5-20.75

Table 5.2.2 summarizes the turbulent-flow parameters extracted from each run and contains eight columns: Entry; Polymeric-Regime Constants, A_p and B_p ; Apparent Slips, S'_1 and S'_3 ; Slope Increment δ ; Onset & Retro-Onset Wall Shear Stresses, T_w^* and $T_w^\#$. The Entry column links each row with Table 5.2.1. The second and third columns give the slope A_p and intercept B_p , respectively, of the best-fit, least-squares line through the data composing the polymeric-regime segment P of the run:

$$\frac{1}{\sqrt{f}} = A_p \log(Re_s \sqrt{f}) - B_p \quad (5.2-1)$$

The fourth and fifth columns, S'_1 and S'_3 , contain the apparent slip S' evaluated at $Re_s \sqrt{f} = 1000$ and 3000 , respectively; for runs in the gravity-driven system, only S'_1 is quoted because $Re_s \sqrt{f}_{\max} < 3000$. In the sixth column is given the slope increment $\delta = A_p - A_n$, the difference between the P-segment slope, A_p , and the slope of the solvent line N, A_n . The seventh column gives the onset wall shear stress T_w^* , dyne/cm², for each run exhibiting onset. Both regressed and visual values of T_w^* are quoted, the latter in parentheses to the right of the former. Regressed T_w^* were calculated from $Re_s \sqrt{f}^*$, determined from (A_n, B_n) and (A_p, B_p) :

$$Re_s \sqrt{f}^* = 10^{\left(\frac{B_p - B_n}{A_p - A_n} \right)} \quad (5.2-2)$$

This $Re_s \sqrt{f}^*$ obtains at the onset point where the P segment, extrapolated backward, would intersect the N baseline. By use of $Re_s \sqrt{f} = \sqrt{2} Du_r / \nu_s$ and $T_w = \rho u_r^2$, the onset wall shear stress is:

$$T_w^* = \rho \left[\frac{\nu_s Re_s \sqrt{f}^*}{\sqrt{2} D} \right]^2 \quad (5.2-3)$$

In the calculating the visual T_w^* , two adjacent data points were selected in an LNP trajectory, one with the highest T_w in the N segment without drag reduction and one with the lowest T_w in the P segment with drag reduction. The visual T_w^* was the geometric mean of these two T_w values. The uncertainty in T_w^* can be as high as $\pm 100\%$ for P segments having small slope increments δ , excess curvature, or more than one linear domain. Mostly, regressed T_w^* either equals or exceeds visual T_w^* because the curvature in a P-segment was usually concave upward. The visual and regressed T_w^* values are not statistically very different and can be considered the best lower and upper bounds bracketing T_w^* . In the eighth column, the retro-onset wall shear stress $T_w^\#$, dyne/cm², is given for each run exhibiting retro-onset. As for T_w^* , both regressed and visual $T_w^\#$ values were calculated, with the latter given in parentheses to the right of the former. Regressed $T_w^\#$ was calculated from $Re_s \sqrt{f}^\#$, determined from (A_p, B_p) and the slope and intercept of the MDR asymptote, (19.0,32.4):

$$Re_s \sqrt{f}^\# = 10^{\left(\frac{32.4 - B_p}{19.0 - A_p} \right)} \quad (5.2-4)$$

This $Re_s \sqrt{f}^\#$ obtains at the retro-onset point where the P segment, extrapolated backward, would intersect the MDR asymptote. The retro-onset wall shear stress $T_w^\#$ is calculated from an equation analogous to equation 5.2-3:

$$T_w^\# = \rho \left[\frac{\nu_s Re_s \sqrt{f}^\#}{\sqrt{2} D} \right]^2 \quad (5.2-5)$$

In the calculating visual $T_w^\#$, two adjacent data points were selected in an LMP trajectory, one with the highest T_w in the M segment of additive-independent, maximum turbulent drag reduction and one with the lowest T_w in the P segment of additive-dependent turbulent drag reduction. The visual $T_w^\#$ was the geometric mean of these two. The uncertainty in $T_w^\#$ can be as high as $\pm 100\%$, especially at large $Re_s \sqrt{f}$ because T_w grows as $(Re_s \sqrt{f})^2$. Regressed $T_w^\#$ does not exceed visual $T_w^\#$ because the regression of a P segment includes the last data point on M and, thus, yields lower $Re_s \sqrt{f}^\#$. The two values are probably not statistically different and represent the best lower and upper values for $T_w^\#$. The appearance of "MDR" in this column indicates that the flow trajectory of the run attained maximum drag reduction at the highest $Re_s \sqrt{f}$, by which point retro-onset did not occur.

Table 5.2.2
Turbulent-Flow Parameters

Entry	Polymeric-Regime Constants		Apparent Slips ^a		Slope Increment	Onset & Retro-Onset Wall Shear Stresses ^b	
	A _p	B _p	S' ₁	S' ₃	δ	T _w [°]	T _w [#]
						(dyne/cm ²)	
Cyanamid 832A = C832A; Pump-Driven System; Pipe ID = 1.458 cm							
1	4.96	1.71	1.5	2.0	0.96	0	
2	7.01	4.89	4.3	5.8	3.01		0.7(1.3)
3	10.9	13.7	7.3	10.1	6.90		0.8(1.8)
4	9.63	3.40	12.0	16.6	5.63		29.8(47)
5	1.74?	-26.1?	11.5	18.5			110?(150?)
6			7.6	18.7			MDR
7			7.6	19.1			MDR
8	4.13	0.82	0	0†	0.13		
9	9.07	14.3	~1.1	3.4	5.07	5.9(6.0)	
10	13.4	25.9	2.1	7.1	9.40	5.4(4.8)	
11	19.5	42.8	3.8	11.1	15.5		
12	21.1	45.4	6.0	14.8	17.1		
13	24.3	53.4	8.2	18.7	20.3		
14			10.2	19.7			MDR
Cyanamid 832A = C832A; Pump-Driven System; Pipe ID = 1.021 cm							
15	4.01	-1.04	1.2	1.6	0.01		
16	6.24	4.46	2.9	3.5	2.24		
17	8.15	6.37	6.6	8.2	4.15		

Entry	Polymeric-Regime Constants		Apparent Slips ^a		Slope Increment	Onset & Retro-Onset Wall Shear Stresses ^b	
	A _p	B _p	S' ₁	S' ₃	δ	T _w [*]	T _w [#]
						(dyne/cm ²)	
18	11.0	8.71	11.9	15.1	7.0		31.9(66)
19	2.06	-26.3	12.7	19.5	-1.94		332(410)
20			~ 12	20.9			MDR
21	5.27	3.86	0.3	0.9	1.27	12.2(22.2)	
22	7.50	9.83	1.2	2.7	3.50	9.7(9.6)	
23	13.4	25.2	3.5	7.0	9.40		
24	18.5	37.1	6.7	11.4	14.5		
25	24.0	50.1	10.9	17.7	20.0		
26	22.9	44.8	12.8	20.2	18.9		MDR
Betz 1120 = B1120; Pump-Driven System; Pipe ID = 1.458 cm							
27	4.01	-0.57	0.5	1.0	~0	3.3(3.8?)	
28	7.43	7.69	3.0	4.4	3.43		
29	5.29	-4.76	8.8	9.5	1.29		
30	7.98	-1.18	13.0	14.7	3.98		23.4(38)
31			11.8	18.2			MDR
32			10.8	19.1			MDR
33			9.7	18.6			MDR
34	4.92	3.14	0.3	0.5	0.92	17.8(22?)	
35	7.70	10.6	0.5	2.7	3.70	6.5(13.5)	
36	12.4	23.9	1.3	5.4	8.40	7.4(6.1)	
37	17.2	36.1	4.0	10.2	13.2	5.1(4.1)	

Entry	Polymeric-Regime Constants		Apparent Slips ^a		Slope Increment	Onset & Retro-Onset Wall Shear Stresses ^b	
	A _p	B _p	S' ₁	S' ₃	δ	T _w [*]	T _w [#]
						(dyne/cm ²)	
38	22.0	48.8	5.6	14.5	18.0		
39			11.0	19.0			MDR
40			11.2	18.6			MDR
Pusher 500-F = P500; Pump-Driven System; Pipe ID = 1.458 cm							
41	8.95	10.7	4.6	7.0	4.95		
42	5.90	-6.21	11.3	13.4	1.90		14.8(14.6)
43			7.3	18.4			MDR
44	10.8	19.7	1.0	4.56	6.80	9.5(9.6)	
45	15.7	32.4	2.5	9.0	11.7	5.9(6.2)	
46	26.2	61.8	5.0	16.0	22.2	6.5(4.1)	
Pusher 500-F = P500; Pump-Driven System; Pipe ID = 1.021 cm							
47	8.58	9.63	4.6	6.6	4.58		
48	9.00	3.35	10.4	14.8	5.00		
49			9.2	19.7			MDR
50	7.60	-1.72	10.1	15.3	3.60		
51	18.0	34.7	7.7	13.8	14.0		
52	10.6	19.0	1.1	4.8	6.60	16.0(14.4)	
53	17.2	35.6	4.2	10.8	13.2		
54	31.2	72.6	9.2	19.4	27.2		MDR

Entry	Polymeric-Regime Constants		Apparent Slips ^a		Slope Increment	Onset & Retro-Onset Wall Shear Stresses ^b	
	A _p	B _p	S' ₁	S' ₃	δ	T _w [*]	T _w [#]
(dyne/cm ²)							
Alcomer 507 = A507; Pump-Driven System; Pipe ID = 1.458 cm							
55	4.27	0.94	0.1?	0.4	0.27	0.19(25.0)	
56	5.61	4.57	0.3?	1.5	1.61	2.9(20.3)	
57	9.03	15.9	0†	2.0	5.03	27.7(25.7)	
58	15.6	39.3	-1.7!	1.4	11.6	90.0(69.3)	
59	4.43	1.78	0†	0.10	0.43	45.2(55.2)	
60	5.32	4.61	0†	0.4	1.32	46.9(68.0)	
61	6.97	9.86	0†	0.9	2.97	45.6(38.8)	
62	9.72	18.7	0†	1.7	5.27	46.8(60.7)	
DSR 1438 = D1438; Pump-Driven System; Pipe ID = 1.458 cm							
63	5.73	5.76	0†	0.6	1.73	29.4(38.8)	
64	8.12	12.7	0.4	1.9	4.12	18.3(12.2)	
65	13.3	29.4	0†	3.2	9.30	33.8(37.6)	
66	20.8	55.1	0†	3.5	16.8	60.5(58.3)	
67	5.36	4.89	0†	0.3	1.36	77.3(68.6)	
68	6.37	7.89	0†	0.8	2.37	40.9(66.4)	
69	8.84	15.3	0†	1.7	4.84	27.7(27.4)	
70	15.4	36.4	0†	3.4	11.4	40.2(38.0)	
Cyanamid 837A = C837A; Gravity-Driven System; Pipe ID = 1.458 cm							
71	3.20	-1.61	0.2		0.22	0(10.9)	

Entry	Polymeric-Regime Constants		Apparent Slips ^a		Slope Increment	Onset & Retro-Onset Wall Shear Stresses ^b	
	A _p	B _p	S' ₁	S' ₃	δ	T _w [*]	T _w [#]
						(dyne/cm ²)	
72	5.97	5.87	0.6		2.43	7.0(9.5)	
73	9.02	13.7	2.4		6.05		
74	13.7	25.2	4.5		10.1		
75	25.0	54.3	9.1		21.4		
76			10.8				MDR
77	3.02	-2.02	0.1		0.05	0(6.2)	
78	5.22	3.90	0.3		1.68	8.77(9.7)	
79	8.25	12.0	1.7		5.28		
80	12.0	21.5	3.1		8.00		
81	2.77	-2.66	0		-0.20		
82	4.02	0.59	0.1		0.48	13.2(14.0)	
83	8.59	14.7	0.2†		5.62	19.4(23.2)	
84	13.5	29.2	0.2†		9.95	24.8(16.4)	
85	20.6	47.0	3.1		17.0	9.24(6.1)	
86	17.9	37.6	5.9		13.9		
Cyanamid 836A = C836A; Gravity-Driven System; Pipe ID = 1.458 cm							
87	6.02	6.32	0.4		2.48	12.1(6.4)	
88	6.51	7.65	0.5		2.97	10.8(6.5)	
89	11.1	18.6	3.1		7.52		
90	13.6	24.7	4.8		10.1		
91	18.0	32.0	10.6		14.4		

Entry	Polymeric-Regime Constants		Apparent Slips ^a		Slope Increment	Onset & Retro-Onset Wall Shear Stresses ^b	
	A _p	B _p	S' ₁	S' ₃	δ	T _w ^c	T _w [#]
						(dyne/cm ²)	
92	5.01	3.43	0.2		1.47	13.1(17.6)	
93	5.44	4.62	0.3		1.90	11.3(13.7)	
94	8.22	11.3	1.8		4.68		
95	12.4	22.1	3.6		8.88		
96	19.8	38.9	9.0		16.3		
97	19.4	42.1	4.4		15.9		
98	3.94	0.40	0		0.40?	23.5(20.0)	
99	4.09	0.79	0		0.54?	17.3(20.8)	
100	8.08	12.6	0.2		4.54	20.1(14.7)	
101	10.7	20.3	0.5		7.20	16.5(15.1)	
102	18.6	42.8	1.4		15.1	13.7(6.6)	
103	18.6	42.0	2.3		15.1	10.8(6.6)	
Cyanamid 832A = C832A; Gravity-Driven System; Pipe ID = 1.458 cm							
104	3.19	-1.75	0.9		0.22		
105	4.72	1.46	1.8		1.74		
106	8.49	10.1	4.7		5.52		
107	4.64	-6.69	9.9		1.66		6.21(6.4)
108			12.8‡				MDR
109	4.78	2.53	0.2		0.78	6.18(8.7)	

Entry	Polymeric-Regime Constants		Apparent Slips ^a		Slope Increment	Onset & Retro-Onset Wall Shear Stresses ^b	
	A _p	B _p	S' ₁	S' ₃	δ	T _w [*]	T _w [#]
						(dyne/cm ²)	
110	6.03	4.92	1.5		2.03		
111	9.78	14.0	3.8		5.78		
112	9.54	8.18	9.0		5.54		3.10(5.2)
113			11.2‡				MDR
114	3.97	0.40	0		0		
115	5.39	3.80	0.8		1.39		
116	8.70	12.5	2.0		4.70		
117	10.5	14.0	5.9		6.49		
118			11.3‡				MDR
119	3.98	0.38	0		0		
120	3.93	0.22	~0.1		0		
121	10.9	19.7	1.2		6.87	10.1(7.7)	
122	20.1	44.8	3.9		16.1	7.44(4.2)	

(a) S'₁ and S'₃ denote S' evaluated at Re_v√f = 1000 and 3000, respectively.
(b) () = visual value.
† = before onset; ‡ = highest Re_v√f < 1000.

Table 5.2.3 summarizes the laminar-flow parameters extracted from each run and contains five columns: Entry; Arithmetic-Mean and Geometric-Mean Estimated Intrinsic Viscosities, η_{sp}/c^a and η_{sp}/c^g , and Pseudo-Power-Law Coefficient and Exponent, K' and n'. The Entry column links the rows to Table 5.2.1. The second and third columns both provide estimates of polymer intrinsic viscosity, $[\eta]$, by listing the arithmetic and geometric means, respectively, of η_{sp}/c in cm³/g for each run. In laminar flow, the relative viscosity η_r at each data point was the $Re_s\sqrt{f}$ ratio of polymer solution to solvent at fixed $1/\sqrt{f}$:

$$\eta_r = \left(\frac{Re_s\sqrt{f_p}}{Re_s\sqrt{f_L}} \right) \frac{1}{\sqrt{f_r}} = \left(\frac{Re_s f_p}{16} \right) \quad (5.2-6)$$

From the specific viscosity $\eta_{sp} = (\eta_r - 1)$, it follows that $\eta_{sp}/c = (\eta_r - 1)/c$. For each laminar-flow data point, η_{sp}/c was calculated, from several of which an average value, either arithmetic or geometric, could be determined. At low salinity the laminar viscosity was usually shear-thinning as η_{sp}/c decreased with increasing $Re_s\sqrt{f}$. At high salinity, shear-thinning behavior was not pronounced, and η_{sp}/c was approximately constant. Whereas an arithmetic mean was appropriate for a set of η_{sp}/c at high salinity, it was not at low salinity; thus, both arithmetic and geometric mean were calculated for each set, their difference reflecting the severity of shear thinning. Significant differences only arose at the highest concentrations and lowest salinities. In the fourth and fifth columns, the pseudo-power-law coefficient K' and exponent n' were determined from the laminar-flow data in each run. Both are defined by the pseudo-power law for polymer-solution viscosity:

$$T_w = K' \left(\frac{8 \langle \bar{U} \rangle}{D} \right)^{n'} \quad (5.2-7)$$

where $8 \langle \bar{U} \rangle / D$ is the laminar-flow shear rate in s^{-1} . At each laminar-flow data point, T_w and $8 \langle \bar{U} \rangle / D$ were determined. For a set of data, the best-fit line for $\log T_w$ vs. $\log 8 \langle \bar{U} \rangle / D$ was calculated, where the slope and intercept were n' and $\log K'$, respectively.

At the highest salinities, corresponding to the random-coiling conformation, and moderate polymer concentrations, the polymer-solutions were virtually indistinguishable from solvent in that they exhibited almost no shear thinning and had relative viscosities very close to unity; thus, their exponents $n' \approx 1.0$, the Newtonian value, and their coefficients $K' \approx 0.009 \text{ g}/(\text{cm} \cdot \text{s})$, about the solvent viscosity. Even at the highest concentrations for which $\eta_r \approx 1.5$; the solutions were Newtonian, having exponents $n' \approx 1.0$. At the lowest salinities at all concentrations, the coefficient K' could be much greater than $0.009 \text{ g}/(\text{cm} \cdot \text{s})$; the exponent n' , much less than unity. For the most extreme example, a 100-wppm solution of additive B1120 with 0.0001 N NaCl (entry 36), K' and n' respectively reached $0.4176 \text{ s}^{0.490} \cdot \text{dyne}/\text{cm}^2$ and a minimum of 0.490.

Table 5.2.3
Laminar-Flow Parameters

Entry	Arithmetic- and Geometric-Mean Estimated Intrinsic Viscosities		Pseudo-Power-Law Coefficient and Exponent	
	η_{sp}/c^a	η_{sp}/c^b	K'	n'
	(cm ³ /g)		(s ^{n'} · dyne/cm ²)	
Cyanamid 832A = C832A; Pump-Driven System; Pipe ID = 1.458 cm				
1	11994	11980	0.0092	0.998
2	106170	105875	0.0120	0.969
3	55215	55167	0.0120	0.989
4	110550	105733	0.0405	0.756
5	86350	79622	0.0560	0.735
6	116644	105897	0.1945	0.566
7	83039	74663	0.2383	0.595
8	0	0	0.0093	0.999
9	19722	19608	0.0099	0.995
10	13326	12818	0.0094	1.015
11	11367	11365	0.0105	0.997
12	5790	5780	0.0103	1.004
13	2547	2633	0.0108	0.994
14	3739	3667	0.0133	0.972
Cyanamid 832A = C832A; Pump-Driven System; Pipe ID = 1.021 cm				
15	62797	59371	0.0106	0.973
16	69357	66187	0.0129	0.935
17	74359	71848	0.0178	0.898
18	57649	55238	0.0209	0.882

Entry	Arithmetic- and Geometric-Mean Estimated Intrinsic Viscosities		Pseudo-Power-Law Coefficient and Exponent	
	η_{sp}/c^a	η_{sp}/c^b	K'	n'
	(cm ³ /g)		(s ^{n'} · dyne/cm ²)	
19	109219	107192	0.0739	0.679
20	59145	57253	0.0818	0.726
21	0	0	0.0092	1.005
22	0	0	0.0095	1.001
23	0	0	0.0096	0.999
24	0	0	0.0097	1.001
25	3172	3086	0.0098	1.002
26	2575	2575	0.0109	0.996
Betz 1120 = B1120; Pump-Driven System; Pipe ID = 1.458 cm				
27	26869	24388	0.0090	1.006
28	84479	80687	0.0119	0.956
29	123199	113391	0.0210	0.861
30	113990	109283	0.0300	0.814
31	54709	52839	0.0296	0.847
32	116809	109491	0.2150	0.543
33	111709	104565	0.4176	0.490
34	0	0	0.0090	1.007
35	0	0	0.0093	0.997
36	7703	7689	0.0097	0.998
37	3658	3585	0.0096	1.002
38	2470	2357	0.0098	1.002
39	3398	3373	0.0109	1.004

Entry	Arithmetic- and Geometric-Mean Estimated Intrinsic Viscosities		Pseudo-Power-Law Coefficient and Exponent	
	η_{sp}/c^a	η_{sp}/c^g	K'	n'
	(cm ³ /g)		(s ^{n'} · dyne/cm ²)	
40	4001	3993	0.0131	1.000
Pusher 500-F = P500; Pump-Driven System; Pipe ID = 1.458 cm				
41	71637	69745	0.0191	0.925
42	75338	73942	0.0695	0.732
43	99572	95219	0.2746	0.565
44	3336	3271	0.0096	1.002
45	3037	2984	0.0100	1.007
46	2091	2088	0.0113	1.001
Pusher 500-F = P500; Pump-Driven System; Pipe ID = 1.021 cm				
47	62981	62074	0.0195	0.892
48	53183	52775	0.0362	0.836
49	72353	70603	0.1683	0.653
50	33358	33143	0.0243	0.892
51	8485	8480	0.0116	0.994
52	0	0	0.0093	1.000
53	1637	1630	0.0099	1.001
54	1829	1829	0.0113	0.995
Alcomer 507 = A507; Pump-Driven System; Pipe ID = 1.458 cm				
55	5398	5385	0.0104	1.008

Entry	Arithmetic- and Geometric-Mean Estimated Intrinsic Viscosities		Pseudo-Power-Law Coefficient and Exponent	
	η_{sp}/c^a	η_{sp}/c^b	K'	n'
	(cm ³ /g)		(s ^{n'} · dyne/cm ²)	
56	32618	32566	0.0454	0.938
57	8973	8952	0.0394	0.969
58	6633	6628	0.0781	0.963
59	0	0	0.0095	0.999
60	0	0	0.0092	1.016
61	347	314	0.0100	1.011
62	360	360	0.0125	1.009
DSR 1438 = D1438; Pump-Driven System; Pipe ID = 1.458 cm				
63	3099	3085	0.0100	1.002
64	8383	8381	0.0170	0.997
65	7733	7732	0.0320	0.986
66	3825	3822	0.0480	0.972
67	0	0	0.0094	1.001
68	436	422	0.0095	1.009
69	461	458	0.0104	1.006
70	441	441	0.0133	1.007
Cyanamid 837A = C837A; Gravity-Driven System; Pipe ID = 1.458 cm				
71	34523	34508	0.0100	0.999
72	25672	25483	0.0099	1.012
73	--	--	--	--
74	--	--	--	--

Entry	Arithmetic- and Geometric-Mean Estimated Intrinsic Viscosities		Pseudo-Power-Law Coefficient and Exponent	
	η_{sp}/c^a	η_{sp}/c^b	K'	n'
	(cm ³ /g)		(s ^{n'} · dyne/cm ²)	
75	21194	21166	0.0139	1.000
76	41727	40122	0.0476	0.803
77	33211	32598	0.0101	0.999
78	7911	7864	0.0099	1.003
79	--	--	--	--
80	--	--	--	--
81	21878	19632	0.0099	0.998
82	2586	2071	0.0100	1.002
83	--	--	--	--
84	--	--	--	--
85	--	--	--	--
86	2775	2648	0.0106	0.994
Cyanamid 836A = C836A; Gravity-Driven System; Pipe ID = 1.458 cm				
87	42155	42024	0.0100	1.003
88	22247	21392	0.0101	1.001
89	49278	47947	0.0148	0.940
90	26550	26392	0.0128	0.989
91	70970	67372	0.0401	0.797
92	33501	33033	0.0098	1.008
93	18797	18391	0.0100	1.003
94	24934	24891	0.0113	1.000

Entry	Arithmetic- and Geometric-Mean Estimated Intrinsic Viscosities		Pseudo-Power-Law Coefficient and Exponent	
	η_{sp}/c^a	η_{sp}/c^b	K'	n'
	(cm ³ /g)		(s ^{n'} · dyne/cm ²)	
95	21058	20967	0.0119	0.998
96	36543	36109	0.0218	0.910
97	8204	8172	0.0115	0.996
98	0	0	0.0095	1.010
99	3957	3768	0.0098	1.004
100	0	0	0.0099	1.004
101	4395	4245	0.0094	1.027
102	2821	2811	0.0106	0.999
103	2569	2543	0.0103	1.003
Cyanamid 832A = C832A; Gravity-Driven System; Pipe ID = 1.458 cm				
104	--	--	--	--
105	116856	112141	0.0195	0.860
106	35364	34285	0.0151	0.949
107	96855	95552	0.0516	0.732
108	199918	146399	0.1158	0.617
109	--	--	--	--
110	47196	46647	0.0102	1.006
111	21957	21956	0.0110	0.997
112	47270	47125	0.0181	0.954
113	58527	58016	0.0564	0.769

Entry	Arithmetic- and Geometric-Mean Estimated Intrinsic Viscosities		Pseudo-Power-Law Coefficient and Exponent	
	η_{sp}/c^a	η_{sp}/c^g	K'	n'
	(cm ³ /g)		(s ^{n'} · dyne/cm ²)	
114	--	--	0.0100	1.001
115	17859	17518	0.0092	1.021
116	21602	21498	0.0104	1.013
117	32795	32767	0.0137	0.994
118	43424	42978	0.0415	0.806
119	--	--	--	--
120	--	--	--	--
121	--	--	--	--
122	5246	5229	0.0109	1.002

Superscripts: a = arithmetic mean; g = geometric mean.

5.2.3 Detailed Descriptions

(1) High Molecular-Weight Additives

Figures 5.2.6 and 5.2.7, each a composite PK plot, presents results from the pump-driven system using the 1.458-cm pipe for additive C832A in 0.3 N NaCl, the initially collapsed conformation, and 0.0001 N NaCl, the initially extended conformation, respectively, at $c = 1, 2, 5, 10, 20, 50,$ and 100 wppm.

The set of runs in Figure 5.2.6 typifies Type-A drag-reduction behavior by initially collapsed HPAM macromolecules. Lines L, N, and M represent Poiseuille's Law for laminar flow, the Newtonian turbulent-flow baseline, and the MDR asymptote, respectively.

For $50 < Re_r\sqrt{f} < 150$, the 1-wppm data follow L closely and for $150 < Re_r\sqrt{f} < 350$, depart downward from L and toward N, completing a laminar-to-turbulent transition like those previously observed in solvent runs. For $400 < Re_r\sqrt{f} < 6000$, the data adhere closely to the baseline N, following an N segment of slope and intercept $(A_p, B_p) = (4.1, 0.8)$ and then appear to show a small amount of flow enhancement for $6000 < Re_r\sqrt{f} < 7000$. The 1-wppm data thus exhibit essentially an LN trajectory.

The 2-wppm and 5-wppm data display LNP trajectories, like that described for the 0.3-N data shown in Figure 5.2.4. For $50 < Re_r\sqrt{f} < 150$, the data follow L closely with viscosities $\eta_r \approx 1.0$ and for $180 < Re_r\sqrt{f} < 350$, undergo laminar-to-turbulent transitions, departing downward from L and dropping toward N. For $Re_r\sqrt{f} > 400$, the 2-wppm and 5-wppm data continue along N, onset respectively at $Re_r\sqrt{f}^* \approx 550$ and

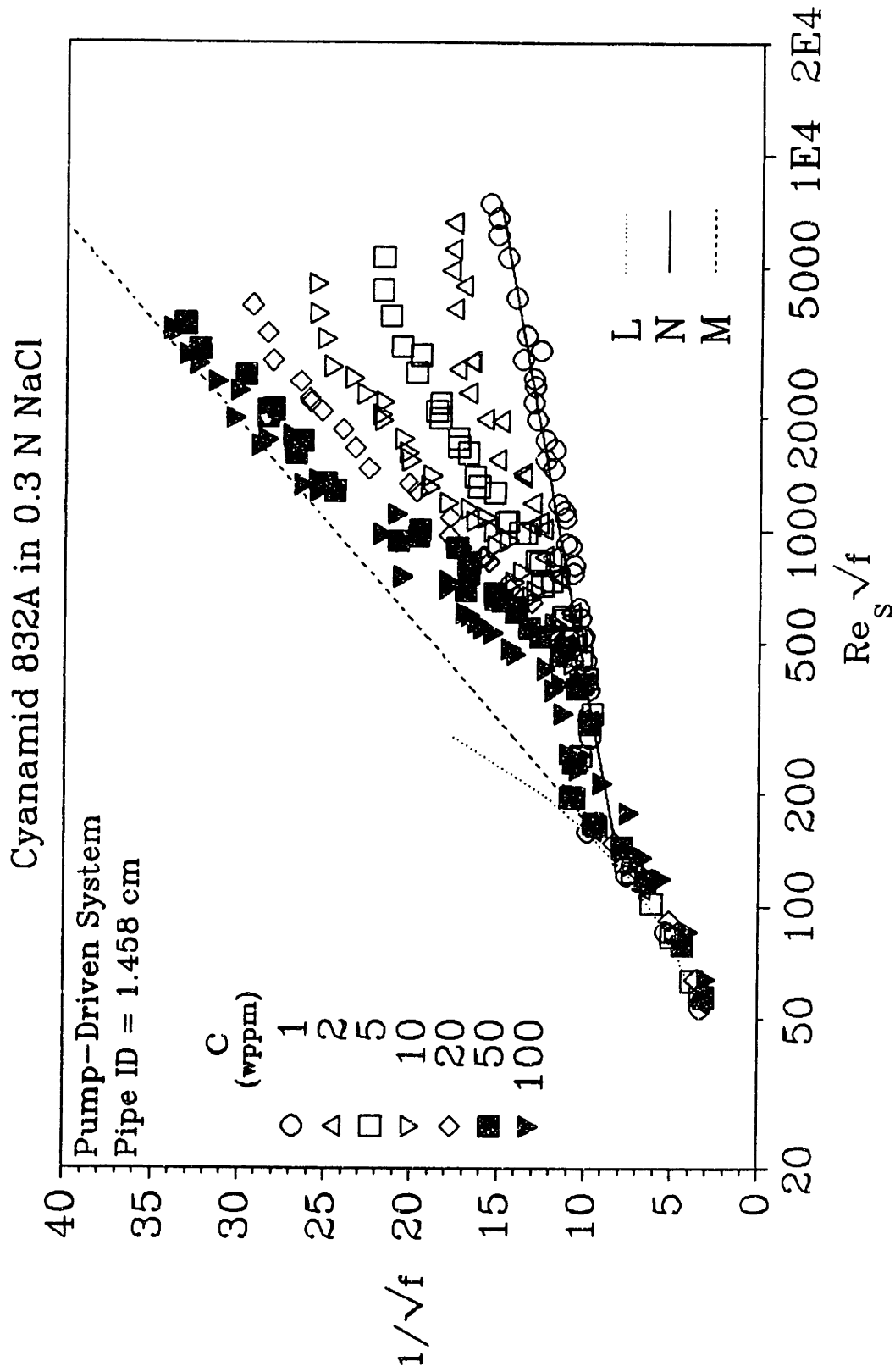


Figure 5.2.6: Cyanamid 832A in 0.3 N NaCl from the 1.458-cm Pipe

520, and ascend into the polymeric regime along linear segments P with slopes and intercepts $(A_p, B_p) = (9.1, 14.3)$ and $(13.4, 25.9)$ and slope increments $\delta = 5.1$ and 9.4 until $Re_p\sqrt{f} \approx 3000$ and 4000 , respectively. For $Re_p\sqrt{f} > 3000$, the 2-wppm data depart downward from their segment P, perhaps because of polymer degradation, and maintain constant $1/\sqrt{f}$ up to $Re_p\sqrt{f} \approx 7600$; similarly, the 5-wppm data level off from their segment P for $4000 < Re_p\sqrt{f} < 5000$.

Data for $c = 10, 20$, and 50 wppm display L(N)P trajectories, with ill-defined Newtonian segments. For $50 < Re_p\sqrt{f} < 150$, their data parallel L closely with $\eta_r \leq 1.1$, exhibiting slight drag enhancement relative to solvent, and at $Re_p\sqrt{f} \approx 180$, depart downward from L toward N, beginning laminar-to-turbulent transitions. Rather than dropping onto, and then following, N upon achieving turbulence, data for $c = 10, 20$, and 50 wppm reach $1/\sqrt{f}$ minima on or very close to N at $Re_p\sqrt{f} \approx 300$ to 400 . From their minima, these data rise into the polymeric regime along respective linear segments with $(A_p, B_p) = (19.5, 42.8)$, $(21.1, 45.4)$, and $(24.3, 53.4)$ and $\delta = 15.5, 17.1$ and 20.3 until $Re_p\sqrt{f} \approx 3000, 3000$, and 1500 . Although these data do not show clear-cut onsets, for a lack of well-defined N segments, nonetheless extrapolating their segments P back to the line N yields apparent regressed $Re_p\sqrt{f}^* \approx 540, 420$, and 410 , respectively. For $Re_p\sqrt{f} > 3000$, the 10-wppm and 20-wppm data depart slightly downward from their segments P, likely on account of polymer degradation, up to $Re_p\sqrt{f} \approx 4400$ and 5100 , respectively; for $Re_p\sqrt{f} > 1000$, the 50-wppm data rise steeply along their segment P toward the MDR asymptote, come closest to M at $Re_p\sqrt{f} \approx 1400$, and then approximately parallel M up to $Re_p\sqrt{f} \approx 4000$.

The 100-wppm data display an LPM trajectory. For $50 < Re_p\sqrt{f} < 150$, they

data follow a slightly shear-thinning, laminar path with $\eta_r \approx 1.3$ and show the greatest drag enhancement relative to solvent. At $Re_s\sqrt{f} \approx 180$, the 100-wppm data suddenly shift rightwards and begin to parallel L as if $\eta_r \approx 1.5$ until $Re_s\sqrt{f} \approx 240$. For $250 < Re_s\sqrt{f} < 400$, the 100-wppm data shift abruptly rightward and slightly upward in apparent transitional behavior and for $450 < Re_s\sqrt{f} < 1200$, rise steeply into the polymeric regime toward the MDR asymptote along a linear segment P with $(A_p, B_p) = (27.5, 59.5)$ and $\delta = 23.5$. Extrapolating the segment P back to the line N gives an apparent regressed $Re_s\sqrt{f}^* \approx 330$ for the 100-wppm data. At $Re_s\sqrt{f} \approx 1300$, the data virtually converge onto M and begin to climb along M up to $Re_s\sqrt{f} \approx 3400$.

To summarize, the flow trajectories displayed in Figure 5.2.6 are: LN by the 1-wppm data; LNP by the 2-wppm and 5-wppm data; L(N)P by the data at $c = 10, 20$, and 50 wppm; and LPM by the 100-wppm data. In laminar flow, all data lie close to L with $\eta_r < 1.4$, typical behavior by solutions of collapsed macromolecules. In turbulent flow, the 1-wppm data show no perceptible drag reduction; all other solutions, with $c = 2, 5, 10, 20, 50$, and 100 wppm exhibit drag reduction, with P segments, the slopes and slope increments of which increase as the concentration increases: $A_p = 9.1, 13.4, 19.5, 21.1, 24.3$, and 27.5 , and $\delta = 5.1, 9.4, 15.5, 17.1, 20.3$, and 23.5 , respectively. These P segments radiate from the turbulent baseline N at their real and apparent $Re_s\sqrt{f}^*$ in the range $330 < Re_s\sqrt{f} < 550$, forming the spokes of a fan-like structure. This "Type-A fan" is the characteristic drag-reduction behavior of solutions of initially collapsed, random-coiling macromolecules. Note that, in the present case, the slopes of the fan spokes are much nearer that of the MDR asymptote, $A_m = 19.0$, than that of the turbulent baseline N, $A_n = 4.0$.

In Figure 5.2.7, results for additive C832A runs at $1 \leq c \leq 100$ wppm in 0.0001 N NaCl exemplify Type-B drag-reduction behavior by initially extended HPAM macromolecules. Newtonian laminar and turbulent baselines and the MDR asymptote are shown by lines L, N, and M, respectively.

The 1-wppm data follow along L for $50 < Re_s\sqrt{f} < 150$ and then depart L beginning a laminar-to-turbulent transition at $Re_s\sqrt{f} \approx 150$. Dropping toward, but never reaching, N, the data attain a $1/\sqrt{f}$ minimum at $Re_s\sqrt{f} \approx 350$ and exhibit flow enhancement immediately. The 1-wppm data remain above and slightly diverge from N along a linear segment P with slope and in $(A_p, B_p) = (5.0, 1.7)$ for $350 < Re_s\sqrt{f} < 2000$. For $2000 < Re_s\sqrt{f} < 7500$, the data exhibit nearly constant $1/\sqrt{f} \approx 13$, weakly departing from P, towards N, perhaps as a result of polymer degradation. Thus, the 1-wppm data display an LP trajectory.

The 2-wppm and 5-wppm data both show LP trajectories; they lie parallel to the right of L for $50 < Re_s\sqrt{f} < 200$, with $\eta_r \approx 1.15$ and 1.3, respectively, the latter slightly shear-thinning and both enhancing drag relative to solvent. At $Re_s\sqrt{f} \approx 300$ data for both solutions shift sharply rightward and somewhat upward into the polymeric regime and for $Re_s\sqrt{f} > 500$ follow along respective linear segments P with $(A_p, B_p) = (7.0, 4.9)$ and $(10.9, 13.7)$ until $Re_s\sqrt{f} \approx 3000$. For $Re_s\sqrt{f} > 3000$ and up to $Re_s\sqrt{f} \approx 6400$ and 5000, respectively, the 2-wppm and 5-wppm data exhibit essentially constant $1/\sqrt{f} \approx 20$ and 24, respectively, declining from their segments P, possibly from polymer degradation.

The 10-wppm and 20-wppm data exhibit LMP trajectories. For $Re_s\sqrt{f} < 300$, the 10-wppm and 20-wppm data follow shear-thinning laminar paths with $\eta_r \approx 2.1$ and 2.7,

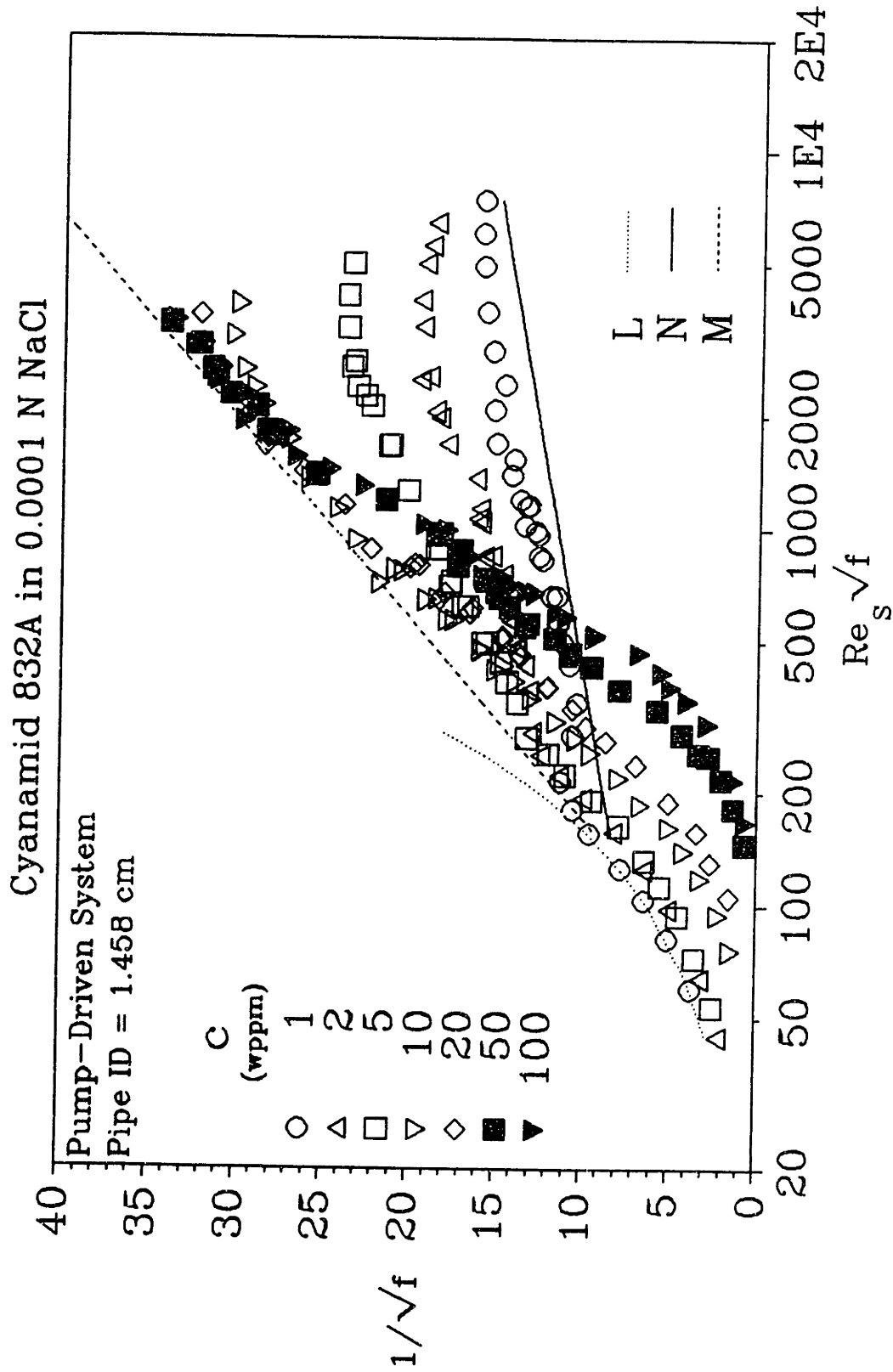


Figure 5.2.7: Cyanamid 832A in 0.0001 N NaCl from the 1.458-cm Pipe

respectively, enhancing drag relative to solvent. At $Re_s\sqrt{f} \approx 300$, these data depart from their laminar courses and ascend toward the MDR asymptote, which is approached most closely at $Re_s\sqrt{f} \approx 800$ and 900 , respectively. For $800 < Re_s\sqrt{f} < 900$, the 10-wppm data are parallel and close to M, shift sharply into the polymeric regime at a retro-onset point $Re_s\sqrt{f}^* \approx 2000$, and then rise along a linear segment P with $(A_p, B_p) = (9.6, 3.4)$ for $2000 < Re_s\sqrt{f} < 3500$. Similarly, the 20-wppm data parallel M for $900 < Re_s\sqrt{f} < 3300$, and then at $Re_s\sqrt{f} \approx 3400$, the final 20-wppm data point shifts horizontally rightward into the polymeric regime, possibly a retro-onset induced by polymer degradation.

The 50-wppm and 100-wppm data display LM trajectories. For $Re_s\sqrt{f} > 150$, the 50-wppm and 100-wppm data trace respective laminar paths, well to the right of L and highly shear-thinning, with average $\eta_r \approx 6.8$ and 9.3 until $Re_s\sqrt{f} \approx 700$; the solutions enhance drag greatly relative to solvent, lying ~ 29 units below L at $Re_s\sqrt{f} \approx 700$, respectively. For $700 < Re_s\sqrt{f} < 1500$, the 50-wppm and 100-wppm data deviate from their apparently laminar paths, and both rise toward the MDR asymptote M, which is reached at $Re_s\sqrt{f} \approx 1500$ and closely adhere to M up to the highest $Re_s\sqrt{f} \approx 3400$.

In Figure 5.2.7, the flow trajectories exhibited are: LP by data at $c = 1, 2$, and 5 wppm; LMP by the 10-wppm and 20-wppm data; and LM by the 50-wppm and 100-wppm data. In laminar flow, as the concentration increases, these solutions have both increasing relative viscosities and drag enhancements relative to solvent, as the data shift farther to the right from L, and are increasingly shear thinning. In turbulent flow, as the concentration increases, these solutions increasingly enhance the flow relative to solvent, opposite to the effect observed in laminar flow. In the polymeric regime, the segments

P for $c = 1, 2, 5,$ and 10 wppm have slopes $A_p = 5.0, 7.0, 10.9,$ and $9.6,$ respectively, nearer that of the turbulent baseline N, $A_n = 4.0,$ than that of the MDR asymptote, $A_m = 19.0.$ Furthermore, as the concentration increases, the segments P achieve higher slips. At $Re_p\sqrt{f} = 1000,$ $S' = 1.9, 4.5, 7.0,$ and $12.0,$ and at $Re_p\sqrt{f} = 3000,$ $S' = 2.0, 5.8, 10.1,$ and $16.6,$ respectively. At each $Re_p\sqrt{f},$ to a rough approximation, S' increases linearly with increasing concentration. The segments P appear to extend from the MDR asymptote into the polymeric regime and to parallel the baseline N with uniform interspacings. The resulting overall structure thus resembles a "ladder", the segments P being the rungs and the MDR asymptote providing support. This "Type-B ladder" is characteristic of drag-reduction by solutions of extended additives. The Type-B ladder in Figure 5.2.7 has no rungs for $c = 20, 50,$ and 100 wppm because the maximum $Re_p\sqrt{f}$ is not large enough to give rise to retro-onset at these concentrations. (The tiny segment P in the 20-wppm data may, in fact, be the retro-onset and incipient segment P corresponding to a degraded polymer solution that has a concentration somewhat less than 20 wppm.)

In summary, Figures 5.2.6 and 5.2.7 respectively illustrate a Type-A fan, which is characteristic of the drag-reduction behavior exhibited by solutions of initially collapsed macromolecules, and a Type-B ladder, which typifies drag-reduction behavior of solutions of initially extended macromolecules. The Type-A fan radiates into the polymeric regime from the turbulent baseline N, the lower limit of turbulent flow, at the individual onset points, which usually occur within a narrow band. The characteristic onset wall shear stress T_w^* reflects the average physical properties of the collapsed macromolecules in solution. The fan spokes have slopes A_p and slope increments δ that

increase with additive concentration. Note that the spokes emerge from the turbulent baseline N and have slopes like that of the MDR asymptote. In contrast, the Type-B ladder is characteristic of the drag-reduction behavior exhibited by solutions of initially extended macromolecules. The segments P forming the ladder rungs extend, or retro-onset, from the MDR asymptote, the upper turbulent-flow limit, into the polymeric regime and approximately parallel the turbulent baseline N, having shallow slopes near to that of N.

The Type-A fan and Type-B ladder structures exhibit some symmetry about the polymeric regime. The former has segments P which onset from N and have steep slopes whereas the latter has segments P which retro-onset from M and have shallow slopes. Both structures may contain LP trajectories, the former lacking an N segment and the latter lacking an M segment.

It is of interest to compare the turbulent flow enhancements observed in the present example of additive C832A in the 1.458-cm pipe. In the Type-A fan for $c = 1, 2, 5, 10,$ and 20 at $Re_t\sqrt{f} \approx 1000$, the respective apparent slips $S' = 0, 1.1, 1.8, 3.8,$ and 6.1 ; in the Type-B ladder at the same conditions, the respective $S' = 1.9, 4.5, 7.1, 12.0,$ and 10.4 . Here the respective apparent slip ratios $S'_A/S'_B = 0, 0.24, 0.25, 0.32,$ and 0.59 . The data for $c = 50$ and 100 wppm are excluded because they exhibit LM trajectories and do not display ladder rungs. At $Re_t\sqrt{f} \approx 3000$ for $c = 1, 2, 5, 10,$ and 20 wppm, the respective apparent slips in the Type-A fan and the Type-B ladder are: $S' = (0, 3.4, 7.1, 11.1, \text{ and } 14.8)$ and $(2.0, 5.8, 10.1, 16.6, \text{ and } 18.5)$; the respective apparent slips ratios $S'_A/S'_B = 0, 0.58, 0.70, 0.67,$ and 0.80 . It is thus seen that the turbulent flow enhancement induced by the collapsed conformation never exceeds that

induced by the extended conformation at the same solution concentration. Also, as $Re_p\sqrt{f}$ increases, the flow enhancement induced by the collapsed conformation approaches that induced by the extended conformation, which suggests that initially collapsed macromolecules are transformed toward extended conformations at the higher $Re_p\sqrt{f}$.

Figures 5.2.8 and 5.2.9 present results, from the pump-driven system using the 1.021-cm pipe, for additive C832A, at $c = 1, 2, 5, 10, 20,$ and 50 wppm, in the collapsed conformation in 0.3 N NaCl and the extended conformation in 0.0001 N NaCl, respectively. In both figures, lines L, N, and M represent the Newtonian laminar and turbulent baselines and the MDR asymptote, respectively.

In Figure 5.2.8, for $30 < Re_p\sqrt{f} < 150$, all data follow laminar paths either along, or just to the right of, L, typical of the behavior of solutions of initially collapsed macromolecules. The 20-wppm and 50-wppm laminar data lie slightly rightward, with respective relative viscosities $\eta_r \approx 1.06$ and 1.13 .

The 1-wppm and 2-wppm data depart downward from L and onto N, completing a laminar-to-turbulent transition for $200 < Re_p\sqrt{f} < 400$. For $400 < Re_p\sqrt{f} < 700$, the 1-wppm data adhere to N, and then onset at $Re_p\sqrt{f} \approx 770$; for $700 < Re_p\sqrt{f} < 3000$, they ascend into the polymeric regime along a linear segment P with slope and intercept $(A_p, B_p) = (5.3, 3.9)$ and slope increment $\delta = 1.3$; for $4000 < Re_p\sqrt{f} < 10000$, the data become downward from the P segment, descending slightly toward N. Similarly, the 2-wppm data follow N briefly, onset at $Re_p\sqrt{f} \approx 500$, and then rise into the polymeric regime along a linear segment P with $(A_p, B_p) = (7.5, 9.8)$; for $4000 < Re_p\sqrt{f} < 10000$, these nearly exhibit constant $1/\sqrt{f} \approx 15$, declining slightly from their linear P segment, possibly on account of polymer degradation. The 1-wppm and 2-wppm

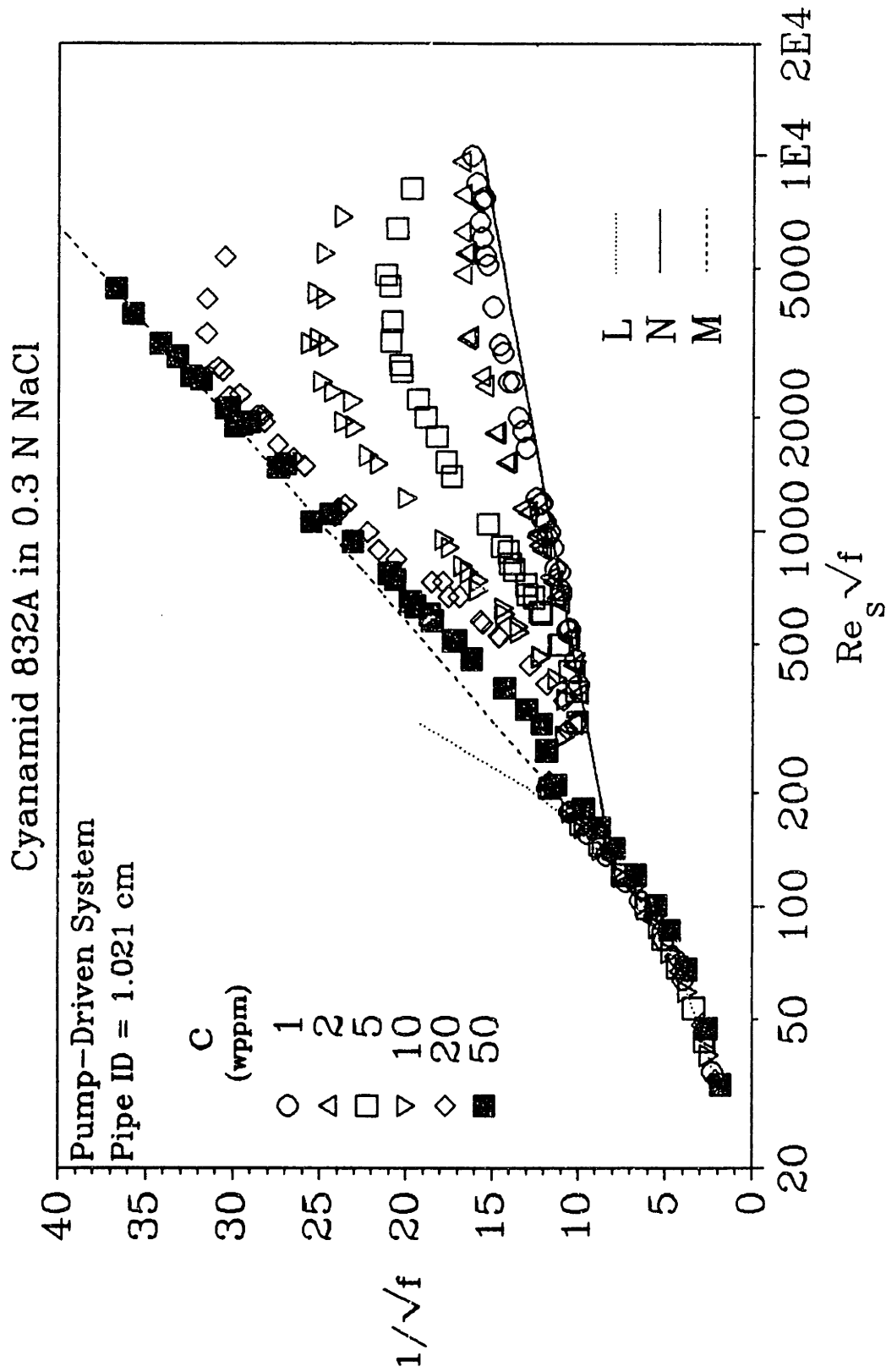


Figure 5.2.8: Cyanamid 832A in 0.3 N NaCl from the 1.021-cm Pipe

data thus exhibit LNP trajectories.

The 5-wppm and 10-wppm data depart downward from L toward N, for $200 < Re_p\sqrt{f} < 800$, in a laminar-to-turbulent transition. Yet, although both solutions either reach, or come very close to, N in the vicinity of $Re_p\sqrt{f} \approx 350$, they do not exhibit well-defined N segments. Rather, immediately after reaching $1/\sqrt{f}$ minima near N at $Re_p\sqrt{f} \approx 350$, the 5-wppm and 10-wppm solutions begin turbulent flow enhancement, rising into the polymeric regime along respective linear segments P with $(A_p, B_p) = (13.4, 25.2)$ and $(18.5, 37.1)$, and $\delta = 9.4$ and 14.5 until $Re_p\sqrt{f} \approx 3000$. Their respective apparent regressed onsets occur at $Re_p\sqrt{f} \approx 420$ and 340 . For $Re_p\sqrt{f} > 3500$, the 5-wppm and 10-wppm data descend markedly from their linear segments P, probably on account of polymer degradation, up to $Re_p\sqrt{f} \approx 5000$ and 6500 , respectively. The 5-wppm and 10-wppm data thus display L(N)P trajectories.

The 20-wppm data undergo a laminar-to-turbulent transition in the region $180 < Re_p\sqrt{f} < 300$, reaching a $1/\sqrt{f}$ minimum slightly above N at $Re_p\sqrt{f} \approx 300$. For $350 < Re_p\sqrt{f} < 750$, the data, already flow enhancing, rise further into the polymeric regime along a linear segment P with $(A_p, B_p) = (24.0, 50.1)$ and $\delta = 20.0$, with an apparent regressed onset at $Re_p\sqrt{f} \approx 300$. At $Re_p\sqrt{f} \approx 1000$, the 20-wppm data approach the MDR asymptote closely and for $1000 < Re_p\sqrt{f} < 3000$, lie parallel to M and about ~ 1.5 units of $1/\sqrt{f}$ beneath it; for $3500 < Re_p\sqrt{f} < 5000$, they depart rightward from M into the P regime and then descend somewhat in a possible manifestation of polymer degradation. The 20-wppm solution exhibit an LPM(P) trajectory.

The 50-wppm data depart rightward from L at $Re_p\sqrt{f} \approx 200$ and exhibit transitional behavior for $200 < Re_p\sqrt{f} < 300$, moving slightly upward into the polymeric

regime. For $300 < Re_s\sqrt{f} < 800$, the data ascend more steeply into the polymeric regime, toward M, along a linear segment with $(A_p, B_p) = (22.9, 44.8)$, $\delta = 18.9$ and apparent regressed onset at $Re_s\sqrt{f} \approx 200$. The 50-wppm data merge with M at $Re_s\sqrt{f} \approx 800$, and then continue along M up to the highest $Re_s\sqrt{f} \approx 5000$. The 50-wppm data, thus, trace an LPM trajectory.

In Figure 5.2.8, the flow trajectories displayed are: LNP by the 1-wppm and 2-wppm data, L(N)P by the 5-wppm and 10-wppm data, LPM(P) by the 20-wppm data, and LPM by the 50-wppm data. The laminar-flow data exemplify the behavior of solutions of initially collapsed macromolecules in that the solutions have low relative viscosities $\eta_r < 1.2$ up to the highest concentrations and show little relatively small drag enhancements relative to solvent. In turbulent flow, all segments P have slopes and slope increments that increase as concentration increases: $A_p = (5.3, 7.5, 13.4, 18.5, 24.0$ and $22.9)$ and $\delta = (1.3, 3.5, 9.4, 14.5, 20.0,$ and $18.9)$ for $c = (1, 2, 5, 10, 20,$ and $50)$ wppm, respectively. The segments P seemingly radiate from the turbulent baseline N within a narrow range of real and apparent onset points, $220 < Re_s\sqrt{f} < 550$, and create a fan structure. This ensemble of segments P constitutes a Type-A "fan", characteristic of the drag-reduction behavior of solutions of collapsed macromolecules.

Figure 5.2.9 presents results for initially extended conformation of additive C832A in 0.0001 N NaCl.

The 1-wppm and 2-wppm data follow laminar paths for $30 < Re_s\sqrt{f} < 150$, shifted slightly rightward from L, to higher $Re_s\sqrt{f}$, corresponding to relative viscosities $\eta_r \approx 1.06$ and 1.14 , respectively; these rightward shifts decrease with increasing $Re_s\sqrt{f}$ showing shear-thinning behavior. Both solutions enhance drag relative to the solvent with

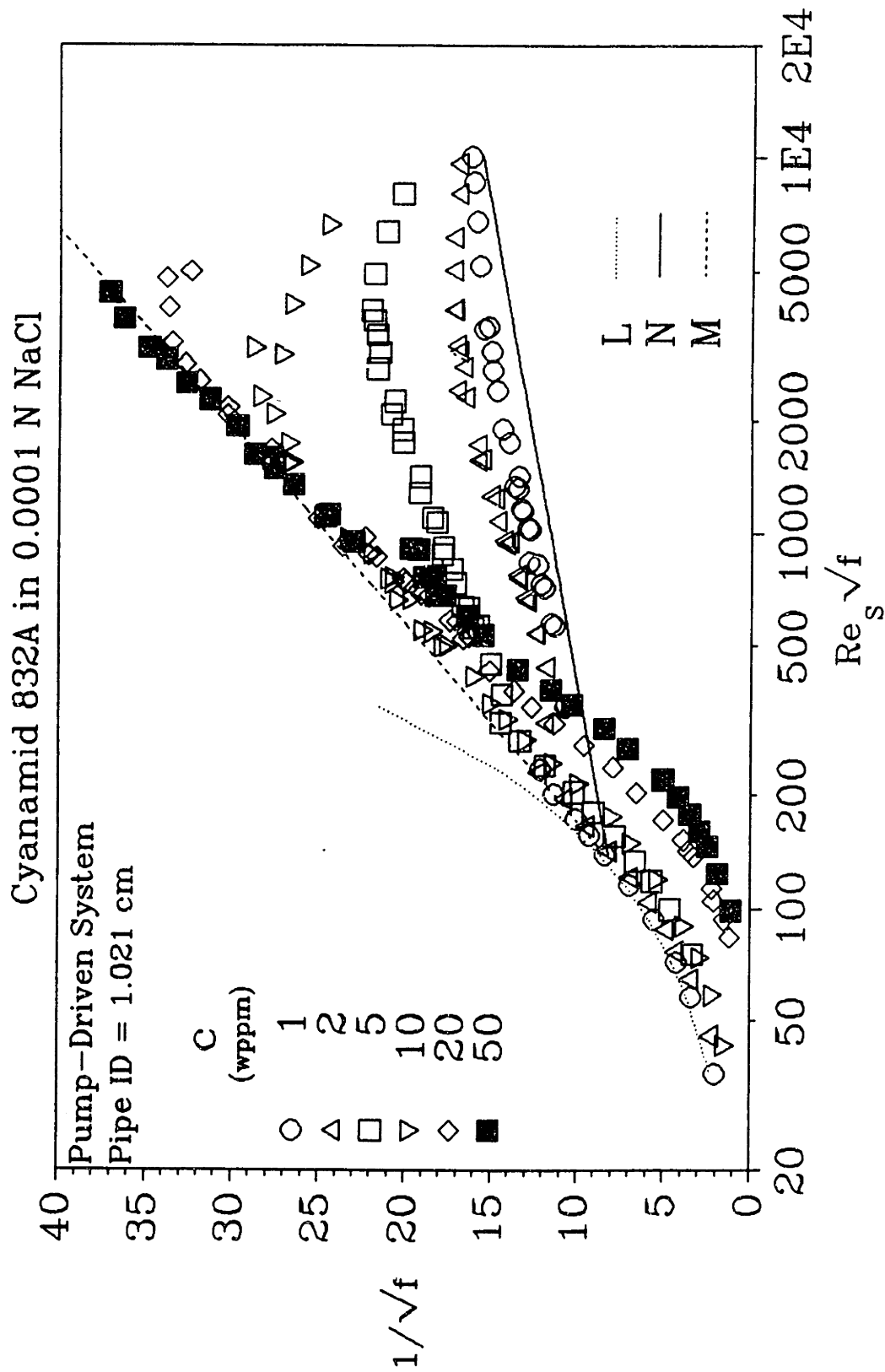


Figure 5.2.9: Cyanamid 832A in 0.0001 N NaCl from the 1.021-cm Pipe

$1/\sqrt{f_p} > 1/\sqrt{f_1}$ at constant $Re_s\sqrt{f}$. For $180 < Re_s\sqrt{f} < 350$, the 1-wppm and 2-wppm data depart downward from L, toward N, but reach $1/\sqrt{f}$ minima above N at $Re_s\sqrt{f} \approx 350$, thus exhibiting laminar-to-turbulent transitions that terminate in the polymeric regime. From these minima at $Re_s\sqrt{f} \approx 350$, the 1-wppm and 2-wppm data rise linearly into the polymeric regime along their respective P segments with slopes and intercepts $(A_p, B_p) = (4.0, -1.0)$ and $(6.2, 4.5)$, virtually parallel to N until $Re_s\sqrt{f} \approx 4000$; for $4000 < Re_s\sqrt{f} < 10000$, both solutions exhibit nearly constant $1/\sqrt{f} \approx 16$ and 17, respectively, declining from their P segments toward N. The 1-wppm and 2-wppm data thus make LP trajectories. The 5-wppm data are similar, but not identical. For $50 < Re_s\sqrt{f} < 200$, they follow a laminar path, to the right of L, corresponding to a relative viscosity $\eta_r \approx 1.4$ with some shear thinning. In the region $200 < Re_s\sqrt{f} < 300$, the data are both parallel to L and very close to M, so they could be following either an L or an M segment. At $Re_s\sqrt{f} \approx 300$, the 5-wppm data shift abruptly rightward, in a brief transition, and then, already flow enhancing, rise into the polymeric regime along a linear segment P, with $(A_p, B_p) = (8.2, 6.4)$ until $Re_s\sqrt{f} \approx 3500$. For $3500 < Re_s\sqrt{f} < 8000$, the data descend significantly from their segment P with $1/\sqrt{f}$ decreasing from 23 to 19, possibly on account of polymer degradation. The 5-wppm data thus display either an LP or an L(M)P trajectory.

The 10-wppm data follow a laminar path for $50 < Re_s\sqrt{f} < 250$ shifted rightward from L with $\eta_r \approx 1.6$ amid shear thinning. At $Re_s\sqrt{f} \approx 300$, the data approach the MDR asymptote from beneath, lie parallel and very close to M for $350 < Re_s\sqrt{f} < 1000$, and then retro-onset at $Re_s\sqrt{f} \approx 1000$. For $1000 < Re_s\sqrt{f} < 3000$, the 10-wppm data rise briefly into the polymeric regime along a linear segment P with $(A_p,$

$B_p) = (11.0, 8.7)$ and for $3500 < Re_s\sqrt{f} < 6500$, decline from the segment P as a probable result of polymer degradation. The 10-wppm data trace an LMP trajectory.

In laminar flow for $90 < Re_s\sqrt{f} < 400$, both the 20-wppm and 50-wppm data exhibit shear-thinning with average $\eta_r \approx 3.2$ and 4.0 , respectively; these solutions also greatly enhance drag relative to L, lying ~ 10 and ~ 12 units below L at $Re_s\sqrt{f} \approx 400$. At $Re_s\sqrt{f} \approx 400$, both solutions exhibit inflections in their slopes, departing their laminar paths and converging upon the MDR asymptote M, with which they merge at $Re_s\sqrt{f} \approx 1000$. For $1000 < Re_s\sqrt{f} < 3000$, the 20-wppm data follow along M, but then at $Re_s\sqrt{f} \approx 3000$ with $1/\sqrt{f} \approx 33$, shift sharply into the polymeric regime, following a short, nearly horizontal, segment with $(A_p, B_p) = (2.1, -26.3)$ up to $Re_s\sqrt{f} \approx 5000$. The sudden departure from M is likely a retro-onset induced by polymer degradation. The 20-wppm data display an LMP trajectory. The 50-wppm data follow M for $1000 < Re_s\sqrt{f} < 4500$ to the highest $Re_s\sqrt{f}$, completing an LM trajectory.

In Figure 5.2.9, the flow trajectories displayed are: LP by data at $c = 1, 2$, and 5 wppm; LMP by the 10-wppm and 20-wppm data; and LM by the 50-wppm data. In laminar flow, relative viscosities and drag enhancements relative to solvent are high and increase with increasing concentration; also all solutions exhibit shear thinning. This behavior is typical of solutions of initially extended macromolecules. In turbulent flow, the data exhibit flow enhancements relative to solvent that increase with increasing concentration, the reverse of the laminar-flow observation. The segments P at $c = 1, 2, 5$, and 10 wppm seemingly extend(i.e. retro-onset) from the MDR asymptote into the polymeric regime and approximately parallel the Newtonian turbulent baseline N with slopes $A_p = 4.0, 6.2, 8.2$, and 11.0 , respectively, until polymer degradation begins to

negate flow enhancement. The separation between a segment P and the baseline N, quantified by the apparent slip S' , is roughly proportional to the concentration: At $Re_s\sqrt{f} \approx 3000$ for $c = 1, 2, 5,$ and 10 , $S' = 1.6, 3.5, 8.2,$ and 15.3 and $S'/c = 1.6, 1.8, 1.6,$ and 1.5 , respectively. These uniformly-spaced and nearly-parallel P segments which extend from the MDR asymptote form the rungs of a "Type-B ladder", characteristic of drag reduction by solutions of initially extended additives. The 20-wppm data are omitted from the ladder because its segment P appears to be a manifestation of polymer degradation; the 50-wppm data, in their LM trajectory, do not contribute a ladder rung.

A comparison between the flow enhancements exhibited by the same polymer concentrations in the Type-A fan, Figure 5.2.8, and the Type-B ladder, Figure 5.2.9, is again interesting. For $c = 1, 2, 5,$ and 10 wppm at $Re_s\sqrt{f} = 1000$, the respective apparent slips are: $S'_A = 0.3, 1.0, 3.5,$ and 6.7 and $S'_B = 1.2, 2.9, 6.6,$ and 11.9 , with slip ratios $S'_A/S'_B = 0.28, 0.36, 0.53,$ and 0.56 . The same concentrations at $Re_s\sqrt{f} = 3000$ respectively provide $S'_A = 0.9, 2.7, 7.0,$ and 11.4 and $S'_B = 1.6, 3.5, 8.2,$ and 13.5 , with slip ratios $S'_A/S'_B = 0.59, 0.79, 0.86,$ and 0.84 . It is seen that, at constant $Re_s\sqrt{f}$, for a given concentration, the flow enhancement induced by the initially collapsed conformation never exceeds that induced by the initially extended conformation. Also at each fixed concentration, the ratio of collapsed to extended flow enhancement increases toward unity with increasing $Re_s\sqrt{f}$. This suggests that, as $Re_s\sqrt{f}$ increases, initially collapsed macromolecules are progressively stretched by the flow toward their extended conformations.

The effect of flow length scale on drag reduction can be inferred by comparing turbulent flow results for additive C832A in the 1.458-cm pipe, Figures 5.2.6 and 5.2.7,

to those in the 1.021-cm pipe, Figures 5.2.8 and 5.2.9.

Data for additive C832A in 0.3 N NaCl, in the initially collapsed conformation, form Type-A fans in Figures 5.2.6 and 5.2.8. Each fan comprises the same kinds of flow trajectories, LNP, LP, and LPM at low, medium, and high concentrations. The fan from the 1.458-cm pipe, in Figure 5.2.6, contains segments P for $2 \leq c \leq 100$ wppm, the 1-wppm solution showing no perceptible drag reduction, whereas the fan from the 1.021-cm pipe, in Figure 5.2.8, contains segments P for all solutions $1 \leq c \leq 50$ wppm. The slope increments δ in the two fans at constant concentrations are similar, being for $c = 2, 5, 10, 20,$ and 50 wppm, $\delta = (5.1, 9.4, 15.5, 17.1, \text{ and } 20.3)$ and $(3.5, 9.4, 14.5, 20.0, \text{ and } 18.9)$, respectively. Also if the entire 1.021-cm-pipe fan is translated rightward, along the Newtonian line N, by a factor of ~ 1.4 , then it virtually superimposes upon the 1.458-cm-pipe fan. Because the superposition factor 1.4 is roughly their pipe-diameter ratio $1.458/1.021$, the structures of the two fans are essentially independent of the pipe diameter and are scaled by the wall shear stress alone. This implies that Type-A fans are essentially independent of the large scales of turbulence imposed by the pipe diameters. Moreover, the foregoing superposition of fans also causes the coincidence of the maxima exhibited by solutions of a given concentration in each pipe, suggesting that degradation, which likely causes these maxima, is also primarily dependent upon the wall shear stress.

Data for additive C832A in 0.0001 N NaCl, the initially extended conformation, create Type-B ladders in Figures 5.2.7 and 5.2.9. Each ladder comprises LP, LMP, and LM trajectories respectively at low, medium, and high concentrations. The ladders from the 1.458-cm pipe in Figure 5.2.7 and from the 1.021-cm pipe in Figure 5.2.9 have the

same qualitative appearance, showing well-developed rungs at $c = 1, 2, 5,$ and 10 wppm with similar P-segment slopes $A_p = (5.0, 7.0, 10.9,$ and $9.6)$ and $(4.0, 6.2, 8.2,$ and $11.0)$, respectively. When compared at constant $Re_s\sqrt{f}$, the rungs in the 1.458-cm ladder are all somewhat higher than those in the 1.021-cm ladder: For example, at $Re_s\sqrt{f} = 3000$, $S' = (2.0, 5.8, 10.1,$ and $16.6)$ and $(1.6, 3.5, 8.2,$ and $13.5)$, respectively. Yet, when compared at equal wall shear stresses, by translating the 1.021-cm rightward along N by the pipe-diameter ratio $1.458/1.021$, the differences between the rungs diminish, and the ladders from both pipes roughly superimpose. Thus, Type-B ladders also appear to be scaled by wall shear stress and are roughly independent of pipe diameter.

Results for additive B1120 from the pump-driven system using the 1.458-cm pipe are shown in Figures 5.2.10 and 5.2.11 for solutions of initially collapsed and initially extended macromolecules in 0.3 N and 0.0001 N NaCl, respectively, with $1 \leq c \leq 100$ wppm. In both figures, the Newtonian laminar and turbulent baselines and the MDR asymptote are given by lines L, N, and M, respectively, the latter two enveloping the polymeric regime.

Figure 5.2.10 presents results for additive B1120 in 0.3 N NaCl at $c = 1, 2, 5, 10, 20, 50,$ and 100 wppm from the pump-driven system using the 1.458-cm pipe. In laminar flow for $30 < Re_s\sqrt{f} < 180$, the data for $c = 1, 2, 5,$ and 10 wppm follow L closely, with $\eta_r < 1.05$; for $180 < Re_s\sqrt{f} < 400$, they complete laminar-to-turbulent transitions, descending from L and alighting onto N. For $Re_s\sqrt{f} > 400$, these data continue along N until they onset at respective $Re_s\sqrt{f} \approx 960, 580, 640,$ and 510 and then rise into the polymeric regime along respective linear segments P with slopes and intercepts $(A_p, B_p) = (4.9, 3.1), (7.7, 10.6), (12.4, 23.9),$ and $(17.2, 36.1)$ and slope

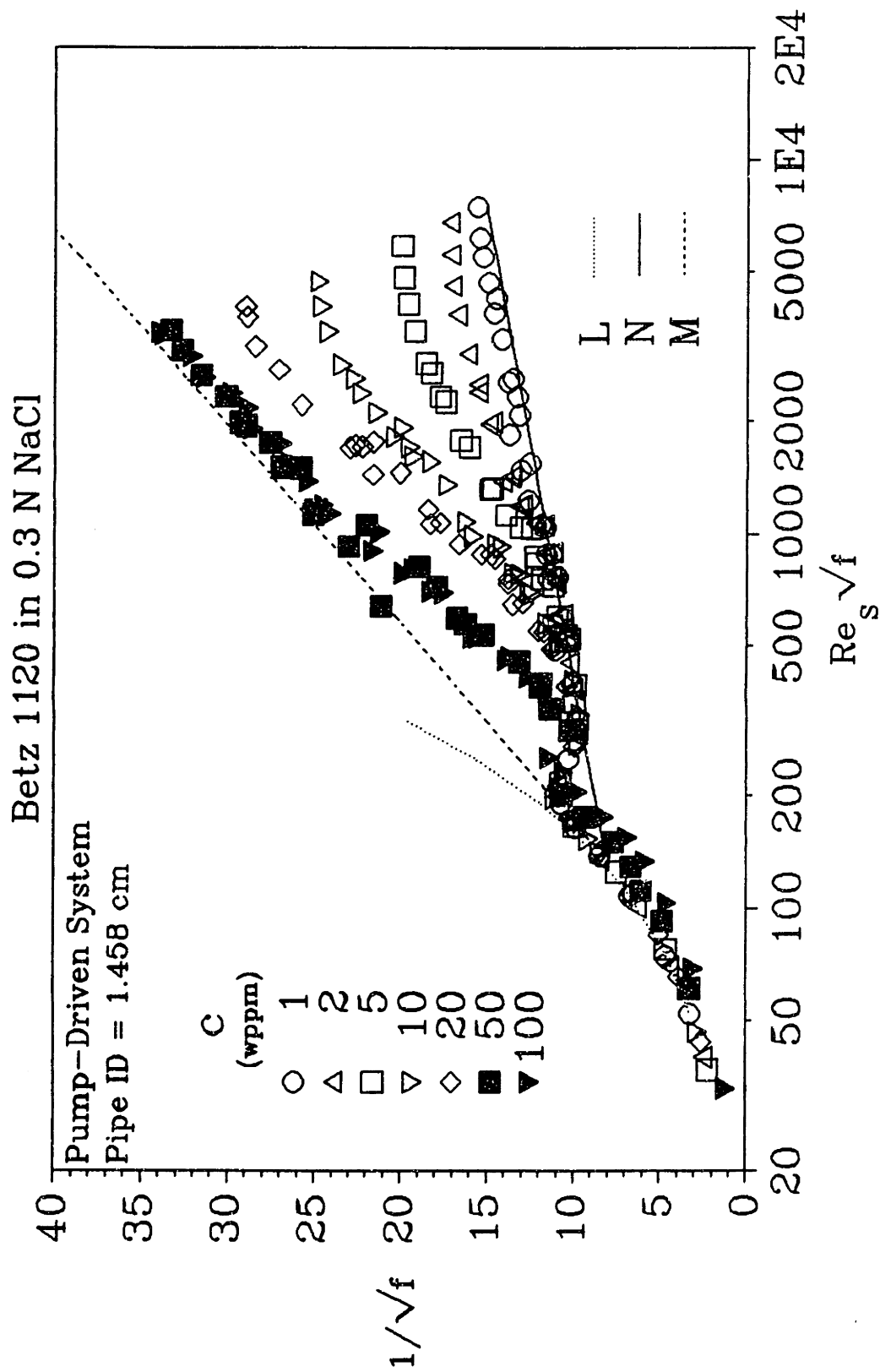


Figure 5.2.10: Betz 1120 in 0.3 N NaCl from the 1.458-cm Pipe

increments $\delta = 0.9, 3.7, 8.4,$ and 13.2 until $Re_s\sqrt{f} \approx 3000$. At $Re_s\sqrt{f} > 4000$, these data decline from their respective P segments, showing essentially constant $1/\sqrt{f} \approx 13, 15, 18,$ and 23 , up to highest $Re_s\sqrt{f} \approx 7500, 6800, 5800$ and 4700 . Data for $c = 1, 2, 5,$ and 10 wppm, thus, display LNP trajectories.

The 20-wppm data follow along L for $40 < Re_s\sqrt{f} < 150$, depart downward from L toward N at $Re_s\sqrt{f} \approx 180$, and reach a $1/\sqrt{f}$ minimum very close to N at $Re_s\sqrt{f} \approx 350 \pm 50$; for $400 < Re_s\sqrt{f} < 3000$, the data ascend linearly into the polymeric regime along a segment P with $(A_p, B_p) = (22.0, 48.8)$, $\delta = 18.0$, and an apparent regressed onset at $Re_s\sqrt{f} \approx 480$. For $3000 < Re_s\sqrt{f} < 4000$, the data fall slightly below their segment P, likely owing to polymer degradation. The 20-wppm data complete an L(N)P trajectory.

The 50-wppm and 100-wppm data parallel L to the right with respective $\eta_r \approx 1.2$ and 1.4 , until $Re_s\sqrt{f} \approx 200$. The 50-wppm and 100-wppm solutions slightly enhance laminar drag relative to the solvent in that they lie beneath L. At $Re_s\sqrt{f} \approx 220$, both solutions commence laminar-to-turbulent transitions, departing to the right and downward to reach $1/\sqrt{f}$ minima at $Re_s\sqrt{f} \approx 300$, close to, but slightly above, N. Already a bit flow enhancing at their minima, both then rise steeply into the polymeric regime toward the MDR asymptote along respective linear segments P with $(A_p, B_p) = (21.8, 44.2)$ and $(24.7, 51.9)$, $\delta = 17.8$ and 20.7 , and apparent regressed onsets at $Re_s\sqrt{f} \approx 290$ and 310 . The 50-wppm and 100-wppm data approach M most closely at $Re_s\sqrt{f} \approx 1500$ and then begin to parallel M up to $Re_s\sqrt{f} \approx 3400$. These data, thus, follow LPM trajectories.

In Figure 5.2.10, LNP, L(N)P, and LPM trajectories are displayed at $c = 1, 2, 5,$ and 10 wppm, at $c = 20$ wppm, and at $c = 50$ and 100 wppm, respectively. The

laminar-flow paths for $c \leq 20$ wppm are virtually indistinguishable from solvent line L and are characteristic of solutions of initially collapsed macromolecules; the 50-wppm and 100-wppm solutions also exhibit Newtonian viscosities, even though they show significant $\eta_r > 1$. In turbulent flow, the segments P for $c \leq 20$ wppm have slopes and slope increments that increase with increasing concentration: $A_p = 4.9, 7.7, 12.4, 17.2,$ and 22.0 and $\delta = 0.9, 3.7, 8.4, 13.2,$ and 18.0 , respectively, the corresponding $Re_s\sqrt{f} \approx 960, 580, 640, 510,$ and 480 (apparent). These five segments appear to radiate from a narrow band on the turbulent baseline N, forming a fan, typical of Type-A drag-reduction behavior by an initially collapsed additive conformation.

Figure 5.2.11 shows results for the initially extended conformation of additive B1120 in 0.0001 N NaCl for $1 \leq c \leq 100$ wppm from the pump-driven system using the 1.458-cm pipe.

The 1-wppm data follow L closely for $50 < Re_s\sqrt{f} < 160$, a little to the right with $\eta_r \approx 1.02$; for $160 < Re_s\sqrt{f} < 320$, they depart downward from L onto N in a laminar-to-turbulent transition. Continuing along N for $320 < Re_s\sqrt{f} < 750$, the 1-wppm data onset at $Re_s\sqrt{f} \approx 750$ and then slowly diverge from N before becoming nearly parallel to N at $Re_s\sqrt{f} \approx 1000$. For $1000 < Re_s\sqrt{f} < 7500$, the data hover just above N, with slope $A_p = 4.0$, descending slightly at the highest $Re_s\sqrt{f}$. The 1-wppm data, thus, display an LNP trajectory.

The 2-wppm data follow a laminar path to the right of L for $50 < Re_s\sqrt{f} < 190$, with $\eta_r \approx 1.2$ and, thus, show drag enhancement relative to solvent. Departing rightwards from L at $Re_s\sqrt{f} \approx 200$, the 2-wppm data exhibit a transitional undulation and reach a $1/\sqrt{f}$ minimum above N at $Re_s\sqrt{f} \approx 400$. For $400 < Re_s\sqrt{f} < 3000$, the data

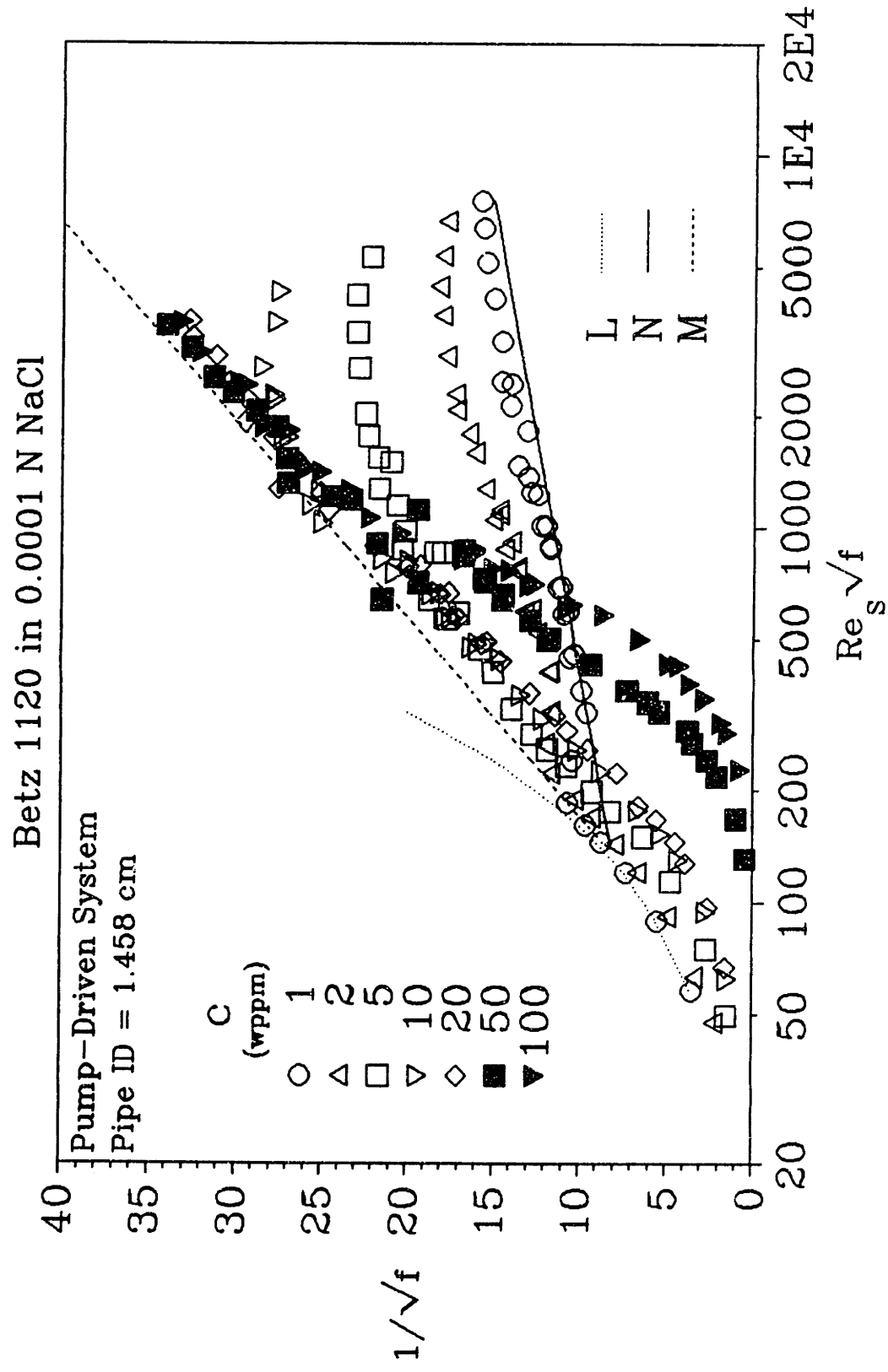


Figure 5.2.11: Betz 1120 in 0.0001 N NaCl from the 1.458-cm Pipe

rise shallowly into the polymeric regime along a linear segment P with slope and intercept $(A_p, B_p) = (7.4, 7.7)$ and for $3000 < Re_s\sqrt{f} < 6500$, decline from their segment P possibly because of polymer degradation, becoming horizontal with $1/\sqrt{f} \approx 17$. The 2-wppm solution follows an LP trajectory.

The 5-wppm data follow a laminar path still farther to the right of L for $50 < Re_s\sqrt{f} < 200$, with $\eta_r \approx 1.6$, showing greater drag enhancement relative to solvent as well, and exhibit distinct shear thinning. Departing from their laminar path at $Re_s\sqrt{f} \approx 300$, the data ascend linearly, parallel and close to M, until $Re_s\sqrt{f} \approx 800$. At $Re_s\sqrt{f} \approx 800$, retro-onset occurs, and the 5-wppm data sharply shift to the right, into the polymeric regime, and ascend along a shallow linear segment P with $(A_p, B_p) = (5.3, -4.8)$ until $Re_s\sqrt{f} \approx 3000$; for $4000 < Re_s\sqrt{f} < 6000$, the data decline slightly from their linear path. Thus, the 5-wppm solution follows an LMP trajectory.

The 10-wppm and 20-wppm data trace laminar paths to the right of L for $60 < Re_s\sqrt{f} < 300$, amidst shear thinning, with $\eta_r \approx 1.8$ and 2.0 , respectively. Both the 10-wppm and 20-wppm solutions enhance drag relative to solvent. At $Re_s\sqrt{f} \approx 320$, these data appear to depart from their L segments, exhibit slight inflections, and then become parallel to the MDR asymptote M. The 10-wppm data retro-onset at $Re_s\sqrt{f} \approx 1500$, continue linearly into the polymeric regime along a segment P with $(A_p, B_p) = (8.0, -1.2)$ until $Re_s\sqrt{f} \approx 3000$, and then decay slightly from their segment P up to $Re_s\sqrt{f} \approx 4300$. The 20-wppm data run parallel to M for $600 < Re_s\sqrt{f} < 3500$. The 10-wppm and 20-wppm trace LMP and LM trajectories, respectively.

The 50-wppm data follow a laminar path far to the right of L for $120 < Re_s\sqrt{f} < 500$, with $\eta_r \approx 7.0$; they exhibit great drag enhancement relative to solvent and

distinct shear-thinning. The 100-wppm data follow a similar laminar path for $200 < Re_s\sqrt{f} < 800$, with $\eta_r \approx 12$, even more drag enhancement, and more severe shear-thinning behavior. For $500 < Re_s\sqrt{f} < 1400$, the 50-wppm data depart from their L segment, inflect, and rise toward the MDR asymptote, widely scattering in apparent transitional behavior at $Re_s\sqrt{f} \approx 1000$. At $Re_s\sqrt{f} \approx 1400$, the data approach M closely and are then parallel to M up to the highest $Re_s\sqrt{f} \approx 3500$. For $1200 < Re_s\sqrt{f} < 1500$, the 100-wppm data leave their L segment, inflect, and rise toward M, closely approaching it at $Re_s\sqrt{f} \approx 1400$ and continuing parallel to M up to the highest $Re_s\sqrt{f} \approx 3500$. The 50-wppm and 100-wppm data both show LM trajectories.

In Figure 5.2.11, the flow trajectories displayed are: LNP by the 1-wppm data; LP by the 2-wppm data; LMP by the 5-wppm and 10-wppm data; and LM by data for $c = 20, 50, \text{ and } 100$ wppm. In laminar flow, these solutions exhibit high relative viscosities, as well as shear-thinning behavior, typically associated with extended macromolecules; also, as the concentration increases, the solutions increasingly enhance drag relative to solvent. In turbulent flow, the opposite holds in that increasing concentration increases flow enhancement relative to solvent. In the polymeric regime, for $c = 1, 2, 5, \text{ and } 10$ wppm, the segments P are approximately parallel to the turbulent baseline N, with respective slopes $A_p = 4.0, 7.4, 5.3, \text{ and } 8.0$; also, as concentration increases, the segments P achieve higher flow enhancements relative to solvent at constant $Re_s\sqrt{f}$, with, for example, $S' = 1.0, 4.4, 9.5, \text{ and } 14.7$, respectively, at $Re_s\sqrt{f} \approx 3000$. The resulting polymeric-regime structure resembles a ladder, the rungs of which are the ascending parallel linear P segments; this Type-B ladder is characteristic of drag reduction by solutions of extended additives.

Figures 5.2.10 and 5.2.11 for additive B1120 in the initially collapsed and initially extended conformations in 0.3 N and 0.0001 N NaCl, respectively, differ significantly in both laminar and turbulent flow. In laminar flow, whereas the former data show Newtonian relative viscosities near unity and small accompanying drag enhancements relative to solvent, the latter data exhibit large, highly shear-thinning relative viscosities, $\eta_r \leq 7.0$, and concomitant large drag enhancements relative to solvent. Consequently, in laminar flow, solutions of a collapsed additive enhance flow relative to solutions of an extended additive.

In turbulent flow for $Re_c \sqrt{f} > Re_c \sqrt{f}^*$, the collapsed and extended conformations exhibit a Type-A fan and a Type-B ladder, respectively. The Type-A fan is characterized by P segments radiating outward from closely clustered onset points on the turbulent baseline N; the P-segment slope increments δ increase with increasing concentration. The Type-B ladder is characterized by P segments of shallow slope, roughly parallel to N, that appear to extend outward from the MDR asymptote at retro-onset points; the displacements S' of the P segments above N increase with increasing concentration. Note that data for $c = 50$ and 100 wppm exhibit LPM trajectories for the initially collapsed macromolecular conformation and LM trajectories for the initially extended macromolecular conformation. Thus, maximum drag reduction is not only independent of the additive's physical properties, it is independent of the additive's initial conformation. By comparing the Type-A fan to the Type-B ladder, it is found that solutions of initially extended macromolecules enhance flow relative to solutions of initially collapsed additive, the opposite of the laminar-flow observation. Between the establishment of turbulent flow and the onset of Type-A drag reduction, $400 < Re_c \sqrt{f}$

$< Re_p\sqrt{f}^*$, Type-B solutions enhance flow relative to solvent infinitely more than do Type-A solutions because the latter exhibit Newtonian turbulent-flow behavior, no drag reduction, prior to onset. For $Re_p\sqrt{f} > Re_p\sqrt{f}^*$, both kinds of solutions enhance flow relative to solvent, but with $S'_A < S'_B$ at equal concentration; as $Re_p\sqrt{f}$ increases further, the flow enhancements S'_A and S'_B approach each other. In Figure 5.2.10, at $Re_p\sqrt{f} \approx 1000$ for $c = 1, 2, 5,$ and 10 wppm, $S'_A = 0.3, 0.5, 1.1,$ and 4.0 , whereas in Figure 5.2.11, at the same $Re_p\sqrt{f}$, $S'_B = 0.5, 3.0, 8.8,$ and 13.0 ; thus, $S'_A/S'_B = (0.52, 0.15, 0.12,$ and $0.31)$, respectively. At $Re_p\sqrt{f} \approx 3000$, $S'_A = 0.45, 2.7, 5.3,$ and 10.2 , $S'_B = 1.0, 4.4, 9.5,$ and 14.7 , and $S'_A/S'_B = 0.47, 0.61, 0.56,$ and 0.69 . The preceding illustrates that, for fixed $Re_p\sqrt{f}$ and c , $S'_A < S'_B$, always and that, for all c , S'_A/S'_B increases toward unity as $Re_p\sqrt{f}$ is increased.

(2) Low Molecular-Weight Additives

Figures 5.2.12 and 5.2.13 show results from the pump-driven system using the 1.458-cm and 1.021-cm pipes, respectively, for additive P500 at $c = 10, 30,$ and 100 wppm in both the initially collapsed conformation, in 0.3 N NaCl(closed symbols), and the initially extended conformation, in 0.0001 N NaCl(open symbols). In Figures 5.2.12 and 5.2.13, the lines L, N, and M represent the Newtonian laminar and turbulent baselines and the MDR asymptote, respectively.

Consider first Figure 5.2.12, in the 1.458-cm pipe. For the initially collapsed-conformation in laminar flow, for $50 < Re_p\sqrt{f} < 150$, data for $c = 10, 30,$ and 100 wppm parallel L with constant rightward displacements that increase as concentration

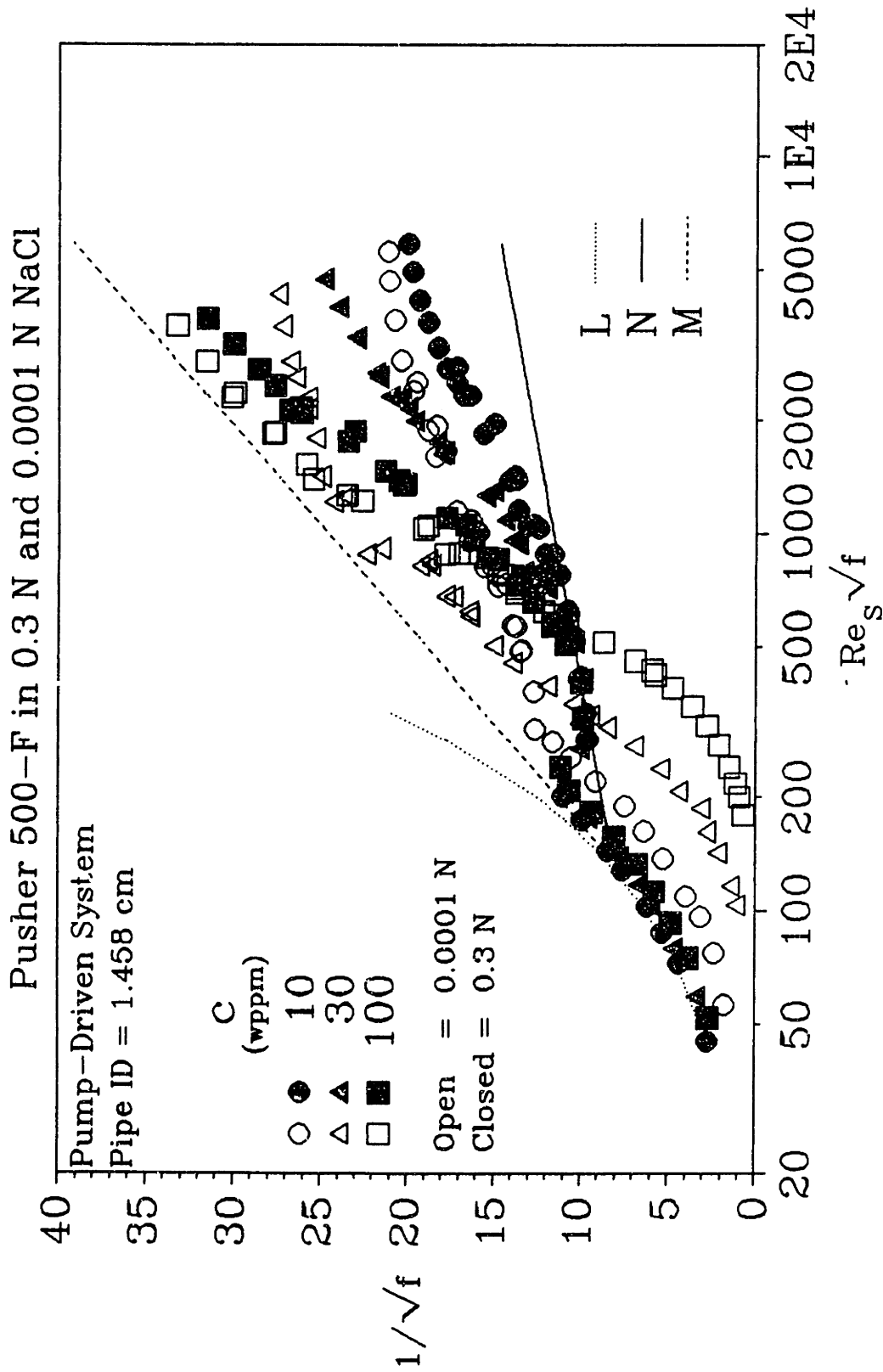


Figure 5.2.12: Pusher 500-F in 0.3 and 0.0001 N NaCl from the 1.458-cm Pipe

increases and that correspond to $\eta_r \approx 1.03, 1.09, \text{ and } 1.21$, respectively; thus, these solutions slightly enhance drag relative to solvent. For $150 < Re_p\sqrt{f} < 320$, these data deviate to the right from their laminar paths and drop onto N, completing laminar-to-turbulent transitions. For $Re_p\sqrt{f} > 320$, the data for $c = 10, 30, \text{ and } 100$ wppm continue along N until they onset at respective $Re_p\sqrt{f}^* \approx 700, 550, \text{ and } 580$. For $Re_p\sqrt{f}^* < Re_p\sqrt{f} < 3500$, the 10-wppm and 30-wppm data rise into the polymeric regime along their respective linear segments P with slopes and intercepts $(A_p, B_p) = (10.8, 19.7)$ and $(15.7, 32.4)$ and slope increments $\delta = 6.8$ and 11.7 , and then for $Re_p\sqrt{f} > 3500$, they decline slightly downward from their segments P, possibly because of polymer degradation, up to $Re_p\sqrt{f} \approx 6000$ and 4700 , respectively. For $600 < Re_p\sqrt{f} < 3000$, the 100-wppm data ascend into the polymeric regime showing slight initial concave-upward curvature before achieving a linear segment P with $(A_p, B_p) = (26.2, 61.8)$ and $\delta = 22.2$. As a result of the initial curvature, the regressed $Re_p\sqrt{f}^* \approx 580$ is much larger than the visual $Re_p\sqrt{f}^* \approx 450$. At $Re_p\sqrt{f} \approx 3000$, the 100-wppm data deviate slightly downward from their segment P up to the highest $Re_p\sqrt{f} \approx 4000$. The data for all three $c = 10, 30, \text{ and } 100$ wppm exhibit LNP trajectories.

In the same Figure 5.2.12, the initially extended conformation data for $c = 10, 30, \text{ and } 100$ wppm follow respective laminar paths with increasing rightward shifts from L that correspond to $\eta_r \approx 1.7, 3.3, \text{ and } 11.0$ for $Re_p\sqrt{f} < 250, 450, \text{ and } 650$; thus, lying below L, the data exhibit large drag enhancements relative to solvent, that increase with concentration. Also, because the rightward shifts from L decrease as $Re_p\sqrt{f}$ increases, these solutions exhibit shear thinning.

The 10-wppm data depart their laminar path at $Re_p\sqrt{f} \approx 300$, shift rightward in

a short transitional undulation for $300 < Re_s\sqrt{f} < 400$, and then ascend linearly into the polymeric regime until $Re_s\sqrt{f} \approx 3000$ along a segment P with slope and intercept $(A_p, B_p) = (9.0, 10.7)$; for $3500 < Re_s\sqrt{f} < 5600$, the data decline slightly from their segment P, perhaps because of polymer degradation. The 10-wppm data exhibit an LP trajectory. Similarly, departing their laminar path at $Re_s\sqrt{f} \approx 450$, the 30-wppm data inflect and then steeply approach the MDR asymptote with some transitional scatter, reaching M at $Re_s\sqrt{f} \approx 800$; after following M briefly, they exhibit retro-onset at $Re_s\sqrt{f} \approx 1000$. For $1000 < Re_s\sqrt{f} < 4300$, the 30-wppm data extend into the polymeric regime along a shallow linear segment P with $(A_p, B_p) = (5.9, -6.2)$ without any apparent polymer degradation. The 30-wppm data display an L(M)P trajectory, with a short, ill-defined, M segment. The 100-wppm data leave their laminar path at $Re_s\sqrt{f} \approx 650$, inflect, and rise steeply toward the MDR asymptote, approaching M closely at $Re_s\sqrt{f} \approx 1400$, after which they are parallel to, and just beneath, M for $1500 < Re_s\sqrt{f} < 3600$. The 100-wppm data, thus, trace an LM trajectory.

Figure 5.2.12 well illustrates the striking differences in flow behavior between solutions of initially collapsed and initially extended macromolecules, the former exhibiting LNP trajectories whereas the latter exhibits LP and LM trajectories. In laminar flow, the former have relative viscosities near unity, thus enhancing drag relative to solvent very little, and show no shear-thinning behavior, whereas the latter have large relative viscosities, thus greatly enhancing drag relative to solvent, and show pronounced shear-thinning behavior. In turbulent flow, the former data have distinct N segments with no flow enhancement whereas the latter do not. The segments P of the collapsed conformation at $c = 10, 30, \text{ and } 100$ wppm burst from closely clustered onset points

with respective $Re_p\sqrt{f} \approx 700, 550, \text{ and } 580$ on the Newtonian turbulent baseline N and have respective slope increments that increase with increasing concentration, $\delta = 6.8, 11.0, \text{ and } 22.2$. The resulting Type-A fan structure exemplifies the drag-reduction behavior of solutions of initially collapsed additives. For the extended conformation, the segments P at $c = 10$ and 30 wppm extend into the polymeric regime roughly parallel to the turbulent baseline N, having respective slopes $A_p = 9.0$ and 5.9 . Their upward displacements from N, measured by the apparent slip S' , are roughly proportional to concentration: At $Re_p\sqrt{f} = 1000$, $S' = 4.6$ and 11.3 and $S'/c = 0.46$ and 0.38 , whereas at $Re_p\sqrt{f} = 3000$, $S' = 7.0$ and 13.4 and $S'/c = 0.70$ and 0.45 . The 30-wppm data exhibit retro-onset from M into the polymeric regime. These result in a Type-B ladder structure, here comprising only two segments P and the MDR asymptote.

By comparing the Type-A fan and Type-B ladder in Figure 5.2.12, it is evident that, for fixed concentration, Type-A flow enhancement is always less than Type-B flow enhancement, with the former approaching the latter at the higher $Re_p\sqrt{f}$. In Figure 5.2.12, at $Re_p\sqrt{f} \approx 1000$, $S'_A = (1.0, 2.5, \text{ and } 5.0)$, $S'_B = (4.6, 11.3, \text{ and } 7.3)$, and the ratios $S'_A/S'_B = (0.22, 0.22, \text{ and } 0.69)$; the last ratio is oddly large because the high relative viscosity of the 100-wppm data with Type-B behavior displaces laminar flow to higher $Re_p\sqrt{f}$, thus reducing S' at $Re_p\sqrt{f} \approx 1000$. At $Re_p\sqrt{f} \approx 3000$, $S'_A = (4.6, 9.0, \text{ and } 16.0)$, $S'_B = (7.0, 13.4, \text{ and } 18.4)$, and the ratios $S'_A/S'_B = (0.65, 0.67, \text{ and } 0.87)$. The last ratio here is also oddly large, this time because the 100-wppm data in both Type-A and Type-B drag reduction closely approach the MDR asymptote at $Re_p\sqrt{f} \approx 3000$.

Figure 5.2.13 presents results for additive P500 in the 1.021-cm pipe at the same concentrations and salinities as shown in Figure 5.2.12 in the 1.458-cm pipe.

Data for the initially collapsed conformation (closed symbols) at $c = 10, 30,$ and 100 wppm follow along or closely to L with respective $\eta_r \approx 1.00, 1.05,$ and 1.18 for $30 < Re_p\sqrt{f} < 150$. At $Re_p\sqrt{f} \approx 180$, the data depart downward from L and drop toward N, commencing a laminar-to-turbulent transition, at the end of which the 10-wppm and 30-wppm data alight onto N at $Re_p\sqrt{f} \approx 350$, whereas the 100-wppm data reach a $1/\sqrt{f}$ minimum just above N at $Re_p\sqrt{f} \approx 350$. The 10-wppm data continue along N until $Re_p\sqrt{f} \approx 600$, then onset at $Re_p\sqrt{f} \approx 640$, and ascend into the polymeric regime along a linear segment P with slope and intercept $(A_p, B_p) = (10.6, 19.0)$ and slope increment $\delta = 6.6$ until $Re_p\sqrt{f} \approx 4000$. For $4100 < Re_p\sqrt{f} < 8000$, the 10-wppm markedly decline from their linear segment P, perhaps because of polymer degradation. The 30-wppm data reside only briefly on N, onset at $Re_p\sqrt{f} \approx 450$, and ascend into the polymeric regime along a P segment, for $450 < Re_p\sqrt{f} < 3000$, with slope and intercept $(A_p, B_p) = (17.2, 35.6)$ and slope increment $\delta = 13.2$; for $3500 < Re_p\sqrt{f} < 6000$, the data exhibit near-constant $1/\sqrt{f} \approx 26$, departing downward from their P segment, possibly owing to polymer degradation. From their minimum, the 100-wppm data rise further into the polymeric regime, from an apparent regressed onset at $Re_p\sqrt{f} \approx 460$, along a linear segment P with $(A_p, B_p) = (31.2, 72.6)$ and $\delta = 27.2$ until $Re_p\sqrt{f} \approx 1500$. The 100-wppm data, approach the MDR asymptote closely at $Re_p\sqrt{f} \approx 1500$ and are then parallel to and just below M, for $1500 < Re_p\sqrt{f} < 4500$.

Data for $c = 10, 30,$ and 100 wppm in 0.3 N NaCl, thus, exhibit LNP, L(N)P, and LPM flow trajectories, respectively. All their laminar-flow data remain proximal to

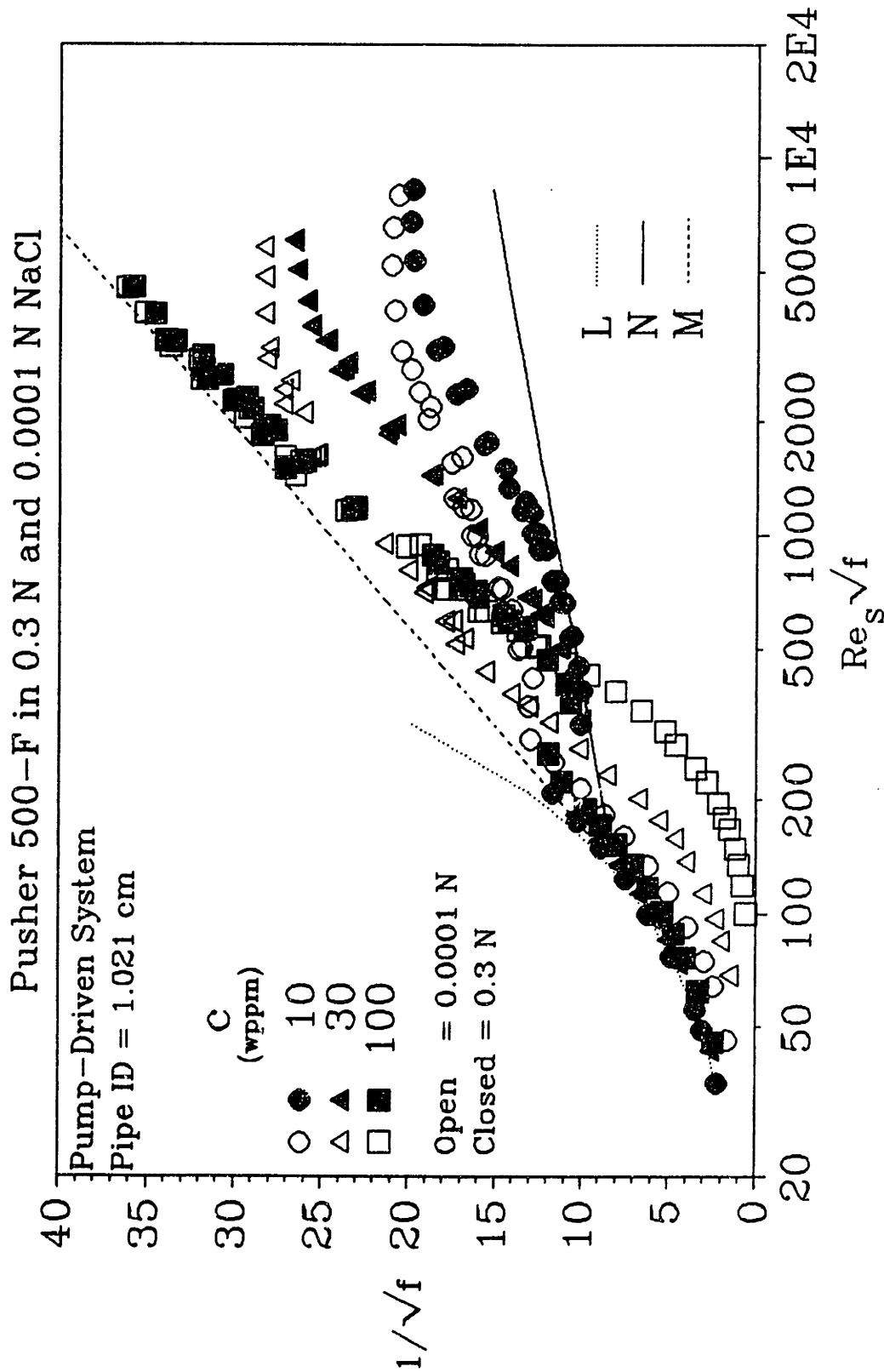


Figure 5.2.13: Pusher 500-F in 0.3 and 0.0001 N NaCl from the 1.021-cm Pipe

L with small Newtonian relative viscosities near unity, typical of solutions of initially collapsed macromolecules. In turbulent flow with drag reduction, the segments P have slope increments that increase with increasing concentration: $\delta = 6.6, 13.2,$ and $27.2,$ respectively. Although only the 10-wppm data show a distinct N segment and onset point, $Re_s\sqrt{f} \approx 640,$ the 30-wppm also reach N and onset at $Re_s\sqrt{f} \approx 450,$ whereas the 100-wppm data, with no N segment, have an apparent regressed onset, $Re_s\sqrt{f} \approx 460,$ close to the others. Thus, the three P segments collectively appear to radiate from the turbulent baseline N near $Re_s\sqrt{f} \approx 500,$ forming a Type-A "fan", that exemplifies drag-reduction behavior of solutions of initially random-coiling macromolecules.

For the initially extended conformation(open symbols) in Figure 5.2.13, data for $c = 10, 30,$ and 100-wppm follow respective laminar paths that are shifted increasingly rightward from L and that correspond to increasingly shear-thinning $\eta_r \approx 1.6, 2.6,$ and 8.2 for $Re_s\sqrt{f} < 180, 250,$ and $500;$ the observed drag enhancements relative to solvent increase greatly as concentration increases. The 10-wppm data depart from their L segment at $Re_s\sqrt{f} \approx 250,$ at which point they are also very close to the MDR asymptote; at $Re_s\sqrt{f} \approx 300,$ they undergo a transition, abruptly shifting rightward from L and M, to reach a $1/\sqrt{f}$ minimum at $Re_s\sqrt{f} \approx 430$ in the polymeric regime with flow enhancement. From this minimum, the 10-wppm data rise into the polymeric regime along a shallow linear segment P with slope and intercept $(A_p, B_p) = (8.6, 9.8)$ until $Re_s\sqrt{f} \approx 3000;$ from $4000 < Re_s\sqrt{f} < 8000,$ the data show nearly constant $1/\sqrt{f} \approx 20,$ declining from their linear segment P, possibly because of polymer degradation. The 10-wppm data describe an I.P trajectory. The 30-wppm data depart from their L segment at $Re_s\sqrt{f} \approx 400,$ exhibit an inflection, and then are parallel, and ~ 2 units of $1/\sqrt{f}$

below, M for $500 < Re_s \sqrt{f} < 1500$. At $Re_s \sqrt{f} \approx 1500$, the data exhibit retro-onset, suddenly shifting away from M toward the polymeric regime, into which they ascend along a linear segment P with $(A_p, B_p) = (9.0, 3.4)$ until $Re_s \sqrt{f} \approx 3100$; for $3500 < Re_s \sqrt{f} < 5800$, the data attain a constant $1/\sqrt{f} \approx 28$, descending somewhat from their segment P , possibly on account of polymer degradation. The 30-wppm data trace an LMP trajectory. The 100-wppm data inflect away from L at $Re_s \sqrt{f} \approx 600$ and ascend steeply toward M , which is reached at $Re_s \sqrt{f} \approx 1500$ and then followed closely for $1500 < Re_s \sqrt{f} < 4500$. The 100-wppm solution follows an LM trajectory.

Data for $c = 10, 30$, and 100 wppm in 0.0001 N NaCl, respectively display LP, LMP, and LM trajectories. In laminar flow, the data exhibit large relative viscosities amidst shear-thinning behavior and, concomitantly, are greatly drag enhancing relative to solvent; this is the characteristic behavior of solutions of initially extended macromolecules. In turbulent flow, the segments P for $c = 10$ and 30 wppm appear to extend linearly from the MDR asymptote into the polymeric regime with similar shallow slopes $A_p = 8.6$ and 9.0 , roughly parallel to the turbulent baseline N . Each segment P lies above N at a distance roughly proportional to its concentration, as shown by the observation that at $Re_s \sqrt{f} \approx 3000$, $S' = 6.6$ and 14.8 and $S'/c = 0.66$ and 0.49 , respectively. The 30-wppm data exhibit retro-onset, from M to P , at $Re_s \sqrt{f} \approx 1500$. The two segments P for $c = 10$ and 30 wppm and the MDR asymptote followed by the 100-wppm data form a Type-B ladder structure, typical of the drag-reduction behavior of extended macromolecules in solution.

Figure 5.2.13 serves to contrast the flow behaviors induced by solutions of initially collapsed and initially extended macromolecules. In laminar flow, the former,

which are less viscous and Newtonian, enhance drag relative to solvent less than the latter, which are more viscous and shear-thinning. In turbulent flow, whereas a Type-A fan, characteristic of initially collapsed macromolecules, comprises segments P that radiate upward from their closely-clustered onset points on the turbulent baseline N into the polymeric regime, a Type-B ladder, characteristic of initially extended macromolecules, comprises segments P that extend rightward from the widely spaced retro-onset points on the MDR asymptote into the polymeric regime above N. Figure 5.2.13 clearly shows that, for fixed concentration, Type-B drag reduction always exceeds Type-A drag reduction, with the latter asymptotically approaching the former as $Re_t\sqrt{f}$ is increased. These statements are illustrated by examples. At fixed $c = 10$ wppm, for $300 < Re_t\sqrt{f} < 400$, the solution of initially extended macromolecules exhibits $S' \approx 3$, enhancing flow infinitely better than the solution of initially collapsed macromolecules because the latter, having yet to onset, exhibits Newtonian turbulent behavior with $S' = 0$. At fixed $c = 30$ wppm and $Re_t\sqrt{f} \approx 460$, the solution of initially extended macromolecules exhibits $S' \approx 6$ and is a much better flow enhancer than the solution of initially collapsed macromolecules, which has barely reached its onset point, $S' \approx 0$. Interestingly, for fixed $c = 100$ wppm, for $300 < Re_t\sqrt{f} < 460$, the solution of initially extended macromolecules is in laminar flow and, thus, drag enhancing, $S' < 0$, whereas solution of initially collapsed macromolecules is slightly flow enhancing, $S' \approx 1$. For fixed $c = 10, 30,$ and 100 wppm, at higher $Re_t\sqrt{f} = 1000$ and 3000 , the results follow: At $Re_t\sqrt{f} = 1000$, the apparent slips are $S'_A = (1.1, 4.2, \text{ and } 9.3)$ and $S'_B = (4.6, 10.4, \text{ and } 9.0)$ with the ratio $S'_A/S'_B = (0.23, 0.41, \text{ and } 1.0)$, respectively; at $Re_t\sqrt{f} = 3000$, $S'_A = (4.8, 10.8, \text{ and } 19.4)$, $S'_B = (6.6, 14.8, \text{ and } 19.7)$, and $S'_A/S'_B = (0.72,$

0.73, and 0.98). For $c = 10$ and 30 wppm, the results show that always $S'_A < S'_B$, and that the ratio S'_A/S'_B increases toward unity with increasing $Re_p\sqrt{f}$. For $c = 100$ wppm, the ratios S'_A/S'_B are about unity because both initial conformations trace the same path for $Re_p\sqrt{f} > 500$, and both are close to the MDR asymptote at $Re_p\sqrt{f} = 1000$ and 3000 .

The effect of pipe diameter on both Types A and B of drag reduction by the collapsed and extended conformations of additive P500 can be inferred by comparisons between Figure 5.2.12, in the 1.458-cm pipe, and Figure 5.2.13, in the 1.021-cm pipe. Direct superposition of figures, as drawn, with identical $1/\sqrt{f}$ vs. $Re_p\sqrt{f}$ coordinates, causes all the polymeric-regime data in the 1.021-cm pipe to lie systematically somewhat higher than the corresponding data in the 1.458-cm pipe. But, if the 1.021-cm-pipe data are translated rightward along the Newtonian line N by an abscissa factor of $1.458/1.021$, the pipe-diameter ratio, then all of the polymeric-regime data are simultaneously superimposed upon the corresponding data in the 1.458-cm pipe. This remarkable coincidence of the entire Type-A fan and Type-B ladder structures in both pipes strongly suggests that, in the polymeric regime, both types of drag reduction are independent of pipe diameter and are scaled only by the wall shear stress. Theoretically, this result implies that drag reduction in the polymeric regime is relatively unaffected by the large scales of turbulence, imposed by the pipe diameter, and is controlled by the finer "wall" scales related to the wall shear stress. It is further noteworthy that the aforementioned superposition of polymeric regimes in both pipes also succeeds in superposing the degradation-induced maxima and declines observed in the many trajectories at the highest $Re_p\sqrt{f}$. Thus the wall shear stress is also important in scaling polymer degradation during drag reduction.

Figures 5.2.14 and 5.2.15 present results, from pump driven-system using the 1.458-cm pipe, for additive A507 in the collapsed conformation, in 0.3 N NaCl, and in the expanded conformation, in 0.0001 N NaCl, at $c = 30, 100, 300,$ and 1000 wppm. The Newtonian laminar and turbulent baselines and the MDR asymptote are represented by the lines L, N, and M, respectively, in both figures.

In Figure 5.2.14, for the collapsed conformation of additive A507, the data for $c = 30, 100, 300,$ and 1000 wppm follow laminar paths either on or to the right of L with respective Newtonian $\eta_r \approx 1.0, 1.0, 1.1,$ and 1.4 for $40 < Re_s\sqrt{f} < 150$. For $180 < Re_s\sqrt{f} < 400$, all data depart from their laminar paths and drop downward onto N in laminar-to-turbulent transitions. All data continue along N, onset respectively at $Re_s\sqrt{f}^* \approx 1520, 1540, 1520,$ and 1540 , and then rise into the polymeric regime along respective linear segments P with slopes and intercepts $(A_p, B_p) = (4.4, 1.8), (5.3, 4.6), (7.0, 9.9),$ and $(9.3, 17.0)$ and slope increments $\delta = 0.4, 1.3, 3.0,$ and 5.3 .

These data all exhibit LNP trajectories. The laminar-flow data trace paths adjacent to L with small relative viscosities and curvatures identical to that of L, as is typical behavior of solutions of random-coiling macromolecules. In turbulent flow, the long segments N, without drag reduction, and the relatively high onsets at $Re_s\sqrt{f}^* \approx 1530$ indicate that high stresses are required to perturb the non-flow-enhancing coiled conformation, implying that the additives are either short or very tightly coiled. The segments P for all $c = 30, 100, 300,$ and 1000 wppm radiate from a single onset point at $Re_s\sqrt{f} \approx 1530$ on the Newtonian turbulent baseline N, with small slope increments that nevertheless increase with increasing concentration, forming a Type-A fan structure typical of drag reduction by solutions of random-coiling macromolecules.

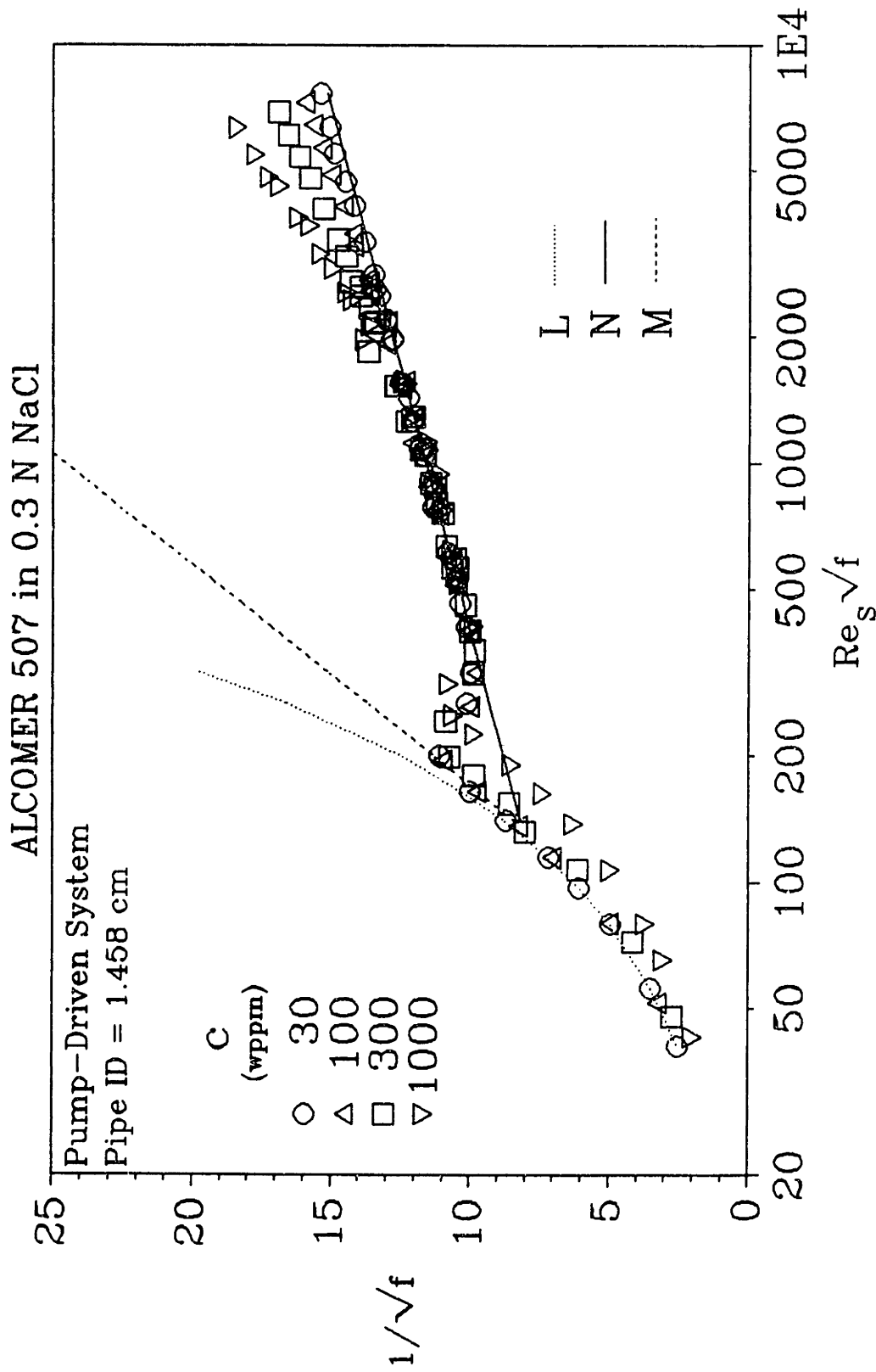


Figure 5.2.14: ALCOMER 507 in 0.3 N NaCl from the 1.458-cm Pipe

Figure 5.2.15 shows results for the expanded conformation of additive A507. The 30-wppm data parallel L for $40 < Re_s\sqrt{f} < 170$ to the right with a Newtonian $\eta_r \approx 1.2$. For $200 < Re_s\sqrt{f} < 400$, they undergo a laminar-to-turbulent transition, departing their laminar path and dropping onto N, to which they adhere for $400 < Re_s\sqrt{f} < 1100$. The data then onset at $Re_s\sqrt{f}^* \approx 1500$ and rise shallowly into the polymeric region above N along a linear segment P with slope and intercept $(A_p, B_p) = (4.3, 0.9)$ and slope increment $\delta = 0.3$ up to $Re_s\sqrt{f} \approx 7200$. The 100-wppm and 300-wppm data follow roughly the same laminar path for $70 < Re_s\sqrt{f} < 550$ far to the right of L with respective, essentially Newtonian, $\eta_r \approx 4.0$ and 4.3 , both greatly drag enhancing relative to solvent. Both sets of data show similar laminar-to-turbulent transitions, $600 < Re_s\sqrt{f} < 900$, that end on N. After briefly following N, the 100-wppm and 300-wppm data onset at $Re_s\sqrt{f}^* \approx 1200$ and then ascend into the polymeric regime along respective linear segments P with $(A_p, B_p) = (5.6, 4.6)$ and $(9.0, 15.9)$ and $\delta = 1.6$ and 5.0 up to $Re_s\sqrt{f} \approx 6200$ and 6900 . The 1000-wppm data trace a laminar path for $100 < Re_s\sqrt{f} < 1100$, farthest right of L, with essentially Newtonian $\eta_r \approx 7.8$; they exhibit the greatest drag enhancement relative to solvent, lying ~ 56 units of $1/\sqrt{f}$ below L at $Re_s\sqrt{f} \approx 1100$. For $1200 < Re_s\sqrt{f} < 1600$, the data seem to undergo laminar-to-turbulent transition, in which the data drop slightly beneath N by $\sim 1/2$ $1/\sqrt{f}$ unit, but then ascend immediately into the polymeric regime along a linear segment P with $(A_p, B_p) = (16.5, 42.4)$ and $\delta = 12.5$ up to $Re_s\sqrt{f} \approx 6000$. The 1000-wppm data appear to onset at $Re_s\sqrt{f}^* \approx 2000$.

In Figure 5.2.15, data for $c = 30, 100,$ and 300 wppm display LNP trajectories similar to those in Figure 5.2.14; the 1000-wppm data display an L(N)P trajectory,

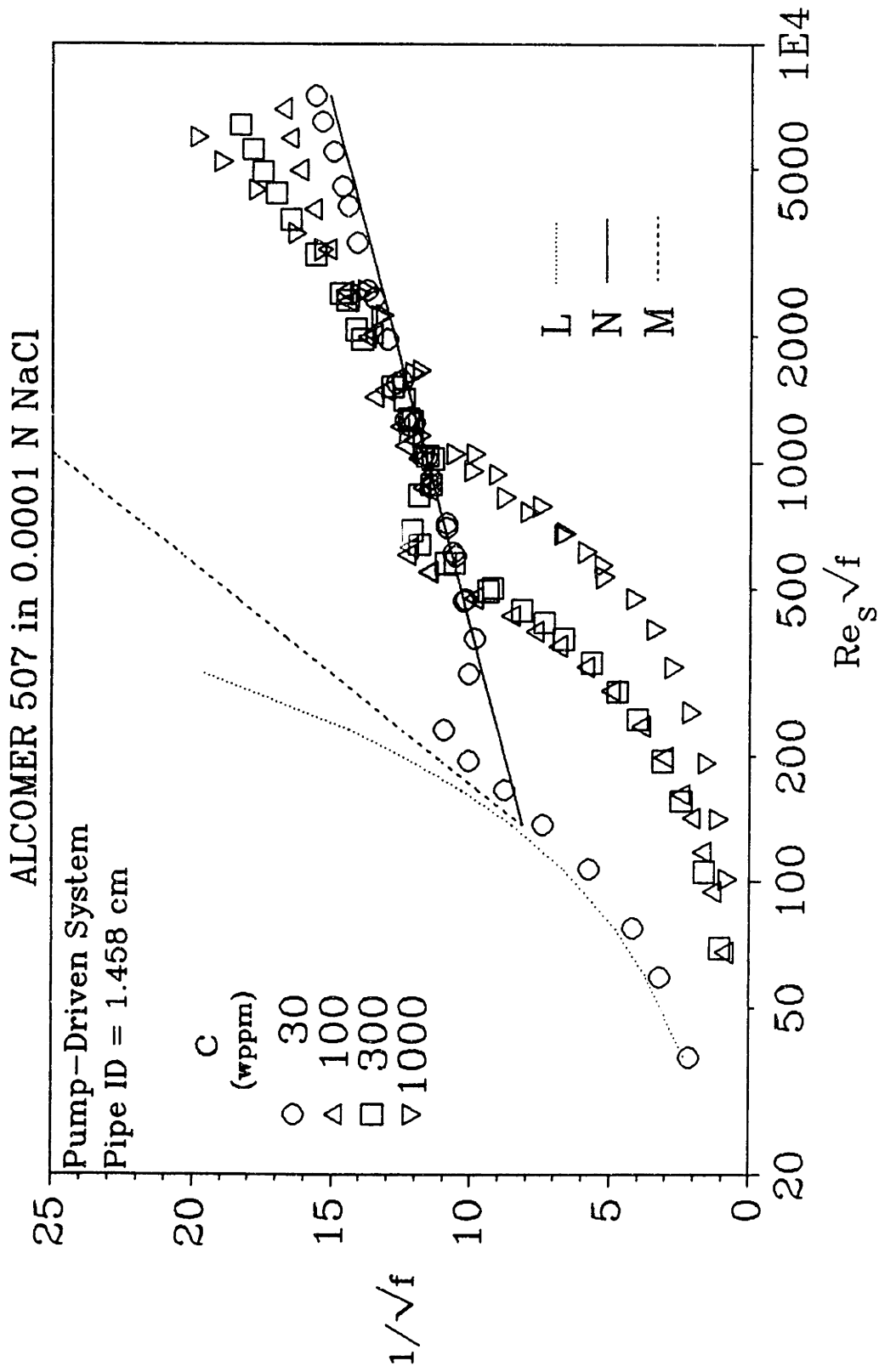


Figure 5.2.15: ALCOMER 507 in 0.0001 N NaCl from the 1.458-cm Pipe

lacking a clearly-defined segment N. The laminar-flow data exhibit only slightly shear thinning, but their relative viscosities, and concomitant drag enhancements, are large and increase as concentration increases. In turbulent flow, the solutions at $c = 20, 100,$ and 300 wppm all exhibit N segments, without flow enhancement before onset in the vicinity of $Re_s\sqrt{f} \approx 1200$; the 1000-wppm solution does not clearly follow N between transition and onset. After onset, the segments P have respective slope increments $\delta = 0.3, 1.6, 5.0,$ and 11.6 that increase with increasing concentration. The segments P form a less-than-perfect Type-A fan, that radiates from an onset region at $Re_s\sqrt{f} \approx 1200$ on the turbulent baseline N.

When juxtaposed, Figures 5.2.14 and 5.2.15 show interesting behavior by additive A507. All solutions exhibit LNP trajectories with normal Newtonian laminar-to-turbulent transitions. In laminar flow, the conformation of the polyelectrolytic additive is clearly influenced by salinity, the data in 0.3 N NaCl showing low relative viscosities and lying very close to L whereas the data in 0.0001 N NaCl exhibit much higher relative viscosities and lie much farther to the right of L. For example, the 1000-wppm solution possesses a relative viscosity $\eta_r \approx 1.4$ at high salinity, whereas at low salinity, $\eta_r \approx 7.8$. Yet, unlike previous additives C832A, B1120, and P500, the high relative viscosities exhibited by A507 solutions at low salinity are not accompanied by significant shear thinning, which suggests that the expanded conformation has no tendency to orient, remaining approximately spherical.

In turbulent flow, the data at both salinities, for both collapsed and expanded conformations, exhibit similar Type-A fans, with respective average onset $Re_s\sqrt{f} \approx 1530$ and 1200 , and respective slope increments $\delta = (0.4, 1.3, 3.0, \text{ and } 5.3)$ and $(0.3,$

1.6, 5.0, 11.6) for $c = 30, 100, 300,$ and 1000 wppm. Thus, in turbulent flow, the additive behaves as though it were initially random-coiling at both salinities, with a somewhat larger coil-size at the lower salinity.

Evidently, both laminar and turbulent results with A507 suggest that the macromolecule retains a random-coiling conformation in 0.3 N and 0.0001 N NaCl, despite the coil expansion at lower salinity.

Figures 5.2.16 and 5.2.17 show results for additive D1438 in 0.3 N and 0.0001 N NaCl, corresponding to its collapsed and expanded conformations, respectively, at $c = 30, 100, 300,$ and 997 wppm, using the pump-driven system with the 1.458 -cm pipe. In both figures, lines L, N, and M respectively represent the Newtonian laminar and turbulent baselines and the MDR asymptote.

Figure 5.2.16 presents results for additive D1438 in 0.3 N NaCl. For $40 < Re_c\sqrt{f} < 150$, all data for $c = 30, 100, 300,$ and 997 wppm trace laminar paths either on or slightly to the right of L with Newtonian $\eta_r \approx 1.00, 1.05, 1.12,$ and 1.45 , respectively. For $180 < Re_c\sqrt{f} < 400$, these data depart from their laminar paths and drop onto N, undergoing laminar-to-turbulent transitions; for $Re_c\sqrt{f} > 400$, all solutions continue along N until they onset respectively at $Re_c\sqrt{f} \approx 2000, 1450, 1200,$ and 1450 , and rise into the polymeric regime along respective linear segments P with slopes and intercepts $(A_p, B_p) = (5.4, 4.9), (6.4, 7.9), (8.8, 15.3),$ and $(15.4, 36.4)$ and slope increments $\delta = 1.4, 2.4, 4.8,$ and 11.4 up to $Re_c\sqrt{f} \approx 5300, 6100, 6500,$ and 7200 .

All solutions display LNP trajectories. Relative viscosities in laminar flow are small, $\eta_r < 1.5$, with Newtonian behavior. The observed laminar-to-turbulent transitions are all akin to those seen in normal Newtonian flows. In turbulent flow with drag

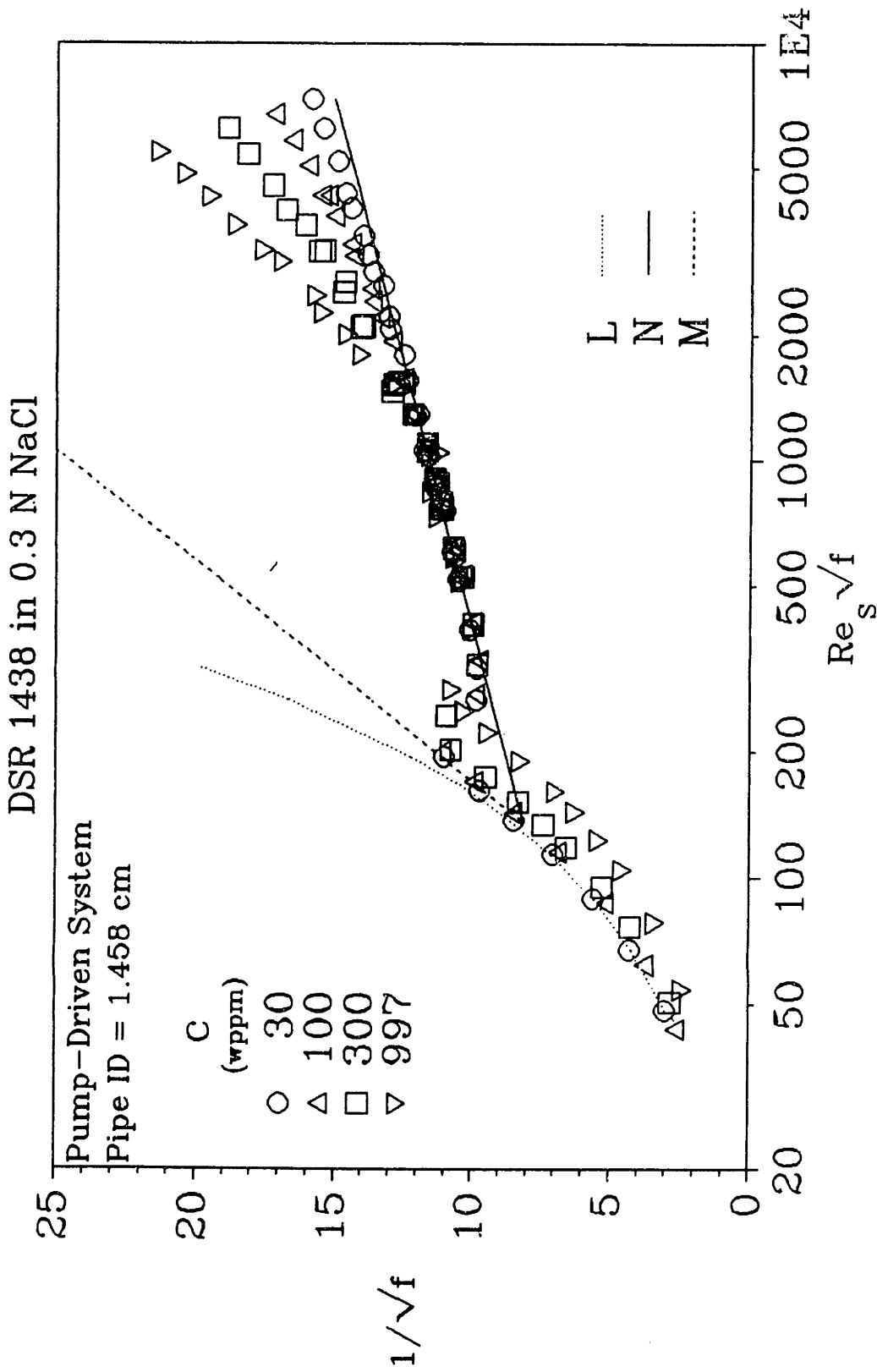


Figure 5.2.16: DSR 1438 in 0.3 N NaCl from the 1.458-cm Pipe

reduction, the segments P for $c = 30, 100, 300,$ and 997 wppm rise from onset points in the vicinity of $Re_s\sqrt{f}^* \approx 1500$ on the Newtonian turbulent baseline N, with increasing respective slopes increments $\delta = 1.4, 2.4, 4.8,$ and 11.4 . The segments P constitute a "Type-A fan" typical of drag reduction by initially random-coiling macromolecules in solution.

Figure 5.2.17 presents results for additive D1438 in the expanded conformation, in 0.0001 N NaCl. The 30-wppm data follow just to the right of L for $40 < Re_s\sqrt{f} < 150$ with $\eta_r \approx 1.08$, showing slight drag enhancement relative to solvent, and for $180 < Re_s\sqrt{f} < 380$, then undergo a laminar-to-turbulent transition, departing L and dropping onto N. Adhering to N for $400 < Re_s\sqrt{f} < 1200$, the 30-wppm data onset at $Re_s\sqrt{f}^* \approx 1250$ and ascend into the polymeric regime along a linear segment P with slope and intercept $(A_p, B_p) = (5.7, 5.8)$ and slope increment $\delta = 1.7$ up to $Re_s\sqrt{f} \approx 5100$. The 100-wppm data trace a laminar path for $45 < Re_s\sqrt{f} < 270$ rightward from L with $\eta_r \approx 1.8$ and for $300 < Re_s\sqrt{f} < 580$, depart their laminar path and drop onto N, in a laminar-to-turbulent transition. These data then follow along N for $600 < Re_s\sqrt{f} < 950$, onset at $Re_s\sqrt{f}^* \approx 1000$, and rise into the polymeric regime along a linear segment P with $(A_p, B_p) = (8.1, 12.7)$ and $\delta = 4.1$ up to $Re_s\sqrt{f} \approx 5600$. The 300-wppm data follow a laminar path for $60 < Re_s\sqrt{f} < 540$ to the right of L with Newtonian $\eta_r \approx 3.4$, enhancing drag greatly relative to solvent; they abruptly undergo a laminar-to-turbulent transition for $620 < Re_s\sqrt{f} < 890$, alighting onto N. The 300-wppm data continue along N for $900 < Re_s\sqrt{f} < 1300$, onset at $Re_s\sqrt{f}^* \approx 1350$, and rise into the polymeric regime along a linear segment P with $(A_p, B_p) = (13.3, 29.4)$ and $\delta = 9.3$ up to $Re_s\sqrt{f} \approx 6200$. The 997-wppm data trace the most drag-enhancing laminar path, farthest to the right of

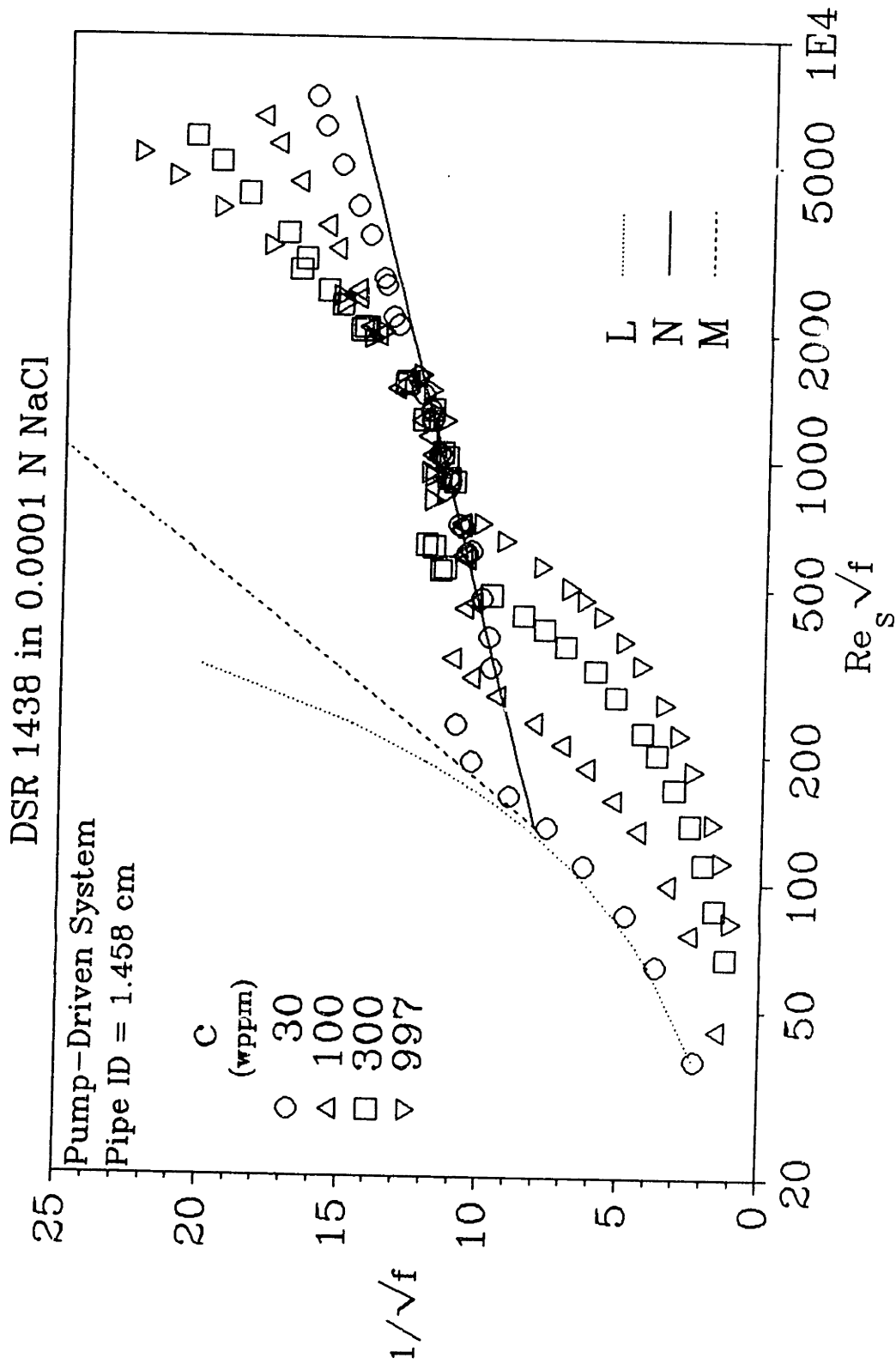


Figure 5.2.17: DSR 1438 in 0.0001 N NaCl from the 1.458-cm Pipe

L, for $80 < Re_s\sqrt{f} < 800$ with Newtonian $\eta_r \approx 5.0$. These data undergo a laminar-to-turbulent transition for $900 < Re_s\sqrt{f} < 1200$, after which they alight onto N; they continue along N for $1300 < Re_s\sqrt{f} < 1700$, onset at $Re_s\sqrt{f} \approx 1800$, and then rise into the polymeric regime along a linear segment P with $(A_p, B_p) = (20.8, 55.1)$ and $\delta = 16.8$ up to $Re_s\sqrt{f} \approx 7000$.

In Figure 5.2.17, data for $c = 30, 100, 300,$ and 997 wppm all display LNP trajectories. In laminar flow, the relative viscosities and concomitant drag enhancements relative to solvent increase greatly as concentration increases, but the behavior remains Newtonian with no shear thinning. The observed laminar-to-turbulent transitions are all Newtonian in nature. In turbulent flow, all solutions possess N segments, without drag reduction. For three solutions, $c = 30, 100,$ and 300 wppm, onsets occur in a narrow band, $Re_s\sqrt{f} \approx 1200$, but the 997 -wppm solution, with the highest viscosity, onsets at $Re_s\sqrt{f} \approx 1800$. Beyond onset, the segments P have slope increments that increase with increasing concentration: $\delta = 1.7, 4.1, 9.3,$ and 16.8 , respectively. The segments P form an imperfect Type-A fan, that radiates from onsets at $Re_s\sqrt{f} \approx 1200$ on the Newtonian turbulent baseline N. This "Type-A-fan" behavior, typical of drag reduction by initially random-coiling macromolecules in solution, suggests that even the expanded conformation of additive D1438 still retains its random-coiling character.

Figures 5.2.16 and 5.2.17 together illustrate the effect of salinity-induced changes in the flow behavior of additive D1438. In laminar flow, data in 0.3 N NaCl, with the collapsed conformation, show Newtonian behavior with small relative viscosities near unity, whereas data in 0.0001 N NaCl, with the expanded conformation, display much larger relative viscosities, but continue to show Newtonian behavior. For example, the

997-wppm solution has a relative viscosity $\eta_r \approx 1.4$ in 0.3 N NaCl and a much larger relative viscosity $\eta_r \approx 5.0$ in 0.0001 N NaCl, but exhibits Newtonian behavior, without shear thinning in both cases. Thus, reduction in salinity from 0.3 N to 0.0001 N NaCl increases the size of the macromolecular coils but do not distort their shape enough to allow significant orientation.

At both salinities, both solutions of D1438 display normal Newtonian laminar-to-turbulent transitions. In turbulent flow, Type-A fans are exhibited at both high and low salinities, with somewhat different respective onsets at $Re_r\sqrt{f} \approx 1500$ and 1200, and respective slope increments $\delta = (1.4, 2.4, 4.8, \text{ and } 11.4)$ and $(1.7, 4.1, 9.3, 16.8)$. At a fixed $Re_r\sqrt{f} \approx 3000$, the fan at low salinity shows slightly more flow enhancement than that at high salinity. The turbulent-flow data suggest that at both high and low salinities, the conformation of D1438 macromolecules retain random-coiling character, despite changes in coil size.

It is seen that salinity-induced conformational changes have similar effects on the turbulent-flow drag-reduction behavior of additives A507 and D1438. For both additives, the expanded conformations at low salinity exhibit Type-A fans with slightly lower onset and higher slope increments than the similar Type-A fans shown by the collapsed conformations at high salinity. This effect of salinity on additives A507 and D1438 contrasts with that of additives C832A, B1120, and P500, all latter of which exhibit Type-A fans at high salinity and Type-B ladders at low salinity.

5.2.4 Comparative Descriptions for Similar Additives of Varying Backbone Charge

Additives C837A, C836A, and C832A — HPAMs of approximately equal, nominal, molecular weights, $M_w \approx (15-18) \times 10^6$ g/mole — possess increasing degrees of hydrolysis ~ 8 , ~ 16 , and ~ 40 percent, respectively. Their drag-reduction results at salinities of 0.1, 0.001, and 0.0003 N NaCl in the 1.458-cm pipe from the gravity-driven system show the influence of backbone charge on polyelectrolytes with approximately equal backbone lengths. Figures 5.2.18 - 27 present these data and are ordered by decreasing salinity overall, corresponding to increasing coil expansions, and by increasing backbone charge at each salinity. The following descriptions focus on turbulent-flow aspects; all relevant laminar- and turbulent-flow parameters have been derived and are given in Tables 5.2.1 - 5.2.3.

Figures 5.2.18 - 5.2.20 respectively show results for the most-collapsed conformations, in 0.1 N NaCl, of additives C837A, C836A, C832A at $1 \leq c \leq 50$ wppm. Each polymer exhibits a Type-A drag-reduction fan that radiates from an onset point near $Re\sqrt{f^*} \approx 600$. For typical $c \approx 10$ and 20 wppm, all additives possess P segments with similar slope increments, $\delta \approx 8.5$ and 16, that attain flow enhancements of roughly the same magnitudes, $S'_1 \approx 0.7$ and 2.5, respectively. Thus, all the polymers show almost quantitatively-identical Type-A drag-reduction behavior, constituting a single fan that presumably is characteristic of the fully-collapsed, random-coiling conformation of their common backbone.

Figures 5.2.21 - 5.2.23 respectively show results for the three polymers in 0.001 N NaCl, at which salinity their conformations are all appreciably larger. Each polymer

Cyanamid 837A in 0.1 N NaCl

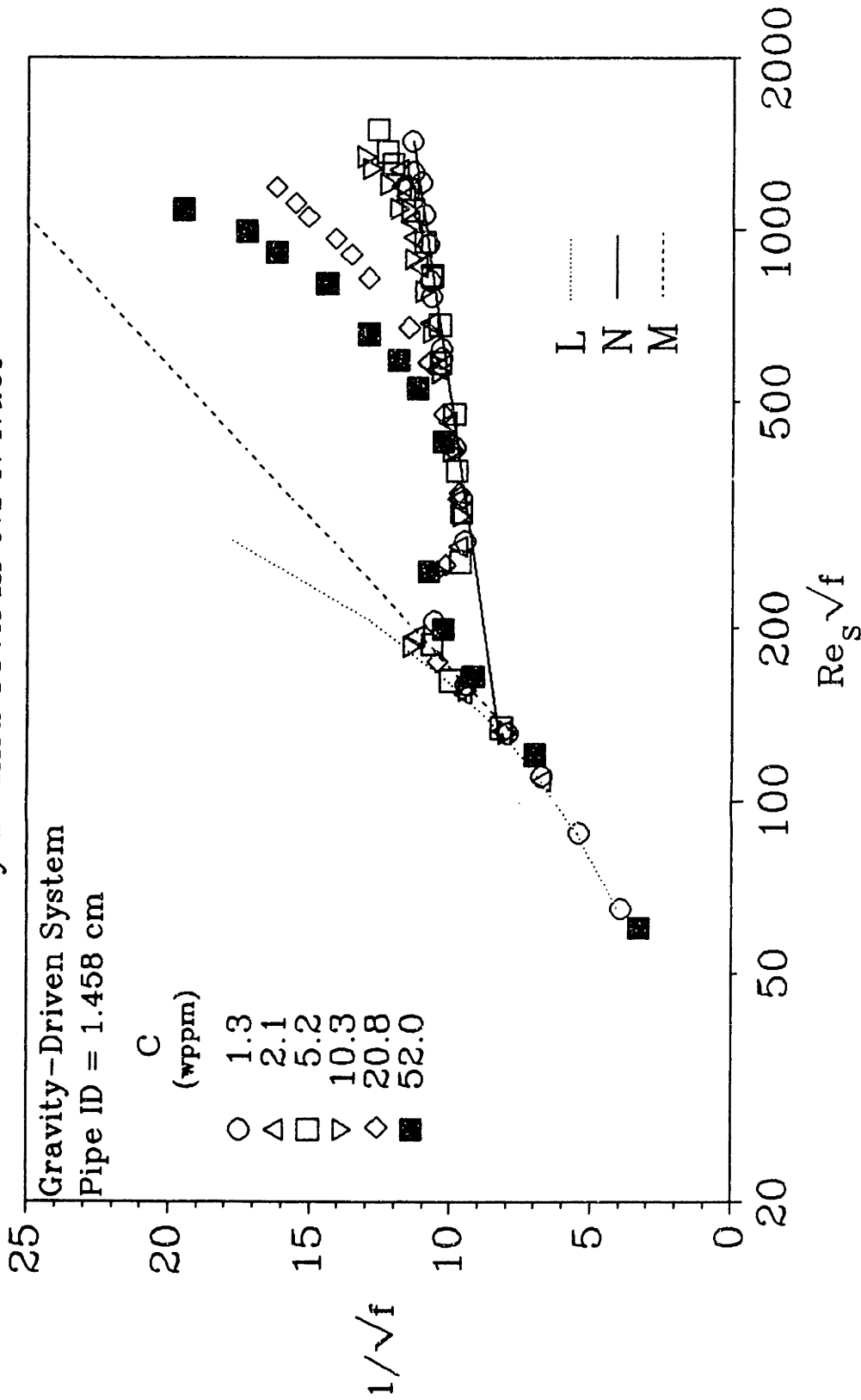


Figure 5.2.18: Cyanamid 837A in 0.1 N NaCl from the 1.458-cm Pipe

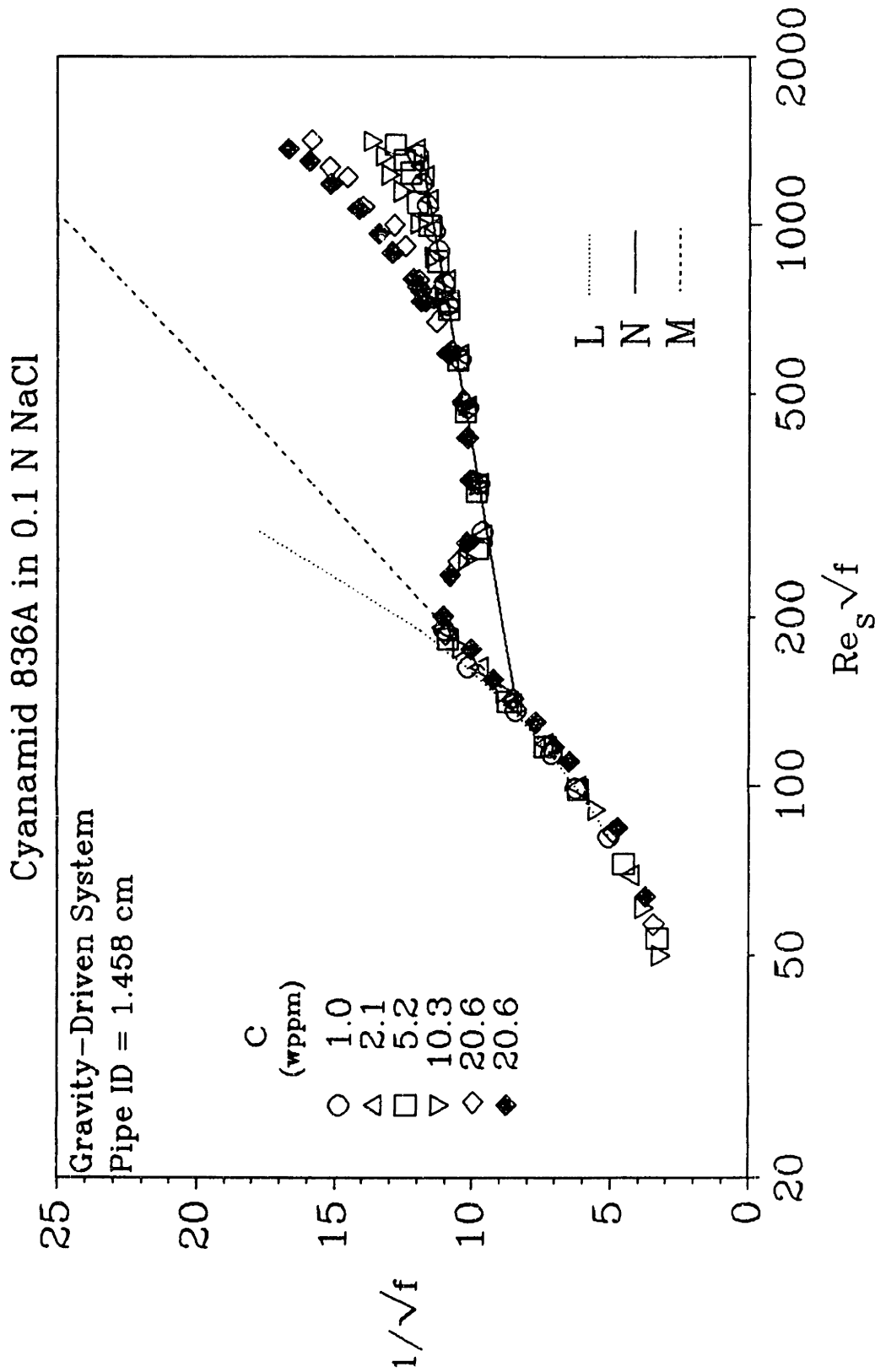


Figure 5.2.19: Cyanamid 836A in 0.1 N NaCl from the 1.458-cm Pipe

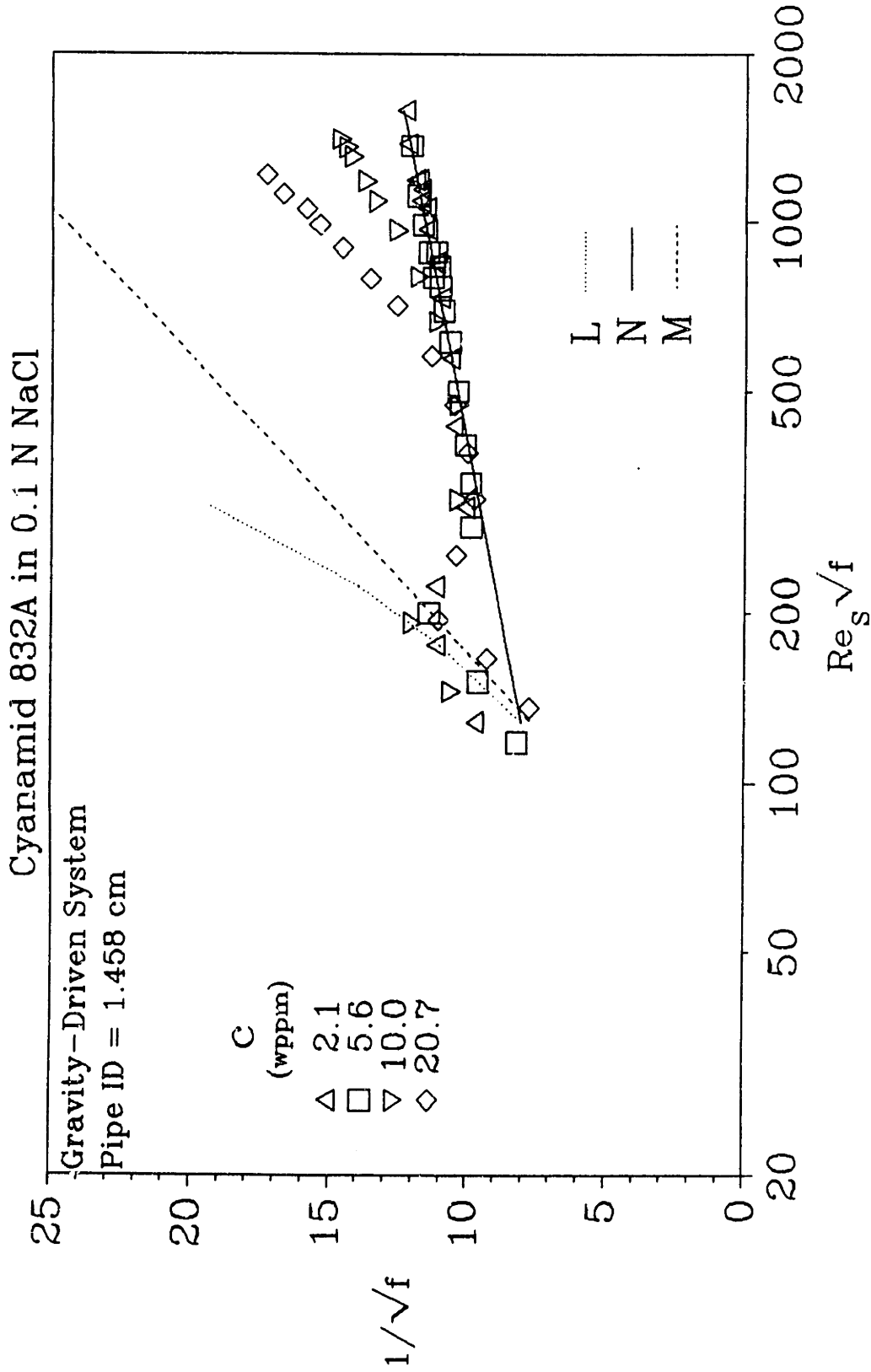


Figure 5.2.20: Cyanamid 832A in 0.1 N NaCl from the 1.458-cm Pipe

Cyanamid 837A in 0.001 N NaCl

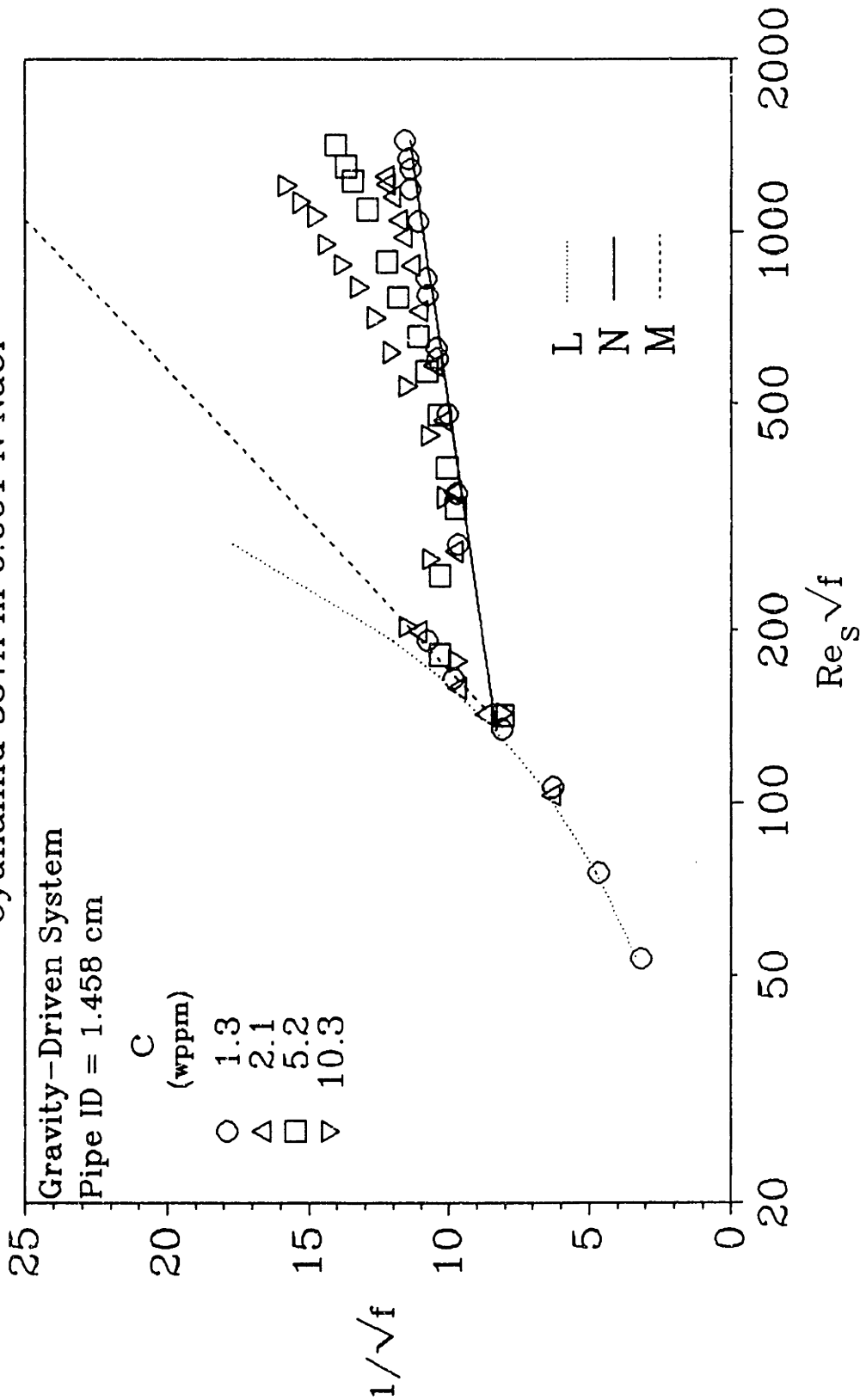


Figure 5.2.21: Cyanamid 837A in 0.001 N NaCl from the 1.458-cm Pipe

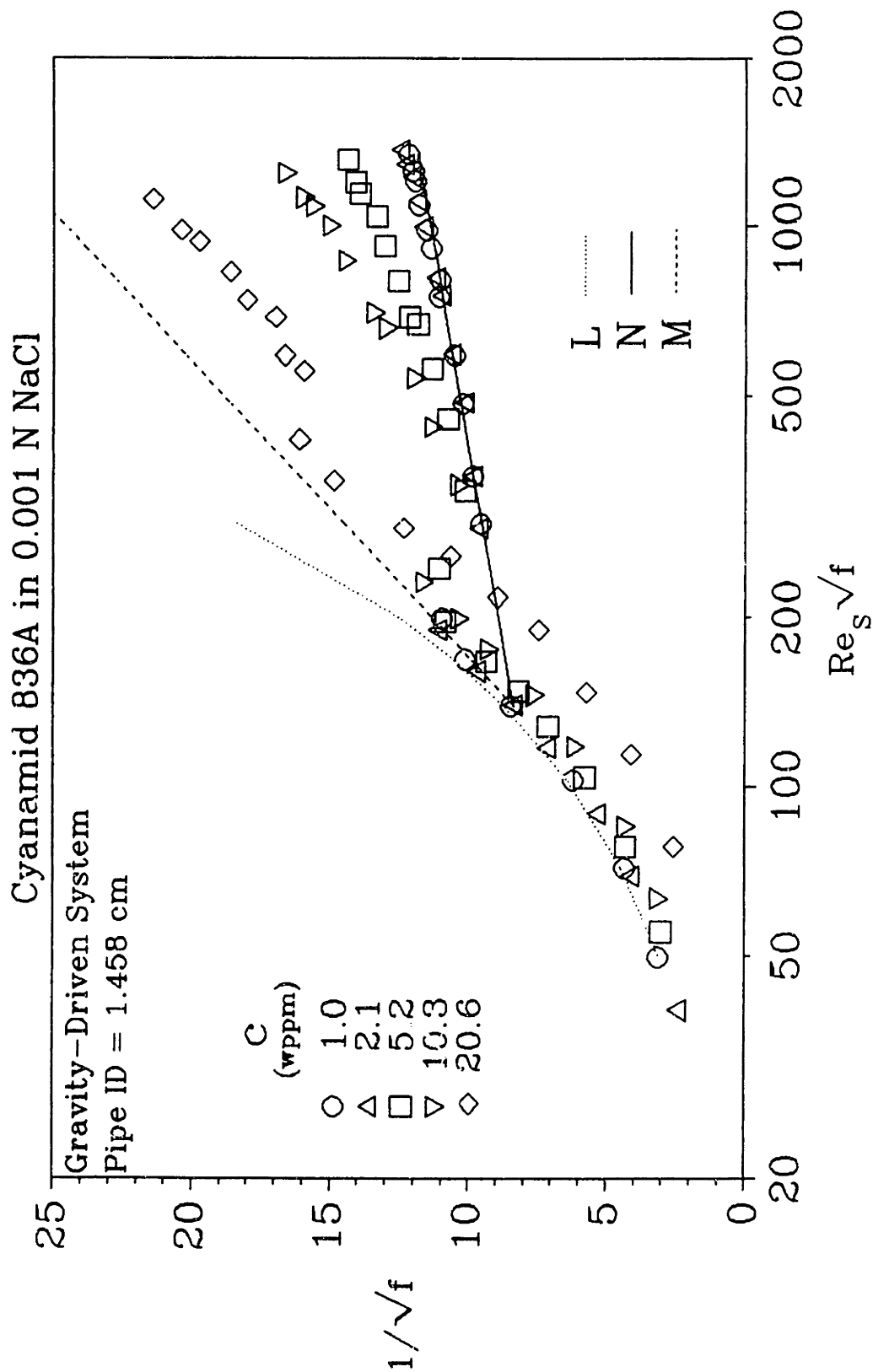


Figure 5.2.22: Cyanamid 836A in 0.001 N NaCl from the 1.458-cm Pipe

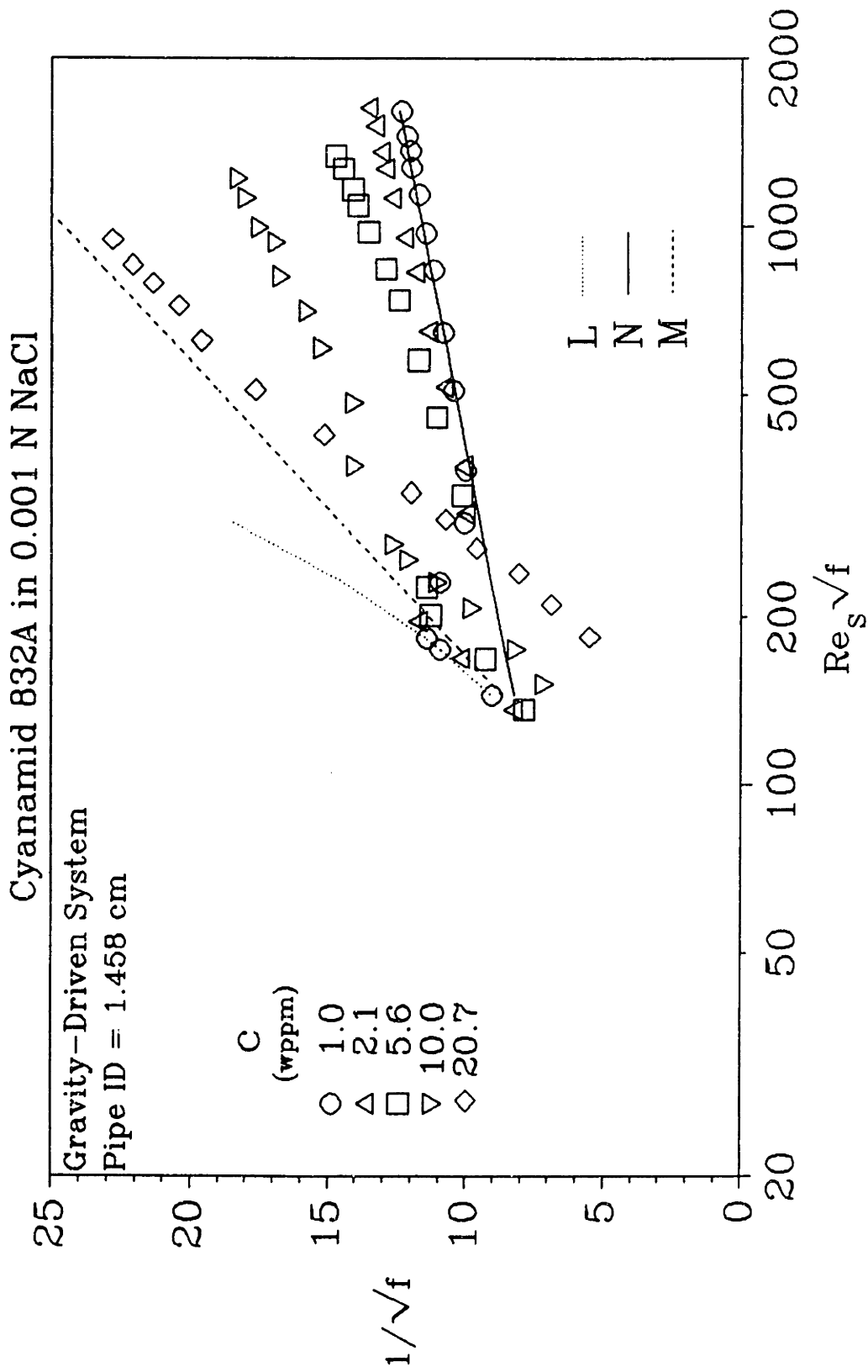


Figure 5.2.23: Cyanamid 832A in 0.001 N NaCl from the 1.458-cm Pipe

here differs from the other two in its drag-reduction behavior, and all three differ from their common collapsed fan obtained in 0.1 N NaCl. Additive C837A, with the lowest backbone charge, shows almost the same Type-A fan, which here is translated to lower $Re_c\sqrt{f}$ relative to the common collapsed fan, with onset at $Re_c\sqrt{f}^* \approx 400$. For $c \approx 10$ wppm, the P segment has roughly the same slope increment as in the collapsed fan, $\delta \approx 8$, but here achieves appreciably greater flow enhancement, $S'_1 \approx 3$, on account of its earlier onset. Next, additive C836A also continues to exhibit a Type-A fan, translated to lower $Re_c\sqrt{f}$ relative to both the common collapsed fan and the preceding C837A fan, with onset at $Re_c\sqrt{f}^* \approx 300$, near the lower limit of fully turbulent flow. For $c \approx 10$ and 20 wppm, the P segments retain approximately the same slope increments as in the collapsed fan, $\delta \approx 9$ and 14, but here attain appreciably greater respective flow enhancements, $S'_1 \approx 4$ and 9, on account of their earlier onsets. Finally, additive C832A, with the highest backbone charge, displays a distorted Type-A fan structure that tends toward, but short of, a Type-B ladder structure. Onsets are visible only at the lowest $c \approx 2$ and 5 wppm, near the lowest turbulent $Re_c\sqrt{f}$. The 10-wppm solution traces an LP trajectory, with a P-segment slope increment $\delta \approx 6.5$, somewhat lower than that in the collapsed fan, whereas the 20-wppm solution follows an LM trajectory, attaining maximum drag reduction; their respective flow enhancements, $S'_1 \approx 5.9$ and 11.3, greatly exceed those observed at $c \approx 10$ and 20 wppm in the common collapsed fan.

Evidently, at this salinity of 0.001 N NaCl, drag reduction by the three polymers depends upon their backbone charges. Most directly, the flow enhancement induced by a fixed concentration increases with increasing backbone charge. In terms of drag-reduction behavior, the additive with the least-charged backbone, C837A, continues to

exhibit a Type-A fan, translated to lower $Re_p\sqrt{f}$ relative to the common collapsed fan; this implies that C837A retains an initially random-coiling conformation that is more expanded than the collapsed conformation. The additive with the next-higher backbone charge, C836A, also continues to exhibit a Type-A fan, translated to lower $Re_p\sqrt{f}$ relative to both the collapsed and C837A fans, again implying an initially random-coiling conformation with a coil size larger than those for both its collapsed conformation and the C837A expanded conformation. Note that in the two Type-A fans exhibited by these expanded conformations of C837A and C836A, the P-segment slope increments at each concentration are essentially the same as those in the common collapsed fan. Finally, the additive with the highest backbone charge, C832A, exhibits a distorted Type-A fan that possesses some Type-B ladder structure, suggesting that its conformation is expanded enough to render it non-random-coiling.

Figures 5.2.24 - 5.2.26 show results for all three polymers in 0.0003 N NaCl, the lowest common salinity, which allowing the most-expanded initial conformations. Additive C837A still exhibits a Type-A fan, translated to lower $Re_p\sqrt{f}$ relative to both the common collapsed fan and the C837A fan in 0.001 N NaCl, with onset in the transitional region at $Re_p\sqrt{f}^* \approx 250$, such that several solutions display either LP or LM trajectories. For $c \approx 10$ and 20 wppm, their respective P segments retain approximately the same slope increments, $\delta \approx 9$ and 16, as in the collapsed fan and the C837A fan in 0.001 N NaCl, but attain appreciably greater flow enhancement, $S'_1 \approx 4$ and 9. Interestingly, this fan for C837A in 0.0003 N NaCl is quantitatively similar to the fan for C836A, with a more highly charged backbone, at the higher salinity of 0.001 N NaCl. Next, additive C836A also continues to exhibit Type-A behavior, translated to

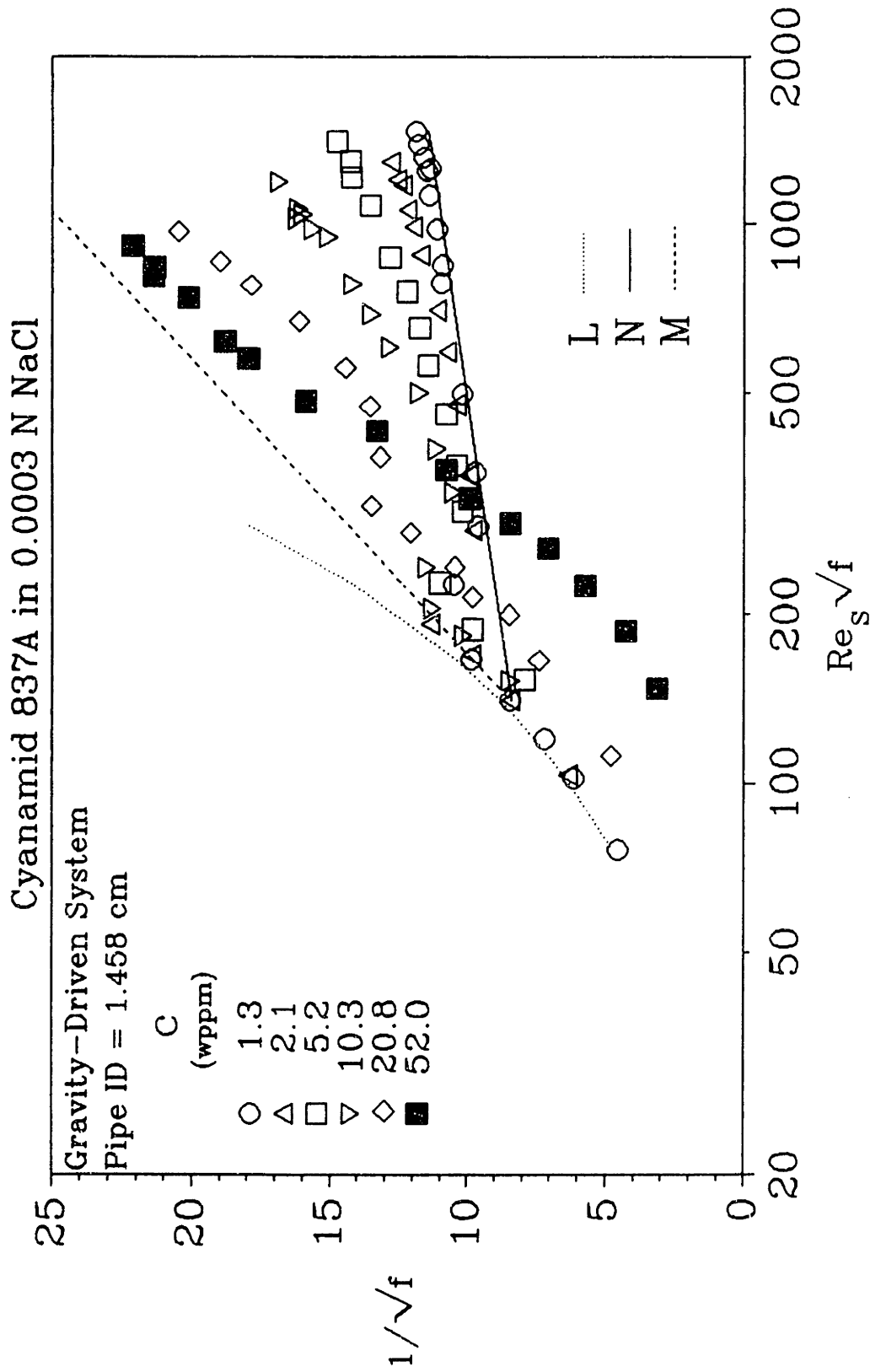


Figure 5.2.24: Cyanamid 837A in 0.0003 N NaCl from the 1.458-cm Pipe

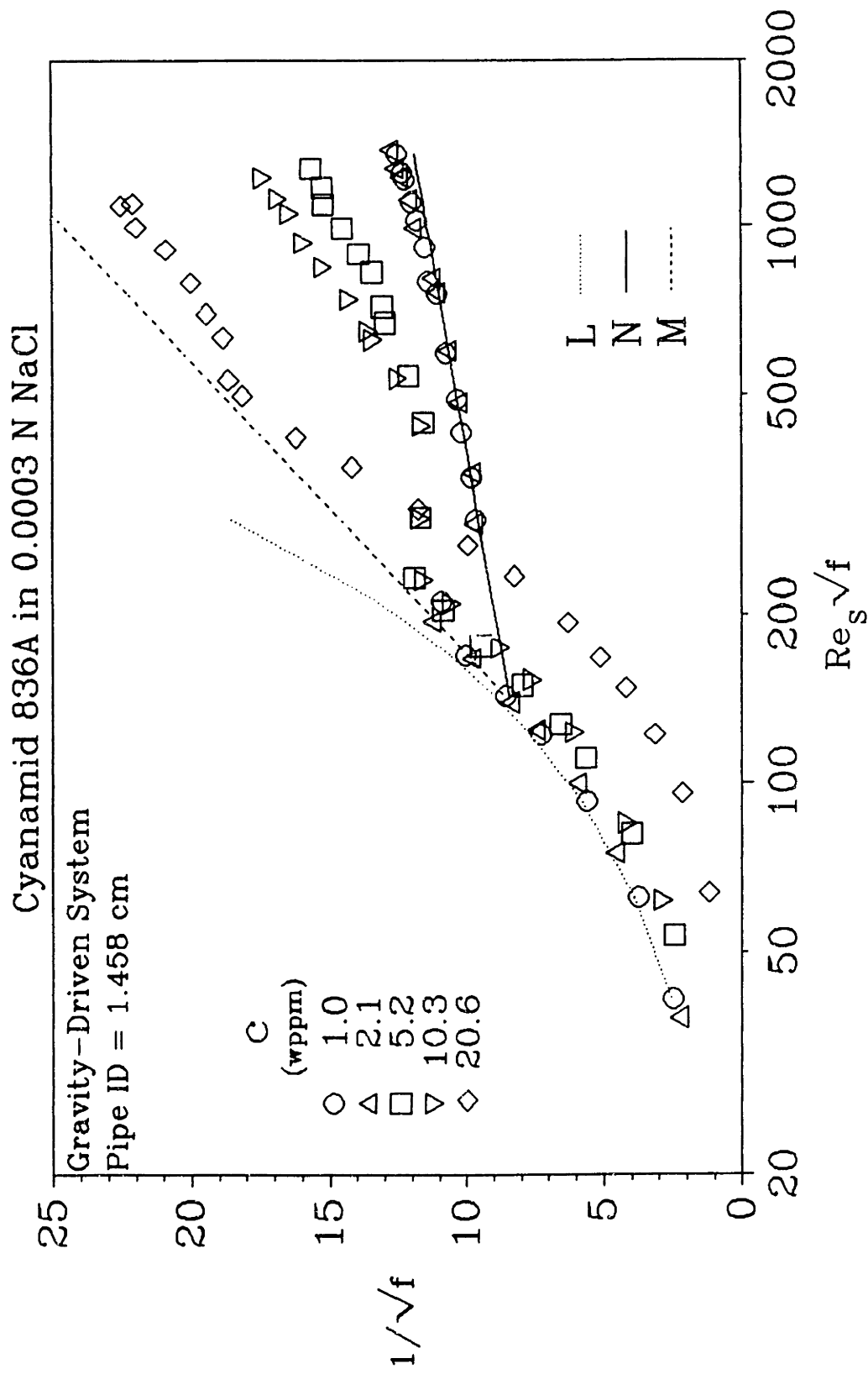


Figure 5.2.25: Cyanamid 836A in 0.0003 N NaCl from the 1.458-cm Pipe

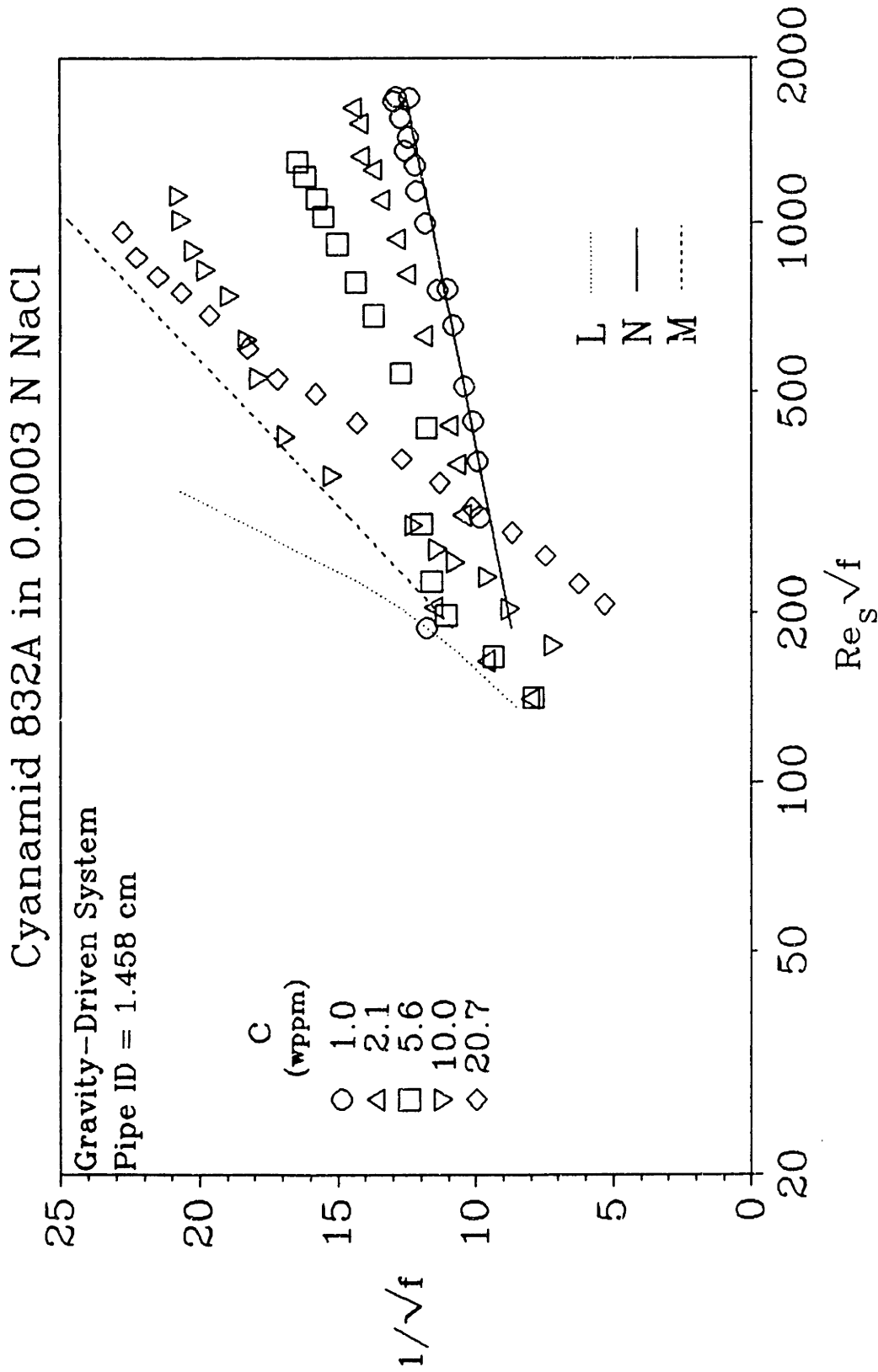


Figure 5.2.26: Cyanamid 832A in 0.0003 N NaCl from the 1.458-cm Pipe

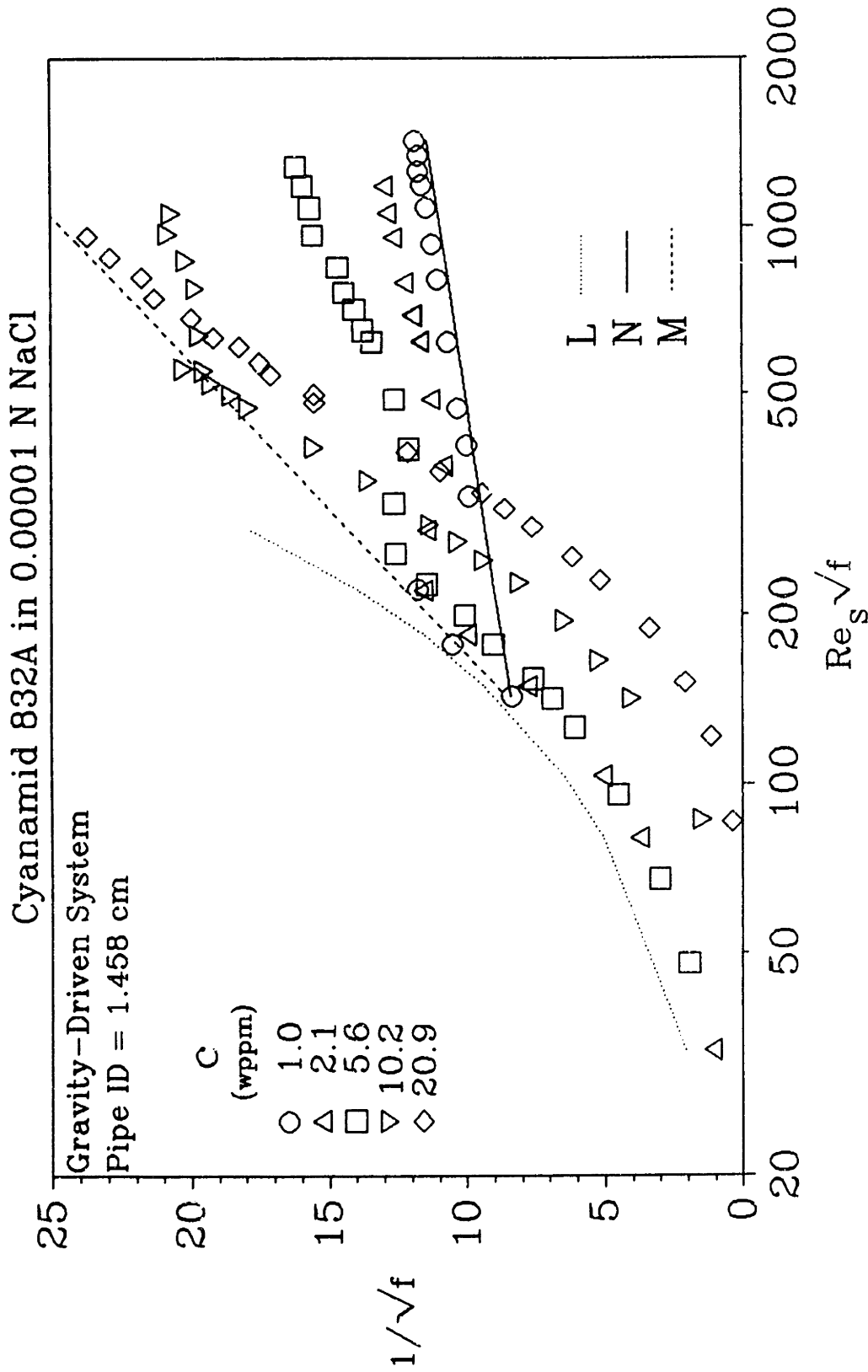


Figure 5.2.27: Cyanamid 832A in 0.00001 N NaCl from the 1.458-cm Pipe

lower $Re_c\sqrt{f}$ relative to both the common collapsed fan and the C836A fan in 0.001 N NaCl; however, only a partial Type-A fan is observed because flow transition masks the onset region of $Re_c\sqrt{f} < 250$. For $c \approx 10$ and 20 wppm, the P segments retain approximately the same slope increments, $\delta \approx 10$ and 14, as in the collapsed fan and the C836A fan in 0.001 N NaCl, but achieve greater flow enhancements, $S'_1 \approx 5$ and 10.5. Finally, for additive C832A, with the highest backbone charge, a Type-B ladder emerges. No onsets are visible. The 10-wppm solution traces an LP trajectory, with a P-segment slope increment, $\delta \approx 5.5$, appreciably lower than that in the collapsed fan, and a flow enhancement, $S'_1 \approx 9$, greater than those exhibited at the same concentrations in all the previous examples. The 20-wppm solution traces an LM trajectory, achieving maximum drag reduction. The preceding description for additive C832A is reinforced in Figure 5.2.27, for additive C832A in 0.00001 N NaCl, in which a Type-B ladder is also clearly visible.

The drag-reduction behavior of each polymer at this salinity of 0.0003 N NaCl is analogous to that seen in 0.001 N, and essentially continues the progression with declining salinity established in the preceding descriptions. Additives C837A and C836A, with the lowest backbone charges, retain Type-A fan structures that are translated to lower $Re_c\sqrt{f}$ relative to both the collapsed fan and their own respective fans in 0.001 N NaCl. Additive C832A, with the highest backbone charge, exhibits Type-B ladders in both 0.0003 and 0.00001 N NaCl, constituting the final progression from the collapsed fan exhibited in 0.1 N NaCl through its intermediate behavior, between Type-A and Type-B, in 0.001 N NaCl. In summary, drag-reduction observations with additives C837A, C836A, and C832A reveal the following influence of increasing backbone

charge. In 0.1 N NaCl, all three polymers exhibit virtually identical Type-A fans, independent of backbone charge. In 0.001 N and 0.0003 N NaCl the polymers with the least backbone charges, C837A and C836A, continue to exhibit Type-A fans, but these are translated to lower $Re_c\sqrt{f}$ relative to the common fan seen in 0.1 N NaCl, the extent of translation increasing separately with increasing backbone charge and decreasing salinity. The most-charged additive, C832A, displays intermediate drag-reduction behavior between Type-A and Type-B in 0.001 N NaCl and exhibits Type-B ladders in both 0.0003 N and 0.00001 N NaCl. At a given concentration, flow enhancement at constant $Re_c\sqrt{f}$ increases monotonically, and significantly, with both increasing backbone charge and decreasing salinity; however, in Type-A fans, the slope increments at constant concentration remain essentially independent of backbone charge and salinity.

The foregoing observations suggest the following physical interpretations. The identical Type-A fans observed at the highest salinity, 0.1 N NaCl, show that all three polymers, regardless of backbone charge, effect a collapsed random-coiling conformation, characteristic of their common backbone. The prevalence of Type-A fans for additives C837A and C836A, with the two least-charged backbones, at all lower salinities, 0.001 N and 0.0003 N NaCl, implies that their conformations remain random-coiling. The observed translations of their fans to lower $Re_c\sqrt{f}$ suggests that their random coils increasingly expand with increasing backbone charge and decreasing salinity. For C832A, with the highest backbone charge, the crossover of drag-reduction behavior from Type A in 0.1 N NaCl, through an intermediate structure in 0.001 N NaCl, to Type B in 0.0003 and 0.00001 N NaCl, reflects marked conformational changes with decreasing salinity, from a collapsed coil toward full extension.

Two further inferences arise from the foregoing. First, although all three polymers exhibit conformational expansion with decreasing salinity, Type-B behavior is displayed only by additive C832A, which has the highest backbone charge; thus, the requisite non-random-coiling, fully extended type of conformation associated with Type-B behavior can only be achieved with backbone charges in excess of a minimum charge that lies between those for additives C836A and C832A, thus corresponding to a $\sim 25\%$ degree of hydrolysis. Second, as observed in all cases, drag reduction at constant concentration always increases separately with increasing backbone charge and decreasing salinity; this implies that the drag-reduction phenomenon is enhanced by macromolecular expansion and thus is intimately associated with extended conformations of the macromolecular additive.

5.2.5 Comparative Descriptions for the Effect of Salinity

Results for solutions of additives P500 and C836A at intermediate salinities, which are not shown in either §5.2.3 or §5.2.4, are presented here in Figures 5.2.28 and 5.2.29, respectively. In each figure, the intermediate results are superposed upon the previously described and shown results for solutions of these additives at the same concentrations at both high and low salinity; the lines L, N, and M represent respectively the Newtonian laminar and turbulent baselines and the MDR asymptote.

Figure 5.2.28 presents the results for solutions of 30-wppm P500 in 0.3, 0.01, 0.001, and 0.0001 N NaCl in the 1.021-cm pipe from the pump-driven system. (Data for the 0.3-N(\blacklozenge) and 0.0001-N(\blacklozenge) solutions are described in §5.2.3 and shown in Figure

30-wppm Pusher 500-F at Various Salinities

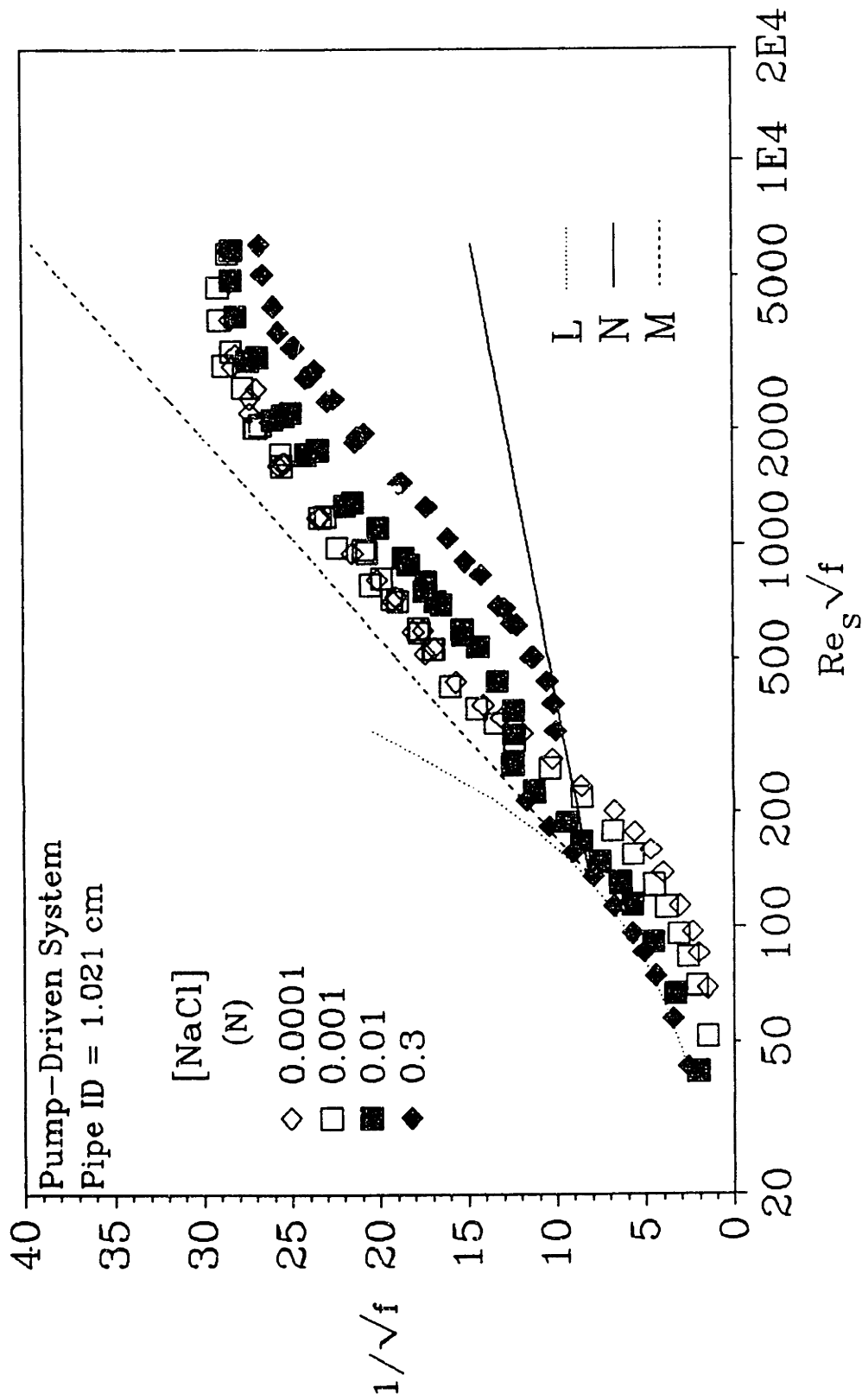


Figure 5.2.28: 30-wppm Pusher 500-F at Various Salinities

5.2.13.) In Figure 5.2.28, symbol shapes indicate polymer solutions from the same set of experimental runs; open and closed symbols denote low and high salinity, respectively.

The 0.3-N data(♦) adhere closely to L for $40 < Re_s\sqrt{f} < 150$, and then undergo a laminar-to-turbulent transition for $180 < Re_s\sqrt{f} < 350$; staying briefly on N, they onset at $Re_s\sqrt{f} \approx 450$ and rise linearly into the polymeric regime for $450 < Re_s\sqrt{f} < 3000$ along a P segment with slope and intercept $(A_p, B_p) = (17.2, 35.6)$ and slope increment $\delta = 13.2$. The data attain a nearly constant $1/\sqrt{f} \approx 26$, declining from their P segment for $3500 < Re_s\sqrt{f} < 6000$, on account of polymer degradation. The 0.3-N solution traces an L(N)P trajectory. The 0.01-N data(■) follow a laminar path for $50 < Re_s\sqrt{f} < 150$ to the right of L with a Newtonian $\eta_r \approx 1.25$, inflect toward M for $180 < Re_s\sqrt{f} < 250$, lying just below it near $Re_s\sqrt{f} \approx 250$, and then abruptly shift horizontally rightward, away from either L or M, in an altered laminar-to-turbulent transition for $250 < Re_s\sqrt{f} < 400$. Enhancing flow immediately after transition, they rise linearly into the polymeric regime for $400 < Re_s\sqrt{f} < 2500$ along a segment P with $(A_p, B_p) = (18.0, 34.7)$ and $\delta = 14.0$. The 0.01-N data maintain a nearly constant $1/\sqrt{f} \approx 28$, declining from their P segment for $3000 < Re_s\sqrt{f} < 5800$ because of polymer degradation. The 0.01-N solution follows an LP trajectory. The 0.001-N(□) and 0.0001-N(◇) data follow adjacent laminar paths for $50 < Re_s\sqrt{f} < 250$ to the right of L with respective average $\eta_r \approx 2.0$ and 2.6 amidst some shear thinning. Both sets of data inflect toward M for $300 < Re_s\sqrt{f} < 450$ and then are about parallel to, and ~ 2 units of $1/\sqrt{f}$ below, M for $500 < Re_s\sqrt{f} < 1300$. At $Re_s\sqrt{f} \approx 1500$, the 0.001-N and 0.0001-N data retro-onset into the polymeric regime and follow respective linear P segments with $(A_p,$

$B_p) = (9.0, 3.4)$ and $(7.6, -1.7)$ for $1500 < Re_s\sqrt{f} < 3000$; these data maintain nearly constant $1/\sqrt{f} \approx 28.5$, declining from their respective P segments for $3100 < Re_s\sqrt{f} < 5800$. The 0.001-N and 0.0001-N solutions exhibit LMP trajectories.

In Figure 5.2.28, the 0.3-N, 0.01-N, 0.001-N, and 0.0001-N data exhibit L(N)P, LP, LMP, and LMP trajectories, respectively. In laminar flow, these 30-wppm solutions of decreasing salinity possess increasing average relative viscosities $\eta_r \approx 1.0, 1.25, 2.0,$ and 2.6 and exhibit increasingly shear-thinning behavior from initial Newtonian behavior at both 0.3 N and 0.01 N NaCl. That relative viscosities and shear thinning increase with decreasing salinity suggests the following progression of initial macromolecular conformations in solution: collapsed random coils that neither increase viscosity nor give rise to shear thinning; expanded random coils that enhance viscosity without the extension and alignment necessary for shear thinning; partially extended macromolecules, the extension and alignment of which give rise to a shear-thinning, enhanced viscosity; fully extended macromolecules, the alignment of which induce a more-shear-thinning, larger viscosity than that observed for the partially extended conformation. As seen in Figure 5.2.28, this progression coincides with L segments that are displaced below the line L by greater $1/\sqrt{f}$ deficits; evidently, drag enhancement relative to solvent directly reflects the extent to which the initial additive conformation departs from the initially collapsed additive conformation.

Similarly, laminar-to-turbulent transitions are influenced by the initial conformation of the additive. The transition observed for a solution of initially collapsed macromolecules appears much like those observed for solvent flows. After transition, the N segment here is ill-defined, with onset immediately ensuing, rather than well-defined,

as for solvent flows, with no subsequent onset. At the next lower salinity of 0.01 N NaCl, in which the macromolecules are somewhat more-expanded relative to those at the highest salinity, the observed transition is altered because the expanded macromolecules interact with the transitional flow, rather than being passive "tracer particles" like the collapsed macromolecules. After commencing transition, the observed horizontal rightward shift of the 0.01-N data (■) away from either L or M, these data lie above the 0.3-N data by ~ 2.5 units of $1/\sqrt{f}$, but displaced to slightly lower $Re_s\sqrt{f}$. Thus, already enhancing flow, they begin to rise linearly into the polymeric regime at $Re_s\sqrt{f} \approx 350$, just to the left of the 0.3-N onset point at $Re_s\sqrt{f} \approx 450$. Moreover, the P segments of the 0.01-N and 0.3-N data possess virtually the same slope increments $\delta \approx 14.0$ and 13.2, respectively, with their subsequent declines due to polymer degradation being the same. Modest coil expansion, short of extension, evidently translates transition and the P segment with ensuing polymer degradation together toward the MDR asymptote, to higher $1/\sqrt{f}$ and lower $Re_s\sqrt{f}$. For the 0.001-N and 0.0001-N solutions, no transitional behavior is observed in that both solutions exhibit LM transitions. Interestingly, these LM transitions coincide with shear-thinning behavior in laminar flow: The 0.3-N and 0.01-N solutions are Newtonian and exhibit transitions whereas the 0.001-N and 0.0001-N solutions are shear-thinning and show no transitional behavior. (To be precise, the absence of gross-flow transition does guarantee the absence of transitional behavior in either the mean-flow or turbulent-flow structure.)

In turbulent flow, the P segment, like a vector, retains both its direction and magnitude, i.e., its slope increment and linear extent prior to polymer degradation. In Figure 5.2.28, the 0.3-N P segment is translated increasingly nearer to the MDR

asymptote as the salinity decreases to 0.001 N, during which translation it becomes a 0.01-N P segment and then a 0.001-N M segment. Evidently, in a given trajectory, laminar flow and transition determine the location, but not the subsequent behavior, of a P segment. In macromolecular terms, this observation is consistent with what is known about Type-A drag reduction. In an LNP trajectory associated with Type-A behavior, the L and N segments are governed by the initially collapsed conformation, and the P segment is governed by the subsequent departure of the additive conformation, after onset, from the initial one. In an LMP trajectory associated with Type-B behavior, the L and N segments, too, are governed by the initial conformation, but with a difference. Because of the initially extended additive conformation, an L segment often lies well to the right of Poiseuille's Law and exhibits shear thinning; because the initially extended conformation coincides with that needed for turbulent flow enhancement, flow enhancement occurs immediately following the L segment, obviating a would-be N segment and giving rise to the observed LM transition. Once both macromolecular extension and turbulent flow are achieved, the subsequent drag-reduction behavior, including flow-enhancement-related polymer degradation, is independent of the prior segments in the trajectory, notwithstanding the change in $(Re_s\sqrt{f}, 1/\sqrt{f})$ due to translation.

It is important to note, however, that flow enhancement efficiency is influenced by salinity. Because P segments are translated to lower $Re_s\sqrt{f}$ and higher $1/\sqrt{f}$, nearer to M, with decreasing salinity, the apparent slip S' must so increase. For example, at $Re_s\sqrt{f} \approx 450, 1000, \text{ and } 3000$, solutions in 0.3, 0.01, 0.001, and 0.0001 N NaCl respectively exhibit flow enhancements $S' \approx (0, 4.2, 10.8), (3.1, 7.7, 13.8), (5.8, 10.1,$

15.3), and (5.5, 10.4, 14.8), corresponding to slip ratios, relative to the 0.0001-N solution, $S'_A/S'_B \approx (0, 0.40, 0.73)$, (0.58, 0.74, 0.93), (1.06, 0.97, 1.03), and (1.0, 1.0, 1.0). For each of the 0.3-N and 0.01-N solutions, the slip ratios increase with increasing $Re_s\sqrt{f}$, implying macromolecular extension in Type-A drag reduction; that the ratios of the latter always exceed those of the former indicates that lower salinities induce larger initial macromolecular conformations. The slip ratios for the 0.001-N and 0.0001-N solution are approximately unity at all $Re_s\sqrt{f}$, implying that their initially extended conformations are essentially the same and greater than those for the 0.3-N and 0.01-N solutions.

Figure 5.2.29 presents the results for solutions of 20.6-wppm C836A in 0.1, 0.01, 0.001, and 0.0003 N NaCl in the 1.458-cm pipe from the gravity-driven system. In Figure 5.2.29, symbol shapes indicate salinity; open and closed symbols denote solutions from the same set of experimental runs.

The 0.1-N data($\nabla, \blacktriangledown$) follow closely to L for $60 < Re_s\sqrt{f} < 150$ with Newtonian $\eta_r \approx 1.05$ and undergo a laminar-to-turbulent transition for $180 < Re_s\sqrt{f} < 450$, dropping onto N. They remain along N for $500 < Re_s\sqrt{f} < 600$, onset at $Re_s\sqrt{f} \approx 700$, and then, rising into the polymeric regime, attain a linear P segment with slope and intercept $(A_p, B_p) \approx (18.6, 42.4)$ and slope increment $\delta = 15.1$. The 0.1-N solution follows an LNP trajectory. The 0.01-N data(\blacksquare) trace a laminar path for $60 < Re_s\sqrt{f} < 150$, rightward of L, with a Newtonian $\eta_r \approx 1.2$, undergo transition for $180 < Re_s\sqrt{f} < 350$, but reach a $1/\sqrt{f}$ minimum slightly above N at $Re_s\sqrt{f} \approx 350$. Rising immediately into the polymeric regime, they attain a linear P segment with $(A_p, B_p) = (19.4, 42.1)$ and $\delta = 15.9$ from an apparent onset at $Re_s\sqrt{f} \approx 500$. The 0.01-N solution exhibits an

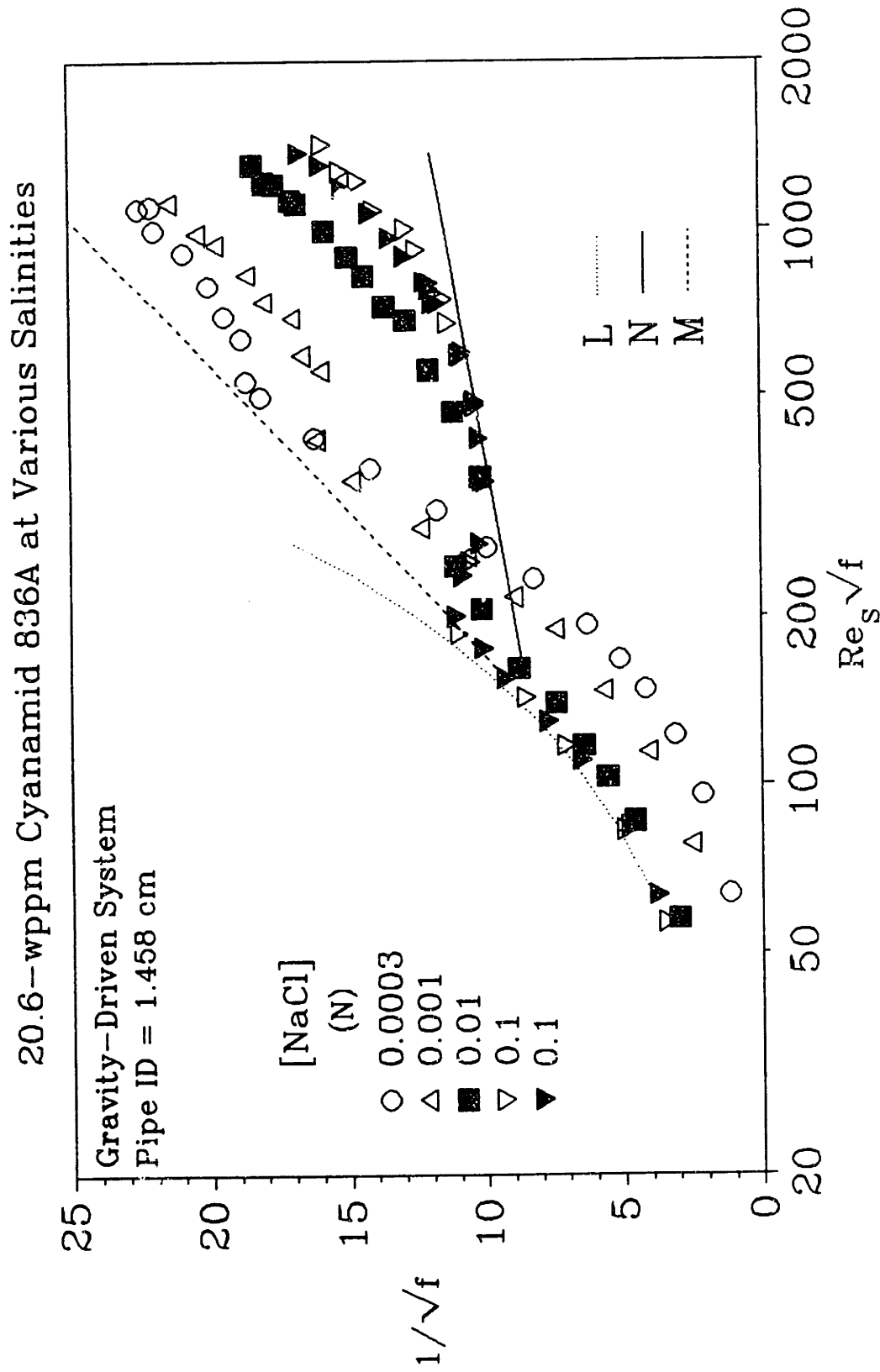


Figure 5.2.29: 20.6-wppm Cyanamid 836A at Various Salinities

L(N)P trajectory, the (N) denoting an ill-defined N segment. The 0.001-N data(∇) trace a laminar path for $70 < Re_s\sqrt{f} < 350$, far rightward from L, with a nearly Newtonian $\eta_r \approx 1.8$, lying just below the MDR asymptote at $Re_s\sqrt{f} \approx 350$. At $Re_s\sqrt{f} \approx 400$, they display transitional behavior as they shift rightward and slightly downward into the polymeric regime, reaching a $1/\sqrt{f}$ minimum at $Re_s\sqrt{f} \approx 500$ well above N by ~ 5.5 unit of $1/\sqrt{f}$. The 0.001-N data, already flow enhancing at this minimum, rise further into the polymeric regime along a linear P segment with $(A_p, B_p) = (19.8, 38.9)$ and $\delta = 16.3$. Although the 0.001-N data shift into the polymeric regime from M, they do not retro-onset because the ensuing P segment possesses a slope increment, $\delta = 16.3$, similar to those of the 0.1-N and 0.01-N P segments, $\delta = 15.1$ and 15.9 , respectively. The 0.001-N solution follows an LP trajectory. The 0.0003-N data(\circ) follow a laminar path for $60 < Re_s\sqrt{f} < 400$, farthest to the right from L, with an average $\eta_r \approx 3.0$ amidst some shear thinning, lying just below M at $Re_s\sqrt{f} \approx 400$. Approaching M most-closely at $Re_s\sqrt{f} \approx 500$, they shift slightly upward into the polymeric regime, exhibiting transitional behavior, and then rise further into the polymeric regime along a somewhat-linear P segment with $(A_p, B_p) = (18.0, 32.0)$ and $\delta = 14.4$. As with the 0.001-N data, the 0.0003-N data do not retro-onset because their P segment has a slope increment, $\delta = 14.4$, similar to those for the previous P segments. The 0.0003-N solution traces an LP trajectory.

In Figure 5.2.29, the 0.1-N, 0.01-N, 0.001-N, and 0.0003-N solutions display LNP, L(N)P, LP, and LP trajectories. In laminar flow, these solutions respectively possess increasingly higher relative viscosities, $\eta_r \approx 1.0, 1.2, 1.8,$ and 3.0 , exhibiting some shear thinning at the two lowest salinities. Thus, as salinity decreases, the initial

conformation of additive C836A progressively departs from a collapsed random coil in 0.1 N NaCl to a highly expanded macromolecule in 0.0003 N NaCl. Moreover, as seen in Figure 5.2.29, the L segments lie farther beneath the line L, over a fixed region of $Re_s\sqrt{f}$, as the salinity decreases. Evidently, solutions of increasingly expanded macromolecules enhance drag to greater extents relative to the solvent in laminar flow.

Laminar-to-turbulent transitions are also influenced by salinity via the initial macromolecular conformation of the additive. As observed in Figure 5.2.28 for P500 solutions of decreasing salinity, such C836A solutions exhibit systematically changing transitions. The 0.1-N solution undergoes a Newtonian transition that appears no different than that for solvent; for the 0.01-N solution, transition appears generally Newtonian but its peak is translated to a higher $Re_s\sqrt{f} \approx 250$ from the lower Newtonian $Re_s\sqrt{f} \approx 200$. The 0.001-N and 0.0003-N solutions, which both contain initially highly expanded macromolecules, undergo transition only when their L segments approach the line M and only at the points of imminent intersection at respective $Re_s\sqrt{f} \approx 450$ and 500, as seen in Figure 5.2.29. These transitions are characterized by rightward horizontal shifts, away from M, into the polymeric regime at $1/\sqrt{f}$ well above N. Thus, increasing coil expansion, short of extension, with decreasing salinity essentially translates transition along the line M, as dictated by the relative viscosity in laminar flow.

In turbulent flow, decreasing salinity evidently reduces the length of an N segment in a flow trajectory, as seen in Figure 5.2.29 by the trajectory progression of LNP to L(N)P to LP. The disappearance of the N segment coincides with the translation of transition to higher $(Re_s\sqrt{f}, 1/\sqrt{f})$ along the line M as salinity decreases. Just as the character of transition is not greatly altered by decreasing salinity, all ensuing P segments

possess approximately the same slope increments $\delta \approx 15.1, 15.9, 16.3,$ and $14.4,$ respectively; thus, all four initial macromolecular conformations are random-coiling, only differing in their expansions, due to decreasing salinity, away from the collapsed conformation. As observed for additive P500, the P segments exhibited by C836A solutions are vector-like in their constant direction, irrespective of their locations on the (PK) coordinate plane, which are determined by the initial conformations in the previous L segments.

Flow enhancement, unlike P segments, does vary with salinity. For example, at $Re_p\sqrt{f} \approx 400$ and $1000,$ the $0.1\text{-N}, 0.01\text{-N}, 0.001\text{-N},$ and 0.0003-N solutions exhibit respective $S' \approx (0, 1.8), (0.7, 4.4), (6.0, 9.0),$ and $(6.1, 10.6),$ having slip ratios, relative to the 0.0003-N solution, $S'_A/S'_B \approx (0, 0.17), (0.11, 0.42), (0.98, 0.85),$ and $(1.0, 1.0),$ respectively. Because these turbulent flow enhancements and slip ratios increase with decreasing salinity as do drag enhancements in laminar flow, larger initial coil sizes induce greater turbulent flow enhancements, all else being equal. It is worth noting that coil expansion produces opposite effects in laminar and turbulent flow, i.e., drag enhancement vis-a-vis flow enhancement.

5.3 Turbulent-Flow Parameters

The turbulent-flow parameters, given in Table 5.2.2, are presented pictorially for each polymer additive. The apparent slips S'_1 and S'_3 at $Re_p\sqrt{f} = 1000$ and $3000,$ slope increments $\delta,$ onset wall shear stresses T_w^* , and the retro-onset wall shear stresses $T_w^\#,$ respectively, are plotted against solution concentration. These summarize the drag-

reduction trends observed in the figures presented in the detailed descriptions.

5.3.1 The Apparent Slip S'

Figures 5.3.1 - 5.3.9, double-logarithmic plots of apparent slip S' vs. concentration c , illustrate the concentration dependence of the apparent slip S' for additives C832A, B1120, P500, A507, D1438, C837A, and C836A, respectively.

As shown in the previous section, Type-B drag-reduction exceeds Type-A drag-reduction at constant $Re_s\sqrt{f}$ with the latter approaching the former at high $Re_s\sqrt{f}$. The apparent slip S' observed for a polymer solution at low salinity, thus, exceeds that observed for a polymer solution at high salinity, with the two becoming closer at high $Re_s\sqrt{f}$. Moreover, as concentration increases, the asymptote of maximum drag reduction is approached; thus, the apparent slips S' for both Type-A and Type-B drag-reduction tend toward these asymptotic maximum values at high concentrations.

Figures 5.3.1 and 5.3.2, which respectively display S'_3 and S'_1 for additive C832A in both the 1.458-cm($\circ \nabla$) and 1.021-cm($\bullet \nabla$) pipes, contain three important observations: (1) pipe diameter has little effect on flow-enhancement efficiency as indicated by the virtually coinciding triangles and circles at both salinities; (2) Type-B drag-reduction is more effective than Type-A drag-reduction with their difference decreasing with increasing concentration, as the open and closed symbols become less separated and overlap; and (3) in Type-B drag reduction, both S'_3 and S'_1 initially increase about linearly with concentration at low flow enhancements and then reach respective constant values ~ 20 and ~ 13 , the maxima permitted by the MDR asymptote

at $Re_3\sqrt{f} = 3000$ and 1000 .

Figure 5.3.3 shows S'_1 for additive C832A from all experiments and serves to compare the results from the gravity-driven and pump-driven systems. At low concentrations, $c < 10$ wppm, data from the gravity-driven system, the 0.00001-N(\circ) and 0.0003-N(∇), lie below the 0.0001-N data(\diamond) from the pump-driven system; at high concentrations, $c \approx 10$ and 20 wppm, data from both systems at these three salinities coincide. The 0.001-N(∇) data, from the gravity-driven system, lie below those at the three lower salinities, from both systems; increasing more rapidly with increasing concentration, they nearly reach the maximum drag-reduction value, $S'_1 \approx 13$, at $c = 20$ wppm. At $c \approx 10$ and 20 wppm, the only 0.1-N data(∇) from the gravity-driven system are much less than the 0.3-N data(\blacklozenge) from the pump-driven system. In summary, data from the gravity-driven system follow the same trends with respect to salinity as observed in Figures 5.3.1 and 5.3.2, the high-salinity data lying below the low-salinity data at fixed concentration, but generally exhibit less flow enhancement than data from the pump-driven system.

Figure 5.3.4 shows both S'_1 and S'_3 for additive B1120 and illustrates the initial near-linear growth of S' with increasing c at low concentrations and low salinity, the merging of the 0.3-N and 0.0001-N data as concentration increases, and the levelling of S' as maximum drag reduction is approached.

Figures 5.3.5 and 5.3.6 present S'_3 and S'_1 , respectively, for additive P500 from both pipes. Pipe diameter has little influence on flow enhancement, as the 0.3-N data($\nabla \nabla$) and 0.0001-N data($\circ \bullet$) separately overlap at almost every concentration. Low-salinity data, again, exceed high-salinity data, and S' appears to increase linearly

with increasing concentration. Note that additive P500 is less effective than additives C832A and B1120, the extended conformation requiring almost fourfold higher c to reach the same S' .

Figure 5.3.7 shows S'_3 for additives A507 and D1438. Additive A507 is slightly more effective than D1438, but both additives are clearly much less effective per unit-mass than additives C832A, B1120, and P500. Unlike the other additives, both A507 and D1438 exhibit Type-A drag-reduction behavior irrespective of salinity. Because the Type-A fan at low salinity is displaced to lower $Re_c\sqrt{f}$ and has steeper spokes, S' at low salinity is generally greater than that at high salinity until $c \approx 1000$ wppm when the two are nearly equal. Note that all the data are well below maximum drag reduction.

Figures 5.3.8 and 5.3.9 present S'_1 for additives C837A and C836A, respectively. As seen in both figures, S' at low salinity is greater than that at high salinity and increases almost linearly with increasing concentration at low concentrations, reaching a constant value, $S'_1 \approx 13$, at high concentrations, corresponding roughly to maximum drag reduction.

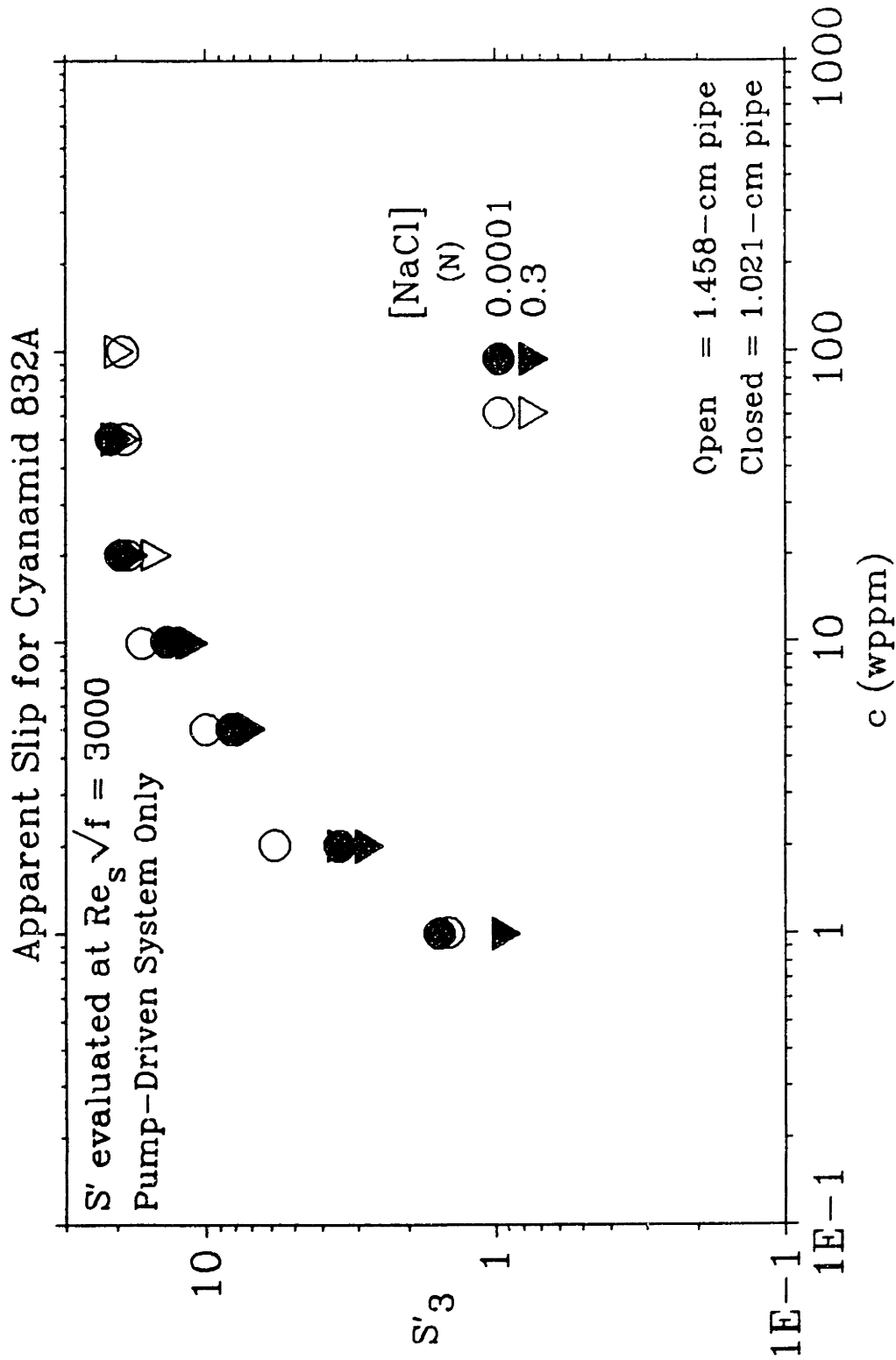


Figure 5.3.1: Apparent Slip S'_3 from the Pump-Driven System in Both Pipes for Additive C832A

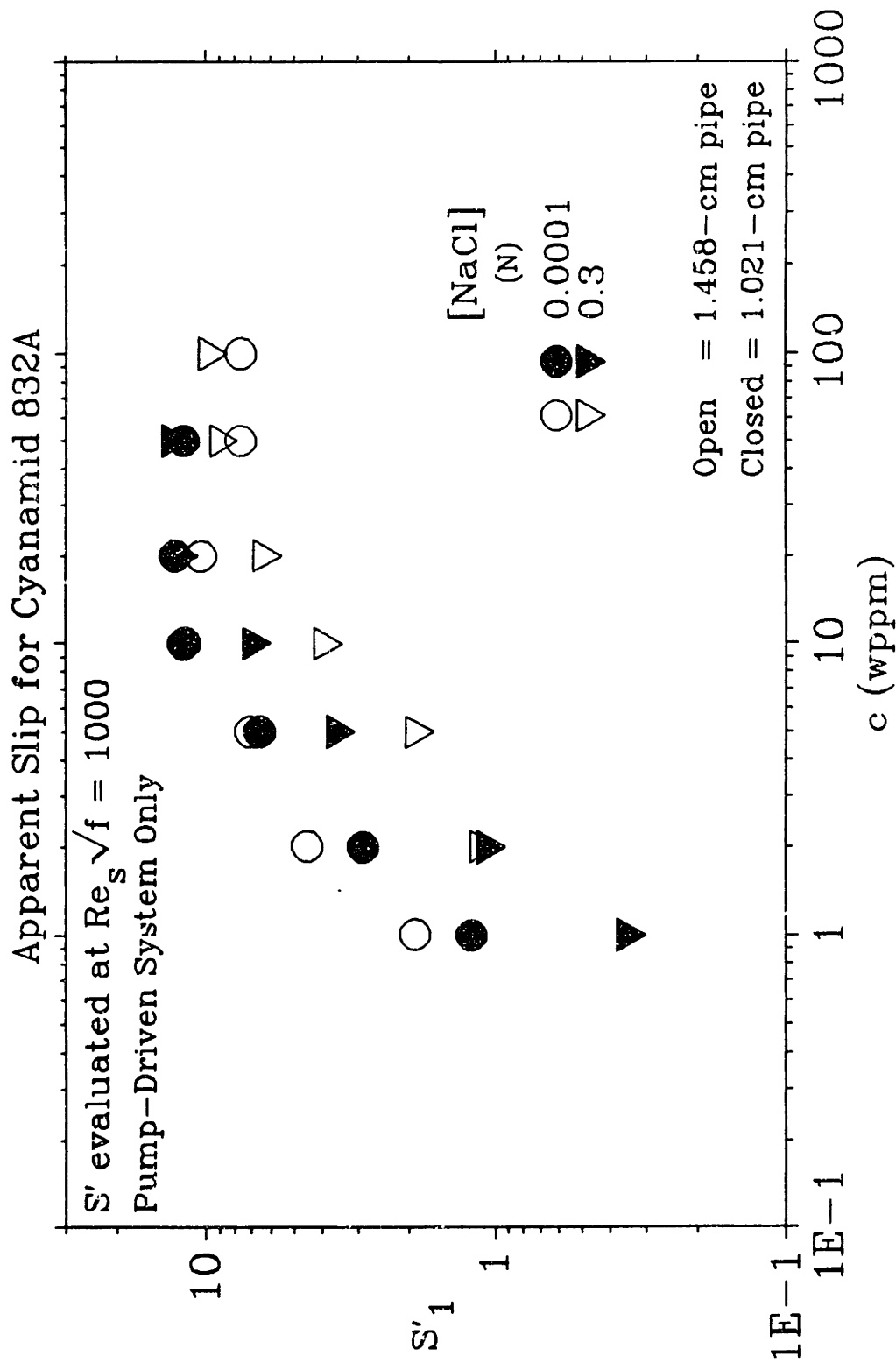


Figure 5.3.2: Apparent Slip S'_i for Cyanamid 832A from Pump-Driven System in Both Pipes

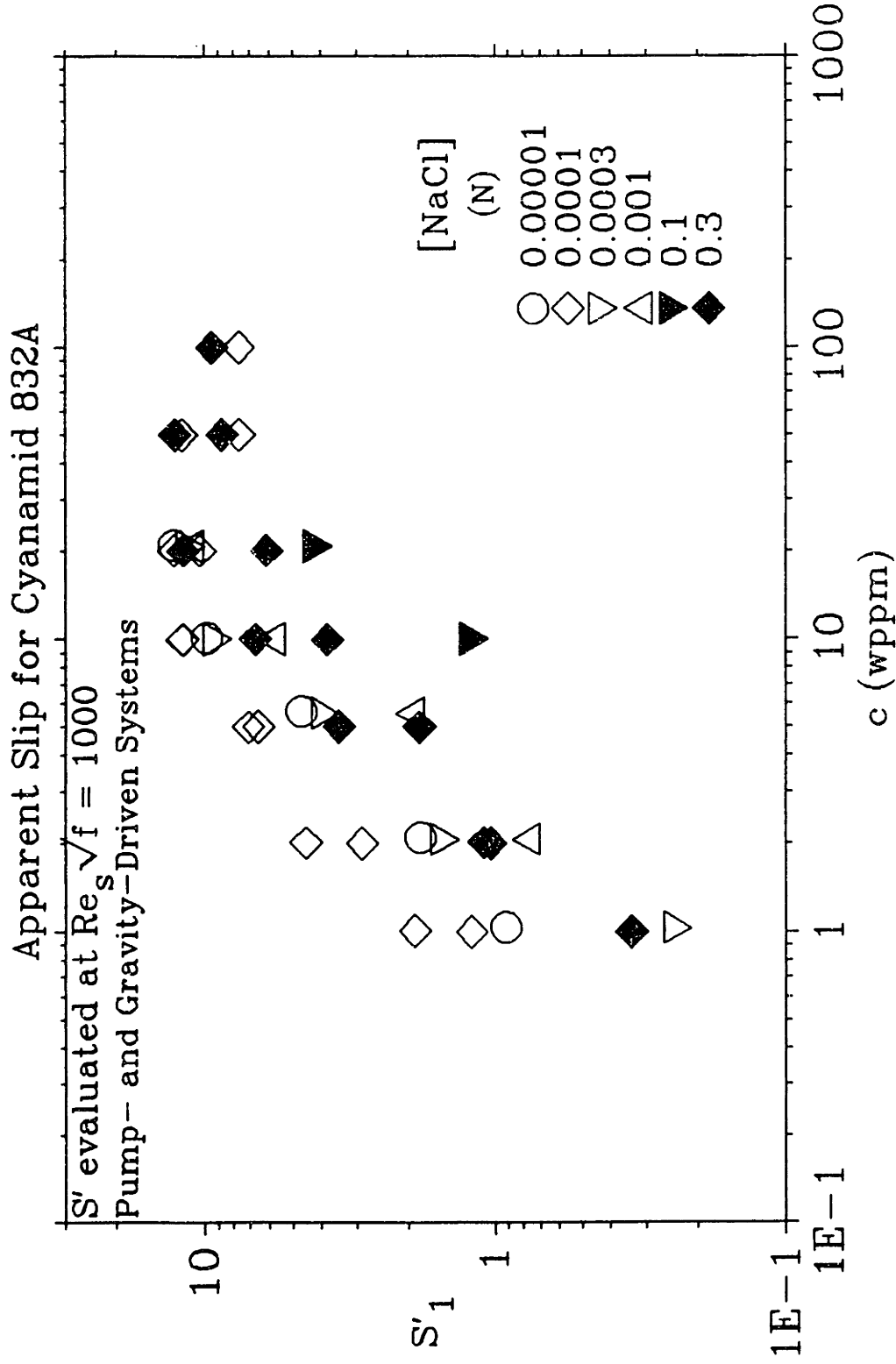


Figure 5.3.3: Apparent Slip S'_1 for Cyanamid 832A from Both Systems in the 1.458-cm Pipe

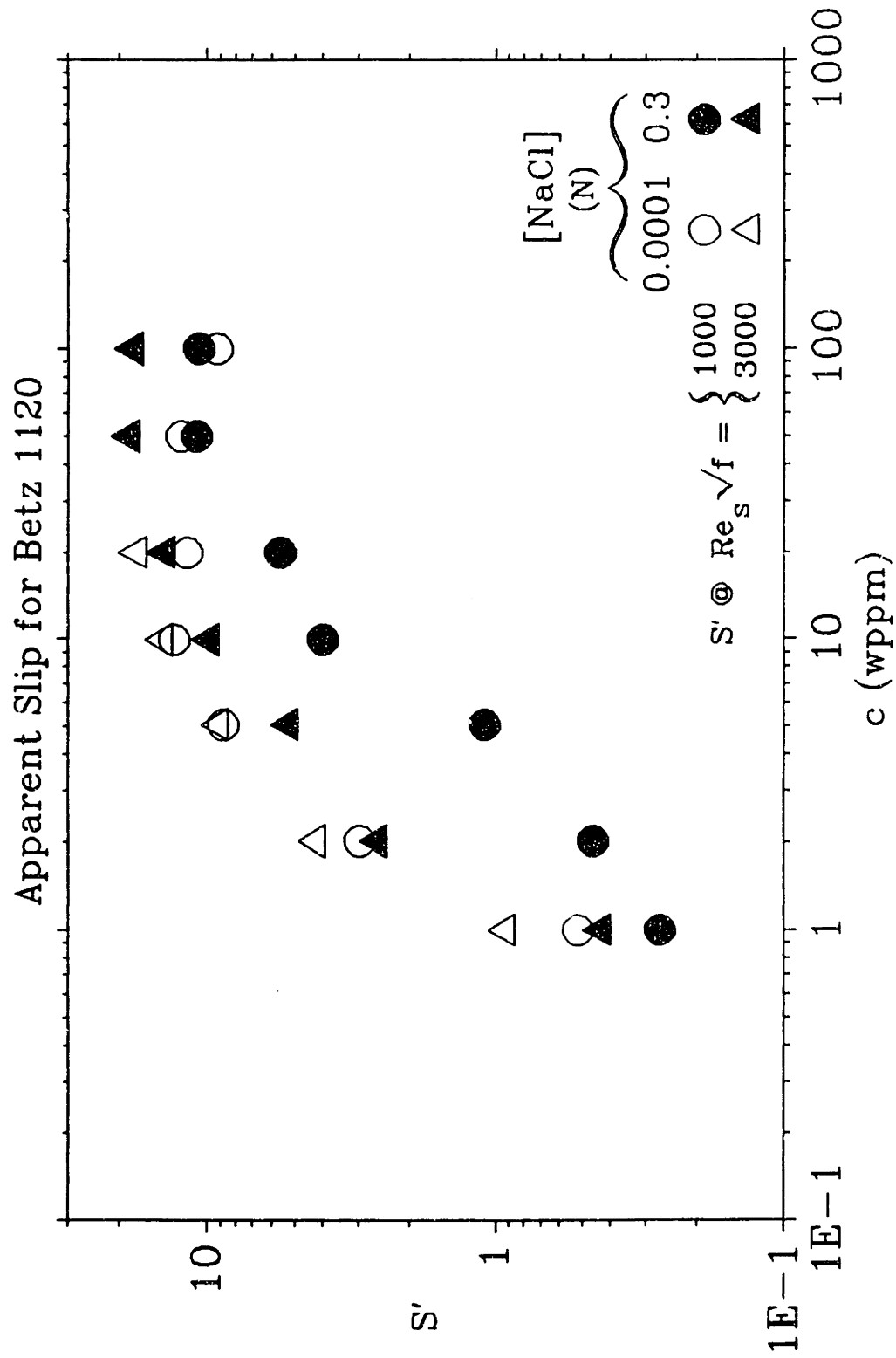


Figure 5.3.4: Apparent Slip S'_3 for Betz 1120

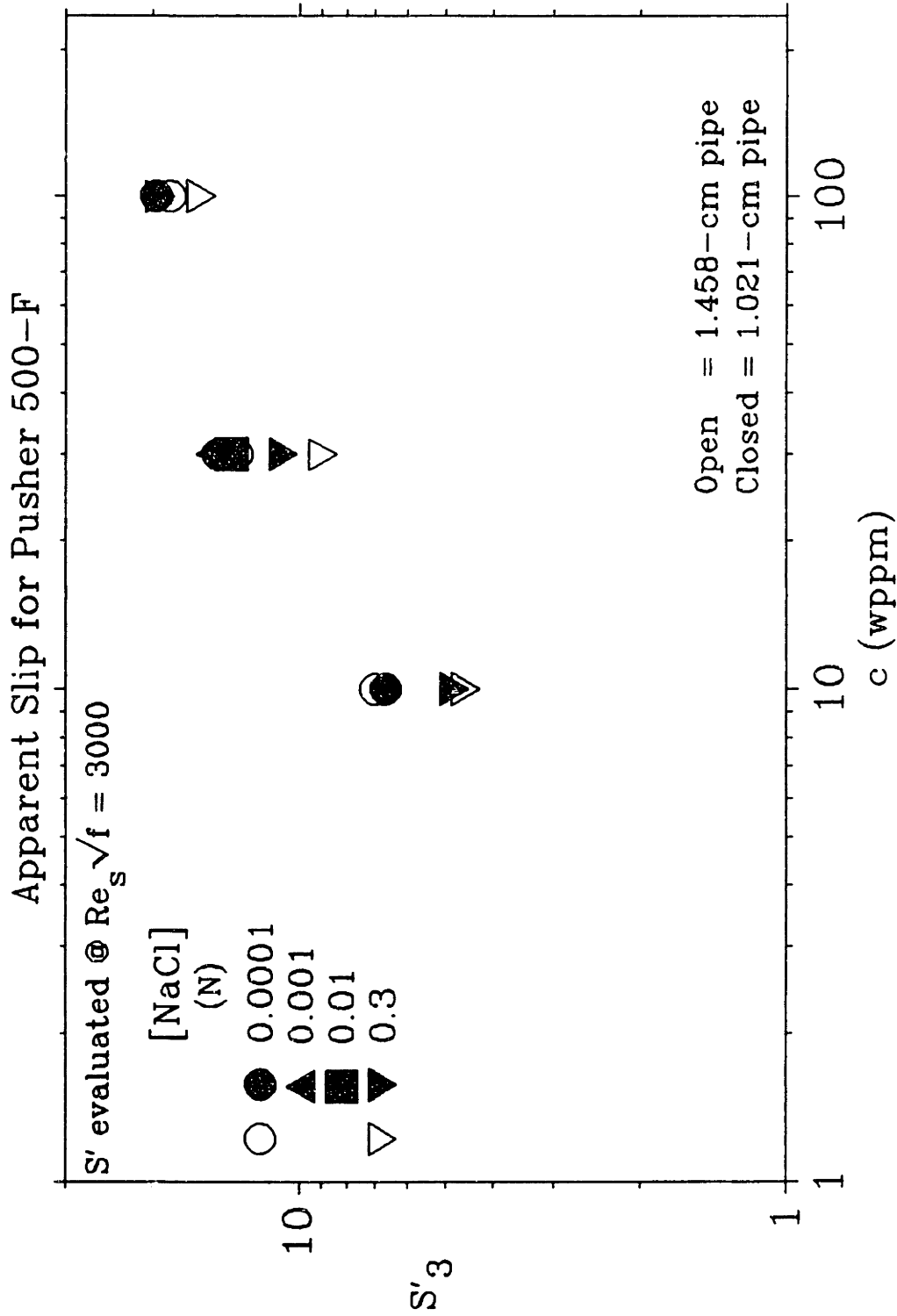


Figure 5.3.5: Apparent Slip S'_3 for Pusher 500-F in Both Pipes

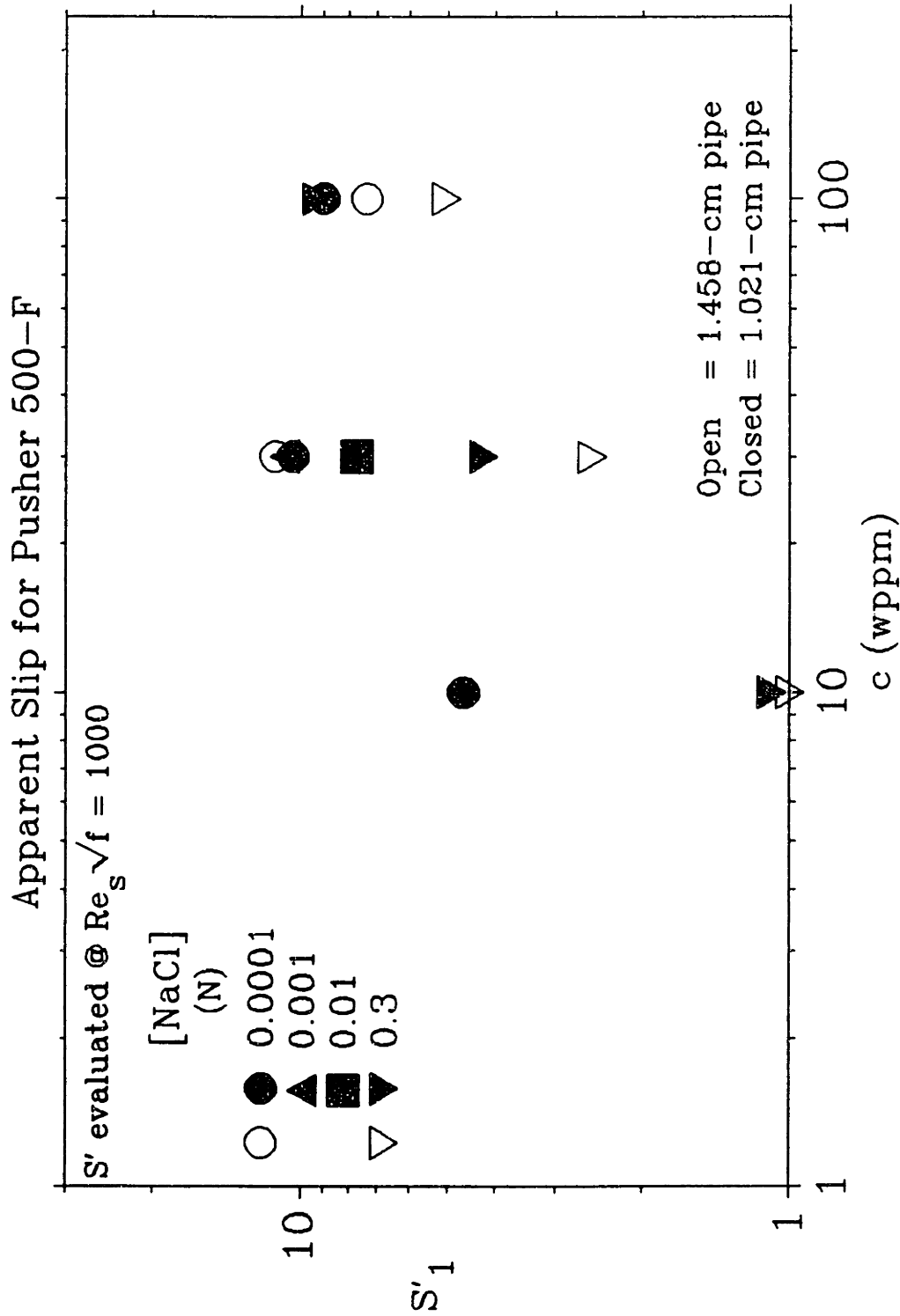


Figure 5.3.6: Apparent Slip S'_1 for Pusher 500-F in Both Pipes

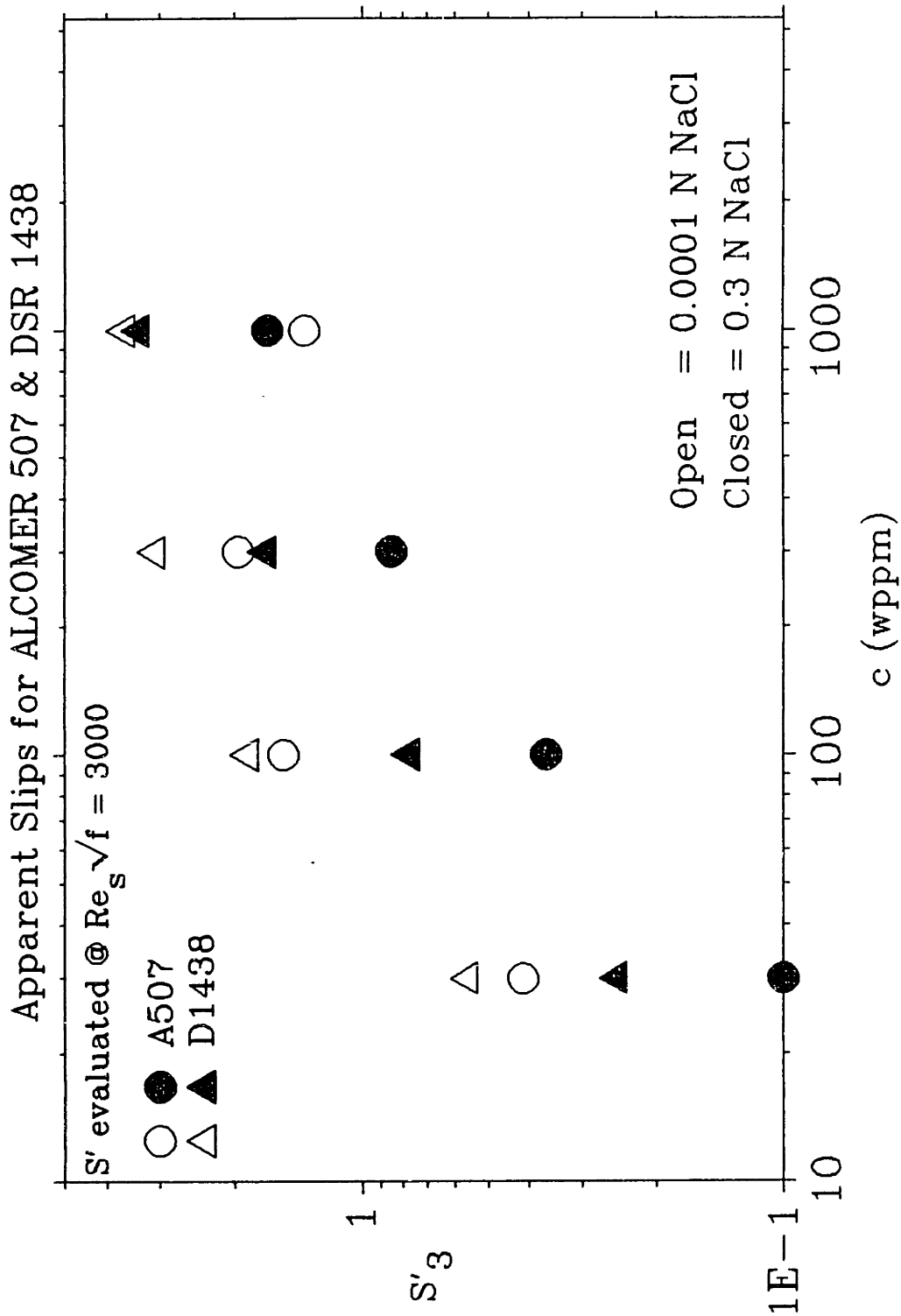


Figure 5.3.7: Apparent Slip S'_3 for Alcomer 507 and DSR 1438

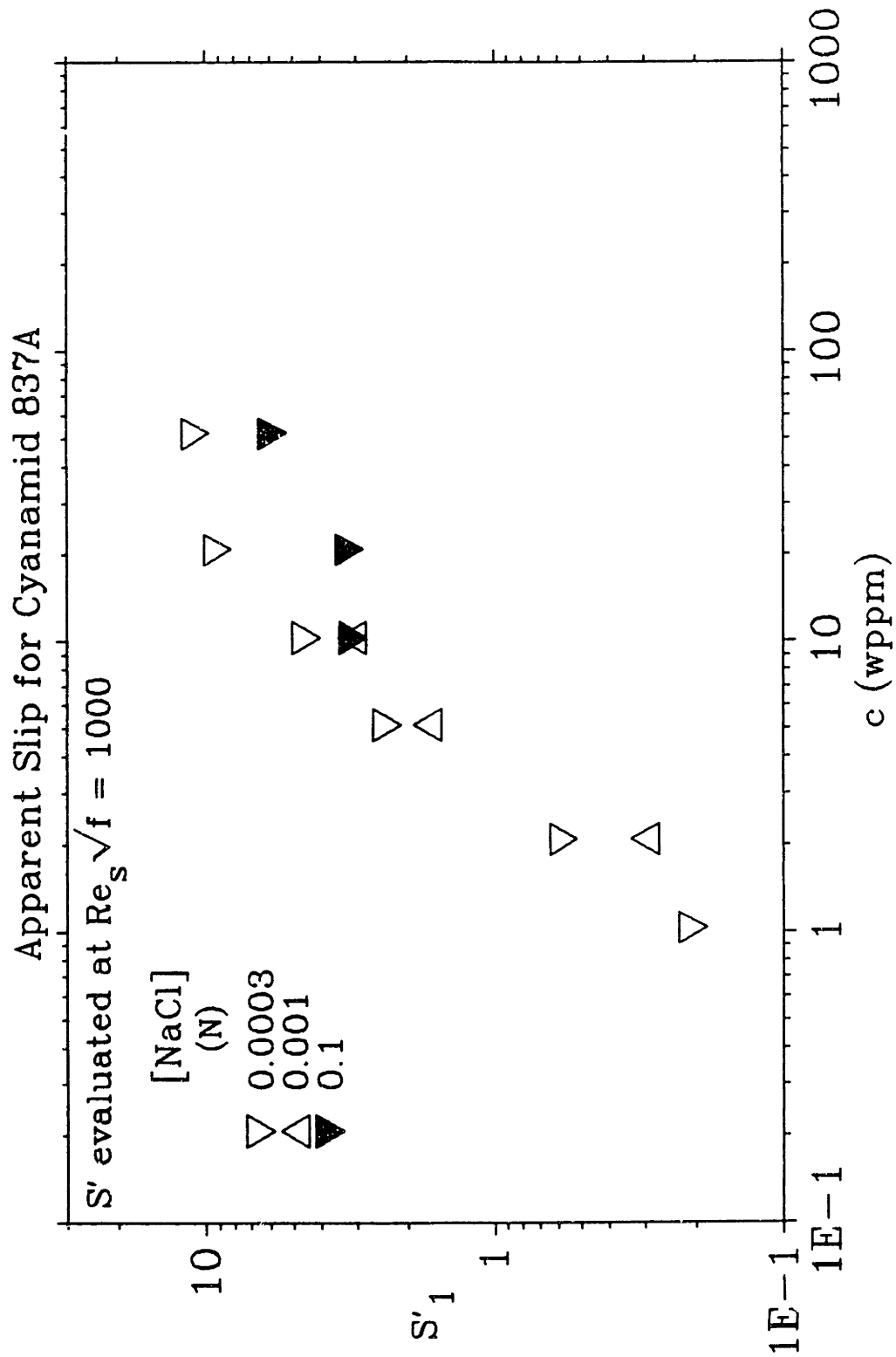


Figure 5.3.8: Apparent Slip S'_1 for Cyanamid 837A

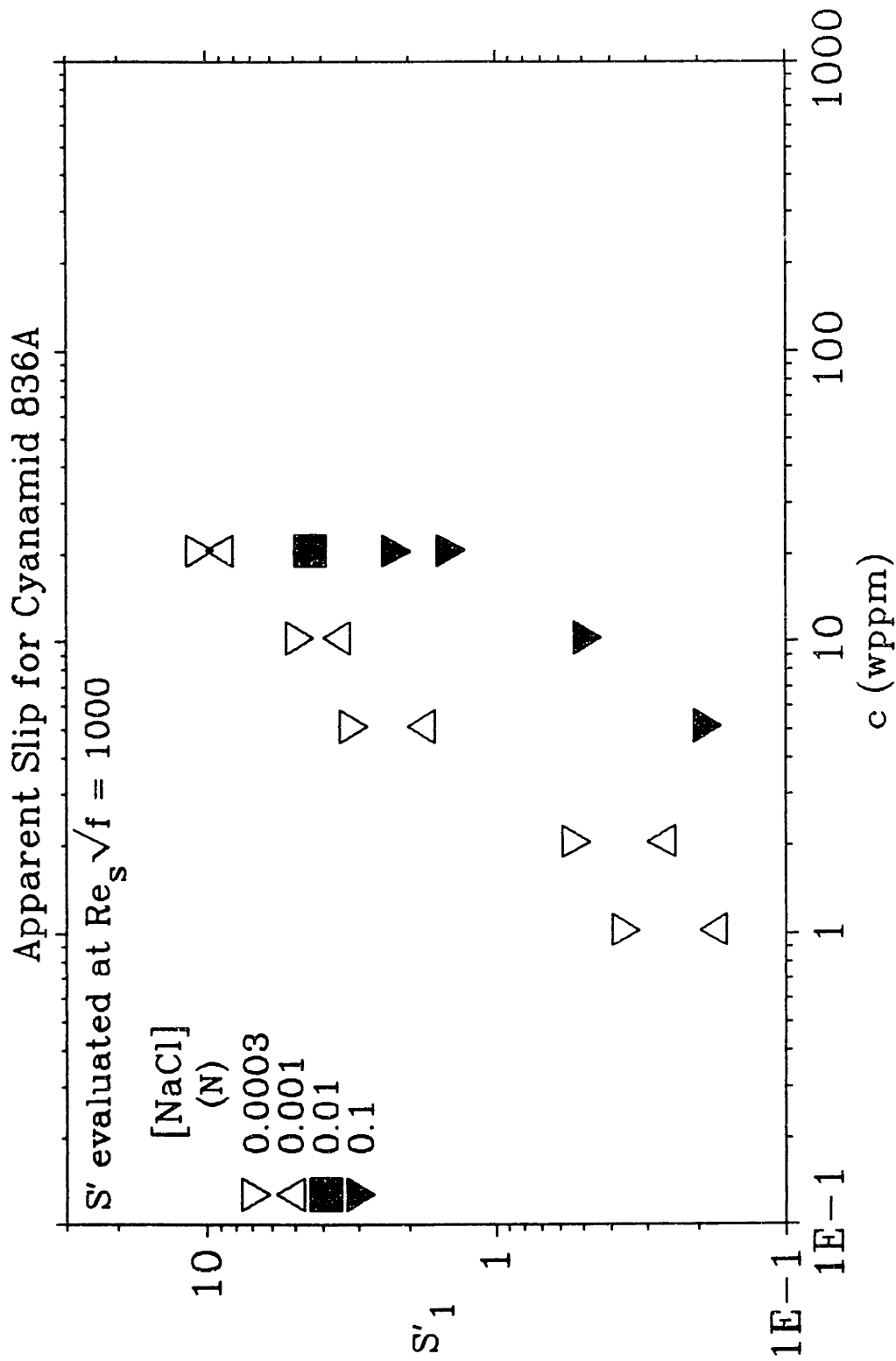


Figure 5.3.9: Apparent Slip S'_1 for Cyanamid 836A

5.3.2 The Slope Increment δ

Figures 5.3.10 - 5.3.16 are double-logarithmic plots of the slope increment δ versus concentration c for additives C832A, B1120, P500, A507 & D1438, C837A, and C836A, respectively, from all runs. Whereas in Type-B drag-reduction the rungs of the ladder have slopes that are only slightly larger than the slope of the turbulent baseline N , in Type-A drag-reduction the spokes of the Type-A fan generally have slopes appreciably steeper than N . Thus the slope increment δ in Type-A behavior, at high salinity, generally exceeds that in Type-B behavior, at low salinity.

In Figure 5.3.10 for additive C832A, values of δ at high salinity are clearly greater than those at low salinity. The slope increments δ observed from the gravity-driven system($\circ \nabla \triangle \blacktriangledown$) and the pump-driven system($\diamond \blacklozenge$) are nearly equal. At high concentration, the data reach nearly a constant value because of the limiting effect of the MDR asymptote.

To discern the effect of pipe diameter, Figure 5.3.11 juxtaposes data in the 1.458-cm($\circ \nabla$) and 1.021-cm($\bullet \blacktriangledown$) pipes, from the pump-driven system, at both 0.3 and 0.0001 N NaCl. For $c > 1$ wppm, data at high salinity($\nabla \blacktriangledown$) and at low salinity($\circ \bullet$) are either adjacent or overlapping, the former exceeding the latter, indicating that pipe diameter has only a weak effect on the shape of the Type-A fan and the Type-B ladder, respectively.

In Figures 5.3.12 and 5.3.13, the slope increments δ for additives B1120 and P500, respectively, show the same trends as in Figure 5.3.10. High-salinity data exceed low-salinity data and reach a limiting MDR value at high concentrations. In Figure

5.3.13 as in Figure 5.3.11, data from the 1.458-cm($\circ \nabla$) and 1.021-cm($\bullet \nabla$) pipes, from the pump-driven system, are compared directly at both high($\nabla \nabla$) and low($\circ \bullet$) salinity. At each concentration, data from each pipe either overlap or lie adjacently, again suggesting that Type-A behavior, as well as Type-B behavior, is influenced little by pipe diameter.

Figure 5.3.14 shows data for additives A507 and D1438. Because each additive exhibits Type-A fans at both high and low salinities, the latter having both lower $Re_{\gamma} \sqrt{f}$ and steeper slopes, the slope increments at low salinity are greater than those at high salinity for both additives. All the slope increments for D1438 slightly exceed all those for A507.

Figures 5.3.15 and 5.3.16, for respective additives C837A and C836A, show nearly-equal slope increments δ at all salinities for $c \geq 2$ wppm, strongly reflecting Type-A drag-reduction behavior.

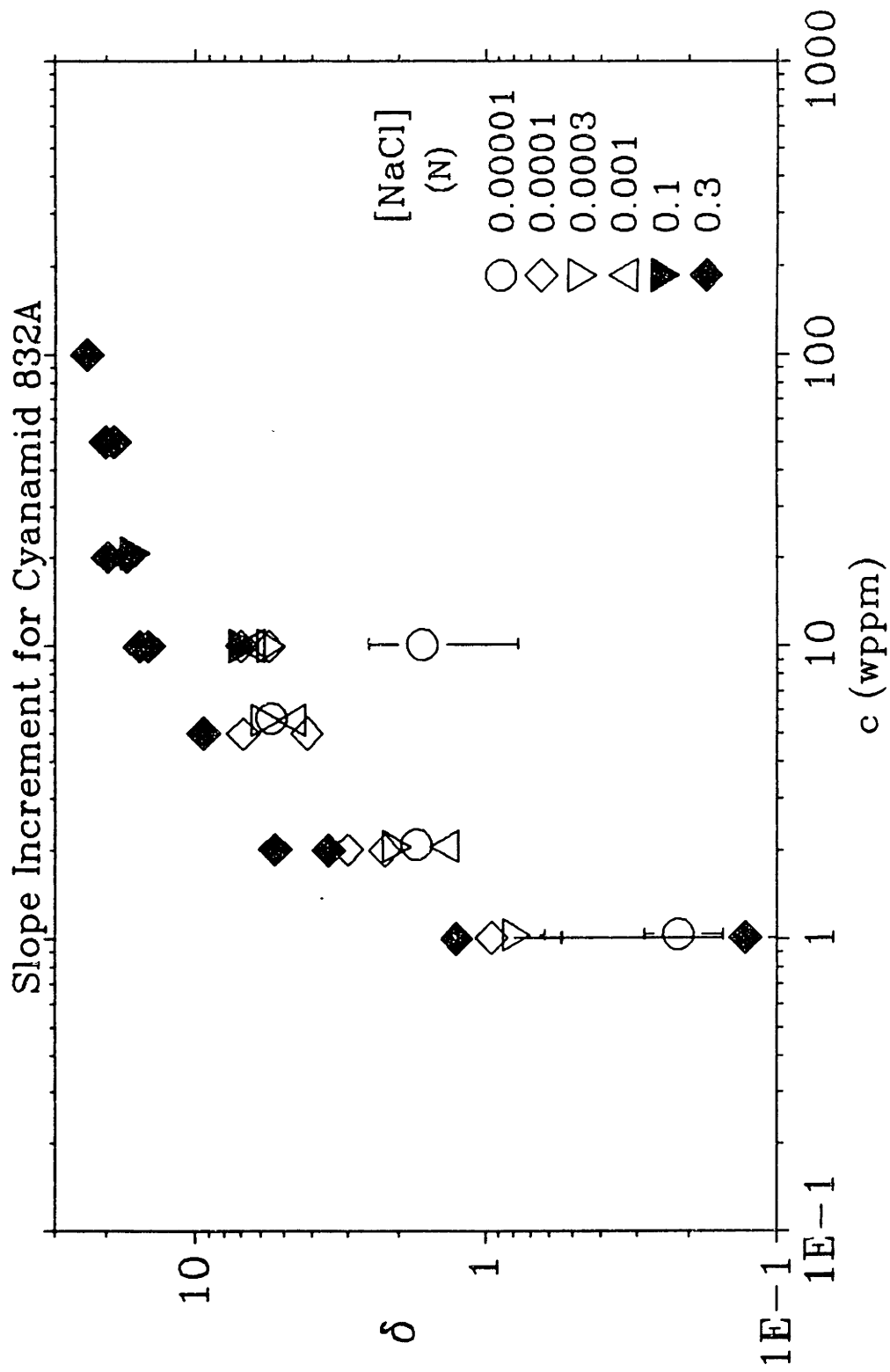


Figure 5.3.10: Slope Increment δ for Cyanamid 832A

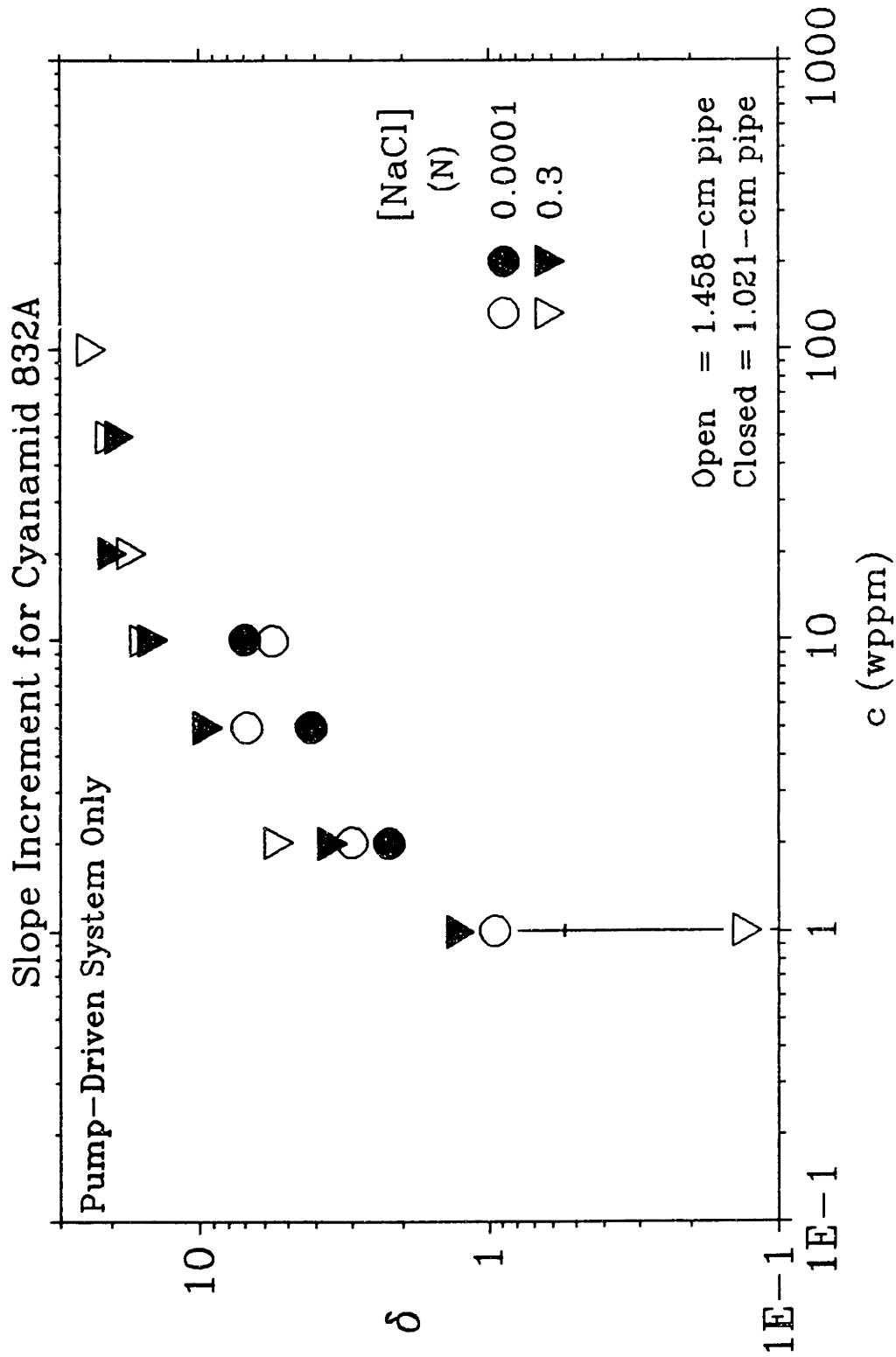


Figure 5.3.11: Slope Increment δ for Cyanamid 832A from the Pump-Driven System in Both Pipes

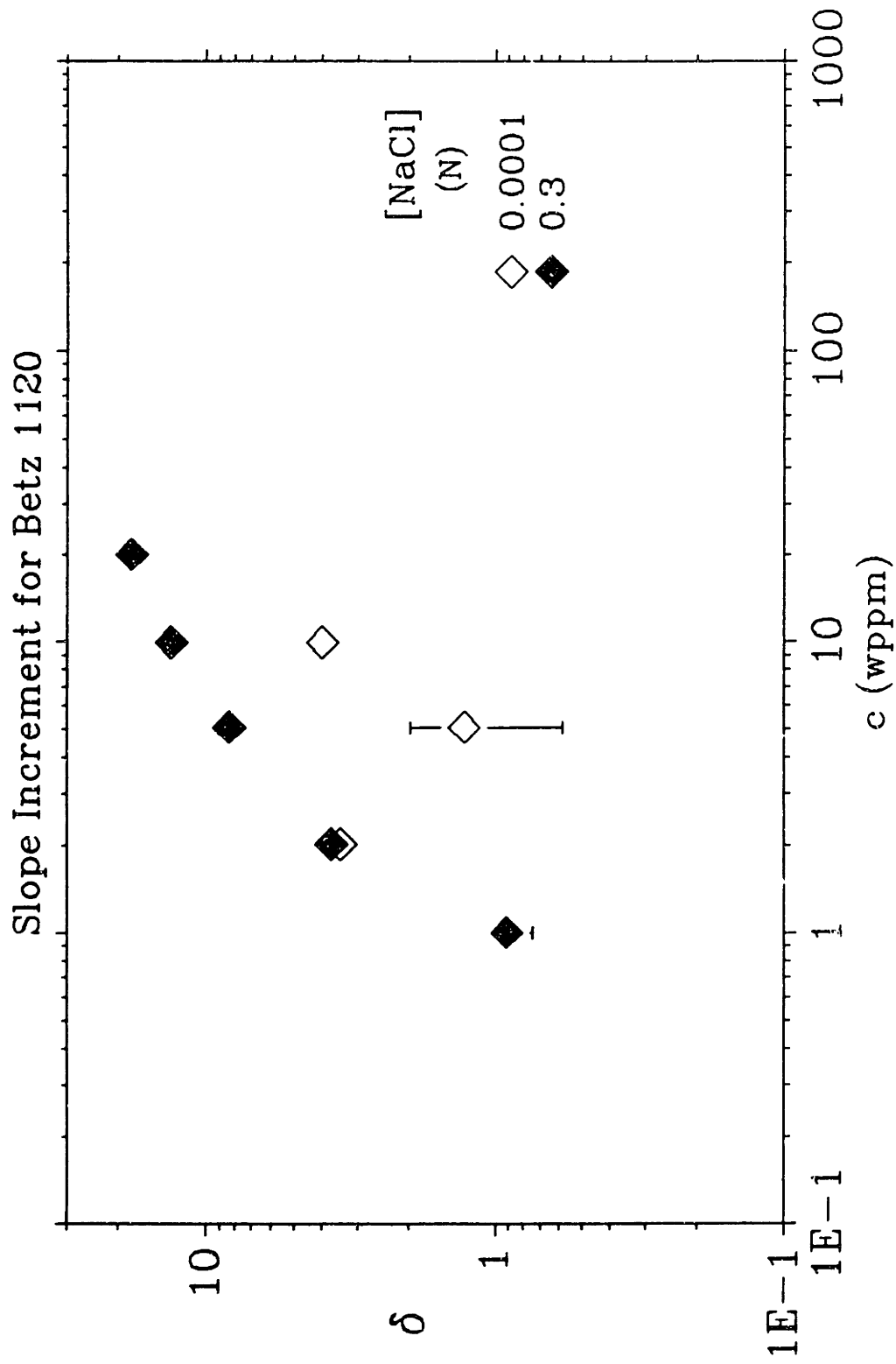


Figure 5.3.12: Slope Increment δ for Betz 1120

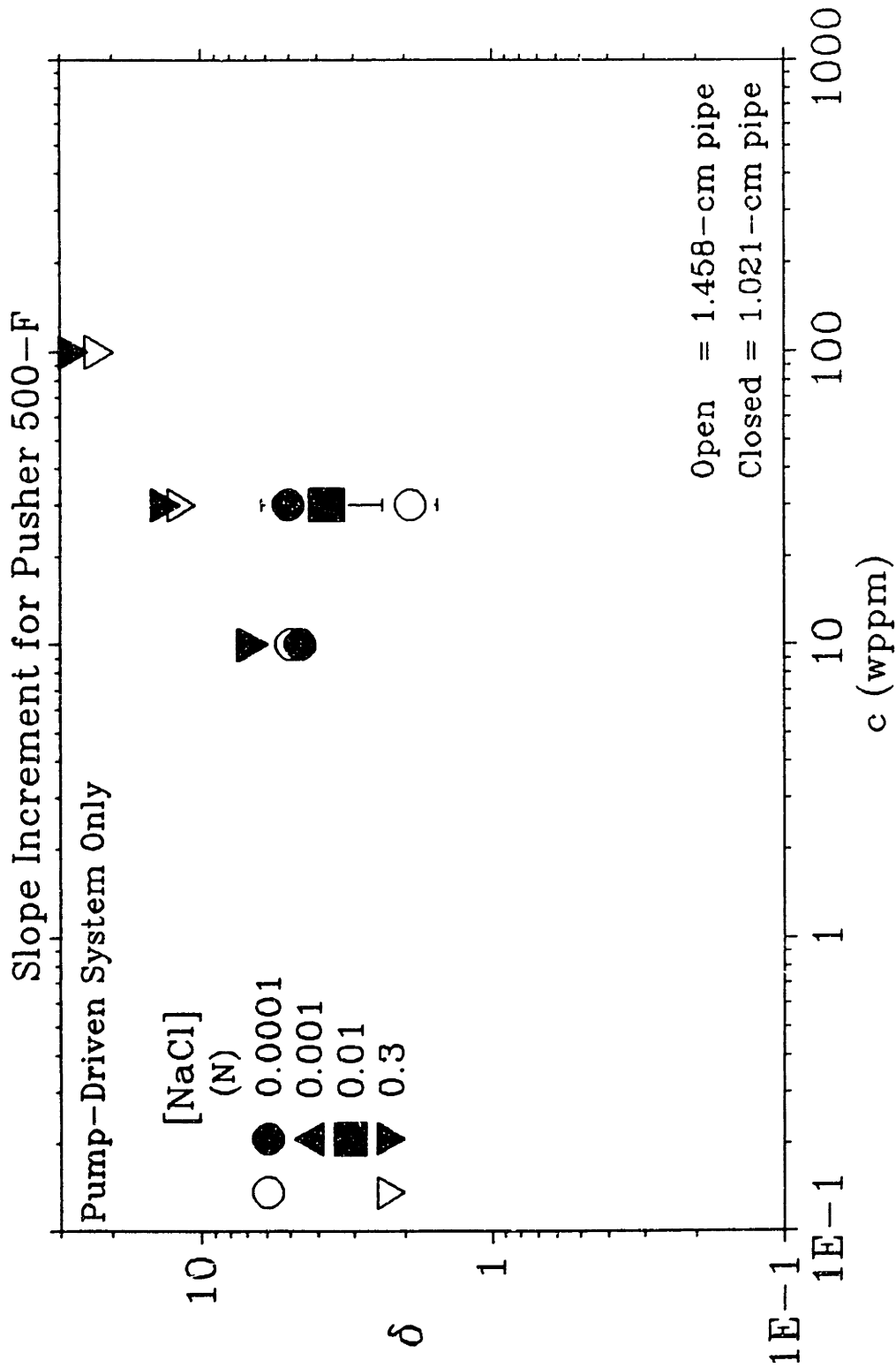


Figure 5.3.13: Slope Increment δ for Pusher 500-F

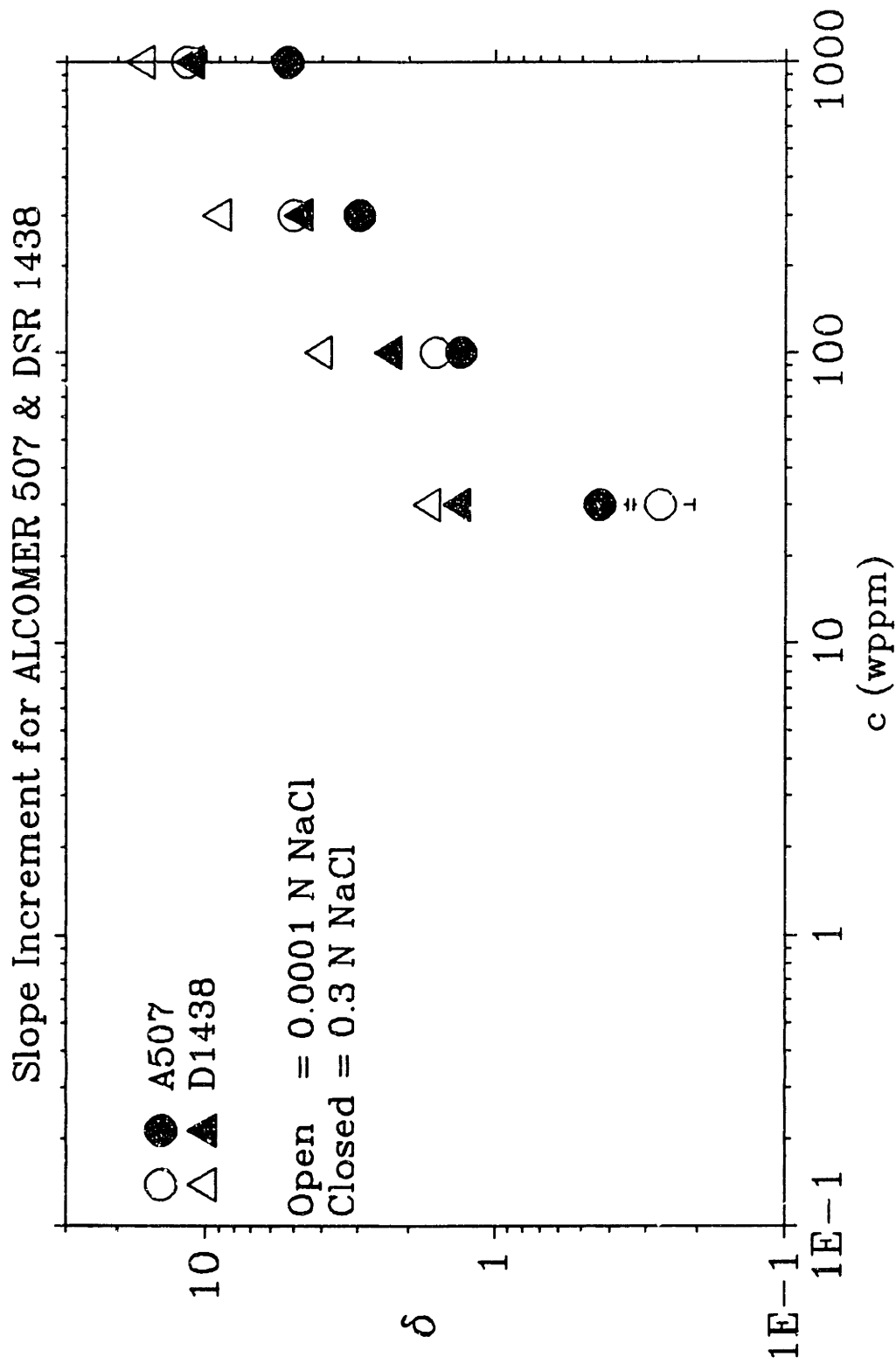


Figure 5.3.14: Slope Increment δ for Alcomer 507 and DSR 1438

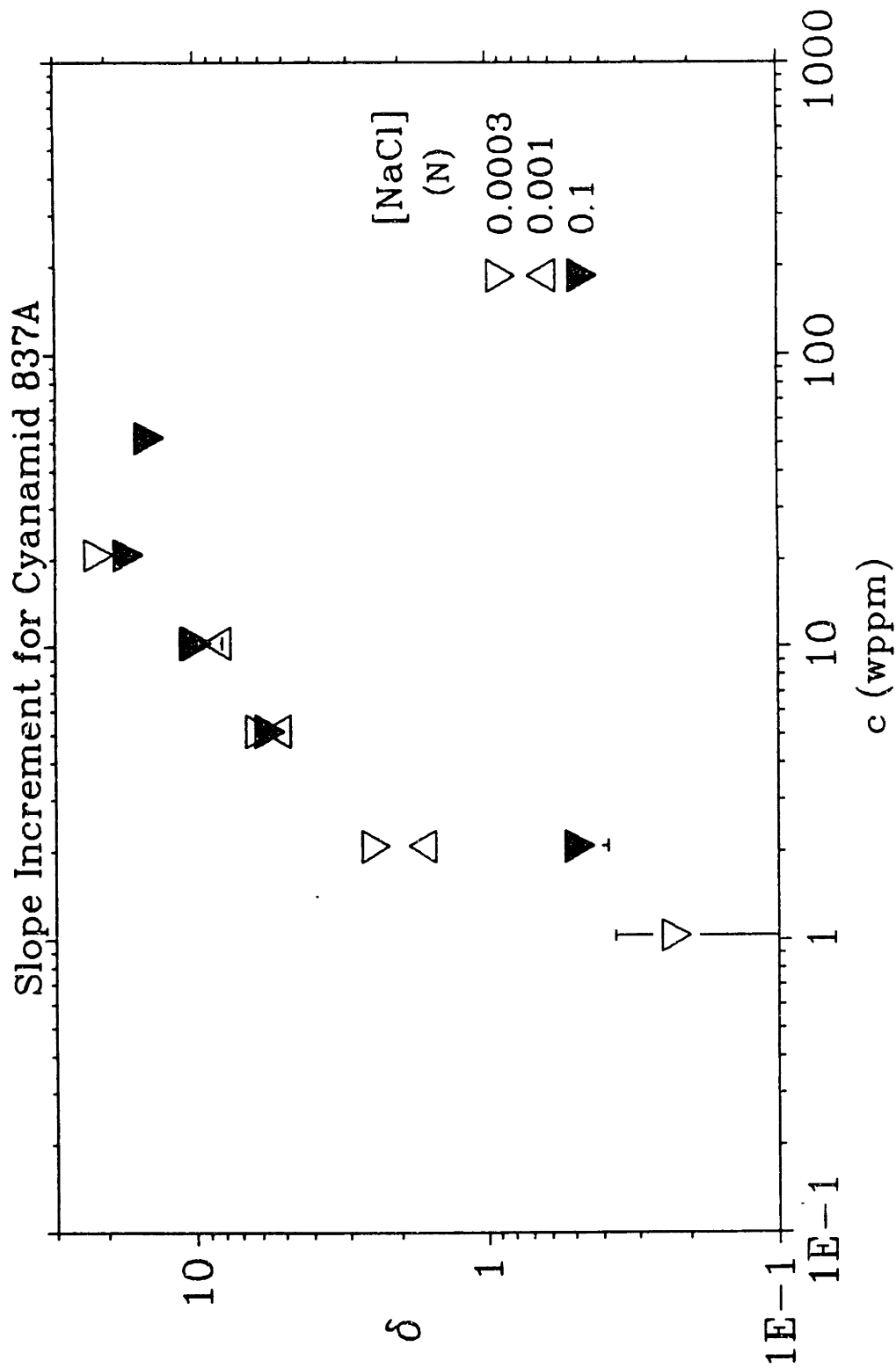


Figure 5.3.15: Slope Increment δ for Cyanamid 837A

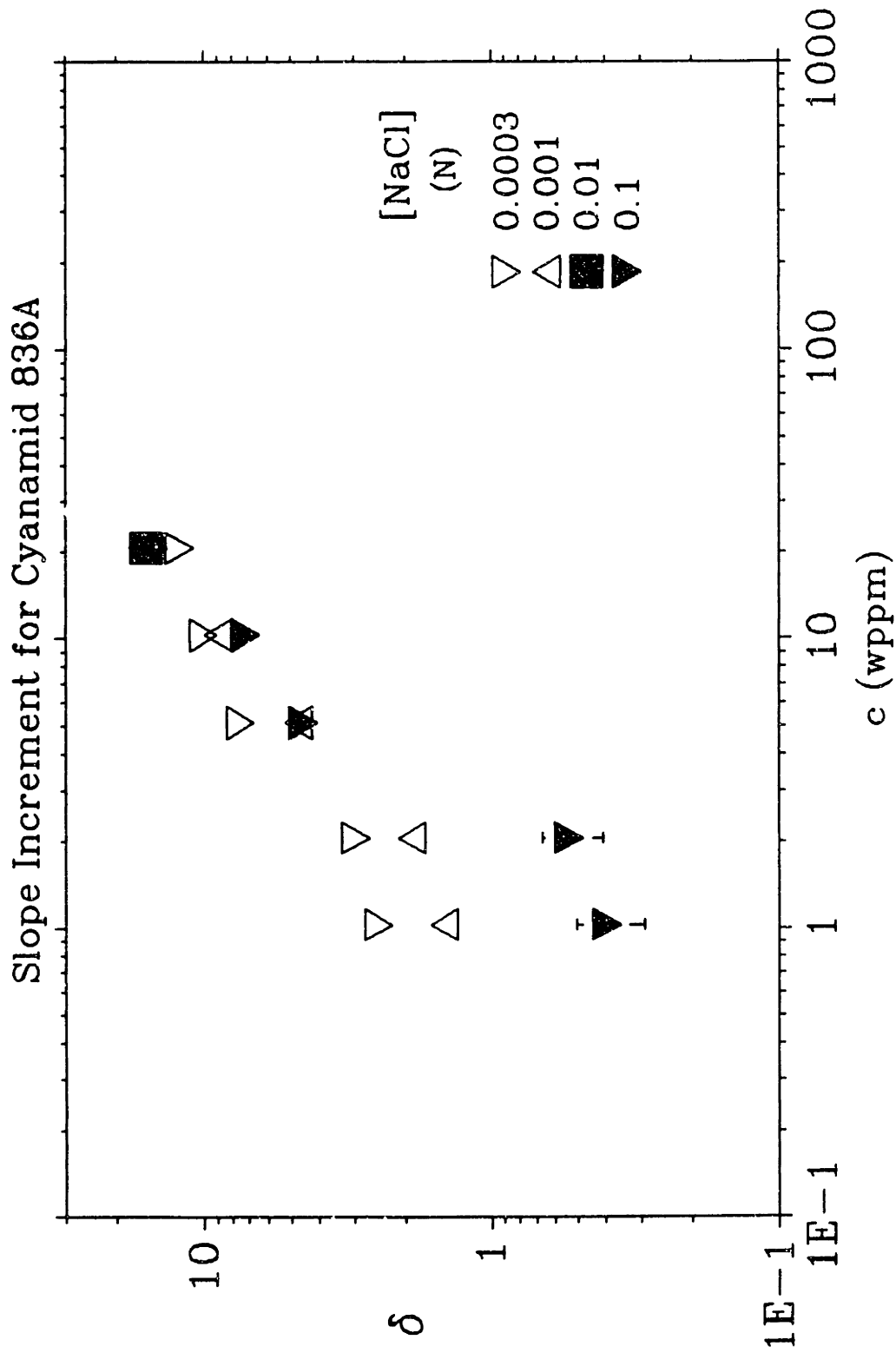


Figure 5.3.16: Slope Increment δ for Cyanamid 836A

5.3.3 The Onset Wall Shear Stress T_w^*

Figures 5.3.17 - 5.3.22 show the concentration dependence of the onset wall shear stress T_w^* for all additives, and average values are summarized in Table 5.3.3.

To provide both consistency and significance to the preceding slope-increment data, the regressed T_w^* are plotted against concentration with the error bars reflecting the uncertainty in the slopes and intercepts (A_p , B_p), from which the slope increments are derived. It should be noted that even the regressed T_w^* derived from (A_p , B_p), for which the standard-error coefficients are small and the square of the regression coefficient $r^2 > 0.999$, has an uncertainty of ± 50 percent. The uncertainty in T_w^* is determined from the minimum and maximum regressed T_w^* , using all combinations of (A_p , B_p) and their standard-error coefficients. (See discussion preceding Table 5.2.2.) Both large standard-error coefficients and small slopes A_p , which occur mostly at low concentrations, increase the difference between minimum and maximum T_w^* values and, thus, the uncertainty in T_w^* . Because the ideal Type-A fan, characterized by T_w^* and (A_p , B_p), radiates from a single point on the turbulent baseline N , the onset wall shear stress T_w^* has one concentration-independent value; however, under the best conditions, the many T_w^* in a given fan lie within a narrow range and have small uncertainties.

In each of Figures 5.3.17 - 5.3.22, the T_w^* data-scatter about an average T_w^* value. Table 5.3.3 summarizes the best overall average T_w^* calculated from the best T_w^* values for each additive; the standard deviation accompanying each value reflects the scatter in the best T_w^* values and not the uncertainty in the overall average, which is at least 100 percent.

Table 5.3.3
Overall Average T_w^* for Each Polymer Additive

Polymer	Ensemble Average Onset Wall Shear Stress	Number of Values
	$T_w^* \dagger$	
	(dyne/cm ²)	
C832A	7.7±2.2	5
B1120	6.4±1.2	3
P500	9.5±4.6	4
A507	50.4±20.1	6
D1438	41.0±19.2	8
C837A	13.7±7.0	6
C836A	15.2±4.6	10
<p>† ±[] are the standard deviations of the averages, not the uncertainties in them.</p>		

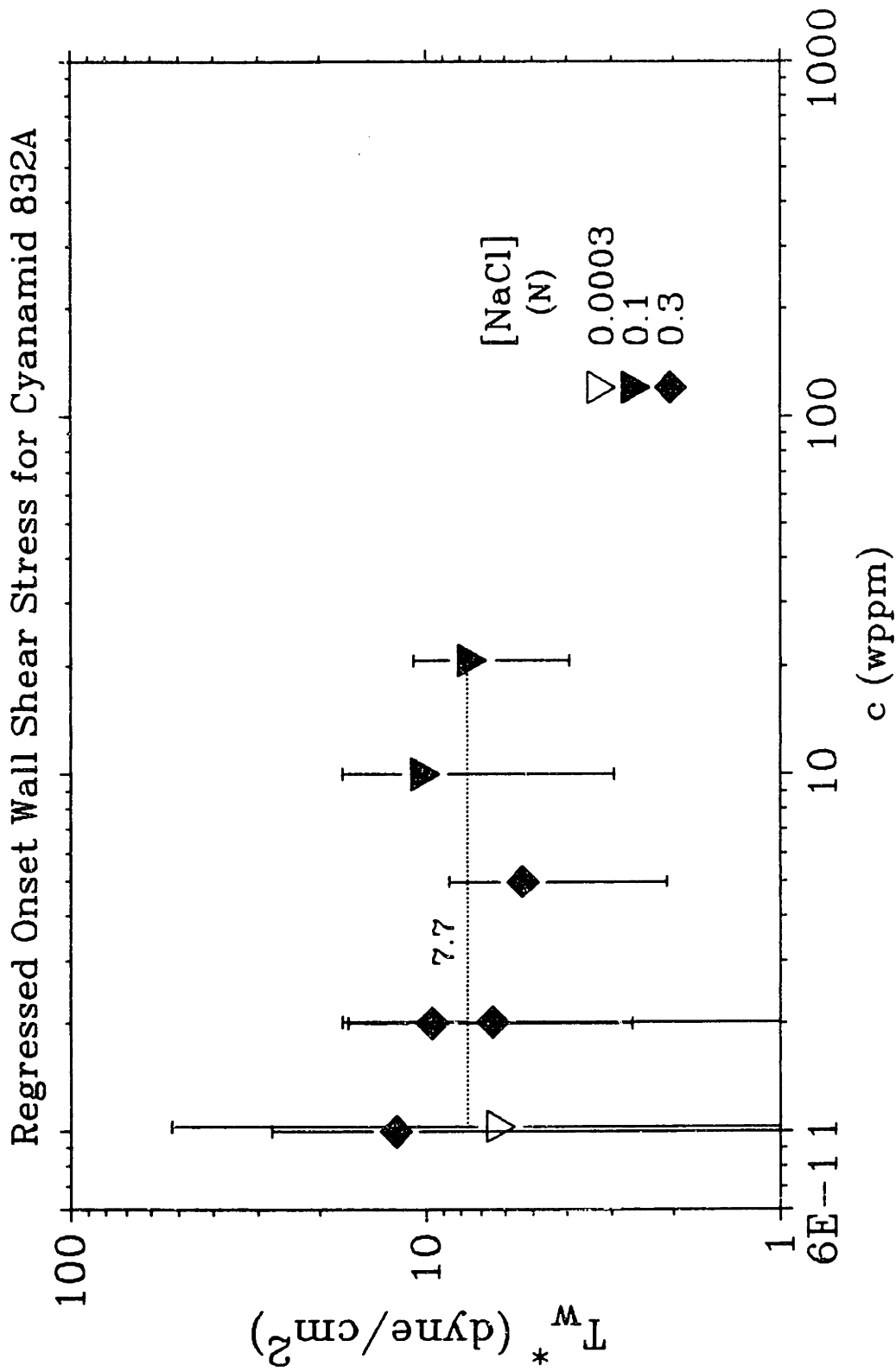


Figure 5.3.17: Regressed Onset Wall Shear Stress T_w^* for Cyanamid 832A

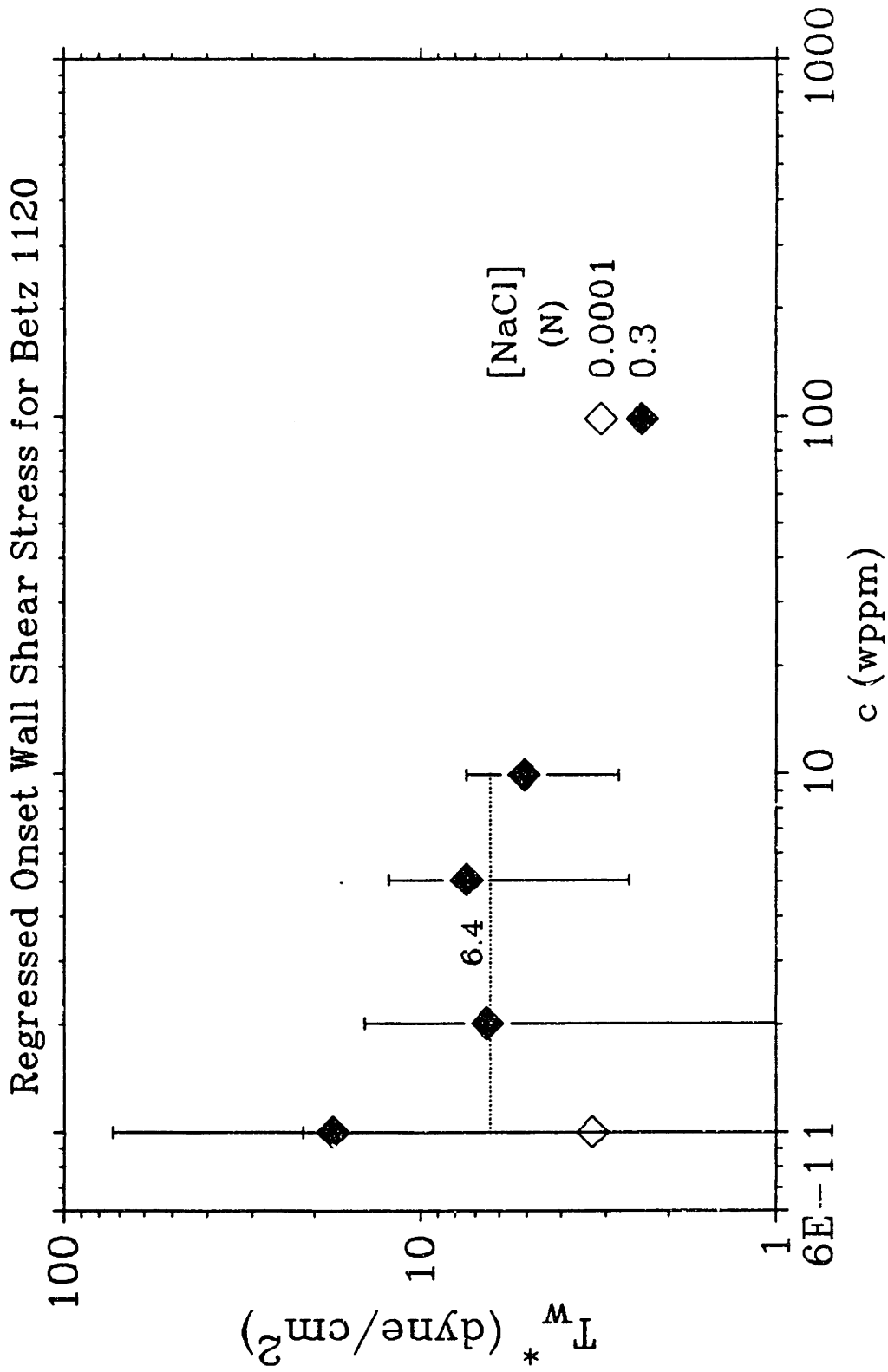


Figure 5.3.18: Regressed Onset Wall Shear Stress T_w^* for Betz 1120

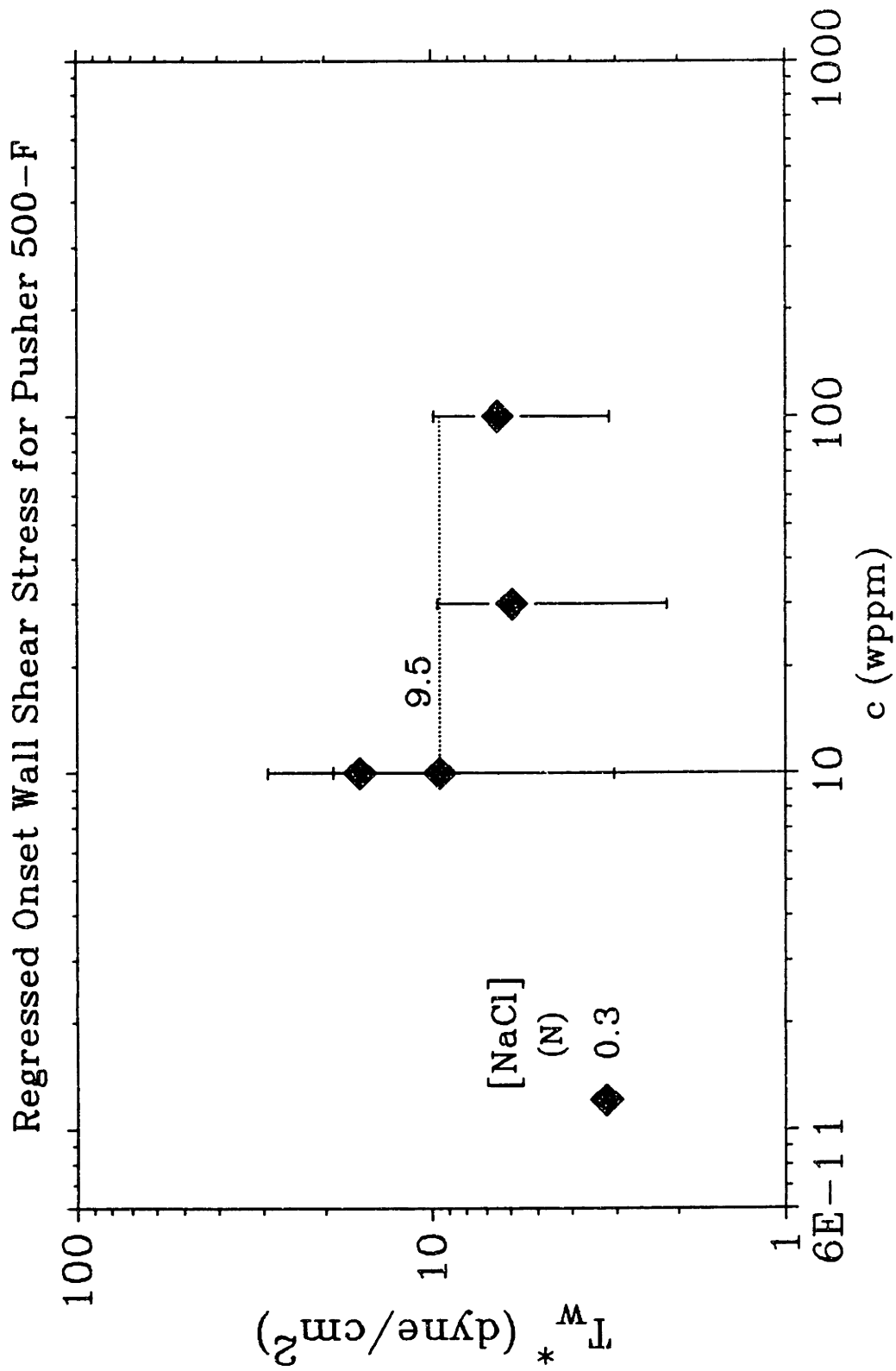


Figure 5.3.19: Regressed Onset Wall Shear Stress T_w^* for Pusher 500-F

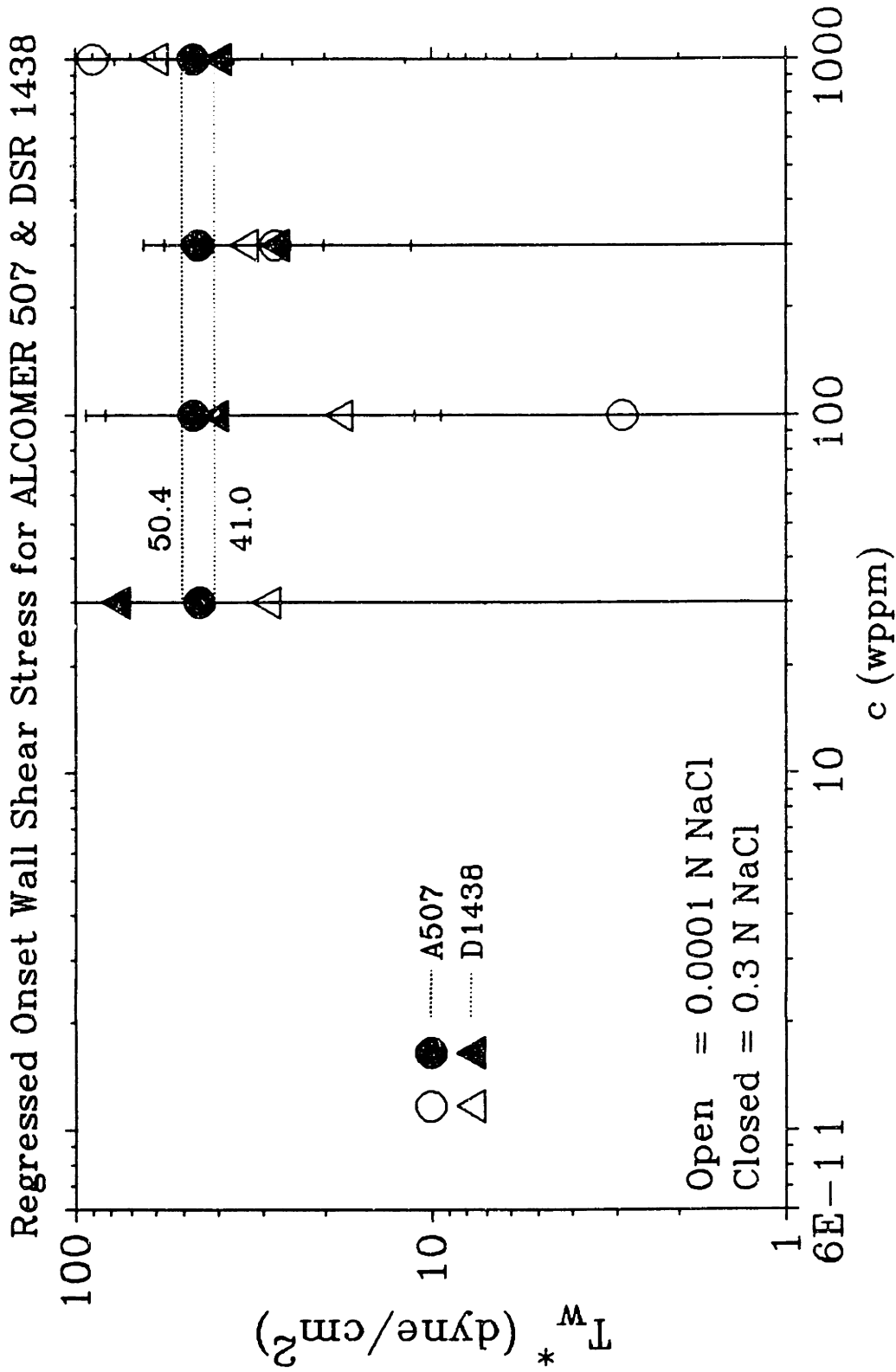


Figure 5.3.20: Regressed Onset Wall Shear Stress T_w^* for Alcomer 507 and DSR 1438

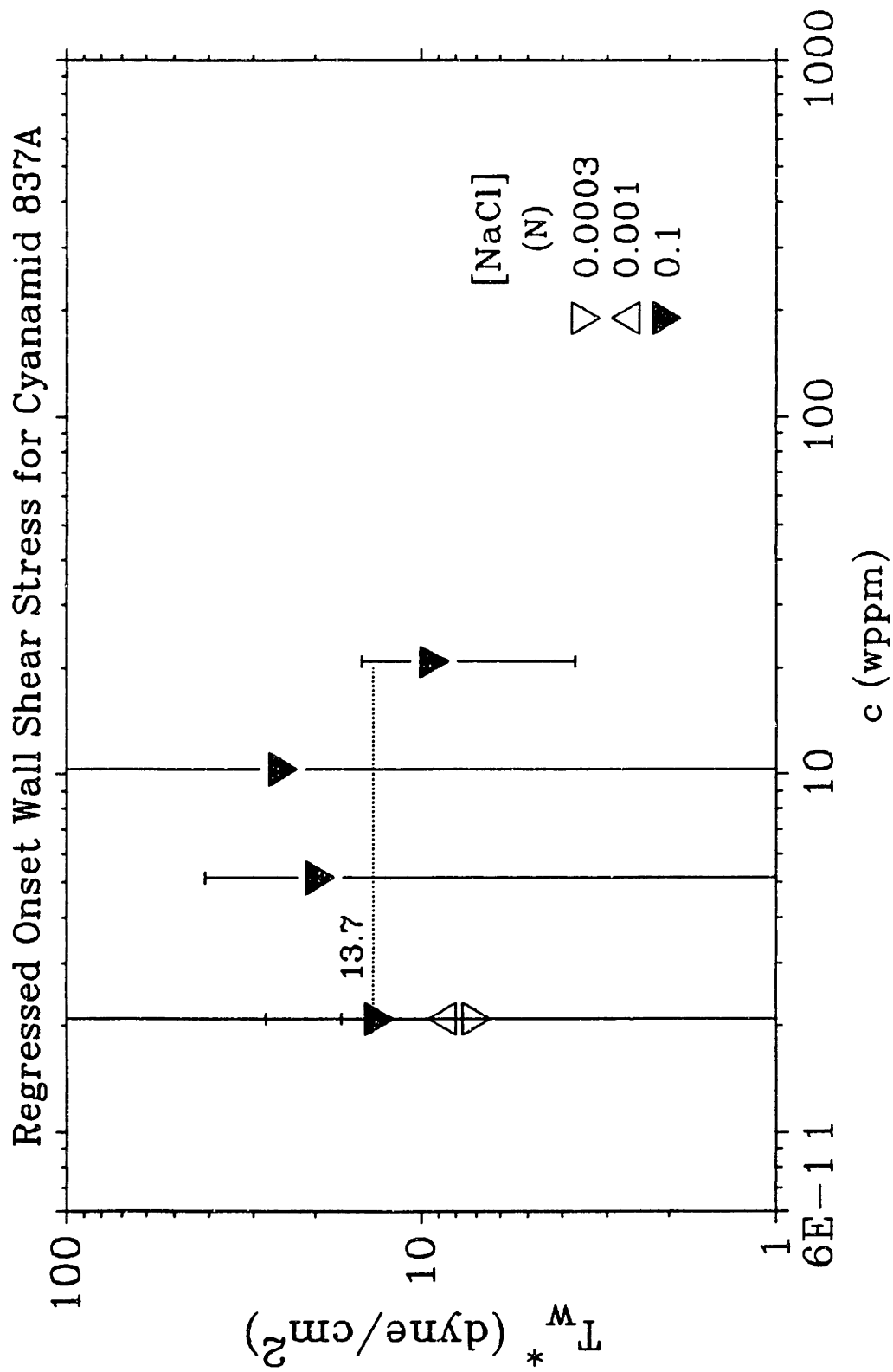


Figure 5.3.21: Regressed Onset Wall Shear Stress T_w^* for Cyanamid 837A

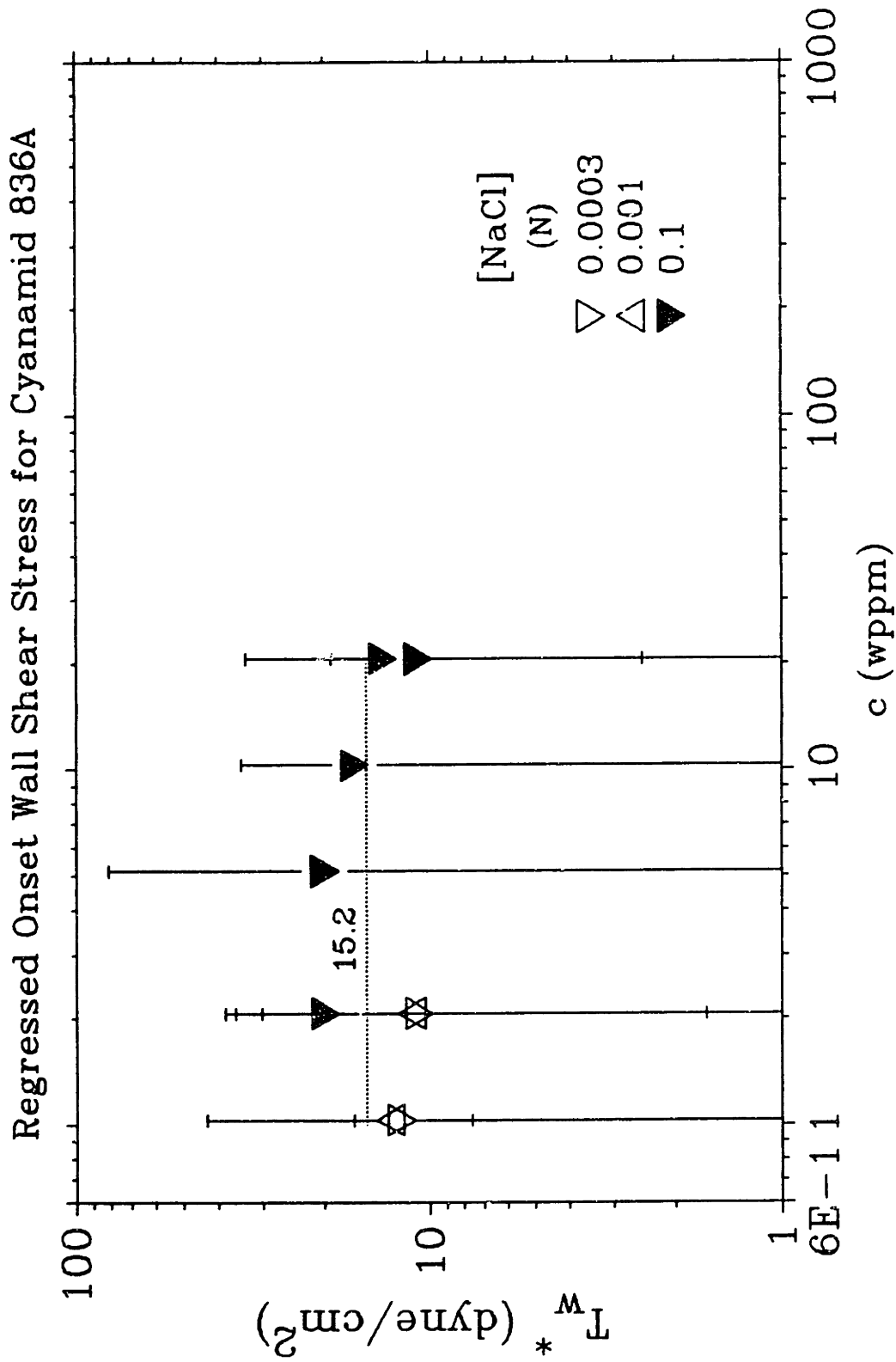


Figure 5.3.22: Regressed Onset Wall Shear Stress T_w^* for Cyanamid 836A

5.3.4 The Retro-Onset Wall Shear Stress $T_w^{\#}$

Figure 5.3.23 illustrates the concentration dependence of the regressed retro-onset wall shear stress $T_w^{\#}$ in semi-logarithmic coordinates. Because the retro-onset phenomenon in Type-B drag-reduction behavior occurs less frequently than the onset phenomenon does in Type-A drag-reduction behavior, all but two of the observed retro-onset points pertain to solutions of C832A with salinities up to 0.0003 N NaCl; solutions of B1120 and P500 with 0.0001 N NaCl account for the rest. Data from the 1.458-cm pipe are represented by open symbols; data from the 1.021-cm pipe, closed symbols.

As for the onset wall shear stress T_w^* , the retro-onset wall shear $T_w^{\#}$ is determined from the slopes and intercepts (A_p , B_p) of the segments P within a Type-B ladder and the slope and intercept of the MDR asymptote, (19.0, 32.4). (See discussion preceding Table 5.2.2.) The uncertainty in $T_w^{\#}$, shown by error bars in the figures, is determined from the lowest and highest regressed $T_w^{\#}$ that can be calculated from combinations of (A_p , B_p) and their standard errors. Because the MDR asymptote is much steeper than the turbulent baseline N, the uncertainty in $T_w^{\#}$ is generally much smaller than that for T_w^* .

In Figure 5.3.23, the \log - $T_w^{\#}$ data for additives C832A and B1120 in the 1.458-cm pipe depends linearly on concentration. The resulting best-fit line through these data is:

$$\log T_w^{\#} = -0.436 + 0.134c \quad (5.3-1)$$

The ordinate intercept corresponds to $T_w^{\#} = 0.37$ dyne/cm², which is very close to the "ideal" value $T_w^{\#} = 0.346$ dyne/cm², at the intersection of N($c = 0$) with M.

Regressed Retro-Onset Wall Shear Stress for All Polymer Additives

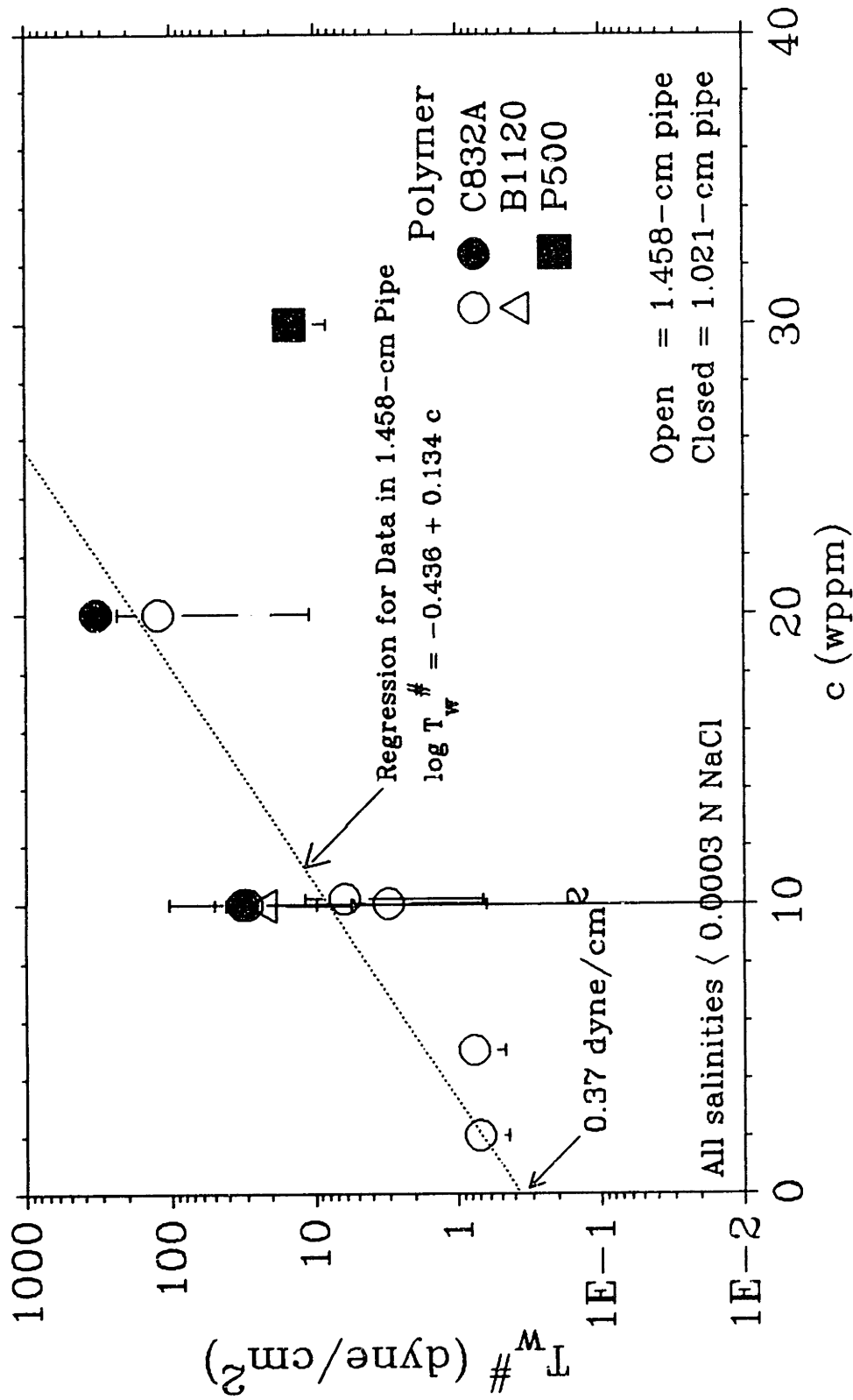


Figure 5.3.23: Regressed Retro-Onset Wall Shear Stress $T_w^{\#}$ for All Polymer Additives

5.4.1 Laminar-Flow Parameters

Figures 5.4.1 - 5.4.7 are double-logarithmic plots of the estimated intrinsic viscosity η_{sp}/c versus concentration c for additives C832A, B1120, P500, A507, D1438, C836A, and C837A, respectively, from all experiments. In each figure, the estimated intrinsic viscosities η_{sp}/c are grouped according to solution salinity. Data at low salinities, $[\text{NaCl}] \leq 0.001 \text{ N}$, are represented by open symbols; data at high salinity, $[\text{NaCl}] \geq 0.01 \text{ N}$, by closed symbols. For all data, it is assumed that the absolute error in pressure-drop measurement $\epsilon = \pm 2\%$, even though laminar-flow data for solvent adhered to Poiseuille's Law to within one percent. Using $\epsilon = \pm 1\%$ approximately halves the reported standard error in η_{sp}/c . The standard error in η_{sp}/c , denoted by bars above and below each data point, is calculated from the equation,

$$s.e. = \epsilon(\pm 2 + \epsilon) \left(\frac{\frac{\eta_{sp}}{c} + \frac{1}{c}}{\frac{\eta_{sp}}{c}} \right) \quad (5.4-1)$$

As seen from equation 5.4-1, data at low concentrations have much greater uncertainty than data at higher concentrations. Thus, to get the best average η_{sp}/c for both the extended and collapsed conformations at low and high salinity, respectively, η_{sp}/c data with low uncertainties and at high concentrations are used to calculate the average η_{sp}/c . From equations 2.4-10 and 2.4-11, the macromolecular parameters for each additive can be inferred from the best average η_{sp}/c at high salinity, under the assumption that the collapsed conformation obtains. These parameters are summarized in Table 5.4.1.

Moreover, the ratio of the average η_{sp}/c at low salinity to that at high salinity approximates the intrinsic-viscosity ratio $[\eta]/[\eta]_0$; from equations 2.4-2 and 2.4-5, it can be shown that $[\eta]/[\eta]_0 = \alpha^3$, the cube of the linear expansion factor α . From these data, the magnitude of macromolecular expansion can be determined.

Table 5.4.1
Inferred Polymer Characteristics

Polymer	Estimated Intrinsic Viscosity at High Salinity	Parameters Inferred Via Equations 2.4-10 and 2.4-11			
		Molecular Weight	Number of Backbone Chain Links	Radius of Gyration	Contour Length
	η_{sp}/c^\ddagger (cm ³ /g)	$M_w \times 10^{-6}$ (g/mole)	$N_{bb} \times 10^{-5}$	R_G (nm)	L_c (μ m)
C832A	3000 \pm 600	18.0 \pm 5.0	5.0 \pm 1.4	280 \pm 50	64 \pm 18
B1120	3300 \pm 800	20.1 \pm 6.4	5.6 \pm 1.8	300 \pm 60	71 \pm 23
P500	1850 \pm 500	9.5 \pm 3.5	2.7 \pm 1.0	190 \pm 40	34 \pm 12
A507	340 \pm 80	1.0 \pm 0.3	0.3 \pm 0.1	50 \pm 10	3.6 \pm 1.1
D1438	440 \pm 150	1.4 \pm 0.6	0.4 \pm 0.2	60 \pm 20	5.0 \pm 2.2
C837A*	2700 \pm 900	15.7 \pm 6.7	4.4 \pm 1.9	260 \pm 70	56 \pm 24
C836A	2700 \pm 1450	15.5 \pm 11.0	4.4 \pm 3.1	260 \pm 110	55 \pm 39

$\ddagger \pm[]$ are average standard errors of $\pm 0.02\Delta P$ in pressure measurement.
 * Only one datum with a small average standard error and of uncertain accuracy.

Table 5.4.2
Macromolecular Expansion

Polymer	Estimated Intrinsic Viscosity		Coil Expansion Ratio	Linear Expansion Factor
	η_{sp}/c			
	Low Salinity	High Salinity	α^3	α
	(cm ³ /g)			
C832A	97000±2000	3000±600	32.4	3.2
B1120	97000±3000	3300±800	29.6	3.1
P500	72000±2000	1850±500	38.7	3.4
A507	7000±500	340±80	20.3	2.7
D1438	5800±400	440±150	13.0	2.4
C837A	31000±2000	2700±900	11.4	2.2
C836A	48000±4000	2700±1450	17.9	2.6
± values are average standard errors.				

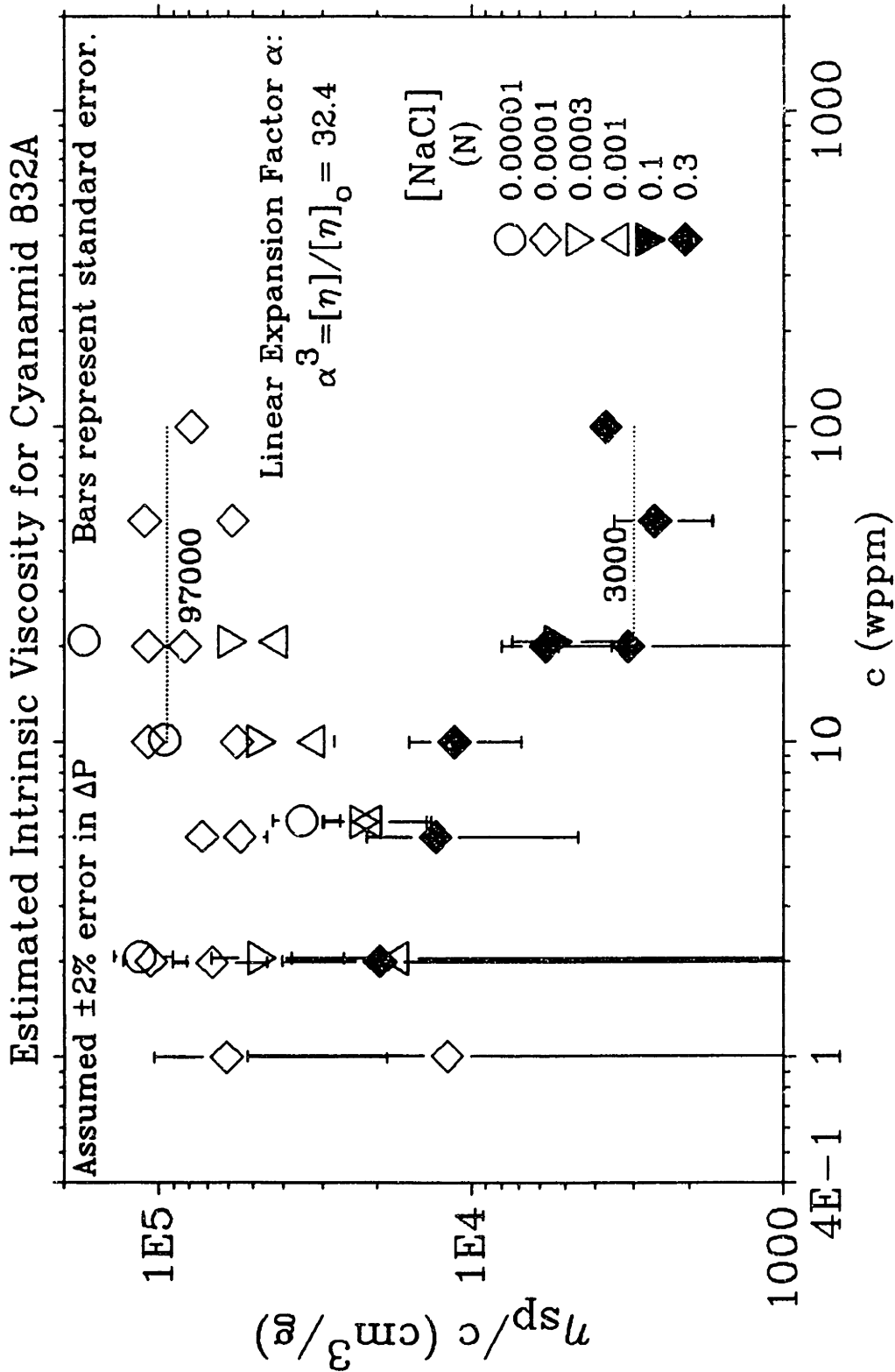


Figure 5.4.1: Estimated Intrinsic Viscosity η_{sp}/c for Cyanamid 832A

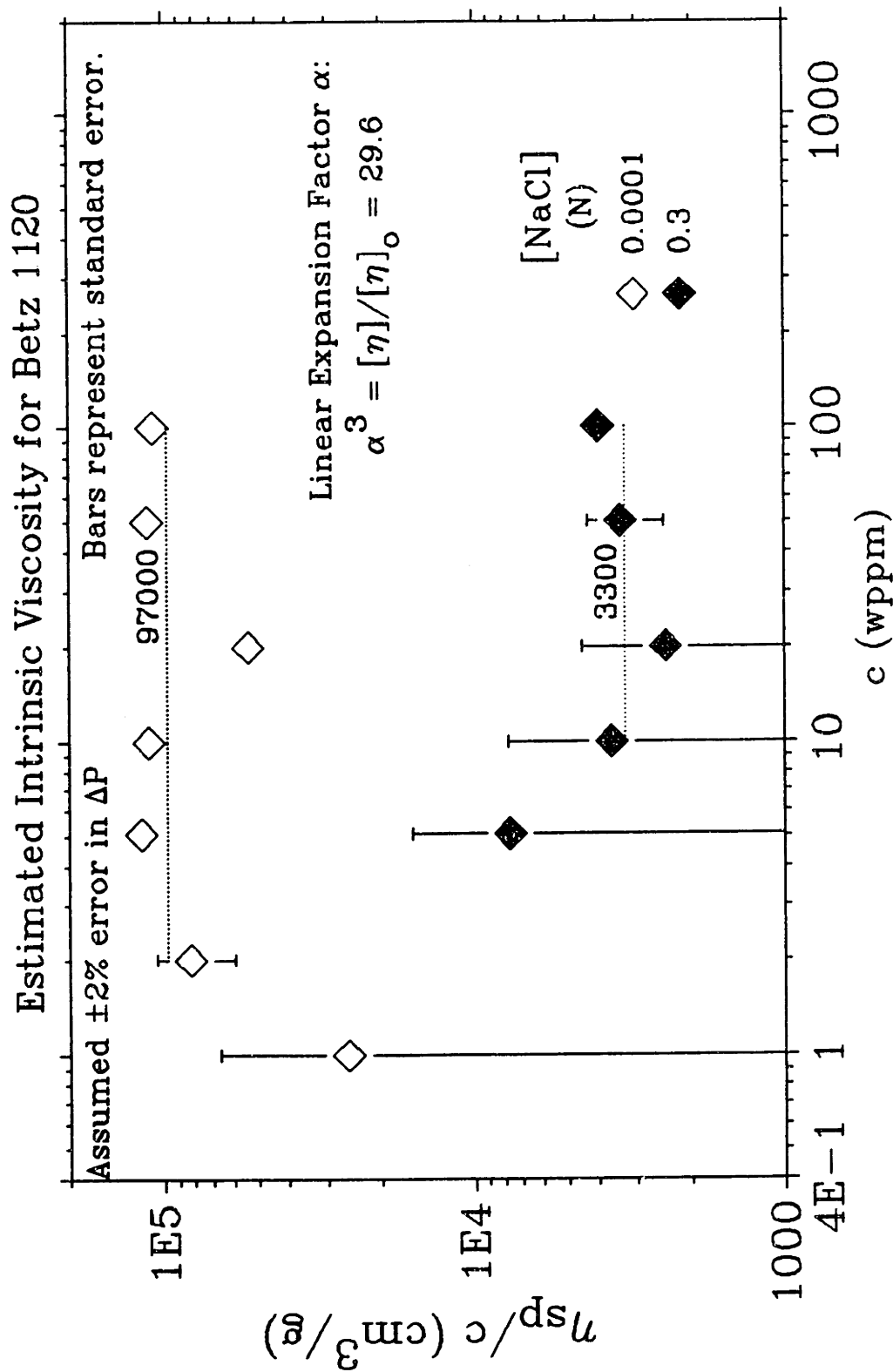


Figure 5.4.2: Estimated Intrinsic Viscosity η_{sp}/c for Betz 1120

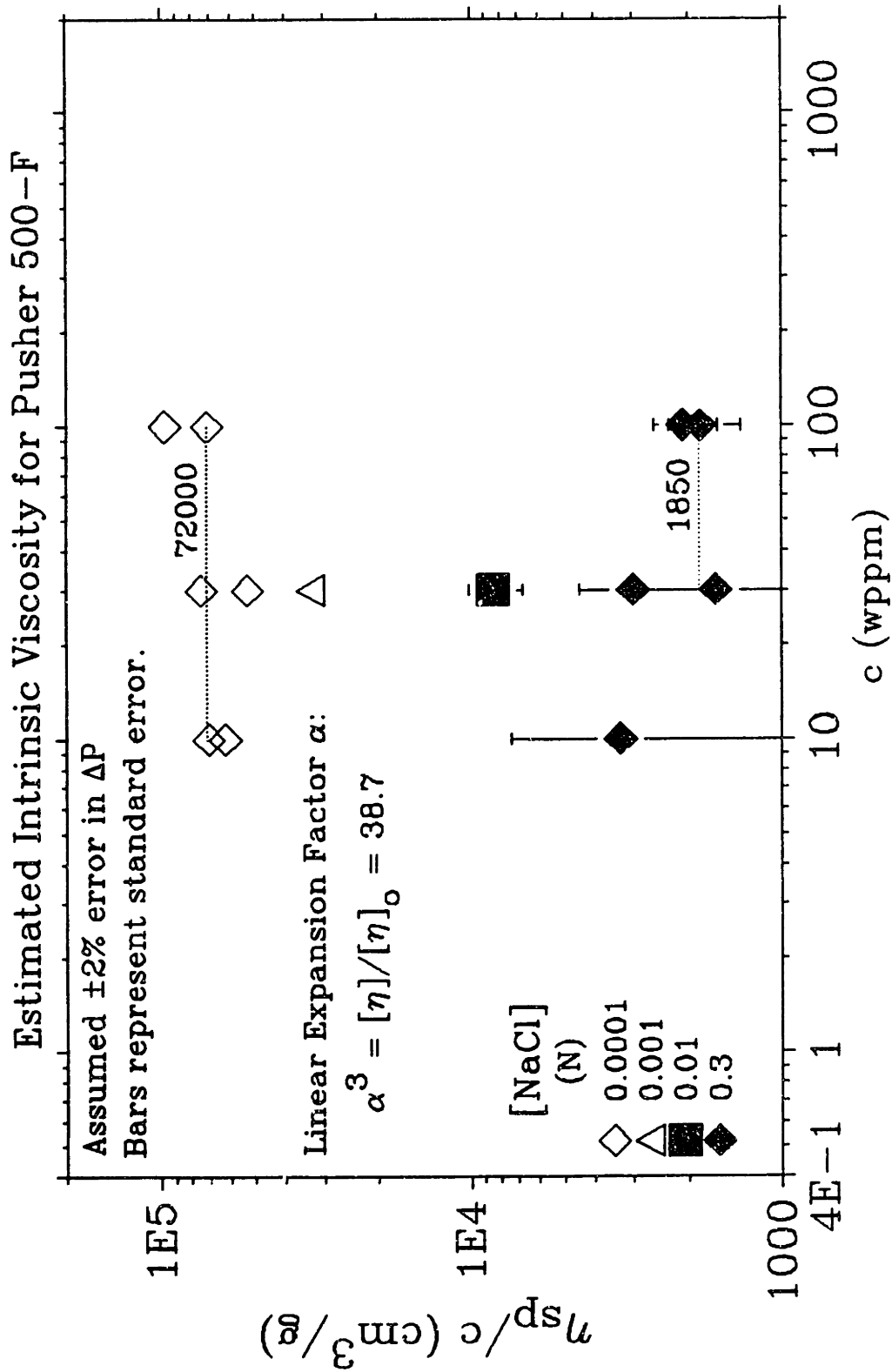


Figure 5.4.3: Estimated Intrinsic Viscosity η_{sp}/c for Pusher 500-F

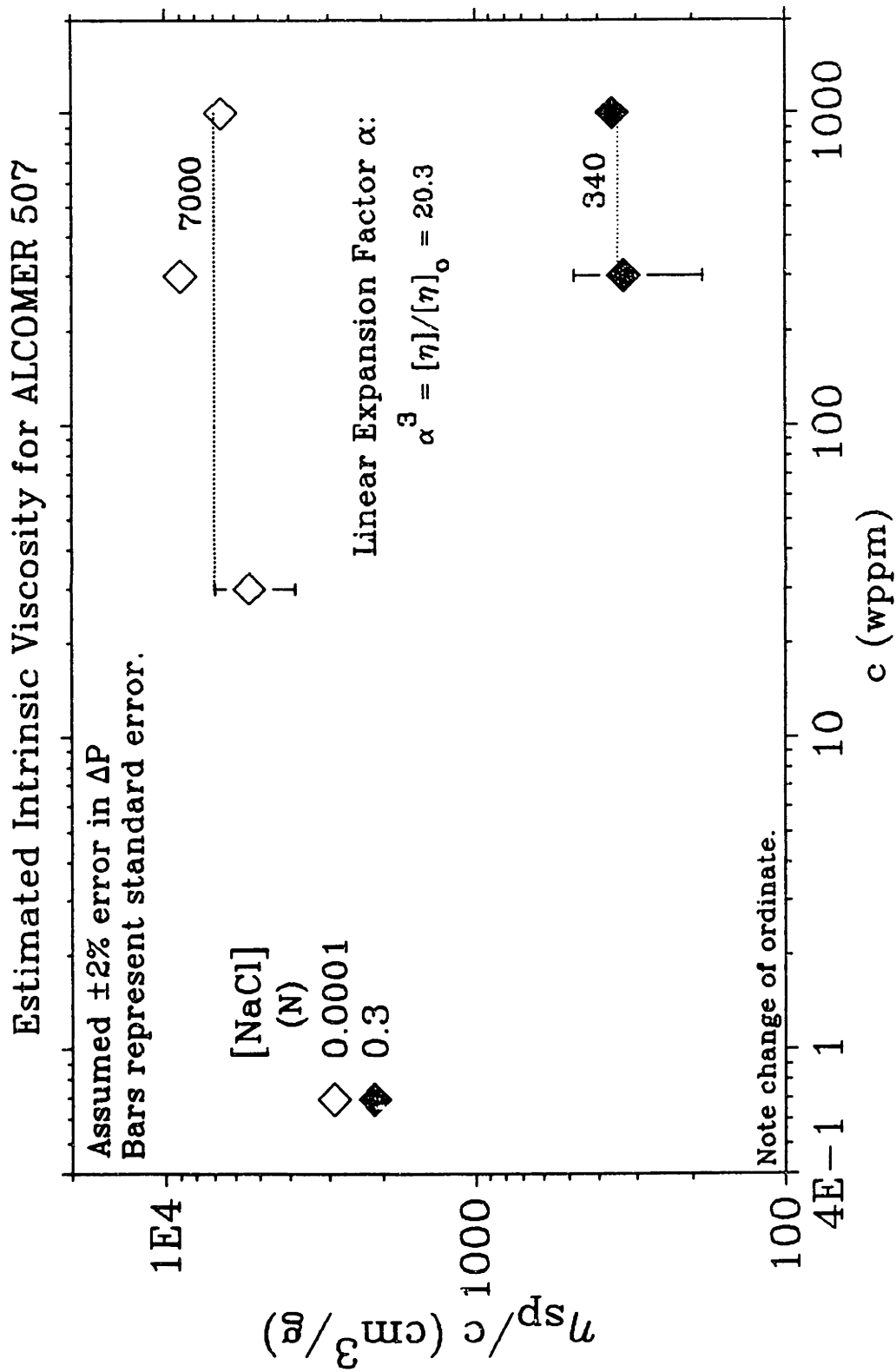


Figure 5.4.4: Estimated Intrinsic Viscosity η_{sp}/c for Alcomer 507

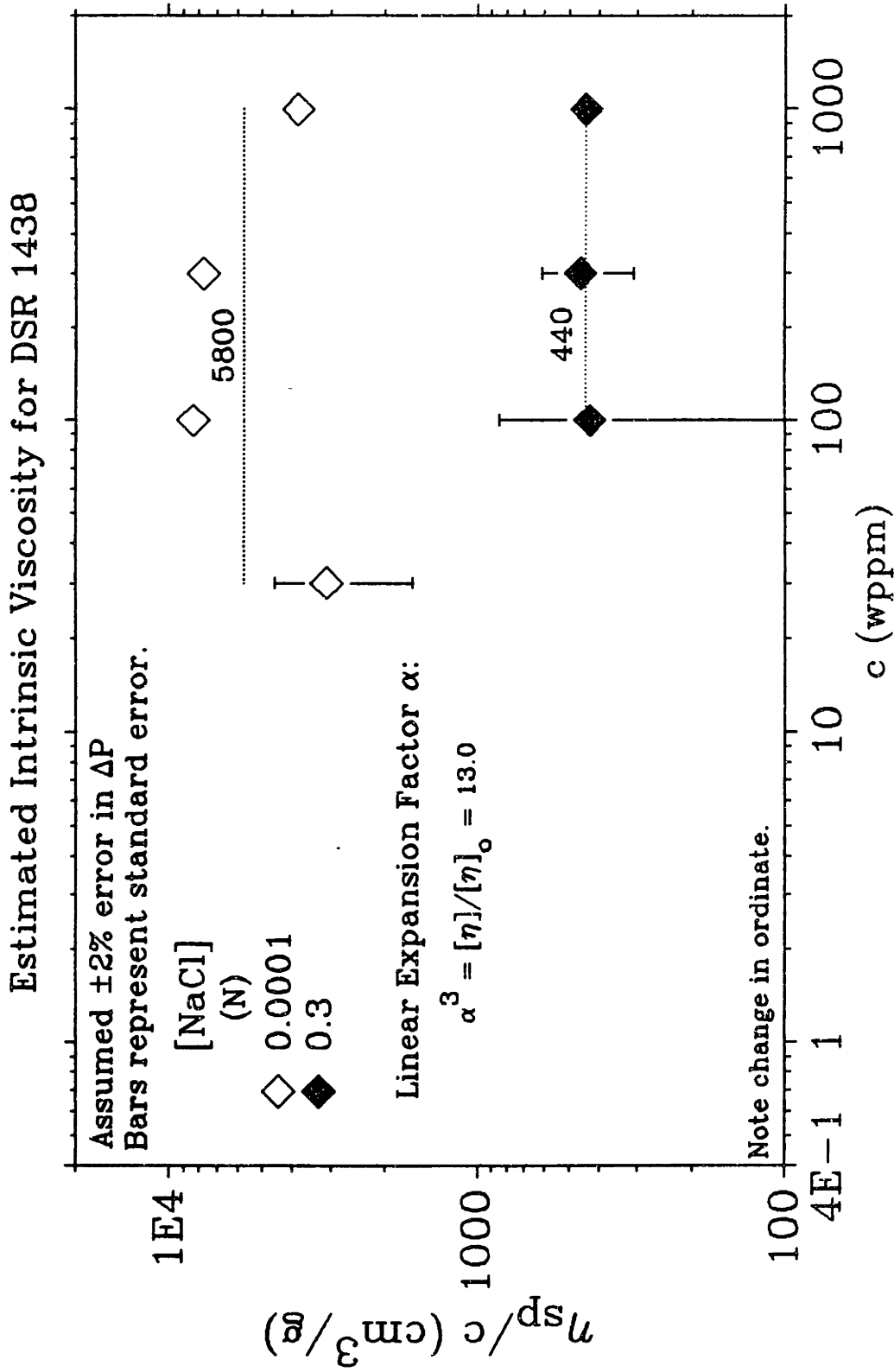


Figure 5.4.5: Estimated Intrinsic Viscosity η_{sp}/c for DSR 1438

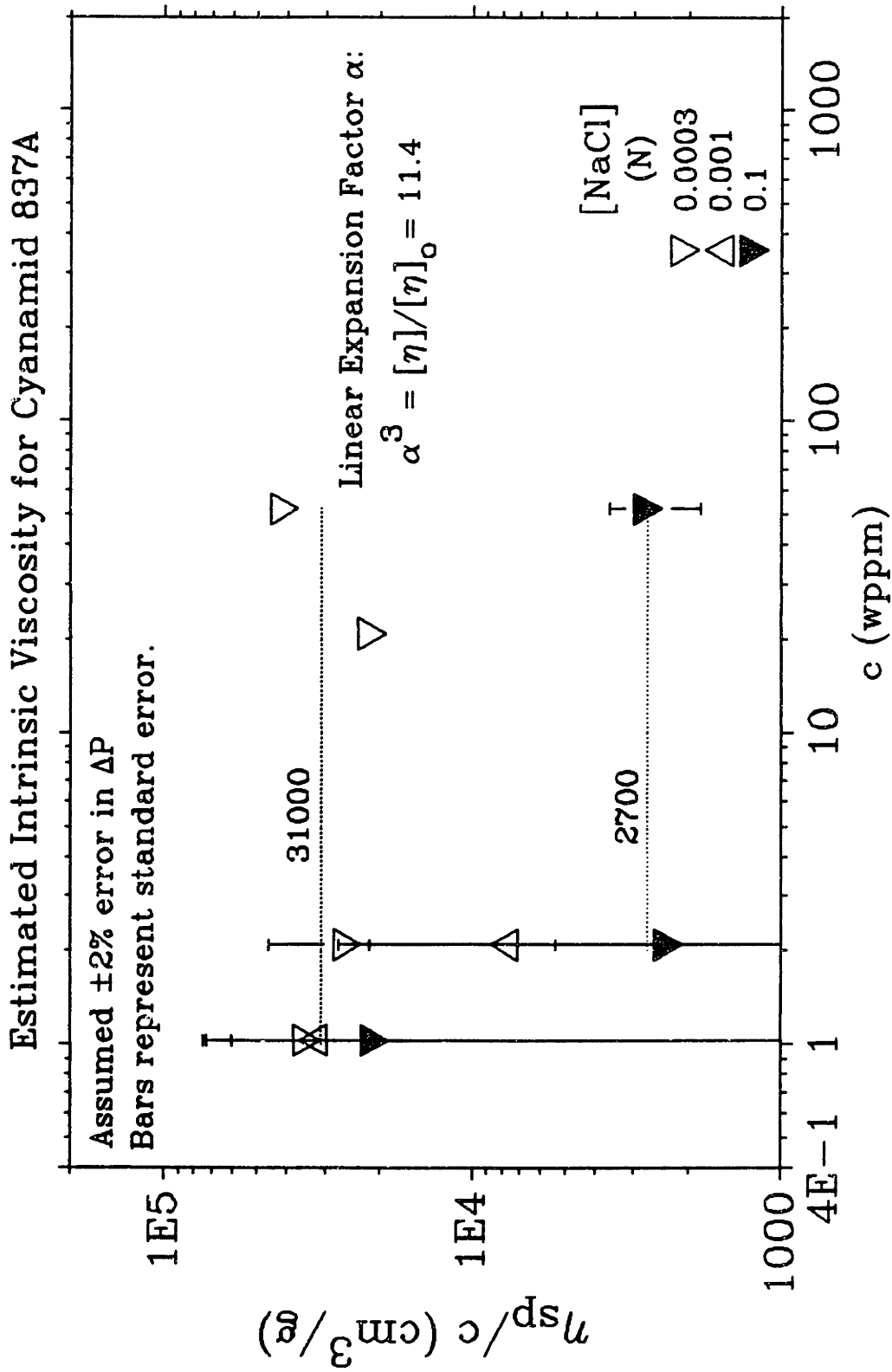


Figure 5.4.6: Estimated Intrinsic Viscosity η_{sp}/c for Cyanamid 837A

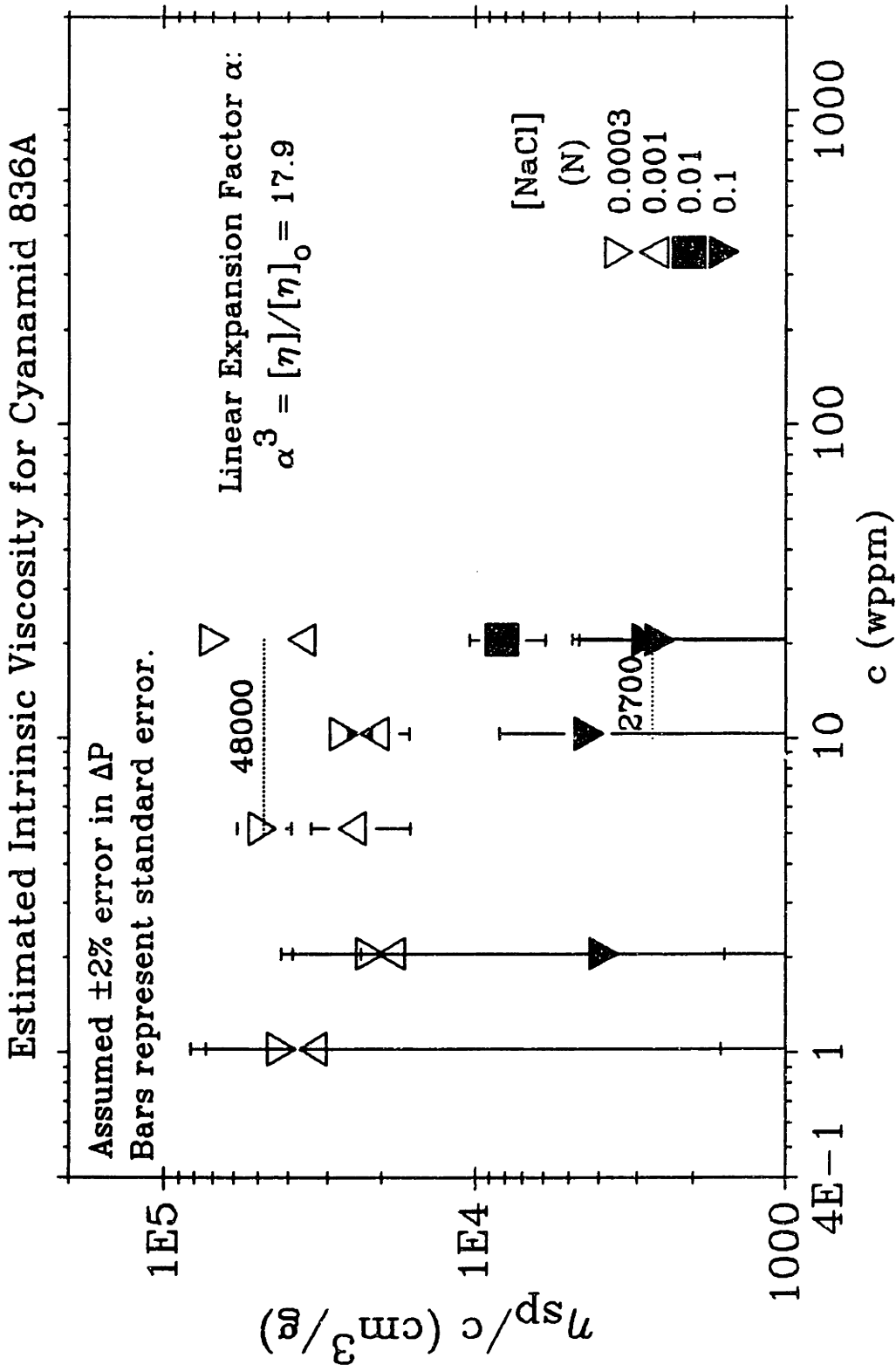


Figure 5.4.7: Estimated Intrinsic Viscosity η_{sp}/c for Cyanamid 836A

CHAPTER VI

DISCUSSION

In this chapter the results presented in Chapter V are analyzed, correlated, and compared with the literature. Wherever possible, the results are physically interpreted in terms of the mechanisms underlying turbulent drag reduction. The discussion comprises seven parts: §6.1, the influence of pipe diameter; §6.2, an overview of the effect of additive initial-conformation on the phenomenon; §6.3, Type-A drag reduction by solutions of collapsed additives; §6.4, Type-B drag reduction by solutions of extended additives; §6.5, comparisons between Type-A and Type-B drag reduction; §6.6, analysis of Type-B flow enhancement and comparison with literature; and §6.7, modelling of both Types A and B of drag reduction.

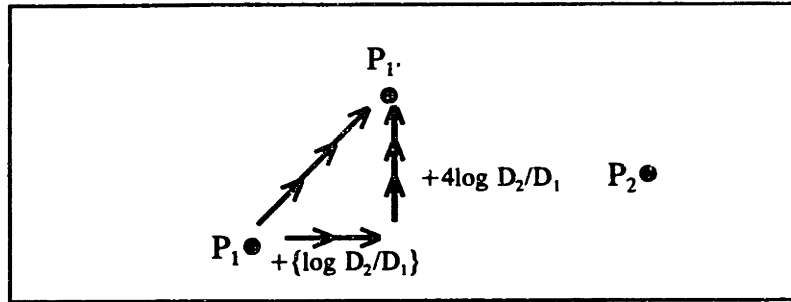
6.1 Influence of Pipe Diameter

In §5.2.3, the pipe diameter was observed to influence gross flow enhancement structure systematically. Data for P500 in 0.3 N NaCl from the 1.458- and 1.021-cm pipes in Figures 5.2.12 and 5.2.13, respectively, virtually superposed on the same PK plot when their abscissae and ordinates were appropriately corrected by the ratio of pipe diameters. Likewise, the P500 data in 0.0001 N NaCl from the 1.458- and 1.021-cm pipes in Figures 5.2.12 and 5.2.13, respectively, also superposed when these data were corrected by the pipe-diameter ratio. This superposition was further supported by the

results for additive C832A in the 1.458- and 1.021-cm pipes, as shown in Figures 5.2.6 and 5.2.8 at 0.3 N NaCl and in Figures 5.2.7 and 5.2.9 at 0.0001 N NaCl.

The transformations that superpose drag reduction data from different pipes are quantitatively effected as follows: On a given set of PK axes, let data point P_1 , from a pipe of diameter D_1 have coordinates $(\log Re_s \sqrt{f}, 1/\sqrt{f})_1$ and data point P_2 , from a pipe of diameter D_2 have coordinates $(\log Re_s \sqrt{f}, 1/\sqrt{f})_2$. In order to put P_1 on the same basis as P_2 for our comparison, P_2 is left unchanged, while the coordinates of P_1 are changed in a two-step process to arrive at a new point P_1' , coordinates $(\log Re_s \sqrt{f}, 1/\sqrt{f})_{1'}$, as shown in Equation 6.1-1 and the accompanying sketch. The net effect is to slide P_1 linearly, parallel to the PK baseline N , by an amount proportional to the pipe-diameter ratio. After transformation, both abscissae become solely dependent upon wall shear stress, sharing the common diameter D_2 in their PK form; also, the ordinate of the transformed point P_1' preserves its original vertical displacement, that is, flow enhancement, relative to solvent.

$$\begin{aligned}
 P_1 \left[\log \frac{\sqrt{2} D_1 u_{\tau_1}}{\nu_s}, \frac{1}{\sqrt{f_1}} \right] &\Rightarrow P_1' \left[\log \frac{\sqrt{2} D_1 u_{\tau_1}}{\nu_s} + \log \frac{D_2}{D_1}, \frac{1}{\sqrt{f_1}} + 4 \log \frac{D_2}{D_1} \right] \\
 P_2 \left[\log \frac{\sqrt{2} D_2 u_{\tau_2}}{\nu_s}, \frac{1}{\sqrt{f_2}} \right] &\Rightarrow P_2 \left[\log \frac{\sqrt{2} D_2 u_{\tau_2}}{\nu_s}, \frac{1}{\sqrt{f_2}} \right]
 \end{aligned} \tag{6.1-1}$$



Coordinate Transformation According to Equation 6.1-1.

Figure 6.1.1 shows original data for additive P500 in 0.3-N NaCl at $c = 10, 30,$ and 100 wppm from the 1.458-cm(open symbols) and 1.021-cm(closed symbols) pipes. In the polymeric-regime, at every concentration, the data in the 1.021-cm pipe lie systematically somewhat higher than the corresponding data in the 1.458-cm pipe. Figure 6.1.2 displays the superposition of these data by the transformation of equation 6.1-1. The 1.021-cm data have been shifted horizontally by a multiplicative factor of $\log(1.458/1.021) \approx 0.155$ and vertically by an additive factor of $4\log(1.428) \approx 0.619$, effectively sliding the 1.021-cm data forward along the baseline N . The two Type-A fans precisely overlap, with coinciding onset points, linear P segments, and regions of polymer degradation. Thus the flow enhancement in both pipes scales with the wall shear stress.

Figure 6.1.3 shows original data for additive P500 in 0.0001-N NaCl at $c = 10, 30,$ and 100 wppm from the 1.458-cm(open symbols) and 1.021-cm(closed symbols) pipes. Figure 6.1.4 shows these same data after the 1.021-cm data are transformed by Equation 6.1-1. The two Type-B ladders are seen to superpose neatly, with their corresponding ladder rungs and regions of polymer degradation coinciding. Again, the flow enhancement in both pipes depends only upon the wall shear stress.

Theoretically, the foregoing results imply that both Type-A and Type-B drag

Superposition of P500 Data at High Salinity from Different Pipes

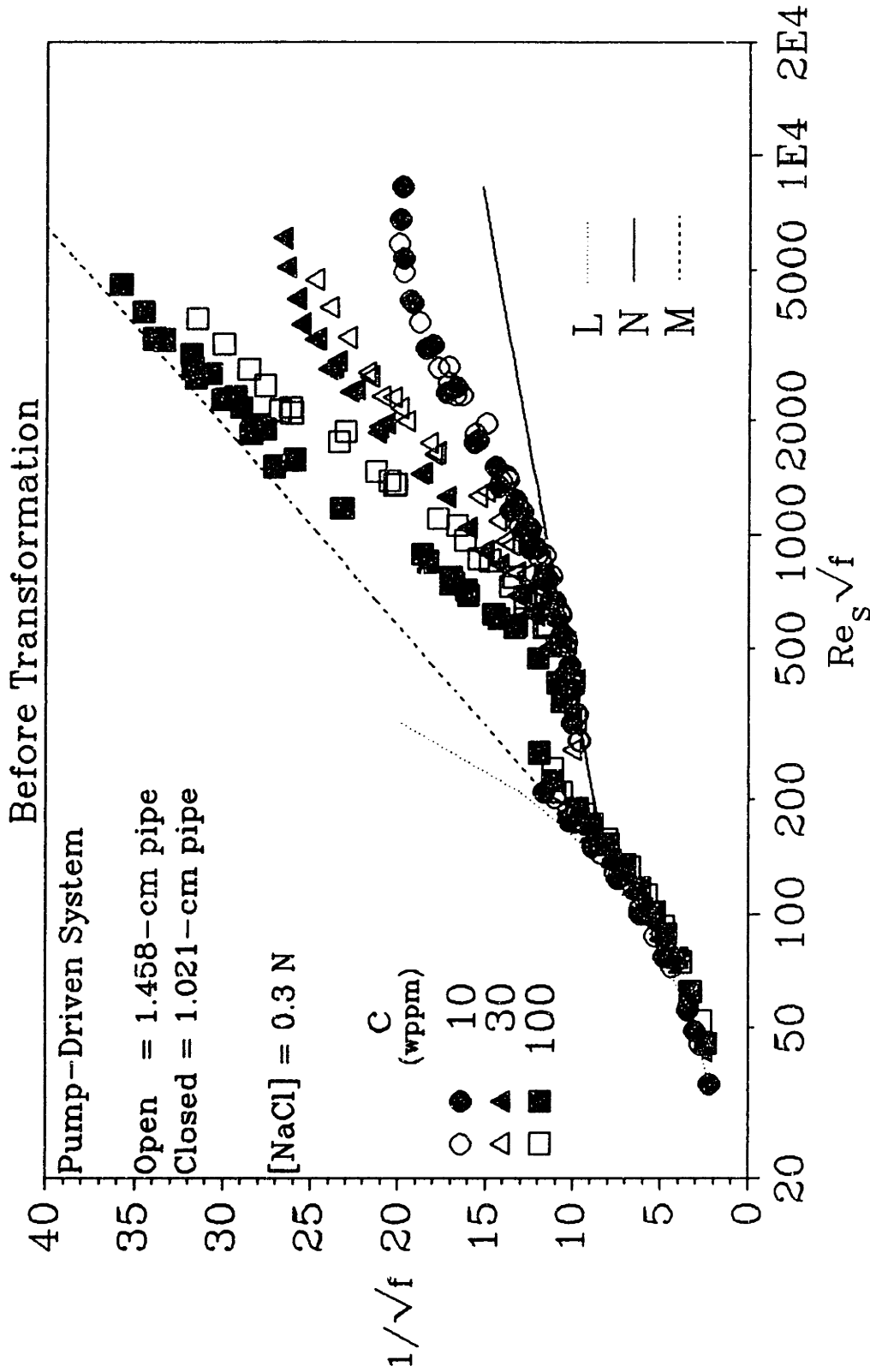


Figure 6.1.1: Superposition of P500 Data at High Salinity from Different Pipes, Before Transformation

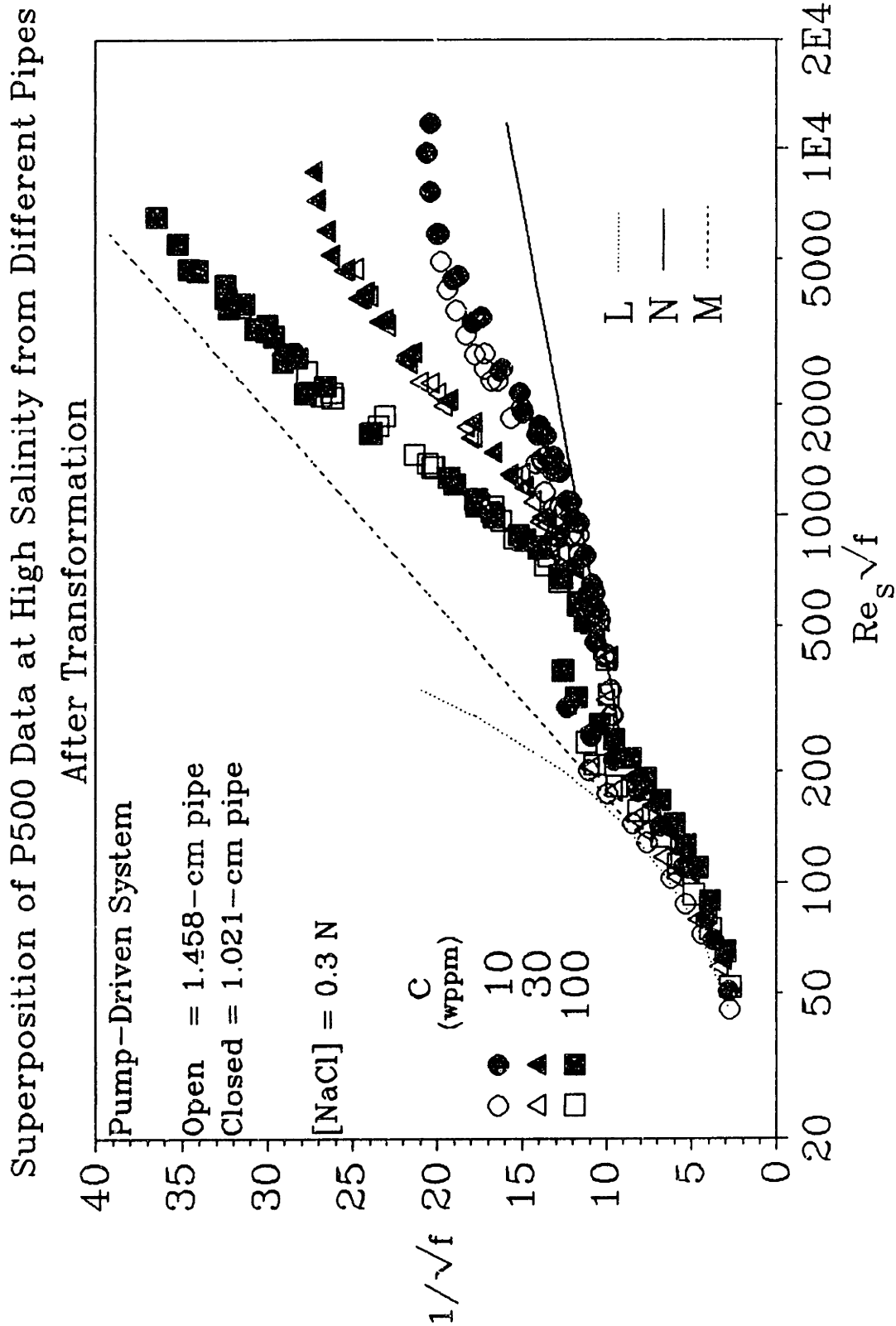


Figure 6.1.2: Superposition of P500 Data at High Salinity from Different Pipes, After Transformation

Superposition of P500 Data at Low Salinity from Different Pipes
Before Transformation

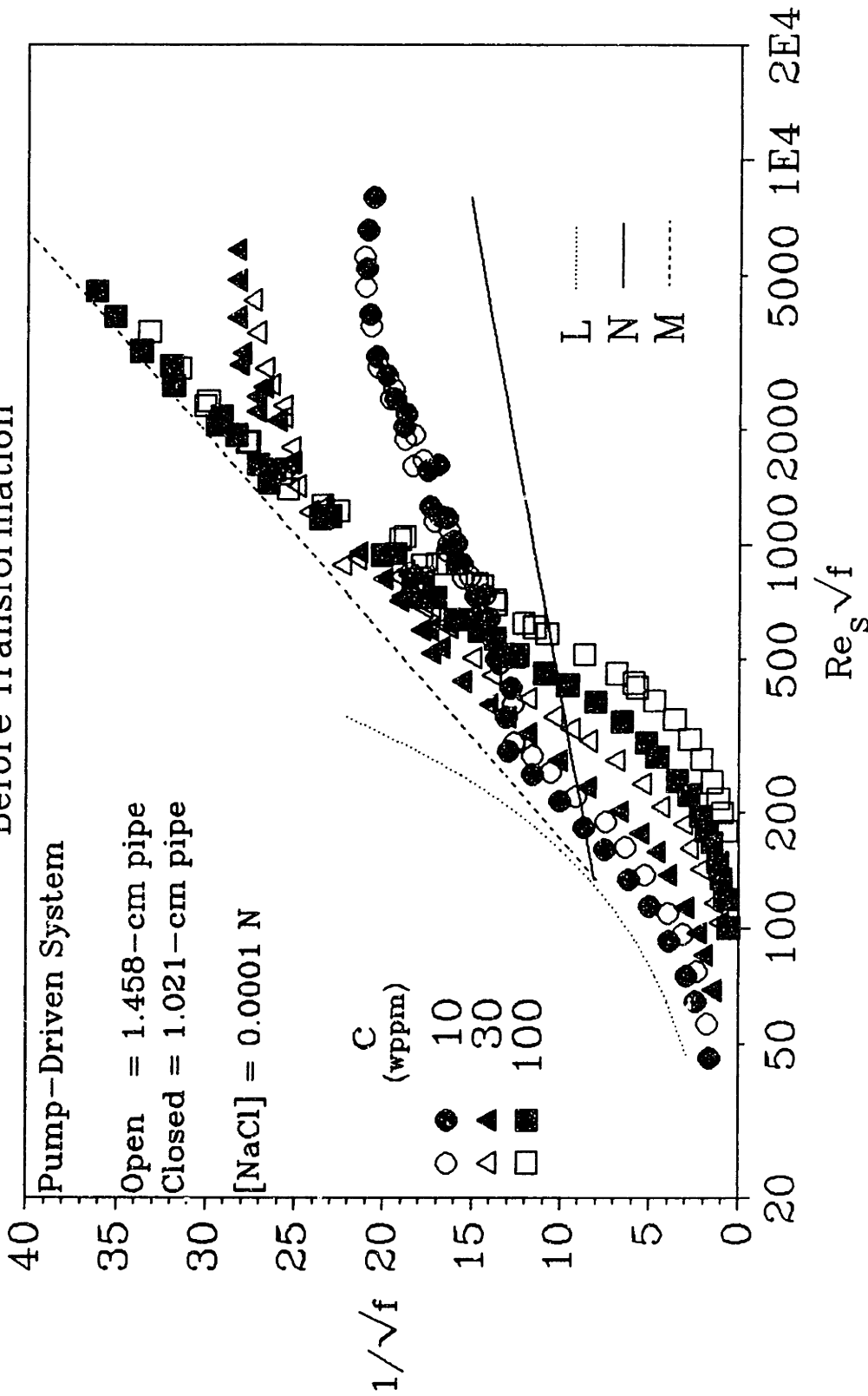


Figure 6.1.3: Superposition of P500 Data at Low Salinity from Different Pipes, Before Transformation

Superposition of P500 Data at Low Salinity from Different Pipes
After Transformation

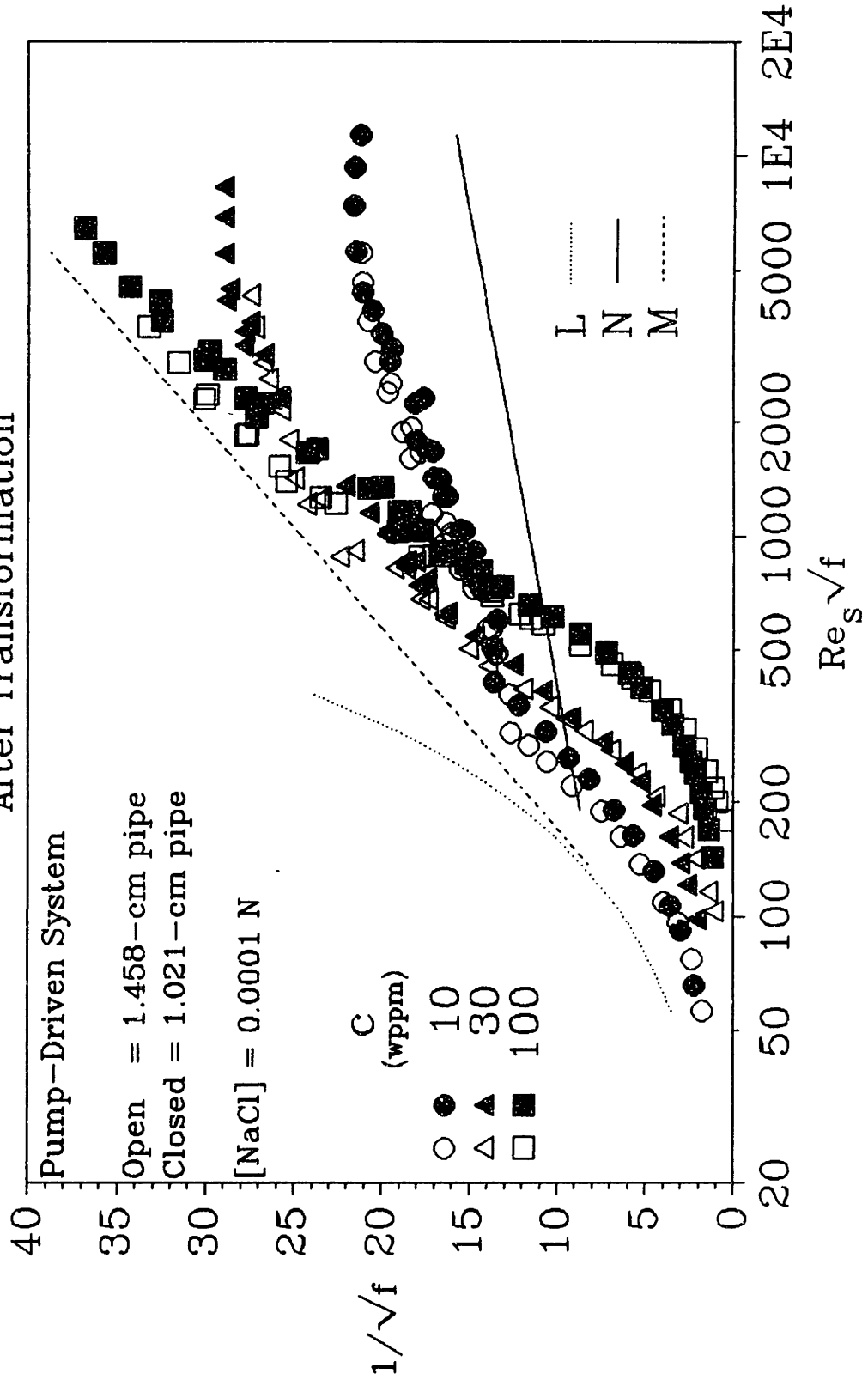


Figure 6.1.4: Superposition of P500 Data at Low Salinity from Different Pipes, After Transformation

reduction in the polymeric regime are controlled by the finer wall-turbulence scales related to the wall shear stress and not by the large scales of turbulence imposed by pipe diameter.

Figures 6.1.5 and 6.1.6 respectively show data for C832A in 0.3 N NaCl at $2 \leq c \leq 50$ wppm in the 1.458-cm(open symbols) and 1.021-cm(closed symbols) pipes, before and after transformation of the 1.021-cm data via equation 6.1-1. In Figure 6.1.6, despite a small mismatch between the 2-wppm data, the two Type-A fans overlap, with their onset points occurring at the nearly same $Re_s\sqrt{f}^*$; also, the corresponding linear P segments superpose, as do the regions of polymer degradation, which follow the linear P segments at higher $Re_s\sqrt{f}$.

Figures 6.1.7 and 6.1.8 respectively show data for C832A in 0.0001N NaCl at $2 \leq c \leq 50$ wppm in the 1.458-cm(open symbols) and 1.021-cm(closed symbols) pipes, before and after transformation of the 1.021-cm data via equation 6.1-1.

In Figure 6.1.8, after transformation, the two Type-B ladders somewhat overlap. While the corresponding ladder rungs at $c = 1, 10,$ and 20 wppm coincide, the 1.458-cm rungs at $c = 2$ and 5 wppm lie above, and nearly parallel to, the corresponding 1.021-cm rungs with an approximately constant upshift. Similarly, while the corresponding regions of polymer degradation at $c = 1$ and 10 wppm occur over the same range of $Re_s\sqrt{f}$, polymer degradation in the 1.458-cm pipe at $c = 2$ and 5 wppm occurs at slightly smaller $Re_s\sqrt{f}$ than it does in the 1.021-cm pipe at the same concentrations. The systematic differences between the corresponding 2- and 5-wppm rungs may arise from experimental factors. Despite these discrepancies, the coinciding P segments(ladder rungs) and polymer-degradation regions at $c = 1, 10,$ and 20 wppm in Figure 6.1.8

Superposition of C832A Data at High Salinity from Different Pipes

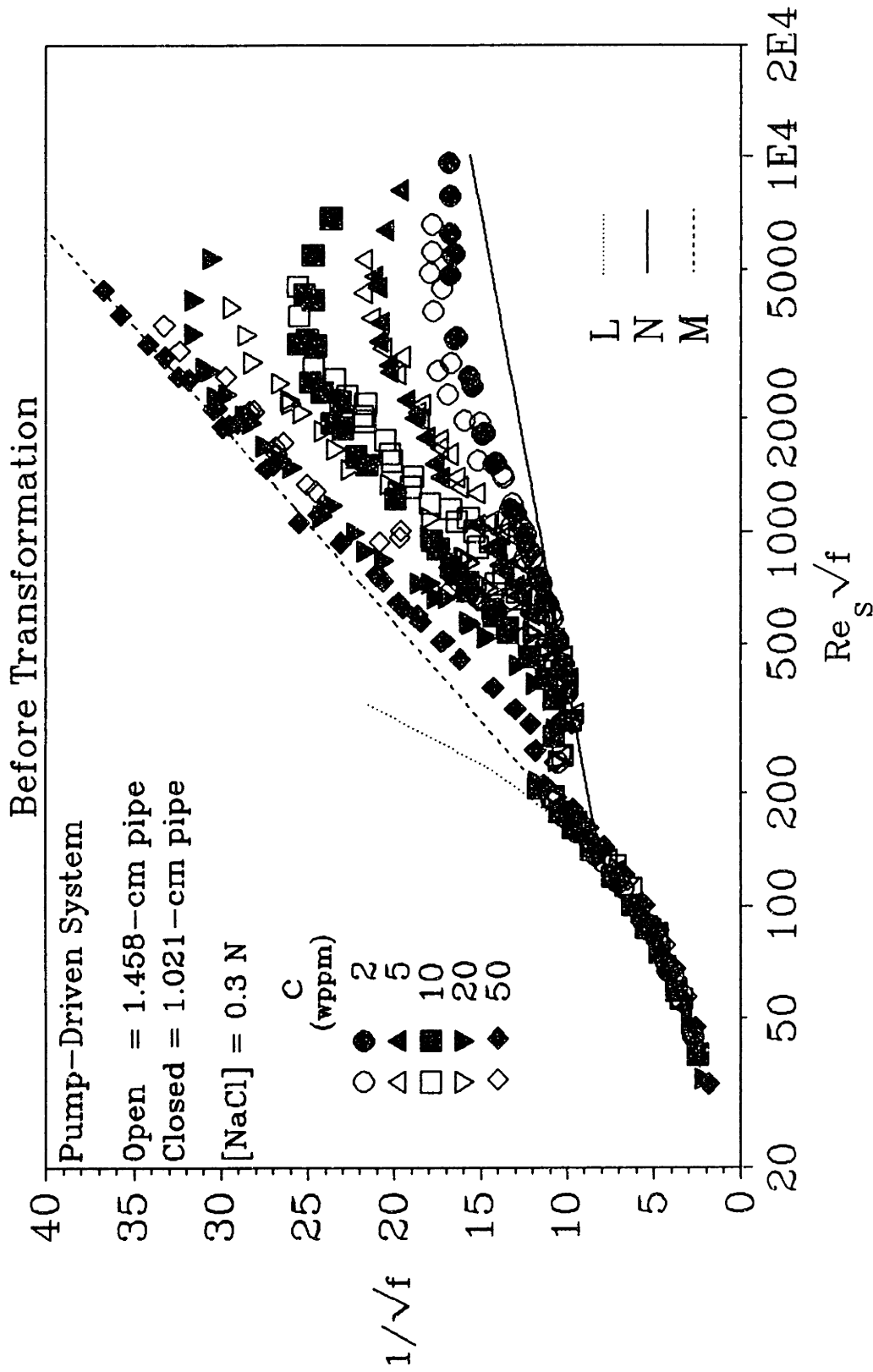
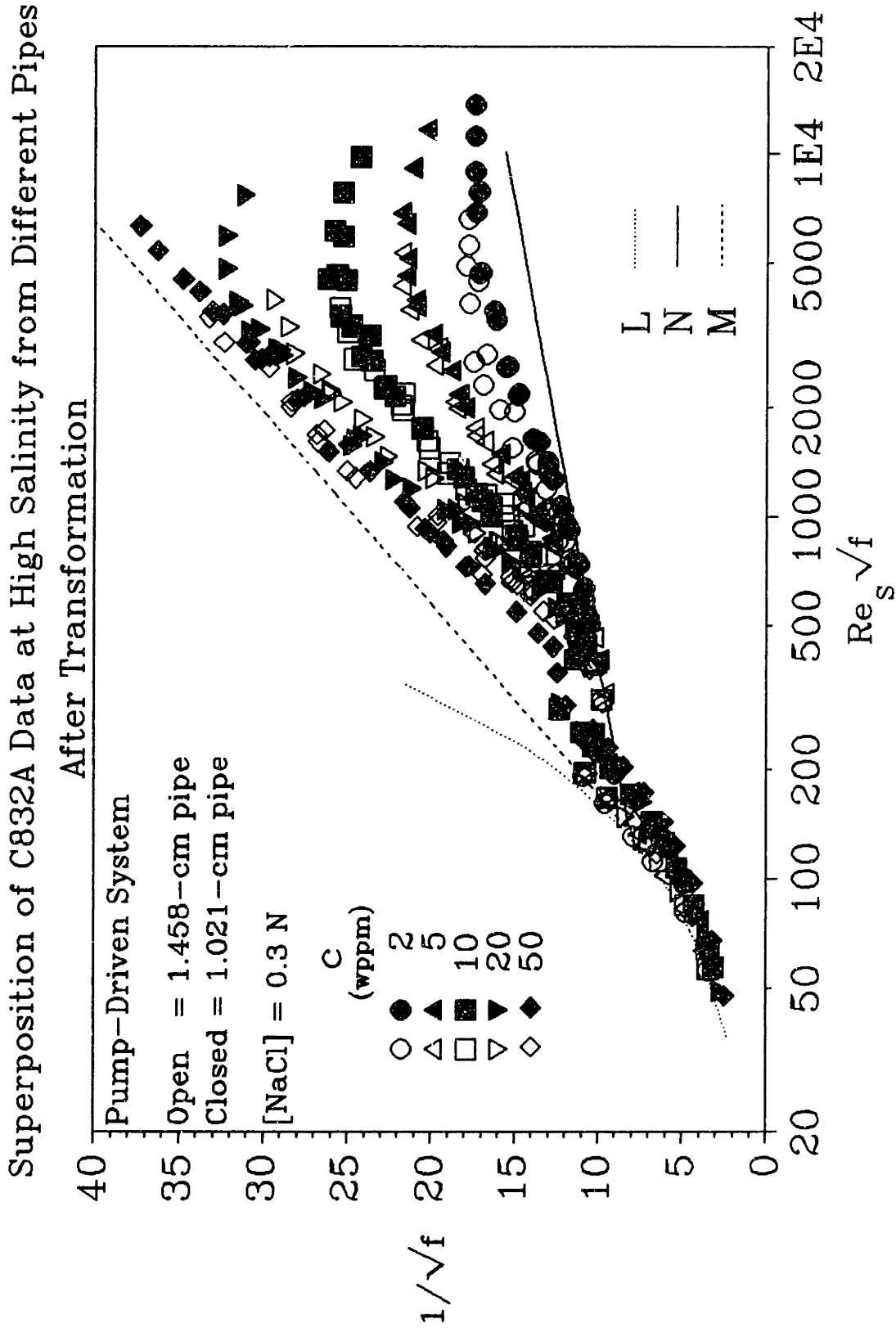
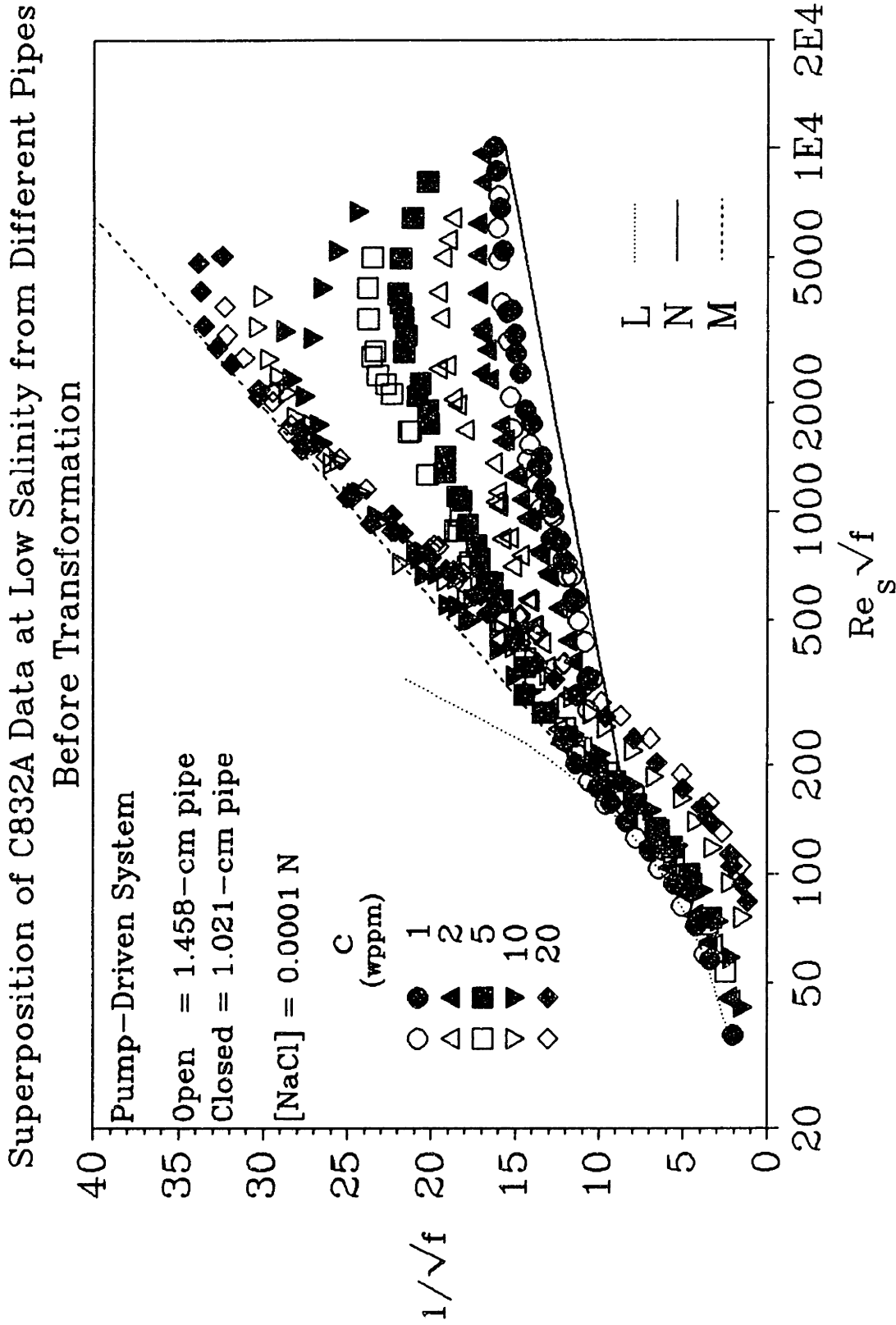


Figure 6.1.5: Superposition of C832A Data at High Salinity from Different Pipes, Before Transformation



451 Figure 6.1.6: Superposition of C832A Data at High Salinity from Different Pipes, After Transformation



452 Figure 6.1.7: Superposition of C832A Data at Low Salinity from Different Pipes, Before Transformation

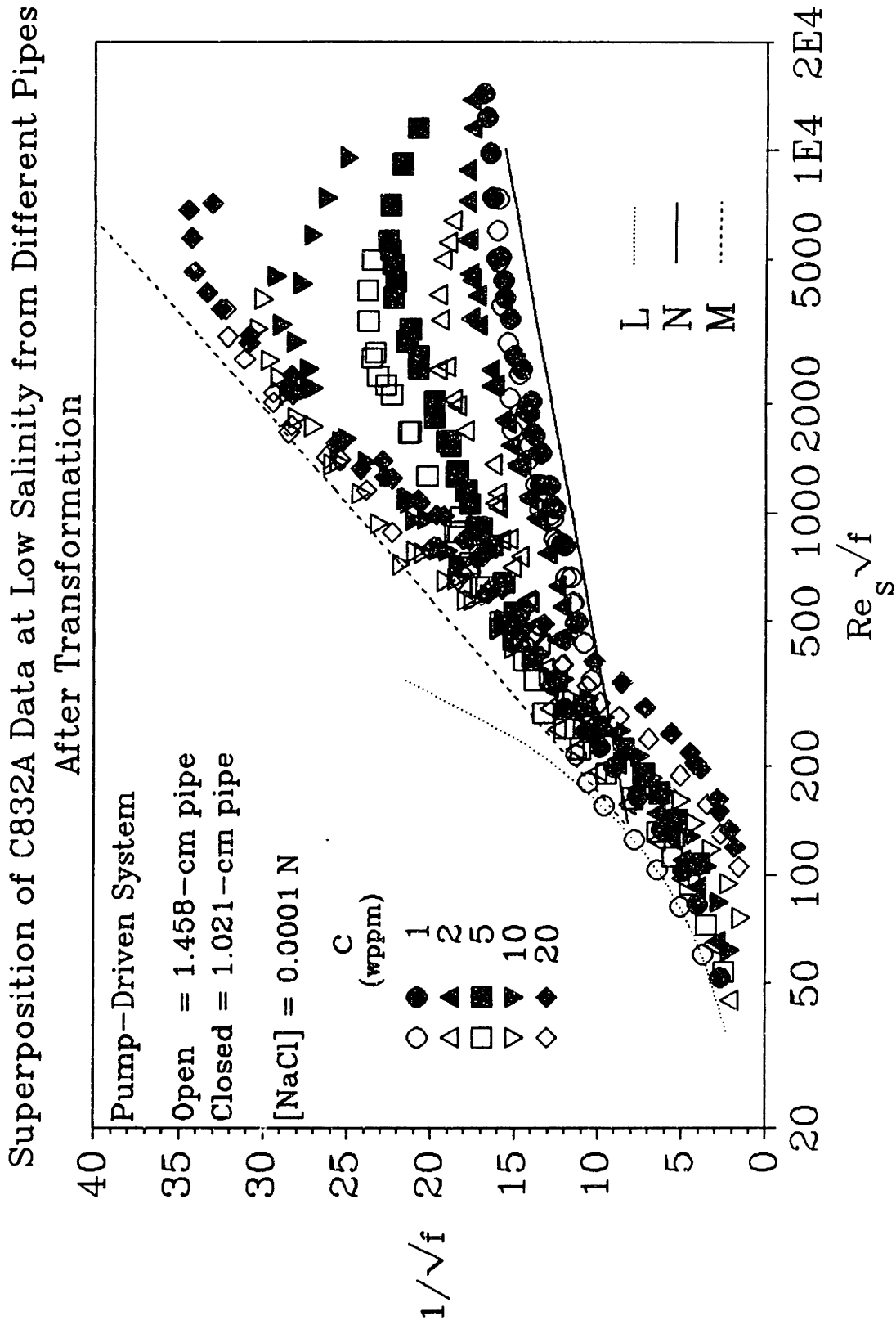


Figure 6.1.8: Superposition of C832A Data at Low Salinity from Different Pipes, After Transformation

suggest that wall shear stress scales flow enhancement in the polymeric regime and that S'/c is independent of pipe diameter.

In summary, the influence of pipe diameter upon both Types A and B of turbulent drag reduction was sought from the experiments with additives P500 and C832A in each of the 1.458- and 1.021-cm pipes. For P500, at all concentrations from 10 to 100 wppm, the respective Type-A fans and Type-B ladders obtained in the polymeric regime at high and low salinities in both pipes scaled with wall shear stress and were independent of pipe diameter. For C832A, polymeric-regime data for $2 \leq c \leq 50$ wppm at both high and low salinities in both pipes were also found to scale with wall shear stress rather than pipe diameter, reinforcing the results obtained with P500. Theoretically, these results imply that drag reduction in the polymeric regime is relatively unaffected by the large scales of turbulence, imposed by the pipe diameter, and is instead controlled by the finer wall-turbulence scales related to the wall shear stress.

6.1.1 Additive Degradation

The aforementioned superposition of polymeric regimes further succeeds in superposing the degradation-induced maxima and downward departures from P segments observed in both pipes at the highest $Re\sqrt{f}$. Thus the wall shear stress also appears to scale polymer degradation during drag reduction. Perusal of Figures 6.1.2 and 6.1.4 shows that for additive P500 at both high and low salinities, degradation becomes significant beyond a characteristic "falloff" wall shear stress, $T_w^* \approx 690$ dynes/cm², corresponding to $Re\sqrt{f}^* \approx 6000$ in the 1.458-cm pipe. Note also that the Type-A fans

in Figure 6.1.2 exhibit onset at $Re_s\sqrt{f^*} \approx 700$, where $T_w^* \approx 9.5$ dynes/cm². For P500, a 70-fold range of wall shear stress thus separates onset from the degradation falloff; this is the region within which its initially-collapsed conformation can effectively reduce turbulent drag. The C832A data exhibited degradation falloffs at $T_w^* \approx 170$ dynes/cm², corresponding to $Re_s\sqrt{f^*} \approx 3000$ in the 1.458-cm pipe, and Type-A onsets at $Re_s\sqrt{f^*} \approx 550$, where $T_w^* \approx 5.7$ dynes/cm²; in this case only a 30 fold range of wall shear stress separated onset from the degradation falloff. Lastly, the molecular weights of additives P500 and C832A are in the ratio $9.5/18 \approx 0.5$ while their falloff shear stresses are in the ratio $690/170 \approx 4$; this provides the following dimensional inverse-square relation for degradation of HPAM additives in the present pipes:

$$T_w^* \approx 5.9 \times 10^{16} M_w^{-2} \quad (6.1-2)$$

where T_w^* and M_w are in dyne/cm² and g/mole, respectively.

Since degradation likely occurs by scission near the midpoints of the extended polymer chains (Merrill & Horn, 1984), the observed dependence of T_w^* on M_w likely reflects an underlying connection to some length scale of the extended additive, such as its contour length L_c , over which the disruptive turbulent flow field acts.

6.2 Effect of Macromolecular Conformation

The effects of macromolecular additive conformation on gross flow physics are summarized in the central kernel of Figure 6.2.1. Observations with any additive and salinity fall into one of three sets, namely, (i) laminar flow that is Newtonian with

Observed Effects of Macromolecular Additive Conformation on Gross-Flow Behavior

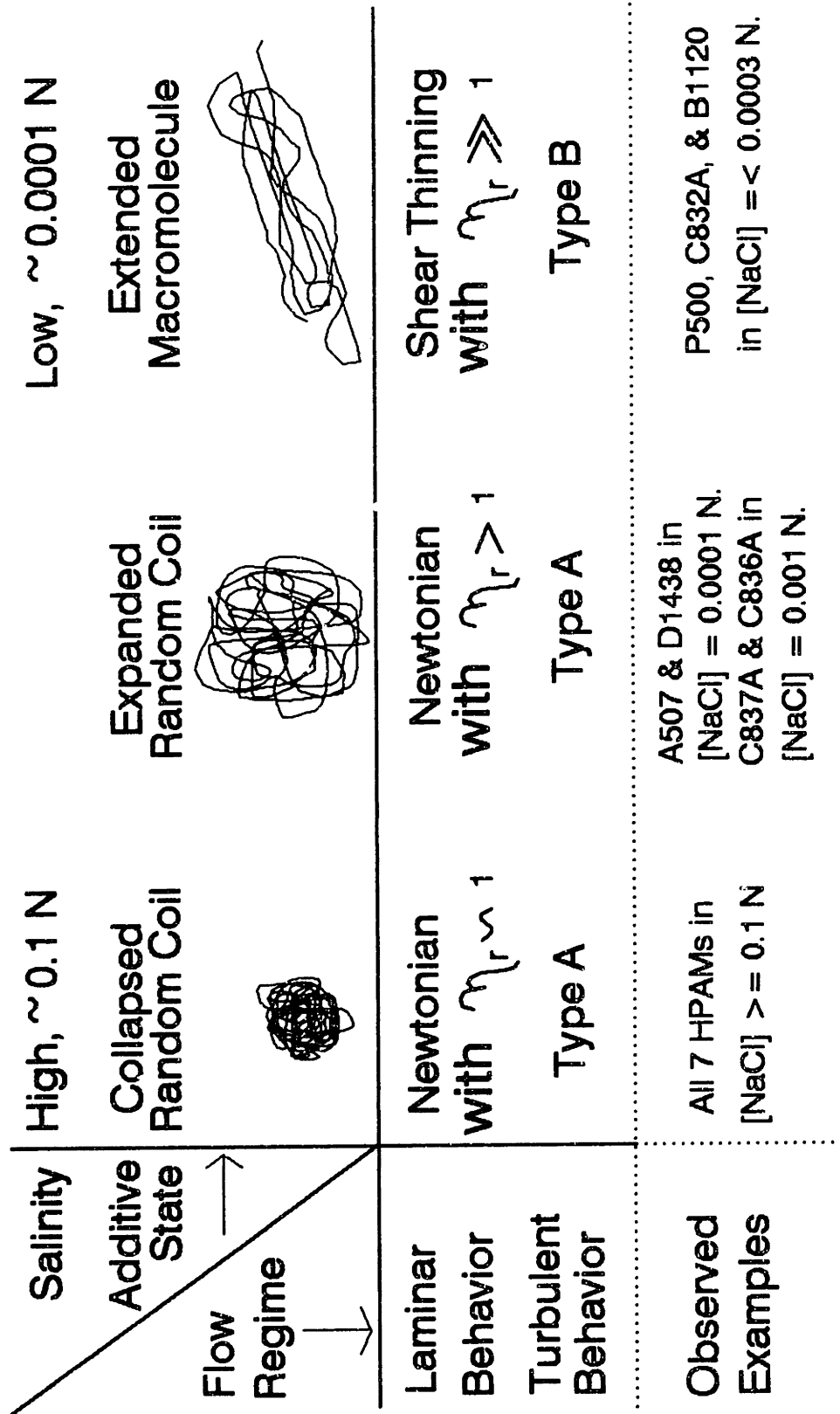


Figure 6.2.1: Observed Effects of Macromolecular Additive Conformation on Gross-Flow Behavior

relative viscosities near unity, and turbulent flow with Type-A drag reduction, (ii) laminar flow that is Newtonian but with relative viscosities appreciably greater than unity, and turbulent flow with Type-A drag reduction, and (iii) laminar flow with shear-thinning and relative viscosities greatly in excess of unity, and turbulent flow with Type-B drag reduction. The preceding are associated with each of three initial conformations of the additive: (i) collapsed random-coil, (ii) expanded random-coil, and (iii) the extended macromolecule. The observed examples actually used to derive the above classification are given in the bottom row of Figure 6.2.1: (i), all seven HPAM additives at high salinities; (ii), A507 & D1438 in 0.0001 N NaCl and C837A & C836A in 0.001 N NaCl; and (iii), P500, C832A & B1120 in <0.0003 N NaCl. Comparisons between these and the HPAM characterization data in Table 6.2 show that, while Type-A drag reduction behavior is achieved by the initially-collapsed conformations of all additives, Type-B drag reduction behavior, associated with the initially-extended macromolecular conformation, is only accessible to additives of the highest molecular weight and backbone charge. The lowest molecular weight additives, D1438 and A507, each with $M_w \approx 1 \times 10^6$ g/mole, do not exhibit Type-B behavior, despite the latter possessing a highly charged backbone, with nominal degree of hydrolysis $\approx 60\%$. The highest molecular weight additives, B1120 and C832A, with $M_w \approx 20 \times 10^6$ g/mole, and high backbone charge $\approx 50\%$, both exhibit Type-B drag reduction. However, P500, with $M_w \approx 10 \times 10^6$ g/mole, and backbone charge $\approx 30\%$ achieves Type-B behavior, whereas C837A and C836A, with $M_w \approx 16 \times 10^6$ g/mole, and backbone charges ≈ 8 and 15% , do not. These data suggest that, at any given molecular weight, a threshold backbone charge must be exceeded to induce Type-B behavior; for these $M_w \times 10^{-6} \approx 1, 10, 16,$

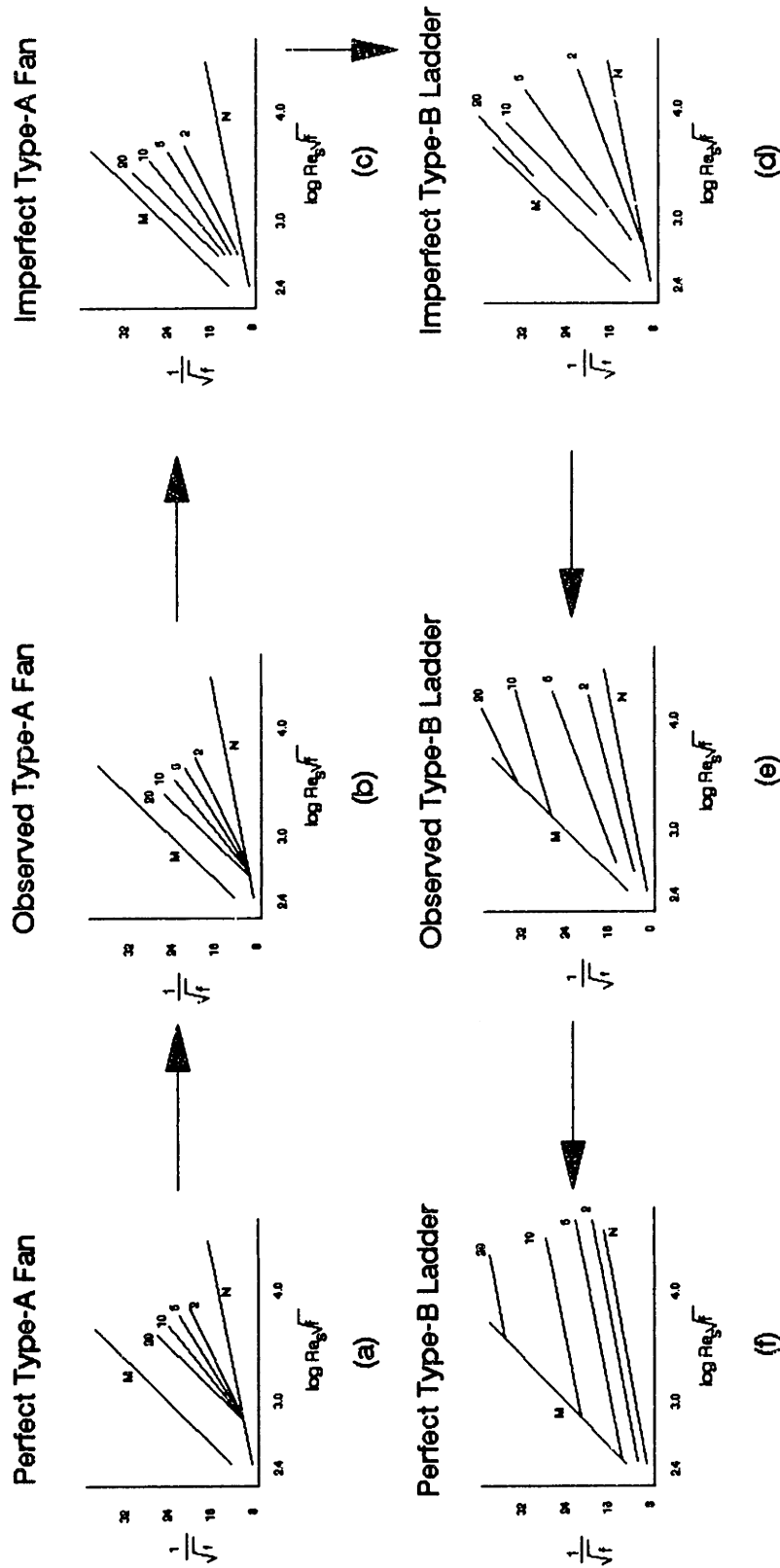
Table 6.2
Inferred Polymer Characteristics†

Polymer	Manufacturer's Data‡		Estimated Intrinsic Viscosity at High Salinity	Parameters Inferred from Equations 2.4-10 and 2.4-11	
	Molecular Weight	Degree of Hydrolysis		Molecular Weight	Radius of Gyration
	$M_w \times 10^{-6}$		η_{sp}/c	$M_w \times 10^{-6}$	R_G
	(g/mole)	(%)	(cm^3/g)	(g/mole)	(nm)
C832A	14 - 17	50(?)	3000 ± 600	18.0 ± 5.0	280 ± 50
B1120	8 - 10	High(?)	3300 ± 800	20.1 ± 6.4	300 ± 60
P500	2 - 3	30	1850 ± 500	9.5 ± 3.5	190 ± 40
A507	1 - 2	60	340 ± 80	1.0 ± 0.3	50 ± 10
D1438	2 - 4	10	440 ± 150	1.4 ± 0.6	60 ± 20
C837A	14 - 17	8(?)	2700 ± 900	15.7 ± 6.7	260 ± 70
C836A	14 - 17	15(?)	2700 ± 1450	15.5 ± 11.0	260 ± 110
Polymer	Number of Backbone Chain Links	Contour Length	Estimated Intrinsic Viscosity at Low Salinity	Coil Expansion Ratio	Linear Expansion Factor
	$N_{bb} \times 10^{-5}$	L_c	η_{sp}/c	α^3	α
		(μm)	(cm^3/g)		
C832A	5.0 ± 1.4	64 ± 18	97000 ± 2000	32.4	3.2
B1120	5.6 ± 1.8	71 ± 23	97000 ± 3000	29.6	3.1
P500	2.7 ± 1.0	34 ± 12	72000 ± 2000	38.7	3.4
A507	0.3 ± 0.1	3.6 ± 1.1	7000 ± 500	20.3	2.7
D1438	0.4 ± 0.2	5.0 ± 2.2	5800 ± 400	13.0	2.4
C837A	4.4 ± 1.9	56 ± 24	31000 ± 2000	11.4	2.2
C836A	4.4 ± 3.1	55 ± 39	48000 ± 4000	17.9	2.6
† \pm values are average standard errors.					
‡ The accuracy of manufacturers' data is unknown.					

and 20 g/mole, the threshold charges are, respectively, $> 60\%$, $< 30\%$, $> 15\%$, and $< 50\%$.

The ranges of turbulent-flow behaviour actually observed are more precisely elaborated in Figure 6.2.2. This shows six composite Prandtl-Karman(PK) plots labelled (a) through (f) that depict the continuous transformation of the Perfect Type-A Fan, (a), to the Perfect Type-B Ladder, (f). In each PK plot, the units on the $\log-Re_p\sqrt{f}$ abscissa and the $1/\sqrt{f}$ ordinate correctly locate the Newtonian turbulent baseline N and the MDR Asymptote M. To begin, (a) displays a Perfect Type-A Fan, the spokes of which have concentrations $c = 2, 5, 10,$ and 20 wppm. From the fan's single onset point, its four spokes radiate with slope increments δ that increase as the square-root of the concentration, \sqrt{c} , as depicted to scale in (a). In a slight departure from ideality, (b) shows the Observed Type-A Fan having the "same" four spokes. While the spokes of the observed fan in (b) continue to obey the \sqrt{c} law, here they radiate from adjacent points along, rather than one point on, the turbulent baseline N, constituting a diffuse onset point. In a further systematic departure from (b), the Imperfect Type-A Fan in (c) now has no discernable onset point, and its spokes, now assuming shallower slopes, no longer obey the \sqrt{c} rule. From (c) to (d), the spokes of the Imperfect Type-A Fan become less steep, attaining slopes near that of N; any remnant of an onset point has completely disappeared. In (d), the Imperfect Type-B Ladder obtains. Its ladder rungs are neither mutually parallel nor parallel to N; moreover, they have neither retro-onset points along M nor apparent slips S' in proportion to their respective concentrations c . In (e), the Observed Type-B Ladder has ladder rungs that are nearly parallel to N and have apparent slips S' nearly in proportion to their concentrations c . While the ladder

The Progression of Turbulent Drag-Reduction Behavior from Type A to Type B, As Seen With HPAM Additives in Solutions of Decreasing Salinity



Note: Concentrations are hypothetical, corresponding to an HPAM Mw ~ 15E6.

Figure 6.2.2: The Progression of Turbulent Drag-Reduction Behavior from Type A to Type B as Seen with HPAM Additives in Solutions of Decreasing Salinity

rungs at high concentrations exhibit sharp retro-onset points, the rungs at low concentrations do not, their retro-onset points obscured by laminar-to-turbulent transitions. Finally in (f), the Perfect Type-B Ladder is reached. In this PK plot, the rungs exhibit distinct retro-onset points from M and have slopes identical to that of N. Their upshifts relative to N, S', are constant, independent of $Re_s\sqrt{f}$, and proportional to their respective concentrations such that $S'_{20}/20 = S'_{10}/10 = S'_5/5 = S'_2/2$. Each PK plot in this sequence of six drag-reduction structures depends intimately on the state of the additive, as shown conceptually in Figure 6.2.1.

Figure 6.2.3 details the dependence of turbulent drag reduction behavior on salinity observed with the present HPAM additives. In the columns of this figure, using the scheme evolved in Figure 6.2.2, each of the two broad categories, the Type-A fan and the Type-B ladder, are amplified into their perfect, observed, and imperfect counterparts, respectively representing their idealized, typical, and distorted (but still recognizable) forms. The rows in the figure represent the HPAM additives studied, arranged by increasing molecular weights. The cells of the matrix contain the salinity at which solutions of the additive represented by that row gives rise to the flow behavior represented by that column. All the kinds of turbulent flow behavior listed, except the perfect Type-A fan, were observed. A prominent feature of Figure 6.2.3 is its general lower-diagonal nature, with high-salinity entries down the left and low-salinity entries along the diagonal to the right. These trends have physical significance, reflecting the influence of additive molecular weight, M_w , and degree of backbone hydrolysis (loosely, "charge"), upon the salinity-induced conformational changes. Thus, at the lowest molecular weights, additives A507 and D1438 with $M_w \approx 1.0 \times 10^6$ g/mole show only

Dependence of Turbulent Drag-Reduction Behavior on Salinity

DRAG-REDUCTION BEHAVIOR	HPAM ADDITIVE					
	Perfect Type-A Fan	Observed Type-A Fan	Imperfect Type-A Fan	Imperfect Type-B Ladder	Observed Type-B Ladder	Perfect Type-B Ladder
A507		 0.3 0.0001				
D1438		 0.3 0.0001				
P500		 0.3			 0.0001	
C836A		 0.1	 0.01 0.001 0.0003			
C837A		 0.1 0.001	 0.0003			
C832A		 0.1 0.3		 0.001	 0.0001 0.0003	 0.00001
B1120		 0.3			 0.0001	

Figure 6.2.3: Dependence of Turbulent Drag-Reduction Behavior on Salinity

Type-A drag reduction at both high and low salinity, apparently unable to extend sufficiently, even in solutions of low salinity, to induce Type-B drag reduction. Additives C832A and B1120, with the highest $M_w \approx 20.1 \times 10^6$ g/mole, and high backbone charges, display Type-A behavior at high salinities and Type-B at low salinities. Additive C832A exhibits the widest range of behaviour, from Observed Type-A in 0.1 and 0.3 N NaCl to Imperfect, Observed and Perfect Type-B Ladders in 0.001, 0.0001 and 0.00001-N aqueous NaCl. Also, additives C832A, C836A and C837A, respectively high-, moderate- and low-charge homologues, exhibit a noteworthy spectrum of behavior. All three exhibit Observed Type-A Fans in 0.1-N aqueous NaCl, but in 0.001 N NaCl they respectively exhibit the Observed Type-A Fan, the Imperfect Type-A Fan, and the Imperfect Type-B Ladder, three adjacent columns in Figure 6.2.3, and in 0.0003 N NaCl, only C832A attains Type-B behaviour. This demonstrates the strong influence of backbone charge in enabling the initial conformational extension required for Type-B behaviour.

6.3 Type-A Drag Reduction

Type-A drag reduction has been known for long, and here the focus is exclusively on the present, new, results for HPAM additives in their variously random-coiling conformations. A Type-A fan is defined by the wall shear stress at its onset point T_w^* , and by the slope increments δ of the P segments emanating therefrom. Both of these parameters have previously been related to the macromolecular properties of the additive (Virk, 1975b), as considered below.

6.3.1 Onset

For a given polymer-solvent pair, the onset wall shear stress T_w^* is not greatly influenced by either polymer concentration or pipe diameter, but is strongly, and inversely, dependent upon the polymer coil-size in solution, as measured by its rms radius of gyration, R_G . determines the two being inversely related. The inverse relationship between T_w^* and R_G was generalized by Virk(1975b):

$$T_w^* \propto R_G^{-g}. \quad (6.3-1)$$

When $g = 2$, $T_w^* \propto R_G^{-2}$, so it follows that $Re_s \sqrt{f}^* \propto R_G^{-1}$ and the length-based onset constant Ω_L , equation 2.3-4, obtains. Because $R_G \propto \eta^{1/3}$ for a polymer of fixed molecular weight, it can be expected that $Re_s \sqrt{f}^* \propto \eta^{-1/3}$ to a good approximation. Figure 6.3.1 shows the observed dependence of $Re_s \sqrt{f}^*$ on η_{sp}/c in doubly-logarithmic coordinates among 20.6-wppm solutions of additive C836A with salinities ranging from 0.0003 to 0.1 N NaCl in the 1.458-cm pipe. The $Re_s \sqrt{f}^*$ data are derived from the slopes and intercepts, (A_p, B_p) , of the observed P segments of these solutions. The η_{sp}/c data are directly determined from the corresponding laminar-flow data. The data shown in Figure 6.3.1 are listed in Table 6.3.1. The best-fit power-law line through these data is:

$$Re_s \sqrt{f}^* = (1.88 \pm 0.13) \times 10^4 \left(\frac{\eta_{sp}}{c} \right)^{-(0.41 \pm 0.02)} \quad (6.3-2)$$

where η_{sp}/c is in cm^3/g . From the exponent of -0.41 in equation 6.3-2, $g \approx 2.5$, which is within the range of commonly observed literature values, $2 \leq g \leq 3$.

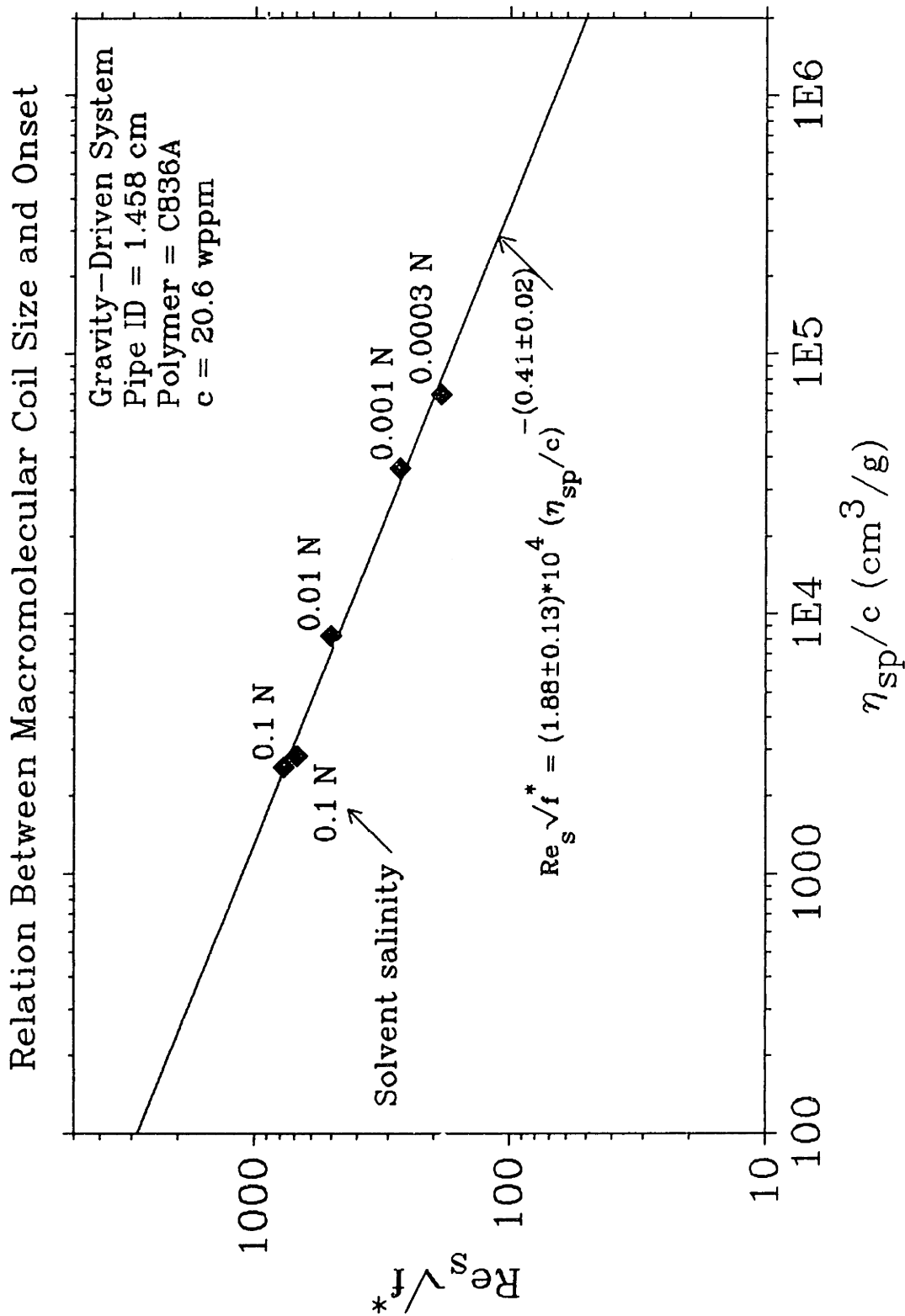


Figure 6.3.1: Relation Between Macromolecular Coil Size and Onset

For the class of HPAM polymers of various molecular weights, Figure 6.3.2 presents average T_w^* values versus R_G in log-log coordinates for all seven HPAMs in saline solutions of at least 0.1 N NaCl and includes individual T_w^* values versus R_G for solutions of additives C836A, P500, A507, and D1438 having salinities less than 0.1 N. These data are listed in Table 6.3.1. The best-fit line through all the data, shown dotted in Figure 6.3.2, has the following power-law form:

$$T_w^* = (0.38 \pm 0.02) \times 10^5 R_G^{-(1.52 \pm 0.20)} \quad (6.3-3)$$

where T_w^* and R_G are in dyne/cm² and nm, respectively. The exponent -1.52 in equation 6.3-3 is somewhat higher than previously quoted in the literature. Another fitted line, obtained by excluding the data for additives A507 and D1438 in 0.3 N NaCl, is shown dashed in Figure 6.3.2:

$$T_w^* = (23.5 \pm 9.4) \times 10^5 R_G^{-(2.24 \pm 0.25)} \quad (6.3-4)$$

This fit has an exponent -2.24, that lies in the range of literature values. To obtain an average value of the "onset constant" Ω_L from among the data represented by equation 6.3-4, equation 6.3-1 with $g = 2$ is assumed to be satisfied by the geometric-mean values of T_w^* and R_G . This "forced" line, shown solid in Figure 6.3.2 has the form:

$$T_w^* = 5.97 \times 10^5 R_G^{-2} \quad (6.3-5)$$

By rearranging equation 6.3-5, $T_w^* R_G^2 = \rho u_r^2 R_G^2 = \rho \nu_s^2 (u_r R_G / \nu_s)^2 = \rho \nu_s^2 (\Omega_L)^2 = 5.79 \times 10^5$ dyne/cm² · nm². With $\rho \approx 1.009$ g/cm³ and $\nu_s \approx 9.801 \times 10^{-3}$ cm²/s for 0.3-N aqueous NaCl at 25 °C, equation 6.3-5 corresponds to $\Omega_L \approx 8.3 \times 10^{-3}$ which is similar to a previous value of $\Omega_L = (8.2 \pm 0.3) \times 10^{-3}$ for HPAM additives in 1.0-m NaCl (Virk,

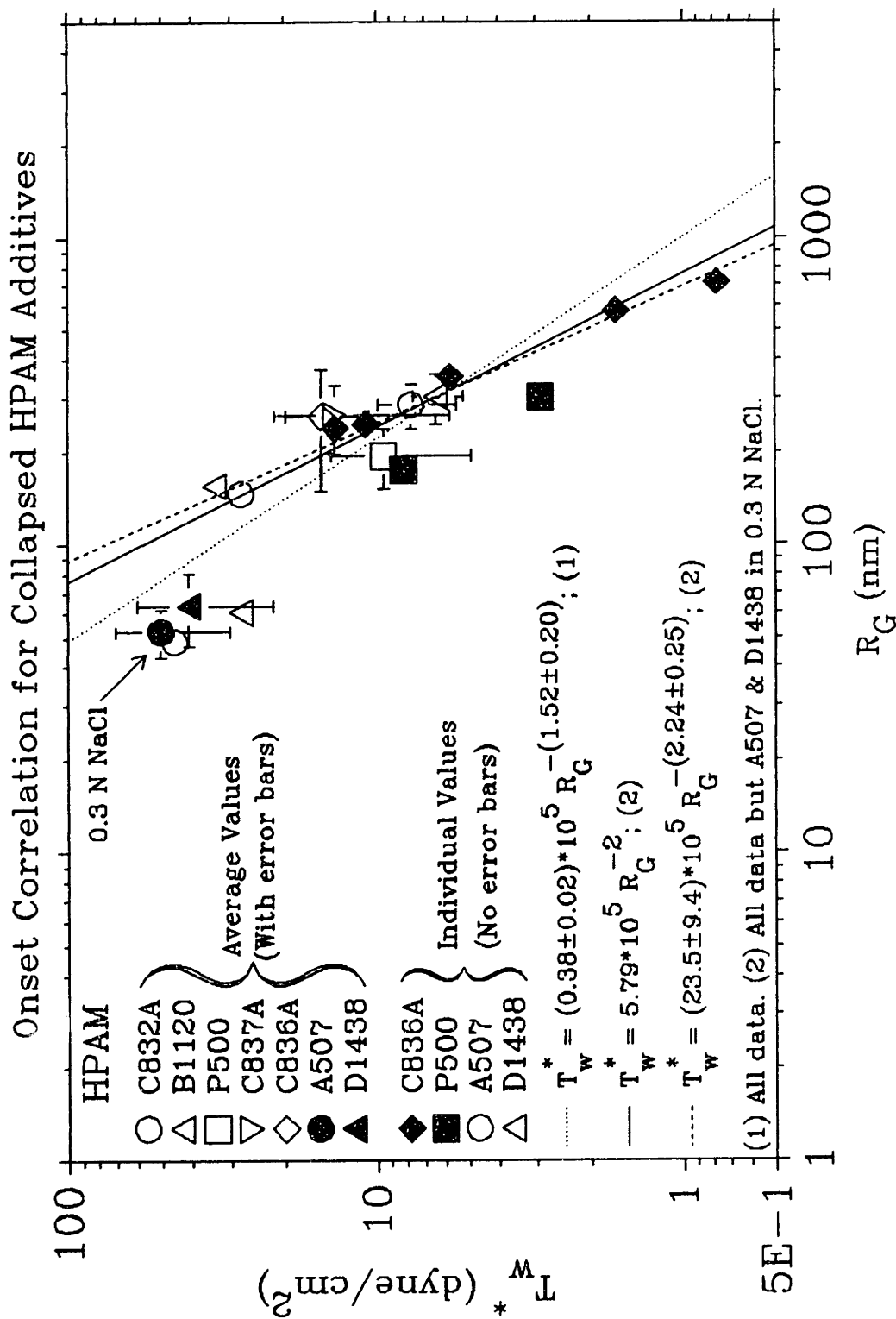


Figure 6.3.2: Onset Correlation for Collapsed HPAM Polymers

1975b). Values of Ω_L for the data points in Figure 6.3.2 are provided in Table 6.3.1; among these data, the average $\Omega_L \approx (8.6 \pm 1.7) \times 10^{-3}$ over a 20-fold range of molecular weights.

6.3.2 Slope Increment

While the macromolecular coil size influences the observed onset of a solution of initially coiled macromolecules, it appears to have little influence on the slope increment, a measure of macromolecular resistance to expansion by the turbulent flow field. Figure 6.3.3 shows the dependence of the slope increment on macromolecular coil size for the same 20.6-wppm solutions of C836A used in Figure 6.3.1. Figure 6.3.3, a log-log plot of δ versus η_{sp}/c shows that the slope increment does not significantly depend on the initial coil size, with $\delta \approx 15.3 \pm 0.7$, roughly constant, for $2500 < \eta_{sp}/c < 70000$. Thus, for initially randomly-coiled macromolecular additives, the turbulent-flow strength, T_w^* , required to excite the macromolecular interaction leading to drag reduction decreases with increasing coil-size, but the molecular deformation processes thereafter associated with δ seem essentially independent of the initial coil size.

For a polymer-solvent pair, the slope increment δ also does not greatly depend on pipe diameter; however, it does depend approximately on the square root of the polymer concentration. Figure 6.3.4 shows the concentration dependence of δ on doubly-logarithmic coordinates for solutions of the seven HPAM additives at high salinity. Except for the concentrations that are very low, with uncertain δ , and those that give rise to nearly maximally drag-reducing turbulent flows, which are independent of

Relation Between Macromolecular Coil Size and Slope Increment

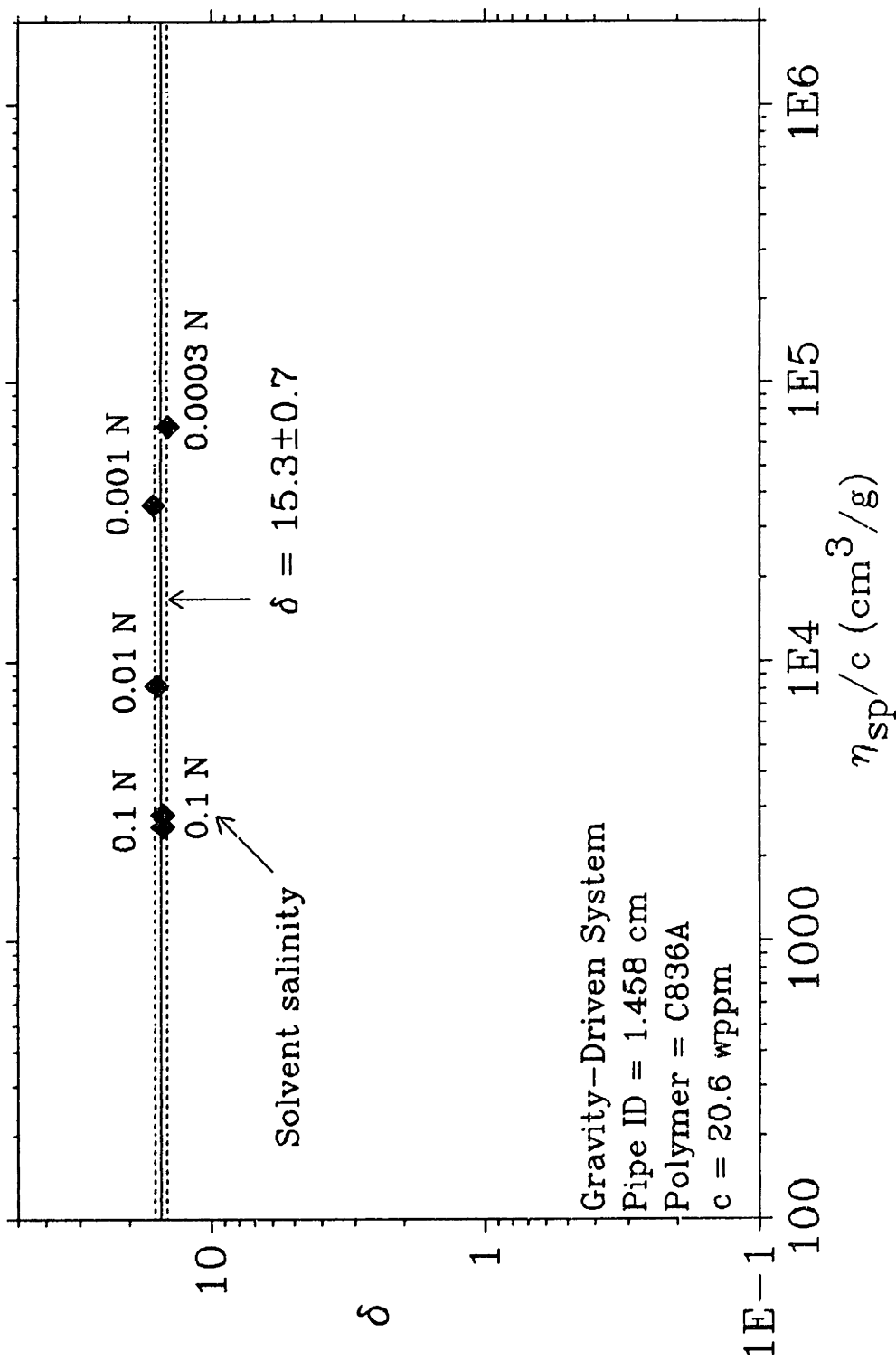


Figure 6.3.3: Relation Between Macromolecular Coil Size and Slope Increment

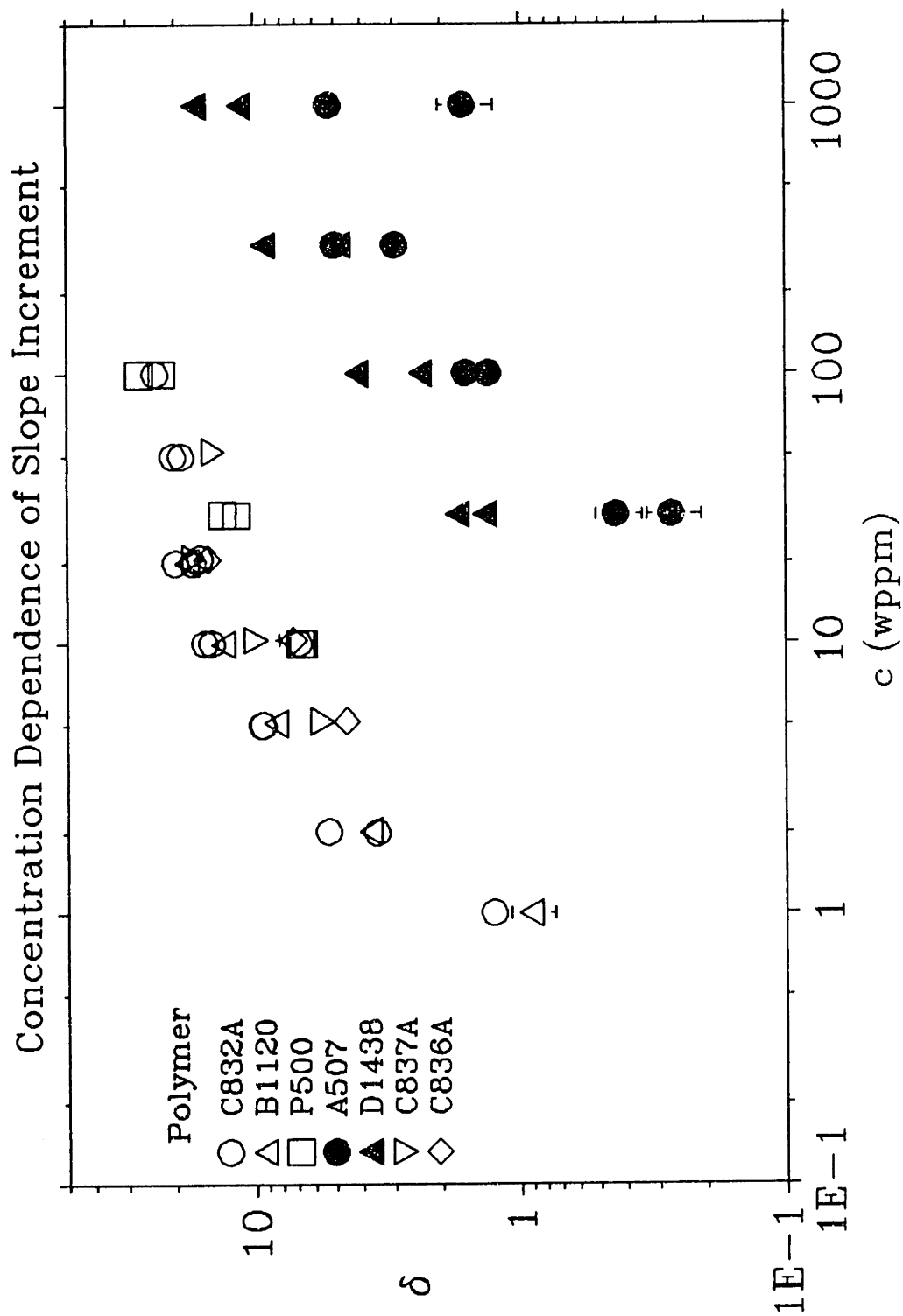


Figure 6.3.4: Concentration Dependence of Slope Increment

Table 6.3.1
Onset Data for Type-A Drag Reduction by HPAM Additives†

HPAM	Concentration Range	Salinity	Estimated Intrinsic Viscosity	Radius of Gyration	Onset Wall Shear Stress ¹	Length-Based Onset Constant
	c		[NaCl]		η_{sp}/c	T_w^*
	(wppm)	(N)	(cm ³ /g)	(nm)	(dyne/cm ²)	
Part A: Average Values						
C832A ²	20-100	0.3	3000	280±50	7.7±2.2	8.5±2.7
B1120	10-100	0.3	3300	300±60	6.4±1.2	8.3±2.4
P500 ²	30-100	0.3	1850	190±40	9.5±4.6	6.5±3.1
A507	300-1000	0.3	340	50±10	50.4±20.1	4.0±1.5
D1438	100-1000	0.3	440	60±20	41.0±19.2	4.4±2.2
C837A	50	0.1	2700	260±70	13.7±7.9	10.8±5.9
C836A	20	0.1	2700	260±110	15.2±4.6	11.2±6.5
Part B: Other Individual Values						
C836A ³	20.6	0.0003	69170	715	0.77(190)	7.1
C836A ³	20.6	0.001	36330	580	1.6(270)	8.3
C836A	20.6	0.01	8190	350	5.8(510)	9.4
C836A ⁴	20.6	0.1	2820	250	10.8(690)	9.0
C836A ⁴	20.6	0.1	2560	240	13.7(770)	9.8
P500	30	0.01	8480	300	2.9	5.8
P500 ⁴	30	0.3	1630	170	8.4	5.4
A507	30-300	0.0001	7000	135	23.7 ⁵	8.6
A507 ⁴	30-300	0.3	330	49	45.6	4.0

HPAM	Concentration Range	Salinity	Estimated Intrinsic Viscosity	Radius of Gyration	Onset Wall Shear Stress ¹	Length-Based Onset Constant
	c	[NaCl]	η_{sp}/c	R_G	T_w^*	$\Omega_L \times 10^3$
	(wppm)	(N)	(cm ³ /g)	(nm)	(dyne/cm ²)	
D1438	30-300	0.0001	5800	140	30	10.1
D1438 ⁴	30-300	0.3	440	60	46.5	4.4

† All solvent physical properties are evaluated at 25°C.
 1 Values in parentheses are the corresponding $Re_p\sqrt{f^*}$.
 2 Data are included from both pipes.
 3 T_w^* and $Re_p\sqrt{f^*}$ are virtual values regressed via (A_p , B_p) data.
 4 Data are incorporated into Part-A averages.
 5 T_w^* data are visual values.

polymer parameters, the data show a slope of one-half, corresponding to a square-root concentration dependence. Data from the 1.458- and 1.021-cm pipes, which are not distinguished for additives C832A(O) and P500(□), either lie adjacently or overlap, showing δ to be essentially independent of pipe-diameter, as previously-established.

To illustrate explicitly the empirical square-root-concentration dependence of δ , the specific slope increment δ/\sqrt{c} is plotted against concentration in Figure 6.3.5 in log-log coordinates. Values of δ/\sqrt{c} for each polymer are approximately constant over concentrations for which turbulent drag reduction in the polymeric regime is not too close to the MDR asymptote. Also, δ/\sqrt{c} does not depend on pipe diameter, or flow length scale, the data for each of additives C832A and P500 in two different pipes showing no obvious differences. Note, however, that the levels of constant δ/\sqrt{c} vary appreciably with additive molecular weight, suggesting a further rescaling of δ/\sqrt{c} on a

macromolecular basis.

To generate a macromolecular-based parameter, Virk(1975b) inserted the molecular weight M_w into the specific slope increment δ/\sqrt{c} to produce an intrinsic slope increment $\Pi = \delta/\sqrt{(c/M_w)}$, equation 2.3-5, which characterizes Type-A drag-reduction efficacy per macromolecule in solution. The intrinsic slope increment Π is found to depend on the number of backbone chain links N_{bb} raised to the 3/2 power for many polymer-solvent systems, with the associated slope modulus κ defined by $\Pi = \kappa N_{bb}^{3/2}$.

Figures 6.3.6 presents the averaged Π versus N_{bb} in doubly-logarithmic coordinates for all HPAM additives. The best-fit line through the data, shown solid in Figure 6.3.6, is:

$$\Pi = (102 \pm 22) \times 10^{-6} N_{bb}^{(1.43 \pm 0.05)} \quad (6.3-6)$$

The exponent of 1.43 and coefficient of $(102 \pm 22) \times 10^{-6}$ in equation 6.3-6 agree well with the literature values of 3/2 and $(80 \pm 20) \times 10^{-6}$ (Virk, 1975b). By assuming an exponent of 3/2 and using the average Π from the Π values of all seven HPAM additives, another line through the data is obtained, shown dotted in Figure 6.3.6:

$$\Pi = 43.5 \times 10^{-6} N_{bb}^{3/2} \quad (6.3-7)$$

While equation 6.3-7 has a coefficient, $\kappa \approx 43.5 \times 10^{-6}$, about half that of equation 6.3-6, $\kappa \approx (102 \pm 22) \times 10^{-6}$, the two lines do not differ greatly in this narrow range of N_{bb} between $\sim 3 \times 10^4$ and $\sim 6 \times 10^5$ backbone links. Table 6.3.2 summarizes the data for Figures 6.3.5 and 6.3.6.

Table 6.3.2
Specific and Intrinsic Slope Increment Data

Polymer	Molecular Weight	Number of Backbone Chain Links	Average Specific Slope Increment	Average Intrinsic Slope Increment	Slope Modulus†
	$M_w \times 10^{-6}$	$N_{bb} \times 10^{-5}$	$\delta N/c$	$\Pi \times 10^{-3}$	$\kappa \times 10^6$
	(g/mole)				
C832A	18.0±5.0	5.0±1.4	4.1±0.7	17.2±5.3	47.9
B1120	20.1±6.4	5.7±1.8	3.6±0.6	16.2±5.4	38.3
P500	9.5±3.5	2.7±1.0	2.3±0.2	7.0±2.0	51.1
A507	1.0±0.3	0.3±0.1	0.16±0.02	0.16±0.04	42.8
D1438	1.4±0.6	0.4±0.2	0.29±0.05	0.35±0.14	56.4
C837A	15.7±6.7	4.4±1.9	2.8±0.6	1.1±0.5	38.1
C836A	15.5±11.0	4.4±3.1	2.5±0.6	9.9±5.9	34.4

† Slope moduli are averages; uncertainties in N_{bb} cause very large uncertainties in the slope moduli.

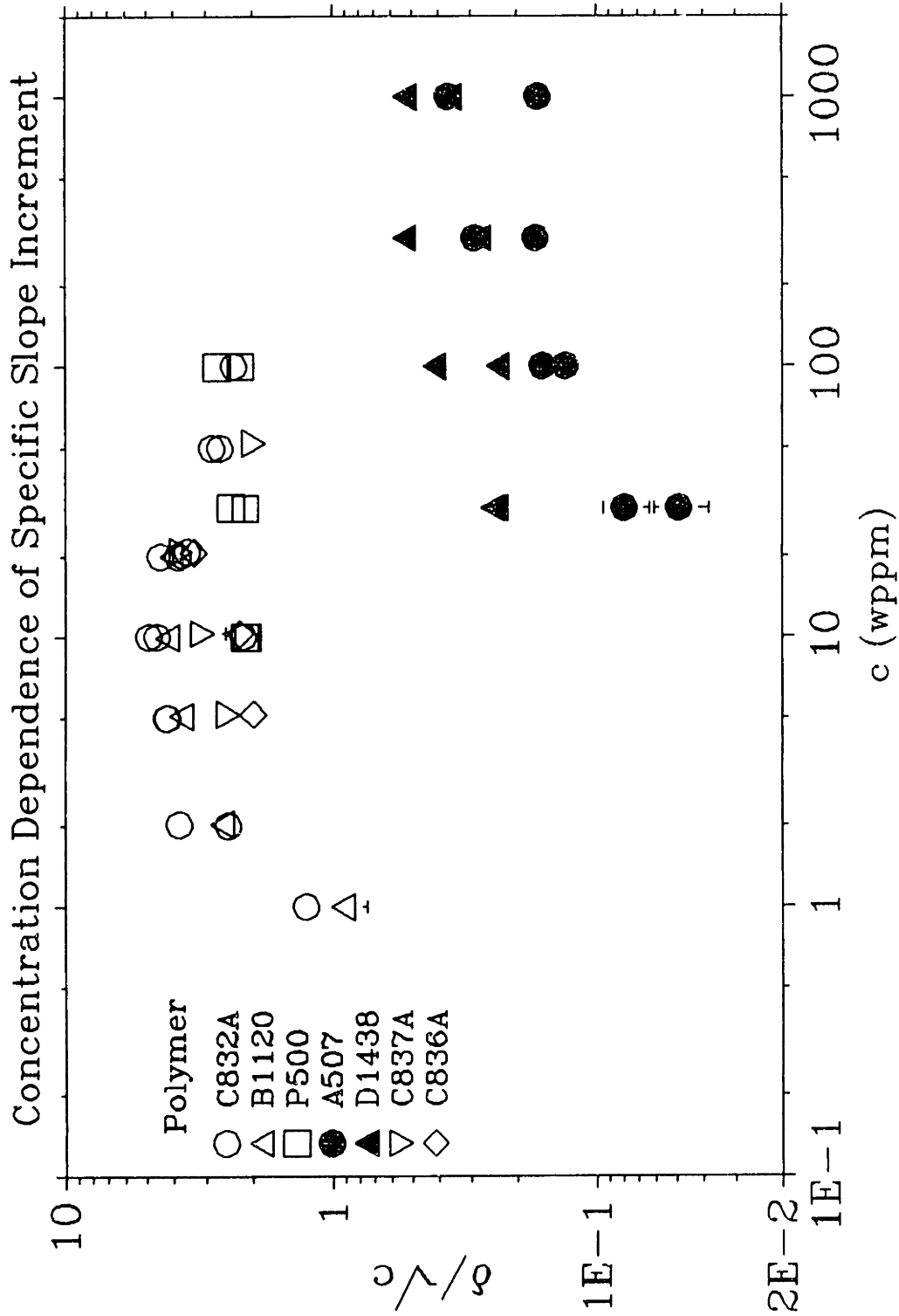


Figure 6.3.5: Concentration Dependence of Specific Slope Increment

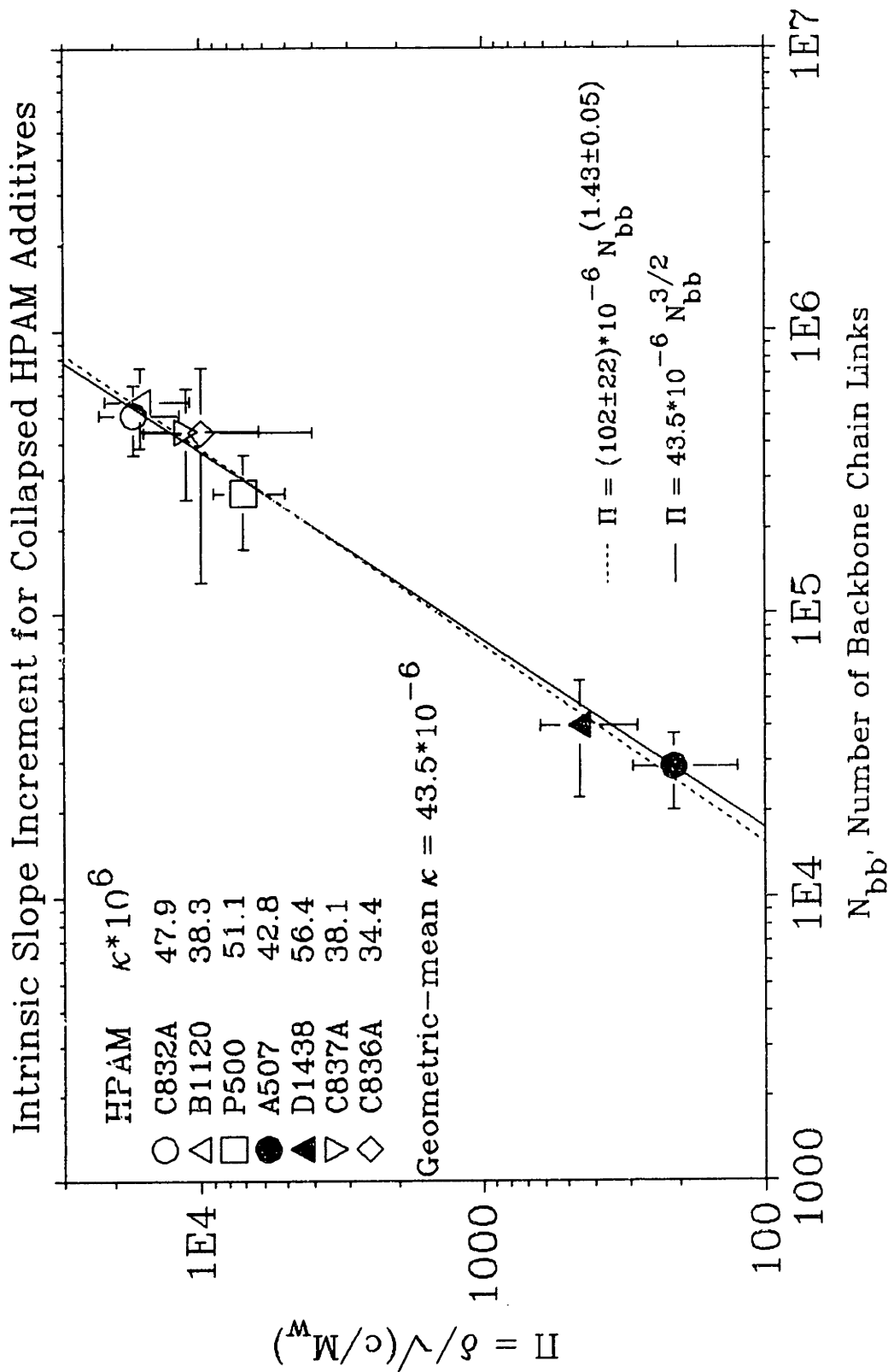


Figure 6.3.6: Intrinsic Slope Increment for Collapsed HPAM Additives

6.4 Type-B Drag Reduction

Type-B drag reduction has hitherto been little studied. Here the new results for HPAM additives in their extended conformations are discussed. A Type-B ladder is primarily defined by the flow enhancements induced by its P segment rungs at a known, high, $Re_c\sqrt{f}$; and secondarily by the wall shear stresses at its retro-onset points, where the rungs intersect the MDR asymptote. The dependence of both these parameters on the molecular properties of the additive are considered.

6.4.1 Flow Enhancement

The observed apparent-slip data for Type-B flow enhancement are analyzed in a manner analogous to the analysis performed on the observed slope-increment data in Type-A flow enhancement.

In Figure 6.4.1, S' at $Re_c\sqrt{f} = 3000$ is plotted against concentration in log-log coordinates for additives C832A, B1120, and P500 in 0.0001 N NaCl solutions from the pump-driven system. For low concentrations of additives C832A and B1120, S' is approximately linear in concentration, having a slope near unity on these coordinates; for $c \geq 20$ wppm, S' becomes constant because of the limiting effect of the MDR asymptote, as shown in Figure 6.4.1. The data for additive P500 show a concentration power dependence less than unity, perhaps because the highest concentrations used are too close to MDR. At $c = 100$ wppm, solutions of all three additives are maximally drag reducing and, thus, reach the asymptotic $S' \approx 20$. Figure 6.4.2 similarly shows the

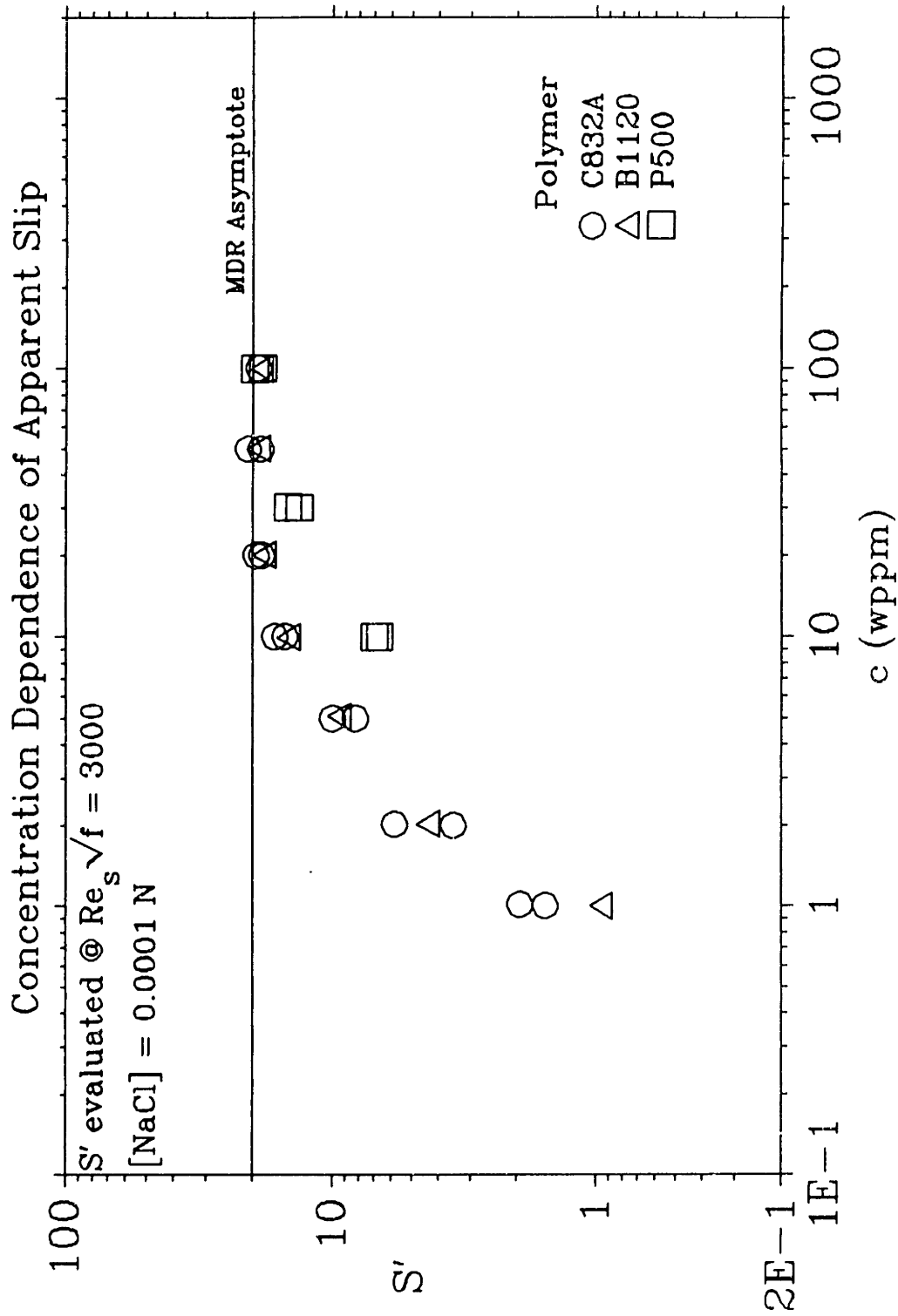


Figure 6.4.1: Concentration Dependence of Apparent Slip at $Re_s \sqrt{f} = 3000$

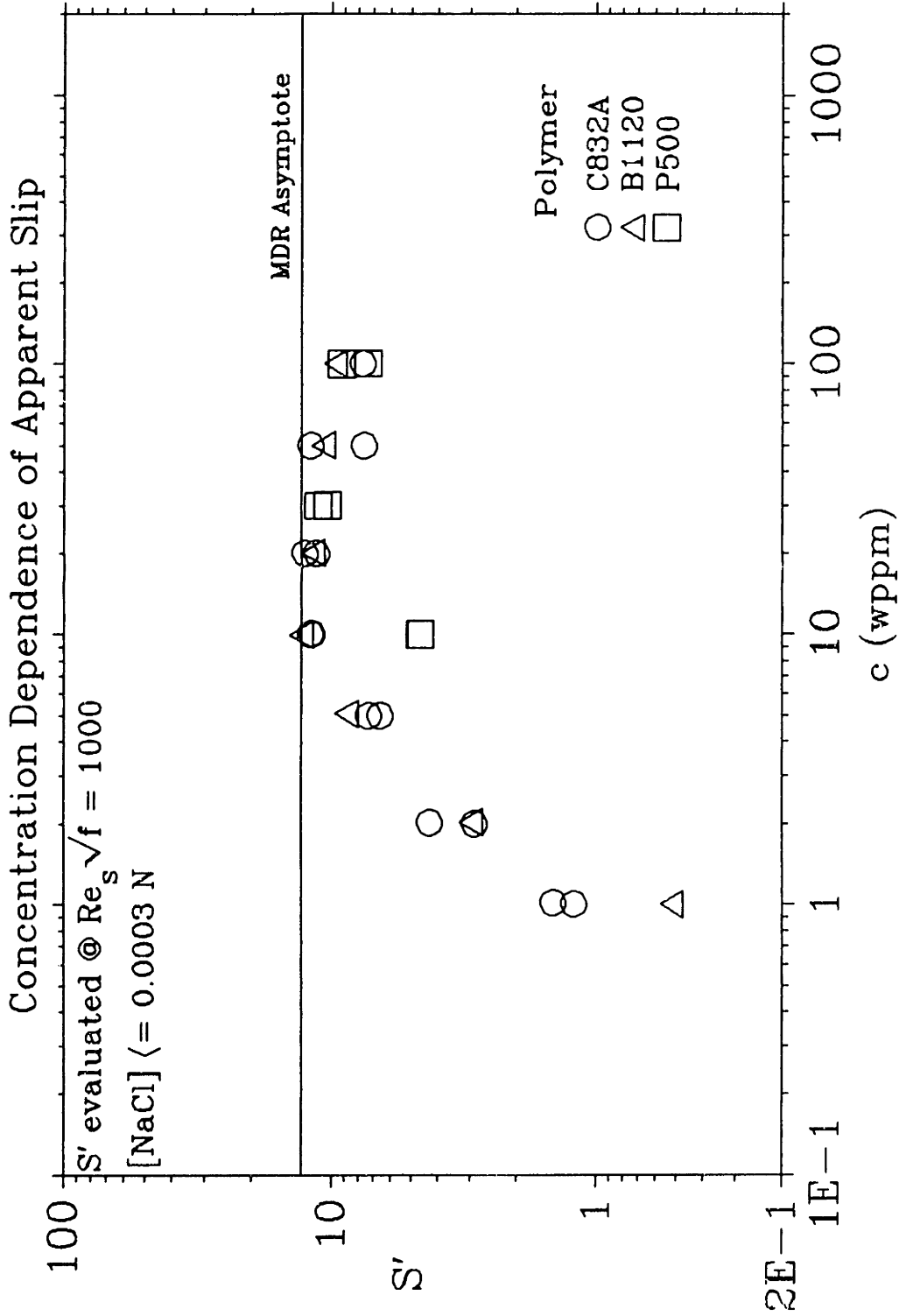


Figure 6.4.2: Concentration Dependence of Apparent Slip at $Re_s \sqrt{f} = 1000$

concentration dependence of S' at $Re_p\sqrt{f} = 1000$ on doubly-logarithmic coordinates for additives C832A, B1120, and P500. For these additives, S' is roughly linear in concentration up to $c = 10$ wppm. At high concentrations, a plateau due to the MDR asymptote is reached at $S' \approx 10$. The data decline from the MDR plateau at the highest concentrations because the associated high laminar viscosities shift the laminar regime to higher $Re_p\sqrt{f}$; thus, these data may not represent fully-turbulent flow.

In Figures 6.4.1 and 6.4.2, data from the 1.458- and 1.021-cm pipes for additives C832A and P500 are not distinguished. To better display the effect of pipe diameter, Figure 6.4.3 displays S' at $Re_p\sqrt{f} \approx 3000$ and 1000 plotted against concentration in log-log coordinates for solutions of additives C832A and P500 with 0.0001 N NaCl from both pipes. With the exception of data at $c = 2$ wppm, S' at respective $Re_p\sqrt{f} = 3000$ and 1000 for additive C832A in the large pipe (\circ, \triangle) and small pipe (\bullet, \blacktriangle) are nearly the same, the difference being less than the ratio of pipe diameters. At high concentrations, S' at $Re_p\sqrt{f} = 3000$ and 1000 reach their respective MDR-asymptote values, $S' \approx 20$ and 13. The wide separation of S' at $Re_p\sqrt{f} = 1000$ from the two pipes for additive C832A at $c = 50$ wppm is likely an artifact, caused by these flows not being fully turbulent, on account of the high laminar viscosity. For additive P500, the same trends for S' are observed at respective $Re_p\sqrt{f} = 3000$ and 1000 in both the large pipe (\square, ∇) and the small pipe ($\blacksquare, \blacktriangledown$). In the two pipes, S' at $Re_p\sqrt{f} = 3000$ are virtually identical and reach the MDR plateau, $S' \approx 20$, at $c = 100$ wppm; similarly, S' at $Re_p\sqrt{f} = 1000$ are nearly the same. Data at $c = 100$ wppm are both more separated and well below the MDR plateau because of the differing, but similar, effects of enhanced laminar viscosity in the two pipes.

Concentration Dependence of Apparent Slip
Effect of Pipe Diameter

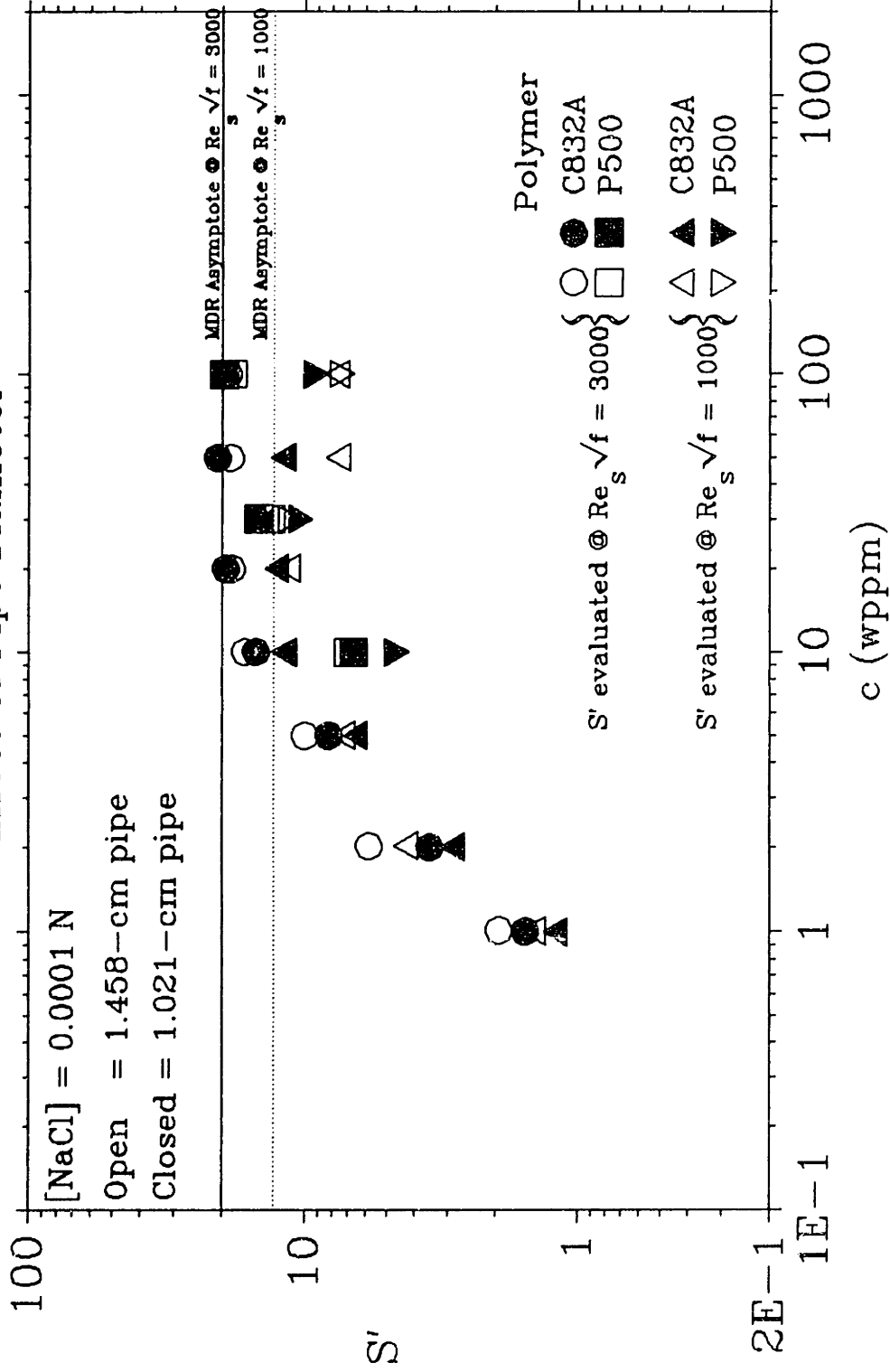


Figure 6.4.3: Concentration Dependence of Apparent Slip, Effect of Pipe Diameter

In summary Figure 6.4.3 suggests that in Type-B drag reduction, the flow enhancement, as measured by the apparent slip S' , is independent of pipe diameter; it can also be seen that S' is only a weak function of $Re_s\sqrt{f}$, increasing slowly therewith.

To better demonstrate the linearity of S' with concentration at low concentrations, Figure 6.4.4 presents the specific slip S'/c at $Re_s\sqrt{f} = 3000$ plotted against concentration on log-log coordinates for the three HPAM additives at low salinity. For $c \leq 10$ wppm, additives C832A and B1120 have respective $S'/c \approx 1.9$ and 1.6 ; the data for $c \geq 10$ wppm rapidly decline along the line corresponding to the MDR asymptote. For additive P500, the initial $S'/c \approx 0.6$ and then declines with increasing concentration, merging into the line determined by the MDR asymptote. Because additives C832A and B1120 are about twice the molecular weight of P500 — respectively 18×10^6 and 20.1×10^6 versus 9.5×10^6 g/mole — the specific slip appears to vary with the molecular weight to a power between one and two, $S'/c \propto M_w^{1-2}$. Also, S'/c is independent of pipe diameter for the data for each of additives C832A and P500 in different pipes. Figure 6.4.5 presents a doubly-logarithmic plot of S'/c at $Re_s\sqrt{f} = 1000$ versus concentration for these three HPAM additives at low salinity. Additives C832A and B1120 with respective $M_w \approx 18 \times 10^6$ and 20.1×10^6 g/mole display similar initial specific slips $S'/c \approx 1.6$; additive P500 with a $M_w \approx 9.5 \times 10^6$ g/mole shows an initial $S'/c \approx 0.4$. In Figure 6.4.5, the specific slip appears to vary more closely with the square of the molecular weight: $S'/c \propto M_w^2$. For $c \geq 20$ wppm, S'/c for these HPAM additives lie adjacent to the line representing the MDR asymptote. The slight divergence at the highest concentrations reflects the large laminar viscosities, which shift the laminar-flow regimes to higher $Re_s\sqrt{f}$.

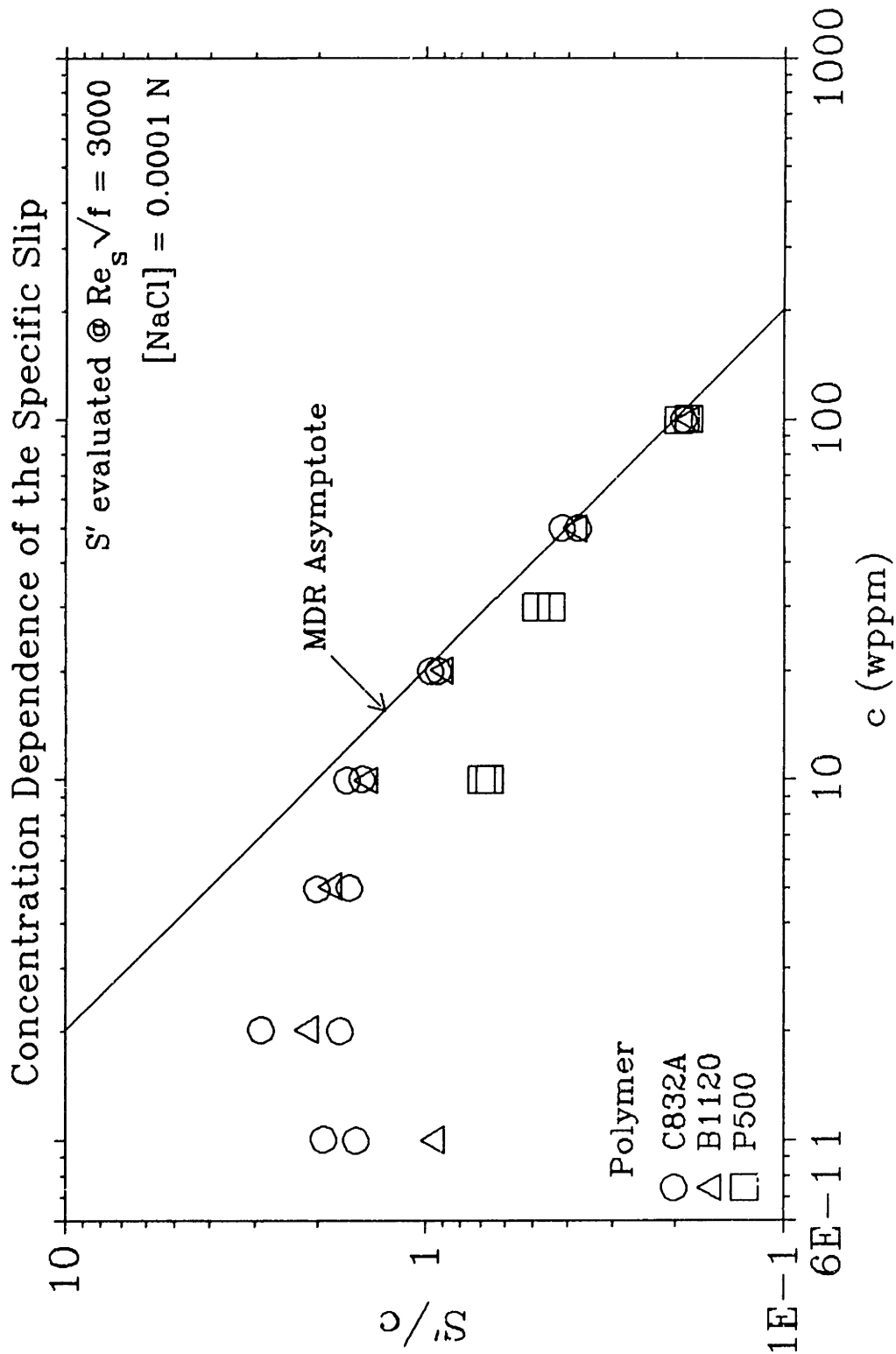


Figure 6.4.4: Concentration Dependence of the Specific Slip at $Re_s \sqrt{f} = 3000$

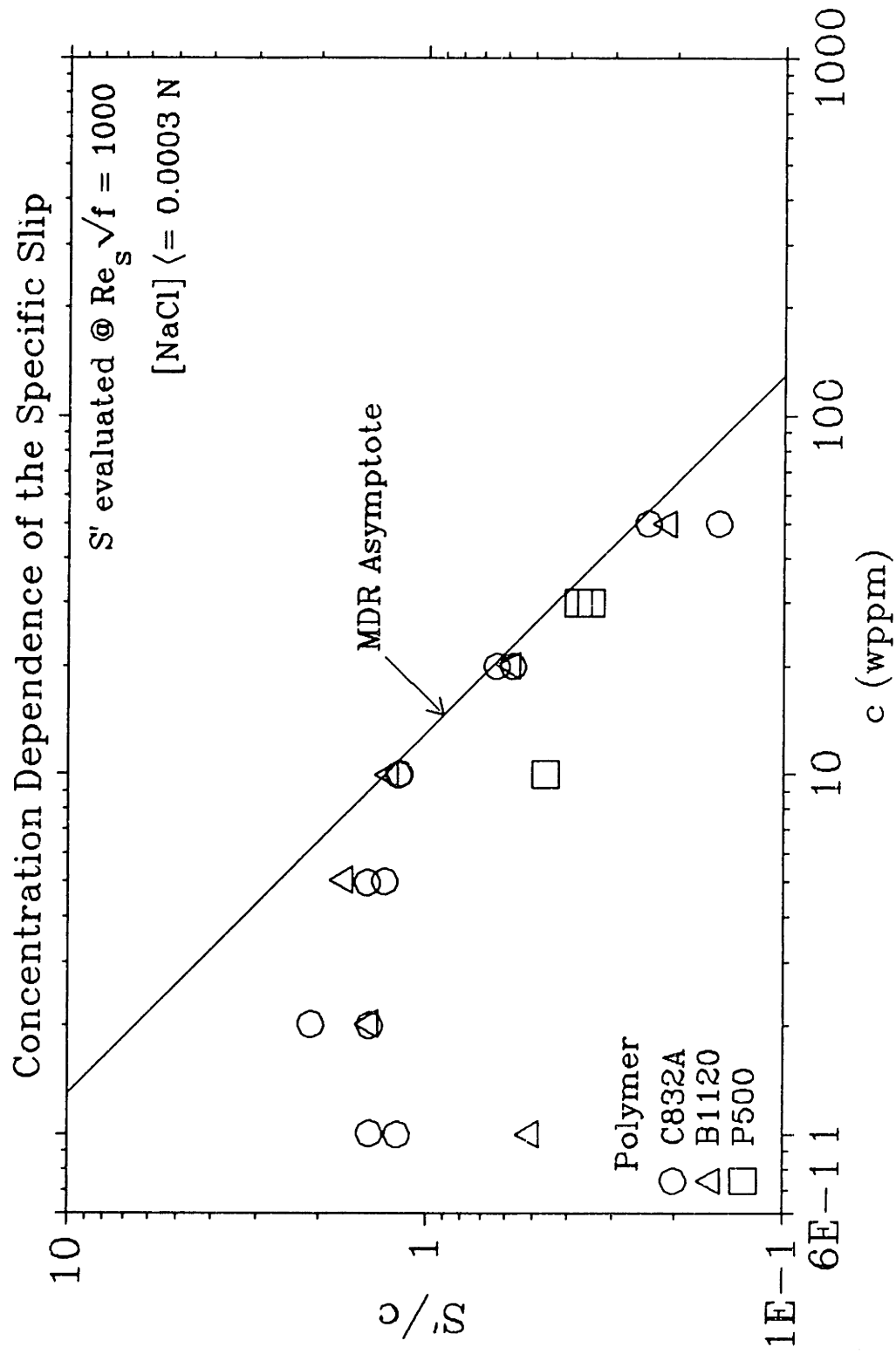


Figure 6.4.5: Concentration Dependence of the Specific Slip at $Re_s \sqrt{f} = 1000$

To further analyze the effect of molecular weight on Type-B drag-reduction, we define an intrinsic slip, a measure of flow enhancement per molecule:

$$\Sigma \equiv \frac{S'}{\left[\frac{c}{M_w} \right]} = \left[\frac{S'}{c} \right] M_w. \quad (6.4-1)$$

Since the intrinsic slip Σ is a molecular quantity, we might expect it to depend upon a molecular attribute of the additive, of which the number of backbone chain links, N_{bb} , is the most fundamental. For any macromolecule, the number of backbone chain links, N_{bb} , and the related contour length, L_c , are derived from molecular weight by $M_w = mN_{bb}$ and $L_c = aN_{bb}$, respectively, where m and a are respectively the molecular weight and length per backbone chain link. For HPAM, specifically, $m = 35.54$ g/mole and $a = 1.26 \times 10^{-8}$ cm. Figure 6.4.6 presents Σ plotted against N_{bb} in log-log coordinates for additives C832A, B1120, and P500 in 0.0001 N NaCl solutions. The best-fit line through the three data points, shown dashed in Figure 6.4.6, is:

$$\Sigma = (1.00 \pm 0.23) \times 10^{-7} N_{bb}^{(2.53 \pm 0.40)} \quad (6.4-2)$$

The N_{bb} exponent of 2.53 in equation 6.4-2 is identically also the molecular-weight dependence of the intrinsic slip, that is, $\Sigma \propto M_w^{2.53}$. Note that because $\Sigma = S'/(c/M_w) = M_w(S'/c)$, the specific slip variation is $S'/c \propto M_w^{1.53}$, as previously observed in Figures 6.4.4 and 6.4.5.

If we assume for the moment (this is justified in §6.6) that the intrinsic slip Σ varies approximately as N_{bb}^3 , then we can define a "slip modulus" λ as the proportionality constant in the relation $\Sigma = \lambda N_{bb}^3$. This is shown by the solid line in

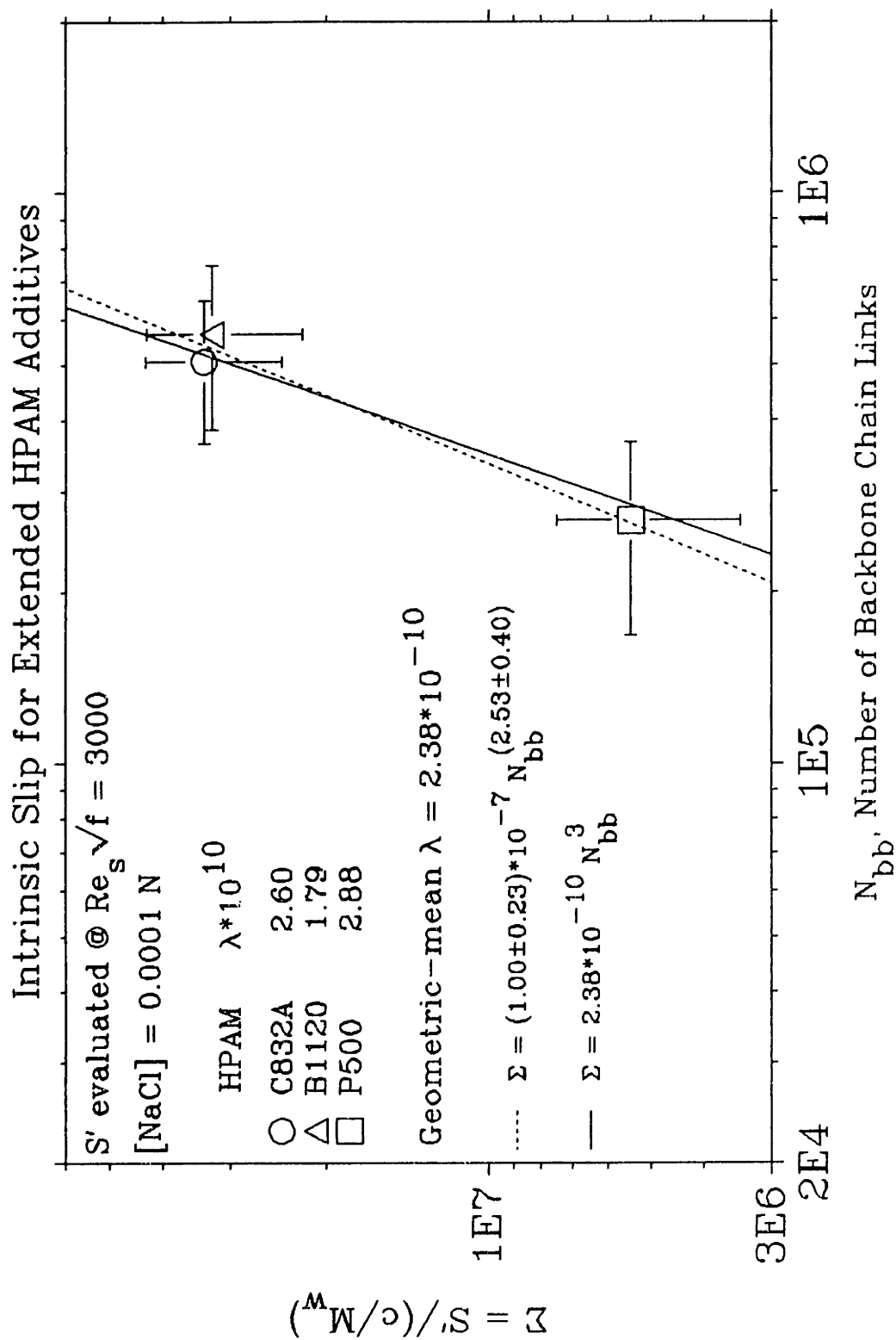


Figure 6.4.6: Intrinsic Slip for Extended HPAM Additives

Figure 6.4.6, corresponding to the equation:

$$\Sigma = 2.38 \times 10^{-10} N_{bb}^3 \quad (6.4-3)$$

where the geometric-mean slip modulus $\lambda = 2.38 \times 10^{10}$ g/mole/wppm. From equation 6.4-3, the specific slip S'/c is seen to vary as macromolecular contour length to the third power, by the expression

$$\frac{S'}{c} = \left[\frac{\lambda}{a^3} \right] \left[\frac{L_c^3}{M_w} \right] \quad (6.4-4)$$

with λ in g/mole/wppm, backbone-link length a and contour length L_c in cm, and M_w in g/mole. If every macromolecule in solution occupied a sphere of diameter equal to its contour length, then this "pervaded" volume fraction per wppm of additive, X_v/c , must also vary as L_c^3 , given by the expression

$$\frac{X_v}{c} = \left[\frac{\pi L_c^3}{6} \right] \left[\frac{\rho N_A}{10^6 M_w} \right] \quad (6.4-5)$$

with L_c in cm, fluid density ρ in g/cm³, M_w in g/mole, and Avogadro's number $N_A = 6.022 \times 10^{23}$ mole⁻¹. Equations 6.4-4 and 6.4-5 both have factors of L_c^3/M_w on their respective right sides, so the maximum pervaded volume fraction per unit of slip, X_v/S' , depends solely on the physical properties of the additive and solvent, and should thus be constant for a given polymer-solvent system. From equations 6.4-4 and 6.4-5, X_v/S' can be written

$$\frac{X_v}{S'} = \left[\frac{\pi L_c^3}{6} \right] \left[\frac{\rho N_A}{10^6 M_w} \right] \left[\frac{c}{S'} \right] = \left[\frac{\pi}{6 \times 10^6} \right] \left[\frac{\rho N_A a^3}{\lambda} \right] \quad (6.4-6)$$

With $\rho \approx 1 \text{ g/cm}^3$, $a \approx 1.26 \times 10^{-8} \text{ cm}$, and $\lambda = 2.38 \times 10^{-10} \text{ g/mole/wppm}$, $X_v/S' \approx 2630$ for the present HPAM additives — C832A, B1120, and P500. Thus, to induce unit flow enhancement, the HPAM additive macromolecules would have to pervade a volume 2630 times greater than that of the solvent surrounding them. Since that is impossible, the additive macromolecules must align themselves to a considerable extent, even in the turbulent flow field. All slip data are summarized in Table 6.4.

Table 6.4
Specific and Intrinsic Slip Data

HPAM	Molecular Weight	Number of Backbone Chain Links	Contour Length
	$M_w \times 10^{-6}$	$N_{bb} \times 10^{-5}$	$L_c \times 10^{-3}$
	(g/mole)		(cm)
C832A	18.0 ± 5.0	5.0 ± 1.4	6.4
B1120	20.1 ± 6.4	5.7 ± 1.8	7.1
P500	9.5 ± 3.5	2.7 ± 1.0	3.4
.			
Average Specific Slip†	Average Intrinsic Slip†	Volume Fraction per wppm	Volume Fraction per unit slip
S'/c	$\Sigma \times 10^{-6}$	X_v/c	X_v/S'
(wppm ⁻¹)	(g/mole/wppm)	(wppm ⁻¹)	
1.87	33.6 ± 9.4	4520	2420
1.62	32.5 ± 10.4	5640	3480
0.58	5.45 ± 2.02	1260	2170
† These parameters are evaluated at $Re_s \sqrt{f} = 3000$.			

6.4.2 Retro-Onset

Here retro-onset data in Type-B drag reduction are analyzed for the first time according to a model of an ideal Type-B ladder.

As mentioned briefly in §5.3, the retro-onset wall shear stress $T_w^\#$ in the idealized Type-B ladder depends on concentration, pipe diameter, and flow-enhancement efficiency of the additive, characterized by the specific slip S'/c .

In an ideal Type-B ladder, each rung, or P segment, is parallel to N and has a constant specific slip, S'/c , that provides a corresponding $1/\sqrt{f_p}$ within the polymeric regime; each rung spans a range of $Re_s\sqrt{f}$, with lower bound at the retro-onset point, $Re_s\sqrt{f}^\#$, where it intersects the MDR asymptote, and an upper bound of $Re_s\sqrt{f}^\wedge$, which denotes the degradation falloff, where the rung begins to deviate downward from its parallel path. Since a rung's parallel displacement above N is proportional to c , the retro-onset $Re_s\sqrt{f}^\#$ increases with increasing c , rungs farther above N intersecting the MDR asymptote M at higher $1/\sqrt{f_p}$ and, therefore, higher $Re_s\sqrt{f}^\#$. In PK coordinates, each rung is described by the equation

$$\frac{1}{\sqrt{f_p}} = 4.0 \log Re_s\sqrt{f} - 0.4 + c \left[\frac{S'}{c} \right] \quad (6.4-7)$$

The intersection of P with M, that is, with equation 2.3-7, provides the retro-onset point:

$$Re_s\sqrt{f}^\# = 10 \left[\frac{c \frac{S'}{c} + 32}{-15} \right] \doteq 136 + 10^{\frac{S'}{15}} \quad (6.4-8)$$

where the constant $136 = Re_s\sqrt{f}^\#_0$ is physically the intersection of the zero concentration

rung, that is, the PK line N, with M. The nondimensional equation 6.4-8 is independent of pipe diameter; however, converting $Re_s \sqrt{f}^\#$ to $T_w^\#$ by the relation $T_w^\# = (\rho \nu_s^2)(Re_s \sqrt{f}^\#)^2 / (2D^2)$ yields a dimensional, general equation in which $T_w^\#$ depends on pipe diameter:

$$\log T_w^\# = \log T_{w_o}^\# + \frac{2c}{15} \left[\frac{S'}{c} \right] \quad (6.4-9)$$

where $T_{w_o}^\#$ represents the stress at the intersection of the Newtonian turbulent baseline N and the MDR asymptote M. Whereas in equation 6.4-8, the pipe-diameter independent $Re_s \sqrt{f}_o^\# = 10^{32/15} \approx 136$, the pipe-diameter dependent $T_{w_o}^\# = (\rho \nu_s^2)(Re_s \sqrt{f}_o^\#)^2 / (2D^2) \approx 0.346$ and 0.705 dyne/cm² for the 1.458- and 1.021-cm pipes, respectively. Recall that the experimentally obtained retro-onset relation 5.3-1 in §5.3 obeyed the form of equation 6.4-9. While equation 5.3-1

$$\log T_w^\# = -0.436 + 0.134c \quad (5.3-1)$$

has approximately the theoretical ordinal intercept, $\log T_{w_o}^\# = -0.436$ or $T_{w_o}^\# = 0.37$ dyne/cm², the coefficient $(2/15)(S'/c)$ yields an $S'/c \approx 1.00$ which is lower than the observed average specific slip of additives C832A and B1120 in the 1.458-cm pipe, $S'/c \approx 1.75$; the differences between these two specific slips are caused by the observed Type-B ladders being less than perfect, with rungs not entirely parallel to N. To account for ladder imperfections, the factor β is incorporated into equation 6.4-9 to give the following expression for the observed Type-B ladders

$$\log T_w^\# = \log T_{w_o}^\# + \left[\frac{2}{15} \right] \beta \left[\frac{S'}{c} \right] c \quad (6.4-10)$$

For the HPAM data shown in Figure 6.4.6, the ladder-imperfection factor $\beta \approx 0.58$.

6.5 Comparisons Between Type-A and Type-B Flow Enhancement

After separate analyses of Type-A and Type-B flow enhancement in §6.3 and §6.4, the two types are directly compared to establish quantitatively the relative effectiveness of initially collapsed and extended macromolecules on flow enhancement. In §6.5.1, the slip ratio at constant concentration, a measure of relative flow enhancement by equally concentrated solutions of initially collapsed and extended additives, is introduced. In §6.5.2, additive equivalence and isoslip are defined to quantify the concentration equivalence at constant flow enhancement between solutions of initially collapsed macromolecules and solutions of initially extended macromolecules.

6.5.1 Slip Ratio at Constant Concentration

In the polymeric regime, Type-A drag reduction is observed never to exceed Type-B drag reduction, that is, $S'_A < S'_B$, with the former approaching the latter as $Re_s\sqrt{f}$ increases. Hence, initially random-coiling macromolecules in Type-A drag reduction are stretched toward the extended conformations present in Type-B drag reduction. Because the extended conformation induces flow enhancement, the slip ratio S'_A/S'_B at fixed concentration, defined as R_{sc} , directly reflects relative macromolecular extension; thus, the dependence of R_{sc} on $Re_s\sqrt{f}$ should provide insight into the dynamics of coil extension by the turbulent flow.

Figure 6.5.1 illustrates in semilogarithmic coordinates the dependence of the slip ratio at constant concentration on $Re_s\sqrt{f}$ and salinity for three 30-wppm P500 solutions

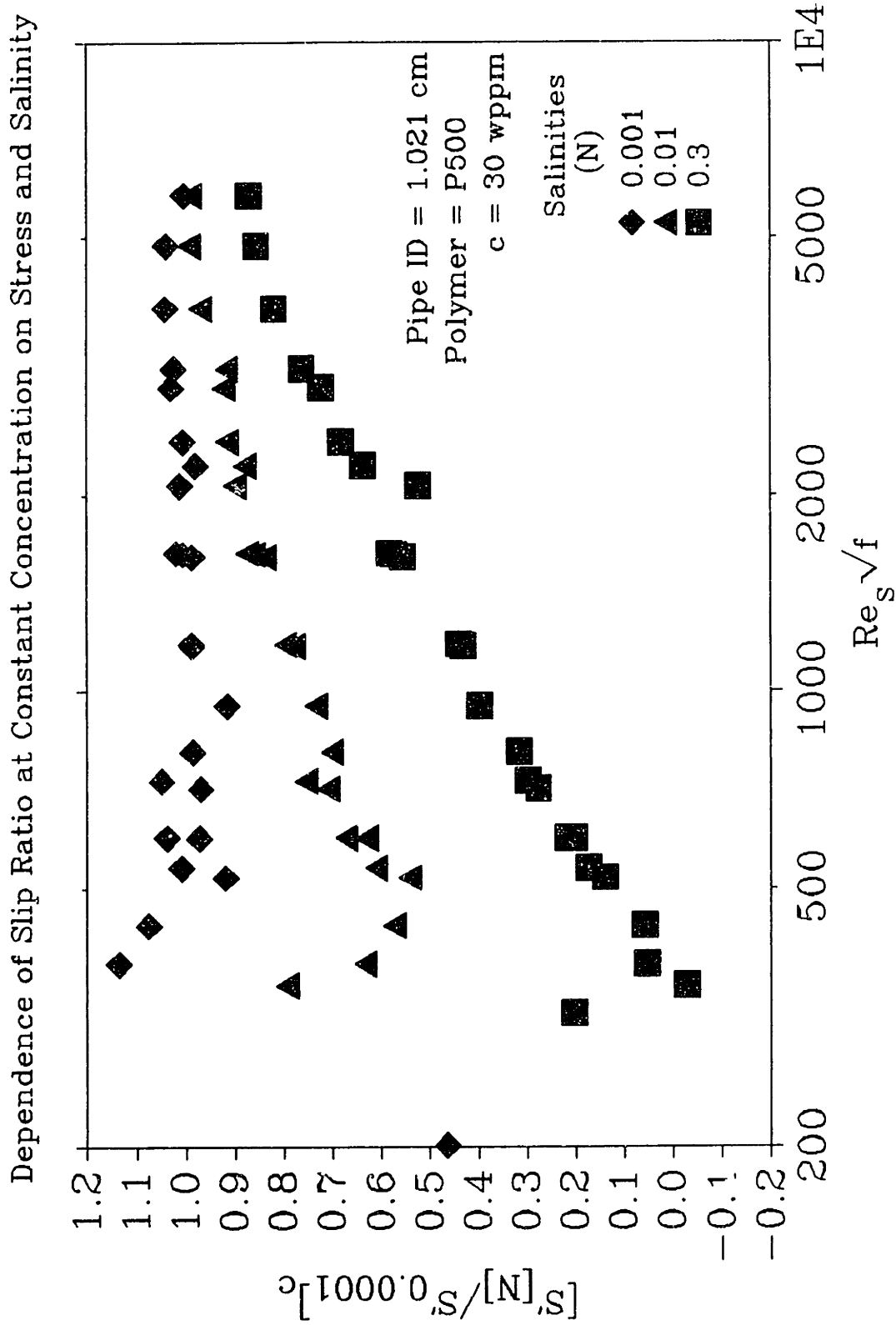


Figure 6.5.1: Dependence of Slip Ratio at Constant Concentration on Stress and Salinity

in the 1.021-cm pipe with 0.3, 0.01, and 0.001 N NaCl, each of which is referenced to a fourth 30-wppm P500 solution also in the 1.021-cm pipe with 0.0001 N NaCl. Because only the 0.3-N P500 solution exhibits Type-A behavior, whereas the 0.01- and 0.001-N P500 solutions exhibit behaviors somewhere between Types A and B, the slip ratio in Figure 6.5.1 is written as $[S'_{[N]}/S'_{0.0001}]_c$. For the 30-wppm P500 solution in 0.3 N NaCl(■), $[S'_{[N]}/S'_{0.0001}]_c \approx 0$ at $Re_s\sqrt{f}^* \approx 450$ and then increases monotonically, but with decreasing slope, to $[S'_{[N]}/S'_{0.0001}]_c \approx 0.85$ at $Re_s\sqrt{f} \approx 5000$. The observed increase in the slip ratio for $Re_s\sqrt{f} > Re_s\sqrt{f}^*$ reflects the progressive extension of the initially-collapsed macromolecular conformation with increasing turbulent flow strength. For the 0.01-N P500 solution(▲), $[S'_{[N]}/S'_{0.0001}]_c \approx 0.55$ at $Re_s\sqrt{f} \approx 450$ and increases with shallow slope up to $Re_s\sqrt{f} \approx 5000$ at which $[S'_{[N]}/S'_{0.0001}]_c \approx 0.95$. For the 0.001-N P500 solution(◆), $[S'_{[N]}/S'_{0.0001}]_c \approx 1.0$, approximately constant, for $500 \leq Re_s\sqrt{f} \leq 5000$. These results suggest that the extended conformations of the additive induce drag reduction, and thence the more closely an initial conformation resembles the active extended form, the more effective it is in drag reduction.

Figure 6.5.2 shows the slip ratio for the extreme conformations, $R_{sc} = S'_A/S'_B$ versus $Re_s\sqrt{f}$ in semilogarithmic coordinates for solution pairs, in 0.3 N and 0.0001 N NaCl, of additives C832A at $c = 2$ and 5 wppm in the 1.458-cm and 1.021-cm pipes, B1120 at $c = 2$ and 5 wppm in the 1.458-cm pipe, and P500 at $c = 10$ and 30 wppm in the two pipes. Data for these additives at $c = 2, (5,10),$ and 30 wppm characterize the relative macromolecular extensions at flow enhancements near the turbulent baseline N, in the polymeric regime P, and near the MDR asymptote M, respectively. In the region $200 < Re_s\sqrt{f} < 500$, R_{sc} declines precipitously from 0.8 ± 0.1 to 0.0 ± 0.1 with

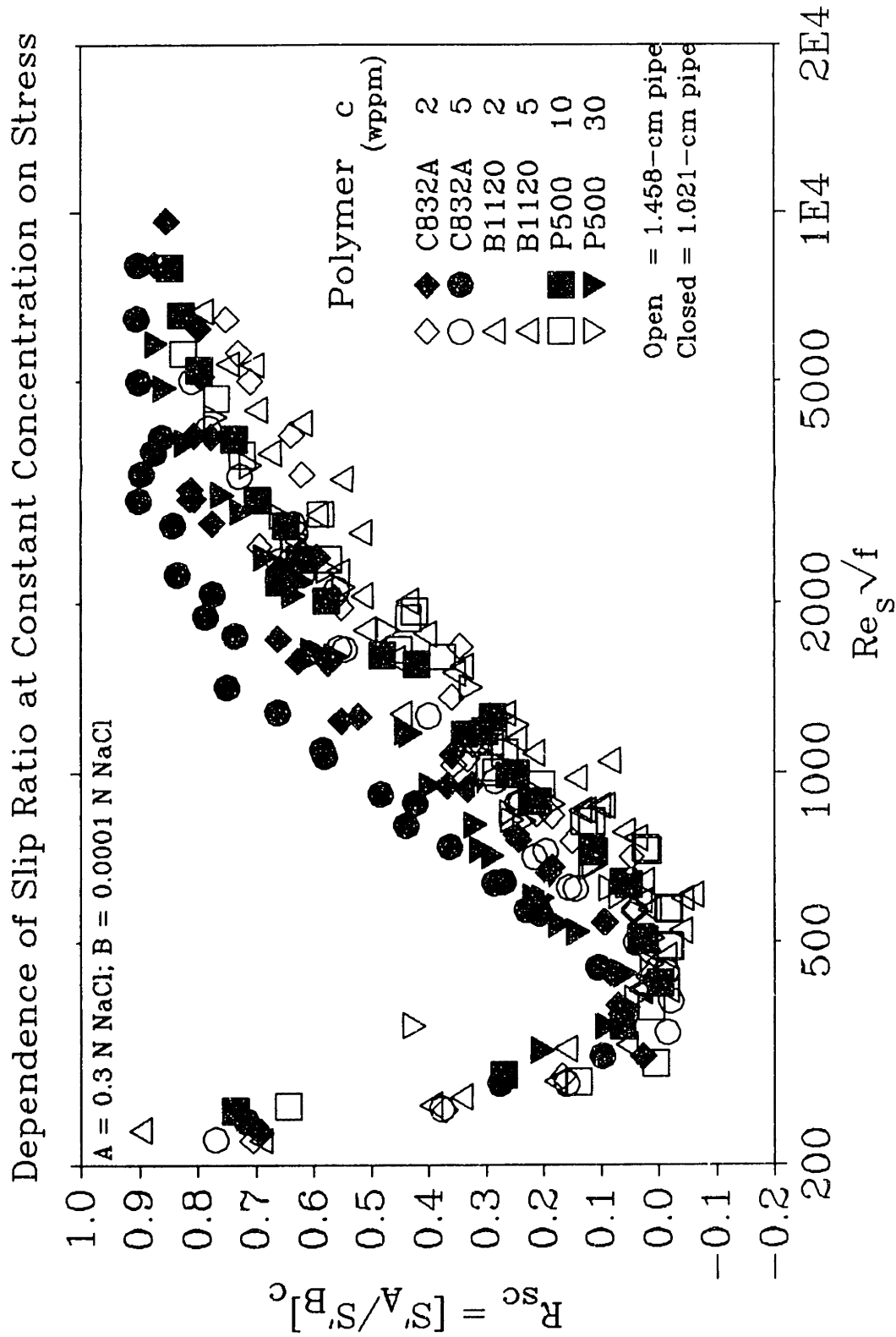


Figure 6.5.2: Dependence of Slip Ratio at Constant Concentration on Stress

increasing $Re_3\sqrt{f}$, for all additives. The behavior in this region arises from the relative positions of laminar-to-turbulent transitions common to Type-A flow trajectories and rightward-shifted, drag-enhancing laminar segments common to Type-B flow trajectories, given that $Re_3\sqrt{f}^* \approx 530 \pm 40$, 610 ± 40 , and 630 ± 70 for additives C832A, B1120, and P500, respectively, at these concentrations. From being approximately zero at $Re_3\sqrt{f} \approx 550 \pm 100$, in the vicinity of the onset points, R_{sc} increases with increasing $Re_3\sqrt{f}$ up to $R_{sc} \approx 0.8$ at $Re_3\sqrt{f} \approx 3000$ for all additives at all concentrations. The near universality of the broad band of R_{sc} -versus- $Re_3\sqrt{f}$ data, combined with the observations that $S'_A \geq 0$ only for $Re_3\sqrt{f} \geq Re_3\sqrt{f}^*$, suggest a more refined plot of R_{sc} versus the normalized flow-strength parameter $Re_3\sqrt{f}/Re_3\sqrt{f}^*$.

Figure 6.5.3, a semilogarithmic plot of R_{sc} vs. $Re_3\sqrt{f}/Re_3\sqrt{f}^*$, presents the data shown in Figure 6.5.2 with an abscissa normalized by $Re_3\sqrt{f}^*$, to remove the influence of differing onset points among the additives. For $0.8 < Re_3\sqrt{f}/Re_3\sqrt{f}^* < 1$, $R_{sc} \approx 0$. At $Re_3\sqrt{f}/Re_3\sqrt{f}^* \approx 1$, all 10 curves are essentially fixed at $R_{sc} \approx 0$. For $Re_3\sqrt{f}/Re_3\sqrt{f}^* > 1$, R_{sc} increases monotonically with increasing $Re_3\sqrt{f}/Re_3\sqrt{f}^*$ up to $R_{sc} \approx 0.6$ at $Re_3\sqrt{f}/Re_3\sqrt{f}^* \approx 5$, with the data in a narrower band than that in Figure 6.5.2. For $Re_3\sqrt{f}/Re_3\sqrt{f}^* > 5$, the rate of increase of R_{sc} declines, and at $Re_3\sqrt{f}/Re_3\sqrt{f}^* \approx 15 \pm 5$, all data attain the final asymptotic $R_{sc} \approx 0.8 \pm 0.1$.

The shape of the data in Figure 6.5.3 suggests a relation that satisfies the boundary conditions $R_{sc} = 0$ at $Re_3\sqrt{f}/Re_3\sqrt{f}^* = 1$ and $R_{sc} \rightarrow 1$ as $Re_3\sqrt{f}/Re_3\sqrt{f}^* \rightarrow \infty$, having the general form: $R_{sc} = 1 - (Re_3\sqrt{f}/Re_3\sqrt{f}^*)^x$. After some trial and error, the following equation, shown in Figure 6.5.3 by the solid curve, is found to well approximate the data:

Dependence of Slip Ratio at Constant Concentration on Normalized Stress

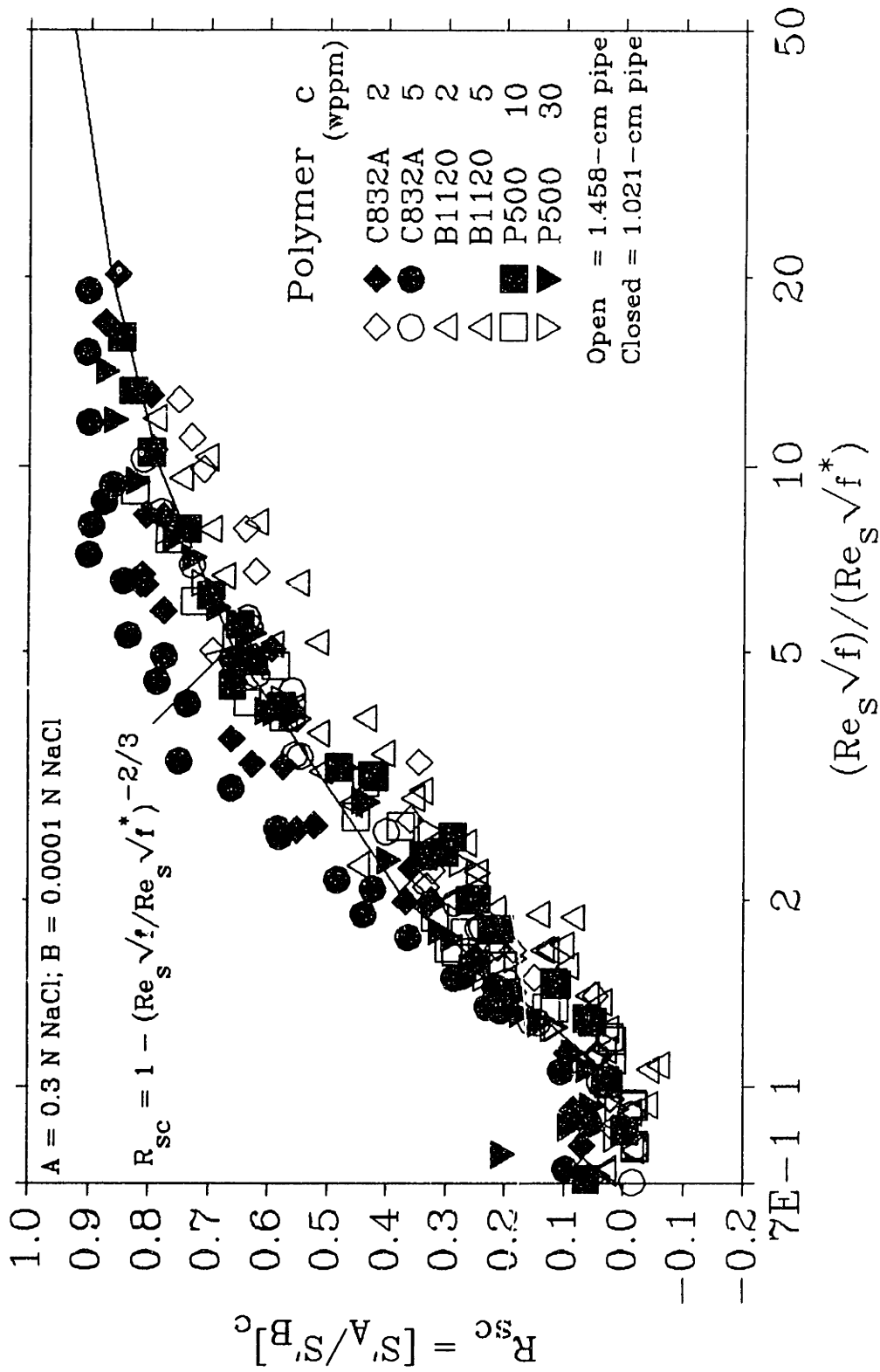


Figure 6.5.3: Dependence of Slip Ratio on Normalized Stress

$$R_{sc} = 1 - \left[\frac{Re_s \sqrt{f}}{Re_s \sqrt{f}^*} \right]^{-2/3} \quad (6.5-1)$$

Equation 6.5-1 physically represents the extension of initially collapsed, random-coiling HPAM macromolecule towards their fully extended conformations by the turbulent flow field. This process seems relatively independent of additive parameters and absolute wall shear stress levels. Relation 6.5-1 provides an indication of the normalized flow strengths required to achieve significant extensions of initially collapsed, random-coiling macromolecules; for $R_{sc} = 0.5$, $T_w/T_w^* = 10$, while for $R_{sc} = 0.8$, $T_w/T_w^* = 125$. These also indicate that macromolecular extension is most facile at low flow strengths, near onset, and then becomes increasingly more difficult at higher flow strength.

6.5.2 Additive Equivalence Between Types A and B Drag Reduction

Figure 6.5.4, a semilogarithmic PK plot with abscissa $Re_s \sqrt{f}$ and ordinate $1/\sqrt{f}$, provides an example of an isoslip point and additive equivalence for additive C832A among a 5.6-wppm solution in 0.00001 N NaCl(\square , abbr 5.6B), a 20.9-wppm solution in 0.00001 N NaCl(\diamond , abbr 20.9B), and a 20.7-wppm solution in 0.1 N NaCl(\blacklozenge , abbr 20.7A). The former two trajectories are part of a Type-B ladder, while the third belongs to a Type-A fan. The lines L, N, and M respectively represent the Newtonian laminar and turbulent baselines and the MDR asymptote. Laminar regimes are omitted to provide the most-expansive view. It is seen that the trajectory 20.7A intersects 5.6B at $(Re_s \sqrt{f}, 1/\sqrt{f}) \approx (950, 15.1)$. This is termed an "isoslip point", since both solutions here exhibit

Example of Additive Equivalence at an Isoslip Point

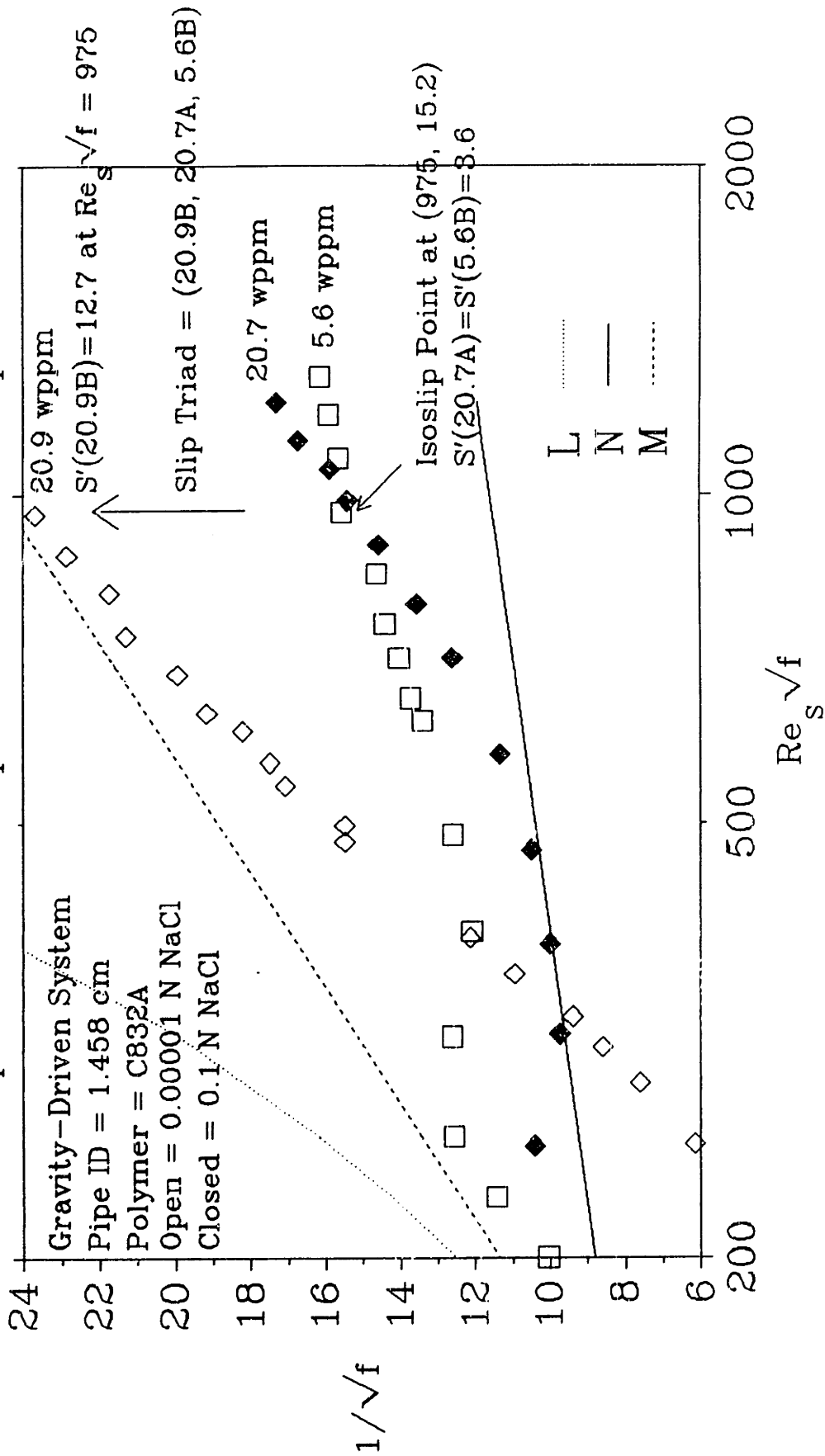


Figure 6.5.4: Example of Additive Equivalence at an Isoslip Point

the identical flow enhancement, $S'(20.7A) = S'(5.6B) \approx 3.6$. At this isoslip point, 20.7 wppm of the initially collapsed conformation and 5.6 wppm of the initially extended conformation are evidently equivalent in their abilities to reduce drag. The term "additive equivalence" is used to describe such a case, where two different additive solutions cause the same drag reduction. Continuing, at the isoslip $Re_s\sqrt{f} \approx 950$, the trajectory 20.9B exhibits $S' = 12.7$, generating a "slip triad" (20.9B, 20.7A, 5.6B) with associated $S'(12.7, 3.6, 3.6)$. Within this triad, the collapsed to extended slip ratio at constant concentration, $R_{sc} = S'(A)/S'(B) = 3.6/12.7 \approx 0.28$, while the extended to collapsed concentration ratio at constant slip $R_{cs} = c_B/c_A = 5.6/20.7 \approx 0.27$. The essential equality between R_{sc} and R_{cs} is striking. Physically, $R_{sc} = R_{cs}$ implies that, for fixed total additive concentration, the collapsed to extended slip ratio R_{sc} at any $Re_s\sqrt{f}$ simply represents the fraction of originally collapsed macromolecules that have become extended in the flow, and thence effective in drag reduction.

6.5.2.1 Analysis of Isoslip Points and Additive Equivalences

The detailed flow trajectories presented in §5.2 for additive solutions at high and low salinity are intercalated to establish isoslip points and additive equivalences. Two PK plots, with the laminar regimes omitted, demonstrate isoslip points for each additive. In each pair of plots, alternate spokes of a Type-A fan are superposed upon an entire Type-B ladder, identifying all isoslip points between the two drag-reduction structures.

Figures 6.5.5 and 6.5.6 illustrate isoslip points among solutions of additive C832A, comprising data at 0.3 N and 0.0001 N NaCl, from the pump-driven system

using the 1.458-cm pipe. In the former, Type-A fan spokes at $c = 5$ and 20 wppm(5A and 20A) are shown with Type-B ladder rungs at $c = 1, 2, 5, 10,$ and 20 wppm(1B, 2B, 5B, 10B, and 20B); in the latter, the 2A and 10A spokes of the Type-A fan are superposed upon the 1B, 2B, 5B, and 10B rungs of the Type-B ladder. The lines L, N, and M, shown for reference in both figures, respectively represent the Newtonian laminar and turbulent baselines and the MDR asymptote.

In Figure 6.5.5, the 5A data onset at $Re_s\sqrt{f}^* \approx 500$ and, rising linearly into the polymeric regime, intersect the 1B and 2B data, forming isoslip points, at $(Re_s\sqrt{f}, 1/\sqrt{f}) \approx (750, 12.5)$ and $(2000, 18.2)$, respectively; the 5B data attain $1/\sqrt{f} \approx 17.5$ and 22.1 at $Re_s\sqrt{f} \approx 750$ and 2000, respectively. Notice that polymer degradation causes both the 5A and 5B data to decline from their P segments at almost the same $Re_s\sqrt{f} \approx 3000$, preventing the intersection of these P segments; therefore, the extended conformation, the only conformation in solutions exhibiting Type-B drag-reduction behavior, not only also obtains for Type-A drag-reduction at high $Re_s\sqrt{f} > Re_s\sqrt{f}^*$, it is responsible for flow enhancement regardless of the type.

At $Re_s\sqrt{f} \approx 750$, the slip triad $S'(5B, 5A, 1B) \approx (6.4, 1.4, 1.4)$ produces $R_{cs} = c_B/c_B = 1/5 = 0.20$ at $S' \approx 1.4$ and $R_{sc} = S'_A/S'_B \approx 1.4/6.4 \approx 0.22$ at $c = 5$ wppm. At $Re_s\sqrt{f} \approx 2000$, the triad $S'(5B, 5A, 2B) \approx (9.3, 5.4, 5.4)$ yields $R_{cs} = 2/5 = 0.40$, and $R_{sc} \approx 5.4/9.3 \approx 0.58$. At the first isoslip point, the ratios R_{cs} and R_{sc} agree well, whereas at the second isoslip point, they differ somewhat because the 2B data exhibit too-large an apparent slip.

The 20A data show an apparent onset at $Re_s\sqrt{f}^* \approx 400$ and, ascending linearly into the polymeric regime, form isoslip points with the 1B, 2B, and 5B data at respective

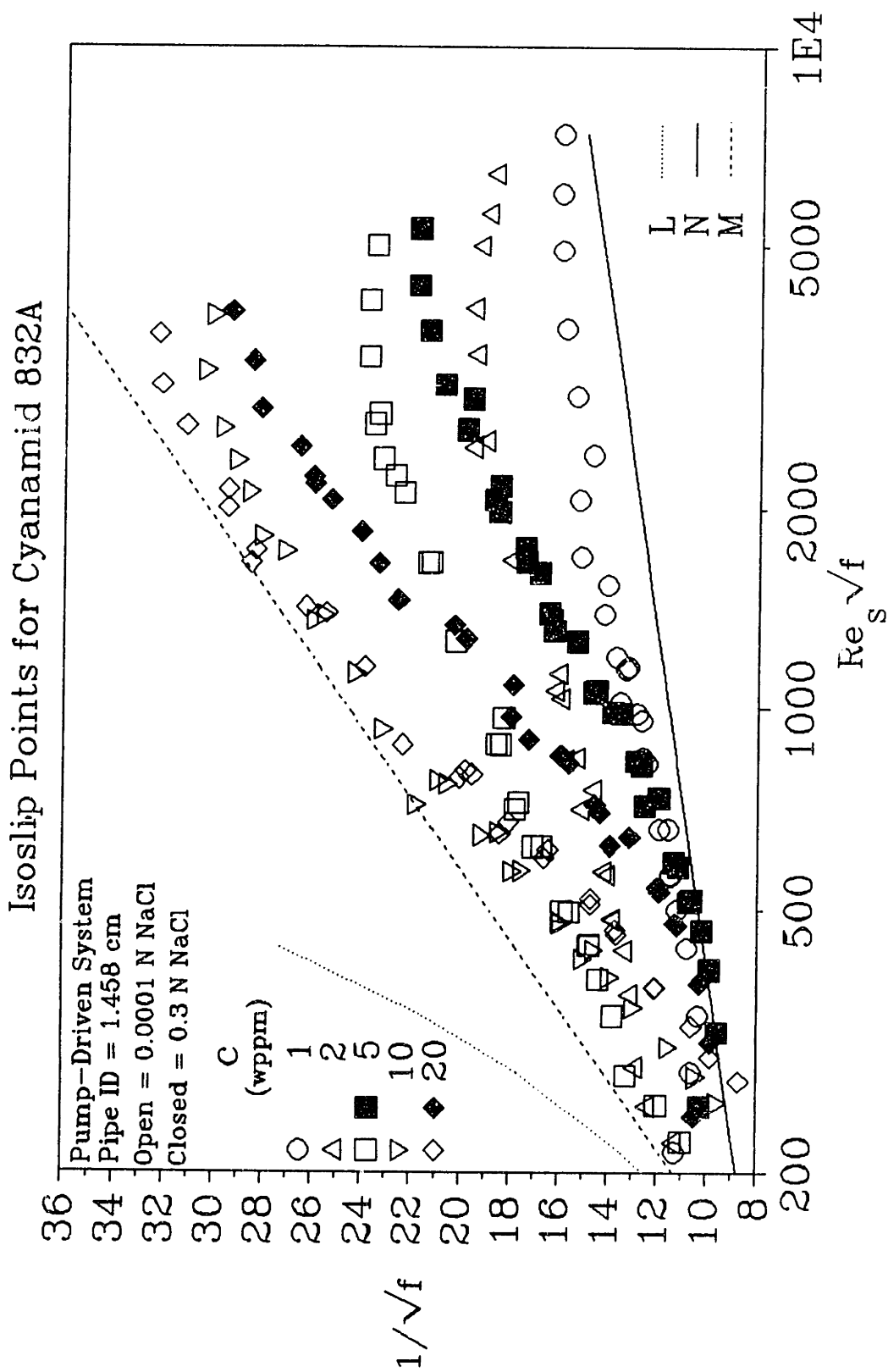


Figure 6.5.5: Isoslip Points for Cyanamid 832A at $c = 5$ and 20 wppm in the 1.458-cm Pipe

$(Re_p\sqrt{f}, 1/\sqrt{f}) \approx (500, 11.6), (750, 15.2)$ and $(1200, 19.9)$. At $Re_p\sqrt{f} \approx 500, 750,$ and $1200,$ the 20B data attain respective $1/\sqrt{f} \approx 14.4, 19.6,$ and 24.7 . As seen in Figure 6.5.5, the first two $1/\sqrt{f}$ data appear somewhat transitional, not yet fully turbulent, and the third is clearly limited by the MDR asymptote. Interestingly, at $Re_p\sqrt{f} \approx 3000,$ where the 20A data decline from their P segment, the 20B data depart from M into the polymeric regime, exhibiting retro-onset; this suggests that the 20B retro-onset is induced by polymer degradation, which is reinforced by the 10B rung lying closely beneath. Moreover, degradation of additive C832A in the 1.458-cm pipe occurs at $Re_p\sqrt{f} \geq 3000,$ irrespective of the concentration, implying that additive length is central to polymer degradation.

At $Re_p\sqrt{f} \approx 500,$ the observed slip triad $S'(20B, 20A, 1B) \approx (4.0, 1.3, 1.3)$ yields $R_{cs} = 1/20 = 0.05$ and $R_{sc} \approx 1.3/4.0 \approx 0.31$. At $Re_p\sqrt{f} \approx 750,$ the slip triad $S'(20B, 20A, 2B) \approx (8.5, 4.1, 4.1)$ gives $R_{cs} = 2/20 = 0.10$ and $R_{sc} \approx 4.1/8.5 \approx 0.48$. At $Re_p\sqrt{f} \approx 1200,$ $S'(20B, 20A, 5B) \approx (12.7, 8.0, 8.0)$ yields $R_{cs} = 5/20 = 0.25$ and $R_{sc} \approx 8.0/12.7 \approx 0.62$. Because the 20B data do represent turbulent-flow enhancement, $R_{sc} \gg R_{cs}$ for these three isoslip points; however, by reversing the analysis under the assumption that $S'/c \approx \text{constant},$ virtual 20B data can be inferred at these $Re_p\sqrt{f}$ that would lie the "forbidden" region above the MDR asymptote.

The 1B, 2B, 5B and 10B data at $Re_p\sqrt{f} = 1000,$ which better account for rung slopes A_p greater than the turbulent baseline slope $A_n,$ yield an average $S'/c \approx 1.6$ and an inferred $S'(20B) \approx 31.3$. The corrected triads at $Re_p\sqrt{f} \approx 500, 750,$ and 1200 are respectively: $S'(20B, 20A, 1B) \approx (31.3, 1.3, 1.3);$ $S'(20B, 20A, 2B) \approx (31.3, 4.1, 4.1);$ and $S'(20B, 20A, 5B) \approx (31.3, 8.0, 8.0).$ Thus, the respective inferred $R_{sc} \approx$

0.04, 0.13, and 0.25 are all much nearer their unchanged complimentary $R_{cs} = 0.05$, 0.10, and 0.25.

In Figure 6.5.6, the 2A data onset at $Re_p\sqrt{f}^* \approx 600$ and, ascending into the polymeric regime, intersect the 1B data, creating an isoslip point at $(Re_p\sqrt{f}, 1/\sqrt{f}) \approx (1150, 13.5)$. The 2B data at $Re_p\sqrt{f} \approx 1150$ attain $1/\sqrt{f} \approx 16.6$. The resulting triad $S'(2B, 2A, 1B) \approx (4.7, 1.6, 1.6)$ yields $R_{cs} = 0.50$ and $R_{sc} \approx 0.34$, the disagreement between which arises from overly flow-enhancing 2A and 2B data. Unsurprisingly, the 2A and 2B data display the effect of polymer degradation at $Re_p\sqrt{f} \approx 3000$, just as do the data pairs 5AB and 20AB in Figure 6.5.5.

The 10A data, which possess an apparent onset at $Re_p\sqrt{f}^* \approx 550$, rise linearly into the polymeric regime and intersect the 1B, 2B, and 5B data at $(Re_p\sqrt{f}, 1/\sqrt{f}) \approx (650, 12.3)$, $(1100, 16.4)$, and $(2400, 23.0)$, respectively, forming three isoslip points. (Because the isoslip coordinates $(Re_p\sqrt{f}, 1/\sqrt{f})$ are derived from (A_p, B_p) of the intersecting P segments, regressed isoslip points may differ somewhat from visual isoslip points. The 10A/1B isoslip point illustrates nicely a poor match between regressed and visual isoslip points, wherein the latter occurs at $(Re_p\sqrt{f}, 1/\sqrt{f}) \approx (500, 10.0)$.) Given that the 10B data at $Re_p\sqrt{f} \approx 650$, 1100, and 2400 achieve respective $1/\sqrt{f} \approx 19.3$, 24.2, and 29.3, the corresponding slip triads, concentration ratios, and slip ratios are observed: $S'(10B, 10A, 1B) \approx (8.4, 1.4, 1.4)$, $R_{cs} = 0.10$, and $R_{sc} \approx 0.16$; $S'(10B, 10A, 2B) \approx (12.5, 4.6, 4.6)$, $R_{cs} = 0.20$, and $R_{sc} \approx 0.37$; and $S'(10B, 10A, 5B) \approx (16.2, 9.9, 9.9)$, $R_{cs} = 0.50$, and $R_{sc} \approx 0.61$. At the 10A/1B and 10A/2B isoslip points, R_{cs} and R_{sc} differ because the 10B data at these $Re_p\sqrt{f}$ are either transitional or limited by the MDR asymptote. With an inferred $S'(10B) \approx 15.6$, obtained from the average

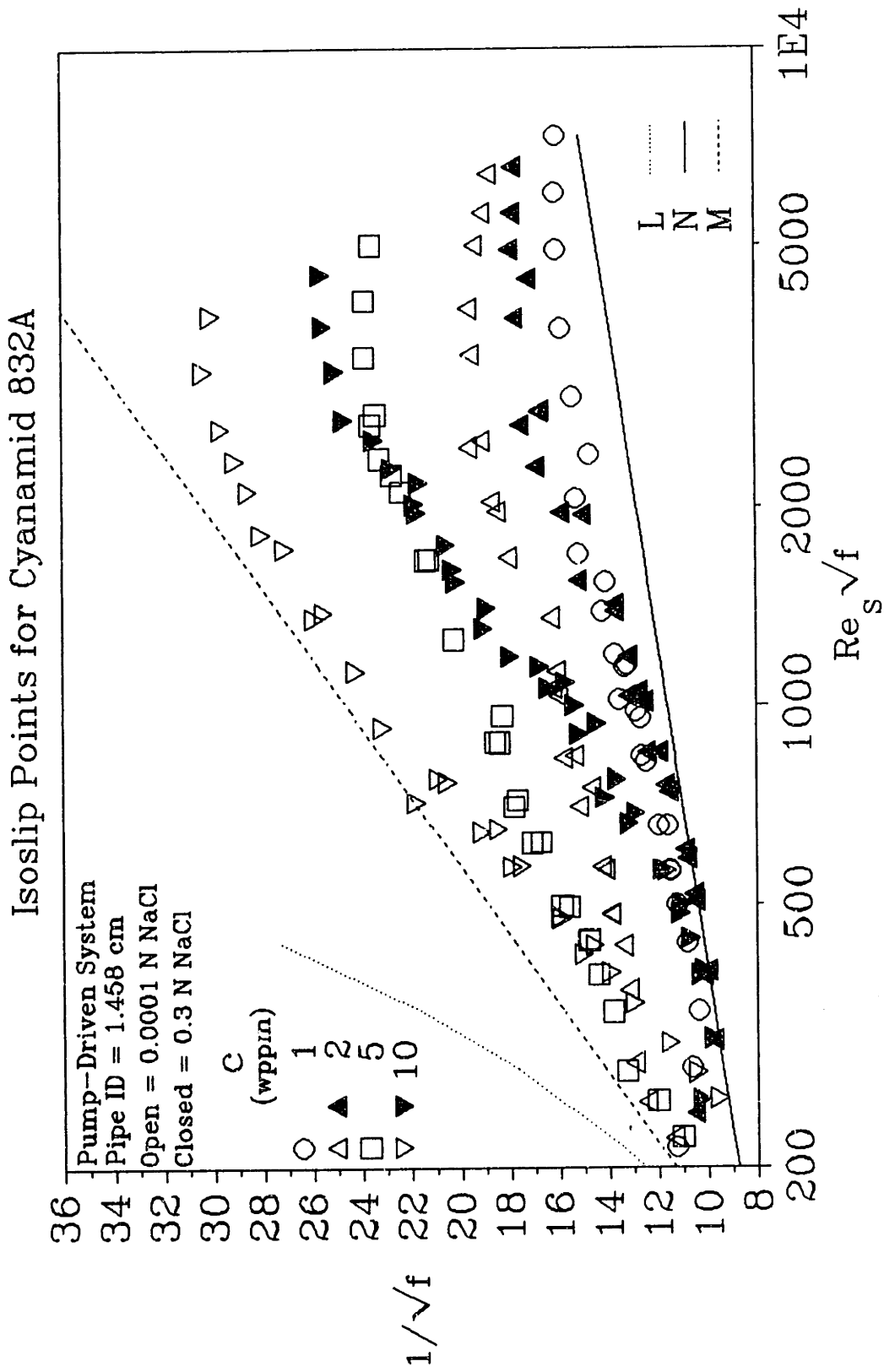


Figure 6.5.6: Isoslip Points for Cyanamid 832A at $c = 2$ and 10 wppm in the 1.458-cm Pipe

$S'/c \approx 1.6$ at $Re_p\sqrt{f} = 1000$, the corrected slip triads at $Re_p\sqrt{f} \approx 650$ and 1100 are respectively: $S'(10B, 10A, 1B) \approx (15.6, 1.4, 1.4)$; and $S'(10B, 10A, 2B) \approx (15.6, 4.6, 4.6)$. The inferred slip ratios and their complimentary concentration ratios, which are unchanged, agree better: $R_{cs} = 0.10$ and $R_{sc} \approx 0.09$; and $R_{cs} = 0.20$ and $R_{sc} \approx 0.30$. Like the P segments of the data pairs 2AB, 5AB, and 20AB, the 10A and 10B P segments, which do not come close to intersecting, show the effect of polymer degradation at $Re_p\sqrt{f} \approx 3000$, which is evidently characteristic for additive C832A in this 1.458-cm pipe.

Figures 6.5.7 and 6.5.8 show the isoslip points among solutions of additive C832A from the pump-driven system with the 1.021-cm pipe. The former superposes 5A and 20A data upon 1B, 2B, 5B, 10B, and 20B data; the latter, 2A and 10A data upon 1B, 2B, 5B, and 10B data. The lines L, N, and M, shown for reference in both figures, respectively represent the Newtonian laminar and turbulent baselines and the MDR asymptote.

In Figure 6.5.7, the 5A data, having an apparent onset at $Re_p\sqrt{f}^* \approx 400$, rise linearly into the polymeric regime and intersect the 1B and 2B data at $(Re_p\sqrt{f}, 1/\sqrt{f}) \approx (600, 12.2)$ and $(750, 13.5)$, respectively. As the 5B data attain respective $1/\sqrt{f} \approx 16.3$ and 17.1 at $Re_p\sqrt{f} \approx 600$ and 750 , the respective slip triads, concentration ratios, and slip ratios are: $S'(5B, 5A, 1B) \approx (5.6, 1.5, 1.5)$, $R_{cs} = 0.20$, and $R_{sc} \approx 0.26$; and $S'(5B, 5A, 2B) \approx (6.0, 2.4, 2.4)$, $R_{cs} = 0.40$, and $R_{sc} \approx 0.40$. That $R_{cs} \approx R_{sc}$ for these isoslip points nicely illustrates additive equivalence. Notice that the 5A and 5B data nearly form an isoslip point at $Re_p\sqrt{f} \approx 3000$; however, both solutions suffer polymer degradation at this point, causing the two to decline along adjacent downward paths as

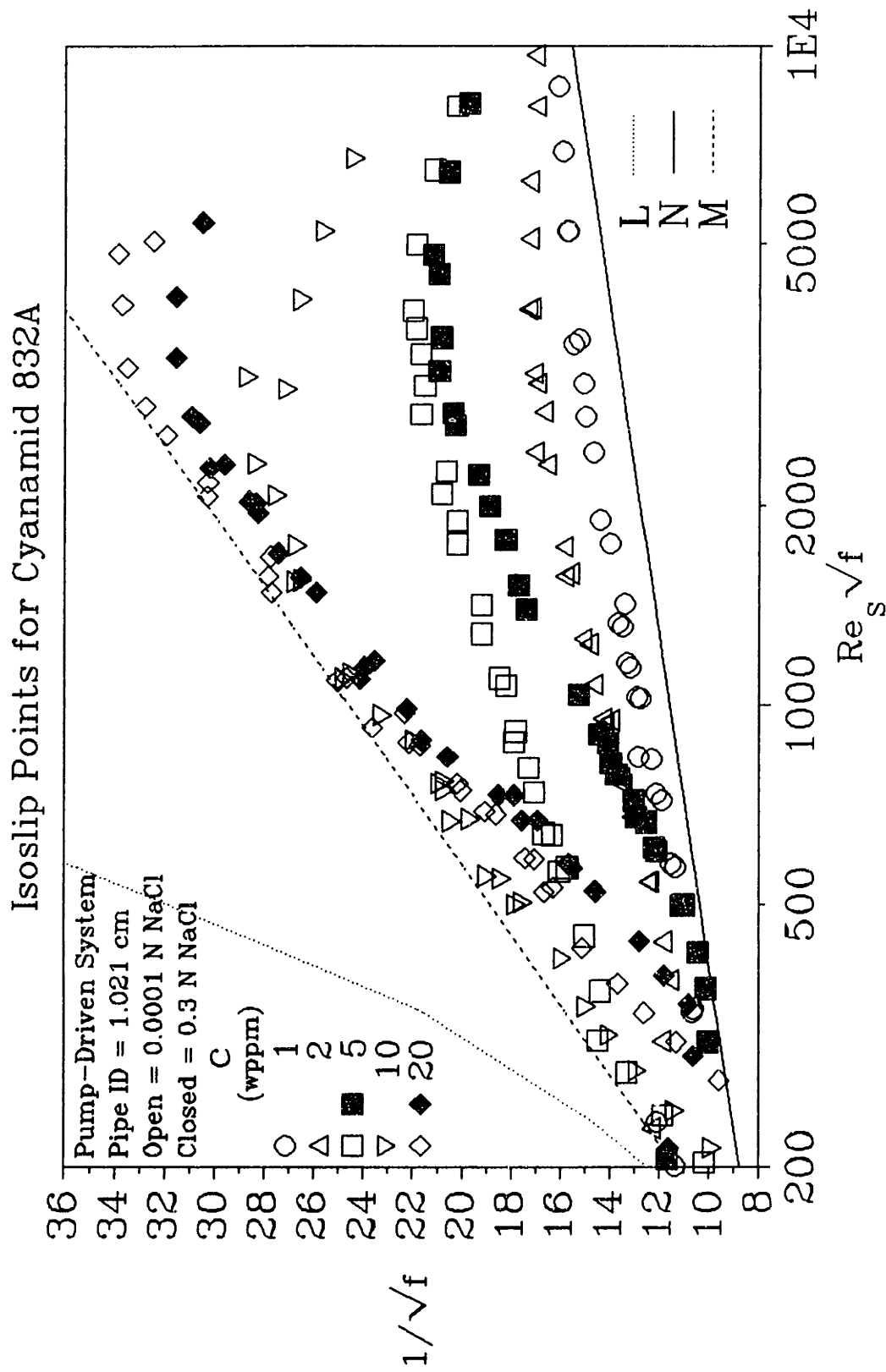


Figure 6.5.7: Isoslip Points for Cyanamid 832A at $c = 5$ and 20 wppm in the 1.021 -cm Pipe

seen in Figure 6.5.7. Their virtual isoslip point, at which $R_{cs} = R_{sc} = 1$, occurs at $(Re_s\sqrt{f}, 1/\sqrt{f}) \approx (3700, 22.7)$, which corresponds to the slip triad $S'(5B, 5A, 5B) \approx (8.8, 8.8, 8.8)$.

The 20A data rise steeply toward the MDR asymptote from an apparent onset point at $Re_s\sqrt{f}^* \approx 300$ and intersect the 1B, 2B, 5B, and 10B data at $(Re_s\sqrt{f}, 1/\sqrt{f}) \approx (360, 11.3)$, $(370, 11.6)$, $(600, 16.2)$, and $(1500, 26.9)$, respectively. The 20B data attain respective $1/\sqrt{f} \approx 13.5$, 13.8 , 17.8 , and 28.0 , of which the first two are transitional and the last two are MDR-limited. The four sets of slip triads, concentration ratios, and slip ratios are respectively: $S'(20B, 20A, 1B) \approx (3.7, 1.5, 1.5)$, $R_{cs} = 0.05$, and $R_{sc} \approx 0.40$; $S'(20B, 20A, 2B) \approx (3.9, 1.7, 1.7)$, $R_{cs} = 0.10$, and $R_{sc} \approx 0.44$; $S'(20B, 20A, 5B) \approx (7.1, 5.5, 5.5)$, $R_{cs} = 0.25$, and $R_{sc} \approx 0.78$; and $S'(20B, 20A, 10B) \approx (15.7, 14.0, 14.0)$, $R_{cs} = 0.50$, and $R_{sc} \approx 0.89$. Poor agreement between R_{cs} and R_{sc} at all isoslip points reflects the unsuitability of the 20B data, which do not characterize turbulent-flow enhancement as seen in Figure 6.5.7. Corrected slip triads can be constructed from inferred 20B data, under the assumption of constant S'/c .

From the 1B, 2B, 5B, and 10B data, the average $S'/c \approx 1.3$ and 1.6 , yielding $S'(20B)/c \approx 25.8$ and 32.3 , at $Re_s\sqrt{f} = 1000$ and 3000 , respectively. The corrected slip triads and inferred slip ratios at $Re_s\sqrt{f} \approx 360$, 370 , 600 , and 1500 are respectively: $S'(20B, 20A, 1B) \approx (25.8, 1.5, 1.5)$ and $R_{sc} \approx 0.06$; $S'(20B, 20A, 2B) \approx (25.8, 1.7, 1.7)$ and $R_{sc} \approx 0.07$; $S'(20B, 20A, 5B) \approx (25.8, 5.5, 5.5)$ and $R_{sc} \approx 0.21$; and $S'(20B, 20A, 10B) \approx (32.3, 14.0, 14.0)$ and $R_{sc} \approx 0.43$. The inferred $R_{sc} \approx 0.06$, 0.07 , 0.21 , and 0.43 agree favorably with their complimentary $R_{cs} = 0.05$, 0.10 , 0.25 , and 0.50 .

Notice that the 20A and 20B data depart from their respective P and M segments

at $Re_s\sqrt{f} \approx 3000$ because of polymer degradation, in a similar manner as the 5A and 5B data. As noted for the 20B data in Figure 6.5.5, the departure of the 20B data from M into the polymeric regime likely results from polymer degradation, lowering the effective concentration; thus, the observed 20B retro-onset, when compared with the 10B retro-onset, must correspond to that for a solution with $10 < c < 20$ wppm.

In Figure 6.5.8, the 2A data, onsetting at $Re_s\sqrt{f}^* \approx 500$, rise linearly into the polymeric regime, and intersect the 1B data at $(Re_s\sqrt{f}, 1/\sqrt{f}) \approx (1300, 13.5)$. As the 2B data attain $1/\sqrt{f} \approx 14.9$, above this isoslip point, at $Re_s\sqrt{f} \approx 1300$, the slip triad $S'(2B, 2A, 1B) \approx (2.9, 1.5, 1.5)$ yields $R_{cs} = 0.50$ and $R_{sc} \approx 0.51$.

As previously observed for the data pairs 5AB and 20AB in Figure 6.5.7, the 2A data approach the 2B data until polymer degradation first appears at $Re_s\sqrt{f} \approx 3000$, after which point they converge up to $Re_s\sqrt{f} \approx 10000$. The 2A and 2B data make a virtual isoslip point at $(Re_s\sqrt{f}, 1/\sqrt{f}) \approx (17000, 22.0)$ with slip triad $S'(2B, 2A, 2B) \approx (5.4, 5.4, 5.4)$ and $R_{cs} = R_{sc} = 1$.

The 10A data, which rise into the polymeric regime from an apparent onset point at $Re_s\sqrt{f}^* \approx 350$, intersect the 1B, 2B, and 5B data at isoslip points with respective $(Re_s\sqrt{f}, 1/\sqrt{f}) \approx (430, 11.6)$, $(460, 12.1)$, and $(950, 17.9)$. As the 10B data achieve $1/\sqrt{f} \approx 16.6, 17.2, \text{ and } 25.7$ above the respective isoslip points, the slip triads, concentration ratios, and slip ratios are: $S'(10B, 10A, 1B) \approx (6.5, 1.5, 1.5)$, $R_{cs} = 0.1$, and $R_{sc} \approx 0.23$; $S'(10B, 10A, 2B) \approx (7.0, 1.9, 1.9)$, $R_{cs} = 0.2$, and $R_{sc} \approx 0.27$; and $S'(10B, 10A, 5B) \approx (14.2, 6.4, 6.4)$, $R_{cs} = 0.5$, and $R_{sc} \approx 0.45$. For the first two slip triads, R_{cs} and R_{sc} do not agree because the 10B data are MDR-limited; however, they do agree for the third because the 10B data occur near the beginning of the 10B ladder rung.

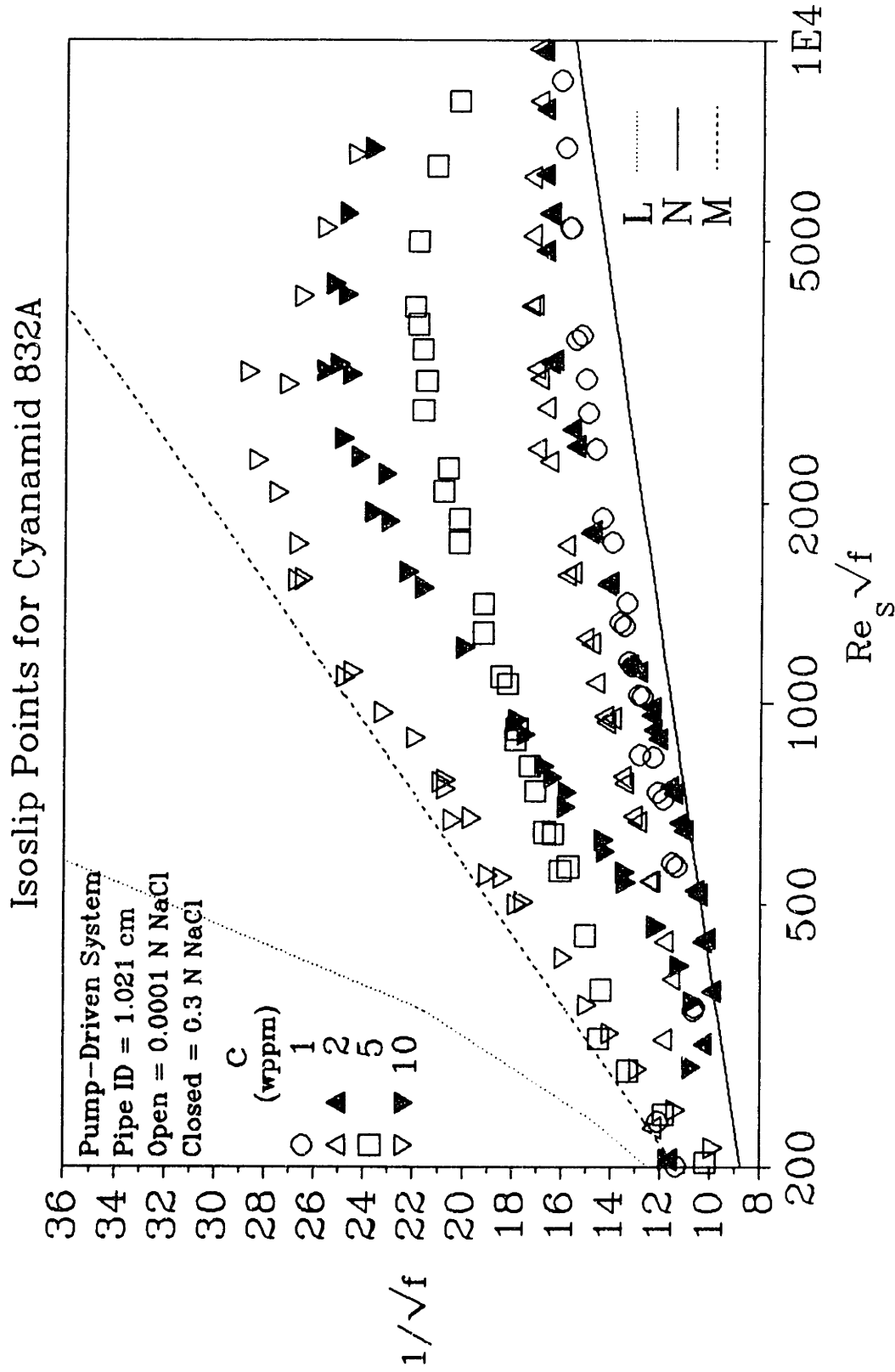


Figure 6.5.8: Isoslip Points for Cyanamid 832A at $c = 2$ and 10 wppm in the 1.021-cm Pipe

Given an average $S'/c \approx 1.3$ at $Re_p\sqrt{f} = 1000$, the corrected slip triads at $Re_p\sqrt{f} \approx 430$ and 460 are $S'(10B, 10A, 1B) \approx (12.9, 1.5, 1.5)$ and $S'(10B, 10A, 2B) \approx (12.9, 1.9, 1.9)$, respectively; the respective inferred $R_{sc} \approx 0.11$ and 0.15 better match their complimentary $R_{cs} = 0.1$ and 0.2 .

Note that as the 10A fan spoke approaches the 10B ladder rung near $Re_p\sqrt{f} \approx 2500$, polymer degradation causes the 10A and 10B data to decline from their P segments beginning at $Re_p\sqrt{f} \approx 2700$, which is slightly lower than that for 2AB, 5AB, and 20AB solutions in this 1.021-cm pipe. The virtual 10A/10B isoslip point, at which the P segments of the 10A and 10B data would intersect in the absence of polymer degradation, occurs at $(Re_p\sqrt{f}, 1/\sqrt{f}) \approx (6000, 32.8)$ and possess the slip triad $S'(10B, 10A, 10B) = (18.1, 18.1, 18.1)$, at which $R_{cs} = R_{sc} = 1$.

Figure 6.5.9 shows the isoslip points among the C832 data at 0.1 N and 0.0003 N NaCl from the gravity-driven system using the 1.458-cm pipe. In the figure, 10A and 20.7A data are superposed over 2.1B, 5.6B, 10B, and 20.7B data; the lines N and M represent respectively the Newtonian turbulent baseline and the MDR asymptote, providing reference.

The 10A data onset at $Re_p\sqrt{f}^* \approx 650$ and, ascending into the polymeric regime, form an isoslip point with the 2.1B data at $(Re_p\sqrt{f}, 1/\sqrt{f}) \approx (1100, 13.5)$. With the 10B data attaining $1/\sqrt{f} \approx 20.9$ above the isoslip point, the resulting slip triad $S'(10B, 10A, 2.1B) \approx (9.1, 1.7, 1.7)$ yields $R_{cs} \approx 0.21$ and $R_{sc} \approx 0.19$, which show good agreement.

The 20.7A data onset at $Re_p\sqrt{f}^* \approx 550$ and, rising into the polymeric regime, intersect the 2.1B and 5.6B data at isoslip points with respective $(Re_p\sqrt{f}, 1/\sqrt{f}) \approx (700, 12.2)$ and $(950, 15.1)$. The 20.7B data attain $1/\sqrt{f} \approx 19.9$ and 22.7 above the respective

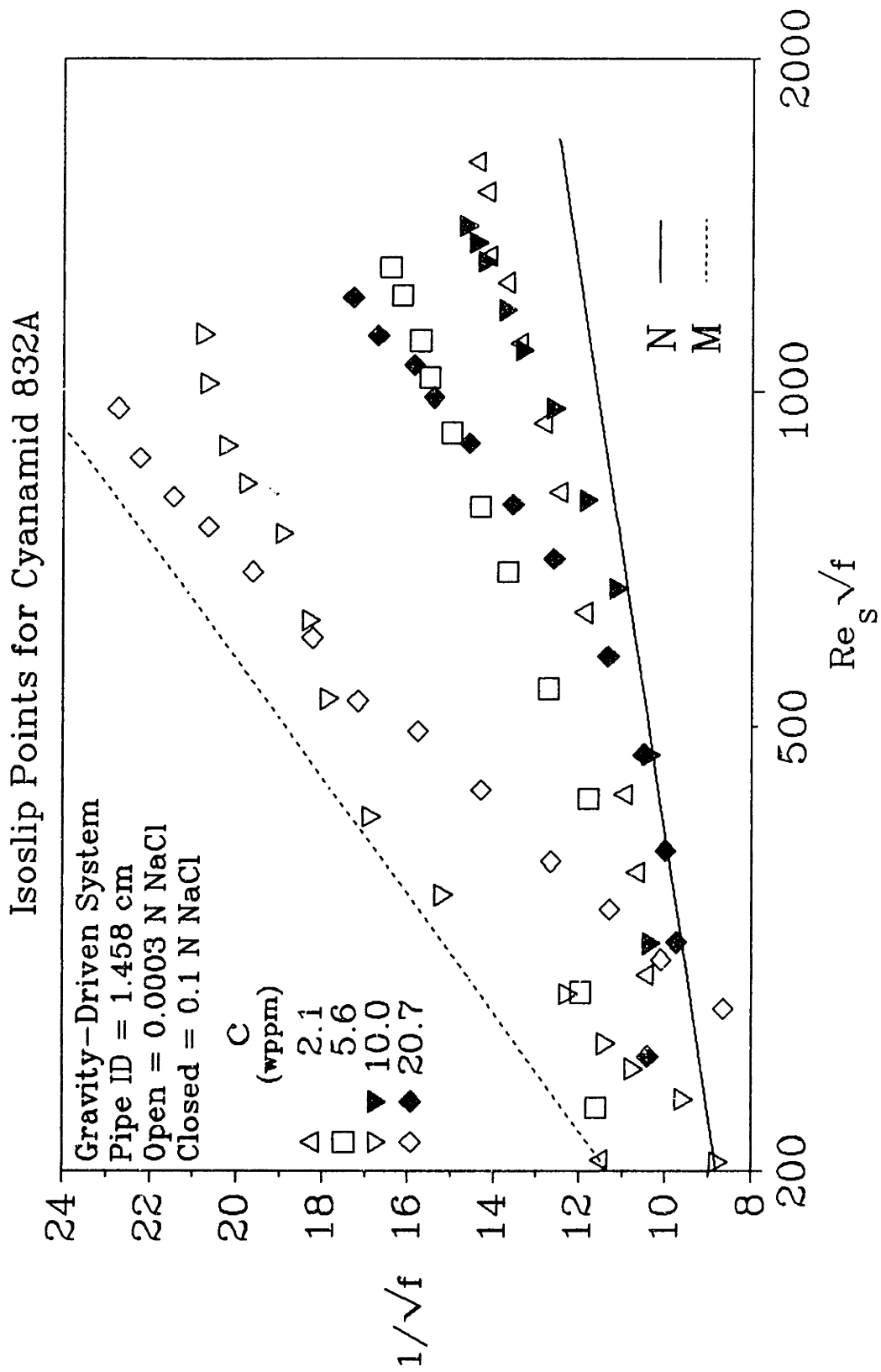


Figure 6.5.9: Isoslip Points for Cyanamid 832A at $c = 10$ and 20.7 wppm in the 1.458-cm Pipe

isoslip points, and the slip triads $S'(20.7B, 20.7A, 2.1B) \approx (9.0, 1.2, 1.2)$ and $S'(20.7B, 20.7A, 5.6B) \approx (11.2, 3.6, 3.6)$ yield $R_{cs} \approx 0.10$ and 0.27 and $R_{sc} \approx 0.14$ and 0.32 , respectively. The complimentary R_{cs} and R_{sc} show favorable agreement.

Figures 6.5.10 and 6.5.11 show the isoslip points among solutions of additive B1120 from the pump-driven system using the 1.458-cm pipe. The former superposes 5A and 20A data upon 1B, 2B, 5B, 10B, and 20B data; the latter, 2A and 10A data upon 1B, 2B, 5B, and 10B data. The lines L, N, and M respectively represent the Newtonian laminar and turbulent baselines and the MDR asymptote, which provide reference.

In Figure 6.5.10, the 5A data, which onset at $Re_p\sqrt{f}^* \approx 650$, rise into the polymeric regime and form isoslip points with the 1B and 2B data at respective $(Re_p\sqrt{f}, 1/\sqrt{f}) \approx (850, 14.2)$ and $(1900, 16.7)$. Above these isoslip points, the 5B data attain $1/\sqrt{f} \approx 20.2$ and 22.1 , respectively. At $Re_p\sqrt{f} \approx 850$, the slip triad $S'(5B, 5A, 1B) \approx (8.9, 2.9, 2.9)$ gives $R_{cs} = 0.20$ and $R_{sc} \approx 0.32$; at $Re_p\sqrt{f} \approx 1900$, the triad $S'(5B, 5A, 2B) \approx (9.4, 4.0, 4.0)$ yields $R_{cs} = 0.4$ and $R_{sc} \approx 0.43$.

Note that the 5A and 5B data, the P segments of which are well separated for $1000 < Re_p\sqrt{f} < 2500$, both exhibit polymer degradation at $Re_p\sqrt{f} \approx 3000$.

Interestingly, additives B1120 and C832A, which both show polymer degradation at $Re_p\sqrt{f} \approx 3000$, have approximately equal molecular weights and, thus, contour lengths; this reinforces the notion that polymer degradation and drag reduction both involve the presence of extended additives in turbulent flow.

The 20A data, which have an apparent onset point at $Re_p\sqrt{f}^* \approx 500$, ascend linearly into the polymeric regime and form isoslip points with the 1B, 2B, 5B, and 10B data at respective $(Re_p\sqrt{f}, 1/\sqrt{f}) \approx (550, 11.5)$, $(650, 13.2)$, $(1600, 21.6)$, and $(3600,$

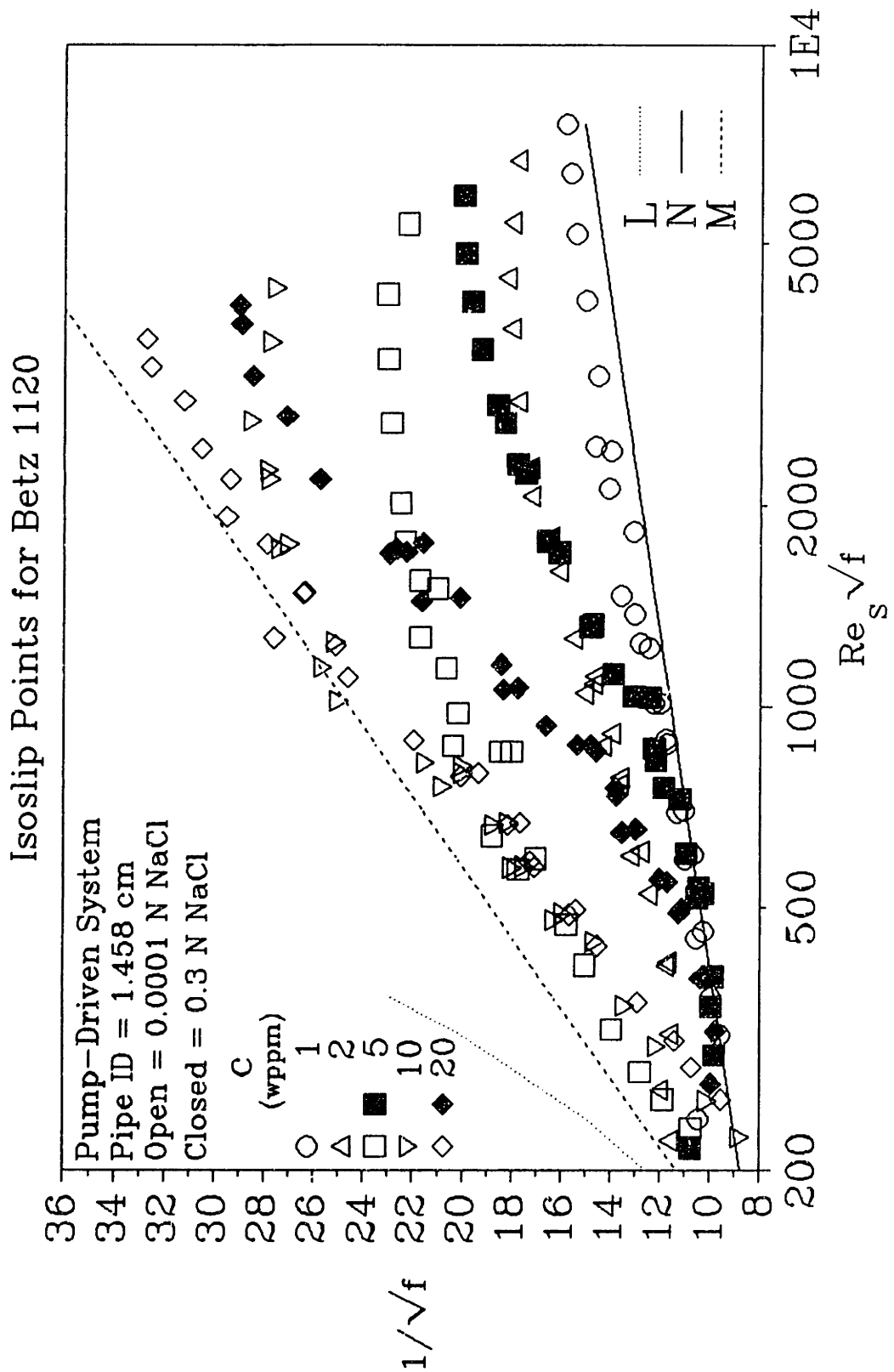


Figure 6.5.10: Isoslip Points for Betz 1120 at $c = 5$ and 20 wppm

29.5). The 20B data have $1/\sqrt{f} \approx 16.7, 18.0, 27.0,$ and 32.7 at $Re_3\sqrt{f} \approx 550, 650, 1600,$ and $3600,$ respectively. For these four isoslip points, the respective sets of slip triads, concentration ratios, and slip ratios are: $S'(20B, 20A, 1B) \approx (6.2, 1.0, 1.0), R_{cs} = 0.05,$ and $R_{sc} \approx 0.16;$ $S'(20B, 20A, 2B) \approx (7.2, 2.4, 2.4), R_{cs} = 0.10,$ and $R_{sc} \approx 0.33;$ $S'(20B, 20A, 5B) \approx (14.6, 9.3, 9.3), R_{cs} = 0.25,$ and $R_{sc} \approx 0.63;$ and $S'(20B, 20A, 10B) \approx (18.8, 15.7, 15.7), R_{cs} = 0.50,$ and $R_{sc} \approx 0.83.$ As seen in Figure 6.5.10, the mismatches between R_{cs} and R_{sc} arise from the MDR-limited 20B data. With average $S'/c \approx 1.3$ and 1.6 at $Re_3\sqrt{f} = 1000$ and $3000,$ respectively, calculated from the 1B, 2B, 5B, and 10B data, the corrected slip triads at $Re_3\sqrt{f} \approx 550, 650, 1600,$ and 3600 are respectively: $S'(20B, 20A, 1B) \approx (25.4, 1.0, 1.0); S'(20B, 20A, 2B) \approx (25.4, 2.4, 2.4); S'(20B, 20A, 5B) \approx (32.5, 9.3, 9.3);$ and $S'(20B, 20A, 10B) \approx (32.5, 15.7, 15.7).$ The respective inferred $R_{sc} \approx 0.04, 0.09, 0.29,$ and 0.48 agree more favorably with their corresponding $R_{cs} = 0.05, 0.10, 0.25,$ and $0.50.$

The 20A and 20B data, which remain well separated up to the highest $Re_3\sqrt{f} \approx 3800,$ appear to be affected similarly by polymer degradation, as seen in Figure 6.5.10. The 20A data decline from their P segment at $Re_3\sqrt{f} \approx 3300;$ the last 20B data point departs into the polymeric regime from their M segment at $Re_3\sqrt{f} \approx 3300.$

In Figure 6.5.11, the 2A data onset at $Re_3\sqrt{f}^* \approx 600$ and then, rising into the polymeric regime, intersect the 1B data at an isoslip point with $(Re_3\sqrt{f}, 1/\sqrt{f}) \approx (1100, 13.6).$ With $1/\sqrt{f} \approx 14.8$ for the 1B data above the isoslip point, the slip triad $S'(2B, 2A, 1B) \approx (3.1, 1.9, 1.9)$ yields $R_{cs} = 0.50$ and $R_{sc} \approx 0.60.$

The 10A data, onsetting at $Re_3\sqrt{f}^* \approx 500,$ rise into the polymeric regime and form isoslip points with the 1B, 2B, and 5B data at respective $(Re_3\sqrt{f}, 1/\sqrt{f}) \approx (600,$

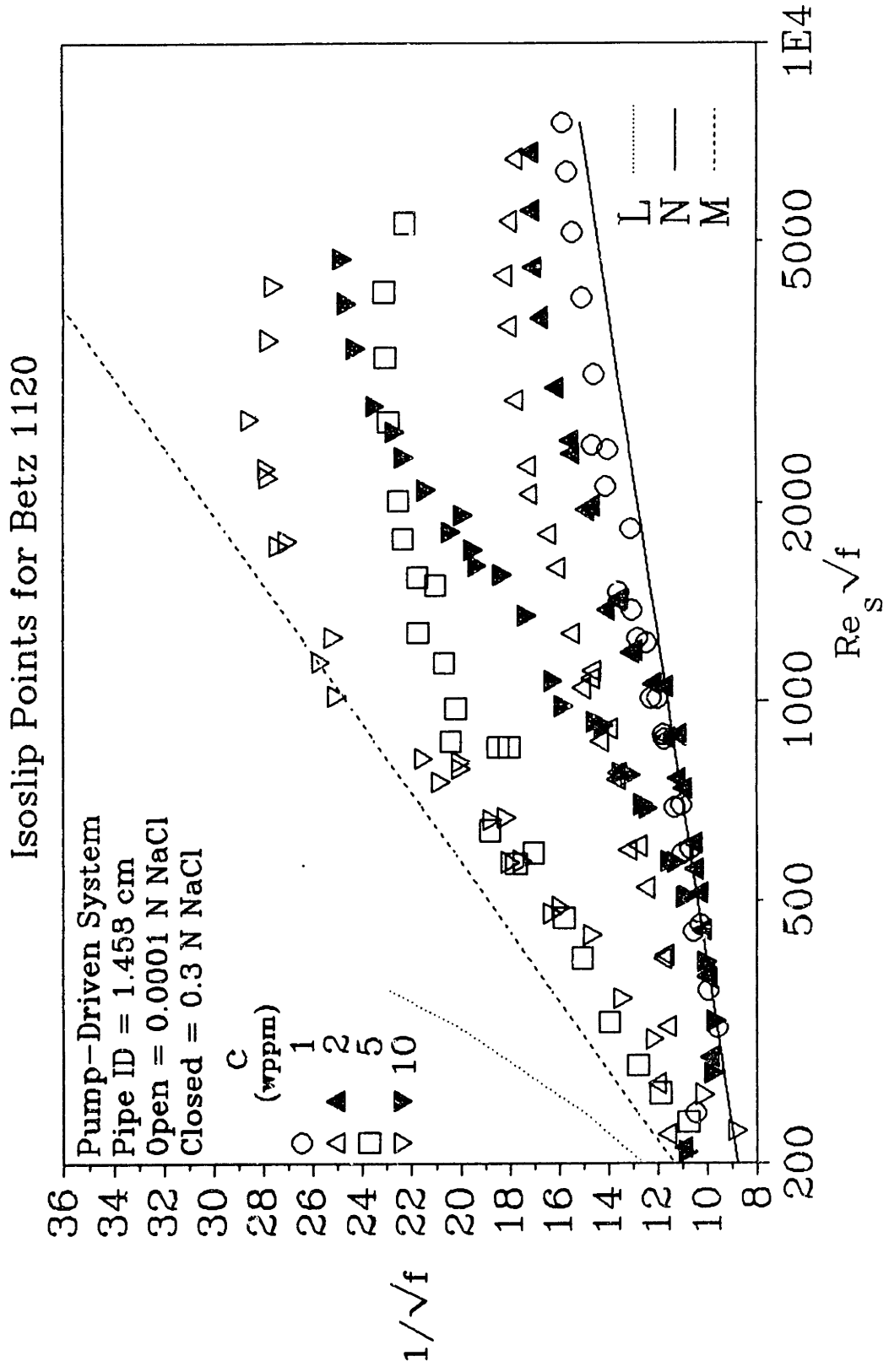


Figure 6.5.11: Isoslip Points for Betz 1120 at $c = 2$ and 10 wppm

11.7), (800, 14.0), and (2700, 22.9). Above these isoslip points, the 10B data achieve respective $1/\sqrt{f} \approx 18.3, 21.9, \text{ and } 28.6$. Thus, the slip triads, concentration ratios, and slips ratios at $Re_s\sqrt{f} \approx 600, 800, \text{ and } 2700$ are respectively: $S'(10B, 10A, 1B) \approx (7.5, 1.0, 1.0)$, $R_{cs} = 0.10$, and $R_{sc} \approx 0.13$; $S'(10B, 10A, 2B) \approx (10.6, 2.7, 2.7)$, $R_{cs} = 0.20$, and $R_{sc} \approx 0.26$; and $S'(10B, 10A, 5B) \approx (15.2, 9.6, 9.6)$, $R_{cs} = 0.50$, and $R_{sc} \approx 0.63$. Despite the MDR-limited 10B data at the first two isoslip points, all three isoslip points have about the same ratios $R_{cs}/R_{sc} \approx 0.76, 0.78, \text{ and } 0.79$, respectively, perhaps indicating that the 10B rung is too low with respect to the 5B data. Corrected slip triads for the 10A/1B and 10A/2B isoslip points are $S'(10B, 10A, 1B) \approx (12.7, 1.0, 1.0)$ and $S'(10B, 10A, 2B) \approx (12.7, 2.7, 2.7)$, and the respective inferred $R_{sc} \approx 0.08$ and 0.21 more closely match their complimentary $R_{cs} = 0.10$ and 0.20 .

Figures 6.5.12 and 6.5.13 show the isoslip points among the P500 data in the 1.458- and 1.021-cm pipes, respectively. In each figure, a partial Type-A fan comprising 30A and 100A data is superposed upon a Type-B ladder comprising 10B, 30B, and 100B data; the accompanying lines L, N, and M respectively represent the Newtonian laminar and turbulent baselines and the MDR asymptote.

In Figure 6.5.12, the 30A data onset at $Re_s\sqrt{f}^* \approx 550$ and, rising into the polymeric regime, make an isoslip point with the 10B data at $(Re_s\sqrt{f}, 1/\sqrt{f}) \approx (1700, 18.2)$. Given that the 30B data attain $1/\sqrt{f} \approx 25.3$ above the isoslip point, the resulting slip triad $S'(30B, 30A, 10B) \approx (12.8, 5.7, 5.7)$ yields $R_{cs} = 0.33$ and $R_{sc} \approx 0.45$. Either the 10B rung is too low or the 10B rung is too high.

The 100A data onset at $Re_s\sqrt{f}^* \approx 600$ and, rising into the polymeric regime, intersect the 10B and 30E data at isoslip points with respective $(Re_s\sqrt{f}, 1/\sqrt{f}) \approx (900,$

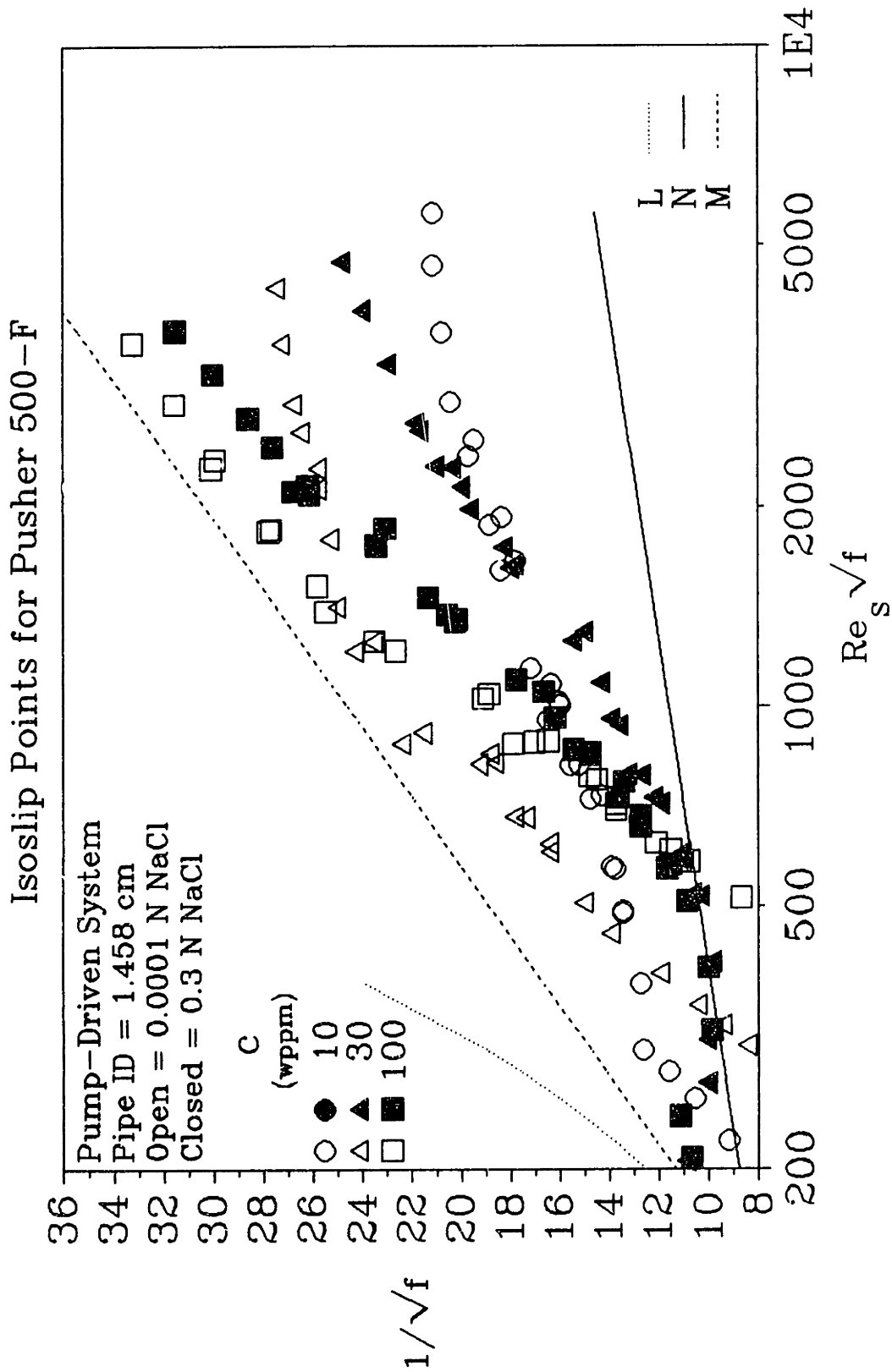


Figure 6.5.12: Isoslip Points for Pusher 500-F in the 1.458-cm Pipe

15.8) and (2200, 26.0). (Even though the 100A data do cross the 100B data at $(Re_p\sqrt{f}, 1/\sqrt{f}) \approx (600, 12)$, the 100B data show either laminar or transitional behavior; thus, the intersection does not constitute a legitimate isoslip point.) The 100B data attain $1/\sqrt{f} \approx 17.2$ and 30.1 at $Re_p\sqrt{f} \approx 900$ and 2200 . The respective slip triads $S'(100B, 100A, 10B) \approx (5.8, 4.3, 4.3)$ and $S'(100B, 100A, 30B) \approx (17.1, 13.0, 13.0)$ give $R_{c_i} = 0.10$ and 0.30 and $R_{s_c} \approx 0.75$ and 0.76 . The large discrepancies between complimentary R_{c_s} and R_{s_c} arise because the 100B data are either transitional or MDR-limited, as seen in Figure 6.5.12. With average $S'/c \approx 0.4$ and 0.6 at $Re_p\sqrt{f} \approx 1000$ and 3000 , respectively, the corrected triads $S'(100B, 100A, 10B) \approx (41.8, 4.3, 4.3)$ and $S'(100B, 100A, 30B) \approx (57.2, 13.0, 13.0)$ give inferred $R_{s_c} \approx 0.10$ and 0.22 that are much closer to their complimentary $R_{c_s} = 0.1$ and 0.3 .

In Figure 6.5.13, the 30A data, rising into the polymeric regime from an apparent onset point at $Re_p\sqrt{f}^* \approx 450$, form an isoslip point with the 10B data at $(Re_p\sqrt{f}, 1/\sqrt{f}) \approx (1000, 16.2)$. The 30B data achieve $1/\sqrt{f} \approx 22.1$ above the isoslip point. The resulting slip triad $S'(30B, 30A, 10B) \approx (10.5, 4.6, 4.6)$ yields $R_{c_s} = 0.33$ and $R_{s_c} \approx 0.43$. That R_{c_s} and R_{s_c} do not agree results from MDR-limited 30B data, as seen in Figure 6.5.13. Given an average $S'/c \approx 0.4$ at $Re_p\sqrt{f} = 1000$, the corrected slip triad $S'(30B, 30A, 10B) \approx (12.2, 4.6, 4.6)$ yields an inferred $R_{s_c} \approx 0.37$ that agrees better with $R_{c_s} = 0.33$.

The 100A data, which have an apparent onset point at $Re_p\sqrt{f}^* \approx 450$, rise steeply into the polymeric regime virtually atop the 100B data and intersect the 10B and 30B data at isoslip points with respective $(Re_p\sqrt{f}, 1/\sqrt{f}) \approx (600, 14.3)$ and $(1300, 24.8)$. The 100B data achieve $1/\sqrt{f} \approx 15.7$ and 25.7 above the respective isoslip points. The resulting slip

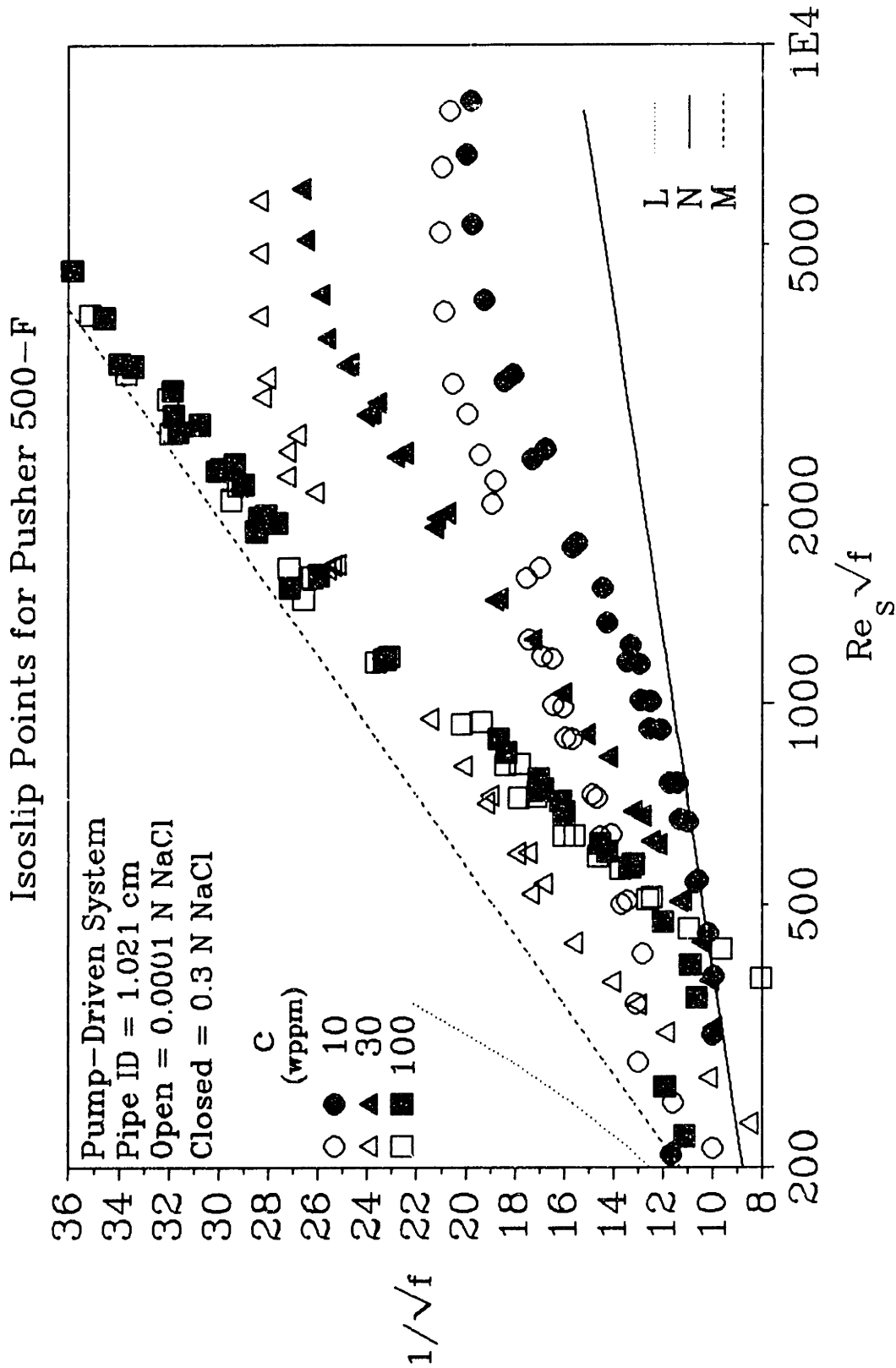


Figure 6.5.13: Isoslip Points for Pusher 500-F in the 1.021-cm Pipe

triads $S'(100B, 100A, 10B) \approx (4.9, 3.6, 3.6)$ and $S'(100B, 100A, 30B) \approx (13.6, 12.7, 12.7)$ have $R_{cs} = 0.10$ and 0.30 and $R_{sc} \approx 0.72$ and 0.93 . The complimentary R_{cs} and R_{sc} greatly differ because the 100B data are either transitional or MDR-limited, as seen in Figure 6.5.13. Given an average $S'/c \approx 0.4$ at $Re_p\sqrt{f} = 1000$, the corrected slip triads $S'(100B, 100A, 10B) \approx (41.8, 3.6, 3.6)$ and $S'(100B, 100A, 30B) \approx (41.8, 12.7, 12.7)$ yield inferred $R_{sc} \approx 0.08$ and 0.30 that almost exactly match their complimentary $R_{cs} = 0.10$ and 0.30 .

6.5.2.2 Summary of Additive Equivalence and Isoslip Points

The 42 isoslip-point coordinates $(Re_p\sqrt{f}, 1/\sqrt{f})$, slip triads (C_B, C_A, c_B) , and R_{sc} and R_{cs} values derived from the flow trajectories shown in Figures 6.5.4 - 6.5.13 are listed in Table 6.5, documenting all additive equivalences observed in the present work. Figure 6.5.14 is a plot of the slip ratio R_{sc} versus the concentration ratio R_{cs} among all slip triads. Evidently, the data collectively adhere to the line $R_{sc} = R_{cs}$, reinforcing the earlier conclusion, from the introductory example in Figure 6.5.4, that for fixed total additive concentration, the collapsed to extended slip ratio R_{sc} is simply the fraction of originally collapsed macromolecules that have become extended in the flow, and thence effective in drag reduction. Thus the extended additive states appear to be the active species responsible for drag reduction, with Type-B drag reduction the inherently fundamental form of the phenomenon. Type-A drag reduction appears to be a special case wherein the initially randomly-coiled and ineffective additives are extended, and hence activated, by the turbulent flow field.

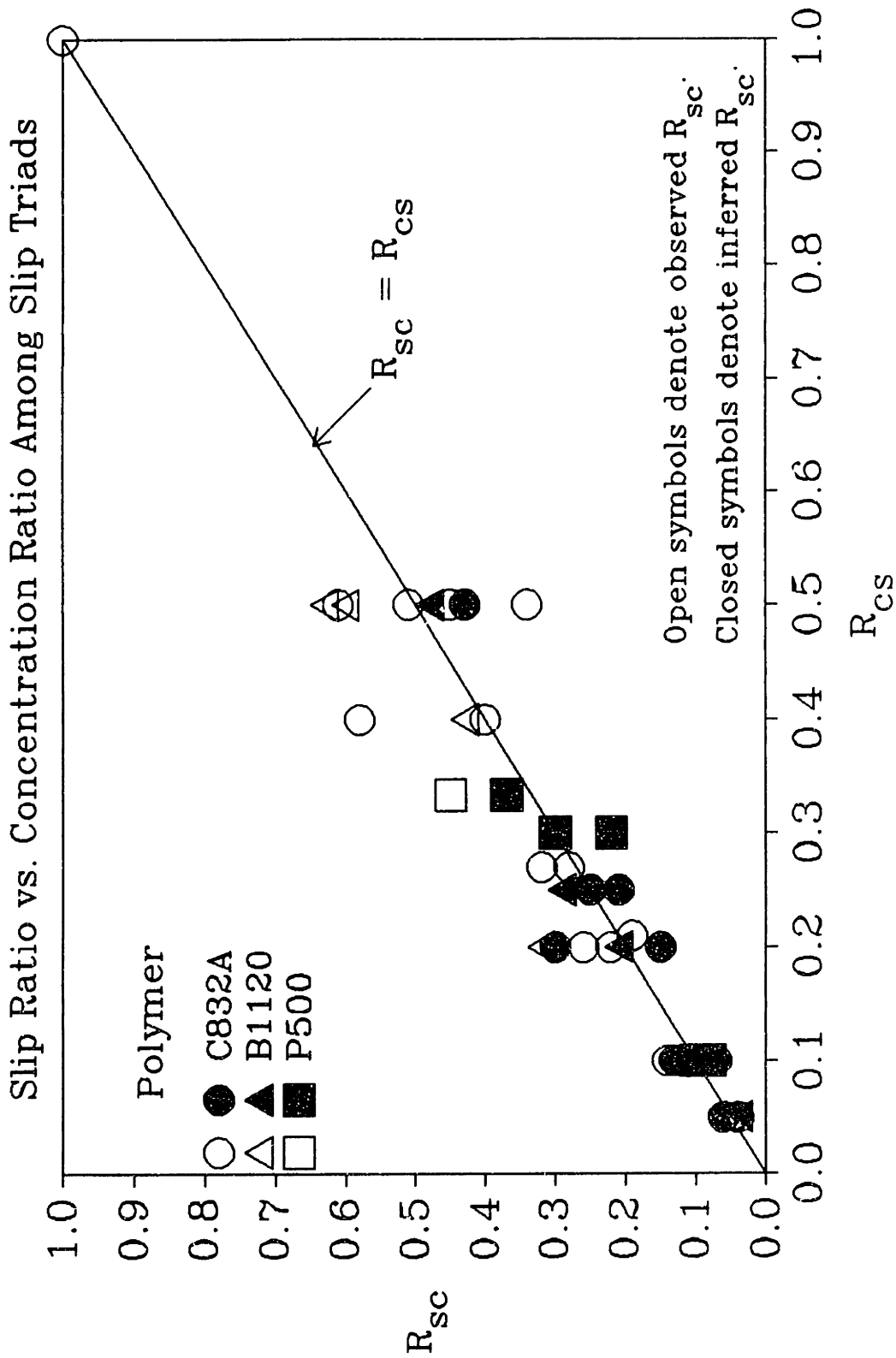


Figure 6.5.14: Slip Ratio versus Concentration Ratio Among Slip Triads

Table 6.5
Summary of Isoslip Points

Polymer	Isoslip Point Coordinates	Slip Triad			Concentration Ratio	Slip Ratio
		$S'(C_B, C_A, c_B) = (Y, X, X)$			R_{cs}	R_{sc}
	$(Re, \sqrt{f}, 1/\sqrt{f})$	(C_B, C_A, c_B)	Y	X	c_B/C_A	X/Y
Figure 6.5.4: Gravity-Driven System with 1.458-cm Pipe						
C832A	(950, 15.1)	(20.9B, 20.7A, 5.6B)	12.7	3.6	0.27	0.28
Figure 6.5.5: Pump-Driven System with 1.458-cm Pipe						
C832A	(750, 12.5)	(5B, 5A, 1B)	6.4	1.6	0.20	0.22
C832A	(2000, 18.2)	(5B, 5A, 2B)	9.3	5.4	0.40	0.58
C832A†	(500, 11.6)	(20B, 20A, 1B)	31.3	1.3	0.05	0.04
C832A†	(750, 15.2)	(20B, 20A, 2B)	31.3	4.1	0.10	0.13
C832A†	(1200, 19.9)	(20B, 20A, 5B)	31.3	8.0	0.25	0.25
Figure 6.5.6: Pump-Driven System with 1.458-cm Pipe						
C832A	(1150, 13.5)	(2B, 2A, 1B)	4.7	1.6	0.50	0.34
C832A†	(650, 12.3)	(10B, 10A, 1B)	15.6	1.4	0.10	0.09
C832A†	(1100, 16.4)	(10B, 10A, 2B)	15.6	4.6	0.20	0.30
C832A	(2400, 23.0)	(10B, 10A, 5B)	16.2	9.9	0.50	0.61
Figure 6.5.7: Pump-Driven System with 1.021-cm Pipe						
C832A	(600, 12.2)	(5B, 5A, 1B)	5.6	1.5	0.20	0.26
C832A	(750, 13.5)	(5B, 5A, 2B)	6.0	2.4	0.40	0.40
C832A‡	(3700, 13.5)	(5B, 5A, 5B)	8.8	8.8	1.0	1.0
C832A†	(360, 11.3)	(20B, 20A, 1B)	25.8	1.5	0.05	0.06
C832A†	(370, 11.6)	(20B, 20A, 2B)	25.8	1.7	0.10	0.07

Polymer	Isoslip Point Coordinates	Slip Triad			Concentration Ratio	Slip Ratio
		$S'(C_B, C_A, c_B) = (Y, X, X)$			R_{cs}	R_{sc}
		(C_B, C_A, c_B)	Y	X	c_B/C_A	X/Y
C832A†	(600, 16.2)	(20B, 20A, 5B)	32.3	5.5	0.25	0.21
C832A†	(1500, 26.9)	(20B, 20A, 10B)	32.3	14.0	0.50	0.43
Figure 6.5.8: Pump-Driven System with 1.021-cm Pipe						
C832A	(1300, 13.5)	(2B, 2A, 1B)	2.9	1.5	0.50	0.51
C832A‡	(17000, 22.0)	(2B, 2A, 2B)	5.4	5.4	1.0	1.0
C832A†	(430, 11.6)	(10B, 10A, 1B)	12.9	1.5	0.10	0.11
C832A†	(460, 12.1)	(10B, 10A, 2B)	12.9	1.9	0.20	0.15
C832A	(950, 17.9)	(10B, 10A, 5B)	14.2	6.4	0.50	0.45
C832A‡	(6000, 32.8)	(10B, 10A, 10B)	18.1	18.1	1.0	1.0
Figure 6.5.9: Gravity-Driven System with 1.458-cm Pipe						
C832A	(1100, 13.5)	(10B, 10A, 2.1B)	9.1	1.7	0.21	0.19
C832A	(700, 12.2)	(20.7B, 20.7A, 2.1B)	9.0	1.2	0.10	0.14
C832A	(950, 15.1)	(20.7B, 20.7A, 5.6B)	11.2	3.6	0.27	0.32
Figure 6.5.10: Pump-Driven System with 1.458-cm Pipe						
B1120	(850, 14.2)	(5B, 5A, 1B)	8.9	2.9	0.20	0.32
B1120	(1900, 16.7)	(5B, 5A, 2B)	9.4	4.0	0.40	0.43
B1120†	(550, 11.5)	(20B, 20A, 1B)	25.4	1.0	0.05	0.04
B1120†	(650, 13.2)	(20B, 20A, 2B)	25.4	2.4	0.10	0.09
B1120†	(1600, 21.6)	(20B, 20A, 5B)	32.3	9.3	0.25	0.29
B1120†	(3600, 29.5)	(20B, 20A, 10B)	32.3	15.7	0.50	0.48

Polymer	Isoslip Point Coordinates	Slip Triad			Concentration Ratio	Slip Ratio
		$S'(C_B, C_A, c_B) = (Y, X, X)$			R_{c_A}	R_{c_c}
	$(Re_i\sqrt{f}, 1/\sqrt{f})$	(C_B, C_A, c_B)	Y	X	c_B/C_A	X/Y
Figure 6.5.11: Pump-Driven System with 1.458-cm Pipe						
B1120	(1100, 13.6)	(2B, 2A, 1B)	3.1	1.9	0.50	0.60
B1120†	(600, 11.7)	(10B, 10A, 1B)	12.7	1.0	0.10	0.08
B1120†	(800, 14.0)	(10B, 10A, 2B)	12.7	2.7	0.20	0.21
B1120	(2700, 22.9)	(10B, 10A, 5B)	15.2	9.6	0.50	0.63
Figure 6.5.12: Pump-Driven System with 1.458-cm Pipe						
P500	(1700, 18.2)	(30B, 30A, 10A)	12.8	5.7	0.33	0.45
P500†	(900, 15.8)	(100B, 100A, 10B)	41.8	4.3	0.10	0.10
P500†	(2200, 26.0)	(100B, 100A, 30B)	57.2	13.0	0.30	0.22
Figure 6.5.13: Pump-Driven System with 1.021-cm Pipe						
P500†	(1000, 16.2)	(30B, 30A, 10B)	12.2	4.6	0.33	0.37
P500†	(600, 14.3)	(100B, 100A, 10B)	41.8	3.6	0.10	0.08
P500†	(1300, 24.8)	(100B, 100A, 30B)	41.8	12.7	0.30	0.30
† Y and R_{c_c} are the inferred values belonging to the corrected slip triad. ‡ The slip triad is a virtual isoslip point with $C_B = C_A = c_B$ and $Y = X$.						

6.6 Comparison of Type-B Drag Reduction with Literature

The results in §6.4 indicate that in Type-B drag reduction — the nondimensional flow enhancement or apparent slip, S' — only depends weakly on flow parameters, such as $Re_p\sqrt{f}$ and pipe diameter, but strongly depends on additive parameters, such as concentration and molecular weight.

In this section, data for HPAM additives from this work and from the available literature are compared quantitatively. The comparison is then broadened to include other types of additives, including fibers. Also, retro-onset data from this work and the few that could be extracted from the literature are compared and correlated.

6.6.1 Present and Literature Flow-Enhancement Data

Figure 6.6.1 depicts the dependence of flow enhancement on concentration by six HPAM additives, including both the present data for additives C832A, B1120, and P500, and literature data for additives AP30(Clarke, 1970), Magnifloc[®] E-10(MagE10)(Oliver & Bakhtiyarov, 1983), and Hydropur[®] SB125 (HSB125)(Interthal & Wilski, 1985) with respective $M_w \times 10^{-6} \approx 9.2, 16.5, \text{ and } 23$ g/mole. The experimental conditions for these data, shown in Figure 6.6.1 and summarized in Table 6.6, are similar, with pipe diameters $0.5 < D < 1.5$ cm and nondimensional stress levels therein corresponding to $Re_p\sqrt{f} \approx 3000$. For all HPAMs at $c < 20$ wppm, S' is observed to be approximately linear in c ; at the highest concentrations $c \geq 20$ wppm, S' attains the MDR asymptote where $S' = S_M$, independent of c . For additives MagE10, C832A, B1120, HSB125,

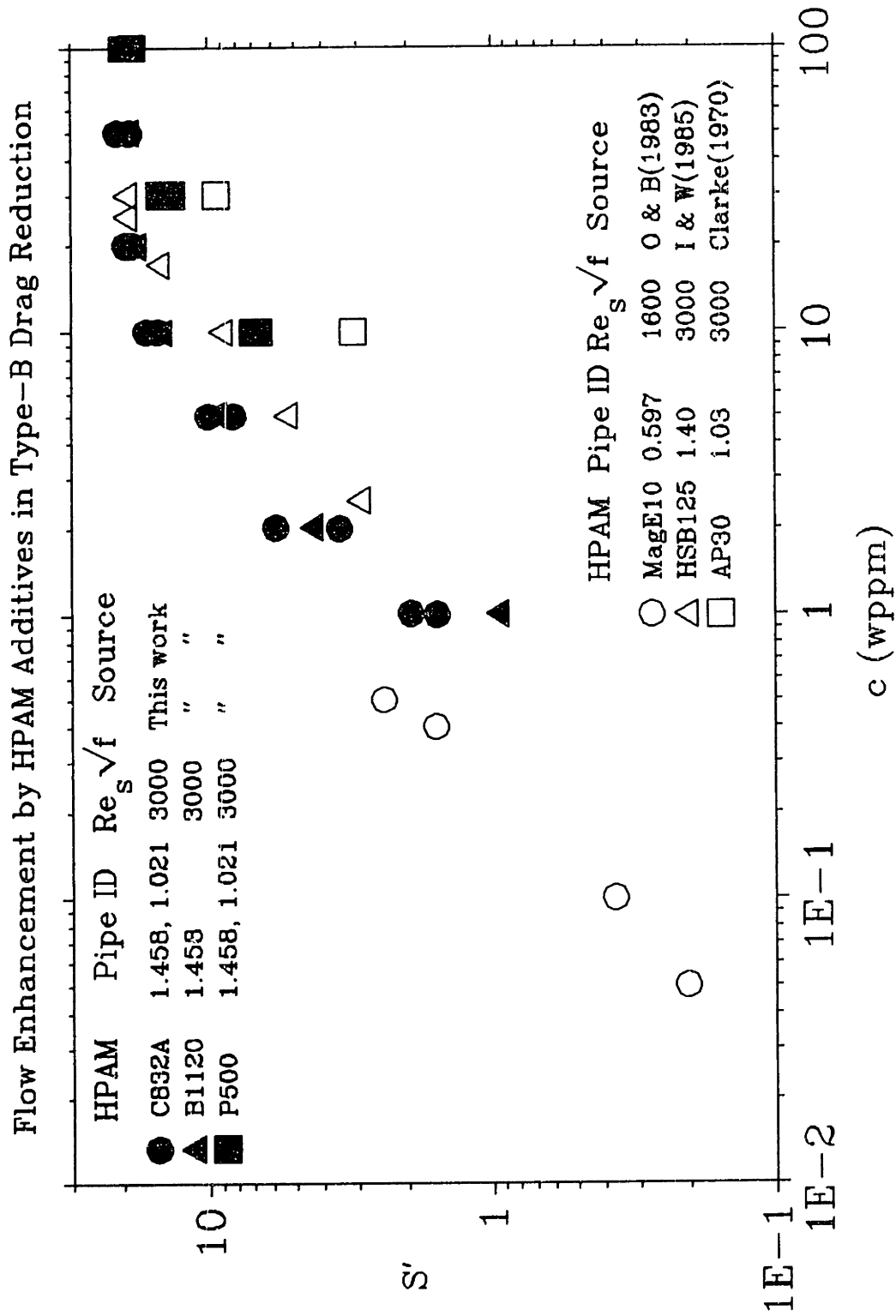


Figure 6.6.1: Flow Enhancement by HPAM Additives in Type-B Drag Reduction

P500, and AP30 with $M_w \times 10^{-6} = 23, 18.0, 20.1, 16.5, 9.5, \text{ and } 9.2$ g/mole, the respective specific slips $S'/c \approx 4.1, 1.87, 1.62, 0.91, 0.58, \text{ and } 0.31$. These data reinforce our earlier finding that HPAM additive efficacy increases with increasing molecular weight. Next, the intrinsic slip $\Sigma = S'/(c/M_w)$, a measure of flow enhancement per molecule developed in §6.4.1, is plotted against N_{bb} , the number of backbone chain links, in Figure 6.6.2, using doubly logarithmic coordinates. The six HPAM data points straddle a line with an approximate slope of three. Figure 6.6.2 contains three correlating lines that lie within the data scatter. Equation 6.4-2, the best-fit line of the present data(closed symbols), is shown dotted:

$$\Sigma = (1.00 \pm 0.23) \times 10^{-7} N_{bb}^{(2.53 \pm 0.40)} \quad (6.4-2)$$

Inclusion of the three HPAM data from the literature leads to the best-fit line for all HPAM additives(open and closed symbols), shown dashed:

$$\Sigma = (1.73 \pm 0.66) \times 10^{-11} N_{bb}^{(3.19 \pm 0.43)} \quad (6.6-1)$$

Finally, the best-fit line of slope 3, having the form of the earlier correlation of equation 6.4-3, is indicated by the solid line in Figure 6.6.2:

$$\Sigma = 2.21 \times 10^{-10} N_{bb}^3 \quad (6.6-2)$$

where the slip modulus $\lambda = 2.21 \times 10^{-10}$ g/mole/wppm, the geometric-mean value of the six individual slip moduli listed in Figure 6.6.2. This mean slip modulus is slightly lower than the value $\lambda = 2.38 \times 10^{-10}$ g/mole/wppm determined in §6.4.1 from only the present data.

The Type-B flow-enhancement comparison is now expanded to encompass

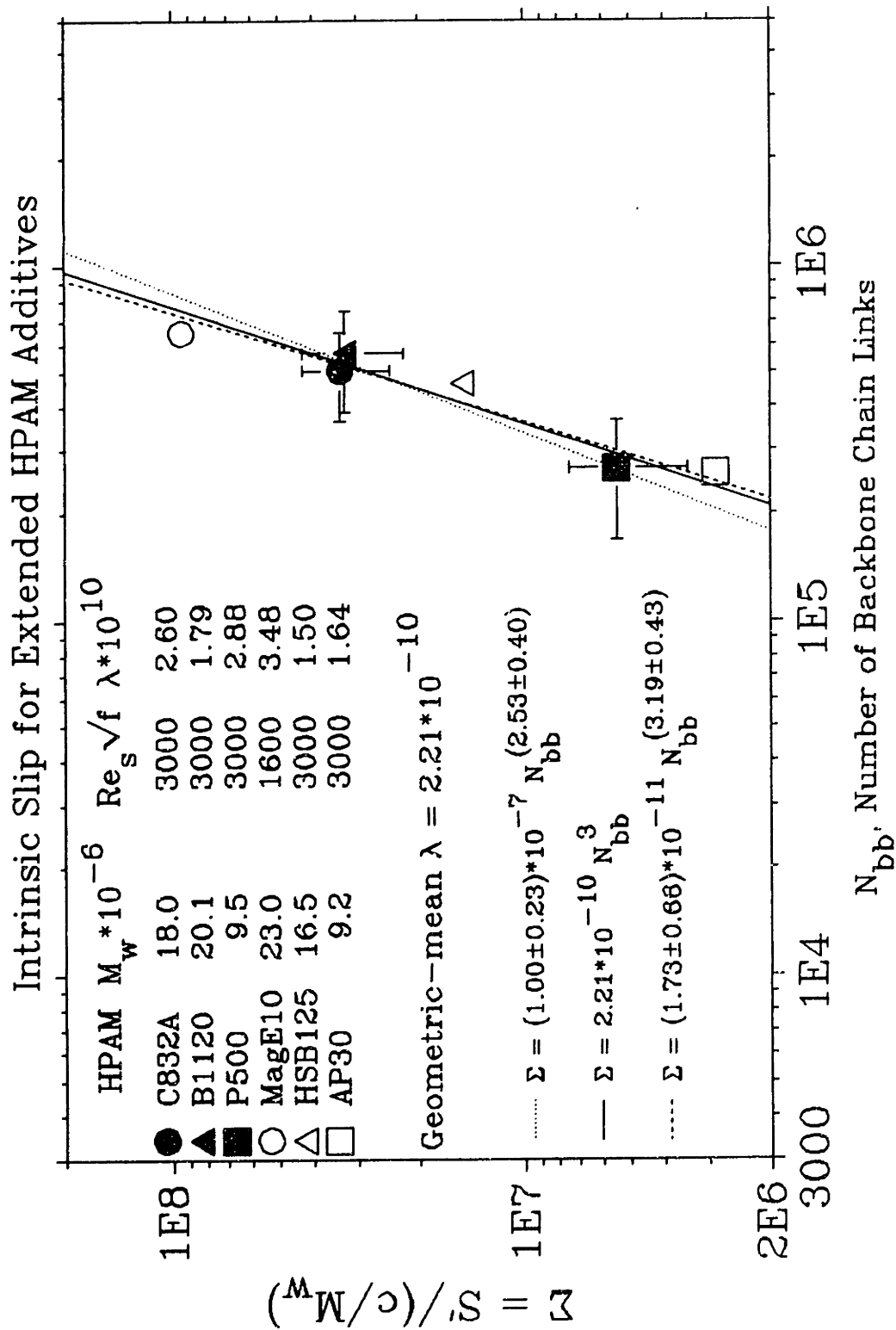


Figure 6.6.2: Intrinsic Slip for Extended HPAM Additives

various other additives, including xanthan gum (Rochefort & Middleman, 1984) with $M_w \approx 2.0 \times 10^6$ g/mole; asbestos fibers with $(d_f, l_f) = (35 \text{ nm}, 1.4 \text{ mm})$ (Sharma et al., 1979); asbestos fibers with $(d_f, l_f) = (50 \text{ nm}, 1.4 \text{ mm})$ (McComb & Chan, 1985); paper fibers with $(d_f, l_f) = (30 \text{ } \mu\text{m}, 2.7 \text{ mm})$ (Lee & Duffy, 1976); and nylon fibers with $(d_f, l_f) = (20 \text{ } \mu\text{m}, 1.0 \text{ mm})$ (Bobkowicz & Gauvin, 1965). Table 6.6 summarizes the physical dimensions of these fiber additives, the prevailing experimental conditions, and the flow-enhancements achieved. Figure 6.6.3 illustrates the observed flow enhancements S' over a seven-decade concentration domain. Data for HPAMs in Figure 6.6.1 occupy the upper left, where the low c and high S' give rise to high specific slips $S'/c \approx O(1)$ as seen in the figure. To the right at higher c and slightly downward at lower S' from the HPAM data, data for xanthan (∇) and asbestos fibers (\diamond \blacklozenge) lie roughly along the same trajectory with $0.03 < S'/c < 0.07$. These additives are clearly less effective per unit mass than HPAM. Farther to the right of the asbestos data, are the data for paper (\blacktriangle) and nylon (\blacktriangledown) fibers, showing the lowest $S'/c \approx 0.0016$ and 0.00021 , respectively. The observed specific slips span nearly five orders of magnitude, from $S'/c \approx 0.00021$ for nylon fibers to $S'/c \approx 4.1$ for the highest molecular-weight HPAM.

Because the most-important physical properties of fibers are their lengths l_f and aspect ratios l_f/d_f , additive efficacies exhibited by fibers and linear-polymer can be compared on an equal basis through their l_f and L_c , respectively.

To help interpret the broad variation in additive efficacy observed above, the additive-pervaded volume fraction per wppm, X_v/c , derived from either the macromolecular contour length L_c or the fiber length l_f and aspect ratio l_f/d_f , and then the additive-pervaded volume fraction required to induce unit slip can be calculated for each

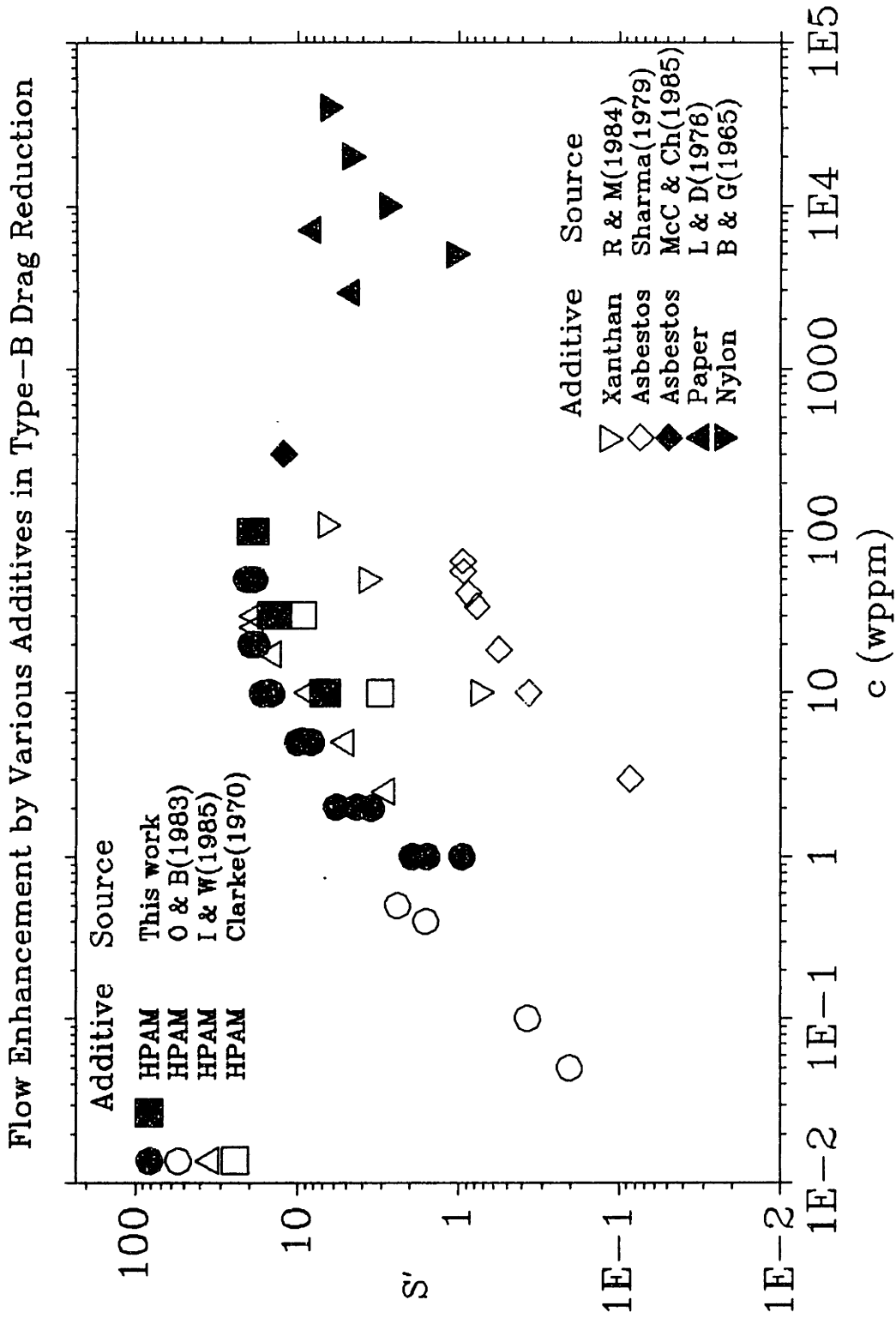


Figure 6.6.3: Flow Enhancement by Various Additives in Type-B Drag Reduction

additive. In §6.4.1, general expressions for X_v/c and X_v/S' are given for polymer additives by equations 6.4-5 and 6.4-6

$$\frac{X_v}{c} = \left[\frac{\pi L_c^3}{6} \right] \left[\frac{\rho N_A}{10^6 M_w} \right] \quad (6.4-5)$$

$$\frac{X_v}{S'} = \left[\frac{\pi L_c^3}{6} \right] \left[\frac{\rho N_A}{10^6 M_w} \right] \left[\frac{c}{S'} \right] = \left[\frac{\pi}{6 \times 10^6} \right] \left[\frac{\rho N_A a^3}{\lambda} \right] \quad (6.4-6)$$

with Avogadro's number $N_A = 6.022 \times 10^{23}$ mole⁻¹, and with densities, concentrations, lengths, and molecular weights in g/cm³, wppm, cm, and g/mole, respectively. Analogous expressions for X_v/c and X_v/S' can be derived for fiber additives using d_f , l_f , and ρ_f in lieu of L_c and M_w . The respective equations for polymer and fiber X_v/S' are:

$$\frac{X_v}{c} = \left[\frac{\pi l_f^3}{6} \right] \left[\frac{4\rho}{10^6 \rho_f \pi d_f^2 l_f} \right] \quad (6.6-3)$$

$$\frac{X_v}{S'} = \left[\frac{\pi l_f^3}{6} \right] \left[\frac{4\rho}{10^6 \rho_f \pi d_f^2 l_f} \right] \left[\frac{c}{S'} \right] \quad (6.6-4)$$

again with Avogadro's number $N_A = 6.022 \times 10^{23}$ mole⁻¹ and with densities, concentrations, and lengths, in g/cm³, wppm, and cm, respectively. The last two columns of Table 6.6 respectively list X_v/c and X_v/S' for each additive. For all HPAM additives, $X_v/S' = 3000 \pm 100$, implying, since X_v cannot physically exceed unity, that these additives must be significantly aligned during drag reduction. Note also that equation 6.6-2, with the slip modulus $\lambda = 2.21 \times 10^{10}$ g/mole/wppm for the six HPAM polymers, yields $X_v/S' \approx 2840$, which agrees with the average value cited above. For the xanthan

data, with uncertain molecular characterization, $X_v/S' \approx 40$, still much greater than unity, but two orders of magnitude lower than that for HPAM. Thus for polymeric additives, the additive-pervaded volume per unit slip seems to increase with increasing number of backbone chain links.

Within the fiber data cited, X_v/S' again assumes larger values for greater additive efficacies. For asbestos(Sharma et al., 1979), asbestos (McComb & Chan, 1985), paper, and nylon fibers with respective aspect ratios $l_f/d_f = 40000, 28000, 90,$ and $51,$ their respective $(S'/c, X_v/S') \approx (0.03, 14000), (0.04, 5000), (0.0016, 4),$ and $(0.00021, 7).$ For fibers, both S'/c and X_v/S' increase with increasing aspect ratio, a suitably normalized measure of the fiber length.

In summary, in Type-B turbulent flow-enhancement by polymer additives, HPAM and xanthan, and fiber additives, asbestos, nylon, and paper, the additive efficacies S'/c and additive-pervaded volume fractions per unit slip X_v/S' seem to respectively depend on the number polymer backbone chain links and the fiber aspect ratio.

Additive†	Fiber Diameter	Aspect Ratio	Fiber Length	Pipe Diameter
	$d_f \times 10^3$	l_f/d_f	l_f	D
	(cm)		(cm)	(cm)
Fiber Additives				
Asbestos ⁵	0.0035	40000	0.14	1.9
Asbestos ⁶	0.005	28000	0.14	1.95
Paper ⁷	3.0	90	0.27	10.0
Nylon ⁸	2.0	51	0.10	4.98
Stress Level of Data				
Stress Level of Data	Specific Slip	Intrinsic Slip	Volume Fraction Per wppm	Volume Fraction Per Unit Slip
$Re_s \sqrt{f}$	S'/c	$\Sigma \times 10^{-6}$	X_v/c	X_v/S'
	(wppm ⁻¹)	(g/mole/wppm)	(wppm ⁻¹)	
1600	0.03	n/a	420	13900
1300	0.041	n/a	205	4980
3000	0.0015	n/a	0.006	4.1
5800	0.00021	n/a	0.0015	7.1
† Note the wrap-around nature of this table in both the HPAM- and Fiber-Additive sections. 1 — Clarke(1970); 2 — Oliver & Bakhtiyarov(1983); 3 — Interthal & Wilski (1985); 4 — Rochefort & Middleman(1984); 5 — Sharma et al.(1979); 6 — McComb & Chan(1985); 7 — Bobkowicz & Gauvin(1965); 8 — Lee & Duffy (1976). n/a = not applicable				

6.6.2 Present and Literature Retro-Onset Data

In §6.4.2, retro-onset data from the present work were analyzed and correlated

In Figure 6.6.4, the $T_w^\#$ data from this work, previously shown in Figure 5.3.23, and the few available $T_w^\#$ data for HPAMs in the literature — AP30(Clarke, 1970) and HSB125(Interthal & Wilski, 1985) — are plotted semilogarithmically against concentration to adhere to the form of equation 6.4-10. The legend in Figure 6.6.4 provides the additive molecular weight and experimental conditions for these data. The dotted line represents equation 5.3-1 for the best-fit line through C832A(● ◆) and B1120(▲) data from the 1.458-cm pipe:

$$\log T_w^\# = -0.436 + 0.134c \quad (5.3-1)$$

While the ordinal intercept, $T_w^\#_o = 0.37$ dyne/cm², closely matches the ideal intercept value for a 1.458-cm pipe, $T_w^\#_o = 0.346$ dyne/cm², the coefficient yields an inferred $S'/c = 1.00$, which differs from the observed average for the two additives, $S'/c \approx 1.75$. The ratio 1.00/1.75 produces a ladder imperfection factor $\beta = 0.58$. Literature data from a 1.40-cm pipe for additive HSB125(▽), of $M_w = 16.5 \times 10^6$ g/mole, lie close to the dotted line in Figure 6.6.4.

Well to the right of the dotted line at $c = 30$ wppm, two data points for additives P500(■) and AP30(□) lie close together. Both data points refer to similar polymer molecular weights — $M_w \times 10^{-6} = 9.5$ and 9.2 g/mole, respectively — and nearly identical pipe diameters — $D = 1.021$ and 1.02 cm, respectively. Equation 6.4-10 can be used to predict the concentration dependence of $T_w^\#$ data for additives with respective

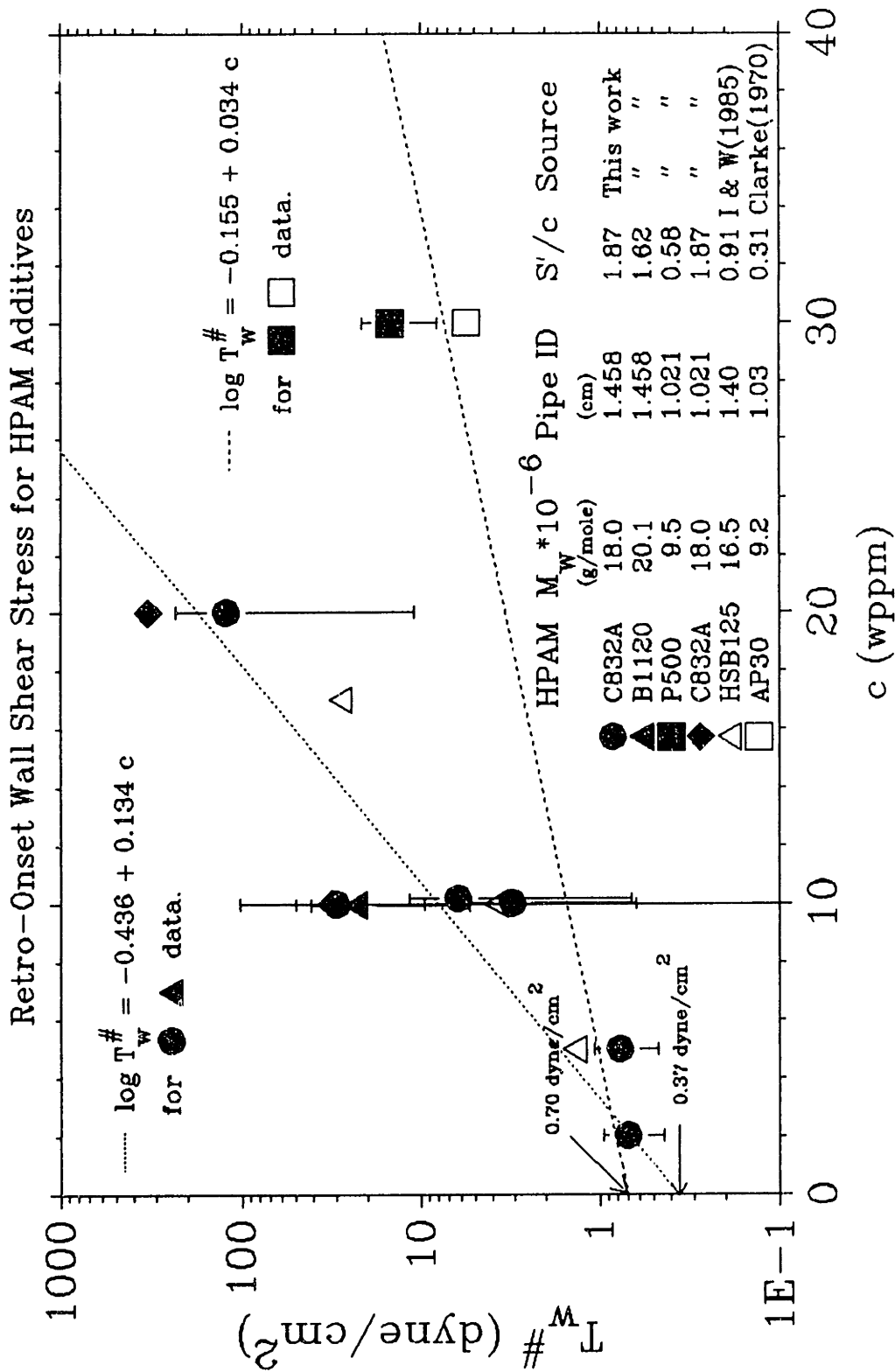


Figure 6.6.4: Retro-Onset Wall Shear Stress for HPAM Additives

$M_w \times 10^{-6} = 9.5$ and 9.2 g/mole in pipes of respective inner diameters of 1.02 and 1.03 cm. With $T_w^{\#_o} = (\rho\nu_s^2)(Re_s\sqrt{f^{\#}})^2/(2D^2)$, the theoretical ordinate intercept for a 1.026 -cm pipe and water solvent at 25°C should be $T_w^{\#_o} \approx 0.70$ dyne/cm², or $\log T_w^{\#_o} \approx -0.155$. The slope of this second line can be predicted from concentration coefficient in equation 6.4-10 for imperfect Type-B ladders, $(2/15)\beta(S'/c)$. With an average $S'/c \approx 0.44$ for additives P500 and AP30 and $\beta = 0.58$, the slope of the line should be ~ 0.034 . In Figure 6.6.4, the dashed line represents retro-onset predictions for HPAM additives of $M_w \approx 9 \times 10^6$ g/mole in a 1.026 -cm pipe, corresponding to the relation:

$$\log T_w^{\#} = -0.155 + 0.034c \quad (6.6-5)$$

As seen in Figure 6.6.4, this line runs close to the data points for additives P500 and AP30.

In conclusion, the retro-onset correlations developed from the present data also accommodate the few retro-onset data available in the literature.

6.7 Modelling Types A and B of Drag Reduction

Prior to this work, only Type-A drag reduction by random-coiling additives was amenable to modelling from knowledge of the additive's macromolecular properties. As a result of this work, preliminary modelling of Type-B drag reduction based on macromolecular parameters can also be undertaken. These approaches are illustrated for HPAM polymers.

6.7.1 Modelling a Perfect Types-A Fan

Type-A drag reduction for collapsed HPAM additives can be predicted from their molecular weights as follows. For known M_w , the rms radius of gyration R_G is obtained from equation 2.4-11, $R_G = 1.5 \times 10^{-2} M_w^{0.59}$; and this yields the onset wall shear stress T_w^* via equation 6.3-5, $T_w^* = 5.79 \times 10^5 R_G^{-2}$; this finally leads to the onset point on N, at $Re_s \sqrt{f}^*$, using the known pipe diameter, D , and solvent physical properties. Next, using $N_{bb} = M_w/m$, the intrinsic slope increment is obtained from equation 6.3-7, $\Pi = 43.5 \times 10^{-6} N_{bb}^{3/2}$, and hence the specific slope increment δ/\sqrt{c} , and for known c , the slope increment δ . A polymeric regime segment P can now be calculated by the following equation:

$$\frac{1}{\sqrt{f_p}} = 4.0 \log(Re_s \sqrt{f}) - 0.4 + \sqrt{c} \left[\frac{\delta}{\sqrt{c}} \right] \log \left[\frac{Re_s \sqrt{f}}{Re_s \sqrt{f}^*} \right] \quad (6.7-1)$$

Equation 6.7-1 allows the construction of a perfect fan comprising any set of additive concentrations. However, it does not account for two important observed physical phenomena: the MDR asymptote which limits the extent of flow enhancement, $1/\sqrt{f_p} \leq 1/\sqrt{f_m}$, at any $Re_s \sqrt{f} > 400$; and polymer degradation which causes fan radii to deviate downward from their linear slopes, as observed in §5.2. The valid domain of $Re_s \sqrt{f}$ and range of $1/\sqrt{f_p}$ for equation 6.7-1 are therefore constrained. The lower bound on $Re_s \sqrt{f}$ is the onset $Re_s \sqrt{f}^*$, described above. The upper bound on $Re_s \sqrt{f}$ is the smaller of two values: either the point where the P segment intersects the line M or the point at which degradation begins. The former is the simultaneous solution of equation 2.4-7 for the

MDR asymptote and equation 6.7-1 for an ideal fan radius:

$$Re_s \sqrt{f} = 10^{\left(\frac{32 - \delta \log Re_s \sqrt{f^*}}{15 - \delta} \right)} \quad (6.7-2)$$

The latter is determined via equation 6.1-2 for T_w^{\wedge} :

$$Re_s \sqrt{f}^{\wedge} \approx 3.4 \times 10^8 \left[\frac{D \sqrt{\rho}}{\eta_s M_w} \right] \quad (6.7-3)$$

This completes the information required to construct, and constrain, a perfect Type-A fan.

Figure 6.7.1 compares the experimentally-observed Type-A fan for additive B1120 and the perfect Type-A fan predicted by the preceding model. For B1120, $M_w \approx 20.1 \times 10^6$ g/mole and $R_G = 300$ nm in 0.3 N NaCl, hence, using the length-based onset constant for HPAM, $\Omega_L = R_G u_r^* / \nu_s = 8.3 \times 10^{-3}$, the onset point $Re_s \sqrt{f^*} \approx 570$ in a 1.458 cm pipe. From equation 6.3-7, the intrinsic slope increment, $\Pi = 43.5 \times 10^{-6} N_{bb}^{3/2}$, and using $N_{bb} \approx 5.7 \times 10^5$, the estimated a specific slope increment $\delta/\sqrt{c} \approx 4.1$. From $Re_s \sqrt{f^*}$ and δ/\sqrt{c} , P segment trajectories can be predicted by equation 6.7-1, for any concentration c . In Figure 6.7.1, the predicted P segments for $1 \leq c \leq 100$ wppm are shown by various kinds of lines, as indicated by the legend, emanating from the predicted onset point on N, labelled $Re_s \sqrt{f^*} = 570$. While the predicted onset point closely matches the observed onset points, as seen by inspection, the predicted fan segments only match the observed radii for $c = 5, 10,$ and 20 wppm. At low concentrations, the model overestimates the slope increments for $c = 1$ and 2 wppm. At high concentration, it misses entirely the fan radii for $c = 50$ and 100 wppm, possibly

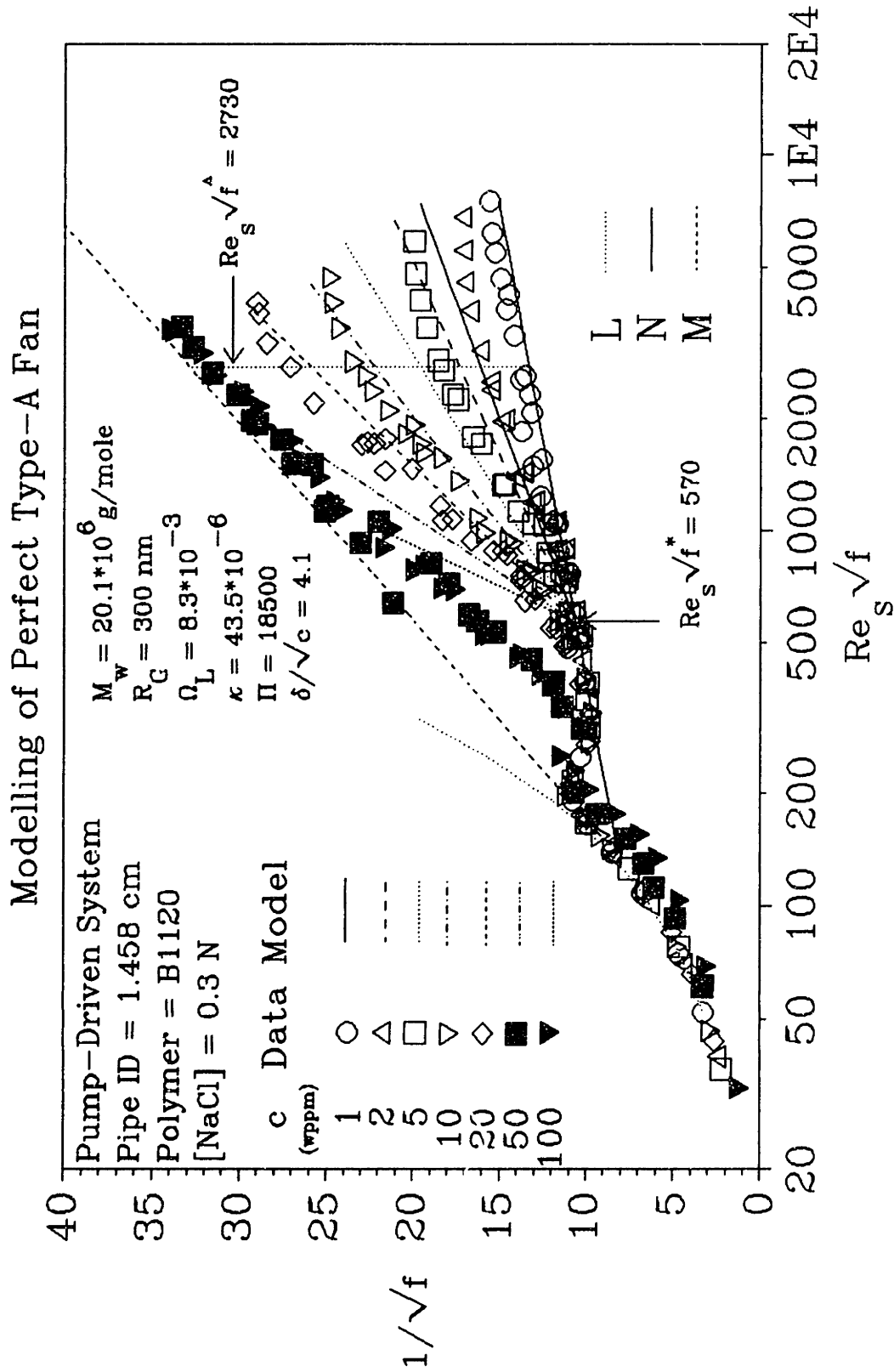


Figure 6.7.1: Modelling of Perfect Type-A Fan

due to the ill-defined onsets observed for these higher concentrations. Also in Figure 6.7.1, the vertical dotted line marks the "degradation falloff", estimated to occur at $Re_p \sqrt{f} = 2730$; at higher $Re_p \sqrt{f}$, the flow data are seen to deviate downwards from their linear paths.

6.7.2 Modelling a Perfect Type-B Ladder

In a perfect Type-B ladder, the P segments, or ladder rungs, run parallel to the Newtonian baseline N and have constant flow enhancements S' above N that depend only on concentration, since the specific slip S'/c is essentially constant. Thus, only knowledge of the specific slip S'/c is required to construct a perfect ladder in a PK coordinates. From the present work, equation 6.6-2 correlates S'/c and M_w by an expression for the intrinsic slip: $\Sigma = S'/(c/M_w) = \lambda N_{bb}^3$, where $\lambda = 2.21 \times 10^{-10}$ g/mole/wppm. For HPAM additives,

$$\frac{S'}{c} = \left[\frac{\lambda}{m^3} \right] M_w^2 \quad (6.7-4)$$

with M_w in g/mole and $\lambda/m^3 \approx 4.9 \times 10^{-15} [(g/mole)^2 \cdot wppm]^{-1}$. Equation 6.4-7 then describes each rung in PK coordinates:

$$\frac{1}{\sqrt{f_p}} = 4.0 \log Re_p \sqrt{f} - 0.4 + c \left[\frac{S'}{c} \right] \quad (6.4-7)$$

The retro-onset point for any rung, its intersection with the line M, is given by equation 6.4-8:

$$Re_s \sqrt{f}^{\#} = 10 \left[\frac{c \left(\frac{S'}{c} \right)^{+32}}{15} \right] \doteq 136 + 10 \frac{S'}{15} \quad (6.4-8)$$

The domain of valid $Re_s \sqrt{f}$ for each Type-B P segment is limited as follows: The lower bound for $Re_s \sqrt{f}$ is given by equation 6.4-8 for the retro-onset point $Re_s \sqrt{f}^{\#}$; the upper bound is set by degradation, using equation 6.7-3. This completes the information to construct a perfect Type-B ladder.

Figure 6.7.2 compares the observed Type-B ladder for additive B1120 at $c = 1, 2, 5,$ and 10 wppm and the perfect Type-B ladder predicted by the preceding model. For B1120, using equation 6.6-2 for the intrinsic slip, $\Sigma = 2.21 \times 10^{-10} N_{bb}^3$, the model estimates a specific slip $S'/c = 2.0$. From this, using equations 6.4-7 and 6.4-8, all P segments can be calculated. The predicted ladder rungs are depicted by various types of line segments in Figure 6.7.2, as noted in the legend. The model accurately predicts ladder rungs at intermediate concentrations of 5 and 10 wppm but overpredicts the rungs at both low and high concentrations, $c = 1$ and 10 wppm. The degradation falloff is predicted to occur at $Re_s \sqrt{f}^{\wedge} = 2800$, beyond which the data begin to fall below from their linear P segments.

In summary, simple models are presented for a perfect Type-A fan and a perfect Type-B ladder during drag reduction by collapsed and extended HPAM additives. These accord reasonably with the observed flow-enhancement behavior of high molecular-weight HPAM additives and may serve to provide preliminary estimates in engineering applications of drag reduction.

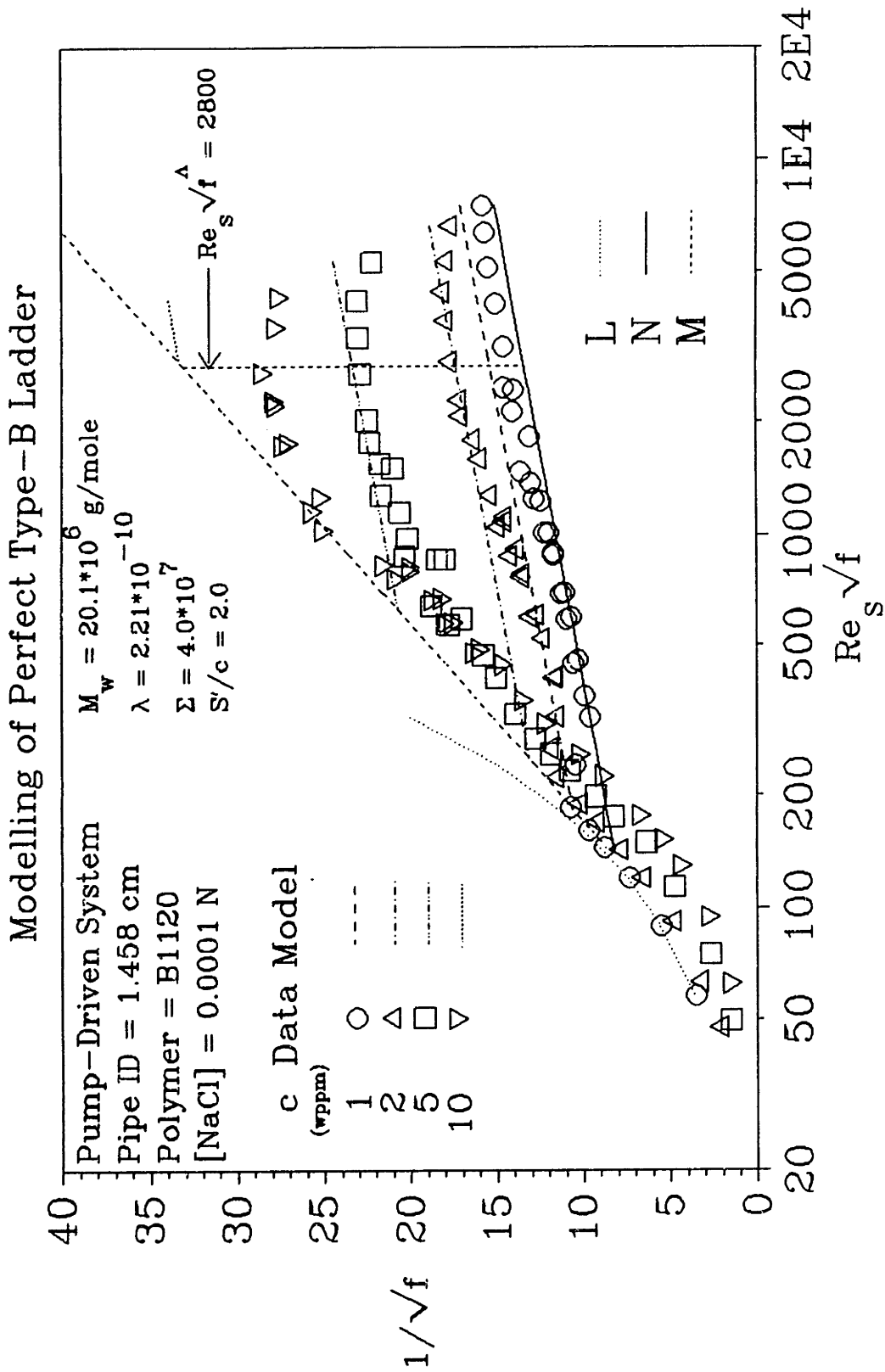


Figure 6.7.2: Modelling of Perfect Type-B Ladder

CHAPTER VII

CONCLUSIONS

1. The drag reduction phenomenon was experimentally studied in two pipes, of diameters 1.46 and 1.02 cm, using seven polyelectrolytic HPAM additives, with molecular weights from 1 to 20×10^6 g/mole and degree of backbone hydrolysis from 8 to 60%, at concentrations from 1 to 1000 wppm, in saline solutions containing from 0.3 to 0.00001 N NaCl.
2. Both laminar and turbulent flow behavior were greatly influenced by salinity-induced changes in the initial conformation of the HPAM additives. Initially collapsed, random-coiling conformations exhibited Newtonian laminar flow and Type-A turbulent drag reduction, while initially extended conformations exhibited shear-thinning in laminar flow and Type-B turbulent drag reduction.
3. The gross-flow physics of Type-B drag reduction were delineated. A characteristic "ladder" structure prevailed, with polymeric-regime segments that were roughly parallel to, but shifted upward from, the Prandtl-Karman line and intersected the maximum drag reduction asymptote at retro-onset points.
4. In the polymeric regime, both Type-A fan and Type-B ladder structures were essentially independent of pipe diameter, and were scaled by the wall shear stress. Thus

both types of drag reduction are insensitive to the large turbulence scales imposed by pipe diameter, and are controlled instead by the finer wall-turbulence scales associated with the wall shear stress. The wall shear stress also scaled incipient degradation during drag reduction.

5. New correlations were presented for Type-A drag reduction by HPAM additives, as follows:

$$\text{(Onset Correlation)} \quad T_w^* = 5.79 \times 10^5 R_G^{-2} \quad (6.3-5)$$

$$\text{(Slope-Increment Correlation)} \quad \Pi = 43.5 \times 10^{-6} N_{bb}^{3/2} \quad (6.3-7)$$

6. In Type-B drag reduction it was found that the flow enhancement S' was proportional to additive concentration, and that the intrinsic slip, $\Sigma = S'/(c/M_w)$, varied roughly as the third power of backbone chain links N_{bb} . New correlations were presented for Type-B drag reduction by HPAM additives:

$$\text{(Intrinsic-Slip Correlation)} \quad \Sigma = 2.21 \times 10^{-10} N_{bb}^3 \quad (6.6-2)$$

$$\text{(Retro-Onset Correlation)} \quad \log T_w^\# = -0.436 + 0.134c \quad (5.3-1)$$

7. Analysis of available literature for Type-B drag reduction by polyelectrolytic and fiber additives revealed a wide range of additive efficacies, with specific slips S'/c from 0.0001 to 4. For the most effective additives, HPAM and asbestos fibers, the additive-pervaded volume fraction per unit flow enhancement, $X_v/S' \approx 3000$, implied that these additives align during drag reduction.

8. The slip ratio R_{sc} , which is the relative flow enhancement induced in Type-A and Type-B drag reduction at constant additive concentration, was found to be a universal function of the normalized turbulent flow strength ($Re_s\sqrt{f}/Re_s\sqrt{f^*}$), as follows:

$$R_{sc} = 1 - \left(\frac{Re_s\sqrt{f}}{Re_s\sqrt{f^*}} \right)^{-2/3} \quad (6.5-2)$$

The extension of initially collapsed, random-coiling, HPAM macromolecules by the turbulent flow field thus seems independent of additive parameters and absolute wall shear stress levels.

9. Gross flow additive equivalence was detected at iso-slip points, where different polymer solutions induced equal flow enhancements. At numerous such points, the collapsed to extended slip ratio at constant concentration, R_{sc} , was essentially equal to the extended to collapsed concentration ratio at constant slip, R_{cs} . Thus, for fixed total additive concentration, the collapsed to extended slip ratio R_{sc} observed at any $Re_s\sqrt{f}$ simply represents the fraction of originally collapsed macromolecules that have become extended in the flow, and thence effective in drag reduction.

10. If extended additive states are the active species responsible for drag reduction, as appears likely, then Type-B behavior should underlie the basic mechanism of additive-turbulence interaction.

CHAPTER VIII

RECOMMENDATIONS

1. Flow-structure measurements under conditions of gross-flow additive equivalence might discover whether gross-flow additive equivalence reflects additive equivalence in the corresponding mean and turbulent flow structures.
2. Experiments conducted in the pump-driven system using additives C837A and C836A, of low and moderate backbone charges respectively, might permit the effect of backbone charge on turbulent drag-reduction behavior to be better identified.
3. Additional polymer-characterization techniques, such as light-scattering and viscometry, might be used on solutions of collapsed HPAM additives, at least, to directly determine additive properties, such as radius of gyration and intrinsic viscosity. This would augment the present in-situ, laminar-flow data from which such properties were inferred.

CHAPTER IX

APPENDICES

- A Linear Polymers: Theory and Experiment
- B Equipement and Vendors
- C Water and Mercury Manometers
- D Manufacturers' Polymer Data
- E Solvent Data Sets 1 - 5
- F Polymer-Solution Data
- G NOMENCLATURE
- H REFERENCES
- I BIOGRAPHICAL NOTE

APPENDIX A

A2.4 Linear Polymers: Theory and Experiment

The following sections present some theory, experimental results, and theoretical calculations for dilute solutions of both nonionic and ionic linear polymers. These provide the bases for inferring physical properties of polymers from experimental data.

A2.4.1 Nonionic Linear Polymers

The static and dynamic properties of nonionic linear polymers have been widely discussed (Flory, 1953; Morawetz, 1975). The relevant macromolecular properties discussed briefly are molecular weight, chain configuration, and intrinsic viscosity. Only vinyl polymers such as PAM are treated.

Free radical polymerization of vinyl monomer ($\text{CH}_2=\text{CXY}$) in solution produces contaminant-free polymer of high molecular weight. Common methods include thermal initiation, redox systems, and electromagnetic and ultrasonic irradiation. Osmometry, light-scattering, ultracentrifugation, and sedimentation provide various average molecular weights for a given polymer sample.

Theoretically, some average chain configuration can be calculated via statistical methods. Such methods require that the chain have a large degree of polymerization to average over the fine details which would otherwise make the calculation virtually impossible. Some assumptions for idealized chains include: infinitely thin, non-

intersecting bonds; equal bond lengths; freely rotating bonds; only short-range intramolecular forces; perfect chain solvation; homogeneity; and isotropy. For a three-dimensional chain of this type, the end-to-end displacement has been calculated,

$$\langle h^2 \rangle^{1/2} = \ell N^{1/2} \quad (\text{A2.4-1})$$

in which ℓ and N are the bond length and number of bonds, respectively. The radius of gyration, R_G , relates simply to the end-to-end displacement:

$$R_G = \langle R^2 \rangle^{1/2} = \left(\frac{\langle h^2 \rangle}{6} \right)^{1/2} = \ell \left(\frac{N}{6} \right)^{1/2} \quad (\text{A2.4-2})$$

While these assumptions greatly simplify the calculations, they apply only random-coiling chains. Fortunately, real chains behave qualitatively the same as these idealized, random-flight chains.

Having restricted bonds and long-range forces, real chains may be expanded and extended enough to invalidate the above statistical calculations. For a restricted angle θ ,

$$\langle h^2 \rangle = N\ell^2 \frac{(1 - \cos\theta)}{(1 + \cos\theta)} \quad (\text{A2.4-3})$$

thus, for tetrahedrally linked vinyl polymers in which $\theta = 109.47^\circ$ and $\cos\theta = -1/3$, $\langle h^2 \rangle^{1/2}$ is $\sqrt{2}$ times that for random-flight chains.

Without the random-flight assumptions, $\langle h^2 \rangle^{1/2}$ and R_G become larger as the spectrum of statistically acceptable configurations shifts to larger values. This expansion is characterized by a linear-expansion factor:

$$\alpha = \frac{\langle h^2 \rangle^{1/2}}{\langle h_o^2 \rangle^{1/2}} = \frac{R_G}{R_{G_o}} \quad (\text{A2.4-4})$$

in which the 0 subscript indicates the unperturbed state.

In thermodynamic calculations of dilute solutions of linear polymers, solvent-polymer interactions and excluded volume effects are very important; these reflect roughly enthalpic and entropic phenomena, respectively. Most importantly, solvent-polymer interactions influence volume exclusion. For example, good solvent-polymer interactions can increase the population of otherwise less-probable chain configurations, leading to chain expansion. Both chemical properties and temperature determine the exact nature of this interaction. Calculating how these affect the statistical configuration of a single polymer chain gives rise to an expression for α :

$$\alpha^5 - \alpha^3 = 2C_M \psi_1 \left(1 - \frac{\Theta}{T}\right) M^{1/2} \quad (\text{A2.4-5})$$

in which C_M is a constant for a given solvent-polymer pair, ψ_1 reflects the entropy of mixing, Θ is the temperature at which enthalpic and entropic effects cancel, and M is the molecular weight of the polymer chain. Clearly, increasing M and T above the Θ temperature leads to macromolecular expansion.

Adopting the random-flight model, an equivalent-chain model accounts for the excluded-volume effect of real chains. Rather than consisting of N C-C bonds of bond-length ℓ , this chain consists of N' Kuhn statistical segments of length ℓ' in which $\ell' = 1/\lambda \equiv \langle h^2 \rangle / L_c$ and $N' \equiv L_c^2 / \langle h^2 \rangle$ as $L_c \rightarrow \infty$. While the contour length remains the same ($L_c = N'\ell' = N\ell$), $\ell' > \ell$, and $N' < N$ so that $\langle h'^2 \rangle^{1/2} / \langle h^2 \rangle^{1/2} = R'_G / R_G = (\ell' / \ell)^{1/2} > 1$. While these larger average sizes are consistent with the excluded-volume effect, N' and ℓ' have no physical meaning, rather they must be determined empirically. To account for excluded-volume effects under the assumption (Peterlin, 1955) that

$\langle h^2 \rangle^{1/2} \propto N^{1+\epsilon}$, a new relation between $\langle h^2 \rangle^{1/2}$ and R_G obtains:

$$R_G = \langle R^2 \rangle^{1/2} = \frac{\langle h^2 \rangle^{1/2}}{[(2+\epsilon)(3+\epsilon)]^{1/2}} \quad (\text{A2.4-6})$$

When $\epsilon = 0$ (i.e. no excluded-volume effects), this reduces to the ideal random-coiling relationship previously derived.

So far, the polymer has been considered an ensemble of unconnected segments, the radial distribution of which is identical to the radial density distribution of a macromolecule composed of the same linear sequence of segments. In addition, it has been at rest with respect to the solvent. The macromolecule is modelled now as a string of beads in a laminar flow field. Strictly speaking, there are N beads and $N-1$ bonds; however, as $N \rightarrow \infty$, $N \approx N-1$, and the distinction loses importance.

In this laminar flow field, the solvent exerts a force at every point of contact along the polymer chain. While in the idealized case the solvent exerts a force at every bead, that is, a free-draining polymer, for real chains the solvent does not penetrate into the inner, more-bead-dense core. The solvent exerts a force on the macromolecule that depends on several parameters: R_G or $\langle h^2 \rangle^{1/2}$; $N = M/m$, the number of beads; the bead distribution; and ζ/η_0 , the ratio of bead friction coefficient to solvent viscosity. While ζ must be inferred experimentally, it can be reasoned that the overall macromolecular frictional coefficient f_0 becomes independent of ζ when ζ/η_0 becomes sufficiently large. Furthermore, it can be shown that $f_0/\eta_0 \sim \langle h^2 \rangle^{1/2}$ (or R_G), independent of both the polymer and solvent!

To describe the contribution of polymer molecules to dilute-solution viscosity, Kraemer(1938) defined the intrinsic viscosity:

$$[\eta] = \lim_{c \rightarrow 0} \frac{\eta_{sp}}{c} = \lim_{c \rightarrow 0} \frac{(\eta_r - 1)}{c} = \lim_{c \rightarrow 0} \frac{\eta - \eta_s}{c\eta_s} \quad (\text{A2.4-7})$$

in which the subscript indicates solvent. Since the intrinsic viscosity $[\eta]$ can depend on the shear rate $\dot{\gamma}$, a stricter definition includes the restriction $\dot{\gamma} \rightarrow 0$. Huggins(1942) included in his definition the observation that the slope of the η_{sp}/c curve varied as $[\eta]^2$:

$$\frac{\eta_{sp}}{c} = [\eta] + k'[\eta]^2 c \quad (\text{A2.4-8})$$

in which the Huggins (slope) coefficient k' varies with M_w and is typically between 0.35 and 0.40. The physical significance of k' has not been elucidated, and experimental k' values vary widely(Fanood & George, 1987). Intrinsic viscosity has also been defined as,

$$[\eta] = \lim_{c \rightarrow 0} \frac{\ln \eta_r}{c} = \lim_{c \rightarrow 0} \frac{\ln(\frac{\eta}{\eta_o})}{c} \quad (\text{A2.4-9})$$

Both definitions can be used to extrapolate dilute solution viscosities down to infinite dilution; the latter is preferred because as $c \rightarrow 0$ the extrapolation has greater linearity. Better methods for extrapolating viscosity data down to infinite dilution have been devised and discussed extensively elsewhere(Bohandecký & Kovář, 1982).

Kirkwood & Riseman(1948) and Debye & Bueche(1948) independently developed theories for intrinsic viscosity. In both treatments, the intrinsic viscosity had the same dependence: $[\eta] \sim \langle h^2 \rangle^{3/2}/M$. The Flory-Fox equation followed from this dependence:

$$[\eta] = \Phi \frac{\langle h^2 \rangle^{3/2}}{M} \quad (\text{A2.4-10})$$

in which the KR constant Φ is 3.62×10^{23} mole⁻¹ for all polymer-solvent systems. The equation obtains if the polymer behaves somewhat like a random coil.

In a solution of random-coiling polymers of diameter $\langle h^2 \rangle^{1/2}$ with concentration c , the volume fraction of coils is:

$$\phi = \frac{\pi \langle h^2 \rangle^{3/2} \rho c N_A}{6M} \quad (\text{A2.4-11})$$

in which ρ and N_A are the solvent density and Avogadro's number, respectively. Substituting for $\langle h^2 \rangle^{1/2}$ via the Flory-Fox equation yields the following equation:

$$\phi = \frac{\pi \rho N_A}{6\Phi} c[\eta] \approx 1.26c[\eta] \quad (\text{A2.4-12})$$

Rearranging and setting $\phi = 1$ gives one definition of diluteness: $c[\eta] = 0.79$. Einstein's limiting law for dilute solutions of hard spheres, $c[\eta] = 2.5$, constitutes a laxer dilute-solution criterion. Other such criteria have been developed elsewhere (Wolff, 1977).

The above value of the KR constant is theoretical; experiments have inferred smaller Φ values. Flory(1953) tabulated Φ values from 10 polymer-solvent systems; Φ ranged between 1.75×10^{23} and 2.6×10^{23} mole⁻¹ with a best value of $(2.1 \pm 0.2) \times 10^{23}$ mole⁻¹. Flory speculated that polymer heterogeneity reduced the experimental value from the probable true value of 2.5×10^{23} mole⁻¹. Fujita(1988) recently discussed both experimental values and theoretical calculations for the KR constant. He tabulated values from several experiments using polystyrene near the Θ condition and showed Φ to range from 1.7 to 2.9×10^{23} mole⁻¹, citing a "most reliable" experimental value of 2.55×10^{23}

mole⁻¹(Miyaki et al., 1980; Fujita, 1988).

On the theoretical side, improved KR techniques(Miyaki et al., 1980), renormalization group methods(Oono & Kohomoto, 1983), and Monte Carlo methods(Zimm, 1980; Garcia de la Torea et al., 1982) have been used to calculate Φ . The respective Φ values are 2.85×10^{23} , 2.36×10^{23} , and 2.51×10^{23} mole⁻¹. The last value has been declared the upper bound by Fixman(1981). To account for good solvents, the Flory-Fox equation has been corrected by introducing a 0.8 factor(Yamakawa, 1971). The Flory-Fox equation in terms of R_G is:

$$[\eta] = (0.8)(6^{3/2}) \frac{\Phi R_G^{3/2}}{M} \quad (\text{A2.4-13})$$

It should be noted no single value for Φ has been accepted, from either experiment or theory. For example, Banijamali et al.(1974) used $\Phi = 2.66 \times 10^{23}$ mole⁻¹ (Pyun & Fixman, 1966) and neglected the 0.8 solvent factor in the Flory-Fox equation. While Virk(1975b) used the same Φ , he did include the 0.8 solvent factor. More recently, Merrill & Horn(1984) and Tam & Tiu(1990) used $\Phi = 2.5 \times 10^{23}$ mole⁻¹ and 2.85×10^{23} mole⁻¹, respectively, without any solvent correction. Coincidentally, using the 0.8 solvent factor with $\Phi = 2.5 \times 10^{23}$ mole⁻¹ yields an effective $\Phi' = 2.0 \times 10^{23}$ mole⁻¹, identical within experimental error to Flory's best Φ value of $(2.1 \pm 0.2) \times 10^{23}$ mole⁻¹.

To relate $[\eta]$ and the linear-expansion factor α , the Flory-Fox equation can be modified:

$$[\eta] = (0.8)(6^{3/2})\Phi \left(\frac{\langle R_o^2 \rangle}{M}\right)^{3/2} M^{1/2} \alpha^3 = KM^{1/2} \alpha^3 \quad (\text{A2.4-14})$$

Under Θ conditions, in which $\alpha \equiv 1$, $[\eta]_{\Theta} = KM^{1/2}$. Experiments indicate that $\log \alpha^3$

varies with $\log M$; thus, intrinsic viscosity may be expressed as $[\eta] = K'M^a$. That $[\eta] = KM^{1/2}\alpha^3$ agrees qualitatively with the empirical Mark-Houwink-Kuhn-Sakurada(MHKS) relation, $[\eta] = K'M_w^a$, is not surprising.

To this point, the theoretical treatment has considered only monodisperse polymers of molecular weight M . For heterogeneous polymer solutions, the relation can be transformed:

$$[\eta] = K'M_v^a \quad (\text{A2.4-15})$$

in which M_v is the viscosity average molecular weight. Because M_v and M_w are not too different, using M_w in the MHKS relation,

$$[\eta] = K'M_w^a \quad (\text{A2.4-16})$$

does not introduce too-unacceptable an error in $[\eta]$.

A2.4.2 Linear Polyelectrolytic Polymers

Linear polyelectrolytic polymers(called henceforth polyions, but also known as ionic polymers and macroions) differ from nonionic linear polymers in that some of the side-chain residues are either acids or salts of the monomer. Making polyions can be achieved either by polymerizing monomers that are either acids or salts or by reacting nonionic polymers with acid or base to alter the residues. For example, HPAM has been made by hydrolyzing PAM in NaOH(Farinato, 1988) and by copolymerizing PAM and sodium acrylate(NaA)(Morgan et al., 1990).

The presence of ionizable residues along the chain drastically alters the static and

dynamic properties of the otherwise nonionic polymer. The physical and transport properties of polyions based on idealized models have been calculated elsewhere (Tanford, 1961; Rice & Nagasawa, 1961; Oosawa, 1970; Bohandecký & Kovář, 1982).

In any model, interactions among polyion charges and between polyion charges and solvent counterions must be considered. Counterion mobility both inside and outside the polyion domain further complicates the problem. Accounting for solvent dielectric effects all but makes this an intractable problem. How the solvent arranges itself near polyion charges and how mobile counterions "bind" themselves to the polyion are not known. Treated as a continuous medium, the solvent is characterized by its bulk dielectric constant (i.e., its relative permittivity, ϵ_r). Counterions in the solvent are modelled to screen polyion charges, reducing the strength of their electrostatic interactions.

Three basic models have been used to describe polyion behavior. The random-flight and cylindrical models represent the extremes of polyion configuration. The former applies only to very weakly ionized polyions and polyions in a solution of high ionic strength (i.e., a large salt concentration) and uses much of the statistics that apply to nonionic linear polymers. The latter model obtains for highly ionized polyions in a solution of low ionic strength; the chain is almost fully extended to which cylindrical symmetry applies. The third model, the worm-like chain model, bridges those two extremes. It best describes real polyion chains by allowing for local rigid-rod behavior amid global flexibility. For a spherical (i.e., random-coiling) polyion, the random-flight model can be modified by including an electrostatic contribution to the radial distribution function of chain segments. The characteristic length across which charges interact in a

dielectric medium is the Debye screening length κ^{-1} :

$$\kappa^2 = \frac{8\pi e^2 I}{(4\pi\epsilon_0\epsilon_r)k_b T} \quad (\text{A2.4-17})$$

in which the ionic strength $I \equiv \frac{1}{2}\sum z_i^2 c_i$, the unit charge $e = 1.602 \times 10^{-19}$ C, the inverse Coloumbic proportionality constant $4\pi\epsilon_0 = 1.113 \times 10^{-10}$ C²/(J·m), ϵ_r is the relative permittivity of the solvent, z_i is the charge on species i , and c_i is the concentration of species i in m⁻³. (The $4\pi\epsilon_0\epsilon_r$ group is the solvent bulk-dielectric constant D .) For 1.0×10^{-4} N aqueous NaCl at 25°C, $\epsilon_r = 78.54$, and $I = 1.2 \times 10^{-23}$ m⁻³; thus, $\kappa^{-1} \approx 300$ Å. For 0.3 N aqueous NaCl at 25°C, $\kappa^{-1} \approx 6$ Å. For a single PAM polymer of $M_w = 15.5 \times 10^6$ g/mole, $\langle h^2 \rangle^{1/2} \approx 1.26$ Å $\times \sqrt{(2 \cdot 15.5 \times 10^6 / 35.54)} = 1170$ Å, and $R_G \approx 480$ Å. Since κ^{-1} for a dilute aqueous salt solution and $\langle h^2 \rangle^{1/2}$ of a neutral PAM are of the same order, a HPAM chain of equal M_w should not be random-coiling at all. Rather, the charges everywhere along the backbone should repel and should coordinate polarizable water molecules around themselves, expanding and swelling the chain. Conversely, since κ^{-1} in concentrated brine and the distance between neighboring charges in a **fully ionized HPAM** are about the same, a HPAM of equal M_w should be nearly random-coiling. Clearly, spherical polyions can exist only when there are very few ionizable backbone groups or when the counterion concentration is so high that κ^{-1} becomes smaller than the distance between ionizable backbone groups.

Highly ionizable polyions in a solvent of low ionic strength will most certainly be expanded. For dilute polyion solutions, each chain can be modelled as having locally cylindrical symmetry. For calculating properties which do not depend upon M_w (via R_G , $\langle h^2 \rangle^{1/2}$, and L_c), the chain may be treated as an infinitely long cylinder (Manning, 1969).

In the limit of zero radius, it may be treated as a line charge. Thus, the electrostatic potential depends only upon radial position from the line charge. The characteristic length scale here is that for a simple electrolyte solution, the Bjerrum length Q . The Bjerrum length and Debye screening length are related by

$$Q = \frac{e^2}{(4\pi\epsilon_0\epsilon_r)k_bT} = \frac{\kappa^2}{8\pi I} \quad (\text{A2.4-18})$$

In this model, the Poisson-Boltzmann equation describes the potential field radially about the line charge, and a Boltzmann distribution function accounts for charge-screening by the solvent and counterions: $\nabla^2\Phi(r) = \kappa^2\sinh\Phi(r)$. Although no general analytical solution exists, it was shown that for high linear charge densities, counterions "condense" onto the chain. The criterion for condensation is

$$\xi = \frac{Q}{A} \geq 1 \quad (\text{A2.4-19})$$

in which A is the distance between neighboring polyion charges. Here, condensation means that enough counterions will associate with the polyion charges to lower ξ to unity. Condensation does not neutralize the line charge; rather, counterions in the bulk solution are still influenced by the significant electrostatic potential of the "condensed" line charge. For a HPAM polyion of $M_w = 15.5 \times 10^6$ g/mole in 1.0×10^{-4} N aqueous NaCl at 25°C, $Q \approx 7$ Å; thus, for condensation to occur the polyion must have about 1/3 of its residues ionizable. Infinite dilution of the polyion solution does not reduce counterion condensation. As $[\text{NaCl}] \rightarrow 0$, the polyion expands so that $\langle h^2 \rangle^{1/2} \rightarrow L_c$. The line charge, albeit condensed, still exerts forces so long in range that other polyions in this "dilute" solution may be influenced. In 1.0×10^{-5} N and 1.0×10^{-6} N aqueous NaCl

at 25°C, κ^{-1} is 962 Å and 3043 Å, respectively. In a 1-ppm solution of PAM of $M_w = 15.5 \times 10^6$ g/mole, the number density is $\sim 3.9 \times 10^{10}$ cm⁻³; with $L_c \approx 55$ μm, each cylindrical polyion has an effective radius $b \approx 0.4$ μm = 4000 Å in a densely packed arrangement of parallel polyions. That b and κ^{-1} are approximately equal implies that in "dilute" solutions, interactions between polyions can occur. Experiments have confirmed the interesting behavior of "dilute" polyion solutions (Kratky & Porod, 1949).

Worm-like chain models have been used to describe stiff nonionic polymers in solution (Kratky & Porod, 1949). This linear chain consists of N bonds of length ℓ connected at bond angle θ . In the limit $N \rightarrow \infty$, two lengths characterize the chain: the persistence length $\mathcal{L} \equiv (2\lambda)^{-1} = \ell/(1+\cos\theta)$ and contour length $L_c = N\ell$. The worm-like chain obtains in the limit $\ell \rightarrow 0$ and $\theta \rightarrow \pi$. As $\mathcal{L}/L_c \rightarrow 0$, the chain exhibits greater flexibility, and $R_G = (\mathcal{L}L_c/3)^{1/2} = (N\ell/6\lambda)^{1/2}$; the random-flight result is recovered if λ^{-1} were equal to ℓ . As $L_c/\mathcal{L} \rightarrow 0$, the chain becomes rigid, and $R_G = L_c/\sqrt{12}$, the exact result for a rigid rod. To apply the worm-like-chain model to polyion chains, \mathcal{L} must be related to the electrostatic potential and charge screening due to the polyion charges and solvent and counterions, respectively. Odijk & Houwaart (1978) calculated excluded-volume effects in a dilute solution of polyions and a 1:1 salt, combining excluded-volume theory, counterion condensation, and cylindrical polyion models. The highly ionizable model polyion ($\xi = Q/A \geq 1$) had an effective persistence length of $\mathcal{L}_T \sim O(L_c)$ and a surrounding impenetrable cylindrical shell of radius $b = 2\kappa^{-1}$, twice the Debye screening length. These dimensions characterized short-range and excluded-volume (long-range) effects, respectively. The effective persistence length can be separated into bare (nonelectrostatic) and electrostatic persistence lengths provided that the latter makes

a small contribution: $\mathcal{L}_T = \mathcal{L}_p + \mathcal{L}_{p,c}$, in which $\mathcal{L}_{p,c} = 1/(4Q\kappa^2)$. With $Q \approx 7 \text{ \AA}$ and $\kappa^{-1} = b/2 \approx 304 \text{ \AA}$ from previous calculations, $\mathcal{L}_{p,c} \approx 3300 \text{ \AA}$; $\mathcal{L}_{p,c}/\mathcal{L}_T \sim \mathcal{L}_{p,c}/L_c \approx 3300 \text{ \AA}/550000 \text{ \AA} = 0.006$, indeed a small perturbation. It follows that the otherwise rigid chain only "collapses" when the salt concentration increases (i.e., κ^{-1} decreases); the smaller radius b enhances chain flexibility. Yet, when the polyion solution is diluted, the chain expands, reaches a maximum when $\kappa^{-1}_{\max} = (2Q\mathcal{L}_p)^{1/2}$, and then drops off upon further dilution. Intrinsic viscosity measurements have exhibited such maxima at low ionic strengths (Takahashi & Nagasawa, 1964; Cohen et al., 1988; Tam & Tiu, 1990).

Recently, Monte Carlo methods have been used to simulate the conformation of polyions in solvents of varying ionic strengths. Carnie et al. (1988) studied fully ionized polyions, characterized by PAA, in solutions of varying ionic strength. The chains contained between 20 and 320 beads of diameter 2.52 \AA and were either freely rotating or hindered. Simple 1:1 salt concentrations ranged between 1.0×10^{-4} and 0.1 N . At 0.1 N , both $\langle h^2 \rangle$ and $\langle R^2 \rangle$ varied as N^ν with ν between 1.3 and 1.6, implying extension even at small screening lengths. At lower salt concentrations, $\langle h^2 \rangle$ went as N^2 (or M_w^2), implying high extension at large screening lengths. Over all salt concentrations and chain lengths, the $\langle R^2 \rangle / \langle h^2 \rangle$ ratio ranged between about $1/7$ and $1/12$, close to the ideal ratios for random-flight ($1/6$) and rigid rods ($1/12$), respectively. If $\langle h^2 \rangle^{1/2} \propto N^\nu = N^{1+\epsilon}$, the $\langle R^2 \rangle / \langle h^2 \rangle$ ratios for $\nu = 0.3$ and 0.6 are $1/7.59$ and $1/9.36$, respectively; thus, these results are consistent with excluded-volume effects treated in §A2.4.1. Brender (1990) calculated thermal effects on coil-to-rod transition in small polyions. The Bjerrum length Q was varied between 1×10^{-4} and 18 \AA , corresponding to temperatures between 2.1×10^7 and $-155 \text{ }^\circ\text{C}$. For water at 25°C , $Q \approx 7.14 \text{ \AA}$. Added

1:1 salt concentrations ranged between 0 to 1.0 N. Without added salt, the polyion proceeds through a coil-to-rod transition as Q increases; transition is indicated by the $\langle R^2 \rangle / \langle h^2 \rangle$ ratio changing from about 1/6 to about 1/11. Only at 0.1 N does the transition disappear with the ratio ranging between about 1/6 and 1/8. At 1.0 N, only random-coiling behavior occurs with the ratio being $\sim 1/6$. At $Q = 8 \text{ \AA}$, the ratio varies from 1/10 at 0 N to $\sim 1/7$ at 1.0 N; thus, a coil-to-rod transition can occur in a solution of short polyions at room temperature. Between 0.01 N and 0.1 N, the polyion collapses with $\langle h^2 \rangle^{1/2} / L_c$ decreasing from 0.8 to 0.2. Qian & Kholodenko(1988) studied polyion rigidity due to electrostatic effects. In the limit $N \rightarrow \infty$, the static properties of polyions are not universal, unlike those of neutral polymers. Einvoll and Hemmer(1988) investigated counterion distributions around polyions; only supercritical polyions(i.e., polyions for which $\xi = Q/A \geq 1$) have universal counterion distributions.

Given that the static properties of polyions differ from those of random-flight polymers, the dynamic properties of polyions also can be expected to differ. While the universal KR constant Φ characterizes very large random-flight polymers under Θ conditions irrespective of polymer and solvent, no such universality has been found for polyelectrolytic polymers, except perhaps in the limit $\lambda^{-1} \rightarrow 0$.

Under certain conditions, two general equations do fit $[\eta]$ data for polyions, the coefficients of which depend on both polyion-solvent pair and temperature. Fuoss & Strauss(1948) proposed the following equation to fit viscosity data of dilute polyion solutions:

$$\frac{\eta_{sp}}{c} = \frac{A}{1+Bc^{1/2}} \quad (\text{A2.4-20})$$

in which A and B are system specific. Recently Ait-Kadi et al.(1987) found that equation A2.4-20 did not obtain for their HPAM samples, claiming that the equation applied only to highly ionized polyions. Noda et al.(1970) empirically determined an expression for the dependence of solution viscosity on solvent ionic strength at moderate 1:1-salt concentrations:

$$[\eta] = [\eta]_{s\infty} + k_{s\infty}[\text{salt}]^{-1/2} \quad (\text{A2.4-21})$$

in which $[\eta]_{s\infty} \equiv [\eta]$ as $[\text{salt}] \rightarrow \infty$. While this equation has been "confirmed" theoretically(Fixman, 1964), it is not universal. Isoionic dilution of polyion solutions(i.e. using a diluent of the same ionic strength as the original polyion solution) shows η_{sp}/c to vary linearly with c as do nonionic polymers according to the Huggins equation. Despite this fact, Φ seems to depend on polyion charge. Clarke(1970) observed that while high-molecular-weight PAM solutions obeyed the linear Huggins equation, high-molecular-weight HPAM solutions did not, displaying great nonlinearity. To date, each polyion-solvent pair must be investigated separately.

APPENDIX B

B3.0 Experimental Equipment

Table B3.0
Equipment and Vendors

Equipment	Vendor
Moyno 3L4-SSQ-AAA pump; Reliance 2 Hp TEFC-XE motor, model #P14G9245; and T. B. Woods 2 Hp E-trAc AC Inverter, Model AFC2002-0B2	Robbins & Myers, Inc. Fluids Handling Group P.O. Box 743 7 - 11 Elm St. Southbridge, MA 01550 1-(508)-765-0628
Unistrut channels and assorted pieces	Unistrut Northeast 55 Shawmut, P.O. Box 157 Canton, MA 02021 (617)-821-1720
316-SS seamless 0.574"-ID and microsmooth 0.402"-ID tubing	Stainless Pipe & Fittings 37 Rogers Street Cambridge, MA 02142 (617)-491-1320
Assorted tools	Kaufman. Co. 110 Second Street Cambridge, MA 02141 (617)-491-5500
Swagelok fittings	Cambridge Valve & Fittings, Inc. 50 Manning Road Billerica, MA 01821 (617)-272-8270
PVC pipe, valves, and fittings	Metro Pipe 303 Binney St. Cambridge, MA 02142 (617)-492-6400
Jamesbury ball valves	Boston Pipe & Fittings Co. 161 - 171 Sidney Street Cambridge, MA 02139 (617)-876-7800

Equipment	Vendor
Stainless-steel pipe stubs, flanges, reducers, and valves	Tek Supply, Inc. 9 Walkup Drive Westboro, MA 01581 1-(800)-343-813
Flexible stainless-steel hose with flanged ends	Northeast Rubber 110 Alexander Street P.O. Box 937 Framingham, MA 01701 1-(508)-626-9300
CJ3D pressure transducers, carrier demodulator, and accessories	C.J. Enterprises, Inc. 9048 Independence Ave. Canoga Park, CA 91304 (818)-996-4131
Micro Motion mass flow meter	Pond Technical 174 North Plain Industrial Rd. Wellingford, CT 06492 (203)-284-1500
Lightning bench mixer	M.A. Olson Co., Inc. Industrial Sales Equipment 414 Old Boston Road Topsfield, MA 01983 (508)-887-2384
55-gallon drum heater	Cole-Parmer Instrument Co. 7425 North Oak Park Ave. Chicago, IL 60648 1-(800)-323-4340
55-gallon flexible drum heater	N.E. Industrial Heat 460 Totten Pond Road Waltham, MA (617)-890-5885
5000Ω thermistors	Omega Eng., Inc. 1 Omega Drive, Box 4047 Stamford, CT 06907-0047 (203)-359-1660

Equipment	Vendor
Electronic parts	E.M.F. 110 - 120 Brookline Avenue Cambridge, MA 02139 (617)-547-1991
Computer supplies	Unitech 24 Thorndike Street Cambridge, MA 02142 (617)-UNI-TECH
Thermal paper	University Stationary Co. 311 Massachusetts Avenue Cambridge, MA 02139 (617)-547-6650
Clear plastic pipe	A.I.N Plastics 1400 Providence Highway Norwood, MA (617)-769-9050
Tricomb Spiral Wrap Honeycomb	ELDIM, Inc. 8 Southside Road Danvers, MA 01923 (617)-774-1777
Large vincon tubing and gaskets	Greene Rubber Co. Inc. 160 Second Street Cambridge, MA 02142 (617)-547-7655
Glass U-tube manometer	Lab Glass, Inc. 1172 N. W. Blvd. P.O. Box 610 Vineland, NJ 08360-0610 1-(609)-691-3200
Cyanamid HPAM samples	American Cyanamid Co. Specialty Polymers Dept. Paper Chemicals Dept. Wayne, NJ 07470 1-(800)-438-5615

Equipment	Vendor
Betz HPAM samples	Betz Laboratories, Inc. 4636 Somerton Road Trevose, PA 19047 (215)-355-3300
Allied Colloid HPAM samples	Allied Colloids Inc. P.O. Box 820 2301 Wilroy Road Suffolk, VA 23434 (804)-934-3700

APPENDIX C

C3.4 Experimental Equipment

(3) The Water and Mercury Manometers

Figure C3.4.3a shows a schematic of the water manometer. Two glass tubes were taped along the outer edges of the meter stick, next to the millimeter markings. The lower end of each tube extended a little below the bottom of the meter stick. The meter stick mounted on a ring stand by two screws. One end of a short length of $\frac{1}{8}$ " flexible tubing slid over the lower end of each glass tube.

Into the other end of the left flexible tube inserted one run of a small plastic tee. The branch run of this tee connected to the left side of the stopcock via a short length of $\frac{1}{4}$ " flexible tubing. The other run inserted into one end of a short length of $\frac{1}{4}$ " flexible tubing. The other end of this short length slid over and was clamped to the stub of a $\frac{1}{4}$ "-stub-to- $\frac{1}{8}$ "-port reducer. One end of a long length of $\frac{1}{8}$ " flexible vincon tubing inserted into the port of the reducer; on its other end were a $\frac{1}{8}$ " stainless-steel nut with nylon ferrules.

Into the other end of the right flexible tube inserted the branch run of a small plastic tee. The left run of this tee connected to the right side of the stopcock. Its right run connected to the left run of another small plastic tee via a short length of $\frac{1}{4}$ " flexible tubing. The branch run of the second tee inserted into one end of a short length of $\frac{1}{4}$ " flexible tubing. The other end of this short length slid over and was clamped to the stub of a $\frac{1}{4}$ "-stub-to- $\frac{1}{8}$ "-port reducer. One end of a long length of $\frac{1}{8}$ " flexible vincon

Water Manometer

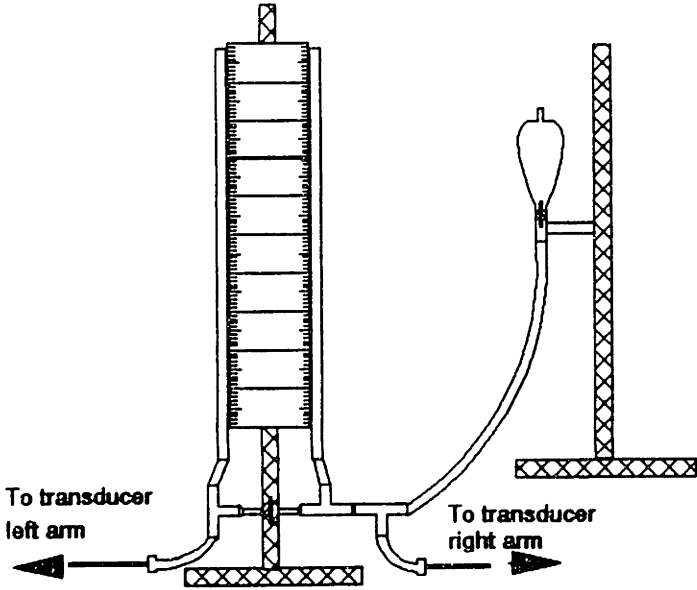


Figure C3.4.3a

Mercury Manometer

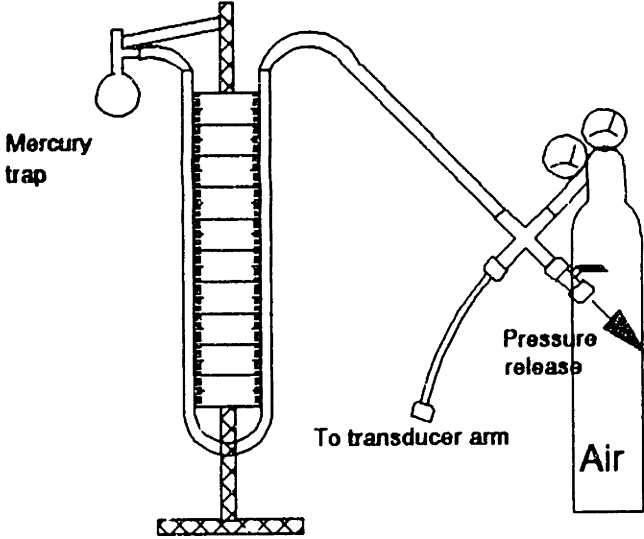


Figure C3.4.3b

tubing inserted into the port of the reducer; on its other end were a 1/8" stainless-steel nut and nylon ferrules. The right run of the second tee inserted into one end of a long length of 1/4" flexible tubing; its other end slid over the tip of the small separation funnel supported by the other ring stand.

The stopcock was held just below the meter stick by a three-prong grip. This grip was held by a regular holder that also clamped onto the ring stand. On the other ring stand, a regular holder clamped onto a three-prong grip. The water reservoir, the small separation funnel, was supported by this three-prong grip.

Figure C3.4.3b is a schematic of the mercury manometer. The U-tube with meter stick, configured much like the two glass tubes on the meter stick in the water manometer, mounted onto a ring stand by two screws. The manometer was filled with enough mercury so that the maximum height difference produced a pressure differential of 10 psid, corresponding to $(760/14.69) \times 10 \text{ psid} \approx 517 \text{ mm Hg}$. To the top of the left arm connected a mercury trap. Over the top of the right arm fitted one end of the compressed-air supply tube.

On the end of the regulating valve attached a 1/4" brass union cross. Onto one arm attached a 1/4" brass toggle valve via a 1/4" brass port connector. This served as a quick release valve in case of overpressure. The arm opposite the toggle-valve connected to one end of a long length of 1/4" flexible vincon tubing via a 1/4" brass port connector. The other end fitted over the top of the right arm of the U-tube. The arm opposite the compressed-air arm held the tube of a 1/4"-stub-to-1/8"-port reducer. One end of a long length of 1/8" flexible vincon tubing inserted into the port of the reducer; on its other end were a 1/8" stainless-steel nut with nylon ferrules.

APPENDIX E

SOLVENT DATA SETS 1 - 5

Page 1

Solvent Set 1: Runs 8000234 - 8000339

Data	PK	L	Data
Log(Ra/f)	1/f	1/f	1/f
3.058215	11.78284	68.24584	11.79687
2.946110	11.44444	87.80837	11.44549
2.910348	11.24147	89.84505	11.14585
2.882582	10.81832	39.64998	10.82931
2.732203	10.32913	33.74142	10.55190
2.626243	10.16868	24.43280	10.05378
3.031306	11.72322	67.17172	11.83259
2.984480	11.43340	54.79117	11.53547
2.984197	11.21679	50.12769	11.16595
2.796942	10.74365	38.42270	10.78149
2.788244	10.75297	38.38174	10.85743
2.714733	10.43961	32.46460	10.62589
2.599487	9.998751	24.84362	10.23872
2.497443	9.589853	19.44913	9.810283
2.402701	9.216804	15.79724	10.44229
2.285805	8.743220	12.04938	11.10361
3.034262	11.73705	67.45051	11.75232
2.941102	11.44440	57.14532	11.42846
2.902216	11.20884	49.89953	11.28402
2.790435	10.74174	38.57584	10.80702
2.791784	10.74713	38.69390	10.74859
2.717777	10.47110	32.43300	10.54584
2.601143	10.00465	24.94863	10.20631
2.492916	9.571644	19.44449	9.913529
2.418433	9.274532	14.30751	10.05803
2.282197	8.728791	11.96954	11.19423
3.033108	11.73243	67.45106	11.79938
2.956537	11.42614	56.54798	11.53177
2.901546	11.20418	49.82258	11.23773
2.790209	10.74083	38.55579	10.80020
2.787698	10.74839	38.28042	10.83583
2.717492	10.44976	32.60787	10.53529
2.602381	10.00952	25.01851	10.14321
2.490511	9.562047	19.33712	9.992695
2.422487	9.290748	14.54120	9.900550
2.275179	8.708717	11.77747	11.37883
3.853246	15.01299	445.7883	15.05011
3.795046	14.77218	388.0844	14.69472
3.707958	14.43183	319.0354	14.57018
3.635020	14.14008	249.7124	14.09598
3.545850	13.78340	219.6494	13.74518
3.487862	13.25144	159.8469	13.29011
3.320978	12.68391	136.8754	12.81594
3.172693	12.29077	93.61946	12.02168

80000234

Tags 14

Tags 12

Tags 23

Tags 34

Tags 14

Page 2

Solvent Set 1: Runs 8000234 - 8000339

Data	PK	L	Data
Log(Ra/f)	1/f	1/f	1/f
3.879419	15.11747	473.4781	15.16218
3.820444	14.98178	413.3577	14.74231
3.733435	14.53374	358.3103	14.65403
3.640207	14.14092	272.9527	14.44561
3.559273	13.75709	216.3481	13.82402
3.482309	13.20973	157.8300	12.88753
3.188978	12.35441	96.51812	12.39657
3.890204	15.14081	485.3829	15.12776
3.825939	14.90373	418.6195	14.90935
3.752232	14.40892	353.2746	14.54939
3.690941	14.03376	306.7757	14.36116
3.595588	13.59999	246.5025	13.91224
3.441721	13.14444	180.9478	13.52498
3.321424	12.63567	131.0098	13.07772
3.212135	12.144854	101.8626	12.01415
3.890444	15.14245	485.8947	15.24875
3.828651	14.91480	421.2415	14.95086
3.770888	14.68335	368.7813	14.73367
3.692822	14.37128	308.1075	14.42870
3.599451	13.99850	248.6175	13.90764
3.487792	13.55116	192.1642	13.49503
3.323849	12.69539	131.7437	13.12276
3.212418	12.144867	101.9290	12.11515
3.859631	15.03852	452.3879	15.10065
3.742741	14.57104	395.4537	14.49329
3.626185	14.10474	264.2809	14.21685
3.450978	13.32391	168.6002	13.53652
3.429817	13.31926	168.1501	13.54217
3.320295	12.88118	130.6698	13.06987
3.180714	12.32285	94.75336	12.01602
3.024946	11.69978	66.19525	11.81808
2.948935	11.39574	55.56478	11.48668
2.909874	11.23949	50.78225	11.24139
2.844479	11.06591	45.95781	11.18724
2.810427	10.84251	40.41177	10.91602
2.718945	10.47578	32.72093	10.57486
2.609690	10.03876	25.44314	10.29535
2.413060	9.252240	16.17857	10.37846
2.309442	8.837771	12.74449	10.99692
2.131359	8.125439	6.457459	8.320147
2.057115	7.828462	7.128459	7.146449
2.003300	7.613200	6.297672	6.494558
1.744053	6.456213	3.630223	3.529578

80000234

80000243

Data	PK	L	Data
Log(Re/ff)	1/ff	1/ff	1/ff
3.849040	14.99616	441.4897	14.95855
3.815977	14.84391	409.1267	14.79644
3.787144	14.74858	382.8480	14.64232
3.748599	14.58293	347.8480	14.53550
3.682253	14.32991	309.7000	14.27544
3.604489	14.02592	252.5575	13.94594
3.527456	13.71049	210.4350	13.58652
3.467277	13.22911	159.6458	13.09950
3.394260	12.77480	123.0487	12.52294
3.125356	12.10220	83.45065	11.87654
3.023164	11.69245	65.92413	11.48725
3.377480	13.10992	149.0599	13.26144
3.271262	12.48513	114.7244	13.17178
3.193994	12.37598	97.69593	12.54503
3.122606	12.09042	82.88692	11.92437
3.037921	11.75168	68.20273	11.27133
3.025407	11.70292	66.29402	11.74574
2.982879	11.31511	47.72449	11.16048
2.771594	10.68437	34.93812	10.45534
2.697726	10.39090	31.16041	10.44308
2.643557	10.18223	27.43341	10.19450
2.582254	9.929019	23.88552	10.05510
2.474593	9.498372	18.64118	9.697407
2.283133	8.732333	11.99334	10.34221
2.927925	11.31170	52.94259	11.42071
2.883452	11.13391	47.78951	11.27471
2.839963	10.95985	43.23577	11.05321
2.798490	10.79476	39.31408	10.84736
2.751746	10.52498	33.69973	10.61890
2.674589	9.506356	18.72704	9.874054
2.254181	8.424724	11.27357	10.74564
2.191363	8.365454	9.710543	9.621582
2.094442	7.978549	7.771812	7.750865
1.991334	7.543336	6.126323	6.198184
1.791445	6.744463	3.848528	3.909549
Data	PK	L	Data
Log(Re/ff)	1/ff	1/ff	1/ff
3.875479	15.10271	469.4177	14.91848
3.801440	14.80444	395.8593	14.74219
3.715985	14.46394	324.9865	14.34572
3.602394	14.00937	250.1926	13.99522
3.448145	13.39264	175.4063	13.30815

50000243

Data	PK	L	Data
Log(Re/ff)	1/ff	1/ff	1/ff
2.920772	11.28308	52.07773	11.37274
2.887209	11.14883	48.20466	11.29514
2.845458	10.98183	43.78633	11.06748
2.795236	10.78094	39.00465	10.84818
2.748410	10.59364	35.01790	10.67543
2.679383	10.31753	29.87193	10.42650
2.565046	9.840185	22.95759	10.02366
2.458238	9.432954	17.95224	9.782378
2.263793	8.655172	11.47289	10.46160
2.190567	8.342249	9.69257	9.203031
1.994144	7.584577	6.194757	5.866763
1.794149	6.784598	3.908675	3.897965
Data	PK	L	Data
Log(Re/ff)	1/ff	1/ff	1/ff
2.992487	11.57075	61.45645	11.89957
2.911222	11.24489	50.94511	11.44182
2.857381	11.05135	45.05245	11.06055
2.738804	10.35521	34.25191	10.67506
2.648908	10.27563	29.16006	10.42829
2.550337	9.801350	22.19307	10.08261
2.447132	9.388529	17.49896	9.909985
2.317834	8.871336	12.99314	11.15809
2.249583	8.598333	11.10358	10.62227

80000243

Data	PK	L	Data
Log(Re/ff)	1/ff	1/ff	1/ff
3.334583	12.933	135.0401	12.94466
3.174723	12.0689	93.88661	12.43166
3.095712	11.98284	77.90985	11.98479
3.394816	13.18726	155.8464	13.38965
3.327248	12.90699	132.7788	13.09652
3.272738	12.49095	117.1165	12.86823
3.173982	12.29592	93.29579	12.42600
3.091574	11.94629	77.17098	12.01793
3.030738	11.72295	67.08395	12.00398
2.948638	11.39459	55.53015	11.40635
2.882951	11.13180	47.73440	11.44939
2.778398	10.71359	37.52137	10.84093
2.780033	10.72013	37.46289	10.73877
2.708320	10.43328	31.93010	10.50190
2.652314	10.20925	28.06693	10.34856
2.584440	9.938541	24.01708	10.29282
2.481975	9.527903	18.94074	10.07846
2.345139	9.060556	14.48835	10.78108
2.246114	8.644458	11.53439	11.16897
2.199324	8.397299	9.890195	9.868805

1.679558 7.118235 4.736296 4.816192
 1.685246 6.340987 3.027797 2.991622

Data PK L Data
 Log(Ra/f) 1//f 1//f 1//f

3.904482 15.21792 501.6054 14.97251
 3.893643 14.95745 431.7613 14.78537
 3.762994 14.65198 362.1399 14.51706
 3.756013 14.62405 356.3657 14.50070
 3.679000 14.31400 298.4558 14.28422
 3.602741 14.01104 250.4040 13.82980
 3.567310 13.46924 183.3117 13.39016
 3.545459 12.98183 138.4648 13.06204
 3.180399 12.32159 94.68458 12.27964
 3.080714 11.92285 75.26519 12.01507

3.448740 13.39494 175.6386 13.38979
 3.382512 13.13005 150.7970 13.11411
 3.225436 12.50174 105.0307 12.55231
 3.137758 12.15103 85.82997 12.26829
 3.102061 12.00824 79.05724 12.50835
 3.033093 11.73237 67.44869 11.48591
 2.975395 11.50158 59.05757 11.47580
 2.864110 11.05644 45.70784 11.02006
 2.790981 10.76592 38.62433 10.72418
 2.737079 10.54831 34.11612 10.48759

2.967519 11.47007 57.99614 11.52784
 2.732250 10.52900 33.75886 10.52722
 2.667187 10.26875 29.04477 10.31255
 2.565197 9.860791 22.96560 10.06778
 2.494442 9.577850 19.51383 9.798645
 2.362817 9.051289 14.81111 10.75756
 2.264183 8.576735 10.96659 10.43042
 2.174173 8.294694 9.333497 9.114597
 2.046598 7.786394 6.937907 6.847004
 1.944472 7.377890 5.499872 5.510991
 1.752103 6.608415 3.531701 3.547791

Data PK L Data
 Log(Ra/f) 1//f 1//f 1//f

3.901414 15.20565 498.0743 14.80896
 3.827658 14.91043 420.2799 14.62510
 3.737621 14.55048 341.5849 14.39249
 3.646282 14.18513 276.7979 14.21198
 3.555779 13.74511 214.6144 13.74737
 3.589845 13.15958 153.3649 12.82512
 3.161735 12.24694 90.70161 12.19818
 3.098820 15.19528 495.1088 14.89746

80000248

80000251

2.187340 8.349440 9.621439 9.250355
 2.653210 7.820941 7.897253 7.820039
 1.745710 6.882840 3.480088 3.448110
 1.932094 7.328579 8.345334 5.354249

Data PK L Data
 Log(Ra/f) 1//f 1//f 1//f

3.644841 18.06756 457.8403 14.98603
 3.815415 14.84164 408.5974 14.83526
 3.769256 14.64102 359.8624 14.61942
 3.714950 14.48932 324.1231 14.46734
 3.633582 14.21432 281.4894 14.22070
 3.532398 13.86959 222.9843 13.84842
 3.453164 13.42845 178.2540 13.47300
 3.375820 13.10328 148.4912 13.09572
 3.266205 12.66482 115.3481 12.86761
 3.130352 12.12140 84.37863 12.19702
 3.037641 11.75044 68.16185 11.74550

3.393460 13.17384 154.6466 13.26211
 3.374272 13.10508 148.6454 13.17273
 3.350444 13.00177 140.6434 13.03538
 3.297428 12.79051 124.0248 12.82751
 3.248047 12.67219 115.8585 12.80415
 3.196743 12.22705 89.64919 12.28308
 3.042880 11.85152 72.23709 11.85894
 3.074559 11.89823 74.20610 11.84882
 2.987343 11.54945 60.70770 11.62504
 2.822331 10.88932 41.51545 10.74247
 2.733818 10.61527 35.45670 10.41742
 2.675929 10.38571 31.03200 10.28973
 2.638993 10.15390 27.21921 9.963989
 2.538697 9.755590 21.61612 9.503857

2.954532 11.42613 54.54741 11.51321
 2.936544 11.33825 53.75812 11.34944
 2.901512 11.20604 49.81849 11.24644
 2.871977 11.08799 46.54552 11.06516
 2.832012 10.92804 42.45142 10.88514
 2.774337 10.69735 37.17215 10.49753
 2.752440 10.52974 33.75361 10.46708
 2.682474 10.33070 30.09928 10.33592
 2.611423 10.04569 25.54487 10.13025
 2.570694 9.883378 23.24883 9.966052
 2.507004 9.628027 19.85577 9.831373
 2.415848 9.263375 14.28279 9.939077
 2.286978 8.747914 12.10203 11.21828
 2.200777 8.403111 9.923338 9.842418
 2.037242 7.754970 6.891049 6.799137

80000245

3. 824984 14. 89993 417.7006 14. 71543
 3. 737373 14. 85829 341.5496 14. 39767
 3. 446990 14. 18794 277.2425 14. 18883
 3. 344411 13. 73764 213.9398 13. 79073
 3. 542972 13. 88934 144.0343 13. 45574
 3. 167679 12. 27071 91.79139 12. 03234
 3. 164137 12. 02483 79.90270 12. 08902
 3. 024842 11. 89937 64.17942 11. 89499
 2. 968148 11. 47239 50.66021 11. 57495
 2. 841204 11. 64513 45.41134 11. 11224
 2. 784652 10. 73860 38.04537 10. 93238
 3. 425438 13. 30255 144.5399 13. 28484
 3. 299294 12. 79717 124.5015 12. 83419
 3. 117309 12. 04923 81.88211 12. 01070
 3. 176977 12. 39391 98.82295 12. 45949
 3. 356025 13. 00010 139.9281 13. 14843
 3. 197047 12. 38827 98.38926 12. 44637
 3. 444574 13. 45829 182.1404 13. 49719
 3. 583316 13. 94124 240.5449 13. 79840
 3. 672655 14. 29062 294.1274 14. 21055

2. 728280 10. 77128 38.78824 10. 47078
 2. 484991 10. 34794 30.39984 10. 21758
 2. 571670 9. 884483 23.31046 9. 890253
 2. 397208 9. 194832 15.47049 10. 24014
 2. 842174 11. 04859 45.50450 10. 98114
 2. 974216 11. 49484 58.89747 11. 37345
 3. 022712 11. 69085 45.85558 12. 03333
 3. 107934 12. 03174 80.13385 11. 98297

Data Log (Re/f) 1//f L 1//f Data 1//f
 3. 894275 15. 17710 489.9545 15. 19085
 3. 812921 14. 85168 408.2572 14. 94172
 3. 754074 14. 61630 334.7776 14. 48519
 3. 451149 14. 20439 279.9173 14. 18100
 3. 548783 13. 87513 231.5600 13. 92824
 3. 448933 13. 47541 183.9441 13. 48401
 3. 373504 13. 09401 147.7015 12. 59775
 3. 204076 12. 42430 100.4513 12. 34895
 3. 115229 12. 04091 81.49089 12. 17774
 2. 984875 11. 54749 60.43924 12. 27394

3. 423113 13. 29245 163.5745 13. 42475
 3. 299242 12. 79494 124.4845 12. 89579
 3. 354116 13. 01644 141.2527 13. 11359
 3. 202675 12. 41070 99.46797 12. 39000
 3. 114907 12. 05943 81.43044 12. 13191

80000252

3. 863222 15. 05289 454.1447 15. 11204
 3. 807432 14. 83033 401.3405 14. 88555
 3. 752498 14. 40999 333.4912 14. 62542
 3. 687122 14. 34848 304.0900 14. 35674
 3. 600088 14. 03235 253.4947 14. 04971
 3. 521228 13. 48491 207.5430 13. 83905
 3. 422200 13. 28880 163.2248 13. 21134
 3. 244594 12. 45838 114.9413 12. 99596
 3. 134553 12. 14621 75.59211 12. 08045
 2. 915400 11. 26140 51.43743 11. 16749

3. 391834 13. 16733 154.0485 13. 39224
 3. 244545 12. 45818 114.9278 12. 94620
 3. 328127 12. 90450 132.4363 12. 98312
 3. 175080 12. 30032 93.53209 12. 25559
 3. 082804 11. 93122 75.42873 12. 12545
 2. 999954 11. 59981 62.49347 11. 68305
 2. 847298 11. 30919 52.86425 11. 27254
 2. 843728 11. 05491 45.66758 11. 02099
 2. 754204 10. 41482 35.48841 10. 56589
 2. 679079 10. 31631 29.85105 10. 29314
 2. 609985 10. 03994 25.46042 10. 25008
 2. 538381 9. 753525 21.59043 10. 11382

3. 013212 11. 45285 44.43070 11. 84946
 2. 936332 11. 34532 33.97745 11. 51029
 2. 869596 11. 07838 46.28882 11. 37445
 2. 745531 10. 46212 34.42400 10. 73728
 2. 688073 10. 35229 30.47571 10. 41644
 2. 538459 9. 753837 21.59431 9. 939724
 2. 472182 9. 488728 18.53796 9. 723701
 2. 317595 8. 870382 12.98400 10. 80399
 2. 246787 8. 587149 11.05323 10. 18938
 2. 184637 8. 338551 9.561320 9. 180304
 2. 034884 7. 747536 4.803996 6. 445777
 1. 888136 7. 152347 4.830774 4. 734096
 1. 670451 6. 281805 2.926384 3. 113877

Data Log (Re/f) 1//f L 1//f Data 1//f
 2. 971981 11. 48792 58.59510 11. 48367
 2. 911149 11. 24459 50.93651 11. 32788
 2. 807958 10. 83183 40.14415 10. 77921
 2. 743561 10. 57424 34.62910 10. 46402
 2. 628886 10. 11554 26.59297 10. 12852
 2. 529630 9. 718523 21.15976 9. 782427
 2. 448892 9. 395568 17.57001 9. 832440
 2. 333099 8. 932398 13.45797 10. 67595

80000255

80000255

2.237487 8.549951 10.79841 9.924409
 2.047491 7.790744 4.975439 4.551272
 2.139171 8.154487 8.419447 8.280477
 1.935298 7.341835 8.384414 5.465851
 1.775339 4.742187 4.727815 3.778943
 1.572372 8.096288 2.333888 2.354280

Data PK L Data
 Log(R_s/f) 1//f 1//f 1//f

3.047492 15.04996 440.4513 15.04502
 3.803425 16.81450 397.4541 14.83449
 3.725789 14.50315 332.4645 14.41462
 3.437263 14.22913 283.8788 14.25996
 3.535999 13.82399 234.8430 13.88987
 3.458394 13.43337 179.5869 13.52544
 3.337851 12.95140 134.0401 12.75107
 3.215675 12.44270 102.4944 12.38942
 3.138950 12.15369 86.04584 12.09554
 3.398734 13.19493 154.5341 13.27044
 3.305027 12.82010 126.1557 12.80722
 3.146737 12.17902 87.22420 13.23113
 3.042274 11.74509 48.88980 11.72674
 3.051142 11.80454 70.31084 11.74618
 2.945432 11.46173 57.71817 11.40185
 2.914437 11.25375 51.32347 11.14822
 2.801994 10.80797 39.41431 10.74351
 2.730464 10.52186 33.40039 10.46844

80000258

3.033475 11.73390 47.50810 12.02306
 2.961448 11.44459 37.21742 11.51432
 2.904452 11.22441 30.41165 11.15284
 2.792716 10.77084 38.77899 10.78461
 2.729828 10.51931 33.55124 10.47628
 2.414072 10.04428 25.91973 10.11030
 2.504082 9.416329 19.95089 9.812277
 2.422524 9.290098 16.53501 9.881748
 2.294924 8.787494 12.38237 10.82652
 2.223800 8.495290 10.44357 10.40261
 2.140416 8.162444 8.639451 8.089704
 2.046054 7.844223 7.274731 4.946443
 1.946783 7.387134 5.529217 5.54279
 1.730418 6.521473 3.359483 3.460735

Data PK L Data
 Log(R_s/f) 1//f 1//f 1//f

3.849759 15.07903 443.0621 15.07215
 3.799041 14.79416 393.4787 14.78128
 3.711780 14.44712 321.8551 14.45449

80000261

3.414205 14.05482 257.0903 14.02617
 3.482370 13.52948 189.7798 13.48453
 3.357899 13.03159 142.4883 13.04183
 3.218199 12.47279 103.2951 12.38728
 3.048873 11.79489 69.92037 11.44548

3.413855 13.25542 162.0821 13.40808
 3.291511 12.74604 122.2901 12.83454
 3.039521 11.75808 68.45442 11.71612
 2.945234 11.44093 57.69184 11.23195
 2.903595 11.21438 50.05825 11.09382
 2.790232 10.74092 38.55781 10.73887
 2.718975 10.47590 32.72315 10.37484

3.015048 11.46019 44.70365 11.77444
 2.938049 11.35319 54.19129 11.47840
 2.886880 11.14752 48.16819 10.99849
 2.774012 10.70404 37.31574 10.57479
 2.705814 10.42325 31.74441 10.28035
 2.593528 9.974114 26.51368 9.980183
 2.492193 9.548773 19.41214 9.728459
 2.403401 9.213404 15.82274 9.988346
 2.274344 8.703457 11.80985 10.71360
 2.204013 8.424033 10.04349 9.369517
 2.127444 8.109787 8.381598 9.900905
 2.024447 7.698670 6.615249 4.327208
 1.843775 6.975100 4.561494 4.366117
 1.699051 6.394204 3.125584 3.086220

Data PK L Data
 Log(R_s/f) 1//f 1//f 1//f

3.871015 15.08406 464.4036 15.04557
 3.834219 14.94487 428.4470 14.94225
 3.800152 14.80060 394.4866 14.74015
 3.757476 14.62990 337.3658 14.65580
 3.713402 14.45340 323.0593 14.41885
 3.642424 14.24969 287.2796 14.18784
 3.602245 14.00898 250.1070 13.94844
 3.531598 13.72639 212.5585 13.69665
 3.447552 13.59020 175.1589 13.29491
 3.447252 13.38901 175.0381 13.30609
 3.332163 12.92865 134.2899 13.00771
 3.305466 12.82184 126.2835 12.81024
 3.182558 12.33023 95.15649 12.23812
 3.139599 12.15839 86.19450 12.15951

80000264

3.400431 13.20172 157.1490 13.33871
 3.289874 12.75950 121.8505 12.42626
 3.175928 12.29571 93.28439 12.48722
 3.050027 11.72011 66.97426 11.71655
 2.950539 11.40215 55.77242 11.41894

2.897535	11.16422	48.48945	11.05104
2.778491	10.71346	37.52144	10.77439
2.789949	10.43979	32.05014	10.39835
3.070003	11.68901	45.44410	11.48903
2.943048	11.38547	35.17301	11.30600
2.887795	11.15118	48.24985	11.04370
2.774207	10.78482	37.33252	10.45101
2.707410	10.43044	31.87798	10.42155
2.597629	9.988118	24.71209	9.980249
2.492479	9.869918	19.42493	9.741674
2.385940	9.143341	15.19248	10.37448
2.273372	8.693489	11.72874	10.86272
2.203543	8.414253	9.987188	9.570427
2.184824	8.019384	7.954207	7.891348
2.029752	7.719910	6.493181	6.720747
1.912100	7.248401	5.104819	5.124193
1.487474	6.350705	3.044782	3.150074

Data	PK	L	Data
Log(Re/f)	1/f	1/f	1/f
3.657383	15.02933	450.0532	15.07460
3.815084	16.84034	408.2881	14.95495
3.745533	14.45413	342.5881	14.45887
3.707484	16.45073	318.8338	14.54239
3.458139	14.15255	271.4544	14.15387
3.542862	13.85144	228.4241	13.84220
3.540615	13.84246	227.2454	13.93410
3.431531	13.32620	148.8230	13.39721
3.345440	12.98236	138.5224	13.06217
3.234649	12.54647	107.7828	12.59064
3.145591	12.24234	91.51044	12.35789
3.078102	11.91240	74.81391	12.09271
3.387318	13.14927	152.4750	13.35024
3.321448	12.88579	131.0173	12.94728
3.247110	12.53884	107.2978	12.64755
3.142934	12.25173	90.95246	12.43374
3.091487	11.94473	77.19115	11.72030
3.010394	11.64158	64.01424	11.71297
2.933247	11.33298	53.59338	11.31578
2.874028	11.09411	46.74341	11.06713
2.872421	11.09048	44.61262	11.03804
2.746172	10.44468	34.47979	10.57508
2.690770	10.34308	30.46551	10.34049
2.585434	9.942544	24.07224	9.882964
2.487460	9.550542	19.20970	9.738615
2.386795	9.139181	15.15917	10.44907
2.274991	8.699944	11.77256	10.84614
2.198269	8.393079	9.646194	9.432115

80000267

2.155547	8.222190	8.941854	8.872932
2.073454	7.894425	7.405192	7.378641
1.982820	7.531280	6.007588	5.948840
1.787038	6.748134	5.827529	5.826207
Data	PK	L	Data
Log(Re/f)	1/f	1/f	1/f
3.880137	15.12053	474.2412	15.17133
3.830708	14.92283	423.2417	15.01680
3.774809	14.69923	372.1252	14.81577
3.712137	14.44853	322.1198	14.51902
3.646481	14.18472	277.0521	14.28376
3.557542	13.85017	225.6433	13.81786
3.460237	13.44095	180.3506	13.39849
3.347984	12.99194	139.2728	12.91541
3.233149	12.53259	106.9128	12.33823
3.109529	12.03811	80.42848	11.92807

80000270

Data	PK	L	Data
Log(Re/f)	1/f	1/f	1/f
3.407004	13.22801	159.5453	13.52940
3.341308	12.94523	137.1475	13.11575
3.257571	12.63028	113.0970	12.73390
3.152737	12.21103	88.84602	12.14772
3.070198	11.88079	73.44459	11.88905
2.972882	11.57153	61.48408	11.46887
2.928214	11.31285	52.97781	11.43449
2.821119	10.88447	41.39994	10.89390
2.821822	10.88729	41.46700	10.82071
2.751820	10.40728	35.29395	10.50670
2.643858	10.17535	27.52442	10.10224
2.543356	9.775425	21.83918	9.870754
2.473228	9.492915	18.58270	9.716861
2.331757	8.927030	13.41444	11.03822
2.250226	8.400907	11.15005	10.55460
2.190530	8.342120	9.491928	9.404834
2.124582	8.098328	8.32492	8.225170
2.041183	7.844733	7.195538	7.107829
1.950901	7.403604	5.581889	5.569239
1.804316	6.817266	3.982875	3.974200
Data	PK	L	Data
Log(Re/f)	1/f	1/f	1/f
3.888644	15.14657	481.4206	15.08120
3.820731	14.88292	413.4294	14.91997
3.744281	14.45704	363.1964	14.45954
3.706542	14.42616	317.9963	14.46008
3.600251	14.00160	248.9609	14.09235
3.493240	13.57294	194.5899	13.48080
3.371887	13.08754	147.1523	13.15715
3.233089	12.53255	104.8981	12.45179

80000272

Date	PK	L	Data
Log(Re/f)	1/f	1/f	1/f
3.151950	12.26780	88.48080	12.28044
3.414185	13.24474	142.75440	13.35434
3.348591	12.99434	139.4670	12.98521
3.345124	12.97280	137.7231	13.14764
3.259451	12.63780	113.5674	12.73497
3.149824	12.19429	88.24802	12.31509
3.046383	11.74153	68.59037	11.85914
2.954328	11.42830	54.52037	11.53037
2.912500	11.25660	51.09528	10.94219
2.785837	10.73535	37.99422	11.02049
3.030554	11.72221	47.05557	11.44142
2.932921	11.41140	54.07913	11.28467
2.891137	11.17453	48.97984	11.12582
2.787868	10.75155	38.33627	10.81281
2.728492	10.51477	33.44359	10.27114
2.642359	10.24943	28.72341	10.34902
2.614157	10.05443	23.76418	9.88727
2.518135	9.472542	20.46703	9.711575
2.422774	9.291094	16.54451	10.02223
2.294850	8.779322	12.32263	11.13243
2.214197	8.444789	10.28199	9.916892
2.143434	8.254539	9.109923	8.963205
2.103198	8.012792	7.924440	7.841558
1.995386	7.58323	6.161042	6.128424
1.824497	6.897989	4.172318	4.177335

80000274

Date	PK	L	Data
Log(Re/f)	1/f	1/f	1/f
2.972659	11.49043	58.48661	11.38574
2.915319	11.26127	51.42793	11.12111
2.864443	10.81777	39.84042	10.72377
2.628840	10.11536	26.59014	10.09174
2.524141	9.494545	20.89598	9.771773
2.359481	8.957925	13.45719	10.79994
2.235127	8.540510	10.74008	10.14891
2.143484	8.254734	9.110942	8.830354
2.090475	7.941900	7.697595	7.508274
1.884883	7.139533	4.794721	4.751950
1.784390	6.737561	3.804261	3.789528

Date	PK	L	Data
Log(Re/f)	1/f	1/f	1/f
3.880471	15.12188	474.6254	15.22825
3.824782	14.89913	417.5062	15.00341
3.749935	14.59974	351.4114	14.74016
3.672033	14.28813	293.7045	14.55503
3.549471	13.87788	231.9270	14.02368
3.454120	13.41448	177.8281	13.54812
3.370539	13.08215	146.4963	13.13864
3.241295	12.54518	108.9349	13.24953
3.186507	12.38602	98.24242	12.25920
3.407229	13.22891	159.4282	13.46150
3.341747	12.96489	137.2845	13.04349
3.263483	12.65393	114.4473	12.49532
3.132430	12.13052	84.82241	12.46667
3.029137	11.71654	66.83704	11.72866
2.954705	11.41882	56.31001	11.23528
2.882451	11.13040	47.70143	11.30444
2.780552	10.72221	37.70794	10.70931
2.709908	10.43963	32.04708	10.48748
3.022880	11.49152	45.88109	11.42316
2.947134	11.38853	55.33680	11.19389
2.783843	10.73545	37.99651	10.50340
2.604273	10.02549	25.24951	9.992158
2.514983	9.459933	20.45800	9.756353
2.421072	9.284290	16.47982	10.10544
2.304740	8.818943	12.40724	10.88983
2.219582	8.478330	10.36245	9.751364
2.143229	8.172918	8.691799	8.148378
2.075086	7.900347	7.429624	7.121120
1.928098	7.512395	5.294375	5.246925
1.667364	6.270257	2.906996	2.881476

80000282

Date	PK	L	Data
Log(Re/f)	1/f	1/f	1/f
3.900127	15.20051	494.4014	14.95375
3.834358	14.93743	424.8141	14.78898
3.747537	14.47015	345.9444	14.54312
3.484472	14.34649	303.7755	14.24009
3.400924	14.00349	249.3473	13.89825
3.490299	13.54119	193.2749	13.44744
3.346509	13.04203	143.3472	12.93114
3.294627	12.61851	100.1149	12.34229
3.119953	12.07981	82.58214	12.01887
3.423381	13.29352	143.4749	13.41645
3.323836	12.89336	131.7397	13.12315
3.264498	12.41749	100.0871	12.35812
3.119584	12.07833	82.31224	12.00197
3.057390	11.83034	71.34257	11.77988
2.975518	11.50207	59.07425	11.49705
2.921071	11.28428	52.11344	11.23747
2.810780	10.84312	40.42593	10.74459
2.450127	10.12051	28.46905	10.12357

80000274

80000282

3.056295 11.80118 70.17381 11.72053

3.816320	14.84408	409.6382	14.97501
3.786099	14.72034	374.6778	14.77752
3.739433	14.85863	343.1724	14.56517
3.672264	14.84682	307.6708	14.39972
3.639908	14.18837	272.1749	14.19078
3.578911	13.91244	237.0234	13.87694
3.486879	13.85381	192.4459	13.56242
3.417858	13.27182	163.3725	13.19529
3.324953	12.90782	132.4891	12.81197
3.269467	12.43786	101.2388	12.34301
3.189378	12.03831	80.43740	11.99814

3.391240	13.16494	133.8581	13.29008
3.291273	12.74817	122.2287	13.01159
3.172818	12.29127	95.06409	12.20893
3.032993	11.73197	67.43311	11.43189
2.958787	11.40314	55.80424	11.42745
2.897175	11.18878	49.32370	11.02400
2.784349	10.73739	38.03901	10.76455
2.716912	10.46745	32.54910	10.50015
2.644113	10.25645	28.83787	10.26379

3.016992	11.44794	64.99386	11.77095
2.944745	11.37904	53.03581	11.31343
2.888749	11.15567	48.37819	11.07349
2.784182	10.73472	38.02440	10.56049
2.645418	10.24247	28.94001	10.19741
2.604589	10.01835	25.14402	9.949427
2.502197	9.488788	19.86498	9.672444
2.434802	9.339211	17.00915	9.65824
2.296416	8.742445	12.20383	11.11141
2.216428	8.465712	10.28746	9.781186
2.155153	8.220412	8.93734	8.498814
2.001943	7.407855	4.278327	4.181479
1.773843	6.695374	3.712988	3.444538

Data PK L Data
Log (Re/f) 1//f 1//f 1//f

3.840921	15.04348	453.7347	14.95428
3.797794	14.79118	392.3527	14.69974
3.721154	14.48461	328.8776	14.44213
3.649727	14.19891	279.0022	14.18654
3.562367	13.84947	228.1444	13.87798
3.431859	13.32743	168.9425	13.38773
3.322541	12.89174	131.6483	12.90286
3.167301	12.26920	91.87171	12.30933
3.027750	11.71100	66.62391	11.88185
3.386774	13.14710	152.2867	13.34693
3.321815	12.88726	131.1279	12.93637
3.263219	12.41287	99.79284	12.44549

80000285

2.992388	11.54955	61.41419	11.67501
2.916964	11.26786	51.42343	11.32726
2.835469	11.02243	44.89178	11.12088
2.751267	10.40507	35.24908	10.58541
2.679173	10.31649	29.85753	10.37890
2.972230	11.48892	58.42871	11.48161
2.901395	11.20558	49.80532	11.47590
2.789713	10.75885	38.51181	10.74635
2.678737	10.31495	29.82755	10.31822
2.563278	9.853115	22.86435	9.987877
2.457495	9.429982	17.92155	9.873868
2.322860	8.891443	13.14440	11.12348
2.437773	9.331093	16.92985	9.646594
2.291541	8.746165	12.22985	11.20011
2.214873	8.459493	10.25049	9.828635
2.142431	8.149725	8.675838	8.591703
2.050139	7.800537	7.014867	4.964791
1.925760	7.301442	5.243087	5.279104
1.75727	4.603309	3.521335	3.543490

Data PK L Data
Log (Re/f) 1//f 1//f 1//f

80000288

3.862135	15.04854	455.0043	15.14992
3.814717	14.85887	407.9413	14.92632
3.758967	14.63587	358.7961	14.72939
3.685441	14.34256	303.0547	14.40579
3.722277	14.48911	329.7293	14.49074
3.651161	14.20444	279.9246	14.37388
3.537249	13.82899	225.4911	13.94042
3.428800	13.31200	167.4481	13.51629
3.341182	13.04473	143.5687	13.13692
3.203618	12.41447	99.88452	12.38830
3.122436	12.09054	82.89270	12.13498

3.426748	13.30707	166.9738	13.52414
3.357781	13.03112	142.4496	13.21038
3.275042	12.70024	117.7449	12.78570
3.202503	12.41001	99.62839	12.59222
3.037514	11.75805	68.13883	11.86921
2.952398	11.40959	56.01163	11.71499
2.910726	11.24290	50.68692	11.01895
3.020001	11.68000	65.44580	11.86675
2.950037	11.40014	55.70798	11.37620
2.894912	11.16564	48.67344	11.09871
2.785284	10.74113	38.12098	10.60462
2.598847	9.995388	24.81573	10.05452
2.515281	9.661127	20.47267	9.780288
2.433197	9.352789	16.94639	9.674030
2.317426	8.870504	12.98691	10.94164

Solvent Set 1:		Runs 80000234 - 80000339		Page 18		Runs 80000234 - 80000339	
2.228798	8.518162	10.58550	10.14524				
2.145404	8.174738	6.760798	8.617564				
2.059652	7.634211	7.160328	7.010824				
1.894486	7.158661	4.792149	4.766497				
1.694507	6.826689	3.107332	3.194515				
3.428475	13.31390	147.4314	13.41044				
3.333797	12.93319	134.7962	12.97108				
3.283337	12.46755	99.59649	12.54050				
3.113769	12.05483	81.26433	12.50342				
3.085193	11.95477	74.74914	12.01151				
3.008044	11.43318	63.64874	11.71155				
2.956424	11.40249	55.78337	11.47335				
2.844811	10.97824	43.72115	10.95472				
2.779024	10.71619	37.57561	10.68974				
2.657548	10.25819	28.40721	10.31872				
Data	PK	L	Data				
Log(Re/f)	1//f	1//f	1//f				
3.074255	15.09702	467.8813	15.20572				
3.810144	14.84064	403.4890	14.98009				
3.753049	14.61227	353.9560	14.73990				
3.684252	14.34493	303.4678	14.45707				
3.574944	13.90777	235.9527	14.07098				
3.502564	13.61001	198.7854	13.71938				
3.390350	13.16140	153.5431	13.12834				
3.290489	12.74195	122.0027	12.43470				
3.188274	12.35309	94.41728	12.29805				
3.404108	13.22443	159.2146	13.40526				
3.503415	12.81444	125.7442	13.20152				
3.187977	12.55191	96.55129	12.30648				
3.012081	11.64832	64.26395	11.79564				
2.924044	11.29425	52.47398	11.43464				
2.853467	11.01464	44.62180	11.24945				
2.750043	10.40017	35.16985	10.64398				
3.056122	11.82449	71.12177	11.76297				
2.977297	11.50902	59.31130	11.38504				
2.923471	11.29368	52.40245	11.43660				
2.788848	10.75547	38.43494	10.74911				
2.741228	10.56491	34.44362	10.48215				
2.742420	10.49748	33.13602	10.38589				
2.675489	10.50275	29.41893	10.19114				
2.615472	10.04188	25.78411	10.04200				
2.520439	9.681736	20.71642	9.841888				
2.449711	9.398044	17.40317	9.840419				
2.317443	8.849775	12.98147	10.94971				
2.231427	8.525709	10.64896	10.15134				
2.195885	8.383543	9.812187	9.444378				
2.148325	8.195303	8.794394	8.513749				
2.084458	7.945834	7.624732	7.464950				
1.984568	7.558275	6.031825	5.975641				
1.814070	6.844283	4.092143	4.077883				
Data	PK	L	Data				
Log(Re/f)	1//f	1//f	1//f				
3.882505	15.13002	476.8544	15.12291				
3.809232	14.83693	402.8216	14.91857				
3.722242	14.48897	329.7029	14.58166				
3.609882	14.03953	254.5440	14.16538				
3.455480	13.42192	178.5857	13.47534				
3.344371	12.97748	138.1184	13.05297				
3.879461	15.11784	473.5230	15.22950				
3.812470	14.84988	405.8360	14.80774				
3.722498	14.48999	329.8968	14.57509				
3.610181	14.04072	254.7190	14.15565				
3.457541	13.43016	179.3344	13.41157				
3.342304	12.96921	137.4624	13.11526				
3.918544	15.27417	518.1129	15.19874				
3.848101	14.98440	438.5119	14.96475				
3.760189	14.64075	359.8072	14.59057				
3.647544	14.19017	277.4031	14.18331				
3.492284	13.58913	194.1620	13.51906				
3.378866	13.11546	149.5361	13.16515				
3.913879	15.23551	512.5778	15.36287				
3.843225	14.97290	435.6176	15.06418				
3.759174	14.63669	358.9668	14.62469				
3.647157	14.18842	277.3558	14.19596				
3.490643	13.56257	193.4300	13.57022				
3.374755	13.10702	148.8110	13.22950				
Data	PK	L	Data				
Log(Re/f)	1//f	1//f	1//f				
3.874568	15.09827	468.2186	15.29795				
3.875312	15.10124	469.0212	15.20302				
3.819287	14.87714	412.2561	15.05998				
3.754616	14.42446	354.8589	14.71928				
3.667440	14.24974	290.6169	14.37351				
3.553156	13.81262	223.3759	13.89529				
3.470789	13.48315	184.7860	13.56690				
3.878439	15.11375	472.4105	15.16220				
3.798298	14.79319	392.8064	14.89187				
3.739119	14.55847	342.7671	14.62786				
3.650507	14.20203	279.5038	14.09437				
3.558708	13.83483	226.2498	13.71879				

Log (Re/f)	PK	L	Data
3.455393	15.42157	178.3500	15.38713
3.874904	15.10743	476.7442	15.21981
3.814433	14.88374	407.4759	14.93433
3.789435	14.48374	389.1831	14.42404
3.691123	14.84449	364.9449	14.39224
3.594973	13.97909	245.9338	14.07584
3.486482	13.58472	192.3582	13.43927

80000302

Log (Re/f)	PK	L	Data
3.871432	15.08452	445.0434	15.14641
3.828473	14.91449	421.2434	15.04302
3.762901	14.73126	379.0372	14.80098
3.731914	14.52744	337.1290	14.43947
3.646057	14.24022	285.7174	14.39472
3.586788	13.93315	242.1944	14.07024
3.482244	13.52965	189.7335	13.62545
3.341127	13.04451	143.5314	13.09738
3.289343	12.72137	119.1854	12.81717
3.185982	12.34393	95.90980	12.25264
3.401141	13.20454	157.4040	13.43744
3.331064	12.92434	133.9371	13.15823
3.182447	12.33647	95.18042	12.34595
3.249823	12.59929	111.0971	12.49259
3.072014	11.94804	77.24945	12.14930
3.041942	11.74774	68.83703	11.88010
2.944514	11.44605	57.84310	11.46260
2.901944	11.26784	49.87084	11.34441
2.794178	10.77471	38.96978	10.86273
2.723384	10.49354	33.05727	10.40400
2.996895	11.58758	62.05477	11.38484
2.934894	11.34733	54.04611	11.13454
2.819543	10.87816	41.23019	10.75934
2.734174	10.54470	34.04524	10.43627
2.679448	10.31859	29.89019	10.25624
2.417651	10.07140	25.92375	10.15244
2.523270	9.493062	20.65214	9.853512
2.533928	9.415713	17.77493	9.949134
2.317485	8.849940	12.98270	11.22109
2.248194	8.592774	11.04812	10.04543
2.174434	8.298344	9.343440	8.619884
2.111448	8.046473	8.082349	7.571428
1.987904	7.551623	6.078360	5.801841
1.806743	6.826974	4.003193	3.911635
1.625424	6.102494	2.439393	2.430346
2.940857	11.45343	57.11335	11.42549
2.903978	11.21591	50.10239	11.32549

Log (Re/f)	PK	L	Data
2.804171	10.81448	39.81548	10.70702
2.753447	10.54247	34.00537	10.48881
2.684121	10.33448	30.19942	10.28494
2.424122	10.09448	24.30292	10.12581
2.524554	9.704223	21.01050	9.879132
2.459170	9.434480	17.99078	9.788134
2.329746	8.918984	13.35445	10.84655
2.240194	8.540784	10.84615	10.30341
2.145438	8.242333	9.152041	9.053807
2.084445	7.938582	7.594642	7.546790
2.003347	7.413471	6.298457	6.228194
1.898078	7.192312	4.942430	4.932235
1.745717	6.582849	3.480145	3.511805

80000303

Log (Re/f)	PK	L	Data
3.869922	15.07949	443.2345	15.18591
3.819938	14.87975	412.8750	15.05046
3.765529	14.44411	345.0983	14.77204
3.711981	14.44792	322.0042	14.56434
3.647343	14.18937	277.4743	14.36641
3.574409	13.89765	234.5791	13.99462
3.481477	13.52591	189.3902	13.61939
3.340857	13.04343	143.4623	13.07599
3.181731	12.32492	94.97543	12.34472
3.402644	13.21045	157.9588	13.33034
3.307452	12.83046	124.9204	12.90352
3.174295	12.29718	93.36311	12.52960
3.094843	11.98377	81.1294	11.98063
3.029382	11.71752	66.87473	11.71190
2.950472	11.40189	55.74386	11.48174
2.884273	11.13709	47.87982	11.31733
2.777451	10.70980	37.43959	10.81201
2.707544	10.43024	31.87449	10.51039
3.014902	11.44740	44.98034	11.78071
2.937430	11.35052	44.13903	11.52222
2.888743	11.15505	40.37754	10.98372
2.774275	10.70510	37.33838	10.40823
2.709041	10.33424	31.98443	10.48577
2.594203	9.984814	24.66514	10.12679
2.498854	9.595416	19.71215	9.811742
2.407941	9.231766	15.98901	10.29888
2.337990	8.733160	12.01331	11.05858
2.208450	8.433800	10.10020	9.646241
2.138484	8.153946	8.597389	8.551855
2.020342	7.681371	6.549722	6.412358
1.924434	7.297744	5.251893	5.254399
1.685190	6.340743	3.027406	3.082498

Data	PK	L	Data
Log(Rn/f)	1/f	1/f	1/f
3.862483	15.07473	441.9143	15.19500
3.813294	14.88317	404.4070	14.94033
3.748237	14.89794	358.9375	14.70443
3.690751	14.54368	304.6418	14.49654
3.611848	14.04747	255.7104	14.18141
3.472923	13.87149	194.4481	13.83483
3.381971	13.12788	150.4692	13.20413
3.183483	12.33393	98.35942	12.24730
3.408898	13.20359	157.3181	13.35444
3.332715	12.93686	134.4407	13.02053
3.258482	12.40273	111.3172	12.58205
3.182710	12.33694	95.10788	12.24144
3.041918	11.74407	48.49074	11.89413
3.042949	11.77179	48.99489	11.98190
2.949404	11.47742	58.24874	11.48428
2.910914	11.24345	50.90895	11.17097
2.860047	10.80018	39.43912	10.82213
2.730513	10.52205	33.60421	10.54544
2.620337	10.08135	26.07442	10.17532
2.945252	11.44100	57.49422	11.40413
2.900298	11.20119	49.67942	11.30034
2.800074	10.80029	39.44141	10.71177
2.726014	10.51205	35.41141	10.52091
2.621314	10.68524	24.13340	10.11712
2.527029	9.708117	21.03339	9.821452
2.454471	9.417885	17.79718	9.794524
2.319140	8.874542	15.03229	10.97547
2.228342	8.513451	10.57409	10.12873
2.150925	8.203703	8.847200	8.701123
2.043902	7.853411	7.240738	7.149281
1.948404	7.474417	5.814123	5.848440
1.728544	6.314259	3.345375	3.335034

Data	PK	L	Data
Log(Rn/f)	1/f	1/f	1/f
3.872814	15.09125	444.3314	15.01721
3.809749	14.83507	402.3917	14.79292
3.741520	14.56498	344.6677	14.56152
3.674057	14.29422	295.0783	14.23941
3.575370	13.90228	255.2048	13.89444
3.465775	13.46310	182.4451	13.41827
3.359724	13.03889	143.0885	13.05113
3.175942	12.30377	93.71793	12.45404
3.599929	13.19971	154.9673	13.38431
3.304816	12.81924	124.0944	12.95878

80000311

3.181822	12.32728	94.99533	12.20457
3.045422	11.78168	49.39883	11.77413
3.038489	11.75475	48.32343	11.84355
2.961298	11.44519	57.17130	11.50441
2.904213	11.21485	50.12955	11.19342
2.789720	10.75888	38.51237	10.98521
2.720727	10.48291	32.85544	10.70315
3.024170	11.49448	44.07703	11.91050
2.958274	11.43310	34.77492	11.34733
2.899287	11.19715	49.56418	11.27047
2.784255	10.74502	38.20434	10.79407
2.724709	10.50483	33.31111	10.51452
2.614807	10.05923	25.74449	10.22450
2.519854	9.479419	20.48878	9.939451
2.437724	9.350907	17.12404	10.00689
2.307525	8.850100	12.48834	11.23245
2.218357	8.474228	10.33801	10.34909
2.139544	8.158187	8.418404	8.745612
2.012131	7.448525	6.427045	6.540478
1.829434	6.917744	4.220035	4.294127
1.457041	4.228147	2.837408	2.827847

Data	PK	L	Data
Log(Rn/f)	1/f	1/f	1/f
3.851583	15.00433	444.0828	15.14204
3.780183	14.72075	374.7584	14.87319
3.493415	14.37346	308.5285	14.53987
3.582810	13.93124	259.1610	14.05814
3.428400	13.31360	167.4025	13.37354
3.319832	12.87932	130.5306	12.87882
3.166267	12.26506	91.6513	12.22784
3.094807	11.97922	77.74761	11.53128
3.383789	13.13515	151.2408	13.30824
3.277748	12.71099	118.4755	13.21346
3.163489	12.24195	91.48911	12.22216
3.085159	11.94043	74.03946	11.74434
2.991572	11.54428	41.29883	11.41688
2.933432	11.33373	53.41824	11.43936
2.883150	11.13240	47.75652	11.31973
2.786440	10.74644	38.24199	11.07881
2.661404	10.24561	28.64052	10.14490
2.486757	10.34703	30.38348	10.83411
2.997371	11.58948	42.12285	11.54445
2.934141	11.41644	56.23951	11.24007
2.845248	10.98107	43.76715	10.84928
2.774228	10.49691	37.16283	10.58465
2.645997	10.26399	28.96528	10.21067
2.573048	9.892194	23.38452	9.801933

80000314

2.50723	9.431675	20.12014	9.752011
2.588990	9.183962	15.30631	10.42741
2.265449	8.641877	11.51726	10.45475
2.291800	8.407203	9.944746	9.421644
2.134990	8.139943	8.328447	8.294924
2.051189	7.894707	7.651846	8.851037
1.934782	7.427129	6.437993	3.540003
1.843426	6.973707	4.358196	4.325384
1.679885	6.119543	2.649421	2.654374

Data	PK	L	Data
Log(Re/f)	1//f	1//f	1//f

80000317

3.873965	15.09584	667.5686	15.04322
3.860765	14.80282	394.9890	14.04149
3.713279	14.46111	324.4584	14.45417
3.483617	14.01447	250.8994	14.01894
3.502002	13.60601	198.5539	13.58118
3.403924	13.21549	158.4180	13.32172
3.335167	12.94042	133.2032	13.06758
3.180758	12.52503	94.74284	12.37241
3.087432	11.95053	76.47385	12.24505
3.402049	13.20827	157.7426	13.37874
3.338477	12.93390	134.2544	12.90704
3.183971	12.33588	95.4654	12.28121
3.021443	11.71277	66.48433	11.86301
2.954349	11.41747	54.26439	11.44904
2.905240	11.22104	50.25054	11.09124
2.789243	10.79703	38.47187	10.80701
2.721800	10.48720	32.93672	10.50395
2.952582	11.41033	54.03542	11.35295
2.894058	11.17423	48.97090	11.15482
2.791759	10.74763	38.69346	10.73524
2.724959	10.50783	33.33032	10.34224
2.607803	10.03121	25.33280	10.21567
2.505907	9.623431	20.03493	9.959472
2.425053	9.300214	16.45158	10.18703
2.310324	8.841304	12.77044	10.96121
2.225689	8.502757	10.50919	10.11613
2.140325	8.161302	8.435872	8.528995
2.048174	7.792497	6.983197	6.979213
1.975404	7.495424	5.878771	5.893407
1.834029	6.934119	4.264909	4.235074
1.654025	6.216103	2.817772	2.830900

Data	PK	L	Data
Log(Re/f)	1//f	1//f	1//f

3.885177	15.14070	479.7949	15.03016
3.828371	14.91348	420.9708	14.84440

80000320

3.752563	14.61025	353.5438	14.61824
3.673317	14.29406	294.7115	14.27384
3.615383	14.05313	256.5449	14.05490
3.527907	13.71162	210.7595	13.48455
3.412722	13.25089	161.6600	13.38257
3.346442	12.98444	138.8489	12.98430
3.191181	12.36472	97.04468	12.38251
3.414448	13.25047	162.3859	13.32275
3.315017	12.84007	129.0915	13.03467
3.192308	12.34923	97.31687	12.35042
3.111450	12.04660	80.82219	11.89477
3.034748	11.74707	68.02189	11.78630
2.953766	11.42504	56.44775	11.52318
2.898273	11.19309	49.44853	11.21165
2.789474	10.75790	38.49076	10.82922
3.028122	11.71249	66.68110	11.73114
2.954117	11.41647	54.23385	11.35711
2.895843	11.18337	48.17266	11.20618
2.788993	10.75597	38.44802	10.76509
2.725370	10.50148	33.20842	10.43380
2.612845	10.05138	25.42862	10.07988
2.523210	9.692841	20.84924	9.826482
2.439690	9.358761	17.20166	9.945390
2.304718	8.818874	12.60662	11.20046
2.224903	8.499613	10.49018	10.19448
2.150729	8.202918	8.843203	8.696066
2.077193	7.908782	7.665786	7.487815
1.952730	7.410923	5.605455	5.651552
1.803935	6.815741	3.979379	4.047597
1.654569	6.218276	2.821298	2.807111

Data	PK	L	Data
Log(Re/f)	1//f	1//f	1//f

3.858942	15.03576	451.6708	15.05654
3.780796	14.72318	377.2914	14.72205
3.701539	14.40615	314.3543	14.42276
3.574649	13.90659	255.7923	13.94005
3.430479	13.32191	168.4047	13.46066
3.327837	12.91135	132.9589	12.78707
3.170649	12.28259	92.58271	12.24238
3.081345	11.92538	75.37466	12.02986
3.391783	13.16715	154.0505	13.24758
3.294118	12.77647	125.0265	12.89809
3.171644	12.28657	92.79489	12.21479
3.084479	11.94591	74.27096	11.88849
3.395193	13.18077	155.2468	13.05137
3.289079	12.75651	121.6071	12.96061
3.168192	12.27277	92.06036	12.22880

80000323

Data	PK	L	Data
Log (Re/f)	1/f	1/f	1/f
3.074308	11.90523	74.50540	12.09009
3.022445	11.69046	49.04046	11.00082
2.944079	11.37431	54.94074	11.46274
2.869276	11.18718	48.43694	11.13327
2.751914	10.60748	38.30163	10.61989
2.641568	10.20443	28.44743	10.31830
2.565222	9.620888	20.06332	9.740793
3.013050	11.45212	64.40370	11.70516
2.942596	11.36988	54.75443	11.31407
2.068970	11.15228	48.30038	11.04111
2.781337	10.72414	37.79352	10.69444
2.713429	10.45371	32.50798	10.38748
2.608329	10.03331	28.34332	9.944452
2.517952	9.671810	20.39835	9.714535
2.304167	8.816449	12.59062	10.90810
2.232845	8.531442	10.48428	9.967624
2.151480	8.204723	8.042591	8.641097
2.008213	7.952852	7.457406	7.424190
2.015909	7.643439	6.483205	6.428877
1.924228	7.304913	5.273414	5.233787
1.806406	6.801627	3.947180	3.934705
1.672786	6.291146	2.942162	2.951649
3.844274	14.97709	434.6712	15.02160
3.780859	14.72343	377.3458	14.77377
3.705359	14.42135	317.1148	14.47937
3.634084	14.13633	269.1316	14.21749
3.556075	13.80030	221.7970	13.80136
3.473448	13.47967	185.7861	13.18848
3.310998	12.84399	127.9024	12.82130
3.157733	12.25893	90.28454	12.10894
3.378184	13.11274	149.3021	13.10032
3.276761	12.70784	118.2411	12.94213
3.152599	12.21039	88.81342	12.50949
3.004652	11.62640	63.46448	12.05828
2.931909	11.40743	55.94866	11.44061
2.872472	11.09989	46.59644	11.16638
2.840530	11.34212	54.50178	11.36465
2.876708	11.10483	47.05314	11.30140
2.774377	10.69750	37.17552	10.85281
3.026071	11.70428	64.36684	11.75683
2.970178	11.48071	58.35241	11.33793
2.905890	11.22354	50.32345	11.16229
2.789659	10.75955	38.50517	10.65443
2.724492	10.50674	33.30983	10.44923
2.620990	10.08394	24.11390	10.02656

80000329

Data	PK	L	Data
Log (Re/f)	1/f	1/f	1/f
2.519279	9.677118	20.66139	9.750896
2.457300	9.429200	17.91349	9.706331
2.350202	8.920810	13.36850	10.77349
2.236549	8.546196	10.77529	10.20940
2.154943	8.219773	8.929424	8.405937
2.040795	7.763181	4.865550	6.798728
1.933945	7.335863	5.549411	5.531997
1.780011	6.720047	3.766099	3.704207
1.658035	6.224141	2.830840	2.846041
3.444039	13.37615	173.7480	13.42903
3.333927	12.93570	134.8365	13.45900
3.222879	12.49151	104.4141	12.41460
3.095985	11.98394	77.95883	11.63924
2.995431	11.58172	61.84599	11.61103
2.935500	11.34200	53.87419	11.41007
2.833589	10.93435	42.40586	10.80383
2.759117	10.43446	35.89195	10.48756
2.647462	10.18984	27.75506	10.28299
3.056794	11.82717	71.23196	11.65854
2.982167	11.52867	59.98567	11.50239
2.918911	11.27364	51.85512	11.35646
2.818530	10.87420	41.15574	10.80405
2.651746	10.20898	28.03023	10.08946
2.561011	9.846046	22.74530	9.823396
2.489487	9.358750	19.30046	9.700457
2.374212	9.104849	14.86231	10.39946
2.254558	8.626235	11.28336	10.43616
2.170890	8.283561	9.263400	8.842129
2.071946	7.887784	7.374097	7.166780
1.951498	7.405995	5.589574	5.571848
1.745742	6.583048	3.480504	3.500396
3.913115	15.25246	511.6767	15.04661
3.833429	14.93371	425.9016	14.76284
3.742220	14.64888	361.4937	14.55746
3.676904	14.30761	297.0188	14.25651
3.582201	13.92880	238.8258	13.96937
3.441935	13.36774	172.9082	13.57996
3.347307	12.98922	139.0551	12.91886
3.214283	12.45713	102.5677	12.53487
3.126812	12.10725	83.69372	12.26576

80000333

Data	PK	L	Data
Log (Re/f)	1/f	1/f	1/f
3.853769	15.01507	466.3222	14.99821
3.781626	14.72650	378.0131	14.75709

3.818765 14.87506 411.7616 14.90234
 3.742776 14.57110 345.6657 14.52425
 3.495622 14.38668 309.6723 14.41103
 3.642552 14.17020 279.4304 14.22896
 5.529991 13.93196 239.2610 13.98900
 3.515085 13.65234 203.6879 13.69343
 3.425243 13.39097 166.3886 13.41046
 3.315046 12.84018 129.1000 12.96291
 3.162193 12.24877 90.79741 12.28751
 3.384925 13.14770 152.3370 13.24232
 3.292732 12.77092 122.6344 12.79419
 3.166759 12.26703 91.75693 12.21401
 3.092861 11.93144 75.63823 11.85347

Data PK L Data
 Log(Ro/f) 1//f 1//f 1//f

80000336

3.893624 15.17449 489.2199 15.00912
 3.811278 14.84511 404.7239 14.81648
 3.741742 14.56697 346.8439 14.55021
 3.679463 14.31785 298.7742 14.33616
 3.591360 13.96544 243.9166 14.04834
 3.478610 13.51944 188.1439 13.65937
 3.352814 13.01125 140.8299 13.03480
 3.198632 12.39452 98.74430 12.39356
 3.419038 13.27615 164.0281 13.29931
 3.321861 12.88744 131.1417 13.03512
 3.194380 12.38552 98.23376 12.42989
 3.111397 12.04558 80.77506 12.09319

Data PK L Data
 Log(Ro/f) 1//f 1//f 1//f

50000339

3.898167 15.15266 483.1111 15.02842
 3.807409 14.82963 401.1336 14.78142
 3.716629 14.46651 325.4686 14.49989
 3.613271 14.05308 256.5377 14.15074
 3.458414 13.42565 178.7698 13.53770
 3.349932 12.99973 139.8983 12.97441
 3.190886 12.36354 96.99882 12.47506
 3.112562 12.05025 80.99214 11.95243
 3.415313 13.26125 162.6274 13.39331
 3.309744 12.83897 127.5334 13.28352
 3.191412 12.36566 97.11630 12.45997
 3.112447 12.05059 81.00795 11.95010
 3.035355 11.74142 67.80690 11.73622
 2.932740 11.45096 57.36153 11.39678
 2.899485 11.19874 49.40922 11.19816
 2.793982 10.77592 38.89219 10.73421

3.029051 11.71220 66.67019 11.68554
 2.951944 11.40785 55.95573 11.41912
 2.893598 11.17439 48.91908 11.16014
 2.796136 10.78462 39.08738 10.67957
 2.725193 10.50078 33.19518 10.46428
 2.611246 10.04498 25.33444 10.08367
 2.523293 9.493175 20.65325 9.715576
 2.449346 9.398187 17.59452 9.643634
 2.322434 8.889738 13.13150 10.81802
 2.231845 8.527460 10.63970 9.970923
 2.157744 8.231046 8.987459 8.413246
 2.091043 7.964173 7.707476 7.434544
 2.018502 7.674008 6.522019 6.334544
 1.941109 7.364437 5.457445 5.424544
 1.855202 7.020810 4.477985 4.634544
 1.738372 6.553489 3.421782 3.26607

Page 1

Solvent Set 2a Runs T0000341 - T0000370

Page 2

Solvent Set 2a Runs T0000341 - T0000370

T0000341

Data	PK	L	Data
Log(Re/f)	1//f	1//f	1//f
4.018862	15.67545	452.7441	15.93942
3.942133	15.34584	547.6355	15.53242
3.844213	16.65606	457.1890	15.17150
3.733927	14.61571	354.4544	14.44823
3.617076	14.84828	258.7917	14.07127
3.485999	13.56395	191.3479	13.59209
3.339447	12.95370	134.5412	12.69805
3.251117	12.60444	111.4288	12.44944
4.019454	15.67841	453.9343	15.91041
3.950389	15.40155	537.5321	15.55122
3.856056	15.02622	440.4093	15.07273
3.754297	14.62519	354.5968	14.58841
3.601167	14.00467	249.4849	13.90101
3.489248	13.53707	192.8182	13.48984
3.333433	12.93373	134.4833	12.87509
3.195330	12.38132	97.99652	12.38659
4.043730	15.77492	451.2111	15.90777
3.973613	15.49445	580.1573	15.57920
3.896642	15.10456	492.4313	15.25213
3.742893	14.65157	342.0542	14.47888
3.597352	13.98933	247.2935	14.08222
3.511047	13.64419	202.7364	13.55913
3.351754	13.00701	140.4844	13.04471
3.219403	12.47741	103.5810	12.38463
3.518312	13.67324	204.1542	13.59238
3.321944	12.68785	131.1730	12.81723
3.405275	14.02110	251.8574	14.09273
3.711588	14.44435	321.7131	14.51670
3.850104	14.92041	422.4534	15.02745
3.893278	15.17311	480.8364	15.28616
3.929087	15.31934	531.8231	15.45347
3.946827	15.38731	552.9777	15.53985
3.948025	15.39210	554.5049	15.46213
3.974006	15.09602	467.6131	15.14655
3.780307	14.73214	379.2425	14.74420
3.658574	14.23430	284.7455	14.40067
3.517561	13.67024	205.7981	13.58522
3.359332	13.03733	142.9593	13.03780
3.215412	12.46145	102.4343	12.71225

T0000341

Data	PK	L	Data
Log(Re/f)	1//f	1//f	1//f
3.458109	13.45243	179.4690	13.77928
3.351965	13.00794	140.5613	13.19506

3.283882	12.73552	120.1605	12.86576
3.194023	12.38409	98.15293	12.59746
3.484259	13.53703	190.4074	13.78495
3.441125	13.36450	172.5860	13.43327
3.390662	13.16245	153.4535	13.07666
3.288972	12.75589	121.5774	12.71286
3.151733	12.20493	88.43672	12.20620
3.483426	13.53370	190.2421	13.81142
3.412549	13.25019	161.5955	13.59044
3.321686	12.88674	131.0890	12.96948
3.243743	12.37497	109.5527	12.69742
3.154869	12.21947	89.27912	12.11837
3.284792	12.73917	120.4128	12.87581
3.321591	12.88436	131.0404	12.97231
3.248412	12.59365	110.7369	12.56163
3.319167	12.87466	130.3309	13.04492
3.246501	12.58600	110.2508	12.61702
3.046045	11.78426	69.49367	11.92322
2.984431	11.53772	60.29918	11.42008
2.944052	11.37421	54.94559	11.46248
2.853440	11.02176	44.80437	11.07113
2.771700	10.78868	39.17878	10.81542
2.695843	10.57545	30.88471	10.45385
2.613829	10.35531	23.68475	10.15413
2.546021	9.784085	21.97361	10.01420
2.599936	9.199745	15.49699	11.32320
2.416027	9.284111	16.28950	10.91888
2.288273	8.753092	12.13816	11.13778
2.230537	8.523148	10.62715	10.01232
2.174858	8.307433	9.591572	9.060778
2.132289	8.129156	8.475572	8.234969
2.081947	7.927790	7.547925	7.349711
2.017786	7.671144	6.511275	6.396376
1.945029	7.380119	5.506934	5.436711
1.905968	7.223872	5.033245	4.738176
1.900690	7.202740	4.972447	4.780385
2.004371	7.617487	6.313234	6.116954
2.117793	8.071172	8.197343	7.853479
2.202231	8.408924	9.956602	9.423877
2.293594	8.774378	12.28781	11.38584
2.418997	9.275990	16.40127	10.81395
2.553292	9.813169	22.34458	9.800849
2.595806	9.983224	24.64257	10.00969
2.695159	10.38063	30.97703	10.31090
2.795405	10.78162	39.01987	10.67134

2. 853496 11.01478 44.62464 10.91849
 2. 915438 11.26178 51.44213 11.20289
 2. 938948 11.38879 54.30334 11.27299
 2. 939935 11.38874 54.42708 11.26815
 2. 984115 11.83444 60.25338 11.40242
 3. 037900 11.73163 48.20041 11.44219

Data PK L Data
 Log(Ra/f) 1//f 1//f 1//f

3. 983874 15.53550 402.2214 15.71480
 3. 914260 15.23734 513.0273 15.37247
 3. 827886 14.91154 420.5002 15.00403
 3. 721107 14.48443 328.8422 14.59878
 3. 564859 13.96735 261.3901 13.92139
 3. 458853 13.43942 180.1919 13.32104
 3. 304027 12.81611 125.8457 12.71380
 3. 170784 12.28314 92.61192 12.09323

10000342

3. 116594 12.04638 81.74797 12.18001
 3. 040503 11.84201 71.84284 11.90342
 3. 013784 11.45394 64.54545 11.73408
 2. 923327 11.30130 52.62681 11.40580
 2. 045784 11.05514 45.67374 11.10147
 2. 745451 10.44240 34.43404 10.43844
 2. 481084 10.32434 29.98934 10.33599
 2. 615735 10.04294 25.79977 10.12729
 2. 537479 9.750717 21.55534 9.915001

3. 034480 11.81872 70.88599 11.80383
 3. 014418 11.64567 64.90811 11.62425
 2. 924704 11.29882 52.53172 11.20590
 2. 839187 11.03674 45.19258 10.97535
 2. 762982 10.45141 34.20419 10.55473
 2. 674651 10.30660 29.48460 10.24099
 2. 537595 9.750380 21.53138 9.939007
 2. 348272 9.073091 14.59328 11.54410
 2. 272147 8.688589 11.49573 11.11844
 2. 219335 8.477341 10.35655 9.919042
 2. 143388 8.173552 8.69472 8.524580
 2. 091873 7.967494 7.722423 7.704562
 2. 032436 7.729745 4.734670 6.702890
 1. 996516 7.542044 6.119994 6.120783
 1. 954494 7.417785 5.627441 5.426102
 1. 912924 7.251706 5.114539 5.140487
 1. 882082 7.128331 4.743902 4.794094
 1. 809442 6.837749 4.030159 4.053246
 1. 740628 6.562512 3.439402 3.437728
 1. 648889 6.195238 2.784130 2.843856

Data PK L Data
 Log(Ra/f) 1//f 1//f 1//f

3. 995704 15.58281 618.8486 15.86320
 3. 927267 15.30907 528.6249 15.47556
 3. 842144 14.94865 434.5531 15.06049
 3. 732262 14.52905 337.3983 14.54979
 3. 998160 15.59264 622.3589 15.80935
 3. 929209 15.31683 530.9936 15.44132
 3. 843755 14.97502 436.1497 15.02356
 3. 735498 14.54199 339.9211 14.50529

10000345
 Log(Ra/f) 1//f 1//f 1//f

4. 000992 15.60396 626.4295 15.74209
 3. 931851 15.32740 534.2340 15.38332
 3. 847112 14.98844 439.5340 14.99101
 3. 745704 14.54321 340.5330 14.51108
 3. 844856 14.98742 439.2755 14.99983

3. 999293 15.59717 623.9835 15.80748
 3. 930799 15.32319 532.9414 15.42322
 3. 845920 14.98368 438.3294 15.00182
 3. 746349 14.58547 348.5378 14.62165
 3. 580081 13.92032 237.6428 13.83418
 3. 449035 13.47414 184.0414 13.39863
 3. 312742 12.85097 128.4171 12.80153

4. 012303 15.44922 642.9430 15.74185
 3. 935433 15.34173 538.4581 15.38472
 3. 848718 14.95487 431.1203 14.88768
 3. 735229 14.54091 339.7107 14.41885
 3. 629415 14.11766 264.2538 13.95625
 3. 478815 13.51526 188.2327 13.45978
 3. 324443 12.89857 131.9846 12.79730

4. 015991 15.66396 648.4429 15.69932
 3. 947180 15.38872 533.4271 15.52890
 3. 840879 15.04351 433.6898 14.95899
 3. 736871 14.54748 340.9981 14.42937
 3. 612984 14.05193 256.3685 13.89812
 3. 480320 13.52128 188.8863 13.47386
 3. 325300 12.90120 132.1843 12.83575

Data PK L Data
 Log(Ra/f) 1//f 1//f 1//f

4. 006749 15.62707 634.8188 15.82045
 3. 938782 15.35512 542.8281 15.41809
 3. 850197 15.00078 442.6672 15.12535
 3. 735107 14.52431 336.4795 14.42654
 3. 606298 14.02519 252.4519 13.92398
 3. 476163 13.50465 187.0870 13.42055
 3. 313404 12.85361 128.6129 13.01482

10000348

3.532689 13.73075 213.0932 15.48924
 3.440624 13.44329 190.3943 13.30222
 3.334683 12.93841 133.0444 12.70424
 3.247904 12.89161 119.4074 12.41097
 3.007941 15.43176 436.3336 15.77803
 3.940122 15.34848 544.3053 15.37040
 3.843727 14.98290 438.1343 14.89979
 3.737742 14.63997 337.7854 14.50313
 3.680307 14.03322 283.4221 13.85974
 3.478566 13.51426 188.1251 13.34450
 3.324897 12.89959 132.9419 12.67492
 3.533510 13.73404 213.4945 13.43240
 3.533937 13.73374 213.7063 13.44997
 3.442149 13.44859 181.1461 13.26170
 3.334269 12.93707 134.9427 12.71401
 3.202733 12.41101 99.46577 12.04939
 4.011541 15.44416 441.8327 15.44774
 3.930104 13.33641 537.0122 15.27336
 3.834374 14.94549 426.7996 14.83378
 3.744745 14.37904 347.2326 14.46101
 3.600464 14.03228 253.4814 13.86743
 3.474323 13.50529 187.1560 13.41541
 3.320451 12.88180 130.7147 12.80533
 3.533493 13.73397 213.4877 13.46395
 3.446653 13.44261 180.5235 13.30744
 3.333843 12.93145 134.9044 12.75725
 3.194794 12.37917 97.87555 12.27225
 3.848227 15.07291 461.4321 15.04359
 3.817264 14.84905 410.3406 14.80208
 3.749048 14.67427 347.2391 14.64913
 3.687895 14.35158 304.4332 14.24174
 3.581451 13.72580 238.4138 13.82997
 3.490790 13.54316 193.4952 13.45303
 3.295034 12.78013 123.2842 12.64855
 3.863170 15.04071 458.2032 15.01350
 3.813709 14.85483 404.9954 14.78947
 3.755166 14.62864 353.4693 14.50624
 3.682833 14.33133 301.1017 14.27929
 3.597748 13.99099 247.5301 13.89575
 3.484223 13.54489 191.4710 13.47312
 3.333090 12.93236 134.5747 12.77939
 3.812948 14.85187 406.3014 14.83165
 3.820320 14.88128 413.2386 14.85131
 3.746091 14.64036 359.7259 14.60386
 3.690250 14.34100 304.2884 14.29314
 3.604423 14.01749 251.3463 13.93300
 3.494072 13.57429 194.9433 13.47276

3.338264 12.95305 136.1897 12.85801
 3.104658 12.01843 79.33138 12.08846
 3.049486 11.79794 70.04323 11.87156
 3.003010 11.61204 62.93488 11.71209
 2.913455 11.25374 51.20332 11.28055
 2.852335 11.00894 44.47490 10.94404
 2.854862 11.01944 44.74475 11.03307
 2.812040 10.84816 40.54342 10.73051
 2.753098 10.61239 35.39796 10.60370
 2.754621 10.61848 35.32235 10.54210
 2.664879 10.25951 28.89078 10.23305
 2.604408 10.02443 25.24320 10.03338
 2.539257 9.757050 21.43404 9.894379
 2.336459 8.938438 13.50640 11.62850
 2.251939 8.407759 11.14400 10.56386
 2.179234 8.316939 9.443106 9.131637
 2.134963 8.147854 8.567294 8.463412
 2.059462 7.838430 7.170389 7.158748
 1.973711 7.494844 5.882895 5.856990
 1.847766 7.071063 4.609420 4.575264
 1.752134 6.408534 3.531946 3.538103
 1.343231 5.772924 2.183288 2.185732

Data PK L Data
 Log (Rr/f) 1/f/f 1/f/f 1/f/f

3.981498 15.52679 599.2093 15.69936
 3.912408 15.25043 511.0793 15.33879
 3.838222 14.95289 430.6284 14.92762
 3.741659 14.56643 344.7776 14.53192
 3.648526 14.19410 278.2314 14.08780
 3.560205 13.84082 227.0311 13.81192
 3.420422 13.38168 164.5517 13.33936
 3.291054 12.74421 122.1616 12.93437
 3.983559 15.53023 600.3978 15.66829
 3.906249 15.22507 503.6734 15.25304
 3.829216 14.91686 421.7902 14.84870
 3.743209 14.57283 366.0104 14.50007
 3.646337 14.13854 289.4742 13.94379
 3.678720 13.51488 188.1919 13.32995
 3.294321 12.77728 123.0840 12.73819
 3.777439 14.71053 374.5584 14.68377
 3.492761 14.37104 308.0645 14.26254
 3.582453 13.93061 239.0743 13.80306
 3.434734 13.41893 178.0796 13.23629
 3.301100 12.80440 125.0202 12.54924
 3.212854 12.45141 102.0315 12.32097
 3.490481 13.56192 193.3578 13.74913
 3.421049 13.28427 164.7972 13.30447

Log(R _r /f)	PK	L	Data
3.294903	12.77993	123.2716	12.70447
3.213090	12.48236	102.0871	12.27245
3.048916	11.74344	68.47443	11.90004
2.963221	11.594889	60.40897	11.61708
2.939461	11.38634	51.31771	11.39981
2.945765	11.38282	53.15505	11.31957
2.653569	11.02203	44.01150	10.95487
2.794721	10.77940	38.97462	10.48427
2.694433	10.38573	31.06798	10.29404
2.409037	10.03414	25.40487	10.04142
2.540234	9.761024	21.68383	9.944490
2.419785	9.279140	16.43194	11.00419
2.293468	8.774473	12.28989	11.20340
2.287284	8.428824	10.07131	9.730417
2.099452	7.997808	7.858361	7.914981
2.012423	7.450263	6.434348	6.449790
1.845419	7.053474	4.543510	4.598573
1.743139	6.572631	3.439705	3.489903
1.569286	5.877146	2.318283	2.391108

Log(R _r /f)	PK	L	Data
4.002613	15.41045	628.7718	15.86505
3.974384	15.49733	589.2017	15.51945
3.922520	15.29011	522.8879	15.26214
3.869908	15.07963	463.2209	15.07455
3.799171	14.79448	393.5971	14.78424
3.728930	14.51572	334.8192	14.40028
3.671310	14.28524	293.2174	14.17333
3.581053	13.92421	238.1953	13.95982
3.474840	13.49944	184.5243	13.37008
3.318714	12.87485	130.1951	12.76993
3.509524	13.63809	202.9248	13.77112
3.445463	13.38185	174.3185	13.14345
3.313788	12.85515	128.7245	12.71325
3.250952	12.52380	104.3732	12.30787
4.001870	15.40748	627.6981	15.89219
3.982913	15.33165	600.8873	15.49452
3.930814	15.32324	532.9621	15.28542
3.854089	15.01435	444.6526	14.68927
3.691954	14.60781	396.1264	14.48985
3.750220	14.52088	335.8152	14.35757
3.441890	14.16674	273.8866	13.96177
3.348147	13.79258	220.8144	13.55278
3.455952	13.42380	178.5798	13.03404
3.289733	12.75893	121.7906	12.28604
3.319280	13.67712	206.6142	13.77246
3.449704	13.39961	174.1101	13.30658
3.322936	12.89174	131.4669	12.73228

3.187452	12.34981	96.23494	12.17353
4.002801	15.61120	629.0443	15.89400
3.939167	15.43658	568.8883	15.23139
3.894081	15.17632	489.7358	14.97111
3.816324	14.86529	409.4536	14.65079
3.745370	14.58148	347.7567	14.37584
3.640253	14.24102	285.9483	13.99048
3.549046	13.87418	231.7000	13.64440
3.477747	13.51107	187.7792	13.31088
3.321459	12.88463	131.0808	12.71230
3.235587	12.54235	107.5147	12.39894
3.523174	13.69270	208.4764	13.77316
3.451176	13.40486	176.8466	13.37128
3.324540	12.89816	131.9534	12.80033
3.512516	13.45006	203.4211	13.80056
3.463539	13.45423	181.7354	13.63000
3.372820	13.17128	154.4190	12.83289
3.316319	12.86526	129.4775	12.73405
3.228323	12.51329	103.7512	12.49484

Log(R _r /f)	PK	L	Data
3.510726	13.64290	202.5847	13.85734
3.467773	13.39110	175.2489	13.19218
3.385447	13.14178	151.8193	13.05263
3.276019	12.48607	116.3857	12.76988

Log(R _r /f)	PK	L	Data
3.990472	15.56188	611.4378	15.77197
3.921416	15.28566	521.5507	15.40830
3.834907	14.93962	427.3535	15.04287
3.726652	14.50661	333.0678	14.47690
3.567815	13.87126	231.0445	13.91301
3.453778	13.42311	178.5084	13.50377
3.304728	12.81891	126.0689	12.74907
3.990996	15.56398	612.1764	15.71744
3.920420	15.28168	520.3354	15.40909
3.833615	14.93446	426.0847	15.05467
3.724709	14.49883	331.3808	14.50905
3.565494	13.84197	229.8131	13.95404
3.452513	13.41005	177.1712	13.57704
3.309192	12.83677	127.3715	12.59026
4.005890	15.62356	633.5355	15.71028
3.935151	15.34040	538.3082	15.40787
3.849747	14.99907	442.2296	15.00430
3.740111	14.56044	343.5514	14.48549
3.580300	13.92120	237.7827	13.95254

3.471172	13.48468	104.9492	13.45372
3.313403	12.85343	128.6132	12.89787
4.012644	15.44825	442.4042	15.46852
3.959291	15.59716	543.6443	15.24169
3.861311	15.60824	643.8040	14.95107
3.758474	14.88449	342.4161	14.53351
3.578654	13.91841	234.9925	13.99904
3.468794	13.47518	185.9403	13.52751
3.307540	12.85824	126.8959	13.07263
3.512645	15.44826	293.2103	13.87733
3.468651	13.47220	183.4248	13.55675
3.392403	13.18141	153.3400	12.81449
3.315009	12.86083	129.0892	12.85631
3.231025	12.52410	104.3912	12.47569
3.510485	13.46274	202.5637	13.92152
3.442879	13.37151	173.2842	13.46209
3.317458	12.84983	129.8190	12.77806
3.235902	12.54361	107.5926	12.33620
3.511474	13.44470	203.0281	13.88981
3.442588	13.37035	173.1681	13.41107
3.315515	12.84206	129.2395	12.85537
3.231748	12.52707	104.5733	12.45217
3.084286	11.94514	76.23708	12.10372
3.032403	11.73042	47.37300	11.74759
2.984487	11.53795	40.30498	11.42441
2.894263	11.17704	48.99433	11.28258
2.837164	10.94842	42.95227	11.04458
2.840149	10.94659	43.25435	10.93954
2.735708	10.54283	34.00456	10.48348
2.445294	10.18118	27.41700	10.16529
2.589562	9.954248	24.23494	9.989557
2.519415	9.477443	20.65788	9.876932
2.327322	8.910063	13.28624	11.82299
2.226909	8.507436	10.53874	10.23464
2.124941	8.099245	8.333768	8.271409
2.024801	7.707207	4.447841	4.442729
1.914248	7.257074	5.130369	5.163173
1.830549	6.922277	4.231042	4.248193
1.477477	6.309909	2.974112	3.003592
1.552047	5.808271	2.228168	2.220375
Log(R _n /f)	1//f	L	Date
	1//f	1//f	1//f
3.992814	15.57125	614.7437	15.45180
3.920059	15.28023	519.9237	15.42189

10000341

3.823822	14.89528	416.5837	15.01307
3.734246	14.53698	338.9426	14.66704
3.631775	14.20710	280.3209	14.30183
3.544680	13.77872	219.0586	13.90914
3.453748	13.41199	177.6759	13.53847
3.303570	12.81428	125.7333	12.75429
3.217071	12.44828	103.0271	12.45218
3.978840	15.51536	595.2790	15.59055
3.908032	15.23213	505.7228	15.29284
3.811055	14.84422	404.5153	14.91284
3.712684	14.49073	322.5260	14.58757
3.553442	13.82177	224.5549	13.77448
3.444628	13.37851	173.9835	13.33564
3.284738	12.73895	120.3978	12.84730
3.982804	15.53121	600.7367	15.65945
3.912307	15.24922	510.7251	15.34947
3.825882	14.90753	419.5295	14.94882
3.713926	14.45570	323.4491	14.54202
3.561190	13.84476	227.5466	13.78062
3.442435	13.36974	173.1072	13.58580
3.294275	12.77710	123.0709	12.73955
3.990410	15.56244	611.6316	15.51993
3.917236	15.26894	516.5549	15.31377
3.826673	14.91469	421.2633	15.02224
3.713378	14.45431	323.1909	14.68526
3.557369	13.82947	225.5534	14.02883
3.449106	13.39442	173.7848	13.49999
3.291551	12.76620	122.3013	12.93592
3.500964	13.60385	198.0817	13.88771
3.433809	13.33523	169.7020	13.74949
3.308867	12.82746	126.6914	12.77258
3.222964	12.49186	104.4352	12.39265
3.498784	13.59513	197.0899	13.86745
3.431482	13.32592	168.7959	13.33070
3.307546	12.83018	126.8897	12.66661
3.175492	12.30197	93.62090	12.01744
3.498494	13.59397	196.9584	13.87271
3.432052	13.32821	169.0179	13.31219
3.307734	12.83093	126.9446	12.66112
3.074466	11.90586	74.53267	12.11109
3.019719	11.67887	65.40334	11.83398
2.974610	11.49844	58.95090	11.61257
2.883350	11.14140	47.99883	11.25658

2. 827334 10.90934 41.99686 10.97904
 2. 833247 10.93398 42.57229 10.70719
 2. 735905 10.33862 33.86768 10.40402
 2. 667326 10.17510 27.75920 10.13347
 2. 535489 9.93337 25.93184 9.969814
 2. 562713 9.611683 19.69724 9.668210
 2. 317325 8.69991 12.97793 11.99210
 2. 234701 8.338897 10.72954 10.22489
 2. 129269 8.117079 8.916853 8.347148
 2. 040389 7.793534 6.984450 6.923048
 1. 948492 7.393971 8.531621 5.513150
 1. 843699 7.056798 4.564459 4.537077
 1. 767509 4.678278 3.674627 3.634495
 1. 629347 4.117389 2.662118 2.715974

Data PK L Data
 Log(Ret/f) 1//f 1//f 1//f

T0000344

3. 972075 15.48830 586.0779 15.62241
 3. 891448 15.14439 484.9995 15.33594
 3. 813124 14.85349 404.4474 15.01783
 3. 717332 14.44932 325.9939 14.51115
 3. 564361 13.85744 229.2143 13.78073
 3. 444627 13.37851 173.9833 13.15636
 3. 265469 12.74187 120.6004 12.63328
 3. 971265 15.48504 584.9865 15.45156
 3. 919231 15.25692 513.0143 15.44343
 3. 835817 14.93527 426.2828 15.03501
 3. 717078 14.44893 322.0743 14.68774
 3. 543257 13.65302 228.4322 14.01432
 3. 423488 13.29475 145.7937 13.60423
 3. 279263 12.71705 118.0895 12.83537

3. 985342 15.54134 604.2374 15.53313
 3. 919231 15.25692 512.9929 15.24714
 3. 824465 14.90564 419.1247 14.92947
 3. 714536 14.45814 323.9038 14.40838
 3. 575538 13.90215 235.1899 13.96787
 3. 434945 13.34784 170.9406 13.72700
 3. 288241 12.75284 121.3727 12.88868
 3. 671720 13.46488 185.1827 13.51603
 3. 396532 13.18413 133.7445 13.05750
 3. 298108 12.78443 123.5915 12.65729
 3. 211739 12.44703 101.7745 12.29646

3. 470996 13.48398 184.8744 13.52331
 3. 343741 13.05494 144.4181 12.98372
 3. 258254 12.63501 113.2750 12.41503
 3. 160464 12.24242 90.46620 12.09070

3. 475778 13.49511 186.0423 13.57407
 3. 394673 13.17869 155.0790 13.23241
 3. 299352 12.79740 124.5179 12.67701
 3. 214352 12.45741 102.3841 12.33406
 3. 055881 11.82352 71.08235 11.96940
 3. 000248 11.40099 62.53578 11.71217
 2. 951632 11.40653 55.91302 11.55551
 2. 844422 11.06569 45.95184 11.19144
 2. 004248 10.82307 40.00815 10.93624
 2. 809237 10.83703 40.28447 10.87720
 2. 707031 10.42812 31.83544 10.41914
 2. 627931 10.11172 26.53451 10.22509
 2. 556710 9.826843 22.52116 9.957052
 2. 442111 9.348445 17.29781 10.70614
 2. 301126 8.804504 12.50276 11.69162
 2. 227923 8.511694 10.56340 10.46540
 2. 152455 8.209820 8.678410 8.817226
 2. 054838 7.819353 7.091178 7.110727
 1. 938603 7.434412 5.681764 5.712933
 1. 852368 7.009555 4.49067 4.484229
 1. 685872 6.343488 3.032159 3.028526

Data PK L Data
 Log(Ret/f) 1//f 1//f 1//f

T0000367

3. 983638 15.53455 601.8921 15.59417
 3. 911781 15.24712 510.1074 15.33338
 3. 823373 14.89349 416.1533 15.03614
 3. 724154 14.49661 331.1576 14.64389
 3. 573012 13.89204 233.8258 14.04976
 3. 430244 13.32097 168.3156 13.94108
 3. 290949 12.74379 122.1320 12.80855
 3. 988953 15.55581 609.3035 15.64968
 3. 919265 15.27706 518.9740 15.31121
 3. 885495 15.54198 604.4707 15.70779
 3. 914736 15.26694 515.9602 15.33142
 3. 80410 14.95344 430.8151 15.02641
 3. 729415 14.51764 335.1937 14.63168
 3. 562755 13.85102 228.3681 13.85553
 3. 449308 13.39723 175.8685 13.49772
 3. 297116 12.78846 123.8785 12.77122
 3. 997727 15.59090 621.7380 15.51068
 3. 919742 15.27897 519.5448 15.15863
 3. 828787 14.91514 421.3733 15.25738
 3. 722878 14.49151 330.1858 14.60326
 3. 566664 13.86665 230.4339 13.94994
 3. 457099 13.42839 179.0522 13.46475

3. 279215 12.77286 124.1925 12.94170
 3. 481796 13.82699 109.4875 13.46341
 3. 490376 13.23359 160.9501 13.14357
 3. 308488 12.89478 127.2239 12.71913
 3. 218779 12.47811 103.4331 12.51574
 3. 494340 13.83824 190.7394 13.57393
 3. 377921 13.11169 149.2113 13.01384
 3. 310243 12.84997 127.4800 12.47349
 3. 221483 12.68878 104.0790 12.43804
 3. 494947 13.53584 170.9180 13.54123
 3. 497983 13.23994 169.4444 13.99493
 3. 309948 12.83307 127.3058 12.71095
 3. 207804 12.43122 106.8524 12.83401

Data PK L Data
 Log(Ra/f) 1//f 1//f 1//f

3. 977465 15.58984 421.3426 13.64073
 3. 923396 15.29358 533.9338 15.16790
 3. 697104 14.98042 439.5284 15.12874
 3. 737514 14.59893 341.5030 14.72221
 3. 548223 13.87269 231.2615 14.02596
 3. 451979 13.40791 174.9435 13.74793
 3. 363339 12.82135 126.2465 12.84654
 3. 223037 12.49215 104.4923 12.42161
 3. 483592 13.53437 190.3148 13.60421
 3. 397945 13.19186 134.2592 13.46244
 3. 358412 12.83445 127.2014 12.72133
 3. 215038 12.44015 102.5460 12.42400
 3. 101674 12.00449 78.98490 11.91404
 3. 104857 12.01942 79.54782 11.84084
 3. 048460 11.79584 69.87797 11.70656
 3. 009869 11.46347 42.62527 11.51113
 2. 910169 11.24647 50.82175 11.30043
 2. 856054 11.00822 44.25239 11.05462

2. 843843 10.98337 43.82512 11.18704
 2. 752217 10.40687 35.32428 10.64002
 2. 671397 10.28559 29.32749 10.27280
 2. 609199 10.03479 23.41439 10.01079
 2. 537175 9.740703 21.53058 9.803210
 2. 361499 8.945999 13.72081 11.81047
 2. 259271 8.457064 11.35407 10.71457
 2. 193950 8.375503 9.748548 9.477785
 2. 118748 8.075075 8.215701 8.048992
 2. 040497 7.761990 6.060847 6.812781
 1. 933437 7.413731 5.414568 5.574537
 1. 845285 6.981140 4.374884 4.348270

1. 640548 6.162193 2.731671 2.752026

Page 1

Solvent Set 3: Runs 80000011 - 80000042

Page 2

Solvent Set 3: Runs 80000011 - 80000042

File/Run
80000011

Data Log (Rr/f)	PK 1/f	L 1/f	Data 1/f
1.411320	6.045260	2.553078	2.462361
1.716678	6.464714	3.235058	3.317172
1.047602	4.991211	4.402333	4.413000
1.952245	7.609054	5.599429	5.444227
2.068912	7.635650	4.379584	4.345922
2.040819	7.793276	6.993372	7.028068
2.667751	7.951304	7.649444	7.679320
2.116763	8.058824	8.139280	8.205801
2.132265	8.209140	8.874935	8.893575
2.224369	8.497522	10.47757	10.35029
2.253156	8.612624	11.19532	10.58339
2.316532	8.658211	12.89534	11.15747
2.399040	9.156160	15.30804	10.31948
2.447774	9.391105	17.52493	9.740202
2.461936	9.447745	18.10574	9.774659
2.486008	9.544033	19.13744	9.847404
2.514424	9.645767	20.52612	9.850592
2.535037	9.740230	21.42582	9.910807
2.557594	9.830387	22.56715	10.00134
2.591143	9.944373	24.37941	10.03350
2.620493	10.08241	24.09053	10.09149
2.640901	10.14840	27.33890	10.22195
2.660810	10.24324	28.62134	10.25950
2.685486	10.34274	30.30844	10.34125
2.702911	10.41164	31.53490	10.43084
2.719239	10.47695	32.74309	10.52484
2.737712	10.55086	34.14583	10.52844
2.755303	10.62121	35.57814	10.64044
2.760728	10.67491	36.69512	10.77859
2.780943	10.72377	37.74189	10.79015
2.798984	10.77933	39.34273	10.79791
2.817706	10.87082	41.07594	10.91293
2.831119	10.92447	42.34426	10.99590

Data Log (Rr/f)	PK 1/f	L 1/f	Data 1/f
3.248781	12.59512	110.8311	12.52020
3.264849	12.50747	110.3642	12.52294
3.240104	12.56041	108.4384	12.50422
3.231437	12.52575	104.4921	12.48627
3.223487	12.49474	104.6095	12.45418
3.217716	12.47084	103.1803	12.38167
3.207941	12.43176	100.6837	12.37839
3.200741	12.46304	99.22962	12.33522
3.187375	12.34950	96.21775	12.30031

80000012

Data Log (Rr/f)	PK 1/f	L 1/f	Data 1/f
3.172404	12.28961	92.93747	12.17827
3.077585	11.99034	78.24667	11.91684
2.986401	11.54640	60.60119	11.43417
2.915512	11.26204	51.45080	11.13995
2.776316	10.70526	37.54190	10.61445
2.697185	10.38874	31.12185	10.35362
2.599950	9.999801	24.87885	9.971679

80000013

Data Log (Rr/f)	PK 1/f	L 1/f	Data 1/f
3.180386	12.32154	94.48185	12.25534
3.175050	12.30020	93.52564	12.15451
3.175050	12.30020	93.52564	12.15451
3.137627	12.15051	85.80404	12.13520
3.137627	12.15051	85.80404	12.13520
3.117319	12.04927	81.88402	12.06050
3.117319	12.04927	81.88402	12.06050
3.089419	11.95767	76.78912	11.90396
3.089419	11.95767	76.78912	11.90396
3.044352	11.77740	69.22013	11.72422
3.044352	11.77740	69.22013	11.72422
3.177943	12.31177	94.15070	12.31597
3.177943	12.31177	94.15070	12.31597
3.168546	12.27418	92.13547	12.19759
3.146607	12.18642	87.59662	12.08879
3.146607	12.18642	87.59662	12.08879
3.118958	12.07599	82.20125	12.09281
3.097177	11.98870	78.17310	12.02318
3.097177	11.98870	78.17310	12.02318
3.068062	11.87225	73.10428	11.79562
3.068062	11.87225	73.10428	11.79562
3.028502	11.71400	66.73942	11.64173
3.005802	11.62321	63.34068	11.47652
2.971413	11.48565	58.51858	11.41637
2.930257	11.32103	53.22771	11.23417
2.887677	11.15071	48.25670	11.03868
2.851603	11.00641	44.41029	10.93444
2.813241	10.85296	40.65567	10.78115
2.770496	10.68198	36.84479	10.57577
2.738758	10.55503	34.24826	10.56970
2.693030	10.37212	30.82554	10.43017
2.658763	10.23505	28.48679	10.25103
2.609408	10.03763	25.42663	10.09267
2.564802	9.859208	22.94469	9.898846
2.500946	9.603787	19.80736	9.657903
2.452478	9.409915	17.71572	9.806958
2.381198	8.964792	13.71128	10.94683
2.237398	8.549595	10.79639	10.63119
2.172668	8.290754	9.501837	9.175411

Data
Log (Rr/f)

PK
1/f

L
1/f

Data
1/f

2.500114 9.600459 19.74946 10.02352
 2.316019 8.864077 12.93894 11.48705
 2.214445 8.487845 10.24109 10.48678
 2.160278 8.241095 9.038498 9.272960
 2.118332 8.061331 8.151036 8.444721
 2.045827 7.882110 7.224359 7.481157
 1.982234 7.466937 5.729468 5.918285
 1.837471 6.949686 4.298943 4.491918
 1.631368 6.128332 2.474457 2.734640

Data PK L Data
 Log (Re/f) 1//f 1//f 1//f

2.912781 11.25192 51.15191 11.04677
 2.864989 11.05993 45.80042 10.92384
 2.777654 10.79041 39.22242 10.72995
 2.682069 10.32827 30.05725 10.28102
 2.601937 10.06775 24.99297 10.00915
 2.513115 9.652461 20.37020 9.480004
 2.399879 9.159518 15.33747 10.42014
 2.310429 8.842518 12.77937 10.95832
 2.244731 8.578926 10.98022 10.45117
 2.170409 8.262438 9.257415 9.053737
 2.064795 7.867182 7.289128 7.340444
 2.013741 7.454965 6.450714 6.340514
 1.884074 7.134307 4.785925 4.710467
 1.690091 6.340364 3.061760 2.950434

Data PK L Data
 Log (Re/f) 1//f 1//f 1//f

1.844493 6.977983 4.348937 4.336394
 2.004381 7.617205 4.312208 4.454480
 2.125446 8.101785 8.343077 8.408921
 2.233387 8.534028 10.70008 10.72332
 2.346878 8.945315 13.70120 11.04468
 2.462600 9.451325 18.14518 9.853323
 2.581739 9.924956 23.85718 10.16674
 2.725434 10.50173 33.21347 10.49244
 2.828418 10.91367 42.10162 10.92614
 2.895332 11.16215 49.13749 11.25399
 2.897714 11.19085 49.38495 11.12124
 2.967026 11.44610 57.95833 11.30950
 3.018532 11.67421 65.22783 11.49744
 3.081493 11.92477 75.43509 11.78960
 3.128543 12.11337 85.98916 12.04939
 3.151911 12.20744 88.67293 12.10462
 3.203545 12.41626 99.87231 12.31049

Data PK L Data
 Log (Re/f) 1//f 1//f 1//f

80000025

1.799589 6.797558 3.957944 3.976037
 1.995063 7.572015 4.150122 4.240640
 2.142532 8.170129 6.677855 8.707590
 2.215970 8.455883 10.22941 10.113598
 2.284086 8.756346 12.02171 11.05304
 2.414600 9.258400 14.23604 10.03249
 2.491524 9.566098 19.58227 10.03662
 2.468821 10.27528 29.15419 10.25778
 2.785991 10.73596 38.00766 10.79554
 2.853012 11.01204 44.55456 10.97272
 2.903673 11.21469 50.06720 11.21743
 2.919129 11.27451 51.88108 11.09537
 2.996502 11.58601 61.99872 11.45949
 3.052378 11.82951 71.32767 11.44194
 3.101639 12.00455 78.98041 11.87410
 3.144233 12.17493 87.11919 11.96440
 3.160494 12.24197 90.44293 11.97454
 3.197413 12.39045 98.51302 12.20181
 3.216399 12.46539 102.8677 12.33444
 3.223870 12.49548 104.4527 12.34602

Data PK L Data
 Log (Re/f) 1//f 1//f 1//f

80000034

3.201667 12.40667 99.45694 12.21632
 3.149840 12.19944 88.25528 11.94282
 3.123438 12.09375 83.04593 11.92045
 3.103855 12.01542 79.38440 11.81686
 3.070446 11.88258 73.54050 11.71679
 3.051399 11.72559 67.18616 11.45224
 2.971694 11.48677 58.55640 11.29501
 2.857529 11.03011 45.02037 10.82805

80000022

2.834690 10.93876 42.71400 10.67243
 2.77245 10.70898 37.42190 10.49175
 2.686434 10.34573 30.36089 10.15451
 2.626770 10.10708 26.46366 10.08665
 2.557939 9.831756 22.58495 9.917160
 2.440270 9.361081 17.22464 9.854488
 2.266768 8.667074 11.55177 11.08290
 2.107458 8.030627 8.008235 7.971127
 1.969413 7.477455 5.824974 5.740973
 1.844658 7.058634 4.574555 4.430496
 1.738193 6.552772 3.420369 3.299742

Data PK L Data
 Log (Re/f) 1//f 1//f 1//f

80000038

1.805928 6.815714 3.979316 3.912053
 1.946352 7.385408 5.523725 5.455952
 2.060796 7.843187 7.189140 6.906283
 2.150027 8.200109 8.828918 8.704182

2.193292 8.373170 9.753772 9.352882
 2.286893 8.722375 11.92542 11.30410
 2.457288 9.439934 17.91177 9.742799
 2.887772 9.931070 24.19093 9.885934
 2.637629 10.91051 42.02520 10.58312
 2.803342 11.13417 47.79942 10.90704
 2.788982 10.58373 34.24199 10.29098
 2.738833 10.58333 34.25415 10.35154
 2.893244 11.17504 48.68177 10.97579
 2.972100 11.48846 58.61122 11.23485
 3.029335 11.71730 44.84669 11.44469
 3.049342 11.67337 73.15142 11.45235
 3.123621 12.09528 83.11920 11.44819
 3.146039 12.18415 87.48210 11.98175
 3.168250 12.27332 92.19540 11.98814
 3.209781 12.40280 99.21600 12.21314
 3.243942 12.57577 109.4030 12.38854
 3.264586 12.42422 100.5425 12.14920

Data	PK	L	Data
Log (Ra/?)	i//i	l//l	l//l
3.254497	12.41879	112.3511	12.87341
3.288022	12.43268	100.9025	12.41578
3.179107	12.26043	92.44720	12.52533
3.151013	12.20405	88.48987	12.18403
3.123489	12.09475	81.07587	11.84494
3.072192	11.86876	73.80269	11.74575
3.013247	11.45299	44.43587	11.51647
2.897640	11.19044	49.37882	11.00138

80000042

2.848854 11.07541 44.20980 10.91535
 2.767823 10.47129 34.61874 10.54032
 2.581467 9.925869 23.84226 10.00974
 2.689047 10.35419 30.54412 10.30985
 2.517926 9.671704 20.59709 9.938809
 2.491118 9.394474 17.57917 9.896904
 2.244045 8.584242 11.01401 10.97482
 2.144425 8.257700 9.126316 8.903498
 1.994079 7.576317 4.165372 6.215074
 1.802268 6.869078 3.944147 3.940869

Page 1

Solvent Set #3 Runs 80000065 - 80000065

Data PK L Data
Log (Re/f) 1/1 1/1 1/1

3.091814 11.96468 77.16033 11.04873
3.092264 11.05098 78.16402 11.01963
3.013214 11.65388 68.45689 11.12158
2.976487 11.49198 58.37393 10.91624
2.082999 11.12839 47.64883 10.52265
2.781417 10.72846 37.78303 10.26984
2.489116 10.35646 30.54898 9.931533
2.568192 9.840771 22.70245 9.617183

Data PK L Data
Log (Re/f) 1/1 1/1 1/1

3.132414 12.12945 84.79018 11.35588
3.122234 12.06394 82.01456 11.28622
3.064878 11.94731 76.34108 11.13309
3.073674 11.82349 71.09108 11.14823
3.017443 11.67837 65.09139 10.94332
2.980992 11.52396 59.82353 10.85053
2.927335 11.31814 53.13931 10.73473
2.887391 11.15934 49.24713 10.54167
2.850462 11.03365 45.11726 10.27644
2.854859 11.02743 44.93103 10.45147
2.795454 10.78181 39.02428 10.19893
2.744647 10.77846 38.93358 10.33502
2.739442 10.55977 34.34178 10.07568
2.701905 10.40742 31.44190 9.978834
2.667869 10.27167 28.69041 9.897392

Data PK L Data
Log (Re/f) 1/1 1/1 1/1

3.158135 12.23254 89.93299 11.44382
3.103318 12.01327 79.28537 11.32899
3.064864 11.85945 72.56786 11.12843
2.974487 11.50594 59.20424 10.93276
2.841562 11.04425 45.54054 10.73082
2.894025 11.17610 48.98723 10.35396
2.736097 10.52038 33.37200 9.982692
2.595200 9.980601 26.60823 9.428523
2.489965 9.537440 19.36834 9.346189
2.218359 8.473436 10.33350 9.702147

Data PK L Data
Log (Re/f) 1/1 1/1 1/1

2.654841 10.22736 28.34102 9.991616
2.568271 9.642908 22.73039 9.780193
2.471460 9.485742 18.56634 9.540397
2.338494 8.933979 13.62619 10.48729

80000065

80000066

80000067

80000068

Page 2

Solvent Set #4: Runs 80000065 - 80000085

2.212304 6.449216 10.19023 9.459414
2.140277 8.161109 8.632911 8.327407
2.065295 7.941181 7.604333 7.410057
2.005018 7.620074 6.322643 6.148794
1.901594 7.208377 4.982811 4.893889
1.755188 6.620753 3.554874 3.410754

Data PK L Data
Log (Re/f) 1/1 1/1 1/1

3.106148 12.02459 79.80478 11.23451
3.105073 12.02029 79.40732 11.29968
3.049855 11.85942 72.54641 11.13596
3.022685 11.69074 65.85143 11.27479
2.954277 11.41710 54.25450 10.90689
2.849594 10.99838 44.20553 10.66324
2.754024 10.61609 35.47354 10.26775
2.647211 10.16884 27.73904 9.959317

80000069

Data PK L Data
Log (Re/f) 1/1 1/1 1/1

3.146386 12.18554 87.55210 11.29784
3.091539 11.94615 77.14681 11.26815
3.049617 11.79846 70.04441 11.22440
2.972871 11.49148 58.71529 10.84723
2.844010 11.04404 45.90819 10.59060
2.846877 10.94350 43.32887 10.54002
2.758325 10.63350 35.82658 10.23718
2.740105 10.54042 34.33462 10.09827
2.638009 10.14403 27.03267 9.856086
2.631458 10.12463 26.76322 9.849011
2.544414 9.785666 21.99361 9.631831
2.474025 9.498101 18.61881 9.350845
2.321734 8.884944 13.11040 10.63483
2.220341 8.481447 10.38104 9.728959
2.158811 8.203246 8.844872 8.502604
2.011370 7.645583 4.415801 6.294362
1.897934 7.191759 4.940999 4.747862
1.779161 6.716447 3.758735 3.574753

80000072

Data PK L Data
Log (Re/f) 1/1 1/1 1/1

3.172080 12.28832 92.88815 11.38121
3.149794 12.17918 87.23206 11.23900
3.123606 12.09442 83.07805 11.24492
3.093793 11.97517 77.56644 11.12922
3.038274 11.74509 67.94447 10.94483
2.938231 11.35392 54.21402 10.78498
2.908748 11.23499 50.5576 10.68755
2.834465 10.93858 42.70966 10.53014

80000077

Solvent Set #j Runn 80000045 - 80000065

2. 881272 10. 92828 62. 37918 10. 44372
 2. 798877 10. 03559 31. 72488 10. 09332
 2. 644428 10. 17089 27. 87488 9. 75113
 2. 543744 9. 887868 28. 84849 9. 79324
 2. 494367 9. 1077898 19. 81044 9. 857861
 2. 319981 8. 69727 13. 63785 10. 62784
 2. 181148 8. 274878 9. 224213 9. 197199
 2. 093184 7. 984744 7. 794887 7. 549462
 1. 991928 7. 847853 4. 133343 5. 883880
 1. 87289 7. 117187 4. 733337 4. 714854
 1. 797287 4. 429287 3. 188887 3. 042859

Date PK L Date
 Log(Ra/f) 1//4 1//4 1//4

80000081

3. 172089 12. 28852 92. 88815 11. 38121
 3. 144794 12. 17918 87. 23304 11. 23900
 3. 123466 12. 09642 83. 07863 11. 24492
 3. 093793 11. 97517 77. 84444 11. 12922
 3. 034274 11. 74909 67. 94497 10. 94483
 2. 938231 11. 33292 54. 21402 10. 78498

Date PK L Date
 Log(Ra/f) 1//4 1//4 1//4

80000065

3. 146173 12. 18469 87. 50900 11. 31425
 3. 113779 12. 05511 81. 21939 11. 18433
 3. 093133 11. 97281 77. 45288 11. 28853
 3. 048407 11. 87443 73. 19601 11. 01914
 3. 011173 11. 64478 64. 12921 10. 88928
 2. 947103 11. 38841 53. 33290 10. 67687
 2. 852642 11. 03444 45. 13798 10. 54542
 2. 745647 10. 58259 34. 78588 10. 27927
 2. 639478 10. 19391 27. 18684 9. 837140
 2. 527554 9. 710217 21. 05883 9. 727424
 2. 454027 9. 416109 17. 77899 9. 601403
 2. 334533 8. 938135 13. 58249 10. 53531
 2. 242721 8. 576884 10. 27952 10. 93321
 2. 164134 8. 264418 9. 142934 8. 654649

Page 1

Solvent Set 5: Runs 80000089 - 80000131

Data	PK	L	Data
Log (Re/f)	1/f	1/f	1/f
3.112021	12.04608	86.89120	11.89807
3.086489	11.94475	76.56795	11.81074
3.046927	11.87376	73.24994	11.69621
3.039153	11.78477	69.60272	11.54967
3.028287	11.70167	66.20415	11.50548
2.974427	11.59576	59.19664	11.27752
2.890367	11.16139	48.55428	10.99957
2.789421	10.73848	38.50342	10.54759
2.684979	10.33991	30.35934	10.29580
2.604096	10.01439	25.11764	9.947027
2.538247	9.717049	21.14204	9.736130
2.475104	9.500738	18.43459	10.03202
2.236407	8.594430	10.82848	10.79105
2.194342	8.363370	9.822314	9.628492
2.092796	7.971185	7.738849	9.345424

80000089

Data	PK	L	Data
Log (Re/f)	1/f	1/f	1/f
3.109553	12.00221	78.78325	11.81843
3.069111	11.84844	71.77801	11.54812
3.022472	11.68989	65.81924	11.38599
2.943255	11.38101	53.09775	11.23162
2.919948	11.27979	51.97901	11.11081
2.826497	10.91878	42.22374	10.68501
2.685743	10.34297	30.31242	10.03327
2.553319	9.813276	22.34594	9.849707
2.395225	9.180094	15.52757	10.04604

80000093

Data	PK	L	Data
Log (Re/f)	1/f	1/f	1/f
3.100455	12.00262	78.80173	11.77754
3.087755	11.95094	74.49191	11.77180
3.074910	11.89944	74.26403	11.72525
3.066330	11.84132	71.81420	11.48758
3.013025	11.69210	65.90298	11.38747
2.944988	11.58793	59.31827	11.08115
2.905014	11.22065	50.22208	10.95079
2.881752	11.12701	47.06281	10.96495
2.844072	10.97428	45.44679	10.74293
2.818616	10.87446	41.16200	10.83999
2.728216	10.51286	33.42894	10.15920
2.640494	10.16193	27.31543	10.15920
2.537454	9.750619	21.55434	9.841297
2.449844	9.399384	17.68865	9.774193
2.258675	8.634500	14.33718	11.23486
2.178893	8.315375	9.435692	9.680409
2.091269	7.965879	7.711693	7.796231

80000100

Page 2

Solvent Set 5: Runs 80000089 - 80000131

3.990134	7.560539	4.109628	6.127747
1.861087	7.044350	4.539078	4.584147
1.765919	6.455679	3.629107	3.751527

Data	PK	L	Data
Log (Re/f)	1/f	1/f	1/f

80000116

3.184288	12.33715	95.53431	12.11000
3.181670	12.32668	94.96205	12.15578
3.150062	12.20024	88.29625	11.97227
3.120202	12.08081	82.42952	11.96941
3.077048	11.90819	74.63255	11.80346
2.998308	11.57723	61.48629	11.52934
2.935425	11.53370	58.61736	11.12226
2.905984	11.22394	50.33458	11.51125
2.881737	11.12894	47.60113	10.98042
2.800729	10.80291	39.50110	10.81204
2.711414	10.44545	32.15843	10.59474
2.609831	10.03932	25.45136	10.06358
2.493856	9.575424	19.48660	9.753502
2.305801	8.815207	12.58003	11.71973
2.224971	8.497885	10.47976	9.938083
2.141614	8.166456	8.65928	8.458289
2.099434	7.997739	7.858051	7.823745
2.029003	7.716014	6.681649	6.708814
1.890019	7.192077	4.941961	5.022760
1.781359	6.725436	3.777800	3.775318

Data	PK	L	Data
Log (Re/f)	1/f	1/f	1/f

80000117

3.170018	12.28007	92.44814	12.05153
3.137180	12.14872	85.71582	11.97729
3.117519	12.07007	81.92181	11.67754
3.048500	11.87400	73.17802	11.63802
3.017531	11.47012	65.07460	11.38411
2.922548	11.29019	52.29119	11.04348
2.893574	11.17349	48.89382	10.95357
2.787118	10.74847	38.28233	10.54891
2.700339	10.40135	31.34847	10.28448
2.462482	9.529930	18.98289	9.649900
2.543055	9.852220	22.85257	9.902820
2.259989	8.799958	12.67008	11.06418
2.235419	8.541678	10.74730	10.08803
2.157684	8.230738	9.985961	8.686156
2.087224	7.948905	7.440230	7.514080
1.938911	7.355464	5.429894	5.504653
1.787411	6.749445	3.830816	3.816162

Data	PK	L	Data
Log (Re/f)	1/f	1/f	1/f

Page 3

Belmont Est 5: Run 80000131 - 80000131

80000125

3.150725 12.15490 84.62127 11.96073
 3.140171 12.03346 86.17737 11.87595
 3.071684 11.80473 73.71647 11.54916
 3.017289 11.64969 65.03232 11.45492
 2.977190 11.50076 59.30215 11.42842
 2.914139 11.24453 51.53321 11.08794
 2.872190 11.08878 46.56412 11.14741
 2.773964 10.49382 37.13954 10.67865
 2.665174 10.34070 30.27310 10.35610
 2.548939 9.783736 21.76944 10.01034
 2.434434 9.424545 17.86413 9.692793
 2.245074 8.660299 11.59460 11.32344
 2.192104 8.367326 9.727173 9.761573
 2.136310 8.122043 6.440940 8.544174
 2.057764 7.831047 7.139154 7.340951
 1.947323 7.470094 3.799674 5.917074
 1.687832 7.031329 4.565183 4.537607

Data PK L Data
 Log (Rn/f) 1/f 1/f 1/f

80000131

3.165715 12.24286 91.53685 12.06050
 3.126816 12.11326 84.09047 11.94044
 3.078118 11.91247 74.81664 11.97960
 3.033328 11.74131 67.79673 11.56917
 2.999419 11.59747 62.41453 11.37594
 2.936124 11.34490 53.95188 11.11112
 2.894063 11.16462 49.19093 11.61244
 2.796743 10.78497 39.14021 10.42125
 2.706422 10.43369 31.93742 10.23618
 2.549445 9.678443 23.20303 9.015135
 2.475765 9.503061 18.49155 9.712102
 2.331044 8.923866 13.49746 10.64191
 2.233304 8.591273 10.49993 10.13394
 2.154565 8.216343 8.722074 7.602339
 2.083354 7.941416 7.407543 7.582334
 2.044310 7.704941 6.936492 6.506994
 1.930234 7.326934 5.322401 5.339715
 1.836790 6.923160 4.233212 4.201248

APPENDIX F

POLYMER-SOLUTION RUN DATA

01P01465 5/19/90 12:58
 10 PSID Taps 14 1.0 PSID Taps 14 0.1 PSID Taps 14
 S = 2.7 S = 7.25 S = 9.9 C (ppm) =
 Z = 2.7 Z = 8.25 Z = 7.5 [NaCl] =

Freq. (Hz)	Dtest (1/s)	Temp (deg C)	<U> (volts)	<U>0 (volts)	<U>f (volts)	<U> corr (volts)
60	1.21416		8.006533	0.0175	0.0915	9.481833
49	0.991564		5.340333	0.0175	0.0915	5.248833
40	0.80944		3.6085	0.0175	0.0915	3.517
30	0.60708		2.116333	0.0175	0.0915	2.024833
23	0.465428		1.34825	0.0175	0.0915	1.25675
16	0.32376		0.710333	0.0175	0.0915	0.618833
11	0.222596		0.435	0.0175	0.0915	0.3435
7	0.141652		0.242833	0.0175	0.0915	0.151333
18	0.364248	24.9	9.495533	0.0135	0.0315	9.481833
15	0.30354	25.15	5.046	0.0275	0.0415	5.0185
13	0.263068	25.15	4.67425	0.0275	0.0415	4.64675
10	0.20236	25.15	3.146166	0.0275	0.0415	3.118666
8	0.161888	25.15	2.173375	0.0275	0.0415	2.145875
		24.85	2.3584	0.0325	0.0205	2.3379
		24.8	1.598	0.0175	0.0155	1.5805
		24.8	1.1798	0.0145	0.0135	1.1652
		24.8	0.750166	0.0125	0.0115	0.717666
		24.7	0.530666	0.0105	0.0095	0.520166
		24.7	3.2116	-0.0145	-0.0355	3.2471
		24.65	2.5096	-0.0445	-0.0465	2.5561
		24.6	1.905857	-0.0535	-0.0545	1.960357
		24.6	1.167	-0.058	-0.0595	1.2265
		24.6	0.7622	-0.062	-0.0635	0.8257
		24.5	0.411666	-0.066	-0.0675	0.478666
		24.5	0.2655	-0.0685	-0.0695	0.335
		24.4	0.1822	-0.0695	-0.07	0.2522
		24.4	0.093733	-0.07	-0.071	0.164733
		24.3	0.041190	-0.071	-0.071	0.112190
		24.25	-0.00109	-0.072	-0.071	0.069909
		24.2	-0.03386	-0.071	-0.0715	0.037633
		24.3	4.4536	-0.07	-0.0835	4.5371
		24.4	7.019	-0.082	-0.0815	7.1005
		24.5	9.4675	-0.081	-0.078	9.5455
		24.6	13.4862	-0.0775	-0.069	13.5587

density viscosity ID(cm) = 1.45796
 cg[NaCl] 1.00088 1.001574 K(V/psi)=1.088055 12.19257
 1.008150 X coeff -0.00025 -0.02281 XS(cm2) = 1.569479
 0.000100 constant 0.003419 -4.14933

Batch Vol (ml)	t(s)	visap (sec)	DP (psid)	U (cm/s)	Re	Tw (dyne/cm2)	f	Log(Re/f)
7	274295	727.2685	118373.2	1026.242	0.003891	3.688794		
4	824051	593.9560	96671.50	680.5669	0.003869	3.779104		
3	222373	484.8457	78915.51	456.0163	0.003890	3.692258		
1	860965	267.6542	59186.63	262.5411	0.003981	3.572268		
1	155042	278.7862	45376.42	162.9509	0.004204	3.468697		
0	568751	193.9282	31566.20	80.2380	0.004278	3.214860		
0	315700	122.3325	21701.76	44.53842	0.005024	3.187026		
0	139086	84.84800	13810.21	19.62197	0.005466	3.009040		
0	777673	218.1805	25431.95	109.7124	0.004622	3.281812		
0	411603	181.8171	29693.63	58.06809	0.003522	3.246116		
0	381113	157.5748	25734.48	52.73664	0.004242	3.229403		
0	255784	121.2114	19795.75	36.08549	0.004925	3.142817		
0	175998	96.96914	15836.60	24.82950	0.005295	3.061631		
14.9	0.191747	97.44627	15807.18	27.05139	0.005712	3.077286		
1939	14.9	0.129628	77.94898	12630.18	18.28766	0.006035	2.991778	
1645	15	0.095574	65.58913	10643.70	13.48346	0.006266	2.925599	
1620	19.9	0.058860	48.76192	7900.965	8.303982	0.007003	2.850342	
1330	19.9	0.042662	40.03293	6471.977	6.018748	0.007531	2.749466	
1329	19.9	0.042837	40.00283	6467.111	6.043478	0.007572	2.750557	
1155	19.9	0.033721	34.76544	5614.065	4.757394	0.007893	2.697905	
1224	25	0.025862	29.22650	4730.424	3.648602	0.008507	2.634791	
1114	30	0.016180	22.24246	3587.753	2.982757	0.009252	2.57958	
1090	35	0.010893	18.65423	3008.964	1.526786	0.008855	2.452035	
1005	39.9	0.006314	15.08731	2438.130	0.890890	0.007848	2.372655	
1186	59.9	0.004419	11.85978	1908.696	0.623499	0.008888	2.255161	
933	59.9	0.003327	9.229829	1498.145	0.469392	0.010812	2.192526	
613	60	0.002175	6.119671	982.6715	0.206600	0.016416	2.100044	
523	89.9	0.001480	4.150947	665.0399	0.208808	0.024299	2.015646	
591	90.1	0.000922	2.599386	415.9886	0.120114	0.036612	1.912442	
280	120	0.000496	1.597641	223.4170	0.070042	0.071896	1.777469	
1593	20	0.059856	47.70947	7643.726	8.444416	0.007438	2.819057	
1509	15	0.093674	64.25156	10317.24	13.21539	0.006419	2.917298	
1885	14.9	0.125970	75.77814	12195.62	17.76601	0.006203	2.982528	
2360	14.9	0.178829	94.87343	15303.27	25.22883	0.005620	3.059877	

Tap DL= 122.2334
40.77743

Solvent	L	MDR	1/f/f	1/f/f	1/f/f/Slv	1/f/f/L
75.79972	1/f/f	1/f/f	1/f/f	1/f/f	1/f/f/Slv	1/f/f/L
0.4						
15.07317	461.5028	41.09759	16.03095	1.063541	0.034736	
14.71641	375.8243	39.40299	16.07657	1.092454	0.042776	
14.34865	307.6378	37.5103	16.03255	1.115801	0.052115	
13.88907	233.4254	35.47309	15.84730	1.140991	0.067890	
13.47479	183.8984	33.50526	15.42170	1.144485	0.083859	
12.85944	129.0447	30.58234	15.28839	1.188885	0.118473	
12.34814	96.14283	28.15370	14.10276	1.142500	0.146737	
11.63616	63.81471	24.77177	13.52569	1.166384	0.211952	
13.12724	150.5539	31.85443	14.70899	1.120473	0.097699	
12.58446	110.1529	29.27620	16.84795	1.338790	0.152950	
12.51761	105.9946	28.95867	15.17440	1.212244	0.143162	
12.17125	86.85475	27.31345	14.24815	1.170639	0.164083	
11.84652	72.02965	25.77099	13.74139	1.159951	0.190774	
11.90914	74.67349	26.04844	13.23024	1.110931	0.177174	
11.56711	61.32791	24.44378	12.87157	1.112773	0.209881	
11.30239	52.65987	23.18639	12.63260	1.117692	0.239890	
10.88136	41.32590	21.18450	11.94917	1.098131	0.289144	
10.59786	35.10322	19.83987	11.52311	1.087305	0.328263	
10.60142	35.17526	19.85679	11.49087	1.083898	0.326674	
10.39162	31.17352	18.18602	11.25567	1.083148	0.361065	
10.15915	27.26917	17.75404	10.84196	1.067210	0.397590	
9.751832	21.56940	15.82120	10.39595	1.046051	0.481977	
9.408141	17.69764	14.18867	10.62628	1.129477	0.600435	
8.930622	13.44422	11.92045	11.28798	1.263963	0.839615	
8.620446	11.24712	10.44806	10.60657	1.230369	0.943047	
8.370105	9.736581	9.258003	9.616720	1.148937	0.987690	
8.000178	7.869093	7.500849	7.804833	0.975582	0.991832	
7.662387	6.879280	5.897288	6.415063	0.837192	0.990088	
7.249771	5.108848	3.936416	5.089070	0.701962	0.996128	
6.709879	3.744121	1.371928	3.739364	0.553813	0.996085	
10.87623	41.20386	21.16210	11.59437	1.066028	0.281290	
11.26919	51.66285	23.02867	12.48146	1.107573	0.241594	
11.53015	60.03693	24.26833	12.69595	1.101109	0.211469	
11.83870	71.70630	25.73386	13.33850	1.126685	0.186015	

01F01465

TW	8<U>/D	Log	Log
dyne/cm ²	(1/sec)	TW	8<U>/D
0.890890	82.78591	-0.05017	1.917956
0.623499	65.07604	-0.20516	1.813431
0.462392	51.19388	-0.32846	1.709218
0.306600	33.57936	-0.51342	1.526072
0.208808	22.77674	-0.68025	1.357491
0.120114	14.26314	-0.88567	1.154215
0.070042	7.669023	-1.15463	0.884740

Regression Output:
 Constant -2.04025
 Std Err of Y Est 0.001118
 R Squared 0.999989
 No. of Observations 4
 Degrees of Freedom 2

X Coefficient(s) 1.000916
 Std Err of Coef. 0.002338

TW vs. K*(8<U>/D)^n

K' = 0.009114
 n = 1.000916

TW = 0.010550
 Res/fz = 23.67377

Regression Output:

Constant -1.71207
 Std Err of Y Est 0.414623
 R Squared 0.918856
 No. of Observations 15
 Degrees of Freedom 12

X Coefficient(s) 4.955447
 Std Err of Coef. 0.408425

t = 24.72282 deg C
 s.d.)t = 0.286387 deg C

02P01462

10 PSID Taps 14 1.0 PSID Taps 14 0.1 PSID Taps 14
 S = 2.7 S = 7.25 S = 9.9 <D> (ppm) =
 Z = 2.7 Z = 8.2 Z = 7.5 [NaCl] =

col(NaCl) 1.00088 1.001574
 2.015260 X coeff -0.00025 -0.02281
 0.000100 constant 0.003419 -4.14933

density viscosity
 ID(cm) = 1.45796
 K(V/psi) = 1.08 12.09067
 X5(ce2) = 1.669479

Freq. (Hz)	Qtest (1/s)	Temp (deg C)	<V> (volts)	<Vo> (volts)	<V>f (volts)	<V>corr (volts)
24	0.485664	25.9	0.914	0.0285	0.0345	0.8855
33	0.467788	25.9	1.631333	0.0285	0.0345	1.602833
39	0.789204	25.9	2.241333	0.0285	0.0345	2.212833
48	0.971328	25.9	3.472333	0.0285	0.0345	3.443833
60	1.21616	25.9	5.733	0.0285	0.0345	5.7045
53	1.072508	25.9	4.366	0.0285	0.0345	4.3375
19	0.384484	25.9	0.612333	0.0285	0.0345	0.577833
11	0.222596	25.9	0.2898	0.0285	0.0345	0.2553
15	0.30354	25.9	0.4226	0.0285	0.0345	0.3881
9	0.182124	25.9	0.210428	0.0285	0.0345	0.175928
18	0.364248	26.1	5.9974	0.0475	0.0465	5.9499
24	0.485664	26.1	9.4268	0.0475	0.0465	9.3793
25.9	1.7878	25.9	1.7878	0.044	0.042	1.7458
25.7	1.135	25.7	1.135	0.0435	0.0415	1.0915
25.8	0.9278	25.8	0.9278	0.0425	0.0415	0.8853
25.7	0.5515	25.7	0.5515	0.0425	0.0415	0.509
25.7	0.406	25.7	0.406	0.0415	0.0405	0.3645
25.6	2.318333	25.6	2.318333	0.0525	0.0375	2.280833
25.5	1.8665	25.5	1.8665	0.017	0.0175	1.849
25.5	1.370666	25.5	1.370666	0.0145	0.0125	1.358166
25.3	0.827	25.3	0.827	0.008	0.0065	0.8205
25.4	0.63975	25.4	0.63975	0.0025	0.0015	0.62825
25.4	0.489545	25.4	0.489545	-0.001	-0.0005	0.490045
25.3	0.367312	25.3	0.367312	-0.0015	-0.0025	0.369812
25.3	0.244380	25.3	0.244380	-0.0025	-0.0015	0.245880
25.2	0.154652	25.2	0.154652	-0.0015	-0.0005	0.155152
25.05	0.098	25.05	0.098	0	0.0015	0.0965
24.9	0.042875	24.9	0.042875	0.0015	0.0015	0.041375
24.8	0.022	24.8	0.022	0.0015	0.0005	0.0205
25.1	3.1892	25.1	3.1892	-0.0005	-0.0105	3.1997
25.3	4.96825	25.3	4.96825	-0.0095	-0.0095	4.97775
25.5	7.0312	25.5	7.0312	-0.0095	-0.0065	7.0377
25.5	10.5858	25.5	10.5858	-0.0055	-0.0045	10.5963

Batch Vol (ml)	t(samp)	DP (psid)	<U> (cm/s)	Re	Tw (dyne/cm2)	f	Log(Re/f)
0.819907	290.9074	48320.51	115.6707	0.002741	7.403148		
1.484104	399.9977	66440.71	209.3743	0.002624	3.531998		
2.048919	472.7245	78520.84	289.0572	0.002594	3.602028		
3.188734	581.8148	96641.03	449.8599	0.002665	3.698074		
5.281944	727.2685	120801.2	745.1655	0.002826	3.807662		
4.016203	642.4205	106707.8	566.5974	0.002753	3.748172		
0.535030	230.3017	38253.71	75.48101	0.002854	3.310455		
0.236388	133.3325	22146.90	33.34924	0.003762	3.133079		
0.359351	181.8171	30200.32	50.69659	0.003076	3.224025		
0.162896	109.0902	18120.19	22.98113	0.003873	3.052222		
0.492106	218.1805	36404.27	69.42537	0.002925	3.294265		
0.775746	290.9074	48359.03	109.4407	0.002594	3.393096		
2594	15	0.144392	103.5851	17205.78	20.37056	0.003808	3.026037
2000	15	0.090276	79.86520	13221.01	12.73597	0.004005	2.922574
1685	15.1	0.073221	66.84083	11077.42	10.32996	0.004637	2.877600
1646	20	0.042098	49.29480	8151.470	5.939177	0.004902	2.756429
1358	20	0.030147	40.67135	6725.210	4.253104	0.005157	2.683918
1692	25	0.030090	40.53958	6688.314	4.245070	0.005180	2.682523
1469	25	0.024393	35.19459	5793.731	3.441345	0.005571	2.635959
1482	29.9	0.017917	29.68902	4887.126	2.527809	0.005732	2.568967
1320	34.9	0.010824	22.65517	3729.280	1.527108	0.005967	2.459530
1278	40.1	0.008288	19.08997	3135.330	1.169294	0.006433	2.400572
1537	59.9	0.006465	15.36971	2524.316	0.912068	0.007743	2.346624
1175	59.9	0.004878	11.74978	1927.604	0.688292	0.009999	2.285004
1183	90	0.003243	7.873378	1290.206	0.457631	0.014806	2.195883
740	89.9	0.002046	4.930499	806.1378	0.288768	0.023823	2.094914
910	180.1	0.001273	3.026541	493.1684	0.179605	0.039333	1.990321
420	200	0.000545	1.257877	204.2759	0.077006	0.097603	1.804948
238	240	0.000270	0.593997	96.24627	0.038154	0.216858	1.631471
1629	20	0.042212	48.78766	7958.818	5.955257	0.005017	2.751104
1960	14.9	0.065669	65.48679	10731.28	9.264551	0.00432	2.849037
2502	14.9	0.092845	78.79319	12970.19	13.09851	0.004231	2.926206
	14.9	0.139714	100.5819	16556.84	19.71058	0.003907	3.014945

75.79972

Tap DL= 122.2234
40.77743

Solvent L MDR
1//4 1//4 1//4 1//4 1//4 1//4 1//4 1//4 1//4 1//4

13.21259	158.1350	32.25981	19.09780	1.445424	0.120768
13.72799	212.7541	34.70796	19.51804	1.421769	0.091739
14.00811	249.9816	36.03853	19.63164	1.401448	0.078532
14.39229	311.8565	37.86342	19.76808	1.345725	0.062105
14.83065	401.3679	39.94558	18.81087	1.268378	0.046866
14.59269	349.9883	38.81529	19.05559	1.305831	0.054446
12.84182	127.7424	30.49864	18.71624	1.457445	0.146515
12.13331	84.91008	27.12950	16.30173	1.343661	0.191988
12.49610	104.6901	28.85648	18.02959	1.442817	0.172218
11.80888	70.48586	25.59221	16.06722	1.360404	0.227949
12.77706	123.0681	30.19104	18.48785	1.446956	0.150224
13.17238	154.5169	32.06882	19.63337	1.490495	0.127062
11.70415	66.36174	25.09471	16.20453	1.384511	0.244184
11.29029	52.29432	23.12891	15.80120	1.399538	0.302158
11.11040	47.14987	22.27441	14.58379	1.321625	0.311428
10.62571	35.67048	19.97215	14.28258	1.344153	0.400403
10.53567	30.18553	18.59445	13.92473	1.347243	0.461304
10.33009	30.08867	18.56793	13.89292	1.344898	0.461732
10.14383	27.02959	17.68523	13.59672	1.320676	0.495631
9.875870	23.16581	16.41038	13.18517	1.335090	0.569165
9.438121	18.00571	14.33107	12.94478	1.271541	0.718926
9.202288	15.71998	13.21087	12.46554	1.354613	0.792972
8.986496	13.88366	12.18585	11.36369	1.264530	0.818494
8.740016	12.04714	11.01507	10.00031	1.144199	0.850098
8.383532	9.812127	9.221780	8.218188	0.980277	0.837554
7.979657	7.776684	7.403374	6.478804	0.811915	0.833106
7.561285	6.112254	5.416106	5.042825	0.666926	0.825035
6.819795	3.988677	1.894029	3.200872	0.469350	0.802489
6.205886	2.801248	-1.02203	2.147396	0.346025	0.766585
10.60441	35.23586	18.97099	14.11703	1.331241	0.400644
10.99614	44.14863	21.73170	15.19198	1.281573	0.344110
11.30682	52.72349	23.19792	15.37233	1.359803	0.291509
11.65978	64.68823	24.88395	15.99677	1.371961	0.247290

02P01462

Tw	B(U)/D	Log	Log
dyne/cm ²	(1/sec)	Tw	B(U)/D
0.912068	84.35548	-0.03997	1.926010
0.488392	64.47247	-0.16222	1.809374
0.457631	43.20216	-0.33948	1.635505
0.288768	27.05423	-0.53945	1.432235
0.179405	16.60699	-0.74568	1.220290
0.077006	6.902121	-1.11247	0.838982
0.038154	3.259334	-1.41845	0.513128

Regression Output:
Constant -1.92195
Std Err of Y Est 0.006467
R Squared 0.999852
No. of Observations 6
Degrees of Freedom 4

X Coefficient(s) 0.968245
Std Err of Coef. 0.005886

Tw vs. K*(B(U)/D)^n

K' = 0.011968
n = 0.968245

Tw)Retro=0.599017
Res/(f)R= 196.6891

Regression Output:
Constant -4.88763
Std Err of Y Est 0.388709
R Squared 0.974677
No. of Observations 23
Degrees of Freedom 21

X Coefficient(s) 7.005665
Std Err of Coef. 0.246414

t = 25.60454 deg C
s.d.(t) = 0.338750 deg C

05P01459

Cyanamid 832A

Page 2

Cyanamid 832A

5/13/90 13:52
 10 PSID Taps 14 1.0 PSID Taps 14 0.1 PSID Taps 14
 S = 2.7 S = 7.25 S = 9.9 C (ppm) =
 Z = 2.7 Z = 7.5 Z = 8.15 [NaCl]=

density viscosity ID(cm) = 1.45796
 co[NaCl] 1.00088 1.001574 K(V/psi)= 1.08 12.03909
 4.991468 X coeff -0.00025 -0.0281 XS(cm2)= 1.669479
 0.000100 constant 0.003419 -4.14933

Batch (ml)	Vol (ml)	t) (sec)	DP (psid)	<U> (cm/s)	Re	Tm (dyne/cm2)	f	Log (Re/f)
0								
	3.371064	727.2685	117840.3	475.5826	0.001803	3.695112		
	2.284259	664.0571	98200.31	322.2584	0.001759	3.614801		
	1.539043	496.9668	80524.25	217.1249	0.001763	3.529053		
	1.032870	399.9977	64812.20	145.7151	0.001826	3.442451		
	0.678472	315.1497	51064.16	95.7142	0.001932	3.351194		
	0.372376	218.1805	33352.11	52.53609	0.002213	3.220919		
	0.214043	157.5748	25532.08	30.19476	0.002438	3.100479		
	0.123925	109.0902	17678.05	17.76536	0.002993	2.985486		
	0.367884	218.1805	35511.98	51.90042	0.002186	3.220254		
	0.597041	290.9074	47349.51	84.22931	0.001996	3.325401		
	0.753974	339.5920	55240.86	106.3691	0.001851	3.374077		
	0.954681	387.8765	63132.41	134.6844	0.001795	3.427228		
2515	14.9	0.104783	101.1045	16382.11	14.78265	0.002900	2.942575	
1973	15	0.070146	78.78702	12765.97	9.896119	0.003197	2.858431	
1642	15	0.053121	65.58933	10600.35	7.353244	0.003429	2.792953	
1629	20	0.033349	48.78766	7887.321	4.704904	0.003963	2.695989	
1345	20	0.026206	40.28201	6512.244	3.697129	0.004569	2.643646	
1680	24.9	0.026466	40.41372	6518.814	3.753893	0.004584	2.644809	
1467	25.1	0.020826	35.00864	5646.964	2.938138	0.004807	2.592764	
1230	25	0.016065	29.47026	4753.612	2.266473	0.005233	2.556404	
1344	35	0.010621	23.00118	3710.136	1.498467	0.005679	2.446552	
1259	40	0.008685	18.85318	3041.055	1.225397	0.006913	2.402867	
1143	44.9	0.006750	15.24820	2459.566	0.952405	0.008214	2.348119	
1122	60	0.004954	11.20109	1802.687	0.699005	0.011171	2.279982	
807	60	0.003630	8.056403	1296.585	0.512164	0.015823	2.213448	
530	60	0.002382	5.291070	851.5370	0.336088	0.024073	2.120970	
580	90	0.001726	3.860151	619.8471	0.243532	0.032772	2.050037	
397	90.1	0.001205	2.639274	422.8487	0.170077	0.048957	1.971095	
240	90	0.000722	1.597304	255.9104	0.101899	0.080083	1.859859	
250	180.1	0.000399	0.831467	133.2127	0.056368	0.163488	1.731289	
1602	19.9	0.033776	48.22012	7754.258	4.765108	0.004109	2.695202	
1634	15.1	0.053182	64.81775	10408.16	7.502812	0.003580	2.794370	
1948	15	0.067515	77.78871	12547.47	9.524980	0.003156	2.848160	
2516	15	0.105492	100.4704	16206.08	14.88272	0.002956	2.945069	

Freq. (Hz)	Q)est (1/s)	Temp (deg C)	<U> (volts)	<U> (volts)	<U>f (volts)	<U>corr (volts)
60	1.21416	24.8	3.67125	0.0285	0.0305	3.64075
50	1.0118	24.8	2.4975	0.0285	0.0305	2.467
41	0.829676	24.8	1.692666	0.0285	0.0305	1.662166
33	0.667788	24.8	1.146	0.0285	0.0305	1.1135
26	0.526136	24.8	0.76325	0.0285	0.0305	0.73275
18	0.364248	24.8	0.432666	0.0285	0.0305	0.402166
13	0.263068	24.8	0.281666	0.0285	0.0305	0.251166
9	0.182124	24.8	0.1665	0.0285	0.0305	0.136
18	0.364248	25	4.4485	0.0195	0.0345	4.429
24	0.485664	25	7.207333	0.0195	0.0345	7.187833
28	0.566608	25	9.096666	0.0195	0.0345	9.077166
32	0.647552	25	11.513	0.0195	0.0345	11.4925
24.8	1.278	24.8	1.278	0.0225	0.0165	1.2615
24.8	0.861	24.8	0.861	0.0165	-0.1	0.8445
24.7	0.489	24.7	0.489	0.0615	0.0565	0.6275
24.7	0.458	24.7	0.458	0.0565	0.0515	0.4015
24.7	0.367	24.7	0.367	0.0515	0.0475	0.3155
24.6	1.984857	24.6	1.984857	-0.0285	-0.0355	2.020357
24.6	1.558285	24.6	1.558285	-0.0315	-0.0315	1.587785
24.6	1.191857	24.6	1.191857	-0.0335	-0.0345	1.226357
24.6	0.7723	24.6	0.7723	-0.0365	-0.0385	0.8108
24.6	0.621545	24.6	0.621545	-0.0395	-0.0415	0.665045
24.6	0.471833	24.6	0.471833	-0.0425	-0.0435	0.515333
24.5	0.333722	24.5	0.333722	-0.0445	-0.0445	0.378222
24.5	0.233625	24.5	0.233625	-0.0445	-0.0435	0.277125
24.5	0.140352	24.5	0.140352	-0.0435	-0.0415	0.181852
24.4	0.094272	24.4	0.094272	-0.0405	-0.0375	0.131772
24.3	0.058526	24.3	0.058526	-0.0375	-0.0355	0.07-026
24.3	0.024136	24.3	0.024136	-0.0335	-0.031	0.055136
24.3	0	24.3	0	-0.0305	-0.0305	0.0305
24.35	2.535333	24.35	2.535333	-0.031	-0.043	2.578533
24.4	0.020166	24.4	0.020166	-0.0415	-0.0395	0.059666
24.6	5.116833	24.6	5.116833	-0.0385	-0.037	5.153833
24.6	8.023333	24.6	8.023333	-0.0355	-0.0295	8.052833

Solvent	L	MDR	Tap DL=	1//f	1//f/Siv	1//f/L
1//f	1//f	1//f	122.2234			
76.33526			40.77743			
0.4						
14.39724	312.7462	37.88692	23.54951	1.635695	0.075299	
14.05920	257.4431	36.28122	23.84029	1.695707	0.092604	
13.71621	211.3167	34.45202	23.81621	1.736354	0.112703	
13.56980	173.1137	33.00657	23.39943	1.750170	0.135168	
13.00477	140.3054	31.27269	22.74687	1.749116	0.162123	
12.48367	103.9440	28.79747	21.25669	1.702758	0.204501	
12.00271	78.80600	26.51290	20.24915	1.687047	0.256949	
11.54194	60.44580	24.32423	18.27676	1.583508	0.302366	
12.48101	103.7850	28.78484	21.38552	1.713443	0.206055	
12.90160	132.2151	30.78262	22.38270	1.734877	0.169290	
13.10430	148.5789	31.74546	23.23716	1.773246	0.156396	
13.30931	167.1892	32.71923	23.60065	1.773243	0.141161	
11.38230	55.13853	23.56593	18.56925	1.631415	0.336774	
11.03372	45.11402	21.91019	17.68570	1.602877	0.392022	
10.77181	38.80014	20.66611	17.07524	1.585178	0.440081	
10.38395	31.03625	18.82379	15.88328	1.529598	0.511765	
10.17458	27.51225	17.82927	14.79396	1.454011	0.537722	
10.17923	27.58605	17.85138	14.76926	1.450920	0.535388	
9.971059	24.47061	16.86253	14.42282	1.446468	0.589393	
9.745616	21.49235	15.79167	13.82355	1.418438	0.643184	
9.386209	17.47561	14.08449	13.26897	1.413667	0.759285	
9.211468	15.80327	13.25447	12.02699	1.305654	0.761044	
8.992558	13.93219	12.21465	11.03364	1.226974	0.791952	
8.719935	11.90868	10.91969	9.460991	1.084984	0.794461	
8.449972	10.19361	9.636516	7.949740	0.940820	0.779874	
8.083882	8.257537	7.898439	6.445149	0.797283	0.780517	
7.800151	7.013227	6.50720	5.23911	0.708179	0.787641	
7.484383	5.847577	5.50823	4.519486	0.603855	0.772881	
7.039436	4.536255	2.937521	3.533695	0.501985	0.780710	
6.525159	3.366432	0.494507	2.473180	0.379022	0.734659	
10.38120	30.98718	8.1073	15.59971	1.502687	0.503424	
10.77748	38.92694	20.69303	16.71105	1.550552	0.429292	
10.99264	44.05962	21.71505	17.79900	1.619173	0.403975	
11.38027	55.07441	23.55652	18.39111	1.616051	0.333932	

05P01459	Tw	8<U>/D	Log Tw	Log 8<U>/D
	dynes/cm2 (1/sec)			
0.952405	83.66872	-0.02117	1.922563	
0.699005	61.46174	-0.15551	1.788604	
0.512164	44.20644	-0.29059	1.645485	
0.336088	29.03273	-0.47354	1.462887	
0.243533	21.18111	-0.61344	1.325948	
0.170077	14.48201	-0.76935	1.160828	
0.101899	8.764598	-0.99182	0.942732	
0.056368	4.562360	-1.24896	0.659189	

Regression Output:	
Constant	-1.92127
Std Err of Y Est	0.003412
R Squared	0.999918
No. of Observations	7
Degrees of Freedom	5

X Coefficient(s)	0.988725
Std Err of Coef.	0.003990

Tw vs. K*(8<U>/D)^n	
K' =	0.011987
n =	0.988725

Tw)Retros=0.775105	
Res(f)/R=	202.0150

Regression Output:	
Constant	-13.6573
Std Err of Y Est	0.273221
R Squared	0.994377
No. of Observations	23
Degrees of Freedom	21
X Coefficient(s)	10.87003
Std Err of Coef.	0.178373

t = 24.66029 deg C	
s.d.)t =	0.202113 deg C

OIP11453 5/7/90 12:28
 10 PSID Taps 14 1.0 PSID Taps 14 0.1 PSID Taps 14
 S = 2.7 S = 7.25 S = 9.9 <C> (ppm) =
 Z = 2.7 Z = 7.65 Z = 8.1 [NaCl] =

Freq. (Hz)	Drest (1/s)	Temp (deg C)	<U> (volts)	<U>0 (volts)	<U>f (volts)	<U>corr (volts)
60	1.21416	24.6	2.26	0.0245	0.0235	2.2365
50	1.0118	24.6	1.545	0.0245	0.0235	1.5215
40	0.80944	24.6	1.0425	0.0245	0.0235	1.02075
31	0.627316	24.6	0.684	0.0245	0.0235	0.6605
24	0.485664	24.6	0.463666	0.0245	0.0235	0.440166
18	0.364248	24.6	0.29375	0.0245	0.0235	0.27025
14	0.283304	24.6	0.21075	0.0245	0.0235	0.18775
11	0.232596	24.6	0.1502	0.0245	0.0235	0.1267
8	0.161888	24.6	0.099	0.0245	0.0235	0.0755
18	0.364248	24.6	3.123	0.0145	0.0185	3.1085
26	0.526136	24.8	5.39025	0.0145	0.0185	5.37575
35	0.70826	24.8	9.063666	0.0145	0.0185	9.049166
		24.5	1.021166	0.0275	0.0265	0.994666
		24.4	0.715714	0.0275	0.0265	0.688214
		24.3	0.568428	0.0275	0.0235	0.540928
		24.3	0.403333	0.0235	0.0235	0.379833
		24.25	0.336	0.0235	0.0235	0.3125
		24.2	1.837428	0.014	-0.066	1.863428
		24.2	1.570714	-0.0665	-0.0665	1.637214
		24.2	1.263	-0.0665	-0.066	1.32925
		24.2	0.94	-0.0645	-0.0645	1.0045
		24.2	0.7567	-0.062	-0.0595	0.81745
		24.1	0.632545	-0.055	-0.054	0.687045
		24	0.46125	-0.0495	-0.0465	0.50925
		23.9	0.239833	-0.0445	-0.0345	0.279333
		23.9	0.334181	-0.0325	-0.0375	0.366681
		23.9	0.18	-0.0355	-0.0195	0.2075
		23.8	0.134090	-0.0185	-0.0133	0.150090
		23.8	0.084666	-0.0125	-0.0095	0.095666
		23.8	0.053428	-0.0095	-0.0075	0.061928
		23.9	2.396166	-0.0075	-0.0395	2.419666
		24	3.465666	-0.0365	-0.0425	3.485166
		24.2	4.45025	-0.0415	-0.0445	4.49325
		24.2	6.203	-0.042	-0.0465	6.24725

densi'ty viscosity ID(ica) = 1.45796 11.97077
 K(V/psid) = 1.08 12.03909
 XS(ica2) = 1.669479

col[NaCl] 1.00088 1.001574
 K(V/psid) = 1.08 12.03909
 XS(ica2) = 1.669479

Batch Vol (ml)	t'samp (sec)	DP (psid)	<U> (cm/s)	Re	Tw (dyne/cm2)	f	Log(Re/f)
2.070833	727.2685	117309.8	292.1487	0.001107	3.591530		
1.408796	606.0571	97758.23	198.7499	0.001085	3.507882		
0.945138	484.8457	78206.58	133.3381	0.001137	3.421205		
0.611574	375.7554	60410.10	86.27957	0.001225	3.326682		
0.407561	290.9074	46923.95	57.49794	0.001362	3.238554		
0.250231	218.1805	35192.96	35.30212	0.001487	3.132639		
0.173379	169.6960	27372.30	24.46003	0.001703	3.052957		
0.117314	133.3325	21306.81	16.55052	0.001866	2.988134		
0.069907	96.96914	15641.31	9.862388	0.002103	2.855719		
0.258200	218.1805	35352.11	36.42638	0.001534	3.141407		
0.446524	315.1497	51064.16	62.99474	0.001271	3.260551		
0.751648	424.2400	68740.22	106.0410	0.001181	3.373436		
14.9	0.082619	101.1045	16271.61	11.65581	0.002286	2.891014	
2570	20	0.057164	76.97009	12359.53	8.064713	0.002729	2.810052
2130	20	0.044931	63.79233	10220.42	4.338772	0.003123	2.756775
1592	20	0.031550	47.67953	7638.928	4.451007	0.003925	2.680002
1648	25	0.025957	39.48535	6318.975	3.661974	0.004709	2.637138
1641	24.9	0.024411	39.47554	6310.282	3.443867	0.004431	2.623311
1431	25	0.021447	34.28613	5480.740	3.025793	0.005161	2.595207
1200	25	0.017413	28.75147	4596.008	2.456633	0.005958	2.549758
1111	29.9	0.013159	22.25675	3557.807	1.856451	0.007514	2.489129
1060	35	0.010708	18.14081	2899.862	1.510758	0.009204	2.444385
1018	40	0.009000	15.24427	2431.350	1.269752	0.010955	2.405662
381	44.9	0.006671	10.91922	1737.613	0.941162	0.015826	2.339649
583	45	0.004803	7.760236	1332.129	0.677877	0.022361	2.267343
275	45	0.002718	3.660488	581.1951	0.383488	0.057381	2.143708
179	44.9	0.001966	2.387951	378.2920	0.277588	0.097527	2.072391
130	60.2	0.001253	1.293498	204.9119	0.174804	0.211862	1.974394
69	59.9	0.000811	0.689987	109.3056	0.114452	0.481984	1.880159
1193	15	0.031697	47.63959	7563.964	4.471871	0.003950	2.67076
1566	14.9	0.045656	62.95415	10018.10	6.441059	0.003258	2.757296
1887	15	0.058862	75.35282	12045.37	8.304133	0.002932	2.814435
2455	14.9	0.081839	98.69249	15776.28	11.54576	0.002376	2.885999

Solvent	L	MDR	1/f/f	1/f/f	1/f/f/Siv	1/f/f/L
74.66555	0.4					
74.33526					122.2334	
76.33526					40.77743	
13.96612	244.0117	35.83908	30.04719	2.151433	0.123138	
13.63152	201.2622	34.24976	30.35785	2.227032	0.150837	
13.28482	164.8488	32.60291	29.65086	2.231935	0.179866	
12.90673	132.6058	30.80697	28.56484	2.213339	0.215426	
12.55421	108.2517	29.13254	27.09191	2.157992	0.250267	
12.13051	84.82212	27.11995	25.95144	2.137703	0.305715	
11.81182	70.60528	25.60618	24.23004	2.051337	0.343176	
11.47253	58.07839	23.99435	23.14416	2.017353	0.398498	
11.02287	44.83320	21.85867	21.80487	1.978146	0.486355	
12.16562	86.55400	27.28675	25.52749	2.098329	0.294931	
12.64140	113.8233	29.54667	28.03915	2.218041	0.246339	
13.09374	147.6780	31.89528	29.09208	2.221831	0.196996	
11.16405	48.62895	22.52928	20.91297	1.873240	0.430051	
10.84021	40.35829	20.99100	19.14033	1.765679	0.474260	
10.62710	35.89897	19.97873	17.89341	1.683753	0.501230	
10.32000	29.91453	18.52004	15.95990	1.546500	0.533516	
10.14855	27.10304	17.70562	14.57164	1.435834	0.537638	
10.09324	26.25373	17.44291	15.02234	1.488356	0.572198	
9.980830	24.60863	16.90894	13.91975	1.394449	0.565645	
9.799832	22.17369	16.04920	12.95456	1.321916	0.584231	
9.556518	19.27568	14.89346	11.53593	1.207127	0.598470	
9.377541	17.38863	14.04332	10.42298	1.111483	0.599413	
9.222649	15.90531	13.30738	9.554001	1.035928	0.600679	
8.958599	13.66249	12.05334	7.948829	0.887284	0.581799	
8.433042	10.09579	9.556950	4.995953	0.592425	0.494854	
8.669375	11.56708	10.67953	6.657519	0.767933	0.375557	
8.174832	8.701382	8.330456	4.174574	0.510661	0.479759	
7.889564	7.383651	6.975432	3.202108	0.405866	0.433675	
7.498377	5.894871	5.117291	2.172566	0.289738	0.368551	
7.120638	4.742851	3.323030	1.440400	0.202285	0.303699	
10.52918	35.74177	19.98862	17.51819	1.648122	0.490132	
10.85774	40.76759	21.07426	18.46652	1.700770	0.452970	
11.14399	48.07056	22.43398	20.51188	1.840622	0.426703	

Tw	8<U>/D	Log	Log
dyne/cm2	(1/sec)	Tw	8<U>/D
1.269752	83.64713	0.103719	1.922451
0.941162	59.91509	-0.02633	1.777536
0.516245	27.88957	-0.28714	1.445441
0.677677	42.58133	-0.16897	1.629219
0.583488	20.08553	-0.41624	1.302883
0.277388	13.10297	-0.55691	1.117369
0.176804	7.097577	-0.75250	0.851110
0.114452	3.786043	-0.94137	0.578185

Regression Output:
 Constant -1.37424
 Std Err of Y Est 0.006784
 R Squared 0.999611
 No. of Observations 5
 Degrees of Freedom 3

X Coefficient(s) 0.736518
 Std Err of Coef. 0.008379

Tw vs. K*(8<U>/D)^n
 K' = 0.042242
 n = 0.736518

Tw)Retros=29.84650
 Res/f)K =1247.887

Regression Output:
 Constant -3.39885
 Std Err of Y Est 0.075995
 R Squared 0.994728
 No. of Observations 5
 Degrees of Freedom 3

X Coefficient(s) 9.632234
 Std Err of Coef. 0.404877

t = 24.29558 deg C
 s.d.)t = 0.211157 deg C

02P11456

5/10/90 9:20(H2O)12:45

10 PSID Taps 14 1.0 PSID Taps 14 0.1 PSID Taps 14
 S = 2.7 S = 7.25 S = 9.9 <C> (ppm) =
 Z = 2.7 Z = 8.15 Z = 7.5 [NaCl] =

24.1 0.1159 -0.0015 -0.0015 0.1174
 24.2 2.1935 -0.0015 -0.0225 2.216
 24.3 2.705833 -0.023 -0.024 2.727833
 24.4 3.728166 -0.0235 -0.0235 3.750666
 24.5 4.383166 -0.0215 -0.0215 4.404666
 24.6 6.5538 -0.0215 -0.015 6.5688

Freq. (Hz)	0)est (1/s)	Temp (deg C)	<U> (volts)	<U>0 (volts)	<U>f (volts)	<U>corr (volts)
60	1.21416	23.3	8.85175	0.0285	0.0395	8.81235
50	1.0118	23.3	6.39325	0.0285	0.0395	6.35375
40	0.80944	23.3	4.3352	0.0285	0.0395	4.2957
30	0.60708	23.3	2.5988	0.0285	0.0395	2.5593
21	0.424956	23.3	1.3874	0.0285	0.0395	1.3479
14	0.283304	23.3	0.691	0.0285	0.0395	0.6515
9	0.182124	23.3	0.364333	0.0285	0.0395	0.324833
7	0.141652	23.3	0.238166	0.0285	0.0395	0.198666
18	0.364248	23.3	11.4115	-0.0265	-0.0265	11.438
13	0.263048	23.3	6.51222	-0.0265	-0.0265	6.57772
15	0.30354	23.3	8.39011	-0.0265	-0.0265	8.41661
11	0.222596	23.3	4.7916	-0.0265	-0.0265	4.8181
8	0.161888	23.3	2.8075	-0.0265	-0.0265	2.834
60	1.21416	25	1.969333	0.0345	0.0365	1.932833
50	1.0118	25	1.39	0.0345	0.0365	1.3535
42	0.849912	25	1.053333	0.0345	0.0365	1.016833
32	0.64752	25	0.697	0.0345	0.0365	0.6605
25	0.5059	25	0.472333	0.0345	0.0365	0.435833
19	0.384484	25	0.32875	0.0345	0.0365	0.29225
14	0.283304	25	0.22875	0.0345	0.0365	0.19225
10	0.20236	25	0.1485	0.0345	0.0365	0.112
8	0.161888	25	0.125625	0.0345	0.0365	0.089125
18	0.364248	25.1	3.1305	0.0125	0.0095	3.118
24	0.485664	25.1	4.4316	0.0125	0.0095	4.4191
30	0.60708	25.1	6.5284	0.0625	0.0095	6.4659
24.8	1.0706	24.8	1.0706	0.0255	0.0195	1.0511
24.7	0.7585	24.8	0.7585	0.0205	0.0175	0.738
24.6	0.455571	24.7	0.634	0.0175	0.0155	0.6165
24.6	0.366666	24.6	0.455571	0.0155	0.0125	0.440071
24.6	0.246444	24.6	0.366666	0.0125	0.0095	0.35166
24.5	1.514111	24.6	0.246444	0.0105	0.0095	0.235944
24.5	1.162	24.5	1.514111	0.0175	0.0085	1.505611
24.5	0.9399	24.5	1.162	0.0135	0.0135	1.1485
24.4	0.798909	24.5	0.9399	0.0125	0.0125	0.9274
24.35	0.603333	24.4	0.798909	0.0075	0.0125	0.786409
24.3	0.269809	24.35	0.603333	0.0025	0.0125	0.589833
24.2	0.3875	24.3	0.269809	-0.0005	0.0125	0.257309
24.2	0.190857	24.2	0.3875	0.0025	0.0125	0.375
24.2	0.190857	24.2	0.190857	-0.0055	0.0125	0.178357

H2O

density viscosity
 co[NaCl] 1.000088 1.001574 ID(cm) = 1.45786
 20.00475 X coeff -0.00025 -0.02281 K(V/psi) = 1.08 12.03909
 0.000100 constant 0.005419 -4.14933 XS(cm²) = 1.669479

Batch	Vol	t ₁ amp	DP	<U>	Re	Tw	f	Log(Re/f)
(ml)	(sec)	(psid)	(cm/s)		dyne/cm ²			
0								
8.159490	727.2685	113919.3	1151.123	0.004362	3.876482			
5.883101	606.0571	94932.81	829.9755	0.004529	3.805453			
3.9775	484.8457	75946.23	561.1372	0.004785	3.720455			
2.349722	363.6342	56959.48	334.3153	0.005068	3.607999			
1.248035	254.5440	39871.78	174.0730	0.005447	3.468767			
0.603240	169.6960	26581.18	85.10392	0.005924	3.310895			
0.300771	109.0902	17087.90	42.43221	0.007147	3.159769			
0.183950	84.84800	13290.59	25.95136	0.007226	3.053001			
0.950071	218.1805	34175.81	134.0341	0.005644	3.409528			
0.546363	157.5748	24682.53	77.07983	0.006223	3.289391			
0.699106	181.8171	28479.84	98.62852	0.005980	3.542922			
0.400206	133.3325	20885.21	56.46002	0.006366	3.221791			
0.235399	96.74914	15189.25	33.20971	0.007080	3.106533			
1.789660	727.2685	118373.2	252.4815	0.000957	3.563784			
1.23240	606.0571	98644.39	176.8045	0.000965	3.486416			
0.941512	509.0880	82841.29	132.8265	0.001027	3.424311			
0.611574	387.8765	63132.41	86.27957	0.001150	3.336623			
0.402549	303.0285	49322.19	56.93189	0.001243	3.240347			
0.270601	230.3017	37484.87	38.17593	0.001443	3.153564			
0.178009	169.6960	27420.43	25.11316	0.001748	3.062620			
0.103703	121.2114	19728.87	14.63029	0.001997	2.945296			
0.082523	96.74914	15783.10	11.64219	0.002483	2.895686			
0.258989	218.1805	35592.16	36.53771	0.001539	3.145025			
0.367062	290.9074	47456.25	51.78441	0.001227	3.220754			
0.537075	363.6342	59320.31	75.76946	0.001149	3.303401			
14.9	0.087307	98.53169	15965.23	12.31712	0.002544	2.905933		
15	0.061300	75.31289	12203.05	8.648116	0.003057	2.829159		
1559	14.9	0.051208	62.67274	10132.07	7.224342	0.003688	2.789113	
1589	20.1	0.033553	47.35291	7638.120	5.156896	0.004611	2.714922	
1315	19.9	0.029418	39.58143	6384.565	4.150237	0.005312	2.667765	
1427	29.9	0.019598	28.58720	4611.173	2.764871	0.006784	2.579566	
1420	29.8	0.019723	28.58243	4593.576	2.782572	0.006849	2.579966	
1095	29.9	0.015045	21.93622	3530.383	2.122583	0.008845	2.521175	
1224	40	0.012149	18.32906	2949.852	1.713960	0.010230	2.474743	
995	60	0.010302	14.89985	2392.556	1.453390	0.013127	2.437949	
1030	60	0.007726	10.28264	1649.283	1.090091	0.020673	2.374997	
425	75	0.003370	3.394271	543.8098	0.475542	0.082764	2.194367	
600	59.9	0.004912	5.998990	959.1003	0.693050	0.038602	2.275170	
330	90	0.002336	2.196293	351.0839	0.329628	0.137010	2.113800	

175 100 0.001537 1.048230 167.1852 0.216971 0.395923 2.022003
 1323 20.2 0.029029 39.23081 6271.162 4.095467 0.005335 2.660979
 1553 20 0.035734 46.81099 7499.777 5.041404 0.004613 2.707046
 1532 14.8 0.049134 62.00346 9956.259 6.931758 0.003615 2.777179
 1864 15 0.057701 74.43437 11979.35 8.140419 0.002946 2.813066
 2416 15 0.086051 96.47717 15561.96 12.14003 0.002615 2.900838

Tap DL= 122.2334
40.77743

76.33526
4
0.4

Solvent L MDR 11/f/S1v 11/f/L
11/f 11/f 11/f

15.10592	470.2860	41.25316	15.15963	1.002231	0.032192
14.82181	399.5317	39.90362	14.85807	1.002446	0.037207
14.48182	358.3490	38.28865	14.45608	0.998222	0.044026
14.03199	253.4424	36.15198	14.04650	1.001033	0.055422
13.47507	183.9278	33.50658	13.54871	1.005465	0.073663
12.84358	127.8721	30.50702	12.99207	1.011561	0.101602
12.23907	90.29194	27.63561	11.82823	0.966431	0.130999
11.81200	70.61244	25.60702	11.76367	0.995908	0.166594
13.25811	160.4755	32.38104	13.31036	1.005457	0.082943
12.75756	121.6946	30.09843	12.67466	0.993642	0.104166
12.97168	137.4583	31.11552	12.93049	0.996824	0.093931
12.48716	104.1529	28.81404	12.53277	1.003652	0.120330
12.02621	79.87919	26.62451	11.88434	0.988220	0.148781
13.85513	228.9097	35.31190	32.31985	2.332698	0.141190
13.54566	191.5561	33.84190	32.18520	2.376031	0.168019
13.29724	166.0320	32.66192	31.19175	2.345729	0.187865
12.92249	133.8145	30.88184	29.48688	2.281826	0.220356
12.56138	108.6994	29.16659	28.35927	2.257634	0.260896
12.21425	89.0113	27.1772	26.32035	2.154887	0.293697
11.85048	72.19385	25.78978	23.91168	2.017781	0.331214
11.38118	55.10310	23.56062	22.37723	1.966160	0.406097
11.18274	49.15490	22.61804	20.04806	1.794556	0.408261
12.18010	87.27811	27.35548	25.48762	2.092562	0.292027
12.48501	103.9044	28.79433	28.54560	2.286753	0.274729
12.81360	125.6845	30.36463	29.49861	2.302132	0.234703
11.22381	50.33079	22.81312	19.82537	1.766367	0.393901
10.91683	42.17352	21.35403	18.08459	1.656608	0.438813
10.75645	38.45856	20.59314	16.46589	1.530791	0.428146
10.45969	32.41924	19.18353	14.72528	1.407812	0.454214
10.27106	29.08340	18.28753	13.72038	1.335829	0.471759
9.918264	23.73811	16.61175	12.14074	1.224079	0.511445
9.919867	23.76001	16.61936	12.08326	1.218087	0.508554
9.684703	20.75180	15.50234	10.63275	1.097892	0.512377
9.498975	18.64764	14.62013	9.886815	1.040829	0.530191
9.331797	17.15284	13.92103	8.727961	0.933292	0.509428
9.099988	14.82099	12.74494	6.955013	0.764288	0.469267
8.377471	9.777952	9.292990	3.475994	0.41921	0.355493
8.700681	11.77742	10.82823	5.089716	0.584979	0.432158
8.095200	8.123318	7.762200	2.701537	0.333378	0.332606

7.688014	6.574816	6.018068	1.589257	0.206718	0.241718
10.24375	28.62988	18.15785	13.69015	1.336438	0.478177
10.42819	31.83676	19.03392	14.72310	1.411853	0.462456
10.70871	37.41617	20.36640	16.63093	1.553028	0.444485
10.83226	40.63936	21.04827	18.42326	1.697642	0.453335
11.20335	49.74146	22.71593	19.55355	1.745330	0.393103

02P11456

Tw	8<U>/D	Log	Log
dyne/cm2	(1/sec)	Tw	8<U>/D
2.122583	120.3666	0.326864	2.080506
1.713960	100.5737	0.234000	2.002484
1.453390	81.75726	0.162382	1.912526
1.090091	56.42210	0.037463	1.751449
0.475542	18.62477	-0.32281	1.270090
0.693050	32.92211	-0.15923	1.517487
0.329628	12.05132	-0.48197	1.081034
0.216971	5.751767	-0.66359	0.739801

Regression Output:
 Constant -1.22219
 Std Err of Y Est 0.022885
 R Squared 0.994726
 No. of Observations 5
 Degrees of Freedom 3

X Coefficient(s) 0.709385
 Std Err of Coef. 0.029822

Tw vs. K*(8<U>/D)^n

K' = 0.059815
 n = 0.709385

Tw)Retro=122.7480
 Res/(R =2457.132

Regression Output:
 Constant 26.11734
 Std Err of Y Est 0.237809
 R Squared 0.992102
 No. of Observations 5
 Degrees of Freedom 3

X Coefficient(s) 1.740428
 Std Err of Coef. 0.883294

t = 24.67031 deg C
 s.d.)t = 0.316933 deg C

OSF11-49

10 FSID Taps 14 1.0 FSID Taps 14 0.1 FSID Taps 14
 S = 2.7 S = 7.25 S = 9.9 C (ppm) =
 Z = 2.7 Z = 7.65 Z = 8.1 [NaCl] =

4/30/90 9:12 (H2O) 12:45

Freq. (Hz)	Dist (1/s)	Temp (deg C)	V ₁ (volts)	V ₂ (volts)	V ₃ (volts)	V ₄ (volts)	V ₅ (volts)
60	1.21416	23.8	9.22425	0.0395	0.0725	9.15175	
50	1.0118	23.8	6.647	0.0395	0.0725	6.5745	
38	0.768960	23.8	4.064	0.0395	0.0725	3.9915	
31	0.627316	23.8	2.8622	0.0395	0.0725	2.7977	
25	0.5059	23.8	1.96975	0.0395	0.0725	1.89725	
18	0.364248	23.8	1.1178	0.0395	0.0725	1.0452	
11	0.222596	23.8	0.52175	0.0395	0.0725	0.44925	
8	0.161888	23.8	0.328	0.0395	0.0725	0.2555	
6	0.121416	23.8	0.2444	0.0395	0.0725	0.1719	
60	0.264248	24.7	11.3555	0.0675	0.0675	11.298	
50	0.283264	24.7	7.2494	0.0675	0.0675	7.2019	
40	0.202326	24.7	3.892833	0.0675	0.0675	3.825333	
30	0.161888	24.7	2.85975	0.0675	0.0675	2.79225	
20	0.121416	24.7	1.680666	0.0675	0.0675	1.613166	
60	1.21416	24.9	1.816	0.0445	0.0445	1.7715	
50	1.0118	24.9	1.4085	0.0445	0.0445	1.364	
40	0.80744	24.9	0.97075	0.0445	0.0445	0.92625	
31	0.627316	24.9	0.6945	0.0445	0.0445	0.65	
25	0.5059	24.9	0.50325	0.0445	0.0445	0.45875	
18	0.364248	24.9	0.3265	0.0445	0.0445	0.282	
12	0.263068	24.9	0.252666	0.0445	0.0445	0.208166	
9	0.182124	24.9	0.178285	0.0445	0.0445	0.133785	
7	0.141652	24.9	0.137428	0.0445	0.0445	0.092928	
18	0.364248	25.1	3.1535	0.0625	0.0795	3.091	
26	0.526126	25.1	5.2532	0.0625	0.0795	5.1907	
35	0.70826	25.1	8.17025	0.0625	0.0795	8.10775	
42	0.849912	25.1	10.99866	0.0625	0.0795	10.93616	
24.7	1.223	24.7	1.223	-0.0055	-0.0075	1.2205	
24.5	0.8724	24.5	0.8724	-0.0075	-0.0075	0.8799	
24.5	0.5812	24.5	0.5812	-0.0085	-0.011	0.6897	
24.45	0.501323	24.45	0.501323	-0.011	-0.011	0.513323	
24.4	0.414857	24.4	0.414857	-0.0115	-0.0115	0.426257	
24.4	0.293	24.4	0.293	-0.0105	-0.0115	0.3035	
24.4	1.919444	24.4	1.919444	0.0015	-0.0015	1.917944	
24.2	1.443525	24.2	1.443525	-0.0215	-0.0215	1.465125	
24.2	1.1082	24.2	1.1082	-0.0295	-0.0295	1.1377	
24.2	0.813225	24.2	0.813225	-0.0355	-0.0355	0.848725	
24.2	0.632912	24.2	0.632912	-0.0415	-0.0415	0.670312	
24.1	0.615882	24.1	0.615882	-0.0445	-0.0445	0.660782	

24	0.454066	-0.0495	-0.0445	0.198566
24	0.7054	-0.0445	-0.0435	0.1379
23.8	0.183705	-0.0435	-0.0435	0.227205
24	2.1912	-0.047	-0.0565	2.2477
24.05	2.232666	-0.0595	-0.0585	2.291166
24.1	2.093625	-0.0595	-0.0605	2.154125
24.1	2.980428	-0.0625	-0.0625	4.042928
24.1	4.7718	-0.0635	-0.0605	4.8722
24.2	5.41	-0.061	-0.061	5.471
24.2	7.2338	-0.061	-0.0575	7.2913

Batch	Vol	t ₁ (sec)	DP	η _{sp} /c	Re	T _w	f	Log (Re/f)
(ml)			(psid)	(cm ² /s)		dyne/cm ²		
				density				
				viscosity				
				co[NaCl] 1.00088	1.001574			
				50.01392 X coeff	-0.00025	-0.02281		
				0.000100 constant	0.003419	-4.14933		
							ID(cm) = 1.45796	
							K (V/psi) ² = 1.097177	11.9-037
							X5(cm ²) = 1.669479	
285	80	0.065831	2.843198	152.7553	9.790115	0.000972	0.000972	2.725115
159	80	0.068819	1.587321	152.5926	0.051841	0.001352	0.001352	2.757221
159	120	0.005999	0.597829	107.9142	0.423139	1.742210	1.742210	2.64089
1571	20	0.039671	21.26706	4991.545	4.186034	0.008530	0.008530	2.553719
1584	20	0.030245	31.62662	5038.530	4.266985	0.008552	0.008552	2.563370
1916	24.9	0.041637	46.07038	7351.161	5.874127	0.005544	0.005544	2.738274
1860	20	0.053370	55.70598	8884.700	7.529402	0.004864	0.004864	2.772192
1593	14.9	0.063791	84.03957	13213.84	8.999497	0.004799	0.004799	2.330911
1775	15	0.072222	70.88037	11230.43	10.13899	0.004066	0.004066	2.358652
2269	15	0.097572	90.50708	14516.52	13.74528	0.003762	0.003762	2.725115

8.341179	727.2685	115211.6	1176.755	0.004460	3.836190			
5.992196	606.0571	96009.71	845.3663	0.004614	3.814369			
3.537772	450.6034	72967.38	513.2374	0.004950	3.765006			
2.542616	375.7554	59526.02	358.7068	0.005093	3.628216			
1.729210	303.0285	48004.85	283.7933	0.005326	3.544500			
0.953717	218.1805	34563.49	134.4073	0.005660	3.415058			
0.409459	133.3325	21122.13	57.76573	0.006514	3.231582			
0.232870	95.96914	15261.55	32.85285	0.007004	3.109132			
0.156674	72.72685	11521.16	22.10375	0.008378	3.022076			
0.946156	218.1805	35272.44	133.4817	0.005523	3.422424			
0.602661	169.6960	27434.12	85.16222	0.005930	3.324039			
0.320638	121.2114	19595.80	45.23496	0.006174	3.187451			
0.234045	93.96914	15676.64	32.01864	0.007041	3.119093			
0.135215	72.72685	11757.48	19.07586	0.007322	3.999956			
1.614598	727.2685	118106.5	227.7840	0.000863	3.540445			
1.243190	606.0571	98422.10	175.3866	0.000957	3.482682			
0.847212	484.8457	78737.68	119.0996	0.001016	3.399639			
0.592429	375.7554	61021.70	82.57869	0.001187	3.322732			
0.418118	303.0285	49211.05	58.98727	0.001288	3.247062			
0.257023	218.1805	35431.95	36.26029	0.001527	3.141599			
0.189729	157.5748	25589.74	26.76661	0.002161	3.075430			
0.121936	109.0902	17715.97	17.20251	0.002598	2.979480			
0.084697	84.84800	13779.09	11.94899	0.003228	2.900250			
0.259083	218.1805	35592.18	136.55139	0.001579	3.145106			
0.435082	315.1497	51410.93	211.78057	0.001239	3.257670			
0.679589	424.2400	69207.03	295.87499	0.001068	3.254507			
0.915656	509.0880	87048.43	329.3213	0.001000	3.419489			
15	0.103140	92.44398	14945.07	0.007414	2.941157			
14.9	0.077352	71.95909	11580.98	0.004090	0.004039	2.866762		
1509	15	0.057810	59.25830	9697.981	8.155574	0.004504	0.004504	2.813475
1545	20	0.042943	46.27190	7478.576	6.058595	0.005573	0.005573	2.748429
1249	20.1	0.025737	37.22076	5976.755	5.041717	0.007297	0.007297	2.708047
1288	20	0.025439	25.71659	4129.464	3.588919	0.010881	0.010881	2.534240
1231	29.9	0.025718	25.66377	4120.757	3.571909	0.010975	0.010975	2.672308
922	30	0.019741	18.62856	2984.556	2.728595	0.015768	0.015768	2.577742
595	29.9	0.015018	11.91968	1909.499	2.118811	0.029902	0.029902	2.518019
782	60.1	0.011204	7.793834	1245.867	1.580657	0.052175	0.052175	2.454205
538	30	0.008848	5.270925	858.5599	1.248265	0.068771	0.068771	2.402958
449	30	0.006717	4.482434	714.9158	1.229872	0.122721	0.122721	2.398732

3.946845 11.57026 11.39751 11.045270 0.577077 0.1555657
 8.572285 11.5846 10.57361 11.388686 0.160740 0.112152
 8.253353 9.119460 8.717597 0.757294 0.091238 0.032302
 10.35487 28.81369 18.21065 10.92719 1.055809 0.375755
 10.27748 29.12397 18.29904 10.81267 1.052483 0.371255
 10.55309 24.21010 19.57221 12.43017 1.272628 0.392579
 10.78873 38.71138 20.45147 14.22705 1.331359 0.370166
 10.72764 42.34400 21.38732 15.07569 1.380097 0.356029
 11.05541 45.15787 21.91821 15.68170 1.421024 0.347263
 11.30066 52.50727 23.17814 17.24633 1.526134 0.327831

15.14476 480.9172 41.42761 14.97290 0.988652 0.031134
 14.05747 407.9144 40.07302 14.72128 0.990833 0.036115
 14.42402 317.5042 38.01411 14.35894 0.995487 0.045210
 14.11285 265.5198 35.53612 14.01167 0.992829 0.052770
 13.77800 218.9679 34.94550 13.70202 0.994485 0.062575
 13.26023 182.5319 32.48611 13.29104 1.002323 0.081774
 12.52672 104.5521 29.00196 12.38955 0.989049 0.116276
 12.05653 80.35514 26.67357 11.94817 0.992358 0.148692
 11.69230 65.91073 25.05344 10.92497 0.934372 0.165754
 13.28969 165.7122 32.62307 13.22554 1.007449 0.080668
 12.89935 132.0443 30.77195 12.98527 1.006660 0.098340
 12.34980 96.23455 28.16156 12.72659 1.030509 0.132245
 12.07637 82.21925 26.86277 11.91679 0.986784 0.144929
 11.59982 62.49266 24.59916 11.75067 1.013694 0.188157
 13.76178 216.9331 34.86847 34.02733 2.472596 0.156856
 12.53473 190.2542 32.78996 32.31543 2.387593 0.169764
 12.19855 156.8626 32.19315 31.37306 2.274921 0.199997
 12.99092 131.4050 30.73190 29.02366 2.251479 0.220871
 12.58825 110.3934 29.29420 27.86116 2.213266 0.252280
 12.16559 86.55256 27.28659 25.58557 2.103108 0.295607
 11.90192 74.36370 26.03413 21.50725 1.807040 0.289217
 11.51792 59.61564 24.21012 19.57312 1.612341 0.311547
 11.20140 49.68554 22.70665 17.52237 1.547284 0.348851
 12.18042 87.29446 27.25702 25.48285 2.092114 0.291918
 12.63068 113.1228 29.49573 28.40438 2.248840 0.251093
 13.01802 141.3798 31.52363 30.59446 2.50161 0.216299
 13.22795 164.1987 32.57030 31.61125 2.380721 0.1922518
 11.36462 54.59046 23.48198 17.11258 1.505863 0.212547
 11.06545 45.94546 22.06089 15.75371 1.423684 0.242878
 10.85290 40.67767 21.05604 14.90049 1.272823 0.266206
 10.59371 35.01948 19.82016 13.27571 1.253168 0.275095
 10.43219 31.91005 19.05290 11.70625 1.122128 0.266851
 10.13696 26.92279 17.65056 9.586356 0.945683 0.256068
 10.12282 26.52892 17.52093 9.589894 0.946519 0.257009
 9.894970 25.42192 16.50111 7.964106 0.804864 0.240027
 9.675276 20.63920 15.45755 5.782903 0.597698 0.280186
 9.416825 17.78622 14.22991 4.277897 0.464901 0.246128
 9.211325 15.00681 12.75621 2.794781 0.368522 0.214679
 9.194920 15.85334 12.17592 2.854448 0.310427 0.182251

Tap DL = 122.2254
 40.77743

Solvent L MDK
 1/1/1 1/1/1 1/1/1 1/1/1/1/1/1/1

05P11447

Tw	B(U)/D	Log	Log
dynes/cm ²	(1/sec)	Tw	B(U)/D
2.728595	102.2171	0.455939	2.009522
2.118811	65.40471	0.326092	1.315609
1.580253	42.76569	0.198836	1.031095
1.248355	29.47096	0.096341	1.469394
1.229872	24.59565	0.089859	1.390858
0.928512	15.61194	-0.07221	1.197456
0.551641	8.709819	-0.18599	0.940009
0.423139	5.807122	-0.37351	0.580596

Regression Output:

Constant -0.71112
 Std Err of Y Est 0.014594
 R Squared 0.997394
 No. of Observations 8
 Degrees of Freedom 6

X Coefficient(s) 0.566092
 Std Err of Coef. 0.011811

Tw vs. K*(B(U)/D)**n

K* = 0.194481
 n = 0.566093
 415309.1

Regression Output:

Constant -39.8827
 Std Err of Y Est 0.339132
 R Squared 0.790507
 No. of Observations 6
 Degrees of Freedom 4

X Coefficient(s) 20.77389
 Std Err of Coef. 1.015835

t = 24.50285 deg C
 s.d.t = 0.393390 deg C

01P21445

4/26/90 12:11
 10 PSID Taps 14 1.0 PSID Taps 14 0.1 PSID Taps 14
 S = 2.7 S = 7.25 S = 9.9 (C. (ppa))=
 Z = 2.7 Z = 8 Z = 7.65 [NaCl]=

density viscosity
 1.00059 1.901574 ID(cm) = 1.45795
 K(U/psi)=1.091557 11.97077
 99.99499 X coeff -0.00035 -0.02281
 0.000100 constant 0.003419 -4.14933 XS(cm2) = 1.669479

Freq. (Hz)	Qtest (1/s)	Temp (deg C)	<V> (volts)	<V>0 (volts)	<V>f (volts)	<V>icorr (volts)	Batch Vol (ml)	t(samp (sec)	DP (psid)	U. (cm/s)	Re	Iw (dyne/cm.2)	f	Log(Re/f)
60	1.21416	25.1	1.931333	0.0235	0.1315	1.799833			1.648722	727.2685	118640.6	232.5983	0.000601	2.545937
50	1.0118	25.1	1.4595	0.0235	0.1315	1.729			1.216502	605.0571	98867.18	171.6217	0.000977	2.480940
39	0.789204	25.1	1.016333	0.0235	0.1315	0.884833			0.810544	472.7245	77116.40	114.3498	0.001026	2.792772
29	0.586844	25.1	0.670666	0.0235	0.1315	0.539166			0.497899	351.5151	57742.97	69.67826	0.001130	2.205203
21	0.424956	25.1	0.482	0.0235	0.1315	0.3505			0.331072	254.5440	41534.21	45.39635	0.001402	2.191685
15	0.30354	25.1	0.3725	0.0235	0.1315	0.24575			0.225117	181.8171	29660.15	31.75507	0.001926	2.114588
9	0.18124	25.1	0.2742	0.0235	0.1315	0.1427			0.120719	109.0902	17796.09	18.44158	0.002107	2.096553
7	0.141652	25.1	0.2325	0.0235	0.1315	0.10175			0.092207	84.84850	12841.40	12.14948	0.002667	2.072109
10	0.20236	25.1	0.285	0.1295	0.1325	0.1525			0.172696	121.2114	19773.47	19.70697	0.003590	2.019776
6	0.121416	25.1	0.213333	0.1295	0.1325	0.080833			0.074046	72.72685	11864.06	10.44635	0.007951	2.87117
18	0.364248	25	3.356	0.0525	0.0715	3.2845			0.275297	218.1805	35511.98	38.82838	0.001526	2.157700
25	0.5059	25	5.3175	0.0525	0.0715	5.246			0.439704	303.0285	49332.19	62.02262	0.001354	2.258979
34	0.688024	25	8.25125	0.0525	0.0715	8.17975			0.585603	412.1188	67078.18	96.72348	0.001142	2.255435
24.5	1.1738	24.5	1.1738	0.0795	0.0355	1.1213	2226	15	0.093984	88.88997	14305.82	13.25909	0.003364	2.919000
24.45	0.9382	24.45	0.9382	0.0595	0.0355	0.9067	1715	15	0.075997	68.52435	11015.77	10.72149	0.004578	2.872778
24.45	0.79825	24.45	0.79825	0.0595	0.0345	0.75625	1420	15	0.063386	56.70429	9115.617	8.942465	0.005576	2.822979
24.4	0.582564	24.4	0.582564	0.0395	0.0285	0.554566	1345	20.1	0.046490	40.08160	6436.138	6.558793	0.008166	2.755170
24.4	0.451867	24.4	0.451867	0.0285	-0.0175	0.446357	1267	25	0.027412	30.35676	4874.563	5.278060	0.011484	2.717995
24.3	2.8242	24.3	2.8242	0.0565	0.0575	2.7667	1258	24.9	0.035237	30.26217	4848.424	5.152601	0.011231	2.711786
24.3	2.337571	24.3	2.337571	0.0575	0.0515	2.286071	931	25	0.020178	19.91039	2189.924	4.257496	0.021534	2.670750
24.3	1.882416	24.3	1.882416	0.0645	0.0915	1.790916	956	40	0.026441	14.31582	2292.597	3.325277	0.023312	2.612747
24.3	1.581769	24.3	1.581769	0.078	0.0805	1.501269	888	45	0.019818	11.85005	1893.737	2.795909	0.040126	2.579074
24.2	1.121916	24.2	1.121916	-0.0495	-0.1595	1.281416	569	45.1	0.01915	8.885225	1420.229	2.383463	0.060611	2.547655
24.2	0.957928	24.2	0.957928	-0.0355	-0.0055	0.963428	458	50.1	0.012718	5.475789	875.2210	1.794254	0.119984	2.481729
24.1	0.498117	24.1	0.498117	-0.0105	0.0045	0.493617	187	59.9	0.006316	1.869965	298.2459	0.919295	0.527122	2.355570
23.9	0.309923	23.9	0.309923	0.0005	0.0145	0.295423	142	120	0.007899	0.708803	112.5401	0.550185	2.195677	2.222086
24.2	3.625333	24.2	3.625333	0.0145	-0.1435	3.768833	1082	14.9	0.049752	43.49705	6953.133	7.018937	0.007436	2.777922
24.3	4.75725	24.3	4.75725	0.0065	0.1835	4.75075	1349	14.9	0.062716	54.23062	8668.925	8.847623	0.005032	2.326201
24.3	5.147666	24.3	5.147666	-0.0075	-0.0385	5.185166	1544	15	0.048463	62.45459	10006.10	9.658527	0.004945	2.848278
24.3	6.916333	24.3	6.916333	0.0005	0.009	6.907333	2194	14.9	0.091183	88.20013	14130.89	12.86396	0.003315	2.910460

Tw 8 U / D Log U u
dyne/cm² (1/sec) Tw 8 U / D
5.152501 166.0521 0.713025 2.220344
4.257496 109.2507 0.529154 2.078424
3.355337 78.55271 0.523179 1.895161
2.795909 64.85802 0.446523 1.811963
2.386463 48.75429 0.377754 1.663012
1.794254 30.04630 0.253382 1.477791
0.719295 10.26072 -0.03654 1.011178
0.550185 3.889290 -0.25949 0.589870

Regression Output:
Constant -0.52294
Std Err of Y Est 0.014747
R Squared 0.998228
No. of Observations 6
Degrees of Freedom 4

X Coefficient(s) 0.595105
Std Err of Coef. 0.012522

Tw vs. K*(8.U./D)^n

K* = 0.238264
n = 0.595105

Regression Output:
Constant -20.0648
Std Err of Y Est 0.080859
R Squared 0.998522
No. of Observations 4
Degrees of Freedom 2

X Coefficient(s) 15.14715
Std Err of Coef. 0.411589

t = 24.62265 deg C
s.d.t = 0.408805 deg C

Tap DL= 122.2234
40.77743

Solvent	L	MDR	1//f	1//f	1//f/Slv	1//f/L
75.75206						
0.4						
13.78783	230.2104	34.99220	33.67250	2.442190	0.1522910	
13.52376	189.1563	33.73787	32.66715	2.415537	0.172699	
13.17109	154.4018	32.06267	31.21578	2.370022	0.202172	
12.74081	120.5257	30.01886	29.73560	2.333886	0.246713	
12.36674	97.17753	28.24203	28.70641	2.159535	0.274820	
12.05835	81.37080	26.77718	27.78163	1.889282	0.279973	
11.58621	62.00601	24.53452	17.93787	1.548207	0.289292	
11.23243	52.35872	23.15907	16.52232	1.463132	0.315560	
11.64390	64.09981	24.80855	19.27992	1.657795	0.300779	
11.09254	46.66777	22.18960	15.38899	1.432402	0.340470	
12.22920	89.78009	27.58870	24.72150	2.021514	0.275356	
12.65591	112.4663	29.52061	27.16832	2.150087	0.239443	
13.02174	141.6822	31.35227	29.59006	2.272358	0.208848	
11.27500	51.85571	23.06100	17.23901	1.528833	0.332377	
11.08951	46.58634	22.17519	14.77870	1.332672	0.317332	
10.93191	42.56608	21.42561	13.39080	1.224926	0.314756	
10.66068	36.39571	20.13823	11.05236	1.036740	0.303672	
10.47198	32.64942	19.24191	9.331259	0.891049	0.285801	
10.44714	32.18595	19.12394	9.414869	0.901190	0.292514	
10.28140	29.25705	18.33665	8.814439	0.862792	0.232916	
10.06937	25.89543	17.23951	5.525721	0.549758	0.213772	
9.916138	23.70907	16.60165	4.992122	0.502434	0.210557	
9.774661	21.85472	15.92964	4.041849	0.415348	0.185856	
9.526919	18.95003	14.75286	2.886937	0.303029	0.152744	
8.942121	13.53350	11.97507	1.377350	0.154029	0.101773	
8.488347	10.42237	9.819648	0.874870	0.079505	0.064752	
10.71169	37.48034	20.38054	11.59463	1.082427	0.309352	
10.91280	42.08052	21.33582	12.87549	1.179852	0.305972	
10.99291	44.06650	21.71634	14.19176	1.290991	0.322052	
11.24184	50.85580	22.89875	17.36637	1.544797	0.341482	

01P03166

5/19/90 15:38

10 PSID Taps 14 1.0 PSID Taps 14 0.1 PSID Taps 14
 S = 2.7 S = 7.25 S = 9.9 C (ppm) =
 Z = 2.7 Z = 8.25 Z = 7.5 [NaCl] =

Freq. (Hz)	Dtest (1/s)	Temp (deg C)	<V> (volts)	<U> (volts)	<U>f (volts)	<U>f corr (volts)
60	1.21416	25.1	8.433666	0.0225	0.0945	8.339166
48	0.971328	25.1	5.748666	0.0225	0.0945	5.654166
53	1.072508	25.1	7.014	0.0225	0.0945	6.9195
40	0.80944	25.1	4.270666	0.0225	0.0945	4.276166
30	0.60708	25.1	2.669666	0.0225	0.0945	2.575166
23	0.465428	25.1	1.733	0.0225	0.0945	1.6385
17	0.344012	25.1	1.05375	0.0225	0.0945	0.95925
11	0.222596	25.1	0.547375	0.0225	0.0945	0.452875
9	0.182124	25.1	0.418	0.0225	0.0945	0.3225
20	0.40472	24.2	1.4525	0.0375	0.0295	1.415
15	0.30354	24.2	0.7855	0.0375	0.0295	0.748
10	0.20236	24.2	0.4095	0.0375	0.0295	0.372
20	0.40472	25.3	13.511	0.0665	0.099	13.4445
16	0.323776	25.3	9.671666	0.0665	0.099	9.605166
12	0.243068	25.3	6.5244	0.0665	0.099	6.4254
10	0.20236	25.3	4.593	0.0665	0.099	4.494
7	0.141652	25.3	2.4026	0.0665	0.099	2.3036
25.05	1.1692	25.1	2.216	0.0775	0.0805	2.1355
25	0.7135	25.1	1.5082	0.0795	0.0745	1.4337
25	0.5215	25.05	1.1692	0.0715	0.0685	1.1007
24.9	2.767833	24.9	2.767833	-0.0645	-0.0645	2.830833
24.9	2.077142	24.9	2.077142	-0.0665	-0.0665	2.143642
24.9	1.440285	24.8	1.440285	-0.072	-0.0745	1.512285
24.8	0.749363	24.8	0.749363	-0.0765	-0.078	0.845863
24.8	0.332571	24.8	0.332571	-0.0815	-0.0835	0.414071
24.7	0.1858	24.7	0.1858	-0.0845	-0.0855	0.2703
24.6	0.070826	24.6	0.070826	-0.0865	-0.0865	0.157226
24.5	-0.00765	24.5	-0.00765	-0.0865	-0.0845	0.07885
24.5	-0.05432	24.5	-0.05432	-0.0855	-0.0845	0.031178
24.5	3.592	24.5	3.592	-0.085	-0.0875	3.6795
24.6	6.276	24.6	6.276	-0.0875	-0.0855	6.2615
24.7	8.7712	24.7	8.7712	-0.0845	-0.081	8.8522
24.7	12.4562	24.7	12.4562	-0.0825	-0.0795	12.5357

density viscosity ID(cm) = 1.45/98
 co[NaCl] 1.01224 1.029478 K(V/psi) = 1.088055 1.099067
 1.008150 X coeff -0.00025 -0.02201 X5(cm2) = 1.669479
 0.300023 constant 0.003419 -4.14932

Batch	Vol (ml)	t)5amp (sec)	DP (psid)	U: (cm/s)	Re	Tu dyne/cm2	f	Log(Re/f)
7.664287	727.2685	116878.9	1081.261	0.004050	3.871270			
5.194581	581.8148	93471.14	733.1227	0.004290	3.786957			
6.359513	642.4205	103207.7	897.1866	0.004307	3.870806			
2.970101	484.8457	77892.52	554.4507	0.004672	3.726296			
2.366761	263.6342	58419.46	333.8976	0.005002	3.516171			
1.505898	278.7862	44788.25	212.4489	0.005415	3.517991			
0.881619	206.0594	33104.26	134.2749	0.005802	3.401724			
0.416224	133.3225	21420.47	58.72005	0.006544	3.228757			
0.297319	109.0902	17525.84	41.94520	0.006987	3.152705			
1.200485	242.4228	28163.51	182.4697	0.006182	3.472280			
0.687465	181.8171	28622.57	96.98612	0.005811	3.278052			
0.241894	121.2114	19081.75	48.23274	0.006502	3.187172			
1.111973	242.4228	29122.43	156.9748	0.005288	3.454111			
0.794427	193.9382	31297.94	112.0762	0.005904	3.281091			
0.531434	157.5748	25429.58	74.97366	0.005982	3.297789			
0.371691	121.2114	19561.21	52.43745	0.007071	3.215155			
0.190527	86.84800	13692.85	26.87915	0.007297	3.071042			
14.9	0.176627	79.42640	12761.81	24.91771	0.007823	3.052618		
1599	14.9	0.118579	64.28077	10326.99	16.72887	0.008021	2.966098	
1369	15.2	0.091037	53.94842	8657.283	12.84322	0.008742	2.908210	
1255	20	0.052677	40.58150	6504.908	7.572743	0.009710	2.795006	
1375	24.9	0.038045	32.07670	5301.945	5.267429	0.009719	2.718262	
1370	24.9	0.037346	32.95642	5270.761	5.268726	0.009510	2.712247	
1177	25	0.028319	28.20040	4510.125	3.995215	0.00952	2.651149	
1167	30.1	0.019951	22.22326	3714.134	2.814654	0.010239	2.577106	
1291	45.1	0.011159	17.14622	2736.027	1.574215	0.010508	2.449924	
1124	49.9	0.005462	13.49225	2152.970	0.770666	0.008287	2.294842	
988	59.9	0.002565	9.879819	1572.978	0.503080	0.010210	2.201241	
867	89.9	0.001020	5.776679	917.6397	0.292814	0.017282	1.982774	
482	100	0.001040	2.887127	457.5927	0.146752	0.024877	1.921750	
228	120	0.000411	1.158079	180.2792	0.058029	0.088752	1.770277	
1265	20	0.048542	27.88605	6004.731	6.848258	0.009451	2.768242	
1295	14.9	0.082925	52.05978	8269.825	11.82997	0.008654	2.883114	
1550	14.9	0.116784	62.21094	9920.601	16.47584	0.008406	2.952845	
1900	14.9	0.165579	76.28115	12160.73	23.33155	0.007922	3.024297	

Tap DL= 122.2234
40.77743

Solvent	L	MDR	1//f	1//f	1//f/Slv	1//f/L
75.79972	0.4					
15.08532	464.7400	41.15527	15.71294	1.041604	0.033810	
14.74781	382.6776	39.55210	15.26597	1.035134	0.039892	
14.92322	423.3369	40.38531	15.23723	1.021041	0.035993	
14.50518	332.7944	38.39962	14.62851	1.008502	0.043956	
14.06468	258.2666	36.30725	14.13794	1.005208	0.054743	
13.67196	206.0022	34.44184	13.58852	0.993896	0.065962	
13.20693	157.6212	32.33295	13.12654	0.993913	0.083279	
12.55503	108.3023	29.13640	12.36149	0.984585	0.114139	
12.26282	91.53473	27.74841	11.96665	0.975848	0.130733	
13.50912	187.5686	35.66852	12.71651	0.941328	0.067796	
12.95541	136.3743	31.03820	13.11767	1.012524	0.096188	
12.34869	96.17307	28.15629	12.40066	1.004208	0.128941	
13.41644	177.8245	33.22812	13.75026	1.024888	0.077325	
13.12436	156.3044	31.84074	13.01439	0.991620	0.086586	
12.77515	122.9332	30.18200	12.92854	1.012006	0.105167	
12.46462	102.8101	28.70696	11.89159	0.954027	0.115665	
11.88417	73.60785	25.94981	11.62655	0.978322	0.157953	
11.81047	70.55029	25.59975	11.30559	0.957251	0.160248	
11.46439	57.80669	23.95586	11.16543	0.973923	0.193131	
11.23284	50.59305	22.85600	10.69475	0.952096	0.211587	
10.77202	38.80406	20.66711	10.47695	0.972607	0.269990	
10.47305	32.66951	19.24699	10.14314	0.968499	0.310477	
10.45298	32.29439	19.15169	10.20061	0.975855	0.315863	
10.21267	28.12224	18.01022	10.02348	0.981474	0.356425	
9.908427	23.60407	16.56503	9.834438	0.992522	0.416641	
9.399819	17.61306	14.14914	9.708834	1.033874	0.551229	
8.779369	12.52517	11.20200	10.91932	1.243747	0.886080	
8.404970	9.933965	9.423610	9.896464	1.177453	0.996224	
7.920939	7.561619	7.171960	7.584683	0.956341	1.003050	
7.327000	5.341092	4.30231	5.354636	0.730808	1.062535	
6.521109	3.358592	0.475269	3.356675	0.514739	0.999429	
10.66497	36.48578	20.15862	10.28608	0.964473	0.281920	
11.14445	48.08329	22.42616	10.74934	0.964596	0.223536	
11.43538	56.84931	25.81805	10.90648	0.953766	0.191852	
11.73757	67.65095	25.25348	11.23481	0.937166	0.166070	

Tw	B U./D	Log	Log
dynes/cm ²	(1/5 th sec)	Tw	B U./D
0.770666	74.03363	-0.11313	1.869429
0.503080	54.21174	-0.29836	1.734093
0.292814	31.59733	-0.53340	1.501022
0.146755	15.84201	-0.83340	1.199810
0.058029	6.244773	-1.23635	0.795516

Regression Output:
 Constant -2.03140
 Std Err of Y Est 0.001211
 R Squared 0.999994
 No. of Observations 4
 Degrees of Freedom 2

X Coefficient(s) 0.998782
 Std Err of Coef. 0.001725

Tw vs. K's (B.U./D)ⁿ
 K' = 0.009302
 n = 0.998782

Tw# = 55.27296
 Res/f# = 1652.073

Regression Output:
 Constant -0.81535
 Std Err of Y Est 0.130490
 R Squared 0.970511
 No. of Observations 5
 Degrees of Freedom 3

X Coefficient(s) 4.129070
 Std Err of Coef. 0.415542

t = 24.89571 deg C
 s.d.) t = 0.318561 deg C

02P03163

Cyanamid 832A

10 FSID Taps 14 1.0 FSID Taps 14 0.1 FSID Taps 14
 S = 2.7 S = 7.25 S = 9.9 <C>(ppm) =
 Z = 2.7 Z = 8.2 Z = 7.5 [NaCl] =

density viscosity

col(NaCl) 1.01224 1.029478 ID(cm) = 1.45786
 2.015260 X coeff -0.00025 -0.02281 K(U/psi) = 1.08 12.09067
 0.300061 constant 0.003419 -4.14933 XS(cm2) = 1.669479

Cyanamid 832A

Freq. (Hz)	Dist (1/s)	Temp (deg C)	<V> (volts)	<V>0 (volts)	<V>f (volts)	<V>corr (volts)	Batch Vol (ml)	t(s) sweep (sec)	DP (psid)	<U> (cm/s)	Re	Tw (dyne/cm2)	f	Log(ke/f)
24	0.485664		25.3 1.203666	0.0315	0.0385	1.172166			1.085339	290.9074	46946.92	153.1173	0.003584	3.448847
35	0.70826		25.3 2.242333	0.0315	0.0385	2.210833			2.047067	424.2400	68464.26	288.7959	0.003179	3.586630
45	0.91062		25.3 3.604333	0.0315	0.0385	3.572833			3.308179	545.4514	88025.47	466.7108	0.003108	3.690859
51	1.032036		25.3 4.663666	0.0315	0.0385	4.632166			4.289905	618.1782	99762.20	605.0891	0.003127	3.747244
60	1.21416		25.3 6.467666	0.0315	0.0385	6.436166			5.959413	727.2685	117367.3	840.7414	0.003149	3.819366
24	0.485664		25.3 1.196333	0.0315	0.0385	1.164833			1.078549	290.9074	46946.92	152.1594	0.003562	3.447484
16	0.322776		25.3 0.61175	0.0315	0.0385	0.57325			0.520787	193.9382	31297.94	74.88230	0.003394	3.29554
12	0.242832		25.3 0.292	0.0315	0.0385	0.2535			0.327214	145.4537	23473.46	46.17687	0.004334	3.188547
8	0.161888		25.3 0.2478	0.0315	0.0385	0.2093			0.193796	96.96914	15648.97	27.34037	0.005761	3.07437
40	0.80944		24.2 3.103666	0.0315	0.0385	3.065166			2.828117	484.8457	76327.03	400.3955	0.003373	3.646742
10	0.20236		24.15 9.340375	0.0315	0.0385	9.301875			0.279513	121.2114	19060.24	39.43322	0.005316	3.162926
24	0.485664		25.2 11.97766	0.0655	0.1035	11.91216			0.985236	290.9074	46841.12	138.9950	0.003254	3.423849
15	0.30354		25.2 6.44325	0.0655	0.1035	6.33975			0.524350	181.8171	29275.70	73.97426	0.004453	3.289890
20	0.40472		25.2 8.998333	0.0655	0.1035	8.894833			0.756677	242.4228	39034.27	103.7878	0.003499	3.353432
10	0.20236		25.2 3.4675	0.0655	0.1035	3.264			0.278231	121.2114	19517.13	39.25224	0.005293	3.152282
7	0.141652		25.2 1.8878	0.0655	0.1035	1.7843	2080	14.9	0.147576	84.84800	13661.99	20.81979	0.005729	3.014588
			25 1.931333	0.0775	0.0745	1.856833	1655	15	0.153575	83.81726	13403.21	21.66613	0.006159	3.021270
			25 1.292666	0.074	0.0715	1.221166	1855	20	0.101000	66.08846	10593.47	14.24897	0.004663	2.930271
			24.9 1.045	0.0705	0.0685	0.9745	1374	19.9	0.080764	55.55623	8885.176	11.39412	0.007313	2.880724
			24.8 0.686166	0.0685	0.0655	0.620666	1426	24.9	0.051234	41.35733	6599.423	7.242140	0.008388	2.781342
			24.7 0.521	0.0655	0.0645	0.4565	1039	25	0.037756	34.30355	5461.510	5.226590	0.008967	2.715448
			24.7 0.331166	0.0655	0.0645	0.266666			0.022055	24.89398	3963.402	3.111553	0.009946	2.596912
			24.6 1.644333	0.018	0.018	1.626333	1040	25	0.021455	24.91794	3958.276	3.026919	0.067657	2.589779
			24.6 1.05232	0.017	0.014	1.041222	965	30.1	0.013726	19.20347	2050.518	1.937915	0.010410	2.492104
			24.5 0.637	0.01	0.006	0.621	1070	39.9	0.008224	16.06311	2545.915	1.174412	0.009016	2.383263
			24.5 0.403666	0.004	0.0015	0.399666	991	44.9	0.005272	13.23044	2095.368	0.745856	0.008420	2.284198
			24.5 0.278462	-0.0005	-0.0025	0.279142	975	59.9	0.003682	9.749822	1545.293	0.519538	0.010826	2.205262
			24.4 0.1806	-0.0055	-0.0065	0.1841	654	59.9	0.002455	6.539880	1034.199	0.346367	0.016042	2.11727
			24.1 0.129333	-0.0075	-0.0075	0.136833	720	90.1	0.001805	4.784594	751.8325	0.254673	0.023017	2.047504
			24.1 0.0652	-0.0085	-0.0065	0.0717	499	120	0.000945	2.490796	391.2310	0.153447	0.042605	1.907168
			24 0.028	-0.0065	-0.0065	0.0345	410	199.9	0.000455	1.228541	192.5330	0.044211	0.084266	1.747322
			24.3 2.7654	-0.0075	-0.0125	2.7759	1396	24.9	0.036621	33.58187	5298.581	5.166484	0.009074	2.707080
			24.3 3.736333	-0.0125	-0.0105	3.746833	1689	25.1	0.049420	40.30647	6359.594	6.973578	0.008502	2.768211
			24.3 6.001714	-0.0115	-0.0085	6.010214	1824	20.1	0.079290	54.25602	8574.346	11.18616	0.007499	2.870622
			24.3 7.89525	-0.012	-0.0105	7.90575	1609	14.9	0.104297	54.68277	10205.71	14.71412	0.006966	2.970750
			24.2 11.2145	-0.0115	-0.011	11.2255	2006	14.9	0.148094	80.64242	12695.16	20.89281	0.006363	3.005496

Solvent	L	MDR	1//f	1//f	1//f/Siv	1//f/L
74.66555					122.2234	
75.79972					40.77743	
	0.4					
	1//f	1//f	1//f	1//f	1//f/Siv	1//f/L
13.39538	175.6820	33.12810	16.70166	1.246821	0.095067	
13.96652	241.2741	35.74598	17.73508	1.271649	0.073505	
14.36343	306.7178	37.72632	17.93697	1.248794	0.058480	
14.58897	349.2406	38.79765	17.85341	1.223760	0.051120	
14.87466	411.6673	40.15466	17.81889	1.197935	0.045284	
13.38993	175.1316	33.10220	16.75415	1.251249	0.095666	
12.77409	122.8583	30.17697	15.92176	1.246409	0.129594	
12.35418	96.47781	28.18240	15.20451	1.230879	0.157616	
11.89994	74.23647	26.02000	13.17493	1.107235	0.177472	
14.18697	277.0911	36.88810	17.21614	1.213517	0.062131	
12.17174	86.85934	27.31579	13.71488	1.126780	0.157897	
13.30739	167.0050	32.71014	17.52983	1.317299	0.104965	
12.75956	121.8345	30.10791	15.01817	1.177013	0.123266	
13.05369	144.3122	31.50503	16.90530	1.295059	0.117143	
12.20912	88.74874	27.49336	13.74465	1.125768	0.154871	
11.65835	64.63506	24.87717	13.21070	1.133153	0.204389	
11.68508	65.63723	25.00413	12.76258	1.092212	0.194441	
11.32108	53.22936	23.27515	12.43848	1.098700	0.233677	
11.12293	47.49137	22.33396	11.69314	1.051263	0.246216	
10.72537	37.77658	20.44551	10.91851	1.018007	0.289028	
10.45459	32.32426	19.15932	10.56000	1.010082	0.326689	
9.987650	24.70544	16.94133	10.02664	1.003904	0.405867	
9.959756	24.31191	16.80884	10.17576	1.021687	0.418550	
9.572424	19.45298	14.96901	9.800933	1.023871	0.503826	
9.133455	15.10928	12.88391	10.53125	1.153041	0.697005	
8.756792	12.02480	10.99976	10.89086	1.246551	0.905699	
8.425049	10.04945	9.518987	9.610552	1.140711	0.956325	
8.048948	8.186857	7.827506	7.895270	0.978475	0.944383	
7.790017	6.972433	6.502583	6.739339	0.865123	0.966549	
7.228672	5.047171	3.836192	4.844682	0.670203	0.959880	
6.589331	3.493114	0.799322	3.444867	0.522794	0.986187	
10.41232	31.54719	18.95853	10.49733	1.008164	0.332750	
10.67284	36.65143	20.19600	10.84472	1.016104	0.295888	
11.08359	46.41985	22.14565	11.54724	1.041860	0.248756	
11.32140	53.33905	23.27665	11.98099	1.058260	0.225041	
11.62198	63.29603	24.70443	12.53550	1.078602	0.198045	

Tw	8.U./D	Log	Log	Log
dyne/cm ²	(1/sec)	Tw	8.U./D	8.U./D
1.174412	88.14022	0.069820	1.945174	
0.743856	72.54217	-0.12851	1.860590	
0.519528	52.49843	-0.28438	1.728341	
0.346367	35.88510	-0.46046	1.554914	
0.254673	26.26461	-0.59401	1.419270	
0.173447	17.66729	-0.97468	1.175682	
0.064211	6.741155	-1.19238	0.828724	

Regression Output:

Constant -2.00529
 Std Err of Y Est 0.001947
 R Squared 0.999959
 No. of Observations 4
 Degrees of Freedom 2

X Coefficient(s) 0.994741
 Std Err of Coef. 0.004492

Tw vs. K's (8.U./D)ⁿ

K' = 0.009878
 n = 0.994741

Tw# = 6.516127
 Res/# = 579.8690

Regression Output:

Constant -15.1892
 Std Err of Y Est 0.410444
 R Squared 0.964582
 No. of Observations 18
 Degrees of Freedom 16

X Coefficient(s) 9.251965
 Std Err of Coef. 0.448004

t = 24.77261 deg C
 s.d.t = 0.453609 deg C

05P03160 5/13/90 16:36
 10 PSID Taps 14 1.0 PSID Taps 14 0.1 PSID Taps 14
 S = 2.7 S = 7.35 S = 9.9 <C> (ppa) =
 Z = 2.7 Z = 7.5 Z = 8.15 <E>= <I>=

Freq. (Hz)	Qrest (1/s)	Temp (deg C)	<U> (volts)	<U> (volts)	<U>f (volts)	<U>icorr (volts)
60	1.21416	24.7	4.329	0.0295	0.0315	4.2975
49	0.991564	24.7	2.891	0.0295	0.0315	2.8595
41	0.829676	24.7	2.117	0.0295	0.0315	2.0855
33	0.667788	24.7	1.466	0.0295	0.0315	1.4345
27	0.546372	24.7	1.080666	0.0295	0.0315	1.049166
19	0.384484	24.7	0.829666	0.0295	0.0315	0.798166
14	0.283304	24.7	0.4216	0.0295	0.0315	0.3921
10	0.202356	24.7	0.2738	0.0295	0.0315	0.2423
8	0.161888	24.7	0.203714	0.0295	0.0315	0.172214
30	0.60708	24.2	1.35525	0.0265	0.0295	1.32575
21	0.424956	24.2	0.763	0.0265	0.0295	0.7355
16	0.323776	24.2	0.507166	0.0265	0.0295	0.477666
12	0.242832	24.2	0.3314	0.0265	0.0295	0.3019
20	0.40472	24.8	7.3475	0.0595	0.17	7.1775
15	0.30354	24.8	4.828	0.0595	0.17	4.658
11	0.222596	24.8	3.046625	0.0595	0.17	2.876625
8	0.161888	24.8	2.0405	0.0595	0.17	1.8705
24.6	1.6588	24.6	1.6588	0.0365	0.0095	1.6493
24.6	1.1776	24.6	1.1776	0.0135	0.0025	1.1751
24.6	0.8622	24.6	0.8622	0.0015	-0.0025	0.8647
24.5	0.5845	24.5	0.5845	-0.0035	-0.0055	0.59
24.5	0.439	24.5	0.439	-0.0065	-0.0075	0.4465
24.5	2.809166	24.5	2.809166	-0.0125	-0.0265	2.835666
24.5	2.258285	24.5	2.258285	-0.0275	-0.0285	2.286785
24.45	1.707285	24.45	1.707285	-0.0315	-0.0345	1.741785
24.4	1.089444	24.4	1.089444	-0.0385	-0.0415	1.127944
24.4	0.852642	24.4	0.852642	-0.0445	-0.0455	0.877142
24.4	0.5614	24.4	0.5614	-0.0475	-0.0495	0.4089
24.3	0.249	24.3	0.249	-0.0505	-0.051	0.2995
24.3	0.135722	24.3	0.135722	-0.0525	-0.054	0.188222
24.2	0.111461	24.2	0.111461	-0.0545	-0.0555	0.165961
24.2	0.057375	24.2	0.057375	-0.056	-0.055	0.112375
24.1	-0.019	24.1	-0.019	-0.0555	-0.0555	0.0745
24.1	-0.012	24.1	-0.012	-0.0555	-0.0555	0.0433
24.2	3.565333	24.2	3.565333	-0.0555	-0.064	3.629333
24.3	5.7166	24.3	5.7166	-0.0665	-0.062	5.7786
24.3	7.156166	24.3	7.156166	-0.0665	-0.0635	7.219666
24.3	10.2755	24.3	10.2755	-0.0665	-0.0645	10.34

density viscosity ID(cm) = 1.45796
 cof(NaCl) 1.01234 1.029478 K(U/ps)= 1.08 11.9307
 4.991468 X coeff -0.00025 -0.02281 XS(cm2)= 1.669479
 0.300067 constant 0.003419 -4.14933

Batch (ml)	Vol (ml)	t (sec)	t/samp	DP (psid)	<U> (cm/s)	Re	Iw dyne/cm2	f	Log(Re/f)
3.979166	727.2685	115789.3	561.3723	0.002102	3.725049				
2.647685	593.9360	94561.28	373.5298	0.002097	3.636586				
1.931018	496.9668	79122.70	272.4259	0.002185	3.568046				
1.328240	399.9977	63684.12	187.3853	0.002320	3.486791				
0.971450	327.2708	52105.19	137.0501	0.002334	3.418863				
0.553858	230.3017	36666.61	78.13711	0.002318	3.296852				
0.363055	169.6960	27017.50	51.21910	0.003523	3.205139				
0.224351	121.2114	19298.22	31.65108	0.004267	3.100618				
0.159457	96.96914	15438.57	22.49595	0.004739	3.024476				
1.227546	363.6342	57245.27	173.1796	0.002594	3.464476				
0.679166	254.5440	40071.69	95.81539	0.002929	3.336215				
0.442283	193.9382	30530.81	62.39648	0.003286	3.243078				
0.279537	145.4537	22898.11	39.43649	0.003692	3.143447				
0.601615	242.4228	38683.61	84.87469	0.002861	3.215798				
0.390432	181.8171	29012.70	55.08133	0.003301	3.221911				
0.241117	132.3325	21275.98	34.01639	0.003790	3.117252				
0.156784	96.96914	15473.44	22.11885	0.004660	3.023790				
15	0.138243	86.25442	13701.72	0.005193	2.994491				
15	0.098496	67.68576	10752.04	0.006008	2.920878				
15	0.072478	56.50463	8975.900	0.006344	2.854273				
1411	20	0.049453	42.25867	6697.767	6.976811	0.007759	2.770282		
1459	25.1	0.037425	34.81773	5518.418	5.279909	0.008627	2.709766		
1452	25	0.037978	34.78928	5513.909	5.357890	0.008769	2.713950		
1255	25.1	0.030627	29.94945	4746.823	4.320799	0.009542	2.66625		
1269	30	0.023327	25.33723	4011.285	3.291041	0.010155	2.608627		
1160	35.2	0.015106	19.73941	3121.537	2.131210	0.010834	2.511781		
1367	50	0.007069	16.27636	2589.713	1.279437	0.009450	2.400977		
1124	50.1	0.005476	13.45839	2125.112	0.772601	0.008474	2.291446		
1010	59.9	0.004011	10.09981	1593.558	0.565894	0.010989	2.222850		
805	75	0.002520	6.429149	1014.197	0.355639	0.017043	2.121987		
575	59.9	0.002222	5.749895	905.1796	0.313578	0.018787	2.093671		
599	89.9	0.001505	3.991039	628.3910	0.212328	0.024404	2.009002		
659	150.1	0.000997	2.629805	413.0652	0.140765	0.040316	1.918760		
309	120	0.000582	1.542396	242.2653	0.082191	0.068433	1.801926		
1384	20.1	0.048607	41.24382	6492.826	6.887495	0.007985	2.763580		
1396	15	0.077393	55.74591	8795.644	10.91845	0.006959	2.865562		
1653	15	0.096693	66.00859	10414.90	13.64130	0.006201	2.915911		
2090	14.9	0.138484	84.01927	13256.64	19.53705	0.005482	2.991912		

Solvent	L	MHR	Tap DL=	1//f	1//f	1//f/Slv	1//f/L
1//f	1//f	1//f	122.2234	1//f	1//f	1//f	1//f
74.66555			40.77743				
74.66555							
0.4							
14.50019	331.8405	38.37594	21.80816	1.50390	0.065718		
14.14634	270.6865	36.49514	21.83367	1.543414	0.080660		
13.87218	231.1674	35.97288	21.39215	1.542089	0.092539		
13.54716	191.7219	35.84904	20.74057	1.532466	0.108284		
13.27545	163.9622	32.55841	19.86173	1.496124	0.121136		
12.78741	123.8034	30.24020	18.51050	1.447556	0.149515		
12.42055	100.2351	28.49765	16.84633	1.356326	0.168068		
12.00247	78.79492	26.51174	15.30731	1.275346	0.194267		
11.70590	66.42875	25.10304	14.52550	1.240869	0.218662		
13.45898	182.3327	33.43018	19.43330	1.458750	0.107737		
12.94486	135.5487	30.98809	18.47660	1.427330	0.136509		
12.57231	109.3850	29.21848	17.44457	1.387539	0.159478		
12.17378	86.96151	27.32549	16.45707	1.351844	0.189245		
12.86319	129.3237	30.60016	18.69514	1.453382	0.144560		
12.48764	104.1816	28.81631	17.40511	1.393786	0.167065		
12.06901	81.87160	26.82781	16.24188	1.345750	0.198382		
11.69516	66.01924	25.05201	14.64861	1.252536	0.224860		
11.37796	61.71221	24.49533	13.87663	1.198538	0.224860		
11.28351	52.09051	23.09669	12.90067	1.143321	0.247658		
11.01709	44.68420	21.83120	12.55463	1.139559	0.280963		
10.68112	36.82663	20.23535	11.36705	1.064218	0.308663		
10.43906	32.03662	19.08556	10.76583	1.031302	0.336047		
10.45180	32.27234	19.14605	10.67847	1.021687	0.330886		
10.26494	28.98115	18.23847	10.23687	0.997265	0.353225		
10.02651	25.24432	17.12592	9.923294	0.989705	0.392278		
9.647126	20.30773	15.33384	9.606984	0.995838	0.473070		
9.203911	15.73467	13.21857	10.28665	1.117638	0.653756		
8.765784	12.22717	11.13747	10.86264	1.239209	0.888401		
8.491403	10.44073	9.834167	9.539314	1.123408	0.913663		
8.087951	8.276904	7.917770	7.659848	0.947069	0.925448		
7.974684	7.754450	7.379749	7.595446	0.914850	0.940833		
7.636008	6.580903	5.771040	6.154017	0.805920	0.964443		
7.275040	5.183704	4.056444	4.980334	0.684578	0.960767		
6.807706	3.961017	1.836607	3.822649	0.561517	0.965067		
10.65432	36.26275	20.10803	11.19059	1.050333	0.308597		
11.06225	45.86103	22.04571	11.98681	1.083578	0.261372		
11.25564	51.26147	22.96431	12.69825	1.128167	0.247715		
11.56765	61.34692	24.44634	13.50581	1.167550	0.220154		

05P03160	Tw	8<U>/D	Log	Log
	dyne/cm ²	(1/sec)	Tw	8<U>/D
	0.772601	73.73808	-0.11204	1.867691
	0.565894	55.41889	-0.24726	1.743657
	0.355639	35.27750	-0.44899	1.547497
	0.213578	31.55035	-0.50365	1.499004
	0.212328	21.89930	-0.67299	1.340430
	0.140765	14.43005	-0.85150	1.159268
	0.082191	8.463315	-1.08517	0.927540

Regression Output:	
Constant	-2.01086
Std Err of Y Est	0.001903
R Squared	0.999957
No. of Observations	3
Degrees of Freedom	1

X Coefficient(s)	
X Coefficient(s)	0.998741
Std Err of Coef.	0.006505

Tw vs. K*(8<U>/D)^n	
K'	= 0.009752
n	= 0.998741

Tw#	
Tw#	= 5.352524
Res/#	= 518.4457

Regression Output:	
Constant	-25.8988
Std Err of Y Est	0.251146
R Squared	0.990353
No. of Observations	16
Degrees of Freedom	14

X Coefficient(s)	
X Coefficient(s)	13.39286
Std Err of Coef.	0.353267

t	
t	= 1.960167 deg C
s.d.t	= 0.224121 deg C

91P13154

5/7/90 15:42

10 PSID Taps 14 1.0 PSID Taps 14 0.1 PSID Taps 14
 S = 2.7 S = 7.25 S = 9.9 <C>(ppm)=
 Z = 2.7 Z = 7.65 Z = 8.1 [NaCl]=

24.2 8.6105 -0.0775 -0.0775 8.689

Freq. (Hz)	Dist Temp (1/s)	Temp (deg C)	<V> (volts)	<U> (volts)	<U>f (volts)	<V>corr (volts)
60	1.21416	24.5	3.141	0.0195	0.0235	3.1175
50	1.0118	24.5	2.200666	0.0195	0.0235	2.177166
42	0.849912	24.5	1.619333	0.0195	0.0235	1.595833
31	0.627316	24.5	1.013333	0.0195	0.0235	0.989833
23	0.465428	24.5	0.653666	0.0195	0.0235	0.630166
17	0.344012	24.5	0.42175	0.0195	0.0235	0.39825
13	0.263068	24.5	0.28375	0.0195	0.0235	0.26425
10	0.20236	24.5	0.2258	0.0195	0.0235	0.2023
8	0.161888	24.5	0.1776	0.0195	0.0235	0.1541
6	0.121416	24.5	0.087	0.0195	0.0235	0.0635
25	0.5059	23.9	0.776	0.0255	0.0205	0.7555
19	0.384484	23.9	0.595833	0.0255	0.0205	0.485333
14	0.283304	23.9	0.331666	0.0255	0.0205	0.311166
9	0.182124	23.9	0.266285	0.0205	0.0205	0.185785
35	0.70826	24.4	12.77733	0.0405	0.0465	12.73083
27	0.546372	24.9	8.977333	0.045	0.0785	8.898833
22	0.45192	24.9	6.562	0.045	0.0785	6.4835
16	0.323776	24.9	4.065	0.045	0.0785	3.9865
11	0.222596	24.9	2.452333	0.045	0.0785	2.373833
9	0.182124	24.9	1.980833	0.045	0.0785	1.902333
7	0.141652	24.9	1.565333	0.045	0.0785	1.486833
		24.7	1.4534	0.074	0.053	1.4004
		24.7	1.0754	0.0535	0.0495	1.0259
		24.6	0.860714	0.0495	0.0475	0.813214
		24.6	0.586833	0.0475	0.0445	0.542333
		24.6	0.4696	0.0445	0.0435	0.4261
		24.6	0.379857	0.0445	0.0435	0.336357
		24.5	0.314285	0.0445	0.0435	0.270785
		24.4	1.646166	0.0095	-0.0175	1.663666
		24.4	1.092	-0.0235	-0.0295	1.0715
		24.4	0.663714	-0.033	-0.0385	0.702214
		24.4	0.384833	-0.0425	-0.0495	0.427333
		24.3	0.257230	-0.0535	-0.0565	0.310730
		24.3	0.124769	-0.0595	-0.0595	0.184269
		24.2	0.0796	-0.0605	-0.0605	0.1401
		24.2	0.026777	-0.0605	-0.0605	0.081277
		24.1	-0.0233	-0.0575	-0.0595	0.037166
		24.1	2.506428	-0.0615	-0.0785	2.584928
		24.3	3.379333	-0.0795	-0.079	3.458333
		24.3	4.7564	-0.0805	-0.0805	4.8369
		24.3	5.725666	-0.0805	-0.0785	5.804166

density viscosity 12.05909
 ID(cm) = 1.45796 11.93037
 K(V/psi) = 1.08 12.03909
 XS(cm2) = 1.669479
 density viscosity
 cof(NaCl) 1.01234 1.029478
 9.97478 X coeff -0.00025 -0.02281
 0.299977 constant 0.003419 -4.14933

Batch Vol (gal)	t ₀ (sec)	DP (psid)	<U> (cm/s)	Re	Tu dyne/cm ²	f	Log (Re/f)
		2.86574	727.2685	115268.0	407.2317	0.001525	3.653374
		2.015895	604.0571	94054.71	284.3921	0.001533	3.575416
		1.477623	509.0880	80687.64	208.4599	0.001593	3.507964
		0.916512	375.7554	59555.16	129.2996	0.001814	3.404252
		0.585487	278.7862	44184.08	82.31720	0.002098	3.306198
		0.36875	206.0594	32659.28	52.02246	0.002427	3.206549
		0.244675	157.5748	24974.74	34.51836	0.002753	3.117478
		0.187514	121.2114	19211.34	26.42597	0.003563	3.059469
		0.142685	96.96914	15369.07	20.12972	0.004240	3.000372
		0.058796	72.72685	11526.80	8.294856	0.003106	2.807858
		0.699537	303.0285	47582.62	98.68920	0.002128	3.339677
		0.449582	230.3017	36010.79	63.39796	0.002367	3.243580
		0.288117	169.6960	24534.27	40.64697	0.002795	3.147056
		0.172023	109.0902	17057.74	24.246875	0.004039	3.035046
		1.057458	424.2400	67088.17	149.1839	0.001641	3.434329
		0.739161	327.2708	52340.82	104.2793	0.001928	3.361493
		0.538537	266.6651	42648.07	75.97571	0.002116	3.292731
		0.331129	193.9382	31014.78	46.71507	0.002460	3.187122
		0.197177	133.3325	21324.03	27.81733	0.003100	3.074552
		0.158013	109.0902	17446.94	22.29214	0.003711	3.026470
		0.123500	84.84800	13569.84	17.42318	0.004794	2.972958
		0.085214	66.68745	10617.39	12.02182	0.005355	2.890409
		20.0	0.67547	54.00547	8894.407	9.539503	0.06018
		20.1	0.045047	41.98883	6670.029	6.555234	0.06
		20.9	0.027938	29.87728	4744.080	3.941539	0.008747
		30	0.022492	25.45703	4034.799	3.173152	0.009699
1275		29.9	0.021794	25.44201	4023.331	3.074680	0.009409
1270		35.2	0.014036	19.39907	3067.718	1.980276	0.010423
1140		40.1	0.009199	16.44605	2600.735	1.297786	0.009504
1013		44.9	0.005598	13.51394	2137.058	0.789769	0.008564
1010		59.9	0.004070	10.09981	1593.558	0.574272	0.011151
596		59.9	0.002413	5.959891	940.3574	0.340554	0.018991
453		59.9	0.001833	4.529917	713.1241	0.258923	0.024994
264		60.1	0.001044	2.631166	414.2123	0.150212	0.042978
379		179.8	0.000486	1.262607	198.3186	0.068489	0.085346
1376		23	0.035862	34.19029	5370.292	4.777297	0.008094
1378		19.9	0.045304	41.41753	6534.898	6.391447	0.007360
1378		14.9	0.063363	55.39643	8740.503	8.939244	0.005770
1433		15	0.076033	65.26994	10288.88	10.72688	0.004996

76.33526
74.66555
76.33526

Tap DL= 122.2234
40.77743

11.39329 55.48872 23.61817 14.97573 1.314433 0.269887

Solvent	L	MDR	1//f	1//f	1//f/Slv	1//f/L
0.4						
14.21349	281.3548	37.01411	25.60557	1.801497	0.091008	
13.90166	235.1240	35.53292	25.53352	1.834723	0.108595	
13.65185	201.5005	34.25133	25.05198	1.837752	0.124450	
13.21700	158.5375	32.28079	23.47833	1.774372	0.148093	
12.82479	126.4966	30.41777	21.83165	1.702300	0.172586	
12.42619	100.5608	28.52443	20.29820	1.631501	0.201849	
12.06991	81.91409	26.83209	19.05559	1.570767	0.232628	
11.83787	71.67192	25.72991	16.75284	1.411190	0.233743	
11.60148	62.55362	24.60707	15.35589	1.321614	0.245483	
10.83143	40.15465	20.94930	17.94117	1.654399	0.446799	
12.95870	136.6335	31.05386	21.67414	1.671554	0.158629	
12.57432	109.5115	29.22802	20.55193	1.631437	0.187669	
12.18822	87.68726	27.39407	18.91257	1.551708	0.215682	
11.74026	67.75574	25.26625	15.73459	1.340224	0.232225	
13.33731	169.9062	32.85225	24.67837	1.850325	0.145247	
13.04597	143.6724	31.46837	22.76916	1.745301	0.158479	
12.77092	122.6342	30.16190	21.73540	1.701944	0.177237	
12.34849	96.16186	28.15533	20.15922	1.612525	0.209438	
11.89820	74.20481	26.01648	17.96045	1.509509	0.242038	
11.70588	66.42786	25.10293	16.41530	1.402312	0.247114	
11.49183	58.72704	24.08620	14.44164	1.256687	0.245911	
11.43193	56.73651	23.80166	13.19395	1.329080	0.267798	
10.95589	43.13739	21.54050	12.88992	1.176529	0.298811	
10.60401	35.22772	19.86908	11.83377	1.115970	0.339222	
10.39450	31.22533	18.87591	11.05758	1.063791	0.354122	
10.18908	27.74289	17.89816	10.69210	1.049368	0.385399	
9.997696	24.83585	16.98478	10.15366	1.015692	0.408831	
9.965473	24.39205	16.83599	10.30902	1.034473	0.422638	
9.583325	19.57543	15.02079	9.794542	1.022040	0.500348	
9.216280	15.8471	13.27333	10.25713	1.11936	0.647256	
8.784874	12.36228	11.22815	10.80432	1.229878	0.873975	
8.504168	10.51773	9.894801	9.469475	1.113509	0.900334	
8.050305	8.099467	7.738952	7.256321	0.901372	0.895901	
7.898335	7.040345	6.589594	6.253501	0.810070	0.897671	
7.335402	5.366989	4.343164	4.823613	0.657579	0.898755	
6.651825	3.621066	1.096172	3.423001	0.514595	0.945332	
10.33641	30.19839	18.59797	11.11460	1.075286	0.368052	
10.59713	35.08839	19.83638	11.64006	1.098416	0.331735	
10.88853	41.49670	21.22053	13.16445	1.209019	0.317240	
11.04687	45.45691	21.97267	13.14648	1.280586	0.311206	

Cyanamid 952A

Page 7

01P13154

Tw	B<U>/D	Log	Log
dyne/cm ²	(1/sec)	Tw	B<U>/D
0.789769	74.15259	-0.10249	1.870126
0.574272	55.41889	-0.24088	1.743657
0.340554	32.70263	-0.46781	1.514582
0.258923	24.85619	-0.58682	1.395434
0.150212	14.43752	-0.82329	1.159492
0.068689	6.928078	-1.16311	0.840612

Regression Output:

Constant	-1.97878
Std Err of Y Est	0.000956
R Squared	0.999989
No. of Observations	4
Degrees of Freedom	2

X Coefficient(s)	0.997100
Std Err of Coef.	0.002269

Tw vs. K*(B<U>/D)^n	
K'	0.010500
n	0.997100
	14397.84

Twt	5.898375
Res/fs	541.7759

Regression Output:

Constant	-42.8489
Std Err of Y Est	0.568876
R Squared	0.961354
No. of Observations	10
Degrees of Freedom	8

X Coefficient(s)	19.52735
Std Err of Coef.	1.384227

t	24.44285	deg C
s.d.\t	0.277010	deg C

02P13157

Cyanamid 832A

5/10/90 15:54

10 PSID Taps 14 1.0 PSID Taps 14 0.1 PSID Taps 14
 S = 2.7-S = 7.25 S = 9.9 <C>(ppa)=
 Z = 2.7 Z = 8.15 Z = 7.5 [NaCl]=

Freq. (Hz)	Dist Temp (1/s)	Temp (deg C)	<U> (volts)	<U> (volts)	<U>f (volts)	<U>corr (volts)
60	1.21416	24.9	2.405666	0.0365	0.0375	2.368166
49	0.991564	24.9	1.717	0.0365	0.0375	1.6795
41	0.829676	24.9	1.258	0.0365	0.0375	1.2005
34	0.688024	24.9	0.96525	0.0365	0.0375	0.92775
27	0.546372	24.9	0.683166	0.0365	0.0375	0.645666
20	0.40492	24.9	0.4524	0.0365	0.0375	0.4149
14	0.283304	24.9	0.3075	0.0365	0.0375	0.27
10	0.20236	24.9	0.215	0.0365	0.0375	0.1775
8	0.161888	24.9	0.15825	0.0365	0.0375	0.12175
30	0.60708	23.9	0.790333	0.0345	0.0315	0.755833
30	0.60708	24.9	8.399	-0.0225	-0.0015	8.4005
23	0.465428	24.9	5.757666	-0.0225	-0.0015	5.759166
17	0.344012	24.9	3.582	-0.0225	-0.0015	3.5835
13	0.243068	24.9	2.721833	-0.0225	-0.0015	2.723333
9	0.182124	24.9	1.585166	-0.0225	-0.0015	1.586666
7	0.141652	24.9	1.210666	-0.0225	-0.0015	1.212166
		24.7	1.2174	0.0055	-0.011	1.2284
		24.7	0.8574	-0.0135	-0.0165	0.8709
		24.7	0.6435	-0.0175	-0.0195	0.661
		24.6	0.47714	-0.0205	-0.0235	0.498214
		24.6	0.363	-0.0235	-0.0255	0.3865
		24.5	0.257125	-0.0255	-0.0255	0.262625
		24.4	1.610571	-0.0125	0.0005	1.623071
		24.4	1.080428	0.0045	0.0065	1.07928
		24.3	0.650666	0.005	0.0025	0.648166
		24.3	0.416615	0.0005	-0.0025	0.419115
		24.2	0.307764	-0.005	-0.0065	0.312764
		24.2	0.233470	-0.0075	-0.0075	0.240970
		24.1	0.085583	-0.0085	-0.0075	0.093083
		24.1	0.1625	-0.0115	-0.0115	0.174
		24	0.035708	-0.0125	-0.0075	0.045708
		24	2.477285	-0.0095	-0.0135	2.490785
		24.1	3.116571	-0.0145	-0.0135	3.130071
		24.1	4.548285	-0.0135	-0.0135	4.561785
		24	5.407833	-0.0145	-0.0085	5.416333
		23.9	7.608	-0.009	-0.009	7.617

Cyanamid 832A

density viscosity

col[NaCl] 1.01234 1.029478 ID(cm) = 1.45796
 20.00475 X coeff -0.00025 -0.02581 K(W/psi) = 1.08 12.03909
 0.300206 constant 0.003419 -4.14933 XS(cm2) = 1.669479

Batch Vol (ml)	t (sec)	DP (psid)	<U> (cm/s)	Re	Tw dyne/cm2	f	Log(Re/f)
2.192746	727.2685	116312.9	309.3480	0.001158	3.597618		
1.555092	593.9360	94988.90	219.3891	0.001232	3.523001		
1.111574	496.9668	79480.51	156.8185	0.001257	3.450093		
0.859027	412.1188	65910.66	121.1898	0.001413	3.394127		
0.597859	327.2708	52340.82	84.34192	0.001560	3.215416		
0.384166	242.4238	38770.98	54.19741	0.001827	3.219282		
0.25	169.6960	27139.68	35.26946	0.002426	3.126093		
0.164551	121.2114	19385.49	23.18641	0.003126	3.035011		
0.112731	96.96914	13508.39	15.90391	0.003350	2.953146		
0.699845	363.6342	56859.15	98.73274	0.001478	3.339772		
0.697768	363.6342	58156.47	98.43972	0.001474	3.348979		
0.478372	278.7862	44586.62	67.48774	0.001720	3.267006		
0.297655	206.0594	32955.33	41.99259	0.001959	3.163980		
0.226207	157.5748	25201.13	31.91288	0.002346	3.104377		
0.131792	109.0902	17446.94	18.59306	0.003095	2.987069		
0.100485	84.84800	13569.84	14.20455	0.003909	2.928088		
15	0.102034	84.85678	13510.15	14.39478	0.003960	2.925234	
15	0.072339	65.52940	10433.01	10.20548	0.004708	2.854840	
20	0.054904	54.68770	8706.896	7.745807	0.005120	2.794957	
25	0.041383	40.92293	6500.708	5.858233	0.006906	2.723579	
25	0.032103	33.95070	5393.152	4.529129	0.007784	2.677446	
30.1	0.021814	25.17346	3989.854	3.077523	0.009650	2.592354	
29.9	0.021262	25.16154	3978.979	2.999655	0.009285	2.586004	
30	0.014068	19.56697	3094.269	1.984765	0.010269	2.496332	
40.2	0.008491	16.22634	2560.208	1.197899	0.009012	2.385893	
39.9	0.005490	13.29093	2112.834	0.774581	0.008556	2.291016	
60	0.004097	9.993134	1573.173	0.578031	0.011465	2.226472	
59.9	0.003156	7.839856	1234.192	0.445346	0.014352	2.169846	
90	0.001219	3.149111	473.5541	0.172030	0.037487	1.962315	
59.9	0.002279	5.619897	882.7210	0.321575	0.020167	2.098154	
100	0.000598	1.479503	231.8628	0.084475	0.076440	1.806892	
247	0.032629	33.92674	5216.887	4.603308	0.007921	2.675062	
1416	0.041004	40.41978	6348.762	5.784795	0.007013	2.725656	
1687	0.059759	53.81871	8453.341	8.430796	0.005765	2.807447	
1788	0.070954	64.03957	10036.07	10.01011	0.004834	2.843747	
1593	0.099783	82.46082	12893.86	14.67724	0.004100	2.916801	
2065							

02P13157

Tw	8<U>/D	Log	Log
dynes/cm ²	(1/sec)	Tw	8<U>/D
0.774581	73.47764	-0.11093	1.866155
0.578031	54.83351	-0.23804	1.739046
0.445346	43.01822	-0.35130	1.633652
0.174030	16.54317	-0.76439	1.218618
0.321575	30.83704	-0.49271	1.489072
0.084475	8.118209	-1.07327	0.909460

02P13157

Tap DL = 122.2234
40.77743

Solvent	L	MDR	1/f/f	1/f/f	1/f/f/S1v	1/f/f/L
76.33526	4					
0.4						

13.99047	247.4560	35.95474	29.37717	2.099798	0.118716
13.59200	208.3924	34.53703	28.48858	2.080672	0.136706
13.40037	176.1866	33.15176	28.19471	2.104024	0.160027
13.17650	158.8843	32.08842	26.59673	2.018496	0.171720
12.36166	129.2100	30.59290	25.31771	1.968463	0.195942
12.47753	103.5770	28.74828	23.39500	1.874970	0.225870
12.10437	85.55526	26.99578	20.30070	1.677137	0.242961
11.74004	67.74716	25.26521	17.88404	1.523356	0.263982
11.41258	56.10821	23.70978	17.27509	1.513487	0.307888
12.95909	156.6636	31.05568	26.00323	2.006563	0.190271
12.99591	139.5916	31.23061	26.03865	2.003402	0.186534
12.66802	115.5810	29.67312	24.11003	1.903219	0.208598
12.25592	91.17183	27.71563	22.59149	1.843312	0.247790
12.01750	79.47991	26.58317	19.81722	1.649029	0.249336
11.54827	60.66662	24.35832	17.97419	1.556439	0.296278
11.31443	53.02591	23.24355	15.99435	1.413624	0.301632
11.31810	53.13815	23.26100	15.89036	1.403977	0.299038
11.01936	44.74255	21.84197	14.57367	1.322551	0.323723
10.77982	38.97959	20.70418	13.96066	1.295072	0.358153
10.53031	33.76443	19.51900	12.03320	1.142719	0.356386
10.30978	29.73898	18.47147	11.33434	1.099377	0.381127
9.970216	24.45874	16.85853	10.19536	1.022582	0.416839
9.944016	24.09262	16.73407	10.32209	1.038020	0.428433
9.585291	19.59760	15.03013	9.868137	1.029508	0.503537
9.142773	15.19054	12.92817	10.53372	1.152136	0.693439
8.764067	12.21509	11.12931	10.81057	1.233510	0.885017
8.305894	10.52819	9.903000	9.339053	1.097950	0.887052
8.279387	9.241168	8.827090	8.347110	1.008179	0.903252
7.449262	5.730540	4.883996	5.164806	0.693331	0.901277
7.992617	7.834914	7.464930	7.041565	0.881008	0.898741
6.827568	4.006564	1.930950	3.616921	0.529752	0.902748
10.30025	29.57621	18.42618	11.23556	1.090804	0.379885
10.50262	33.23049	19.38747	11.94076	1.136931	0.359331
10.82978	40.11687	20.94149	13.16986	1.216077	0.328287
10.97498	43.61412	21.63119	14.39191	1.310426	0.329753
11.26720	51.60374	23.01922	15.61643	1.386008	0.302622

Regression Output:

Constant -1.97833
Std Err of Y Est 0.001674
R Squared 0.999985
No. of Observations 4
Degrees of Freedom 2

X Coefficient(s) 0.995396
Std Err of Coef. 0.002667

Tw vs. K*(8<U>/D)^n

K' = 0.010511
n = 0.995396

Tw = 3.494575
Res/fs = 420.8153

Regression Output:

Constant -45.3727
Std Err of Y Est 0.651620
R Squared 0.989413
No. of Observations 28
Degrees of Freedom 26

X Coefficient(s) 21.13878
Std Err of Coef. 0.428818

t = 24.53611 deg C
s.d.)t = 0.368293 deg C

05F13150

4/30/90 15:54

10 FSID Taps 14 1.0 FSID Taps 14 0.1 FSID Taps 14
 S = 2.7 S = 7.25 S = 7.9 C (ppm) =
 Z = 2.7 Z = 7.65 Z = 8.1 [NaCl] =

Density viscosity
 ID(cm) = 1.4579
 K((psi)/=1.097177 11.93377
 XS(cm2) = 1.569479

Batch Vol (ml)	t (sec)	DP (psid)	U (cm/s)	Re	Tw (dyne/cm2)	f	Log(Re/f)
60	1.21416	25.5	1.9205	0.0405	0.0445	1.874	
50	1.0118	25.5	1.415	0.0405	0.0445	1.3715	
39	0.789204	25.5	1.03665	0.0405	0.0445	0.992163	
30	0.60708	25.5	0.688	0.0405	0.0445	0.6435	
23	0.465428	25.5	0.4664	0.0405	0.0445	0.4221	
17	0.24012	25.5	0.30966	0.0405	0.0445	0.265166	
10	0.20526	25.5	0.19422	0.0405	0.0445	0.149325	
7	0.141552	24	0.145322	0.0405	0.0445	0.100822	
30	0.60708	24	0.6834	0.0405	0.0445	0.5429	
10	0.485664	24	0.51	0.0405	0.0445	0.4755	
10	0.20226	24	0.1622	0.0405	0.0445	0.1487	
30	0.60708	25.35	7.22575	0.0625	0.1045	7.12125	
22	0.445192	25.35	4.2212	0.0625	0.1045	4.2167	
16	0.232776	25.35	2.76428	0.0625	-0.1045	2.662928	
10	0.20226	25.35	1.542	0.0625	0.1045	1.4375	
8	0.161388	25.35	1.42075	0.0625	0.1045	1.31525	
6	0.121416	25.35	0.895	0.0625	0.1045	0.7805	
24.9	0.795	25	1.1038	0.0265	0.0265	1.0672	2093
24.8	0.677	24.8	0.795	0.0295	0.0295	0.7665	1520
24.8	0.479325	24.8	0.479325	0.0205	0.0205	0.6525	1363
24.7	0.412142	24.7	0.412142	0.0175	0.0175	0.458822	1392
24.7	0.27025	24.7	0.27025	0.0125	0.0115	0.294642	1425
24.5	1.6005	24.5	1.6005	0.0455	0.0515	1.555	1264
24.4	0.673666	24.4	0.673666	0.049	0.0485	0.63566	1258
24.4	0.45325	24.4	0.45325	0.0465	0.0465	0.450822	946
24.4	0.33220	24.4	0.33220	0.0395	0.041	0.31225	1091
24.2	0.264928	24.2	0.264928	0.0375	0.039	0.294220	1313
24.2	0.19125	24.2	0.19125	0.0405	0.042	0.224929	976
24	0.117086	24	0.117086	0.047	0.0445	0.151125	717
24	0.081909	24	0.081909	0.0455	0.0445	0.063566	484
24.2	0.421166	24.2	0.421166	0.0465	0.0455	0.26409	220
24.2	0.346222	24.2	0.346222	0.0545	0.051	0.272166	231
24.2	0.407	24.2	0.407	0.0555	0.054	0.292222	1412
24.2	0.6708	24.2	0.6708	0.052	0.0505	0.9785	1554
24.2	0.7853	24.2	0.7853	0.0515	0.052	4.5198	1742
24.1	6.4702	24.1	6.4702	0.051	0.051	4.7746	1580
				0.0505	0.0505	6.4197	2044
1.709842	727.2685	117998.0	241.2209	0.000993	0.000993	2.549217	
1.250025	506.0571	98748.38	174.2510	0.000951	0.000951	2.481194	
0.904290	472.7245	76577.73	127.5753	0.001121	0.001121	2.411380	
0.586595	363.8342	58949.03	82.74290	0.001259	0.001259	2.317170	
0.394714	278.7832	45194.25	54.27471	0.001793	0.001793	2.225694	
0.241660	206.0594	33404.45	34.09582	0.001591	0.001591	2.124856	
0.128562	121.2114	19649.67	19.26596	0.002593	0.002593	2.000709	
0.091902	94.84800	13754.77	12.96541	0.003588	0.003588	2.914670	
0.585958	363.6342	56987.57	82.66275	0.001210	0.001210	2.302190	
0.433784	290.9074	45590.05	61.14102	0.001421	0.001421	2.225397	
0.135529	121.2114	18995.85	19.12023	0.002577	0.002577	2.984274	
0.597729	363.6342	58749.88	84.22773	0.001263	0.001263	2.719811	
0.252442	266.6651	42083.24	49.86292	0.001789	0.001789	2.505715	
0.222205	193.9382	31333.27	31.48941	0.001658	0.001658	2.105909	
0.120490	121.2114	19585.29	16.99858	0.002292	0.002292	2.972074	
0.110727	96.96914	15666.63	15.56479	0.002279	0.002279	2.752999	
0.065421	72.72685	11749.97	9.229494	0.003457	0.003457	2.329413	
14.9	0.089460	84.13987	12486.98	12.62093	0.00352	2.907425	
15.0	0.062427	64.69081	10246.08	9.062947	0.004270	2.871052	
14.9	0.054692	54.79343	8743.432	7.715881	0.005091	2.795101	
20.1	0.029459	41.48222	6619.252	5.425251	0.006245	2.713679	
25	0.023078	34.14237	5425.849	4.666397	0.007930	2.684928	
30	0.021520	25.23740	4018.078	3.076095	0.009443	2.591531	
29.9	0.020527	25.20161	3994.316	2.892975	0.009022	2.549750	
30	0.013401	18.98812	2986.717	1.990609	0.010497	2.485767	
40	0.008227	16.22742	2592.557	1.174841	0.008719	2.282427	
60	0.005942	13.10787	2072.844	0.757757	0.003851	2.290010	
60	0.003884	9.742555	1540.819	0.547994	0.011422	2.134444	
59.9	0.003269	7.169869	1121.263	0.418898	0.016141	2.152627	
59.9	0.001994	4.829111	761.9251	0.281449	0.022799	2.070196	
90	0.000905	2.196293	344.1958	0.127646	0.052435	1.895416	
119.8	0.000480	1.154978	181.0045	0.067806	0.100491	1.759184	
24.9	0.021214	33.79082	5251.019	4.417823	0.007574	2.668193	
20.1	0.042461	46.20990	7290.255	6.121521	0.005697	2.776744	
14.9	0.052493	57.94921	8492.979	7.405668	0.005046	2.706269	
15	0.060972	61.25661	9642.248	8.601884	0.004504	2.812794	
14.9	0.062501	62.51696	9999.184	9.317546	0.004239	2.818171	
15	0.084746	81.62224	12820.46	11.95551	0.003554	2.895777	

Density viscosity
 ID(cm) = 1.4579
 K((psi)/=1.097177 11.93377
 XS(cm2) = 1.569479

05P13150

Tw 8<U>/D Log Log
 dyne/cm² (1/sec) Tw 8<U>/D

 0.767759 71.92448 -0.11477 1.856876
 0.547964 53.46404 -0.26124 1.728061
 0.418898 39.34192 -0.37789 1.594855
 0.281449 26.55717 -0.55059 1.424181
 0.127696 12.05132 -0.89382 1.081024
 0.067806 6.337506 -1.16872 0.801918

Regression Outputs
 Constant -1.95939
 Std Err of Y Est 0.006384
 R Squared 0.999783
 No. of Observations 5
 Degrees of Freedom 3

 X Coefficient(s) 0.987127
 Std Err of Coef. 0.008396

 Tw vs. K'*(8<U>/D)^n
 K' = 0.010979
 n = 0.987127

 Regression Outputs
 Constant -53.2586
 Std Err of Y Est 0.115907
 R Squared 0.996677
 No. of Observations 6
 Degrees of Freedom 4

X Coefficient(s) 24.29819
 Std Err of Coef. 0.701470

 t = 24.75526 deg C
 s.d.t = 0.574890 deg C

Tap DL= 122.2274
 40.77745

Solvent	L	MDK	1//f	1//f	1//f	1//f	1//f	1//f	1//f
75.75206									
0.4									
0.4									
13.79805	221.5098	35.04074	35.26546	2.410881	0.150175				
13.52597	189.3976	35.74839	32.42133	2.396967	0.171181				
13.24475	161.0701	32.41259	29.73247	2.244848	0.184570				
12.86868	129.7331	30.52624	28.39917	2.206843	0.218904				
12.59241	105.0713	28.88448	26.88207	2.150230	0.255855				
12.09862	83.27111	26.96846	25.06964	2.072107	0.301031				
11.60280	62.50094	24.51331	19.61799	1.690797	0.315381				
11.25879	51.35452	22.97927	16.73997	1.486835	0.225968				
12.80876	125.3344	30.34161	28.41775	2.218618	0.226275				
12.54677	107.7888	29.09718	26.43480	2.106900	0.245246				
11.53709	60.27755	24.30120	19.69630	1.707214	0.326761				
12.87925	130.5248	30.57444	28.13156	2.184254	0.215526				
12.42286	100.3383	28.50861	26.82831	2.159583	0.267297				
12.02263	79.75089	26.61223	24.55250	2.042019	0.307826				
11.48813	58.60223	24.06864	20.88582	1.818034	0.356399				
11.41159	56.07651	23.70508	17.46138	1.530135	0.311284				
10.95766	43.18139	21.54891	17.00671	1.552037	0.393943				
11.21570	50.09656	22.77458	16.82623	1.500248	0.325880				
10.92421	42.25775	21.39000	15.26591	1.397439	0.360404				
10.78040	38.99257	20.70693	14.01457	1.300004	0.359416				
10.47455	32.69784	19.25414	12.65250	1.207927	0.386952				
10.33971	30.25579	18.61764	11.22894	1.086001	0.371133				
9.966326	24.40403	16.84005	10.39050	1.032527	0.421672				
9.917403	23.72575	16.50766	10.52183	1.060946	0.443466				
9.543077	19.12710	14.82961	9.740091	1.022740	0.510275				
9.129851	15.07779	12.86670	10.70927	1.172998	0.710267				
8.740323	12.19879	11.11153	10.62883	1.213292	0.872016				
8.467378	10.29733	9.70048	9.352058	1.104480	0.908202				
8.230150	8.982924	8.593216	7.870967	0.956357	0.876214				
7.880793	7.346464	6.933768	6.482073	0.822515	0.882339				
7.186445	4.926021	3.625710	4.367051	0.607678	0.886529				
6.656658	3.589589	1.024129	3.151553	0.474870	0.877970				
10.27241	29.10601	18.39395	11.49026	1.118555	0.394776				
10.55712	34.23957	19.54635	12.38821	1.258995	0.387529				
10.72112	37.58432	20.42533	14.08572	1.312829	0.373782				
10.85117	40.61390	21.04310	14.83997	1.367590	0.365391				
10.87248	41.11988	21.14526	15.19821	1.397834	0.369607				
11.13320	47.77298	22.38274	16.77263	1.506540	0.351090				

01P23147

10 PSID Taps 14 1.0 PSID Taps 14 0.1 PSID Taps 14
 S = 2.7 S = 7.25 S = 9.9 C: (ppm) =
 Z = 2.7 Z = 8 Z = 7.65 [NaCl]=

Cyanamid 832A

4/26/90 15:09

Freq. (Hz)	D'est (1/s)	Temp (deg C)	<V> (volts)	<V>0 (volts)	<V>f (volts)	<V>corr (volts)
60	1.21416	24.9	1.896	0.118	0.1065	1.7895
50	1.0118	24.9	1.4205	0.118	0.1065	1.314
40	0.80944	24.9	1.0405	0.118	0.1065	0.934
31	0.627316	24.9	0.706	0.118	0.1065	0.5995
25	0.5059	24.9	0.538333	0.118	0.1065	0.431833
18	0.364268	24.9	0.37325	0.118	0.1065	0.26675
11	0.222596	24.9	0.2328	0.118	0.1065	0.1463
8	0.161888	24.9	0.193	0.118	0.1065	0.0865
60	1.21416	24.15	1.916	0.0375	0.0945	1.8215
47	0.951092	24.15	1.3	0.0375	0.0945	1.2055
37	0.74872	24.15	0.96325	0.0375	0.0945	0.86875
26	0.526126	24.15	0.5745	0.0375	0.0945	0.48
17	0.344012	24.15	0.3504	0.0375	0.0945	0.2559
10	0.20236	24.15	0.231333	0.0375	0.0945	0.136833
25	0.5059	24.8	5.479666	-0.0005	0.1215	5.358166
18	0.364268	24.8	3.242666	-0.0005	0.1215	3.121166
12	0.242832	24.8	2.17975	-0.0005	0.1215	2.05825
8	0.161888	24.8	1.064333	-0.0005	0.1215	0.942833
11	0.222596	24.7	0.980333	0.0775	0.0765	0.903833
8	0.161888	24.6	0.6725	0.0665	0.0645	0.609
24.6	0.562833	24.6	0.562833	0.0605	0.0565	0.506333
24.6	0.428	24.6	0.428	0.0565	0.0565	0.3715
24.5	0.362166	24.5	0.362166	0.0535	0.0515	0.311666
24.5	0.30975	24.5	0.30975	0.0505	0.049	0.25925
24.3	1.5468	24.3	1.5468	0.0085	0.0125	1.5343
24.3	1.162111	24.3	1.162111	0.0115	0.0145	1.147611
24.3	0.7141	24.3	0.7141	0.0135	0.0075	0.7066
24.3	0.58825	24.3	0.58825	0.0075	0.0045	0.58375
24.3	0.5	24.3	0.5	0.0045	0.0045	0.4955
24.2	0.358166	24.2	0.358166	0.0055	0.009	0.345166
24.2	0.0888	24.2	0.0888	0.0085	0.014	0.0803
24.15	0.165692	24.15	0.165692	0.0125	0.0115	0.154192
24.1	0.2132	24.1	0.2132	0.0115	0.0125	0.2007
24	0.0578	24	0.0578	0.0115	0.0125	0.0457
24.2	2.566333	24.2	2.566333	0.0085	0.0105	2.555833
24.2	3.126	24.2	3.126	0.0095	0.0115	3.1145
24.2	3.559	24.2	3.559	0.0215	0.0215	3.5275
24.2	3.86025	24.2	3.86025	0.0135	0.0225	3.83775
24.2	5.4232	24.2	5.4232	0.019	0.029	5.3942

Cyanamid 832A

density viscosity

col/NaCl ID(cm) = 1.45796
 99.99499 X coef K(W/psi) = 1.09165
 0.299995 constant 0.003419 -4.14933 XS(cm2) = 1.669479

Batch Vol (ml)	t (sec)	DP (psid)	W (cm/s)	Re	Tw (dyne/cm2)	f	Log(Re/f)
1.639257	727.2685	116312.9	231.2629	0.000866	3.574447		
1.203679	606.0571	96927.45	169.8125	0.000915	3.467279		
0.855583	484.8457	77541.96	120.7038	0.001017	3.392254		
0.549167	375.7554	60095.02	77.47534	0.001087	3.296976		
0.395577	303.0285	48463.72	55.80733	0.001204	3.225739		
0.244254	218.1805	34893.88	34.47297	0.001424	3.121122		
0.134016	133.3325	21324.03	18.90882	0.002107	2.990703		
0.079237	96.96914	15508.39	11.17867	0.002355	2.876589		
1.668570	727.2685	114761.4	235.2983	0.000881	3.570907		
1.104288	569.6937	89583.16	155.7906	0.000950	3.441276		
0.795811	448.4822	70522.91	112.2713	0.001105	3.270179		
0.459700	315.1497	49556.64	62.03196	0.001327	3.241313		
0.234415	206.0594	32402.42	33.07079	0.001542	3.104727		
0.125345	121.2114	19060.24	17.48541	0.002384	2.968788		
0.449106	303.0285	48354.51	63.35897	0.001266	3.252312		
0.261607	218.1805	34815.25	36.90700	0.001535	3.14963		
0.172516	145.4537	23210.16	24.33828	0.002279	3.044554		
0.079035	96.96914	15473.44	11.14876	0.003348	2.875032		
15	0.075756	82.82022	13185.90	10.68760	0.007086	2.864864	2074
15	0.051044	64.29149	10212.86	7.201271	0.003451	2.778143	1610
15	0.042439	54.90733	8722.164	5.987264	0.003924	2.728052	1275
15	0.031138	41.41011	6578.097	4.328893	0.005074	2.670814	1077
20.1	0.06127	33.22750	5266.376	3.685379	0.006612	2.631694	1115
19.9	0.021729	28.23375	4474.894	3.065565	0.007618	2.591708	938
20.1	0.020254	28.16142	4443.337	2.857424	0.007137	2.574470	945
29.9	0.015149	23.23837	3666.572	2.137269	0.007839	2.511412	1160
40	0.009327	17.67017	2788.017	1.315946	0.008348	2.466102	1180
40	0.007705	15.27422	2409.981	1.087154	0.009230	2.446628	1020
40	0.006541	12.18942	1933.259	0.923801	0.012302	2.39027	814
59.9	0.004556	8.449845	1330.220	0.642825	0.017833	2.249544	845
59.9	0.001060	2.199959	346.296	0.149547	0.061206	1.972887	220
60	0.002035	2.22872	644.0380	0.287162	0.031897	2.074068	423
60	0.002549	5.731191	900.2020	0.37776	0.023540	2.110818	476
179.8	0.000598	1.219299	191.0845	0.084365	0.112400	1.805308	179.8
20.1	0.032739	4.295566	619.759	4.759890	0.004879	2.684396	1475
19.9	0.041114	52.15311	8207.078	5.800331	0.004227	2.727224	1722
20.1	0.046698	58.85589	9265.413	6.588111	0.00767	2.754878	1975
19.9	0.050661	62.78850	9884.506	7.147285	0.007591	2.772568	2086
20	0.071208	80.23452	12635.67	10.04596	0.007088	2.846492	2680

Y1P01443 10/31/90 12:37
 10 PSID Taps 14 1.0 PSID Taps 14 0.1 PSID Taps 14
 S = 2.7 S = 7.25 S = 9.9 C: (ppm) =
 Z = 2.85 Z = 9.15 Z = 6.9 [NaCl] =
 FlowCo = 0.019693

Tap Pair	Freq. (Hz)	Dist (1/s)	Temp (deg C)	<U> (volts)	<U>0 (volts)	<U>f (volts)	<U>corr (volts)
23	60	1.181580	24.9	9.736	0.0505	0.0535	9.6855
23	51	1.004343	24.9	7.199	0.0505	0.0535	7.1485
23	40	0.787720	24.9	4.505	0.0505	0.0535	4.49
23	30	0.590790	24.9	2.64225	0.0505	0.0535	2.59175
23	20	0.393860	24.9	1.277	0.0505	0.0535	1.2265
14	15	0.293395	24.9	2.1954	0.0505	0.0535	2.1449
14	10	0.196930	24.9	1.08325	0.0505	0.0535	1.03275
14	20	0.393860	24.9	3.613	0.0505	0.0535	3.5625
14	30	0.590790	24.9	7.803333	0.0505	0.0535	7.752833
23	17	0.334781	24.7	10.9405	0.0305	0.019	10.91
23	13	0.256009	24.7	6.7486	0.0305	0.019	6.7181
22	9	0.177237	24.7	3.574	0.0305	0.019	3.5435
23	7	0.137851	24.7	2.37125	0.0305	0.019	2.34075
14	14		24.5	6.246333	0.0425	0.0245	6.203833
14	14		24.4	4.7312	0.0115	0.0045	4.7197
14	14		24.3	3.753	-0.0035	-0.0095	3.7565
14	14		24.4	2.441142	-0.0105	-0.0145	2.451642
14	14		24.3	1.88175	-0.0155	-0.0215	1.89725
14	14		24.15	1.147714	-0.0245	-0.0265	1.172214
14	14		24.2	0.4085	-0.0245	-0.0245	0.433
14	14		24.1	2.627846	-0.0025	-0.0075	2.635346
14	14		24.1	1.215529	-0.0055	-0.004	1.219529
14	14		24	0.898333	-0.005	-0.001	0.899333
14	14		24.05	0.673347	0.0005	0.0045	0.668847
14	14		24	0.55832	0.0045	0.0065	0.55182
14	14		24	0.444625	0.0075	0.0105	0.434125
14	14		23.9	0.312304	0.0095	0.0145	0.297804
14	14		23.8	0.210708	0.0135	0.0145	0.196208
14	14		23.7	0.131807	0.0145	0.0155	0.116307
14	14		23.65	0.091909	0.0155	0.0155	0.076409
14	14		23.6	0.044347	0.0155	0.0145	0.029847
14	14		23.7	0.307385	0.015	0.0015	0.292285
14	14		23.8	1.58566	0.0135	0.004	1.58166
14	14		23.9	10.231	0.0015	0.0055	10.2255
23	24	7.80725	24	7.80725	0.002	0.0065	7.80075
23	24.1	9.645	24.1	9.645	0.0015	0.0075	9.6375
23	24.2	12.7415	24.2	12.7415	0.0025	0.0105	12.731

density viscosity ID(cm) = 1.02108
 co[NaCl] 1.00088 1.001574 K(U/psi)=1.098348 13.19632
 0.999734 X coeff -0.00025 -0.02281 XS(cm2) = 0.818859
 0.000100 constant 0.003419 -4.14933

Batch	Vol (ml)	t samp (sec)	DP (psid)	<U> (cm/s)	Re	Tw dyne/cm2	f	Log(Re/f)							
8.818243	1442.958	164114.5	5914.435	0.003770	4.003332	8.818243	1442.958	164114.5	5914.435	0.003770	4.003332				
6.508410	1225.514	139497.3	2889.096	0.003851	3.937779	6.508410	1225.514	139497.3	2889.096	0.003851	3.937779				
4.087957	961.9723	109409.6	1814.652	0.003932	3.826395	4.087957	961.9723	109409.6	1814.652	0.003932	3.826395				
2.359680	721.4792	82057.27	1047.466	0.004035	3.717068	2.359680	721.4792	82057.27	1047.466	0.004035	3.717068				
1.116677	480.9861	54704.84	495.6950	0.004296	3.554605	1.116677	480.9861	54704.84	495.6950	0.004296	3.554605				
1.932841	360.7396	41028.63	288.8935	0.004452	3.437367	1.932841	360.7396	41028.63	288.8935	0.004452	3.437367				
0.940275	240.4930	27352.42	139.0996	0.004823	3.278661	0.940275	240.4930	27352.42	139.0996	0.004823	3.278661				
3.243507	480.9861	54704.84	479.8280	0.004159	3.547541	3.243507	480.9861	54704.84	479.8280	0.004159	3.547541				
7.058651	721.4792	82057.27	1044.218	0.004023	3.716394	7.058651	721.4792	82057.27	1044.218	0.004023	3.716394				
0.826745	408.8382	46289.78	366.8618	0.004401	3.487279	0.826745	408.8382	46289.78	366.8618	0.004401	3.487279				
0.509088	312.6409	35398.07	285.9041	0.004634	3.381990	0.509088	312.6409	35398.07	285.9041	0.004634	3.381990				
0.268521	216.4437	24506.35	119.1544	0.005100	3.243083	0.268521	216.4437	24506.35	119.1544	0.005100	3.243083				
0.177378	168.3451	19060.50	78.71052	0.005569	3.152044	0.177378	168.3451	19060.50	78.71052	0.005569	3.152044				
15	0.470118	161.7697	18233.53	69.54694	0.005329	3.124196	15	0.470118	161.7697	18233.53	69.54694	0.005329	3.124196		
1686	15	0.357652	137.2640	15436.58	52.90933	0.005630	3.063878	1686	15	0.357652	137.2640	15436.58	52.90933	0.005630	3.063878
1458	15	0.284662	118.7016	13318.99	42.11155	0.005992	3.013287	1458	15	0.284662	118.7016	13318.99	42.11155	0.005992	3.013287
1556	19.9	0.185782	95.48762	10738.44	27.48369	0.006094	2.921610	1556	19.9	0.185782	95.48762	10738.44	27.48369	0.006094	2.921610
1625	25	0.143771	79.37869	8906.735	21.24877	0.006768	2.864958	1625	25	0.143771	79.37869	8906.735	21.24877	0.006768	2.864958
1210	24.9	0.088828	59.34397	6636.232	13.14089	0.007481	2.758921	1210	24.9	0.088828	59.34397	6636.232	13.14089	0.007481	2.758921
1220	44.9	0.032812	33.18211	3714.829	4.854067	0.008859	2.543154	1220	44.9	0.032812	33.18211	3714.829	4.854067	0.008859	2.543154
1216	44.9	0.032114	33.07332	3694.306	4.750896	0.008708	2.537504	1216	44.9	0.032114	33.07332	3694.306	4.750896	0.008708	2.537504
1248	59.9	0.014861	25.44358	2842.061	2.198518	0.006809	2.370181	1248	59.9	0.014861	25.44358	2842.061	2.198518	0.006809	2.370181
1006	60	0.010959	20.47563	2281.984	1.621282	0.007753	2.302060	1006	60	0.010959	20.47563	2281.984	1.621282	0.007753	2.302060
1155	99.9	0.008150	15.67220	1748.619	1.205771	0.009842	2.239256	1155	99.9	0.008150	15.67220	1748.619	1.205771	0.009842	2.239256
1070	99.9	0.006724	13.08003	1457.753	0.994798	0.011658	2.194999	1070	99.9	0.006724	13.08003	1457.753	0.994798	0.011658	2.194999
854	99.9	0.005290	10.53448	1174.055	0.782623	0.014139	2.162080	854	99.9	0.005290	10.53448	1174.055	0.782623	0.014139	2.162080
591	99.9	0.003629	7.224579	803.3561	0.536869	0.020622	2.062080	591	99.9	0.003629	7.224579	803.3561	0.536869	0.020622	2.062080
283	100	0.002391	4.677236	518.9256	0.353716	0.024416	1.970488	283	100	0.002391	4.677236	518.9256	0.353716	0.024416	1.970488
236	104.9	0.001417	2.747432	304.1326	0.209674	0.055689	1.855949	236	104.9	0.001417	2.747432	304.1326	0.209674	0.055689	1.855949
146	100	0.000931	1.782967	197.1467	0.137747	0.086870	1.764224	146	100	0.000931	1.782967	197.1467	0.137747	0.086870	1.764224
111	199.9	0.000363	0.678110	74.89572	0.053808	0.234594	1.559615	111	199.9	0.000363	0.678110	74.89572	0.053808	0.234594	1.559615
1195	25	0.088865	58.37586	6461.814	13.14623	0.007734	2.754576	1195	25	0.088865	58.37586	6461.814	13.14623	0.007734	2.754576
1265	20	0.141136	77.24157	8569.725	20.87896	0.006597	2.918018	1265	20	0.141136	77.24157	8569.725	20.87896	0.006597	2.918018
1126	15	0.124609	91.67321	10193.72	27.65313	0.007610	2.856615	1126	15	0.124609	91.67321	10193.72	27.65313	0.007610	2.856615
1456	15.1	0.095061	117.7538	13123.51	42.19786	0.006101	3.010776	1456	15.1	0.095061	117.7538	13123.51	42.19786	0.006101	3.010776
1658	15	0.117444	134.9844	15077.83	52.13369	0.005736	3.057376	1658	15	0.117444	134.9844	15077.83	52.13369	0.005736	3.057376
1948	15	0.155142	158.5945	17755.10	68.86787	0.005490	3.119110	1948	15	0.155142	158.5945	17755.10	68.86787	0.005490	3.119110

Solvent	L	MDR	DATA	1/f/f/SIV	1/f/f/L
1/f	1/f	1/f	1/f		
82.06026					
4					
0.4					
15.54911	629.8150	43.64332	16.28598	1.043082	0.025858
15.34951	541.0774	42.41020	16.11337	1.049764	0.029780
14.94558	428.8201	40.49150	15.94632	1.066959	0.037186
14.46827	325.7780	38.22430	15.74158	1.088007	0.048317
13.81842	224.1226	35.13750	15.25527	1.103980	0.068066
13.34946	171.0989	32.90997	14.98717	1.122679	0.087593
12.71464	118.7248	29.89456	14.59906	1.152478	0.121281
13.79016	220.5064	35.00328	15.50545	1.124385	0.070317
14.46557	325.2925	38.21148	15.76605	1.089901	0.048467
13.54911	191.9372	33.85830	15.07321	1.112486	0.078531
13.12796	150.6156	31.85781	14.68890	1.118902	0.097525
12.57233	109.3863	29.21857	14.00217	1.113729	0.128006
12.21217	88.90464	27.50784	13.39953	1.097227	0.150718
12.09678	83.19106	26.95973	13.89853	1.132412	0.164663
11.85335	72.39667	25.81293	13.32639	1.124082	0.184074
11.65315	64.44184	24.85247	12.91765	1.108511	0.200454
11.28644	52.17831	23.11059	12.86268	1.139657	0.246513
11.05983	45.79715	22.03421	12.15514	1.099034	0.265412
10.63568	35.87582	20.01951	11.56111	1.087011	0.322253
9.772619	21.82905	15.91994	10.63613	1.088360	0.487246
9.750018	21.54689	15.81258	10.71589	1.099063	0.497328
9.080727	14.65756	12.63345	12.11857	1.334537	0.826779
8.812243	12.55859	11.35815	11.35668	1.288739	0.904296
8.557027	10.84268	10.14588	10.07948	1.177919	0.929611
8.387997	9.837577	9.342987	9.261575	1.104146	0.941467
8.179632	8.725453	8.353252	8.409701	1.028127	0.963812
7.848323	7.210426	6.779537	6.963493	0.887258	0.965753
7.481955	5.839409	5.039289	5.554132	0.742336	0.951146
7.023796	4.485489	2.863035	4.237540	0.603311	0.944679
6.656899	3.631658	1.120273	3.392849	0.509674	0.934242
5.838464	2.267233	-2.76729	2.064623	0.353624	0.910635
10.61830	35.51868	19.93696	11.37044	1.070834	0.320125
11.02406	44.86576	21.86429	11.93853	1.082952	0.266106
11.27207	51.74860	25.04235	12.31160	1.092521	0.237911
11.64310	64.07032	24.80476	12.80186	1.099523	0.199809
11.83070	71.37664	25.69584	13.20270	1.115969	0.184972
12.07644	82.22244	26.86309	13.49623	1.117567	0.164142

Tw	8(U)/D	Log	Log
dyne/cm2	(1/sec)	Tw	8(U)/D
0.782623	82.53601	-0.10644	1.916643
0.536869	56.60343	-0.27013	1.752842
0.353716	36.64540	-0.45134	1.564019
0.209674	21.52570	-0.67845	1.332957
0.137747	13.96926	-0.86091	1.145173
0.053808	5.312891	-1.26914	0.725330

Regression Output:

Constant -1.97516
Std Err of Y Est 0.001150
R Squared 0.999993
No. of Observations 5
Degrees of Freedom 3

X Coefficient(s) 0.973236
Std Err of Coef. 0.001449

Tw vs. K's(8(U)/D)^n

K' = 0.010508
n' = 0.973236

Regression Output:

Constant 1.039455
Std Err of Y Est 0.164353
R Squared 0.976134
No. of Observations 16
Degrees of Freedom 14

X Coefficient(s) 4.008034
Std Err of Coef. 0.167492

t = 24.31756 deg C
s.d.t = 0.433903 deg C

Page 1

Cyanamid 832A

Y2P01446

10 PSID Taps 14 1.0 PSID Taps 14 0.1 PSID Taps 14
 S = 2.7 S = 7.25 S =
 Z = 2.85 Z = 9.15 Z =
 FlowCo = 0.019693

11/4/90 12:55

col(NaCl) 1.00088 1.001574 ID(cc) = 1.02108
 K(U/psi) = 1.098348 13.19632
 X5(ccm2) = 0.818859
 density viscosity
 1.999589 X coeff 0.00025 -0.02281
 0.000100 constant 0.003419 -4.14933

Page 2

Cyanamid 832A

col(NaCl) 1.00088 1.001574 ID(cc) = 1.02108
 K(U/psi) = 1.098348 13.19632
 X5(ccm2) = 0.818859
 density viscosity
 1.999589 X coeff 0.00025 -0.02281
 0.000100 constant 0.003419 -4.14933

Tap Pair	Freq. (Hz)	Dist (l/s)	Temp (deg C)	<U> (volts)	<U>0 (volts)	<U>f (volts)	<U>corr (volts)	Batch Vol (ml)	t(samp (sec))	DP (psid)	<U> (cm/s)	Re	Tw (dyne/cm2)	f	Log(Ker/f)
23	60	1.181580	25.1	8.847	0.0345	0.0295	8.8125	8.023413	1442.958	164856.7	3561.608	0.003430	3.984791		
23	50	0.984650	25.1	6.191333	0.0345	0.0295	6.156833	5.605539	1202.465	137580.5	2488.309	0.002451	3.904921		
23	39	0.748027	25.1	3.6565	0.0345	0.0295	3.622	3.297679	937.9229	107156.8	1463.846	0.003337	3.791716		
23	32	0.630176	25.1	2.473333	0.0345	0.0295	2.438833	2.220455	749.5778	87923.57	985.6446	0.003337	3.705833		
23	25	0.493325	25.1	1.558333	0.0345	0.0295	1.508333	1.369177	601.3326	68690.29	607.7805	0.003372	3.600842		
23	19	0.374167	25.1	0.9285	0.0345	0.0295	0.894	0.813949	456.9368	52204.62	361.3138	0.003470	3.487911		
23	15	0.295395	25.1	0.585	0.0345	0.0295	0.5505	0.501207	360.4930	41214.17	232.4868	0.003428	3.382621		
23	10	0.196930	25.1	0.317166	0.0345	0.0295	0.282666	0.257356	240.4930	27476.11	114.2409	0.003961	3.237879		
23	25	0.493325	25.2	4.481	0.0285	0.0275	4.4525	4.053815	601.3326	68845.43	599.7009	0.003327	3.598921		
14	19	0.374167	25.2	2.701333	0.0285	0.0275	2.672833	2.433503	456.9368	52322.52	360.0001	0.003458	3.488105		
14	9	0.177237	25.2	0.719166	0.0285	0.0275	0.690666	0.628823	216.4437	24784.35	93.02491	0.003982	3.194253		
23	17	0.334781	24.9	8.917333	0.0415	0.0635	8.875833	0.672599	408.8382	46499.12	298.4605	0.003580	3.444441		
23	20	0.393860	24.9	11.724	0.0415	0.0635	11.6825	0.885284	480.9861	54704.84	392.8380	0.002405	3.504105		
23	14	0.275702	24.9	6.142	0.0415	0.0635	6.1005	0.462287	336.6903	38293.39	205.1366	0.003629	3.363020		
23	9	0.177237	24.9	2.894666	0.0415	0.0635	2.853166	0.216209	216.4437	24617.18	95.94114	0.004107	3.198000		
14	14	5.5992	24.5	5.5992	0.0655	-0.0205	5.5337	15.7	0.419336	168.4803	18989.93	62.03453	0.004382	3.099374	
14	24.2	4.0902	24.2	4.0902	-0.0145	-0.0635	4.1047	14.9	0.311048	141.1358	15800.55	46.01499	0.004631	3.031551	
14	24.2	3.3108	24.2	3.3108	0.0785	0.0645	3.2323	15	0.244939	122.0396	13662.67	36.23511	0.004878	2.979666	
14	24.2	2.190666	24.2	2.190666	0.0625	0.0645	2.128166	20	0.161269	93.91109	10513.60	23.85742	0.005424	2.888913	
14	24.2	1.687333	24.2	1.687333	0.0645	0.0605	1.622833	20	0.122976	79.25657	8872.992	18.19247	0.005807	2.830047	
14	24.1	1.099875	24.1	1.099875	0.0605	0.0585	1.039375	25	0.078762	60.32780	6738.645	11.65172	0.006419	2.732211	
14	24	6.554142	24	6.554142	-0.0455	-0.0405	6.594642	25	0.079319	60.27895	6718.016	11.73416	0.006474	2.732857	
14	24	4.30275	24	4.30275	-0.0425	-0.0425	4.34525	29.9	0.052264	46.72458	5207.597	7.731712	0.007100	2.642369	
14	24	3.2986	24	3.2986	-0.0485	-0.0475	3.3461	40.1	0.040246	39.98627	4456.421	5.953877	0.007466	2.585531	
14	24	2.1373	24	2.1373	-0.0555	-0.0565	2.1938	40	0.026386	33.30852	3712.193	3.903534	0.007054	2.493860	
14	24	1.127235	24	1.127235	-0.0585	-0.0595	1.186735	60	0.014273	25.34012	2824.125	2.111615	0.004593	2.360439	
14	23.9	0.808904	23.9	0.808904	-0.0605	-0.0605	0.869404	75	0.010472	19.01832	2114.792	1.546973	0.008575	2.291887	
14	23.9	0.562772	23.9	0.562772	-0.061	-0.0585	0.621272	90.1	0.007472	14.20453	1579.510	1.105460	0.010984	2.218918	
14	23.8	0.401090	23.8	0.401090	-0.06	-0.0595	0.460390	90	0.005539	10.55668	1171.233	0.819551	0.014743	2.152949	
14	23.7	0.274458	23.7	0.274458	-0.0615	-0.0615	0.335958	100	0.004040	7.693627	831.6617	0.597786	0.020247	2.082449	
14	23.5	0.18364	23.5	0.18364	-0.0645	-0.0655	0.24914	100.1	0.002996	5.563157	613.0527	0.443306	0.028715	2.016557	
14	23.4	0.110041	23.4	0.110041	-0.0675	-0.0705	0.180541	100	0.002171	3.968934	436.3858	0.321246	0.040882	1.945639	
14	23.3	0.066291	23.3	0.066291	-0.0715	-0.074	0.137791	100	0.001657	3.052026	334.9249	0.243179	0.052750	1.885977	
14	23.2	0.018666	23.2	0.018666	-0.0765	-0.0795	0.098166	100	0.001180	2.074058	227.2357	0.174672	0.081240	1.811260	
14	23.1	-0.03555	23.1	-0.03555	-0.0805	-0.0845	0.048947	150.1	0.000588	0.976317	106.6224	0.087094	0.183156	1.659260	
14	23.3	10.1014	23.3	10.1014	-0.086	-0.103	10.2044	20	0.122737	78.15748	8574.079	18.15718	0.005958	2.820759	
14	23.5	13.2545	23.5	13.2545	0	-0.0045	13.259	20	0.159478	92.81200	10327.76	23.59337	0.005490	2.879591	
14	23.6	13.37035	23.6	13.37035	-0.0375	-0.0375	13.40775	15.2	0.161267	110.4338	13301.63	35.78811	0.004946	2.971060	
24	23.8	6.838	23.8	6.838	-0.0115	-0.0115	6.8515	19.9	0.082409	119.7891	13290.24	36.58161	0.005111	2.977792	
23	23.9	11.5288	23.9	11.5288	-0.0235	-0.0115	11.5503	14.9	0.138925	165.2322	18373.43	61.64950	0.004528	3.092181	

Y2F01446

Solvent	L	MDR	DATA	1/f/fL	
1/f/f	1/f/f	1/f/f	1/f/f	1/f/f/Slv 1/f/fL	
83.13996					
4					
0.4					
15.53916	603.4926	43.31104	17.07318	1.098719	0.028290
15.23768	504.4302	41.83150	17.02175	1.117816	0.033744
14.76886	386.8981	39.64261	17.31025	1.172335	0.044741
14.42333	317.4778	39.01083	17.30899	1.200069	0.054520
14.00336	249.2999	36.01600	17.22079	1.229760	0.069076
13.55164	192.2167	33.87031	16.87453	1.252581	0.085309
13.13048	150.8346	31.86979	17.07755	1.300603	0.113220
12.55151	108.0835	29.11971	15.88823	1.245841	0.146999
13.99568	248.1997	35.97950	17.33619	1.238681	0.069847
13.52242	192.3027	33.87400	17.00526	1.254776	0.088429
12.37701	97.75381	28.29081	15.84615	1.280289	0.162102
13.37776	173.9089	33.04439	16.71101	1.249163	0.096090
13.61642	199.5194	36.17799	17.13643	1.258512	0.085888
13.05208	144.1783	31.49738	16.59983	1.271815	0.115134
12.39200	98.60090	28.36201	15.60405	1.259203	0.158254
11.99749	78.56958	26.48811	15.10598	1.259094	0.192262
11.72620	67.20966	25.19948	14.69354	1.253034	0.218619
11.51864	59.64126	24.21267	14.31755	1.242987	0.240061
11.15565	48.59426	22.48936	13.57806	1.217146	0.280571
10.92017	42.25985	21.37091	13.12266	1.201688	0.310523
10.52924	33.74364	19.51392	12.48132	1.185395	0.369886
10.53143	33.78607	19.52429	12.42748	1.180037	0.367828
10.16907	27.42518	17.80312	11.86728	1.166996	0.432714
9.942126	24.06642	16.72510	11.57323	1.164060	0.480886
9.575442	19.48680	14.98325	11.90611	1.243400	0.610983
9.041756	14.33240	12.44834	12.31529	1.362047	0.859262
8.787531	12.23962	11.14587	10.79890	1.231690	0.882290
8.475672	10.34661	9.759443	9.541233	1.125719	0.922160
8.211797	8.888519	8.506039	8.235576	1.002895	0.926540
7.933797	7.574069	7.185535	7.027775	0.885802	0.927873
7.666231	6.492887	5.914599	5.901194	0.769764	0.908870
7.382558	5.514672	4.567154	4.945736	0.669921	0.896832
7.143908	4.806813	3.433567	4.354820	0.609585	0.905948
6.845450	4.048019	2.013889	3.508440	0.512521	0.866705
6.237040	2.851937	0.87405	2.336622	0.374636	0.819310
10.98303	41.34561	21.19443	12.95471	1.190358	0.313176
11.11836	47.36652	22.31223	13.49550	1.213802	0.284916
11.48424	58.47097	24.05014	14.21819	1.238061	0.243166
11.51117	59.38444	24.17806	13.98750	1.215124	0.235541
11.98872	77.27904	26.35145	14.85965	1.241540	0.192285

Tw	B(U)/D	Log	Log
dynes/cm2	(1/sec)	Tw	B(U)/D
1.546973	149.0055	0.189482	2.173202
1.105460	111.2902	0.043543	2.046457
0.819551	82.70997	-0.08642	1.917557
0.597786	60.27834	-0.22349	1.780161
0.443306	43.58645	-0.35329	1.639351
0.321246	31.09597	-0.49316	1.492704
0.245179	23.91997	-0.61051	1.378760
0.174672	16.26558	-0.75777	1.211269
0.087094	7.649293	-1.06000	0.885621

Regression Output:
 Constant -1.89022
 Std Err of i Est 0.005671
 R Squared 0.999713
 No. of Observations 6
 Degrees of Freedom 4

X Coefficient(s) 0.935276
 Std Err of Coef. 0.007917

Tw vs. K's (B(U)/D)^n

K' = 0.012875
 n = 0.935276

Tw Retro=0.912706
 Res/f/R =154.5732

Regression Output:
 Constant -4.45987
 Std Err of Y Est 0.221595
 R Squared 0.985366
 No. of Observations 23
 Degrees of Freedom 21

X Coefficient(s) 6.256909
 Std Err of Coef. 0.165859

t = 24.2835 deg C
 s.d.)t = 0.673010 deg C

Y5P01449

10 PSID Taps 14 1.0 PSID Taps 14 0.1 PSID Taps 14
 S = 2.7 S = 7.25 S = 9.9 <C> (ppm) =
 Z = 2.7 Z = 9.15 Z = 6.9 [NaCl] =
 FlowCo = 0.019693

density viscosity ID (cm) = 1.02108
 colNaCl] 1.000088 1.001574 K (V/psi) = 1.098248 13.19632
 5.000475 X coeff -0.00025 -0.02281 XS (cm2) = 0.818859
 0.000100 constant 0.003419 -4.14933

Tap Pair	Freq. (Hz)	Dist (1/s)	Temp (deg C)	<V> (volts)	<V>0 (volts)	<V>f (volts)	<V>corr (volts)	Batch Vol (ml)	t) (sec)	DP (psid)	<U> (cm/s)	Re	Tu (dyne/cm2)	f	Log (Ref/f)
12	60	1.181580	24.7	6.285666	-0.0145	0.0265	6.259166	5.688709	1442.958	163375.7	2528.757	0.002435	3.906481		
12	50	0.984650	24.7	4.013	-0.0145	0.0265	3.9865	3.629541	1202.465	136146.4	1610.580	0.002333	3.808519		
12	40	0.787720	24.7	2.412666	-0.0145	0.0265	2.386166	2.172505	961.9723	108917.1	964.0519	0.002089	3.697075		
12	32	0.630176	24.7	1.534	-0.0145	0.0265	1.5075	1.372515	769.5778	87133.72	609.0430	0.002062	3.597252		
14	30	0.590790	24.6	4.05275	0.0255	0.0255	4.02725	3.666642	721.4792	81503.78	542.4246	0.002089	3.571512		
14	22	0.432246	24.6	2.2305	0.0255	0.0255	2.205	2.007560	529.0847	59769.44	296.9883	0.002127	3.440412		
14	16	0.315088	24.6	1.286	0.0255	0.0255	1.2605	1.147632	384.7889	43468.68	169.7749	0.002299	3.218979		
14	10	0.196930	24.6	0.604333	0.0255	0.0255	0.580833	0.528824	240.4930	27167.92	78.25162	0.002712	3.150734		
14	13	0.256009	24.6	0.9128	0.0255	0.0255	0.8873	0.807849	312.6409	35318.30	119.5091	0.002451	3.242743		
23	17	0.334781	25	5.890666	0.0665	0.0905	5.800166	0.439529	408.8382	46604.14	195.0375	0.002340	3.352042		
23	24	0.472632	25	10.732	0.0665	0.0905	10.6415	0.806399	577.1833	65794.08	357.8331	0.002154	3.484823		
23	27	0.531711	25	13.347	0.0665	0.0905	13.2565	1.004560	649.3313	74018.34	445.7657	0.002120	3.525356		
23	14	0.275702	24.9	4.20125	0.0795	0.0835	4.11775	0.312037	356.6903	38295.39	138.4642	0.002449	3.277667		
23	9	0.177237	24.9	1.96575	0.0795	0.0835	1.88225	0.142634	216.4437	24617.18	63.29291	0.002709	3.107675		
23	24.7	1.455	24.7	1.455	0.0575	0.0575	1.3975	15	0.105900	179.3531	20307.08	46.99261	0.002929	3.041042	
14	24.5	2.9826	24.5	2.9826	0.0575	0.0455	2.9251	15	0.221660	144.5913	16297.32	32.79130	0.003145	2.960936	
14	24.1	2.352666	24.1	2.352666	0.0445	0.0405	2.308166	15	0.174909	124.7263	13931.99	25.87528	0.003334	2.905559	
14	24.1	1.495166	24.1	1.495166	0.0435	0.0315	1.451666	20	0.110003	95.37655	10653.60	16.27364	0.003586	2.804859	
14	24.1	1.152	24.1	1.152	0.0345	0.0415	1.1175	19.9	0.084682	80.51398	8993.452	12.52733	0.003874	2.748049	
14	24	7.173	24	7.173	-0.0415	-0.0415	7.2145	20.1	0.087381	80.13815	8931.299	12.92681	0.004035	2.753877	
14	24	4.4634	24	4.4634	-0.046	-0.0475	4.4909	25	0.054393	60.42550	6734.348	8.046716	0.004418	2.650941	
14	24	3.030111	24	3.030111	-0.0515	-0.0535	3.083611	30	0.037348	47.95287	5344.289	5.525160	0.004817	2.569304	
14	24	2.136888	24	2.136888	-0.0555	-0.0555	2.192388	35	0.026554	40.64886	4530.266	3.928284	0.004766	2.495233	
14	23.9	1.699181	23.9	1.699181	-0.0585	-0.0585	1.757681	40	0.021288	33.49170	3724.198	3.149383	0.005629	2.446259	
14	23.85	1.236666	23.85	1.236666	-0.0595	-0.0595	1.296166	50	0.015699	25.59657	2843.069	2.322448	0.007106	2.379626	
14	23.8	0.87875	23.8	0.87875	-0.0605	-0.0605	0.938375	60	0.011365	18.70487	2075.230	1.681363	0.009634	2.308992	
14	23.7	0.676357	23.7	0.676357	-0.0615	-0.0605	0.736857	70.1	0.008924	14.73814	1631.469	1.320287	0.012186	2.255510	
14	23.6	0.495909	23.6	0.495909	-0.0615	-0.0595	0.555409	90.1	0.006727	11.06002	1221.552	0.995172	0.016310	2.193140	
14	23.5	0.349	23.5	0.349	-0.06	-0.0595	0.4085	90.1	0.004947	8.037490	885.7210	0.731943	0.022714	2.125444	
14	23.3	0.2635	23.3	0.2635	-0.06	-0.06	0.3235	90	0.003916	6.119622	671.3385	0.579641	0.031027	2.072815	
14	23.2	0.169695	23.2	0.169695	-0.06	-0.0595	0.229695	99.9	0.002782	4.217394	461.6165	0.411564	0.046384	1.997469	
14	23.1	0.072695	23.1	0.072695	-0.0595	-0.0605	0.133195	100	0.001613	2.295876	250.7297	0.238657	0.090759	1.878152	
14	23	0.004125	23	0.004125	-0.0605	-0.0605	0.064625	99.9	0.000782	1.026843	111.8876	0.115793	0.220131	1.720122	
14	23.3	9.235166	23.3	9.235166	-0.0605	-0.0695	9.304666	19.9	0.012697	94.56711	10374.25	16.67193	0.003737	2.802228	
14	23.6	12.30475	23.6	12.30475	-0.0695	-0.0695	12.37425	15	0.149876	113.9796	12588.77	22.17196	0.003421	2.867092	
24	23.8	11.63125	23.8	11.63125	-0.0695	-0.0685	11.69975	15	0.141706	142.1489	15771.00	31.44733	0.003120	2.948953	
23	24.1	8.47325	24.1	8.47325	-0.0695	-0.0575	8.53075	15	0.103524	174.7959	19524.79	45.86577	0.003009	3.029861	

Solvent	L	MDR	DATA	1/f/f	1/f/f	1/f/f/Siv	1/f/f/L
82.563							
0.4							
0.4							
15.22592	503.9700	41.82315	20.26310	1.330838	0.040210		
14.83407	402.1603	39.96186	21.15860	1.426351	0.052612		
14.38829	311.1385	37.84440	21.87875	1.520593	0.070318		
13.98940	247.3045	35.94968	22.02085	1.574109	0.089043		
13.88485	232.8587	35.45303	21.87586	1.575520	0.093944		
13.36165	172.3028	32.96783	21.68036	1.622581	0.125827		
12.87591	130.2745	30.66061	20.85435	1.619460	0.160080		
12.20293	88.43293	27.46394	19.20094	1.573468	0.217124		
12.57097	109.3008	29.21212	20.19558	1.606524	0.184770		
13.01217	140.9038	31.30781	20.67196	1.588663	0.166709		
13.53229	190.8551	33.81165	21.54581	1.591353	0.112890		
13.73014	213.0183	34.71820	21.71712	1.581711	0.101949		
12.71066	118.4533	29.87567	20.20489	1.589600	0.170572		
12.03070	80.08588	26.64584	19.21154	1.596876	0.239886		
11.76417	68.69464	25.37981	18.67586	1.570519	0.268956		
11.44374	57.12378	23.85780	17.83115	1.558156	0.312149		
11.22233	50.28511	22.80562	17.31624	1.543029	0.344361		
10.81943	39.87854	20.89232	16.89696	1.543237	0.418695		
10.59219	34.98884	19.81294	16.06485	1.516668	0.459142		
10.61550	35.46152	19.92367	15.74117	1.482847	0.443894		
10.20376	27.97828	17.96787	15.04369	1.474328	0.537691		
9.877216	23.18377	16.41677	14.40740	1.458650	0.621443		
9.580932	19.54848	15.00942	14.48407	1.511760	0.740930		
9.385037	17.46383	14.07892	13.32826	1.420160	0.763192		
9.118507	14.97983	12.81291	11.86207	1.300878	0.791869		
8.85968	12.73128	11.47085	10.18775	1.152986	0.800214		
8.622041	11.25616	10.45469	9.058756	1.050650	0.804781		
8.372560	9.750346	9.289660	7.830187	0.935220	0.803067		
8.101777	8.343041	7.983442	6.635178	0.819978	0.795294		
7.891260	7.390862	6.983486	5.677099	0.719416	0.768124		
7.589876	6.215683	5.551913	4.643144	0.611754	0.747245		
7.112610	4.720984	3.284898	3.519351	0.466685	0.703105		
6.480490	3.260972	0.282329	2.131372	0.328890	0.649616		
10.80891	39.63769	20.84233	16.35794	1.513375	0.412686		
11.06837	46.02279	22.07476	17.09584	1.544567	0.371464		
11.37981	55.05962	23.55411	17.90218	1.573153	0.325141		
11.71944	66.94856	25.16736	18.22741	1.555314	0.272260		

Tw	B<U>/D	Log	Log
dyne/cm2	(1/sec)	Tw	8<U>/D
2.322448	200.5451	0.365946	2.302212
1.681365	146.5497	0.225661	2.165985
1.320287	115.4710	0.120668	2.062473
0.995172	86.65351	-0.00210	1.937786
0.731943	62.97246	-0.13552	1.799150
0.579641	47.94627	-0.23684	1.680754
0.411564	33.04261	-0.38556	1.519074
0.238657	17.98782	-0.62222	1.254978
0.115793	8.045158	-0.93631	0.905534

Regression Output:

Constant	-1.74953
Std Err of Y Est	0.002109
R Squared	0.999967
No. of Observations	5
Degrees of Freedom	3

X Coefficient(s)	0.898279
Std Err of Coef.	0.002946

Tw vs. K*(8<U>/D)^n

K' =	0.017801
n =	0.898279

Tw)Retro=2.451489
Res/f)R =251.0400

Regression Output:

Constant	-6.36946
Std Err of Y Est	0.221248
R Squared	0.990509
No. of Observations	20
Degrees of Freedom	18

X Coefficient(s)	8.152781
Std Err of Coef.	0.188096

t = 24.15810 deg C
s.d.t = 0.579784 deg C

Y1P11452

10 PSID Taps 14 1.0 PSID Taps 14 0.1 PSID Taps 14
 S = 2.7 S = 7.25 S = 9.9 <D> (ppm) = 9.9
 Z = 2.85 Z = 9.15 Z = 6.9 [NaCl] = 6.9
 FlowCo = 0.019693

11/11/90 12:48
 density viscosity
 1.000088 1.001574 ID(cm) = 1.02108
 K(V/psi) = 1.098348 13.45545
 0.000100 constant 0.003419 -4.14933
 XS(cm2) = 0.818859

Tap Pair	Freq. (Hz)	Dist (1/s)	Temp (deg C)	<U> (volts)	<V> (volts)	<W> (volts)	<U>f (volts)	<U>corr (volts)	Batch Vol (ml)	t) sump (sec)	DP (psid)	<U> (cm/s)	Re	Tw (dyne/cm2)	f	Log (Re/f)
14	60	1.181580	24.7	13.082	0.0875	0.0985	0.0985	12.9835	11.82093	1442.958	163375.7	1748.729	0.001684	3.826389		
14	49	0.964957	24.7	7.9355	0.0875	0.0985	7.837	7.837	7.135261	1178.416	133423.5	1055.534	0.001524	3.716768		
14	40	0.787720	24.7	4.9805	0.0875	0.0985	4.882	4.882	4.444857	961.9723	108917.1	637.5496	0.001424	3.613992		
14	30	0.590790	24.7	2.725	0.0875	0.0985	2.6265	2.6265	2.391318	721.4792	81687.86	333.7595	0.001362	3.479382		
14	21	0.413553	24.7	1.345666	0.0875	0.0985	1.247166	1.247166	1.135493	505.0354	57181.50	167.9791	0.001320	3.317655		
14	15	0.295395	24.7	0.7854	0.0875	0.0985	0.6869	0.6869	0.625393	360.7396	40843.93	92.51759	0.001425	3.188140		
14	10	0.196930	24.7	0.4468	0.0875	0.0985	0.3483	0.3483	0.317112	240.4930	27229.28	46.91203	0.001626	3.040670		
12	17	0.354781	24.9	3.5855	0.0395	0.0425	3.546	3.546	0.263536	408.8382	46499.12	116.9421	0.001403	3.240984		
12	24	0.472632	24.9	6.316	0.0395	0.0425	6.2765	6.2765	0.466465	577.1833	65645.81	206.9902	0.001246	3.364973		
12	33	0.649869	24.9	11.61966	0.0395	0.0425	11.58016	11.58016	0.860630	793.6271	90262.99	381.8978	0.001215	3.497972		
12	15	0.295395	24.9	2.7994	0.0425	0.0435	2.7569	2.7569	0.204890	360.7396	41028.63	90.91873	0.001401	3.186335		
12	10	0.196930	24.9	1.5025	0.0425	0.0435	1.46	1.46	0.108506	240.4930	27352.42	48.14877	0.001669	3.048291		
12	12	24.6	1.1465	0.0395	0.0345	1.112	1.112	1.112	0.082643	199.4097	22526.84	36.67221	0.001849	2.986211		
12	12	24.3	0.7508	0.0345	0.0345	0.6963	0.6963	0.6963	0.051748	141.9046	15922.50	22.96300	0.002286	2.881401		
14	24	2.15625	0.0315	2.12475	0.0315	0.0245	2.12475	2.12475	0.157909	141.6604	15859.27	23.36040	0.002334	2.884342		
14	24.1	1.6408	0.027	1.6138	0.0235	1.6138	1.6138	1.6138	0.119936	121.7954	13604.60	17.74280	0.002398	2.823627		
14	24.1	1.1504	0.0275	1.1069	0.0235	1.1069	1.1069	1.1069	0.082264	93.74766	10471.66	12.16972	0.002776	2.741757		
14	24	0.931666	0.0265	0.907166	0.0265	0.0245	0.907166	0.907166	20.1	0.067420	79.68399	8880.684	9.973776	0.003149	2.697561	
14	23.8	5.767	0.0605	5.7075	0.0595	5.7075	5.7075	5.7075	20	0.069129	79.37069	8806.852	10.22659	0.003253	2.701026	
14	23.8	3.9505	0.055	3.8955	0.055	3.8955	3.8955	3.8955	25	0.047182	59.59507	6611.898	6.979888	0.003940	2.618085	
14	23.8	2.860125	0.0515	2.797125	0.0515	2.797125	2.797125	2.797125	30	0.033878	47.43267	5261.517	5.011839	0.004467	2.544159	
14	23.8	2.3707	0.063	2.3017	0.063	2.3017	2.3017	2.3017	35	0.027878	40.33484	4475.032	4.124145	0.005082	2.505828	
14	23.7	1.85727	0.0675	1.788227	0.0675	1.788227	1.788227	1.788227	40	0.021658	32.66738	3616.182	3.204114	0.006019	2.498030	
14	23.6	1.420266	0.069	1.352266	0.069	1.352266	1.352266	1.352266	55	0.016378	25.09032	2771.166	2.423967	0.007716	2.386364	
14	23.6	1.117	0.067	1.0485	0.0685	1.0485	1.0485	1.0485	60.1	0.012899	19.20206	2120.821	1.878683	0.010214	2.331117	
14	23.5	0.772318	0.0675	0.702818	0.0675	0.702818	0.702818	0.702818	90	0.008512	12.61917	1390.616	1.259297	0.015853	2.243269	
14	23.3	0.531954	0.0205	0.516954	0.015	0.516954	0.516954	0.516954	90	0.006261	9.308338	1021.149	0.926270	0.021430	2.174604	
14	23.1	0.359681	0.02	0.333181	0.0265	0.333181	0.333181	0.333181	90.9	0.002306	5.129428	340.2224	0.341191	0.069833	1.953793	
14	22.9	0.2292	0.0285	0.19042	0.0325	0.19042	0.19042	0.19042	99.9	0.002306	5.746873	627.6088	0.596989	0.036234	2.077248	
14	22.8	0.163478	0.0335	0.129978	0.036	0.129978	0.129978	0.129978	99.9	0.001574	1.943668	210.8338	0.232892	0.133564	1.869887	
14	22.7	0.117391	0.0365	0.084891	0.0355	0.084891	0.084891	0.084891	100	0.000991	1.160150	125.5603	0.146731	0.218507	1.768585	
14	22.5	0.081147	0.0355	0.046467	0.0345	0.046467	0.046467	0.046467	150	0.000540	0.586181	63.15541	0.079997	0.466621	1.634892	
14	23	7.048714	0.0365	7.011214	0.0375	7.011214	7.011214	7.011214	25	0.084919	92.32522	10059.81	12.56257	0.002994	2.77818	
14	23.3	10.469	0.0215	10.4315	0.0275	10.4315	10.4315	10.4315	15	0.126345	120.3299	13200.50	18.69097	0.002587	2.827031	
14	23.6	12.6024	0.0245	12.5689	0.0335	12.5689	12.5689	12.5689	15	0.152234	139.0351	15358.31	23.52073	0.002334	2.870482	
13	23.7	12.009	0.0533	11.906	0.105	11.906	11.906	11.906	14.9	0.144205	175.7331	19452.03	32.00068	0.002077	2.947755	

YIP11452

Cyanamid 832A

Page 3

Tw 8<U>/D Log Log
dyne/cm2 (1/sec) Tw 8-U>/D
2.422967 196.5787 0.384347 2.293536
1.878683 150.4451 0.273853 2.177378
1.259297 98.86924 0.100128 1.995061
0.926270 72.92936 -0.03326 1.862902
0.596989 45.02584 -0.22403 1.653461
0.341191 24.51857 -0.46700 1.389495
0.232892 15.22833 -0.63284 1.182652
0.146731 9.089592 -0.83347 0.958544
0.079997 4.592636 -1.09692 0.662062

Regression Output:
Constant -1.68075
Std Err of Y Est 0.006826
R Squared 0.999756
No. of Observations 6
Degrees of Freedom 4

X Coefficient(s) 0.881684
Std Err of Coef. 0.006875

Tw vs. K*(8<U>/D)^n

K' = 0.020856 133482.4
n = 0.881684

Tw)Retro=31.86297
Res/f)R= 905.0614

Regression Output:

Constant -8.71213
Std Err of Y Est 0.283324
R Squared 0.964923
No. of Observations 7
Degrees of Freedom 5

X Coefficient(s) 10.98835
Std Err of Coef. 0.936928

t = 23.97777 deg C
s.d.)t = 0.715351 deg C

Solvent	L	MDR	DATA
1//f	1//f	1//f	1//f/5lv 1//f/L
82.563			
4			
0.4			
14.90555	419.0533	40.30139	24.36678 1.634744 0.058147
14.46707	325.5730	38.21859	25.61320 1.770448 0.078671
14.05596	256.7640	36.26585	26.49134 1.884703 0.103093
13.51752	188.4786	33.70826	27.08790 2.003909 0.143718
12.87062	129.8780	30.63545	27.51692 2.137963 0.211867
12.35256	96.38739	28.17466	26.48422 2.144027 0.274768
11.76268	68.63572	25.37273	24.79511 2.107947 0.361256
12.56393	108.8589	29.17869	26.69689 2.124882 0.245243
13.05989	144.8282	31.53449	28.32915 2.169172 0.195505
13.59188	196.7216	34.06146	28.67726 2.109880 0.145775
12.34530	95.98539	28.14017	26.71541 2.164014 0.278327
11.79316	69.85075	25.51753	24.47398 2.075269 0.350375
11.54484	60.54683	24.33801	23.25353 2.014191 0.384958
11.12640	47.58627	22.35043	20.91267 1.879553 0.439468
11.13736	47.88751	22.40250	20.69860 1.858482 0.432233
10.89451	41.63973	21.24893	20.42010 1.874348 0.490399
10.56702	34.48556	19.69338	18.97833 1.795995 0.550327
10.39024	31.14881	18.85366	17.81906 1.714980 0.572062
10.40410	31.39835	18.91951	17.53044 1.684953 0.558323
10.07234	25.93973	17.34362	15.93091 1.581649 0.614150
9.78639	21.98061	15.97703	14.96067 1.528995 0.680630
9.615313	19.93922	15.17273	14.02709 1.458829 0.703492
9.392120	17.53517	14.11257	12.88903 1.373323 0.735038
9.145458	15.21404	12.94092	11.39407 1.244779 0.748261
8.924470	13.35669	11.89123	9.894330 1.108674 0.738564
8.573079	10.94333	10.22212	7.942142 0.926404 0.725751
8.298416	9.342952	8.91478	6.831011 0.823170 0.731140
7.908992	7.666691	7.067715	5.253404 0.664231 0.703578
7.415173	5.619186	4.722075	3.784160 0.510326 0.673435
7.079549	4.631986	3.127858	2.844808 0.401834 0.614165
6.674342	3.668306	1.205127	2.139276 0.320522 0.563178
6.139571	2.696328	-1.33703	1.463921 0.238440 0.542931
10.55127	34.17424	19.61856	18.39801 1.743677 0.538359
10.90820	41.96926	21.51397	19.65800 1.802129 0.468390
11.08192	46.38335	22.13916	20.69480 1.867436 0.446168
11.39102	55.41606	23.60735	21.93862 1.925957 0.395889

Y2P11455 10 PSID Taps 14 1.0 PSID Taps 14 0.1 PSID Taps 14 9.9 <C>(ppa)= 2.7 S = 7.25 E = 2.8 Z = 9.2 Z = 6.9 [NaCl]= FlowCo= 0.019693

11/15/90 11:37

Tap Pair	Freq. (Hz)	Qrest (1/s)	Temp (deg C)	<U> (volts)	<U> (volts)	<U>f (volts)	<U>corr (volts)
12	60	1.181580	24.7	2.993	0.0585	0.0905	2.9345
14	60	1.181580	24.7	9.6775	0.0585	0.0905	9.587
14	50	0.984650	24.7	6.261	0.0585	0.0905	6.1705
14	40	0.787720	24.7	4.085333	0.0585	0.0905	3.994833
14	30	0.590790	24.7	2.566666	0.0585	0.0905	2.476166
14	23	0.452939	24.7	1.706666	0.0585	0.0905	1.616166
14	16	0.315088	24.7	1.016333	0.0585	0.0905	0.925833
14	10	0.196930	24.7	0.518666	0.0585	0.0905	0.460166
14	8	0.157544	24.7	0.418666	0.0585	0.0905	0.360166
12	17	0.354781	24.9	3.33675	0.0285	0.041	3.28575
12	24	0.472632	24.9	5.544	0.0285	0.041	5.503
12	34	0.669562	24.9	9.46225	0.0285	0.041	9.42125
14	15	0.295395	24.9	7.770333	0.0365	0.0705	7.699833
14	10	0.196930	24.9	4.253	0.0365	0.0705	4.1825
14	8	0.157544	24.9	3.082571	0.0365	0.0705	3.012071
14	24.6	2.7768	0.0365	0.0365	0.0705	0.0705	2.7485
14	24.4	2.1066	0.0285	0.0285	0.0245	0.0245	2.0781
14	24.4	1.7352	0.0285	0.0285	0.0265	0.0265	1.7047
14	24.4	1.263166	0.0295	0.0295	0.0275	0.0275	1.233666
14	24.3	1.009	0.0285	0.0285	0.0275	0.0275	0.9805
14	24.2	6.227	0.0695	0.0695	0.0725	0.0725	6.1545
14	24.2	6.1	0.0735	0.0735	0.0735	0.0735	6.0265
14	24.3	3.235444	0.0735	0.0745	0.0745	0.0745	3.160944
14	24.2	2.667272	0.074	0.0745	0.0745	0.0745	2.592772
14	24.2	2.190416	0.073	0.0745	0.0745	0.0745	2.115916
14	24.2	1.691941	0.073	0.0745	0.0745	0.0745	1.616441
14	24.15	1.310090	0.073	0.0745	0.0745	0.0745	1.233590
14	24.1	0.982	0.0735	0.0735	0.0735	0.0735	0.9065
14	24	0.73296	0.0755	0.0785	0.0785	0.0785	0.65446
14	23.8	0.594166	0.078	0.077	0.077	0.077	0.517166
14	23.7	0.528083	0.075	0.0735	0.0735	0.0735	0.454583
14	23.65	0.49908	0.0735	0.0735	0.0735	0.0735	0.42558
14	23.6	0.318053	0.0715	0.0695	0.0695	0.0695	0.248555
14	23.5	0.359458	0.0695	0.0685	0.0685	0.0685	0.309958
14	23.4	0.265041	0.0675	0.0665	0.0665	0.0665	0.198541
14	23.4	0.22552	0.0655	0.0655	0.0655	0.0655	0.160052
14	23.65	7.73725	0.0625	0.0515	0.0515	0.0515	7.67475
14	23.9	10.39166	0.0475	0.0435	0.0435	0.0435	10.34816
14	24.05	8.22125	0.0415	0.01235	0.01235	0.01235	8.09775
14	24.1	11.1235	0.0335	0.003	0.003	0.003	11.09

density viscosity ID(cm) = 1.02108
 co[NaCl] 1.00088 1.001574 K(W/psi)=1.440482 13.4881
 20.00475 X coeff -0.00025 -0.02281 XS(cm2)= 0.818859
 0.000100 constant 0.003419 -4.14953

Batch	-Vol	t/saap	DP	<U>	Re	Tw	f	Log
(ml)	(sec)	(psid)	(cm/s)		dyne/cm2			(Re/f)
2.036882	1442.958	163375.7	903.8504	0.000870	3.685076			
6.854487	1442.958	163375.7	984.4311	0.000948	3.701620			
4.283040	1202.465	136146.4	633.6114	0.000878	3.605939			
2.772876	961.9723	108917.1	410.2053	0.000888	3.511528			
1.718746	721.4792	81687.86	254.2626	0.000979	3.407669			
1.121806	553.1340	62627.36	165.9544	0.001087	3.315022			
0.642435	384.7889	43566.86	95.06823	0.001287	3.194045			
0.319408	240.4930	27229.28	47.25173	0.001638	3.042236			
0.249997	192.3944	21783.43	36.98334	0.002003	2.989031			
0.243603	408.8382	46499.12	108.0971	0.001296	3.221905			
0.407989	577.1833	65645.81	181.0420	0.001089	3.355888			
0.698486	817.6764	92998.24	309.9476	0.000929	3.452642			
0.570861	560.7396	41028.63	84.45032	0.001301	3.170299			
0.310088	240.4930	27352.42	45.87287	0.001590	3.027774			
0.223313	192.3944	21881.93	33.03583	0.001789	2.966491			
14.9	0.203757	172.4447	19480.67	30.14283	0.002032	2.943624		
14.9	0.154069	136.4641	15346.62	22.79220	0.002454	2.880965		
15	0.126385	116.9105	13147.65	18.69682	0.003742	2.87956		
20	0.091465	90.98019	10231.54	13.53062	0.003277	2.767731		
20	0.072693	77.48581	8694.344	10.75393	0.003591	2.716871		
20.1	0.075515	77.28258	8651.999	11.17135	0.003750	2.724155		
25	0.049404	57.93423	6500.546	7.508712	0.004366	2.657007		
29.9	0.038784	46.47952	5215.263	5.737596	0.005325	2.580452		
40.3	0.031813	38.78783	4342.405	4.706278	0.006272	2.536440		
44.9	0.025962	31.44141	3519.953	3.840711	0.007790	2.492207		
60.1	0.019833	23.28631	2606.967	2.934087	0.010849	2.433838		
80	0.015126	16.80691	1879.459	2.259155	0.015894	2.374651		
100.1	0.011122	11.90710	1330.029	1.645435	0.022269	2.307257		
100	0.008030	7.718051	860.1674	1.187944	0.039984	2.235529		
100	0.006345	5.512266	589.3803	0.938736	0.066692	2.182433		
100.1	0.005577	4.611564	510.4865	0.825138	0.077787	2.153439		
99.9	0.005221	4.046253	447.4033	0.772492	0.094593	2.138630		
100.1	0.003049	2.025184	223.6767	0.451166	0.220534	2.021359		
100	0.003570	2.295876	253.0025	0.528123	0.200865	2.054577		
100	0.002436	1.294483	142.3289	0.360383	0.431141	1.970602		
150	0.001963	0.911837	100.2568	0.290519	0.700468	1.922808		
19.9	0.094168	90.21003	9974.725	13.95084	0.003421	2.766672		
15.1	0.126971	114.5570	12716.23	18.78350	0.002879	2.834034		
15	0.099358	123.3562	14879.16	22.04883	0.002485	2.870117		
15	0.136073	169.0155	18879.12	30.19623	0.002119	2.957993		

Solvent	L	MDR	DATA	T _w	B(U)/D	Log T _w	Log 8(U)/D
1//4	1//4	1//4	1//4	dyne/cm ²	(1/sec)		
81.5				1.645435	93.29031	0.216280	1.969836
4				1.187944	60.46970	0.074796	1.781537
0.4				0.938736	41.62076	-0.02745	1.619310
				0.825138	36.13087	-0.08347	1.557878
				0.772492	31.70175	-0.11210	1.501083
				0.451166	15.86689	-0.34566	1.200494
				0.528133	17.98782	-0.27725	1.254978
				0.260383	10.14207	-0.44323	1.006126
				0.290519	7.144100	-0.53682	0.853947

Regression Output:
 Constant -1.13168
 Std Err of Y Est 0.013828
 R Squared 0.997278
 No. of Observations 9
 Degrees of Freedom 7

X Coefficient(s) 0.678567
 Std Err of Coef. 0.013397
 T_w vs. K's (B(U)/D)ⁿ
 K' = 0.073877
 n = 0.678567

T_w Retro=331.9457
 Res/f)R= 2921.202

Regression Output:
 Constant 26.32042
 Std Err of Y Est 0.000460
 R Squared 0.999996
 No. of Observations 7
 Degrees of Freedom 1

X Coefficient(s) 2.056016
 Std Err of Coef. 0.003791
 t = 24.305 deg C
 s.d.)t = 0.457684 deg C

Solvent	L	MDR	DATA	T _w	B(U)/D	Log T _w	Log 8(U)/D
1//4	1//4	1//4	1//4	dyne/cm ²	(1/sec)		
14.35230	301.2703	37.57845	33.89309	2.364803	0.112500		
14.40448	314.4131	37.93079	32.47631	2.254285	0.103291		
14.02375	252.2432	36.11285	33.73391	2.405483	0.133735		
13.64611	202.9591	34.31704	33.54034	2.457867	0.165256		
13.23067	159.7898	32.34571	31.95127	2.414938	0.199958		
12.86008	129.0929	30.58542	30.32087	2.357749	0.234876		
12.37618	97.70702	28.28686	27.86830	2.251768	0.285223		
11.76894	68.88377	25.40250	24.70582	2.099238	0.358659		
11.55612	60.94121	24.39159	22.34061	1.933227	0.366592		
12.49562	104.6611	28.85420	27.76764	2.22190	0.265309		
12.94355	135.4866	30.98187	30.29137	2.360267	0.233640		
13.41057	177.2240	33.20020	32.79684	2.445596	0.185058		
12.28119	92.50796	27.83568	27.71966	2.257081	0.299646		
11.75110	68.17991	25.31775	25.07375	2.133735	0.367758		
11.46596	57.85902	23.96333	23.63712	2.061503	0.408529		
11.37453	54.89274	23.52906	22.18038	1.950002	0.404067		
11.12386	47.51663	22.33834	20.18586	1.814644	0.424816		
10.95182	43.03645	21.52117	19.09377	1.743432	0.443665		
10.67092	36.61098	20.18489	17.46666	1.636845	0.477088		
10.46748	32.56499	19.22034	16.68652	1.594129	0.512406		
10.49662	33.11578	19.35894	16.32907	1.555650	0.493090		
10.13203	26.84650	17.62714	15.13339	1.493639	0.563708		
9.921809	23.78659	16.62859	13.70326	1.381125	0.576091		
9.745763	21.49418	15.79237	12.62668	1.295608	0.587446		
9.569231	19.41725	14.95385	11.52997	1.184000	0.583500		
9.335354	16.97143	13.84293	9.600569	1.058409	0.565689		
9.098606	14.80920	12.71838	7.931975	0.871778	0.535611		
8.829029	12.48052	11.43788	6.553473	0.742490	0.516971		
8.542119	10.75003	10.07506	5.00957	0.585446	0.465203		
8.329732	9.512904	9.066229	3.87242	0.464869	0.407051		
8.215757	8.988533	8.513348	3.585460	0.436518	0.402926		
8.154522	8.600242	8.233982	3.251386	0.398721	0.378057		
7.685436	6.565067	6.005824	2.129421	0.277072	0.324356		
7.818310	7.084922	6.636975	2.231244	0.285387	0.314839		
7.482411	5.840942	5.041455	1.522966	0.203539	0.260739		
7.295233	5.244311	4.152360	1.194828	0.163782	0.227833		
10.66668	36.52180	20.16677	17.06981	1.600291	0.467386		
10.93613	42.64958	21.44666	18.63476	1.703961	0.436927		
11.08126	46.36572	22.13602	20.05678	1.809972	0.432577		
11.35637	54.32168	23.44277	21.72143	1.912708	0.399866		

YSP11459

11/8/90 12:40

10 PSID Taps 14 1.0 PSID Taps 14 0.1 PSID Taps 14
 S = 1 S = 7.25 S = 9.9 <C> (ppm) =
 Z = 5.3 Z = 7.2 Z = 6.8 [NaCl] =
 FlowCo = 0.019693

Tap Pair	Freq. (Hz)	Qtest (1/s)	Temp (deg C)	<U> (volts)	<U>0 (volts)	<U>f (volts)	<U>icorr (volts)
12	60	1.181580	24.9	2.017	0.0155	0.0225	2.0015
12	50	0.984650	24.9	1.469666	0.0155	0.0225	1.454166
12	40	0.787720	24.9	1.02525	0.0155	0.0225	1.00975
12	30	0.590790	24.9	0.661	0.0155	0.0225	0.6455
12	21	0.413553	24.9	0.39625	0.0155	0.0225	0.38075
14	21	0.413553	24.9	1.168333	0.0215	0.0215	1.146833
14	15	0.295395	24.9	0.700555	0.0215	0.0215	0.679055
14	10	0.196930	24.9	0.401375	0.0215	0.0215	0.379875
14	8	0.157544	24.9	0.299	0.0215	0.0215	0.2775
12	17	0.334781	25	3.133666	-0.0155	-0.0135	3.147166
12	26	0.512018	25	6.16925	-0.0155	-0.0135	6.18275
12	36	0.708948	25.1	10.14933	-0.0135	0.0005	10.14883
12	16	0.315088	25.1	2.992833	-0.0135	0.0005	2.992333
12	10	0.196930	25.1	1.5062	-0.0135	0.0005	1.5057
12	13	0.256009	25	2.1574	-0.0075	-0.0075	2.1649
14	24.7	3.0006	-0.0245	-0.0245	-0.0405	0.30251	3.0251
14	24.5	2.1124	-0.0345	-0.0345	-0.0425	2.1469	2.1469
14	24.4	1.7016	-0.0375	-0.0375	-0.0435	1.7391	1.7391
14	24.4	1.29325	-0.0395	-0.0395	-0.0465	1.33275	1.33275
14	24.3	8.2786	0.0775	0.0805	0.0805	8.1981	8.1981
14	24.3	6.565	0.0805	0.0865	0.0865	6.4785	6.4785
14	24.4	4.320857	0.0855	0.0925	0.0925	4.228357	4.228357
14	24.3	3.409	0.0905	0.0965	0.0965	3.3125	3.3125
14	24.3	2.743454	-0.0225	-0.0185	-0.0185	2.761954	2.761954
14	24.2	2.059	-0.0195	-0.0155	-0.0155	2.0745	2.0745
14	24.15	1.607176	-0.0175	-0.0135	-0.0135	1.620676	1.620676
14	24	1.096476	-0.0155	-0.0125	-0.0125	1.108976	1.108976
14	23.9	0.887206	-0.0135	-0.0095	-0.0095	0.896706	0.896706
14	23.8	0.723376	-0.0105	-0.0105	-0.0105	0.734076	0.734076
14	23.8	0.581592	-0.0115	-0.0115	-0.0115	0.593092	0.593092
14	23.65	0.488	-0.0135	-0.0135	-0.0135	0.5015	0.5015
14	23.55	0.392187	-0.0145	-0.0165	-0.0165	0.358687	0.358687
14	23.5	0.211482	-0.0185	-0.0175	-0.0175	0.228982	0.228982
14	23.75	10.843	-0.0205	-0.0215	-0.0215	10.8645	10.8645
14	23.9	4.542666	-0.0345	-0.0015	-0.0015	4.544166	4.544166
12	24	6.25625	-0.0095	0.0055	0.0055	6.25075	6.25075

density viscosity
 col[NaCl] 1.000088 1.001574 ID[cm] = 1.02108
 50.01221 X coeff -0.00025 -0.03281 K(U/psi)=1.180945 13.84846
 0.000100 constant 0.003419 -4.14933 XS[cm2]= 0.818859

Batch	Vol	t[samp]	DP	<U>	Re	Tw	f	Log(Re/f)
(ml)	(sec)	(psid)	(cm/s)	dyne/cm2				
1440	20	0.096865	87.92716	9865.922	14.32985	0.003716	2.779208	2.779208
1210	20	0.076547	73.88324	8290.115	11.32408	0.004159	2.728088	2.728088
1068	25.1	0.049980	51.96226	5843.627	7.390931	0.005488	2.636422	2.636422
1127	35	0.039139	39.32298	4412.259	5.790079	0.007508	2.582429	2.582429
1050	40	0.032634	32.05677	3596.950	4.827754	0.009419	2.542959	2.542959
932	50	0.024511	22.76336	2548.422	3.626119	0.014031	2.479833	2.479833
839	60	0.019149	16.87306	1886.856	2.832859	0.019951	2.425721	2.425721
810	75	0.013103	9.932513	1106.966	1.938433	0.039395	2.341857	2.341857
729	119.9	0.010595	4.25042	825.6471	1.567397	0.057001	2.294736	2.294736
504	110	0.008673	5.595365	620.7892	1.283128	0.082168	2.250296	2.250296
383	110	0.007007	4.252033	471.7505	1.036695	0.114960	2.203986	2.203986
333	120	0.005925	3.287091	363.4611	0.876596	0.162648	2.166083	2.166083
209	120	0.004228	2.126941	234.6507	0.626967	0.277841	2.092320	2.092320
99	150	0.002705	1.007498	111.0250	0.400250	0.790498	1.994371	1.994371
1351	15.1	0.128371	109.2619	12108.62	18.99058	0.003189	2.834937	2.834937
1554	15	0.053692	126.5174	14068.43	23.83554	0.002984	2.885667	2.885667
1920	15	0.073856	156.3149	17421.11	32.77333	0.002689	2.955891	2.955891
1951	15	0.218443	158.8387	17984.16	32.31536	0.022568	2.959772	2.959772
1594	15.1	0.155028	128.9145	14530.35	22.93406	0.002767	2.883298	2.883298
1361	14.9	0.125580	111.5481	12544.60	18.57778	0.002993	2.836569	2.836569
1433	19.9	0.096238	87.93943	9889.585	14.23698	0.003691	2.778781	2.778781
1440	20	0.096865	87.92716	9865.922	14.32985	0.003716	2.779208	2.779208
1210	20	0.076547	73.88324	8290.115	11.32408	0.004159	2.728088	2.728088
1068	25.1	0.049980	51.96226	5843.627	7.390931	0.005488	2.636422	2.636422
1127	35	0.039139	39.32298	4412.259	5.790079	0.007508	2.582429	2.582429
1050	40	0.032634	32.05677	3596.950	4.827754	0.009419	2.542959	2.542959
932	50	0.024511	22.76336	2548.422	3.626119	0.014031	2.479833	2.479833
839	60	0.019149	16.87306	1886.856	2.832859	0.019951	2.425721	2.425721
810	75	0.013103	9.932513	1106.966	1.938433	0.039395	2.341857	2.341857
729	119.9	0.010595	4.25042	825.6471	1.567397	0.057001	2.294736	2.294736
504	110	0.008673	5.595365	620.7892	1.283128	0.082168	2.250296	2.250296
383	110	0.007007	4.252033	471.7505	1.036695	0.114960	2.203986	2.203986
333	120	0.005925	3.287091	363.4611	0.876596	0.162648	2.166083	2.166083
209	120	0.004228	2.126941	234.6507	0.626967	0.277841	2.092320	2.092320
99	150	0.002705	1.007498	111.0250	0.400250	0.790498	1.994371	1.994371
1351	15.1	0.128371	109.2619	12108.62	18.99058	0.003189	2.834937	2.834937
1554	15	0.053692	126.5174	14068.43	23.83554	0.002984	2.885667	2.885667
1920	15	0.073856	156.3149	17421.11	32.77333	0.002689	2.955891	2.955891

Solvent	L	MDR	DATA	1//f/Siv	1//f/L
1//f	1//f	1//f	1//f		
84.65346					
82.65316					
84.65346					
4					
0.4					
14.18050	276.0620	34.85740	37.15526	2.620164	0.134590
13.90502	235.3076	35.53936	36.32535	2.612766	0.154373
13.58622	196.0911	34.03456	34.87385	2.566654	0.177854
13.19758	156.7750	32.18854	32.71297	2.478708	0.208661
12.73907	120.4062	30.01060	29.81578	2.340498	0.247626
12.74267	120.6560	30.02771	29.75404	2.334991	0.246602
12.28748	92.84333	27.84556	27.61947	2.247772	0.297484
11.78295	69.44154	25.46904	24.61820	2.089306	0.354517
11.51020	59.35133	24.17345	23.04280	2.001946	0.388244
12.43923	101.3183	28.58635	28.74858	2.311121	0.283745
13.02575	142.0100	31.57234	31.56966	2.408279	0.220897
13.46016	182.3565	33.43578	33.90130	2.518639	0.185906
12.59935	99.01897	28.39692	27.74833	2.237885	0.280232
11.80281	70.23969	25.56334	24.44852	2.071415	0.348072
12.11426	84.03247	27.04277	26.50446	2.188036	0.315431
11.43893	56.96558	23.83491	19.73139	1.724933	0.346373
11.13319	47.77252	22.38266	19.00981	1.707490	0.397923
10.94627	42.89921	21.49481	18.27626	1.669632	0.426027
10.71512	37.55445	20.39684	16.45874	1.536028	0.438263
10.71683	37.59137	20.40495	16.40323	1.530604	0.436356
10.51235	33.41710	19.43368	15.50499	1.474931	0.463983
10.14569	27.05843	17.69202	13.49770	1.330387	0.498835
9.929718	23.89513	16.66616	11.54068	1.162236	0.482972
9.771839	21.81925	15.91623	10.30325	1.054382	0.472209
9.519292	18.86701	14.71643	8.442056	0.886836	0.447450
9.302887	16.45719	13.68871	7.079732	0.761025	0.425025
8.967428	13.73210	12.09528	5.038222	0.561835	0.366893
8.778944	12.32015	11.19998	4.188499	0.477107	0.339971
8.601185	11.12183	10.35563	3.488573	0.405592	0.313668
8.415947	9.996935	9.475750	2.949345	0.350447	0.295024
8.244333	9.161430	8.755582	2.479560	0.300031	0.270652
7.969282	7.730378	7.354093	1.897148	0.238037	0.245414
7.577485	6.169520	5.493056	1.124733	0.148430	0.182304
10.93975	42.73836	21.46381	17.70748	1.618637	0.414333
11.14267	48.03390	22.43268	18.30534	1.642815	0.381092
11.42356	56.46404	23.76194	19.28341	1.688037	0.341516

Tw	8<U>/D	Log	Log
dynes/cm2	(1/sec)	Tw	8<U>/D
3.626119	178.3473	0.559442	2.251266
2.832859	132.1977	0.452224	2.121224
1.938433	77.81966	0.287450	1.891089
1.567397	58.17402	0.195179	1.744729
1.283128	43.83879	0.108270	1.641858
1.036695	33.31400	0.015651	1.522626
0.876596	25.75384	-0.05720	1.410842
0.626967	16.66425	-0.20275	1.221785
0.400250	7.893593	-0.39766	0.897274

Regression Output:

Constant -1.09192
 Std Err of Y Est 0.003547
 R Squared 0.999679
 No. of Observations 6
 Degrees of Freedom 4

X Coefficient(s) 0.729733
 Std Err of Coef. 0.006533

Tw vs. K*(8<U>/D)^n
 K' = 0.080924
 n = 0.729733
 161141.7

Regression Output:

Constant -41.4883
 Std Err of Y Est 0.313166
 R Squared 0.996593
 No. of Observations 9
 Degrees of Freedom 7

X Coefficient(s) 21.72891
 Std Err of Coef. 0.480123

t = 24.45 deg C
 s.d.(t) = 0.500277 deg C

Page 1

Cyanamid 852A

YIP05144

10 PSID Taps 14 1.0 PSID Taps 14 0.1 PSID Taps 14
 S = 2.7 S = 7.25 S = 9.9 <D>(ppm) =
 Z = 2.85 Z = 9.15 Z = 6.9 [NaCl] =
 FlowCo= 0.019693

10/31/90 15:34

Page 2

Cyanamid 852A

24.4 10.70066 -0.0845 0.1385 10.56216
 24.4 10.903 -0.0845 0.1385 10.7645
 24.4 10.87033 -0.0845 0.1385 10.73183

12
 23
 34

Tap Pair	Freq. (Hz)	Q'est (1/s)	Temp (deg C)	<V> (volts)	<V> (volts)	<V> (volts)	<V>f (volts)	<V>corr (volts)
23	60	1.181580	24.9	9.925666	0.0475	0.0945	9.878166	
23	50	0.984650	24.9	7.126333	0.0475	0.0945	7.078833	
23	39	0.769027	24.9	4.48575	0.0475	0.0945	4.40825	
23	31	0.610483	24.9	2.965	0.0475	0.0945	2.9175	
14	35	0.689255	24.9	10.897	0.0495	0.055	10.8475	
14	29	0.571097	24.9	7.823666	0.0495	0.055	7.768666	
14	22	0.43246	24.9	4.733	0.0495	0.055	4.678	
14	16	0.315088	24.9	2.721666	0.0495	0.055	2.666666	
14	10	0.194930	24.9	1.2425	0.0495	0.055	1.1875	
14	8	0.157544	24.9	0.867	0.0495	0.055	0.8175	
12	45	0.886185	24.1	6.040333	0.0445	0.0515	5.995833	
23	45	0.886185	24.1	5.983333	0.0445	0.0515	5.940833	
34	45	0.886185	24.1	6.116333	0.0445	0.0515	6.071833	
14	13	0.256009	24.1	1.971	0.0525	0.0465	1.9185	
23	17	0.334781	24.9	11.863	0.0275	0.0415	11.8215	
23	13	0.256009	24.9	7.450666	0.0275	0.0415	7.409166	
23	9	0.177337	24.9	4.059	0.0275	0.0415	4.0175	
14	14		24.7	5.3448	0.0345	-0.0195	5.3643	
14	14		24.7	4.0696	-0.0325	-0.0375	4.1071	
14	14		24.7	3.2868	-0.0445	-0.0475	3.3343	
14	14		24.7	2.21833	-0.0525	-0.0575	2.269333	
14	14		24.7	1.667166	-0.0605	-0.0665	1.733666	
14	14		24.6	1.0045	-0.0665	-0.069	1.0735	
14	14		24.5	6.767635	-0.0025	-0.0345	6.802125	
14	14		24.5	4.6772	-0.04	-0.0355	4.7127	
14	14		24.5	3.3921	-0.0455	-0.0425	3.4376	
14	14		24.5	2.089461	-0.0485	-0.0505	2.137961	
14	14		24.4	0.914823	-0.0545	-0.0575	0.969323	
14	14		24.4	0.66245	-0.0585	-0.0575	0.72095	
14	14		24.4	0.49856	-0.0585	-0.0545	0.55706	
14	14		24.3	0.37315	-0.0575	-0.0565	0.42965	
14	14		24.2	0.25696	-0.0565	-0.0545	0.31146	
14	14		24.1	0.19275	-0.0545	-0.0525	0.24625	
14	14		24.1	0.09976	-0.0535	-0.0525	0.15326	
14	14		24	0.042125	-0.0535	-0.053	0.095125	
14	14		23.9	-0.02288	-0.0535	-0.053	0.030611	
14	14		24.1	10.54514	-0.0555	-0.0615	10.60644	
13	13		24.3	9.088166	-0.0805	-0.1185	9.206666	
13	13		24.2	12.3708	-0.0205	-0.0485	12.4193	
12	12		24.3	7.4584	-0.0585	-0.0605	7.5189	
12	12		24.7	8.282	-0.0745	-0.0745	8.3565	

20.1 0.128712 130.0194 14399.81 57.11507 0.006692 3.071157
 20.1 0.131177 130.0194 14399.81 58.23016 0.006823 3.075256
 20.1 0.130779 130.0194 14399.81 58.03626 0.006800 3.074632

2140
 2140
 2140

density viscosity ID(cm) = 1.02108
 col(NaCl) 1.01234 1.029478 K(W/psi)=1.098348 13.19
 0.999734 X coeff -0.00025 -0.02281 XS(cm2)= 0.818859
 0.299950 constant 0.003419 -4.14933

Batch Vol (gal)	t)saap (sec)	DP (psid)	<U> (cm/s)	Re	Ta dyne/cm2	f	Log(Re/f)
8.993658	1442.758	161622.2	3992.302	0.003798	3.998320		
6.444982	1202.465	134685.2	2860.940	0.003919	3.925962		
4.013527	937.9229	105054.4	1781.612	0.004012	3.823115		
2.656261	745.5285	83504.84	1179.119	0.004202	3.733487		
9.876195	841.7257	94279.66	1461.034	0.004085	3.780039		
7.073046	697.4299	78117.43	1046.350	0.004261	3.707547		
4.259123	529.0847	59261.50	630.0732	0.004439	3.597404		
2.427888	384.7889	43099.27	359.1695	0.004805	3.475358		
1.081169	240.4930	26937.04	159.9426	0.005478	3.299690		
0.744299	192.3944	21549.63	110.1079	0.005895	3.218617		
5.458955	1082.218	119048.6	2422.368	0.004096	3.881947		
5.408880	1082.218	119048.6	2401.012	0.004060	3.880024		
5.528150	1082.218	119048.6	2453.230	0.004149	3.884694		
1.746714	512.6409	34391.82	258.4000	0.005236	3.395973		
1.896247	408.8382	45792.97	397.8458	0.004715	3.497565		
0.561726	312.6409	35018.15	249.3512	0.005054	3.396114		
0.304586	216.4437	24243.34	135.2066	0.005717	3.263207		
15	0.406694	135.7986	15141.99	60.16432	0.006463	3.085407	
15	0.311379	115.6893	12899.74	46.06395	0.006818	3.027418	
15	0.252789	101.7675	11347.42	37.39647	0.007761	2.982153	
1320	20	0.172049	80.59990	8967.157	25.45213	0.007761	2.898600
1400	25	0.131437	68.38779	7625.467	19.44426	0.008236	2.840133
1274	30	0.081387	51.86074	5769.615	12.04004	0.008868	2.735066
1266	29.9	0.082891	51.70744	5739.597	12.26259	0.009085	2.738058
1372	40	0.057429	41.88752	4449.572	8.495866	0.007592	2.658571
1142	39.9	0.041891	34.95294	3879.824	6.197167	0.010048	2.589864
1150	50	0.026053	28.08784	3117.789	3.854231	0.009677	2.486736
1078	60	0.011812	21.94108	2430.002	1.747457	0.007190	2.313985
1033	74.9	0.008785	16.84259	1865.338	1.299699	0.009075	2.249704
1091	100	0.006788	13.52340	1475.583	1.004245	0.011206	2.193702
934	109.9	0.005335	10.37862	1146.855	0.774255	0.014243	2.136323
627	100	0.003795	7.656990	844.2034	0.561487	0.018970	2.045482
496	100	0.003000	6.057204	666.3179	0.443929	0.023966	2.013483
309	99.9	0.001867	3.777318	415.5208	0.276290	0.038356	1.910510
191	100.2	0.001159	2.327856	255.4969	0.171487	0.062682	1.805958
93	150	0.000373	0.757150	82.91478	0.055184	0.190862	1.558765
1113	20	0.129254	67.96037	7475.925	19.12122	0.008200	2.830584
1860	29.1	0.112193	78.05676	8625.401	24.89707	0.008094	2.889871
1148	15	0.151343	93.46332	10304.57	33.58482	0.007615	2.933883
1290	15	0.091626	105.0241	11605.33	40.65856	0.007301	2.996373
1385	15	0.101833	112.7584	12572.94	45.18789	0.007040	3.023249

11.88463 73.62713 25.95199 12.22359 1.028521 0.166020
 11.90142 74.34239 26.03177 12.10599 1.017188 0.162841
 11.89852 74.21851 26.01801 12.12619 1.019134 0.163305

82.06026	0.4	Solvent	L	MDR	1//f	1//f	1//f/Siv	1//f/L
		1//f	1//f	1//f	1//f	1//f	1//f	1//f
15.59328	622.5872	43.54688	16.22486	1.040503	0.026040			
15.30385	527.0391	42.19329	15.97191	1.043653	0.030304			
14.89246	415.9059	40.23918	15.78499	1.040066	0.037958			
14.53594	338.3510	38.53626	15.42496	1.061305	0.045588			
14.72015	374.6333	39.42073	15.44513	1.062837	0.041539			
14.43018	318.7330	38.04339	15.31795	1.061521	0.048058			
13.98961	247.3341	35.95067	14.97306	1.070441	0.060545			
13.50143	186.7404	33.63180	14.42466	1.068394	0.077245			
12.79876	124.6151	30.29412	13.51012	1.055580	0.108414			
12.47447	103.3945	28.75373	13.02633	1.044239	0.125986			
15.12778	476.2412	41.35699	15.62346	1.052765	0.032805			
15.12009	474.1373	41.32045	15.69279	1.037876	0.033097			
15.13878	479.2654	41.40922	15.52488	1.025503	0.032393			
13.18389	155.5439	32.12349	13.81916	1.048185	0.088844			
13.59026	196.5377	34.05375	14.56240	1.071531	0.074094			
13.18445	155.5945	32.12617	14.06627	1.064882	0.090403			
12.65283	114.3743	29.60094	13.22467	1.045194	0.115424			
11.94163	76.08300	26.22274	12.43871	1.041626	0.163488			
11.70967	66.57309	25.12095	12.11051	1.034231	0.181913			
11.52861	59.98372	24.26091	11.82343	1.025573	0.197110			
11.19440	49.48576	22.67340	11.35068	1.013961	0.229372			
10.96053	43.25276	21.56234	11.01875	1.005311	0.254752			
10.54026	33.95837	19.56627	10.61890	1.007461	0.312703			
10.55223	34.19313	19.62312	10.49113	0.994209	0.306819			
10.23348	28.46109	18.10905	10.21036	0.977741	0.358748			
9.959437	24.30772	16.80742	9.975801	1.001641	0.410396			
9.546946	19.14975	14.84799	10.16506	1.064745	0.530265			
8.855943	12.87851	11.56573	11.79290	1.331637	0.915703			
8.598816	11.10667	10.34437	10.49671	1.220716	0.945082			
8.374809	9.762981	9.280346	9.446293	1.127941	0.967362			
8.145294	8.534678	8.190149	8.378858	1.028674	0.979447			
7.861928	7.267118	6.844161	7.260473	0.923497	0.999085			
7.653935	6.447094	5.856195	6.459479	0.843942	1.001921			
7.242041	5.086163	3.899653	5.106020	0.705052	1.003904			
6.823832	3.997956	1.913202	3.994180	0.585338	0.999055			
5.835060	2.262794	-2.78346	2.290165	0.392483	1.012086			
10.92253	42.31212	21.36111	11.04282	1.011031	0.260984			
11.15948	48.50109	22.50755	11.14495	0.996009	0.229169			
11.41553	56.20353	23.72378	11.45899	1.003807	0.203883			
11.58569	61.98025	24.53109	11.70265	1.010112	0.188812			
11.69299	65.93700	25.04173	11.91757	1.019205	0.180741			

Y1P03146

Tw	B<U>/D	Log	Log
dyne/ea2	(1/sec)	Tw	B<U>/D
0.774555	81.31487	-0.11094	1.910169
0.561487	59.99130	-0.25065	1.778088
0.443929	47.45723	-0.35268	1.676302
0.276290	29.59468	-0.55863	1.471213
0.171487	18.23838	-0.76576	1.260986
0.055186	5.932154	-1.25818	0.773212

Regression Output:

Constant	-2.03586
Std Err of Y Est	0.003147
R Squared	0.999954
No. of Observations	6
Degrees of Freedom	4

X Coefficient(s)	1.005452
Std Err of Coef.	0.003393

Tw vs. $K^* \cdot (B<U>/D)^n$

K'	= 0.009207
n	= 1.005452

Res/ft	= 546.0208
Tw	= 12.21470

Regression Output:

Constant	-3.86420
Std Err of Y Est	0.065299
R Squared	0.997971
No. of Observations	9
Degrees of Freedom	7

X Coefficient(s)	5.265597
Std Err of Coef.	0.089726

t	= 24.51818 deg C
s.d.t	= 0.316423 deg C

YZP03147 10 PSID Taps 14 1.0 PSID Taps 14 0.1 PSID Taps 14
 S = 2.7 S = 7.25 S = 9.9 C<(ppm)>= 6.9
 Z = 2.8 Z = 9.15 Z = 6.9 [NaCl]=
 FlowCo= 0.019693

density viscosity ID(cm) = 1.02108
 col[NaCl] 1.01234 1.029478 K(V/psi)=1.098348 13.19348
 1.999589 X coeff -0.00025 -0.02281 XS(cm2)= 0.818859
 0.300236 constant 0.003419 -4.14933

Tap Pair	Freq. (Hz)	Q'est (1/s)	Temp (deg C)	<U> (volts)	<U> (volts)	<U>f (volts)	<U>corr (volts)	Batch Vol (ml)	t[samp (sec)	DP (psid)	<U> (cm/s)	Re	Tw (dyne/cm2)	f	Log(Re/f)	
23	60	1.181580	24.9	9.233666	0.0635	0.0685	9.160166	8.339949	1442.958	161622.2	3702.119	0.003522	3.981933			
23	49	0.764957	24.9	6.21375	0.0635	0.0685	6.152225	5.601366	1178.416	151991.5	2486.437	0.003347	3.895499			
23	39	0.768027	24.9	3.948	0.0635	0.0685	3.8845	3.536675	937.9229	105054.4	1569.936	0.003353	3.795649			
23	30	0.590790	24.9	2.37425	0.0635	0.0685	2.31075	2.103841	721.4792	80811.13	933.8992	0.003354	3.682858			
23	20	0.593860	24.9	1.1184	0.0635	0.0685	1.0549	0.960442	480.9861	53874.09	426.3422	0.003651	3.512587			
23	14	0.275702	24.9	0.653333	0.0635	0.0685	0.589833	0.537018	336.4903	37711.86	238.3836	0.004166	3.386346			
23	10	0.196950	24.9	0.393	0.0635	0.0685	0.3295	0.299995	240.4930	26937.04	133.1687	0.004561	3.259909			
23	8	0.157544	24.9	0.291333	0.0635	0.0685	0.227833	0.207432	192.3944	21549.63	92.07979	0.004928	3.179790			
35	35	0.689255	23.3	3.262	0.0635	0.0665	3.1985	2.912100	841.7257	90937.22	1292.221	0.003611	3.737613			
35	35	0.689255	23.3	3.267	0.0635	0.0665	3.2033	2.916653	841.7257	90937.22	1294.707	0.003618	3.738031			
34	35	0.689255	23.3	3.2965	0.0635	0.0665	3.233	2.943511	841.7257	90937.22	1306.243	0.003651	3.739957			
23	20	0.393860	25	12.9006	0.0205	0.1	12.8801	0.976247	480.9661	53995.76	433.3580	0.003711	3.517117			
23	15	0.295375	25	7.9542	0.0205	0.1	7.9337	0.601334	360.7396	40496.82	266.9337	0.004063	3.411895			
23	10	0.196950	25	3.9912	0.0205	0.1	3.8912	0.294933	240.4930	26997.88	130.9215	0.004484	3.257199			
23	8	0.157544	25	2.872	0.0205	0.1	2.772	0.210103	192.3944	21598.30	93.26547	0.004991	3.182554			
14	24.7	4.8392	0.0845	0.0775	0.0845	0.0775	4.7617	15	0.360913	136.9384	15289.09	0.005640	3.059474			
14	24.6	3.4262	0.0815	0.0765	0.0815	0.0765	3.3497	15	0.253890	107.3037	11937.75	0.006462	2.982111			
14	24.6	3.0914	0.0735	0.0755	0.0735	0.0755	3.0159	19.9	0.228590	101.0730	11244.47	0.006537	2.959317			
14	24.4	2.08	0.0345	0.0225	0.0345	0.0225	2.0575	19.9	0.155948	78.85706	8733.517	0.007349	2.874308			
14	24.4	1.614	0.0225	0.0175	0.0225	0.0175	1.5965	35	0.121006	67.11773	7433.371	0.007871	2.819222			
14	24.4	1.017	0.017	0.0145	0.017	0.0145	1.0025	30	0.075984	50.19175	5558.798	0.008838	2.718180			
14	24.35	0.7227	0.0145	0.0145	0.0145	0.0145	0.7082	40	0.0533678	40.91053	4525.786	0.009398	2.642223			
14	24.3	4.5005	-0.0175	-0.0585	-0.0175	-0.0585	4.559	40	0.054875	40.94108	4524.057	0.009586	2.646262			
14	24.25	3.098166	-0.0725	-0.0765	-0.0725	-0.0765	3.174666	50	0.038184	33.36347	3682.562	0.010052	2.567284			
14	24.2	2.206333	0.0105	0.0095	0.0105	0.0095	2.196833	60	0.026423	28.67809	3161.835	0.009414	2.486841			
14	24.1	0.989619	0.0015	0.0005	0.0015	0.0005	0.988119	75	0.011885	21.81896	2400.177	0.007315	2.312362			
14	24	0.704952	-0.0015	-0.0015	-0.0015	-0.0015	0.704452	75	0.008497	16.20139	1778.205	0.007024	2.228515			
14	23.9	0.575384	-0.0035	-0.0035	-0.0035	-0.0035	0.579884	100	0.006974	13.51880	1480.430	0.011182	2.194657			
14	23.85	0.440307	-0.0015	-0.0015	-0.0015	-0.0015	0.441807	105	0.005314	10.45588	1143.722	0.011829	2.16242			
14	23.7	0.32116	-0.0015	0.0015	0.0015	0.32266	659	99.9	0.003880	7.689104	838.2352	0.0124	2.063589			
14	23.6	0.20532	0.0025	0.0085	0.0025	0.20282	377	100.2	0.002439	4.848206	527.3409	0.030887	1.963048			
14	23.5	0.121375	0.0095	0.0145	0.0095	0.109375	216	100.2	0.001315	2.632549	285.6980	0.194616	0.056615	1.828505		
14	23.4	0.067937	0.0155	0.0245	0.047937	0.0245	0.047937	100	0.000576	1.155725	122.9771	0.085297	0.130963	1.648398		
14	23.5	6.43375	0.0265	0.0205	6.41375	0.0205	6.41375	30.1	0.077137	49.98443	5424.571	0.085297	0.130963	1.648398		
14	23.7	9.8712	0.0185	0.0205	9.8597	0.0205	9.8597	20.1	0.118483	65.43501	7133.462	0.085297	0.130963	1.648398		
14	23.7	12.783	0.0145	0.0155	12.7685	0.0155	12.7685	15.1	0.149317	98.26297	10724.32	0.085297	0.130963	1.648398		
24	23.75	12.4775	0.0535	0.0695	12.4425	0.0695	12.4425	20	0.092539	111.9850	12233.72	0.085297	0.130963	1.648398		
23	23.8	7.7592	0.0625	0.0655	7.6937	0.0655	7.6937	15	0.119506	132.8677	14484.70	0.085297	0.130963	1.648398		
23	23.7	10.00125	0.0575	0.0655	9.93575	0.0655	9.93575	15	0.119506	132.8677	14484.70	0.085297	0.130963	1.648398		

Solvent	L	MDR	1/f/f	1/f/f	1/f/f/Slv	1/f/f/L
83.13996	4					
0.4						
15.52773	599.5338	43.25674	16.84874	1.085074	0.028103	
15.18199	491.3365	41.61448	16.78985	1.105905	0.034171	
14.78259	390.4178	39.71734	16.81763	1.137664	0.043075	
14.33143	301.1192	37.57431	16.77307	1.170369	0.055702	
13.65035	203.4546	34.33916	16.54978	1.212407	0.081343	
13.14538	152.1341	31.94058	15.49284	1.178576	0.101836	
12.63963	113.7076	29.53828	14.80608	1.171400	0.130211	
12.31916	94.55199	28.01602	14.24456	1.156293	0.150653	
14.55045	341.5811	38.61466	16.63902	1.143539	0.048711	
14.55212	341.9095	38.62259	16.62304	1.142310	0.048618	
14.55982	343.4293	38.65919	16.54947	1.136653	0.048188	
13.64846	205.5877	34.42522	16.41506	1.200943	0.079844	
13.24758	161.3524	32.42601	15.68648	1.184101	0.097218	
12.62879	113.0002	29.48678	14.93242	1.182410	0.132145	
12.33621	95.37491	28.08752	14.13355	1.147503	0.148399	
11.85789	71.67287	25.73002	13.31491	1.124769	0.185773	
11.52844	59.97794	24.26011	12.43973	1.079047	0.207405	
11.43726	56.91111	23.82702	12.34872	1.079691	0.216982	
11.09723	46.79378	22.21185	11.66490	1.051154	0.249283	
10.87689	41.21949	21.16533	11.27101	1.036255	0.273439	
10.47272	32.66332	19.24542	10.63654	1.015442	0.325441	
10.16889	27.42228	17.80224	10.31502	1.014370	0.376155	
10.18545	27.68487	17.88088	10.21328	1.002733	0.368912	
9.869137	23.07619	16.37840	9.973920	1.010617	0.432216	
9.547364	19.17437	14.84998	10.30619	1.079480	0.537498	
8.849448	12.83045	11.53487	11.69179	1.321189	0.911253	
8.554054	10.82414	10.13175	10.26758	1.200317	0.948581	
8.378631	9.784481	9.296498	9.456492	1.128644	0.966478	
8.140444	8.530825	8.167109	8.379338	1.029346	0.982242	
7.861556	7.265561	6.842394	7.210688	0.917208	0.992447	
7.454347	5.747339	4.908149	5.734620	0.769298	0.997787	
6.914021	4.211000	2.341599	4.240352	0.613297	1.006970	
6.193594	2.781497	-1.08042	2.763284	0.446152	0.993452	
10.45034	32.24521	19.13912	10.51429	1.006119	0.326072	
10.83100	40.14488	20.94725	11.10580	1.041194	0.251870	
11.05634	45.70530	22.01764	11.51181	1.041194	0.251870	
11.38612	55.25994	23.58407	12.12940	1.065279	0.219497	
11.57471	61.59672	24.47987	12.41515	1.072610	0.201555	
11.79290	69.84013	25.51627	12.96237	1.099167	0.185400	

dyne/cm ²	Tw	8<U>/D	Log Tw	Log 8<U>/D
1.257024	126.9353	0.099343	2.103582	
1.031816	105.9176	0.013602	2.024968	
0.786129	81.92023	-0.10450	1.913391	
0.574124	60.24291	-0.24099	1.779905	
0.360887	37.98492	-0.44262	1.579611	
0.194616	20.62561	-0.71082	1.314406	
0.085297	8.898232	-1.06906	0.949303	

Regression Output:

Constant	-2.02230
Std Err of Y Est	0.003437
R Squared	0.999940
No. of Observations	5
Degrees of Freedom	3

X Coefficient(s) 1.000917
Std Err of Coef. 0.004464

Tw vs. R*(8<U>/D)^n

K' =	0.009499	17289.45
n =	1.000917	

116.5581 Tw# = 9.665741
Res/fg = 490.1467

Regression Output:

Constant	-9.82628
Std Err of Y Est	0.162904
R Squared	0.993608
No. of Observations	21
Degrees of Freedom	19

X Coefficient(s) 7.503770
Std Err of Coef. 0.138073

t = 24.24358 deg C
s.d.)t = 0.581022 deg C

Y5P03150 10 PSID Taps 14 1.0 PSID Taps 14 0.1 PSID Taps 14 11/8/90 12:40

S = 2.7 S = 7.25 S = 9.9 <C> (ppm) = 9.9 <C> (ppm) = 9.9

Z = 2.7 Z = 9.15 Z = 6.9 [NaCl] = 6.9 [NaCl] = 6.9

FlowCo = 0.019493

Tap Pair	Freq. (Hz)	Qlent (1/s)	Temp (deg C)	<U> (volts)	<U> (volts)	<U>f (volts)	<U>corr (volts)
12	60	1.181580	24.7	6.707333	0.0265	0.0315	6.675833
12	49	0.964957	24.7	4.126	0.0265	0.0315	4.0945
12	38	0.748334	24.7	2.349333	0.0265	0.0315	2.317833
14	35	0.689235	24.8	6.0633	0.0325	0.0325	6.033
14	28	0.551404	24.8	3.933	0.0325	0.0325	3.9025
14	21	0.413533	24.8	2.331666	0.0325	0.0325	2.299166
14	14	0.275702	24.8	1.223666	0.0325	0.0325	1.191166
14	10	0.196930	24.8	0.7227	0.0325	0.0325	0.6902
12	30	0.590790	22.7	1.553	0.0355	0.0315	1.5215
23	30	0.590790	22.7	1.601	0.0355	0.0315	1.5695
12	20	0.393860	24.9	8.457	0.0425	0.0645	8.4145
12	25	0.492325	24.9	12.40133	0.0425	0.0645	12.35883
12	16	0.315088	24.9	6.002	0.0425	0.0645	5.9375
12	12	0.236316	24.9	3.822	0.0425	0.0645	3.7575
12	9	0.177237	24.9	2.3885	0.0425	0.0645	2.324
14	24.6	3.9424	0.0335	-0.2965	-0.2965	-0.2965	3.9089
14	24.45	2.9902	0.0025	0.0015	0.0015	2.9887	1438
14	24.4	2.4362	0.0005	-0.0045	-0.0045	2.4407	1264
14	24.3	1.6795	-0.0055	-0.0045	-0.0045	1.684	1306
14	24.2	1.337666	-0.0045	-0.0075	-0.0075	1.365166	1103
14	24.15	0.909333	-0.0085	-0.0095	-0.0095	0.918833	1030
14	24	5.80175	0.0155	-0.0015	-0.0015	5.80325	1234
14	24	4.186777	0.0065	0.0085	0.0085	4.178277	1157
14	24	3.2783	0.0095	0.0115	0.0115	3.2668	1131
14	23.9	2.273307	0.0085	0.0085	0.0085	2.264807	1167
14	23.85	1.003375	0.0065	0.0045	0.0045	0.998875	1081
14	23.75	0.641375	0.0015	-0.0025	-0.0025	0.639875	1097
14	23.86	0.495045	-0.0015	-0.0055	-0.0055	0.497545	858
14	23.5	0.343444	-0.0055	-0.0055	-0.0055	0.348944	612
14	23.4	0.2245	-0.0075	-0.0075	-0.0075	0.232	406
14	23.3	0.13083	-0.0085	-0.0085	-0.0085	0.162083	320
14	23.1	0.10075	-0.013	-0.0165	-0.0165	0.1155	225
14	23	0.051275	-0.0165	-0.019	-0.019	0.070275	165
14	22.9	0.024689	-0.0205	-0.0225	-0.0225	0.047189	110
14	23.2	8.707571	-0.0235	-0.0265	-0.0265	8.731071	950
14	23.2	10.6575	-0.0275	-0.0245	-0.0245	10.682	1053
14	23.35	12.3114	-0.0305	-0.0325	-0.0325	12.3439	1230
24	23.2	10.056	-0.0895	-0.0955	-0.0955	9.9605	1408
24	23.2	12.5344	0.0905	0.0955	0.0955	12.4389	1408

density viscosity ID(cm) = 1.02108
 K(U/psi)=1.098348 13.19348
 XS(cm2)= 0.818859

col(NaCl) 1.01234 1.029478
 S.000475 X coeff -0.00025 -0.02281
 0.300029 constant 0.003419 -4.14933

Batch Vol (ml)	t(samp (sec)	DP (psid)	<U> (cm/s)	Re	Tw (dyne/cm2)	f	Log(Re/f)
6.078067	1442.958	160894.6	2697.094	0.002566	3.911186		
3.727871	1178.416	131397.3	1654.213	0.002359	3.805033		
2.110290	913.8736	101899.9	956.4246	0.002221	3.681474		
5.492794	841.7257	94067.20	812.5762	0.002272	3.651655		
3.553063	673.3806	75253.76	525.6222	0.002296	3.557060		
2.093295	505.0354	56440.32	309.6715	0.002405	3.442173		
1.084507	336.6903	37626.88	160.4365	0.002803	3.299374		
0.628398	240.4930	26876.34	92.96206	0.003184	3.180876		
1.385262	721.4792	76898.22	614.6991	0.002338	3.570365		
1.428964	721.4792	76898.22	634.3199	0.002412	3.577188		
0.637777	480.9861	53874.09	283.0085	0.002423	3.423608		
0.936737	601.2326	67342.61	415.6700	0.002278	3.507082		
0.450032	384.7889	43099.27	199.6985	0.002672	3.347895		
0.288799	288.3916	32324.45	126.3776	0.003006	3.248543		
0.176147	216.4437	24243.34	78.16410	0.003305	3.144212		
15	0.296275	142.3117	15832.47	43.82944	0.004287	3.015635	1748
14.9	0.226578	117.8591	13067.77	33.51148	0.004779	2.955871	1438
15	0.184992	103.9073	11397.11	27.36691	0.005119	2.911395	1264
20.1	0.127638	79.34831	8768.119	18.88223	0.005940	2.829824	1306
20	0.103472	67.34976	7425.489	15.30724	0.006684	2.783260	1103
25	0.069642	50.31387	5540.984	10.30263	0.008061	2.696793	1030
30.1	0.070288	50.06557	5495.012	10.39816	0.008216	2.697220	1234
35	0.050607	40.36973	4430.832	7.486565	0.009099	2.625983	1157
40	0.039567	34.52973	3789.855	5.853395	0.009724	2.572545	1131
50	0.027431	28.50305	3121.340	4.058042	0.009893	2.492014	1167
60	0.012074	22.00214	2406.716	1.786183	0.007308	2.313326	1081
90	0.007750	14.88520	1624.556	1.146516	0.010248	2.216068	1097
90	0.006026	11.64220	1273.776	0.891493	0.013027	2.152521	858
90.1	0.004226	8.295015	900.2183	0.625232	0.017996	2.081936	612
90	0.002809	5.509016	596.5199	0.415693	0.027125	1.992317	406
100	0.001963	3.907874	422.1936	0.309418	0.037660	1.913457	320
100.1	0.001398	2.744978	295.2232	0.206950	0.054389	1.827908	225
119.9	0.000851	1.18510	119.7546	0.084532	0.133830	1.641570	165
120.1	0.000571	0.818510	81.7546	0.084532	0.133830	1.641570	110
15	0.129379	77.34334	8327.085	19.13982	0.006336	2.821929	950
14.9	0.149508	86.30434	9234.555	22.11758	0.005880	2.854804	1053
15	0.120641	100.1392	10794.33	26.77246	0.005287	2.894804	1230
15	0.150659	114.6309	12356.43	33.43406	0.005038	2.943054	1408

YS03150

Tw dyn/cm² (1/sec) Log Tw 8<U>/D Log 8<U>/D

0.891493 91.21485 -0.04988 1.940065
0.625232 64.99013 -0.20395 1.812847
0.415693 43.16227 -0.38122 1.635104
0.290418 30.61757 -0.53697 1.485970
0.206950 21.50647 -0.88413 1.332569
0.125919 13.16696 -0.89990 1.119485
0.084553 8.763356 -1.07286 0.942670

Regression Output: -2.01700
Constant 0.003086
Std Err of Y Est 0.999927
R Squared 6
No. of Observations 4
Degrees of Freedom 4

X Coefficient(s) 0.999316
Std Err of Coef. 0.004261

Tw vs. K'(8<U>/D)^n

K' = 0.007616
n = 0.999316

Tw = 7.304254
Kes/fe = 424.1564

Regression Output: -25.1818
Std Err of Y Est 0.173880
R Squared 0.994746
No. of Observations 14
Degrees of Freedom 12

X Coefficient(s) 13.43161
Std Err of Coef. 0.281777

t = 24.02076 deg C
s.d.}t = 0.719245 deg C

82.563
4
0.4

Solvent L HDR 1/ff 1/ff 1/ff 1/ff/S1v 1/ff/L

15.24474 509.4085 41.91253 19.74037 1.294897 0.038751
14.82013 398.9457 39.89564 20.58508 1.388994 0.051598
14.52589 300.1612 37.54801 21.21775 1.481076 0.070687
14.20662 280.2433 36.98145 20.97890 1.476699 0.074859
13.82824 225.3928 35.18414 20.86738 1.509041 0.092582
13.56869 173.0031 33.00130 20.58992 1.525199 0.117858
12.79749 124.5245 30.28812 18.88527 1.475700 0.151459
12.32350 94.78862 28.03664 17.72123 1.438002 0.186955
13.88146 232.4050 35.43694 20.68001 1.489757 0.088982
13.90873 236.0849 35.56657 20.35766 1.463658 0.086230
13.29443 165.7632 32.64855 20.31288 1.527924 0.122541
13.62833 200.8921 34.23457 20.95111 1.537320 0.104290
12.99158 139.2438 31.21002 19.34523 1.489059 0.138930
12.59417 110.7703 29.32232 18.23843 1.448164 0.164650
12.17684 87.11485 27.34003 17.39323 1.428385 0.199658
11.66254 66.79118 24.89708 15.27259 1.309542 0.235720
11.42348 56.46144 23.76156 14.46537 1.266283 0.256199
11.24558 50.96540 22.91651 13.97653 1.242846 0.274235
10.91929 42.23807 21.36665 12.97425 1.188195 0.307169
10.73304 37.94378 20.48195 12.23106 1.139571 0.322347
10.38717 31.09378 18.83907 11.13764 1.072249 0.358195
10.38928 31.13149 18.84908 11.05185 1.061850 0.354363
10.10593 26.41575 17.49367 10.48340 1.037556 0.396861
9.890182 23.35746 16.47836 10.14091 1.025351 0.434161
9.568059 19.40416 14.94828 10.05370 1.050757 0.518121
8.855307 12.85899 11.55321 11.69763 1.321272 0.709684
8.464275 10.27895 9.705310 9.877926 1.167013 0.940985
8.250085 9.086601 8.687908 8.761562 1.061972 0.964206
7.927746 7.547733 7.156794 7.454376 0.940289 0.987631
7.569268 6.140407 5.434026 6.071664 0.802146 0.988804
7.253928 5.120792 3.956866 5.152932 0.710374 1.006276
6.951634 4.303171 2.520263 4.287873 0.616815 0.996445
6.516142 3.349002 0.451674 3.365516 0.445300 0.998522
6.166282 2.738108 -1.21015 2.735516 0.516489 1.004930
10.71254 37.49873 20.38459 12.12727 1.132063 0.333405
10.88771 41.47716 21.21665 12.56276 1.153847 0.302883
11.01922 44.73905 21.84132 13.04027 1.183411 0.291474
11.17921 49.05312 22.60128 13.75280 1.230212 0.280354
11.37221 54.81946 23.51804 14.08764 1.238777 0.256982

YIP13153 11/11/90 15:35
 10 PSID Taps 14 1.0 PSID Taps 14 0.1 PSID Taps 14
 S = 2.7 S = 7.25 S = 9.9 <D>(ppm)=
 Z = 2.7 Z = 9.1 Z = 6.9 [NaCl]=
 FlowCd= 0.019693 0.020236

Tap Pair	Freq. (Hz)	Qtest (1/s)	Temp (deg C)	<V> (volts)	<U>o (volts)	<U>f (volts)	<U>corr (volts)
13	60	1.181580	25.1	9.359666	0.09	0.0985	9.269666
13	50	0.986650	25.1	6.00375	0.09	0.0985	5.91375
13	40	0.787720	25.1	3.724	0.09	0.0985	3.634
13	30	0.590790	25.1	2.159333	0.09	0.0985	2.069333
13	21	0.415533	25.1	1.17675	0.09	0.0985	1.08675
13	16	0.315088	25.1	0.7978	0.09	0.0985	0.6993
13	13	0.256009	25.1	0.5922	0.09	0.0985	0.4937
13	9	0.177237	25.1	0.392571	0.09	0.0985	0.294071
14	30	0.590790	22.6	3.325	0.0675	0.0845	3.2405
14	40	0.787720	22.6	5.795	0.0675	0.0845	5.675
14	20	0.393860	22.6	1.706	0.0675	0.0845	1.6215
12	30	0.590790	25	11.91525	0.0115	0.0235	11.90375
12	23	0.45939	25	7.437	0.0115	0.0235	7.4255
12	17	0.334781	25	4.513	0.0115	0.0235	4.4895
12	12	0.236316	25	2.698	0.0115	0.0235	2.6745
12	9	0.177237	25	1.78714	0.0115	0.0235	1.764214
14	24.6	3.219	-0.0115	-0.0115	-0.0155	3.2345	
14	24.45	2.349	-0.0155	-0.0155	-0.0195	2.3685	
14	24.4	1.985	-0.0185	-0.0185	-0.0215	1.98	
14	24.2	1.407166	-0.0205	-0.0205	-0.0235	1.430666	
14	24.2	1.122142	-0.0235	-0.0235	-0.0245	1.146642	
14	24.05	0.774714	-0.0245	-0.0245	-0.0235	0.798214	
14	23.95	4.963833	0.0435	0.0435	0.0035	4.960333	
14	23.9	3.797111	0.003	0.003	-0.0125	3.809611	
14	23.9	2.950545	-0.0085	-0.0085	-0.0185	2.959045	
14	23.8	1.858687	-0.017	-0.017	-0.0265	1.875687	
14	23.7	0.974937	-0.0245	-0.0245	-0.0295	0.999437	
14	23.6	0.716695	-0.0295	-0.0295	-0.0315	0.746195	
14	23.6	0.590523	-0.0305	-0.0305	-0.0295	0.620023	
14	23.45	0.44708	-0.0305	-0.0305	-0.0295	0.47758	
14	23.25	0.312235	-0.0315	-0.0315	-0.0305	0.342735	
14	23.1	0.211058	-0.0335	-0.0335	-0.0335	0.244558	
14	22.9	0.153166	-0.0335	-0.0335	-0.0355	0.188666	
14	22.8	0.100434	-0.0375	-0.0375	-0.0375	0.137934	
14	22.7	0.045708	-0.0405	-0.0405	-0.0415	0.086708	
14	22.5	-0.00458	-0.0435	-0.0435	-0.0445	0.039913	
14	22.7	7.0888	-0.0465	-0.0465	-0.0465	7.1533	
14	22.9	8.6646	-0.062	-0.062	-0.0885	8.7531	
14	23	11.7128	-0.0885	-0.0885	-0.0915	11.8043	
13	23	9.7036	0.0135	0.0135	0.0225	9.6811	

Batch	Vol	t) samp	DP	<U>	Re	Tw	f	Log (Re/f)
(ml)	(sec)	(psid)	(cm/s)	(cm/s)	dynes/cm2			
			density	viscosity				
			co[NaCl] 1.01234	1.029478	ID(cm) = 1.02108			
			9.999572 X coeff -0.00025	-0.02281	K(U/psi) = 1.098348			13.19
			0.300099 constant 0.003419	-6.14933	XS(cm2) = 0.818859			
1843			8.439644	1442.958	162353.1	1872.849	0.001782	3.835930
1481			5.384222	1202.465	135294.3	1194.818	0.001637	3.738329
1707			3.308605	961.9725	108235.4	734.2158	0.001571	3.632590
1323			1.884041	721.4792	81176.58	418.0895	0.001591	3.510313
1390			0.989440	505.0354	56823.60	219.5677	0.001705	3.370463
1050			0.636683	384.7889	43294.17	141.2870	0.001890	3.274730
			0.449493	312.6409	35176.51	99.74749	0.002021	3.199129
			0.267739	216.4437	24352.97	59.41439	0.002512	3.086624
			2.950339	721.4792	76724.95	436.4583	0.001660	3.495020
			5.166850	961.9725	102299.9	764.3577	0.001635	3.616697
			1.476308	480.9861	51149.95	218.3975	0.001869	3.344672
			0.902482	721.4792	80993.65	400.4696	0.001524	3.499978
			0.562964	553.1340	62095.13	249.8109	0.001617	3.397499
			0.340371	408.8382	45896.40	151.0371	0.001790	3.288335
			0.202767	288.3916	32397.46	89.97636	0.002140	3.175757
			0.133753	216.4437	24298.09	59.35224	0.002510	3.085412
14.9			0.245223	151.0531	16804.96	36.27714	0.003149	2.974569
14.9			0.179567	121.3834	13458.53	26.56435	0.003571	2.905424
19.9			0.150115	104.7540	11601.64	22.20706	0.004008	2.866028
20			0.108466	80.78308	8906.548	16.04591	0.004870	2.795494
25			0.086932	67.89931	7486.078	12.86038	0.005525	2.745439
25			0.060516	51.29084	5635.847	8.952523	0.006740	2.665307
35			0.060447	51.24159	5617.791	8.942289	0.006745	2.664073
35			0.046424	41.45137	4539.297	6.867813	0.007916	2.606265
1281			45	0.036059	34.76379	3806.947	5.334448	0.008742
1368			60	0.022857	27.84360	3042.253	3.81414	0.008638
1086			60	0.012179	22.10391	2409.679	1.801745	0.007303
1251			89.9	0.009093	16.99370	1848.411	1.345211	0.009225
1059			89.8	0.007555	14.40158	1566.464	1.117754	0.010673
924			99.9	0.005819	11.29528	1224.440	0.860962	0.013344
603			90	0.004176	8.182111	882.9713	0.617869	0.018277
428			90.1	0.002980	5.801089	625.9088	0.440880	0.025943
365			99.9	0.002599	4.451880	477.7162	0.340120	0.033830
270			100	0.001680	3.297268	352.2302	0.248663	0.045289
177			105	0.001056	2.058612	219.4153	0.156514	0.073035
93			120	0.000486	0.946438	100.4211	0.071954	0.159051
1105			19.9	0.087171	67.81094	7227.569	12.89568	0.005553
985			15.1	0.106666	79.66175	8529.074	15.77973	0.004923
1263			15	0.143849	102.8259	11034.03	21.28031	0.003985
1458			15.1	0.117975	117.9155	12653.27	26.18005	0.003728

11.41096 56.05586 23.70208 17.46439 1.530492 0.311553

82.06026	4								
0.4									
Solvent	L	MDR	1//f	1//f	1//f	1//f	1//f	1//f	1//f
1//f	1//f	1//f	1//f	1//f	1//f	1//f	1//f	1//f	1//f
14.94372	428.3614	40.48267	23.68810	1.585154	0.055299				
14.55331	342.1447	38.62826	24.71437	1.698195	0.072333				
14.13036	268.2074	36.61922	25.22195	1.784947	0.094038				
13.64125	202.3921	34.29595	25.06785	1.837650	0.123857				
13.08185	146.6706	31.63879	24.21395	1.850957	0.165090				
12.69892	117.6549	29.81987	22.99849	1.811058	0.195474				
12.39651	98.85756	28.38346	22.23939	1.794003	0.224964				
11.94649	76.29652	26.24587	19.94928	1.669885	0.261470				
13.58008	195.3891	34.00538	24.54235	1.807231	0.125607				
14.06678	258.5695	36.31724	24.72737	1.757854	0.095631				
12.97869	138.2142	31.14878	23.12983	1.782138	0.167347				
13.59991	197.6325	34.09959	25.61370	1.883372	0.129602				
13.18999	156.0915	32.15248	24.86326	1.885008	0.159286				
12.75294	121.5711	30.07647	23.63431	1.853244	0.194727				
12.30303	93.67806	27.93940	21.61489	1.756875	0.230735				
11.94164	76.08381	26.22283	19.95997	1.671458	0.262341				
11.49827	58.94534	24.11682	17.81838	1.549656	0.302286				
11.22169	50.26952	22.80307	16.75296	1.491126	0.333845				
11.06411	45.91008	22.05453	15.79397	1.427495	0.344019				
10.77397	38.84850	20.67639	14.32897	1.329961	0.368842				
10.58175	34.77916	19.76334	13.45287	1.271327	0.386808				
10.26122	28.91923	18.24083	12.18013	1.187005	0.421177				
10.25629	28.83722	18.21739	12.17564	1.187139	0.422219				
10.02506	25.24328	17.11905	11.23387	1.121077	0.445252				
9.805605	22.24750	16.07642	10.69487	1.090689	0.480722				
9.405682	17.67260	14.17698	10.75907	1.143890	0.600799				
8.854931	12.87101	11.56092	11.70109	1.321421	0.909103				
8.597184	11.09625	10.33662	10.41123	1.211005	0.938266				
8.436296	10.11472	9.572407	9.679357	1.147346	0.956957				
8.203660	8.84682	8.467387	8.650130	1.054423	0.977749				
7.907604	7.460726	7.061121	7.396827	0.935406	0.991435				
7.608542	6.280808	5.640375	6.208483	0.813988	0.988484				
7.375284	5.491627	4.532600	5.436869	0.737174	0.990028				
7.099300	4.684952	3.221678	4.698956	0.661890	1.002989				
6.672134	3.706069	1.287637	3.700270	0.552928	0.998435				
6.010376	2.503077	-1.95070	2.507442	0.417185	1.001744				
10.32502	33.66172	19.49387	13.41948	1.275007	0.398657				
10.70821	37.06541	20.36403	14.25106	1.330853	0.380989				
10.97191	43.53703	21.61659	15.84001	1.443687	0.363828				
11.15150	48.28976	22.47152	16.37675	1.468517	0.339135				

Cyanamid 832A

Page 7

YIP13153

Tw	B(U)/D	Log	Log
dyne/cm2 (1/sec)	Tw	B(U)/D	Tw
0.860962	88.49674	-0.06501	1.946927
0.617869	64.10554	-0.20910	1.806895
0.440880	45.45061	-0.35567	1.657539
0.340120	34.95812	-0.46836	1.543548
0.248663	25.83357	-0.60438	1.412184
0.156314	16.12890	-0.80600	1.207604
0.071954	7.415193	-1.14293	0.870122

Regression Outputs

Constant -2.01440
 Std Err of Y Est 0.001567
 R Squared 0.999984
 No. of Observations 7
 Degrees of Freedom 5

X Coefficient(s) 1.000776
 Std Err of Coef. 0.001741

Tw vs. $K^*z(B(U)/D)^n$

K* = 0.009673
 n = 1.000776

Twz = 4.431038
 Res/fg = 340.5648

Regression Outputs

Constant -37.1138
 Std Err of Y Est 0.143522
 R Squared 0.998573
 No. of Observations 18
 Degrees of Freedom 16

X Coefficient(s) 18.49878
 Std Err of Coef. 0.174807

t = 23.93048 deg C
 s.d.)t = 0.957229 deg C

Y2P13156

10 PSID Taps 14 1.0 PSID Taps 14 0.1 PSID Taps 14
 S = 2.7 S = 7.25 S = 9.9 <C> (ppm) =
 Z = 2.8 Z = 9.2 Z = 6.9 [NaCl] =
 FlowCo = 0.019693

density viscosity

ID (cm) = 1.02108
 K(V/psi) = 1.44082 13.4081
 XS (cm²) = 0.818859

Tap Pair	Freq. (Hz)	Q'est (1/s)	Temp (deg C)	<U> (volts)	<U>o (volts)	<U>f (volts)	<U>corr (volts)	Batch Vol (ml)	t ₀ (sec)	DP (psid)	<U> (cm/s)	Re	T _w (dyne/cm ²)	f	Log(Re/f)
14	60	1.181580	25.5	11.1005	0.0785	0.1115	10.989			7.627637	1442.958	163824.8	1128.594	0.001073	3.729850
14	48	0.945264	25.5	6.68575	0.0785	0.1115	6.57625			4.563290	1154.366	131059.8	675.0700	0.001003	3.618294
14	39	0.768027	25.5	4.48725	0.0785	0.1115	4.35575			3.009512	937.9229	106486.1	445.2120	0.001002	3.527903
14	31	0.610483	25.5	2.967333	0.0785	0.1115	2.85833			1.982278	745.5285	84642.84	293.2482	0.001045	3.437237
14	21	0.413553	25.5	1.669	0.0785	0.1115	1.5575			1.081085	505.0354	57338.70	159.9502	0.001242	3.305585
14	25	0.492325	25.6	2.1215	0.1025	0.0995	2.022			1.403501	601.2326	68414.53	207.6269	0.001138	3.362346
14	17	0.334781	25.6	1.18925	0.1025	0.0995	1.08975			0.756412	408.8382	46521.88	111.9998	0.001326	3.229019
14	14	0.275702	25.6	0.9298	0.1025	0.0995	0.8503			0.576324	336.6903	38312.13	85.25849	0.001490	3.169973
14	10	0.195930	25.6	0.595166	0.1025	0.0995	0.495666			0.344050	240.4930	27365.81	50.89701	0.001743	3.057951
14	7	0.137851	25.6	0.39675	0.1025	0.0995	0.29725			0.206325	168.3451	19156.06	30.52280	0.002134	3.046917
14	31	0.610483	24.05	2.96475	0.0555	0.0545	2.90925			2.019356	745.5285	81918.80	298.7333	0.001064	3.426976
14	22	0.433246	24.05	1.734333	0.0555	0.0545	1.678833			1.165304	529.0847	58155.92	172.3892	0.001219	3.307589
14	10	0.196930	24.1	0.51725	0.0295	0.0545	0.48775			0.338554	240.4930	26455.24	50.08410	0.001715	3.079476
12	25	0.492325	25.9	6.07375	0.0065	0.0135	6.06725			0.449822	601.2326	68879.13	199.6051	0.001094	3.357646
12	20	0.393860	25.9	4.4475	0.0065	0.0135	4.441			0.329253	480.9861	55103.30	146.1034	0.001251	3.289890
12	15	0.293395	25.9	2.845	0.0065	0.0135	2.8315			0.209925	360.7396	41327.47	95.15290	0.001418	3.192158
12	10	0.196930	25.9	1.612	0.0065	0.0135	1.5985			0.118511	240.4930	27551.65	52.58870	0.001801	3.068006
12	8	0.157544	25.9	1.159	0.0065	0.0135	1.1455			0.084926	192.3944	22041.32	37.68555	0.002017	2.995647
14	25	6.157544	25.6	2.516	0.0385	-0.0125	2.4775	1856	15	0.183680	151.1044	17194.24	27.17275	0.002358	2.921671
14	14	0.8858	25.5	1.8858	-0.0125	-0.0165	1.9023	1473	15.1	0.141035	119.1286	13525.15	20.86406	0.003913	2.863219
14	10	0.57075	25.5	1.57075	-0.0155	-0.0215	1.59225	1271	15	0.118048	103.4772	11748.18	17.46349	0.003251	2.824685
14	7	0.433246	25.4	1.1655	-0.0205	-0.0235	1.189	1307	20	0.088151	79.80611	9040.290	13.04072	0.004057	2.760285
14	5	0.334781	25.35	0.964	-0.0225	-0.0225	0.9865	1388	25	0.073138	67.80161	7671.784	10.81974	0.004663	2.719250
14	25	6.0134	25.2	6.0134	0.0555	0.0555	5.9579	1384	25	0.073103	67.60622	7623.832	10.81449	0.004688	2.717667
14	20	4.295	25.15	4.295	0.0775	0.0615	4.2355	1228	30	0.051944	49.98822	5630.727	7.684448	0.006092	2.642977
14	15	2.845	25.2	3.435	0.0835	0.0835	3.3515	1178	35	0.041122	41.10246	4635.051	6.083484	0.007134	2.592740
14	10	1.612	25.1	2.6866	0.0165	-0.0775	2.7641	1118	40	0.033915	34.13283	3840.425	5.017263	0.008532	2.549912
14	8	0.157544	25	1.95525	0.0255	0.0115	1.92975	1150	50.1	0.023677	28.03178	3146.863	3.502790	0.008831	2.470900
14	25	6.0134	25	1.019277	0.0085	0.0065	1.010777	1274	70	0.012402	22.22603	2495.106	1.834715	0.007358	2.330478
14	24.85	0.721863	24.85	0.721863	0.0085	0.0145	0.707363	1064	80	0.006679	16.24210	1817.187	1.283972	0.009642	2.251493
14	24.8	0.598363	24.8	0.598363	0.0165	0.0255	0.572863	975	100	0.005341	13.24449	1480.141	1.039834	0.011743	2.205205
14	24.7	0.475842	24.7	0.475842	0.0295	0.0385	0.45342	839	100	0.005341	13.24449	1480.141	1.039834	0.011743	2.205205
14	24.6	0.341103	24.6	0.341103	0.0425	0.0515	0.289603	618	110	0.003553	6.860983	763.2985	0.525674	0.021222	2.055111
14	24.5	0.260148	24.5	0.260148	0.0545	0.0595	0.200648	430	109.9	0.002461	4.778167	530.3830	0.364207	0.031601	1.874441
14	24.4	0.189875	24.4	0.189875	0.0625	0.0675	0.123375	239	100	0.001501	2.918693	323.2488	0.222129	0.051855	1.866085
14	24.3	0.12532	24.3	0.12532	0.0685	0.0715	0.05382	104	100	0.000660	1.270059	140.3436	0.097691	0.119968	1.588725
14	24.2	0.101785	24.2	0.101785	0.0725	0.0745	0.027285	64	119.9	0.000354	0.651855	71.86879	0.049527	0.030883	1.538236
24	24.4	7.351	24.4	7.351	0.0755	-0.0175	7.2755	1296	19.9	0.089269	79.53210	8808.278	13.20614	0.004135	2.753170
23	24.5	10.0445	24.5	10.0445	-0.0165	-0.0375	10.061	1252	15	0.123447	101.9503	11314.41	18.26225	0.003481	2.824544
23	24.5	11.98066	24.5	11.98066	-0.0335	-0.0535	12.01416	1444	15	0.147413	117.5618	13049.52	21.80754	0.003125	2.863071

81.5
4
0.4

Solvent	L	MDR	1/f	1/f	1/f	1/f	1/f	1/f	1/f	1/f	1/f	1/f
14.	51940	335.5290	38.46715	30.51614	2.101750	0.090949						
14.	07317	259.5219	36.34758	31.56281	2.242743	0.121619						
13.	71161	210.7575	34.63015	31.57839	2.303040	0.149852						
13.	34894	171.0477	32.90751	30.92807	2.316891	0.180815						
12.	82234	126.3179	30.40611	28.37022	2.212562	0.226593						
13.	05298	144.2536	31.50168	29.64159	2.270866	0.205482						
12.	51607	105.9009	28.95137	27.45602	2.153660	0.239261						
12.	27989	92.43868	27.82950	25.90375	2.109444	0.280226						
11.	83180	71.42184	25.70107	23.94734	2.023980	0.335294						
11.	38766	55.30917	23.59142	21.64657	1.900878	0.391374						
13.	30790	167.0537	32.71254	30.64837	2.303020	0.183464						
12.	83035	126.9022	30.44419	28.63233	2.231400	0.225524						
11.	75870	68.47891	25.35386	24.14542	2.053408	0.332596						
13.	03058	142.4053	31.39538	30.23022	2.319943	0.212282						
12.	75956	121.8346	30.10792	28.26746	2.215394	0.232015						
12.	36863	97.28338	28.25101	26.35096	2.146636	0.272923						
11.	87202	73.09484	25.89212	23.55813	1.984339	0.322295						
11.	58259	61.87681	24.51731	22.26330	1.922135	0.359800						
11.	28668	52.18572	23.11176	20.59260	1.824504	0.394602						
11.	05327	45.62461	22.00306	18.52777	1.676234	0.404091						
10.	89874	41.74123	21.26902	17.59079	1.614021	0.421424						
10.	64114	35.98863	20.04542	15.69990	1.475396	0.436246						
10.	47700	32.74390	19.26575	14.64353	1.397683	0.447214						
10.	47066	32.62475	19.23567	14.60515	1.394863	0.447670						
10.	17191	27.46995	17.81657	12.81110	1.259459	0.466368						
9.	970961	24.46922	16.86206	11.83897	1.187345	0.483831						
9.	799649	22.17136	16.04833	10.82597	1.104730	0.488286						
9.	483603	18.48335	14.54711	10.64086	1.122027	0.575699						
8.	921912	13.37698	11.87908	11.65764	1.306631	0.871470						
8.	605975	11.15254	10.37838	10.18370	1.183329	0.913128						
8.	420822	10.02502	9.49804	9.22788	1.095829	0.920475						
8.	178440	8.719469	8.347590	8.188990	1.001290	0.939161						
7.	820445	7.095636	6.647115	6.733309	0.859709	0.947527						
7.	497767	5.892802	5.114395	5.625327	0.750266	0.934609						
7.	044361	4.591615	3.055623	4.399988	0.622844	0.958266						
6.	346902	3.058125	-0.35221	2.887134	0.454888	0.950301						
5.	752945	2.158522	-3.17350	2.081153	0.361754	0.944245						
10.	61268	35.40385	19.91023	15.54964	1.465194	0.439207						
10.	89817	41.72774	21.26635	16.94677	1.555009	0.406127						
11.	05228	45.59856	21.99835	17.88643	1.618347	0.392258						

Y2P13156

Tw dynes/cm² (1/sec) 8(U)/D Log Log
 Tw 8(U)/D

0.790212 80.27545 -0.10225 1.904582
 0.525674 53.75471 -0.27928 1.730416
 0.364207 37.43618 -0.43865 1.573291
 0.222129 22.86750 -0.65339 1.339218
 0.097691 9.950711 -1.01014 0.997854
 0.049527 5.107184 -1.30515 0.708181

Regression Output:
 Constant -2.01232
 Std Err of Y Est 0.002512
 R Squared 0.999973
 No. of Observations 5
 Degrees of Freedom 3

X Coefficient(s) 1.000947
 Std Err of Coef. 0.003000

Tw vs. K * 8(U)/D ^ n

K' = 0.009720
 n = 1.000947

Tw = 3.696873
 Res/fg = 307.9797

Regression Output:
 Constant -50.0767
 Std Err of Y Est 0.413400
 R Squared 0.994681
 No. of Observations 10
 Degrees of Freedom 8

X Coefficient(s) 23.96233
 Std Err of Coef. 0.619472

t = 25.12375 deg C
 s.d.t = 0.575973 deg C

YSP13160 11/24/90 15:40

10 PSID Taps 14 1.0 PSID Taps 14 0.1 PSID Taps 14 9.9 <C> (ppm) =
 S = 1 S = 7.25 S = 6.8 [NaCl] =
 Z = 5.3 Z = 9.2 Z =
 FlowCo= 0.019693 0.020236

Tap Pair	Freq. (Hz)	Qtest (1/s)	Temp (deg C)	<V> (volts)	<V>0 (volts)	<V>f (volts)	<V>corr (volts)
12	60	1.181580	25.1	2.099333	0.0165	0.0255	2.073833
12	50	0.984650	25.1	1.54575	0.0165	0.0255	1.52025
12	40	0.787720	25.1	1.08825	0.0165	0.0255	1.06275
12	31	0.610483	25.1	0.73425	0.0165	0.0255	0.70875
12	21	0.413553	25.1	0.40775	0.0165	0.0255	0.38225
14	21	0.413553	25	1.233666	0.0245	0.0215	1.212166
14	15	0.295395	25	0.7398	0.0245	0.0215	0.7183
14	10	0.194930	25	0.412666	0.0245	0.0215	0.391166
12	25	0.492325	22.9	0.547	0.0215	0.0175	0.5295
14	25	0.492325	22.9	1.589	0.0215	0.0175	1.5715
12	36	0.708948	24.9	10.662	-0.0285	-0.0375	10.4905
12	30	0.590790	24.9	8.055	-0.0285	-0.0375	8.0835
12	21	0.413553	24.9	4.561333	-0.0285	-0.0375	4.598833
12	15	0.295395	24.9	2.68725	-0.0285	-0.0375	2.72475
12	10	0.194930	24.9	1.359285	-0.0285	-0.0375	1.396785
12	8	0.157544	24.9	1.053	-0.0285	-0.0375	1.0905
14	24.6	1.515	24.7	2.16675	-0.0565	-0.075	2.24175
14	24.6	1.2672	24.6	1.515	-0.0815	-0.0875	1.6035
14	24.6	1.2672	24.6	1.2672	-0.0715	-0.0995	1.3667
14	24.5	1.019666	24.5	1.019666	0.0385	0.0355	0.984666
14	24.4	6.072166	24.4	6.072166	-0.0055	-0.0635	6.135666
14	24.4	4.833714	24.4	4.833714	-0.0335	-0.0555	4.889214
14	24.2	3.408666	24.2	3.408666	-0.0005	-0.0625	3.471166
14	24.2	2.597222	24.2	2.597222	-0.0595	-0.0685	2.656722
14	24.1	2.1845	24.1	2.1845	-0.055	-0.0565	2.24
14	24.1	1.557428	24.1	1.557428	-0.0555	-0.0565	1.612928
14	24	1.0144	24	1.0144	-0.0505	-0.0485	1.0629
14	23.9	0.747473	23.9	0.747473	-0.0435	-0.0385	0.790973
14	23.8	0.6014	23.8	0.6014	-0.0335	-0.029	0.6304
14	23.75	0.467434	23.75	0.467434	-0.0255	-0.0165	0.492934
14	23.6	0.342916	23.6	0.342916	-0.0165	-0.0115	0.356916
14	23.5	0.24124	23.5	0.24124	-0.0085	-0.0035	0.24724
14	23.4	0.18248	23.4	0.18248	-0.0025	0.0015	0.18298
14	23.3	0.118636	23.3	0.118636	0.0015	0.0045	0.114136
14	23.2	0.061114	23.2	0.061114	0.0055	0.006	0.055614
14	23.1	0.033419	23.1	0.033419	0.0055	0.0055	0.027919
14	23.3	8.18925	23.3	8.18925	0.0035	-0.0375	8.22675
14	23.3	9.71	23.3	9.71	-0.0345	-0.0355	9.7455
14	23.3	13.4785	23.3	13.4785	-0.0275	-0.0275	13.504

density viscosity ID(cm) = 1.02108
 K(V/psi)=1.180945 13.84846
 XS(cm2) = 0.818859

co[NaCl] 1.01234 1.029478
 50.01221 X coeff -0.00025 -0.02281
 0.29986 constant 0.003419 -4.14933

Batch Vol (ml)	t(samp)	DP (psid)	<U> (cm/s)	Re	Tw (dyne/cm2)	f	Log(Re/f)
1768	14.9	0.161877	144.9060	16157.50	23.94729	0.002259	2.885366
1416	15	0.157116	115.2822	12825.39	17.11856	0.002351	2.811486
1234	15	0.098689	100.4649	11176.93	14.59965	0.002865	2.776924
1294	20	0.071102	79.01232	8770.476	10.51861	0.003337	2.704746
1295	20	0.072496	79.07338	8757.474	10.72483	0.003397	2.707977
1369	25.1	0.057769	66.60706	7376.814	8.546095	0.003815	2.658666
1214	29.9	0.041014	49.58360	5466.723	6.067421	0.004888	2.582314
1130	35	0.031390	39.42765	4347.003	4.643813	0.005917	2.524249
1111	40.2	0.026467	33.75037	3712.682	3.915404	0.006808	2.486215
1143	49.9	0.019057	27.97282	3077.127	2.819316	0.007136	2.414898
1066	59.9	0.012558	21.73306	2385.340	1.857894	0.007791	2.323352
920	70	0.009345	16.05019	1757.640	1.382381	0.010630	2.258201
1065	100	0.007448	13.00589	1421.052	1.101906	0.012902	2.207943
846	100	0.005824	10.33144	1127.563	0.861624	0.015987	2.154037
607	99.9	0.004217	7.420168	807.0941	0.623871	0.022448	2.082448
419	99.9	0.002921	5.121994	555.8655	0.432162	0.02624	2.001739
311	100	0.002162	3.797965	411.2461	0.319839	0.043912	1.955396
213	109.9	0.001348	2.366859	255.7075	0.199504	0.070521	1.831921
141	150	0.000637	1.147938	133.7399	0.097210	0.146088	1.674817
71	150	0.000229	0.578039	62.16833	0.048801	0.289231	1.524191
1205	14.9	0.097204	98.76233	10669.95	14.37993	0.002919	2.760823
1382	14.9	0.115149	113.2693	12237.23	17.03463	0.002629	2.797611
1738	15	0.159538	141.4976	15286.92	23.60429	0.002334	2.868440

YSP13160

Tw 8(U)/D Log Log
 dyne/cm2 (1/sec) Tw 8(U)/D

0.861624 80.94521 -0.06468 1.908191
 0.622871 58.13584 -0.20490 1.744443
 0.432162 40.13001 -0.36435 1.603469
 0.319839 29.75645 -0.49506 1.473581
 0.199504 18.54396 -0.70004 1.268202
 0.097210 8.993912 -1.01228 0.953948
 0.048801 4.528849 -1.31156 0.655987

Regression Output:
 Constant -1.96389
 Std Err of Y Est 0.001527
 R Squared 0.999990
 No. of Observations 7
 Degrees of Freedom 5

X Coefficient(s) 0.996524
 Std Err of Coef. 0.001392

Tw vs. K'z(8(U)/D)^n

K' = 0.010866
 n = 0.996524

Twk = 2.078633
 Res/fk = 223.2111

Regression Output:
 Constant -44.8353
 Std Err of Y Est 0.137432
 R Squared 0.998318
 No. of Observations 8
 Degrees of Freedom 6

X Coefficient(s) 23.91901
 Std Err of Coef. 0.385977

t = 24.22948 deg C
 s.d.t = 0.724101 deg C

Solvent	L	NDR	1/f/f	1/f/f	1/f/f	1/f/f/S1v	1/f/f/L
84.63346							
82.65316							
84.63346							
0.4							
14.18206	276.3098	36.86480	36.72353	2.589434	0.132907		
13.91234	256.5739	35.58365	35.74313	2.569166	0.151086		
13.60137	197.7993	34.10455	34.19987	2.514441	0.172901		
13.24950	161.5310	32.43514	32.45602	2.449602	0.200927		
12.71321	118.6268	29.98775	29.93819	2.354888	0.252372		
12.75758	121.6957	30.09851	29.11746	2.283365	0.239264		
12.30366	93.68006	27.93937	27.01803	2.196040	0.288407		
11.77518	69.13137	25.43210	24.40813	2.072845	0.353068		
12.90955	132.8213	30.82037	30.29051	2.346364	0.228054		
12.90032	132.1181	30.77656	30.45175	2.360540	0.230488		
13.46028	182.3694	33.43636	33.23382	2.469028	0.182233		
13.21749	158.5816	32.28308	31.84919	2.409624	0.200837		
12.72758	119.6125	29.95604	29.55781	2.323342	0.247112		
12.27294	92.06963	27.79649	27.42867	2.234889	0.297912		
11.69255	65.92611	25.03942	25.53947	2.184251	0.387430		
11.47734	58.24597	24.01833	23.12352	2.014675	0.396997		
11.14146	48.00056	22.42196	21.03817	1.888277	0.438290		
10.84594	40.49175	21.01824	19.79630	1.825225	0.488897		
10.70789	37.39419	20.36155	18.68092	1.744626	0.499567		
10.41898	31.66846	18.99019	17.30916	1.661309	0.546574		
10.43191	31.90492	19.05157	17.15541	1.644512	0.537704		
10.23466	28.48042	18.11466	16.18834	1.581717	0.568402		
9.929256	23.88879	16.66396	14.30253	1.440443	0.598713		
9.696998	20.89919	15.56074	12.99991	1.340612	0.622029		
9.544861	19.14675	14.83809	12.11916	1.269705	0.632961		
9.239595	16.24721	13.48307	11.83713	1.278364	0.728564		
8.93409	13.15928	11.74369	11.32917	1.273884	0.860926		
8.633807	11.32613	10.50383	9.699027	1.123507	0.856340		
8.431775	10.08843	9.550931	8.803722	1.044112	0.872654		
8.216151	8.910823	8.526718	7.908665	0.962575	0.887534		
7.929794	7.556639	7.16625	6.673372	0.841808	0.883378		
7.666957	6.275082	5.633049	5.536436	0.727812	0.882288		
7.341586	5.386128	4.378637	4.772051	0.650002	0.885989		
6.927686	4.244257	2.406512	3.765493	0.543542	0.887197		
6.299270	2.955934	-0.57846	2.616327	0.415338	0.885104		
5.696767	2.089642	-3.44035	1.859418	0.326398	0.889826		
10.64329	36.03328	20.05365	18.50711	1.738851	0.513611		
10.79044	39.21857	20.75462	19.50166	1.807308	0.497255		
11.07376	46.16585	22.10037	20.69566	1.868891	0.448289		

B1P01496

B1120

7/23/90 12:06

10 PSID Taps 14 1.0 PSID Taps 14 0.1 PSID Taps 14
 S = 2.7 S = 7.25 S = 9.9 <C>(ppm) =
 Z = 2.7 Z = 9.05 Z = 7.05 [NaCl] =

density viscosity
 co) [NaCl] 1.00088 1.001574
 1.000181 X coeff -0.00025 -0.02381
 0.000100 constant 0.003419 -4.14933

ID (cm) = 1.45796
 K (U/psi) = 1.08859 12.79427
 XS (cm2) = 1.669479

Freq. (Hz)	Q'est (1/s)	Temp (deg C)	<V> (volts)	<V>0 (volts)	<V>f (volts)	<V>corr (volts)	Batch Vol (ml)	t(samp) (sec)	DF (psid)	U (cm/s)	Re	Tw (dyne/cm2)	f	Log(Re/f)
60	1.21416	25.5	8.152	0.0215	0.0375	8.1145								
50	1.0118	25.5	5.775	0.0215	0.0375	5.74								
40	0.80944	25.5	3.81575	0.0215	0.0375	3.77825								
31	0.627316	25.5	2.43235	0.0215	0.0375	2.39575								
23	0.465428	25.5	1.4464	0.0215	0.0375	1.4089								
17	0.344012	25.5	0.8686	0.0215	0.0375	0.8511								
12	0.242832	25.5	0.511	0.0215	0.0375	0.4755								
9	0.182124	25.5	0.306222	0.0215	0.0375	0.268722								
18	0.364248	25.5	10.2564	0.0185	0.1865	10.0699								
15	0.30354	25.6	7.5735	0.0435	0.059	7.5145								
10	0.202336	25.6	3.643888	0.0435	0.059	3.584888								
8	0.161888	25.6	2.64125	0.0435	0.059	2.58225								
23.4	2.5652	25.4	2.5652	0.0315	0.0205	2.5337	2338	15	0.198032	35.26243	15333.80	27.93799	0.006428	3.089707
25.4	1.7345	25.4	1.7345	0.0175	0.0155	1.717	1880	14.9	0.134199	75.57714	12412.76	18.93260	0.006648	3.005215
25.4	1.54925	25.4	1.54925	0.0145	0.013	1.33475	1600	15	0.104323	63.89216	10493.62	14.71769	0.007231	2.950520
25.4	0.8134	25.4	0.8134	0.0135	0.0105	0.7999	1590	20	0.062519	47.61963	7821.029	8.820144	0.007801	2.839348
25.3	0.5942	25.3	0.5942	0.0125	0.0115	0.5817	1311	19.9	0.045465	39.46103	6466.461	6.414149	0.008261	2.769194
25.3	0.350714	25.3	0.350714	0.0125	0.0115	0.338214	1206	25	0.026434	28.89523	4755.047	3.729339	0.008958	2.651441
25.2	2.282	25.2	2.282	0.0045	0	2.282	1200	24.9	0.027798	28.86694	4719.752	3.921818	0.009439	2.661783
25.2	1.443428	25.2	1.443428	-0.0085	-0.0125	1.455928	1116	30	0.017735	22.28239	3643.176	2.502141	0.010107	2.562795
25.25	1.094444	25.25	1.094444	-0.0165	-0.0185	1.112944	1252	39.9	0.015557	18.79534	3076.511	1.912693	0.010859	2.505955
25.2	0.596615	25.2	0.596615	-0.0225	-0.0255	0.622115	1153	45	0.007578	15.34743	2509.308	1.069160	0.009103	2.379161
25.2	0.344333	25.2	0.344333	-0.0265	-0.0295	0.373833	1215	60	0.004553	12.13952	1983.180	0.642465	0.008758	2.258564
25.2	0.248777	25.2	0.248777	-0.0305	-0.0315	0.280277	1190	75	0.003414	9.503959	1553.899	0.481682	0.010695	2.205020
25.2	0.196928	25.2	0.196928	-0.0325	-0.0335	0.230428	784	60	0.002807	7.826790	1279.682	0.396011	0.012965	2.162493
25.2	0.122	25.2	0.122	-0.0345	-0.0345	0.1565	675	75	0.001906	5.390901	881.4136	0.268959	0.018561	2.079482
25.1	0.0508	25.1	0.0508	-0.036	-0.036	0.0868	378	75	0.001057	3.018904	492.4793	0.149173	0.032826	1.950500
25.05	-0.0002	25.05	-0.0002	-0.037	-0.037	0.0249	189	89.9	0.000448	1.259276	205.1964	0.065244	0.079984	1.762671
25.1	3.8528	25.1	3.8528	-0.0385	-0.0445	3.8973	1311	20	0.047476	39.26373	6405.163	6.697853	0.008712	2.776622
25.2	5.22025	25.2	5.22025	-0.0445	-0.0445	5.26475	1181	15	0.064134	47.16040	7710.737	9.047937	0.008159	2.843914
25.3	8.339666	25.3	8.339666	-0.0445	-0.0375	8.384166	1581	15	0.102174	63.13344	10345.64	14.40893	0.007250	2.943940
25.3	11.0502	25.3	11.0502	-0.0375	-0.0305	11.0807	1860	15	0.134982	74.27464	12171.34	19.04316	0.006923	3.005494

82.0894

4

0.4

Solvent L MDR
1///f 1///f 1///f

Tap DL= 122.2234
40.77743

1///f 1///f 1///f

15.11409	472.5020	41.29194	15.83539	1.047733	0.033513
14.81339	397.4007	39.86362	15.68998	1.059175	0.039481
14.45015	322.4171	38.13822	15.47116	1.070657	0.047984
14.05445	256.7399	36.25865	15.05738	1.071360	0.058648
13.59333	196.8851	34.06852	14.56787	1.071892	0.073991
12.13487	151.2165	31.89066	14.01944	1.067344	0.092711
12.64621	114.1386	29.56950	13.11081	1.036738	0.114867
12.15417	85.98536	27.23234	13.05266	1.073924	0.151801
13.16131	153.5352	32.01623	14.61994	1.110827	0.095222
12.91100	132.9323	30.82726	14.10332	1.092349	0.106094
12.26815	91.81603	27.77373	13.61264	1.109591	0.148259
11.98319	77.92554	26.42019	12.83131	1.070775	0.144661
11.95883	76.84009	26.30444	12.47217	1.042923	0.162313
11.62086	63.25508	24.69909	12.26458	1.055394	0.193890
11.40212	55.77123	23.66007	11.75967	1.031358	0.210855
10.95739	43.17458	21.54761	11.52180	1.033257	0.262233
10.67677	36.73454	20.21469	11.00201	1.030461	0.299500
10.20576	28.01051	17.97737	10.56533	1.035232	0.377191
10.24553	28.65917	18.16638	10.29284	1.004617	0.359146
9.855183	22.89158	16.31212	9.946833	1.009298	0.436518
9.623820	20.03711	15.21314	9.596292	0.997139	0.478925
9.116645	14.96377	12.80406	10.48076	1.149629	0.700408
8.674259	11.39964	10.70273	10.68556	1.251870	0.921197
8.424080	10.04384	9.514382	9.669474	1.147837	0.962726
8.253975	9.106971	8.706385	8.782297	1.044008	0.964348
7.917931	7.505212	7.110176	7.340013	0.927011	0.977988
7.402061	5.576741	4.659508	5.519345	0.745655	0.989708
6.654687	3.627036	1.109766	3.535882	0.531337	0.974868
10.70649	37.36823	20.35582	10.71291	1.000600	0.286685
10.97165	43.53040	21.61537	11.07085	1.099041	0.254323
11.37976	55.05806	23.55387	11.74401	1.032008	0.213302
11.63197	63.29575	24.70439	12.01833	1.034103	0.189875

BIP01496

Tw	8<U>/D	Log	Log
dyne/cm2	(1/sec)	Tw	8<U>/D
1.069160	84.21318	0.029042	1.925380
0.642465	66.55616	-0.19215	1.823188
0.481682	52.14935	-0.31723	1.717248
0.396011	42.94653	-0.40229	1.632928
0.268959	29.58051	-0.57031	1.471005
0.149173	16.56509	-0.82430	1.219193
0.063244	6.909798	-1.19898	0.839465

Log Tw vs. Log 8<U>/D

Regression Output:
 Constant -2.04722
 Std Err of Y Est 0.004440
 R Squared 0.999073
 Degrees of Freedom 5

X Coefficient(s) 1.005978
 Std Err of Coef. 0.006536

Tw = K'(8<U>/D)^n'
 K' = 0.008969
 n' = 1.005978

Regression Output:
 Constant 0.566011
 Std Err of Y Est 0.281963
 R Squared 0.925815
 No. of Observations 11
 Degrees of Freedom 9

X Coefficient(s) 4.009097
 Std Err of Coef. 0.378285

t = 25.35 deg C
 s.d.t = 0.159589 deg C

B2P-01494

B1120 7/21/90 12:25
 10 PSID Taps 14 1.0 PSID Taps 14 0.1 PSID Taps 14
 S = 2.7 S = 7.25 S = 9.9 C:(ppm) =
 Z = 2.7 Z = 7.05 [NaCl] =

density viscosity
 coj[NaCl] 1.000888 1.001574
 2.017038 X coeff -0.00025 -0.02381
 0.000100 constant 0.003419 -4.14933

ID(cm) = 1.45776
 K(U/psi) = 1.08859 12.56699
 XS(CM2) = 1.669479

Freq. (Hz)	Dist Temp (1/s)	Temp (deg C)	<V> (volts)	<V>0 (volts)	<V>f (volts)	<V>corr (volts)	Batch Vol (ml)	t)swamp (sec)	DP (psid)	<U> (cm/s)	Re	Tw (dyne/cm2)	f	Log(fRe/f)
60	1.21416	25	6.42375	0.0135	0.0225	6.40325	5.882150	727.2685	118373.2	829.8412	0.003146	3.822166		
49	0.991564	25	4.183	0.0135	0.0225	4.1605	3.821916	593.9360	96671.50	539.1878	0.003063	3.728539		
41	0.829676	25	2.872353	0.0135	0.0225	2.849833	2.617912	496.9668	80888.40	369.3295	0.003999	3.646376		
34	0.688024	25	2.024666	0.0135	0.0225	2.002166	1.829229	412.1188	67078.18	259.4745	0.003063	3.569716		
26	0.526136	25	1.225666	0.0135	0.0225	1.203166	1.105252	315.1497	51295.08	155.9266	0.003148	3.459129		
20	0.40472	25	0.776666	0.0135	0.0225	0.754166	0.62792	242.4228	39457.75	97.73765	0.00335	3.357700		
15	0.30354	25	0.489666	0.0135	0.0225	0.467166	0.429148	181.8171	29593.31	60.54334	0.003672	3.252702		
10	0.20236	25	0.256875	0.0135	0.0225	0.234375	0.215301	121.2114	19728.87	30.37427	0.004146	3.103922		
18	0.364248	25.1	7.18	0.0655	0.085	7.1145	0.566126	218.1805	25592.18	79.86785	0.003364	3.314840		
13	0.263068	25.1	4.3226	0.0655	0.085	4.2376	0.337300	157.5748	25705.46	47.57158	0.003842	3.202328		
10	0.20236	25.1	2.061875	0.0655	0.085	1.976875	0.157306	121.2114	19773.43	22.19253	0.003029	3.036758		
8	0.161880	25.1	1.92075	0.0655	0.085	1.83575	0.146077	96.96914	15818.75	20.60825	0.004631	3.047215		
24.9	2.1648	0.0715	0.0595	2.0932	2526	15	0.166571	100.8697	16380.98	23.49952	0.004631	3.047215		
24.9	1.4642	0.0615	0.0565	1.4027	1971	15	0.111617	78.70716	12781.83	15.74680	0.005097	2.960380		
24.8	1.0972	0.0605	0.0655	1.0367	1623	15	0.082493	65.96866	10688.99	11.63806	0.005262	2.892639		
24.8	0.561	0.0615	0.0605	0.5995	1624	20	0.047704	48.63791	7880.871	6.730027	0.005705	2.774707		
24.8	0.5252	0.0635	0.0635	0.4617	1538	19.9	0.036739	40.27373	6525.611	5.183075	0.006408	2.717992		
24.8	0.353285	0.0645	0.0655	0.288785	1497	30	0.022979	29.88955	4843.047	3.241927	0.007277	2.616100		
24.7	1.8815	0.0405	0.0405	1.841	1489	29.9	0.022569	29.82925	4822.385	3.183996	0.007175	2.611200		
24.7	1.181285	0.0385	0.0355	1.145785	1162	30	0.014046	23.20084	3750.794	1.981628	0.007382	2.508225		
24.7	0.806090	0.0335	0.0315	0.774590	1316	40	0.009495	19.70674	3185.916	1.339449	0.006917	2.422209		
24.6	0.5711	0.0285	0.026	0.5451	1070	40	0.006682	16.02295	2584.535	0.942746	0.007263	2.345226		
24.6	0.420846	0.0245	0.0245	0.396346	911	45	0.004858	12.12620	1955.980	0.685477	0.009348	2.276725		
24.6	0.241388	0.0235	0.0235	0.317888	820	50	0.003897	9.823420	1584.537	0.549786	0.011424	2.228825		
24.55	0.2516	0.0225	0.0235	0.2281	714	60	0.002796	7.127969	1148.459	0.394497	0.015569	2.156258		
24.5	0.185214	0.0235	0.0235	0.161714	500	59.9	0.001982	4.999908	804.6779	0.279683	0.02334	2.081077		
24.5	0.117	0.0235	0.0235	0.0935	423	89.9	0.001146	2.818380	453.5859	0.161707	0.03822	1.962108		
24.4	0.068272	0.0235	0.0235	0.044772	221	100	0.000548	1.323765	212.5648	0.077434	0.088606	1.801224		
24.4	0.046	0.0225	0.0205	0.0255	224	200.1	0.000312	0.670532	107.6713	0.044102	0.196686	1.678987		
24.4	4.0975	0.0205	0.0115	4.086	1200	14.9	0.050090	48.24073	7746.296	7.066708	0.006088	2.781366		
24.3	6.493	0.0105	0.0095	6.4835	1627	15	0.079482	64.97034	10456.23	11.21316	0.005226	2.882307		
24.6	8.4475	0.0075	0.0075	8.44	1948	15	0.103467	77.78871	12547.47	14.59492	0.004837	2.940859		
24.6	13.009	0.0055	0.0105	12.9985	2462	14.9	0.159350	98.97389	15964.68	22.48081	0.004602	3.034634		

Tap DL= 122.2234
40.77743

Solvent	L	MDR	1/f/f	1/f/f	1/f/f/Slv	1/f/f/L
81.57181						
0.4						
14.88866	414.9989	40.22117	17.82734	1.197376	0.042957	
14.51415	334.5180	38.44225	18.06171	1.244420	0.053393	
14.18550	276.8576	36.88115	18.26037	1.287256	0.065955	
13.87886	232.0581	35.42462	18.06610	1.301698	0.077851	
13.43651	179.8911	33.23460	17.82157	1.326333	0.099068	
13.03080	142.4231	31.39630	17.31537	1.328803	0.121577	
12.61481	112.0940	29.42035	16.50026	1.308007	0.147200	
12.01568	79.39669	26.57452	15.53030	1.292502	0.195603	
12.85936	129.0389	30.58197	17.23907	1.340585	0.133595	
12.40931	99.58834	28.44424	16.13232	1.300017	0.161990	
11.74703	68.02023	25.29840	18.16870	1.546663	0.267107	
11.68270	65.54737	24.99283	15.08331	1.291081	0.250113	
11.78885	69.67770	25.49706	14.69353	1.246391	0.210878	
11.44112	57.03750	23.84532	14.00595	1.224177	0.245556	
11.17455	48.92372	22.57914	13.65518	1.221988	0.279111	
10.69883	37.20381	20.31944	13.23935	1.237457	0.355860	
10.47197	32.64922	19.24186	12.49189	1.192888	0.382609	
10.06440	25.82145	17.30591	11.72243	1.164742	0.453980	
10.04480	25.53172	17.21280	11.80488	1.175223	0.462361	
9.632900	20.14211	15.25627	11.63853	1.208206	0.577820	
9.29237	16.56111	13.64098	12.02333	1.293827	0.725997	
8.983704	13.86137	12.17259	11.65349	1.297181	0.840717	
8.706901	11.81967	10.85778	10.34282	1.187887	0.875051	
8.515303	10.58536	9.947689	9.355709	1.098693	0.883834	
8.225032	8.956496	8.568904	8.014152	0.974361	0.894786	
7.924308	7.532811	7.140464	6.676440	0.842526	0.886314	
7.448434	5.727811	4.880065	4.949380	0.644486	0.844096	
6.804897	3.954617	1.823265	3.359440	0.495679	0.849498	
6.315951	2.984474	-0.49923	2.254822	0.357004	0.755317	
10.72546	37.77869	20.44597	12.81525	1.194843	0.339219	
11.15043	47.69662	22.36954	13.70148	1.230992	0.287263	
11.36343	56.54304	23.47632	14.37795	1.245281	0.263607	
11.75853	67.68847	25.25805	14.74095	1.255774	0.217776	

52P01494

Tw	8<U>/D	Log	Log
dyne/cm2	(1/sec)	Tw	8<U>/D
0.942746	87.91987	-0.02560	1.944087
0.685477	66.53790	-0.16400	1.823069
0.549786	53.90227	-0.25980	1.731607
0.394497	39.11201	-0.40395	1.592310
0.279683	27.43509	-0.55333	1.438306
0.161707	15.46478	-0.79126	1.189343
0.077434	7.263660	-1.11106	0.861155
0.044102	3.679291	-1.35554	0.565764

Log Tw vs. Log 8<U>/D

Regression Output:
 Constant -1.89797
 Std Err of Y Est 0.013716
 R Squared 0.999080
 No. of Observations 5
 Degrees of Freedom 3

X Coefficient(s) 0.934091
 Std Err of Coef. 0.016359

Tw = K'(8<U>/D)^n'
 K' = 0.012648
 n' = 0.934091

Tw)Retro=0.353158
 Res/f|R =136.9791

Regression Output:
 Constant -7.68893
 Std Err of Y Est 0.199089
 R Squared 0.989337
 No. of Observations 18
 Degrees of Freedom 16

X Coefficient(s) 7.424693
 Std Err of Coef. 0.192955

t = 24.78030 deg C
 s.d.)t = 0.228943 deg C

BSP01490

10 PSID Taps 14 1.0 PSID Taps 14 0.1 PSID Taps 14

S = 2.7 S = 7.25 S = 9.9 (C)(ppm)

Z = 2.7 Z = 9 Z = 7.1 [NaCl]=

60	49	39	31	23	17	14	10	20	16	12	9	24.7	24.6	24.6	24.6	24.6	24.5	24.5	24.5	24.4	24.4	24.4	24.5			
1.21416	0.991564	0.789204	0.627316	0.465428	0.344012	0.285304	0.20236	0.40472	0.333776	0.242852	0.182124	3.75575	2.4115	1.827	1.181833	0.884	0.737428	0.611142	0.455875	0.365875	0.275909	0.173857	0.096214	0.0625	0.952666	
25.05	25.05	25.05	25.05	25.05	25.05	25.05	25.05	25	25	25	25	24.7	24.6	24.6	24.6	24.6	24.5	24.5	24.5	24.4	24.4	24.4	24.5	24.4	24.5	24.5
4.134	2.568	1.640333	1.094666	0.609	0.364666	0.25423	0.158166	5.3235	3.871	2.296	1.366142	3.75575	2.4115	1.827	1.181833	0.884	0.737428	0.611142	0.455875	0.365875	0.275909	0.173857	0.096214	0.0625	9.52666	
0.0145	0.0145	0.0145	0.0145	0.0145	0.0145	0.0145	0.0145	0.0745	0.0745	0.0745	0.0745	0.0315	0.0295	0.0285	0.0295	0.0305	0.0315	0.0315	0.0325	0.0325	0.0325	0.0335	0.0335	0.0355	0.0355	0.036
4.1145	2.5485	1.620833	1.035166	0.5895	0.345166	0.23475	0.138666	5.231	3.7785	2.2035	1.273642	3.72425	2.382	1.7985	1.152333	0.8535	0.705928	0.579642	0.433375	0.333375	0.243409	0.140357	0.061214	0.027	7.91666	
0.0195	0.0195	0.0195	0.0195	0.0195	0.0195	0.0195	0.0195	0.0925	0.0925	0.0925	0.0925	0.0275	0.0285	0.0295	0.0305	0.0315	0.0315	0.0315	0.0325	0.0325	0.0325	0.0335	0.0335	0.0355	0.0355	0.036
4.1145	2.5485	1.620833	1.035166	0.5895	0.345166	0.23475	0.138666	5.231	3.7785	2.2035	1.273642	3.72425	2.382	1.7985	1.152333	0.8535	0.705928	0.579642	0.433375	0.333375	0.243409	0.140357	0.061214	0.027	7.91666	

density viscosity

co[NaCl]=1.00088 1.001574 ID(cm) = 1.45796

5.068321 X coeff -0.00225 -0.02281 K(V/psi)= 1.08859 12.56699

0.000100 constant 0.003419 -4.14933 XS(cm2)= 1.669479

Batch	Vol	t ₀ samp	DP	<U>	Re	T _w	f	Log(Re/f)
(ml)	(sec)	(psid)	(cm/s)			dynes/cm ²		
3.779659	727.2685	118506.8	533.2264	0.002021	3.722617			
2.341101	593.9360	96780.61	330.2776	0.001877	3.522501			
1.488929	472.7245	77029.46	210.0549	0.001885	3.524328			
0.950924	375.7554	61228.55	134.1543	0.001905	3.426964			
0.541526	278.7862	45427.63	76.39736	0.001971	3.204701			
0.317076	206.0594	33576.94	44.73252	0.002112	3.188472			
0.215645	169.6960	27651.60	30.42286	0.002118	3.104762			
0.127281	121.2114	19751.14	17.97076	0.002453	2.990445			
0.416249	242.4228	39457.75	58.72355	0.002003	3.247075			
0.300668	193.9282	31566.20	42.41769	0.002261	3.176442			
0.175340	145.4537	23674.65	24.73663	0.002344	3.059779			
0.101348	109.0902	17755.99	14.29800	0.002409	2.946307			
14.9	0.098201	97.28547	15798.90	0.002935	2.932473			
1855	15	0.054865	74.07498	12002.47	7.740373	0.002828	2.805080	
1560	15	0.043582	62.29486	10093.72	6.148517	0.003177	2.755084	
1557	15	0.047031	62.17506	10051.61	6.635086	0.003441	2.770637	
1154	15	0.030080	46.08222	7433.155	4.243747	0.004007	2.672602	
1272	20	0.022712	38.09570	6144.913	3.204189	0.004427	2.611587	
946	20	0.014552	28.33218	4570.038	2.052985	0.005128	2.514921	
746	20	0.010778	22.34229	3603.856	1.520587	0.006108	2.449724	
791	25.1	0.008914	18.87650	3044.818	1.257675	0.007077	2.408512	
646	25	0.007319	15.47787	2490.986	1.032685	0.008643	2.364727	
570	29.9	0.005246	11.41885	1837.733	0.754280	0.011599	2.296509	
525	35	0.004209	8.984836	1446.006	0.593937	0.014753	2.244615	
466	45	0.003073	5.936647	955.4352	0.433655	0.024673	2.175215	
337	60	0.001772	3.364321	540.2288	0.250058	0.044299	2.055779	
126	60.1	0.000773	1.555784	201.5485	0.109058	0.138671	1.875588	
156	200	0.000340	0.752211	75.02288	0.048102	0.441876	1.697844	
2382	14.9	0.099974	95.75785	15411.12	14.10425	0.003084	2.972418	

BSP01490

79.1865
4
0.4

Solvent L MDR 1//f 1//f 1//f 1//f/Slv 1//f/l

Tap DL= 122.2234
40.77743

14.50647	333.0411	38.40574	22.23953	1.533076	0.066777
14.09040	262.1088	36.42943	23.07739	1.637808	0.088045
13.69731	209.0299	34.56224	23.03182	1.681484	0.110184
13.30785	167.0492	32.71232	22.90812	1.721398	0.137133
12.81880	126.0611	30.38932	22.52261	1.756998	0.178664
12.35389	96.46145	28.18100	21.75541	1.761016	0.225534
12.01904	79.55036	26.59048	21.72491	1.807940	0.273096
11.56178	61.13999	24.41846	20.19049	1.746313	0.330233
12.58830	110.3965	29.29443	22.33864	1.774555	0.202349
12.30577	93.82596	27.95241	21.02710	1.708718	0.234107
11.83735	71.65060	25.72745	20.65113	1.744572	0.288219
11.36122	54.47373	23.46583	20.37219	1.753132	0.373981
11.32989	53.49994	23.31699	18.45668	1.629025	0.344985
10.82032	39.89882	20.89652	18.80142	1.737603	0.471227
10.62033	35.56020	19.94660	17.74055	1.670432	0.498887
10.68254	36.85676	20.24210	17.04506	1.595598	0.462467
10.39041	29.40921	18.37946	15.79682	1.535100	0.537138
10.04635	25.55452	17.22016	15.02892	1.495958	0.588112
9.659486	20.45510	15.38351	13.96362	1.445556	0.682647
9.398937	17.60412	14.14495	12.79479	1.361301	0.726806
9.234651	16.01006	13.36174	11.88634	1.287230	0.742429
9.058910	14.47463	12.52982	10.75582	1.187320	0.743080
8.786039	12.37057	11.23368	9.284800	1.056767	0.750555
8.578435	10.97725	10.24766	8.232965	0.959725	0.750001
8.305263	9.379847	8.949999	6.366276	0.766535	0.678718
7.823117	7.106560	6.459809	4.751143	0.607321	0.668557
7.102354	4.693194	3.236182	2.685385	0.378097	0.572187
6.391376	3.116908	-0.14096	1.504352	0.235372	0.482642
11.32967	53.49319	23.31595	18.00594	1.589272	0.336602

BSP01490

Tw B<U>/D Log B<U>/D

dyne/cm2 (1/sec) Tw Log B<U>/D

0.593937	49.30086	-0.22625	1.692854
0.433655	32.57508	-0.36285	1.512885
0.250058	18.46043	-0.60195	1.266241
0.109058	6.890636	-0.96233	0.838359
0.048102	2.563644	-1.31782	0.408857

Log Tw vs. Log B<U>/D

Regression Output:

Constant -1.67442

Std Err of Y Est 0.012545

R Squared 0.999408

No. of Observations 5

Degrees of Freedom 3

X Coefficient(s) 0.856928

Std Err of Coef. 0.012037

Tw = K' (B<U>/D)^n'

K' = 0.021163

n' = 0.856928

Tw)Retro=4.896452

Res/f)R =512.1444

Regression Output:

Constant 4.756168

Std Err of Y Est 0.389394

R Squared 0.877390

No. of Observations 10

Degrees of Freedom 8

X Coefficient(s) 5.286162

Std Err of Coef. 0.698653

t = 24.76896 deg C

s.d.)t = 0.247892 deg C

10 PSID Taps 14 1.0 PSID Taps 14 11:53
 S = 2.7 S = 7.25 S = 7.5 S = 9.9 C (ppm) =
 Z = 2.7 Z = 8.9 Z = 7.15 [NaCl] =

Freq. (Hz)	Qtest (1/s)	Temp (deg C)	<U> (volts)	<V> (volts)	<V>0 (volts)	<U>f (volts)	<U>corr (volts)
60	1.21416	24.9	2.715666	0.0365	0.0385	2.677166	0.0385
50	1.01118	24.9	1.874666	0.0365	0.0385	1.836166	0.0385
39	0.789204	24.9	1.094	0.0365	0.0385	1.0555	0.0385
31	0.627316	24.9	0.7416	0.0365	0.0385	0.7031	0.0385
24	0.485664	24.9	0.4844	0.0365	0.0385	0.4459	0.0385
16	0.333776	24.9	0.267	0.0365	0.0385	0.2385	0.0385
13	0.263068	24.9	0.2464	0.0365	0.0385	0.2079	0.0385
8	0.161888	24.9	0.122	0.0365	0.0385	0.0835	0.0385
18	0.364248	24.9	3.595	0.0325	0.034	3.561	0.034
24	0.485664	24.9	4.9985	0.0325	0.034	4.9645	0.034
32	0.647552	24.9	8.568333	0.0325	0.034	8.534333	0.034
15	0.30354	24.9	2.249375	0.036	0.0435	2.208875	0.0435
9	0.182124	24.9	1.1752	0.036	0.0435	1.1317	0.0435
13	0.263068	24.9	1.7873	0.036	0.0435	1.7438	0.0435
24.7	1.1704	24.7	1.1704	0.0635	0.06	1.1104	0.06
24.6	0.804	24.6	0.804	0.0635	0.0625	0.7415	0.0625
24.5	0.6174	24.5	0.6174	0.0655	0.0635	0.5591	0.0635
24.5	0.451833	24.5	0.451833	0.0665	0.0635	0.388353	0.0635
24.4	2.632	24.4	2.632	0.0445	0.0445	2.5875	0.0445
24.4	2.2112	24.4	2.2112	0.0665	0.0745	2.1367	0.0745
24.4	1.462	24.4	1.462	0.0815	0.085	1.377	0.085
24.4	1.127555	24.4	1.127555	0.0905	0.094	1.035555	0.094
24.3	0.6927	24.3	0.6927	-0.0185	-0.0165	0.7092	-0.0165
24.3	0.538214	24.3	0.538214	-0.0145	-0.0125	0.548714	-0.0125
24.2	0.333692	24.2	0.333692	-0.012	-0.0065	0.340192	-0.0065
24.2	0.249733	24.2	0.249733	-0.0055	-0.0045	0.254233	-0.0045
24.1	0.1846	24.1	0.1846	-0.0035	-0.0015	0.1861	-0.0015
24.1	0.098363	24.1	0.098363	-0.0005	0.0005	0.097863	0.0005
24	0.043666	24	0.043666	-0.001	0.0005	0.043166	0.0005
24.2	3.5934	24.2	3.5934	0.0005	-0.0105	3.6039	-0.0105
24.3	4.854	24.3	4.854	-0.0105	-0.0075	4.8615	-0.0075
24.4	6.8355	24.4	6.8355	-0.007	-0.0065	6.862	-0.0065

density viscosity ID (cm) = 1.45796
 co[NaCl] = 0.00088 1.001574 K(V/psi) = 1.086516 12.44018
 9.963670 X coeff -0.00025 -0.02381 XS(ca2) = 1.669479
 0.000099 constant 0.003419 -4.14733 1.085095

Batch Vol (ml)	t (sec)	DP (psid)	<U> (cm/s)	Re	Tw (dyna/cm2)	f	Log(Re/f)
2.463991	727.2685	118106.5	347.6147	0.001318	3.632232		
1.689958	606.0571	98422.10	238.4157	0.001301	3.550251		
0.971453	472.7245	76769.24	137.0506	0.001290	3.430124		
0.647114	375.7554	61021.70	91.29350	0.001296	3.341904		
0.410394	290.9074	47242.61	57.89756	0.001372	3.243014		
0.210305	193.9582	31495.07	29.66941	0.001581	3.097828		
0.191345	157.5748	25589.74	26.99462	0.002180	3.07322		
0.076851	96.96914	15747.53	10.84199	0.002312	2.879238		
0.286249	218.1805	35431.95	40.38352	0.001701	3.164786		
0.399069	290.9074	47242.61	56.29991	0.001334	3.226938		
0.686029	387.8765	62990.14	96.78361	0.001290	3.354585		
0.177318	181.8171	29526.43	25.01572	0.001517	3.060790		
0.090971	109.0902	17715.97	12.83404	0.002162	2.915866		
0.140174	157.5748	25589.74	19.77556	0.001597	3.009748		
15	0.089259	100.4305	16236.22	12.59249	0.002503	2.909769	
14.9	0.059605	76.82336	12391.76	8.408981	0.003857	2.821100	
15	0.044541	63.89216	10282.71	6.283771	0.003086	2.756853	
20	0.031216	48.36836	7784.333	4.403894	0.003774	2.679661	
19.8	0.032676	48.43340	7777.236	4.609864	0.003940	2.688602	
20	0.026983	40.43176	6492.364	3.806723	0.004669	2.647032	
25	0.017389	29.73381	4774.533	2.453249	0.005564	2.551629	
30	0.013052	23.30067	3741.525	1.841572	0.006800	2.489329	
40	0.008956	16.09783	2579.097	1.263503	0.009776	2.404561	
49.9	0.006929	12.30388	1971.254	0.977583	0.012948	2.350850	
60	0.004296	7.297683	1166.556	0.606083	0.022819	2.246054	
60	0.003210	5.071440	810.6848	0.453939	0.035311	2.182808	
59.9	0.002350	3.489936	556.6195	0.331553	0.054581	2.114079	
90	0.001235	1.590648	253.6969	0.174352	0.138166	1.974517	
99.9	0.000545	0.575605	91.59796	0.076905	0.465392	1.795795	
15	0.045511	62.77405	10034.61	6.420672	0.002267	2.758578	
15.1	0.061393	75.56782	12107.02	8.661199	0.003041	2.824562	
14.9	0.086403	98.85329	15873.45	12.18963	0.002501	2.899753	

Solvent	L	MDR	1//f	1//f	1//f/Slv	1//f/L
79.1365			Tap DL=	122.2534		
0.4				40.77743		
14.12893	267.9867	36.61243	27.54485	1.949535	0.102784	
13.80140	221.9390	35.05668	27.71666	2.008249	0.124884	
13.32049	168.2692	32.77237	28.51428	2.140631	0.169466	
12.94761	137.3359	31.09618	27.77027	2.141509	0.202206	
12.57205	109.3690	29.21727	26.99724	2.147400	0.246845	
11.99135	78.29225	26.45893	25.14223	2.096696	0.321133	
11.90929	74.67976	26.06913	21.41623	1.798279	0.286774	
11.11695	47.32808	22.30553	20.79570	1.870629	0.439394	
12.25914	91.34113	27.73094	24.24425	1.977645	0.265425	
12.54775	107.8495	29.10182	27.37762	2.181874	0.253850	
13.01834	141.4051	31.33711	27.84116	2.138510	0.196889	
11.84316	71.89039	25.75502	25.66983	2.167481	0.357069	
11.26346	51.49274	23.00145	21.50300	1.909093	0.417592	
11.63899	63.91882	24.78522	25.02172	2.149818	0.391460	
11.25907	50.77497	22.88562	19.98551	1.778216	0.393609	
10.88440	41.39810	21.20090	18.70822	1.718811	0.451910	
10.62741	35.70538	19.98022	17.99923	1.693660	0.594104	
10.31864	29.89110	18.51357	16.27644	1.577381	0.544524	
10.35440	30.51282	18.48344	15.93026	1.538590	0.522084	
10.18813	27.72770	17.89364	14.63419	1.436396	0.527782	
9.806516	22.25918	14.08095	13.40607	1.367058	0.602271	
9.557516	19.28453	14.89725	12.12605	1.268772	0.628797	
9.226245	15.93827	13.32466	10.11361	1.096179	0.634548	
9.003400	14.01942	12.26615	8.788056	0.976081	0.626848	
8.584216	11.01372	10.27502	6.619904	0.771171	0.601059	
8.331232	9.52120	9.073352	5.321622	6.638755	0.558928	
8.056319	8.129552	7.767315	4.280343	0.531502	0.526646	
7.490069	5.893825	5.115828	2.690282	0.358796	0.456457	
6.783182	3.905491	1.720117	1.465852	0.216100	0.375331	
10.63431	35.84744	20.01298	17.49335	1.645179	0.488050	
10.89824	41.72940	21.26668	18.13323	1.663866	0.434543	
11.19901	49.61736	22.69532	19.99482	1.785409	0.402980	

Tw	(δ) ² /D	Log Tw	Log (δ) ² /D
1.263503	88.53071	0.101576	1.946111
0.977583	67.51287	-0.00984	1.829386
0.606083	40.04325	-0.21746	1.602529
0.452939	27.82759	-0.34395	1.444475
0.331553	19.14969	-0.47944	1.282161
0.174352	8.728079	-0.75857	0.940918
0.076905	3.158413	-1.11404	0.499469

Log Tw vs. Log (δ) ² /D	
Constant	-1.52221
Std Err of Y Est	0.062184
R Squared	0.999972
No. of Observations	5
Degrees of Freedom	3

Regression Output:	
Constant	0.814203
X Coefficient(s)	0.814203
Std Err of Coef.	0.002480

Tw = K' (δ) ² /D ^{n'}	
K' =	0.030045
n' =	0.814203

(Tw)Retrom=33.45511	Res/(f)R =1113.741
Constant	1.175836
Std Err of Y Est	0.196362
R Squared	0.979521
No. of Observations	7
Degrees of Freedom	5

Regression Output:	
Constant	7.979911
X Coefficient(s)	7.979911
Std Err of Coef.	0.516009

t = 24.58125 deg C	s.d.)t = 0.310682 deg C
--------------------	-------------------------

BSP11483

10 PSID Taps 14 1.0 PSID Taps 14 0.1 PSID Taps 14
 S = 2.7 S = 7.25 S = 9.9 C (ppm) =
 Z = 2.7 Z = 8.9 Z = 7.2 [NaCl] =

B1120 7/4/90 12:38
 density viscosity
 col[NaCl]=1.00088 1.001574
 20.01199 X coeff -0.00025 -0.02281
 0.000100 constant 0.003419 -4.14933

ID(cm) = 1.45796
 K (N/psi) = 1.086516 12.44018
 XS(cm2) = 1.669479

Freq. (Hz)	Qtest (L/s)	Temp (deg C)	<U> (volts)	<U>0 (volts)	<U>f (volts)	<U>corr (volts)	Batch Vol (ml)	t(swap) (sec)	DP (psid)	<U> (cm/s)	Re	Tw (dyne/cm2)	f	Log (Re/f)	
20	0.40472	24.7	0.364666	0.041	0.04	0.324666	0.298814	242.4228	39191.61	42.15610	0.001428	3.172144			
29	0.586844	24.7	0.5845	0.041	0.04	0.5445	0.501143	351.5131	5827.83	70.70020	0.001147	3.284424			
38	0.768968	24.7	0.9144	0.041	0.04	0.8744	0.804774	460.6034	74464.05	113.5358	0.001073	3.287280			
46	0.930856	24.7	1.26325	0.041	0.04	1.22325	1.125846	557.5725	90140.70	158.8330	0.001024	3.460182			
54	1.092744	24.7	1.5915	0.041	0.04	1.5515	1.427958	654.5417	105817.3	201.4533	0.000942	3.511801			
60	1.21416	24.7	1.933666	0.041	0.04	1.893666	1.742879	727.2685	117574.8	245.8817	0.000932	3.555077			
20	0.40472	24.6	0.363	0.0495	0.0405	0.3225	0.296820	242.4228	39103.29	41.87477	0.001428	3.169704			
14	0.283304	24.6	0.22428	0.0495	0.0405	0.181928	0.167442	169.6960	27372.30	23.62238	0.001444	3.045230			
10	0.20236	24.6	0.157333	0.0495	0.0405	0.116833	0.107330	121.2114	19551.64	15.17013	0.002070	2.949223			
18	0.364248	24.5	2.76975	0.0255	0.0645	2.74425	0.220595	218.1805	35113.65	31.12117	0.001310	3.104271			
16	0.323776	24.5	2.677	0.0255	0.0645	2.6125	0.210004	193.9382	31212.14	29.62705	0.001579	3.095587			
11	0.222596	24.5	2.504625	0.0255	0.0645	2.460125	0.196168	133.3325	21458.34	27.67224	0.003121	3.078745			
7	0.141652	24.5	0.593857	0.0255	0.0645	0.529357	0.042552	84.84800	13655.31	6.003175	0.001672	2.746934			
25	0.5059	24.6	5.211333	0.0645	0.0245	5.168833	0.416941	303.0285	48879.11	58.82129	0.001284	3.243495			
33	0.667788	24.6	8.162	0.0645	0.0245	8.1375	0.654130	399.9977	64520.43	92.28332	0.001156	3.341290			
24.2	0.7884	24.3	1.07725	0.0335	0.0295	1.05375	15	0.084705	98.23420	15738.49	11.95005	0.002483	2.894438		
24.2	0.618	24.2	0.7884	0.0325	0.029	0.7559	14.9	0.060762	75.37614	12049.09	8.572284	0.003025	2.821336		
24.2	0.4516	24.2	0.4516	0.0305	0.0275	0.5865	14.9	0.047145	63.11495	10089.11	6.651204	0.003347	2.766239		
24.1	2.561166	24.1	2.561166	-0.0385	-0.0425	2.603666	20	0.032880	47.76937	7618.869	4.638666	0.004075	2.686999		
24.1	2.076166	24.1	2.076166	-0.0275	-0.029	2.105166	20.1	0.026584	39.93260	6368.960	3.750543	0.004715	2.640849		
23.95	1.409142	23.95	1.409142	-0.0245	-0.0275	1.436642	25.1	0.018142	29.33353	4646.784	2.559508	0.006004	2.556403		
23.9	1.076444	23.9	1.076444	-0.0265	-0.0265	1.102944	30	0.013928	22.66175	3598.113	1.964994	0.007671	2.498513		
23.9	0.884125	23.9	0.884125	-0.0285	-0.0285	0.912625	30	0.011525	19.40724	3081.380	1.625923	0.008655	2.457582		
23.9	0.699111	23.9	0.699111	-0.0285	-0.0285	0.727611	29.9	0.009188	15.42547	2449.175	1.296304	0.010922	2.408185		
23.8	0.521625	23.8	0.521625	-0.0295	-0.0285	0.550125	59.9	0.006947	11.05979	1752.059	0.980097	0.016064	2.346481		
23.8	0.339266	23.8	0.339266	-0.0285	-0.0265	0.365766	59.9	0.004619	7.569861	1199.194	0.651646	0.022799	2.257853		
23.75	0.282368	23.75	0.282368	-0.0275	-0.0275	0.309868	75	0.003913	5.870092	928.8738	0.552058	0.032120	2.221247		
23.7	0.155428	23.7	0.155428	-0.0275	-0.0255	0.180928	90	0.002284	3.134709	495.4720	0.322340	0.065765	2.104019		
23.6	0.077832	23.6	0.077832	-0.0255	-0.0285	0.106333	99.9	0.001342	1.630881	257.1961	0.189442	0.142791	1.987615		
23.5	0.022555	23.5	0.022555	-0.0285	-0.0315	0.051055	100.1	0.000644	0.688149	108.2791	0.090960	0.385073	1.827216		
23.5	0.207454	23.5	0.207454	-0.0325	-0.0335	0.239954	70	0.003050	4.158695	654.3640	0.427500	0.049554	2.162559		
23.7	3.632285	23.7	3.632285	-0.0355	-0.045	3.677285	15	0.046428	61.93547	9789.517	6.551415	0.003424	2.758029		
23.9	4.916166	23.9	4.916166	-0.0455	-0.035	4.951166	15	0.063525	74.27464	11792.93	8.820949	0.003205	2.824589		
24	6.9344	24	6.9344	-0.0365	-0.0275	6.9619	15	0.087917	96.43724	15346.37	12.40325	0.002673	2.899585		

BSP11480

10 PSID Taps 14 1.0 PSID Taps 14 0.1 PSID Taps 14
 S = 2.7 S = 7.25 S = 9.9 C (ppa) =
 Z = 2.7 Z = 8.9 Z = 7.4 [NaCl] =

6/28/90 13:02

density viscosity

co) [NaCl] 1.00088 1.001574 ID (cm) = 1.45796
 49.91302 X coeff -0.00025 -0.02281 K (V/psi) = 1.085095 12.37189
 0.000099 constant 0.003419 -4.14933 XS (cm2) = 1.669479

Freq. (Hz)	Qtest (1/s)	Temp (deg C)	<U> (volts)	<U> (volts)	<U>f (volts)	<U>corr (volts)	Batch (ml)	Vol (ml)	t (sec)	DP (psid)	<U> (cm/s)	Re	Tw (dyne/cm2)	f	Log (Re/f)
60	1.21416	25.1	1.78475	0.0325	0.0375	1.74725				1.610227	727.2685	118640.6	227.1675	0.000861	3.541827
50	1.0118	25.1	1.558666	0.0325	0.0375	1.521166				1.217558	606.0571	98867.18	171.7705	0.000937	3.481139
40	0.80944	25.1	0.953666	0.0325	0.0375	0.916166				0.844319	484.8457	79093.75	119.1147	0.001016	3.401637
30	0.60708	25.1	0.644333	0.0325	0.0375	0.606833				0.559244	363.6342	59320.31	78.89701	0.001196	3.312184
21	0.424956	25.1	0.3755	0.0325	0.0375	0.338				0.311493	254.5440	41524.21	43.94483	0.001260	3.195108
14	0.283304	25.1	0.2398	0.0325	0.0375	0.2023				0.186435	169.6960	27682.81	24.30189	0.001831	3.072648
10	0.20236	25.1	0.155714	0.0325	0.0375	0.118214				0.108943	121.2114	19773.43	15.36934	0.002098	2.956985
7	0.141652	25.1	0.110428	0.0325	0.0375	0.072928				0.067209	84.84800	13841.40	9.481757	0.002641	2.852099
18	0.364248	25.2	2.8475	-0.0035	0.0035	2.844				0.239875	218.1805	35672.57	32.43041	0.001366	3.120116
26	0.526136	25.2	5.485	-0.0035	0.0035	5.4815				0.459226	315.1497	51527.05	64.78670	0.001308	3.270382
35	0.70826	25.2	8.605	-0.0035	0.0035	8.6015				0.695245	424.2400	69363.34	98.08375	0.001092	3.360438
15	0.30354	25	2.4316	0.0025	0.0165	2.4151				0.195208	181.8171	29593.31	27.53962	0.001670	3.082348
11	0.222596	25	2.044	0.0025	0.0165	2.0475				0.165496	133.3325	21701.76	23.34784	0.002633	3.046792
7	0.141652	25	0.6944	0.0025	0.0165	0.6779				0.054793	84.84800	13810.21	7.730160	0.002153	2.806762
24.8	1.2825	0.0235	1.2825	-0.0055	0.0055	1.259	2235	14.9	0.101762	89.84836	14538.25	14.32650	0.002566	2.939223	
24.7	0.88125	-0.0035	0.88125	-0.0035	-0.0045	0.88475	1750	14.9	0.071512	79.35106	11373.39	10.08889	0.004087	2.861635	
24.7	0.7238	-0.0035	0.7238	-0.0035	-0.0035	0.7273	1982	20.1	0.058786	59.06449	9548.739	8.293473	0.004767	2.819082	
24.6	0.528571	-0.0035	0.528571	-0.0035	-0.0035	0.532071	1495	19.9	0.043006	44.99943	7258.498	6.067262	0.006008	2.750225	
24.6	0.422375	-0.003	0.422375	-0.003	-0.0015	0.425375	1524	24.9	0.034382	36.66101	5913.495	4.850592	0.007237	2.701626	
24.5	2.587333	-0.0395	2.587333	-0.0395	-0.0645	2.626833	1526	25	0.035643	36.56229	5884.281	4.746534	0.007119	2.695922	
24.5	1.890571	-0.0725	1.890571	-0.0725	-0.073	1.963071	1037	24.9	0.025142	24.94585	4014.748	3.547006	0.011429	2.623674	
24.5	1.357777	-0.077	1.357777	-0.077	-0.076	1.434777	836	30	0.018376	16.69182	2686.358	2.592450	0.018658	2.564598	
24.5	1.158777	-0.0795	1.158777	-0.0795	-0.0785	1.238277	753	35	0.015859	12.92105	2079.494	2.237401	0.026872	2.522615	
24.4	1.028916	-0.0805	1.028916	-0.0805	-0.0805	1.109416	731	40.1	0.014208	10.91922	1753.364	2.004566	0.033712	2.507768	
24.4	0.795538	-0.0835	0.795538	-0.0835	-0.081	0.879038	567	50	0.011258	6.792536	1090.717	1.588304	0.069028	2.457225	
24.25	0.67275	-0.0905	0.67275	-0.0905	-0.0865	0.76325	585	59.9	0.009775	5.849893	936.1782	1.379090	0.080804	2.425076	
24.2	0.5316	-0.09	0.5316	-0.09	-0.0885	0.6216	405	60	0.007961	4.043176	646.3137	1.123147	0.137760	2.380006	
24.2	0.418866	-0.0905	0.418866	-0.0905	-0.0895	0.509266	284	60	0.006523	2.835214	453.2175	0.920357	0.229571	2.325768	
24.1	0.214045	-0.0905	0.214045	-0.0905	-0.0905	0.304545	157	90	0.003900	1.044903	166.6544	0.550272	1.010530	2.224091	
23.9	0.096541	-0.0905	0.096541	-0.0905	-0.0905	0.187041	66	100	0.002395	0.395332	62.76885	0.337959	4.335511	2.115264	
24	4.3844	-0.0905	4.3844	-0.0905	-0.112	4.4749	1466	15	0.007312	58.54119	9315.856	8.085542	0.004730	2.806672	
24.2	7.51	-0.114	7.51	-0.114	-0.106	7.624	2215	15	0.007644	88.45071	14139.10	13.77554	0.003520	2.924742	
24.2	5.4125	-0.1095	5.4125	-0.1095	-0.1065	5.522	1740	15	0.007023	69.48273	11107.02	9.977511	0.004143	2.854299	

Tap DL= 122.2233
40.77743

Solvent	L	MDR	1//f	1//f	1//f	1//f/Siv	1//f/L
78.07879							
4							
0.4							
13.76731	217.6245	34.89472	34.07262	2.474893	0.156566		
13.52451	189.2383	33.74145	32.65300	2.414356	0.172549		
13.20454	157.5859	32.23111	31.36928	2.375282	0.199061		
12.84873	128.2522	30.53151	28.90802	2.249872	0.225399		
12.34043	95.71689	28.11706	27.11395	2.197165	0.283272		
11.89459	74.05053	25.99931	23.36479	1.964520	0.315535		
11.62794	56.60636	23.78271	21.83217	1.910420	0.385684		
11.00839	44.46098	21.78988	19.45723	1.767490	0.437624		
12.08046	82.41307	26.88220	27.05318	2.239415	0.328263		
12.68153	116.4830	29.73727	27.64728	2.180121	0.237350		
13.04175	143.3238	31.44832	30.24764	2.319292	0.211044		
11.93059	75.60116	26.17032	24.46499	2.050610	0.323606		
11.78717	69.61020	25.48906	19.48508	1.655075	0.279917		
10.82705	40.05380	20.92851	21.54947	1.990335	0.538013		
11.35689	54.33796	23.44524	16.74503	1.474438	0.308164		
11.04654	45.44808	21.97107	15.64064	1.415885	0.344143		
10.87632	41.20615	21.16256	14.48317	1.331623	0.351480		
10.60090	35.16455	19.85427	12.90095	1.216957	0.366873		
10.40650	31.44170	18.93089	11.75487	1.129570	0.373862		
10.38369	31.03149	18.82253	11.85142	1.141350	0.381916		
10.13069	26.82591	17.62081	9.353708	0.923303	0.348681		
9.88394	22.93394	16.32737	7.320912	0.742606	0.319217		
9.730461	21.30568	15.71969	6.100175	0.626915	0.286316		
9.631074	20.12095	15.24760	5.446325	0.565495	0.270679		
9.428900	17.91039	14.28727	3.806159	0.403669	0.212511		
9.300307	16.63247	13.67645	3.517885	0.378254	0.211507		
9.120025	14.99292	12.82012	2.694244	0.295420	0.179731		
8.947064	13.57207	11.99855	2.087087	0.233270	0.153778		
8.496366	10.47060	9.857742	0.994775	0.117082	0.095006		
8.045057	8.168539	7.809033	0.480263	0.059548	0.058794		
10.82668	40.04535	20.92676	14.53934	1.342935	0.365076		
11.29736	52.50761	23.16250	16.82983	1.489712	0.320521		
11.01719	44.68677	21.83168	15.53454	1.410027	0.347631		

BSP11480

Tw	B<U>/D	Log	Log
dyne/cm2	(1/sec)	Tw	B<U>/D
2.237401	70.89933	0.349743	1.850642
2.004566	59.91509	0.302020	1.777536
1.588304	37.27145	0.200933	1.571376
1.379090	32.09906	0.139592	1.506492
1.123147	22.18538	0.050436	1.346067
0.920357	15.55716	-0.03604	1.191930
0.550272	5.733507	-0.25942	0.758420
0.337959	2.169238	-0.47113	0.336307

Log Tw vs. Log B<U>/D

Regression Output:
Constant -0.66765
Std Err of Y Est 0.013784
R Squared 0.997953
No. of Observations 8
Degrees of Freedom 6

X Coefficient (e) 0.543339
Std Err of Coef. 0.010045

Tw = K'(B<U>/D)^n'

K' = 0.214954
n' = 0.543329

Regression Output:

Constant -41.2077
Std Err of Y Est 0.442050
R Squared 0.994154
No. of Observations 8
Degrees of Freedom 6

X Coefficient (s) 21.28429
Std Err of Coef. 0.666289

t = 24.68636 deg C
s.d.t = 0.402882 deg C

Page 1

Betz 1120

B1P21477 6/18/90 13:08
 10 PSID Taps 14 1.0 PSID Taps 14 0.1 PSID Taps 14
 S = 2.7 S = 7.25 S = 9.9 <D> (ppm) =
 Z = 2.7 Z = 8.95 Z = 7.4 [NaCl] =

Freq. (Hz)	Qtest (1/s)	Temp (deg C)	<V> (volts)	<V>0 (volts)	<V>f (volts)	<V>corr (volts)
60	1.21416	24.9	1.9095	0.0325	0.0575	1.852
48	0.971338	24.9	1.328	0.0325	0.0575	1.2705
37	0.748732	24.9	0.926	0.0325	0.0575	0.8685
27	0.546372	24.9	0.56725	0.0325	0.0575	0.50975
19	0.384484	24.9	0.362	0.0325	0.0575	0.3045
12	0.242832	24.9	0.22333	0.0325	0.0575	0.164833
7	0.141652	24.9	0.164	0.0325	0.0575	0.1065
18	0.364248	24.9	3.3945	0.082	0.085	3.3095
25	0.5059	24.9	5.605	0.082	0.085	5.52
36	0.728496	24.9	9.705	0.082	0.085	9.62
15	0.30354	24.9	2.749	0.084	0.1105	2.6385
10	0.20336	24.9	1.653571	0.084	0.1105	1.543071
7	0.141652	24.9	1.2392	0.084	0.1105	1.1187
24.7	1.289333	24.7	1.289333	0.0305	0.0125	1.276833
24.7	1.6235	24.7	1.6235	0.0175	0.0125	1.611
24.7	0.8324	24.7	0.8324	0.0175	0.0145	0.8179
24.65	0.624	24.65	0.624	0.0185	0.0095	0.6145
24.6	4.1025	24.6	4.1025	-0.0025	-0.0015	4.105
24.6	3.608	24.6	3.608	-0.0105	-0.0135	3.6215
24.6	2.6557	24.6	2.6557	-0.0195	-0.0185	2.6742
24.6	1.949	24.6	1.949	-0.021	-0.021	1.97
24.55	1.917071	24.55	1.917071	-0.0175	-0.0155	1.934571
24.5	1.540562	24.5	1.540562	-0.017	-0.0115	1.552062
24.5	1.279375	24.5	1.279375	-0.0115	-0.0105	1.289875
24.5	0.959	24.5	0.959	-0.0155	-0.0055	0.9645
24.5	0.851066	24.5	0.851066	-0.0065	-0.0055	0.856566
24.45	0.541852	24.45	0.541852	-0.0075	-0.0065	0.548152
24.4	5.3502	24.4	5.3502	0.0045	-0.0195	5.3377
24.5	6.252	24.5	6.252	-0.0275	-0.0355	6.2835
24.6	7.8668	24.6	7.8668	-0.0345	-0.0285	7.8983

Page 2

Betz 1120

density viscosity
 co[NaCl]=1.000088 1.001574 ID(cm) = 1.45796
 100.0044 X coeff -0.00025 -0.02381 K(V/psi)=1.091022 12.7189
 0.000099 constant 0.003419 -4.14933 XS(cm2) = 1.669479

Batch Vol (ml)	t(s)swap	DP (psid)	U (cm/s)	Re	Iw (dyne/cm2)	f	Log(Re/f)
1.697489	727.2685	118106.5	239.4782	0.000908	3.551217		
1.164503	581.8148	94485.22	164.2856	0.000973	3.469484		
0.796041	448.4822	72832.35	112.3038	0.001119	3.286881		
0.467222	327.2708	53147.93	85.91469	0.001234	3.271175		
0.279095	230.3017	37400.40	39.37425	0.001488	3.159290		
0.151081	145.4537	23621.30	21.31424	0.002020	3.026019		
0.097614	84.84800	13779.09	13.77128	0.002836	2.931171		
0.267501	218.1805	35431.95	37.73855	0.001589	3.150076		
0.446172	303.0285	49211.05	62.94510	0.001274	3.261165		
0.777569	436.3611	70863.91	109.5978	0.001155	3.381782		
0.213265	181.8171	29526.63	30.08707	0.001825	3.100874		
0.134723	121.2114	19684.42	17.59579	0.002401	2.984288		
0.090422	84.84800	13779.09	12.75664	0.002552	2.914552		
0.103204	86.89334	14047.72	14.53985	0.003866	2.941292		
15	0.081717	72.47767	11.71719	0.004401	2.890600		
1815	15	0.066109	56.14524	9.076794	9.326594	0.005933	2.844575
1406	20	0.049669	40.31196	6.509739	7.007203	0.008646	2.781993
1346	20	0.052575	40.19216	6.483077	7.417183	0.009207	2.792848
1040	19.9	0.046382	31.30395	5.049390	6.543563	0.013390	2.766635
1184	34.8	0.034250	20.37939	3.387237	4.831919	0.022330	2.700788
977	45	0.025230	13.00471	2.097487	3.559525	0.042205	2.624624
947	50	0.024777	11.54485	1.827484	3.495510	0.054460	2.629991
875	60	0.019878	8.735257	1.405489	2.804368	0.072697	2.581661
611	59.9	0.016520	6.109888	983.3164	2.330630	0.125191	2.561480
350	60.1	0.012552	3.488289	561.4000	1.742721	0.287190	2.478357
261	59.9	0.010970	2.609952	420.0418	1.547700	0.455605	2.452587
174	99	0.007020	1.052768	169.2400	0.990437	1.791936	2.355164
1390	15	0.068362	55.50632	8912.974	9.644506	0.006276	2.848898
1685	15	0.080476	67.28643	10828.97	11.33343	0.005038	2.885207
2122	14.8	0.101158	85.88208	13852.95	14.27116	0.003880	2.955958

Tap DL= 122.2234
40.77743

Solvent	L	MDR	1/f/f	1/f/f	1/f/f/Slv	1/f/f/L
78.07879						
0.4						
11.32468	53.35982	25.29226	16.14541	1.425682	0.302589	
12.20030	88.29923	27.45146	25.07946	2.055641	0.284028	
12.64466	114.0368	29.56213	26.97102	2.152996	0.236511	
13.12713	150.5439	31.85388	29.41994	2.241155	0.195424	
12.00349	78.84139	26.51661	25.40667	1.949987	0.296883	
11.53755	60.29325	24.50338	20.40487	1.768561	0.338427	
11.25821	51.33724	22.97649	16.77521	1.490043	0.326765	
11.36516	54.59746	23.48455	16.08102	1.414939	0.294537	
11.16240	48.58261	22.52141	15.07380	1.350408	0.310271	
10.97830	43.69738	21.64693	12.98246	1.182556	0.297099	
10.72797	37.83325	20.45787	10.75399	1.002425	0.284247	
10.77539	38.88017	20.68311	10.42156	0.967163	0.268043	
10.66654	36.51874	20.16608	8.641777	0.810175	0.236639	
10.40315	31.38112	18.91498	6.547003	0.629328	0.208628	
10.13769	26.93424	17.65406	4.867612	0.480149	0.180722	
10.11996	26.60669	17.56983	4.285064	0.423426	0.160725	
9.926444	23.85289	16.65155	3.683618	0.371084	0.154430	
9.765920	21.74504	15.88812	2.826266	0.289400	0.129972	
9.513430	18.80345	14.68879	1.866014	0.196145	0.099237	
9.410348	17.72013	14.19915	1.481513	0.157434	0.083606	
9.020657	14.15938	12.34812	0.747031	0.082813	0.052758	
10.99559	44.13451	21.72906	12.62188	1.147904	0.285986	
11.14122	47.99403	22.42083	14.10198	1.265747	0.293827	
11.34383	55.93099	23.38321	16.05402	1.415220	0.297677	

81P21477

Tw	8<U>/D	Log Tw	Log 8<U>/D
dyne/cm2	(1/sec)		
3.559525	71.35843	0.551392	1.853445
3.495510	62.25055	0.563510	1.794143
2.804368	47.93139	0.447835	1.680620
2.330630	33.52568	0.367473	1.525377
1.742721	19.14065	0.241228	1.281956
1.547700	14.32111	0.189687	1.155976
0.990437	5.776666	-0.00417	0.761677

Log Tw vs. Log 8<U>/D

Regression Output:
Constant -0.37927
Std Err of Y Est 0.005238
R Squared 0.999323
No. of Observations 5
Degrees of Freedom 3

X Coefficient (s) 0.489946
Std Err of Coef. 0.007359

Tw = K' (8<U>/D)^n'
K' = 0.417569
n' = 0.489946

Regression Output:
Constant -32.1506
Std Err of Y Est 0.347174
R Squared 0.989161
No. of Observations 5
Degrees of Freedom 3

X Coefficient (s) 18.42598
Std Err of Coef. 1.112593

t = 24.71166 deg C
s.d.t = 0.177325 deg C

B1P03197

10 PSID Taps 14 1.0 PSID Taps 14 0.1 PSID Taps 14
 S = 2.7 S = 7.25 S = 9.9 C (ppm) =
 Z = 2.7 Z = 9.05 Z = 7.05 [NaCl] =

81120 7/23/90 15:00

density viscosity ID (cm) = 1.45796
 co [NaCl] 1.01234 1.029478 K (U/psi) = 1.08859 12.79437
 1.000181 X coeff -0.00025 -0.02281
 0.299990 constant 0.003419 -4.14933 XS (cm²) = 1.669479
 1.085095

Batch Vol (ml) t (sec) DP (psid) U (cm/s) Re Tw dyne/cm² f Log (Re/f)

Batch Vol (ml)	t (sec)	DP (psid)	U (cm/s)	Re	Tw dyne/cm ²	f	Log (Re/f)	
60	1.21414	25.1	8.438	0.0315	8.4065	0.0315	8.4065	
49	0.991564	25.1	5.7725	0.0315	5.741	0.0315	5.741	
43	0.870148	25.1	4.561	0.0315	4.5295	0.0315	4.5295	
36	0.728496	25.1	3.328666	0.0315	3.297166	0.0315	3.297166	
29	0.586844	25.1	2.280666	0.0315	2.249166	0.0315	2.249166	
24	0.485664	25.1	1.6635	0.0315	1.632	0.0315	1.632	
18	0.364248	25.1	1.04225	0.0315	1.01075	0.0315	1.01075	
14	0.283304	25.1	0.6775	0.0315	0.64625	0.0315	0.64625	
10	0.20236	25.1	0.391	0.0315	0.3595	0.0315	0.3595	
32	0.647552	24.6	2.8225	0.0465	2.777	0.0465	2.777	
16	0.323776	24.5	0.872	0.0465	0.8255	0.0465	0.8255	
18	0.364248	25	11.2955	-0.076	11.3715	-0.076	11.3715	
13	0.263068	25	5.942666	-0.076	6.018666	-0.076	6.018666	
10	0.20236	25	3.844111	-0.076	3.920111	-0.076	3.920111	
8	0.161888	25	2.604666	-0.076	2.680666	-0.076	2.680666	
		25	2.044666	0.0745	1.977166	0.0675	1.977166	
		24.9	1.4395	0.0645	1.376	0.0635	1.376	
		24.9	1.073	0.0615	0.945	0.0605	1.0125	
		24.9	0.8526	0.0595	0.5941	0.0585	0.5941	
		24.9	0.481142	0.0585	0.422642	0.0585	0.422642	
		24.9	3.021833	-0.027	3.048833	-0.027	3.048833	
		24.9	1.752857	-0.0285	1.783357	-0.0305	1.783357	
		24.85	1.107142	-0.0305	1.138442	-0.0315	1.138442	
		24.8	0.892083	-0.0325	0.925583	-0.0335	0.925583	
		24.8	0.584571	-0.0345	0.620071	-0.0355	0.620071	
		24.8	0.276266	-0.0355	0.313766	-0.0375	0.313766	
		24.8	0.183285	-0.0375	0.220785	-0.0375	0.220785	
		24.8	0.097	-0.0375	0.1345	-0.0375	0.1345	
		24.7	0.025642	-0.0385	0.064142	-0.0385	0.064142	
		24.7	-0.00759	-0.0395	-0.041	-0.041	0.031909	
		24.7	4.0604	-0.0425	4.1019	-0.0425	4.1019	
		24.7	6.7314	-0.0435	6.7749	-0.0435	6.7749	
		24.65	8.897	-0.0445	8.9415	-0.0445	8.9415	
		24.6	12.5275	-0.0445	12.572	-0.0445	12.572	
		7.222274	727.2685	116830.9	1089.456	0.004080	3.872969	
		5.273794	597.9760	95418.46	744.0157	0.004178	3.790155	
		4.160887	521.7091	82734.57	587.0091	0.004281	3.778687	
		3.028841	456.3611	70103.56	427.5025	0.004446	3.669772	
		2.066128	351.5121	56472.15	291.4850	0.004673	3.506672	
		1.499187	290.9074	46735.57	211.5021	0.004951	3.517032	
		0.928494	218.1805	35051.68	130.9900	0.005451	3.412793	
		0.593657	169.6960	27262.41	83.75199	0.005752	3.315862	
		0.330243	121.2114	19473.15	48.59008	0.006282	3.188511	
		2.551006	387.8765	61615.14	359.8905	0.004738	3.627522	
		0.758320	193.9382	30738.14	106.9822	0.005634	3.565109	
		0.888789	218.1805	34972.69	125.3885	0.005218	3.402508	
		0.470415	157.5748	25258.05	66.36518	0.005295	3.264749	
		0.306593	121.2114	19429.27	43.22533	0.005828	3.171248	
		0.209519	96.96914	15543.41	29.55852	0.006228	3.088720	
		15	0.154534	78.62729	12603.36	21.80134	0.006986	3.072621
		15.1	0.107547	63.82605	10207.77	15.17254	0.007378	2.942923
		15.0	0.079136	54.14861	8660.053	11.16439	0.007542	2.876511
		13.46	0.046634	40.31196	4447.141	6.550878	0.007986	2.760544
		1412	0.023033	33.69611	5389.061	4.660296	0.008131	2.686601
		1400	0.037140	33.54338	5364.634	5.239689	0.008226	2.712047
		1241	0.021724	24.77818	3962.804	3.064856	0.009889	2.595599
		989	0.013870	19.34754	3090.756	1.956858	0.010256	2.497681
		1080	0.008828	16.21323	2587.159	1.246978	0.009397	2.399258
		1076	0.005117	12.89024	2056.906	0.721929	0.008507	2.280656
		1026	0.003822	10.24271	1634.438	0.539235	0.010182	2.217298
		740	0.002489	7.387531	1178.834	0.379439	0.012773	2.140980
		575	0.001628	4.592249	732.7890	0.221150	0.021714	2.037256
		350	0.000781	2.196293	349.6745	0.110235	0.045233	1.871584
		181	0.000388	1.085255	172.7848	0.054838	0.092240	1.719967
		1320	0.049968	29.73193	6325.770	7.049477	0.008846	2.744502
		1523	0.082550	52.85083	9411.262	11.66326	0.008264	2.887461
		2076	0.108923	62.1506	9887.808	15.36675	0.007874	2.943222
		1930	0.153150	76.55953	12161.66	21.60609	0.007502	3.013726

Tap DL = 122.2234
40.77743

Solvent	L	NDR	1//f	1//f	1//f/Siv	1//f/L
82.0894						
4						
0.4						
15.09187	466.4978	41.18642	15.65373	1.037228	0.033555	
14.76062	385.5101	59.61296	15.46951	1.048025	0.040127	
14.55474	342.4263	38.63505	15.28331	1.050057	0.044632	
14.27892	292.1544	37.32491	14.99706	1.050293	0.051332	
13.94669	241.2975	35.74678	14.62720	1.048794	0.060618	
13.66808	205.5427	34.42342	14.21102	1.039723	0.069129	
13.25193	161.7575	32.44669	13.54331	1.021987	0.085726	
12.86344	129.3428	30.60138	13.17352	1.024105	0.101849	
12.55404	96.46982	28.18171	12.61609	1.021211	0.130777	
14.11009	265.0965	36.52295	14.52658	1.029517	0.054797	
13.05243	144.2080	31.49907	13.32196	1.020649	0.092380	
13.21003	157.9022	32.24766	13.84269	1.047892	0.087666	
12.65729	114.8761	29.62264	13.74200	1.085689	0.119624	
12.28499	92.71946	27.85372	13.09808	1.066185	0.141279	
11.95488	76.66567	26.28569	12.67142	1.059937	0.165281	
11.69048	65.84172	25.02980	11.96369	1.033369	0.181703	
11.37169	54.80290	23.51554	11.64146	1.023723	0.212424	
11.10524	47.01017	22.24992	11.51353	1.036765	0.244915	
10.64217	36.01008	20.05033	11.18981	1.051459	0.310741	
10.24640	30.37234	18.64542	11.08950	1.071821	0.365115	
10.44818	32.20528	19.12889	10.41101	0.994442	0.323270	
9.982397	24.63085	16.91638	10.05548	1.007322	0.408247	
9.590725	19.65900	15.05594	9.826148	1.024546	0.499829	
9.197354	15.67540	13.18743	10.31536	1.121557	0.658060	
8.722626	11.92714	10.93247	10.77849	1.235693	0.903693	
8.469193	10.30809	9.728670	9.909916	1.170113	0.961372	
8.163922	8.646902	8.278630	8.520641	1.043694	0.985398	
7.753424	6.748950	6.233767	6.786138	0.877507	1.005510	
7.086336	4.650118	3.160096	4.699806	0.663220	1.010685	
6.479868	3.279798	0.279374	3.292597	0.508127	1.003902	
10.69800	37.18625	20.31554	10.63190	0.993820	0.285909	
11.15384	47.79047	22.38576	11.00018	0.987994	0.230175	
11.37288	54.84063	23.52122	11.26879	0.990847	0.205482	
11.66690	64.95414	24.91781	11.70216	1.003022	0.180160	

dyne/cm ²	T _w	8<U>/D	Log T _w	Log 8<U>/D
0.721929	70.73030	-0.14150	1.849605	
0.559235	56.20298	-0.26822	1.749759	
0.379439	40.53626	-0.42085	1.607843	
0.231150	25.19821	-0.63610	1.401369	
0.110225	12.05132	-0.95767	1.081034	
0.054838	5.954925	-1.26091	0.774876	

Log T_w vs. Log 8<U>/D

Regression Output:
 Constant -2.04384
 Std Err of Y Est 0.004455
 R Squared 0.999902
 No. of Observations 4
 Degrees of Freedom 2

X Coefficient(s) 1.007135
 Std Err of Coef. 0.007059

T_w = K' (8<U>/D)^{n'}

K' = 0.009059
 n' = 1.007135

T_w = 17.82578
 Res/fs = 963.4034

Regression Output:

Constant -3.13742
 Std Err of Y Est 0.101088
 R Squared 0.990347
 No. of Observations 10
 Degrees of Freedom 8

X Coefficient(s) 4.917425
 Std Err of Coef. 0.171643

t = 24.89117 deg C
 s.d.) t = 0.173404 deg C

82P03195	10 PSID	Taps 14	1.0 PSID	Taps 14	0.1 PSID	Taps 14	9.9	<C: (ppm)=					
S =	2.7	S =	7.25	S =	7.05	[NaCl]=							
Z =	2.7	Z =	9	Z =	7.05	[NaCl]=							
B1120	7/21/90	15:01											
Batch	Vol	Temp	<V>	<V>	<V>	<U>	DP	Re	T _w	f	Log (Re/f)		
(Hz)	(l/s)	(deg C)	(volts)	(volts)	(volts)	(volts)	(psid)	(cm/s)	dyne/cm ²				
60	1.21416	25.1	6.969	0.0135	0.0245	6.9445	6.379353	727.2685	116838.9	899.9856	0.003271	3.831482	
49	0.991564	25.1	4.67525	0.0135	0.0245	4.65075	4.272269	593.9360	95418.46	602.7227	0.003285	3.744423	
40	0.80944	25.1	3.160666	0.0135	0.0245	3.136166	2.880943	484.8457	77892.62	406.4374	0.003425	3.658861	
33	0.667788	25.1	2.2356	0.0135	0.0245	2.2115	2.051537	399.9977	64261.41	286.6035	0.003549	3.583095	
25	0.5039	25.1	1.378666	0.0135	0.0245	1.365166	1.254068	303.0285	48882.88	176.9213	0.003817	3.478254	
19	0.384484	25.1	0.87875	0.0135	0.0245	0.85425	0.784770	230.3017	36998.99	110.7081	0.004155	3.376454	
15	0.30354	25.1	0.6004	0.0135	0.0245	0.5759	0.539033	181.8171	29209.73	74.63484	0.004473	3.290830	
10	0.20236	25.1	0.3115	0.0135	0.0245	0.287	0.263643	121.2114	19473.15	37.19430	0.005015	3.139602	
8	0.161888	25.1	0.236428	0.0135	0.0245	0.211928	0.194681	96.96914	15578.52	27.46528	0.005787	3.073756	
30	0.60708	24.3	2.107333	0.0135	0.0125	2.093833	1.923436	267.6342	57274.57	271.3542	0.004065	3.563251	
15	0.30354	24.2	0.656666	0.0105	0.0155	0.641166	0.588988	181.8171	28622.63	83.09320	0.004978	3.305280	
20	0.40472	25.1	10.886	0.0125	0.005	10.8735	0.865724	242.4228	38946.31	122.1345	0.004117	3.297784	
15	0.30354	25.1	6.864111	0.0125	0.005	6.851611	0.545510	181.8171	29209.73	76.95945	0.004612	3.297495	
10	0.20236	25.1	3.5896	0.0125	0.005	3.5771	0.284800	121.2114	19473.15	40.17911	0.005418	3.156364	
10	0.20236	25	3.538428	-0.0005	0.0015	3.536928	0.281602	121.2114	19429.27	39.72789	0.005357	3.152927	
8	0.161888	25	2.50375	-0.0005	0.0015	2.50425	0.199382	96.96914	15543.41	28.12852	0.005926	3.077953	
24.8	2.0746	24.8	2.0746	0.0745	0.0675	2.0001	15	0.159243	81.70210	13037.27	22.46575	0.006667	3.027169
24.7	1.4474	24.7	1.4474	0.0645	0.0635	1.3839	15	0.110183	64.85055	10324.93	15.54440	0.007322	2.946210
24.6	1.10675	24.6	1.10675	0.0615	0.0605	1.04625	15.1	0.082300	54.34526	8632.894	11.75180	0.007882	2.884491
24.6	0.72	24.6	0.72	0.0595	0.0585	0.6615	15.1	0.052667	40.69952	6465.218	7.430176	0.008886	2.784928
24.5	0.5296	24.5	0.5296	0.0585	0.0585	0.4711	20	0.037507	33.51343	5311.695	5.291543	0.009233	2.710244
24.5	0.3215	24.5	0.3215	0.0575	0.0575	0.264	25	0.021019	24.43875	3873.407	2.965331	0.009835	2.584490
24.7	1.703428	24.7	1.703428	0.0235	0.0245	1.678928	29.9	0.020586	23.99962	3821.010	2.904236	0.009989	2.581929
24.6	0.992333	24.6	0.992333	0.0215	0.0195	0.972833	25	0.011928	18.12369	2878.993	1.682822	0.010149	2.462457
24.5	0.537083	24.5	0.537083	0.0185	0.0165	0.520583	40	0.006383	14.67523	2325.943	0.900513	0.008283	2.325698
24.6	0.3655	24.6	0.3655	0.0165	0.0145	0.351	50	0.004303	11.38079	1807.866	0.607165	0.009286	2.241092
24.5	0.227866	24.5	0.227866	0.014	0.014	0.213866	59.9	0.002622	7.249867	1149.064	0.369949	0.013943	2.12524
24.5	0.1324	24.5	0.1324	0.0135	0.0145	0.1179	59.9	0.001445	4.009926	635.2512	0.203945	0.025125	2.002210
24.5	0.0705	24.5	0.0705	0.0135	0.0145	0.057	60.1	0.000698	1.943475	308.0301	0.098599	0.051712	1.845390
24.4	0.33235	24.4	0.33235	0.0145	0.0145	0.318735	100	0.000229	0.634928	100.4058	0.032408	0.159249	1.602798
24.4	2.3778	24.4	2.3778	0.0135	0.008	2.3643	25	0.028989	29.13482	4607.303	4.089802	0.009544	2.62219
24.5	3.6228	24.5	3.6228	0.0075	0.0065	3.6153	20	0.044328	37.16727	5890.807	6.253801	0.008968	2.746525
24.5	6.373833	24.5	6.373833	0.0055	0.0055	6.360333	20	0.078084	51.51306	8164.536	11.01604	0.008223	2.869466
24.5	9.258166	24.5	9.258166	0.0145	0.0145	9.243666	15.1	0.113340	63.11202	10002.90	15.98983	0.007952	2.950375
24.3	13.0615	24.3	13.0615	0.0075	0.0105	13.054	15	0.160060	78.66723	12412.19	22.58100	0.007227	3.023354

density viscosity ID(cm) = 1.45796
 K(U/psi) = 1.08859 12.56
 XS(cm2) = 1.669479
 1.085095

col[NaCl] 1.01274 1.029478
 2.017038 X coeff -0.00025 -0.02281
 0.300079 constant 0.003419 -4.14932

T-p DL= 122.2234
40.77743

Solvent	L	MDR	1///f	1///f	1///f/Slv	1///f/L
81.55661						
4						
0.4						
14.92593	423.9967	40.39816	17.22285	1.153888	0.040620	
14.57769	346.9792	38.74404	17.18734	1.179016	0.049534	
14.23544	284.9322	37.11837	17.08577	1.200227	0.059964	
13.93202	239.2684	35.67710	16.78590	1.204843	0.070135	
13.51301	187.9900	33.68684	16.18532	1.197757	0.086096	
13.10581	148.7080	31.75263	15.55017	1.186509	0.104568	
12.76334	122.0999	30.12587	14.95175	1.171460	0.122454	
12.15841	86.19518	27.25745	14.11995	1.161332	0.163813	
11.89502	74.06905	26.00137	13.14527	1.105106	0.177473	
13.85200	228.6291	35.30177	15.68440	1.132201	0.068601	
12.82112	126.2294	30.40033	14.17192	1.105357	0.112271	
13.19113	156.1939	32.15789	15.58411	1.181408	0.099774	
12.78998	123.9868	30.25241	14.72420	1.151229	0.118756	
12.22545	89.58698	27.57093	13.58536	1.111335	0.151644	
12.21170	88.88067	27.50561	13.66247	1.118800	0.153716	
11.91181	74.78819	26.08110	12.98953	1.090474	0.173684	
11.70867	66.53492	25.11622	12.24664	1.045945	0.184063	
11.38484	55.21930	23.57800	11.68628	1.026477	0.211634	
11.13796	47.96393	22.40533	11.26329	1.011252	0.235122	
10.73975	38.09064	20.51382	10.60827	0.987758	0.278500	
10.44097	32.07190	19.09465	10.35114	0.991596	0.322748	
9.957960	24.00878	16.70531	10.08330	1.014625	0.419984	
9.927759	23.86821	16.65685	10.00548	1.007829	0.419197	
9.449831	18.12749	14.38669	9.926196	1.050409	0.547576	
8.902794	13.23057	11.78827	10.98754	1.234167	0.830466	
8.564268	10.88860	10.18075	10.37705	1.211654	0.953020	
8.150099	8.480178	8.11974	8.468748	1.041653	0.998652	
7.612841	6.296371	5.660996	6.308705	0.828692	1.001958	
6.981563	4.577950	2.662426	4.397464	0.629868	1.004457	
6.011193	2.504254	-1.94682	2.505882	0.416869	1.000649	
10.21327	38.13193	18.01307	10.23593	1.002217	0.363854	
10.58610	34.86628	19.78398	10.55964	0.997500	0.302841	
11.07786	46.27499	22.11986	11.02119	0.995426	0.238297	
11.40150	55.75137	23.65713	11.21374	0.983532	0.201138	
11.69341	63.95304	25.04374	11.76233	1.005893	0.178344	

82F03195

Tw	8:U./D	Log Tw	Log 8:U./D
dyne/cm ² (1/sec)			
0.607165	62.44776	-0.21669	1.795516
0.269949	39.78088	-0.43185	1.599674
0.203945	22.00294	-0.69048	1.242480
0.032408	3.483927	-1.48933	0.542069
0.098599	10.66408	-1.00612	1.027923
0.032408	3.483927	-1.48933	0.542069

Log Tw vs. Log 8:U./D

Regression Output:
 Constant -2.03025
 Std Err of Y Est 0.000996
 R Squared 0.999995
 No. of Observations 4
 Degrees of Freedom 2

X Coefficient(s) 0.997452
 Std Err of Coef. 0.001463

Tw = K' (8:U./D)^{n'}

K' = 0.009327
 n' = 0.997452

T_∞ = 6.497072
 Res/fs = 576.5994

Regression Output:

Constant -10.6178
 Std Err of Y Est 0.140911
 R Squared 0.989342
 No. of Observations 9
 Degrees of Freedom 7

X Coefficient(s) 7.701142
 Std Err of Coef. 0.302104

t = 24.74 deg C
 s.d.t = 0.302560 deg C

B5P03191

10 PSID Taps 14 1.0 PSID Taps 14 0.1 PSID Taps 14

S = 2.7 S = 7.25 S = 9.9 <C> (ppm) = 9.9

Z = 2.7 Z = 9 Z = 7.1 [NaCl] = 7.1

7/16/90 15:37

Freq. (Hz)	Dtest (1/s)	Temp (deg C)	<V> (volts)	<V>0 (volts)	<V>f (volts)	<V>corr (volts)
60	1.21416	25.3	5.183666	0.03	0.0365	5.147166
49	0.991564	25.3	3.500333	0.03	0.0365	3.463833
41	0.827676	25.3	2.529333	0.03	0.0365	2.492833
34	0.688024	25.3	1.8205	0.03	0.0365	1.784
27	0.546372	25.3	1.236	0.03	0.0365	1.206
21	0.424956	25.3	0.834333	0.03	0.0365	0.797833
14	0.283304	25.3	0.469	0.03	0.0365	0.4325
10	0.20236	25.3	0.296625	0.03	0.0365	0.260125
25	0.5059	24.6	1.23	0.0285	0.0315	1.1985
19	0.384484	24.6	0.821	0.0285	0.0315	0.7895
15	0.30354	24.6	0.532	0.0285	0.0315	0.5217
10	0.20236	24.6	0.311285	0.0285	0.0315	0.279785
25	0.5059	25.3	12.428	0.0735	0.0905	12.3375
20	0.40472	25.3	8.7568	0.0735	0.0905	8.6663
15	0.30354	25.3	5.5	0.0735	0.0905	5.4095
10	0.20236	25.3	3.130444	0.0735	0.0905	3.039944
8	0.161888	25.3	2.2705	0.0735	0.0905	2.18
		25.15	1.9586	0.0845	0.0795	1.8741
		25.1	1.37835	0.0735	0.0725	1.30575
		25.1	1.0578	0.0685	0.0685	0.9893
		25	0.6946	0.0655	0.0635	0.6311
		25	0.5278	0.0625	0.0615	0.4663
		24.9	3.0878	0.0635	0.055	3.0328
		24.9	1.763142	0.0505	0.05	1.713142
		24.9	1.038444	0.0465	0.046	0.992444
		24.8	0.563153	0.0435	0.0435	0.519653
		24.8	0.3475	0.0425	0.0415	0.306
		24.7	0.213846	0.0405	0.0385	0.175346
		24.65	0.105166	0.0375	0.0375	0.067666
		24.6	0.051933	0.0365	0.0365	0.015433
		24.6	1.445	0.036	0.0345	1.4105
		24.6	3.222	0.0325	0.033	3.189
		24.6	5.90225	0.0305	0.0295	5.87275
		24.7	7.72525	0.0295	0.0275	7.69775
		24.7	11.98866	0.029	0.0315	11.95716

density viscosity

col[NaCl] 1.0123, 1.029478 ID(cm) = 1.45796

5.068331 X coeff -0.00025 -0.02281 K(V/psi) = 1.08859 12.56699

0.300099 constant 0.003419 -4.14933 XS(cm2) = 1.669479

Batch Vol (ml)	t/samp (sec)	DP (psid)	<U> (cm/s)	Re	Tw (dyne/cm2)	f	Log(Re/f)
4.728287	727.2685	117267.3	667.0567	0.002498	3.768416		
3.181944	593.9360	95849.96	448.9020	0.002521	3.482410		
2.289985	496.9668	80200.99	323.0634	0.002591	3.610979		
1.638817	412.1188	66508.13	231.2008	0.002697	3.528229		
1.107855	327.2708	52815.28	156.2938	0.002891	3.452206		
0.732905	234.5440	41078.55	103.5967	0.003161	3.365588		
0.397302	169.6960	27385.70	56.05065	0.003856	3.230625		
0.238955	121.2114	19561.21	33.71139	0.004546	3.120232		
1.100965	303.0017	48136.83	155.3218	0.003350	3.445055		
0.752520	230.3017	36583.99	102.3167	0.003821	3.354412		
0.479243	181.8171	28882.09	67.61069	0.004051	3.264446		
0.257016	121.2114	19254.73	36.25935	0.004889	3.129148		
0.981738	303.0285	48903.04	138.5016	0.002988	3.427062		
0.689608	242.4228	39122.43	97.28846	0.003280	3.350365		
0.430453	181.8171	29341.82	60.72741	0.003639	3.248027		
0.241899	121.2114	19561.21	34.12662	0.004602	3.122881		
0.173470	96.96914	15648.97	24.47282	0.005156	3.050577		
14.9	0.169138	84.42127	13577.96	21.02877	0.005848	3.015267	
15	0.103903	66.08846	10617.40	14.65843	0.006649	2.937408	
14.8	0.078722	55.64932	8940.311	11.10594	0.007105	2.877142	
20	0.050218	41.06070	6581.719	7.084771	0.008325	2.778542	
19.9	0.037105	33.92264	5437.543	5.234715	0.009012	2.712825	
19.9	0.038299	33.65174	5381.964	5.403206	0.009452	2.718720	
30	0.021634	24.33892	3892.553	3.052118	0.010207	2.594695	
34.9	0.012533	18.29874	2942.534	1.748129	0.010348	2.476151	
45.1	0.006562	14.60948	2331.248	0.925810	0.008593	2.324670	
59.9	0.003804	10.37981	1656.314	0.545166	0.010024	2.219673	
60	0.002214	5.939974	945.7107	0.312394	0.017540	2.097775	
75	0.000854	2.26158	361.9814	0.120554	0.046096	1.890522	
100.1	0.000194	0.520599	82.69857	0.027495	0.200789	1.569072	
25	0.017812	23.33447	7532.000	2.512932	0.010069	2.549529	
20	0.040272	35.10075	5575.841	5.681490	0.009135	2.726669	
15	0.074163	51.07380	8131.522	10.46283	0.007946	2.860248	
15	0.097210	63.52277	10115.13	13.71423	0.006730	2.919009	
15.1	0.131000	80.84369	12817.22	21.50276	0.006457	3.014641	

Tap DL= 122.2234
40.77743

79.1865

0.4

4

Solvent	L	MDR	1/f/f	1/f/f	1/f/f	1/f/f	1/f/f	1/f/f	1/f/f
14.67366	366.6878	39.19991	20.00463	1.363301	0.054554				
14.32964	300.8090	37.56580	19.91503	1.389778	0.066204				
14.04391	255.1873	36.20860	19.64267	1.398660	0.074973				
13.75331	215.8787	34.82826	19.25506	1.400030	0.089193				
13.41322	177.4949	33.21281	18.59745	1.386501	0.104777				
13.05435	144.3671	31.50818	17.78388	1.362295	0.123185				
12.52250	106.2932	28.98188	16.10269	1.285900	0.151493				
12.08089	82.43345	26.88424	14.83106	1.27644	0.179915				
13.38022	174.1546	33.05604	17.27517	1.291097	0.099194				
13.01764	141.3488	31.33383	16.17629	1.242643	0.114442				
12.65778	114.9017	29.62448	15.71022	1.241150	0.136727				
12.11659	84.14509	27.03382	14.30173	1.180342	0.169945				
13.30825	167.0869	32.71418	18.29251	1.374524	0.109478				
13.00146	140.0379	31.25695	17.46063	1.342974	0.124685				
12.59211	110.6388	29.31252	16.57523	1.316318	0.149813				
12.09152	82.93957	26.93475	14.74056	1.219082	0.177726				
11.80270	70.23558	25.56286	13.92343	1.179850	0.198267				
11.66547	64.90042	24.91098	13.07576	1.120894	0.201474				
11.34963	54.11137	23.41076	12.26336	1.080507	0.226631				
11.10857	47.10018	22.26570	11.86342	1.067952	0.251876				
10.71416	37.53379	20.39230	10.95965	1.022912	0.291994				
10.45130	32.26309	19.14369	10.53359	1.007873	0.326490				
10.47488	32.70394	19.25568	10.28538	0.981909	0.314499				
9.978780	24.57961	16.89920	9.897820	0.991886	0.402684				
9.504605	18.70817	14.64687	9.830376	1.034275	0.525458				
8.938680	13.50672	11.95873	10.78744	1.206826	0.798471				
8.478694	10.36462	9.773801	9.987784	1.177986	0.965641				
7.991103	7.82892	7.457743	7.550615	0.944877	0.964553				
7.162090	4.857384	3.519929	4.657615	0.650315	0.958872				
5.876290	2.317141	-2.58762	2.330619	0.379596	0.982660				
9.798116	22.15180	16.04105	9.963328	1.017065	0.449865				
10.50667	33.30810	19.40672	10.46262	0.995806	0.314116				
11.04099	45.30317	21.94472	11.21820	1.016050	0.247625				
11.27403	51.86683	23.06118	12.18882	1.080949	0.275002				
11.65856	64.64307	24.87819	12.44451	1.067413	0.192311				

B5P03191

Tw	8<U>/D	Log	Log
dyne/cm ²	(1/sec)	Tw	8<U>/D
3.052118	122.5505	0.484401	2.125645
1.788129	100.9561	0.247513	2.004132
0.925810	80.16400	-0.03347	1.903979
0.545166	56.95525	-0.26347	1.755533
0.312394	32.59334	-0.50529	1.513128
0.120554	12.48955	-0.91881	1.096546
0.027495	2.856593	-1.56073	0.455848

Log Tw vs. Log 8<U>/D

Regression Output:

Constant	-2.0146
Std Err of Y Est	0.000003
R Squared	0.99995
No. of Observations	4
Degrees of Freedom	2

X Coefficient(s)	0.997905
Std Err of Coef.	0.001465

Tw = K' (8<U>/D)^{n'}

K' =	0.009664
n' =	0.997905

Tw* = 7.451550
Res/f* = 641.2683

Regression Output:

Constant	-23.8737
Std Err of Y Est	0.194827
R Squared	0.993206
No. of Observations	11
Degrees of Freedom	9

X Coefficient(s)	12.36246
Std Err of Coef.	0.340796

t = 24.97714 deg C
s.d.t = 0.288182 deg C

BIP13187
 10 PSID Taps 14 1.0 PSID Taps 14 0.1 PSID Taps 14
 S = 2.7 S = 7.25 S = 9.9 <C> (ppm) =
 Z = 2.7 Z = 8.95 Z = 7.2 [NaCl] =

density viscosity
 col[NaCl] 1.01234 1.029478
 9.963670 X coeff -0.00025 -0.02281
 0.500097 constant 0.003419 -4.14933

s.d.t = 0.310682 deg C
 ID(cm) = 1.45796
 K(U/psi)=1.086516 12.44018
 XS(cm2)= 1.669479

Freq. (Hz)	Qiest (1/s)	Temp (deg C)	<U> (volts)	<U>o (volts)	<U>f (volts)	<U>corr (volts)	Batch Vol (gal)	t(samp (sec))	DP (psid)	<U> (cm/s)	Re	Tw (dyne/cm2)	f	Log(Re/f)
60	1.21416		25 3.383	0.0345	0.039	3.344			3.07727	727.2685	116575.6	434.1992	0.001626	2.672224
51	1.032036		25 2.493	0.0345	0.039	2.454			2.25895	618.1782	99089.29	318.6378	0.001651	2.605038
43	0.870148		25 1.838	0.0345	0.039	1.799			1.65251	521.2091	83545.87	233.5898	0.001703	2.537606
34	0.688024		25 1.24025	0.0345	0.039	1.20125			1.105598	412.1188	66059.53	155.9754	0.001819	2.449907
27	0.546372		25 0.8735	0.0345	0.039	0.839			0.772192	327.2708	52459.03	108.9393	0.002015	2.371971
19	0.384484		25 0.53475	0.0345	0.039	0.49575			0.456274	230.3017	36915.62	64.37029	0.002404	2.257722
16	0.323776		25 0.4306	0.0345	0.039	0.3916			0.360418	192.9382	31086.83	50.84701	0.002678	2.206512
12	0.242832		25 0.244666	0.0345	0.039	0.210166			0.193431	145.4527	23215.12	27.28892	0.002553	2.071372
9	0.182124		25 0.214444	0.0345	0.039	0.175444			0.161474	109.0902	17486.34	22.78045	0.003792	2.032160
20	0.40472		24.2 0.615333	0.0375	0.0385	0.576833			0.530901	242.4228	38165.51	74.89850	0.002534	2.282734
15	0.30354		24.1 0.421666	0.0375	0.0385	0.383166			0.352656	181.8171	28558.13	49.75199	0.002981	2.192918
30	0.60708		25.1 1.547	0.0885	0.1055	11.4585			0.921087	375.6342	58419.46	129.9451	0.001947	2.411244
23	0.465428		25.1 7.6785	0.0885	0.1055	7.573			0.608753	268.7862	44788.25	85.88161	0.002189	2.321314
17	0.344012		25.1 5.08	0.0885	0.1055	4.9745			0.399873	206.0594	33104.36	56.41332	0.002632	2.230055
12	0.242832		25.1 3.2551	0.0885	0.1055	3.1496			0.253179	145.4537	23367.78	35.71804	0.003344	2.120808
8	0.161888		25.1 1.780714	0.0885	0.1055	1.675214			0.134661	96.96914	15578.52	18.99776	0.004002	2.093716
			25 1.5405	0.0385	0.031	1.5095	2115	15	0.121360	84.45745	13537.89	17.11848	0.004754	2.070112
			24.9 1.087	0.0315	0.0225	1.0645	1640	14.9	0.085569	65.92899	10544.10	12.07196	0.005502	2.092282
			24.8 0.87125	0.0235	0.0165	0.85475	1381	15	0.068708	55.14692	8799.840	9.693293	0.006314	2.844644
			24.8 0.0886	0.0185	0.0125	0.0761	825	35	0.006117	14.11902	2252.984	0.865012	0.008576	2.319417
			24.75 0.5856	0.0145	0.0095	0.5761	1379	19.9	0.046309	41.50783	6615.972	6.533262	0.007512	2.758481
			24.75 0.4542	0.0135	0.0085	0.4457	1151	20	0.035827	34.47182	5494.495	5.054441	0.008426	2.702753
			24.6 2.8594	-0.029	-0.07	2.8884	1151	20	0.036475	34.47182	5475.933	5.145944	0.008578	2.705171
			24.6 1.839833	0.0105	0.0055	1.829333	1061	25	0.023101	25.42109	4038.203	3.259122	0.009990	2.605989
			24.6 1.20925	-0.002	-0.002	1.21125	1165	35	0.015296	19.93777	3167.165	2.157950	0.010754	2.516459
			24.55 0.842666	-0.0055	-0.006	0.848666	1126	40	0.010717	16.86154	2675.477	1.511976	0.010525	2.428718
			24.5 0.42225	-0.0085	-0.009	0.43125	1066	50.1	0.005446	13.68947	2159.705	0.768310	0.008121	2.291221
			24.5 0.314	-0.0125	-0.0135	0.3275	1066	60	0.004135	10.64203	1686.704	0.583470	0.010205	2.214462
			24.45 0.250285	-0.015	-0.0175	0.265285	887	60	0.003350	8.855055	1401.895	0.472630	0.011940	2.185221
			24.4 0.207857	-0.0175	-0.0175	0.225357	759	60	0.002845	7.577211	1198.240	0.401494	0.013852	2.149707
			24.4 0.116214	-0.019	-0.0195	0.135714	457	60	0.001713	4.562300	721.4699	0.241787	0.023010	2.059185
			24.3 0.049266	-0.0195	-0.0195	0.068766	234	60	0.000868	2.556057	368.5854	0.122514	0.044470	1.890576
			24.25 0.003956	-0.0205	-0.0215	0.024956	140	100.2	0.000315	0.836910	131.8997	0.044462	0.125742	1.669986
			24.3 3.67925	-0.0215	-0.004	3.70075	1012	14.9	0.046734	40.68301	6419.005	6.593219	0.007890	2.756031
			24.3 5.379	-0.0185	0.0005	5.3975	1345	14.9	0.046161	54.06981	8531.188	9.616132	0.006515	2.827982
			24.3 6.8586	-0.0155	-0.011	6.8741	1605	14.9	0.086808	64.52197	10180.34	12.24682	0.005827	2.890494
			24.3 9.6336	-0.0195	-0.0195	9.6531	2057	14.9	0.121903	82.69265	13047.32	17.19786	0.004981	2.944220

Tap DL= 122.2234
40.77743

Solvent	L	MDR	1//f	1//f	1//f/Siv	1//f/L
79.1865						
4						
0.4						
14.28889	295.8353	37.37225	24.79612	1.735341	0.084387	
14.02011	251.7145	36.09553	24.60359	1.754878	0.097744	
13.75042	215.5194	34.81452	24.23805	1.761985	0.112416	
13.59963	174.1114	33.14824	23.44379	1.749584	0.133119	
13.08788	147.1810	31.66746	22.27657	1.702075	0.151354	
12.65088	113.1343	29.49672	20.39331	1.614559	0.180254	
12.42604	100.5223	28.52373	19.32254	1.555002	0.192163	
11.88549	73.66358	25.95608	19.78176	1.664362	0.268541	
11.72864	67.30398	25.21105	16.25821	1.384492	0.241266	
12.73093	119.8435	29.97195	19.90278	1.565340	0.166073	
12.37167	97.45363	28.26544	18.31520	1.480415	0.187937	
13.24497	161.1108	32.41365	22.66276	1.711045	0.140665	
12.88525	130.9769	30.70498	21.37220	1.658655	0.165175	
12.52022	106.1538	28.97105	19.49080	1.556745	0.183609	
12.12323	84.46729	27.08536	17.29055	1.426233	0.204701	
11.57486	61.60217	24.48060	15.80557	1.365508	0.256574	
11.48044	58.34346	24.03213	14.50236	1.263222	0.248568	
11.17315	48.88361	22.57238	13.48113	1.204566	0.275780	
10.97857	43.70436	21.64825	12.58432	1.146261	0.287942	
8.877670	13.04060	11.66893	10.79793	1.216502	0.828024	
10.63392	35.82947	20.01115	11.53750	1.084971	0.321921	
10.41101	31.52346	18.95232	10.89365	1.046358	0.345572	
10.42068	31.69942	18.99825	10.79659	1.036073	0.340592	
10.02395	25.22720	17.11379	10.00458	0.998067	0.396579	
9.665838	20.52766	15.41273	9.642977	0.997634	0.469755	
9.354874	17.16321	13.93565	9.742776	1.041465	0.567654	
8.764887	12.22086	11.13321	11.09631	1.265996	0.907981	
8.525852	10.64984	9.997798	9.898648	1.161015	0.929464	
8.340887	9.574184	9.119213	9.151531	1.097189	0.955854	
8.197231	8.814302	8.436850	8.496418	1.036498	0.963935	
7.756740	6.840140	6.344515	6.592243	0.849872	0.963758	
7.162504	4.857983	3.520944	4.742005	0.662078	0.976126	
6.279945	2.923253	-0.67025	2.820054	0.449057	0.964697	
10.62412	35.63788	19.94660	11.25734	1.059601	0.315881	
10.95193	43.03912	21.52168	12.38871	1.131189	0.287847	
11.16197	48.57077	22.51940	13.09988	1.173616	0.269707	
11.45688	57.55730	23.92018	14.16775	1.236615	0.246150	

BIP13187

Tw	B<U>/D	Log	Log
dyne/cm2	(1/sec)	Tw	B<U>/D
0.768310	75.11575	-0.11446	1.875731
0.583470	58.39413	-0.23398	1.766269
0.472630	48.58874	-0.32547	1.686535
0.401494	41.57706	-0.39632	1.618853
0.241787	25.03388	-0.61656	1.398528
0.122514	12.81822	-0.91181	1.107827
0.044462	4.592229	-1.35200	0.662023

Log Tw vs. Log B<U>/D

Regression Output:
Constant -2.01768
Std Err of Y Est 0.003089
R Squared 0.999959
No. of Observations 5
Degrees of Freedom 3

X Coefficient(s) 1.001928
Std Err of Coef. 0.003680

Tw = K'(B<U>/D)^n'

K' = 0.009600
n' = 1.001928

Tw = 5.111821
Res/ft = 510.1141

Regression Output:

Constant -36.1219
Std Err of Y Est 0.399325
R Squared 0.992176
No. of Observations 23
Degrees of Freedom 21

X Coefficient(s) 17.19286
Std Err of Coef. 0.333158

t = 24.70675 deg C
s.d.t = 0.318391 deg C

B2F13184 B1120 7/4/90 15:17
 10 PSD Taps 14 1.0 PSD Taps 14 0.1 PSD Taps 14
 S = 2.7 S = 7.25 S = 9.9 <C> (ppa)=
 Z = 2.7 Z = 8.9 Z = 7.2 [NaCl]=

Freq. (Hz)	Drest (1/s)	Temp (deg C)	<U> (volts)	<U>0 (volts)	<U>f (volts)	<U>corr (volts)
20	0.40472	25.2	0.483333	0.0375	0.0395	0.443833
29	0.586844	25.2	0.761	0.0375	0.0395	0.7215
38	0.788988	25.2	1.160666	0.0375	0.0395	1.121166
46	0.950856	25.2	1.52925	0.0375	0.0395	1.48975
56	1.133216	25.2	2.171	0.0375	0.0395	2.1335
60	1.21816	25.2	2.475	0.0375	0.0395	2.4355
15	0.30354	25.2	0.357333	0.0375	0.0395	0.317833
10	0.20236	25.2	0.208888	0.0375	0.0395	0.169388
20	0.40472	24	0.5246	0.033	0.0355	0.4891
20	0.40472	24	0.496333	0.033	0.0355	0.460833
10	0.20236	24	0.216	0.0475	0.035	0.181
20	0.40472	25.1	4.980333	0.0245	0.0325	4.955833
16	0.232776	25.1	3.5955	0.0245	0.0325	3.563
11	0.252596	25.1	2.356625	0.0245	0.0325	2.324125
8	0.161888	25.1	1.544714	0.0245	0.0325	1.512214
24.8	1.374	0.0285	0.0295	0.0295	1.3455	
24.7	1.0286	0.0315	0.0285	0.0285	1.0001	
24.6	0.7552	0.0315	0.0195	0.0195	0.7357	
24.6	0.55325	0.0225	0.0205	0.0205	0.53275	
24.5	0.456	0.0235	0.0195	0.0195	0.4365	
24.4	2.805	0.0905	0.1325	0.1325	2.7145	
24.3	1.7516	0.0145	0.0145	0.0145	1.7371	
24.3	1.213833	0.0125	0.0075	0.0075	1.206333	
24.3	0.833571	0.003	0.0005	0.0005	0.833071	
24.3	0.448666	-0.0025	-0.003	-0.003	0.451666	
24.2	0.322062	-0.0095	-0.012	-0.012	0.334062	
24.2	0.217076	-0.0145	-0.0145	-0.0145	0.231576	
24.1	0.120333	-0.0175	-0.0175	-0.0175	0.137833	
24.05	0.063222	-0.0195	-0.02	-0.02	0.083222	
24	-0.00104	-0.0215	-0.0235	-0.0235	0.02452	
23.8	0.025	-0.0295	-0.0275	-0.0275	0.0505	
23.9	3.4065	-0.0295	-0.015	-0.015	3.436	
24	4.90975	-0.0155	0.003	0.003	4.92525	
24.1	6.205	0.001	0.0165	0.0165	6.204	
24.1	8.8412	0.0135	0.0215	0.0215	8.8277	
24.1	8.4165	0.0175	0.0255	0.0255	8.399	

Triggered

density viscosity ID(cm) = 1.45796
 c0[NaCl] 1.01234 1.029478 K(U/psi)=1.086516 12.44018
 20.01199 X coeff -0.00025 -0.02281 XS(cm2) = 1.669479
 0.300113 constant 0.003419 -4.14933

Batch Vol (ml)	t(samp (sec))	DP (psid)	<U> (cm/s)	Re	Tw dyne/cm2	f	Log (Re/f)
0	408492	242.4228	39034.27	57.62921	0.001942	3.255671	
0.664049	351.5131	56599.69	93.68264	0.001502	3.241179		
1.031891	460.6034	74165.12	145.5770	0.001559	3.436895		
1.371125	557.5725	89778.82	193.4555	0.001232	3.498618		
1.963615	678.7840	109295.9	277.0227	0.001191	3.576607		
2.241568	727.2685	117102.8	316.2357	0.001184	3.605355		
0.293525	181.8171	29275.70	41.26883	0.002473	3.163161		
0.155900	121.2114	19517.13	21.99417	0.002966	3.036502		
0.450154	242.4228	37991.71	63.50683	0.002140	3.244937		
0.424128	242.4228	37991.71	59.83656	0.002016	3.222010		
0.166587	121.2114	18995.85	23.50181	0.003168	3.039078		
0.398373	242.4228	38946.31	56.20163	0.001894	3.229229		
0.286410	193.9282	31157.04	40.40620	0.002126	3.157588		
0.186824	133.3325	21420.47	26.35674	0.002937	3.064810		
0.121558	96.96914	15578.52	17.14926	0.002613	2.971487		
15	0.108157	84.49739	13483.31	15.25864	0.004233	2.963167	
15	0.080392	65.48947	10426.65	11.34163	0.005238	2.877761	
14.9	0.059139	55.15523	8761.544	8.343206	0.005433	2.810105	
15	0.042824	41.64970	6616.158	6.041652	0.006899	2.740016	
15.1	0.025087	34.90797	5522.721	4.950128	0.008047	2.695761	
15.1	0.034279	34.86830	5513.980	4.856126	0.007879	2.689717	
19.9	0.021936	25.73546	4060.565	3.094800	0.009256	2.591799	
25	0.015234	20.17395	3183.065	2.149191	0.010460	2.512620	
30	0.010520	17.07118	2693.508	1.484191	0.010088	2.422259	
45	0.005703	13.79005	2175.808	0.804684	0.008382	2.299296	
60	0.004218	10.78180	1697.329	0.595162	0.010141	2.223815	
59.9	0.002924	7.649860	1204.282	0.412575	0.013965	2.155249	
60	0.001740	4.652148	730.7160	0.245563	0.022474	2.059592	
75	0.001050	2.763336	433.5497	0.148267	0.038440	1.929563	
90	0.000283	0.758753	115.7749	0.040000	0.145176	1.544562	
180	0.000657	1.653875	258.0230	0.089970	0.065147	1.818606	
15.1	0.043391	40.85819	6388.732	6.121543	0.007263	2.75972	
15	0.062198	54.14861	8485.992	8.774776	0.005927	2.815145	
15	0.078246	64.49115	10129.66	11.05298	0.005263	2.866252	
15	0.111479	82.70042	12989.81	15.72734	0.004554	2.942840	
15	0.106066	79.50581	12488.03	14.96357	0.004688	2.920200	

Triggered

Tap DL= 122.2234
40.77743

79.1865

0.4

Solvent

L

1//f

MDR

1//f

1//f

1//f/Slv

1//f/L

12.54268	107.5353	29.0775	22.6868	1.80873	0.210971
12.96471	137.1069	31.08241	25.80088	1.990084	0.188180
13.34758	170.9135	32.90103	27.12084	2.031891	0.158681
13.59447	197.0144	34.07374	28.48104	2.095045	0.144563
13.90643	235.7695	35.55554	28.97320	2.083439	0.122887
14.02142	251.7042	36.10175	29.05440	2.072143	0.115339
12.25264	90.99993	27.70006	20.10695	1.641029	0.220955
11.70601	66.43299	25.10357	18.36167	1.568567	0.276393
12.57975	109.8544	29.25381	21.61479	1.718221	0.196758
12.52804	104.6328	29.00820	22.26763	1.777439	0.208827
11.71631	66.82797	25.15248	17.76563	1.516315	0.265841
12.51695	105.9544	28.95554	22.97349	1.835390	0.214824
12.23035	89.83980	27.59418	21.67542	1.772264	0.241267
11.85924	72.55888	25.83140	18.45093	1.553827	0.254289
11.48595	58.52852	24.05826	16.63561	1.448344	0.284230
11.37266	54.83364	23.52017	15.36843	1.351348	0.280273
11.11104	47.16738	22.27747	13.81603	1.243450	0.292914
10.84042	40.36317	20.99199	13.56673	1.251495	0.336114
10.56006	34.34761	19.66031	12.03896	1.140046	0.350503
10.38304	31.02000	18.81947	11.14748	1.073623	0.359364
10.35886	30.59124	18.70462	11.26543	1.087516	0.368236
9.967197	24.41627	16.84418	10.39410	1.042831	0.425703
9.650482	20.34701	15.33979	9.777433	1.013154	0.480534
9.328912	16.90862	13.81233	9.956122	1.067232	0.588819
8.797184	12.45019	11.28662	10.92256	1.241598	0.877300
8.531262	10.68306	10.02349	9.930029	1.163957	0.929511
8.212997	8.894663	8.511740	8.462114	1.030331	0.951369
7.758375	6.846581	6.352281	6.670445	0.859773	0.974273
7.318174	5.314628	4.261330	5.099119	0.896774	0.959558
6.178250	2.757037	-1.15330	2.624532	0.424801	0.951939
6.874427	4.116108	2.153528	3.917886	0.569921	0.951842
10.54289	34.02928	19.58348	11.73388	1.112861	0.344817
10.86058	40.83434	21.08776	12.98844	1.195924	0.318076
11.06501	45.93382	22.05879	13.78296	1.245335	0.290061
11.37136	54.79241	23.51396	14.81707	1.303016	0.270421
11.32812	53.44541	23.30857	14.60372	1.289156	0.273245

B2P13184

Tw dyne/cm2 (1/sec)
Log 8(U)/D
Log Tw
Log 8(U)/D

1.484191	93.67164	0.171490	1.971608
0.804684	75.66769	-0.09437	1.878910
0.595162	59.16103	-0.22536	1.772035
0.412375	41.97569	-0.38449	1.622997
0.245562	25.52689	-0.60983	1.406997
0.148267	15.16275	-0.82893	1.180778
0.089970	9.075011	-1.04590	0.957047
0.040000	4.053626	-1.39792	0.607843

Log Tw vs. Log 8(U)/D

Regression Output:
Constant -2.00914
Std Err of Y Est 0.007164
R Squared 0.999782
No. of Observations 6
Degrees of Freedom 4

X Coefficient(s) 1.001839
Std Err of Coef. 0.007396

Tw = K' (8(U)/D)^n'

K' = 0.009791
n' = 1.001839

Tw# = 4.490478
Res/fe = 480.2819

Regression Output:

Constant -48.8089
Std Err of Y Est 0.640957
R Squared 0.982633
Ho. of Observations 17
Degrees of Freedom 15

X Coefficient(s) 22.05294
Std Err of Coef. 0.758964

t = 24.5375 deg C
s.d.t = 0.493059 deg C

85F15181

10 PSID Taps 14 1.0 PSID Taps 14 6/28/90 15:40
 S = 2.7 S = 7.25 S = 9.9 <C>pp
 Z = 2.7 Z = 8.9 Z = 7.4 [NaCl]

density viscosity ID(cm) = 1.45796
 co)[NaCl] 1.01234 1.029478 K(V/psi)=1.085095 12.37189
 49.91302 X coeff -0.00225 -0.02281 XS(cm2)= 1.669479
 0.300037 constant 0.007*19 -4.14933

Freq. (Hz)	Dist (1/s)	Temp (deg C)	<U> (volts)	<U>o (volts)	<U>f (volts)	<U>ico (volts)	Batch Vol (ml)	t ₀ (sec)	DP (psid)	Re (cm/s)	Tw (dyne/cm2)	f	Log(Re/f)
60	1.21416	24.9	1.883333	0.0385	0.0395	1.8438	1.699236	727.2685	116312.9	239.7247	0.000897	2.542250	
52	1.052272	24.9	1.47925	0.0385	0.0395	1.439	1.328842	630.2994	100804.5	187.1881	0.000933	3.488522	
43	0.870148	24.9	1.0945	0.0385	0.0395	1.0	0.972265	521.2091	83257.61	137.1650	0.001000	3.421016	
36	0.728496	24.9	0.852	0.0385	0.0395	0.81	0.748782	426.2611	69787.76	105.6366	0.001099	3.264201	
29	0.586844	24.9	0.6075	0.0385	0.0395	0.5	0.524378	351.5131	56217.92	73.97814	0.001186	3.286946	
21	0.424956	24.9	0.384	0.0385	0.0395	0.34	0.317483	254.5440	40709.53	44.78992	0.001269	3.177984	
15	0.30354	24.9	0.2446	0.0385	0.0395	0.20	0.189015	181.8171	29078.23	26.66593	0.001598	3.065372	
11	0.222596	24.9	0.169	0.0385	0.0395	0.12	0.119244	133.3325	21324.03	16.83685	0.001876	2.965524	
7	0.141652	24.9	0.100666	0.0385	0.0395	0.0621	0.057291	84.84800	12569.84	8.082556	0.002224	2.806168	
15	0.30354	23.7	0.2406	0.0375	0.0395	0.20	0.187172	181.8171	28301.59	26.40590	0.001582	3.051422	
30	0.60708	24.8	6.813	0.0115	0.0105	6.80	0.549754	363.6342	58025.41	77.55817	0.001162	3.296222	
25	0.5059	24.8	5.3315	0.0115	0.0105	5.3	0.430087	303.0285	48354.51	60.67588	0.001309	3.242917	
20	0.40472	24.8	3.903	0.0115	0.0105	3.89	0.314624	242.4228	38683.61	44.38656	0.001496	3.175034	
15	0.30354	24.7	2.3685	0.0115	0.0105	2.3	0.190189	181.8171	28947.33	26.83149	0.001607	3.064746	
12	0.242832	24.7	1.947666	0.0115	0.0105	1.9321	0.156173	145.4537	23157.86	22.03268	0.002063	3.021957	
8	0.161888	24.7	1.169166	0.0115	0.0105	1.1536	0.093249	96.96914	15438.37	13.15537	0.002771	2.909975	
24.8	0.9138	24.8	0.9138	0.0185	-0.0075	0.89	0.073265	80.74372	12884.34	10.20919	0.003102	2.855904	
24.8	0.604	24.8	0.604	-0.0045	-0.0075	0.61	0.049426	62.47733	9969.559	6.972994	0.003579	2.773118	
24.8	0.4942	24.8	0.4942	-0.0065	-0.0075	0.50	0.040551	51.40992	8203.523	5.720934	0.004288	2.70142	
24.8	0.349166	24.8	0.349166	-0.0065	-0.0065	0.3556	0.028747	37.28706	5949.928	4.055701	0.005779	2.655442	
24.8	0.263166	24.8	0.263166	-0.0065	-0.0065	0.2694	0.021796	29.27858	4672.007	3.075035	0.007106	2.595224	
24.2	1.644666	24.2	1.644666	-0.0465	-0.15	1.6911	0.021659	29.34563	4619.748	3.055710	0.007028	2.588054	
24.2	1.26	24.2	1.26	-0.039	-0.1265	1.24	0.016657	24.57646	3868.959	2.347118	0.007697	2.520765	
24.1	0.99	24.1	0.99	-0.0105	-0.0145	1.00	0.012865	19.39420	3046.260	1.814996	0.009538	2.473950	
24.1	0.437285	24.1	0.437285	-0.0165	-0.0195	0.45671	0.005850	13.66770	2146.795	0.825350	0.008751	2.302871	
24.05	0.325875	24.05	0.325875	-0.0222	-0.0245	0.35033	0.004487	10.51558	1649.828	0.633080	0.011340	2.244749	
24	0.229111	24	0.229111	-0.0275	-0.028	0.25711	0.002792	7.427464	1164.007	0.464565	0.016679	2.177050	
23.9	0.15725	23.9	0.15725	-0.0315	-0.033	0.190	0.002436	5.560668	866.3555	0.343756	0.023179	2.110667	
23.9	0.1076	23.9	0.1076	-0.0345	-0.035	0.14	0.001826	4.352653	680.5964	0.257659	0.026937	2.048055	
23.8	0.061785	23.8	0.061785	-0.036	-0.036	0.09771	0.001252	2.900263	452.4735	0.176685	0.041603	1.965157	
23.8	0.006	23.8	0.006	-0.0365	-0.037	0.04	0.000550	1.291154	201.4345	0.077695	0.092308	1.786754	
23.8	3.236	23.8	3.236	-0.039	-0.048	3.271	0.041901	52.21171	8161.213	5.911341	0.004278	2.727400	
23.8	3.6932	23.8	3.6932	-0.0495	-0.0515	3.742	0.047934	59.69924	9313.750	6.762555	0.003758	2.756612	

85P13181

Tw 8<U>/D Log Log
dyne/cm2 (1/sec) Tw 8<U>/D

0.85350 74.99632 -0.08336 1.87504
0.633080 57.70027 -0.19854 1.761177
0.464565 40.75538 -0.33295 1.610184
0.343756 30.40219 -0.46374 1.482905
0.257659 23.88353 -0.58895 1.378098
0.176685 15.91408 -0.75279 1.201781
0.077695 7.084716 -1.10960 0.850322

Log Tw vs. Log 8<U>/D

Regression Output:
Constant -1.96156
Std Err of Y Est 0.008931
R Squared 0.599458
No. of Observations 7
Degrees of Freedom 5

X Coefficient(s) 1.004084
Std Err of Coef. 0.010449

Tw = K' (8<U>/D)^{n'}
K' = 0.010925
n' = 1.004084

Res/ft = 288.7293
Tw# = 1.652584

Regression Output:
Constant -44.2435
Std Err of Y Est 0.441555
R Squared 0.988503
No. of Observations 10
Degrees of Freedom 8

X Coefficient(s) 21.81904
Std Err of Coef. 0.851931

t = 24.48333 deg C
s.d.t = 0.445289 deg C

Betz 1120

Tap DL= 122.2234
40.77743

78.07879
0.4
0.4

Solvent L MDR
1///f 1///f 1///f 1///f/S1v 1///f/L

13.76900 217.8365 34.90276 33.37162 2.423677 0.153195
13.55413 192.4923 33.88213 32.73005 2.414765 0.170032
13.28406 164.7768 32.59950 31.61761 2.380116 0.191881
13.05720 144.6044 31.52173 30.16321 2.310082 0.208591
12.74778 121.0113 30.05197 29.03546 2.277686 0.239940
12.31193 94.15958 27.98170 27.02163 2.194750 0.286976
11.86149 72.65286 25.84208 25.01470 2.108900 0.344304
11.46209 57.73043 23.94497 23.08578 2.014097 0.399889
10.82467 39.99896 20.91720 21.20343 1.958805 0.530099
11.80569 70.35622 25.57702 25.14133 2.129594 0.357343
12.78489 123.6240 30.22823 29.33562 2.294554 0.237297
12.57166 109.3445 29.21542 27.63884 2.198502 0.252768
12.30013 93.52224 27.92566 25.85188 2.101755 0.276424
11.85898 72.54815 25.83018 24.93803 2.102880 0.343744
11.68783 65.74121 25.01719 22.01612 1.883679 0.334890
11.23990 50.79904 22.88953 18.99466 1.689951 0.375917
11.02361 44.85231 21.86219 17.95384 1.628670 0.400287
10.69247 37.06797 20.28925 16.80959 1.572095 0.453480
10.52057 33.57551 19.47271 15.27065 1.451504 0.454815
10.22176 28.26976 18.05340 13.15435 1.286896 0.465315
9.981336 24.61581 16.91135 11.86231 1.188449 0.481897
9.952216 24.20661 16.77302 11.92790 1.198517 0.492753
9.723061 21.21511 15.68454 11.39800 1.172264 0.537258
9.495802 18.61361 14.60506 10.22860 1.077171 0.549522
8.811327 12.55197 11.35380 10.68953 1.213158 0.851621
8.578998 10.98069 10.25024 9.390506 1.094592 0.855183
8.308203 9.395738 8.963967 7.742923 0.931961 0.824088
8.042670 8.063946 7.702684 6.714729 0.834888 0.822685
7.792260 6.981441 6.513256 6.092908 0.781917 0.872729
7.460631 5.768166 4.937998 4.902700 0.657142 0.849958
6.747017 3.825025 1.548332 3.291391 0.487829 0.860488
10.50960 33.26416 19.42060 15.28813 1.454682 0.458220
10.62645 35.68556 19.97563 16.31217 1.535054 0.457108

BIP33178 B1120 6/18/90 14:47
 B1120 10 PSID Taps 14 1.0 PSID Taps 14 0.1 PSID Taps 14
 S = 2.7 S = 7.25 S = 9.9 <U> (ppm) =
 Z = 2.7 Z = 8.85 Z = 7.4 [NaCl] =

Batch Vol (ml)	t (sec)	DP (psid)	<U> (cm/s)	Re	Tw (dyne/cm2)	f	Log(Re/f)
60	1.21416	25.1	1.828666	0.0345	0.0385	1.790166	
49	0.991564	25.1	1.374	0.0345	0.0385	1.3355	
42	0.849912	25.1	1.06775	0.0345	0.0385	1.02925	
32	0.647552	25.1	0.7425	0.0345	0.0385	0.704	
24	0.485664	25.1	0.48975	0.0345	0.0385	0.45525	
18	0.364248	25.1	0.3265	0.0345	0.0385	0.298	
14	0.283304	25.1	0.232	0.0345	0.0385	0.1935	
10	0.20236	25.1	0.161	0.0345	0.0385	0.1225	
8	0.161888	25.1	0.1325	0.0345	0.0385	0.098	
60	1.21416	24.3	1.842666	0.032	0.0315	1.810666	
36	0.728496	25.1	9.51175	0.0095	0.019	9.50225	
28	0.566608	25.1	6.230166	0.0095	0.019	6.211166	
21	0.424956	25.1	4.11725	0.0095	0.019	4.09825	
15	0.30354	25.1	2.451142	0.0095	0.019	2.432142	
11	0.222596	25.1	1.76225	0.0095	0.019	1.74325	
8	0.161888	25.1	1.0725	0.0095	0.019	1.0535	
25	0.608888	24.9	0.8515	0.0135	0.0055	0.838	
24.9	0.4782	24.9	0.608888	0.0085	0.0055	0.603388	
24.9	0.3762	24.9	0.4782	0.0055	-0.0055	0.4817	
24.9	0.3762	24.9	0.3762	-0.0015	-0.0015	0.3777	
24.9	2.319	24.9	2.319	0.0295	-0.0225	2.2895	
24.8	1.8342	24.8	1.8342	-0.023	-0.0255	1.8572	
24.8	1.219444	24.8	1.219444	-0.0275	-0.026	1.245444	
24.8	0.6704	24.8	0.6704	-0.0275	-0.0275	0.6979	
24.7	0.553181	24.7	0.553181	-0.029	-0.029	0.582181	
24.7	0.429928	24.7	0.429928	-0.03	-0.0305	0.460428	
24.7	0.30665	24.7	0.30665	-0.033	-0.0325	0.33965	
24.6	0.230666	24.6	0.230666	-0.034	-0.034	0.264666	
24.6	0.165428	24.6	0.165428	-0.0335	-0.033	0.198428	
24.5	0.085333	24.5	0.085333	-0.033	-0.0335	0.118833	
24.5	0.019333	24.5	0.019333	-0.033	-0.0335	0.052833	
24.5	-0.02526	24.5	-0.02526	-0.0355	-0.0445	0.012230	
24.5	3.0602	24.5	3.0602	-0.045	-0.0385	3.0987	
24.5	5.2962	24.5	5.2962	-0.033	-0.033	5.3292	

density	viscosity	ID(cm)	K(U/psi)	XS(cm2)
1.00044	X coeff	-0.00025	-0.02381	12.37189
0.300112	constant	0.003919	-4.14933	1.669479
1.640814	727.2685	116838.9	231.4826	0.000867
1.224080	593.9360	95418.46	172.5906	0.000769
0.943380	509.0880	81787.25	133.0901	0.001017
0.645265	387.8765	62314.09	91.03275	0.001198
0.417268	290.9074	46735.57	58.86741	0.001278
0.263972	218.1805	35051.68	37.24067	0.001549
0.177256	169.6960	27262.41	25.02107	0.001721
0.112279	121.2114	19473.15	15.84021	0.002126
0.089823	96.96914	15578.52	12.67217	0.002670
1.659604	727.2685	114749.1	234.1334	0.000876
0.768051	436.3611	70103.36	108.3550	0.001127
0.502038	339.3920	54524.83	70.82654	0.001218
0.331254	254.5440	40893.62	46.73274	0.001429
0.196586	181.8171	29209.73	27.73396	0.001662
0.140904	133.3325	21420.47	19.87845	0.002215
0.085152	96.96914	15578.52	12.01316	0.002531
19.9	0.067734	79.43377	12761.39	9.555796
20.9	0.048770	61.60171	9874.288	6.880502
15	0.038925	52.47144	8391.821	5.492872
19.9	0.030528	39.94263	6388.074	4.306950
25	0.029322	39.82079	6368.587	4.136818
25.1	0.023786	32.45518	5178.900	3.355710
30	0.015951	23.46040	3743.596	2.250350
35	0.008958	18.03812	2878.358	1.261011
45	0.007456	15.32080	2439.244	1.031924
60	0.005896	12.61870	2009.039	0.831932
74.9	0.004350	9.116789	1451.495	0.613701
60.1	0.003389	6.717448	1067.083	0.478217
59.9	0.002541	4.929910	783.1283	0.358533
90	0.001521	2.994945	474.6823	0.214715
90	0.000676	1.331086	210.9699	0.095462
170	0.000156	0.249578	39.55686	0.023099
15	0.039686	51.95231	8234.156	5.598934
15.3	0.068254	76.73324	12161.79	9.629148

BIP11499

10 PSID Taps 14 1.0 PSID Taps 14 0.1 PSID Taps 14
 S = 2.7 S = 7.25 S = 9.9 <C> (ppa) =
 Z = 2.7 Z = 9.05 Z = 7.05 [NaCl]=

B1120 7/26/90 12:35

24.05 -0.01155 -0.0815 -0.0815 0.069944
 24 -0.03266 -0.083 -0.084 0.049333
 23.95 -0.05625 -0.0845 -0.086 0.02825

	Freq. (Hz)	D)est (1/s)	Temp (deg C)	<U> (volts)	<U>0 (volts)	<U>f (volts)	<U>corr (volts)
Taps 23	60	1.21416	25	1.0835	0.0225	0.0215	1.062
	50	1.0118	25	0.7225	0.0225	0.0215	0.701
	40	0.80944	25	0.4515	0.0225	0.0215	0.43
	30	0.60708	25	0.2542	0.0225	0.0215	0.2327
	20	0.40472	25	0.1445	0.0225	0.0215	0.123
Taps 12	60	1.21416	24.8	1.061333	0.0175	0.0205	1.040833
	48	0.971328	24.8	0.6154	0.0175	0.0205	0.5949
	40	0.80944	24.8	0.4138	0.0175	0.0205	0.3933
	30	0.60708	24.8	0.232666	0.0175	0.0205	0.212166
	20	0.40472	24.8	0.13375	0.0175	0.0205	0.11325
Taps 34	60	1.21416	24.85	1.036666	0.0205	0.0195	1.017166
	50	1.0118	24.85	0.716333	0.0205	0.0195	0.696833
	42	0.849912	24.85	0.52075	0.0205	0.0195	0.50125
	35	0.70826	24.85	0.374	0.0205	0.0195	0.3545
	27	0.546372	24.85	0.23125	0.0205	0.0195	0.21175
	19	0.384484	24.85	0.11725	0.0205	0.0195	0.09775
Taps 34	25	0.5059	24.7	2.101	0.0325	-0.0055	2.1065
	20	0.40472	24.7	1.306333	0.0325	-0.0055	1.311833
	16	0.323776	24.7	0.903833	0.0325	-0.0055	0.909333
	10	0.20236	24.7	0.4468	0.0325	-0.0055	0.4523
	28	0.566608	24.7	2.464333	0.0325	-0.0055	2.469833
	43	0.870148	24.7	5.729333	0.0325	-0.0055	5.734833
Taps 23	25	0.5059	25	1.96575	0.0285	-0.3525	1.93725
	20	0.40472	25	1.4915	0.0285	-0.3525	1.463
	15	0.30354	25	0.838	0.0285	-0.3525	0.8095
	10	0.20236	25	0.45575	0.0285	-0.3525	0.42725
			24.7	0.2956	-0.0145	-0.0245	0.3101
			24.6	0.165666	-0.0285	-0.0295	0.194166
Taps 23	24.5	1.42825			-0.0505	1.165	1.47875
	24.5	1.142			-0.0205	-0.0485	1.1625
	24.4	0.71625			-0.0555	-0.0565	0.7175
	24.4	0.5634			-0.0625	-0.064	0.5259
	24.3	0.3324			-0.0675	-0.069	0.3399
	24.3	0.222714			-0.0715	-0.071	0.294214
	24.2	0.17025			-0.0745	-0.0745	0.24475
	24.2	0.129			-0.076	-0.076	0.205
	24.2	0.0758			-0.078	-0.0795	0.1538
	24.1	0.031125			-0.081	-0.081	0.112125

40 0.000852 4.717038 751.4853 0.260777 0.032510 2.151930
 39.9 0.000600 3.182598 506.4575 0.254464 0.050370 2.055631
 74.9 0.000344 1.339422 260.5926 0.145715 0.108700 1.934077

315
 212
 205

density viscosity 12.79437
 cc) [NaCl] 1.000088 1.001574 ID (cm) = 1.45796 12.56946
 10.04584 X coeff -0.00025 -0.02281 K (V/psi) = 1.08859 12.56946
 0.000100 constant 0.003419 -4.14933 XS (cm²) = 1.669479

Batch	Vol	t ₁	samp	DP	<U>	Re	Tw	f	Log (Re/f)
(ml)	(sec)	(psid)	(cm/s)	(cm/s)		dyne/cm ²			
0.975573	727.2685	118373.2	413.0796	0.001566	3.670686				
0.643952	406.0571	98644.39	272.6637	0.001488	3.580483				
0.395006	484.8457	78915.51	167.2544	0.001426	3.474358				
0.213762	363.6342	59186.63	90.51190	0.001372	3.341022				
0.112990	242.4228	39457.75	47.84256	0.001632	3.202576				
0.956129	727.2685	117840.3	404.3061	0.001522	3.664054				
0.546486	581.8148	94272.30	231.0857	0.001368	3.542585				
0.361293	484.8457	78560.25	152.7752	0.001303	3.452725				
0.194900	363.6342	58920.18	82.41499	0.001249	3.318702				
0.104033	242.4228	39280.12	43.99135	0.001501	3.182382				
0.934389	727.2685	117973.3	395.6411	0.001500	3.659842				
0.640124	606.0571	98311.14	271.0430	0.001479	3.577710				
0.460458	509.0880	82581.36	194.9681	0.001508	3.506173				
0.325650	424.2400	68817.80	137.8877	0.001536	3.430954				
0.194517	327.2708	53088.02	82.36311	0.001542	3.319058				
0.089795	239.3017	37598.23	38.02122	0.001437	3.151204				
0.167588	303.0285	48989.51	70.96080	0.001549	3.285223				
0.104366	242.4228	39191.61	44.19119	0.001507	3.182381				
0.073344	193.9382	31353.28	30.63233	0.001633	3.102803				
0.053984	121.2114	19595.80	15.23644	0.002079	2.951155				
0.194694	339.3920	54868.25	83.20026	0.001448	3.319776				
0.456251	521.2091	84261.96	193.1869	0.001426	3.502702				
0.154123	303.0285	49322.19	65.25934	0.001425	3.269990				
0.116393	242.4228	39457.75	49.28348	0.001681	3.209020				
0.064402	181.8171	29593.31	27.26929	0.001654	3.080506				
0.033991	121.2114	19728.87	14.39259	0.001964	2.941739				
15 0.024670	96.85656	15655.21	10.44621	0.002333	2.865193				
1845 14.9 0.015347	74.17012	11963.78	6.540812	0.002384	2.766544				
1851 15.1 0.018013	73.42574	11817.03	7.627484	0.002836	2.798934				
1538 15 0.014121	51.41624	7684.255	3.976247	0.003187	2.746683				
1156 15 0.009401	46.16209	7412.517	3.980734	0.003745	2.656739				
960 14.9 0.007624	38.59258	6197.037	3.228431	0.004346	2.611254				
709 15.1 0.004871	28.12471	4505.973	2.065228	0.005228	2.512992				
912 25 0.003584	21.85112	3500.855	1.517575	0.006372	2.446348				
772 24.9 0.002981	18.57106	2968.640	1.262435	0.007339	2.405392				
645 24.9 0.002497	15.51598	2480.275	1.057402	0.008806	2.366908				
575 29.9 0.001873	11.51902	1841.349	0.793309	0.011987	2.304509				
609 30.1 0.001365	8.139087	1298.125	0.578347	0.017504	2.234877				

Page 5	Betz 1120				Page 6	Betz 1120					
82-0894	Tap 14	Tap 12	Tap 23	Tap 34	8.127720	7.822524	7.336509	5.369771	4.347471		
0.4	122.2234	40.77743	40.72299	40.72299	8.468569	7.104132	6.456989	4.455659	0.682372		
Solvent	L	MDR	1//f	1//f	1//f	1//f	1//f	1//f	1//f		
1//f	1//f	1//f	1//f	1//f	1//f	1//f	1//f	1//f	1//f		
14.28274	292.7968	37.34304	25.26779	1.769112	0.086298	14.92193	237.8828	35.62917	25.91727	1.861614	0.108949
13.49743	186.3109	33.61280	26.47305	1.961339	0.142090	12.96408	137.0573	31.07942	26.98990	2.081897	0.196924
12.41030	99.64527	28.44895	24.74888	1.994220	0.246369	14.25621	288.3594	37.21703	25.54111	1.791577	0.088573
13.77034	218.0645	34.90912	27.02704	1.962699	0.123974	13.41090	177.2579	33.20178	27.69983	2.065471	0.156268
12.87480	130.1913	30.65534	28.28537	2.196954	0.217239	12.32953	95.11801	28.06527	25.81012	2.093358	0.271348
14.23926	285.5764	37.13700	25.81913	1.813221	0.090410	13.91084	236.3691	35.57450	25.99512	1.868695	0.109976
13.62469	200.4719	34.21729	25.74592	1.889651	0.128426	13.32381	168.5910	32.78813	25.51210	1.914774	0.151325
12.87633	130.2980	30.66210	25.46469	1.977651	0.195434	12.20481	88.52883	27.47288	26.37434	2.160977	0.297918
12.74089	120.5322	30.01923	25.40270	1.993793	0.210754	12.52952	95.11779	28.06525	25.75202	2.088646	0.270738
12.01121	79.19248	26.55327	24.74452	2.069118	0.312460	11.40462	55.85161	23.67195	21.92842	1.922766	0.392619
12.87910	130.5137	30.67574	26.27513	2.040136	0.201320	13.61081	198.8762	34.15133	26.48063	1.945360	0.133151
12.67996	116.3779	29.72982	26.48814	2.088976	0.227604	12.43608	101.1346	28.57138	24.38440	1.960779	0.241108
11.92202	75.22920	26.12962	24.58596	2.062230	0.326814	11.56695	54.65363	23.49304	22.56126	1.984811	0.412804
11.07677	46.24590	22.11467	21.15756	1.910083	0.457501	10.66617	36.51107	20.16434	20.47972	1.929062	0.560918
10.66617	36.51107	20.16434	20.47972	1.929062	0.560918	10.79573	39.33817	20.77974	18.77475	1.759089	0.477265
10.58673	34.87894	19.78698	17.71171	1.673010	0.507805	10.22695	28.53436	18.07805	16.33901	1.597641	0.576243
10.04501	25.53489	17.21382	15.16805	1.510008	0.594012	9.651968	20.36442	15.34684	13.82918	1.432783	0.679085
9.385393	17.46740	14.08061	12.52538	1.334668	0.717129	9.221570	15.89544	13.30245	11.67253	1.265785	0.734331
9.067622	14.54749	12.57125	10.65594	1.175162	0.732493	8.818027	12.60054	11.38567	9.133282	1.033750	0.724832
8.539588	10.73436	10.06304	7.558218	0.885079	0.704112						

Page 7

Betz 1120

B1P11499

Tw	8<U>/D	Log	Log
dynes/cm2	(1/sec)	Tw	8<U>/D
1.517575	119.8997	0.181150	2.078818
1.262435	101.9016	0.101209	2.008181
1.057402	85.13803	0.024240	1.930123
0.793309	63.20633	-0.10055	1.800759
0.578347	44.66014	-0.23781	1.649920
0.360777	25.88295	-0.44276	1.415013
0.234464	17.46329	-0.59437	1.242126
0.145715	8.995707	-0.83649	0.954035

Log Tw vs. Log 8<U>/D

Regression Output:

Constant	-1.66942
Std Err of Y Est	0.004331
R Squared	0.999833
Na. of Observations	5
Degrees of Freedom	3

X Coefficient(s) 0.869016
 Std Err of Coef. 0.006482

Tw = K' (8<U>/D)^n'
 K' = 0.021407
 n' = 0.869016

t = 24.65121 deg C
 s.d.)t = 0.315163 deg C

BSP01401

10 PSID Taps 14 1.0 PSID Taps 14 0.1 PSID Taps 14
 S = 2.7 S = 7.25 S = 9.9 C (ppm) =
 Z = 2.7 Z = 9.05 Z = 7.05 [NaCl] =

24.15 0.044277 -0.0715 -0.0715 0.115777
 24.1 0.006315 -0.0725 -0.0725 0.078815
 24 -0.03016 -0.0735 -0.0735 0.04324
 23.9 -0.055 -0.0735 -0.0735 0.0185
 24.2 2.926 -0.0735 -0.0735 2.9995

81120

7/30/90 13:17
 1.0 PSID Taps 14 0.1 PSID Taps 14
 S = 7.25 S = 9.05 Z =

Tap	Freq. (Hz)	Dist (1/s)	Temp (deg C)	<U> (volts)	<U> (volts)	<U>f (volts)	<U>corr (volts)	
Taps 23	60	1.21416	24.9	1.473	0.0185	0.0245	1.4485	
	50	1.0118	24.9	0.99075	0.0185	0.0245	0.96625	
	40	0.80944	24.9	0.66175	0.0185	0.0245	0.63725	
	30	0.60708	24.9	0.3865	0.0185	0.0245	0.362	
	21	0.424956	24.9	0.2322	0.0185	0.0245	0.2077	
	15	0.30354	24.9	0.147142	0.0185	0.0245	0.122642	
	10	0.20236	24.9	0.078428	0.0185	0.0245	0.053928	
	Taps 12	60	1.21416	24.9	1.400666	0.0235	0.0265	1.37166
		50	1.0118	24.9	0.96975	0.0235	0.0265	0.94625
		39	0.789204	24.9	0.60475	0.0235	0.0265	0.58125
31		0.67316	24.9	0.397	0.0235	0.0265	0.3735	
24		0.485664	24.9	0.269833	0.0235	0.0265	0.246333	
18		0.364248	24.9	0.169666	0.0235	0.0265	0.146166	
14		0.283304	24.9	0.117888	0.0235	0.0265	0.094388	
10		0.20236	24.9	0.079428	0.0235	0.0265	0.055928	
Taps 34		60	1.21416	25	1.437333	0.027	0.027	1.410333
		49	0.991564	25	0.945	0.027	0.027	0.918
	41	0.829676	25	0.676	0.027	0.027	0.649	
	33	0.67788	25	0.4526	0.027	0.027	0.4256	
	26	0.526136	25	0.314	0.027	0.027	0.287	
	20	0.40472	25	0.20875	0.027	0.027	0.18175	
	10	0.20236	25	0.087	0.027	0.027	0.06	
	Taps 23	30	0.60708	24.9	4.303666	0.0185	0.009	4.285166
		22	0.445192	24.9	2.4665	0.0185	0.009	2.448
		16	0.323776	24.9	1.440428	0.0185	0.009	1.421928
10		0.20236	24.9	0.692071	0.0185	0.009	0.673571	
Taps 23		8	0.161888	24.9	0.479	0.0185	0.009	0.4605
		24.7	0.4694	-0.0095	-0.0095	-0.0095	0.4789	
		24.6	0.3106	-0.0185	-0.0205	0.3291		
		24.4	2.001	-0.0425	-0.045	2.0435		
		24.4	1.39725	-0.0495	-0.0495	1.44675		
		24.4	0.844	-0.0535	-0.054	0.8975		
	24.3	0.54775	-0.0575	-0.0585	0.60525			
	24.3	0.4545	-0.0605	-0.0605	0.515			
	24.3	0.327285	-0.0625	-0.063	0.38785			
	24.2	0.213	-0.0675	-0.0685	0.2805			
24.2	0.175583	-0.0695	-0.0695	0.245083				
24.2	0.125846	-0.0695	-0.0695	0.195346				
24.2	0.077333	-0.0705	-0.0705	0.147833				

density viscosity
 co(NaCl) 1.000088 1.001574
 4.992685 X coeff -0.00025 -0.02281
 0.000100 constant 0.003419 -4.14933

75 0.001453 8.924916 1426.982 0.615580 0.015453 2.248977
 89.9 0.000989 5.829982 929.8399 0.419056 0.024720 2.164939
 476 99.9 0.000544 2.854042 454.1732 0.230435 0.056720 2.074091
 181 99.9 0.000232 1.085255 172.3111 0.098362 0.167443 1.848247
 2386 15 0.037664 95.27919 15230.66 15.94807 0.003522 2.956142

Batch Vol (ml)	t(samp)	DP (psid)	$\langle U \rangle$ (cm/s)	Re	Tw (dyne/cm ²)	f	Log(Ra/f)
1867	15	0.025660	74.55417	11971.59	10.86511	0.003919	2.874775
1569	15	0.018166	62.65425	10060.76	7.692243	0.003929	2.799784
1184	15.2	0.011269	46.65809	7492.163	4.771929	0.004395	2.696105
1271	20	0.007600	38.06575	6098.667	3.218061	0.004453	2.609570
1391	25	0.004666	35.32775	5339.572	2.758210	0.004943	2.574506
1399	30	0.004894	27.93285	4475.234	2.072456	0.005325	2.514015
1460	40.1	0.003522	21.80857	3486.166	1.491394	0.006287	2.441564
1438	44.8	0.003077	19.22647	3075.409	1.303086	0.007068	2.412274
1266	50	0.002452	15.16640	2424.394	1.038638	0.009053	2.363030
1167	60	0.001856	11.65033	1862.341	0.786018	0.011611	2.302503
2450	15	0.038100	97.83488	15816.60	16.13250	0.003379	2.963564
1848	14.9	0.026182	75.09473	12112.93	11.08625	0.003942	2.881221
1867	15	0.025660	74.55417	11971.59	10.86511	0.003919	2.874775
1569	15	0.018166	62.65425	10060.76	7.692243	0.003929	2.799784
1184	15.2	0.011269	46.65809	7492.163	4.771929	0.004395	2.696105
1271	20	0.007600	38.06575	6098.667	3.218061	0.004453	2.609570
1391	25	0.004666	35.32775	5339.572	2.758210	0.004943	2.574506
1399	30	0.004894	27.93285	4475.234	2.072456	0.005325	2.514015
1460	40.1	0.003522	21.80857	3486.166	1.491394	0.006287	2.441564
1438	44.8	0.003077	19.22647	3075.409	1.303086	0.007068	2.412274
1266	50	0.002452	15.16640	2424.394	1.038638	0.009053	2.363030
1167	60	0.001856	11.65033	1862.341	0.786018	0.011611	2.302503
1.330620	727.2685	118106.5	563.4142	0.002136	3.737098		
0.887616	606.0571	98422.10	375.8363	0.002052	3.649183		
0.585390	484.8457	78737.68	247.8672	0.002114	3.558793		
0.332540	363.6342	59033.26	140.8049	0.002335	3.435993		
0.190797	254.5460	41337.28	80.78780	0.002500	3.315357		
0.112662	181.8171	29526.63	47.70364	0.002893	3.200980		
0.049539	121.2114	19684.42	20.97626	0.002863	3.022548		
1.265092	727.2685	118106.5	534.9529	0.002028	3.725842		
0.869243	606.0571	98422.10	367.5657	0.002006	3.644351		
0.533947	472.7245	76749.24	225.7834	0.002026	3.538520		
0.343104	375.7554	61021.70	145.0840	0.002060	3.442494		
0.226286	290.9074	47242.61	95.68685	0.002267	3.352110		
0.134271	218.1805	35431.95	56.77765	0.002391	3.238773		
0.083707	169.6960	27558.18	36.66485	0.002533	3.143809		
0.051377	121.2114	19684.42	21.72515	0.002965	3.030165		
1.295559	727.2685	118375.2	548.5687	0.002079	3.732285		
0.843292	593.9360	96671.50	357.0688	0.002029	3.639045		
0.596184	495.9668	80888.40	252.4375	0.002049	3.563746		
0.390964	399.9977	65105.30	165.5430	0.002074	3.472124		
0.263643	315.1497	51295.08	111.6326	0.002254	3.386565		
0.166959	242.4228	39457.75	70.89419	0.002412	3.287361		
0.055117	121.2114	19728.87	23.33783	0.003185	3.046699		
0.340918	363.6342	59033.26	144.3526	0.002189	3.441396		
0.194757	266.6651	43305.72	82.46477	0.002325	3.319818		
0.113125	193.9582	31495.07	47.89992	0.002533	3.201851		
0.053587	121.2114	19684.42	22.69032	0.003097	3.039604		
0.036636	96.96914	15747.53	15.51267	0.003308	2.957027		
15	0.038100	97.83488	15816.60	16.13250	0.003379	2.963564	
1848	14.9	0.026182	75.09473	12112.93	11.08625	0.003942	2.881221
1867	15	0.025660	74.55417	11971.59	10.86511	0.003919	2.874775
1569	15	0.018166	62.65425	10060.76	7.692243	0.003929	2.799784
1184	15.2	0.011269	46.65809	7492.163	4.771929	0.004395	2.696105
1271	20	0.007600	38.06575	6098.667	3.218061	0.004453	2.609570
1391	25	0.004666	35.32775	5339.572	2.758210	0.004943	2.574506
1399	30	0.004894	27.93285	4475.234	2.072456	0.005325	2.514015
1460	40.1	0.003522	21.80857	3486.166	1.491394	0.006287	2.441564
1438	44.8	0.003077	19.22647	3075.409	1.303086	0.007068	2.412274
1266	50	0.002452	15.16640	2424.394	1.038638	0.009053	2.363030
1167	60	0.001856	11.65033	1862.341	0.786018	0.011611	2.302503

8.595750 11.08709 10.32981 8.044152 0.925820 0.735543
 8.259756 9.137325 8.733842 6.360175 0.770019 0.696065
 7.736366 6.760389 6.247742 4.198844 0.582741 0.621095
 6.992991 4.406846 2.716710 2.443798 0.349463 0.554545
 11.42456 56.49657 23.76670 16.84909 1.474812 0.298232

Tap 14 122.2234
 Tap 12 40.77743
 Tap 23 40.72299
 Tap 34 40.72299

79.65686
 4
 0.4

Solvent	L	MDR	1//f	1//f	1//f/Slv	1//f/t/L
14.54839	341.1757	38.60486	21.63593	1.487170	0.663415	
14.19673	278.6529	36.93449	22.07541	1.554964	0.079221	
13.85517	226.2944	35.21708	21.74647	1.571824	0.096098	
13.34397	170.5584	32.88387	21.63967	1.621681	0.126875	
12.86142	129.1924	30.59178	19.99791	1.554875	0.154791	
12.40384	99.27504	28.41824	18.58890	1.498641	0.187246	
11.69019	65.83069	25.02841	18.66849	1.598646	0.283887	
14.50326	332.4467	38.39099	22.20403	1.530956	0.066789	
14.17740	275.5699	36.84268	22.32239	1.574505	0.081004	
13.75412	215.9784	34.83207	22.21554	1.615191	0.102860	
13.36997	173.1307	33.00738	22.02876	1.647629	0.127237	
13.00844	140.6016	31.29009	21.00020	1.614351	0.149339	
12.55309	108.3061	29.13668	20.46664	1.628554	0.188785	
12.17323	87.03406	27.33337	19.78980	1.625413	0.227379	
11.72066	66.99551	25.17314	18.36356	1.566768	0.274101	
14.52914	337.4155	38.51341	21.92444	1.509137	0.064983	
14.15618	272.2234	36.74186	22.19489	1.567858	0.081531	
13.85498	228.8898	35.31118	22.08715	1.594166	0.096496	
13.48849	185.3352	33.57037	21.95287	1.627525	0.118434	
13.14626	152.2106	31.94473	21.06233	1.602169	0.138377	
12.74944	121.1271	30.05963	20.35968	1.596907	0.168085	
11.78679	69.59527	25.48729	17.71750	1.503165	0.234579	
13.36558	172.6937	32.98653	21.37210	1.599039	0.123757	
12.87927	130.5284	30.67653	20.73608	1.610035	0.158865	
12.40740	99.47906	28.43518	19.78750	1.594813	0.198911	
11.75841	68.46752	25.35248	17.96875	1.528160	0.262442	
11.42811	56.61188	23.78352	17.38541	1.521284	0.307098	
11.45425	57.47048	23.90773	17.20079	1.501693	0.299297	
11.12448	47.53365	22.34130	15.92678	1.431687	0.335063	
11.09910	46.84415	22.22073	15.97264	1.439093	0.340974	
10.79913	39.41529	20.79591	15.95313	1.477259	0.404744	
10.38442	31.04434	18.62600	15.08349	1.452511	0.485866	
10.03828	25.43608	17.16183	14.98527	1.492812	0.589134	
9.898025	23.46315	16.51562	14.22328	1.436982	0.606196	
9.656063	20.41248	15.36630	13.70256	1.419057	0.671280	
9.366326	17.27683	13.99009	12.61141	1.346462	0.729961	
9.249098	16.14933	13.43321	11.89449	1.286016	0.736531	
9.052080	14.41783	12.49738	10.50952	1.151006	0.728925	
8.810015	12.54249	11.34757	9.280157	1.053344	0.739897	

BSP01401
BSP01401

Tw	B(U)/D	Log	Log
dynes/cm ²	(1/sec)	Tw	B(U)/D
1.303086	105.4979	0.114973	2.023244
1.038638	83.21985	0.016484	1.920226
0.786016	63.92678	-0.10456	1.805682
0.615580	49.03792	-0.21071	1.690532
0.419056	31.98980	-0.37772	1.505011
0.230435	15.66046	-0.63745	1.194804
0.098362	5.954925	-1.00716	0.774876

Log Tw vs. Log B(U)/D

Regression Output:

Constant	-1.67707
Std Err of Y Est	0.004784
R Squared	0.999873
No. of Observations	4
Degrees of Freedom	2

X Coefficient(s) 0.866416
Std Err of Coef. 0.006898

Tw = K' (B(U)/D)^{n'}

K' = 0.021034
n' = 0.866416

Tw/Retro=0.856597
Res/f)R =212.8495

Regression Output:

Constant	-8.41594
Std Err of Y Est	0.477739
R Squared	0.975533
No. of Observations	32
Degrees of Freedom	30

X Coefficient(s) 8.597891
Std Err of Coef. 0.251490

t = 24.67159 deg C
s.d.)t = 0.343676 deg C

VIF11434
 10 PSID Taps 14 1.0 PSID Taps 14 0.1 PSID Taps 14
 S = 2.7 S = 7.25 S = 9.9 C (ppm) =
 Z = 2.7 Z = 9.1 Z = 6.8 [NaCl] =

density viscosity
 col[NaCl] 1.00088 1.001574 ID(cm) = 1.45796
 10.01047 X coeff -0.00025 -0.02281 K(V/psi)=1.085245 12.35245
 0.000100 constant 0.007419 -4.14933 XS(cm2) = 1.669479

Fusher 500 9/22/90 12:56
 10 PSID Taps 14 1.0 PSID Taps 14 0.1 PSID Taps 14
 S = 2.7 S = 7.25 S = 9.9 C (ppm) =
 Z = 2.7 Z = 9.1 Z = 6.8 [NaCl] =

Freq. (Hz)	Dist (1/s)	Temp (deg C)	<V> (volts)	<V> o (volts)	<V> f (volts)	<V> corr (volts)	Batch Vol (ml)	t (sec)	DF (psid)	U (cm/s)	Re	Tw (dyne/cm2)	f	Log(keft)	
60	1.21416	24.9	4.632322	0.0805	0.1045	4.527833	1365		4.172176	727.2685	118106.5	588.6017	0.002221	3.745595	
50	1.01118	24.9	3.253666	0.0805	0.1045	3.149166	1249		2.901802	606.0571	98422.10	409.3801	0.002225	3.667747	
39	0.789204	24.9	2.086	0.0805	0.1045	1.9815	1191		1.825854	472.7245	76759.24	257.5877	0.002211	3.57146	
30	0.60708	24.9	1.307666	0.0905	0.0925	1.215166	1185		1.189716	333.5342	59053.26	157.9372	0.002295	3.460967	
24	0.485664	24.9	0.927333	0.0905	0.0925	0.834833	1123		0.789257	290.9074	47242.61	108.5252	0.002571	3.379449	
18	0.364248	24.9	0.607	0.0905	0.0925	0.5145	1056		0.474086	218.1805	35431.95	66.98311	0.002017	3.274542	
15	0.30354	24.9	0.4915	0.0905	0.0925	0.399	883		0.367458	181.8171	29523.53	51.86853	0.003146	3.219176	
10	0.20236	24.9	0.28325	0.0905	0.0925	0.190625	863		0.175651	121.2114	19684.42	24.78055	0.00332	3.059729	
8	0.161888	24.9	0.225	0.0905	0.0925	0.1325	1335		0.122092	96.96914	15747.53	17.22451	0.00367	2.979757	
18	0.364248	24.9	6.43525	-0.0145	0.0025	6.43275	1365		0.500507	218.1805	25431.95	70.81056	0.002974	2.281119	
25	0.5059	24.9	10.99466	-0.0145	0.0025	10.99216	1249		0.855258	303.0285	49211.05	120.6580	0.002675	2.492462	
15	0.30354	24.9	4.436888	-0.0145	0.0025	4.434388	1191		0.345032	181.8171	29526.63	48.67509	0.002952	2.295337	
9	0.182124	24.9	2.02525	-0.0145	0.0025	2.02275	1185		0.157283	109.0902	17715.97	22.20318	0.003741	2.044991	
25.5		24.9	1.7866	-0.0195	-0.0335	1.8061	2556		15	0.140525	101.2390	1371.80	19.82507	0.003876	2.009321
19.76		24.4	1.13575	-0.0275	-0.0405	1.16325	1976		15	0.090508	78.93682	12727.82	12.76868	0.004112	2.911801
16.61		24.6	0.882	-0.0355	-0.0415	0.9175	1661		15	0.071387	66.33805	10698.84	10.07115	0.004590	2.860268
12.41		24.5	0.5376	-0.0385	-0.0395	0.5761	1241		15	0.044824	49.55636	7975.527	6.323694	0.005167	2.758238
13.65		24.5	0.386166	-0.0385	-0.0415	0.426666	1365		19.9	0.032041	41.08643	6612.590	4.661451	0.005537	2.692004
13.65		24.5	2.6992	0.0705	0.0765	2.6227	1365		20	0.032525	40.88100	6579.329	4.588621	0.005505	2.688584
24.5	1.590285	24.5	1.590285	0.0835	0.0855	1.604735	1249		24.8	0.019901	20.16382	4855.004	2.807700	0.006186	2.581918
24.5	1.095875	24.5	1.095875	0.0875	0.0875	1.008375	1191		30	0.012505	23.77986	3827.096	1.744222	0.006356	2.481021
24.5	0.957	24.5	0.957	0.0875	0.0875	0.8695	1185		35	0.010782	20.28005	3263.842	1.521259	0.007417	2.468845
24.4	0.809181	24.4	0.809181	0.0855	0.0865	0.722681	1123		40	0.008962	16.91661	2700.342	1.234389	0.008965	2.407698
24.4	0.526153	24.4	0.526153	0.0855	0.0855	0.540653	1056		50	0.006704	12.85064	2031.388	0.945916	0.011351	2.344684
24.4	0.479125	24.4	0.479125	0.0845	0.0845	0.394625	883		59.9	0.004893	8.28928	1417.858	0.690427	0.017755	2.275317
24.3	0.375869	24.3	0.375869	0.0835	0.0845	0.291369	964		90	0.002612	4.415828	1027.907	0.509774	0.023022	2.209462
24.2	0.296090	24.2	0.296090	0.0825	0.0845	0.211590	686		90.1	0.002624	4.560560	729.0191	0.370195	0.036688	2.139001
24.2	0.21555	24.2	0.21555	0.0815	0.0815	0.13405	452		100	0.001562	2.707400	422.7908	0.234531	0.064157	2.079988
24.1	0.148391	24.1	0.148391	0.0815	0.0805	0.066891	686		100	0.000829	1.38079	181.5152	0.117031	0.100168	1.887954
24.1	0.182083	24.1	0.182083	0.0805	0.0785	0.103583	190		100	0.000829	1.380795	302.3440	0.181227	0.100782	1.982914
24	0.113344	24	0.113344	0.0775	0.0755	0.055844	156		150	0.000444	0.623948	99.17189	0.062712	0.224017	1.751497
24	3.7032	24	3.7032	0.0745	0.0625	3.6347	1251		15	0.045075	49.15702	7822.523	6.359196	0.005276	2.754518
24.2	6.0494	24.2	6.0494	0.0615	0.0605	5.9884	1646		15	0.074265	35.72906	10503.98	10.47718	0.004862	2.363910
24.3	7.48	24.3	7.48	0.0585	0.0585	7.4215	1942		15	0.092027	77.58905	1240.85	12.98450	0.004224	2.912485
24.5	11.16033	24.5	11.16033	0.0575	0.0595	11.10182	2498		15	0.137579	99.75164	16052.88	19.42353	0.003914	3.301707

Tap DL= 122.2334
40.77743

80.65331

0.4

0.4

Solvent L MDR
l/l/f l/l/f l/l/f

Solvent	L	MDR	l/l/f	l/l/f	l/l/f	l/l/f	l/l/f	l/l/f
14.58638	348.7185	38.78530	21.16795	1.451213	0.060702			
14.27099	290.8222	37.28720	21.15168	1.482145	0.072730			
13.86958	230.5890	35.37579	20.79890	1.499712	0.090159			
13.44387	180.6540	33.35838	20.43036	1.519678	0.113091			
13.11779	149.7372	31.80954	19.71896	1.503222	0.131690			
12.69737	117.5499	29.81250	18.83877	1.483675	0.160261			
12.47654	103.5181	28.76358	17.82697	1.428838	0.172211			
11.83495	71.55167	25.71605	17.19423	1.452834	0.240305			
11.51903	59.55375	24.21539	16.49889	1.432316	0.276577			
12.74447	120.7811	30.03626	18.33479	1.438646	0.151801			
13.20984	157.8855	32.24678	19.48050	1.474695	0.133283			
12.42135	100.2807	28.50141	18.40247	1.481519	0.183509			
11.73956	67.73956	25.25294	16.34832	1.392583	0.241380			
11.63328	63.70907	24.75810	16.06109	1.380615	0.252100			
11.24720	51.01310	22.92823	15.59382	1.386461	0.305682			
11.04107	45.30522	21.94509	14.75940	1.356772	0.325777			
10.63291	35.81862	20.00634	13.91651	1.308814	0.388537			
10.36801	30.75275	18.74807	13.43861	1.296160	0.436988			
10.35433	30.51157	18.68310	13.47711	1.301591	0.441704			
9.927675	25.86705	16.65645	12.71366	1.280638	0.522686			
9.524085	18.91913	14.73940	12.64293	1.327470	0.668261			
9.395380	17.56811	14.12805	11.61138	1.235861	0.660935			
9.230794	15.98007	13.34627	10.56136	1.144145	0.660908			
8.978759	13.82180	12.14901	9.185615	1.023040	0.664574			
8.705269	11.80857	10.85003	7.504393	0.862051	0.635503			
8.437848	10.12376	9.57978	6.345880	0.752073	0.626850			
8.156012	8.607623	8.241061	5.293411	0.649019	0.614967			
7.759552	6.851223	6.357874	3.948115	0.508807	0.576264			
7.451817	4.828746	3.471133	2.349411	0.328505	0.486546			
7.331657	6.008893	5.275375	3.149956	0.418228	0.524215			
6.605990	3.526773	0.878454	1.756773	0.265936	0.498124			
10.61807	35.51392	19.93582	13.76664	1.296529	0.387640			
11.05984	45.79205	22.03329	14.34062	1.296662	0.312168			
11.24994	51.09351	22.93722	15.20600	1.331351	0.297611			
11.60763	62.77514	24.62624	15.98351	1.376983	0.254615			

VIF11434

Tw j U / D Log Log
dyne/cm2 (1/sec) Tw 8:U/D

1.764332	130.4829	0.246555	2.115553
1.521259	111.2790	0.182203	2.046413
1.264389	92.27478	0.101880	1.965082
0.945916	59.41561	-0.02414	1.841457
0.590427	48.45037	-0.16088	1.685297
0.509774	35.20446	-0.39262	1.546597
0.370195	25.02433	-0.43156	1.398362
0.234531	14.85599	-0.62979	1.171901
0.117031	5.244776	-0.92169	0.795516

Log Tw vs. Log 8(U)/D

Regression Output:

Constant	-1.71925
Std Err of Y Est	0.007629
R Squared	0.999429
No. of Observations	7
Degrees of Freedom	5

X Coefficient(s) 0.925249
Std Err of Coef. 0.009888

Tw = K' (8(U)/D)^n'
K' = 0.019087
n' = 0.925249

Tw Retro=0.395342
Res/f/R =144.6008

Regression Output:

Constant	-10.6865
Std Err of Y Est	0.308318
R Squared	0.982997
No. of Observations	21
Degrees of Freedom	19

X Coefficient(s) 8.948258
Std Err of Coef. 0.269989

t = 24.53205 deg C
s.d.(t) = 0.302452 deg C

USF11437

Pusher 500

9/26/90 11:55

10 PSID Taps 14

1.0 PSID Taps 14

0.1 PSID Taps 14

7.25 S =

9.9 C (ppm) =

6.85 [NaCl] =

2.7 S =

9.05 Z =

2.7 Z =

1.0 (cm) =

1.45/72

K(V/psi)=1.085245

col[NaCl]=0.00088

density viscosity

29.98515 X coeff -0.00231

0.000100 constant 0.003419 -4.14933

Freq. (Hz)	Dtest (1/s)	Temp (deg C)	<V> (volts)	<V>0 (volts)	<V>f (volts)	(V)corr (volts)	Batch Vol (ml)	t(samp (sec)	DF (psid)	U (cm/s)	Re	Tu dyne/cm2	f	Log (Re/f)
18	0.264248	24.9	3.507	-0.0535	0.0545	3.4535	1599	20	0.036219	47.88917	7637.976	5.109667	0.004467	2.707999
28	0.566608	24.9	7.916	-0.0535	0.0545	7.8615	1599	20	0.036219	47.88917	7637.976	5.109667	0.004467	2.707999
35	0.708226	24.9	11.69766	-0.0535	0.0545	11.64316	1599	20	0.036219	47.88917	7637.976	5.109667	0.004467	2.707999
15	0.30354	24.9	2.485	0.0735	-0.0545	2.5395	1599	20	0.036219	47.88917	7637.976	5.109667	0.004467	2.707999
10	0.20236	24.9	1.382371	0.0735	-0.0545	1.427071	1599	20	0.036219	47.88917	7637.976	5.109667	0.004467	2.707999
18	0.264248	24.5	1.2258	-0.0365	-0.0505	1.2633	1901	15	0.064042	75.91188	12162.14	9.034946	0.002143	2.832735
28	0.566608	24.5	0.7766	-0.0465	-0.0605	0.8231	1600	15	0.053297	63.89215	10213.35	7.519060	0.003693	2.792889
35	0.708226	24.2	0.6295	-0.0555	-0.0605	0.685	1599	20	0.036219	47.88917	7637.976	5.109667	0.004467	2.707999
15	0.30354	24.1	0.41	-0.0555	-0.0575	0.4655	1599	20	0.036219	47.88917	7637.976	5.109667	0.004467	2.707999
10	0.20236	24.1	0.41	-0.0555	-0.0575	0.4655	1599	20	0.036219	47.88917	7637.976	5.109667	0.004467	2.707999
18	0.264248	24.05	2.7265	-0.0805	-0.0815	2.808	1595	20	0.035582	47.76927	7610.280	5.019914	0.004410	2.707658
28	0.566608	24.1	2.18	-0.0815	-0.0845	2.2645	1329	20	0.028695	39.80282	6348.261	4.048389	0.005123	2.557478
35	0.708226	24	1.630714	-0.0875	-0.0905	1.721314	1235	24.9	0.021810	29.70889	4727.675	3.077047	0.006989	2.596884
15	0.30354	24	1.375444	-0.0075	-0.0105	1.385944	1166	30	0.017562	23.28070	3704.736	2.477679	0.009165	2.549840
10	0.20236	24	1.1905	-0.0155	-0.0145	1.202	1147	35	0.015331	19.62972	3123.744	2.148837	0.011181	2.518919
18	0.264248	23.9	1.033	-0.0155	-0.0145	1.0435	1230	45	0.012210	16.37236	2599.518	1.863696	0.013739	2.487019
28	0.566608	23.9	0.806176	-0.0205	-0.0245	0.820676	1202	60	0.010526	11.99974	1905.256	1.485015	0.020677	2.474897
35	0.708226	23.8	0.60055	-0.0255	-0.0285	0.628855	1025	75	0.007964	8.186184	1296.830	1.123670	0.037617	2.376166
15	0.30354	23.75	0.45075	-0.038	-0.0385	0.47925	962	100.1	0.005072	5.756518	910.9019	0.856784	0.051035	2.316785
10	0.20236	23.6	0.26295	-0.0395	-0.0385	0.29345	476	100	0.003718	2.951187	449.6431	0.524606	0.129775	2.208797
18	0.264248	23.5	0.358791	-0.0305	-0.0345	0.391291	680	110	0.004955	3.702841	582.6561	0.699519	0.102379	2.270291
28	0.566608	23.4	0.193478	-0.0355	-0.0355	0.228978	330	100	0.002901	1.976663	310.2240	0.409348	0.210027	2.152953
35	0.708226	23.2	0.115142	-0.037	-0.04	0.152642	177	100.2	0.001946	1.058094	165.7399	0.274670	0.491312	2.065726
15	0.30354	23.2	0.081	-0.04	-0.0425	0.12225	123	100.1	0.001549	0.756020	115.0304	0.218540	0.800712	2.014709
10	0.20236	23.5	4.043	-0.0445	-0.0585	4.0945	1565	14.9	0.051884	62.91595	9899.409	7.219814	0.003707	2.780141
18	0.264248	23.75	5.0862	-0.0585	-0.0645	5.1477	1870	15	0.065220	74.67397	1181.628	9.202639	0.003708	2.372310
28	0.566608	24	7.400333	-0.065	-0.0675	7.466583	2416	15	0.094615	98.47717	15352.73	15.34815	0.003375	2.915528

Tap DL = 122.2234
40.77743

78.91503

0.4

Solvent	L	MDR	1/f/f	1/f/f	1/f/f	1/f/f	1/f/f	1/f/f	1/f/f
14.13599	269.0787	36.64598	27.49503	1.945037	0.102182				
13.79653	221.3161	35.03353	27.50016	1.978770	0.123353				
13.42987	179.2046	33.29191	26.83475	1.998138	0.149743				
13.04226	143.3656	31.45073	25.80331	1.978362	0.179975				
12.61188	111.9056	29.40646	25.34301	2.009454	0.226467				
11.99631	78.51599	26.48248	23.55675	1.963666	0.300024				
11.57775	54.99432	23.54431	22.42149	1.970643	0.407705				
11.25208	51.15651	22.94739	19.28286	1.713714	0.376928				
12.20395	88.48458	27.46876	25.02692	2.050723	0.282839				
12.91869	133.5222	30.86379	25.79925	1.997048	0.193220				
13.25982	162.4936	32.48417	26.49929	1.998465	0.163078				
11.92717	75.88831	26.20160	24.51750	2.037133	0.320438				
11.44263	57.08736	23.85353	21.55076	1.883373	0.377505				
11.31424	53.02019	23.24266	18.84092	1.665238	0.355353				
10.92494	42.62024	21.44098	17.83504	1.631014	0.418464				
10.77147	38.79267	20.66452	16.45502	1.527648	0.424178				
10.43199	31.90649	19.05198	14.96164	1.434206	0.468921				
10.41463	31.58917	18.96950	15.05713	1.445767	0.476654				
10.22975	28.40000	18.09133	13.97064	1.365686	0.491923				
9.987578	24.70384	16.94080	11.96087	1.197580	0.484170				
9.799360	22.16766	15.04696	10.44521	1.045907	0.471191				
9.575577	20.64426	13.45946	9.457058	0.977405	0.458096				
9.548079	19.18226	14.85337	8.469796	0.887068	0.441542				
9.350791	17.12292	13.91625	6.954335	0.743716	0.406141				
5.104666	14.86095	12.74716	5.454017	0.599035	0.367003				
8.867140	12.96179	11.61891	4.392246	0.495359	0.328860				
8.455173	10.10818	9.567074	2.780190	0.329594	0.275043				
8.681165	11.54585	10.73553	3.126842	0.360186	0.268494				
8.211812	8.88593	8.506107	2.182038	0.245719	0.245487				
7.861307	7.264520	6.841211	1.425936	0.181386	0.196287				
7.558839	6.465319	5.879489	1.111995	0.145191	0.171993				
10.72053	27.67225	20.42268	16.43357	1.531959	0.435959				
10.92924	42.48061	21.41390	17.38482	1.590670	0.409241				
11.26211	51.45238	22.99503	18.64909	1.655914	0.362451				

VTP11137

T_w 3 U/D Log Log
dyne/cm² (1/sec) T_w 3 U/D

3.077047	163.0162	0.488134	2.212220
2.477578	127.7440	0.594045	2.106340
2.140837	107.7106	0.522203	2.032258
1.863696	89.83713	0.270275	1.953455
1.485015	65.84404	0.171731	1.818516
1.123670	44.91956	0.050639	1.652423
0.856754	31.58670	-0.06713	1.499504
0.524606	15.54480	-0.28016	1.194370
0.399519	20.21793	-0.15520	1.307879

Log T_w vs. Log 3 U/D

Regression Output:

Constant	-1.15829
Std Err of Y Est	0.004095
R Squared	0.999742
No. of Observations	6
Degrees of Freedom	4

X Coefficient(s) 0.731725
Std Err of Coef. 0.005872

$T_w = K'(3U/D)^{0.731725}$

$K' = 0.069455$

$n' = 0.731725$

T_w Retro = 14.84337
Res/(f)R = 888.0546

Regression Output:

Constant	6.212058
Std Err of Y Est	0.183724
R Squared	0.974151
No. of Observations	9
Degrees of Freedom	7

X Coefficient(s) 5.904251
Std Err of Coef. 0.363515

$t = 24.275$ deg C

s.d.t = 0.599417 deg C

viscosity

VIP21431

Fusher 500
Taps 14 1.0 PSID Taps 14 0.1 FSID Taps 14
S = 2.7 S = 7.25 S = 9.9 C (ppm) =
Z = 2.7 Z = 9.1 Z = 6.85 [NaCl] =

9/15/90 12:42

density viscosity ID(cm) = 1.45793
K(V/psi) = 1.085245 12.85245
XS(cm2) = 1.559479

co[NaCl] 1.00088 1.001574
100.1166 X coeff -0.00025 -0.0231
0.000100 constant 0.003419 -4.14933

• Freq. (Hz)	D'est Temp (1/s)	Temp (deg C)	<V> (volts)	<V> (volts)	<V>f (volts)	<V>corr (volts)	Batch Vol (ml)	t)saap (sec)	DP (psid)	U' (cm/s)	Re	Iw (dyne/cm2)	f	Log (Re/f)	
60	1.21416	24.9	1.909666	0.0875	0.0755	1.854166	1.690094	727.2585	118106.5	238.4749	0.000704	3.550269			
46	0.930856	24.9	1.272	0.0875	0.0755	1.1965	1.102516	557.5725	90548.33	155.5406	0.001003	3.457606			
36	0.728496	24.9	0.889	0.0875	0.0755	0.8135	0.749600	436.3611	70863.91	105.7520	0.001113	3.372838			
25	0.526136	24.9	0.5885	0.0875	0.0755	0.493	0.454375	315.1497	51179.49	64.08819	0.001294	3.265077			
20	0.40472	24.9	0.41325	0.0875	0.0755	0.33775	0.311220	242.4228	39368.84	43.90626	0.001498	3.182947			
14	0.283504	24.9	0.291	0.0875	0.0755	0.2155	0.198572	169.8950	27558.18	28.01421	0.001950	3.065273			
10	0.20236	24.9	0.2295	0.0875	0.0755	0.154	0.141903	121.2114	19684.42	20.01943	0.002732	3.012410			
8	0.161888	24.9	0.18825	0.0875	0.0755	0.11275	0.103893	93.96914	15747.53	14.65708	0.003123	2.944708			
25	3.3414	24.8	1.0806	0.0115	0.0095	1.348	0.257047	218.1805	35511.98	36.54592	0.001579	3.144088			
25	5.90475	24.7	0.8938	0.0115	0.0065	1.0691	0.458492	315.1497	51295.08	64.68312	0.001705	2.268064			
25	9.04533	24.7	0.685833	0.0115	0.0065	0.8833	0.701720	424.2400	69051.07	98.99730	0.001107	3.3260481			
15	0.30254	25	2.745333	0.0115	0.0265	2.718833	0.211542	181.8171	29593.21	29.84390	0.001810	3.100097			
10	0.20236	25	1.89975	0.0115	0.0265	1.87335	0.145750	121.2114	19728.87	20.56216	0.002806	3.019207			
24.9	1.3645	24.9	1.0806	0.0165	0.0095	1.348	14.9	0.104882	92.86340	15080.77	14.79663	0.003440	2.946765		
24.8	1.0806	24.8	1.0806	0.0115	0.0065	1.0691	14.9	0.083182	71.75808	11627.06	11.73522	0.004570	2.895444		
24.7	0.8938	24.7	0.8938	0.0115	0.0065	0.8833	14.8	0.068648	50.54646	9788.223	9.684769	0.005297	2.852758		
24.7	0.685833	24.7	0.685833	0.0115	0.0065	0.674333	19.9	0.052467	46.71512	7552.262	7.401975	0.006801	2.794787		
24.6	0.6045	24.6	0.6045	0.0115	0.0095	0.593	19.9	0.046139	39.03962	6297.172	6.509201	0.008564	2.765492		
24.6	0.325362	24.6	0.325362	0.0125	0.0145	0.310862	40	0.024187	14.92980	2408.207	3.412266	0.030698	2.625250		
24.45	2.9386	24.5	2.9386	0.0115	0.0135	2.9251	24.9	0.036143	27.80848	4470.411	5.099075	0.03322	2.710996		
24.5	2.74975	24.5	2.74975	0.0135	0.0205	2.72925	34.9	0.028781	19.66881	3165.469	4.060381	0.021046	2.662025		
24.5	2.110583	24.5	2.110583	0.0205	0.0245	2.086083	44.9	0.023776	15.92857	2563.521	3.634489	0.028740	2.638084		
24.4	1.718555	24.4	1.718555	0.0255	0.0295	1.699055	64.9	0.020870	11.55522	1855.490	2.944385	0.044217	2.591255		
24.4	1.585045	24.4	1.585045	0.0285	0.0305	1.56545	80	0.016762	7.906655	1259.517	2.364749	0.075849	2.543350		
24.3	1.106772	24.3	1.106772	0.0295	0.0325	1.074272	80	0.013274	5.405876	866.0970	1.872487	0.128482	2.492005		
24.2	0.884260	24.2	0.884260	0.0335	0.0355	0.850760	100	0.010512	3.529873	580.2460	1.483058	0.225688	2.440767		
24.1	0.682535	24.1	0.682535	0.0305	0.0325	0.650035	120.1	0.008032	2.269275	361.9350	1.133151	0.441201	2.380946		
24	0.563318	24	0.563318	0.0295	0.0295	0.553918	100	0.006596	1.587321	252.5956	0.930559	0.740507	2.337189		
23.9	0.481714	23.9	0.481714	0.0275	0.0275	0.454214	99.9	0.005312	1.163202	184.6870	0.791792	1.173287	2.301158		
23.8	0.387636	23.8	0.387636	0.0245	0.0235	0.344126	99.9	0.004499	0.809444	128.2397	0.634767	1.942267	2.252154		
23.9	4.180833	23.9	4.180833	0.0205	-0.0005	4.170833	19.9	0.351336	44.00613	6987.061	7.270655	0.007527	2.782619		
24.1	5.462	24.1	5.462	-0.0005	-0.0025	5.4635	14.9	0.067509	59.92910	9559.852	9.524050	0.005215	2.843213		
24.2	6.7445	24.2	6.7445	-0.0055	-0.0105	6.7525	15	0.083436	70.36124	11247.45	11.77105	0.004767	2.890195		
24.4	8.739	24.4	8.739	-0.0105	-0.0145	8.7515	15	0.108136	91.08627	14626.25	15.25573	0.003687	2.948474		

VIF21431

Tw 8:U/D Log Log
dyne/cm2 (1/sec) Tw 8:U/D

2.63489 87.40197 0.560582 1.941521
2.94385 65.40491 0.468994 1.802122
2.64749 45.38476 0.373785 1.537337
1.872687 29.66268 0.272465 1.472210
1.483058 19.91754 0.171158 1.299235
1.133151 12.45178 0.054387 1.095231
0.930559 8.709819 -0.03125 0.940009
0.791792 6.382627 -0.10138 0.804999
0.534767 4.441519 -0.19738 0.647531

Log Tw vs. Log 8:U/D

Regression Output:
Constant -0.53127
Std Err of Y Est 0.003444
R Squared 0.999687
No. of Observations 6
Degrees of Freedom 4

X Coefficient (s) 0.564852
Std Err of Coef. 0.004991

Tw = K'(8:U/D)^{n'}
K' = 0.274615
n' = 0.564852

Tw# = 0.636630
Res/fs = 183.4965

Regression Output:

Constant -74.7083
Std Err of Y Est 0.060220
R Squared 0.999553
No. of Observations 4
Degrees of Freedom 2

X Coefficient (s) 19.15634
Std Err of Coef. 0.286211

t = 24.57794 deg C
s.d.t = 0.372035 deg C

Tap DL= 122.2234
40.77743

Solvent L MDR 1/1/f 1/1/f 1/1/f/Siv 1/1/f/L
1/1/f 1/1/f

80.92975
4
0.4

13.80147 221.9459 35.05701 33.25865 2.409789 0.149849
13.43042 179.2611 37.29451 31.56997 2.350631 0.176111
13.09531 147.8116 31.70274 29.96377 2.288129 0.202715
12.66029 115.0676 29.63639 27.79858 2.195729 0.241584
12.33179 95.24178 28.07600 25.83480 2.094975 0.271254
11.94149 76.07702 26.22209 22.64004 1.895913 0.297593
11.64964 64.31173 24.83579 19.12988 1.642101 0.297455
11.37883 55.02855 23.54945 17.88534 1.571834 0.325024

12.17635 87.09013 27.33749 25.48507 2.092997 0.292528
12.67225 115.8630 29.69333 27.67010 2.183517 0.238817
13.04192 143.3379 31.44914 30.10851 2.308594 0.210052
12.00028 78.70046 26.50184 23.50154 1.958398 0.298620
11.67681 65.32566 24.96487 19.87550 1.616494 0.288944
11.38706 55.39989 22.58854 17.04739 1.497084 0.308327
11.18177 49.12751 22.61345 14.79194 1.322861 0.301092
11.01103 44.52854 21.80241 13.73883 1.247733 0.308539
10.77755 38.92850 20.69336 12.13521 1.125043 0.311473
10.66197 36.42273 20.14435 10.80570 1.013480 0.296674
10.10100 26.37121 17.47975 5.70740 0.565040 0.216428

10.44398 32.12747 19.10893 8.696627 0.832692 0.270691
10.24810 28.70165 18.17851 6.892046 0.672616 0.240161
10.15233 27.16218 17.73260 5.898644 0.581013 0.217163
9.965022 24.38572 16.83385 4.755576 0.477226 0.195014
9.774603 21.83399 15.92936 3.830966 0.371469 0.166146
9.568022 19.40375 14.94810 2.789721 0.291567 0.143772
9.361468 17.22848 13.96697 2.104966 0.224854 0.123179
9.157786 15.02542 12.87798 1.505502 0.135008 0.100197
8.948758 13.58531 12.00660 1.162080 0.129859 0.085539
8.804552 12.50311 11.32132 0.923205 0.104855 0.073838
8.608618 11.16952 10.39093 0.717520 0.083349 0.064239
10.73047 37.98777 20.46976 11.52591 1.074129 0.304212
10.97285 43.56057 21.62105 13.71632 1.250023 0.314879
11.16078 48.53729 22.51371 14.48300 1.297669 0.298389
11.39289 55.50791 23.62102 16.46865 1.445392 0.296690

V1F13135

Fusher 500

9/22/90 15:32

10 PSID Taps 14 1.0 PSID Taps 14 0.1 PSID Taps 14
 S = 2.7 S = 7.25 S = 9.9 <C (ppm) =
 Z = 2.7 Z = 9.1 Z = 5.8 [NaCl] =

24.5 12.21275 0.0615 0.0055 12.23725

Freq. (Hz)	D'est (1/s)	Temp (deg C)	<V> (volts)	<V>o (volts)	<V>f (volts)	<V>corr (volts)
60	1.21416	25.3	5.212	0.089	0.0975	5.1145
50	1.0118	25.3	3.735	0.089	0.0975	3.6375
41	0.829676	25.3	2.656333	0.089	0.0975	2.558833
35	0.70826	25.3	2.057666	0.097	0.0925	1.965166
29	0.586844	25.3	1.53725	0.097	0.0925	1.44025
22	0.445192	25.3	1.031	0.097	0.0925	0.9385
15	0.30354	25.3	0.575	0.097	0.0925	0.4825
10	0.20236	25.3	0.37787	0.097	0.0925	0.28537
8	0.161888	25.3	0.29	0.097	0.0925	0.1975
25	0.5059	24.2	1.28833	0.091	0.0785	1.20983
20	0.40472	24.2	0.9255	0.091	0.0785	0.847
15	0.30354	24.2	0.605	0.091	0.0785	0.5265
10	0.20236	24.2	0.3816	0.091	0.0785	0.3031
25	0.5059	25.3	13.35033	-0.0495	-0.0255	13.37583
20	0.40472	25.3	9.577	-0.0495	-0.0255	9.6025
15	0.30354	25.3	6.7185	-0.0495	-0.0255	6.744
10	0.20236	25.3	3.525	-0.0495	-0.0255	3.5505
7	0.141652	25.3	1.9045	-0.0495	-0.0255	1.93
25.1	1.9646	-0.0165	-0.0235	1.9811		
25.1	1.3606	-0.0225	-0.0205	1.3831		
25	1.0652	-0.0285	-0.0225	1.0937		
25	0.67475	-0.0175	-0.0265	0.70125		
25	0.485833	-0.0215	-0.0295	0.515333		
24.9	0.2795	-0.0255	-0.0305	0.305		
24.9	2.023	0.0645	0.0765	1.9585		
24.8	1.55725	0.0855	0.0915	1.57175		
24.8	1.026714	0.0955	0.0995	0.97214		
24.8	0.928625	0.0085	0.0105	0.918125		
24.8	0.471785	0.0115	0.0135	0.458285		
24.7	0.260733	0.0135	0.0155	0.247233		
24.7	0.253304	0.0155	0.0165	0.236804		
24.6	0.20568	0.0165	0.0165	0.18918		
24.5	0.133740	0.0165	0.0175	0.121240		
24.5	0.105777	0.0175	0.0185	0.088277		
24.4	0.07595	0.0165	0.0155	0.06045		
24.3	0.037272	0.0155	0.0135	0.03772		
24.4	3.111	0.0125	0.0055	3.102		
24.5	4.287	0.0025	0.0015	4.2855		
24.5	6.37175	0.0005	0.0015	6.37025		
24.5	8.350666	0	0.0045	8.346166		

Batch	Vol	t ₁ saap	DP	<U>	Re	T _w	f	Log (Re/f)
(ml)	(sec)	(psid)	(cm/s)			dyne/cm ²		
			density	viscosity			ID(cm) = 1.45796	
			col[NaCl]	1.01234	1.029478		K(V/psi)=1.085245	12.85245
			10.01047	X coeff	-0.00075	-0.02281	XS(cm ²)= 1.669479	
			0.300147	constant	0.003419	-4.14933		
2072	14.9	0.154141	83.29566	13281.81	21.74600	0.006209	3.023054	
1665	15.1	0.107613	66.04747	10610.82	15.18191	0.006895	2.945028	
1416	15	0.085096	56.54456	9063.666	12.00525	0.007439	2.893065	
1049	14.9	0.054561	42.17043	6759.601	7.697432	0.063575	2.796552	
1458	25	0.040096	34.93304	5599.502	5.556675	0.009183	2.729660	
1086	25	0.023730	26.02008	4161.423	3.347902	0.009796	2.614730	
1299	29.9	0.024288	26.02297	4161.885	3.426551	0.010024	2.619822	
1190	34.9	0.015771	20.42398	3259.071	2.225027	0.010567	2.525076	
1150	39.9	0.011498	17.26409	2754.845	1.622235	0.010783	2.456466	
1150	40	0.011386	17.22095	2747.958	1.606332	0.010750	2.454333	
1166	50.1	0.035683	13.94054	2224.503	0.801807	0.008173	2.303444	
1095	60.1	0.004306	10.91336	1737.529	0.607512	0.010105	2.242201	
1025	89.8	0.002926	7.627444	1215.966	0.414308	0.014071	2.159085	
805	119.9	0.001503	4.021569	637.3963	0.212120	0.025981	2.011744	
494	100	0.001094	2.959006	468.9861	0.154448	0.034943	1.942346	
335	100	0.000749	2.006613	317.3204	0.102762	0.052021	1.859623	
130	99.9	0.000294	0.777465	122.9847	0.041592	0.135605	1.655989	
1140	20	0.038469	34.14237	5399.184	5.427195	0.009222	2.714725	
1049	15.2	0.053146	41.33812	6551.845	7.497823	0.008691	2.785921	
1375	15	0.085201	54.90733	8702.509	12.02004	0.007898	2.888406	
1615	15	0.109705	64.49115	10221.49	15.47707	0.007371	2.943297	

11.55291 04.45714 24.85135 12.45353 1.068705 0.193278

80.63 Tap DL= 122.2224
 80.65331 40.77743

Solvent	L	HDR	L	HDR	L	HDR	L	HDR
1///f	1///f	1///f	1///f	1///f	1///f	1///f	1///f	1///f
0.4								
14.67080	366.0853	39.18634	20.03756	1.365811	0.054734			
14.37480	308.7324	37.78034	19.79993	1.377404	0.064132			
14.06928	258.9413	36.32911	19.35789	1.375897	0.074757			
13.84000	226.9239	35.24000	18.85660	1.362471	0.083096			
13.57007	194.2672	33.95787	18.25047	1.344905	0.093945			
13.19807	156.8187	32.19083	17.15144	1.299541	0.109371			
12.62019	112.4422	29.44593	16.30939	1.292324	0.145046			
12.16398	86.47191	27.27890	14.13841	1.162318	0.163502			
11.84433	71.93897	25.76060	13.59570	1.147865	0.188989			
13.37530	173.6626	33.03269	17.16869	1.283594	0.098861			
13.06562	145.3065	31.56169	16.41308	1.256337	0.112968			
12.65265	114.5625	29.60009	15.61517	1.234142	0.136302			
12.17302	86.92336	27.32187	13.72024	1.127102	0.157843			
13.55892	172.0331	32.95490	17.76657	1.329940	0.102274			
13.07105	145.7618	31.58751	16.77498	1.283368	0.115084			
12.76412	122.1547	30.12937	15.01262	1.176138	0.122898			
12.30686	88.63319	27.48261	13.79365	1.129991	0.152626			
11.67740	65.34769	24.96765	13.09614	1.121495	0.200407			
11.69221	65.90744	25.03803	12.68997	1.085335	0.192342			
11.38011	55.06910	23.55533	12.04261	1.056216	0.218681			
11.17226	48.85906	22.56823	11.59414	1.037761	0.237297			
10.78620	39.12303	20.73449	10.79862	1.001151	0.276017			
10.51864	33.53823	19.46354	10.43492	0.992041	0.311135			
10.05912	25.74369	17.28083	10.10325	1.004386	0.392464			
10.07929	26.04371	17.37663	9.98737	0.990916	0.383498			
9.700307	20.93904	15.57646	9.727854	1.002839	0.464579			
9.425864	17.87911	14.27285	9.630110	1.021668	0.538623			
9.417507	17.79125	14.23221	9.633467	1.025077	0.542595			
8.813776	12.56967	11.36543	11.06086	1.254951	0.879943			
8.568805	10.91645	10.20182	9.947885	1.160941	0.911274			
8.236342	9.014997	8.62626	8.430166	1.023532	0.935126			
8.037372	8.039392	7.677520	7.582169	0.943264	0.943127			
7.646978	6.421325	5.823148	6.203904	0.811288	0.966140			
7.371384	5.479312	4.514075	5.349509	0.725712	0.976310			
7.038533	4.523903	3.933033	4.383941	0.622848	0.969061			
6.223957	2.830541	-0.93619	2.715575	0.436310	0.959383			
10.45902	32.40679	19.18036	10.41290	0.995590	0.221318			
10.74268	38.17694	20.53250	10.72614	0.998367	0.280958			
11.15362	48.33777	22.47972	11.25321	1.008838	0.232782			
11.37319	54.85016	23.52266	11.64706	1.024080	0.212343			

VIP13135

Tw	8<U>/D	Log Tw	Log 8<U>/D
dynes/cm ² (1/sec)			
0.414308	41.90756	-0.38267	1.622292
0.330985	33.68892	-0.48019	1.527487
0.212120	22.06683	-0.67281	1.343739
0.134448	16.23641	-0.81121	1.210490
0.105762	11.01052	-0.97567	1.041808
0.041592	4.277018	-1.38098	0.631141

Log Tw vs. Log 8<U>/D

Regression Output:

Constant -2.01701
 Std Err of Y Est 0.006224
 R Squared 0.999730
 No. of Observations 5
 Degrees of Freedom 3

X Coefficient(s) 1.001548
 Std Err of Coef. 0.009131

$Tw = K'(8<U>/D)^n$

K' = 0.009615
 n' = 1.001548

Tw = 9.524208
 Res/ft = 701.0509

Regression Output:

Constant -19.6566
 Std Err of Y Est 0.326817
 R Squared 0.981955
 No. of Observations 18
 Degrees of Freedom 16

X Coefficient(s) 10.76679
 Std Err of Coef. 0.364880

t = 24.86097 deg C
 s.d.t = 0.391294 deg C

10 PSID	Pusher 500	9/26/90	14:42	10 PSID	1.0 PSID	Taps 14	0.1 PSID	Taps 14	9.9	<V>	corr	Batch	Vol	t _{1/2}	DF	<U>	Re	T _w	f	Log (Re/f)	
S =	2.7 S =	7.25 S =	9.1 Z =	2.7 S =	7.25 S =	9.1 Z =	6.8	[NaCl] =	0.0895	0.0905	0.0895	(ml)	(sec)	(psid)	(cm/s)	(dyne/cm ²)					
Z =	2.7 Z =	9.1 Z =	6.8	[NaCl] =	0.0895	0.0905	0.0895	0.0895	0.0895	0.0905	0.0895										
60	1.21416	25.2	3.412333	0.0905	0.0895	3.322833	2.061827	727.2685	117102.8	431.9561	0.001618	3.673069									
49	0.991564	25.2	2.4605	0.0905	0.0895	2.371	2.184760	593.9360	95633.97	308.2213	0.001721	3.599781									
39	0.789204	25.2	1.727	0.0905	0.0895	1.6375	1.508875	472.7245	73116.83	212.8690	0.001887	3.519403									
29	0.586844	25.2	1.10825	0.0905	0.0895	1.01875	0.938738	351.5131	56599.69	132.4337	0.002123	3.416249									
22	0.445192	25.2	0.77975	0.0905	0.0895	0.69025	0.636031	266.6651	42937.70	89.72997	0.002500	3.231818									
15	0.30354	25.2	0.4835	0.0905	0.0895	0.394	0.365051	181.8171	29275.70	51.21855	0.003069	3.210067									
10	0.20236	25.2	0.326714	0.0905	0.0895	0.237214	0.218581	121.2114	19517.13	30.83698	0.004158	3.099885									
26	0.526136	23.4	0.9554	0.0875	0.0885	0.8679	0.799727	315.1497	48725.19	112.8238	0.002249	3.263816									
17	0.344012	23.4	0.579	0.0875	0.0885	0.4915	0.452893	206.0594	31858.78	62.89320	0.002980	3.240343									
30	0.60708	25.2	12.683	-0.0495	-0.0275	12.7105	0.988955	263.6342	58551.41	139.5197	0.002090	3.427667									
20	0.40472	25.2	6.96725	-0.0495	-0.0275	6.99475	0.544334	242.4228	39034.27	76.77948	0.002588	3.297972									
15	0.30354	25.2	4.731888	-0.0495	-0.0275	4.759388	0.370309	181.8171	29275.70	52.24252	0.003121	3.214262									
10	0.20236	25.2	2.965	-0.0495	-0.0275	2.9925	0.322834	121.2114	19517.13	32.84786	0.004429	3.113603									
8	0.161888	25.2	2.067	-0.0495	-0.0275	2.0945	0.162985	96.96914	15613.70	22.99076	0.004894	3.036126									
24	0.485664	25.2	9.325666	-0.0495	-0.0275	9.353166	0.727734	290.9074	46841.12	102.6671	0.002402	3.361045									
24.9	1.6386	24.9	1.6386	-0.0245	-0.0155	1.6551	14.9	0.126777	83.81826	13405.15	18.16758	0.005123	2.982042								
24.9	1.101	24.9	1.101	-0.0215	-0.0225	1.1235	15	0.087415	65.60926	10492.97	12.33275	0.005675	2.897917								
24.8	0.9286	24.8	0.9286	-0.0225	-0.0265	0.9351	15	0.074312	55.70598	8889.049	10.48387	0.006693	2.861670								
24.8	0.6135	24.8	0.6135	-0.0265	-0.0355	0.649	20	0.050496	41.62974	6642.891	7.123898	0.008143	2.777367								
24.8	0.4598	24.8	0.4598	-0.0305	-0.0315	0.4913	20.2	0.030223	34.87183	5564.527	5.392867	0.008785	2.717319								
24.6	0.264	24.6	0.264	-0.0315	-0.0445	0.3085	29.9	0.024003	25.56220	4060.619	3.386321	0.010266	2.614302								
24.5	1.882	24.5	1.882	0.0525	0.0275	1.8295	30	0.02183	25.57683	4053.787	3.270631	0.009904	2.605749								
24.5	1.1248	24.5	1.1248	0.0235	0.0125	1.1043	35	0.01393	19.93777	3160.028	1.974177	0.009858	2.493146								
24.5	0.817090	24.5	0.817090	0.0065	0	0.817090	39.9	0.010254	17.12898	2714.849	1.460728	0.009862	2.430738								
24.4	0.477071	24.4	0.477071	-0.0025	-0.0005	0.477571	1184	0.006051	14.21248	2247.524	0.853763	0.008372	2.212177								
24.4	0.344466	24.4	0.344466	-0.0045	-0.0085	0.354966	1076	0.004498	10.74187	1698.690	0.634580	0.010894	2.248711								
24.3	0.241166	24.3	0.241166	-0.0105	-0.0105	0.251666	987	0.002189	7.882696	1243.739	0.449909	0.014242	2.17045								
24.2	0.205263	24.2	0.205263	-0.0115	-0.0115	0.216763	1025	0.002746	6.821820	1073.927	0.387511	0.016494	2.139640								
24.05	0.143611	24.05	0.143611	-0.0135	-0.0135	0.157111	750	0.001990	4.997127	784.0172	0.280870	0.022278	2.068272								
23.9	0.108363	23.9	0.108363	-0.0145	-0.0145	0.122863	590	0.001556	3.922347	613.2122	0.219645	0.028277	2.013401								
23.8	0.057238	23.8	0.057238	-0.0155	-0.0165	0.073238	360	0.000728	2.392297	373.3811	0.130929	0.043273	1.900375								
23.7	0.02175	23.7	0.02175	-0.0175	-0.019	0.04075	216	0.000516	1.293816	201.3949	0.073849	0.086193	1.771785								
23.8	3.082	23.8	3.082	-0.0195	-0.0735	3.1015	1146	0.003901	34.32207	5354.627	5.544609	0.009232	2.764941								
22.9	3.8394	22.9	3.8394	-0.0735	-0.0935	3.9129	1372	0.004958	40.88521	6393.114	6.995164	0.008288	2.764941								
22.8	5.88025	22.8	5.88025	-0.0165	-0.0025	5.89675	1366	0.004722	54.54793	8510.089	10.54173	0.007017	2.853013								
23.9	7.1856	23.9	7.1856	0.0065	0.0115	7.1791	1606	0.009072	64.13176	10027.87	12.85421	0.006180	2.896723								
23.9	10.1404	23.9	10.1404	0.0185	0.0225	10.1219	2041	0.012823	81.50244	12743.01	18.09511	0.005395	2.971222								

co) [NaCl] 1.01274 1.029473 ID (ca) = 1.45776
 29.98515 X coeff -0.00025 -0.02281 K (V/psi) = 1.085245
 0.300052 constant 0.003419 -4.14933 XS (ca2) = 1.669479

10 PSID Taps 14 1.0 PSID Taps 14 0.1 PSID Taps 14 9.9 <V> (ppa) =
 S = 2.7 S = 7.25 S = 9.1 Z = 6.8 [NaCl] =
 Z = 2.7 Z = 9.1 Z = 6.8

V.F.15138
 Tw dyne/cm² (1/sec) Log Tw 8-U./D
 0.634580 58.94192 -0.197751 1.770424
 0.449909 43.25329 -0.74687 1.536019
 0.387511 37.43213 -0.41171 1.573244
 0.280870 27.41983 -0.55149 1.438064
 0.219445 21.52239 -0.58827 1.372890
 0.130929 13.12230 -0.88296 1.118240
 0.072849 7.099324 -1.13757 0.851217

Tap DL= 122.2234
 40.77743

Solvent L MDR 1/1/f 1/1/f 1/1/f/Siv 1/1/f/L
 1/1/f 1/1/f 1/1/f

14.29227 294.4081 37.38832 24.85979 1.739386 0.084439
 13.99912 248.6917 35.99584 24.03425 1.716840 0.096462
 13.67762 206.6741 34.46871 23.01875 1.682921 0.111375
 13.26539 163.0156 32.51063 21.70025 1.635853 0.133117
 12.92727 134.1823 30.90455 19.99954 1.547081 0.149046
 12.44025 101.3779 28.59120 18.04860 1.450823 0.178032
 11.99954 78.66217 26.49783 15.50708 1.292306 0.197135
 13.05526 144.4431 31.51251 21.08321 1.614920 0.145962
 12.56137 108.6985 29.16453 18.31831 1.458304 0.168523
 13.31067 167.3199 32.72568 21.87104 1.643121 0.130713
 12.79189 124.1230 30.26147 19.65502 1.536522 0.158331
 12.45744 102.3863 28.67287 17.87085 1.434551 0.174543
 12.05441 81.18644 26.75846 15.02493 1.246425 0.185067
 11.74450 67.92140 25.28640 14.36744 1.223333 0.211530
 13.04426 143.5310 31.46024 20.39677 1.563658 0.142107
 11.52817 59.98847 24.25881 13.97104 1.211904 0.232973
 11.19166 49.40801 22.56043 13.27326 1.136004 0.268648
 11.04668 45.45169 21.97173 12.23320 1.104505 0.268927
 10.71107 37.46692 20.37759 11.08126 1.034561 0.295761
 10.46927 32.59860 19.22906 10.66864 1.019043 0.327273
 10.05721 25.71478 17.27175 9.869371 0.981322 0.383801
 9.02307 25.21444 17.10961 10.04827 1.002514 0.398512
 9.586586 19.58965 15.02678 10.08194 1.051991 0.514656
 9.322953 16.85071 13.78402 10.06948 1.080075 0.597570
 8.822548 12.85327 11.54960 10.22867 1.234522 0.850256
 8.594846 11.08132 10.32552 9.580817 1.114716 0.864591
 8.292182 9.309484 8.887866 8.349948 1.006964 0.896929
 8.158561 8.20259 8.253165 7.786365 0.954379 0.902263
 7.937092 7.313971 6.897191 6.699655 0.850955 0.916007
 7.652614 6.445901 5.854659 5.948727 0.776982 0.922559
 7.200301 4.965412 3.701430 4.699775 0.652719 0.946502
 6.687141 3.695435 1.263922 3.406145 0.509367 0.921717
 10.45297 32.31255 19.15626 10.33706 0.990730 0.320526
 10.65976 36.37653 20.13388 10.98426 1.020441 0.201960
 11.01205 44.53466 21.80724 11.93770 1.084058 0.267934
 11.13690 49.27277 22.62781 12.71984 1.137029 0.238151
 11.48529 58.50635 24.05513 13.61392 1.185335 0.232691

Log Tw vs. Log 8-U./D
 Regression Output:
 Constant -2.00171
 Std Err of Y Est 0.006506
 R Squared 0.999612
 No. of Observations 5
 Degrees of Freedom 3

X Coefficient(s) 1.008362
 Std Err of Coef. 0.011461

Tw = K * (8-U./D)ⁿ
 Kⁿ = 0.009960
 nⁿ = 1.008362

Twⁿ = 5.927007
 Res/ftⁿ = 551.7821

Regression Output:
 Constant -32.4486
 Std Err of Y Est 0.552739
 R Squared 0.986728
 No. of Observations 26
 Degrees of Freedom 24

X Coefficient(s) 15.68904
 Std Err of Coef. 0.371412

t = 24.56081 deg C
 s.d.t = 0.596287 deg C

V1P23132

Pusher 500 9/15/90 15:48
 10 PSID Taps 14 1.0 PSID Taps 14 0.1 PSID Taps 14
 S = 2.7 S = 7.25 S = 9.9 C (ppm) =
 Z = 2.7 Z = 9.1 Z = 6.85 [NaCl] =

density viscosity
 [NaCl] 1.0124 1.029475 ID(cc) = 1.45775
 100.1166 X coeff -0.00025 -0.00291 K(V/psi) = 1.085245
 0.300060 constant 0.003419 -4.14933 XS(cc2) = 1.669479

Freq. (Hz)	Qest Temp (1/s)	Temp (deg C)	<V> (volts)	<V>0 (volts)	<V>f (volts)	<V>corr (volts)	Batch Vol (ml)	t(samp (sec)	DP (psid)	U. (cm/s)	Re	Tw (dyne/cm2)	f	Log (Re/f)	
50	1.21416	25.2	2.158333	0.074	0.0765	2.061833	1.899878	727.2685	117102.8	268.0307	0.001004	3.559442			
49	0.991544	25.2	1.5955	0.074	0.0765	1.519	1.399687	592.9360	95633.97	197.4644	0.001109	3.507094			
40	0.80944	25.2	1.19175	0.074	0.0765	1.11525	1.037648	484.9457	78068.54	144.9784	0.001221	3.45001			
29	0.586844	25.2	0.77475	0.074	0.0765	0.69825	0.645403	351.5131	56599.69	90.76994	0.001455	3.35420			
21	0.424956	25.2	0.531333	0.074	0.0765	0.457333	0.421410	254.5440	40985.98	59.45165	0.001817	3.242471			
14	0.283304	25.2	0.349	0.074	0.0765	0.2725	0.251095	169.6960	27233.99	35.42400	0.002437	3.129998			
10	0.20236	25.2	0.257071	0.074	0.0765	0.180571	0.166387	121.2114	19517.15	23.47362	0.003185	3.040540			
8	0.161888	25.2	0.2156	0.074	0.0765	0.1391	0.128172	96.96914	15613.70	18.08249	0.003810	2.987979			
30	0.60708	23.85	0.815	0.0865	0.1	0.715	0.550827	567.5342	56795.05	92.94728	0.001392	3.356168			
15	0.30354	23.8	0.408333	0.0725	0.1045	0.303833	0.279967	181.8171	28765.51	39.49722	0.002366	3.159840			
35	0.70826	25.2	10.87366	0.0185	0.0445	10.82916	0.842576	424.2400	68309.97	118.8688	0.001308	3.372883			
28	0.566608	25.2	7.794333	0.0185	0.0445	7.749833	0.603984	339.3920	54647.98	85.06783	0.001467	3.302323			
22	0.445192	25.2	6.1818	0.0185	0.0445	6.1373	0.477519	266.5651	42937.70	67.36748	0.001877	3.269575			
16	0.323776	25.2	3.84025	0.0185	0.0445	3.79575	0.295322	192.9382	31227.41	41.66492	0.002194	3.165225			
14	0.283304	25.2	3.30428	0.0185	0.0445	3.259928	0.232642	169.6960	27233.99	35.78325	0.002462	3.122190			
9	0.182124	25.2	2.017428	0.0185	0.0445	1.972928	0.133506	109.0902	17565.42	21.65630	0.002605	3.021142			
		25	1.3404	0.0125	0.0085	1.3279	14.9	0.103318	82.95445	13113.00	0.004186	2.95198			
		24.9	1.0688	0.0085	0.0035	1.0633	15	0.082886	64.53108	10320.53	0.005351	2.885766			
		24.8	0.84375	0.0055	0.0015	0.84225	15.1	0.055522	54.54370	8703.583	0.006156	2.834766			
		24.8	0.6044	0.0035	0.0015	0.6029	20	0.046909	41.62974	6642.891	0.007545	2.761748			
		24.7	3.7445	0.0445	0.0155	3.7	19.9	0.045718	41.58843	6637.267	0.007352	2.755200			
		24.6	2.9826	0.0195	0.0195	2.9621	20	0.026613	34.77121	5523.508	0.008462	2.705987			
		24.6	1.891857	0.0205	0.0225	1.869357	29.9	0.023098	25.44201	4041.525	0.009973	2.605900			
		24.5	1.27525	0.0225	0.0225	1.21275	35	0.014965	20.21160	2902.427	0.010251	2.511014			
		24.5	0.688333	0.0225	0.0215	0.66833	45	0.008239	16.23142	2382.537	0.010433	2.391137			
		24.45	0.523125	0.0215	0.0205	0.501625	49.9	0.005198	14.05645	2225.256	0.0087439	2.319825			
		24.4	0.403812	0.0195	0.0195	0.384312	60	0.004718	10.30176	1708.162	0.006993	0.11174	2.260485		
		24.3	0.304142	0.0195	0.0195	0.286642	80	0.002522	5.870074	892.6128	0.005712	0.152112	2.194708		
		24.2	0.2235	0.0185	0.0185	0.205	89.9	0.002522	5.870074	892.6128	0.005712	0.152112	2.194708		
		24.1	0.16404	0.0175	0.0175	0.14854	100.1	0.001253	4.152831	652.2879	0.005837	0.039739	2.051109		
		24	0.117133	0.0165	0.0155	0.101625	99.9	0.001253	4.152831	652.2879	0.005837	0.039739	2.051109		
		23.8	0.081208	0.0155	0.0145	0.068708	100	0.000824	1.862856	290.6284	0.004266	0.042366	1.96721		
		23.7	0.045541	0.0135	0.0125	0.023541	100	0.000402	0.910463	141.7224	0.005627	0.15556	1.717467		
		23.9	5.135166	0.0115	-0.0065	5.141866	19.9	0.025222	52.2531	8402.877	8.967025	0.006142	2.013769		
		24	6.2404	-0.0075	-0.0075	6.2479	14.9	0.077201	62.25315	9928.939	16.89142	0.005274	2.362039		
		24	8.5568	-0.0195	-0.0295	8.5863	15.1	0.106095	50.40774	12501.17	14.96775	0.004585	2.971105		

Tap DL = 122.2234
40.77743

Solvent	L	MDR	1/f/f	1/f/f	1/f/f/Siv	1/f/f/L
80.92975						
0.4						
4						
13.87776	231.9115	35.41940	31.55915	2.274078	0.136082	
13.61227	199.0556	34.15879	30.02740	2.205889	0.150849	
13.34400	170.5617	32.88403	28.40714	2.143319	0.167713	
12.93728	134.9587	30.95209	26.21157	2.026049	0.194219	
12.56972	109.3224	29.20620	23.45327	1.865853	0.214729	
12.11999	84.30993	27.06997	20.25561	1.671255	0.240251	
11.76256	68.63095	25.37216	17.77562	1.511034	0.258973	
11.33591	60.23641	24.29560	16.20044	1.404348	0.268947	
12.90467	132.4489	30.79719	26.80045	2.076802	0.202345	
12.15936	86.24232	27.25696	20.55654	1.690594	0.238357	
13.17153	154.4414	32.06479	27.64595	2.098764	0.178993	
12.88093	130.6509	30.68441	26.14216	2.029524	0.200091	
12.67830	116.2666	29.72192	23.08148	1.820550	0.198521	
12.24094	91.43558	27.73946	21.34523	1.740912	0.233445	
12.12876	84.73649	27.11161	20.15364	1.661640	0.237839	
11.69256	65.92074	25.03970	16.65392	1.424316	0.252435	
11.34079	53.83673	22.36877	15.45529	1.362805	0.287077	
11.14546	48.11127	22.44096	13.40711	1.202921	0.278668	
10.93746	42.68213	21.45295	12.74476	1.165239	0.298597	
10.64707	36.11173	20.07359	11.49711	1.079838	0.318376	
10.62080	35.56969	19.94880	11.66243	1.098074	0.327875	
10.42394	31.75903	19.01375	10.86995	1.042786	0.342253	
10.02284	25.22552	17.11324	10.01348	0.998966	0.396958	
9.644058	20.27190	15.30927	9.876438	1.024095	0.487198	
9.124550	15.03202	12.84161	11.15758	1.222808	0.742253	
8.675303	13.02284	11.65769	10.68005	1.203345	0.820101	
8.441943	11.38586	10.54923	9.376555	1.085005	0.823526	
8.377234	9.776618	9.291864	8.08879	0.944633	0.826551	
8.088201	8.278092	7.918954	6.739277	0.833223	0.814110	
7.804439	7.030558	6.571086	5.798685	0.742998	0.824782	
7.470884	5.802311	4.986699	4.858351	0.650304	0.827313	
7.097290	4.579533	3.212129	3.881615	0.546915	0.829487	
6.469868	3.240972	0.331877	2.716259	0.419832	0.822959	
10.87507	41.17452	21.15662	12.75889	1.173223	0.309858	
11.04827	45.49356	21.97932	13.64062	1.234637	0.299836	
11.32442	53.33176	23.29101	14.76743	1.304034	0.276897	

VIF:23122

Tw	B-U/D	Log	Log
dyne/cm ² (1/sec)	Tw	8-U/D	8-U/D
0.669938	59.27059	-0.27596	1.772839
0.496193	43.95993	-0.30434	1.643057
0.357358	31.11237	-0.44689	1.492933
0.258937	22.78707	-0.58680	1.357688
0.177158	15.79206	-0.75161	1.198479
0.116286	10.22171	-0.93446	1.009523
0.056727	4.995820	-1.24620	0.698606

Log Tw vs. Log 8-U/D

Regression Output:

Constant -1.94679

Std Err of Y Est 0.003608

R Squared 0.999922

No. of Observations 7

Degrees of Freedom 5

X Coefficient(s) 1.000576

Std Err of Coef. 0.003943

Tw = K * (B-U/D)^n

K' = 0.011303

n' = 1.000576

Tw# = 6.497523

Res/# = 577.7285

Regression Output:

Constant	-61.7698
Std Err of Y Est	0.513013
R Squared	0.989325
No. of Observations	17
Degrees of Freedom	15
X Coefficient(s)	26.22155
Std Err of Coef.	0.703274

t = 24.5833 deg C

s.d.t = 0.528690 deg C

WIP11462 Fuser 500-F 11/28/90 11:25
 10 PSID Taps 14 1.0 PSID Taps 14 0.1 PSID Taps 14
 S = 1 S = 7.25 S = 9.9 C: (ppa)=
 Z = S Z = 8.85 Z = 8.9 [NaCl]=
 FlowCo= 0.019693 0.020236

density viscosity/
 col[NaCl] 1.000039 1.001574 ID(cm) = 1.02106
 0.00012 X const -0.00025 -0.02291 K(V/psi)= 1.17915 1.177591
 1.000100 constant 0.003419 -4.14933 XS(cm2)= 0.818859

Tap	Fair	Freq.	Dist	Temp	<V>	<V>	<V>	<V>	DP	U:	Re	Tw	r	Log(Re/r)
		(Hz)	(1/s)	(deg C)	(volts)	(volts)	(volts)	(volts)	(paid)	(cm/s)		dyne/cm2		
12	60	1.191580	25	6.5195	0.0495	0.0595	6.46	5.478522	1442.950	164485.2	2431.951	0.002541	2.900880	
12	50	0.984550	25	4.4155	0.0495	0.0595	4.356	2.694186	1202.465	137071.0	1639.265	0.002273	2.815208	
12	40	0.787720	25	2.824	0.0495	0.0595	2.7445	2.244485	961.9723	109556.8	1040.740	0.002354	2.715572	
12	30	0.590770	25	1.53975	0.0495	0.0595	1.59035	1.40160	721.4792	82242.50	594.3355	0.002591	2.595127	
12	20	0.392860	25	0.831666	0.0495	0.0595	0.772166	0.54850	480.9861	54828.40	290.5846	0.002519	2.49417	
12	15	0.295295	25	0.54625	0.0495	0.0595	0.48675	0.412797	360.7296	41121.20	182.1755	0.002822	2.379417	
12	10	0.196730	25	0.325	0.0495	0.0595	0.255	0.225152	240.4730	27414.20	99.91593	0.003464	2.267796	
12	8	0.157544	25	0.245833	0.0495	0.0595	0.185333	0.158023	192.3944	21921.26	70.12164	0.003799	2.175909	
12	17	0.234781	24.9	6.885333	0.0065	0.0275	6.857833	0.497055	408.9382	46499.12	220.5545	0.003346	2.755374	
12	23	0.452937	24.9	11.3125	0.0065	0.0275	11.285	0.817926	552.1340	62910.57	262.9529	0.002779	2.436723	
12	14	0.275702	24.9	4.9298	0.0065	0.0275	4.9021	0.255504	336.6903	38293.39	157.6674	0.002789	2.705863	
12	10	0.195730	24.9	2.9388	0.0065	0.0275	2.9113	0.211011	240.4920	27252.42	92.53446	0.002246	2.192718	
12	8	0.157544	24.9	1.9135	0.0065	0.0275	1.886	0.135697	192.3944	21891.92	60.65822	0.002396	2.092442	
14	14		24.8	5.018665	-0.0195	-0.0305	5.049166	15	0.355963	176.2614	20001.87	54.17880	0.003494	2.622257
14	14		24.8	3.5428	-0.0305	-0.0425	3.583	15.1	0.259862	144.2807	16372.76	38.44274	0.003703	2.999420
14	14		24.7	2.8268	-0.0395	-0.0505	2.8773	15	0.208546	125.2776	14195.59	20.85134	0.003925	2.949655
14	14		24.6	1.8878	-0.0475	-0.0565	1.9443	15	0.140922	96.23139	10871.03	20.84741	0.004514	2.863568
14	14		24.7	1.387333	-0.0545	-0.0665	1.443833	19.9	0.104649	81.12766	9185.497	15.48124	0.004715	2.799971
14	14		24.6	0.863	-0.054	-0.0555	0.9185	20.1	0.066572	60.87826	6877.271	9.848454	0.005239	2.700723
14	14		24.5	5.724333	0.0475	0.0195	5.704833	24.9	0.068415	60.71721	6843.622	10.12123	0.005505	2.735374
14	14		24.5	3.936857	0.0345	0.0155	3.921357	30.1	0.047027	47.97470	5396.102	6.957081	0.006083	2.534271
14	14		24.5	2.795818	0.0355	0.0235	2.772318	40	0.022247	41.12426	4635.241	4.918512	0.005811	2.548974
14	14		24.5	1.857083	0.0315	0.0045	1.850933	44.9	0.022193	33.24520	3758.450	3.28215	0.005921	2.431207
14	14		24.4	1.444352	0.0315	0.0045	1.399852	60	0.016788	25.91001	2912.816	2.483551	0.007418	2.799600
14	14		24.4	1.089411	0.0785	0.0715	1.017911	60	0.012207	19.09159	2147.022	1.905929	0.009925	2.720422
14	14		24.3	0.829652	0.0815	0.0825	0.747152	70	0.008960	14.19318	1592.554	1.225561	0.012194	2.252287
14	14		24.25	0.667045	0.0835	0.0915	0.575545	89.9	0.006902	10.78577	1210.224	1.021104	0.017600	2.295622
14	14		24.2	0.281	-0.0115	-0.0115	0.2925	90	0.004807	7.254401	824.2749	0.711472	0.026392	2.125377
14	14		24.1	0.18026	-0.0125	-0.0125	0.19286	100	0.002507	5.116872	572.8480	0.513979	0.03741	2.057350
14	14		24	0.1105	-0.0155	-0.0165	0.127	99.9	0.002312	3.214998	359.1169	0.342162	0.066277	1.966277
14	14		23.95	0.072571	-0.0185	-0.0215	0.094071	100	0.001523	1.990572	221.8469	0.225317	0.114012	1.34529
14	14		23.9	0.020553	-0.0225	-0.0255	0.048555	100	0.001123	1.392180	154.9818	0.166896	0.172649	1.8793
14	14		24.1	9.136	-0.0275	-0.0295	9.1625	150	0.000582	0.675726	75.14030	0.086144	0.278247	1.534731
14	14		24.2	11.71475	0.0035	0.0025	11.71225	20	0.109895	80.52884	8996.228	13.25743	0.002025	2.894542
14	14		24.3	5.9002	0.0095	0.0135	5.8637	15.1	0.140682	94.32360	10593.27	20.77920	0.004652	2.923911
12	12		24.3	7.28525	0.0425	0.0125	7.27275	15	0.070282	122.9121	12902.84	21.22147	0.004078	2.948283
12	12		24.4	10.1755	0.0425	0.0125	10.153	15	0.087220	141.4161	15902.52	23.70240	0.003380	2.975947
12	12		24.4	10.1755	0.0425	0.0125	10.153	15.1	0.121782	171.6972	19208.92	24.02122	0.002675	2.631794

WIP11462
Tw 8 U / D Log Log
dynerca2 (1/3cc) Tw 8 U / D

2.48551 207.0008 0.395073 2.707497
1.80529 149.5798 0.256700 2.174872
1.25561 111.2013 0.122399 2.046109
1.02104 84.50484 0.009070 1.925881
0.711473 57.62057 -0.14784 1.760577
0.518979 40.08988 -0.28488 1.507034
0.342162 25.18900 -0.46576 1.401211
0.225317 15.59582 -0.54720 1.193008
0.166876 10.70751 -0.77755 1.037725
0.085144 5.294288 -1.05477 0.772807

Regression Output:
Constant -1.71012
Std Err of Y Est 0.006048
R Squared 0.999811
No. of Observations 8
Degrees of Freedom 6

X Coefficient(s) 0.891564
Std Err of Coef. 0.004993

Tw vs. K*(8.U./D)^n

K* = 0.019492
n = 0.891564

Tw)Retro=0.905542
Res/f)R =152.6165

Regression Output:
Constant -9.62828
Std Err of Y Est 0.220677
R Squared 0.991288
No. of Observations 21
Degrees of Freedom 19

X Coefficient(s) 8.585017
Std Err of Coef. 0.184529

t = 24.57621 deg C
s.d.)t = 0.343862 deg C

WIP11462

Solvent	L 1/1f	MDR 1/1f	DATA 1/1f	1/1f/Slv	1/1f/L
85.38349					
4					
0.4					
15.20352	497.4628	41.71673	20.66551	1.259258	0.041541
14.86123	408.4965	40.09085	20.97187	1.411179	0.051339
14.46639	325.4263	38.21488	21.06021	1.455813	0.084715
13.98050	246.0409	35.90741	20.89149	1.494330	0.084970
13.55847	171.9887	32.95277	19.92441	1.491518	0.115847
12.95746	136.5517	31.04893	18.82129	1.432521	0.137822
12.43118	100.9501	28.54813	16.98943	1.366678	0.184462
12.12363	84.48696	27.08723	15.22392	1.338205	0.192038
13.11506	149.5017	31.79655	19.43920	1.482204	0.120025
13.54769	191.7801	33.85154	20.50217	1.513333	0.106904
12.82345	126.3990	30.41141	18.93476	1.478572	0.149801
12.37086	97.40838	28.26160	17.55009	1.418663	0.180170
11.99377	78.40137	26.47042	17.44384	1.454407	0.222494
11.89107	73.90053	25.99258	16.91621	1.422597	0.226905
11.59368	62.27309	24.56998	16.43241	1.417359	0.263975
11.39866	55.66024	23.64363	15.94001	1.398411	0.286380
11.05427	45.65086	22.00781	14.88338	1.346391	0.326025
10.79972	39.42857	20.79868	14.56034	1.348214	0.369284
10.40290	31.37667	18.91391	13.69901	1.316844	0.436598
10.42269	31.77616	19.00781	13.47756	1.293097	0.424675
10.09708	26.31183	17.46115	12.81766	1.269442	0.487144
9.795898	22.12253	16.07051	13.09476	1.326760	0.591892
9.444829	18.07577	14.36293	12.99575	1.375965	0.718975
9.198476	15.68516	13.19257	11.61055	1.262221	0.740225
8.921691	13.37528	11.87803	10.03260	1.124518	0.750085
8.649148	11.43318	10.58345	8.705771	1.006546	0.751447
8.423489	10.02465	9.506826	7.537782	0.894958	0.751175
8.166895	8.36695	8.006805	6.157410	0.759546	0.735942
7.830541	7.177405	6.695546	5.016249	0.640592	0.702811
7.464933	5.782468	4.958432	3.881527	0.519968	0.671257
7.098115	4.681757	3.216048	2.961507	0.417235	0.632590
6.835453	4.024790	1.968402	2.406675	0.352087	0.597762
6.259045	2.888293	-0.74953	1.625946	0.259778	0.562950
10.81857	39.85868	20.88821	14.10644	1.303910	0.353911
11.07567	45.16454	21.91943	14.55941	1.328366	0.224579
11.39553	55.49623	23.61928	15.65831	1.374316	0.282151
11.58278	61.91994	24.33299	16.05264	1.385785	0.259250
11.87357	73.16020	25.89950	16.49540	1.389252	0.225469

WSP11465 Pusher 500-F 12/4/90 12:08
 10 PSID Taps 14 1.0 PSID Taps 14 0.1 PSID Taps 14
 S = 1 S = 7.25 S = 9.9 C (ppm) =
 Z = 4.7 Z = 9.2 Z = 6.8 [NaCl] =
 FlowCo= 0.019693

density viscosity ID(cm) = 1.02108
 col(NaCl) 1.000088 1.001574 K(U/psi) = 1.17915 1.77691
 30.00571 X coeff -0.00231 XS(cm2) = 0.818859
 0.000100 constant 0.003419 -4.14923

Tap Pair	Freq. (Hz)	Oldest Temp (1/s)	Temp (deg C)	<U> (volts)	<U> (volts)	<U>f (volts)	<U>corr (volts)	Batch Vol (ml)	t(s)saep (sec)	DF (psid)	'U' (cm/s)	Re	Tw (dyne/cm2)	f	Log (Re/f)	
12	60	1.191580	25.2	3.436	0.0145	0.0195	3.4165	2.897426	1442.958	165229.0	1285.709	0.001278	3.744525			
12	50	0.984650	25.2	2.395333	0.0145	0.0195	2.375833	2.014869	1202.465	137690.8	894.0823	0.001240	3.685642			
12	40	0.787720	25.2	1.54	0.0145	0.0195	1.5205	1.289483	961.9733	110152.6	572.2001	0.001240	3.588728			
12	30	0.590790	25.2	0.98325	0.0145	0.0195	0.86375	0.725219	721.4792	82614.51	325.0495	0.001252	3.465928			
12	22	0.432246	25.2	0.5182	0.0145	0.0195	0.4987	0.422971	529.0847	60582.98	187.6726	0.001344	3.346654			
12	15	0.295395	25.2	0.286571	0.0145	0.0195	0.267071	0.226494	360.7396	41307.25	100.5053	0.001548	3.211048			
14	15	0.295395	25.2	0.8055	0.0145	0.0195	0.786	0.666581	360.7396	41307.25	98.61074	0.001519	3.206918			
14	10	0.196930	25.2	0.443	0.0145	0.0195	0.4225	0.259157	240.4930	27538.17	52.13187	0.001842	3.072671			
14	25	0.492325	25.2	2.008	0.0145	0.0195	1.9885	1.686384	601.2326	68845.43	249.4751	0.001384	3.408467			
12	15	0.295395	25.1	3.2225	0.0345	0.0575	3.145	0.229799	360.7396	41214.17	101.7940	0.001568	3.212820			
12	24	0.472632	25.1	7.00975	0.0345	0.0575	6.95235	0.507899	577.1833	65942.68	223.6012	0.001246	3.382705			
12	32	0.630176	25.1	11.7025	0.0345	0.0575	11.645	0.844029	769.5778	87923.37	374.5314	0.001268	3.495712			
12	20	0.392860	25.1	5.15475	0.0545	0.0565	5.09825	0.769521	480.9861	54952.23	163.9720	0.001421	3.316253			
12	10	0.196930	25.1	1.69174	0.0545	0.0565	1.635214	0.118520	240.4930	27476.11	52.59245	0.001823	3.069430			
14	14	3.30375	24.9	3.30375	0.0645	0.0575	3.24625	15	0.252288	179.5179	20417.43	34.80736	0.001166	2.977822		
14	24.8	2.40725	24.8	2.40725	0.0595	0.0525	2.35475	15.1	0.170672	143.0676	16235.09	25.24839	0.002472	2.907120		
14	24.7	1.9865	24.7	1.9865	0.0555	0.0565	1.93	15	0.139886	122.6095	13882.19	20.69408	0.002760	2.862951		
14	24.7	1.3455	24.7	1.3455	0.0565	0.0535	1.292	15	0.092644	94.50311	10711.22	13.85224	0.002104	2.775803		
14	24.7	1.0324	24.7	1.0324	0.0555	0.0545	0.9779	20	0.070878	79.68399	9022.041	10.48536	0.003311	2.715219		
14	24.6	6.555	24.6	6.555	0.0745	0.0775	6.4775	1505	0.076215	80.08441	9046.944	11.27487	0.003225	2.720098		
14	24.6	4.367833	24.6	4.367833	0.0745	0.0735	4.294333	991	0.050527	60.51098	6835.781	7.474809	0.004091	2.540842		
14	24.6	3.39875	24.6	3.39875	0.0705	0.0685	3.271375	1171	0.028491	47.66792	5384.931	5.694225	0.005025	2.581760		
14	24.6	2.8665	24.6	2.8665	0.0645	0.0645	2.802	1235	0.023968	40.86005	4615.862	4.877221	0.005858	2.548129		
14	24.5	2.371	24.5	2.371	0.0585	0.0575	2.3135	1108	0.027220	33.82753	3812.804	4.026928	0.007056	2.505544		
14	24.45	1.744257	24.45	1.744257	0.0555	0.0555	1.688857	1012	0.019871	24.71720	2782.821	2.939661	0.009648	2.456713		
14	24.4	1.284705	24.4	1.284705	0.0555	0.0545	1.230205	873	0.014474	17.72904	1994.916	2.141322	0.013645	2.357413		
14	24.4	0.976227	24.4	0.976227	0.0545	0.0575	0.918727	896	0.010809	12.14433	1365.740	1.599156	0.021742	2.304017		
14	24.3	0.766818	24.3	0.766818	0.0555	0.0555	0.711318	650	0.008369	8.819854	989.6372	1.238135	0.031914	2.247471		
14	24.2	0.491545	24.2	0.491545	0.0555	0.0585	0.435045	363	0.005095	4.931028	552.0423	0.753768	0.062158	2.138720		
14	24.2	0.63036	24.2	0.63036	0.0575	0.0545	0.57286	594	0.006740	6.594537	758.2767	0.997132	0.045974	2.199478		
14	24.15	0.349083	24.15	0.349083	0.0535	0.0545	0.294583	254	0.003466	3.101875	346.8720	0.512758	0.106854	2.054565		
14	24.1	0.269378	24.1	0.269378	0.0535	0.0535	0.215875	148	0.002540	2.051633	239.1685	0.375756	0.178990	1.986570		
14	24	0.218038	24	0.218038	0.0525	0.0515	0.166538	132	0.001959	1.535226	171.1002	0.289880	0.246593	1.929241		
14	24	0.159416	24	0.159416	0.0505	0.0495	0.109416	76	0.001287	0.928120	103.4378	0.190453	0.443294	1.838025		
14	24.1	8.245	24.1	8.245	0.0495	0.0325	8.2125	1158	0.096629	93.45310	10461.09	14.29485	0.003267	2.776705		
14	24.3	11.4675	24.3	11.4675	0.0275	0.0135	11.454	1490	0.1346769	121.5069	13611.51	19.93707	0.002716	2.850918		

WSP11465

Solvent	L	MDR	DATA
1/f/f	1/f/f	1/f/f	1/f/f/Slv 1/f/f/L
84.98972			
0.4			
4			
14.65810	363.4172	39.12598	28.41586 1.938577 0.078190
14.34257	303.9559	37.62721	28.39633 1.979863 0.093699
13.95491	242.4421	35.78583	28.39664 2.034885 0.117127
13.46371	182.7295	33.45264	28.25709 2.087759 0.154638
12.98661	139.8463	31.18643	27.27114 2.099941 0.196412
12.44419	101.6081	28.60992	25.40843 2.041790 0.250062
12.42766	100.6459	28.53140	25.65134 2.064052 0.254867
11.89052	73.87740	25.98000	23.29718 1.959306 0.315349
13.23387	140.0839	32.36088	26.87864 2.031049 0.167903
12.45132	102.0258	28.64377	25.24739 2.027687 0.247460
13.13482	151.2118	31.89041	27.25590 2.075087 0.180249
13.58385	195.7009	34.01854	28.07969 2.067289 0.1433482
12.86541	129.4892	30.61072	26.52354 2.061615 0.204831
11.87772	73.53487	25.91918	23.41665 1.971476 0.319311
11.51133	59.39007	24.17884	21.48657 1.866558 0.361787
11.22852	50.46730	22.83547	20.10596 1.790615 0.398395
11.05180	45.58594	21.99607	19.03298 1.722160 0.417518
10.70321	37.29784	20.34027	17.94879 1.676953 0.481228
10.46127	32.44888	19.19107	17.57741 1.661117 0.535531
10.52039	33.57211	19.47187	16.84237 1.600925 0.501677
10.16337	27.33524	17.77401	15.62950 1.537826 0.571771
9.727040	23.85833	16.65344	14.10652 1.421019 0.591261
9.792516	22.08051	16.01445	13.06543 1.334226 0.591717
9.622178	20.01818	15.20534	11.90419 1.237161 0.594669
9.346854	17.08416	13.89756	10.18056 1.089196 0.595906
9.049454	14.56443	12.58085	8.560738 0.943888 0.587783
8.816071	12.58629	11.37634	6.781882 0.769263 0.558870
8.589885	11.04972	10.30195	5.597636 0.651654 0.506586
8.154883	8.602031	8.335498	4.010988 0.491851 0.466283
8.397913	9.893694	9.390091	4.663808 0.555353 0.471391
7.818262	7.086727	6.636748	3.039169 0.391283 0.431675
7.546280	6.059687	5.344834	2.363658 0.313221 0.390062
7.316964	5.310325	4.255581	2.013767 0.275219 0.379217
6.952102	4.304330	2.522486	1.501944 0.216041 0.348938
10.70682	37.37547	20.35742	17.49325 1.633840 0.468040
11.00367	44.34024	21.76744	19.18590 1.743590 0.432697

Tw	8(U)/D	Log	Log
dyne/cm ²	(1/sec)	Tw	8 U/D
1.258125	69.10216	0.092768	1.839491
0.997132	51.66715	-0.00124	1.713214
0.752768	38.63382	-0.12276	1.586967
0.512758	24.30269	-0.39008	1.385654
0.335756	16.07422	-0.42509	1.206130
0.289880	12.02833	-0.53778	1.080205
0.190453	7.271673	-0.72021	0.861634

Regression Output:
 Constant -1.44127
 Std Err of Y Est 0.007797
 R Squared 0.999317
 No. of Observations 6
 Degrees of Freedom 4

X Coefficient(s) 0.835928
 Std Err of Coef. 0.010923

Tw vs. K'*(8(U)/D)^n

K' = 0.036201
 n = 0.835928

Tw Retro=24.65887
 Res/f/R =805.2684

Regression Output:
 Constant -3.35237
 Std Err of Y Est 0.459649
 R Squared 0.891827
 No. of Observations 9
 Degrees of Freedom 7

X Coefficient(s) 9.004054
 Std Err of Coef. 1.185241

t = 24.71111 deg C
 s.d.t = 0.416351 deg C

W1921468 Pusher 500-F

10 PSID Taps 14 1.0 PSID Taps 14 0.1 PSID Taps 14
S = 1 S = 7.25 S = 9.9 C (ppm) =
Z = 4.5 Z = 9.2 Z = 5.7 [NaCl] =
FlowCo = 0.018693

12/11/70 12:55

density viscosity
cofNaCl 1.00098 1.001574 ID(CM) = 1.01135
K.V.(psi) = 1.12785 1.17557
K.S(CM2) = 0.018207
72.78646 X coeff -0.00025 -0.00031
0.000160 constant 0.003419 -3.14977

Batch Vol (ml) t(samp) (sec) DF (psid) U (cm/s) Re (re) Iw (dyne/cm2) f Log(Iw/f)

Tap Pair	Freq. (Hz)	Dist Temp (l/s)	Temp (deg C)	V1 (volts)	V2 (volts)	V3 (volts)	V4 (volts)	V5 (volts)	V6 (volts)	V7 (volts)	V8 (volts)	V9 (volts)	V10 (volts)	V11 (volts)	V12 (volts)	V13 (volts)	V14 (volts)	V15 (volts)	V16 (volts)	V17 (volts)	V18 (volts)	V19 (volts)	V20 (volts)	V21 (volts)	V22 (volts)	V23 (volts)	V24 (volts)	V25 (volts)	V26 (volts)	V27 (volts)	V28 (volts)	V29 (volts)	V30 (volts)	V31 (volts)	V32 (volts)	V33 (volts)	V34 (volts)	V35 (volts)	V36 (volts)	V37 (volts)	V38 (volts)	V39 (volts)	V40 (volts)	V41 (volts)	V42 (volts)	V43 (volts)	V44 (volts)	V45 (volts)	V46 (volts)	V47 (volts)	V48 (volts)	V49 (volts)	V50 (volts)	V51 (volts)	V52 (volts)	V53 (volts)	V54 (volts)	V55 (volts)	V56 (volts)	V57 (volts)	V58 (volts)	V59 (volts)	V60 (volts)	V61 (volts)	V62 (volts)	V63 (volts)	V64 (volts)	V65 (volts)	V66 (volts)	V67 (volts)	V68 (volts)	V69 (volts)	V70 (volts)	V71 (volts)	V72 (volts)	V73 (volts)	V74 (volts)	V75 (volts)	V76 (volts)	V77 (volts)	V78 (volts)	V79 (volts)	V80 (volts)	V81 (volts)	V82 (volts)	V83 (volts)	V84 (volts)	V85 (volts)	V86 (volts)	V87 (volts)	V88 (volts)	V89 (volts)	V90 (volts)	V91 (volts)	V92 (volts)	V93 (volts)	V94 (volts)	V95 (volts)	V96 (volts)	V97 (volts)	V98 (volts)	V99 (volts)	V100 (volts)
12	60	1.181580	25	2.015	-0.0545	-0.0425	2.0625	0.0235	1.79277	1442.958	164485.2	791.7591	0.000762	2.557200																																																																																									
12	50	0.984650	25	1.468666	-0.0545	-0.0425	1.522166	0.0235	1.31241	1202.455	127071.0	582.7402	0.000808	2.590721																																																																																									
12	39	0.768027	25	0.9545	-0.0545	-0.0425	1.009	0.0235	0.86937	927.7229	103915.3	393.0280	0.000880	2.501397																																																																																									
12	30	0.592770	25	0.611666	-0.0545	-0.0425	0.666166	0.0235	0.57424	721.4792	82242.50	254.8552	0.000981	2.411173																																																																																									
12	22	0.432246	25	0.365	-0.0545	-0.0425	0.4195	0.0235	0.35187	529.0847	59711.24	160.4945	0.001149	2.319717																																																																																									
14	22	0.432246	25	1.204333	-0.0545	-0.0425	1.258833	0.0235	1.08576	529.0847	59711.24	160.5595	0.001150	2.319301																																																																																									
14	14	0.275702	25	0.573233	-0.0545	-0.0425	0.627833	0.0235	0.541204	253.6703	38379.38	80.07780	0.001416	2.159777																																																																																									
14	10	0.196930	25	0.349571	-0.0545	-0.0425	0.404071	0.0235	0.348281	240.4970	27414.20	51.52780	0.001737	2.024046																																																																																									
12	16	0.315088	24.9	3.1912	0.0695	0.02	3.1117	0.02	0.225576	384.7889	47633.37	100.0798	0.001755	2.207171																																																																																									
12	22	0.452939	24.9	5.62433	0.0695	0.02	5.55433	0.02	0.402614	552.1740	62910.57	178.9539	0.001171	2.277033																																																																																									
12	34	0.68562	24.9	10.17565	0.0695	0.02	10.10616	0.02	0.52494	817.6784	92998.24	235.0788	0.000874	2.404966																																																																																									
12	20	0.393860	24.8	4.47735	0.0235	0.0185	4.45525	0.0185	0.322916	480.7861	54581.57	142.2916	0.001242	2.234127																																																																																									
12	15	0.295395	24.8	2.948	0.0235	0.0185	2.9295	0.0185	0.21270	300.7256	40923.17	94.21982	0.001451	2.197194																																																																																									
12	10	0.196930	24.8	1.7	0.0235	0.0185	1.6815	0.0185	0.121976	240.4970	27290.78	54.0811	0.001875	2.072576																																																																																									
14	24.6	2.2245	24.6	7.2245	0.0485	0.0505	7.174	0.0505	0.230051	168.5510	18314.67	34.0265	0.002760	2.956990																																																																																									
14	24.4	2.47025	24.4	2.47025	0.0565	0.0565	2.4175	0.0565	0.174943	122.6234	14914.70	25.08100	0.002950	2.705567																																																																																									
14	24.2	1.9922	24.2	1.9922	0.0605	0.0595	1.927	0.0595	0.140082	115.1194	12917.05	20.72203	0.00312	2.859225																																																																																									
14	24.2	1.5508	24.2	1.5508	0.0645	0.0605	1.4907	0.0605	0.108016	90.69524	10176.51	15.97947	0.003895	2.902868																																																																																									
14	24.2	1.352666	24.2	1.352666	0.0625	0.0615	1.292166	0.0615	0.092655	77.11945	8653.25	12.85502	0.004671	2.771370																																																																																									
14	24.2	1.023142	24.2	1.023142	0.0655	0.0635	0.959642	0.0635	0.069554	57.25477	6425.482	10.28960	0.006272	2.707286																																																																																									
14	24.2	5.94	24.2	5.94	-0.0105	-0.0055	5.9455	-0.0055	0.070914	57.20150	6403.067	10.49078	0.006429	2.710306																																																																																									
14	24.2	4.748125	24.2	4.748125	-0.0115	-0.0105	4.758625	-0.0105	0.056759	45.07467	5041.757	8.296551	0.008301	2.662152																																																																																									
14	24.2	4.120545	24.2	4.120545	-0.0145	-0.0135	4.131045	-0.0135	0.049272	36.8053	4129.881	7.299192	0.010745	2.571441																																																																																									
14	24.25	3.752230	24.25	3.752230	-0.0145	-0.0135	3.762730	-0.0135	0.040144	27.86802	3123.424	5.828802	0.015232	2.507444																																																																																									
14	24.2	2.664941	24.2	2.664941	-0.0155	-0.0145	2.67441	-0.0145	0.034825	20.25516	2263.741	4.727350	0.02008	2.377477																																																																																									
14	24.1	2.059954	24.1	2.059954	-0.0155	-0.0145	2.069454	-0.0145	0.0304825	14.18170	1584.059	3.572708	0.026518	2.481310																																																																																									
14	24	1.521692	24	1.521692	-0.0155	-0.0065	1.529192	-0.0065	0.021577	11.52008	1283.899	2.122854	0.047220	2.446101																																																																																									
14	24	1.763	24	1.763	-0.0085	-0.0125	1.7755	-0.0125	0.016470	8.739542	921.2891	1.542976	0.215420	2.291726																																																																																									
14	23.9	0.85596	23.9	0.85596	-0.0155	-0.0095	0.87146	-0.0095	0.015275	5.68722	530.2277	2.008247	0.125347	2.343354																																																																																									
14	23.8	1.128642	23.8	1.128642	-0.0085	-0.0095	1.138142	-0.0095	0.0098737	2.92905	252.1755	1.299971	0.207407	2.257128																																																																																									
14	23.8	0.72524	23.8	0.72524	-0.0115	-0.0085	0.73574	-0.0085	0.006828	2.210798	256.0429	1.138519	0.423265	2.221226																																																																																									
14	23.75	0.629093	23.75	0.629093	-0.0105	-0.0105	0.639593	-0.0105	0.006068	1.638422	191.1471	0.897023	0.671272	2.171517																																																																																									
14	23.7	0.496875	23.7	0.496875	-0.0115	-0.0115	0.508375	-0.0115	0.005007	1.221210	174.3797	0.40792	0.975828	2.129279																																																																																									
14	23.6	0.407233	23.6	0.407233	-0.0125	-0.0125	0.419833	-0.0125	0.003912	0.846706	97.20590	0.573252	1.618402	2.074452																																																																																									
14	23.5	0.3155	23.5	0.3155	-0.0125	-0.0125	0.328	-0.0125	0.002792	0.521049	57.22962	0.412597	2.057202	2.004439																																																																																									
14	23.4	0.219878	23.4	0.219878	-0.0135	-0.0145	0.22478	-0.0145	0.002094	0.329426	37.80426	0.215471	0.005294	2.252802																																																																																									
14	23.9	9.1752	23.9	9.1752	-0.0335	-0.0255	9.2107	-0.0255	0.019786	89.04223	9901.297	18.22219	0.004109	2.802562																																																																																									
14	24	11.9302	24	11.9302	-0.0395	-0.0295	11.9697	-0.0295	0.0142738	111.2647	12411.68	21.12047	0.003414	2.950482																																																																																									
14	24.1	4.9714	24.1	4.9714	-0.0195	-0.0265	4.9979	-0.0265	0.0059612	122.7729	13495.31	23.45211	0.001147	2.911756																																																																																									
12	24.2	6.63625	24.2	6.63625	-0.0295	-0.0295	6.66575	-0.0295	0.0079505	132.7626	18244.14	25.27978	0.001345	2.971366																																																																																									

Solvent	L	HDR	DATA
1/f/f	1/f/f	1/f/f	1/f/f
14.22912	283.8965	37.08832	26.21151
15.76288	243.5573	35.82370	35.17421
13.50517	198.3316	34.12456	33.70909
13.24455	161.0715	32.41163	31.91238
12.84285	127.8184	30.50355	29.49053
12.84230	127.8443	30.50523	29.48469
12.33895	90.28586	27.63505	26.56830
11.85618	72.43135	25.81688	23.65532
12.42868	100.7051	28.53626	27.16089
12.92203	134.5514	30.92715	29.22236
13.45186	181.4872	33.39635	32.02644
12.72649	120.2274	29.99834	28.37411
12.37223	97.49097	28.26860	26.24357
11.89014	72.86115	25.97818	23.09297
11.47998	58.32715	24.02982	20.16092
11.23425	50.63409	22.86269	18.40991
11.02725	45.20577	21.92696	17.85968
10.81147	39.59616	20.85450	16.82251
10.87756	36.96332	20.26592	16.63145
10.42914	31.85418	19.03844	12.62633
10.44202	32.09120	19.09961	12.47200
10.24861	28.70895	18.18089	10.97562
10.12576	26.74987	17.59739	9.646952
9.949775	24.17264	16.76145	8.075824
9.749735	21.54338	15.81124	6.581896
9.524440	18.94480	14.75059	5.225902
9.138802	15.15586	12.90931	3.428258
9.384407	17.45748	16.07593	4.596521
8.765304	12.22379	11.13519	2.154547
8.992418	13.94551	12.22353	2.824551
8.612512	11.19458	10.40943	1.815471
8.487707	10.41854	9.816612	1.535980
8.286311	9.278076	8.859980	1.220252
8.116156	8.412384	8.051742	1.002092
7.997809	7.418777	7.014594	0.785061
7.501957	6.257046	5.609298	0.572251
7.011154	5.580666	4.950483	0.474369
7.01041	59.67185	20.84944	15.59889
11.04193	45.27763	21.94917	17.11352
11.24140	50.84290	22.89665	17.81937
11.49246	58.64997	24.10245	19.37559
			1.685507

1/f/f	U/D	1/f/f	U/D
dyne/cm ² (1/1sec)	1/f/f	U/D	1/f/f
3.122854	90.25505	0.495740	1.955485
1.542976	29.69046	0.188359	1.472517
2.008243	44.40570	0.303816	1.647438
1.299971	22.96319	0.113933	1.361032
1.158579	18.10160	0.052516	1.257717
0.897033	12.82110	-0.04719	1.107925
0.740792	9.567991	-0.12030	0.980820
0.573752	6.623807	-0.22750	0.821752
0.412559	4.032743	-0.30346	0.610909

Regression Output:
 Constant -0.77739
 Std Err of Y Est 0.004910
 R Squared 0.999712
 No. of Observations 9
 Degrees of Freedom 7

X Coefficient(s) 0.652753
 Std Err of Coef. 0.004154

Tw vs. K*(B U/D)^m
 K* = 0.158267
 n = 0.552753

Regression Output:
 Constant -33.9491
 Std Err of Y Est 0.287448
 R Squared 0.991330
 No. of Observations 5
 Degrees of Freedom 3

X Coefficient(s) 19.24555
 Std Err of Coef. 1.039073
 t = 24.74024 deg C
 s.d.t = 0.489427 deg C

WSP11371

Pusher 500-F

12/25/90 12:30

10 PSID Taps 14 1.0 PSID Taps 14 0.1 PSID Taps 14
 S = 1 S = 7.25 S = 9.9 <C> (ppm) =
 Z = 4 Z = 9.3 Z = 6.95 [NaCl] =
 FlowCo = 0.019693

col[NaCl] 1.000125 1.001657
 density viscosity
 30.00705 X coeff -0.00025 -0.02281
 0.001000 constant 0.003419 -4.14933

ID(cm) = 1.02108
 K(V/psii)=1.159853 13.79691
 XS(cm2)= 0.818859

Tap Pair	Freq. (Hz)	Dist Temp (1/s)	Temp (deg C)	<U> (volts)	<U>e (volts)	<U>f (volts)	<U>corr (volts)	Batch Vol (gal)	t/samp (sec)	DP (psid)	<U> (cm/s)	Re	Tw (dyne/cm2)	f	Log (Re/f)
12	60	1.181580	24.8	3.3375	-0.0005	0.0115	3.328	2.877950	1442.958	163737.2	1277.067	0.001229	3.759092		
12	50	0.984650	24.8	2.2335	-0.0005	0.0115	2.2335	1.925675	1202.465	136447.6	854.5030	0.001185	3.671842		
12	41	0.807413	24.8	1.50625	-0.0005	0.0115	1.50675	1.299087	986.0216	111887.0	576.4595	0.001188	3.586269		
12	31	0.610483	24.8	0.8752	-0.0005	0.0115	0.8757	0.755009	745.5285	84597.55	335.0294	0.001208	3.468526		
12	20	0.393860	24.8	0.4156	-0.0005	0.0115	0.4161	0.358752	480.9861	54579.06	159.1935	0.001279	3.206947		
14	20	0.393860	24.8	1.24125	-0.0005	0.0115	1.24175	1.070609	480.9861	54579.06	158.3805	0.001372	3.205826		
14	15	0.295395	24.8	0.783	-0.0005	0.0115	0.7825	0.675516	360.7396	40934.30	99.93251	0.001539	3.205828		
14	10	0.196930	24.8	0.426	-0.0005	0.0115	0.4265	0.367719	240.4930	27269.53	54.59849	0.001886	3.073778		
12	16	0.315088	25.15	3.587166	0.0595	0.0395	3.527666	0.255685	384.7889	44009.38	113.4583	0.001576	3.276851		
12	26	0.512018	25.15	7.993	0.0595	0.0395	7.9335	0.575020	625.2819	71515.25	255.1605	0.001308	3.412840		
12	33	0.649869	25.15	12.241	0.0595	0.0395	12.1815	0.882915	793.6271	90769.35	391.7865	0.001247	3.505958		
12	20	0.393860	25.1	5.099333	0.0565	0.0345	5.042833	0.365504	480.9861	54949.71	162.1897	0.001405	3.312952		
12	10	0.196930	25.1	1.707666	0.0565	0.0345	1.651166	0.119676	240.4930	27474.85	53.10552	0.001841	3.071510		
12	8	0.157544	25.1	1.204333	0.0565	0.0345	1.147833	0.083194	192.3944	21979.88	36.91710	0.002000	2.992554		
14	24.8	3.44425	0.6375	0.0355	3.40875			2207	15.1	0.247066	178.4908	20253.93	36.54972	0.002300	2.987427
14	24.7	2.645333	0.0355	0.0305	2.414833			1754	15	0.173027	142.8002	16167.49	23.89262	0.002596	2.911588
14	24.6	1.923	0.0305	0.0255	1.8925			1498	14.9	0.137168	122.7767	13869.15	20.29199	0.002699	2.857677
14	24.6	1.3616	0.0285	0.0195	1.3221			1164	15	0.095825	94.76594	10704.99	14.17598	0.003165	2.779791
14	24.6	1.0515	0.0205	0.0175	1.034			1301	19.9	0.074944	79.83894	9018.801	11.08488	0.003487	2.726419
14	24.5	6.4166	0.0155	0.0185	6.3981			1307	20	0.075678	79.80611	8994.777	11.19548	0.003524	2.727551
14	24.5	4.111	0.0125	0.0145	4.0965			1237	25	0.048454	60.42550	6810.429	7.168111	0.002936	2.650732
14	24.5	3.1469	0.0085	0.008	3.1389			1374	35	0.037127	47.94124	5403.255	5.492489	0.004791	2.572914
14	24.4	2.6266	0.0005	0.0035	2.6231			1167	35	0.031026	40.71865	4578.970	4.589935	0.005550	2.532947
14	24.4	2.113454	-0.0015	0.0015	2.111954			1100	40.1	0.024980	33.49954	3767.153	3.695526	0.006602	2.489582
14	24.4	1.506	-0.0015	0	1.506			1164	60	0.017813	23.69148	2664.199	2.63219	0.009413	2.412452
14	24.35	1.081714	-0.0025	-0.0005	1.082214			1092	80	0.012800	16.66952	1872.439	1.893673	0.013684	2.340204
14	24.3	0.715545	-0.0025	0.001	0.714545			799	90	0.008451	10.84163	1216.436	1.250321	0.021338	2.249570
14	24.2	0.5405	-0.0005	0.0025	0.541			637	99.8	0.006399	7.794701	872.5983	0.946649	0.031339	2.188168
14	24.1	0.3755	0.0005	0.003	0.3725			422	100.1	0.004406	5.148360	575.0480	0.651805	0.049304	2.106147
14	24	0.291875	0.0015	0.0015	0.290375			315	100	0.003434	3.846813	428.7030	0.508102	0.068840	2.051079
14	24	0.21076	0.0005	0.0005	0.21026			220	100.1	0.002487	2.683979	299.1125	0.367915	0.102396	1.980977
14	23.9	0.159	-0.0005	-0.0015	0.1605			160	100	0.001898	1.953937	217.2632	0.280845	0.147479	1.921551
14	23.8	0.109964	-0.0025	-0.0035	0.113464			130	119.9	0.001342	1.274081	146.8962	0.198541	0.227026	1.845058
14	23.75	0.056896	-0.0045	-0.0055	0.062396			89	120	0.000738	0.702196	77.81519	0.109182	0.443920	1.714716
14	23.95	7.957	-0.0065	0.0065	7.9505			1532	20	0.094040	93.54473	10413.21	13.91189	0.003187	2.769304
14	24	11.5648	-0.0045	0.019	11.5458			1490	15.1	0.136566	120.5035	13429.35	20.20299	0.002789	2.850811
12	24.2	4.691	0.0155	0.0355	4.6555			1760	15	0.055066	143.2887	16040.83	24.43531	0.002386	2.894082
12	24.3	6.885	0.0315	0.0335	6.8525			2156	15	0.081053	175.5286	19694.4	35.56670	0.002340	2.979009

84.54326

0.4

4

Solvent	L 1//f	L 1//f	MDR 1//f	DATA 1//f	1//f/Siv	1//f/L
14.63636	358.8990	39.02275	28.51379	1.948147	0.079447	
14.28756	295.5770	37.36499	29.04852	2.033161	0.098946	
13.94547	241.1291	35.74102	29.00081	2.079585	0.120270	
13.47410	183.8259	33.50200	28.76279	2.134671	0.156467	
12.82779	126.7149	30.43201	26.92019	2.098583	0.212446	
12.82334	126.3910	30.41088	26.98918	2.104691	0.213537	
12.42335	100.3965	28.51093	25.48289	2.051208	0.253822	
11.89511	74.07279	26.00179	23.02594	1.955747	0.310855	
12.54740	107.8280	29.10018	25.50901	2.035010	0.236571	
13.25156	161.7038	32.44396	27.64129	2.085921	0.170937	
13.62383	200.3725	34.21320	28.31268	2.078172	0.141300	
12.85581	128.7753	30.56509	26.64937	2.074499	0.207100	
11.88604	73.68697	25.95870	23.30369	1.960592	0.316252	
11.57021	61.43766	24.45853	22.35994	1.932542	0.363945	
11.54970	60.71658	24.36111	20.84885	1.805140	0.343379	
11.24635	50.98802	22.92017	19.81775	1.762149	0.388674	
11.03070	45.03574	21.89586	19.24743	1.744895	0.427381	
10.71916	37.64189	20.41603	17.77439	1.658188	0.472197	
10.50567	33.28891	19.40197	16.93281	1.611777	0.508662	
10.51020	33.37575	19.42347	16.84377	1.602611	0.504670	
10.12292	26.70619	17.58390	15.93831	1.574476	0.596802	
9.891657	23.37729	16.48537	14.44605	1.460427	0.617952	
9.731791	21.32199	15.72600	13.42208	1.379200	0.629494	
9.543530	19.13210	14.83177	12.30639	1.289500	0.643232	
9.249811	16.15596	13.43660	10.30656	1.114245	0.637941	
8.96817	13.67994	12.06388	8.554472	0.956675	0.625343	
8.598280	11.10325	10.34183	6.847301	0.796357	0.616693	
8.352674	9.639569	9.175203	5.657776	0.677361	0.586944	
8.024591	7.980460	7.616810	4.503562	0.561220	0.564523	
7.604316	7.030063	6.570505	3.811336	0.488362	0.542148	
7.523911	5.982158	5.238580	3.125047	0.415348	0.523394	
7.285407	5.214731	4.105686	2.603959	0.357421	0.499346	
6.980233	4.374604	2.656117	2.098707	0.300664	0.479747	
6.458867	3.240387	0.179621	1.500885	0.232375	0.463180	
10.47721	36.74381	20.21678	17.71253	1.658909	0.482054	
11.00324	44.32937	21.76542	18.93405	1.720770	0.427122	
11.17633	48.97372	22.58757	20.47122	1.831658	0.418004	
11.51603	59.55108	24.20118	20.66965	1.794857	0.347091	

WSP11371

Tw dyne/cm2	8(U)/D (1/sec)	Log Tw	Log 8(U)/D
1.893673	130.6030	0.277305	2.115953
1.250321	84.94250	0.097021	1.929125
0.946649	61.07024	-0.02381	1.785829
0.508102	30.13917	-0.29404	1.479131
0.651805	40.33658	-0.18588	1.605699
0.367915	21.02855	-0.43425	1.322809
0.280845	15.30878	-0.55153	1.184940
0.198541	10.37396	-0.70214	1.015944
0.109182	5.501595	-0.96184	0.740488

Regression Outputs

Constant -1.61444
 Std Err of Y Est 0.005571
 R Squared 0.999746
 No. of Observations 7
 Degrees of Freedom 5

X Coefficient(s) 0.891927
 Std Err of Coef. 0.006353

Tw vs. R*(8(U)/D)^n

K' = 0.024296
 n = 0.891927

Tw)Retro=37.35936
 Res/f)R =982.1663

Regression Output:

Constant 1.728273
 Std Err of Y Est 0.145225
 R Squared 0.979781
 No. of Observations 6
 Degrees of Freedom 4

X Coefficient(s) 7.594196
 Std Err of Coef. 0.545460

t = 24.53331 deg C
 s.d.)t = 0.401925 deg C

Page 3

Dow Pusher 500-F

84.54326
82.58
84.54326
4

0.4

Solvent	L 1/f/f	MDR 1/f/f	1/f/f	1/f/f	1/f/f/SIV	1/f/f/L
14.67397	366.7522	39.20136	28.27025	1.926558	0.077082	
14.35588	305.3883	37.69047	28.29233	1.970782	0.092643	
15.98384	246.5133	35.92324	28.03953	2.005138	0.113744	
13.52536	189.3308	33.74548	27.38112	2.024427	0.146620	
12.91203	133.0115	30.83217	25.98516	2.012321	0.195345	
12.95375	136.2447	31.03035	25.36656	1.958239	0.186183	
12.54130	107.4501	29.07121	24.12323	1.923502	0.224506	
12.00521	78.91926	26.52475	21.89617	1.823889	0.277450	
13.72295	212.1384	34.68404	27.43745	1.999383	0.129337	
13.76595	217.4566	34.88828	26.76668	1.944411	0.123090	
13.56202	193.3688	33.91962	26.00934	1.976794	0.138643	
12.98372	138.6135	31.17270	24.93270	1.920304	0.179869	
12.59170	110.6129	29.31059	23.43346	1.861024	0.211850	
12.04182	80.60017	26.69866	21.43953	1.780422	0.265998	
11.77242	69.02197	25.41904	20.02875	1.701327	0.290179	
11.45907	57.63007	23.93041	18.60343	1.623467	0.322807	
11.20284	49.72698	22.71352	17.31527	1.545613	0.348206	
11.00334	44.33706	21.76685	16.80216	1.526976	0.378964	
10.71547	37.56192	20.39848	15.27283	1.425307	0.406604	
10.52818	33.72304	19.50888	14.40793	1.368510	0.427242	
10.52999	33.75817	19.51747	14.36823	1.364505	0.425622	
10.16768	27.39336	17.79354	13.31302	1.309426	0.485994	
9.869333	23.08146	16.38028	12.39845	1.256235	0.537160	
9.617024	19.95887	15.18086	12.36450	1.285689	0.619499	
9.293919	16.57142	13.64611	12.41546	1.335869	0.749209	
9.016459	14.12520	12.32818	11.19547	1.241670	0.792588	
8.698002	11.75927	10.81551	9.413168	1.082221	0.800488	
8.494132	10.45714	9.847128	8.568278	1.008729	0.819370	
8.270837	9.195795	8.706476	7.536455	0.911208	0.819554	
8.050277	8.099334	7.738816	6.411127	0.796460	0.791636	
7.828976	7.130570	6.687640	5.708348	0.729130	0.800345	
7.442562	5.708482	4.852172	4.578074	0.615120	0.801977	
6.900277	4.177817	2.276319	3.348553	0.485249	0.801459	
6.092175	2.633758	-1.56216	2.072474	0.340186	0.789887	
10.65981	36.37336	20.13316	15.24481	1.430146	0.419120	
10.96978	43.48369	23.60648	16.47195	1.501574	0.378807	
11.11228	47.20098	22.28335	17.42723	1.568285	0.369213	
11.38802	55.32054	23.59312	18.32311	1.608981	0.331217	

Page 4

Dow Pusher 500-F

W3711272

Tw	8(U)/D	Log	Log	Log
dyne/cm ²	(1/sec)	Tw	8(U)/D	8(U)/D
1.100457	99.70249	0.041573	1.998704	
0.850992	77.11801	-0.07007	1.887155	
0.664662	57.98203	-0.17759	1.763292	
0.516340	45.49814	-0.28706	1.657993	
0.332429	29.27805	-0.47830	1.466542	
0.178865	15.70721	-0.74747	1.192099	
0.070867	6.119435	-1.14955	0.786711	

Regression Output:

Constant	-1.92379
Std Err of Y Est	0.005386
R Squared	0.999862
No. of Observations	7
Degrees of Freedom	5

X Coefficient(s)	0.985289
Std Err of Coef.	0.005169

Tw vs. K*(8(U)/D)^n

K'	0.011918
n	0.985289

Tw* = 2.910660
Res/ft* = 277.7211

Regression Output:

Constant	-34.6655
Std Err of Y Est	0.366634
R Squared	0.992509
No. of Observations	19
Degrees of Freedom	17

X Coefficient(s)	18.02250
Std Err of Coef.	0.379730

t = 24.79210 deg C
s.d.t = 0.548745 deg C

WIP13163 Pusher 500-F 11/28/90 14:48
 10 PSID Taps 14 1.0 PSID Taps 14 0.1 PSID Taps 14
 S = 1 S = 7.25 S = 9.9 C (ppm)=
 Z = 5 Z = 6.85 Z = 6.9 [NaCl]=
 FlowCo = 0.019693 0.020236

24.7 6.463 0.0255 0.0655 6.7975
 24.7 7.87 0.0695 0.0715 7.7985
 24.7 10.1576 0.0835 0.0845 10.6721

Tap Pair	Temp (Hz)	Diest (l/s)	Temp (deg C)	<V> (volts)	<V>0 (volts)	<V>f (volts)	<V> corr (volts)
12	60	1.181580	25.3	7.188333	0.0495	0.0725	7.115833
12	50	0.984650	25.3	4.9385	0.0495	0.0725	4.866
12	59	0.748027	25.3	3.0885	0.0495	0.0725	3.016
12	29	0.571097	25.3	1.8316	0.0495	0.0725	1.7591
12	21	0.413553	25.3	1.077666	0.0495	0.0725	1.005166
12	15	0.295395	25.3	0.655666	0.0495	0.0725	0.583166
12	10	0.194930	25.3	0.388428	0.0495	0.0725	0.319728
12	7	0.137851	25.3	0.258666	0.0495	0.0725	0.186166
12	25	0.492325	24.6	1.54	0.0275	0.0625	1.4775
23	25	0.492325	24.6	1.539333	0.0275	0.0625	1.476833
34	25	0.492325	24.6	1.54475	0.0275	0.0625	1.48225
12	15	0.295395	24.55	0.68	0.0585	0.0165	0.6215
23	15	0.295395	24.55	0.693333	0.0585	0.0165	0.634833
34	15	0.295395	24.55	0.69725	0.0585	0.0165	0.63875
12	21	0.413553	25.4	1.2485	-0.0195	0.0085	12.24
12	15	0.295395	25.4	0.727333	-0.0195	0.0085	7.26833
12	10	0.194930	25.4	0.378666	-0.0195	0.0085	3.778166
12	8	0.157544	25.4	0.2780333	-0.0195	0.0085	2.771833
12	6	0.118158	25.4	1.852	-0.0195	0.0085	1.8435
14	25.25	4.913	-0.0425	-0.036	4.949		
14	25.2	3.749	-0.0365	-0.0405	3.7895		
14	25.2	3.0848	-0.0405	-0.0425	3.1273		
14	25.1	2.113	-0.0425	-0.0425	2.1555		
14	25.1	1.6335	-0.0405	-0.0425	1.676		
14	25	1.044571	-0.0395	-0.0405	1.085071		
14	25	6.712333	0.0135	0.0045	6.707833		
14	25	4.625875	6.0085	0.0015	4.624375		
14	25	3.4397	0.0045	0.0045	3.4332		
14	25	2.271538	0.0055	0.0075	2.266038		
14	24.9	0.999941	6.0085	0.0105	0.991441		
14	24.9	0.71175	0.0135	0.0195	0.69825		
14	24.9	0.53175	0.0225	0.0305	0.50925		
14	24.8	0.38264	0.0345	0.0435	0.34814		
14	24.7	0.2776	0.0465	0.0555	0.2266		
14	24.6	0.200888	0.0595	0.0655	0.136588		
14	24.5	0.127111	0.0675	0.0725	0.055611		
14	24.5	0.10604	0.0745	0.0785	0.02914		
14	24.4	0.154035	0.0805	0.0835	0.07175		
14	24.55	10.243	0.0845	0.0303	10.2135		
14	24.7	13.2358	0.0315	0.0295	13.2063		

15 0.976723 99.22513 11075.08 74.04553 0.006576 2.941735
 14.9 0.993525 117.2512 12639.04 41.50157 0.003398 2.004758
 14.9 0.120804 133.3496 14868.93 53.60603 0.005972 3.040344

1520
 1533
 1627

density viscosity
 1.01234 1.029478
 10.00012 X coeff -0.00025 -0.02281
 0.300100 constant 0.003419 -4.14933
 ID(cm) = 1.02108
 K(V/psi) = 1.17915 13.79691
 XS(cm2) = 0.818859

Batch Vol (ml)	t)saap (sec)	DP (psid)	(U) (cm/s)	Re	Tw (dyne/cm2)	f	Log(Re/f)
6.034714	1442.958	163087.3	2677.856	0.002548	3.215542		
4.136701	1202.465	135906.1	1831.191	0.002509	3.833016		
2.537774	927.9229	106006.7	1134.992	0.002556	3.729145		
1.491837	697.4299	78825.55	661.9910	0.002596	3.611075		
0.852450	505.0354	57080.57	378.2680	0.002938	3.490549		
0.494565	360.7356	40771.83	219.4594	0.003341	3.372326		
0.257929	260.4930	27181.22	118.8914	0.004072	3.239224		
0.157882	168.3451	19024.85	70.05892	0.004898	3.124381		
1.257021	601.2326	66888.37	556.0182	0.003047	3.567297		
1.253455	601.2326	66888.37	555.9675	0.003046	3.567277		
1.257049	601.2326	66888.37	557.8415	0.003057	3.568008		
0.527074	360.7396	40087.78	233.8851	0.003560	3.378761		
0.528382	360.7396	40087.78	238.9888	0.003638	3.383449		
0.541703	360.7396	40087.78	240.3921	0.003659	3.384720		
0.887155	505.0354	57209.49	393.6680	0.003058	3.500199		
0.526845	360.7396	40863.92	233.7833	0.003559	3.397041		
0.273841	240.4930	27242.61	121.5150	0.004162	3.244949		
0.200902	192.3944	21794.09	89.14888	0.004772	3.177692		
0.133616	144.2958	16345.56	59.29143	0.005642	3.089130		
15 0.358703	138.0782	15588.40	53.06478	0.005514	3.063559		
15 0.274662	115.9335	13073.62	40.63224	0.005989	3.005099		
15 0.226666	102.1746	11522.04	33.53192	0.006363	2.963393		
19.9 0.156230	79.34800	8927.769	23.11196	0.007272	2.881597		
20 0.121476	67.47188	7591.538	17.97061	0.007820	2.826940		
25 0.078345	51.29084	5737.973	11.63448	0.008761	2.715667		
35 0.080445	51.38854	5768.906	11.90071	0.008928	2.725480		
35 0.955459	41.10246	4614.184	8.204341	0.009621	2.655715		
40.2 0.041173	34.66172	3891.144	6.091016	0.010044	2.591028		
1157 49.9 0.027176	28.31544	3178.767	4.020295	0.009934	2.500822		
60 0.011890	21.85967	2448.448	1.758966	0.007292	2.320237		
89.9 0.008373	16.06999	1799.960	1.238801	0.009503	2.244209		
99.9 0.006107	11.94317	1337.725	0.903486	0.012548	2.175649		
99.9 0.004175	8.26347	923.5053	0.617833	0.017918	2.092095		
120 0.002717	5.525978	616.1549	0.402022	0.026031	1.997862		
343 99.9 0.001828	3.537242	371.2751	0.242229	0.043104	1.886955		
273 120 0.000866	1.263685	151.3709	0.098662	0.105100	1.690845		
134 120.5 0.000349	0.710596	78.87716	0.051698	0.203821	1.550507		
157 109.9 0.000860	1.744536	193.2151	0.127270	0.082834	1.745145		
1080 20 0.122476	55.94537	7238.288	18.11852	0.008253	2.822221		
1275 20 0.158380	77.85217	8680.777	22.42997	0.007658	2.880324		

83.30349

0.4

Solvent	L	MDR	1//f	1//f	1//f/Slv	1//f/L
15.26217	514.5445	41.99531	19.80967	1.297959	0.038499	
14.93206	425.4966	40.42750	19.96286	1.334912	0.046916	
14.31658	334.9853	38.45376	19.77825	1.362459	0.059042	
14.04830	255.8322	36.22943	19.25713	1.370780	0.075272	
13.56219	193.3878	33.92043	18.44757	1.360220	0.095391	
13.08930	147.3012	31.67420	17.29951	1.321652	0.117443	
12.55689	108.4187	29.14526	15.66911	1.247849	0.144524	
12.09752	83.22638	26.96323	14.28848	1.181107	0.171682	
13.86918	230.7689	35.37865	18.11562	1.306177	0.078501	
13.86911	230.7584	35.37827	18.11644	1.306244	0.078508	
13.87203	231.1470	35.39215	18.08599	1.303773	0.078244	
13.11504	149.5001	31.79647	16.75908	1.277851	0.112100	
13.13379	151.1225	31.88553	16.57917	1.263329	0.109706	
13.13888	151.5655	31.90968	16.55071	1.258152	0.109066	
13.40079	197.7332	34.10379	18.08291	1.329548	0.091451	
13.14816	152.3776	31.95378	16.76095	1.274775	0.109996	
12.57979	109.8574	29.25403	15.49884	1.232042	0.141081	
12.31076	94.09628	27.97615	14.47592	1.175874	0.153841	
11.85433	72.35022	25.80763	13.46610	1.135973	0.186123	
11.62039	63.23820	24.69689	12.92101	1.111924	0.204322	
11.49557	57.44779	23.90447	12.53534	1.094448	0.218204	
11.12638	47.58580	22.35035	11.72583	1.053880	0.244415	
10.90784	41.96047	21.31224	11.30757	1.036646	0.269481	
10.52626	33.68583	19.49977	10.68315	1.014904	0.317140	
10.54592	34.06906	19.59312	10.58510	1.005523	0.310636	
10.22286	28.28756	18.05859	10.19481	0.997256	0.360399	
9.964154	24.37354	16.82973	9.977890	1.001378	0.409373	
9.603290	19.80171	15.11563	10.03293	1.044738	0.506669	
8.881349	13.06824	11.68640	11.70991	1.318483	0.896058	
8.576837	10.96703	10.23997	10.25778	1.195987	0.935328	
8.302677	9.365897	8.937718	8.928838	1.075175	0.953121	
7.968382	7.726372	7.349816	7.470398	0.937505	0.966870	
7.591453	6.219327	5.559404	6.192037	0.815659	0.995612	
7.147823	4.817657	3.452162	4.816592	0.673854	0.999778	
6.363375	3.067071	-0.27396	3.084598	0.484742	1.005714	
5.802031	2.220178	-2.94035	2.220462	0.382704	1.000128	
6.580582	3.475566	0.757766	3.474525	0.527996	0.999700	
10.89328	41.61038	21.24311	11.00730	1.010466	0.264532	
11.12249	47.47927	23.35185	11.42706	1.027382	0.240674	

11.44707 57.23326 25.07760 12.09423 1.055535 0.211314
 11.61707 53.19008 24.07080 12.50101 1.075904 0.197831
 11.84137 71.81662 25.74655 12.94093 1.092779 0.180181

WIP13163

Tw	8<U>/D	Log	Log
dyna/cm2 (1/sec)	Tw	8<U>/D	8<U>/D
0.617653	64.74436	-0.20925	1.811202
0.402022	43.29516	-0.39574	1.636439
0.243329	26.14676	-0.61559	1.417417
0.127270	13.66855	-0.89527	1.135722
0.098662	10.68425	-1.00584	1.028744
0.051698	5.567410	-1.28651	0.746553

Regression Output:

Constant	-2.03292
Std Err of Y Est	0.001529
R Squared	0.999985
No. of Observations	5
Degrees of Freedom	3

X Coefficient(s) 1.000281
 Std Err of Coef. 0.002214

Tw vs. K*(8<U>/D)^n

K*	0.009269	958.4034
n	1.000281	

Tw# = 16.04068
 Res/ft# = 637.1778

Regression Output:

Constant	-18.9566
Std Err of Y Est	0.267569
R Squared	0.989581
No. of Observations	15
Degrees of Freedom	13

X Coefficient(s) 10.61729
 Std Err of Coef. 0.302153

t = 24.95930 deg C
 s.d.)t = 0.321080 deg C

Tap Pair	Freq. (Hz)	Dist (1/s)	Temp (deg C)	<V> (volts)	<W> (volts)	<X>f (volts)	<Y>corr (volts)
12	60	1.181580	25.4	2.096	-0.0445	-0.0405	2.1365
12	47	0.764957	25.4	1.49	-0.0445	-0.0405	1.5705
12	41	0.807413	25.4	1.070666	-0.0445	-0.0405	1.111166
12	32	0.530176	25.4	0.7315	-0.0445	-0.0405	0.772
12	23	0.452939	25.4	0.439	-0.0445	-0.0405	0.4795
12	25	0.493325	25.4	0.493	-0.0445	-0.0405	0.5335
14	25	0.493325	25.4	1.533	-0.0425	-0.0465	1.5795
14	20	0.393860	25.4	1.0918	-0.0425	-0.0465	1.1383
14	15	0.293395	25.4	0.8528	-0.0425	-0.0465	0.8993
14	10	0.196930	25.4	0.3744	-0.0425	-0.0465	0.4209
14	30	0.590790	25.4	2.0135	-0.0425	-0.0465	2.06
14	40	0.787720	25.4	3.228	-0.0425	-0.0465	3.2745
12	20	0.393860	23.5	0.754	-0.0745	-0.0455	0.3995
14	20	0.393860	23.5	1.08425	-0.0745	-0.0455	1.12975
12	30	0.590790	25.35	8.7035	0.0725	0.0325	8.631
12	25	0.493325	25.35	6.6485	0.0725	0.0325	6.576
12	20	0.393860	25.35	4.677	0.0725	0.0325	4.6045
12	15	0.293395	25.35	3.1005	0.0725	0.0325	3.028
12	10	0.196930	25.35	1.7535	0.0725	0.0325	1.681
12	35	0.689255	25.35	11.0305	0.0725	0.0325	10.958
14	25.1	2.9442	25.1	2.9442	0.0295	0.0285	2.9157
14	25	2.25075	25	2.25075	0.0285	0.0255	2.22725
14	25	1.9242	25	1.9242	0.0245	0.0235	1.9017
14	25	1.447166	25	1.447166	0.0245	0.0235	1.423666
14	24.9	1.261	24.9	1.261	0.0245	0.0235	1.2385
14	24.9	7.482833	24.9	7.482833	0.0195	0.0255	7.457333
14	24.8	5.136428	24.8	5.136428	0.0195	0.0195	5.116928
14	24.8	3.811625	24.8	3.811625	0.0185	0.0175	3.793125
14	24.7	3.0495	24.7	3.0495	0.0155	0.0155	3.034
14	24.7	1.647	24.7	1.647	0.0145	0.0135	1.6397
14	24.6	1.176437	24.6	1.176437	0.0125	0.0125	1.16397
14	24.5	0.8455	24.5	0.8455	0.0115	0.0115	0.834
14	24.5	0.700227	24.5	0.700227	0.0115	0.0125	0.688727
14	24.4	0.558227	24.4	0.558227	0.0115	0.0125	0.545727
14	24.3	0.440043	24.3	0.440043	0.0125	0.0135	0.428745
14	24.2	0.329136	24.2	0.329136	0.0125	0.0135	0.325836
14	24.1	0.257818	24.1	0.257818	0.0125	0.0125	0.245318
14	24	0.201681	24	0.201681	0.0125	0.0125	0.189781
14	23.9	0.153636	23.9	0.153636	0.0115	0.0115	0.142136
14	23.8	0.105045	23.8	0.105045	0.0105	0.0095	0.094545

14	23.8	0.058818	0.0095	0.0005	0.050218
14	24.1	8.6148	0.0075	0.0015	8.6132
14	24.1	11.52175	-0.0045	-0.0045	11.52625
14	24.1	13.1175	-0.0065	-0.0065	13.127
12	23.9	4.518	0.0515	0.0495	4.4685
12	23.8	5.8448	0.0485	0.0485	5.7963

84.78139

C. 4

Solvent	L	MDR	1//f	1//f	1//f/Siv	1//f/L
---------	---	-----	------	------	----------	--------

14.23539	284.9244	37.11814	35.85504	2.518724	0.125840	
17.94565	241.1542	35.74188	34.59631	2.480794	0.147461	
13.66755	205.4792	34.42087	33.97384	2.485730	0.145339	
13.55122	171.2722	32.91833	31.81206	2.382706	0.185739	
12.93757	134.9810	30.95345	29.01242	2.242493	0.214937	
13.03026	142.3788	31.39374	29.39670	2.294405	0.209979	
13.01891	141.4517	31.33983	30.09266	2.311457	0.212741	
12.73438	120.0816	29.96833	28.35842	2.226916	0.236159	
12.31120	94.11962	27.97820	27.13563	2.204141	0.288310	
11.87033	73.01933	25.98359	23.31978	1.964408	0.319339	
13.24960	161.5407	32.43563	31.62045	2.386519	0.195742	
13.65216	203.6671	34.34777	33.44012	2.449437	0.164190	
12.70415	118.0097	29.94472	27.64555	2.176107	0.234234	
12.65296	114.5831	29.60157	28.47228	2.250246	0.248485	
13.29538	165.8543	32.45309	30.76322	2.313834	0.185484	
13.05918	144.7695	31.33114	29.36985	2.248979	0.202873	
12.74963	121.1399	30.06074	28.07898	2.203337	0.231789	
12.38557	98.33680	28.33149	25.96904	2.096716	0.264751	
11.87440	73.19478	25.99340	23.33586	1.956802	0.317452	
13.50272	186.8796	33.63795	31.85261	2.358976	0.170444	
11.38877	55.34454	23.59670	18.66183	1.638616	0.337193	
11.15089	48.26170	22.46673	17.02498	1.526782	0.352783	
11.01263	44.59521	21.81477	16.15747	1.467042	0.362312	
10.76218	38.58534	20.62030	14.55620	1.352534	0.377246	
10.63720	35.90715	20.02671	13.21386	1.242231	0.368000	
10.61924	35.54392	19.94282	13.34890	1.257013	0.375560	
10.38845	29.37603	18.37014	11.99790	1.166152	0.408424	
10.02842	25.29222	17.13503	10.89315	1.086227	0.430691	
9.83024	22.56892	16.19498	10.34342	1.082691	0.471596	
9.292199	16.55502	13.63794	11.94171	1.285132	0.721234	
8.994411	13.94706	12.22345	11.15172	1.239851	0.799575	
8.700943	11.77920	10.82948	9.773735	1.123524	0.929914	
8.574705	10.70425	10.03985	8.925064	1.045737	0.833786	
8.328621	9.506824	9.040933	7.992629	0.959658	0.840725	
8.111063	8.39758	8.027551	7.061029	0.870543	0.841825	
7.872988	7.312687	6.895743	6.195384	0.786936	0.847210	
7.622307	6.330775	5.705961	5.363913	0.703712	0.847275	
7.392666	5.456851	4.615164	4.702832	0.536283	0.848018	
7.140376	4.797050	3.416790	4.046222	0.566667	0.847481	
6.782307	3.903533	1.715959	3.303230	0.487036	0.946217	

5.234475	2.947730	-0.38624	2.407857	0.386216	0.845535	
10.71318	37.51257	20.39763	14.26754	1.331774	0.380340	
10.95103	43.01650	21.51734	16.01811	1.462705	0.373371	
11.07891	46.30294	22.12484	17.05716	1.539603	0.368381	
11.08940	46.38353	22.17469	16.80299	1.522443	0.362424	
11.31144	52.93486	23.22937	18.74849	1.622117	0.346623	

WIP23169

Tw	B<U>/D	Log	Log
dyne/cm2 (1/sec)	Tw	B<U>/D	
0.744624	67.18856	-0.12806	1.827295
0.330103	29.80019	-0.48135	1.474219
0.568551	51.51176	-0.24523	1.711906
0.428055	38.69721	-0.36850	1.587679
0.330103	29.80019	-0.48135	1.474219
0.248013	22.21900	-0.60552	1.346724
0.164972	14.79366	-0.78258	1.170075
0.087800	7.867015	-1.05650	0.895810

Regression Output:

Constant -1.94712
 Std Err of Y Est 0.001210
 R Squared 0.999985
 No. of Observations 8
 Degrees of Freedom 6

X Coefficient(s) 0.994774
 Std Err of Coef. 0.001530

Tw vs. K's(B<U>/D)^n

K' = 0.011294
 n = 0.994774

Tw# = 8.152721
 Res/4# = 455.2875

Regression Output:

Constant -72.6186
 Std Err of Y Est 0.298369
 R Squared 0.992233
 No. of Observations 13
 Degrees of Freedom 11

X Coefficient(s) 31.16738
 Std Err of Coef. 0.831407

t = 24.75869 deg C
 s.d.)t = 0.623742 deg C

AZF11409

ALCOFER 507 8/10/90 12:11

10 PSD Taps 14 1.0 PSD Taps 14 0.1 PSD Taps 14

S = 2.7 S = 7.25 S = 9.9 C (ppm) =

Z = 2.7 Z = 9.05 Z = 6.85 [NaCl] =

Freq. (Hz)	Dist Temp (1/s)	Temp (deg C)	<U> (volts)	<U> (volts)	<U> (volts)	<U>f (volts)	<U>corr (volts)
60	1.21416	24.8	8.278233	0.0245	0.0455	8.253833	
51	1.032036	24.8	6.184	0.0245	0.0455	6.1595	
42	0.849912	24.8	4.415666	0.0245	0.0455	4.391166	
34	0.688024	24.8	3.027	0.0245	0.0455	3.0025	
30	0.60708	24.8	2.451333	0.0395	0.0385	2.412833	
24	0.485644	24.8	1.6545	0.0395	0.0385	1.616	
17	0.344012	24.8	0.919666	0.0395	0.0385	0.881166	
13	0.263068	24.8	0.618	0.0395	0.0385	0.5795	
10	0.20236	24.8	0.3846	0.0395	0.0385	0.3461	
8	0.161888	24.8	0.271	0.0395	0.0385	0.2325	
18	0.364248	24.8	11.3605	0.0375	0.0665	11.294	
13	0.263068	24.8	6.84725	0.0375	0.0665	6.58075	
10	0.20236	24.8	4.281125	0.0375	0.0665	4.214625	
8	0.161888	24.8	2.903	0.0375	0.0665	2.8365	
24.6	2.7774	24.6	2.7774	0.0735	0.0635	2.7139	
24.6	1.946	24.6	1.946	0.0645	0.0635	1.8815	
24.5	1.5126	24.5	1.5126	0.0635	0.0625	1.4491	
24.5	0.957	24.5	0.957	0.0645	0.0625	0.8925	
24.45	0.70425	24.45	0.70425	0.0605	0.0585	0.64375	
24.4	0.4452	24.4	0.4452	0.0605	0.0605	0.3847	
24.3	2.486285	24.3	2.486285	0.0075	0.0095	2.476785	
24.2	1.638571	24.2	1.638571	0.0105	0.0145	1.624071	
24.2	1.118888	24.2	1.118888	0.0155	0.0165	1.102388	
24.2	0.612833	24.2	0.612833	0.0175	0.0175	0.596333	
24.15	0.443928	24.15	0.443928	0.0175	0.0175	0.426428	
24.1	0.3276	24.1	0.3276	0.0185	0.0185	0.3091	
24.1	0.228818	24.1	0.228818	0.0185	0.0185	0.210318	
24	0.14976	24	0.14976	0.0185	0.0195	0.13026	
23.9	0.08775	23.9	0.08775	0.0195	0.0195	0.06825	
23.8	0.0361	23.8	0.0361	0.0195	0.0195	0.0166	
23.7	0.05712	23.7	0.05712	0.0195	0.017	0.04012	
23.8	4.088	23.8	4.088	0.017	0.0125	4.071	
24	5.531	24	5.531	0.0115	0.0145	5.5165	
24.1	8.894	24.1	8.894	0.0135	0.0165	8.8805	
24.2	11.93475	24.2	11.93475	0.0155	0.0165	11.91925	

density viscosity

co) [NaCl] = 1.00088 1.001574 ID (cm) = 1.45796

29.97317 X coeff -0.00025 -0.02281 K (V/psi) = 1.077888 12.75206

0.000100 constant 0.003419 -4.14933 XS (cm2) = 1.669479

Batch Vol (ml)	t (sec)	DP (psid)	<U> (cm/s)	Re	Tu dyne/cm2	f	Log (Re/f)
7.657412	727.2685	117840.3	1080.291	0.004095	3.877469		
5.714415	618.1782	100164.3	806.1776	0.004230	3.813914		
4.073861	509.0880	82488.25	574.7317	0.004447	3.740431		
2.785539	412.1188	66776.21	392.9780	0.004640	3.657887		
2.258482	363.6342	58920.18	315.8003	0.004789	3.610405		
1.499228	290.9074	47136.15	211.5079	0.005012	3.523362		
0.817493	206.0594	33388.10	115.3302	0.005447	3.391670		
0.557625	157.5748	25532.08	75.84705	0.006125	3.300568		
0.321090	121.2114	19640.06	45.29881	0.006183	3.188742		
0.215699	96.96914	15712.05	30.43044	0.006489	3.102353		
0.885660	218.1805	35352.11	124.9471	0.005263	3.409062		
0.516053	157.5748	25532.08	72.80378	0.005880	3.291776		
0.330505	121.2114	19640.06	46.62700	0.006364	3.195017		
0.222434	96.96914	15712.05	31.38060	0.006692	3.109029		
15.1	0.212820	93.81517	15132.57	0.00840	3.097464		
15	0.147544	76.03167	12264.06	0.00720	3.017920		
15	0.113626	64.23041	10449.80	0.007625	2.960271		
15	0.069988	48.55804	7814.860	0.008397	2.854986		
20	0.050482	40.19216	6461.175	0.008840	2.783548		
20	0.030167	30.09920	4833.204	0.009419	2.671258		
25	0.030601	30.09321	4821.353	0.009559	2.673777		
29.9	0.020066	23.51883	3759.555	0.010261	2.580750		
35.2	0.013620	19.82449	3169.004	0.009803	2.496615		
40	0.007368	15.82828	2530.198	0.009463	2.363192		
49.9	0.005268	12.32789	1968.428	0.009806	2.289878		
60.1	0.003819	9.129350	1456.065	0.012961	2.219512		
59.8	0.002598	6.380535	1017.549	0.016603	2.155901		
100	0.001609	3.893428	619.5743	0.0227055	2.030883		
100	0.000843	2.048542	325.2538	0.018965	0.056837	1.889543	
100.1	0.000205	0.520599	82.47184	0.028975	0.214047	1.581541	
99.9	0.000495	1.205173	190.4894	0.068932	0.096529	1.772202	
20	0.050299	39.82277	6310.186	7.096124	0.008966	2.776357	
15	0.068159	47.91912	7625.520	9.615763	0.008296	2.844309	
15	0.109723	63.93210	10196.70	15.47952	0.007593	2.948681	
14.9	0.147268	74.97413	11984.83	20.77634	0.007411	3.01572	

Tap DL= 122.2234
40.77743

Solvent	L	MDR	1/f/f	1/f/f	1/f/f/Slv	1/f/f/L
80.95545						
4						
0.4						
15.10987	471.3565	41.27192	15.62516	1.034102	0.033149	
14.85565	407.1875	40.06437	15.37441	1.034919	0.037757	
14.56172	363.8046	38.66820	14.99548	1.029787	0.043616	
14.23153	284.2910	37.09978	14.68042	1.031541	0.051638	
14.04162	254.8504	36.19770	14.44969	1.029061	0.056698	
13.69344	208.5654	34.54388	14.12510	1.031522	0.067725	
13.16668	154.0106	32.04174	13.54943	1.029069	0.087977	
12.80267	124.8959	30.31270	12.77667	0.997969	0.102298	
12.35497	96.52116	28.18610	12.71745	1.029339	0.131758	
12.00941	79.11033	26.54471	12.41308	1.033612	0.156908	
13.23624	160.3032	32.37218	13.78329	1.041329	0.085982	
12.76710	122.2646	30.14374	13.04097	1.021451	0.106574	
12.38007	97.92596	28.20533	12.53502	1.012515	0.128005	
12.03611	80.33592	26.67156	12.22371	1.015585	0.152157	
11.98985	78.22488	26.45183	12.09060	1.008402	0.154562	
11.57168	65.13285	24.94048	11.76831	1.008279	0.180481	
11.44092	57.03112	23.84440	11.45186	1.000955	0.200800	
11.01994	44.75761	21.84475	10.91275	0.990272	0.243818	
10.73419	37.96897	20.48742	10.63561	0.990816	0.280113	
10.28503	29.31829	18.35391	10.30330	1.001776	0.351429	
10.29350	29.46167	18.39417	10.22802	0.993637	0.347163	
9.925002	23.80293	16.63426	9.871564	0.994816	0.414750	
9.586461	19.61080	15.03569	10.09967	1.053535	0.515905	
9.052770	14.42356	12.50065	10.96382	1.211101	0.740132	
8.759514	12.18312	11.10769	10.09813	1.152818	0.828862	
8.478049	10.36077	9.77033	8.783519	1.036030	0.847766	
8.143604	8.546360	8.182122	7.442123	0.913861	0.870794	
7.723532	6.710627	6.186779	5.770458	0.747126	0.859898	
7.158174	4.864449	3.501330	4.194524	0.585976	0.865483	
5.926244	2.384741	-2.35033	2.161446	0.344724	0.906345	
6.488809	3.498984	1.271846	3.218613	0.481193	0.870134	
10.70543	37.34545	20.35079	10.56049	0.986461	0.282778	
10.97723	43.67062	21.64187	10.91341	0.994185	0.249902	
11.39472	55.53432	23.62494	11.47567	1.007104	0.206641	
11.65428	64.48407	24.85787	11.61608	0.996721	0.180138	

ASF11409

Tw	g(U)/D	Log	Log
dyne/cm2	(1/sec)	Tw	g(U)/D
1.921564	108.7793	0.283654	2.036546
1.039463	86.85169	0.016809	1.938778
0.743303	67.34460	-0.12883	1.830233
0.538789	50.09383	-0.26858	1.699784
0.227055	21.36370	-0.64386	1.329676
0.118965	11.24059	-0.92457	1.050789
0.069932	6.612928	-1.15331	0.820393
0.028935	2.856593	-1.53857	0.455848

Log Tw vs. Log g(U)/D

Regression Output:
 Constant -1.98364
 Std Err of Y Est 0.001319
 R Squared 0.999992
 No. of Observations 4
 Degrees of Freedom 2

X Coefficient(s) 1.008488
 Std Err of Coef. 0.002011

Tw = K'(g(U)/D)^n'

K' = 0.010383
 n' = 1.008488

Tw = 0.189848
 Res/fg = 99.97756

Regression Output:
 Constant -0.94047
 Std Err of Y Est 0.026063
 R Squared 0.998909
 No. of Observations 7
 Degrees of Freedom 5

X Coefficient(s) 4.270249
 Std Err of Coef. 0.063104

t = 24.42857 deg C
 s.d.(t) = 0.362390 deg C

AIP21603

ALCOER 507

8/4/90 12:25

0.1 PSID Taps 14

9.9 C>(ppm)

6.9 [NaCl]=

9.9 C>(ppm)

7.25 S =

9 Z =

2.7 S =

2.7 Z =

10 PSID

1.0 PSID Taps 14

0.1 PSID Taps 14

density viscosity

ID(cm) = 1.45795

K(V/psi)= 1.08859

12.79437

AS(cm2)= 1.669479

col[NaCl]1.00088

1.001574

99.94837 X coeff

-0.00025 -0.02281

0.000100 constant

0.003419 -4.14933

Batch	Vol	t	saep	DP	U>	Re	Tw	f	Log				
(ml)	(sec)	(psid)	(cm/s)						(Re/f)				
60	1.21416	24.8	7.231666	0.0245	0.0345	7.187164	6.602271	727.2685	117840.3	931.4344	0.003531	3.845275	
50	1.0118	24.8	5.175666	0.0245	0.0345	5.141164	4.722775	606.0571	98200.31	666.2792	0.003437	3.772527	
41	0.829676	24.8	3.644	0.0245	0.0345	3.6095	3.315757	494.9568	80524.25	467.7799	0.003798	3.595719	
32	0.647552	24.8	2.374	0.0245	0.0345	2.3395	2.149110	387.8785	62848.20	303.1919	0.004041	3.601557	
25	0.5059	24.7	1.554	0.0335	0.0315	1.5225	1.398598	303.0385	48989.51	197.3112	0.004308	3.507389	
19	0.384484	24.7	0.98875	0.0325	0.0315	0.95722	0.879348	230.3017	37232.02	124.0566	0.004690	3.406535	
14	0.283304	24.7	0.61375	0.0335	0.0315	0.58221	0.524866	169.6760	27434.12	75.45778	0.005254	3.298565	
10	0.20236	24.7	0.557166	0.0335	0.0315	0.355664	0.299165	121.2114	19595.80	42.20538	0.005760	3.172397	
7	0.141652	24.7	0.220571	0.0335	0.0315	0.189071	0.175684	84.84800	13717.06	24.50306	0.006825	3.054324	
18	0.364248	24.4	10.2885	0.0395	0.0575	10.231	0.799648	218.1805	35034.53	112.8127	0.004752	3.282927	
14	0.283304	24.4	7.1415	0.0395	0.0575	7.084	0.553681	169.6760	27249.07	78.11214	0.005439	3.203117	
10	0.20236	24.4	3.687909	0.0395	0.0575	3.630405	0.283750	121.2114	19463.62	40.03092	0.005463	3.157956	
7	0.141652	24.4	2.16325	0.0395	0.0575	2.10572	0.164584	84.84800	13624.53	23.21917	0.006467	3.039481	
23.8	2.7208	23.8	2.7208	0.0315	0.0205	2.6872	15	0.210194	97.23589	15403.81	29.65372	0.006388	3.086886
23.8	1.89875	23.8	1.89875	0.0175	0.0155	1.88121	14.9	0.147037	77.10476	12214.70	20.74371	0.006995	3.009290
23.75	1.388	23.75	1.388	0.0145	0.013	1.3731	15	0.107351	65.09014	10299.75	15.14497	0.007166	2.940488
23.8	0.721666	23.8	0.721666	0.0135	0.0105	0.708164	19.9	0.055349	48.61142	7700.873	7.808641	0.006625	2.797134
23.7	0.554	23.7	0.554	0.0125	0.0115	0.5411	20	0.042323	40.13226	6343.204	5.970881	0.007432	2.737881
23.6	3.424166	23.6	3.424166	0.0185	0.0195	3.404664	20	0.042797	40.13226	6329.010	6.037731	0.007515	2.729213
23.6	2.58	23.6	2.58	0.0195	0.0205	2.5595	25	0.032173	29.94945	4723.141	4.538938	0.010144	2.677353
23.6	2.12222	23.6	2.12222	0.0205	0.0205	2.101721	30	0.026418	23.46040	3699.794	3.727129	0.013576	2.634563
23.6	1.79633	23.6	1.79633	0.0195	0.0195	1.776863	40	0.022335	19.42222	3062.957	3.151035	0.016746	2.598102
23.55	1.554583	23.55	1.554583	0.0175	0.0175	1.517082	44.9	0.019069	16.00861	2521.773	2.690349	0.021045	2.563298
23.5	1.22675	23.5	1.22675	0.0165	0.0165	1.21021	60.1	0.015213	12.27891	1925.773	2.146220	0.028724	2.513728
23.4	0.949187	23.4	0.949187	0.0145	0.0145	0.934687	60	0.011749	9.094650	1427.803	1.657346	0.040173	2.456639
23.3	0.6514	23.3	0.6514	0.0125	0.0155	0.6355	59.9	0.007993	5.849893	916.3375	1.127485	0.066058	2.372015
23.1	0.318	23.1	0.318	0.0125	0.0145	0.3021	106	0.003815	2.575653	401.6341	0.538217	0.162629	2.209429
23.05	0.475235	23.05	0.475235	0.0145	0.0135	0.460731	74.8	0.005791	3.943898	617.4131	0.817053	0.104225	2.299583
22.95	0.247041	22.95	0.247041	0.0125	0.0135	0.233541	100	0.002935	1.916745	297.8807	0.414155	0.225956	2.151034
22.85	0.17504	22.85	0.17504	0.0135	0.0125	0.16154	99.9	0.002030	1.295111	200.8172	0.286470	0.342336	2.070027
22.75	0.117583	22.75	0.117583	0.0125	0.0115	0.105082	100.1	0.001320	0.852779	127.7550	0.186251	0.547749	1.975669
22.6	0.064666	22.6	0.064666	0.0105	0.0095	0.054164	300.1	0.000480	0.405180	62.47214	0.096057	1.172719	1.870290
22.8	4.233	22.8	4.233	0.0095	0.0045	4.2281	20	0.035152	47.91912	7421.861	7.498692	0.006545	2.778487
23.1	8.6026	23.1	8.6026	0.003	0.0055	8.5971	20	0.108066	64.09183	9994.151	15.24583	0.007429	2.925526
23.4	11.4785	23.4	11.4785	0.0025	0.0045	11.474	15	0.144229	75.29275	11826.19	20.24763	0.007176	3.001163

ALP21403
 Tw 8<U>/D Log Log 8<U>/D
 dyne/cm2 (1/sec) Tw 8<U>/D
 2.690349 87.84118 0.429808 1.943698
 2.146220 67.15636 0.331574 1.827087
 1.657546 49.90343 0.219465 1.698120
 1.127655 32.09906 0.052188 1.506492
 0.528217 14.13291 -0.26904 1.150231
 0.817033 21.75038 -0.08774 1.337466
 0.414355 10.51751 -0.38283 1.021913
 0.286470 7.106430 -0.54292 0.851651
 0.186351 4.531148 -0.72966 0.656208
 0.096057 2.223275 -1.01746 0.346993

Log Tw vs. Log 8<U>/D

Regression Output:
 Constant -1.34315
 Std Err of Y Est 0.002817
 R Squared 0.999943
 No. of Observations 6
 Degrees of Freedom 4

X Coefficient(s) 0.937511
 Std Err of Coef. 0.003531

Tw = K' (8<U>/D)^{n'}
 K' = 0.045377
 n' = 0.937511

Tw* = 2.900532
 Res/# = 390.7851

Regression Output:
 Constant -4.57007
 Std Err of Y Est 0.119655
 R Squared 0.993003
 No. of Observations 8
 Degrees of Freedom 6

X Coefficient(s) 5.608864
 Std Err of Coef. 0.192205

t = 23.82571 deg C
 s.d.t = 0.698403 deg C

Tap DL= 122.2234
 40.77743

Solvent	L	MDR	1//f	1//f	1//f	1//f	1//f	1//f	1//f
79.55358									
4									
0.4									
14.98110	437.6785	40.66022	16.82747	1.123246	0.038447				
14.69010	370.1751	39.27801	16.58004	1.128653	0.044789				
14.38287	310.1700	37.81867	16.22582	1.128134	0.052312				
14.00623	249.7111	36.02960	15.73022	1.123087	0.062993				
13.62915	200.9878	34.23850	15.23397	1.117748	0.075795				
13.22609	159.3690	32.32395	14.60134	1.103979	0.091619				
12.79426	124.2927	30.27275	13.79511	1.078226	0.110988				
12.29959	92.95609	27.87555	13.17544	1.072061	0.141738				
11.81729	70.82278	25.63215	12.10422	1.024280	0.170896				
13.13174	150.9445	31.87580	14.50637	1.104679	0.096104				
12.81247	125.6023	30.35923	13.55920	1.058281	0.107953				
12.23182	89.91581	27.60116	13.52906	1.106054	0.150463				
11.75872	68.47968	25.35395	12.43483	1.057498	0.181584				
11.94754	76.34256	26.25084	12.61076	1.055510	0.165186				
11.63716	63.85139	24.77651	11.95618	1.027413	0.187250				
11.36195	54.49653	23.46928	11.81239	1.039644	0.216755				
10.78853	39.17552	20.74556	12.28584	1.138786	0.313610				
10.55152	34.17914	19.61974	11.59937	1.099307	0.339369				
10.55725	34.29206	19.64695	11.53512	1.092625	0.336378				
10.30941	29.73266	18.46972	9.928350	0.963037	0.333920				
10.13625	26.94287	17.65671	8.582496	0.846545	0.318544				
9.992413	24.77327	16.96396	7.727474	0.773334	0.311927				
9.853153	22.86485	16.30248	6.893147	0.699587	0.301473				
9.654914	20.39899	15.36084	5.900322	0.611122	0.289246				
9.426556	17.88624	14.27614	4.989183	0.529268	0.278939				
9.088060	14.71957	12.66828	3.890770	0.428118	0.264326				
8.437718	10.12301	9.579163	2.479710	0.293883	0.244957				
8.798333	12.45843	11.29208	3.097365	0.252039	0.248615				
8.204218	8.849826	8.470039	2.103719	0.256419	0.227713				
7.880109	7.343572	6.930520	1.709124	0.216890	0.232737				
7.502676	5.909477	5.137712	1.351166	0.180091	0.228644				
6.921161	4.228345	2.375317	0.923427	0.133420	0.218389				
10.71395	37.52908	20.39127	12.36018	1.153453	0.329249				
11.34210	53.87736	23.37500	11.59363	1.022176	0.215185				
11.60465	62.66764	24.52210	11.80453	1.017224	0.186267				

ALCOLMER 507 B/6/90 11:55
 10 PSID Taps 14 1.0 PSID Taps 14 0.1 PSID Taps 14
 S = 2.7 S = 7.25 S = 9.9 C<(pna)>=
 Z = 2.7 Z = 6.9 [NaCl]=

Freq. (Hz)	Q _{est} (1/s)	Temp (deg C)	<V> (volts)	<V> ₀ (volts)	<V> _f (volts)	<V> _{corr} (volts)
60	1.21416	24.7	6.088666	0.0395	0.0565	6.049166
51	1.032036	24.7	4.633	0.0395	0.0565	4.5935
44	0.890384	24.7	3.60375	0.0395	0.0565	3.56425
38	0.768968	24.7	2.850666	0.0395	0.0565	2.811666
32	0.647552	24.6	2.155333	0.0375	0.0375	2.117833
25	0.5059	24.6	1.4815	0.0375	0.0375	1.444
19	0.384484	24.6	0.975	0.0375	0.0375	0.969166
14	0.283304	24.6	0.606666	0.0375	0.0375	0.599166
9	0.182124	24.6	0.333333	0.0375	0.0375	0.295833
18	0.364248	24.6	10.33625	0.0495	0.0765	10.25975
15	0.30354	24.6	7.519833	0.0495	0.0765	7.443333
10	0.20336	24.6	4.092142	0.0495	0.0765	4.015642
8	0.161888	24.6	2.893125	0.0495	0.0765	2.816625
24	2.89725	24	2.89725	0.0445	0.0445	2.83275
24	1.9844	24	1.9844	0.0595	0.0385	1.9249
23.9	1.4578	23.9	1.4578	0.0465	0.0375	1.4113
23.9	0.772	23.9	0.772	0.0445	0.0365	0.7275
23.8	0.634428	23.8	0.634428	0.0415	0.0355	0.592928
23.8	0.48	23.8	0.48	0.0405	0.0355	0.4395
23.7	2.831714	23.7	2.831714	0.0125	0.0065	2.825214
23.6	2.250222	23.6	2.250222	0.0015	0	2.250222
23.55	1.9555	23.55	1.9555	-0.004	-0.004	1.9595
23.5	1.634	23.5	1.634	-0.006	-0.006	1.64
23.5	1.25425	23.5	1.25425	-0.0075	-0.0075	1.26175
23.4	0.916058	23.4	0.916058	-0.0085	-0.0085	0.924558
23.4	0.6715	23.4	0.6715	-0.0085	-0.0085	0.68
23.3	0.426727	23.3	0.426727	-0.0085	-0.0075	0.434227
23.25	0.27124	23.25	0.27124	-0.0085	-0.0085	0.27974
23.05	0.118916	23.05	0.118916	-0.0085	-0.0115	0.128916
22.9	0.042590	22.9	0.042590	-0.0115	-0.0135	0.056079
23	3.854666	23	3.854666	-0.0135	-0.0195	3.854166
23.2	5.4254	23.2	5.4254	-0.0195	-0.0255	5.4509
23.45	7.914	23.45	7.914	-0.0255	-0.0215	7.9355
23.4	11.8768	23.4	11.8768	-0.0215	-0.0145	11.8913

density viscosity ID(cm) = 1.45795
 co)[NaCl]=1.000088 1.001574 K(V/psi)= 1.08859 12.79437
 299.7153 X coeff -0.00025 -0.02201 XS(cm2)= 1.689479
 0.000100 constant 0.003419 -4.14933

Batch	Vol (ml)	t ₀ (sec)	t ₁ (sec)	DP (psid)	<U> (cm/s)	Re	T _w (dyne/cm ²)	f	Log(Re/f)						
5.556882	727.2685	117574.8	783.9531	0.002972	3.806858	4.219678	618.1782	99938.60	595.3033	0.002123	3.747087				
3.274189	533.3302	86231.54	461.9157	0.003256	3.691995	2.583392	460.6034	74464.05	364.2184	0.003447	3.540454				
1.945482	387.8765	63565.26	274.4646	0.002658	3.577971	1.326486	303.0285	48879.11	187.1379	0.004086	3.494809				
0.861205	270.3017	37148.12	121.4970	0.004593	3.401011	0.523847	189.8960	27372.30	75.76222	0.005136	3.292345				
0.271758	109.0902	17596.48	38.33907	0.008460	3.150549	0.801895	218.1805	35192.96	113.1297	0.004765	3.385517				
0.581766	181.8171	29327.47	82.07435	0.004978	3.315832	0.313860	121.2114	19551.64	44.27872	0.006043	3.181823				
0.220145	98.96914	15641.31	31.05768	0.006823	3.104813	14.9	0.221405	96.15985	15302.22	31.23548	0.00772	3.100141			
1896	15	0.150448	75.71221	13048.33	21.22502	0.007423	3.016241	15	0.150448	75.71221	13048.33	21.22502	0.007423	3.016241	
1593	14.9	0.110306	64.03957	10167.86	15.56178	0.007607	2.947861	20	0.054860	47.67953	7570.304	8.021821	0.007074	2.803968	
1315	19.9	0.046342	39.58143	6270.370	6.537961	0.008366	2.758568	24.9	0.034351	29.32400	4645.418	4.846172	0.011399	2.693546	
1219	24.9	0.035513	29.27589	4627.346	5.010148	0.011719	2.699787	30	0.028034	23.08104	3639.968	3.955007	0.014883	2.647450	
1156	35	0.024631	19.47570	3067.929	3.474917	0.018266	2.618856	39.9	0.020615	16.13817	2339.316	2.908325	0.022386	2.579713	
1075	60	0.015860	12.03968	1894.424	2.237548	0.030945	2.522777	69.9	0.011621	8.603505	1350.697	1.639584	0.044404	2.454273	
1004	80	0.008547	6.251948	981.5172	1.205891	0.061847	2.387560	89.9	0.005458	3.877771	607.4142	0.770045	0.102657	2.289179	
835	100	0.003516	2.461845	385.1887	0.493082	0.164082	2.193205	100	0.001620	1.108129	172.6012	0.228616	0.273195	2.023012	
582	100	0.000705	0.479191	74.58623	0.099469	0.868294	1.840823	185	0.000705	0.479191	74.58623	0.099469	0.868294	1.840823	
411	80	0.004847	39.28043	6111.287	6.834860	0.008879	2.760730	1705	19.9	0.048447	39.28043	6111.287	6.834860	0.008879	2.760730
1505	15	0.068518	53.54962	8369.113	9.866458	0.006757	2.837589	1586	15	0.099750	53.53311	9954.128	14.07257	0.007073	2.921585
1341	15.1	0.149475	74.17944	11345.71	21.08766	0.007682	3.008920	1870	15.1	0.149475	74.17944	11345.71	21.08766	0.007682	3.008920

A3F21406

Tap DL= 122.2234
40.77743

79.55358

Solvent L MDR
1//f 1//f 1//f

0.4
14.82743 400.6258 39.93032 18.34236 1.237055 0.045784
14.58833 349.1106 38.79457 17.89164 1.226435 0.051249
14.36798 307.5213 37.74790 17.52348 1.219620 0.056982
14.16181 273.1080 36.76863 17.04088 1.203298 0.062396
13.91188 236.5112 35.58146 16.53337 1.188434 0.069905
13.57923 195.2943 34.00138 15.64277 1.151962 0.080098
13.20404 157.3590 32.21922 14.75452 1.117424 0.093763
12.77058 122.6099 30.16026 13.95293 1.092284 0.113799
12.20219 88.39537 27.46044 12.44160 1.019619 0.140749

13.14206 151.8438 31.92482 14.48567 1.102237 0.095398
12.86332 129.3339 30.60081 14.17335 1.101764 0.109579
12.32730 94.99620 28.05469 12.86343 1.043491 0.135410
12.01925 79.55971 26.59145 12.28740 1.022310 0.154442
12.00056 78.70850 26.50269 12.15103 1.012338 0.154380
11.66696 64.88161 24.90859 11.60607 0.994951 0.178880
11.39144 55.42963 23.60937 11.46483 1.006442 0.206835
10.81587 39.79684 20.87540 11.88887 1.099215 0.298741
10.53427 35.84662 20.01279 10.93263 1.028056 0.304983
10.37418 30.86217 18.77738 9.407588 0.906826 0.304825

10.39914 31.30885 18.89595 9.237294 0.888274 0.295037
10.18980 27.75430 17.90155 8.196853 0.804417 0.295736
10.07542 25.98581 17.35827 7.578854 0.732361 0.283937
9.918852 23.74614 16.61454 6.683496 0.673817 0.281456
9.691111 20.82849 15.53277 5.684594 0.586578 0.272923
9.417092 17.78906 14.23119 4.745530 0.503927 0.266766
9.150241 15.25599 12.96364 4.021022 0.439445 0.263570
8.756717 12.16352 11.09440 3.121085 0.356421 0.256593
8.372821 9.751814 9.270902 2.468699 0.294846 0.253152
7.693049 6.590104 6.037333 1.656936 0.212808 0.248393
6.963304 4.332177 2.575697 1.073164 0.154117 0.247719
10.64132 35.99236 20.04627 10.61229 0.997272 0.294848
10.95027 42.99813 21.51382 12.16493 1.110924 0.282917
11.28634 52.17538 23.11012 11.92387 1.056487 0.228554
11.63568 63.79705 24.76949 11.40894 0.980513 0.178831

Tw 8<U>/D Log 8<U>/D
dyne/cm2 (1/sec) Tw 8<U>/D
2.908225 88.55209 0.463643 1.947198
2.237548 66.06315 0.349772 1.819959
1.639584 47.20845 0.214733 1.674019
1.205891 34.30518 0.081308 1.575359
0.770045 21.27779 -0.11348 1.327926
0.496082 13.50843 -0.30444 1.130305
0.228616 6.080439 -0.64089 0.783935
0.099469 2.629379 -1.00230 0.419853

Log Tw vs. Log 8<U>/D

Regression Output:
Constant -1.40432
Std Err of Y Est 0.004638
R Squared 0.999918
No. of Observations 6
Degrees of Freedom 4

X Coefficient(s) 0.969315
Std Err of Coef. 0.004378

Tw = K' (8<U>/D)^{n'}

K' = 0.039416
n' = 0.969315

Tw8 = 27.67825
Res/ft = 1204.434

Regression Output:

Constant -15.9009
Std Err of Y Est 0.104478
R Squared 0.997557
No. of Observations 9
Degrees of Freedom 7

X Coefficient(s) 9.031505
Std Err of Coef. 0.168910

t = 23.93529 deg C
s.d.t = 0.601411 deg C

ALF31412 ALCOLMER 507 8/12/90 12:46
 10 PSID Taps 14 1.0 PSID Taps 14 0.1 PSID Taps 14
 S = 2.7 S = 7.25 S = 9.9 (C) (ppm) =
 Z = 2.7 Z = 9.05 Z = 6.9 [NaCl] =

Freq. (Hz)	Dist Temp (1/s)	Temp (deg C)	<V> (volts)	<V>0 (volts)	<V>f (volts)	<V>corr (volts)
60	1.21416	24.9	5.173333	0.0425	0.0425	5.170833
50	1.01118	24.9	3.945	0.0425	0.0425	3.9025
40	0.80944	24.9	2.898333	0.0425	0.0425	2.855833
29	0.586844	24.9	1.814666	0.0425	0.0425	1.772166
25	0.5059	24.9	1.5333	0.0485	0.0485	1.485
18	0.364248	24.9	1.003	0.0485	0.0485	0.9545
15	0.30354	24.9	0.761666	0.0485	0.0485	0.713166
10	0.20236	24.9	0.43325	0.0485	0.0485	0.38475
18	0.364248	24.7	10.953	0.0225	0.0535	10.8995
15	0.30354	24.7	8.681833	0.0225	0.0535	8.628333
10	0.20236	24.7	4.796	0.0225	0.0535	4.7425
7	0.141652	24.7	2.37925	0.0225	0.0535	2.32575
		24.2	2.5172	0.0685	0.062	2.4487
		24.1	2.0208	0.0615	0.0595	1.9593
		24	1.6942	0.0615	0.0595	1.6327
		24	1.274	0.0615	0.0565	1.2125
		24	1.091	0.0575	0.0575	1.0335
		22.9	0.869428	0.0575	0.0575	0.811928
23.9	5.1468	-0.0025	-0.0085	-0.0085	5.1533	
23.9	4.17022	-0.0135	-0.0105	-0.0105	4.180722	
23.9	3.582625	-0.0135	-0.0125	-0.0125	3.595125	
23.9	3.158818	-0.0145	-0.0145	-0.0145	3.173318	
23.85	2.509846	-0.0155	-0.0145	-0.0145	2.524746	
23.8	1.788428	-0.0165	-0.0165	-0.0165	1.804928	
23.7	1.175133	-0.0175	-0.0165	-0.0165	1.191633	
23.6	0.717066	-0.0165	-0.0165	-0.0165	0.733566	
23.3	0.409260	-0.0195	-0.0185	-0.0185	0.427760	
23.2	0.207272	-0.0195	-0.0225	-0.0225	0.229772	
23.1	0.094695	-0.0235	-0.0245	-0.0245	0.119195	
23.3	7.07525	-0.0255	-0.0275	-0.0275	7.10075	
23.33	9.926	-0.0305	-0.0305	-0.0305	9.9565	
23.6	12.49825	-0.0315	-0.0305	-0.0305	12.52975	

density viscosity ID(cm) = 1.45786
 co[NaCl] 0.000888 1.001574 K(U/psi)=1.077888 12.75147
 999.6909 X coeff -0.00025 -0.02281 XS(cm2) = 1.669479
 0.000100 constant 0.000419 -4.14933

Batch Vol (ml)	t(samp)	DP (psid)	<U> (cm/s)	Re	Tw (dyne/cm2)	f	Log(Re/f)
4.76080	727.2485	118106.5	671.5420	0.002546	3.775220		
3.520506	606.0571	98422.10	510.7733	0.002788	3.715798		
2.549471	484.8457	78737.68	373.7817	0.003188	3.647992		
1.644110	351.5121	57084.82	231.9475	0.003764	3.544379		
1.377694	303.0285	49211.05	194.3621	0.004244	3.505990		
0.88527	218.1805	25431.95	124.9284	0.005263	3.410014		
0.661633	181.8171	29526.63	93.34183	0.005662	3.346722		
0.356948	121.2114	19684.42	50.35747	0.006873	3.212715		
0.854764	218.1805	35272.44	120.5883	0.005079	3.400366		
0.576554	181.8171	29593.70	95.46091	0.005790	3.349623		
0.371917	121.2114	19595.80	53.46938	0.007161	3.219566		
0.182390	84.84800	13717.06	35.73129	0.007167	3.064944		
15	0.192032	90.48728	14464.66	27.09157	0.005674	3.071205	
1757	15.1	0.153652	69.69594	11116.15	21.67702	0.008947	3.021802
1486	14.9	0.128040	59.73810	9506.323	18.06363	0.010148	2.981220
1143	15.1	0.095087	45.34069	7215.216	13.41468	0.013083	2.916607
1261	19.9	0.081049	37.95604	6040.071	11.43428	0.015912	2.881922
1184	25	0.063673	28.36812	4504.141	8.982898	0.022379	2.828540
1182	25	0.064671	28.32020	4496.532	9.123764	0.022807	2.831919
1130	30	0.052446	22.56192	3582.263	7.398972	0.029142	2.786418
1096	35	0.045099	18.75691	2978.124	6.362592	0.036258	2.753649
1161	39.9	0.039808	17.42923	2767.321	5.616085	0.037066	2.726549
1024	50	0.031667	12.26729	1945.540	4.467545	0.059520	2.676774
713	49.9	0.022462	8.558701	1355.843	3.194332	0.087428	2.602027
561	60.1	0.014948	5.591239	883.7494	2.108932	0.135247	2.511893
337	59.9	0.009202	3.59938	531.4520	1.298254	0.229184	2.405556
285	90	0.005366	1.896798	297.1146	0.757044	0.421808	2.285481
169	99.9	0.002882	1.013304	158.3664	0.406647	0.792897	2.149545
86	100	0.001495	0.515130	80.23682	0.210950	1.59252	2.066041
1242	19.9	0.089076	37.38414	5855.853	12.56678	0.018033	2.895522
1790	19.9	0.124901	53.87891	8487.329	17.62084	0.012168	2.971397
1656	15.1	0.157182	65.69045	10359.62	22.17494	0.010302	2.921907

Solvent	L 1/f/f	LDR 1/f/f	MDR 1/f/f	1/f/f/Slv	1/f/f/L
79.71477	122.2234				
0.4	40.77743				
Tap DL=					
14.70088	372.4782	39.32919	19.81768	1.348061	0.052204
14.46319	324.8466	38.20016	18.92626	1.309272	0.058292
14.19197	277.8902	36.91187	17.70880	1.247804	0.063723
13.77751	218.9067	34.94320	16.29826	1.182961	0.074453
13.62396	200.3872	34.21381	15.34873	1.126598	0.076595
13.24005	160.6552	32.39028	13.78415	1.041094	0.085799
12.98488	138.8480	31.18772	13.28897	1.023260	0.095694
12.45086	101.9990	28.48160	12.06164	0.968739	0.118252
13.20146	157.1254	32.20696	14.03036	1.062788	0.089294
12.99850	139.7998	31.24290	13.14097	1.010960	0.093998
12.47866	103.6446	28.77367	11.81670	0.946952	0.114011
11.85977	73.58130	25.83394	11.81180	0.995955	0.162739
11.88482	73.63512	25.95289	12.27730	1.033024	0.166731
11.58721	65.71772	25.01424	10.57187	0.904568	0.160867
11.52488	59.85494	24.24318	9.924418	0.861303	0.165841
11.26643	51.58075	23.01594	8.742620	0.775988	0.169493
11.12768	47.62139	22.35651	7.927203	0.712385	0.166463
10.91416	42.11342	21.34227	6.684538	0.612464	0.158727
10.92767	42.44234	21.40646	6.621531	0.605941	0.156012
10.74567	38.22064	20.54194	5.857866	0.545137	0.152264
10.61459	35.44291	19.91933	5.251621	0.494754	0.148171
10.50619	33.29884	19.40443	5.194101	0.494384	0.155984
10.30549	29.66567	18.45111	4.098888	0.397738	0.158169
10.01214	25.05631	17.05770	3.581990	0.337788	0.134975
9.22226	15.90144	13.30557	2.088851	0.226501	0.131362
8.741926	12.06400	11.02415	1.539722	0.176130	0.127667
8.198180	8.819119	8.441359	1.123333	0.136899	0.127260
7.624164	6.337344	5.714779	0.792172	0.103902	0.124996
11.18213	49.13752	22.61513	7.448295	0.666088	0.151580
11.48559	58.51639	24.05655	9.065119	0.789260	0.154915
11.68723	65.71855	25.01435	9.852271	0.842994	0.149916

A1F51412

Tw dyne/cm2	8<U>/D (1/sec)	Log Tw	Log 8<U>/D
6.362592	102.9214	0.803634	2.012505
5.616085	95.63626	0.749433	1.980622
4.467545	67.51211	0.650069	1.828093
3.194332	46.96261	0.504380	1.671752
2.108932	30.67973	0.324062	1.486851
1.298254	18.49125	0.113359	1.266966
0.757044	10.40796	-0.12087	1.017365
0.406647	5.560124	-0.39078	0.745084
0.210950	2.826582	-0.67581	0.451261

Log Tw vs. Log 8<U>/D

Regression Output:

Constant -1.10736

Std Err of Y Est 0.003694

R Squared 0.999951

No. of Observations 7

Degrees of Freedom 5

X Coefficient(s) 0.963220

Std Err of Coef. 0.003012

Tw = Y' (8<U>/D)^n'

K' = 0.078097

n' = 0.963220

Tw = 90.01278

Res/f# = 2181.907

Regression Output:

Constant -39.2712

Std Err of Y Est 0.176747

R Squared 0.995681

No. of Observations 9

Degrees of Freedom 7

X Coefficient(s) 15.64214

Std Err of Coef. 0.389344

t = 24.15 deg C

s.d. t = 0.586299 deg C

ALCOER 507 B/10/90 14:53

10 PSID Taps 14 1.0 PSID Taps 14 0.1 PSID Taps 14
 S = 2.7 S = 7.25 S = 9.9 <C> (ppm) =
 Z = 2.7 Z = 9 Z = 6.9 [NaCl] =

density viscosity
 co) [NaCl] 1.01234 1.029478
 K(V/psi) = 1.077888 12.75206
 XS(cm2) = 1.669479
 1.085095

Freq. (Hz)	Drest (1/s)	Temp (deg C)	<U> (volts)	<U>0 (volts)	<U>f (volts)	<U>corr (volts)	Batch Vol (ml)	t(samp (sec))	DP (psid)	<U> (cm/s)	Re	Tw (dyne/cm2)	f	Log(Re/f)	
60	1.21416	25.2	8.696333	0.0365	0.0615	8.634833			8.010881	727.2685	117102.8	1130.158	0.004233	3.881919	
49	0.991264	25.2	6.047	0.0365	0.0615	5.9855			5.52988	593.9360	95633.97	783.4038	0.004400	3.802742	
42	0.949912	25.2	4.571	0.0365	0.0615	4.5095			4.182644	509.0880	81971.97	590.2196	0.004512	3.740856	
35	0.70826	25.2	3.354666	0.0365	0.0615	3.293166			3.055203	424.2400	68309.97	431.0215	0.004744	3.672599	
30	0.60708	25.2	2.578	0.0405	0.0405	2.5375			2.354140	363.6342	58551.41	332.1171	0.004976	3.615995	
24	0.485664	25.2	1.748	0.0405	0.0405	1.7075			1.584116	290.9074	46841.12	233.4827	0.005232	3.539972	
17	0.344012	25.2	0.97	0.0405	0.0405	0.9295			0.862334	206.0594	33179.13	121.6563	0.005676	3.397917	
13	0.263068	25.2	0.621	0.0405	0.0405	0.5805			0.538553	157.5748	25372.27	75.97793	0.006062	3.295693	
9	0.192124	25.2	0.346571	0.0405	0.0405	0.306071			0.283954	109.0902	17565.42	40.05973	0.006669	3.156703	
20	0.40472	24.1	1.2845	0.0375	0.0555	1.249			1.158747	242.4228	38077.51	165.4736	0.005509	3.451236	
15	0.30254	24.1	0.786285	0.0375	0.0555	0.750785			0.696574	181.8171	28558.13	98.26554	0.005887	3.340713	
10	0.20236	24.1	0.405375	0.0375	0.0555	0.369875			0.343147	121.2114	19038.75	48.41057	0.006526	3.186982	
8	0.161888	24.1	0.282	0.0375	0.0555	0.2465			0.228687	96.76914	15231.00	32.26281	0.006796	3.093863	
18	0.364248	25.1	1.207875	0.0485	0.0745	1.200425		1990	0.941357	218.1805	35051.68	132.8047	0.005527	3.415971	
13	0.263068	25.1	0.978363	0.0485	0.0745	0.903863		1620	0.541392	157.5748	25315.10	76.37843	0.006094	3.295850	
10	0.20236	25.1	0.431363	0.0485	0.0745	0.266863		1865	0.336601	121.2114	19473.15	47.20492	0.006365	3.191358	
7	0.141652	25.1	2.54	0.0485	0.0745	2.4655		1166	0.195341	84.84800	13631.20	27.27618	0.007506	3.072256	
		25	2.158166	0.0685	0.0725	2.085666		1045	14.9	0.165523	79.99921	12833.26	33.07403	0.007143	3.034941
		24.9	1.5336	0.0695	0.0665	1.4671		1620	0.115048	65.12498	10415.51	16.23073	0.007581	2.937563	
		24.9	1.171285	0.0635	0.0615	1.109785		1865	20	0.087027	55.85573	8933.074	12.27771	0.007796	2.896957
		24.8	0.7346	0.0605	0.0585	0.6761		1393	20	0.053018	41.71958	6657.228	7.479791	0.008513	2.788353
		24.28	0.5595	0.0585	0.0565	0.503		1455	25	0.039444	34.86116	5497.947	5.564761	0.009070	2.719009
		24.7	3.211142	-0.0045	-0.0055	3.215642		1425	25	0.039750	34.86116	5550.288	5.605159	0.009137	2.724717
		26.7	2.434833	-0.0075	-0.009	2.442333		1253	24.9	0.030176	30.14189	4798.928	4.237209	0.009282	2.664986
		24.65	1.87275	-0.0115	-0.0115	1.88425		1276	30	0.033280	25.87632	4115.157	3.284419	0.009717	2.608160
		23.6	1.186111	-0.014	-0.017	1.200111		1186	35	0.014828	20.29717	3152.330	2.091903	0.010056	2.499957
		24.5	0.802333	-0.017	-0.0185	0.819333		1278	45	0.010123	17.01128	2696.195	1.428172	0.009726	2.435843
		24.5	0.438642	-0.0205	-0.0225	0.459142		1166	50	0.005672	12.96842	2213.918	0.800327	0.008125	2.300087
		24.45	0.291187	-0.0235	-0.025	0.314687		1045	59.9	0.003888	10.44980	1654.369	0.548529	0.009950	2.217560
		24.4	0.204733	-0.0255	-0.0255	0.230233		780	60	0.002844	7.786857	1231.392	0.401317	0.01110	2.149212
		24.3	0.1285	-0.027	-0.028	0.1555		660	75	0.001921	5.271103	821.6798	0.271050	0.019324	2.065008
		24.2	0.083	-0.0285	-0.0285	0.1115		589	90.1	0.001377	3.782738	595.4992	0.194354	0.026904	1.989795
		24.15	0.043857	-0.03	-0.031	0.074857		300	90.1	0.000924	2.526258	397.2488	0.110482	0.040498	1.902192
		23.6	0.004785	-0.0315	-0.0325	0.037285		210	99.9	0.000460	1.259136	195.5550	0.044992	0.081189	1.746018
		23.5	-0.014	-0.0325	-0.034	0.02		111	99.9	0.000247	0.665543	103.1318	0.034861	0.155871	1.609776
		23.6	4.2265	-0.0335	-0.037	4.2635		1026	15	0.052677	40.97085	6363.136	7.431669	0.008768	2.7375139
		23.8	6.986	-0.039	-0.039	7.025		1375	15	0.086797	54.90733	8566.158	12.34521	0.008044	2.892540
		23.8	9.15575	-0.039	-0.039	9.19475		1601	15	0.113605	63.92210	9974.133	16.02728	0.007766	2.943987
		23.8	12.91075	-0.0415	-0.0415	12.95225		1961	15	0.160031	78.30783	12216.89	22.57695	0.007292	3.019189

Solvent	L	MDR	Tap DL=	1/1'	1/1'	1/1'/Siv	1/1'/L
1/1'	1/1'	1/1'	122.2234				
80.93545			40.77743				
0.4							
15.12767	476.2111	41.35647	15.36907	1.015957	0.032272		
14.80937	396.4813	39.80451	15.07541	1.017964	0.038023		
14.56342	344.1412	38.67627	14.88704	1.022221	0.043258		
14.29029	294.0894	37.37938	14.51726	1.015875	0.049363		
14.06398	258.1520	36.30391	14.17561	1.007937	0.054911		
13.71989	211.7643	34.86948	13.82465	1.007436	0.065282		
13.19166	156.2418	32.16042	13.27234	1.006115	0.084947		
12.78277	123.4734	30.21818	12.84297	1.004709	0.104014		
12.22681	89.65695	27.57737	12.24488	1.001477	0.136574		
13.40494	176.6512	33.17349	13.47199	1.005002	0.076263		
12.96285	136.9598	31.07355	13.03216	1.005346	0.095153		
12.34793	96.13087	28.15267	12.37815	1.002467	0.128763		
11.99545	78.47727	26.47841	12.13011	1.011225	0.154568		
13.26388	162.8739	32.50345	13.45046	1.014066	0.082582		
12.78240	123.5179	30.22115	12.80942	1.002035	0.103704		
12.36543	97.10429	28.23580	12.53366	1.013604	0.129074		
11.88902	73.81362	25.97287	11.54191	0.970804	0.156365		
11.73976	67.73627	25.26388	11.83198	1.007854	0.174677		
11.43035	56.58178	23.79370	11.48464	1.004758	0.202616		
11.18781	49.29844	22.64211	11.32524	1.012384	0.229728		
10.75341	38.39139	20.57872	10.83776	1.007843	0.282296		
10.47603	32.72373	19.26117	10.50004	1.002291	0.320849		
10.49887	33.15873	19.36964	10.46158	0.996448	0.315500		
10.25994	28.89791	18.23474	10.37905	1.011609	0.359162		
10.03264	25.35366	17.15505	10.14438	1.011137	0.400115		
9.599430	19.75775	15.09729	9.971814	1.038792	0.504703		
9.302275	16.66187	13.69103	10.11363	1.087093	0.608992		
8.900350	12.47290	11.30166	11.09363	1.260590	0.889419		
8.470243	10.31432	9.735554	10.02471	1.183521	0.971921		
8.196850	8.812666	8.435038	8.733415	1.065459	0.991040		
7.852033	7.225841	6.977160	7.193624	0.916147	0.995541		
7.559181	6.104856	5.406113	6.096572	0.806512	0.998643		
7.211128	4.994456	3.752859	4.969132	0.589092	0.994531		
6.584072	3.482555	2.74343	3.509545	0.333035	1.007749		
6.039106	2.544817	-1.81424	2.532889	0.419414	0.995212		
10.70051	37.24062	20.32746	10.67926	0.998013	0.286768		
11.14216	48.01980	22.42526	11.14925	1.000626	0.232180		
11.37594	54.93728	23.53575	11.34716	0.997470	0.206547		
11.67355	65.20324	24.94940	11.71028	1.005154	0.179597		

Tw	8<U>/D	Log	Log
dyne/cm2 (1/sec)	Tw	8<U>/D	8<U>/D
0.800327	76.64641	-0.09673	1.884491
0.548529	57.33924	-0.26080	1.758452
0.401317	42.72741	-0.39651	1.630706
0.271050	28.92317	-0.56694	1.461245
0.194354	20.75633	-0.71140	1.317150
0.130482	13.86187	-0.88444	1.141822
0.064992	6.909030	-1.18713	0.839417
0.034861	3.651915	-1.45764	0.562520

Log Tw vs. Log 8<U>/D

Regression Output:

Constant	-2.02472
Std Err of Y Est	0.004281
R Squared	0.999916
No. of Observations	7
Degrees of Freedom	5

X Coefficient(s)	0.999178
Std Err of Coef.	0.004072

Tw = K' (8<U>/D)^n'

K' =	0.009455
n' =	0.999178

Tw8 = 45.23642
Res/ft = 1524.362

Regression Output:

Constant	-1.78092
Std Err of Y Est	0.051532
R Squared	0.997740
No. of Observations	8
Degrees of Freedom	6

X Coefficient(s)	4.433821
Std Err of Coef.	0.086132

t = 24.55717 deg C
s.d.t = 0.562466 deg C

AIP23104

ALCOHER 507

8/4/90 15:34

10 PSID Taps 14 1.0 PSID Taps 14 0.1 PSID Taps 14

density viscosity

co[NaCl] 1.01234 1.029478

ID(cm) = 1.45795

S = 2.7 Z =

7.25 S =

9.9 <C>[ppm] =

6.95 [NaCl] =

99.94837 X coeff -0.00025 -0.02281

XS(cm2) = 1.669479

1.085095

Batch	Vol	t _{saap}	(sec)	DP	(psid)	<U>	(cm/s)	Re	T _w	f	Log(re/f)		
60	1.21416	24.8	8.128	0.0285	0.0385	8.0895	7.431172	727.2685	116050.8	1048.374	0.003926	3.861667	
52	1.052372	24.8	6.343	0.0285	0.0385	6.3045	5.791436	630.2994	100577.3	817.0435	0.004074	3.807531	
45	0.91062	24.8	4.954666	0.0285	0.0385	4.916166	4.516086	545.4514	87038.12	637.1199	0.004242	3.755519	
38	0.768968	24.8	3.699	0.0285	0.0385	3.6605	3.32606	460.6034	73498.86	474.3894	0.004429	3.689476	
31	0.627316	24.8	2.6138	0.0285	0.0385	2.5853	2.374906	375.7554	59959.60	335.0468	0.004701	3.615961	
26	0.526136	24.8	1.946	0.0285	0.0385	1.9075	1.752266	315.1497	50388.69	247.2060	0.004931	3.547938	
19	0.384484	24.8	1.15	0.0285	0.0385	1.1115	1.021045	230.3017	36749.43	144.0469	0.005380	3.430361	
15	0.30354	24.8	0.732	0.0285	0.0385	0.7347	0.674909	181.8171	29012.70	95.21483	0.005706	3.340761	
10	0.20236	24.8	0.41275	0.0285	0.0385	0.37425	0.343793	121.2114	19341.80	48.50163	0.006540	3.194287	
8	0.161888	24.8	0.2905	0.0285	0.0385	0.232	0.231492	96.96914	15473.44	32.65841	0.006880	3.108406	
20	0.40472	23.5	1.259	0.0345	0.0415	1.2175	1.118419	242.4228	37565.57	157.7842	0.005317	3.457533	
15	0.30354	23.5	0.8034	0.0345	0.0415	0.7619	0.499896	181.8171	28174.18	98.73987	0.005915	3.352847	
10	0.20236	23.5	0.409333	0.0345	0.0415	0.367833	0.337898	121.2114	18782.78	47.67005	0.006425	3.177724	
25	0.5059	23.5	1.8135	0.0345	0.0415	1.772	1.627793	303.0285	46956.96	229.6456	0.004752	3.519130	
18	0.364248	24.7	11.763	0.0445	0.0675	11.6955	0.914113	118.1805	34736.79	128.9411	0.005366	3.405653	
13	0.263068	24.7	6.7406	0.0445	0.0675	6.6731	0.521565	157.5748	25087.68	73.58133	0.005870	3.283807	
10	0.20236	24.7	4.311384	0.0445	0.0675	4.243884	0.331699	121.2114	19298.22	46.79544	0.006309	3.185535	
7	0.141652	24.7	2.3095	0.0445	0.0675	2.242	0.175233	84.94800	13508.75	24.72154	0.006802	3.046961	
24.4	2.1664	24.2	2.1664	0.0375	0.0315	2.1349	0.175233	84.94800	13508.75	24.72154	0.006802	3.046961	
24.2	1.465	24.2	1.465	0.0285	0.0235	1.4415	0.151	0.112666	64.85742	10210.20	0.007484	2.945125	
24.1	1.1138	24.1	1.1138	0.0215	0.0185	1.0953	0.149	0.085607	55.47684	8713.784	0.007739	2.885499	
24.1	0.6826	24.1	0.6826	0.0185	0.0155	0.6671	0.20	0.052140	41.47999	6515.290	0.008468	2.777838	
24	0.5016	24	0.5016	0.0155	0.0145	0.4871	0.249	0.038071	34.54410	5413.639	0.008915	2.708556	
23.9	3.095833	23.9	3.095833	-0.0155	-0.0165	3.111333	0.914113	118.1805	34736.79	128.9411	0.005366	3.405653	
23.9	1.816571	23.9	1.816571	-0.0205	-0.0235	1.837071	0.521565	157.5748	25087.68	73.58133	0.005870	3.283807	
23.8	1.133777	23.8	1.133777	-0.0295	-0.0325	1.163277	0.331699	121.2114	19298.22	46.79544	0.006309	3.185535	
23.8	0.766	23.8	0.766	-0.0355	-0.036	0.8015	0.175233	84.94800	13508.75	24.72154	0.006802	3.046961	
23.7	0.408928	23.7	0.408928	-0.0405	-0.043	0.449428	0.151	0.112666	64.85742	10210.20	0.007484	2.945125	
23.6	0.274066	23.6	0.274066	-0.0455	-0.0475	0.319566	0.149	0.085607	55.47684	8713.784	0.007739	2.885499	
23.55	0.1715	23.55	0.1715	-0.0495	-0.05	0.221	0.20	0.052140	41.47999	6515.290	0.008468	2.777838	
23.4	0.106266	23.4	0.106266	-0.0515	-0.0545	0.157766	0.249	0.038071	34.54410	5413.639	0.008915	2.708556	
23.2	0.0235	23.2	0.0235	-0.0535	-0.0535	0.077	0.901	0.001983	5.251957	812.0035	0.279778	0.020087	2.041023
23.2	-0.0226	23.2	-0.0226	-0.0545	-0.0555	0.0319	0.521565	157.5748	25087.68	73.58133	0.005870	3.283807	
23.3	4.0994	23.3	4.0994	-0.0565	-0.0575	4.1559	0.331699	121.2114	19298.22	46.79544	0.006309	3.185535	
23.5	6.76975	23.5	6.76975	-0.0595	-0.06	6.82925	0.175233	84.94800	13508.75	24.72154	0.006802	3.046961	
23.5	8.88075	23.5	8.88075	-0.0615	-0.061	8.94225	0.151	0.112666	64.85742	10210.20	0.007484	2.945125	
23.6	12.7458	23.6	12.7458	-0.0625	-0.0645	12.8063	0.149	0.085607	55.47684	8713.784	0.007739	2.885499	

AlF23104
 Tw 8(U)/D Log Tw 8(U)/D
 dyne/cm2 (1/sec) Log Tw 8(U)/D
 0.797003 75.66039 -0.09854 1.878848
 0.566709 56.73577 -0.24663 1.733856
 0.391914 39.76656 -0.40680 1.601696
 0.279778 28.81811 -0.55318 1.459665
 0.136549 14.18769 -0.86471 1.151911
 0.056570 5.954925 -1.24741 0.774876

Log Tw vs. Log 8(U)/D
 Regression Output:
 Constant -2.03285
 Std Err of Y Est 0.000382
 R Squared 0.999999
 No. of Observations 3
 Degrees of Freedom 1

X Coefficient(s) 1.013824
 Std Err of Coef. 0.000789

Tw = K' (8(U)/D)^n'

K' = 0.009271
 n' = 1.013824

Tw# = 46.87517
 Res/ft# = 1537.751

Regression Output:
 Constant -4.61408
 Std Err of Y Est 0.034967
 R Squared 0.999252
 No. of Observations 9
 Degrees of Freedom 7

X Coefficient(s) 5.323233
 Std Err of Coef. 0.055037

t = 24.09594 deg C
 s.d.t = 0.583139 deg C

Tap DL= 122.2234
 40.77743

79.55558
 4
 0.4
 Solvent L MDR
 1//f 1//f 1//f 1//f/slv 1//f/l

15.04666 454.5140 40.97167 15.95809 1.060573 0.035110
 14.83012 401.2469 39.94310 15.66637 1.056388 0.039044
 14.61407 354.3233 38.91687 15.35287 1.050553 0.043330
 14.35790 305.7430 37.70005 15.02463 1.046436 0.049141
 14.05584 256.9460 36.26527 14.58467 1.037623 0.056761
 13.79175 220.7083 35.01083 14.24071 1.032352 0.064522
 13.52264 168.4772 32.78256 13.63293 1.023290 0.080918
 12.96304 136.9750 31.07446 13.23813 1.021221 0.096646
 12.37714 97.76138 28.29145 12.36544 0.999034 0.126485
 12.03362 80.22075 26.65972 12.05536 1.001806 0.150277
 13.35053 171.2037 32.91503 13.71376 1.027207 0.080101
 12.94339 135.4340 30.98110 13.00179 1.004512 0.096000
 12.31089 94.10320 27.97676 12.47485 1.013318 0.132565
 13.67652 206.5431 34.46348 14.20918 1.038947 0.048795
 13.22261 159.0498 32.30741 13.65011 1.032331 0.085822
 12.73233 120.1400 29.99234 13.05127 1.024816 0.108633
 12.34210 95.80887 28.12498 12.58900 1.020005 0.131397
 11.78784 69.63727 25.92227 12.12421 1.028534 0.174105
 11.73350 67.49275 25.73416 11.77388 1.003441 0.174446
 11.38450 55.20841 23.57638 11.58870 1.015302 0.209344
 11.14199 48.01526 22.42448 11.34246 1.017992 0.236226
 10.71131 37.47211 20.37873 10.86689 1.014525 0.289999
 10.43422 31.94748 19.06257 10.59089 1.015014 0.331509
 10.45366 32.30689 19.15488 10.44219 0.998903 0.323218
 9.996019 24.82475 16.98109 10.06093 1.006493 0.405278
 9.595193 19.70963 15.07717 9.828414 1.024305 0.498660
 9.271634 16.36019 13.54026 10.01821 1.080523 0.612352
 8.765207 12.22311 11.13473 10.97484 1.252091 0.897876
 8.465068 10.28364 9.709075 9.759818 1.152952 0.949062
 8.142759 8.542203 8.178108 8.267399 1.015306 0.967829
 7.844094 7.192893 6.759448 7.053605 0.899479 0.980913
 7.213163 5.002314 3.762528 4.972257 0.689351 0.993991
 6.447763 3.219741 0.12877 3.242412 0.502873 1.007041
 10.68145 36.83353 20.23690 10.65212 0.997253 0.289196
 11.12075 47.43159 22.32356 11.14615 1.002284 0.234994
 11.35489 54.27559 23.43576 11.36528 1.000914 0.209399
 11.67079 65.09958 24.93626 11.71265 1.003586 0.179918

ALCOHER 507 8/6/90 14:50
 10 PSID Tap. 14 1.0 PSID Taps 14 0.1 PSID Taps 14
 S = 2.7 S = 7.35 S = 9.9 <C> (ppm) =
 Z = 2.7 Z = 9 Z = 6.9 [NaCl] =

Freq. (Hz)	Diest (1/s)	Temp (deg C)	<U> (volts)	<U> (volts)	<U>f (volts)	<U>corr (volts)
60	1.21416	24.9	7.254666	0.0465	0.0435	7.211166
52	1.052272	24.9	5.677666	0.0465	0.0435	5.634166
45	0.91062	24.9	4.4855	0.0465	0.0435	4.442
39	0.789204	24.9	3.539333	0.0465	0.0435	3.495833
32	0.647552	24.9	2.550333	0.0465	0.0445	2.505833
26	0.526136	24.9	1.819	0.0445	0.0445	1.7745
19	0.384484	24.9	1.1046	0.0445	0.0445	1.0601
15	0.30254	24.9	0.757	0.0445	0.0445	0.7125
10	0.20236	24.9	0.400625	0.0445	0.0445	0.356125
8	0.161888	24.9	0.28625	0.0445	0.0445	0.24175
24	0.485664	23.5	1.597666	0.0255	0.0235	1.574166
17	0.344012	23.5	0.912333	0.0255	0.0235	0.888833
12	0.242832	23.5	0.5544	0.0275	0.0225	0.5269
20	0.40472	24.9	13.195	0.0515	0.0825	13.1125
15	0.30354	24.9	8.379	0.0515	0.0825	8.2965
18	0.364248	24.9	11.2722	0.0515	0.0825	11.1897
13	0.243068	24.9	6.1652	0.0515	0.0825	6.0827
10	0.20236	24.9	4.244	0.0515	0.0825	4.1615
8	0.161888	24.9	3.053333	0.0515	0.0825	2.970833
		24.6	2.177142	0.0695	0.0585	2.118642
		24.5	1.521333	0.0565	0.0535	1.467833
		24.4	1.234	0.0535	0.0495	1.1845
		24.3	0.789	0.0505	0.0485	0.7405
		24.25	0.6276	0.0485	0.0485	0.5791
		24.1	3.73625	0.0455	-0.0045	3.68075
		24	2.433666	-0.0045	-0.0035	2.438166
		24	1.818857	-0.0055	-0.0065	1.824357
		24	1.4685	-0.0085	-0.0085	1.477
		24	1.130875	-0.0095	-0.0105	1.140375
		24	0.661916	-0.0115	-0.0115	0.673416
		23.9	0.447461	-0.0135	-0.0145	0.460961
		23.9	0.36175	-0.0145	-0.0155	0.37625
		23.9	0.262133	-0.0155	-0.0155	0.277633
		23.8	0.189	-0.0165	-0.0165	0.2055
		23.8	0.119166	-0.0165	-0.0165	0.135666
		23.6	0.04384	-0.0175	-0.0185	0.06134
		23.5	0.007478	-0.0185	-0.0195	0.026978
		23.6	4.13775	-0.0205	-0.0195	4.15725
		23.8	6.792	-0.0195	-0.0195	6.8115
		23.8	8.930666	-0.0165	-0.0145	8.967166

23.8 12.78875 -0.0135 -0.0095 12.80225

1966 15.1 0.160925 77.98758 12166.93 22.70311 0.007393 3.019599

Batch	Vol	t/samp	DP	<U>	Re	Tw	f	Log(Re/f)
(ml)	(sec)	(psid)	(cm/s)		dynes/cm ²			
			density viscosity					
			co)[NaCl] 1.01234 1.029478	ID(cm) = 1.45796				
			299.7163 X coeff -0.00025 -0.02281	K(U/psi) = 1.08859 12.79437				
			0.300062 constant 0.003419 -4.14933	X5(cm2) = 1.669479				
				1.085095				
2020	15.1	0.165591	80.12966	12728.79	23.36134	0.007207	3.033687	
1619	15.0	0.114724	64.65088	10246.80	16.18515	0.007670	2.953011	
1410	14.8	0.092579	57.06585	9024.241	13.06095	0.007944	2.905455	
1450	19.9	0.057877	45.64493	6886.339	8.165167	0.008490	2.802465	
1271	20.1	0.045262	37.87637	5969.433	6.385480	0.008816	2.748587	
1258	20	0.046267	37.67611	5917.859	6.527329	0.009108	2.751880	
1241	25	0.030648	29.73331	4659.786	4.323769	0.009486	2.661458	
1265	29.9	0.022932	25.34134	3971.490	3.235258	0.009978	2.598482	
1123	30	0.018566	22.42215	3513.926	2.619266	0.010319	2.552617	
1160	35.1	0.014534	19.95665	3102.309	2.022306	0.010221	2.496451	
1115	39.9	0.008464	16.75866	2623.228	1.194216	0.008442	2.382069	
1140	50	0.005794	13.65495	2135.449	0.817455	0.008681	2.298774	
1135	59.9	0.004729	11.34979	1774.694	0.667230	0.010259	2.254680	
850	59.9	0.003489	8.499844	1329.066	0.492346	0.013497	2.188677	
685	60.1	0.002583	6.827080	1065.150	0.264427	0.015486	2.122362	
705	100	0.001705	4.222872	658.8154	0.240587	0.026721	2.052193	
322	100	0.000771	1.928744	299.5511	6.108778	0.057912	1.857858	
140	100.1	0.000359	0.837746	129.8163	0.647842	0.135007	1.678508	
1345	20	0.052257	40.28201	8391.595	12.07930	0.008269	2.862578	
1338	14.9	0.085521	53.78841	8391.595	12.07930	0.008269	2.862578	
1580	15	0.112467	63.09351	9843.295	15.86663	0.007894	2.941799	

Tap DL= 122.2234
40.77743

79.55358
0.4
4

Solvent	L	MDR	1//f	1//f	1//f/Slv	1//f/L
14.	95077	470.1049	40.51619	16.90182	1.130498	0.0392396
14.	73642	380.1775	39.49802	16.57195	1.124557	0.043590
14.	53992	337.5677	38.51713	16.15133	1.111591	0.047846
14.	32186	299.4656	37.52887	15.77881	1.101728	0.052689
14.	03267	253.5407	36.15518	15.29181	1.089729	0.060313
13.	73391	213.3583	34.73136	14.76456	1.075121	0.069200
13.	28546	164.9092	32.60593	13.95935	1.050724	0.084648
12.	94033	135.1960	30.96659	13.44282	1.038815	0.099430
12.	33797	95.58128	28.10536	12.67604	1.027401	0.132620
12.	00149	78.75078	26.50712	12.30812	1.025548	0.156292
13.	57369	194.6723	33.97506	14.47261	1.066225	0.074343
13.	07723	146.2813	31.61987	13.64268	1.043239	0.093263
12.	62305	112.6271	29.45949	12.50772	0.990863	0.111054
13.	32982	169.1753	32.81668	14.32351	1.074546	0.084666
12.	93324	134.5680	30.92817	13.50536	1.044316	0.100360
13.	19209	156.2800	32.16244	13.95486	1.057820	0.089292
12.	66265	115.2238	29.64758	13.66985	1.079325	0.118635
12.	33295	95.30579	28.08154	12.71269	1.030790	0.133388
12.	04021	80.52351	26.69101	12.03686	0.999721	0.149478
11.	73475	67.54102	25.24006	11.77876	1.003750	0.174394
11.	41304	56.09084	23.70722	11.41764	1.000490	0.203556
11.	22182	50.27312	22.80366	11.21901	0.999749	0.223161
10.	80986	39.65936	20.84684	10.85332	1.003927	0.273638
10.	59434	35.03219	19.82315	10.64990	1.005243	0.304003
10.	60752	35.39884	19.88572	10.47813	0.987802	0.296840
10.	24583	28.66413	18.16771	10.16031	0.991653	0.354460
9.	99328	24.79488	16.97115	10.01086	1.001694	0.403747
9.	810469	22.30989	16.09975	9.844083	1.003426	0.441243
9.	585804	19.60338	15.02356	9.890860	1.031823	0.504548
9.	128276	15.06430	12.85931	10.88346	1.192280	0.722466
8.	795097	12.43594	11.27671	10.73284	1.220321	0.863099
8.	618720	11.23466	10.43892	9.873866	1.145514	0.878785
8.	354711	9.650677	9.184877	8.607336	1.030237	0.891889
8.	089450	8.284049	7.924891	8.035781	0.993365	0.970030
7.	728773	6.730903	6.211673	6.117450	0.791516	0.908860
7.	031433	4.505451	2.899307	4.155399	0.590974	0.922304
6.	314032	2.981179	-0.50834	2.721580	0.431036	0.912920
10.	69355	37.09107	20.29439	10.54187	0.985815	0.284215
11.	13031	47.69338	22.36898	10.99680	0.988004	0.230572
11.	36719	54.66124	23.49419	11.25488	0.990119	0.205902

11.67839 65.38527 24.97229 11.63004 0.995859 0.177869

63F23107

Tw	8<U>/D	Log	Log
dyne/cm2 (1/sec)	Tw	8<U>/D	8<U>/D
1.194216	91.84705	0.077083	1.943065
0.817455	74.93731	-0.08753	1.874698
0.667230	62.27766	-0.17572	1.794332
0.492346	46.63966	-0.30772	1.668755
0.364427	37.46100	-0.43838	1.573579
0.240587	23.17140	-0.61872	1.364952
0.108778	10.58325	-0.96345	1.024619
0.047842	4.596817	-1.32018	0.662457

Log Tw vs. Log 8<U>/D

Regression Output:
 Constant -1.99959
 Std Err of Y Est 0.015996
 R Squared 0.998900
 No. of Observations 5
 Degrees of Freedom 3

X Coefficient(s) 1.006351
 Std Err of Coef. 0.019273

Ta = K' (8<U>/D)^n'

K' = 0.010009
 n' = 1.006351

Tw = 45.63800
 Res/ft = 1520.749

Regression Output:
 Constant -9.85783
 Std Err of Y Est 0.032642
 R Squared 0.999362
 No. of Observations 8
 Degrees of Freedom 6

X Coefficient(s) 6.972239
 Std Err of Coef. 0.071915

t = 24.30365 deg C
 s.d.)t = 0.533327 deg C

ALP33113	ALCOLMER 507	8/13/90	15:25	10 PSID	1.0 PSID	Taps 14	0.1 PSID	Taps 14	9.9	<C>	[ppm]=	density	viscosity	ID(cm)	K(U/psi)	X5(cm2)	1.45796	1.07788	12.75147
S =	2.7 S =	7.25 S =	9.9	<C>	[ppm]=	999.6909	X coeff	-0.0025	-0.0201	0.300123	constant	0.003419	-4.14933	1.669479					
Z =	2.7 Z =	9 Z =	6.95	[NaCl]=															
Freq. (Hz)	Qtest (1/s)	Temp (deg C)	<U> (volts)	<U> (volts)	<U>f (volts)	<U>corr (volts)	Batch Vol (ml)	t (sec)	DP (psid)	Re (cm/s)	Tw (dyne/cm2)	f	Log(Re/f)						
60	1.21416	25.05	6.062	0.0585	0.0405	6.0215	5.586387	727.2685	116707.2	788.1156	0.002952	3.802167							
50	1.0118	25.05	4.536333	0.0585	0.0405	4.495833	4.170965	606.0571	97256.01	588.4509	0.003173	3.78719							
40	0.80944	25.05	3.216	0.0585	0.0405	3.1755	2.946038	484.8457	77804.80	415.6209	0.003502	3.662320							
30	0.60708	25.05	2.084666	0.0585	0.0405	2.044166	1.894655	363.6342	58353.60	267.5479	0.004008	3.567572							
25	0.5059	25	1.539333	0.0475	0.0445	1.491833	1.384033	203.0285	48573.18	195.2565	0.004212	3.498682							
19	0.384484	25	1.0242	0.0475	0.0445	0.9797	0.908907	230.3017	36915.62	128.2366	0.004789	3.407268							
14	0.283304	25	0.625666	0.0475	0.0445	0.581166	0.539171	169.5960	27200.98	76.06519	0.005233	3.292972							
10	0.20236	25	0.414875	0.0475	0.0445	0.370375	0.343611	121.2114	19429.27	48.47601	0.006556	3.196143							
8	0.161888	25	0.295285	0.0475	0.0445	0.250785	0.232663	96.96914	15543.41	32.82374	0.006915	3.111472							
23	0.465428	23.9	1.384	0.0535	0.0425	1.3415	1.244565	278.7862	43592.01	175.5803	0.004474	3.644780							
22	0.667788	23.9	2.39075	0.0535	0.0425	2.34825	2.178565	599.9977	62545.06	307.3474	0.003804	3.586357							
44	0.890384	23.9	3.72	0.0535	0.0425	3.6775	3.411764	533.3302	83393.42	481.5244	0.003351	3.683761							
10	0.20236	24	0.415	0.0425	0.0395	0.3755	0.348366	121.2114	18995.85	49.14679	0.006625	3.189275							
18	0.364248	24.9	10.70225	0.0515	0.0555	10.64675	0.834942	218.1805	74893.88	117.7919	0.004902	3.387952							
15	0.30754	24.9	8.19525	0.0515	0.0555	8.13975	0.638338	181.8171	29078.23	90.05539	0.005297	3.329649							
10	0.20236	24.9	4.3953	0.0515	0.0555	4.3397	0.540337	121.2114	19385.49	48.01405	0.006474	3.192078							
8	0.161888	24.9	2.954285	0.0515	0.0555	2.898785	0.227329	96.96914	15508.39	32.07116	0.006757	3.105451							
24.7	2.3235	24.7	2.3235	0.0565	0.0525	2.267	0.177783	81.30378	12944.31	25.08130	0.007516	3.050099							
24.7	1.646333	24.7	1.646333	0.0475	0.0435	1.598833	0.123384	65.60926	10445.73	17.68894	0.008140	2.974274							
24.6	1.206833	24.6	1.206833	0.0395	0.0385	1.167333	0.091545	55.70598	8849.032	12.91497	0.008244	2.904974							
24.5	0.7348	24.5	0.7348	0.0365	0.0345	0.6983	0.054762	41.71853	6612.157	7.725751	0.008793	2.792423							
24.5	0.543	24.5	0.543	0.0335	0.0325	0.5095	0.039956	34.76532	5510.112	5.636932	0.009239	2.723974							
24.4	0.3308	24.4	0.3308	0.0315	0.0315	0.2993	0.022471	25.70861	4065.490	3.211352	0.009924	2.607471							
24.3	1.918857	24.3	1.918857	0	-0.0005	1.918857	25.3	0.024071	25.64052	4045.586	3.395961	0.010232	2.611964						
24.3	1.001888	24.3	1.001888	-0.0045	-0.0065	1.006388	34.9	0.012624	20.26951	3198.143	1.781090	0.008587	2.471826						
24.2	0.7066	24.2	0.7066	-0.0115	-0.0145	0.7181	40	0.009008	16.84656	2652.077	1.270881	0.008870	2.397550						
24.2	0.566307	24.2	0.566307	-0.0175	-0.0205	0.583907	50.1	0.007223	14.11988	2222.828	1.033213	0.010265	2.352592						
24.1	0.3984	24.1	0.3984	-0.022	-0.024	0.4204	60	0.005273	10.35252	1637.913	0.744016	0.013750	2.280796						
24.1	0.28175	24.1	0.28175	-0.0265	-0.0285	0.30825	59.9	0.003866	7.689859	1207.851	0.545535	0.018273	2.212924						
24	0.192526	24	0.192526	-0.0395	-0.0405	0.22026	75	0.002785	5.558618	871.1284	0.392938	0.025189	2.140689						
23.9	0.102454	23.9	0.102454	-0.0325	-0.0345	0.134954	90	0.001692	3.414237	533.8623	0.28840	0.040582	2.031596						
23.8	0.04024	23.8	0.04024	-0.0345	-0.0375	0.07474	99.9	0.000937	1.894700	295.5944	0.132273	0.072978	1.902292						
23.7	0.013708	23.7	0.013708	-0.0365	-0.0375	0.050208	100	0.000629	1.275846	198.5978	0.088857	0.108116	1.818491						
23.55	-0.01883	23.55	-0.01883	-0.0395	-0.0415	0.021662	150.1	0.000271	0.554692	86.05168	0.038337	0.246769	1.630905						
23.7	5.081428	23.7	5.081428	-0.0625	-0.0435	5.125928	20	0.039188	34.53172	5375.194	5.28676	0.009182	2.711882						
23.8	4.182	23.8	4.182	-0.045	-0.044	4.227	19.9	0.05026	41.14663	6419.236	7.480874	0.008751	2.779552						
23.9	6.987	23.9	6.987	-0.046	-0.0475	7.033	15.1	0.08827	54.5833	8574.850	12.44688	0.008274	2.890072						
24	9.074	24	9.074	-0.0485	-0.0465	9.123	15	0.11439	64.21162	10063.03	16.14484	0.007755	2.947544						
24	13.4824	24	13.4824	-0.049	-0.045	13.5314	15	0.169747	79.50615	12428.59	23.94764	0.007541	3.033158						

Page 3

Alcoar 507

Tap DL= 122.2234
40.77743

79.71477

0.4

Solvent	L	MDR	1//f	1//f	1//f	1//f	1//f	1//f	1//f
	1//f	1//f	1//f	1//f	1//f	1//f	1//f	1//f	1//f
14.80866	396.3210	39.84117	18.40477	1.242838	0.046439				
14.55487	342.4521	38.65567	17.74992	1.219517	0.051831				
14.25288	287.8066	37.20119	16.89406	1.185448	0.058706				
13.87029	230.9134	35.38388	15.79409	1.138499	0.068397				
13.59472	197.0436	34.07496	15.40686	1.133296	0.078190				
13.22947	159.6793	32.34000	14.44912	1.092191	0.090488				
12.77589	122.9851	30.18547	13.82331	1.081984	0.112398				
12.38457	98.18000	28.32671	12.36840	0.998694	0.125976				
12.04589	80.78925	26.71799	12.02466	0.998237	0.148839				
13.45912	182.2469	33.43082	14.94949	1.110733	0.082038				
13.94542	241.1222	35.74078	16.21197	1.162529	0.067235				
14.33504	301.7458	37.59146	17.27340	1.204956	0.057243				
12.35710	96.63961	28.19622	12.28524	0.994184	0.127124				
13.15180	152.6976	31.97109	14.28226	1.085954	0.093533				
12.91859	133.5147	30.86333	13.61190	1.053667	0.101950				
12.37231	97.48965	28.26849	12.42791	1.004493	0.127479				
12.02180	79.67677	26.60358	12.16508	1.011917	0.152480				
11.80039	70.14214	25.55188	11.53400	0.977425	0.164437				
11.49709	58.90537	24.11122	11.08317	0.963997	0.188152				
11.21994	50.21870	22.79472	11.01311	0.981566	0.219303				
10.76969	38.75287	20.65605	10.66397	0.990183	0.275179				
10.49589	33.10205	19.35552	10.40384	0.991210	0.314289				
10.02988	25.31343	17.14194	10.03787	1.000797	0.396543				
10.04785	25.57670	17.22732	9.885915	0.985862	0.386520				
9.487304	18.52377	14.56469	10.79125	1.137441	0.582593				
9.190201	15.61099	13.15345	10.61783	1.155342	0.680150				
9.010371	14.07579	12.29926	9.869905	1.095393	0.701196				
8.735187	11.93099	10.95513	8.53752	0.977595	0.714755				
8.431597	10.20479	9.645583	7.397570	0.875276	0.724911				
8.162759	8.641116	8.273107	6.300751	0.771889	0.729159				
7.726384	6.71654	6.200337	4.94015	0.642475	0.738510				
6.859679	4.990841	3.743581	3.70170	0.513472	0.741700				
6.209175	4.083478	3.041267	0.443354	0.745168					
6.135620	2.671684	-1.41280	2.013048	0.328734	0.753475				
10.44733	32.19308	19.12576	10.43546	0.998844	0.324152				
10.71413	37.53300	20.39213	10.68948	0.997699	0.284802				
11.16029	48.52357	22.51138	10.99317	0.985025	0.226553				
11.39017	55.38913	23.60334	11.55492	0.996905	0.205002				
11.75263	67.45886	25.23002	11.51498	0.981448	0.170696				

Page 4

Alcoar 507

A1F33113

Tw	8<U>/D	Log	Log
dyne/cm2	(1/sec)	Tw	8<U>/D
0.744016	56.80555	-0.12841	1.754390
0.545335	42.19517	-0.26317	1.625262
0.392938	30.50080	-0.40567	1.484311
0.238840	18.73432	-0.62189	1.272638
0.132273	10.39644	-0.87852	1.016884
0.088837	7.000722	-1.05130	0.845142
0.058337	3.043668	-1.41637	0.483397

Log Tw vs. Log 8<U>/D

Regression Output:
Constant -1.90421
Std Err of Y Est 0.001128
R Squared 0.999993
No. of Observations 5
Degrees of Freedom 3

X Coefficient(s) 1.008803
Std Err of Coef. 0.001459

Tw = K' (8<U>/D)^n'

K' = 0.012467
n' = 1.008803

Tw8 = 46.76978
Res/88 = 1544.737

Regression Output:

Constant -18.6712
Std Err of Y Est 0.162296
R Squared 0.993377
No. of Observations 14
Degrees of Freedom 12

X Coefficient(s) 9.729725
Std Err of Coef. 0.229525

t = 24.39743 deg C
s.d.t = 0.488187 deg C

DSR1438 8/22/90 12:38
 Taps 14 1.0 PSID Taps 14 0.1 PSID Taps 14
 S = 2.7 S = 7.25 S = 9.9 C (ppm) =
 Z = 2.7 Z = 9.05 Z = 6.85 [NaCl] =

co) [NaCl] 1.00008 1.001574 ID (cm) = 1.45796
 29.99008 X coeff -0.00025 -0.02281 K (V/psi) = 1.077888 12.72682
 0.000100 constant 0.003419 -4.14933 XS (cm²) = 1.669479

density viscosity

Freq. (Hz)	Dist Temp (1/s)	Temp (deg C)	<U> (volts)	<U> (volts)	<U> (volts)	<U> corr (volts)	Batch Vol (ml)	t (sec)	DF (psid)	U (cm/s)	Re	Tw (dyne/cm ²)	f	Log(Re/f)
60	1.21416	24.7	7.6275	0.0515	0.0895	7.53725	6.992609	737.2685	117574.8	984.5025	0.003740	3.856762		
50	1.0118	24.7	5.532666	0.0515	0.0895	5.443166	5.049844	606.0571	97979.02	712.4213	0.003889	3.786082		
39	0.789204	24.7	3.663	0.0515	0.0895	3.5775	3.35229	472.7245	74423.54	467.7125	0.004197	3.594707		
30	0.60708	24.7	2.3845	0.0515	0.0895	2.295	2.129163	363.6342	58787.41	300.3778	0.004555	3.598547		
25	0.5059	24.6	1.7545	0.0545	0.0575	1.597	1.574375	303.0285	48879.11	222.1094	0.004850	3.533012		
19	0.384484	24.6	1.11275	0.0545	0.0575	1.05525	0.978997	230.3017	37148.12	138.1149	0.005221	3.423849		
15	0.30254	24.6	0.750428	0.0545	0.0575	0.692928	0.642857	181.9171	29327.47	90.59299	0.005501	3.337515		
9	0.182124	24.6	0.35525	0.0545	0.0575	0.29775	0.276234	109.0902	17596.48	38.97059	0.005566	3.154097		
7	0.141652	24.6	0.258714	0.0545	0.0575	0.201214	0.186674	84.84800	12686.15	26.33565	0.007255	3.069000		
18	0.364248	35	11.329	0.0405	0.0625	11.2665	0.885255	218.1805	35511.98	124.8900	0.005261	3.410973		
14	0.283304	25	7.3915	0.0405	0.0625	7.329	0.575870	169.6960	27620.43	81.24252	0.005657	3.317561		
10	0.20236	25	4.2304	0.0405	0.0625	4.1679	0.327489	121.2114	19728.87	46.20148	0.006306	3.194997		
8	0.161888	25	2.9545	0.0405	0.0625	2.892	0.227226	92.96914	15782.10	32.05803	0.006837	3.115637		
24.3	2.7035	24.3	1.892	0.0425	0.0425	2.6605	14.9	0.209046	92.46140	14813.61	29.49184	0.005917	3.090624	
24.3	1.892	24.3	1.4662	0.0425	0.0425	1.8495	15	0.145322	75.23302	12033.38	20.50184	0.007263	3.011669	
24.3	1.4662	24.3	1.062	0.0425	0.0425	1.4237	15	0.111866	64.33142	10306.79	15.78182	0.007646	2.954851	
24.2	0.91925	24.2	0.6856	0.0425	0.0425	0.87675	1226	0.068889	48.63315	7774.153	9.718840	0.008739	2.848595	
24.2	0.6856	24.2	0.4925	0.0425	0.0425	0.6411	1349	0.050373	40.40181	6458.349	7.196642	0.008729	2.780620	
24	4.184	24	4.184	0.031	0.022	4.152	1346	0.051692	40.31196	6414.977	7.292711	0.008997	2.784262	
24	2.503	24	2.503	0.0215	0.0235	2.4795	1001	0.030862	29.97940	4770.722	4.354027	0.009713	2.672262	
24	1.661333	24	1.661333	0.024	0.027	1.634332	1181	0.020342	23.65906	3764.946	2.869906	0.010279	2.581751	
24	1.18275	24	1.18275	0.027	0.028	1.15475	1311	0.014373	19.68106	3131.914	2.027753	0.010496	2.506235	
23.95	0.649538	23.95	0.649538	0.0275	0.0275	0.622038	1221	0.007742	16.25257	2583.409	1.092306	0.008291	2.371497	
23.9	0.443933	23.9	0.443933	0.027	0.027	0.416923	1160	0.005189	12.61029	2002.196	0.732139	0.009230	2.284129	
23.9	0.312615	23.9	0.312615	0.0265	0.0265	0.28115	909	0.003561	9.074684	1440.830	0.502421	0.012232	2.203366	
23.8	0.231722	23.8	0.231722	0.026	0.026	0.205722	870	0.002560	6.505873	1030.640	0.261250	0.017111	2.129751	
23.65	0.1625	23.65	0.1625	0.0255	0.025	0.13725	735	0.001708	4.402569	695.0854	0.241012	0.024928	2.040389	
23.5	0.1062	23.5	0.1062	0.0245	0.0245	0.0817	431	0.001016	2.581642	406.2173	0.143466	0.043153	1.926266	
23.4	0.070625	23.4	0.070625	0.0245	0.023	0.046875	250	0.000583	1.495976	234.8590	0.082312	0.073733	1.804640	
23.2	0.039882	23.2	0.039882	0.023	0.023	0.016882	93	0.000210	0.557059	87.06124	0.029645	0.191505	1.580915	
23.2	5.5615	23.2	5.5615	0.0215	0.0175	8.957	1200	0.068956	47.91912	7506.053	9.728297	0.008492	2.839979	
23.6	8.9745	23.6	8.9745	0.0175	0.017	8.957	1595	0.111488	63.69250	10044.54	15.72958	0.007772	2.947221	
23.7	11.5718	23.7	11.5718	0.0155	0.0165	11.5553	1843	0.143829	74.08972	11710.61	20.29122	0.007410	3.005516	

Tap DL= 122.2224
40.77743

80.34
4

0.4

Solvent L MDR
1//f 1//f 1//f

1//f/slv 1//f/l

15.02705	449.4102	40.87849	16.25126	1.088121	0.053563
14.74432	381.9111	39.53556	16.03432	1.087491	0.041984
14.37881	309.4449	37.79936	15.43562	1.073498	0.049881
13.99419	247.9864	35.97240	14.81618	1.058738	0.059745
13.72804	212.7611	34.70823	14.35856	1.045929	0.067486
13.31539	167.7756	32.74813	13.83946	1.039283	0.082481
12.95006	125.9551	31.01279	13.48214	1.041087	0.099166
12.21638	89.12042	27.52784	12.34038	1.010149	0.138468
11.87600	75.26233	25.91101	11.67563	0.983128	0.159367
13.24373	160.9953	32.40773	13.78610	1.040953	0.085630
12.87024	129.8497	30.63366	13.29441	1.032957	0.102383
12.37998	97.92136	28.30495	12.59239	1.017149	0.128596
12.06255	81.56765	26.79712	12.09356	1.002571	0.148264
11.96349	77.00236	26.32185	12.02366	1.005113	0.156146
11.64667	64.20215	24.82172	11.73381	1.007482	0.182763
11.41940	56.32895	23.74218	11.43394	1.001448	0.203020
10.99438	44.10371	21.72330	11.01686	1.002045	0.249794
10.72248	37.71378	20.43178	10.70289	0.998173	0.283792
10.73704	38.03137	20.50097	10.54224	0.981856	0.277198
10.28905	29.38617	18.37299	10.14661	0.986156	0.345285
9.927005	23.85785	16.65327	9.862962	0.993548	0.413405
9.625300	20.05418	15.22017	9.760786	1.014076	0.486720
9.085988	14.70202	12.65844	10.98337	1.208715	0.746997
8.736516	12.02289	10.99845	10.40824	1.191349	0.865701
8.409465	9.959705	9.444942	9.041624	1.075172	0.907245
8.119005	8.426190	8.065274	7.644621	0.941571	0.907245
7.761556	6.859130	6.567391	6.333578	0.816019	0.923379
7.305064	5.274072	4.199055	4.813848	0.658974	0.912728
6.818562	3.985846	1.888169	3.682704	0.540099	0.923945
5.923663	2.281200	-2.36259	2.285119	0.385761	0.959650
10.95975	43.23341	21.55885	10.85105	0.990081	0.250987
11.20888	55.24795	23.59720	11.34250	0.995927	0.204930
11.61406	63.00805	24.66680	11.61619	1.000183	0.184260

DSF11418

Tw	B<U>/D	Log	Log
dyne/cm ² (1/sec)	Tw	B<U>/D	B<U>/D
1.093206	89.17978	0.038244	1.950266
0.72139	69.19419	-0.13540	1.840069
0.50421	49.79387	-0.29893	1.697175
0.361250	35.69850	-0.44219	1.552650
0.241012	24.15742	-0.61796	1.383050
0.143466	14.16578	-0.84325	1.151240
0.082212	8.208602	-1.08453	0.914269
0.029445	3.056653	-1.52803	0.485246

Log Tw vs. Log B<U>/D

Regression Output:

Constant	-2.00012
Std Err of Y Est	0.003109
R Squared	0.999926
No. of Observations	5
Degrees of Freedom	3

X Coefficient (s) 1.002293
Std Err of Coef. 0.004969

Tw = K'(B<U>/D)^{n'}

K' = 0.009997
n' = 1.002293

Tw# = 29.39713
Res/ft# = 1241.270

Regression Output:

Constant	-5.76053
Std Err of Y Est	0.085168
R Squared	0.996613
No. of Observations	8
Degrees of Freedom	6

X Coefficient(s) 5.732631
Std Err of Coef. 0.136377

t = 24.072 deg C
s.d.t = 0.519823 deg C

D1F21415
 Tw 3-U/D Log Log
 dyne/cm² (1/sec) Tw 8-U/D
 1.109654 67.18354 0.045187 1.927262
 0.878880 52.53235 -0.05607 1.720426
 0.683353 40.67815 -0.16535 1.609361
 0.487086 28.98502 -0.31239 1.462173
 0.349533 20.54202 -0.45638 1.312643
 0.195390 11.53640 -0.70909 1.062070
 0.115277 6.744529 -0.93825 0.828951
 0.040319 2.396911 -1.39448 0.379652

Log Tw vs. Log 8-U/D

Regression Output:
 Constant -1.77159
 Std Err of Y Est 0.003676
 R Squared 0.999944
 No. of Observations 5
 Degrees of Freedom 3

X Coefficient(s) 1.000366
 Std Err of Coef. 0.004305

Tw = K'(8-U/D)^{n'}
 K' = 0.016920
 n' = 1.000366

Tw# = 18.27988
 Res/fs = 981.0379

Regression Output:
 Constant -12.7263
 Std Err of Y Est 0.123504
 R Squared 0.994126
 No. of Observations 7
 Degrees of Freedom 5

X Coefficient(s) 8.120185
 Std Err of Coef. 0.279125

t = 24.3088
 s.d.t = 0.415687 deg C

Tap DL= 122.2234
 40.77743

80.1597	L	MDR	1///f	1///f/Siv	1///f/L
4	1///f	1///f			
14.83880	403.2572	39.98434	18.26383	1.230815	0.045290
14.57370	346.1843	38.72512	17.72904	1.216509	0.051212
14.21753	282.0095	37.03329	16.97554	1.193986	0.060194
13.80942	222.9444	35.09475	15.96560	1.156138	0.071606
13.59115	196.6390	34.05800	15.57088	1.145663	0.079185
13.19972	156.9684	32.19871	14.82464	1.123102	0.094443
12.84666	128.0988	30.52163	14.34131	1.116346	0.111955
12.25694	91.75222	27.76799	13.34831	1.088153	0.145482
13.12080	149.9961	31.82380	14.76269	1.125213	0.098427
12.76866	122.4749	30.15117	14.06317	1.101381	0.114824
12.30763	92.92792	27.96137	13.09808	1.064222	0.139448
11.81338	70.66850	25.61357	12.18638	1.031574	0.172444
11.96354	77.04881	26.32683	12.45570	1.041138	0.161659
11.63544	63.78846	24.76838	12.05070	1.033689	0.188916
11.41065	56.04597	23.70062	11.64718	1.020728	0.207814
10.99870	44.21363	21.74384	10.93858	0.994534	0.247402
10.70015	37.32210	20.22571	10.87390	1.016238	0.292057
10.19875	27.89770	17.94408	10.76701	1.055718	0.385946
10.24766	28.69426	18.17638	10.42618	1.018396	0.363702
9.717574	21.14821	15.65847	11.18688	1.151201	0.529975
9.536758	19.05766	14.79960	10.47911	1.098813	0.549863
9.355667	17.17105	13.93942	9.551697	1.020953	0.556267
9.105386	14.86882	12.75153	8.208480	0.901477	0.552059
8.89129	12.20268	11.77086	7.212092	0.810426	0.546259
8.680560	11.64180	10.73266	6.333412	0.729608	0.544023
8.382541	9.806531	9.317072	5.345339	0.637675	0.545079
8.094555	8.208439	7.949139	4.471377	0.552393	0.538173
7.582226	6.189941	5.520224	3.359164	0.442972	0.543681
7.120965	4.742745	3.524586	2.556806	0.359053	0.538984
6.206528	2.802203	-1.01899	1.526447	0.247553	0.548284
10.66807	36.55105	20.17337	10.74142	1.006875	0.292874
10.87877	43.70917	21.64915	10.89088	0.991994	0.249166
11.40706	55.92006	22.68354	11.38436	0.998010	0.203546
11.60780	62.78133	24.63705	11.88378	1.023775	0.189288

DSF21421
 Tw 8(U)/D Log Log
 dyne/cm2 (1/sec) Tw 8(U)/D

2.011490	66.44779	0.302518	1.822480
1.510815	50.39643	0.179211	1.702399
1.035945	34.00512	0.015336	1.531544
0.814815	26.58594	-0.08894	1.424652
0.568227	18.45698	-0.24547	1.256160
0.384188	12.35808	-0.41545	1.091951
0.252974	8.079863	-0.59592	0.907404
0.156304	5.043847	-0.80402	0.702761
0.092302	2.928222	-1.03478	0.466504

Log Tw vs. Log 8(U)/D

Regression Output:
 Constant -1.49457
 Std Err of Y Est 0.002906
 R Squared 0.999963
 No. of Observations 9
 Degrees of Freedom 7

X Coefficient(s) 0.985859
 Std Err of Coef. 0.002238

Tw = K'(8(U)/D)^{n'}
 K' = 0.032020
 n' = 0.985859

Tw = 35.82628
 Res/ft = 1340.592

Regression Output:
 Constant -29.2868
 Std Err of Y Est 0.113496
 R Squared 0.998378
 No. of Observations 8
 Degrees of Freedom 6

X Coefficient(s) 15.26898
 Std Err of Coef. 0.218298

t = 24.14 deg C
 s.d.t = 0.718013 deg C

Tap DL= 122.2234
 40.77743

Solvent	L	MDR	1/f/f	1/f/f	1/f/f/Slv	1/f/f/L
79.692						
4						
0.4						
14.63724	359.0792	39.02689	20.60361	1.407615	0.057379	
14.39783	312.8522	37.88972	19.70666	1.368723	0.062990	
14.10032	283.6110	36.47658	18.71021	1.328934	0.070976	
13.73515	213.6239	34.74197	17.31551	1.260671	0.081052	
13.49171	185.6982	33.58563	16.63773	1.233182	0.089595	
13.19086	156.1699	32.15663	15.82685	1.199834	0.101343	
12.84532	128.0011	30.51534	14.48337	1.127442	0.113142	
12.53674	95.51603	28.09955	12.93883	1.048803	0.135465	
13.05473	144.2989	31.50999	15.30140	1.172096	0.105966	
13.38964	175.1018	33.10080	16.82454	1.256534	0.096084	
12.81881	126.0620	30.38938	14.60595	1.139414	0.115863	
12.31616	94.38907	28.00179	13.00472	1.055906	0.137777	
12.06848	81.84686	26.82531	11.99805	0.994163	0.146591	
11.97191	77.42090	26.36658	12.35902	1.032334	0.159634	
11.66147	64.75137	24.89201	11.63272	0.997534	0.179452	
11.42232	56.42391	23.75608	11.39096	0.997254	0.201881	
10.80069	39.45065	20.80330	12.16106	1.125951	0.308260	
10.55378	34.22366	19.63048	11.63981	1.102904	0.340110	
10.58081	34.74025	19.75885	11.48290	1.085257	0.330345	
10.32109	29.93225	18.52520	9.791358	0.948674	0.327106	
10.15999	26.81500	17.61746	8.623682	0.851302	0.321599	
9.999069	24.86837	16.99558	7.860318	0.786105	0.316076	
9.839981	22.69214	16.23991	7.101533	0.721701	0.312951	
9.610424	19.88319	15.14951	6.030199	0.627464	0.303281	
9.557870	17.19283	13.94988	5.277275	0.563939	0.306946	
9.026180	14.20447	12.57455	4.300282	0.476423	0.302741	
8.813684	12.56901	11.36500	3.790956	0.430121	0.301611	
8.492728	10.44859	9.840462	3.151641	0.371098	0.301630	
8.148831	8.572113	8.206950	2.566385	0.314939	0.299387	
7.781955	6.940151	6.464289	2.067825	0.265720	0.297951	
7.359804	5.442908	4.459069	1.642214	0.223152	0.301716	
6.894411	4.162732	2.984452	1.240683	0.179954	0.297973	
10.77387	38.91247	20.68996	11.88919	1.103218	0.305576	
11.39106	55.41751	33.60757	11.19541	0.982824	0.202019	
11.61991	63.22061	34.69459	11.48343	0.988254	0.181640	

DIFS1424

DSR1438

8/29/90 12:37

10 PSID Taps 14 1.0 PSID Taps 14 0.1 PSID Taps 14

density viscosity

ID(cm) = 1.45796 12.72382

S = 2.7 S = 7.25 S = 9.9

Z = 2.7 Z = 9.05 Z = 6.85

co[NaCl]=1.00088 1.001574

996.8529 X coeff -0.00025 -0.02281

0.000099 constant 0.003419 -4.14933

K(W/psi)=1.077088 12.8687

XS(cm2)= 1.669479

Freq. (Hz)	Q'est (1/s)	Temp (deg C)	<V> (volts)	<U> (volts)	<V>f (volts)	<V>corr (volts)	Batch Vol (ml)	t (sec)	DP (psid)	<U> (cm/s)	Re	Tw (dyne/cm2)	f	Log(Re/f)	
60	1.21416	24.7	4.055666	0.0545	0.0575	3.998166	3.70259	727.2685	117574.8	523.2945	0.001924	2.719086			
50	1.01118	24.7	3.166333	0.0545	0.0575	3.108833	2.884189	606.0571	97979.02	406.8953	0.002221	2.664455			
39	0.789204	24.7	2.268666	0.0545	0.0575	2.211166	2.051388	472.7245	74423.64	289.4054	0.002597	2.590487			
29	0.586844	24.7	1.543	0.0545	0.0575	1.4855	1.378158	351.5131	56827.83	194.4276	0.003155	2.504092			
19	0.384484	24.7	0.918666	0.0545	0.0575	0.861166	0.798938	230.3017	37232.02	112.7126	0.004261	2.385700			
14	0.283304	24.7	0.63725	0.0545	0.0575	0.57975	0.537857	169.6960	27434.12	75.87977	0.005284	2.299773			
9	0.182124	24.7	0.371	0.0545	0.0575	0.3135	0.290846	109.0902	17636.22	41.03201	0.006914	2.166275			
18	0.364248	24.9	9.4716	0.0675	0.085	9.3866	0.729413	218.1805	35431.95	102.9040	0.004335	2.267900			
14	0.283304	24.9	6.5951	0.0675	0.085	6.5101	0.505886	169.6960	27558.18	71.36937	0.004970	2.288440			
10	0.20236	24.8	4.43025	0.0875	0.0905	4.33975	0.337332	121.2114	19640.06	47.57611	0.006493	2.199393			
8	0.161888	24.8	3.05	0.0875	0.0905	2.9595	0.229976	96.96914	15712.05	32.44461	0.006919	2.116270			
		24.4	2.804666	0.1035	0.106	2.698666	15	0.209707	88.73024	14247.93	29.58513	0.007535	2.092295		
		24.3	1.6448	0.0995	0.0995	1.5453	1745	0.120082	70.15006	11239.02	16.94092	0.006902	2.270241		
		24.3	1.2452	0.0995	0.0995	1.1457	1485	0.089029	59.69790	9564.440	12.56015	0.007066	2.905270		
		24.2	7.45675	0.0445	-0.1425	7.59925	1481	0.095231	59.53710	9517.192	13.43503	0.007599	2.918907		
		24.2	5.5362	0.0205	0.0085	5.5277	1111	0.069271	44.96465	7187.733	9.772656	0.009691	2.849794		
		24.2	4.596666	0.0095	0.014	4.582666	1242	0.057428	37.38414	5975.966	8.101891	0.011627	2.809081		
		24.1	3.503714	0.0135	0.0145	3.489214	1160	0.043725	28.01723	4468.345	6.168730	0.015753	2.748900		
		24.1	2.784375	0.0145	0.0145	2.749875	1083	0.034711	21.69582	3460.326	4.896980	0.020859	2.698766		
		24.1	2.446333	0.0135	0.0135	2.432833	940	0.030487	18.76832	2993.411	4.301109	0.024482	2.670592		
		24	2.057666	0.0105	0.0075	2.050166	908	0.025692	15.49521	2465.805	3.624577	0.030267	2.632446		
		23.95	1.562181	0.0075	0.0045	1.557681	781	0.019520	11.69526	1859.007	2.753892	0.040267	2.572298		
		23.8	1.206818	0.0025	0	1.206818	604	0.015123	9.022179	1429.266	2.133585	0.052550	2.515402		
		23.7	0.793388	0	0	0.793388	735	0.009942	5.877930	929.0653	1.402366	0.081392	2.423329		
		23.6	0.571045	-0.0005	-0.0015	0.572545	634	0.007174	4.219545	665.4382	1.012327	0.113975	2.351515		
		23.6	0.382833	-0.0035	-0.0035	0.386333	431	0.004841	2.868492	452.3720	0.683015	0.166414	2.266091		
		23.5	0.213578	-0.0045	-0.0045	0.218078	306	0.002732	1.527422	240.3274	0.355551	0.231300	2.140929		
		23.4	0.136	-0.0085	-0.0095	0.1445	201	0.001810	1.004143	157.6443	0.255467	0.507916	2.050574		
		23.3	0.065909	-0.0105	-0.0125	0.076409	107	0.000957	0.534098	83.66122	0.135086	0.949307	1.911227		
		23.6	9.50175	-0.0145	-0.0165	9.51825	1731	0.119279	69.12333	10901.01	16.82771	0.007060	2.961889		

79.692 Tap DL= 122.2234
79.79777 40.77743
0.4

Solvent	L	MDR	1/f/f	1/f/f	1/f/f	1/f/f/S1v	1/f/f/L
14.47634	327.3158	38.26265	22.45057	1.550844	0.068589		
14.25782	288.6258	37.22464	21.21670	1.488074	0.073509		
13.96186	243.4149	35.81887	19.62277	1.405454	0.080614		
13.61637	199.5137	34.17776	17.80187	1.307395	0.089223		
13.14280	151.9078	31.92830	15.31851	1.165543	0.100840		
12.79910	124.6398	30.79576	13.75669	1.074817	0.110371		
12.26510	91.65482	27.75923	12.02625	0.980526	0.131212		
13.07160	145.8077	31.59011	15.18779	1.161892	0.104163		
12.75376	121.4283	30.08036	14.18438	1.112172	0.116812		
12.39757	98.91760	28.38847	12.40935	1.000950	0.125451		
12.06508	81.68652	26.80913	12.02160	0.998396	0.147167		
11.76918	77.29921	26.35360	11.52011	0.962481	0.149032		
11.48096	58.36085	24.03459	12.03612	1.048355	0.206226		
11.22108	50.25169	22.80014	11.89566	1.060117	0.236721		
11.27562	51.85440	23.05923	11.47099	1.017326	0.221214		
10.99917	44.22565	21.74609	10.15775	0.923501	0.229680		
10.82632	40.26809	20.97254	9.275279	0.855943	0.230338		
10.59560	35.05747	19.83911	7.966462	0.751865	0.227240		
10.39506	31.23538	18.87657	6.923891	0.666074	0.221668		
10.28237	29.27338	18.34126	6.391068	0.621555	0.218323		
10.12978	26.81181	17.61647	5.747945	0.567430	0.214381		
9.889193	23.34416	16.47366	4.977174	0.507794	0.213208		
9.661608	20.47774	15.39264	4.362254	0.451303	0.213024		
9.293356	16.56605	13.64344	3.505154	0.377167	0.211586		
9.006063	14.04092	12.27879	2.962047	0.328894	0.210958		
8.644267	11.53378	10.65574	2.451341	0.282922	0.212535		
8.163729	8.645945	8.27717	1.737356	0.212814	0.200944		
7.802297	7.021895	6.560912	1.403149	0.179838	0.199824		
7.244910	5.094572	3.913326	1.026352	0.141665	0.201459		
11.44755	57.24919	23.87589	11.90083	1.039596	0.207877		

DIF31424

Tw	8<U>/D	Log	Log
dyne/cm2	(1/sec)	Tw	8<U>/D
2.753892	64.17329	0.439946	1.307254
2.135585	49.50577	0.329110	1.594655
1.402666	32.25290	0.146954	1.508568
1.012227	23.15314	0.005278	1.264610
0.683015	15.73975	-0.16556	1.196998
0.385551	8.281147	-0.41391	0.923303
0.255467	5.509854	-0.59266	0.741140
0.135086	2.930662	-0.86938	0.466965

Log Tw vs. Log 8<U>/D

Regression Output:
 Constant -1.21874
 Std Err of Y Est 0.006098
 R Squared 0.999848
 No. of Observations 8
 Degrees of Freedom 6

X Coefficient(s) 0.971772
 Std Err of Coef. 0.004884

Tw = K'(8<U>/D)^n'

K' = 0.048001
 n' = 0.971772

Tw# = 60.52745
 Res/# = 1781.107

Regression Output:

Constant -55.0788
 Std Err of Y Est 0.105409
 R Squared 0.999223
 No. of Observations 6
 Degrees of Freedom 4

X Coefficient(s) 20.82069
 Std Err of Coef. 0.290197

t = 24.22166 deg C
 s.d.(t) = 0.485057 deg C

D:P13119

DSR1438

B/22/90 15:40

10 PSID Taps 14 1.0 PSID Taps 14 0.1 PSID Taps 14
 S = 2.7 S = 7.25 S = 9.9 <C>(ppm) =
 Z = 2.7 Z = 9.1 Z = 6.85 [NaCl] =

density viscosity

col[NaCl] 1.01234 1.029478

29.99008 X coeff -0.00035 -0.02381

0.300133 constant 0.003419 -4.14933

ID(cm) = 1.45796
 K(U/psi)=1.07888 12.72683
 XS(cm2)= 1.569479
 1.085095

Freq. (Hz)	Q'est (1/s)	Temp (deg C)	<V> (volts)	<V>o (volts)	<V>f (volts)	<V>corr (volts)	Batch Vol (ml)	t)swamp (sec)	DP (psid)	<U> (cm/s)	Re	Tw (dyne/cm2)	f	Log (ke/f)	
60	1.21416	24.9	8.171	0.0555	0.0785	8.0925			7.507737	727.2685	116312.9	1059.175	0.005967	3.864878	
50	1.0118	24.9	5.98225	0.0555	0.0785	5.90375			5.477146	606.0571	96927.45	772.7041	0.004167	3.796400	
40	0.80944	24.9	4.1225	0.0555	0.0785	4.067			3.773119	484.8457	77541.96	532.3036	0.004486	3.715474	
30	0.60708	24.9	2.5235	0.0555	0.0785	2.445			2.368324	355.6342	58136.47	320.0104	0.004794	3.604976	
25	0.5059	24.9	1.861665	0.058	0.0585	1.803166			1.672870	303.0285	48463.72	233.0049	0.005091	3.523854	
20	0.40472	24.9	1.2725	0.058	0.0585	1.214			1.126276	242.4228	38770.98	158.8927	0.005356	3.452946	
15	0.30354	24.9	0.801428	0.058	0.0585	0.743928			0.689244	181.8171	29078.23	97.23717	0.005827	3.346310	
10	0.20236	24.9	0.38125	0.058	0.0585	0.368625			0.342915	121.2114	19385.49	48.37785	0.006523	3.194717	
8	0.161888	24.9	0.306	0.058	0.0585	0.2475			0.229615	96.96914	15508.39	32.39369	0.006825	3.107624	
23	0.465428	23.5	1.633666	0.0645	0.0705	1.563166			1.450212	278.7862	43200.41	204.5929	0.005213	3.494046	
34	0.688024	23.5	3.1185	0.0645	0.0705	3.048			2.827752	412.1188	63861.47	398.9332	0.004651	3.639051	
12	0.242832	23.4	0.582	0.0615	0.0625	0.5195			0.481761	145.4537	22488.55	67.99402	0.006264	3.255851	
18	0.364248	24.9	1.234033	0.0535	0.0825	1.235783			0.963148	218.1805	34893.88	135.8790	0.005555	3.418970	
14	0.283204	24.9	0.790125	0.0535	0.0825	0.707625			0.605620	169.6960	27139.48	85.43960	0.005878	3.318222	
10	0.20236	24.9	0.42225	0.0535	0.0825	0.35975			0.240992	121.2114	19385.49	48.10645	0.006486	3.197496	
8	0.161888	24.9	0.3059833	0.0535	0.0825	0.2977333			0.233941	96.96914	15508.39	33.00396	0.006953	3.111677	
24.5	2.073	24.5	2.073	0.0555	0.056	2.017	1963		15	0.158484	78.38770	12424.01	22.35859	0.007208	3.023175
24.4	1.48475	24.4	1.48475	0.0555	0.0545	1.43025	1594		15	0.112380	63.65257	10065.84	15.85442	0.007751	2.947543
24.4	1.15075	24.4	1.15075	0.0545	0.0535	1.09725	1380		15	0.086215	55.10699	8714.472	12.16309	0.007734	2.889990
24.3	0.7158	24.3	0.7158	0.0535	0.0535	0.6623	1367		20	0.052039	40.94090	6459.695	7.341645	0.008676	2.779279
24.25	0.542166	24.25	0.542166	0.0535	0.0535	0.488666	1146		19.9	0.038396	34.49454	5436.447	5.416907	0.009017	2.712866
24.1	3.1132	24.1	3.1132	0.029	0.0295	3.0837	1147		20	0.038469	34.35202	5395.695	5.427189	0.009109	2.711800
24.1	1.8408	24.1	1.8408	0.0385	0.041	1.8023	1056		25	0.022483	25.30129	3974.091	3.171976	0.009814	2.595177
24.05	1.215142	24.05	1.215142	0.0455	0.0435	1.171642	1157		35	0.014616	19.90086	3106.639	2.62044	0.010417	2.501169
24	0.879416	24	0.879416	0.0475	0.0475	0.831916	1264		45.1	0.010278	16.78763	2630.902	1.464140	0.010290	2.426318
24	0.494812	24	0.494812	0.0495	0.05	0.446812	1376		60	0.005574	13.73681	2152.788	0.786372	0.008254	2.291341
24	0.354705	24	0.354705	0.0495	0.0495	0.305205	1250		75	0.003807	10.01509	1599.533	0.537150	0.010607	2.208575
23.9	0.273409	23.9	0.273409	0.0505	0.0505	0.222909	1120		90	0.002780	7.434086	1165.547	0.392311	0.010784	2.159257
23.8	0.20325	23.8	0.20325	0.0505	0.05	0.15225	862		100	0.001911	5.153285	805.5304	0.269713	0.020037	2.057008
23.6	0.1454	23.6	0.1454	0.05	0.05	0.0954	647		120	0.001190	3.229549	501.5776	0.167900	0.021882	1.952112
23.5	0.104454	23.5	0.104454	0.05	0.05	0.058454	310		100	0.000679	1.856866	287.7378	0.095837	0.055048	1.859370
23.4	0.077083	23.4	0.077083	0.05	0.049	0.028083	158		100	0.000350	0.946402	146.3220	0.049425	0.109284	1.684592
23.6	4.1612	23.6	4.1612	0.048	0.0475	4.1137	1346		20	0.051218	40.31196	6260.805	7.239948	0.008623	2.769454
23.7	6.89225	23.7	6.89225	0.0475	0.05	6.84225	1248		15	0.085257	52.82915	8779.026	12.04208	0.008221	2.836922
23.8	8.7225	23.8	8.7225	0.0495	0.0505	8.7225	1571		15	0.108817	62.73412	9787.235	15.35169	0.007735	2.934635
23.7	12.43	23.7	12.43	0.0495	0.05	12.38	1912		15	0.154441	76.35114	11884.79	21.78850	0.007403	3.009682

80.1597 Tap DL= 122.2234
 0.4 40.77743

Solvent	L	MDR	1/f/f	1/f/f	1/f/f/Siv	1/f/f/L
15.05951	457.8870	41.03268	15.87631	1.054238	0.034672	
14.78560	391.0938	39.73161	15.48980	1.047627	0.039606	
14.46189	324.6041	38.19400	14.93010	1.032374	0.045994	
14.01990	251.6844	36.09455	14.44181	1.030093	0.057380	
13.75541	216.1398	34.83824	14.01399	1.018797	0.064837	
13.41178	177.3480	33.20598	13.66345	1.018764	0.077043	
12.98524	138.7364	31.17989	13.09958	1.008805	0.094420	
12.37887	97.85830	28.59983	12.58109	1.000179	0.126520	
12.05049	80.07641	26.64486	12.10437	1.006140	0.151160	
13.57618	194.9516	33.98689	13.84972	1.020148	0.071041	
14.15620	272.2273	36.74198	14.66179	1.035715	0.053858	
12.61540	112.1325	29.62318	12.53457	0.993592	0.111783	
13.27588	164.0025	32.56044	13.29776	1.001648	0.081082	
12.87289	130.0480	30.64625	13.04310	1.013221	0.100294	
12.37398	97.58342	28.27642	12.41597	1.003593	0.127234	
12.04670	80.82718	26.72187	11.99193	0.995453	0.148365	
11.69270	65.92586	25.04034	11.77839	1.007328	0.178661	
11.39017	55.38902	23.60332	11.58812	0.997186	0.205060	
11.15996	48.51438	22.50981	11.25666	1.005976	0.231408	
10.71751	37.60623	20.40821	10.73574	1.001700	0.285477	
10.45146	32.26608	19.14445	10.53049	1.007561	0.326564	
10.44720	32.18698	19.12420	10.47724	1.002875	0.325511	
9.980710	24.60694	16.90837	10.09392	1.011343	0.410306	
9.604676	19.81751	15.1221	9.797611	1.020087	0.494391	
9.305375	16.68011	13.70005	9.857932	1.059391	0.590999	
8.785366	12.22423	11.15549	11.00676	1.255710	0.900405	
8.434301	10.10311	9.562933	9.709459	1.151187	0.961035	
8.157430	8.61651	8.247795	8.456142	1.036618	0.981600	
7.828035	7.126706	6.88167	7.064364	0.902444	0.991252	
7.408449	5.597478	4.690135	5.600486	0.755959	1.000537	
6.917480	4.219394	3.58031	4.262122	0.616139	1.010129	
6.538568	3.023236	-0.39274	3.024966	0.477246	1.000572	
11.13369	47.51195	22.33753	11.02226	0.990881	0.231989	
11.33854	55.76694	23.35807	11.37690	1.003383	0.211596	
11.63873	65.90925	24.78399	11.62272	0.998624	0.181862	

DP13119

Tw	S.U./D	Log	Log
dyne/cm ²	(1/sec)	Tw	S.U./D
0.786272	75.27554	-0.10437	1.877230
0.537150	54.95403	-0.26990	1.739999
0.392511	40.90185	-0.40636	1.611738
0.269713	28.33156	-0.56909	1.452270
0.167900	17.72092	-0.77494	1.248486
0.095837	10.18884	-1.01846	1.008124
0.049425	5.193024	-1.30504	0.715420

Log Tw vs. Log S.U./D

Regression Output:
 Constant -2.02501
 Std Err of Y Est 0.003767
 R Squared 0.999906
 No. of Observations 4
 Degrees of Freedom 2

X Coefficient(s) 1.001306
 Std Err of Coef. 0.006852

Tw = K' (S.U./D)^{n'}

K' = 0.009440
 n' = 1.001306

Tw* = 77.28853
 Res/† = 1979.027

Regression Output:
 Constant -4.88857
 Std Err of Y Est 0.054415
 R Squared 0.997551
 No. of Observations 10
 Degrees of Freedom 8

X Coefficient(s) 5.361639
 Std Err of Coef. 0.093705

t = 24.04074 deg C
 s.d.t = 0.471411 deg C

DIP23116

DSR1438 8/18/90 13:33
 10 PSID Taps 14 1.0 PSID Taps 14 0.1 PSID Taps 14 9.9 C<(ppm)=
 S = 2.7 S = 7.25 S = 9.1 Z = 6.85 [NaCl]=
 Z = 2.7 Z = 9.1 Z = 6.85 [NaCl]=

density viscosity
 (g/ml) (cP) (cm/s)
 99.83178 X coeff -0.00025 -0.02281
 0.300128 constant 0.003419 -4.14933
 ID(cm) = 1.45796
 K(V/psi)=1.07888 12.72682
 XS(cm2) = 1.669479
 1.085095

Freq. (Hz)	Qest (1/s)	Temp (deg C)	<U> (volts)	<U>0 (volts)	<U>f (volts)	<U>corr (volts)	Batch Vol (ml)	t (sec)	DP (psid)	<U> (cm/s)	Re	Tw (dyne/cm2)	f	Log(Re/f)	
60	1.21416	24.9	6.866333	0.0465	0.0155	6.850833	6.55793	727.2685	116312.9	896.6618	0.00358	3.828708			
50	1.0118	24.9	5.157	0.0465	0.0155	5.1415	4.76976	506.0571	9697.45	672.9381	0.003539	3.766281			
42	0.849912	24.9	3.934	0.0465	0.0155	3.8875	3.506589	509.0880	81419.06	508.8100	0.003889	3.705572			
34	0.688024	24.9	2.818	0.0465	0.0155	2.8025	2.599991	412.1188	5910.56	366.8013	0.004278	3.534609			
30	0.60708	24.8	2.300333	0.0515	0.0525	2.247833	2.085405	363.5342	58035.41	294.2045	0.004478	3.585773			
25	0.465428	24.8	1.50125	0.0515	0.0525	1.44875	1.344063	278.7862	44486.15	189.6175	0.004833	3.490248			
17	0.344012	24.8	0.9292	0.0515	0.0525	0.8767	0.813349	206.0594	2881.07	114.7456	0.005333	3.381277			
13	0.263068	24.8	0.6226	0.0515	0.0525	0.5701	0.528904	157.5748	25144.24	74.61574	0.005953	3.287827			
10	0.20236	24.8	0.41575	0.0515	0.0525	0.36335	0.337001	121.2114	19341.80	47.54367	0.006410	3.189954			
25	0.5059	24.3	1.73325	0.0475	0.0415	1.69175	1.569504	303.0285	47812.14	231.4232	0.004776	3.519097			
35	0.70826	24.3	2.916	0.0475	0.0415	2.8745	2.666789	424.2400	66956.99	376.2249	0.004140	3.64206			
10	0.20236	24.3	0.3945	0.0615	0.03	0.3645	0.328161	121.2114	19124.85	47.70707	0.006432	3.185774			
18	0.364248	25.7	11.51775	0.0405	0.0655	11.45225	0.899850	218.1805	35529.36	125.9490	0.005284	3.412090			
15	0.30354	25.7	8.44525	0.0405	0.0655	8.37975	0.658421	181.8171	29607.80	92.89016	0.005568	3.344260			
10	0.20236	25.7	4.34875	0.0405	0.0655	4.28325	0.325522	121.2114	19738.53	47.48015	0.006403	3.198531			
8	0.161888	25.7	2.927857	0.0405	0.0655	2.86357	0.224907	96.96914	15790.82	31.72944	0.006686	3.111007			
		25.4	2.0902	0.0205	0.019	2.0712	14.9	0.162742	79.07459	12789.95	22.95940	0.007275	3.037800		
		25.3	1.42325	0.0125	0.0125	1.42075	14.9	0.111634	63.99936	10328.27	15.74912	0.007618	2.954967		
		25.3	1.1062	0.0105	0.0095	1.0967	14.9	0.086172	54.91403	8862.079	12.15700	0.007987	2.898748		
		25.3	0.6754	0.0085	0.0075	0.6679	20	0.052479	41.09035	5631.248	7.403722	0.008688	2.791060		
		25.2	0.490833	0.0065	0.0065	0.484333	25	0.038056	34.28613	5520.660	5.348871	0.009049	2.720291		
		25.1	3.145666	0.0045	0.0285	3.117166	25	0.038886	34.23821	5500.521	5.486089	0.009272	2.723996		
		25.1	1.887833	0.0295	0.034	1.853833	25	0.023126	25.44505	4087.861	3.263672	0.007984	2.611151		
		25	1.267428	0.0385	0.0385	1.238928	35	0.015331	20.19448	2227.022	2.162865	0.010507	2.529894		
		25	0.890125	0.0415	0.0415	0.848625	39.9	0.010586	16.96385	2719.176	1.493546	0.010382	2.440488		
		24.95	0.492384	0.0425	0.0425	0.449884	50	0.005612	13.87258	2221.163	0.791778	0.008151	2.202188		
		24.8	0.3368	0.0425	0.0425	0.3255	59.9	0.004060	10.56980	1686.632	0.572367	0.010158	2.230436		
		24.75	0.27382	0.0425	0.0425	0.231723	74.9	0.002885	7.629313	1216.043	0.407120	0.013856	2.155777		
		24.6	0.193894	0.0425	0.0425	0.151394	75	0.001888	4.991575	792.9240	0.266448	0.021184	2.062245		
		24.5	0.129055	0.0425	0.0425	0.086555	80	0.001079	2.845198	450.9482	0.152234	0.037277	1.939852		
		24.4	0.084571	0.0425	0.0425	0.044071	90	0.000549	1.464195	231.5439	0.077563	0.071668	1.792298		
		24.25	0.064388	0.0425	0.0425	0.021888	90	0.00027	0.732097	115.3808	0.038523	0.142377	1.638852		
		24.4	4.2258	0.0415	0.0395	4.1863	19.9	0.052324	40.57473	6416.380	7.567721	0.008865	2.781174		
		24.6	6.3386	0.0395	0.0395	6.7991	15	0.084819	53.90901	8563.579	11.96614	0.008156	2.888415		
		24.6	8.988666	0.0395	0.0385	8.950166	15	0.111654	63.17338	10035.24	15.75193	0.007019	2.948105		
		24.6	12.59825	0.0385	0.0385	12.55975	15.1	0.156684	77.11488	12249.88	22.10465	0.007363	3.021680		

80.1597
4
0.4

Solvent L NDR
1//f 1//f 1//f 1//f 1//f/SIV 1//f/L

Tap DL= 122.2234
40.77743

14.91483	421.2973	40.34546	17.25517	1.156913	0.040957
14.66552	364.9739	39.16125	16.59834	1.131793	0.045478
14.42268	317.3600	38.00777	16.03444	1.111751	0.050524
14.13843	269.4572	36.45758	15.28783	1.081295	0.056735
13.94293	240.7763	35.72894	15.06206	1.080264	0.062556
13.56139	193.2985	33.91662	14.38389	1.060669	0.074412
13.12510	150.2686	31.84424	13.66685	1.041275	0.090889
12.75130	121.2571	30.06871	12.98024	1.016385	0.106882
12.35981	96.79092	28.20913	12.48942	1.010486	0.129035
13.67637	206.5256	34.46278	14.46919	1.057969	0.070060
14.13682	269.2073	36.64993	15.54029	1.099277	0.057726
12.34309	95.86378	28.12971	12.46877	1.010181	0.130067
13.24876	161.4249	32.42972	13.75614	1.038328	0.085216
12.97704	138.0831	31.14095	13.40125	1.032689	0.097052
12.39412	98.72155	28.37210	12.49634	1.008247	0.126581
12.04402	80.70253	26.70913	12.22919	1.015373	0.151534
11.75120	68.18372	25.31821	11.72379	0.997688	0.171944
11.41985	56.34343	23.74430	11.45683	1.063228	0.203339
11.19499	49.50264	22.67621	11.18889	0.999455	0.226026
10.76424	38.63127	20.65014	10.72840	0.996670	0.277712
10.48116	32.82248	19.38553	10.51234	1.002974	0.320278
10.49598	33.10367	19.35592	10.38502	0.989428	0.313712
10.04460	25.52886	17.21187	10.00793	0.996349	0.392024
9.683577	20.73875	15.49699	9.755546	1.007432	0.470410
9.361955	17.23331	13.96928	9.861627	1.053372	0.572241
8.808755	12.53340	11.34158	11.07622	1.257410	0.883736
8.521744	10.62468	9.978285	9.921662	1.164276	0.935831
8.232111	8.946597	8.559779	8.495152	1.053082	0.949540
7.848982	7.213160	6.782665	6.870463	0.875331	0.952490
7.359409	5.441673	4.457196	5.179337	0.703770	0.951791
6.769192	3.874167	1.855668	3.735382	0.551820	0.964176
6.155415	2.721033	-1.26177	2.650208	0.430549	0.975971
10.72453	37.75852	20.44156	10.62074	0.990322	0.281280
11.15366	48.33880	22.47990	11.07234	0.992708	0.229056
11.29242	55.46075	23.61400	11.30895	0.992673	0.203909
11.68672	65.69929	25.01193	11.65336	0.997145	0.177374

DIP23116

Tw	8-U/D	Log	Log
dyne/cm2	(1/sec)	Tw	8<U>/D
0.791778	76.12053	-0.10139	1.881501
0.573867	57.99778	-0.24194	1.763411
0.407120	41.86295	-0.39027	1.621829
0.266448	27.38936	-0.57438	1.437582
0.152334	15.61194	-0.81720	1.192456
0.077563	8.034215	-1.11034	0.904943
0.038523	4.017107	-1.41427	0.603913

Log Tw vs. Log 8<U>/D

Regression Output:
Constant -2.02309
Std Err of Y Est 0.002338
R Squared 0.999978
No. of Observations 5
Degrees of Freedom 4

X Coefficient(s) 1.008639
Std Err of Coef. 0.002356

Tw = K' (8<U>/D)^n'
K' = 0.009482
n' = 1.008639

Tw# = 40.89822
Res/f# = 1439.615

Regression Output:
Constant -7.89313
Std Err of Y Est 0.072396
R Squared 0.994515
No. of Observations 10
Degrees of Freedom 8

X Coefficient(s) 6.373561
Std Err of Coef. 0.187318

t = 24.90138 deg C
s.d.t = 0.411211 deg C

DSR1438 8/25/90 15:49
 10 PSID Taps 14 0.1 PSID Taps 14
 S = 2.7 S = 7.25 S = 9.9 <C> (ppa) =
 Z = 2.7 Z = 9.05 Z = 6.85 [NaCl] =

Freq. (Hz)	Q>est (1/s)	Temp (deg C)	<V> (volts)	<V>o (volts)	<V>f (volts)	<V>corr (volts)
60	1.21416	25.5	5.7435	0.049	0.0475	5.696
50	1.0118	25.5	4.323	0.049	0.0475	4.2755
40	0.80944	25.5	3.081333	0.049	0.0475	3.023833
30	0.60708	25.5	2.012666	0.049	0.0475	1.95166
25	0.5059	25.5	1.526	0.049	0.0475	1.4885
19	0.384484	25.5	0.991	0.049	0.0475	0.9435
15	0.30354	25.5	0.691	0.049	0.0475	0.6435
10	0.20236	25.5	0.388375	0.049	0.0475	0.340875
35	0.70826	24.2	2.512	0.0525	0.0535	2.4585
26	0.524136	24.2	1.62575	0.0525	0.0535	1.57225
10	0.20236	24	0.393833	0.0525	0.0535	0.338333
20	0.40472	25.5	12.46666	0.0135	0.0405	12.42616
15	0.30354	25.5	7.730444	0.0135	0.0405	7.689944
10	0.20236	25.5	4.165222	0.0135	0.0405	4.124722
8	0.161868	25.5	2.925833	0.0135	0.0405	2.885333
		25.1	2.121	0.0065	0.0035	2.1175
		25	1.445	0.0005	-0.0025	1.4475
		24.9	1.10325	-0.0035	-0.0065	1.10975
		24.8	0.6688	-0.0065	-0.0075	0.6763
		24.7	4.27425	0.047	-0.0585	4.22725
		24.6	3.1502	0.0455	-0.0425	3.1047
		24.5	1.866833	0.0085	-0.002	1.858333
		24.5	1.1829	-0.0065	-0.0065	1.1894
		24.4	0.677	-0.0065	-0.0065	0.6825
		24.4	0.464333	-0.0045	-0.004	0.468333
		24.3	0.345142	-0.0025	-0.0025	0.347442
		24.2	0.263263	-0.0025	-0.0025	0.265763
		24.15	0.205363	-0.0015	-0.0015	0.206863
		24	0.162363	-0.0005	0	0.162863
		23.9	0.105941	0	0.001	0.105941
		23.75	0.069863	0.0015	0.0025	0.068363
		23.6	0.032833	0.0025	0.003	0.030333
		24	6.779	0.0035	-0.0045	6.7835
		24.1	8.985	-0.0035	-0.0095	8.9905
		24.2	12.76275	-0.0105	-0.0155	12.77825

density viscosity
 co[NaCl] 1.01234 1.029478
 K(V/psi)=1.077888 12.72687
 XS(cm2)= 1.569479
 0.300065 constant 0.007419 -4.14933 1.085095

Batch Vol (ml)	t(samp (sec))	DP (psid)	<U> (cm/s)	Re	Tw (dyne/cm2)	f	Log(Re/f)
5.284408	727.2685	117898.0	745.5130	0.002792	3.794522		
3.966553	606.0571	98248.38	559.5928	0.003018	3.732241		
2.814609	484.8457	78598.70	397.0790	0.003347	3.557744		
1.823164	363.6342	58949.03	257.2081	0.003854	3.563447		
1.389941	305.0285	49124.19	194.8202	0.004203	3.503122		
0.873222	230.3017	37354.38	123.4886	0.004613	3.404119		
0.597000	181.8171	29474.51	84.22360	0.005048	3.321022		
0.316243	121.2114	19649.67	44.61495	0.006017	3.183645		
2.280849	424.2400	56786.15	321.7773	0.003541	3.599375		
1.458659	315.1497	49612.57	205.7817	0.004104	3.502201		
0.313885	121.2114	18995.85	44.28228	0.005969	3.166642		
0.976375	242.4228	39299.35	137.7450	0.004644	3.427845		
0.604230	181.8171	29474.51	85.24361	0.005109	3.327653		
0.324096	121.2114	19649.67	45.72285	0.006166	3.188272		
0.226712	96.96914	15719.74	31.98413	0.006739	3.110772		
15	0.166280	79.62561	12792.20	0.007264	3.029645		
15	0.113736	64.17169	10286.23	0.007719	2.956058		
15	0.087197	54.94726	8787.782	0.008072	2.897376		
1368	19.9	0.053139	41.17673	0.008566	2.788948		
1374	20	0.053044	41.15054	0.008754	2.787475		
1431	25.1	0.038958	34.14953	0.009326	2.719470		
1275	30	0.033318	25.45703	0.009787	2.670327		
1339	40	0.014924	20.05115	0.010581	2.510159		
1411	49.9	0.008576	16.93774	0.010992	2.388859		
1265	54.9	0.005876	13.80184	0.011528	2.241071		
1005	59.9	0.004362	10.49980	0.011548	2.110157		
947	75	0.003334	8.026453	0.011445	2.181767		
746	90	0.002595	6.302496	0.011826	2.125889		
485	90.1	0.002043	4.959443	0.012215	2.073461		
383	90.1	0.001329	3.224303	0.012544	1.979096		
154	100.1	0.000380	2.085571	0.012023	1.862499		
1366	14.9	0.005121	54.11001	0.008794	12.00875		
1573	14.9	0.112815	63.23555	9922.451	15.91578	0.007883	2.945426
1941	14.9	0.160345	78.02938	12282.80	21.52119	0.007359	3.022755

79.692
4
0.4

Solvent	L	MDR	Tap DL=	1//f	1//f	1//f/Slv	1//f/L
	1//f	1//f	122.2234 40.77743				
14.77813	389.4154	39.69613	18.92228	1.280424	0.048591		
14.52896	337.3817	38.51259	18.20051	1.252705	0.053946		
14.23097	284.1999	37.09713	17.28507	1.214609	0.060820		
13.85379	228.7325	35.30550	16.10752	1.162679	0.070420		
13.61249	199.0685	34.15932	15.42314	1.133013	0.077476		
13.21647	158.4890	32.27826	14.72278	1.115971	0.092894		
12.88408	130.8887	30.59942	14.07421	1.092371	0.107528		
12.33218	95.26333	28.07786	12.89168	1.045369	0.135326		
13.99710	248.4023	35.98623	16.80392	1.200528	0.067648		
13.60880	198.6467	34.14182	15.60954	1.147018	0.078579		
12.26657	91.73237	27.76620	12.94244	1.055098	0.141089		
13.31137	167.3876	32.72902	14.67377	1.103348	0.087663		
12.89454	131.6789	30.74909	13.98975	1.084936	0.106241		
12.35348	96.43889	28.17907	12.73453	1.030845	0.132047		
12.04309	80.65900	26.70468	12.18070	1.011427	0.151014		
11.75858	68.47401	25.35326	11.67615	0.992989	0.170519		
11.42423	56.48565	23.76510	11.38146	0.996256	0.201493		
11.18950	49.34649	22.65014	11.13020	0.994700	0.225552		
10.75539	38.43511	20.58811	10.68457	0.993415	0.277989		
10.74990	38.31378	20.56202	10.68745	0.994191	0.278945		
10.47788	32.76051	19.26994	10.34923	0.987721	0.315905		
10.02814	25.28817	17.13711	9.972051	0.994405	0.394336		
9.640558	20.25110	15.29265	9.817796	1.018384	0.485282		
9.155438	15.30170	12.98833	10.94006	1.194925	0.714957		
8.827071	12.66624	11.42859	10.74969	1.220075	0.850267		
8.566287	10.88809	10.18036	9.509640	1.110383	0.873397		
8.327069	9.498334	9.03581	8.314405	0.998478	0.873353		
8.107478	8.370464	8.010521	7.400171	0.912758	0.884081		
7.893846	7.401875	6.995772	6.562759	0.831376	0.886634		
7.516387	5.956304	5.203840	5.290229	0.703826	0.888173		
7.129997	4.768472	3.367485	4.259823	0.597450	0.893330		
6.418275	3.165548	-0.01318	2.823744	0.440265	0.892655		
11.13210	47.77014	22.38225	11.09472	0.996552	0.232352		
11.58170	55.11989	23.56310	11.26236	0.989514	0.204325		
11.69102	65.86212	25.03235	11.65674	0.997067	0.174987		

B3F2:122

Tm	g(U)/D	Log	Log
dyne/cm ²	(1/sec)	Tm	8(U)/D
0.829085	75.73235	-0.08140	1.879281
0.615428	57.61369	-0.21082	1.760525
0.470477	44.04210	-0.32746	1.643868
0.366208	34.58364	-0.43627	1.529870
0.288315	27.21305	-0.54013	1.434777
0.187546	17.69213	-0.72689	1.247780
0.121023	11.44377	-0.91713	1.058569

Log Tm vs. Log 8(U)/D

Regression Output:
Constant -1.98270
Std Err of Y Est 0.001314
R Squared 0.999979
No. of Observations 6
Degrees of Freedom 4

X Coefficient(s) 1.006118
Std Err of Coef. 0.002267

Tm = K * (8(U)/D)^n

K' = 0.010406

n' = 1.006118

Tm = 27.69786
Res/ft = 1200.960

Regression Output:

Constant -15.2927
Std Err of Y Est 0.190557
R Squared 0.988963
No. of Observations 14
Degrees of Freedom 12

X Coefficient(s) 8.836043
Std Err of Coef. 0.269457

t = 24.72857 deg C
s.d.t = 0.658445 deg C

Solvent	L	MDR	1//f	1//f	1//f/Slv	1//f/L
79.79777						
79.592					122.2234	
79.692					40.77743	
0.4						
14.55494	342.4656	38.63600	21.32311	1.465007	0.062263	
14.54919	304.2137	37.65867	20.40364	1.421936	0.067070	
14.12994	268.1432	36.61725	19.51721	1.381266	0.072786	
13.86091	229.6722	35.33934	18.58898	1.341108	0.080937	
13.50559	187.1878	33.65152	16.94305	1.254521	0.090513	
13.18214	155.2088	32.10569	15.71844	1.192585	0.101272	
12.81038	125.4517	30.34933	14.58514	1.138540	0.116261	
12.33791	95.57805	28.10508	12.76256	1.034418	0.133530	
13.61735	199.6272	34.18245	17.60198	1.292613	0.088174	
13.02229	141.7277	31.35592	15.47475	1.188327	0.109186	
12.62116	112.5050	29.45054	14.07918	1.115521	0.125142	
12.32683	94.97053	28.05246	12.82972	1.040796	0.135091	
12.03349	80.21457	26.65909	12.15186	1.009836	0.151491	
11.67017	65.07652	24.93334	11.23396	0.962621	0.172627	
11.74998	68.13588	25.31242	11.68713	0.994650	0.171526	
11.40972	56.01590	23.69619	11.34906	0.994683	0.202604	
11.14513	48.10215	22.43940	11.18520	1.003595	0.232570	
10.72172	37.69730	20.42817	10.67784	0.995907	0.283352	
10.43606	31.98138	19.07132	10.43135	1.001454	0.326791	
10.44658	32.17566	19.12130	10.35305	0.991046	0.321766	
9.979989	24.59673	16.90494	10.01092	1.003099	0.407002	
9.401966	17.63483	14.15933	10.74203	1.142531	0.609137	
9.191977	15.62695	13.16189	10.27699	1.118039	0.657645	
8.987411	13.89098	12.19020	9.414469	1.047517	0.677739	
8.719793	11.90771	10.91902	8.228150	0.943617	0.690993	
8.424378	10.04556	9.515796	6.951263	0.825136	0.691973	
8.227331	8.968357	8.579824	6.246172	0.759197	0.694667	
7.961325	7.695048	7.316295	5.388919	0.676887	0.700310	
7.674472	6.523761	5.953742	4.543589	0.592039	0.696467	
7.170845	4.881927	3.561514	3.371760	0.470204	0.690651	
6.534946	3.385451	0.540995	2.468798	0.368602	0.711514	
10.66189	36.42125	20.14402	10.65069	0.998949	0.292430	
11.05690	45.72002	22.02030	11.25882	1.018261	0.246355	
11.29348	52.39025	23.14403	11.49137	1.017523	0.219341	
11.64580	64.16997	24.81758	11.54749	0.991558	0.179951	

Log Tw vs. Log B<U>/D	Tw	B<U>/D	Log Tw	Log B<U>/D
	dyne/cm ²	(1/sec)		
	1.010835	73.09674	0.004680	1.863898
	0.746176	54.88829	-0.12715	1.739479
	0.531048	39.11896	-0.27486	1.592387
	0.425188	31.45253	-0.37141	1.497655
	0.314447	23.33574	-0.50245	1.368021
	0.226006	16.68037	-0.64587	1.222205
	0.127138	9.284026	-0.89572	0.967733
	0.061697	4.620245	-1.20972	0.664665

Log Tw vs. Log B<U>/D

Regression Output:

Constant -1.87652

Std Err of Y Est 0.003946

R Squared 0.999918

No. of Observations 8

Degrees of Freedom 6

X Coefficient(s) 1.006742

Std Err of Coef. 0.003717

Tw = K' (B<U>/D)^{n'}

K' = 0.013288

n' = 1.006742

Tw = 40.19538

Res/ft = 1433.690

Regression Output:

Constant -24.7365

Std Err of Y Est 0.132750

R Squared 0.998033

No. of Observations 9

Degrees of Freedom 7

X Coefficient(s) 15.40092

Std Err of Coef. 0.258394

t = 24.46285 deg C

s.d.(t) = 0.633960 deg C

Solvent	L	MDR	1//f	1//f	1//f/Slv	1//f/L
79.79777						
79.592					122.2234	
79.692					40.77743	
0.4						
14.55494	342.4656	38.63600	21.32311	1.465007	0.062263	
14.54919	304.2137	37.65867	20.40364	1.421936	0.067070	
14.12994	268.1432	36.61725	19.51721	1.381266	0.072786	
13.86091	229.6722	35.33934	18.58898	1.341108	0.080937	
13.50559	187.1878	33.65152	16.94305	1.254521	0.090513	
13.18214	155.2088	32.10569	15.71844	1.192585	0.101272	
12.81038	125.4517	30.34933	14.58514	1.138540	0.116261	
12.33791	95.57805	28.10508	12.76256	1.034418	0.133530	
13.61735	199.6272	34.18245	17.60198	1.292613	0.088174	
13.02229	141.7277	31.35592	15.47475	1.188327	0.109186	
12.62116	112.5050	29.45054	14.07918	1.115521	0.125142	
12.32683	94.97053	28.05246	12.82972	1.040796	0.135091	
12.03349	80.21457	26.65909	12.15186	1.009836	0.151491	
11.67017	65.07652	24.93334	11.23396	0.962621	0.172627	
11.74998	68.13588	25.31242	11.68713	0.994650	0.171526	
11.40972	56.01590	23.69619	11.34906	0.994683	0.202604	
11.14513	48.10215	22.43940	11.18520	1.003595	0.232570	
10.72172	37.69730	20.42817	10.67784	0.995907	0.283352	
10.43606	31.98138	19.07132	10.43135	1.001454	0.326791	
10.44658	32.17566	19.12130	10.35305	0.991046	0.321766	
9.979989	24.59673	16.90494	10.01092	1.003099	0.407002	
9.401966	17.63483	14.15933	10.74203	1.142531	0.609137	
9.191977	15.62695	13.16189	10.27699	1.118039	0.657645	
8.987411	13.89098	12.19020	9.414469	1.047517	0.677739	
8.719793	11.90771	10.91902	8.228150	0.943617	0.690993	
8.424378	10.04556	9.515796	6.951263	0.825136	0.691973	
8.227331	8.968357	8.579824	6.246172	0.759197	0.694667	
7.961325	7.695048	7.316295	5.388919	0.676887	0.700310	
7.674472	6.523761	5.953742	4.543589	0.592039	0.696467	
7.170845	4.881927	3.561514	3.371760	0.470204	0.690651	
6.534946	3.385451	0.540995	2.468798	0.368602	0.711514	
10.66189	36.42125	20.14402	10.65069	0.998949	0.292430	
11.05690	45.72002	22.02030	11.25882	1.018261	0.246355	
11.29348	52.39025	23.14403	11.49137	1.017523	0.219341	
11.64580	64.16997	24.81758	11.54749	0.991558	0.179951	

Tap DL= 122.2234

L	MDR	1//f	1//f	1//f/Slv	1//f/L
---	-----	------	------	----------	--------

91.90414	27.78164	11.86989	1.039426	0.129155	
87.09188	27.33785	11.80813	1.040350	0.135582	
82.29481	26.87055	11.59863	1.028523	0.140936	
77.82182	26.40920	11.46248	1.023003	0.147291	
78.60941	26.49229	11.34764	1.011579	0.144354	
70.28095	25.56819	11.39887	1.029426	0.162190	
60.97520	24.39619	11.08853	1.018277	0.181853	
52.62520	23.18096	10.90456	1.019193	0.207211	
40.38577	20.99661	10.41079	1.005180	0.257783	
48.99147	22.59056	10.95665	1.032988	0.223644	
31.06340	18.83101	10.16681	1.014852	0.327292	
22.49415	16.16760	9.705741	1.010915	0.431478	
17.94861	14.30486	9.611925	1.032514	0.535524	
14.13797	12.33563	10.51662	1.168401	0.743856	
10.41607	9.814661	9.866314	1.148433	0.947219	
8.797104	8.420734	8.415977	1.003358	0.956675	
7.531486	7.139012	7.195649	0.878901	0.955408	
6.405845	5.803232	6.139994	0.769623	0.958498	
4.760182	3.353128	4.545904	0.598599	0.954985	
3.119444	-0.13425	2.983647	0.423324	0.956467	

P1F03478

Log	Log	Log
dyne/cm ²	(1/s)	80U/D
0.427272	42.73140	-0.36929
0.312464	31.24279	-0.50519
0.226043	22.67553	-0.64580
0.125104	12.48955	-0.90272
0.053735	5.371897	-1.26982

Regression Output:

Constant -1.99941

Std Err of Y Est 0.000850

R Squared 0.999995

No. of Observations 5

Degrees of Freedom 3

X Coefficient(s) 0.999445

Std Err of Coef. 0.001191

K' = 0.010013

n' = 0.999445

Twd = 0.061357

Res/fk = 53.21779

Regression Output:

Constant 1.607649

Std Err of Y Est 0.109634

R Squared 0.981722

No. of Observations 12

Degrees of Freedom 10

X Coefficient(s) 3.199992

Std Err of Coef. 0.138072

t = 21.96 deg C

s.d.t = 0.056124 deg C

P2F05497

2/17/89 11:51

1.0 FSID Taps 14

S = 10.05

Z = 4.9

HMD-40 HMD-40

0.187 0.188

0.17 0.171

0.163 0.164

0.145 0.146

0.116 0.117

0.133 0.134

0.087 0.088

0.07 0.072

0.055 0.056

0.039 0.04

0.03 0.031

0.024 0.025

0.018 0.019

0.012 0.013

<C>(ppm)= 2.08962

[NaCl]= 0.000309

constant

co)NaCl

X coeff

Batch

Vol (ml)

<U> (volts)

<U>o (volts)

<U>corr (volts)

1440

1130

1196

1259

1114

1137

1075

756

-0.0035

0.02488

-0.0025

density viscosity

1.000096 1.001592

-0.00025 -0.02281

0.003419 -4.14933

0

t)samp

(sec)

DP

(psid)

<U>

(cm/s)

Ke

Tw

dyne/cm2

f

Log (Re/f)1/4

Solvent

3.539999

-0.79424

0.273438

0.233742

0.224005

0.182713

0.124807

0.159131

0.079982

20.1

20.2

30

40.2

45.2

60.1

80

102

112.6

102.4271

98.23420

87.45240

70.08172

80.26453

52.71103

42.91265

33.50780

0.0205

0.012989

0.005994

0.004686

0.003340

0.001745

38.57613

33.25807

31.60326

25.77682

17.88966

11.802.89

11.28375

6.234.556

4.932.882

2.892096

1.872527

1.845642

0.661192

0.457131

0.246317

0.006093

0.006350

0.006560

0.006751

0.006980

0.008135

0.008696

0.009289

0.010160

0.010431

0.007773

0.007773

0.014135

0.025035

2.110996

11.80717

11.69488

11.65553

11.49900

11.21822

11.39278

10.86397

10.60250

10.27120

9.822710

9.451722

8.877484

8.588343

8.404635

7.929209

Tap DL= 122.2254

L 1//f	MDR 1//f	1//f	1//f	1//f/Slv	1//f/L
80.70051	26.70892	12.81018	1.084949	0.158737	
75.01675	26.10628	12.54878	1.073014	0.167279	
73.12547	25.89558	12.34656	1.059261	0.168838	
66.04261	25.05494	12.17005	1.058356	0.184275	
55.01874	23.54798	11.70682	1.043552	0.212778	
61.63355	24.48480	11.96882	1.050561	0.194193	
43.69546	21.64657	11.08690	1.020519	0.253731	
36.86173	20.24322	10.72344	1.011406	0.290909	
29.71580	18.46504	10.37512	1.010117	0.349144	
22.19497	16.05786	9.920868	1.009992	0.446946	
17.65902	14.17531	9.790854	1.035666	0.554125	
10.51331	9.969451	9.866192	1.133264	0.927730	
8.824858	8.446726	8.410934	1.000749	0.953095	
6.477904	5.895536	6.320050	0.797049	0.975631	

P2P03497

Tw dyne/cm2	8-U/D (1/s)	Log Tw	Log 8<U>/D
0.845642	81.00466	-0.07281	1.908510
0.641192	62.17979	-0.17967	1.793649
0.457131	44.16535	-0.35995	1.645081
0.246317	24.36042	-0.60850	1.386684

Regression Output:
 Constant -2.01057
 Std Err of Y Est 0.007835
 R Squared 0.998302
 No. of Observations 3
 Degrees of Freedom 1

X Coefficient(s) 1.017211
 Std Err of Coef. 0.041950

K' = 0.009759
 n' = 1.017211

Tw# = 7.026210
 Res/fs = 551.7101

Regression Output:
 Constant -5.87387
 Std Err of Y Est 0.067940
 R Squared 0.992318
 No. of Observations 8
 Degrees of Freedom 6

X Coefficient(s) 5.972103
 Std Err of Coef. 0.214504

t = 20.56666 deg C
 s.d.)t = 0.074535 deg C

Page 1

Cyanaamid 837A

Page 2

Cyanaamid 837A

P5P03486 2/8/89 11:49
 1.0 PS10 Taps 14
 S = 10.05
 Z = 4.9

MHD-40 MHD-40
 0)1 0)h Temp <U> <U> <U>corr Batch Vol
 (1/s) (1/s) (deg C) (volts) (volts) (volts) (ml)
 0.231 0.232 21.2 4.3495 -0.1165 4.4695 1250
 0.205 0.206 21.2 3.649111 -0.1235 3.774111 1250
 0.191 0.192 21.2 3.175416 -0.1265 3.301916 1250
 0.162 0.163 21.2 2.494857 -0.1265 2.622357 1250
 0.123 0.125 21.2 1.587916 -0.1285 1.716416 1250
 0.102 0.103 21.2 1.16375 -0.1285 1.29175 1250
 0.07 0.071 21.35 0.5694 -0.1275 0.6974 1250
 0.084 0.085 21.35 0.821666 -0.1285 0.949666 1250
 0.053 0.055 21.3 0.342 -0.1275 0.4695 1250
 0.042 0.042 21.33 0.178857 -0.1275 0.306357 1250
 0.033 0.034 21.35 0.0813 -0.1275 0.2088 1123
 0.027 0.028 21.4 -0.0112 -0.1275 0.1158 1123
 0.019 0.02 21.4 -0.04726 -0.1265 0.079233 1230
 0.012 0.013 21.4 -0.07415 -0.1265 0.05233 1150

density viscosity ID(cm) = 1.45796
 1.000096 1.001592 K(V/psi) = 14.24
 -0.00025 -0.02281 XS(cm2) = 1.669479 2.97533
 0.003419 -4.14933 -1.99543 Solvent

t)saap DP <U> Re Tw f Log(Re/f)1/f/f
 (sec) (psid) (cm/s) (dyne/cm2)

0.313869 138.9654 20760.13 44.28002 0.004594 3.148329 11.36275
 0.265035 123.3917 18433.56 37.39070 0.004920 3.111507 11.25248
 0.231876 115.0059 17180.80 32.71259 0.004955 3.082582 11.16712
 0.184154 97.63521 14585.78 25.98009 0.005460 3.022546 11.01825
 0.120534 74.87263 11185.41 17.00480 0.006077 2.940511 10.74442
 0.090712 61.69587 9216.784 12.79756 0.006736 2.878789 10.56077
 17.5 0.048974 42.54183 6376.894 6.909249 0.007649 2.746419 10.16693
 14.7 0.066690 50.93444 7634.921 9.408494 0.007366 2.913462 10.36641
 22.6 0.032970 32.83838 4916.826 4.651408 0.008642 2.560003 9.909817
 29.3 0.021513 25.55414 3828.761 3.035127 0.009212 2.559595 9.54872
 32.5 0.014662 20.69737 3102.474 2.068615 0.009675 2.484543 9.287765
 40.3 0.008132 16.67656 2502.589 1.147248 0.008265 2.357025 9.008357
 59.9 0.005564 12.39977 1845.780 0.784976 0.010396 2.274624 8.763189
 85.4 0.003676 8.066012 1210.435 0.518639 0.015972 2.184629 8.495422

Tap DL= 122.2334

L 1//f	HDR 1//f	1//f	1//f/Slv	1//f/L
87.94474	27.41826	14.75367	1.298425	0.167760
80.81421	26.72054	14.25613	1.266818	0.176406
75.58984	26.16908	14.20561	1.272091	0.187930
67.36376	25.21837	13.53267	1.228204	0.200889
54.49940	23.46972	12.82745	1.193870	0.235368
47.27914	22.29700	12.18399	1.153702	0.257703
34.85773	19.78196	11.43378	1.124605	0.328012
40.57652	21.05581	11.73115	1.131650	0.288401
28.56823	18.14006	10.75675	1.085464	0.376528
23.09272	16.38430	10.36246	1.075516	0.448732
19.07319	14.80632	10.16634	1.082935	0.533017
14.23017	12.38347	10.99928	1.221009	0.773498
11.76263	10.81787	9.807431	1.119162	0.833778
9.561128	9.107953	7.912479	0.931381	0.827567

P5P03486

Twe = 3.529210
Res/f# = 397.2507

Regression Output:

Constant -11.7201
Std Err of Y Est 0.098389
R Squared 0.992802
No. of Observations 7
Degrees of Freedom 5

X Coefficient(s) 9.021940
Std Err of Coef. 0.518622

t = 21.29142 deg C
s.d.t = 0.083397 deg C

PIP13490

2/12/89 12:37

1.0 PSID Taps 14
S = 10.05
Z = 4.9

<C>(ppm)= 10.325 X coeff
[NaCl]= 0.000309 constant

co)NaCl

MHD-40 Q11 (1/s)	MHD-40 Q1h (1/s)	Temp (deg C)	<V> (volts)	<V> (volts)	<V> (volts)	<V>corr (volts)	Batch Vol (ml)
0.225	0.226	20.75	3.243571	-0.0005	3.246571		
0.193	0.194	20.7	2.6	-0.0055	2.6065		
0.186	0.187	20.7	2.404333	-0.0075	2.412333		
0.16	0.161	20.7	2.0559	-0.0085	2.0654		
0.124	0.125	20.7	1.394888	-0.0085	1.403888		
0.104	0.105	20.7	1.0864	-0.0095	1.0969		
0.085	0.086	20.7	0.821666	-0.0115	0.833666		1132
0.065	0.066	20.75	0.561375	-0.0125	0.574375		1316
0.048	0.049	20.8	0.345875	-0.0135	0.359375		1258
0.038	0.039	20.8	0.258125	-0.0135	0.251625		1176
0.03	0.031	20.8	0.122	-0.0135	0.135		1255
0.025	0.026	20.8	0.084	-0.0125	0.0965		1055
0.02	0.021	20.85	0.0646	-0.0125	0.0771		1197
0.013	0.014	20.85	0.041941	-0.0125	0.053441		1092
0.172	0.173	20.75	2.1996	-0.0115	2.2131		
0.187	0.188	20.65	2.4825	-0.0155	2.498		

density viscosity
1.000096 1.001592
-0.00025 -0.0281
0.003419 -4.14933

ID(cm) = 1.45796
K(V/psi) = 14.25
XS(cm2) = 1.669479

3.539999
-0.79424
Solvent

t)saap (usec)	DP (psid)	UJ (cm/s)	Re	Tw dyne/cm2	f	Log(Re/f)1/f
0	0	0	0	0	0	0
0.227829	135.3715	20018.96	32.14171	0.007513	3.074327	11.67726
0.182912	116.2038	17165.05	25.80487	0.007828	3.026150	11.50681
0.162286	112.0109	16545.69	25.88258	0.007813	3.009740	11.44731
0.144940	96.43724	14245.22	20.44787	0.004404	2.975624	11.32795
0.098518	74.87363	11059.95	17.89878	0.004966	2.891798	11.03117
0.076975	62.89385	9290.362	10.85953	0.005499	2.828205	10.84149
13	0.058502	52.15812	7704.555	8.253468	0.006077	2.778618
19.9	0.040307	39.61153	5857.820	5.86428	0.007260	2.698212
25.4	0.025219	29.66646	4392.078	3.557885	0.008098	2.596881
30	0.017657	23.48037	3476.235	2.491138	0.009052	2.519484
40	0.009473	18.79328	2782.318	1.336527	0.007581	2.384274
40.4	0.006771	15.61226	2311.373	0.955369	0.007852	2.311370
57.1	0.005410	12.55674	1861.105	0.763305	0.009698	2.263126
75.4	0.003750	8.675014	1285.773	0.529078	0.014084	2.183527
	0.155305	103.6251	15324.25	21.91013	0.004087	2.991115
	0.175298	112.6099	16615.42	24.73070	0.003906	3.016425
						11.47239

Tap DL= 122.2234

L 1//f	MDR 1//f	1//f	1//f/Slv	1//f/L
74.16637	26.01221	16.86998	1.444674	0.227461
66.37902	25.09686	16.16195	1.404555	0.243480
63.85878	24.77747	16.19363	1.414623	0.233585
59.08865	24.13685	15.06763	1.350128	0.255000
48.71563	22.54397	14.18943	1.286302	0.291270
43.06113	21.52590	13.48426	1.243764	0.313142
37.54034	20.59374	12.82709	1.206625	0.341688
31.19552	18.86603	11.73609	1.134370	0.376210
24.70364	16.94074	11.11191	1.112615	0.449808
20.67112	15.47019	10.51054	1.082086	0.508465
15.14098	12.90120	11.48504	1.243700	0.758540
12.80120	11.51604	11.28494	1.257165	0.881553
11.45331	10.59941	10.15416	1.153133	0.886415
9.537131	9.087217	8.426098	0.988518	0.883504
61.23434	24.43118	15.64099	1.274090	0.255428
64.90910	24.91208	15.99873	1.374542	0.246479

P1P13490

Int# = 3.140475
Res/ft# = 370.9285

Regression Output:

Constant -25.2099
Std Err of Y Est 0.181332
R Squared 0.989755
No. of Observations 10
Degrees of Freedom 8

X Coefficient(s) 12.66116
Std Err of Coef. 0.491372

t = 20.75 deg C
s.d.(t) = 0.058630 deg C

F2P13494 2/15/89 12:26

1.0 FSID Taps 14
S = 10.05
Z = 4.9

<C>(ppm)= 20.9137 X coeff
[NaCl]= 0.000312 constant

ID(cm) = 1.45786
K(V/psi) = 14.25
XS(cm²) = 1.669479

density viscosity
1.000096 1.001592
-0.00023 -0.02281
0.003419 -4.14933

D1 (1/s)	D1h (1/s)	Temp (deg C)	<V> (volts)	<V> (volts)	<V> (volts)	<V>corr (volts)	Batch Vol (ml)	t)samp (sec)	DP (psid)	U (cm/s)	Re	Tw dyne/cm ²	f	Log(Re/f)/f	Solvent
0.218	0.219	21.8	2.027333	-0.033	2.068581		1162	16.5	0.034292	42.18335	6394.887	4.837898	0.005448	2.573958	10.25005
0.178	0.179	21.8	1.5534	-0.0495	1.6049		1157	20.9	0.022456	33.15934	5032.545	3.168064	0.005773	2.582519	9.976362
0.152	0.153	21.8	1.270428	-0.0535	1.324928		1166	25.1	0.015060	27.82354	4223.042	2.124693	0.005499	2.495770	9.659272
0.118	0.119	21.8	0.927888	-0.0555	0.984888		1055	28.4	0.012015	22.25117	3377.028	1.695134	0.006860	2.446774	9.455549
0.087	0.088	21.8	0.614	-0.0585	0.672		1121	40.1	0.009058	16.74480	2541.334	1.277887	0.009133	2.385768	9.238450
0.069	0.07	21.85	0.430666	-0.0575	0.488666		1160	50	0.007100	13.89654	2109.058	1.001720	0.010394	2.322495	9.051279
0.034	0.035	21.9	0.2615	-0.0585	0.32		1157	59.9	0.006109	11.14979	1696.010	0.861976	0.013894	2.200845	8.979377
0.045	0.046	21.9	0.156111	-0.0585	0.216111		1166	90.1	0.004201	8.064081	1226.637	0.592720	0.018265	2.219522	8.851591
0.026	0.027	21.9	0.113222	-0.0585	0.171222		1055	180.1	0.001927	3.555399	537.7741	0.271874	0.043589	2.050291	8.052279
0.022	0.023	21.9	0.072076	-0.0575	0.129076		1121								
0.018	0.019	22	0.051582	-0.0555	0.087062		1115								
0.012	0.013	22	-0.02703	-0.0545	0.027461		1065								

Tsp DL= 122.2234

L	MDR	1//f	1//f/Slv	1//f/L
60.62833	24.34911	20.47713	1.801375	0.337748
53.40269	23.30197	19.00162	1.709764	0.355817
48.52163	22.51105	17.87544	1.621349	0.368401
41.83432	21.28740	16.12556	1.493515	0.385462
34.55602	19.71023	14.43642	1.374478	0.417768
29.50109	18.40520	13.54798	1.320459	0.459236
23.90007	16.66786	13.16037	1.224466	0.550641
19.57268	15.01963	13.48512	1.400430	0.688976
17.48253	14.08776	12.07286	1.276788	0.690557
15.17919	12.92200	10.46389	1.132645	0.689357
13.43926	11.91741	9.808383	1.083634	0.729822
12.49467	11.31605	8.483661	0.949036	0.678981
10.36126	9.771119	7.399183	0.852259	0.714120
7.017331	6.555547	4.789696	0.594824	0.682552

P2P13494

Tw	BAU/D	Log	Log
dyne/cm2	(1/s)	Tw	BAU/D
2.124693	152.6820	0.327296	2.183788
1.695134	122.0948	0.229204	2.086697
1.277887	91.88074	0.106492	1.943224
0.861936	61.18026	-0.06452	1.786611
0.52720	44.24857	-0.22714	1.445899
0.271874	19.39915	-0.56563	1.287782

Regression Output:

Constant	-1.86082
Std Err of Y Est	0.008624
R Squared	0.999449
No. of Observations	6
Degrees of Freedom	4

X Coefficient(s)	1.001517
Std Err of Coef.	0.011752

K' =	0.013777
n' =	1.001517

Twa = 2.964849
Res/fb = 369.0952

Regression Output:

Constant	-54.2601
Std Err of Y Est	0.175983
R Squared	0.995870
No. of Observations	5
Degrees of Freedom	3

X Coefficient(s)	24.98583
Std Err of Coef.	0.928925

t = 21.88214 deg C
s.d.t = 0.074659 deg C

Page 1

Cyanamid 837A

FSP13401 2/21/89 12:01
 1.0 PSID 1.0 PSID
 S = 10.05 S = 10.05 \C.(ppm)=52.04769 X coeff
 Z = 4.77 Z = 4.82 [NaCl]= 0.000312 constant

HMD-40 011 (1/s)	Q/h (1/s)	Temp (deg C)	<V> (volts)	<V> (volts)	<V> (volts)	<V>corr (volts)	Batch (ml)
0.211	0.212	23.95	1.676285	0.003	1.665025		
0.186	0.188	23.8	1.42325	0.0195	1.40525		
0.18	0.181	23.8	1.3195	0.0165	1.3005		
0.155	0.156	23.8	1.11385	0.0315	1.089785		
0.121	0.122	23.8	0.789444	0.0255	0.762944		
				0.0275			
0.106	0.107	23.85	3.430571	0.0065	3.475071	1139	
0.078	0.079	23.9	2.408714	-0.0445	2.448714	1136	
0.058	0.059	23.9	1.8785	-0.0355	1.914	1150	
0.04	0.041	23.9	1.355	-0.0355	1.3885	1228	
0.032	0.033	23.95	1.059181	-0.0315	1.089681	1170	
0.025	0.026	23.95	0.862384	-0.0295	0.890384	1128	
0.018	0.019	24	0.693733	-0.0255	0.719733	1166	
0.013	0.014	24	0.506947	-0.0255	0.531447	1080	
		24	0.342565	-0.0255	0.366065	753	
		24.05	0.204291	-0.0255	0.228291	485	
		24.1	0.10732	-0.0245	0.13232	237	
		24.1	0.037478	-0.0255	0.062478	223	
				-0.0245			

Page 2

Cyanamid 837A

density viscosity
 1.000096 1.001592
 -0.00025 -0.02281
 0.003419 -4.14933

ID(cm) = 1.45796
 K(V/psi) = 14.29
 XS(cm2) = 1.569479

75.06

Solvent
 3.579999
 -0.79424

t) samp (sec)	DF (psid)	U (cm/s)	Re	Tw dyne/cm2	f	Log(Re/f)1/4	
0							
0.116517	126.9856	20184.67	16.45804	0.002043	2.950243	11.27750	
0.098337	112.6099	17839.14	13.87331	0.002193	2.921931	11.13789	
0.091007	108.4170	17174.92	12.85917	0.002189	2.905109	11.07377	
0.076262	92.44229	14802.69	10.75889	0.002470	2.856724	10.91245	
0.053390	73.07666	11576.46	7.532161	0.002827	2.789700	10.56837	
10.5	0.046297	64.97605	10204.82	6.531517	0.002101	2.758840	10.54054
14.1	0.052622	48.25897	7662.229	4.602443	0.003962	2.683720	10.29719
19.3	0.025499	35.69105	5666.781	3.597429	0.005662	2.629822	10.10781
29.9	0.018498	24.60062	3905.918	2.609733	0.008645	2.560124	9.857085
34.9	0.014517	20.08072	3191.877	2.048094	0.010183	2.507993	9.672547
43.7	0.011862	15.46131	2457.612	1.673508	0.014035	2.464132	9.517275
60	0.009588	11.64035	1852.349	1.352763	0.020016	2.418422	9.353460
79.9	0.007080	8.094473	1288.405	0.998873	0.030551	2.352566	9.123271
90	0.004876	5.011541	797.4954	0.688032	0.054925	2.271615	8.835765
100.1	0.003041	2.902194	462.3525	0.429082	0.102141	2.169574	8.474528
99.8	0.001762	1.422449	226.8680	0.248700	0.243446	2.051634	8.057032
239.9	0.000832	0.556792	88.80350	0.117430	0.759472	1.888686	7.480195

Tap DL= 122.2234

L 1//f	MDR 1//f	1//f	1//f	1//f/Slv	1//f/L
57.03270	23.84463	22.11962	1.962088	0.387841	
52.21691	22.11669	21.35221	1.917080	0.408913	
50.33305	22.79708	21.36904	1.928904	0.423398	
45.98381	22.06777	20.11943	1.838659	0.437533	
38.47519	20.59671	18.80507	1.762694	0.488758	
35.86911	20.01797	17.95559	1.700253	0.500586	
30.14397	18.58308	15.88673	1.543420	0.527028	
26.65031	17.56662	13.28966	1.315311	0.498668	
22.69887	16.24226	10.75471	1.091064	0.473799	
20.13139	15.25188	9.909515	1.024499	0.492241	
18.19754	14.41852	8.440742	0.886886	0.463839	
16.37956	13.55002	7.068066	0.755501	0.431517	
14.07494	12.29876	5.721184	0.627162	0.406480	
11.68142	10.74070	4.266898	0.482912	0.365272	
9.235369	8.821910	3.128952	0.359218	0.338801	
7.039058	6.581056	2.014367	0.250013	0.286170	
4.836891	3.485039	1.147476	0.153401	0.237234	

PSP13401

Tw dyne/cm2
8-U/D (1/s)
Log Tw
Log 8-U/D

1.352763	63.87200	0.131221	1.805310
0.998873	44.42531	-0.00048	1.647640
0.688032	27.49892	-0.16239	1.439215
0.429082	15.92468	-0.36745	1.202070
0.248700	7.805146	-0.60432	0.892381
0.117430	3.055187	-0.93022	0.485037

Regression Output:
Constant -1.32270
Std Err of Y Est 0.006137
R Squared 0.999908
No. of Observations 6
Degrees of Freedom 4

X Coefficient(s) 0.803268
Std Err of Coef. 0.005562

K' = 0.047565
n' = 0.803368

Regression Output:
Constant -36.7177
Std Err of Y Est 0.208443
R Squared 0.980837
No. of Observations 5
Degrees of Freedom 3

X Coefficient(s) 19.89530
Std Err of Coef. 1.605540

t = 23.93235 deg C
s.d.)t = 0.098430 deg C

Page 1

Cyanamid 837A

Page 2

Cyanamid 837A

F1F01379	2/3/89	14:51				Co)NaCl		
1.0 PSID Taps 14	0.1 PSID Taps 14	10.05	<C>(ppm)=	1.3203	X coeff			
S =	8 S =	7.27	[NaCl]=	0.001035	constant			
Z =	4.9 Z =							
MHD-40	MHD-40	<U>	<V>o	<V>corr	Batch Vol			
(l/s)	(l/s)	(volts)	(volts)	(volts)	(ml)			
0.184	0.185	21.7 2.983125	-0.077	3.059375				
0.169	0.17	21.7 2.5695	-0.0755	2.64525				
0.161	0.162	21.7 2.352571	-0.076	2.428821				
0.148	0.149	21.7 1.990428	-0.0765	2.066928				
0.127	0.128	21.7 1.522	-0.0765	1.599				
0.097	0.099	21.7 0.930777	-0.0775	1.008277				
0.071	0.072	21.7 0.491	-0.0775	0.569				
			-0.0785					
0.09	0.091	21.8 7.7242	-0.0845	7.8232	1246			
0.067	0.068	21.8 4.5915	-0.1135	4.7075	1170			
0.036	0.037	21.8 1.4641	-0.1185	1.58335	1204			
0.052	0.053	21.8 2.906375	-0.12	3.026375	1182			
0.029	0.03	21.8 0.9342	-0.12	1.05255	1335			
0.022	0.023	21.8 0.37075	-0.1165	0.48675	1076			
0.017	0.018	21.8 0.240058	-0.1155	0.356058	1077			
		21.8 0.122944	-0.1165	0.256944	1077			
		21.85 0.0386	-0.1115	0.1491	664			
		21.85 -0.0347	-0.1095	0.0752	350			
		21.85 -0.07311	-0.1105	0.037588	280			

density	viscosity	ID(cm)	K(V/psi)	KS(cm ²)	DP (psid)	<U> (cm/s)	Re	Tw dyne/cm ²	f	Log (Re/f)1/4	Solvent
1.000125	1.001657	1.45796	9.48	85.14							2.97553
-0.00025	-0.02281										-1.99542
0.003419	-4.14933										
0.322718	110.8129	16741.60	45.52849	0.007429	3.159271	11.39530					
0.279034	101.8281	15384.18	39.36562	0.007607	2.777173	10.25842					
0.256204	97.03622	14660.21	36.14482	0.00768	2.540566	9.554452					
0.218030	89.24927	13483.78	30.75927	0.0077	2.581279	9.973001					
0.168670	76.67060	11583.38	22.79573	0.008	2.451899	9.290679					
0.106358	59.29991	8959.023	15.00481	0.00850	2.918245	10.67817					
0.060021	43.12721	6515.653	8.467549	0.009122	2.794011	10.50853					
12.6	0.091886	54.87796	8209.681	12.96312	0.008625	2.887470	10.58660				
17	0.055291	41.22454	6242.264	7.800377	0.009197	2.777173	10.25842				
32.4	0.018597	22.23872	3270.440	2.623627	0.010611	2.540566	9.554452				
22.2	0.035545	31.89212	4829.139	5.014735	0.009879	2.581279	9.973001				
44.1	0.013362	18.12266	2745.667	1.744086	0.010629	2.451899	9.290679				
47	0.005717	13.71302	2076.441	0.806549	0.008594	2.284430	8.792765				
60.2	0.004182	10.71613	1632.648	0.589993	0.010292	2.216538	8.590364				
89.9	0.002782	7.175875	1086.578	0.392619	0.015278	2.128101	8.527222				
90	0.001751	4.419208	669.9165	0.247060	0.025349	2.028009	8.029428				
90.1	0.000884	2.326816	352.7267	0.124772	0.046180	1.879667	7.588062				
149.9	0.000439	1.118858	169.6100	0.061953	0.099170	1.727641	7.155734				

Page 3

Cyanamid 837A

Tap DL= 122.2234

L 1//f	MDR 1//f	1//f	1//f/PK	1//f/L
90.18860	27.62616	11.60180	1.018121	0.128639
83.86237	27.02608	11.44530	1.014509	0.136715
80.35874	26.67390	11.40216	1.013869	0.141890
74.13069	26.00824	11.36825	1.020311	0.153354
65.20179	24.94921	11.10339	1.011597	0.170292
51.77563	23.04666	10.81471	1.012787	0.208876
38.89479	20.68621	10.46999	1.015662	0.269187
48.23364	22.46193	10.76748	1.017085	0.223335
37.41562	20.36628	10.42723	1.016454	0.278686
21.69933	15.87076	9.70790	1.016048	0.447377
29.99986	18.54354	10.06075	1.008798	0.335360
17.69209	14.18608	9.699485	1.044006	0.548238
12.03125	11.00418	10.78670	1.224826	0.896557
10.29007	9.714235	9.855660	1.147292	0.957782
8.394235	8.033921	8.090216	0.971537	0.963782
6.666368	6.132176	6.280748	0.782216	0.942154
4.737486	3.513690	4.653400	0.613252	0.982250
3.338272	0.425192	3.175482	0.445011	0.951235

Page 4

Cyanamid 837A

PIP01379

TW dyne/cm2	8:U/D (1/s)	Log TW	Log 8(U)/D	//
0.589993	58.80069	-0.22915	1.769382	
0.392619	39.37488	-0.40602	1.595219	
0.247060	24.24872	-0.60719	1.384688	
0.124772	12.76751	-0.90387	1.106106	
0.061953	6.139511	-1.20793	0.788119	

Regression Output:
 Constant -2.00140
 Std Err of Y Est 0.007801
 R Squared 0.999701
 No. of Observations 5
 Degrees of Freedom 3

X Coefficient(s) 1.001402
 Std Err of Coef. 0.009987

K' = 0.009967
 n' = 1.001402

TW# = 0.000002
 Res/ft# = 0.321111

Regression Output:
 Constant 2.019581
 Std Err of Y Est 0.030170
 R Squared 0.997708
 No. of Observations 10
 Degrees of Freedom 8

X Coefficient(s) 2.024284
 Std Err of Coef. 0.051243

t = 21.76944 deg C
 s.d.t = 0.058068 deg C

Tap DL= 125.2234

L	MDR	1//f	1//f	1//f/Siv	1//f/L
77.96044	26.42389	12.31522	1.047741	0.157967	
75.57014	26.16693	12.28301	1.049275	0.162537	
71.98688	25.76609	12.05513	1.036421	0.167462	
65.49092	24.98572	11.82514	1.029516	0.180561	
61.13044	24.41717	11.68030	1.026372	0.191071	
54.51355	23.47186	11.38524	1.016171	0.208851	
45.18061	21.92237	11.08759	1.015779	0.245406	
36.59327	20.13768	10.56416	0.998235	0.290278	
29.08103	18.28686	10.23345	0.999554	0.351894	
21.84022	15.92416	9.865621	1.006922	0.451718	
17.21397	13.96145	9.827382	1.041906	0.570796	
12.44684	11.28440	11.13874	1.246873	0.894904	
9.911410	9.404853	9.737374	1.134498	0.982461	
8.932095	8.546393	8.776671	1.041965	0.982401	
6.448651	5.858180	6.355714	0.802251	0.985588	

P2P01398

Tw	B<U>/D	Log	Log
dyne/cm2	(1/s)	Tw	B<U>/D
0.909468	82.49751	-0.04121	1.916440
0.576886	57.42905	-0.23906	1.759131
0.468355	46.64762	-0.32942	1.668839
0.244676	24.41566	-0.61140	1.387668

Regression Output:
 Constant -2.00253
 Std Err of Y Est 0.000119
 R Squared 0.999999
 No. of Observations 3
 Degrees of Freedom 1

X Coefficient(s) 1.002511
 Std Err of Coef. 0.000437

K' = 0.009941
 n' = 1.002511

Tw# = 8.766974
 K 1/f# = 614.8575

Regression Output:
 Constant -3.90361
 Std Err of Y Est 0.061878
 R Squared 0.991178
 No. of Observations 8
 Degrees of Freedom 6

X Coefficient(s) 5.224561
 Std Err of Coef. 0.201216

t = 20.51 deg C
 s.d.t = 0.105198 deg C

Tap DL= 122.2234

L	MDR	1//f	1//f	1//f/Siv	1//f/L
88.39249	27.46017	14.06157	1.236801	0.159091	
81.30126	26.77012	13.68870	1.21557	0.168370	
76.77796	26.29777	13.43898	1.201273	0.175036	
68.44335	25.54957	12.91018	1.189527	0.188625	
55.29123	23.58874	12.23871	1.137103	0.221349	
47.77056	22.38232	11.82408	1.118208	0.247518	
35.55442	19.94525	10.79258	1.058874	0.303551	
40.82374	21.08562	11.09465	1.069768	0.271769	
24.05473	16.72109	10.07476	1.039963	0.418826	
29.74422	18.47292	10.35981	1.039939	0.348296	
20.45097	15.38184	9.762268	1.030004	0.677349	
15.61205	13.15401	10.33208	1.131784	0.661801	
11.33913	10.51456	10.32403	1.184533	0.910558	
8.885190	8.502947	8.056945	0.959082	0.906783	

P5F01387

Tw# = 4.651762
Res/ft# = 456.5433

Regression Output:

Constant -12.0445
Std Err of Y Est 0.095029
R Squared 0.994747
No. of Observations 8
Degrees of Freedom 6

X Coefficient(s) 8.254546
Std Err of Coef. 0.244865

t = 21.26785 deg C
s.d.t = 0.067101 deg C

density viscosity ID(cm) = 1.45796
 1.000125 1.001657 K(V/psi)= 14.25
 -0.00025 -0.02281 XS(cm2)= 1.669479
 0.003419 -4.14933

t)samp (sec)	DP (psid)	<U> (cm/s)	Re	Tw dyne/cm2	f	Log(Re/f)/f	Solvent
0							
13.7	0.061659	50.31508	7398.565	8.698741	0.006882	2.788035	10.66789
17	0.046994	41.83353	6149.928	6.629835	0.007592	2.729059	10.45511
22	0.031382	31.77246	4677.245	4.927370	0.008785	2.641873	10.14647
30.1	0.019124	23.48196	3456.795	2.699455	0.009806	2.574438	9.766157
34.9	0.011585	19.25689	2858.019	1.634523	0.008829	2.425988	9.382344
42.9	0.006740	15.83341	2333.478	0.950869	0.007597	2.308353	8.965816
66.7	0.005101	11.61872	1714.262	0.719744	0.010680	2.248374	8.753492
80.1	0.003344	7.784614	1148.566	0.471822	0.015596	2.156674	8.428875
	0.207759	116.8028	17175.24	29.31023	0.004303	3.051817	11.59767
	0.125175	82.06150	12053.10	17.65948	0.005253	2.941304	11.20646

MND-40 Q1 (1/s)	MND-40 Q1h (1/s)	Temp (deg C)	<U> (volts)	<U>corr (volts)	Batch Vol (ml)
0.214	0.215	20.55	3.360666	-0.0115	3.374666
0.177	0.178	20.5	2.630333	-0.0165	2.647833
0.154	0.155	20.45	2.08925	-0.0185	2.10825
0.119	0.12	20.45	1.472125	-0.0195	1.492125
0.1	0.101	20.45	1.140571	-0.0205	1.161071
0.083	0.084	20.5	0.857142	-0.0205	0.878642
0.068	0.069	20.5	0.647166	-0.0225	0.669666
0.052	0.052	20.55	0.4247	-0.0225	0.4472
0.038	0.039	20.55	0.250666	-0.0225	0.272666
0.031	0.032	20.6	0.1436	-0.0215	0.1651
0.025	0.026	20.6	0.075345	-0.0215	0.096045
0.018	0.019	20.65	0.0522	-0.0205	0.0727
0.012	0.013	20.65	0.027157	-0.0205	0.047657
0.194	0.195	20.5	2.938571	-0.0205	2.960571
0.136	0.137	20.45	1.75975	-0.0235	1.78375
				-0.0245	

<C> (ppm)= 10.325 X coeff
 [NaCl]= 0.001037 constant
 col/NaCl
 constant

Tap DL= 122.2234

L 1//f	MDR 1//f	1//f	1//f/Slv	1//f/L
75.26927	26.13401	15.74196	1.345460	0.209141
66.59705	25.12392	14.71340	1.278108	0.220931
59.35784	24.17436	14.35859	1.266754	0.241898
49.93668	22.74825	13.21356	1.193719	0.264606
44.05006	21.71326	12.60762	1.159172	0.286211
38.36329	20.57238	12.05345	1.130305	0.314192
33.49184	19.45212	11.47654	1.097696	0.342666
27.40016	17.79559	10.66883	1.051481	0.389371
21.39529	15.75432	10.09799	1.033978	0.471972
16.66742	13.69377	10.64209	1.134280	0.638496
12.71256	11.45871	11.47229	1.279559	0.902437
11.07272	10.31911	9.676151	1.105404	0.873872
8.965095	8.576823	8.007209	0.949973	0.893153
70.42023	25.58453	15.24352	1.314359	0.216465
54.59892	23.48477	13.79732	1.231193	0.252703

PIP11391

iwr = 4.162903
Res/ft = 425.1071

Regression Output:
Constant -21.4729
Std Err of Y Est 0.154078
R Squared 0.990285
No. of Observations 9
Degrees of Freedom 7

X Coefficient(s) 12.01146
Std Err of Coef. 0.449657

t = 20.53 deg C
s.d.)t = 0.067823 deg C

Page 1

Cyanamid 837A

2/3/89 16:38
 PIP01180 1.0 PSID Taps 14 0.1 PSID Taps 14
 S = 8 S = 10.05 <C> (ppm) = 1.3203 X coeff
 Z = 4.9 Z = 7.27 [NaCl] = 0.104494 constant

MHD-40 Q1 (l/s)	MHD-40 Q2 (l/s)	Temp (deg C)	<V> (volts)	<V> (volts)	<V>corr (volts)	Batch Vol (ml)
0.18	0.181	21.55	2.931285	-0.0795	3.011285	1085
0.157	0.159	21.5	2.267875	-0.0805	2.348375	1216
0.148	0.149	21.45	2.08675	-0.0805	2.16725	1245
0.129	0.13	21.4	1.600714	-0.0805	1.681214	1091
0.113	0.114	21.4	1.2411	-0.0805	1.3211	1094
0.096	0.097	21.45	0.894444	-0.0815	0.976444	1075
0.069	0.071	21.5	0.4821	-0.0825	0.5646	1086
0.088	0.089	21.6	7.311333	-0.3365	7.647833	1045
0.067	0.068	21.55	4.34275	-0.3375	4.70025	1045
0.044	0.045	21.6	1.9237	-0.3375	2.2612	1045
0.035	0.036	21.6	1.166444	-0.3395	1.526944	1091
0.029	0.03	21.6	0.706636	-0.3415	1.068136	1075
0.023	0.024	21.6	-0.02333	-0.3415	0.337666	1086
0.016	0.017	21.65	-0.13384	-0.3605	0.227153	1045
		21.65	-0.19975	-0.3615	0.16225	748
		21.65	-0.26028	-0.3625	0.102214	650
		21.65	-0.30757	-0.3625	0.055428	592
				-0.3635		

Page 2

Cyanamid 837A

density viscosity
 1.00417 1.010869 ID(cm) = 1.45796
 -0.00025 -0.02281 K(V/psi) = 9.48 85.14
 0.003419 -4.14933 XS(cm2) = 1.669479

0 Solvent

t) samp (sec)	DP (psid)	<U> (cm/s)	Re	Tw dyne/cm2	f	Log(Re/f)1/f
0.317646	108.4170	16349.29	44.81284	0.007539	3.155045	11.3827
0.247718	95.23926	14345.90	34.94785	0.007720	3.100560	11.25062
0.228612	89.24927	13428.48	32.25221	0.008113	3.083628	11.18729
0.177343	77.86857	11702.92	25.01921	0.008268	3.027003	11.00176
0.139462	68.28475	10262.56	19.87500	0.008455	2.974823	10.84651
0.103000	58.10194	8742.034	14.53108	0.008625	2.909507	10.65217
0.059556	42.52822	6406.030	8.402169	0.009309	2.791047	10.29971
12	0.089949	54.15859	8176.339	12.68993	0.008669	2.881566
17.8	0.055206	40.91970	6170.695	7.788363	0.009321	2.775067
27.4	0.024805	27.21683	4108.934	3.781629	0.010300	2.618676
30.1	0.017934	21.71086	3277.696	2.530163	0.010756	2.531410
36.5	0.012545	17.95326	2710.409	1.769913	0.011004	2.452812
44.5	0.006604	14.48342	2186.566	0.931737	0.008901	2.314483
64.8	0.003966	10.03861	1515.532	0.559517	0.011126	2.203743
89.9	0.001905	4.983802	753.2553	0.268849	0.031691	2.045084
123	0.001200	3.165389	478.4191	0.169370	0.033874	1.944747
210	0.000651	1.688578	252.2129	0.091845	0.064552	1.811858
						7.386307

Tap DL= 122.2234

L	MDR	1//f	1//f	1//f/PK	1//f/L
89.31520	27.54586	11.44073	1.005095	0.128093	
78.78445	26.51065	11.38065	1.014262	0.144453	
75.59946	26.17013	11.10167	0.994123	0.146848	
66.50942	25.11305	10.99742	0.999605	0.165351	
58.97986	24.12165	10.87506	1.002632	0.184386	
50.74438	22.88065	10.76724	1.010802	0.212185	
38.63022	20.62989	10.56434	1.006274	0.268296	
47.58241	22.34976	10.73970	1.016147	0.225707	
37.33464	20.33627	10.35778	1.010391	0.278175	
25.97503	17.35484	9.886738	1.010205	0.380624	
21.24667	15.09680	9.641791	1.012028	0.453802	
17.77021	14.22244	9.532837	1.025440	0.536450	
12.89327	11.57518	10.59935	1.193381	0.822083	
9.991333	9.471125	9.480294	1.108598	0.948851	
8.204120	7.844887	7.990208	0.962950	0.975926	
6.933688	6.456601	6.789814	0.840299	0.979250	
5.503358	4.550207	5.433264	0.698210	0.987263	
4.052647	2.025317	3.935899	0.532864	0.971192	

PIP01180

TW	8XU/D	Log	Log
dyne/cm2	(1/s)	TW	8XU/D
0.559517	55.08306	-0.25218	1.741018
0.376396	38.07790	-0.42435	1.580673
0.268849	27.34671	-0.57049	1.436905
0.169370	17.36886	-0.77116	1.239771
0.091845	9.265432	-1.03694	0.966865

Regression Output:

Constant -2.00474
Std Err of Y Est 0.003809
R Squared 0.999862
No. of Observations 4
Degrees of Freedom 2

X Coefficient(s) 0.998431
Std Err of Coef. 0.008274

K' = 0.009891
n' = 0.998431

TW = 74.89090
Res/ft = 1831.333

Regression Output:

Constant 2.661654
Std Err of Y Est 0.048100
R Squared 0.990732
No. of Observations 11
Degrees of Freedom 9

X Coefficient(s) 2.771139
Std Err of Coef. 0.089340

t = 21.55555 deg C
s.d.t = 0.083147 deg C

Tap DL= 122.2234

L	MDR	1//f	1//f	1//f/Slv	1//f/L
79.49551	26.58478	11.90673	1.010411	0.149778	
74.42442	26.04087	11.84092	1.013543	0.159099	
71.5723	25.71900	11.62793	1.000447	0.162452	
64.70096	24.88558	11.51849	1.004451	0.178026	
60.42603	24.32153	11.43314	1.004229	0.189208	
55.84172	23.36954	11.21476	1.002661	0.208291	
42.77138	21.47619	10.82284	0.999237	0.253039	
35.65606	19.94881	10.52434	0.997437	0.293162	
28.86807	18.22621	10.10024	0.987634	0.349876	
21.15178	15.65987	9.801370	1.005417	0.463382	
17.42766	14.06182	9.767886	1.033549	0.560481	
12.11800	11.06346	11.29382	1.270085	0.931987	
9.613356	9.152905	9.588579	1.133283	0.997422	
8.287565	7.928392	8.199872	0.984977	0.989418	
6.794579	6.277215	6.769815	0.846182	0.997823	

P2P01199

Tw	8 U./D	Log	Log
dyne/cm2	(1/s)	Tw	8<U>/D
1.825102	102.2745	0.261287	2.009767
0.880410	82.13150	-0.05531	1.914509
0.554081	55.31809	-0.25642	1.742867
0.410858	40.73634	-0.38630	1.609982

Regression Output:
 Constant -2.14813
 Std Err of Y Est 0.011850
 R Squared 0.997475
 No. of Observations 3
 Degrees of Freedom 1

X Coefficient(s) 1.090939
 Std Err of Coef. 0.054883

K' = 0.007109
 n' = 1.090939

Tw# = 13.19078
 Res/# = 746.9501

Regression Output:
 Constant -0.59374
 Std Err of Y Est 0.043275
 R Squared 0.995706
 No. of Observations 9
 Degrees of Freedom 7

X Coefficient(s) 4.023065
 Std Err of Coef. 0.099845

t = 20.34333 deg C
 s.d.t = 0.138884 deg C

PSP01188 2/8/89 15:59

1.0 PSID Taps 14

S = 10.05

Z = 4.9

col/NaCl

<C>(ppm)=5.156122 X coeff

[NaCl]= 0.1044 constant

HMD-40 Q1 (l/s)	HMD-40 Q2 (l/s)	Temp (deg C)	<V> (volts)	<V> (volts)	<V> (volts)	<V>corr (volts)	Batch Vol (ml)
0.211	0.212	21.3	4.977285	-0.133	5.113785		
0.188	0.189	21.2	4.143285	-0.14	4.283785		
0.176	0.177	21.2	3.7395	-0.141	3.8805		
0.152	0.153	21.2	3.019428	-0.141	3.161428		
0.116	0.117	21.3	1.922373	-0.143	2.066125		
0.137	0.138	21.3	2.515142	-0.1445	2.659142		
0.098	0.099	21.3	1.401666	-0.1435	1.545916		
0.078	0.079	21.4	0.903285	-0.145	1.048785		1182
0.067	0.068	21.4	0.527	-0.146	0.77275		1127
0.052	0.053	21.45	0.365125	-0.1455	0.511125		1173
0.04	0.0415	21.5	0.177222	-0.1465	0.323222		1195
0.033	0.034	21.5	0.085777	-0.1455	0.231277		1040
0.027	0.028	21.5	0.0095	-0.1455	0.1545		1130
0.021	0.022	21.5	-0.06486	-0.1445	0.079633		1210
0.017	0.018	21.5	-0.08507	-0.1445	0.059428		1093
0.012	0.012	21.6	-0.10395	-0.1445	0.040547		1104
0.098	0.099	21.6	1.401	-0.1445	1.567		
					-0.1475		

density viscosity

1.00417 1.010889 ID(cm) = 1.45796

-0.00025 -0.02281 K(V/psi)= 14.24

0.003419 -4.14933 XS(cm2)= 1.669479

2.97533

-1.99543

Solvent

t)isamp (sec)	DP (psid)	<U> (cm/s)	Re	Tw dyne/cm2	f	Log(ke/f)/f
0						
0.359114	124.9856	18915.56	50.66306	0.006269	3.175435	11.46339
0.300827	113.2089	16825.40	42.44012	0.006607	3.135993	11.32604
0.272507	106.0210	15757.12	38.44471	0.006824	3.114522	11.26216
0.232010	91.64532	13620.56	31.22076	0.007441	3.070020	11.12975
0.145093	70.08172	10439.25	20.46941	0.008316	2.978642	10.85787
0.186737	82.66049	12312.96	26.34453	0.007693	3.033435	11.02090
0.108561	59.29991	8833.212	15.21563	0.008691	2.915657	10.67047
14.9	0.073650	47.51711	7094.053	10.39048	0.009183	2.832392
16.6	0.054266	40.66630	6071.263	7.855753	0.009228	2.766089
22.3	0.035893	31.50726	4709.191	5.063794	0.010179	2.676805
28.9	0.022698	24.76788	3706.065	3.202212	0.010417	2.577785
30.2	0.016241	20.62743	3086.522	2.291304	0.010746	2.505101
40	0.010849	16.92144	2531.987	1.530655	0.010667	2.417498
5*	0.005592	13.42179	2008.328	0.788939	0.008739	2.275583
60.2	0.004173	10.87533	1627.296	0.588768	0.009934	2.210032
90	0.002847	7.347599	1101.918	0.402711	0.014849	2.128002
	0.108637	59.29791	8893.198	15.32636	0.008697	2.918765
						10.67971

Tap DL= 122.2234

L 1//f	MDR 1//f	1//f	1//f/Slv	1//f/L
93.60857	27.93327	12.62943	1.103643	0.134917
85.48167	27.18386	12.30190	1.086161	0.143912
81.35851	26.77593	12.10469	1.074811	0.148782
73.43461	25.93039	11.59242	1.041570	0.157860
59.50077	24.19420	10.96545	1.009908	0.184290
67.50177	25.23526	11.40059	1.034451	0.168893
51.46801	22.99749	10.72658	1.005258	0.208412
42.48864	21.41546	10.43321	1.001197	0.245600
36.47111	20.15531	10.40423	1.017489	0.285273
29.69516	18.49530	9.911528	0.995152	0.333775
23.64097	16.57792	9.797782	1.013718	0.414440
19.99777	15.19693	9.646455	1.020904	0.482376
16.34477	13.55248	9.681943	1.053726	0.592357
11.73443	10.79806	10.69676	1.221079	0.911570
10.13706	9.590615	10.03308	1.170583	0.989741
8.392331	8.032049	8.206288	0.985310	0.977831
51.83762	23.05653	10.72242	1.003998	0.206846

P5F01188

Tws = 19.43554
Res/fs = 927.6587

Regression Output:
Constant -14.6790
Std Err of Y Est 0.064012
R Squared 0.991487
No. of Observations 6
Degrees of Freedom 4
X Coefficient(s) 8.594574
Std Err of Coef. 0.598174
t = 21.39705 deg C
s.d.) t = 0.131138 deg C

2/12/89 16:34

PIP11192

1.0 PSID Taps 14
S = 10.05
Z = 4.9

<C> (ppm) = 10.325 X coeff
[NaCl] = 0.103522 constant
co)NaCl

density viscosity ID(cm) = 1.45796
1.00417 1.010869 K(V/psi) = 14.25
-0.00025 -0.02281 XS(cm2) = 1.669479
0.003419 -4.14933

MHD-40 Q1 (1/s)	MHD-40 Q/h (1/s)	Temp (deg C)	<U> (volts)	<U> (volts)	<U> (volts)	<U> (volts)	<U> (volts)	DP (psid)	<U> (cm/s)	Re	Tw dyne/cm2	f	Log (Re/f)1/1/f	Solvent
0.2	0.201	20.25	4.2875	-0.0215	4.312	-0.0215	4.312	0.302596	120.3968	17514.26	42.68967	0.005875	3.127906	11.86703
0.188	0.189	20.2	3.908	-0.0275	3.5355	-0.0275	3.5355	0.276175	113.2089	16450.07	38.96224	0.006064	3.107574	11.79505
0.168	0.169	20.2	3.434	-0.0275	3.4615	-0.0275	3.4615	0.242912	101.2291	14709.52	34.26954	0.006671	3.079706	11.69540
0.147	0.148	20.2	2.802444	-0.0275	2.830444	-0.0275	2.830444	0.198637	88.65038	12881.52	28.02197	0.007113	3.036002	11.54169
0.115	0.116	20.2	1.863666	-0.0285	1.892666	-0.0285	1.892666	0.132818	69.48273	10096.34	18.73778	0.007742	2.948611	11.22233
0.097	0.098	20.2	1.420166	-0.0295	1.449666	-0.0295	1.449666	0.101730	58.70092	8529.668	14.55199	0.008309	2.890708	11.02725
0.08	0.081	20.3	1.012166	-0.0295	1.042166	-0.0295	1.042166	0.073124	48.54039	7069.185	10.31766	0.008736	2.820638	10.77714
0.066	0.067	20.3	0.724	-0.0305	0.755	-0.0305	0.755	0.052982	40.14652	5846.755	7.474652	0.009252	2.756033	10.52976
0.046	0.047	20.35	0.367571	-0.0315	0.399071	-0.0315	0.399071	0.028005	27.95282	4075.514	3.950887	0.010087	2.612077	10.04100
0.034	0.035	20.4	0.205	-0.0315	0.2365	-0.0315	0.2365	0.016596	20.78411	3034.030	2.341397	0.010811	2.498960	9.640566
0.029	0.03	20.45	0.118888	-0.0315	0.149888	-0.0315	0.149888	0.010518	17.95343	2623.519	1.483930	0.009184	2.400422	9.291741
0.023	0.024	20.45	0.051375	-0.0305	0.081875	-0.0305	0.081875	0.005745	14.50884	2120.164	0.810579	0.007682	2.269113	8.856907
0.016	0.017	20.5	0.027307	-0.0305	0.057807	-0.0305	0.057807	0.004056	10.06673	1472.702	0.572307	0.011267	2.194033	8.561087
0.012	0.012	20.55	0.009923	-0.0325	0.040923	-0.0325	0.040923	0.002871	7.187868	1052.728	0.405146	0.015665	2.119507	8.297300

Tap DL= 122.2234

P1P11192

Twe = 24.83040
Res/f# = 1023.851

L 1//f	HDR 1//f	1//f	1//f/Siv	1//f/L
83.90478	27.03022	13.04623	1.099367	0.155488
80.06721	26.64391	12.84083	1.088661	0.160375
75.09083	26.11443	12.24294	1.046726	0.163041
67.90192	25.28403	11.85675	1.027297	0.174615
55.52541	23.62362	11.36455	1.011771	0.204672
48.59469	22.52346	10.97042	0.994837	0.225753
41.29605	21.18054	10.69894	0.992743	0.259079
35.14903	19.85063	10.39636	0.997368	0.295779
25.58337	17.22947	9.956453	0.991579	0.389176
19.71699	15.08025	9.617434	0.997600	0.487773
15.71456	13.20802	10.43426	1.122961	0.663986
11.61430	10.71315	11.40922	1.292550	0.982341
9.770193	9.286439	9.420886	1.100431	0.964427
8.229758	7.870634	7.994833	0.963546	0.971454

Regression Output:
 Constant -29.1543
 Std Err of Y Est 0.123329
 R Squared 0.965986
 No. of Observations 4
 Degrees of Freedom 2

X Coefficient(s) 13.48892
 Std Err of Coef. 1.789802

t = 20.325 deg C
 s.d.(t) = 0.120638 deg C

Tap DL= 122.2234

L	MDR	1//f	1//f	1//f/Siv	1//f/L
74.18156	26.01390	16.23027	1.389854	0.218791	
65.79247	25.02362	15.08485	1.312679	0.229309	
69.64487	25.49317	15.54799	1.342583	0.223246	
60.25294	24.29786	14.13386	1.244402	0.234575	
51.36063	22.98025	12.95728	1.166013	0.252280	
56.46475	23.76205	13.58387	1.206384	0.240572	
42.06690	21.53197	11.53140	1.067193	0.274159	
36.52574	20.16766	10.83280	1.023079	0.296580	
29.63148	18.44159	10.29928	1.003160	0.347579	
25.84107	17.31218	10.00716	0.995103	0.387258	
21.64949	15.85178	9.729659	0.994413	0.449417	
16.18151	13.44964	10.21513	1.094077	0.631284	
10.95325	10.22960	10.49858	1.201649	0.958490	

P2P11195

Tap = 9.241802
Res/f# = 640.4543

Regression Output:

Constant -47.0544
Std Err of Y Est 0.097967
R Squared 0.994951
No. of Observations 6
Degrees of Freedom 4

X Coefficient (s) 20.55662
Std Err of Coef. 0.732123

t = 21.88076 deg C
s.d.)t = 0.082131 deg C

PSP11102		2/21/89 15:28		1.0 PSID		1.0 PSID		10.05 <C>(ppm)=52.04769 X coeff		co/NaCl	
S =	Z =	10.05 S =	4.77 Z =	10.05 <C>(ppm)=52.04769 X coeff	4.82 [NaCl]= 0.106855 constant	co/NaCl	X	coeff	constant		
HMD-40	HMD-40	Temp	<U>	<U>0	<U>corr	Batch	Vol				
D)1	Q)h	(deg C)	(volts)	(volts)	(volts)	(ml)					
(1/s)	(1/s)										
0.223	0.224	23.85	2.443428	0.0455	2.398928						
0.181	0.182	23.8	2.061833	0.0435	2.017533						
0.156	0.157	23.8	1.744142	0.0455	1.699142						
0.122	0.123	23.75	1.3665	0.0445	1.321						
0.089	0.09	23.8	0.924125	0.0465	0.876125						
				0.0495							
0.028	0.029	23.85	0.71075	0.034	0.6785	1057					
0.021	0.022	23.9	0.452330	0.0305	0.426230	1086					
0.015	0.016	23.9	0.319562	0.0295	0.290662	1046					
		24	0.185071	0.0295	0.154571	534					
		24	0.068875	0.0305	0.038375	125					
0.06	0.0615	24	2.970666	0.0295	2.944666	1064					
0.045	0.046	23.95	1.942666	0.0225	1.920666	1090					
0.072	0.075	23.9	3.729166	0.0215	3.707166	1128					
				0.0225							

density	viscosity	ID(cm)	K(V/psi)	XS(cm ²)	75.06	3.539999	-0.79424
1.00417	1.010869	1.45796	14.29	1.569479			
-0.00025	-0.02281						
0.003419	-4.14933						

t)saap	DP	<U>	Re	Tw	f	Log(Re/f)1/f	Solvent
(sec)	(psid)	(cm/s)		dyne/cm ²			
0							
0.167874	134.1735	21169.74	23.68339	0.002626	3.035434	11.55968	
0.141170	109.0160	17181.02	19.91610	0.003346	2.997231	11.40476	
0.118904	94.04128	14820.99	16.77477	0.003787	2.960048	11.27281	
0.092442	73.67565	11598.22	13.04155	0.004797	2.904891	11.07756	
0.061310	52.90991	8496.111	8.649535	0.005942	2.816216	10.76565	
36.7	0.009039	17.25153	2721.927	1.275264	0.008556	2.401012	9.297829
50	0.005678	13.01004	2055.035	0.801115	0.009450	2.300552	8.978201
65.1	0.003864	9.624309	1520.226	0.545182	0.011752	2.216975	8.642340
59.9	0.002059	5.339902	845.2794	0.290522	0.020344	2.081279	8.161977
59.9	0.000511	1.249977	197.8884	0.072127	0.092180	1.778739	7.090984
17.1	0.039230	37.27043	5900.417	5.534603	0.007956	2.721233	10.42741
23.6	0.025588	27.66517	4374.826	3.609959	0.009418	2.627948	10.09718
15.2	0.049389	44.45129	7021.388	6.967748	0.007041	2.770251	10.60097

Tap DL= 122.2234

L 1//f	HDR 1//f	1//f	1//f/Slv	1//f/L
67.81322	25.27325	19.51107	1.690780	0.287717
62.11578	24.54911	17.28729	1.515796	0.278307
57.00698	23.84091	16.24909	1.441441	0.285036
50.20788	22.79294	14.43779	1.303337	0.287560
40.93513	21.10810	12.97191	1.205159	0.316889
15.73593	13.21923	10.81095	1.163239	0.487023
12.48626	11.31049	10.28643	1.150839	0.823819
10.30044	9.722543	9.224274	1.067335	0.895521
7.536331	7.148319	7.010866	0.858966	0.930275
5.785083	1.396051	3.293676	0.464487	0.877124
32.89375	19.30343	11.21112	1.075159	0.340828
26.53559	17.53102	10.30417	1.020499	0.388315
36.82402	20.23477	11.91713	1.124158	0.325623

PSP11102

Tw dyne/cm2	B(U)/D (1/s)	Log Tw	Log B(U)/D
0.800175	71.38765	-0.09681	1.853623
0.554597	52.80973	-0.25602	1.722713
0.294382	29.30068	-0.53108	1.466877
0.072127	6.858773	-1.14190	0.836246

Regression Output:

Constant	-1.97624
Std Err of Y Est	0.015387
R Squared	0.999424
No. of Observations	3
Degrees of Freedom	1

X Coefficient(s) 0.993514
Std Err of Coef. 0.033848

K' = 0.010562
n' = 0.993514

Tw = 4.396551
Res/ff = 467.4858

Regression Output:

Constant	-37.5790
Std Err of Y Est	0.121313
R Squared	0.995024
No. of Observations	4
Degrees of Freedom	2

X Coefficient(s) 17.91327
Std Err of Coef. 0.895670

t = 23.88461 deg C
s.d.(t) = 0.081770 deg C

P1P01404

5/2/89 12:22
 1.0 FSID Taps 14 0.1 PSID Taps 14
 S = 10.05 B = 10.05 <C> (ppm) = 1.031289 X coeff
 Z = 4.9 Z = 4.92 [NaCl] = 0.000309 constant

MHD 40 0)1 (1/s)	MHD-40 0)h (1/s)	Temp (deg C)	<V> (volts)	<V>0 (volts)	<V>(corr)	Batch Vol (ml)
0.187	0.188	21.3	4.102111	0.0225	4.087111	1096
0.17	0.171	21.2	3.5034	0.0075	3.4971	1134
0.164	0.165	21.2	3.309714	0.0055	3.304714	1092
0.147	0.148	21.2	2.758466	0.0045	2.754666	1106
0.117	0.118	21.2	1.907428	0.0035	1.90428	1094
0.114	0.115	21.2	2.372666	0.0015	2.371666	1106
0.1	0.101	21.2	1.452166	0.0005	1.450166	1078
0.092	0.093	21.4	6.601833	0.0435	6.558333	1096
0.07	0.071	21.45	4.158714	0.0265	4.053214	1134
0.055	0.056	21.4	2.875666	0.1055	2.772666	1092
0.047	0.048	21.4	2.201428	0.1005	2.103428	1106
0.037	0.038	21.4	1.547	0.0955	1.4565	1094
0.031	0.032	21.5	1.091610	0.0855	1.011310	1106
0.025	0.026	21.5	0.587769	0.0755	0.517269	1078
0.018	0.019	21.5	0.391071	0.0455	0.350071	1128
0.013	0.013	21.5	0.28825	0.0565	0.23675	1087
		21.55	0.21725	0.0465	0.17225	1183
		21.6	0.14075	0.0435	0.09925	692
		21.6	0.084305	0.0395	0.044805	313
		21.45	0.053535	0.0365	0.019335	204
				0.0315		

density	viscosity	ID(cm)	K(U/psi)	X3(cm2)	0	t)seep (sec)	DP (paid)	-U. (cm/s)	Re	lw dynes/cm ²	I	l)uq(Kn/1)1/1/7	Solvent
1.000096	1.001592	1.41796	14.29	1.669479	0.286011	112.6099	16860.86	40.3496	0.006375	1.129132	11.87137		
-0.00025	-0.02281				0.244723	102.4271	15301.65	39.5200	0.006595	3.094397	11.74804		
0.003419	-4.14933				0.231260	98.83319	14744.75	32.62575	0.006692	3.002006	11.70454		
					0.192768	88.65038	13241.53	27.19741	0.006733	3.042477	11.56460		5.539999
					0.133305	70.68071	10559.07	18.80638	0.007542	3.26278	11.28106		0.79474
					0.163966	80.86353	12080.25	23.41425	0.007174	3.009766	11.44952		
					0.100081	60.49789	9037.818	14.11930	0.007729	2.900132	11.06071		
					11.8	0.089156	55.63491	8348.920	12.57797	0.008142	3.877001	10.97887	
					16	0.055100	42.45335	6378.002	7.77502	0.008642	2.727997	10.61065	
					19.4	0.037492	33.71639	5059.675	5.517570	0.007729	2.690057	10.31707	
					22.9	0.028594	28.92934	4341.316	4.034004	0.009658	2.630068	10.10438	
					28.2	0.019800	23.23737	3487.144	2.792365	0.010365	2.560360	9.822166	
					34.9	0.013748	18.98238	2855.033	1.939268	0.010785	2.472074	9.545245	
					42	0.007031	15.37405	2312.336	0.992050	0.008409	2.326440	9.029877	
					60	0.004487	11.26099	1693.711	0.633031	0.010002	2.228894	8.684570	
					79.9	0.003218	8.148950	1225.643	0.454057	0.011700	2.156775	8.439088	
					119.9	0.002341	5.909958	889.8917	0.330351	0.011951	2.088162	8.106340	
					119.9	0.001349	3.457051	520.5450	0.190347	0.021913	1.768447	7.762751	
					170.4	0.000609	1.557172	234.7356	0.085930	0.071010	1.796341	7.152940	
					179.0	0.000265	0.679809	102.5632	0.037466	0.163548	1.616482	6.516594	

Tap DL= 122.2236

L	HDR	1//f	1//f	1//f/81v	1//f/L
84.14197	27.05352	12.52411	1.054984	0.148845	
77.63569	26.39157	12.31530	1.048285	0.158588	
75.48944	26.15811	12.22418	1.044396	0.161932	
68.92135	25.40700	12.00964	1.038403	0.174251	
57.31372	23.88319	11.51451	1.026493	0.200903	
63.95081	24.78935	11.80419	1.031151	0.184613	
49.64067	22.70251	11.37446	1.028366	0.229043	
47.08490	22.26303	11.08226	1.009421	0.235367	
37.05740	20.28694	10.75690	1.013783	0.290275	
30.61494	18.71102	10.32925	1.001184	0.337392	
26.66544	17.57130	10.17542	1.007000	0.381595	
22.18912	16.05494	9.822223	1.000005	0.442659	
18.53144	14.56844	9.628911	1.008765	0.519592	
13.25343	11.90252	10.90441	1.207593	0.822761	
10.58702	9.94897	9.998740	1.151327	0.944433	
8.96638	8.577967	8.543369	1.013557	0.952826	
7.656717	7.275084	7.263980	0.887329	0.948707	
5.812031	5.000511	5.597709	0.721117	0.963124	
3.909500	1.728583	3.752448	0.524650	0.959879	
2.584416	-1.08683	2.480327	0.380617	0.959724	

PIP03404

Tw	8(U)/D	Log	Log
dyn/cm ²	(1/s)	Tw	8 U / D
0.633031	61.79041	-0.19857	1.790921
0.454033	44.71425	-0.34289	1.650446
0.330351	32.42864	-0.48102	1.510928
0.190347	18.96925	-0.72045	1.278050
0.085930	8.544391	-1.06585	0.931481
0.037466	3.729097	-1.42635	0.571603

Regression Output:
 Constant 2.00187
 Std Err of Y Est 0.002308
 R Squared 0.999979
 No. of Observations 5
 Degrees of Freedom 4

X Coefficient(s) 1.005066
 Std Err of Coef. 0.002627

K' = 0.009956
 n' = 1.005066

Tw8 = 12.06977
 Res/8 = 736.3099

Regression Output:
 Constant -6.32431
 Std Err of Y Est 0.008874
 R Squared 0.999531
 No. of Observations 6
 Degrees of Freedom 4

X Coefficient(s) 6.022181
 Std Err of Coef. 0.065215

t = 21.395 deg C
 s.d.t = 0.148239 deg C

Page 3

Cyanamid 836

Tap DL= 122.2234

L 1//4	MDR 1//4	1//4	1//4/81v	1//4/L
84.14197	27.05352	12.52411	1.054904	0.148845
77.85569	26.39157	12.31530	1.048265	0.158589
75.48944	26.15811	12.22418	1.044396	0.161932
68.92135	25.40700	12.00964	1.038483	0.174251
57.31372	23.88519	11.51451	1.020495	0.200903
63.95081	24.78935	11.80619	1.051151	0.184613
49.60067	22.70251	11.37446	1.028366	0.229043
47.08490	22.26303	11.08226	1.009421	0.233367
37.05760	20.28694	10.75690	1.013783	0.290275
30.61496	18.71102	10.32973	1.001184	0.337392
26.66544	17.57130	10.17342	1.007060	0.381595
22.18912	16.05494	9.82223	1.006605	0.442659
18.53164	14.56864	9.62891	1.008745	0.519592
13.25343	11.80252	10.90441	1.207593	0.822761
10.58702	9.948987	9.998740	1.151327	0.944433
8.966338	8.577967	8.583369	1.013557	0.952826
7.656712	7.275084	7.263980	0.887329	0.948707
5.812031	5.000511	5.597709	0.721117	0.963124
3.909500	1.728583	3.752648	0.524430	0.959879
2.584416	-1.68683	2.480327	0.380617	0.959724

Page 4

Cyanamid 836

PIP03404

Tw dyne/cm2	B(U)/D (1/s)	Log Tw	Log B U./D
0.633031	61.79041	-0.19857	1.790921
0.454053	44.71425	-0.34289	1.650446
0.330351	32.42864	-0.48102	1.510928
0.190347	18.96925	-0.72045	1.278050
0.085930	8.544391	-1.06585	0.931481
0.037466	3.729097	-1.42635	0.571603

Regression Output:
 Constant 2.00187
 Std Err of Y Est 0.003708
 R Squared 0.999979
 No. of Observations 5
 Degrees of Freedom 4

X Coefficient(s) 1.005066
 Std Err of Coef. 0.002627

K' = 0.009954
 n' = 1.005066

Tw = 12.06977
 Res/1/s = 736.3099

Regression Output:
 Constant -6.32231
 Std Err of Y Est 0.008874
 R Squared 0.999531
 No. of Observations 6
 Degrees of Freedom 4

X Coefficient(s) 6.022181
 Std Err of Coef. 0.065215

t = 21.395 deg C
 s.d.t = 0.148239 deg C

P2P03407	3/4/89	13.22	1.0 P810	Temp 14	10.05	<C>(ppm)=2.065943	X coeff	co)MaCl	density	viscosity	ID(cm)	K(V/psi)	X8(cm2)	14.29	73.56	3.539999	-0.79424	Solvent
S =	10.05	B =	4.86	Z =	4.92	[NaCl]=	0.000309	constant	0.000076	1.001592	1.45796	14.29	1.669479					
Z =	4.86	Z =	4.92	[NaCl]=	0.000309	constant			-0.00025	-0.02281								
NHD-40	01	01	Temp C)	<U>	<U>	<U>	corr	Batch	Vol	t)amp	DP	<U>	Re	Tw	f	Loq(Re/f)1/f/f		
(l/s)	(l/s)	(l/s)	(deg C)	(volts)	(volts)	(volts)	(volts)	(ml)	(sec)	(psid)	(cm/s)	(cm/s)	(dynes/cm2)					
0.196	0.197	20.95	4.296166	0.003	4.295416				0.300588	118.0008	17529.07	42.40645	0.006101	5.176470	11.89778			
0.176	0.18	20.9	3.694	-0.0015	3.6965				0.258677	107.8180	15998.35	36.49765	0.006789	3.10379	11.78020			
0.17	0.171	20.8	3.68571	-0.0033	3.441071				0.240802	102.4271	15164.19	33.97194	0.006487	5.086845	11.72167			
0.151	0.152	20.8	2.855142	-0.0015	2.855642				0.199835	91.04633	13479.28	28.19230	0.00681	3.046350	11.57852			
0.132	0.133	20.9	2.2533	0.0005	2.2545				0.157767	79.66554	11821.00	22.25753	0.007076	2.996008	11.40011			
0.101	0.102	20.85	1.48675	0.0015	1.486				0.103988	61.09588	9055.515	14.67051	0.007873	2.905000	11.07794			
0.093	0.094	21.05	6.765714	0.0225	6.743214			1194	12.7	0.091669	56.40873	8398.467	12.92254	0.008142	2.879590	10.98799		
0.07	0.072	21	4.2084	0.004	4.2071			1228	17.1	0.057192	43.01512	6397.126	8.068634	0.008726	2.776655	10.62760		
0.055	0.054	21	2.749714	0.0015	2.747714			1133	20.3	0.037312	33.43126	4971.833	5.263981	0.009426	2.683912	10.29529		
0.038	0.039	21.3	1.522285	0.0085	1.513285			1174	29.7	0.020372	23.67721	3545.141	2.902272	0.010377	2.557480	9.848079		
0.031	0.032	21.4	0.997333	0.0095	0.986833			1099	34.8	0.013415	18.91635	2838.704	1.892609	0.010797	2.463726	9.533918		
0.023	0.024	21.35	0.451461	0.0115	0.439961			1094	44.9	0.005980	14.66122	2197.673	0.843785	0.007065	2.287819	8.900207		
0.017	0.018	21.4	0.335333	0.0115	0.323333			1094	60	0.004398	10.92156	1638.958	0.620492	0.010433	2.225564	8.665667		
0.012	0.013	21.35	0.239136	0.0125	0.226636			1114	85.4	0.003080	7.827538	1173.774	0.434657	0.014714	2.145777	8.390796		
		21.25	0.192538	0.0125	0.181038			1076	103.9	0.002461	6.203197	927.7454	0.347206	0.018078	2.096012	8.174170		
		21.3	0.127384	0.0105	0.116384			1203	180.2	0.001382	3.998800	598.7324	0.233209	0.027268	2.000567	7.876254		
		21.3	0.077	0.0115	0.0655			1150	299.9	0.000890	2.296890	343.9088	0.126619	0.047708	1.875740	7.474367		
		21.3	0.028454	0.0115	0.014954			292	399.9	0.000230	0.583210	87.33294	0.025516	0.171544	1.588762	6.295456		

Top DL= 122.2234

L	1/f	1/f	1/f	1/f	1/f	1/f	1/f	1/f	1/f
85.57737	27.19509	12.80206	1.076040	0.149596					
79.28741	26.54420	12.60945	1.070393	0.159014					
74.33528	26.25006	12.41577	1.059215	0.162447					
69.55952	25.48065	12.11980	1.046536	0.174215					
61.92825	24.52414	11.95014	1.046493	0.192646					
50.22043	22.77500	11.26970	1.017310	0.224404					
47.36638	22.31221	11.08178	1.008335	0.233958					
37.37107	20.35445	10.49966	1.007044	0.266281					
30.18510	18.59434	10.29444	0.999919	0.341044					
22.56629	16.19402	9.818687	0.997015	0.435104					
18.24446	14.44880	9.713894	1.020054	0.531846					
12.18146	11.10637	11.27570	1.266903	0.925643					
10.45789	9.867724	9.794976	1.130320	0.934410					
8.742932	8.369745	8.387445	0.999686	0.959545					
7.796372	7.424258	7.437314	0.905429	0.953945					
6.258172	5.610782	5.979504	0.759181	0.953471					
4.494835	3.239047	4.578284	0.615827	0.975175					
2.386594	-3.33700	2.284891	0.357267	0.956583					

P2P03407

Tw	B(U)/D	Log	Log
dyne/cm ²	(1/s)	Tw	B(U)/D
0.620472	59.92794	-0.20726	1.777629
0.434657	42.95063	-0.36185	1.655969
0.347206	34.03788	-0.45941	1.531960
0.125619	12.60331	-0.90094	1.100484
0.032514	3.200145	-1.48789	0.505169
0.225209	21.94189	-0.65128	1.341274

Regression Output:
 Constant -1.99403
 Std Err of Y Est 0.005371
 R Squared 0.999927
 No. of Observations 4
 Degrees of Freedom 2

X Coefficient(s) 1.000723
 Std Err of Coef. 0.006042

K' = 0.010091
 n' = 1.000723

Tw = 10.77046
 Res/fs = 690.7054

Regression Output:
 Constant -7.64699
 Std Err of Y Est 0.060259
 R Squared 0.990454
 No. of Observations 6
 Degrees of Freedom 4

X Coefficient(s) 6.513269
 Std Err of Coef. 0.319704

t = 21.12222 deg C
 s.d.t = 0.216809 deg C

PS903010 3/7/89 12:15
 1.0 P81D Tape 14 0.1 P81D Tape 14
 S = 10.05 B = 10.05 <C> (ppm) = 5.158589 X coeff
 Z = 4.95 Z = 4.95 [NaCl] = 0.000309 constant

MWD-40 01 (1/s)	MWD-40 01 (1/s)	Temp (deg C)	<U> (volts)	<V> (volts)	<U><V> (volts)	Batch Vol (ml)
0.226	0.227	20.1	3.797	0.0625	3.808	
0.203	0.204	20.1	3.2375	-0.0245	3.2505	
0.189	0.19	20.1	2.797	-0.0313	2.8285	
0.164	0.165	20.1	2.2994	-0.0365	2.3376	
0.141	0.142	20.1	1.84375	-0.0395	1.88325	
0.106	0.107	20.1	1.170555	-0.0425	1.213555	
0.126	0.127	20.1	1.573625	-0.0435	1.617125	
0.097	0.098	20.2	5.559833	0.0605	5.515333	1132
0.073	0.074	20.2	3.617166	0.0445	3.571666	1158
0.057	0.058	20.2	2.4675	0.0465	2.4195	1163
0.039	0.04	20.2	1.154555	0.0495	1.195055	1198
0.03	0.032	20.25	0.715166	0.0495	0.665166	1254
0.024	0.025	20.25	0.561909	0.0505	0.509409	1141
0.018	0.019	20.25	0.435928	0.0545	0.380928	1142
0.013	0.014	20.25	0.331157	0.0535	0.275657	1089
		20.25	0.255130	0.0555	0.200130	860
		20.3	0.205812	0.0545	0.151312	1144
		20.3	0.134833	0.0545	0.080333	664
		20.35	0.0858	0.0515	0.0348	358

density	viscosity	ID(cm)	K(U/ps)	XS(cm2)	3.559999	-0.79424	Solvent
1.000096	1.301592	1.45796	14.24	7.95			
-0.00025	-0.02281						
0.003419	-4.14933						
0.267415	135.9705	19814.84	37.72644	0.004087	3.102711	11.77784	
0.228247	122.1937	17897.17	32.20072	0.004319	3.068321	11.65610	
0.198630	113.8079	14585.11	28.02238	0.004733	3.028161	11.54926	
0.164137	98.83319	14402.85	23.15896	0.004748	2.996748	11.40277	
0.132250	85.95644	12395.18	18.65764	0.005165	2.949817	11.27659	
0.085221	64.99183	9340.035	12.02288	0.005862	2.854791	10.89879	
0.113562	76.07161	11085.83	16.02110	0.005545	2.916735	11.11948	
11.4	0.074581	59.47856	8687.325	10.52185	0.005957	2.876430	10.79977
15.5	0.048298	44.75028	6556.140	6.815835	0.006015	2.720689	10.46577
19.8	0.032718	35.18304	5138.768	4.615793	0.007469	2.647497	10.16638
29.9	0.014943	23.99962	3505.340	2.108166	0.007731	2.477326	9.563910
39.6	0.008994	18.96798	2773.554	1.268969	0.007064	2.367572	9.175521
45.2	0.004888	15.12049	2210.963	0.971823	0.008514	2.309660	8.970443
59.9	0.005151	11.41979	1669.835	0.726715	0.011162	2.246540	8.747028
80.1	0.003727	8.143559	1190.775	0.525885	0.015804	2.176312	8.498770
89.9	0.002064	4.285450	627.3783	0.381798	0.023397	2.106783	8.252259
159.9	0.002064	4.285450	627.3783	0.381798	0.023397	2.106783	8.252259
180.1	0.001086	2.208377	323.2790	0.153333	0.043394	1.907067	7.531344
239.9	0.000470	0.893864	130.9986	0.066389	0.166441	1.777901	6.911018

Tap DL= 122.2234

L	MR	1/14	1/4	1/4/81v	1/4/L
79.17566	26.55152	15.44151	1.328046	0.197554	
75.14785	25.89811	15.21504	1.365328	0.206004	
68.23722	25.52468	15.19047	1.315293	0.222615	
62.03379	24.53821	14.51110	1.272398	0.233922	
55.47974	23.64452	13.91348	1.258229	0.249884	
44.69445	21.83346	13.04037	1.198331	0.292201	
51.59588	23.01796	13.42868	1.207471	0.260244	
41.90831	21.50198	12.95584	1.199440	0.309147	
33.72487	19.50932	12.11299	1.157591	0.359171	
27.75729	17.90244	11.57074	1.138139	0.414854	
18.75885	14.66920	11.67894	1.221138	0.622583	
14.57042	12.58425	11.89719	1.294423	0.816530	
12.75088	11.48354	10.83730	1.208112	0.949925	
11.02627	10.28442	9.465095	1.082092	0.858413	
9.379749	8.949930	7.934444	0.933643	0.845912	
7.992147	7.628886	6.552238	0.793593	0.819836	
6.957239	6.484581	5.635662	0.701035	0.810042	
5.049293	5.872280	5.985741	0.527751	0.786235	
3.340271	0.430135	2.451123	0.354648	0.733809	

PSP03410

Tw	B(U)/D	Log	Log
dynes/cm ²	(1/s)	Tw	B-U./D
0.726715	62.66175	-0.13867	1.797002
0.525885	44.68467	-0.27910	1.650150
0.381798	31.44141	-0.41816	1.497502
0.288665	23.51477	-0.57960	1.371740
0.153255	12.11762	-0.81458	1.083417
0.066389	4.904740	-1.17790	0.690616

Regression Output:
 Constant -1.82947
 Std Err of Y Est 0.002945
 R Squared 0.999955
 No. of Observations 6
 Degrees of Freedom 4

X Coefficient (s)	0.940523
Std Err of Coef.	0.003147
K' =	0.014808
n' =	0.940523

Tw = 3.460/99
 Res/fs = 584.1301

Regression Output:
 Constant -18.6782
 Std Err of Y Est 0.153981
 R Squared 0.9799610
 No. of Observations 7
 Degrees of Freedom 5

X Coefficient (s) 11.05892
 Std Err of Coef. 0.717521

t = 20.19473 deg C
 s.d.t = 0.080939 deg C

PIP15413	3/7/89	12:07	1.0 P81D	Tap 14	0.1 P81B	Tap 14	10.05	<C>(ppm)=10.3123	X coeff	col/NaCl	density	viscosity	ID(cm)	K(U/psi)	X8(ccg?)	75.95	0.539999	0.79424	Solvent
Z =	0.9	Z =	4.9	[NaCl]=	0.000509	constant													
MWB-40	MWB-40	Temp	<V>	<V>	<V>	corr	Batch	Vol			t)naep	DP	<U>	Re	Tm				
(1/s)	(1/s)	(deg C)	(volts)	(volts)	(volts)	(volts)	(ml)	(ml)			(sec)	(psid)	(cm/s)	(dyne/cm2)	(l/ft)				
0.236	0.237	21.1	3.359142	0.0115	3.368142		1196				0.236526	141.9604	21159.76	33.36871	0.005317	3.085910	11.71836		
0.21	0.211	21.1	2.807333	-0.0295	2.842833		1134				0.199637	126.3866	18838.43	28.16438	0.003572	3.049709	11.58002		
0.193	0.194	21	2.4894	-0.0415	2.5279		1168				0.177521	116.2038	17281.61	25.04429	0.003715	3.023609	11.49428		
0.164	0.167	21	1.929371	-0.0455	1.980071		1142				0.139049	99.73168	14831.90	19.61687	0.003951	2.989570	11.0652		
0.193	0.144	21	1.561333	-0.0653	1.619833		1114				0.113752	86.23442	12827.59	16.04793	0.004321	2.925965	11.15216		
0.117	0.118	21	1.178375	-0.0615	1.240375		1074				0.097104	70.68071	10511.49	12.28858	0.004928	2.868006	10.94698		
0.093	0.094	21.05	0.8255	-0.0625	0.8885		1046				0.062394	56.30497	8383.018	8.802506	0.005562	2.796051	10.69226		
0.097	0.098	21.2	4.936	0.0465	4.897		1196				12	0.066220	58.70092	8769.367	9.342236	0.005472	2.810451	10.74324	
0.073	0.074	21.2	3.376425	0.0313	3.345625		1134				15.2	0.045241	44.48773	6675.928	6.382605	0.006403	2.737724	10.45039	
0.055	0.054	21.2	2.290888	0.0345	2.258088		1168				20.5	0.030505	34.12776	5098.368	4.303664	0.007407	2.642145	10.14743	
0.038	0.039	21.2	1.0967	0.0355	1.0482		1142				29.3	0.019174	23.34626	3487.712	1.999700	0.007350	2.475708	9.558353	
0.029	0.03	21.3	0.643425	0.0375	0.626125		1114				37.4	0.009466	17.84154	2671.379	1.194487	0.007518	2.364802	9.165644	
0.024	0.024	21.3	0.550909	0.0375	0.512909		1074				43.7	0.008935	16.74856	2208.273	0.978500	0.009013	2.221491	9.012326	
0.016	0.017	21.3	0.396647	0.0385	0.359147		1046				66.7	0.004856	10.25555	1535.593	0.685161	0.013052	2.264107	8.738386	
0.012	0.013	21.3	0.310283	0.0345	0.274785		1080				83.2	0.003715	7.775338	1164.186	0.524221	0.017373	2.185968	8.535574	
		21.4	0.21155	0.0345	0.17805		1074				128.9	0.002407	4.990801	748.9505	0.339674	0.027324	2.092727	8.202501	
		21.4	0.12	0.0325	0.0835		1037				270	0.001129	2.544931	351.8949	0.159296	0.058046	1.928399	7.620427	
		21.45	0.080666	0.0365	0.044166		352				180	0.000597	1.171356	175.9793	0.084258	0.123066	1.790496	7.133604	

Tap DL= 122.2234

L	1//4	MDR	1//4	1//4	1//4/8lv	1//4/L
76.17114	26.23229	17.36202	1.481407	0.227934		
69.97951	25.53272	16.82495	1.451926	0.240424		
65.84002	25.02958	16.40493	1.427225	0.249163		
58.27072	24.02183	15.96039	1.407010	0.273008		
52.70419	23.19333	15.21177	1.364020	0.298635		
46.11970	22.09212	14.24484	1.301258	0.300867		
39.07790	20.72487	13.40754	1.253997	0.343097		
40.39334	20.99857	13.56803	1.262936	0.335881		
33.38911	19.42677	12.49645	1.193788	0.374267		
27.41333	17.80075	11.42213	1.143327	0.423897		
18.68910	14.63845	11.46359	1.220264	0.624085		
14.47711	12.53123	11.53274	1.258260	0.796620		
13.10202	11.70834	10.53321	1.148757	0.803876		
10.96447	10.23804	8.752953	1.601664	0.798301		
9.590661	9.133402	7.586716	0.809147	0.791052		
7.737625	7.361825	6.049583	0.737529	0.781839		
5.298829	4.237698	4.150620	0.544670	0.783308		
3.858127	1.619435	2.850789	0.397584	0.758904		

P1P13413

Tw	8.U./D	Log	Log
dynes/cm2	(1/s)	Tw	8.U./D
1.194487	97.89868	0.077181	1.990776
0.978500	80.92712	-0.00943	1.908094
0.683161	56.27345	-0.16420	1.750303
0.524221	42.66420	-0.28048	1.630063
0.339674	27.38511	-0.46893	1.437514
0.159296	12.86691	-0.79779	1.109474
0.084258	6.427372	-1.07438	0.808033

Regression Outputs
 Constant -1.89720
 Std Err of Y Est 0.002591
 R Squared 0.999948
 No. of Observations 6
 Degrees of Freedom 4

X Coefficient(s) 0.988739
 Std Err of Coef. 0.003560

K' = 0.012787
 n' = 0.988739

Tw = 2.562297
 Res/8 = 3.7.7256

Regression Outputs
 Constant -24.7470
 Std Err of Y Est 0.084282
 R Squared 0.997852
 No. of Observations 9
 Degrees of Freedom 7

X Coefficient(s) 15.64109
 Std Err of Coef. 0.239170

t = 21.19444 deg C
 s.d.t = 0.146143 deg C

P2P13426
S = 10.05 g = 10.05 C (ppm) = 20.58907 X coeff
Z = 4.62 Z = 4.72 [NaCl] = 0.000309 constant

MWD-40 (l/s)	MWD-40 (l/s)	Temp (deg C)	<U> (volts)	<U>0 (volts)	<U> (volts)	<U>corr (volts)	Batch Vol (ml)
0.271	0.272	21.5	2.590166	0	2.587916	0	2.587916
0.21	0.211	21.5	1.8109	0.0045	1.8063	0.0045	1.8063
0.242	0.243	21.5	2.176166	0.0045	2.171666	0.0045	2.171666
0.175	0.176	21.5	1.367428	0.0045	1.362928	0.0045	1.362928
0.149	0.15	21.5	1.058142	0.0025	1.054442	0.0025	1.054442
0.131	0.132	21.5	0.870426	0.0005	0.870178	0.0005	0.870178
0.109	0.11	21.5	0.616144	0	0.616916	0	0.616916
0.268	0.269	21.5	2.633166	-0.0015	2.632166	-0.0015	2.632166
				0.0035	0.0035	0.0035	0.0035

density	viscosity	ID (cm)	K (V/psi)	KS (cm ²)	1w	Re	<U> (cm/s)	DP (psid)	t (sec)	t (sec)	DP (psid)	Re	1w (dyne/cm ²)	f	1w (dyne/cm ²)	solvent
1.000096	1.001592	1.45796	17.971	84.66												1.539999
-0.00025	-0.02281															0.79424
0.003419	-4.14933															Solvent
0.185181	162.9250	24504.75	26.12506	0.001972	2.076710	11.54419										
0.159252	126.3866	19009.20	18.23463	0.002787	2.958650	11.26779										
0.153396	145.3543	21892.11	21.92201	0.002073	2.998631	11.40940										
0.077597	105.1225	15810.97	15.76888	0.00496	2.897630	11.05185										
0.075609	89.84836	13513.65	10.66682	0.002647	2.842199	10.85567										
0.042266	79.06655	11892.01	8.784468	0.007015	2.800059	10.70638										
0.044144	65.88879	9910.012	6.227784	0.007874	2.725548	10.44197										
0.188348	161.1280	24234.48	26.57177	0.002000	3.040391	11.55723										
11.7	0.038594	59.89890	9029.449	5.444812	0.002040	3.677158	10.74218									
14.6	0.027175	44.88809	6766.647	2.853843	0.002011	2.629987	10.07252									
21.9	0.021314	36.81794	5248.625	3.007028	0.004970	3.568373	9.885799									
26.7	0.015024	24.22877	3652.361	2.119575	0.007254	2.472391	9.616956									
40	0.011100	17.59530	2652.400	1.565972	0.010175	2.426558	9.384263									
59.9	0.008601	12.82976	1934.020	1.713476	0.014772	2.721183	9.188751									
60	0.005844	8.086352	1218.975	0.024592	0.035268	3.107384	8.891739									
90	0.004524	4.126369	622.0387	0.483164	0.056860	2.17214	8.480344									
60	0.004384	3.690396	857.7977	0.610593	0.07879	2.274869	8.670387									
120	0.002344	2.585669	386.7614	0.770781	0.100690	2.088937	8.187087									
170.2	0.001435	1.370399	206.5805	0.702468	0.216070	1.903745	7.811747									
179.8	0.000633	0.503044	75.83130	0.089430	0.708144	1.804209	7.187675									

MWD-40 (l/s)	MWD-40 (l/s)	Temp (deg C)	<U> (volts)	<U>0 (volts)	<U> (volts)	<U>corr (volts)	Batch Vol (ml)
0.099	0.1	21.6	3.3084	0.0485	3.2674	0.0485	1180
0.074	0.074	21.6	2.335666	0.0335	2.300666	0.0335	1244
0.057	0.058	21.6	1.843	0.0365	1.8045	0.0365	1273
0.031	0.04	21.6	1.314444	0.0405	1.271944	0.0405	1080
0.021	0.029	21.6	0.985230	0.0405	0.939730	0.0405	1175
0.02	0.021	21.6	0.7762	0.0465	0.7282	0.0465	1283
0.015	0.014	21.6	0.543333	0.0495	0.494833	0.0495	810
		21.6	0.341444	0.0515	0.289944	0.0515	620
		21.6	0.423714	0.0525	0.371214	0.0525	570
		21.6	0.251	0.0525	0.1985	0.0525	514
		21.6	0.173	0.0515	0.1215	0.0515	275
		21.6	0.105166	0.0515	0.053666	0.0515	151
				0.0495	0.0495	0.0495	

Tap DL= 122.2234

L	NDR	1//4	1//4	1//4/81v	1//4/L
48.01273	25.29749	22.51853	1.950636	0.331092	
56.82115	23.81397	20.90903	1.855445	0.347979	
62.30338	26.57400	21.94120	1.924834	0.352488	
49.37583	22.65498	20.01371	1.810891	0.405337	
43.45894	21.60178	19.43451	1.790270	0.447172	
39.43839	20.80074	18.84507	1.740295	0.477653	
33.20690	19.38161	18.45202	1.786253	0.581691	
68.59173	25.36744	22.68218	1.910481	0.321934	
31.11990	18.84600	18.13439	1.753439	0.582724	
26.11342	17.39869	16.19332	1.607870	0.620191	
23.12679	16.39447	14.18437	1.434822	0.613330	
19.41650	14.93353	11.75462	1.222489	0.605496	
16.68932	13.70461	9.932999	1.058474	0.595170	
14.69137	12.65246	8.227705	0.895441	0.580636	
12.11062	11.05844	6.290838	0.707332	0.519447	
9.270314	8.853074	4.193467	0.494518	0.452378	
10.48934	9.872518	5.11113	0.589497	0.487264	
7.670387	7.289808	3.151414	0.384831	0.410834	
6.001021	5.264558	2.191514	0.275420	0.358524	
3.988714	1.893277	1.188335	0.165422	0.297954	

P2P13424

Tm	8(U)/D	Log	Log
dyna/cm2	(1/s)	Tm	8(U)/D
1.565972	96.54752	0.194784	1.984741
1.213476	70.39845	0.084031	1.847563
0.824592	44.37077	-0.08376	1.447097
0.483164	22.64187	-0.31590	1.354912
0.618593	31.22388	-0.20959	1.494486
0.330781	14.07813	-0.48045	1.148545
6.202468	7.519543	-0.69364	0.876191
0.089430	2.760263	-1.04851	0.440950

Regression Outputs
 Constant -1.40199
 Std Err of Y Est 0.004159
 R Squared 0.999912
 No. of Observations 8
 Degrees of Freedom 6

X Coefficient(s) 0.802618
 Std Err of Coef. 0.001057
 K' = 0.039628
 n' = 0.802618

Tms = 0.774560
 Res/ts = 187.3739

Regression Outputs
 Constant 31.9668
 Std Err of Y Est 0.080108
 R Squared 0.996189
 No. of Observations 4
 Degrees of Freedom 2

X Coefficient(s) 17.95500
 Std Err of Coef. 0.774818

t = 21.56 deg C
 s.d.t = 0.048989 deg C

PIP01305	3/2/89	15:09	1.0 P81D	Tap 14	0.1 P81B	Tap 14	10.05	<C>	(ppm)=1.031289	X coeff	col/MaCl
S =	10.05	B =	4.9	Z =	4.9	Z =	4.92	[NaCl]=	0.001035	constant	
MHD-40	MMB-40	Temp	<V>	<U>	<U>	corr	Batch	Vol			
(1/e)	(1/s)	(deg C)	(volts)	(volts)	(volts)	(volts)	(ml)				
0.181	0.182	21.35	4.018142	0.0105	4.032442		1190				
0.147	0.148	21.2	3.517833	-0.0145	3.534533		1190				
0.159	0.16	21.2	3.2225	-0.0185	3.242		1172				
0.143	0.144	21.1	2.664454	-0.0205	2.687954		1150				
0.126	0.127	21.15	2.14425	-0.0225	2.18775		1095				
0.098	0.099	21.15	1.425888	-0.0245	1.450888		1149				
0.115	0.116	21.2	1.8598	-0.0255	1.8853		1144				
				-0.0255			1144				
0.09	0.091	21.3	4.532714	0.0305	4.458214		1190				
0.068	0.069	21.3	4.143857	0.1185	4.025357		1190				
0.058	0.059	21.3	1.604375	0.1225	1.483375		1172				
0.054	0.055	21.4	2.824285	0.1195	2.705285		1150				
0.03	0.031	21.4	1.123	0.1225	1.002		1095				
0.023	0.025	21.4	0.5799	0.1195	0.4614		1149				
0.018	0.019	21.35	0.4688	0.1175	0.3313		1144				
0.012	0.013	21.4	0.340431	0.1175	0.225131		1053				
		21.45	0.233428	0.1135	0.121928		712				
		21.45	0.148664	0.1095	0.059164		416				
		21.5	0.1338	0.1055	-0.0281		412				
				-0.0975							

density	viscosity	ID (cm)	Re	Tu	t	Lout(Re/t)1/4	Solvent
1.000125	1.001657	1.45796					
-0.00025	-0.02281	14.29					
0.003419	-4.14933	1.649479					
							3.539999
							0.79424
t)saap	DP	<U>	Re	Tu	t	Lout(Re/t)1/4	Solvent
(sec)	(paid)	(cm/s)	dyn-cm ²				
0.282200	109.0160	16340.58	39.81222	0.004711	3.126690	11.86272	
0.247329	100.4301	15032.64	34.89266	0.004903	3.096571	11.75610	
0.228871	95.83825	14316.82	32.00661	0.006981	3.077823	11.68974	
0.188100	86.25442	12856.10	26.57680	0.007146	3.056142	11.54219	
0.153096	74.07141	11351.16	21.59853	0.007477	3.031925	11.38565	
0.101531	59.29991	8848.546	14.32388	0.008160	2.902741	11.06395	
0.131931	69.48273	10379.69	18.61760	0.007724	2.960107	11.27702	
12.9	0.087795	55.25558	8273.011	12.38575	0.008127	2.877654	10.96544
17.2	0.054494	41.44168	6204.750	7.716741	0.009001	2.769097	10.59966
24.9	0.020165	23.47876	3515.303	2.844707	0.01040	2.557227	9.87055
20.9	0.036749	32.95872	4945.811	5.184527	0.009769	2.468529	10.29747
34.9	0.013621	18.79549	2820.167	1.921697	0.010901	2.469016	9.52465
47	0.006272	14.64337	2197.396	0.884901	0.008268	2.308621	8.978446
60	0.004503	11.42072	1711.871	0.655387	0.009760	2.228707	8.687077
80.1	0.003060	7.874350	1181.631	0.431771	0.017952	2.144801	8.384842
100.3	0.001657	4.252046	638.7855	0.235842	0.025914	2.012128	7.917180
120.1	0.000804	2.074766	311.6925	0.113477	0.057817	1.855114	7.561550
240	0.000384	1.028264	154.6507	0.054275	0.102853	1.695461	6.796179

Tap DL= 122.2234

L	1/f	RDR	1/f	1/f/f	1/f/f/f	1/f/f/L
83.67005	27.00711	12.20611	1.028947	0.145083		
78.66406	26.43485	12.03551	1.023767	0.154174		
74.76595	24.07865	11.94803	1.023904	0.160073		
67.92398	25.28671	11.82949	1.024891	0.174157		
61.34895	24.44654	11.54423	1.015494	0.188300		
49.95993	22.75209	11.04955	0.999944	0.221548		
57.01480	23.86204	11.37829	1.009337	0.199567		
46.61590	22.18042	11.09199	1.011725	0.237944		
36.79358	20.22795	10.53981	0.994353	0.286457		
22.34103	14.11124	9.834210	1.000158	0.440185		
30.22797	18.60605	10.22606	0.993045	0.338298		
18.40335	14.51132	9.577428	1.004316	0.520428		
12.48825	11.31181	10.99731	1.230358	0.830612		
10.57015	9.935821	10.12208	1.165859	0.937410		
8.723309	8.351223	8.444049	1.009444	0.970508		
6.427001	5.830439	6.211932	0.784614	0.944534		
4.477073	2.847169	4.351231	0.591091	0.971891		
3.099855	-0.18623	3.118103	0.458802	1.005884		

PIP0005

dynn/cm2	(1/s)	Im	B/U /D
0.633387	62.66687	-0.19496	1.797038
0.431771	43.20749	-0.38474	1.635559
0.233842	23.33148	-0.63107	1.367942
0.113473	11.38449	-0.94510	1.056313
0.054275	5.642710	-1.26539	0.751449

Regression Outputs
 Constant -2.00995
 Std Err of Y Est 0.002596
 R Squared 0.999957
 No. of Observations 4
 Degrees of Freedom 2

X Coefficient(s) 1.007693
 Std Err of Coef. 0.004619

R² = 0.009773
 n^o = 1.007693

Im = 13.10746
 Res/fs = /65.5319

Regression Outputs:
 Constant -2.43248
 Std Err of Y Est 0.076295
 R Squared 0.999233
 No. of Observations 7
 Degrees of Freedom 5

X Coefficient(s) 5.005598
 Std Err of Coef. 0.184744

t = 21.3111 deg C
 s.d.t = 0.116136 deg C

P2P01308	3/4/89	15150	1.0	0.1	1618	14	10.05	10.05	4.92	0.001035	constant	col/NaCl
B =	10.05	B =	10.05	C>(ppm)=	2.065943	X coeff	4.86	Z =	0.001035	constant		
0.19	0.171	21.05	4.246571	<U>	(volts)	<U>	(volts)	<U>	corr	Batch Vol		
0.177	0.178	20.93	3.796111	(volts)	(volts)	(volts)	(volts)	(volts)	(ml)			
0.165	0.166	20.9	3.49225									
0.147	0.142	20.9	2.832									
0.13	0.131	20.9	2.303428									
0.1	0.102	20.9	1.513111									
0.117	0.118	20.95	1.926875									
0.091	0.092	21.1	6.6568									
0.089	0.07	21.1	4.126									
0.054	0.055	21.1	2.782714									
0.038	0.039	21.15	1.520333									
0.03	0.031	21.2	0.9998									
0.023	0.024	21.2	0.633634									
0.014	0.017	21.2	0.3318									
0.012	0.013	21.3	0.191914									
		21.35	0.122571									
		21.4	0.065142									
		21.45	0.047									

density	viscosity	ID(cm)	K (U/psi)	MS(cm ²)	t)saap (sec)	DP (psid)	<U> (cm/s)	Re	fw dyne/cm ²	Log(Re/t)1/2f	Solvent
1.000125	1.001657	1.45796	14.59	7.1.1.6	0.294785	114.4069	17032.96	41.86993	0.006408	5.124677	11.89100
-0.00025	-0.02281				0.243988	106.6200	15857.88	37.29936	0.006571	5.108591	11.79845
0.003419	-4.14933				0.239415	99.43218	14753.51	33.77625	0.006844	5.086534	11.72064
					0.196675	88.65038	13133.73	27.74663	0.007071	5.047853	11.56948
					0.159722	78.46756	11662.83	22.53325	0.00721	5.020660	11.40920
					0.104701	61.09688	9065.410	14.78515	0.007935	5.907161	11.001559
12	0.089920	55.60615	8288.020	12.48722	0.00810	5.875901	10.92491				
16.5	0.055818	42.25595	6298.192	7.874730	0.008035	5.77336	10.60011				
21.9	0.037530	33.17688	4944.968	5.294667	0.008617	5.61618	10.30317				
29.9	0.020355	23.59896	3521.363	2.87167	0.01030	5.52779	9.874624				
40.1	0.013251	18.67172	2789.281	1.869531	0.010743	5.461070	9.504334				
45	0.005765	14.22931	2125.650	0.813434	0.008049	5.380365	8.866739				
60.9	0.004102	10.47493	1564.800	0.578810	0.010568	5.206472	8.605157				
90.1	0.003113	7.871288	1178.510	0.479190	0.013707	5.147515	8.396456				
120.1	0.002187	5.635783	843.8044	0.308615	0.019467	5.070090	8.125334				
120.1	0.001258	3.201923	479.7414	0.177539	0.074696	1.751308	7.101950				
170	0.000756	1.911773	286.8822	0.104715	0.083501	1.841287	7.213404				
240	0.000251	0.048904	97.48508	0.035480	0.160878	1.602661	6.467668				

Top DL = 122.2334

L	1//4	MDR	1//4	1//4	1//4	1//4	1//4
85.22311	27.15887	12.49145	1.050494	0.146373			
60.25493	26.48324	12.33404	1.045374	0.153483			
76.28415	26.24952	12.08763	1.031310	0.158433			
69.14067	25.43321	11.89037	1.027739	0.171973			
67.30751	24.57654	11.47890	1.023402	0.187438			
50.47093	22.83606	11.22602	1.012468	0.222425			
46.94565	22.24214	11.02931	1.004954	0.234834			
37.04129	20.27440	10.43844	1.002041	0.287514			
36.34018	18.63462	10.18650	0.988474	0.335743			
22.34945	14.12180	9.838560	1.000400	0.439817			
18.06967	14.36033	9.647657	1.014855	0.533914			
11.91915	10.92694	11.14618	1.257078	0.933149			
10.05431	9.523972	9.727174	1.150398	0.947443			
8.778000	8.402795	8.391077	0.993340	0.955921			
7.358314	6.947048	7.167100	0.882080	0.974013			
5.587389	4.675249	5.348379	0.697041	0.940638			
4.336787	2.584447	4.134432	0.543399	0.953340			
2.503464	-1.94943	2.433753	0.376295	0.972154			

P2P01308

Tw	B(U)/D	Log	Log
dyne/cm ²	(1/s)	Tw	B U / D
0.578810	57.47719	-0.23746	1.759495
0.439190	43.19069	-0.35734	1.635390
0.308615	30.92421	-0.51058	1.490298
0.177539	17.56933	-0.75070	1.244755
0.106715	10.49012	-0.97177	1.020780
0.035480	3.540618	-1.45001	0.551525

Regression Output
 Constant 2.00029
 Std Err of Y Est 0.004106
 R Squared 0.999972
 No. of Observations 6
 Degrees of Freedom 4

X Coefficient(s) 1.002810
 Std Err of Coef. 0.004107

K' = 0.009993
 n' = 1.002810

Tw = 11.70084
 Res/fs = 708.4050

Regression Output
 Constant -4.62435
 Std Err of Y Est 0.056170
 R Squared 0.991197
 No. of Observations 7
 Degrees of Freedom 5

X Coefficient(s) 5.441076
 Std Err of Coef. 0.229303

t = 21.12631 deg C
 s.d.t = 0.174995 deg C

Tap DL= 122.2234

L	1/4	1/4	1/4	1/4	1/4	1/4	1/4	1/4	1/4
81.80584	26.82118	14.37205	1.215078	0.175484					
74.54842	26.05461	14.09185	1.205951	0.189029					
71.11440	25.66547	13.93038	1.199576	0.195887					
64.97123	24.91998	13.32045	1.160956	0.205023					
57.62683	23.93015	13.03478	1.154599	0.226182					
49.80982	22.72726	12.56701	1.135711	0.252299					
41.77652	21.27994	11.85087	1.097744	0.283537					
42.90129	21.49521	12.15771	1.121998	0.283588					
36.83188	19.77384	11.33739	1.078167	0.325489					
28.29557	18.04093	10.76081	1.055405	0.380300					
21.68061	15.63204	10.14072	1.040781	0.481044					
15.50798	12.99172	11.07840	1.197479	0.723701					
12.28617	11.17720	10.85347	1.217485	0.883405					
10.44170	9.834952	9.373251	1.081951	0.897474					
9.252698	8.837379	8.183473	1.045325	0.884441					
8.019043	7.656408	7.117018	0.861893	0.887514					
4.502489	5.927044	5.783831	0.728894	0.889452					
4.893798	5.581555	4.276403	0.573019	0.877948					
3.443989	0.482455	3.037805	0.434589	0.882059					

PC501311

Tm	8(U)/D	Log	Log
dyne/cm2	(1/a)	Tm	8(U)/D
0.904418	80.15824	-0.04363	1.903948
0.511784	43.44430	-0.29091	1.657470
0.384410	34.28771	-0.41520	1.534882
0.252776	22.58255	-0.59726	1.353773
0.078904	4.281831	-1.14932	0.798086
0.142842	12.61089	-0.84514	1.100745
0.651748	58.76597	-0.18590	1.749125

Regression Output:
 Constant -1.94852
 Std Err of Y Est 0.001823
 R Squared 0.999985
 No. of Observations 5
 Degrees of Freedom 3

X Coefficient(s) 0.999710
 Std Err of Coef. 0.002194

R^2 = 0.01258
 R^2 = 0.999710

Tm = 3.406163
 Res/fe = 379.7645

Regression Output:
 Constant -11.2784
 Std Err of Y Est 0.108984
 R Squared 0.990775
 No. of Observations 9
 Degrees of Freedom 7

X Coefficient(s) 8.220211
 Std Err of Coef. 0.299791

t = 20.13421 deg C
 s.d.t = 0.111275 deg C

density 1.00125 1.001657
 viscosity 1.45796
 K(9/psi)= 14.24
 XB(cm2)= 1.669479
 7.95
 3.539999
 -0.79424
 Solvent

P1P11314 3/9/89 14:02
 1.0 PSID Taps 14 0.1 PSID Taps 14
 S = 10.65 B = 10.05 <C>(ppm)=10.31423 X coeff
 Z = 4.9 [NaCl]= 0.001037 constant

MMD-40 (1/s)	RHD-40 (1/s)	Temp (deg C)	<U> (volts)	<U> (volts)	<U> (volts)	Batch Vol (ml)
0.229	0.23	21.1	3.47075	-0.0015	3.48725	
0.199	0.2	21.1	2.83833	-0.0155	2.85183	
0.188	0.189	21	2.642375	-0.0115	2.674875	
0.167	0.168	21	2.2616	-0.0135	2.2741	
0.139	0.14	21	1.693222	-0.0155	1.709222	
0.104	0.105	21	1.079625	-0.0145	1.116125	
0.094	0.095	21.15	5.117833	0.04	5.085083	1084
0.071	0.071	21.1	3.433125	0.0255	3.406125	1345
0.054	0.055	21.2	2.290265	0.0285	2.260035	1218
0.039	0.04	21.3	1.42325	0.032	1.3905	1102
0.029	0.029	21.25	0.6594	0.0335	0.6254	1180
0.022	0.023	21.25	0.501333	0.0345	0.466333	1085
0.017	0.018	21.25	0.3984	0.0355	0.3619	1084
0.011	0.012	21.3	0.286875	0.0375	0.248375	1157
		21.35	0.202923	0.0395	0.162423	990
		21.35	0.125875	0.0415	0.084375	485
		21.45	0.088	0.0415	0.0465	373

t) ramp (snc)	DP (psid)	<U> (cm/s)	Re	Tw dyne/cm?	f	Log (Re/f) 1/f
0	0.244891	137.7674	20534.05	34.54872	0.003646	3.093424
	0.200269	119.7978	17853.69	28.25335	0.003944	3.049755
	0.187842	115.2089	14835.61	26.50039	0.004142	3.034859
	0.159838	100.6301	14764.98	22.54967	0.004461	2.999803
	0.120029	83.85847	12470.82	16.93352	0.004824	2.937607
	0.078379	62.89385	9353.117	11.05762	0.005600	2.845064
	11.3	0.068763	56.90396	8491.029	9.701051	0.006002
	19	0.066059	43.03263	6413.953	6.498024	0.007030
	22	0.030561	33.16221	4953.945	4.311575	0.007854
	27.7	0.018803	23.82981	3567.863	2.652721	0.009759
	39.4	0.008457	17.9326	2682.884	1.191104	0.007427
	47.1	0.006306	13.79836	2063.599	0.889645	0.009761
	59.8	0.004893	10.87796	1626.841	0.690413	0.011689
	93.9	0.003358	7.390315	1105.030	0.473836	0.017428
	123.3	0.002196	4.809401	720.8970	0.309862	0.026840
	120	0.001140	2.420914	362.8747	0.160966	0.055020
	180.3	0.000628	1.305616	196.1430	0.088710	0.104270

Tap DL= 122.2234

L	1//f	MDR	1//f	1//f	1//f/8lv	1//f/L
77.50234	26.37524	16.55921	1.409894	0.213660		
70.08444	25.54535	5.92287	1.373801	0.227189		
67.72357	25.26233	15.33704	1.344649	0.229418		
62.47176	24.59627	14.97175	1.311752	0.239634		
54.15415	23.41454	14.39752	1.284253	0.265750		
43.74662	21.65622	13.36262	1.229790	0.305455		
41.11505	21.14429	12.96742	1.198416	0.313934		
33.61162	19.48158	11.92659	1.140143	0.354835		
27.44113	17.90791	11.28311	1.111771	0.411175		
21.57322	15.82266	10.33449	1.057020	0.479135		
14.45160	12.51668	11.46289	1.266286	0.602879		
12.47915	11.30579	10.33522	1.156411	0.828199		
10.99338	10.25977	9.248990	1.057940	0.941322		
9.117643	8.716067	7.574790	0.895914	0.830781		
7.381524	6.973055	6.103828	0.730772	0.826906		
5.520214	4.270932	4.262924	0.556933	0.801249		
3.938529	1.831423	3.094891	0.431790	0.782321		

P1P11314

Tw	B(U)/D	Log	Log
dyne/cm2	(1/s)	Tw	B-U/D
1.193104	98.43489	0.076678	1.993149
0.689445	75.71328	-0.05078	1.879172
0.490413	59.68867	-0.16089	1.775891
0.473836	40.49776	-0.32437	1.607431
0.309862	24.58975	-0.50881	1.421435
0.160966	13.28384	-0.79326	1.123323
0.088710	7.164074	-1.05202	0.855160

Regression Output:
 Constant 1.08031
 Std Err of Y Est 0.002304
 R Squared 0.997946
 No. of Observations 5
 Degree of Freedom 4

X Coefficient(s) 0.967414
 Std Err of Coef. 0.003218

K' = 0.013172
 n = 0.967414

Tw = 1.179418
 Res/fg = 372.8035

Regression Output:
 Constant 22.0567
 Std Err of Y Est 0.144099
 R Squared 0.997080
 No. of Observations 8
 Degree of Freedom 6

X Coefficient(s) 12.42230
 Std Err of Coef. 0.423333

t = 21.18529 deg C
 s.d.t = 0.138916 deg C

P2P11327

4/13/89 15h16

1.0 PS10 Taps 14

5 = 10.05 B = 4.62 Z = 10.05 <C> (ppm)=20.58907 X coeff
4.72 [NaCl]= 0.001037 constant

WMD-40 Q1 (1/s)	WMD-40 Q1 (1/s)	Temp (deg C)	<U> (volts)	<U> (volts)	<U> (volts)	<U> (volts)	Batch Vol (gal)	density (g/cm3)	viscosity (cp)	DP (paie)	<U> (cm/s)	Re	Iw dyne/cm2	f	1000k(Re)1/4	Solvent
0.264	0.245	21.4	2.708164	-0.0065	2.713644			0.194180	158.7321	23817.46	27.39451	0.002178	0.046006	11.57710		
0.222	0.223	21.4	2.115	-0.0045	2.119			0.151627	133.5745	20044.30	21.39134	0.00403	0.077292	11.38696		
0.204	0.206	21.4	1.9232	-0.0035	1.9267			0.137867	123.3917	18516.26	19.45007	0.00519	0.077165	11.31303		
0.171	0.172	21.4	1.4985	-0.0035	1.502			0.107477	102.7266	15415.23	15.16271	0.007878	0.07562	11.12541		
0.146	0.148	21.4	1.1914	-0.0035	1.1949			0.085502	88.65038	13302.94	12.06257	0.007075	0.067872	10.94658		
0.129	0.13	21.4	1.0354	-0.0035	1.0391			0.074354	77.86857	11685.02	10.48973	0.007466	0.067556	10.87919		
0.108	0.109	21.4	0.7562	-0.0045	0.7607			0.054432	65.28980	9797.441	7.679380	0.007609	0.067498	10.57946		
0.096	0.098	21.4	4.14025	0.0825	4.05775			0.047929	58.70092	8808.708	6.761856	0.007971	0.071207	10.50165		
0.072	0.074	21.4	2.370833	0.0735	2.295833	1243		16.7	0.027118	44.58343	6690.26	0.007056	0.061874	10.06305		
0.039	0.04	21.4	1.189090	0.0745	1.111590	1188		29.9	0.013150	23.79929	3571.341	1.853761	0.006559	0.046107	9.506317	
0.037	0.038	21.4	1.716428	0.0785	1.637928	1218		21	0.019347	34.74136	5213.317	2.729452	0.004531	0.045311	9.804396	
0.029	0.03	21.4	0.9405	0.0785	0.8805	1075		35.2	0.010400	18.29299	2745.060	1.462769	0.008789	0.041043	9.527165	
0.021	0.022	21.4	0.71	0.0815	0.6385	1083		50	0.007423	12.97410	1946.904	1.047335	0.017466	0.077217	9.047995	
0.015	0.016	21.4	0.568066	0.0845	0.483066	949		60	0.005703	9.474010	1421.677	0.804904	0.017763	0.078068	8.865687	
		21.4	0.375153	0.0855	0.289653	845		90.1	0.003421	5.617600	862.9815	0.482680	0.070649	0.149094	0.477521	
		21.4	0.259375	0.0855	0.173875	448		89.8	0.002053	3.121680	468.4418	0.289746	0.059571	0.078110	0.080214	
		21.4	0.164666	0.0855	0.081166	268		119.9	0.000958	1.338857	200.9101	0.133356	0.15118	1.070771	7.474597	

ID(cm) = 1.45796
K(U/psi) = 13.975
XS(cm2) = 1.669479

Tap DL= 122.2234

L	MDR	1//f	1//f	1//f/81v	1//f/L
69.48423	25.47411	21.42524	1.850654	0.304346	
61.40072	24.43357	20.40316	1.791808	0.332295	
58.54840	24.06106	19.74598	1.747043	0.337400	
51.69433	23.03349	18.43748	1.675448	0.340532	
46.10773	22.08998	18.03242	1.647309	0.391095	
42.99685	21.51357	16.98528	1.567024	0.395035	
36.78872	20.22685	16.44477	1.570341	0.452442	
34.52132	19.70194	15.94794	1.518612	0.461973	
25.96659	17.35216	16.10296	1.400078	0.420141	
18.06829	14.55970	12.35341	1.299516	0.683717	
21.93270	15.95903	14.85400	1.515254	0.677344	
16.08086	13.39815	10.44897	1.143859	0.643457	
13.58618	12.00713	8.956270	0.987479	0.659219	
11.91100	10.92129	7.459897	0.841434	0.624303	
9.223259	8.811083	5.712335	0.674219	0.619340	
7.144005	6.705483	4.097060	0.507048	0.573335	
4.882403	3.562318	2.571864	0.343162	0.526762	

P2P11327

Tw	B(U)/D	Log	Log
dyne/cm2	(1/s)	Tw	B(U)/D
1.852361	130.5895	0.267725	2.115908
2.729452	190.6300	0.436075	2.280091
1.447249	100.3758	0.166510	2.001629
1.047335	71.19044	0.020085	1.852421
0.804984	51.98502	-0.09421	1.715878
0.482480	30.82444	-0.31634	1.488895
0.289746	17.12903	-0.53798	1.233732
0.135256	7.346475	-0.84884	0.866078

Regression Outputs
 Constant -1.66085
 Std Err of Y Est 0.007195
 R Squared 0.999719
 No. of Observations 6
 Degrees of Freedom 4

X Coefficient(s) 0.910001
 Std Err of Coef. 0.007622
 X' = 0.021834
 n' = 0.910001

Tw = 1.445860
 Res/fs = 272.5027

Regression Outputs
 Constant -38.8728
 Std Err of Y Est 0.246519
 R Squared 0.981003
 No. of Observations 6
 Degrees of Freedom 4

X Coefficient(s) 19.82792
 Std Err of Coef. 1.379400

t = 21.4 deg C
 s.d.t = 0.000000 deg C

P2P11229

4/15/89 13:08
 1.0 PSIB Taps 14 0.1 PSIB Taps 14
 S = 10.05 B = 10.05 <C>(ppm)=20.55048 X coeff
 Z = 6.62 Z = 4.84 [NaCl]= 0.010334 constant

density viscosity
 1.000493 1.002495
 -0.00025 -0.02281
 0.003619 -4.14933

0
 (t)amp DP (cm/s) Re Im f Log(Kc/f)1/f
 0.268220 159.9300 23880.00 37.83991 0.007961 5.117895 11.81747
 0.231592 145.5543 21733.49 32.67257 0.007089 5.082012 11.70456
 0.194227 124.5897 18603.15 27.40124 0.005535 5.041005 11.56971
 0.200894 128.1836 19139.78 28.34176 0.003454 5.051174 11.59529
 0.228128 141.3614 21107.42 32.18397 0.003225 5.070740 11.69290
 0.155858 104.8230 15651.69 21.98821 0.004469 5.096015 11.40014
 0.126001 89.24937 13326.29 17.77606 0.004469 5.094470 11.37667
 0.107219 79.06655 11807.84 15.12626 0.004845 5.091478 11.11258
 0.082754 65.88879 9838.205 11.67488 0.005209 5.085047 10.91250

MHD-60 MHD-60
 (l/s) (l/s) Temp (deg C) <V> <V> <V> <V> Batch Vol
 (l/s) (l/s) (l/s) (volts) (volts) (volts) (volts) (ml)
 0.266 0.267 21.2 3.742375 -0.0075 3.748375
 0.242 0.243 21.2 3.233 -0.0045 3.2365
 0.207 0.208 21.2 2.711333 -0.0025 2.714333
 0.213 0.214 21.2 2.804 -0.0035 2.8075
 0.235 0.236 21.2 3.1844 -0.0035 3.1881
 0.174 0.175 21.2 2.174125 -0.0035 2.178125
 0.148 0.149 21.2 1.755875 -0.0045 1.760875
 0.131 0.132 21.2 1.491888 -0.0055 1.498388
 0.109 0.11 21.2 1.149 -0.0075 1.1565

11.7 0.073740 58.70092 8764.946 10.40309 0.006046 5.813301 10.87484
 15 0.048811 44.64465 6666.129 6.886253 0.006919 5.747912 10.50769
 21.1 0.034402 34.74704 5188.265 4.853405 0.008050 5.667944 10.21076
 29.8 0.02072 24.18064 3610.543 2.831722 0.009699 5.560946 9.894574
 39.9 0.009653 18.29994 2732.461 1.761953 0.008145 5.52001 9.76192
 49.8 0.006785 14.01249 2092.279 0.957349 0.009745 5.51456 9.990260
 60.3 0.004171 9.526210 1422.409 0.388518 0.010988 5.499800 9.616941
 80.2 0.003114 6.960820 1039.357 0.439471 0.018163 5.146766 8.792981
 89.8 0.002194 5.062725 755.9423 0.209448 0.034195 5.07055 8.13710
 120 0.001173 2.645335 395.0188 0.165527 0.047367 4.97458 7.641874
 180.1 0.000525 1.160728 173.145 0.074155 0.110233 4.759971 7.024614
 90 0.001689 3.853496 575.3059 0.238771 0.092149 5.01348 7.922206

1168
 1118
 1224
 1203
 1219
 1165
 939
 932
 759
 530
 349
 579
 1.188 6.242833
 -0.0065 4.1324
 -0.0275 2.9125
 -0.0295 1.6993
 -0.0295 0.8173
 -0.0285 0.5745
 -0.0285 0.533166
 -0.0285 0.2637
 -0.0285 0.185818
 -0.0275 0.099333
 -0.0295 0.0445
 -0.0315 0.143045
 -0.0335

Tap DL= 122.2256

P2P11229

L	MDR	1//6	1//4	1//6/8lv	1//6/L
81.24110	26.76402	18.37124	1.554588	0.226132	
75.49046	26.15822	17.99357	1.537311	0.238355	
69.13307	25.43231	16.81824	1.433493	0.243273	
70.30952	25.57154	17.01385	1.467311	0.241985	
74.92388	26.09606	17.60738	1.505807	0.235003	
61.92923	24.52429	15.79594	1.385392	0.255044	
55.68248	23.64693	14.95791	1.331148	0.268628	
51.34491	22.98094	14.36516	1.292692	0.279468	
45.17602	21.91239	13.62601	1.248346	0.301954	
42.59728	21.43653	12.64018	1.188025	0.301901	
34.65710	19.73433	12.02157	1.144073	0.346872	
29.09338	18.29093	11.14493	1.088505	0.383048	
22.27419	16.06797	10.15375	1.035503	0.434878	
15.41281	13.04803	11.06031	1.196328	0.718903	
12.92218	11.59366	10.11960	1.125531	0.783118	
10.13166	9.586217	8.774524	1.018287	0.846049	
8.754798	6.380956	7.419909	0.884124	0.847524	
7.349117	6.936748	6.428652	0.791408	0.874778	
5.373269	4.352812	4.594722	0.601255	0.855107	
3.596425	1.039830	3.011922	0.428767	0.837474	
6.448045	5.857413	5.577135	0.703987	0.864934	

Tw	8(U)/D	Log Tw	Log 8(U)/D
0.588518	52.27145	-0.23023	1.718264
0.439431	58.19485	-0.35710	1.582004
0.309648	27.77977	-0.50913	1.443728
0.165529	14.51636	-0.78132	1.161857
0.074155	6.369054	-1.12985	0.804074
0.238371	21.14459	-0.62274	1.325199

Regression Output:
 Constant -1.91025
 Std Err of Y Est 0.001014
 R Squared 0.999990
 No. of Observations 4
 Degrees of Freedom 3

X Coefficient(s) 0.971126
 Std Err of Coef. 0.002106

K' = 0.012295
 n' = 0.971126

Tw = 5.716257
 Res/ft = 506.9800

Regression Output:
 Constant -42.0941
 Std Err of Y Est 0.186487
 R Squared 0.991604
 No. of Observations 10
 Degrees of Freedom 8

X Coefficient(s) 19.39527
 Std Err of Coef. 0.630976

t = 21.2 deg C
 s.d.t = ERK deg C

PIP01106	3/2/89	16554	1.0 P81D Taps 14		0.1 P81D Taps 14	10.05 <C>(ppm)=1.031289 X coeff	col/NaCl		
B =	10.05	8 =	4.9	Z =	4.9	Z =	4.92 E[NaCl] = 0.105538 constant		
PHD-40	PHD-40	Temp	<V>	<V>	<V>	<V>	corr	Batch	Vol
(1/s)	(1/s)	(deg C)	(volts)	(volts)	(volts)	(volts)	(volts)	(ml)	(ml)
0.178	0.18	21.1	4.640888	-0.027	4.097388	0.0295	6.166	1154	
0.16	0.161	21	3.447833	-0.0365	3.484333	0.1425	3.929571	1095	
0.134	0.159	21	3.221111	-0.0365	3.258111	0.1455	2.6358	1123	
0.14	0.142	21	2.6749	-0.0375	2.7129	0.1445	1.914875	1102	
0.124	0.125	21	2.153555	-0.0385	2.192055	0.1395	0.9525	1251	
0.096	0.098	21	1.398	-0.0395	1.437	0.1375	0.428576	1184	
0.113	0.114	21	1.841444	-0.0395	1.880944	0.1355	0.315166	1119	
						0.1305	0.2185	1158	
0.087	0.088	21.15	6.3085	0.0295	6.166	0.1275	0.115333	1041	
0.067	0.068	21.15	4.673571	0.1425	3.929571	0.1255	0.154428	1038	
0.053	0.054	21.2	2.7808	0.1455	2.6358	0.1255	0.154428	1038	
0.037	0.038	21.2	1.534875	0.1445	1.914875	0.1165	0.0771	554	
0.03	0.031	21.2	1.991	0.1395	0.9525	0.1165	0.0771	234	
0.022	0.023	21.2	0.544076	0.1375	0.428576	0.1315	0.016428	288	
0.018	0.018	21.3	0.450666	0.1355	0.315166	0.1315	0.016428	288	
0.012	0.013	21.3	0.369	0.1305	0.2185	0.1315	0.016428	288	
		21.35	0.241833	0.1275	0.115333	0.1315	0.016428	288	
		21.35	0.275428	0.1255	0.154428	0.1315	0.016428	288	
		21.45	0.1936	0.1165	0.0771	0.1315	0.016428	288	
		21.5	0.170277	0.1145	0.047277	0.1315	0.016428	288	
		21.5	0.155428	0.1315	0.016428	0.1315	0.016428	288	

density	viscosity	ID(cm)	K(V/psi)	X5(cm2)	7.56	
1.00417	1.010849	1.45796	14.29	1.669479	7.56	
-0.00025	-0.02281					
0.003419	-4.14933					
t)amp	DP	<U>	Re	lw	f	Log(ku/1)1/1/f
(sec)	(psid)	(cm/s)		dyne/cm2		
0.286731	107.8180	15986.08	40.45142	0.00694	3.124586	11.85528
0.243830	94.43724	14268.22	34.39904	0.007780	3.088407	11.72720
0.227999	94.64077	14002.36	32.18566	0.007165	3.073870	11.67540
0.189846	85.05644	12584.40	26.78307	0.007386	3.04064	11.53483
0.153397	74.87343	11077.81	21.64104	0.007703	2.987773	11.37094
0.100559	58.70092	8685.009	14.18674	0.008215	2.896076	11.04623
0.131626	68.28475	10102.96	18.56960	0.007946	2.954535	11.25330
15.1	0.083822	52.85735	7846.941	11.82553	0.008441	2.858022
16.2	0.053419	40.48722	6010.532	7.516313	0.009174	2.760197
20.8	0.035831	32.33965	4806.402	5.055098	0.009484	2.673969
29	0.019234	22.74158	3382.885	2.713534	0.010451	2.528072
40	0.012948	18.43388	2739.492	1.826762	0.010717	2.452945
50.2	0.009826	14.12755	2099.673	0.821951	0.008217	2.279527
60.1	0.004284	11.15255	1661.265	0.604445	0.009697	2.217288
89.8	0.002970	7.724157	1150.577	0.419052	0.014015	2.140794
130.1	0.001567	4.15214	619.5030	0.221127	0.025277	1.997948
133.1	0.002099	5.497353	819.8004	0.296172	0.019556	2.039354
120.6	0.001048	2.751575	411.2591	0.147467	0.028974	1.909502
89.8	0.000642	1.560840	233.5514	0.090672	0.074742	1.107997
250.1	0.000223	0.689759	103.2100	0.031507	0.122158	1.574268

Tap DL= 122.2234

L	1/f	H/R	1/f	1/f	1/f	1/f	1/f
83.	26375	24.	94714	12.	00079	1.	012274
74.	61035	26.	27974	11.	64025	0.	992585
74.	08165	26.	00278	11.	81328	1.	011792
67.	59964	25.	24722	11.	63596	1.	008497
60.	76498	24.	36749	11.	39612	1.	002636
49.	19897	22.	62544	11.	03301	0.	998792
34.	28797	23.	73617	11.	21794	0.	994858
45.	07154	21.	90242	10.	88122	0.	997212
33.	98100	20.	04347	10.	44046	0.	988181
29.	50186	18.	40542	10.	18241	0.	992429
21.	41485	15.	83857	9.	78175	0.	999785
17.	73477	14.	20596	9.	655083	1.	018718
11.	89618	10.	91102	11.	03123	1.	244530
10.	22465	9.	641603	10.	15477	1.	176549
8.	51422	8.	150259	8.	446787	1.	011664
7.	145308	4.	72742	7.	156777	0.	884519
5.	074385	3.	880565	5.	045381	0.	670566
3.	978115	1.	872150	3.	669316	0.	311049
2.	345032	-2.	48887	2.	750742	0.	432823

P1P01104

Ta	B(U)/B	Log	Log
dyno/cm2	(1/s)	Tw	B(U)/D
0.	604445	61.	19541
0.	419052	42.	38337
0.	221193	22.	79467
0.	296172	30.	16463
0.	147867	15.	09821

Regression Output:
 Constant -2.02285
 Std Err of Y Est 0.002660
 R Squared 0.999905
 No. of Observations 5
 Degrees of Freedom 3

X Coefficient(s) 1.009946
 Std Err of Coef. 0.005657

K' = 0.009487
 n' = 1.009946

Tw = 23.50472
 Res/fs = 1013.238

Regression Output:
 Constant -0.40152
 Std Err of Y Est 0.044246
 R Squared 0.994949
 No. of Observations 9
 Degrees of Freedom 7

X Coefficient(s) 3.937832
 Std Err of Coef. 0.106041

t = 21.1975 deg C
 s.d.t = 0.167686 deg C

P2701107

3/4/89 15h50
 1.0 P919 Taps 14 0.1 P919 Taps 14 col)NaCl
 S = 10.05 B = 10.05 <C>(ppm)=2.065943 K coeff
 Z = 4.86 Z = 4.92 [NaCl]= 0.104712 constant

MHD-40 01 (1/s)	MHD-40 01 (1/s)	Temp (deg C)	<U> (volts)	<U> (volts)	<U> (volts)	<U>corr (volts)	Batch Vol (ml)
0.185	0.186	21	4.3316	-0.0015	4.3241		
0.171	0.172	20.9	3.8025	0.0165	3.786		
0.161	0.162	20.9	3.484714	0.0165	3.464714		
0.144	0.145	20.9	2.875625	0.0235	2.852125		
0.127	0.128	20.9	2.393	0.0235	2.2795		
0.115	0.116	20.9	1.94375	0.0235	1.9225		
0.098	0.099	20.9	1.5051	0.0235	1.4811		
0.088	0.09	21.1	4.4435	0.0495	4.394		1192
0.068	0.069	21.1	4.138428	0.0365	4.100428		1257
0.054	0.055	21.1	2.73325	0.0395	2.68375		1204
0.037	0.038	21.15	1.454664	0.0395	1.414664		1144
0.029	0.03	21.2	0.949090	0.0405	0.927590		1209
0.023	0.024	21.2	0.4817	0.0425	0.4392		1102
0.017	0.018	21.2	0.361	0.0445	0.3165		1077
0.012	0.013	21.3	0.2754	0.0445	0.2309		1084
		21.35	0.212333	0.0445	0.167333		1184
		21.4	0.16115	0.0455	0.11665		832
		21.4	0.10025	0.0435	0.05625		1100
				0.0445			

density viscosity
 1.00417 1.010869 ID(cm) = 1.45796
 -0.00025 -0.02281 K(U/psl) = 14.29
 0.003419 -4.14933 XB(cm2) = 1.469474 7.556
 3.579999
 0.79424
 Solvent

t)saap (sec)	DP (psid)	<U> (cm/s)	Re	Iw dyne/cm2	I	Lou(kc/f)l/l/f			
0.302576	111.4119	16483.79	42.48963	0.006861	3.133795	11.87119			
0.244940	103.0261	15208.72	37.37724	0.007076	3.105452	11.78754			
0.242457	97.03622	14324.49	34.20535	0.007548	3.086176	11.71937			
0.199588	86.85341	12821.31	28.15757	0.007447	3.045946	11.56981			
0.159517	76.67060	11318.12	22.50434	0.007638	2.995282	11.39754			
0.135916	69.48273	10257.04	19.17484	0.007974	2.940514	11.27446			
0.103643	59.29991	8753.860	14.62214	0.008296	2.701654	11.06610			
13.3	0.086922	53.68383	7940.651	12.26280	0.004470	2.865414	10.97181		
18.1	0.053742	41.59830	6168.515	7.864053	0.009068	2.768942	10.59670		
22.1	0.036483	32.68691	4867.066	5.147060	0.009612	2.676892	10.27046		
30.2	0.019231	22.72985	3374.360	2.713134	0.010478	2.538347	7.779976		
39.8	0.012609	18.19542	2704.250	1.778990	0.010727	2.447191	9.457303		
45.7	0.005957	14.44389	2146.689	0.840406	0.008073	2.284349	8.480842		
		60	0.004302	10.75185	1597.968	0.607007	0.010477	2.213700	8.630744
		80.7	0.003138	8.045900	1198.503	0.442834	0.017650	2.146210	8.791870
		119.9	0.002274	5.924946	883.5658	0.320927	0.010241	2.076782	8.146055
		120	0.001585	4.152990	620.0195	0.223718	0.035084	1.978926	7.870444
		329.8	0.000764	1.997841	298.2670	0.107879	0.053976	1.840544	7.309775

Tap DL= 122.2234

L 1//f	MDR 1//f	1//f	1//f/81v	1//f/L
85.34449	27.17061	12.07151	1.014993	0.141444
79.67695	26.60360	11.92999	1.012064	0.149729
76.22126	26.23772	11.74501	1.002256	0.154101
69.15349	25.43498	11.50739	1.001519	0.167535
61.02473	24.51036	11.44174	1.003027	0.185067
57.04830	23.84978	11.23330	0.996348	0.194839
49.83501	22.73143	10.97853	0.992008	0.220297
45.84525	22.04287	10.85261	0.992210	0.236722
38.71324	20.20991	10.50117	0.991022	0.284032
29.70155	18.46108	10.19952	0.993092	0.343400
21.58876	15.82840	9.76858	0.998841	0.452497
17.50134	14.09643	9.457294	1.021146	0.551802
12.62899	11.00263	11.15371	1.255930	0.927235
10.22304	9.660302	9.749403	1.151930	0.955625
8.751660	8.377978	8.559114	1.019934	0.977998
7.458485	7.058643	7.403832	0.906895	0.992443
6.234563	5.579594	6.215546	0.789732	0.994949
4.329372	2.570353	4.305844	0.589033	0.994570

P2P01109

dyne/cm2	B(U)/D (1/s)	Log 1e	Log 1e	Log 8 U/D
0.840406	79.25536	-0.07551	1.899023	
0.607003	58.99670	-0.21680	1.770827	
0.442334	44.14881	-0.35375	1.644919	
0.320922	32.51088	-0.49360	1.512028	
0.223718	22.78795	-0.65029	1.357705	
0.107879	10.96239	-0.96706	1.039905	

Regression Outputs
 Constant -2.00936
 Std Err of Y Est 0.001551
 R Squared 0.999979
 No. of Observations 7
 Degrees of Freedom 1

X Coefficient(s) 1.001919
 Std Err of Coef. 0.004556

K' = 0.009786
 n' = 1.001919

Twe = 17.26820
 Res/fg = 868.4781

Regression Outputs
 Constant -0.78062
 Std Err of Y Est 0.058708
 R Squared 0.992964
 No. of Observations 9
 Degrees of Freedom 7

X Coefficient(s) 4.078619
 Std Err of Coef. 0.129764

t = 21.10555 deg C
 s.d.t = 0.177081 deg C

3/7/69 14350
 1.0 P01D Taps 14 0.1 P01D Taps 14
 S = 10.95 S = 10.05 <C>(ppa)=5.158589 X coeff
 Z = 4.93 Z = 4.95 [NaCl]= 0.165423 constant

MWD-40 D11 (1/s)	MWD-60 D11 (1/s)	Temp (deg C)	<V> (volts)	<V> (volts)	<U>corr (volts)	Batch Vol (ml)
0.205	0.206	19.9	4.6154	-0.0755	4.6909	1152
0.188	0.188	19.9	4.642833	-0.0755	4.119333	1121
0.174	0.175	19.9	3.625833	-0.0775	3.704333	1168
0.152	0.153	19.9	2.8355	-0.0835	2.919	1132
0.132	0.133	19.9	2.3188	-0.0835	2.4023	1196
0.111	0.112	19.9	1.712428	-0.087	1.798178	1150
0.088	0.089	19.9	1.133166	-0.0845	1.217166	1133
				-0.0833		1196
0.09	0.091	20.05	4.707	0.0555	4.6575	838
0.068	0.069	20.05	4.135466	0.0435	4.112144	567
0.054	0.055	20.05	2.736833	0.0435	2.693833	794
0.037	0.038	20.1	1.446	0.0425	1.4025	
0.029	0.03	20.15	0.917353	0.0445	0.872055	
0.022	0.023	20.15	0.466181	0.0445	0.419431	
0.013	0.014	20.2	0.296415	0.0445	0.250115	
		20.2	0.22	0.0465	0.17225	
		20.15	0.170181	0.049	0.121181	
		20.2	0.112	0.0465	0.0635	
		20.25	0.078555	0.043	0.035555	
				0.044		

density	viscosity	ID(cm)	K(V/psi)	KB(cm2)	73.95	3.539999	-0.79424	Solvent
1.00417	1.010869	1.45796	14.24	1.669479				
-0.00025	-0.02281							
0.003419	-4.14933							
t)amp (sec)	DP (psid)	<U> (cm/s)	Re	fw dyne/cm2	f	Loa(f/r)1/f		
0.329417	123.3917	17808.77	46.47347	0.006088	1.142899	11.72010		
0.289279	112.6099	14252.66	40.81087	0.006419	1.114685	11.87022		
0.260276	104.8230	13128.81	36.71921	0.006666	1.091742	11.73701		
0.204985	91.04633	13140.45	28.91898	0.006979	1.039888	11.55545		
0.168700	79.66554	11497.89	23.79995	0.007480	1.097505	11.40569		
0.126276	67.08677	9682.439	17.81483	0.007895	1.074687	11.18304		
0.082475	53.31002	7694.081	12.05865	0.008464	1.0849946	10.88305		
12.6	0.090027	54.74471	7930.824	12.70082	0.008447	10.97817		
16.1	0.0558607	41.70400	6039.710	7.844972	0.008997	10.55781		
21.3	0.034427	32.84597	4756.432	5.139152	0.007802	10.27266		
29.8	0.018945	22.73554	3298.802	2.675614	0.010709	9.732672		
40	0.011792	17.90977	2599.485	1.663661	0.010746	9.369161		
50	0.005675	13.77674	1999.604	0.800466	0.008415	8.265400		
79.9	0.003382	8.493800	1254.207	0.477156	0.011194	7.151581		
120.3	0.002329	5.955036	865.309	0.278409	0.018485	6.070592		
150	0.001638	4.182940	607.1261	0.171194	0.026258	5.097739		
389.9	0.000480	1.219793	177.4447	0.067830	0.048626	1.060633		
						1.728459		
						6.912992		

Tap DL= 122.2234

L 1//4	MDR 1//4	1//4	1//4/81v	1//4/L
84.85197	27.31509	12.81544	1.075112	0.147555
81.36887	28.77901	12.48871	1.055877	0.133346
77.20116	26.34313	12.24788	1.043348	0.158648
68.51231	25.35788	11.90730	1.037372	0.174945
62.15344	24.55911	11.56200	1.031704	0.186023
53.77346	23.35907	11.23373	1.026321	0.209280
44.24117	21.74898	10.84951	0.998753	0.245487
45.55865	21.99112	10.87994	0.995588	0.238812
35.80557	20.00334	10.54254	0.998553	0.294438
28.98015	18.25819	10.25838	1.002513	0.353979
20.92434	15.57440	9.84859	1.011917	0.470454
16.52618	13.62355	9.830934	1.049286	0.594870
11.44464	10.60413	10.90092	1.237741	0.950830
8.86603	8.40082	8.705744	1.035041	0.982522
7.353137	6.941281	7.354936	0.985318	1.000244
6.160546	5.481044	6.159418	0.784431	0.999817
4.534336	2.952040	4.534842	0.614605	1.000116
3.544563	0.440728	3.515918	0.479644	0.991435

PSP01112

Tw dyne/cm2	B(U)/D (1/s)	Log Tw	Log B(U)/D
1.463661	98.27305	0.221064	1.992434
0.800446	75.59465	-0.09655	1.878491
0.477156	46.60649	-0.32133	1.668446
0.328409	32.67599	-0.48332	1.514228
0.231184	22.95229	-0.63404	1.340826
0.124957	12.42381	-0.90323	1.094255
0.047830	6.693149	-1.16857	0.825630

Regression Output:
 Constant -1.99914
 Std Err of Y Est 0.003633
 R Squared 0.999913
 No. of Observations 5
 Degrees of Freedom 3

X Coefficient(s) 1.003071
 Std Err of Coef. 0.005401

K' = 0.010019
 n' = 1.003071

Tw = 20.05719
 Res/fg = 912.9188

Regression Output:
 Constant -12.6390
 Std Err of Y Est 0.079370
 R Squared 0.979241
 No. of Observations 5
 Degrees of Freedom 3

X Coefficient(s) B.077606
 Std Err of Coef. 0.679013

t = 20.04722 deg C
 s.d.t = 0.128530 deg C

PIP11115 3/9/89 14:08
 1.0 PSID Temp 14 0.1 PSID Temp 14
 S = 10.05 B = 10.05 C = 10.31423 X coeff
 Z = 4.82 Z = 4.9 [NaCl] = 0.105428 constant

MHD-40 011 (1/s)	MHD-40 01a (1/s)	Temp (deg C)	<V> (volts)	<V> (volts)	<V> (volts)	<V>corr (volts)	Batch Vol (ml)
0.216	0.217	20.85	4.44375	0.0045	0.0045	4.416	1319
0.198	0.199	20.7	4.188285	0.051	4.138535		1304
0.18	0.181	20.7	3.578285	0.0485	3.529285		1374
0.162	0.163	20.7	3.150571	0.0695	3.081571		1307
0.135	0.136	20.7	2.416222	0.0485	2.367222		1170
0.112	0.113	20.7	1.839428	0.0475	1.791428		1245
0.092	0.093	20.85	6.021644	0.1935	6.707164		1144
0.069	0.071	20.9	4.297833	0.0355	4.253833		1129
0.054	0.055	20.9	2.86025	0.0525	2.74325		674
0.037	0.038	20.9	1.492333	0.0615	1.430833		464
0.028	0.029	20.9	0.839666	0.0615	0.778166		746
0.02	0.021	20.95	0.458722	0.0615	0.377222		
0.014	0.015	21	0.320727	0.0615	0.259227		
		21	0.2282	0.0615	0.1667		
		21.05	0.159375	0.0605	0.098875		
		21.05	0.1035	0.0595	0.044		
		21.1	0.007164	0.0575	0.029666		

Cyanamid 876

density 1.00417 1.010869
 viscosity 1.00025 -0.02281
 K(V/psi)^{1/2} 14.24
 XS(cm²) = 1.669479
 75.75
 3.539999
 -0.79424
 Solvent

t)amp (sec)	DP (psid)	<U> (cm/s)	Re	Tw dyne/cm ²	Luq(kc/f)1/1/1
0.324157	129.9806	19166.12	45.73142	0.005400	3.148763
0.290427	119.1988	17516.92	41.00111	0.005757	3.12576
0.247843	108.4170	15932.48	34.96517	0.005757	3.040996
0.216402	97.63521	14348.03	30.52960	0.006389	3.039539
0.166307	81.46251	11971.36	23.46234	0.007034	3.007361
0.125872	67.68576	9946.798	17.75786	0.007753	2.941074
14.2	0.090698	55.70598	8214.052	12.79557	0.008202
18.5	0.057523	42.22063	6232.614	8.115277	0.009087
25	0.037096	32.92043	4859.719	5.233426	0.009635
34.3	0.019348	22.82445	3369.348	2.729667	0.010454
40	0.010522	17.52043	2586.367	1.484544	0.009649
59.9	0.005101	12.44977	1839.911	0.719644	0.009264
79.9	0.003505	8.741192	1293.290	0.494540	0.012914
119.9	0.002254	5.640189	874.4858	0.318021	0.01994
119.7	0.001337	3.377119	500.2206	0.180628	0.037001
180.1	0.000594	1.543203	228.5800	0.083940	0.070331
419.9	0.000401	1.064172	157.8026	0.056576	0.099733

Tap BL= 122.2234

L	1//f	nDR	1//f	1//f	1//f/81v	1//f/L
68.03266	27.42651	13.60725	1.159552	0.154570		
83.07235	26.94795	13.17887	1.111989	0.158444		
76.71434	26.29693	12.98036	1.106462	0.167203		
71.68351	25.73124	12.50988	1.076117	0.174315		
62.84118	24.64972	11.90437	1.042356	0.189467		
54.67063	23.49560	11.37127	1.014524	0.207996		
46.56573	22.17154	11.02480	1.005749	0.236758		
37.12613	20.30219	10.49228	0.988580	0.282412		
29.81415	18.49230	10.18753	0.991363	0.341701		
21.53198	15.80487	9.780649	1.000421	0.454211		
15.87909	13.29394	10.17992	1.093703	0.441089		
11.06929	10.51581	10.38953	1.186985	0.938475		
9.185758	8.777644	8.799560	1.039568	0.937954		
7.366182	6.955886	7.080379	0.871239	0.961200		
5.679505	4.810179	5.504667	0.712385	0.969216		
3.788729	1.449658	3.770724	0.530736	0.995247		
3.114542	-0.14722	3.166649	0.665450	1.016734		

PIP11115

Tw	B(U)/D	Log	Log
dyne/cm ²	(1/s)	Tw	8:U/D
1.484544	96.17248	0.171597	1.982884
0.719444	48.31338	-0.14288	1.834505
0.494560	47.96394	-0.30579	1.680915
0.318021	30.94838	-0.49734	1.490638
0.188428	18.53065	-0.72439	1.267890
0.083940	8.467740	-1.07402	0.927767
0.056596	5.839238	-1.24721	0.766356

Regression Outputs
 Constant 2.03261
 Std Err of Y Est 0.003459
 R Squared 0.999941
 No. of Observations 5
 Degrees of Freedom 3

X Coefficient(s) 1.029106
 Std Err of Coef. 0.004546

K' = 0.009276
 n' = 1.029106

Tw = 16.47566
 Res/fs = 845.4306

Regression Outputs
 Constant -20.2790
 Std Err of Y Est 0.088272
 R Squared 0.991077
 No. of Observations 6
 Degrees of Freedom 4

X Coefficient(s) 10.73637
 Std Err of Coef. 0.509361

t = 20.87941 deg C
 s.d.t = 0.134009 deg C

Page 1

Cyanamid 836

P2P11129 4/13/89 17:08
 1.0 P819 Taps 14 0.1 P819 Taps 14
 S = 10.05 B a 10.05 <C>(ppm)=20.58707 X coeff
 Z = 4.62 Z = 4.75 [NaCl]= 0.105631 constant
 col/NaCl
 MHD-40 MHD-40
 Q1 Q1h Temp C <U> <U> <U>corr Batch Vol
 (1/s) (1/s) (deg C) (volts) (volts) (volts) (ml)
 0.252 0.253 20.9 4.5495 -0.0015 4.549 1180
 0.216 0.217 20.9 3.44333 0.0025 3.44333 1154
 0.199 0.2 20.9 3.3735 0.0035 3.3695 1177
 0.169 0.17 20.9 2.44733 0.0045 2.44233 1205
 0.144 0.145 20.9 2.2755 0.0055 2.27 1200
 0.129 0.129 20.9 1.922857 0.0055 1.916357 922
 0.107 0.108 20.9 1.454164 0.0075 1.449664 827
 0.095 0.096 20.95 7.628 0.0395 7.5885 540
 0.071 0.072 21 4.9098 0.0295 4.8753 413
 0.038 0.039 21 1.721285 0.0395 1.68285 330
 0.053 0.054 21 3.2348 0.0325 3.2018 1020
 0.029 0.03 21 0.902543 0.0335 0.867583 932
 0.022 0.023 21 0.52 0.0365 0.4795
 0.013 0.014 21 0.3244 0.0405 0.2824
 21 0.2332 0.0435 0.1897
 21 0.138833 0.0445 0.094333
 21 0.089464 0.0465 0.046164
 0.055 0.056 21 3.180571 0.0455 3.138071
 0.083 0.084 21 6.2624 0.0395 6.2234
 0.101 0.102 21 8.0225 0.0385 7.984

Page 2

Cyanamid 836

density viscosity ID(cm) = 1.45796
 1.00417 1.010869 K(V/psi)= 13.975 84.66
 -0.00025 -0.02281 XS(cm2)= 1.669479
 0.003419 -4.14933
 0.325509 151.5442 22421.50 45.92223 0.003989 3.151145 11.94970
 0.260703 129.9806 19187.75 36.77951 0.00443 3.101952 11.77515
 0.241109 119.7978 17684.56 34.01516 0.004759 3.084985 11.71509
 0.189075 101.8281 15051.88 26.47440 0.005133 3.073196 11.52832
 0.162332 86.85341 12821.31 22.91569 0.006061 3.999715 11.41146
 0.137127 77.26959 11406.54 19.34566 0.006465 3.967440 11.28128
 0.103752 64.69081 9549.666 14.63441 0.006977 3.901876 11.06674
 12.3 0.089635 57.46399 8492.415 12.64551 0.007641 2.870409 10.95670
 15.9 0.057586 43.47379 6432.101 8.124226 0.008577 2.775025 10.61783
 29.9 0.019906 23.57895 3488.586 2.808369 0.010079 2.544361 9.801284
 21.3 0.037819 33.88647 5013.622 5.335426 0.00971 2.683731 10.39463
 40.2 0.010247 17.88027 2645.449 1.445745 0.009023 2.400180 9.290883
 39.9 0.005663 15.84130 2047.569 0.799041 0.008733 2.371418 9.15068
 60 0.003335 8.256064 1221.514 0.470597 0.01377 2.156456 8.420103
 59.9 0.002240 5.595897 828.5245 0.316117 0.020114 2.070058 8.122352
 89.8 0.001114 2.754816 407.5847 0.157197 0.041331 1.918757 7.585770
 149.9 0.000521 1.318455 195.0996 0.075599 0.084456 1.757571 7.001890
 18.3 0.037046 33.38657 4939.617 5.229299 0.009361 2.679756 10.77916
 11.1 0.073310 51.37275 7600.780 10.37070 0.007840 2.828078 10.80550
 0.094306 61.09688 9039.499 13.30450 0.007111 2.882174 10.99700

Tap DL= 122.2236

L	1//4	1//8	1//4	1//6/8lv	1//4/L
68.51682	27.47177	15.83138	1.324879	0.176851	
79.03750	24.53708	15.17302	1.206562	0.191972	
74.00904	24.21472	14.54149	1.241241	0.191312	
67.50951	25.21173	13.95779	1.210780	0.207367	
62.58721	24.58509	12.84449	1.125577	0.205083	
57.32193	23.80437	12.43483	1.102439	0.214944	
49.85391	22.73489	11.97158	1.081741	0.240123	
46.39700	22.14158	11.43987	1.044145	0.246564	
37.23105	20.32548	10.79740	1.016931	0.290014	
21.88977	15.94284	9.940459	1.014240	0.432037	
30.17183	18.59071	10.58556	1.008833	0.344213	
15.70580	13.20342	10.52735	1.133084	0.470284	
11.67413	10.75493	10.94183	1.240718	0.938624	
8.960397	8.572482	0.520037	1.010708	0.950833	
7.344074	6.931167	7.050941	0.868101	0.940083	
5.178894	4.043784	4.918817	0.448473	0.949781	
3.543659	0.917866	3.440999	0.491438	0.971030	
29.87005	18.50774	10.33543	1.005493	0.346020	
42.04474	21.33273	11.29327	1.045140	0.268473	
47.44473	22.36056	11.85794	1.078289	0.248882	

P2P11128

Tm	8<U>/D	1op	Log
dynes/cm2	(1/s)	Tm	8<U>/D
0.799041	75.94884	-0.09743	1.880521
0.470592	45.30201	-0.32735	1.656117
0.316117	30.72730	-0.50015	1.487524
0.157197	15.11400	-0.80355	1.179436
0.073599	7.255617	-1.13312	0.859475

Regression Outputs
 Constant -1.99759
 Std Err of Y Est 0.004104
 R Squared 0.999910
 No. of Observations 4
 Degrees of Freedom 2

X Coefficient(s) 1.008417
 Std Err of Coef. 0.006742

R² = 0.010055
 R = 1.008417

Tms = 13.68447
 Res/ls = 773.1224

Regression Outputs
 Constant -42.7827
 Std Err of Y Est 0.214078
 R Squared 0.978930
 No. of Observations 6
 Degrees of Freedom 4

X Coefficient(s) 18.62769
 Std Err of Coef. 1.366414

t = 20.9675 deg C
 s.d.t = 0.045483 deg C

4/15/89 15:52
 F2F11130 1.0 P819 Tape 14 0.1 P819 Tape 14
 S = 10.05 S = 10.03 <C> (ppm) = 20.55048 X coeff
 Z = 4.55 Z = 4.82 [NaCl] = 0.10479 constant
 (c) NaCl

RWD-60 (l/s)	Q1 (l/s)	Q2h (l/s)	Temp (deg C)	<U> (volts)	<U> (volts)	<U> (volts)	<U> (volts)	Batch (gal)	Vol (ml)
0.254	0.257	21	4.216285	-0.0245	4.227285				
0.232	0.233	21	3.808164	0.0025	3.812664				
0.2	0.202	21	3.1469	-0.0115	3.1755				
0.17	0.171	20.95	2.544833	-0.0185	2.553333				
0.145	0.146	20.95	2.087428	-0.0255	2.113928				
0.129	0.13	21	1.780675	-0.0275	1.808375				
0.109	0.11	21	1.430285	-0.0275	1.458285				
0.094	0.098	21	7.330164	-0.0165	7.344664			3108	
0.071	0.072	21	4.734	-0.039	4.77725			1184	
0.054	0.057	21	3.209125	-0.0435	3.251625			1214	
0.039	0.04	21	1.4558	-0.0415	1.4973			1275	
0.03	0.031	21	0.9702	-0.0415	1.0107			1242	
0.024	0.025	21	0.515434	-0.0395	0.554634			1124	
0.015	0.016	21	0.294437	-0.0385	0.332437			1135	
		21.05	0.194117	-0.0375	0.231617			790	
		21.05	0.13125	-0.0365	0.16775			489	
		21.1	0.0604	-0.0345	0.0949			404	
		21.1	0.017125	-0.0375	0.055125			830	
		21.1	7.2354	-0.0395	7.2759				
		21.1	8.1825	-0.0425	8.21225				
		21	4.71875	-0.0435	4.75875				
		21	2.3492	-0.0445	2.3942				
		21	0.728714	-0.0455	0.774214				
		21	0.381444	-0.0455	0.426944				
		21		-0.0455	-0.0455				

density viscosity
 1.00417 1.010849
 -0.00025 -0.02281
 0.003419 -4.14933

l_v(cc) = 1.45/94
 K(V/psi) = 13.975
 MS(cm²) = 1.6694/9

U4.66
 1.519999
 0.79424
 Solvent

(t)amp (sec)	DP (psid)	<U> (cm/s)	Re	T _w dyne/cm ²	f	Lu(Re-t)1/f
0.302489	153.9401	22775.99	42.67452	0.003591	2.135218	11.89291
0.272820	139.5444	20449.05	38.48897	0.003942	3.112802	11.81556
0.227227	120.9957	17901.75	32.05673	0.004349	3.073093	11.67299
0.184997	102.1276	15093.10	26.09898	0.004992	3.027953	11.51320
0.151245	87.45240	12924.30	21.34014	0.005567	2.984240	11.35845
0.129400	77.88857	11520.93	18.25357	0.006007	2.950032	11.24017
0.104349	65.88879	9748.479	14.77142	0.006765	2.904109	11.07479
11.5	0.086778	58.73273	8689.714	12.34252	0.007081	2.864069
16.5	0.054428	43.50939	6437.367	7.94075	0.008390	2.770613
21.4	0.038408	33.98003	5027.465	5.418525	0.009363	2.687074
31.9	0.020048	23.94078	3542.123	2.838389	0.009846	2.545903
39.6	0.011938	18.69207	2745.557	1.684275	0.009618	2.433335
44.9	0.006551	15.02141	2222.471	0.974749	0.00173	2.307028
70	0.003924	9.712179	1436.951	0.553975	0.011718	2.191879
70	0.002735	6.740019	1001.297	0.385968	0.016853	2.115905
60.4	0.001981	4.849431	718.3002	0.279539	0.02718	2.047048
89.9	0.001144	2.691786	399.1587	0.161474	0.044468	1.925171
310.2	0.000651	1.402710	237.6622	0.091860	0.071358	1.802684
	0.083942	57.50295	8526.979	12.12459	0.007316	2.863975
	0.097002	62.59435	9281.972	13.68497	0.006949	2.808940
	0.056210	43.12721	6380.823	7.930006	0.008507	2.769771
	0.028280	28.75167	4253.882	5.989707	0.009630	2.620604
	0.009144	17.57068	2570.053	1.290154	0.008571	2.575455
	0.005043	11.97978	1772.450	0.711462	0.009891	2.546310

Tap DL= 122.2334

L	1//f	1//f	1//f	1//f/81v	1//f/L
85.32939	27.14915	14.48240	1.462717	0.195505	
81.03679	28.74324	15.92567	1.368083	0.194524	
73.95608	25.98878	15.12870	1.296042	0.204563	
66.45312	25.13111	14.15224	1.229218	0.212320	
60.27266	24.30056	13.40191	1.179904	0.222354	
55.81000	23.66580	12.90195	1.147841	0.231174	
50.11747	22.77807	12.15703	1.097723	0.242570	
45.70353	22.01732	11.68324	1.064911	0.240007	
36.85476	20.24165	10.91678	1.029649	0.296210	
30.40568	18.65442	10.33413	1.002482	0.339875	
21.96766	15.97217	10.07764	1.027623	0.458749	
16.93179	13.83337	10.19440	1.083772	0.601493	
12.55744	11.35754	11.06133	1.234322	0.880843	
9.722089	9.245712	9.237649	1.079987	0.950173	
8.174245	7.764157	7.703003	0.930599	0.948150	
6.915985	6.433120	6.493181	0.808648	0.939137	
5.260798	4.178262	4.721335	0.623198	0.901409	
3.967931	1.850997	3.743485	0.521685	0.943635	
45.58617	21.99611	11.49074	1.069689	0.254953	
48.43071	22.49557	11.97841	1.086757	0.247330	
36.78333	20.22564	10.84190	1.022895	0.294750	
24.09044	17.39149	10.19015	1.011812	0.390567	
14.83662	12.73344	10.82447	1.174361	0.729712	
11.01768	10.27799	10.05457	1.149442	0.912585	

P2P11130

Tw	B(U)/D	Log	Log
dynes/cm ²	(1/g)	Tu	8(U)/D
0.924249	82.42431	-0.03421	1.916055
0.533975	53.29188	-0.25650	1.726661
0.385968	37.09303	-0.41344	1.569292
0.279539	26.60940	-0.55355	1.425035
0.091840	8.794265	-1.03487	0.944199
0.161474	14.77015	-0.79189	1.149384

Regression Output:
 Constant -1.97777
 Std Err of Y Est 0.001305
 R Squared 0.999968
 No. of Observations 4
 Degrees of Freedom 3

X Coefficient(s) 0.997415
 Std Err of Coef. 0.007939
 K' = 0.010526
 n' = 0.997415

Tw = 10.85401
 Res/ts = 488.5404

Regression Output:
 Constant -42.0416
 Std Err of Y Est 0.192790
 R Squared 0.989497
 No. of Observations 8
 Degrees of Freedom 6

X Coefficient(s) 18.63405
 Std Err of Coef. 0.783738
 t = 21.01666 deg C
 s.d.t = 0.042491 deg C

Page 1

Cyanamid 832A

PIF01334 1/4/89 16:27

1.0 PSID Taps 14 1.00085 density viscosity
 S = 0 <C>(ppm)= 1.0009 X coeff -0.00025 1.001565
 Z = 5.05 [NaCl]= 0.00010 constant 0.003419 -4.14933

MWD-40 Q1 (1/s)	MWD-40 Q2 (1/s)	Temp (deg C)	<V> (volts)	<U> (volts)	<U>corr (volts)	Batch Vol (ml)
0.189	0.19	20.8	2.9853	-0.0855	3.0710	
0.174	0.177	20.8	2.431428	-0.0875	2.719428	
0.165	0.166	20.8	2.301714	-0.0885	2.390214	
0.155	0.154	20.8	2.055625	-0.0885	2.144125	
0.139	0.14	20.8	1.491425	-0.0885	1.780125	
0.117	0.118	20.8	1.224111	-0.0885	1.312111	
0.099	0.1	20.8	0.8859	-0.0885	0.9744	
0.074	0.075	20.8	0.493111	-0.0885	0.581611	
0.054	0.055	20.8	0.245222	-0.0885	0.355222	
0.045	0.046	20.8	0.157714	-0.0715	0.247714	
0.054	0.057	20.8	0.0735	-0.0885	0.163	
0.029	0.03	20.8	-0.0136	-0.0705	0.0754	
0.021	0.021	20.8	-0.03977	-0.0875	0.047722	
0.013	0.014	20.8	-0.05633	-0.0875	0.031166	

Page 2

Cyanamid 832A

IS(cm) = 1.45794 Tap BL =
 K (V/pal) = 9.4 -1.99533
 XB(cm2) = 1.669479 Solvent

t)seep (sec)	BP (psid)	<U> (cm/s)	Re	Te dyne/cm2	f	Log(Re/f)1/ff
0.328787	113.5084	14805.02	44.10244	0.007168	3.153154	11.37711
0.289360	105.7215	15452.17	40.81395	0.007315	3.124498	11.29639
0.234378	99.13249	14676.48	35.87301	0.007313	3.098678	11.21502
0.228898	93.14280	13789.87	32.17963	0.007431	3.075085	11.14482
0.189375	83.55877	12376.98	26.71642	0.007465	3.034685	11.02462
0.159439	70.59121	10420.00	19.76004	0.007967	2.968528	10.82778
0.103459	59.59941	8233.749	14.42407	0.008248	2.903828	10.63527
0.041873	44.42468	4404.724	8.728985	0.008781	2.791774	10.30188
0.033461	32.44490	4833.108	5.031110	0.009458	2.672124	9.945887
0.024352	27.25400	4034.960	3.717744	0.010237	2.464435	9.750435
0.017340	21.84310	3234.852	2.444350	0.01253	2.515533	9.480032
0.006021	17.47017	2416.084	1.131624	0.007260	2.348145	8.981938
0.005074	12.57877	1842.298	0.716228	0.009068	2.248820	8.684412
0.003315	8.084352	1197.192	0.467758	0.014331	2.154305	8.411149

TMS = 0.004401
Res/48 = 13.90323

PIP01354

Regression Output:
Constant 1.745537
Std Err of Y Est 0.030220
R Squared 0.997074
No. of Observations 9
Degrees of Freedom 7

X Coefficient(s) 3.193936
Std Err of Coef. 0.045342

t = 20.8 deg C
s.d.t = 0.000000 deg C

122.2234

L	RMR	1//4	1//4/PR	1//4/L
88.92758	27.50997	11.61069	1.038127	0.132814
83.67174	27.00727	11.69165	1.034807	0.139732
78.44376	26.67468	11.69363	1.042674	0.149070
74.29593	26.02661	11.60946	1.040883	0.156138
67.69635	25.25901	11.42179	1.035989	0.168715
58.13103	24.06203	11.20314	1.034466	0.192722
50.08511	22.77274	11.01094	1.033322	0.219846
38.69513	20.64375	10.47112	1.035841	0.275774
29.37492	18.37049	10.38233	1.033847	0.350020
23.25314	17.12227	9.986331	1.024193	0.395448
20.49489	15.39552	9.879728	1.041739	0.482098
13.93239	12.21474	11.73543	1.306581	0.842327
11.08409	10.32758	10.50094	1.208895	0.947389
8.957444	8.569798	8.353311	0.993123	0.932552

P2F01570

1/22/69 12:02

1.0 P81D 0.1 P81D Taps 14

S = 10.05

Z = 4.9 7.27

density 1.00085

<C>(ppm)=2.086688 X coeff -0.00025

[NaCl]= 0.000010 constant 0.003419

<U>NaCl 2.213481

<V>corr (volts)

<V>0 (volts)

Temp (deg C)

Temp (deg C)

Temp (deg C)

Temp (deg C)

Temp (deg C)

Temp (deg C)

WMD-40 Bl (l/s)	WMD-40 Bl (l/s)	Temp (deg C)	<V> (volts)	<V>0 (volts)	<V>corr (volts)	Batch Vol (ml)	density	BP (psid)	<U> (cm/s)	Re	Tm dyne/cm2	f	Log(Re/f)1/4	Top Bl =	
0.176	0.177	19.9	2.175181	-0.0405	2.213481	2634	1.001549	105.8886	15361.78	33.25894	0.005941	3.073381	11.13975	2.97533	
0.154	0.155	19.9	1.7308	-0.0365	1.7488	2486	1.000085	93.45326	13586.76	26.57492	0.006068	3.024643	10.99480	-1.99543	
0.137	0.138	19.9	1.4045	-0.0395	1.444	2536	0.99970	83.39776	12098.94	21.69504	0.006247	2.980607	10.86372		
0.11	0.111	19.9	0.946	-0.0395	0.986	2503	0.9986	64.45420	9446.972	14.81392	0.006682	2.897762	10.61723		
0.082	0.083	19.95	0.5678	-0.0405	0.6083	1864	0.9986	49.64444	7259.551	9.139262	0.007368	2.793375	10.30664		
0.093	0.094	19.95	0.7078	-0.0405	0.7478	1745	0.9986	54.49923	8295.891	11.23514	0.007049	2.838209	10.44004		
0.093	0.094	20.05	4.754571	0.245	4.523821	1077	0.9986	54.58870	8237.467	11.19531	0.007002	2.838423	10.44067		
0.082	0.083	20.05	5.463285	0.2165	5.249785	1082	0.9986	49.47375	7201.745	9.008984	0.007372	2.791243	10.30030		
0.062	0.063	19.9	3.50425	0.2105	3.29425	1019	0.9986	37.91117	5499.971	5.653154	0.007879	2.488573	9.94822		
0.045	0.046	20	2.104222	0.2095	1.894222	567	0.9986	27.61193	4014.855	3.251870	0.008542	2.549452	9.640399		
0.034	0.037	20	1.3254	0.2095	1.1159	456	0.9986	22.30844	3235.394	1.919959	0.007452	2.454492	9.298355		
0.028	0.029	20	0.8086	0.2095	0.6786	542	0.9986	17.44413	2545.508	1.144523	0.007492	2.366486	8.977002		
0.02	0.021	20	0.681543	0.2105	0.470113	446	0.9986	12.64532	1838.666	0.806746	0.010105	2.266781	8.759852		
0.012	0.013	20.15	0.520074	0.212	0.308826	536	0.9986	8.603732	1148.105	0.526535	0.016452	2.175604	8.468571		
		20.2	0.36125	0.2145	0.14625	362	0.9986	5.467887	526.9494	0.250974	0.038621	2.015198	7.991310		
		20.25	0.10375	0.2155	0.087875	308	0.9986	3.001048	2.052153	300.0767	0.150799	0.67127	1.905075	7.665658	
		20.25	0.230714	0.2155	0.015214	75	0.9986	0.000165	0.249301	36.45422	0.026108	0.841476	1.524268	6.536632	
0.176	0.177	19.9	2.175181	-0.0405	2.213481	2634	1.001549	106.0210	15403.79	33.25894	0.005926	3.074042	11.895617		
0.154	0.155	19.9	1.7308	-0.0365	1.7488	2486	1.000085	92.84330	13489.19	26.57492	0.006175	3.025326	11.70129		
0.137	0.138	19.9	1.4045	-0.0395	1.444	2534	0.99970	82.64049	12009.73	21.69504	0.006360	2.981268	11.52369		
0.11	0.111	19.9	0.946	-0.0395	0.986	2503	0.9986	64.45420	9446.972	14.81392	0.006682	2.899823	11.19369		
0.082	0.083	19.95	0.5678	-0.0405	0.6083	1864	0.9986	49.64444	7259.551	9.139262	0.007406	2.794036	10.77614		
0.093	0.094	19.95	0.7078	-0.0405	0.7478	1745	0.9986	54.50497	8189.777	11.23514	0.007098	2.838870	10.93548		
0.093	0.094	20.05	4.754571	0.245	4.523821	1077	0.9986	54.50497	8189.777	11.23514	0.007098	2.838870	10.93548		
0.082	0.083	20.05	5.463285	0.2165	5.249785	1082	0.9986	49.47375	7201.745	9.008984	0.007301	2.791904	10.76761		
0.062	0.063	19.9	3.50425	0.2105	3.29425	1019	0.9986	37.9331	5482.705	5.653154	0.007952	2.689233	10.35693		
0.045	0.046	20	2.104222	0.2095	1.894222	567	0.9986	27.55349	4012.286	3.251470	0.008579	2.570113	9.880453		
0.034	0.037	20	1.3254	0.2095	1.1159	456	0.9986	22.14259	3227.274	1.914959	0.007809	2.455153	9.420513		
0.028	0.029	20	0.8086	0.2095	0.6786	542	0.9986	17.37068	2529.485	1.144523	0.007730	2.347147	8.988590		
0.02	0.021	20	0.681343	0.2105	0.470113	446	0.9986	12.57877	1831.676	0.806746	0.010213	2.267442	8.669768		
0.012	0.013	20.15	0.520074	0.212	0.308826	536	0.9986	8.603732	1137.750	0.526535	0.017595	2.176265	8.305060		
		20.2	0.36125	0.2145	0.14625	362	0.9986	5.478453	517.750	0.250974	0.038624	2.015859	7.443436		
		20.25	0.10375	0.2155	0.087875	308	0.9986	3.407887	527.7494	0.230974	0.038624	2.015859	7.443436		
		20.25	0.30375	0.2155	0.087875	308	0.9986	2.052153	300.5208	0.150799	0.071733	1.905376	7.222945		
		20.25	0.230714	0.2155	0.015214	75	0.9986	0.249301	36.50816	0.026108	0.841567	1.524929	5.699717		

122.2234

L	1/f	MDR	1/f	1/f	1/f/PK	1/f/L
74.00515	25.99425	12.97357	1.144619	0.175306		
66.15211	25.06861	12.83667	1.147521	0.194047		
59.77064	24.23155	12.65142	1.164557	0.211666		
49.39093	22.45749	12.23285	1.152169	0.247676		
38.83791	20.47414	11.64995	1.130333	0.299963		
43.06155	21.52598	11.91011	1.140811	0.274583		
45.08277	21.53004	11.95003	1.144564	0.277375		
38.44747	20.43362	11.64667	1.130492	0.301349		
30.51074	18.48288	11.24445	1.127239	0.349261		
23.19171	16.41960	10.81974	1.122333	0.466535		
17.79804	14.23534	11.43152	1.229413	0.642298		
13.87928	12.18325	11.55277	1.286930	0.832375		
11.35211	10.66884	9.947674	1.138197	0.861112		
9.34499	8.93486	7.796100	0.920392	0.832516		
6.47293	5.880749	5.068469	0.636750	0.786156		
5.022913	3.79437	3.733848	0.487214	0.743363		
2.090012	-3.43889	1.090131	0.166925	0.521591		
74.11782	24.00680	12.98927	1.091887	0.175251		
66.25282	25.08116	12.72511	1.087495	0.192049		
59.86164	24.24410	12.53905	1.087980	0.209467		
49.44542	22.47004	12.20545	1.090386	0.246746		
38.89703	20.48469	11.61945	1.078257	0.298723		
43.12711	21.53853	11.84866	1.083353	0.275201		
43.14836	21.54260	11.86960	1.085180	0.275551		
38.70651	20.44617	11.70302	1.086872	0.302352		
30.55721	18.49544	11.21401	1.082754	0.346984		
23.22701	16.43215	10.79638	1.092701	0.464820		
17.82515	14.24791	11.31572	1.201166	0.634817		
13.90041	12.19580	11.37324	1.265398	0.818195		
11.56970	10.68149	9.894898	1.141310	0.855242		
9.37876	8.949039	7.581967	0.912953	0.808419		
6.482448	5.90321	5.088253	0.663965	0.784727		
5.030560	3.808990	3.733689	0.516920	0.742201		
2.075194	-3.42633	1.090685	0.191252	0.520776		

P20-01570

Tu	8(U)/D	Log Tu	Log 8(U)/D
1.164523	94.81546	0.046148	1.985944
0.806745	49.38640	-0.09326	1.841274
0.526535	43.93227	-0.27857	1.642783
0.250116	19.79690	-0.40185	1.296597
0.150799	11.26041	-0.82160	1.051554
0.026108	1.347948	-1.58321	0.136069

Regression Outputs: -1.70902
Constant 0.019193
Std Err of Y Est 0.999201
R Squared 4
No. of Observations 4
Degrees of Freedom 2

X Coefficient(s) 0.860391
Std Err of Coef. 0.017193

K' = 0.019562
N' = 0.860391

Tw2 = 0.222873
Res/fs = 94.92975

Regression Outputs: -1.46490
Constant of Y Est 0.051761
R Squared 0.995263
No. of Observations 9
Degrees of Freedom 7

X Coefficient(s) 4.717294
Std Err of Coef. 0.146839

t = 20.02058 deg C
a.d.t = 0.118890 deg C

1/25/89 12:25
 1.0 PBID Taps 14 2.1 PBID Taps 14
 S = 0.02
 Z = 4.9 Z = 10.05 $\langle C \rangle_{(PBID)} = 5.430432 \times \text{coeff}$
 constant = 7.27 [NaCl] = 0.000010

WMD-40 01 (1/s)	WMD-40 01h (1/s)	Temp (deg C)	$\langle U \rangle$ (volts)	$\langle U \rangle_{(corr)}$ (volts)	Batch Vol (ml)
0.233	0.234	20.5	2.474636	-0.044	2.520386
0.212	0.213	20.5	2.196875	-0.0435	2.152125
0.191	0.192	20.4	1.744272	-0.043	1.807022
0.169	0.17	20.5	1.590818	-0.0425	1.433318
0.139	0.14	20.5	1.054666	-0.0425	1.097466
0.1	0.101	20.5	0.406222	-0.0435	0.449722
0.123	0.124	20.45	0.845230	-0.0435	0.888730
0.111	0.112	20.5	4.8025	0.0375	6.7745
0.093	0.094	20.55	5.203625	0.0185	5.184125
0.068	0.069	20.55	3.240125	0.0165	3.225125
0.053	0.054	20.4	2.14375	0.0135	2.131
0.044	0.045	20.4	1.3833	0.012	1.37205
0.034	0.037	20.4	0.914083	0.0105	0.905083
0.028	0.029	20.4	0.71	0.0075	0.7015
0.022	0.023	20.4	0.552928	0.0095	0.542428
0.017	0.018	20.65	0.438	0.0115	0.426
0.012	0.013	20.45	0.334083	0.0125	0.320583
		20.45	0.208125	0.0145	0.273125
		20.75	0.139164	0.0135	0.123164
		20.8	0.078714	0.0165	0.061714
		20.8	0.0472	0.0175	0.0307
		20.9	0.2283	0.0155	0.2128
				0.0155	0.0155

density viscosity
 1.00085 1.000134
 -0.00025 -0.02281
 0.003619 -0.14933
 t/error = 0

1)temp (sec) DP (paid) $\langle U \rangle$ (ca/s) Re I_m dyne/cm² f Log(Re/f^{1/3})/f

0.264925	140.1634	20640.38	37.58676	0.003832	3.104667	11.23819	
0.227497	127.5844	18786.04	32.09484	0.003949	3.072167	11.13414	
0.191017	115.0659	16897.53	28.94830	0.004081	3.033230	11.02029	
0.151513	101.8201	14995.13	21.37321	0.004129	2.983905	10.87353	
0.114932	83.65867	12348.94	16.36980	0.004643	2.923949	10.70115	
0.048480	40.49789	8908.884	9.489369	0.005303	2.812097	10.36234	
0.093946	74.27464	10923.50	13.25372	0.004812	2.879624	10.56326	
10.1	0.081404	67.31213	9912.345	11.48440	0.005077	2.849004	10.47215
11.7	0.042318	54.31521	8302.304	8.791726	0.005353	2.791479	10.30100
15.1	0.038734	41.49122	4144.354	5.467561	0.006301	2.688331	9.994103
19.9	0.025404	32.50794	4797.913	3.412556	0.006848	2.598842	9.727844
24.5	0.016487	27.23566	4019.744	2.325954	0.006281	2.503235	9.443382
29.6	0.010873	22.01689	3249.517	1.534333	0.006340	2.412895	9.174589
37.3	0.008429	17.44765	2604.449	1.189210	0.007449	2.357564	9.009962
44.4	0.004518	13.43214	2011.998	0.915446	0.009912	2.301722	8.843812
42.3	0.003118	10.64525	1602.480	0.722172	0.012300	2.249748	8.689173
79.8	0.003652	7.903933	1167.874	0.443012	0.020953	2.153224	8.401982
94.8	0.003281	4.453328	983.0842	0.343445	0.017427	2.188013	8.505493
149.9	0.001480	2.917024	431.9889	0.208797	0.049159	1.961275	7.890377
180	0.000741	1.581002	204.7466	0.104620	0.109899	1.831714	7.445383
246.1	0.000348	0.424181	92.83736	0.052043	0.265910	1.480090	6.994253
120.2	0.002357	5.177617	749.3444	0.340747	0.626960	2.101492	8.248062

1.0 PBID Taps 14 2.1 PBID Taps 14
 S = 0.02
 Z = 4.9 Z = 10.05 $\langle C \rangle_{(PBID)} = 5.430432 \times \text{coeff}$
 constant = 7.27 [NaCl] = 0.000010

WMD-40 01 (1/s)	WMD-40 01h (1/s)	Temp (deg C)	$\langle U \rangle$ (volts)	$\langle U \rangle_{(corr)}$ (volts)	Batch Vol (ml)
0.233	0.234	20.5	2.474636	-0.044	2.520386
0.212	0.213	20.5	2.196875	-0.0435	2.152125
0.191	0.192	20.4	1.744272	-0.043	1.807022
0.169	0.17	20.5	1.590818	-0.0425	1.433318
0.139	0.14	20.5	1.054666	-0.0425	1.097466
0.1	0.101	20.5	0.406222	-0.0435	0.449722
0.123	0.124	20.45	0.845230	-0.0435	0.888730
0.111	0.112	20.5	4.8025	0.0375	6.7745
0.093	0.094	20.55	5.203625	0.0185	5.184125
0.068	0.069	20.55	3.240125	0.0165	3.225125
0.053	0.054	20.4	2.14375	0.0135	2.131
0.044	0.045	20.4	1.3833	0.012	1.37205
0.034	0.037	20.4	0.914083	0.0105	0.905083
0.028	0.029	20.4	0.71	0.0075	0.7015
0.022	0.023	20.4	0.552928	0.0095	0.542428
0.017	0.018	20.65	0.438	0.0115	0.426
0.012	0.013	20.45	0.334083	0.0125	0.320583
		20.45	0.208125	0.0145	0.273125
		20.75	0.139164	0.0135	0.123164
		20.8	0.078714	0.0165	0.061714
		20.8	0.0472	0.0175	0.0307
		20.9	0.2283	0.0155	0.2128
				0.0155	0.0155

Top BL= 122.2234

L	M	1/14	1/14	1/14/PR	1/14/L
79.04334	24.62288	14.15289	1.437329	0.262254	
73.79852	25.97118	15.91160	1.428823	0.215609	
67.46997	25.23138	15.65282	1.420344	0.231994	
60.22617	24.29419	15.56129	1.431116	0.258380	
52.70440	23.19341	14.44403	1.348454	0.277850	
40.54878	21.02985	13.73173	1.373154	0.338647	
47.37033	22.31290	14.61475	1.344611	0.304299	
44.14528	21.73108	14.03369	1.340094	0.317898	
39.64871	20.63411	13.41876	1.302484	0.347023	
30.49379	18.67829	12.59754	1.260498	0.413118	
24.81547	16.97800	12.06397	1.242204	0.486953	
19.91204	15.14108	12.41725	1.334095	0.633649	
16.17242	13.64500	12.55889	1.348791	0.774512	
14.23785	12.39372	11.93344	1.269600	0.903045	
12.51993	11.33272	10.04397	1.135706	0.902238	
11.10780	10.34521	9.016433	1.037485	0.811738	
9.63936	9.17284	7.975069	0.890601	0.784120	
8.894144	8.311259	6.908240	0.822215	0.776717	
5.986255	5.249229	4.510214	0.571409	0.733428	
4.294228	2.402567	3.016496	0.405149	0.711043	
2.992040	-0.47828	1.939283	0.277262	0.648129	
7.895345	7.528352	6.090316	0.738393	0.771378	

PSP01573

Tu	0(U)/B	Log	Log
dym/co2	(1/e)	Tm	0(U)/B
0.722172	59.50923	-0.14335	1.774584
0.543465	43.34993	-0.26482	1.437106
0.443012	34.50740	-0.33440	1.542303
0.360747	28.41020	-0.44279	1.453474
0.289797	18.00404	-0.68027	1.204284
0.164420	7.57723	-0.78038	0.879538
0.052943	3.435934	-1.28343	0.534044

Regression Outputs
 Constant -1.82198
 Std Err of Y Est 0.093934
 R Squared 0.999720
 No. of Observations 5
 Degrees of Freedom 3

X Coefficient(s) 0.949467
 Std Err of Coef. 0.009171

R' = 0.015064
 R' = 0.949467

Tes = 0.549327
 Res/fs = 157.2644

Regression Outputs
 Constant -10.1244
 Std Err of Y Est 0.151312
 R Squared 0.988854
 No. of Observations 11
 Degrees of Freedom 9

X Coefficient(s) 8.492920
 Std Err of Coef. 0.300551

t = 20.59772 deg C
 s.d.t = 0.121968 deg C

PIP11574 1/26/89 13:00
 1.0 PS18 Taps 14 0.1 P818 Taps 14
 S = 8 g = 10.05 <C>(ppm)=10.17577 X coeff
 Z = 4.9 Z = 7.27 [NaCl] = 0.000010 constant
 colNaCl

MWD-40	0/1	0/h	Temp	<U>	<V>	<U>corr	Batch	Vol
(l/s)	(l/s)	(deg C)	(volts)	(volts)	(volts)	(volts)	(mi)	(mi)
0.244	0.245	21.1	1.634857	-0.0515	1.683357			
0.224	0.226	21.1	1.368142	-0.0455	1.414142			
0.194	0.196	21.1	1.084714	-0.0445	1.133714			
0.169	0.171	21.1	0.846	-0.0475	0.89375			
0.139	0.14	21.1	0.559444	-0.048	0.608194			
0.116	0.12	21.1	0.404444	-0.0495	0.453444			
0.099	0.103	21.1	0.322818	-0.0485	0.371818			
0.124	0.125	21.15	3.991571	-0.0545	4.055071			1154
0.11	0.112	21.1	3.522	-0.0705	3.594			1156
0.093	0.094	21.15	2.840144	-0.0775	2.928444			1140
0.068	0.069	21.15	2.023571	-0.0995	2.114071			1208
0.052	0.053	21.2	1.527	-0.0815	1.6085			1174
0.035	0.034	21.2	1.03575	-0.0815	1.11725			1101
0.03	0.031	21.25	0.886727	-0.0815	0.948227			1057
0.025	0.026	21.3	0.746492	-0.0815	0.826492			1161
0.02	0.021	21.3	0.610470	-0.0785	0.687470			1220
0.013	0.014	21.3	0.450414	-0.0755	0.504414			1122
		21.3	0.29025	-0.0725	0.34125			490
		21.3	0.194571	-0.0695	0.244571			255
		21.3	0.0282	-0.0705	0.0982			228
				-0.0695				

density	viscosity	ID(cm)	f	Log(Re(f))/f
1.000085	1.000154	1.65796	83.22	
-0.00025	-0.02201	K(U/psi)= 9.46		
0.003419	-4.14933	MS(ca2)= 1.649479		
1)error=	0			
t)temp	(psid)	Re	Tm	f
(sec)		(cm/s)	dync/ca2	
0.177944	146.7523	21905.17	25.10406	0.002335
0.149484	135.3715	20204.40	21.08924	0.002305
0.119042	117.4018	17524.13	16.90718	0.002457
0.094474	102.4271	15288.91	13.32837	0.002545
0.044271	83.65847	12517.24	9.070041	0.002584
0.047932	71.87848	10729.06	6.742240	0.002422
0.039304	41.48587	9209.112	5.544959	0.002918
				2.694810
				10.01933
9.2	0.04827	75.13404	11227.43	6.874319
10.3	0.043210	67.22434	10034.42	6.094083
12.1	0.035191	56.43348	8433.151	4.964793
17.4	0.025403	41.58498	6214.241	3.583858
22.2	0.019328	31.47424	4738.877	2.724793
29.9	0.013425	22.05642	3299.715	1.894004
33.9	0.011634	18.67444	2797.212	1.641377
44.4	0.009933	15.44275	2348.493	1.401441
59.5	0.008240	12.32321	1847.738	1.165427
79.3	0.004061	8.453657	1247.552	0.855107
80.2	0.003179	3.799557	549.7104	0.448512
141.4	0.001180	0.844155	126.8736	0.166472
				0.465668
				1.937502
				7.740140

Tap No. 122.2234

L	M	N	1//4	1//4	1//4	1//4	1//4	1//4
44.16270	25.06993	20.49252	1.061992	0.312752				
60.64175	24.35094	20.62558	1.913690	0.343419				
54.29713	23.43904	20.17157	1.078239	0.371503				
48.20955	22.45780	19.62090	1.072374	0.411140				
39.78915	20.86966	19.47171	1.902990	0.494647				
34.33894	19.45823	19.52785	1.924390	0.548679				
31.09499	18.83939	18.51003	1.047432	0.595273				
34.64160	19.73540	20.24509	1.992497	0.584078				
32.60368	19.23034	19.23598	1.908227	0.589994				
29.45872	18.59278	17.89309	1.798410	0.607456				
25.02702	17.04805	15.51882	1.593582	0.620082				
21.85508	15.92977	13.55198	1.417023	0.620083				
18.21449	14.42620	11.32241	1.213778	0.621615				
14.97552	13.04692	10.29869	1.114913	0.604678				
13.70359	13.20228	9.546955	1.023024	0.595211				
14.32037	12.44161	8.044379	0.894310	0.583140				
12.24653	11.14399	6.958364	0.732459	0.526504				
10.38080	9.786671	5.185183	0.402808	0.499497				
8.883798	8.501655	4.008072	0.477124	0.451164				
5.412313	4.412554	1.465103	0.188798	0.276498				

PIP11574

Tw	8<U>/b	Log	Log
dyna/ca2	(1/s)	Tw	8<U>/b
1.401461	55.94339	0.146575	1.934212
1.165427	67.61894	0.044485	1.830048
0.855107	44.38422	-0.04797	1.444389
0.612405	31.51653	-0.21294	1.498538
0.949512	26.84842	-0.34822	1.319077
0.166472	4.442956	-0.77845	0.666794

Regression Output:
 Constant -1.28701
 Std Err of Y Est 0.023232
 R Squared 0.996182
 No. of Observations 4
 Degrees of Freedom 4

X Coefficient(s) 0.732169
 Std Err of Coef. 0.022642

K' = 0.051439
 n' = 0.732169

Tw)Retrom=4.204043
 Res/(IR= 526.3433

Regression Output:
 Constant 6.687405
 Std Err of Y Est 0.214454
 R Squared 0.872459
 No. of Observations 4
 Degrees of Freedom 4

X Coefficient(s) 4.634333
 Std Err of Coef. 0.086344

t = 21.165 deg C
 s.d.t = 0.085293 deg C

Page 1

P2P-11575

1/29/89 14:10

Cyanamid 832A

col:NaCl

1.0 P81D Taps 14 0.1 P81D Taps 14 10.05 <C> (ppm) = 20.859 X coeff

B = 4.9 Z = 7.27 [NaCl] = 0.000010 constant

MHD-40 MHD-40

Q1 Q1

(1/s) (1/s)

Temp (deg C) <U> <U> <U>

(volts) (volts) (volts)

<U> corr Batch Vol

(volts) (ml)

0.252 0.253 21.35 1.316 -0.0445 1.3615 1074

0.223 0.226 21.3 1.0975 -0.0465 1.145 1176

0.194 0.196 21.3 0.898714 -0.0485 0.947714 1270

0.175 0.176 21.2 0.744375 -0.0495 0.814375 1178

0.151 0.152 21.2 0.64175 -0.0505 0.69275 1090

0.122 0.123 21.3 0.492444 -0.0515 0.544144 1232

0.085 0.086 21.3 0.316090 -0.0515 0.367590 1148

0.132 0.133 21.25 5.1513 -0.0765 5.2618 1108

0.11 0.111 21.25 4.154688 -0.1245 4.284388 797

0.081 0.082 21.3 2.93575 -0.1305 3.064275 642

0.052 0.053 21.3 1.918688 -0.1305 2.043388 425

0.043 0.044 21.3 1.614 -0.1325 1.749 282

0.034 0.035 21.3 1.350538 -0.1325 1.483538 178

0.029 0.03 21.3 1.155272 -0.1325 1.287772 1337

0.023 0.024 21.3 0.977928 -0.1325 1.09928 1135

0.014 0.016 21.3 0.750333 -0.1315 0.860333 642

0.012 0.013 21.4 0.581818 -0.1285 0.674071 425

0.014 0.016 21.4 0.179487 -0.1245 0.304687 282

0.014 0.016 21.45 0.069844 -0.1235 0.193344 178

0.012 0.013 21.45 -0.024 -0.1255 0.0975 1337

0.012 0.013 21.35 3.743 -0.1215 3.8725 1074

0.012 0.013 21.35 3.743 -0.1375 -0.1375 1176

Page 2

Cyanamid 832A

density viscosity

1.000065 1.001343

-0.000275 -0.02281

0.003419 -4.14983

t) error = 0

t) temp (sec)

EP (ppm)

<U> (cm/s)

Re

Tw (dyne/cm²)

f

Log (Re/f) 1/4

0.144840 151.5442 22716.39 20.43377 0.001782 2.981887 10.86752

0.121808 134.1735 20089.64 17.18448 0.001912 2.943788 10.75417

0.106826 117.4618 17578.62 14.22354 0.002067 2.902724 10.63199

0.094435 105.4220 15749.32 12.22337 0.002203 2.868812 10.53109

0.073494 91.04433 13401.68 10.39498 0.002313 2.833489 10.42659

0.057890 73.47545 11031.48 8.167008 0.0025014 2.782251 10.27354

0.039165 51.51306 7713.071 5.516709 0.004165 2.497068 10.02009

0.062504 80.54403 12049.28 8.818269 0.002722 2.798438 10.32170

10.8 0.0508975 44.33249 9720.794 7.180238 0.003249 2.753815 10.18894

15.3 0.034424 49.72000 7444.597 5.130750 0.004145 2.481447 9.974274

22.2 0.029274 31.78419 4739.040 3.424530 0.006792 2.593539 9.712045

24.4 0.020776 26.54037 3973.930 2.931161 0.008338 2.559758 9.611537

33.4 0.017385 20.84417 3121.504 2.452754 0.011309 2.521045 9.494433

38.4 0.015297 17.90727 2681.244 2.158187 0.013484 2.493283 9.413771

45.2 0.013165 14.46318 2198.519 1.840137 0.017288 2.461011 9.317751

64.9 0.010220 10.47338 1570.254 1.441838 0.026329 2.404189 9.159438

69.9 0.009432 7.94332 1192.044 1.189589 0.037779 2.346922 9.031855

89.9 0.005431 4.277541 441.9246 0.794499 0.087010 2.272720 8.771042

119.9 0.003419 2.123188 318.6239 0.510628 0.226984 2.181274 8.485647

179.9 0.002320 0.938937 141.0441 0.327382 0.746180 2.085244 8.195719

486.1 0.001158 0.222078 33.54647 0.163400 6.639177 1.935344 7.750741

13 0.044092 61.60372 9234.541 6.488951 0.003426 2.732832 10.12654

Page 2

Cyanamid 832A

density viscosity

1.000065 1.001343

-0.000275 -0.02281

0.003419 -4.14983

t) error = 0

t) temp (sec)

EP (ppm)

<U> (cm/s)

Re

Tw (dyne/cm²)

f

Log (Re/f) 1/4

0.144840 151.5442 22716.39 20.43377 0.001782 2.981887 10.86752

0.121808 134.1735 20089.64 17.18448 0.001912 2.943788 10.75417

0.106826 117.4618 17578.62 14.22354 0.002067 2.902724 10.63199

0.094435 105.4220 15749.32 12.22337 0.002203 2.868812 10.53109

0.073494 91.04433 13401.68 10.39498 0.002313 2.833489 10.42659

0.057890 73.47545 11031.48 8.167008 0.0025014 2.782251 10.27354

0.039165 51.51306 7713.071 5.516709 0.004165 2.497068 10.02009

0.062504 80.54403 12049.28 8.818269 0.002722 2.798438 10.32170

10.8 0.0508975 44.33249 9720.794 7.180238 0.003249 2.753815 10.18894

15.3 0.034424 49.72000 7444.597 5.130750 0.004145 2.481447 9.974274

22.2 0.029274 31.78419 4739.040 3.424530 0.006792 2.593539 9.712045

24.4 0.020776 26.54037 3973.930 2.931161 0.008338 2.559758 9.611537

33.4 0.017385 20.84417 3121.504 2.452754 0.011309 2.521045 9.494433

38.4 0.015297 17.90727 2681.244 2.158187 0.013484 2.493283 9.413771

45.2 0.013165 14.46318 2198.519 1.840137 0.017288 2.461011 9.317751

64.9 0.010220 10.47338 1570.254 1.441838 0.026329 2.404189 9.159438

69.9 0.009432 7.94332 1192.044 1.189589 0.037779 2.346922 9.031855

89.9 0.005431 4.277541 441.9246 0.794499 0.087010 2.272720 8.771042

119.9 0.003419 2.123188 318.6239 0.510628 0.226984 2.181274 8.485647

179.9 0.002320 0.938937 141.0441 0.327382 0.746180 2.085244 8.195719

486.1 0.001158 0.222078 33.54647 0.163400 6.639177 1.935344 7.750741

13 0.044092 61.60372 9234.541 6.488951 0.003426 2.732832 10.12654

Tm <U>/B Log Log
 dyno/ca2 (1/a) Tm <U>/D
 1.040137 80.54837 0.269545 1.906144
 1.441838 57.47969 0.158916 1.759514
 1.187589 45.58401 0.075397 1.639347
 0.794499 23.47137 -0.09990 1.370538
 0.510628 11.45019 -0.29189 1.044333
 0.327382 5.152043 -0.48494 0.711981
 0.143400 1.216573 -0.78674 0.085831

P2P11378

Top BL= 123.2334

L M 1//4 1//4 1//4/PK 1//4/L
 1//4 1//4
 59.94699 24.25584 23.48382 2.179320 0.395079
 54.91218 23.53198 22.84589 2.126234 0.414488
 49.93796 22.75176 21.96177 2.049452 0.440205
 44.20542 22.10744 21.36339 2.022904 0.461058
 42.61544 21.44009 19.94819 1.913204 0.468095
 37.85375 20.46278 18.21302 1.772897 0.481114
 31.11346 18.84429 15.49583 1.546274 0.497778

Regression Outputs
 Constant -0.95631
 Std Err of Y Est 0.012980
 R Squared 0.998184
 No. of Observations 3
 Degrees of Freedom 3

X Coefficient(s) 0.616874
 Std Err of Coef. 0.015180

K' = 0.115794
 n' = 0.616874

Regression Outputs
 Constant -40.0500
 Std Err of Y Est 0.002937
 R Squared 0.999993
 No. of Observations 3
 Degrees of Freedom 1

X Coefficient(s) 21.37324
 Std Err of Coef. 0.052461

t = 21.32045 deg C
 o.d.t = 0.066842 deg C

39.29329 20.77033 19.16561 1.856826 0.487757
 33.45449 19.92249 17.48762 1.716333 0.493213
 30.82947 18.53168 15.49435 1.553431 0.515971
 24.51429 16.87724 12.13338 1.249509 0.494951
 22.47977 16.23541 10.95119 1.139377 0.482841
 20.74655 15.59025 9.603085 0.990170 0.453236
 19.46092 14.97238 8.411049 0.914728 0.442478
 18.04722 14.35921 7.405343 0.816220 0.420944
 15.92444 13.51740 6.142828 0.673191 0.386999
 14.48113 12.53553 5.144814 0.569430 0.353277
 11.85452 10.86814 3.590104 0.386310 0.286458
 9.487401 9.044251 2.098949 0.247358 0.221230
 7.685434 7.219438 1.159237 0.141375 0.152422
 5.373888 4.532533 0.386899 0.050072 0.072239
 33.78544 19.52419 17.68262 1.486911 0.505617

Page 1

Cyanamid 832A

PIPO3443 12/23/88 13108 Taps 14 col/MoCl
 <C>(ppm)= 1.03135 X coeff
 [NaCl] = 0.000308 constant

HWB-40 Q1 (1/s)	HWB-40 Q2 (1/s)	Temp (deg C)	<U> (volts)	<V> (volts)	<U>corr (volts)	Batch Vol (ml)
0.227	0.228	22.1	4.1655	0.0415	4.124	
0.236	0.235	22.1	4.058	0.0415	4.0165	
0.238	0.239	22.1	4.226664	0.0415	4.191664	
0.213	0.216	22.1	3.541714	0.0285	3.514714	
0.194	0.195	22.1	3.0255	0.0255	3.0095	
0.186	0.184	22.1	2.7	0.0245	2.6745	
0.149	0.17	22.1	2.4004	0.023	2.37815	
0.151	0.152	22.1	1.932714	0.0215	1.911444	
0.129	0.13	22.1	1.4914	0.021	1.47115	
0.094	0.095	22.1	0.8706	0.0195	0.85135	
				0.019		

PIPO3443

12/23/88 12136 Meter 0.1 PSIB transducer has cal

0.095	0.095	20.7	0.952625	0.045	0.909125	
0.06	0.061	20.35	0.654428	0.042	0.612678	
0.061	0.062	20.25	0.7342	0.0415	0.6932	
0.05	0.052	20.25	0.351666	0.0405	0.311166	
0.042	0.043	20.2	0.266444	0.0405	0.226144	
0.033	0.034	20.2	0.182375	0.0405	0.140875	
0.025	0.024	20.2	0.079444	0.0425	0.036944	
0.017	0.018	20.2	0.081375	0.0425	0.038875	
0.012	0.013	20.2	0.070571	0.0425	0.028071	
				0.0425		

Page 2

Cyanamid 832A

density viscosity ID(cm) = 1.45796
 K(U/psi) = 9.6176 70.31
 XB(cm2) = 1.66979
 t)error = 0.4

t)saap (sec)	DP (psid)	<U> (cm/s)	Re	Tm dync/cm2	f	Log(Re/f)1/4	Solvent
0.428797	136.5695	20820.68	60.49379	0.006499	3.226948	12.49979	
0.417619	140.7624	21459.91	58.91691	0.005958	3.219212	12.47485	
0.435832	143.1583	21825.19	61.48638	0.006012	3.228482	12.51392	
0.365946	129.3816	19724.85	51.55635	0.006172	3.190233	12.36093	
0.311980	116.8028	17807.16	46.01369	0.006465	3.155885	12.22354	
0.278245	111.4119	16985.29	39.25716	0.006338	3.131052	12.12420	
0.247270	101.8281	15524.19	34.88441	0.006742	3.105408	12.02163	
0.198746	91.04633	13880.45	28.03873	0.006778	3.05971	11.83188	
0.152964	77.84857	11871.44	21.57988	0.007132	3.001117	11.60446	
0.088520	56.90396	8675.284	12.48821	0.007728	2.882342	11.12937	

functioned. It does not bleed.

0.094527	56.90396	8405.566	13.33569	0.008250	2.882807	11.13123	
0.042908	36.23883	5310.917	6.053466	0.009233	2.707853	10.43141	
0.072076	48.81740	7138.256	10.16833	0.008546	2.819491	10.87796	
0.032353	30.54894	4464.883	6.564416	0.009797	2.645559	10.18223	
0.023307	25.45703	3718.206	5.288237	0.010163	2.573855	9.895422	
0.014447	20.04613	2930.821	2.066453	0.010280	2.472987	9.491948	
0.005920	15.27422	2230.923	0.835302	0.007171	2.276295	8.705182	
0.004042	10.48230	1531.026	0.570246	0.010395	2.193405	8.373621	
0.002918	7.487363	1093.590	0.411771	0.014712	2.122702	8.098809	

Tap BL=

L	HDR	1/14	1/14	1/14/PR	1/14/L
104.9127	28.87401	12.40337	0.972362	0.118227	
103.5363	28.76504	12.95434	1.038278	0.125118	
105.7699	28.94116	12.89641	1.038981	0.121938	
94.85316	28.21444	12.72058	1.029742	0.131421	
89.48917	27.54182	12.43481	1.017447	0.138977	
84.31448	27.08999	12.50098	1.036018	0.148623	
79.44893	26.40276	12.17849	1.013044	0.152844	
71.42527	25.70144	12.14593	1.026544	0.176051	
62.44099	24.62132	11.84894	1.026377	0.188948	
47.46755	22.34451	11.37472	1.022843	0.238424	

47.71841	22.37334	11.09728	0.989044	0.230712	
31.87582	19.04922	10.46674	0.977434	0.324275	
41.24504	21.17034	10.81693	0.994379	0.242237	
27.43371	17.04542	10.10288	0.992206	0.345000	
23.42802	16.50323	9.91828	1.002405	0.423391	
18.57235	14.58675	9.842847	1.039075	0.531049	
11.80798	10.84941	11.80834	1.356472	1.000030	
9.756302	9.274699	9.807929	1.171288	1.009291	
8.296530	7.931344	8.244270	1.016947	0.994420	

PIP03443

Tw dyne/cm2 B(U)/D (1/s) Log Tw Log B(U)/D

0.835302 83.81147 -0.07815 1.921107
 0.570246 57.51767 -0.24393 1.759801
 0.411771 41.08405 -0.38534 1.613673

Regression Output:
 Constant -1.986023
 Std Err of Y Est 0.002911
 R Squared 0.999820
 No. of Observations 3
 Degrees of Freedom 1
 X Coefficient(s) 0.992539
 Std Err of Coef. 0.013294
 R² = 0.010274
 n² = 0.992539

Tw = 6.185549
 Res/fit = 536.7420

Regression Output:
 Constant -2.51487
 Std Err of Y Est 0.121149
 R Squared 0.989110
 No. of Observations 12
 Degrees of Freedom 10
 X Coefficient(s) 4.782067
 Std Err of Coef. 0.158671

t = 21.23947 deg C
 s.d.t = 0.915290 deg C

Tap DL= 4
0.4
Solvent

ID(cm) = 1.45796
K(U/psi) = 9.6176
XS(cm2) = 1.669479

t)saap (sec)	DP (pa)	<U> (cm/s)	Re	Iw dyne/cm2	f	Log(Re/f)1/f
0.396891	153.0417	23279.37	55.99259	0.004790	3.207172	12.42869
0.348186	141.0619	21457.11	49.12135	0.004947	3.178742	12.31497
0.246514	123.0922	18723.72	37.59959	0.004972	3.120699	12.08279
0.238677	112.9094	17174.80	33.47204	0.005292	3.096742	11.98674
0.185652	97.33572	14805.86	26.19140	0.005539	3.042186	11.76874
0.134348	79.36605	12072.47	18.93355	0.006029	2.971952	11.48781
0.100726	66.78728	10159.09	14.21032	0.006384	2.909409	11.23763
0.060855	49.91659	7516.822	8.58392	0.007045	2.799987	10.79995
0.028957	31.94692	4778.040	4.085238	0.008278	2.638233	10.15289
0.020945	26.05602	3958.947	2.954932	0.008722	2.567888	9.871594
0.013733	20.66512	3139.854	1.937493	0.009091	2.476335	9.504940
0.006436	15.57371	2366.267	0.907993	0.007502	2.311656	8.846625
0.004193	10.48230	1590.884	0.591638	0.010790	2.218150	8.472601
0.003086	7.487363	1136.346	0.433394	0.015563	2.151563	8.206254

12/29/88 13:54
1.0 PSID Taps 14
S = B <C>(ppm) = 2.0433 X coeff -0.00025 -0.02281
Z = 5.05 [NaCl] = 0.000308 constant 0.003419 -4.14933

density viscosity
1.000096 1.001592

MWD-40 (l/s)	Q)h (l/s)	Temp (deg C)	<U> (volts)	<U>e (volts)	<U>(corr (volts)	Batch Vol (ml)
0.255	0.254	22	3.796142	-0.018	3.817142	
0.235	0.236	22	3.322714	-0.024	3.348714	
0.205	0.204	22	2.5365	-0.028	2.56525	
0.189	0.189	22	2.2495	-0.0255	2.2955	
0.162	0.163	22	1.758777	-0.0265	1.785527	
0.132	0.133	22	1.244857	-0.027	1.292107	
0.111	0.112	22	0.94125	-0.0275	0.96875	
0.082	0.083	22	0.557285	-0.0275	0.585285	
0.052	0.053	21.95	0.25	-0.0285	0.2785	
0.043	0.044	21.95	0.173444	-0.0285	0.201444	
0.034	0.035	21.95	0.104833	-0.0275	0.132083	
0.024	0.024	21.95	0.0394	-0.027	0.0619	
0.017	0.018	21.9	0.014333	-0.026	0.040333	
0.012	0.013	21.9	0.004181	-0.026	0.029681	
					-0.025	

122.2234

L	MDR	1/f	1/f	1/f	1/f	1/f
100.7054	28.53428	14.44769	1.162466	0.143464		
94.32410	27.99411	14.21747	1.134503	0.150732		
82.52377	26.89328	14.18055	1.173414	0.171835		
78.99482	26.43810	13.74314	1.146374	0.176005		
48.87584	25.40155	13.43328	1.141404	0.195045		
58.39126	24.06710	12.87785	1.121601	0.219771		
50.73287	22.87877	12.51542	1.113704	0.244692		
39.43370	20.79974	11.91370	1.103123	0.362119		
27.17087	17.72624	10.97972	1.082526	0.404503		
23.10833	16.38988	10.70757	1.084489	0.643344		
18.71177	14.44844	10.48756	1.103380	0.560479		
12.80962	11.52147	11.54534	1.305058	0.901303		
10.32833	9.744858	9.624938	1.134243	0.932089		
8.860203	8.477709	8.015801	0.974791	0.904697		

P2P03445

Tw	8 U./D	log	log
dynes/cm ²	(1/s)	Tw	8 U./D
0.907993	85.45483	0.04191	1.931776
0.591638	57.51767	0.22794	1.759801
0.435394	41.08405	-0.36111	1.613367

Regression Output:
 Constant -1.90909
 Std Err of Y Est 0.010991
 R Squared 0.997649
 No. of Observations 7
 Degrees of Freedom 1

X Coefficient(s) 1.005861
 Std Err of Coef. 0.048818
 K' = 0.010254
 n' = 1.005861

tw = 0.196175
 Res/ft = 166.7626

Regression Output:
 Constant 4.91727
 Std Err of Y Est 0.127250
 R Squared 0.997077
 No. of Observations 10
 Degrees of Freedom 8

X Coefficient(s) 6.034059
 Std Err of Coef. 0.190689
 t = 21.97142 deg C
 s.d.t = 0.06421 deg C

PSP03448

12/30/88 12:38

1.0 PBID Taps 14

B <C>(ppm)=5.577168 X coeff -0.00025 -0.02281

Z = 5.05 [NaCl]= 9.000308 constant 0.003419 -4.14933

density viscosity

co)NaCl 1.000096 1.001592

1.000096 1.001592

-0.00025 -0.02281

0.003419 -4.14933

MHD-40 D1 (1/s)	MHD-40 D1h (1/s)	Temp (deg C)	<V> (volts)	<V> (volts)	<V>corr (volts)	Batch Vol (ml)
0.235	0.234	21.45	2.467444	-0.0335	2.506444	
0.218	0.219	21.5	2.187428	-0.0405	2.228428	
0.195	0.194	21.5	1.803333	-0.0415	1.844833	
0.177	0.177	21.5	1.544466	-0.0415	1.586166	
0.153	0.153	21.5	1.226142	-0.0415	1.248642	
0.125	0.126	21.4	0.8934	-0.0435	0.9369	
0.104	0.105	21.4	0.667888	-0.0435	0.711388	
0.076	0.077	21.4	0.397444	-0.0435	0.440944	
0.056	0.057	21.4	0.237375	-0.0435	0.280375	
0.038	0.039	21.4	0.083425	-0.0425	0.126125	
0.029	0.03	21.4	0.034571	-0.0425	0.078821	
0.024	0.025	21.4	0.017664	-0.042	0.039664	
0.017	0.018	21.4	0.001727	-0.0415	0.042727	
0.012	0.013	21.4	-0.01	-0.0405	0.0305	

ID(ce) = 1.45796
K(V/psi) = 9.6176
KS(ce2) = 1.669479

Tap DL = 4
0.4

t) samp (sec)	DP (psid)	<U> (cm/s)	Re	Tw dyne/cm2	f	Log(Re/f)/f	Solvent
0	0.260610	141.0619	21192.51	36.76633	0.003702	3.110414	12.04165
0.251703	130.8791	19684.88	32.68819	0.003823	3.085376	11.94150	
0.191818	115.9043	17432.61	27.06134	0.004056	3.044356	11.77742	
0.165131	106.0210	15946.11	23.29637	0.004152	3.011825	11.64730	
0.131908	91.64532	13785.92	18.60936	0.004439	2.963047	11.45218	
0.097415	75.17312	11280.94	13.74312	0.004872	2.896239	11.18495	
0.073967	62.59435	9393.296	10.43516	0.005336	2.836445	10.94578	
0.045867	45.82266	6876.452	6.468090	0.006172	2.732584	10.53033	
0.029152	33.84288	5078.672	4.112742	0.007194	2.634262	10.13704	
0.013113	23.06107	3460.688	1.850092	0.006970	2.460793	9.443172	
0.008195	17.67017	2651.696	1.156309	0.007419	2.358714	9.034858	
0.006203	14.67523	2202.256	0.875233	0.008142	2.298158	8.793033	
0.004442	10.48230	1573.040	0.626754	0.011429	2.725745	8.502980	
0.003171	7.487363	1123.600	0.447395	0.015990	2.152342	8.210169	

Page 3

Cyanamid 832A

122.2234

L	MDR	1//4	1//4	3//4/PR	1//4/L
80.59239	26.69786	16.43495	1.346841	0.203926	
76.07763	26.22216	16.17171	1.354243	0.212548	
69.22073	25.44276	15.74905	1.334466	0.227389	
64.22523	24.82468	15.51774	1.332305	0.241614	
57.40203	23.89789	15.09869	1.310500	0.261455	
49.21744	22.62854	14.32538	1.290772	0.291063	
42.88703	21.49247	13.68901	1.250619	0.319187	
33.76481	19.51910	12.72854	1.206750	0.376976	
24.92415	17.65097	11.78930	1.162991	0.437870	
18.05814	14.35504	11.97759	1.248386	0.643279	
14.27560	12.41357	11.60938	1.284954	0.813232	
12.42047	11.26690	11.08178	1.240290	0.892218	
10.51953	9.889155	9.353944	1.100078	0.669958	
8.880192	8.498304	7.906650	0.943201	0.890326	

Page 4

Cyanamid B72A

PSF03448

Tw	B U / D	Log	Log	Log
dynes/cm ²	(1/s)	lw	hw	H U / D
0.875233	80.52474	0.05787	1.205929	
0.626754	57.51767	0.20790	1.759801	
0.447395	41.00405	-0.34930	1.617677	

Regression Output:
 Constant 1.95870
 Std Err of Y Est 0.000762
 R Squared 0.999992
 No. of Observations 1
 Degrees of Freedom 1

X Coefficient(s) 0.997180
 Std Err of Coef. 0.002723

R² = 0.011010
 R² = 0.997180

Tw = 1.170894
 Res/ft = 0.05.1496

Regression Output:

Constant 14.0087
 Std Err of Y Est 0.076276
 R Squared 0.999556
 No. of Observations 9
 Degrees of Freedom 7

X Coefficient(s) 9.784681
 Std Err of Coef. 0.078394

t = 21.43214 deg C
 s.d.(t) = 0.044749 deg C

PIP13431 1/2/89 13s59 density viscosity
 1.0 P81B Page 14 c)/NaCl 1.000096 1.001592
 S = g <C>(ppm)= 10.017 X cosff -0.00025 -0.02281
 Z = 5.05 ENaCl]= 0.000308 constant 0.003919 -4.14933

MWD-40 (1/s)	D/h (1/s)	Temp (deg C)	<U> (volts)	<U> (volts)	<U>corr (volts)	Batch Vol (ml)
0.267	0.248	20	2.002571	-0.0275	2.030071	
0.24	0.241	20	1.6194	-0.0375	1.6569	
0.207	0.206	20	1.2475	-0.0405	1.288	
0.187	0.188	20	1.0595	-0.0405	1.1005	
0.161	0.162	20	0.8501	-0.0415	0.8916	
0.13	0.131	20	0.590727	-0.0415	0.622727	
0.108	0.109	20	0.4088	-0.0425	0.4508	
0.08	0.081	20	0.236353	-0.0415	0.270055	
0.061	0.062	20	0.1593	-0.0415	0.2003	
0.04	0.041	20	0.0934	-0.0405	0.1334	
0.033	0.033	20	0.069644	-0.0395	0.109144	
0.03	0.031	20	0.059	-0.0395	0.0985	
0.025	0.024	20	0.0479	-0.0395	0.0869	
0.02	0.021	20	0.028868	-0.0385	0.066868	
0.014	0.015	20	0.012222	-0.0375	0.049722	

ID(ca) = 1.45796
 K(U/psi) = 9.6176
 XB(ca2) = 1.669679

t)ssap (sec)	EP (psid)	<U> (cm/s)	Re	Tm dyne/cm2	f	Log(Re/f)1/f	Tap BL = c 0.4 Solvent
0.211078	160.2295	23297.47	29.77854	0.002323	3.050355	11.80142	
0.172834	146.0568	20945.95	24.32953	0.002348	3.006470	11.62588	
0.133921	126.2902	18071.87	19.89331	0.002449	2.951557	11.40623	
0.114425	112.3104	16330.00	16.14292	0.002563	2.917394	11.26957	
0.092705	96.73673	14065.57	13.07863	0.002799	2.871684	11.08673	
0.064748	78.14807	11345.68	9.134611	0.002994	2.793348	10.77499	
0.046872	64.99031	9449.628	6.612658	0.003135	2.723591	10.49436	
0.028911	48.21842	7011.014	4.078718	0.003513	2.618665	10.07466	
0.020824	36.83782	5356.241	2.938144	0.004336	2.547440	9.789760	
0.013870	24.25905	3527.280	1.954807	0.006660	2.439177	9.436710	
0.011350	20.36562	2961.173	1.601335	0.007733	2.415444	9.262578	
0.010241	18.26916	2656.347	1.444868	0.008670	2.393317	9.173271	
0.009035	15.27422	2320.880	1.274711	0.010943	2.366109	9.064438	
0.006934	12.27927	1785.413	0.981174	0.013033	2.309276	8.837104	
0.005169	8.685341	1262.853	0.729361	0.019366	2.244874	8.579499	

122.2234

L	MBR	1/f	1/f	1/f	1/f	1/f	1/f
70.18355	25.55675	20.74491	1.756001	0.295609			
63.45815	24.72293	20.43619	1.775921	0.325296			
55.49332	23.67959	20.20437	1.771345	0.361616			
51.67431	23.03049	19.75111	1.752604	0.382223			
46.51194	22.16200	18.90047	1.704782	0.404357			
39.87124	20.68122	18.27455	1.696015	0.470130			
33.07285	19.34824	17.65740	1.701636	0.539947			
25.97439	17.35464	16.87001	1.674499	0.449484			
22.04551	14.60136	15.18518	1.551128	0.688810			
17.99109	14.32437	12.23356	1.278499	0.681090			
16.27513	13.49724	11.37153	1.227484	0.498704			
15.45958	13.07303	10.73907	1.170692	0.694685			
14.52074	12.53408	9.539049	1.054548	0.658303			
12.73942	11.47625	8.739154	0.991179	0.487551			
10.98385	10.25262	7.185888	0.837560	0.454218			

PIP13451

Tw	B(U)/D	Log	Log
dyne/cm ²	(1/s)	Tw	B(U)/D
1.956807	135.1123	0.291548	2.124218
1.601335	111.7486	0.204482	2.048342
1.444868	100.2450	0.159828	2.001063
1.274711	83.81147	0.105411	1.973307
0.981174	67.37784	-0.00825	1.828517
0.729361	47.65750	-0.13705	1.678131

Regression Output:
 Constant -1.74171
 Std Err of Y Est 0.010553
 R Squared 0.996358
 No. of Observations 6
 Degrees of Freedom 4

X Coefficient(s) 0.953702
 Std Err of Coef. 0.029220

R² = 0.018125
 n² = 0.953702

Tw = 3.098975
 Res/fg = 362.3575

Regression Output:
 Constant 8.18127
 Std Err of Y Est 0.205817
 R Squared 0.981757
 No. of Observations 8
 Degrees of Freedom 6

X Coefficient(s) 9.535890
 Std Err of Coef. 0.530728

t = 20 deg C
 s.d.t = 0 deg C

ID(co) = 1.45796
 R(V/psi) = 9.407
 X3(cm2) = 1.669479

Tap DL = 4
 Solvent

t) samp (sec)	DP (psid)	<U> (co/s)	Re	Te (dyne/cm ²)	f	Log(Re/f) ^{1/3}
0						
0.152662	149.4677	21974.29	21.53735	0.001931	2.986925	11.53970
0.128736	132.0770	19378.16	17.59761	0.002020	2.940071	11.36028
0.106232	117.7013	17268.97	14.98711	0.002167	2.905203	11.22081
0.093684	106.3205	15599.20	13.21674	0.002342	2.877906	11.11162
0.077441	91.9482	13490.01	10.95351	0.002595	2.837121	10.94848
0.059104	74.57413	10941.41	8.338396	0.003003	2.777885	10.71154
0.045393	61.69587	9051.932	6.432263	0.003385	2.721526	10.48610
0.040365	53.31002	7821.572	5.694738	0.004013	2.692081	10.38032
0.031718	42.82771	6283.622	4.474784	0.004866	2.642729	10.17091
0.023493	32.64490	4789.614	3.314362	0.006229	2.577544	9.910177
0.019262	24.35531	3866.844	2.717477	0.007836	2.534427	9.757709
0.015650	21.26411	3123.361	2.207908	0.009781	2.489827	9.559310
0.012791	14.47219	2419.505	1.804653	0.013323	2.446033	9.384135
0.010518	12.87826	1893.748	1.483881	0.017923	2.404029	9.216116
0.008344	9.583825	1409.301	1.177273	0.025676	2.353768	9.015073
0.007049	7.487363	1101.016	0.994581	0.035539	2.317149	8.868598

1/8/89 13:01
 1.0 PSD Taps 14
 S = B <C> (ppm) = 20.6882 K coeff -0.00025 -0.02281
 Z = 5.03 [Mac1] = 0.000309 constant 0.003419 -4.14933

density viscosity
 1.000096 1.001592
 -0.00025 -0.02281
 0.003419 -4.14933

MWD-60 (1/s)	MWD-40 (1/s)	Temp (deg C)	<V> (volts)	<U> (volts)	<U>corr (volts)	Batch Vol (ml)
0.249	0.25	20.5	1.3116	-0.1245	1.4361	
0.22	0.221	20.4	1.0404	-0.1245	1.1734	
0.196	0.197	20.4	0.872833	-0.1255	0.999333	
0.177	0.178	20.4	0.753285	-0.1275	0.881285	
0.153	0.154	20.4	0.601875	-0.1285	0.730375	
0.124	0.125	20.4	0.4275	-0.1285	0.556	
0.102	0.104	20.4	0.2999	-0.1285	0.4289	
0.088	0.09	20.4	0.250222	-0.1295	0.379722	
0.071	0.072	20.4	0.168875	-0.1295	0.298375	
0.056	0.055	20.4	0.092	-0.1295	0.221	
0.043	0.045	20.4	0.0527	-0.1285	0.1812	
0.035	0.036	20.45	0.019222	-0.1285	0.147222	
0.027	0.028	20.45	-0.00466	-0.1275	0.120333	
0.021	0.022	20.5	-0.02755	-0.1265	0.098944	
0.016	0.016	20.5	-0.048	-0.1265	0.0785	
0.012	0.013	20.5	-0.06018	-0.1265	0.064318	
				-0.1265		

L	1//t	MDR	1//t	1//t	1//t/PM	1//t/L
60.36786	24.31158	22.75247	1.971648	0.374897		
54.44415	23.46135	22.24545	1.958177	0.408392		
50.24391	22.79886	21.48143	1.914427	0.427542		
47.18311	22.28022	20.64311	1.859594	0.437954		
42.95376	21.50530	19.42848	1.792822	0.454972		
37.47707	20.37982	18.24684	1.703475	0.486860		
32.91594	19.30899	17.18759	1.639082	0.522146		
30.97143	18.60654	15.78384	1.520534	0.509425		
27.45424	17.81185	14.30476	1.446437	0.521040		
23.42786	16.57334	12.64940	1.278423	0.536206		
21.39475	15.75411	11.27612	1.160037	0.527985		
19.50667	14.90372	10.11101	1.057713	0.523795		
17.45475	14.07446	8.643489	0.923205	0.994339		
15.84561	13.27455	7.467528	0.810485	0.471393		
14.11394	12.52159	6.240732	0.692235	0.442147		
12.97268	11.62584	5.304495	0.598121	0.406897		

Yw	8<U>/D	Log	Log
dynes/cm2	(1/g)	Tw	8<U>/D
2.207908	116.6787	0.343981	2.066991
1.804653	90.38491	0.256393	1.956095
1.483881	70.64457	0.171399	1.849201
1.177273	52.58758	0.070877	1.730883
0.994581	41.08405	-0.00235	1.613673

Regression Output:
 Constant -1.24819
 Std Err of Y Est 0.004299
 R Squared 0.999282
 No. of Observations 5
 Degrees of Freedom 3

X Coefficient(s) 0.769132
 Std Err of Coef. 0.011902

K' = 0.056467
 n' = 0.769132

Regression Output:
 Constant -34.7115
 Std Err of Y Est 0.234639
 R Squared 0.955974
 No. of Observations 4
 Degrees of Freedom 2

X Coefficient(s) 19.30190
 Std Err of Coef. 2.930358

t = 20.43125 deg C
 s.d.t = 0.042847 deg C

Page 1

Cyanamid 832A

PIP01346 12/25/88 14506
 1.0 P810 Taps 14 Taps 14
 B = 8
 Z = 5.05

<C>(ppm)= 1.03135 X coeff
 [NaCl] = 0.001033 constant

PHD-40 0)1 (1/s)	PHD-40 0)h (1/s)	Temp (deg C)	<U> (volts)	<V> (volts)	<U>corr (volts)	Batch Vol (ml)
0.226	0.227	20.15	4.164571	0.0435	4.126071	
0.202	0.202	20.05	3.396833	0.0335	3.363333	
0.187	0.188	20.08	3.0125	0.0315	2.9815	
0.174	0.175	20	2.433833	0.0305	2.403833	
0.152	0.153	20	2.114571	0.0295	2.085071	
0.127	0.128	20	1.556	0.0295	1.527	
0.106	0.107	20	1.147333	0.0285	1.119333	
0.08	0.08	20	0.6978	0.0275	0.6698	
0.06	0.061	20.1	0.445	0.0285	0.4165	
0.041	0.042	20.05	0.244666	0.0285	0.215666	
0.033	0.034	20.1	0.149375	0.0295	0.139875	
0.024	0.024	20.1	0.083555	0.0295	0.054055	
0.014	0.015	20.1	0.0432	0.0295	0.0337	
0.021	0.022	20.1	0.07925	0.0295	0.04925	
0.028	0.029	20.1	0.116	0.0305	0.086	
				0.0295	0.0295	

Page 2

Cyanamid 832A

density viscosity
 1.000125 1.001657
 -0.00025 -0.02281
 0.003419 -4.14933
 t)error= 0

IP(cm) = 1.45796
 K(U/psi) = 9.6176
 XB(cm2) = 1.669479
 0.4

t)temp (sec)	BP (psid)	<U> (cm/s)	Re	Tw dyne/cm2	f	Log(Re/f)1/f	Solvent
0.429012	135.9705	19834.49	60.52418	0.006557	3.205823	12.42329	
0.349810	120.9957	17612.08	49.35066	0.006751	3.160519	12.24207	
0.510004	112.6099	16391.44	43.73478	0.006907	3.134287	12.13715	
0.270734	104.8230	15240.78	38.19490	0.006962	3.104384	12.01753	
0.216797	91.64532	13324.80	30.58532	0.007293	3.056138	11.82455	
0.158771	76.67060	11147.54	22.39913	0.007631	2.988497	11.55398	
0.116383	64.09183	9318.633	16.41918	0.008005	2.921057	11.28422	
0.069643	47.91912	6967.217	9.825108	0.008570	2.809550	10.83820	
0.043306	36.53833	5324.502	6.109521	0.009166	2.707370	10.42948	
0.022424	25.15754	3661.917	3.163553	0.010011	2.563961	9.855847	
0.019543	20.38562	2967.755	2.051787	0.009908	2.470433	9.481732	
0.005620	14.37573	2094.886	0.792923	0.007685	2.263983	8.655932	
0.003503	8.984836	1309.303	0.494335	0.012265	2.161377	8.245511	
0.003120	13.17775	1920.312	0.722434	0.008332	2.243766	8.575064	
0.008941	17.37068	2531.320	1.261509	0.008373	2.364812	9.059248	

Tap BL=

L	MDR	1//4	1//4	1//4	1//4/PK	1//4/L
100.3931	28.51043	12.34926	0.994040	0.123009		
90.64819	27.64987	12.17000	0.994112	0.134532		
85.14469	27.15146	12.03176	0.991317	0.141306		
79.48119	26.58330	11.98458	0.997258	0.150785		
71.12434	25.86642	11.78907	0.990234	0.144628		
60.86635	24.59144	11.44674	0.990718	0.188863		
52.11197	23.10009	11.17423	0.990429	0.214465		
40.31163	20.90145	10.80212	0.996471	0.267945		
31.06034	19.04003	10.44500	1.001488	0.327837		
22.90033	14.31527	9.99169	1.014034	0.436420		
18.46345	14.53822	10.04604	1.059315	0.546104		
11.47791	10.61567	11.40715	1.317842	0.993834		
9.042707	8.66180	9.029475	1.095077	0.996333		
10.95585	10.23155	10.95483	1.277521	0.999907		
14.47745	12.53143	10.92785	1.206245	0.754818		

PIP01344

Tm	B U/D	Lon	log
dyna/co2	(1/s)	Tm	B U/D
0.792925	78.88138	-0.10076	1.896974
0.494335	49.30086	0.30597	1.92854
0.722434	72.30793	-0.14120	1.859186

Regression Output:
 Constant 2.00062
 Std Err of Y Est 0.001875
 R Squared 0.99981
 No. of Observations 3
 Degrees of Freedom 1
 X Coefficient(s) 1.000902
 Std Err of Coef. 0.012209
 K' = 0.009985
 n' = 1.000902

Tm = 0.000020
 Res/18 = 0.925987

Regression Output:
 Constant 0.40088
 Std Err of Y Est 0.013512
 R Squared 0.99617
 No. of Observations 6
 Degrees of Freedom 6
 X Coefficient(s) 7.977577
 Std Err of Coef. 0.100536

t = 20.06 dfr 6
 s.d.t = 0.048987 deg t

P2P01346

12/29/88 15:26 density viscosity

1.0 P81D Taps 14 0 NaCl 1.000125 1.001657

S = 0 <C> (ppm) = 2.0433 X coeff -0.00025 -0.02281

Z = 5.05 [NaCl] = 0.001034 constant 0.003419 -4.14933

WHD-40 Q1 (1/s)	WHD-40 Q/h (1/s)	Temp (deg C)	<U> (volts)	<U>e (volts)	<U>corr (volts)	Batch Vol (ml)
0.243	0.244	21.7	3.914333	-0.0245	3.942335	
0.222	0.224	21.7	3.387857	-0.0315	3.419107	
0.196	0.198	21.7	2.727371	-0.031	2.759071	
0.181	0.182	21.7	2.345428	-0.032	2.394928	
0.157	0.158	21.7	1.845428	-0.031	1.877428	
0.129	0.13	21.7	1.329375	-0.033	1.362375	
0.108	0.109	21.7	0.9885	-0.033	1.0215	
0.081	0.082	21.7	0.591285	-0.033	0.624285	
0.061	0.062	21.7	0.342875	-0.033	0.393875	
0.041	0.042	21.7	0.173428	-0.033	0.206178	
0.034	0.034	21.7	0.104425	-0.0325	0.140875	
0.025	0.024	21.7	0.0244	-0.032	0.0574	
0.019	0.019	21.7	0.011923	-0.031	0.042423	
0.012	0.013	21.65	-0.0627	-0.0305	0.0278	

ID(cm) = 1.45794 Tap DL=

K(U/psi) = 9.6176 4

XS(cm2) = 1.669479 0.4

0	PP (paid)	<U> (cm/s)	Re	Tw dyne/cm2	f	Log(Re/f)1/4	Solvent
0.409908	145.8538	22035.57	57.82898	0.005444	3.211202	13.44481	
0.355505	133.5745	20180.42	50.15392	0.005632	3.180282	12.32112	
0.284877	118.0008	17827.55	40.47204	0.005824	3.133707	12.13483	
0.249223	108.7165	16424.87	35.15987	0.005960	3.103153	12.01241	
0.195207	94.34077	14252.99	27.53947	0.006200	3.050107	11.80043	
0.141454	77.54908	11719.12	19.98429	0.006455	2.980474	11.52189	
0.104211	64.99031	9618.727	14.98409	0.007108	2.917945	11.27178	
0.06910	48.81760	7375.357	9.157472	0.007699	2.811017	10.84407	
0.041161	36.83782	5565.453	5.806979	0.008574	2.712105	10.44842	
0.021437	24.85804	3755.550	3.824375	0.009807	2.570447	9.881791	
0.014647	20.34562	3076.836	2.864455	0.009983	2.487743	9.550972	
0.005989	15.27422	2307.437	0.844918	0.007256	2.295537	8.774149	
0.004410	11.38079	1719.408	0.622292	0.009627	2.237127	8.508508	
0.002890	7.487363	1129.914	0.407790	0.014575	2.134855	8.139423	

122.2234

L	MDR	1//f	1//f/PM	1//f/L
101.6442	28.61285	13.54944	1.088742	0.133302
94.65912	28.07534	13.32440	1.061427	0.140761
85.03302	27.14044	13.10340	1.079817	0.154097
79.25628	26.55991	12.95234	1.078228	0.163423
70.14354	25.55204	12.69783	1.074218	0.181054
59.75227	24.22901	12.25603	1.043870	0.205147
51.73986	23.04093	11.84648	1.052244	0.229234
40.44807	21.00933	11.39433	1.050927	0.281732
32.20958	19.12999	10.79929	1.033501	0.335281
23.24491	16.43650	10.09777	1.021854	0.434407
19.21423	14.86711	10.00832	1.047898	0.520880
12.28619	11.17721	11.73692	1.337898	0.955454
10.54404	9.915416	10.19182	1.197838	0.946595
8.525815	8.162262	8.283038	1.017444	0.971524

P2P01346

Tw	B U /D	Log	Log	Log
dyne/cm ²	(1/s)	Tw	Tw	B U /D
0.844918	87.61147	0.07318	1.923307	
0.622292	62.44776	-0.20600	1.795516	
0.407790	41.08405	-0.38956	1.612672	

Regression Output:

Constant -2.07766
 Std Err of Y Est 0.001827
 R Squared 0.999977
 No. of Observations 1
 Degrees of Freedom 1
 X Coefficient(s) 1.020955
 Std Err of Coef. 0.008107
 K = 0.009169
 n = 1.020955

Tw = 1.646760
 Res,fe = 274.4386

Regression Output:

Constant 5.79709
 Std Err of Y Est 0.041116
 R Squared 0.991117
 No. of Observations 10
 Degrees of Freedom 9

X Coefficient(s) 5.79709
 Std Err of Coef. 0.065049

t = 21.69442 deg C
 s.d.)t = 0.012876 deg C

PSP01349 12/30/88 14:17 density viscosity
 1.0 PB10 Taps 14 colNaCl 1.000125 1.001457
 8 = @ (C)(ppm)=5.577148 X coeff -0.00025 -0.02281
 Z = 5.05 [NaCl]= 0.001034 constant 0.003419 -4.14933

#MB-40 @1 (1/a)	#h (1/a)	Temp (deg C)	<V> (volts)	<U> (volts)	<U>corr (volts)	Batch Vol (ml)
0.22	0.221	21.1	2.69557	-0.0355	2.73107	
0.205	0.206	21.1	2.424857	-0.041	2.466107	
0.183	0.185	21.1	2.632333	-0.0415	2.075333	
0.17	0.17	21.1	1.78	-0.0405	1.82075	
0.168	0.149	21.1	1.927	-0.041	1.46775	
0.121	0.122	21.1	1.03775	-0.0405	1.079	
0.102	0.103	21.1	0.788	-0.042	0.82975	
0.075	0.074	21.1	0.4475	-0.0415	0.50625	
0.054	0.057	21.1	0.277	-0.0415	0.318	
0.037	0.038	21.1	0.127	-0.0405	0.1675	
0.028	0.03	21.1	0.058272	-0.0405	0.078522	
0.025	0.024	21.1	0.022875	-0.04	0.042375	
0.017	0.018	21.1	0.005	-0.039	0.0435	
0.012	0.012	21.1	-0.01	-0.0385	0.0285	
				-0.038		

DP (psid) 132.0770 19685.90 40.10585 0.004606 3.125829 12.10331
 K(V/psi)= 9.6176
 XB(cc2)= 1.669479
 Tap DL= 4
 0.4

t) samp (sec)	DP (psid)	<U> (cc/a)	Re	Iw dyne/cm2	f	Log(Re/f)1/f	Solvent
0.284281	132.0770	19685.90	40.10585	0.004606	3.125829	12.10331	
0.234414	123.0922	18346.75	36.17443	0.004783	3.103427	12.01370	
0.215574	110.2139	14427.24	30.41314	0.005016	3.065755	11.84502	
0.189314	101.8281	15177.34	26.70807	0.005140	3.037544	11.75018	
0.152410	88.94987	13257.85	21.53001	0.005451	2.990747	11.56298	
0.112190	72.77717	10847.33	15.82754	0.005987	2.923931	11.29572	
0.066274	61.39638	9151.045	12.17137	0.004469	2.864894	11.06757	
0.052437	45.22367	6740.528	7.426039	0.007274	2.759603	10.63841	
0.033044	33.64289	5044.234	4.644652	0.008159	2.658654	10.23453	
0.017415	22.44209	3347.943	2.457010	0.009756	2.519428	9.677714	
0.004485	15.27422	2276.601	0.914961	0.007857	2.304926	8.819706	
0.004522	10.48230	1562.373	0.438089	0.011634	2.226665	8.506663	
0.002943	7.187848	1071.341	0.418058	0.016211	2.134843	8.139374	

Page 3

Cyanasid 832A

122.2234

L	MDR	1//f	1//f	1//f/PM	1//f/L
83.50433	26.99075	14.73419	1.217349	0.174448	
79.50621	26.56511	14.45877	1.203322	0.182315	
72.71697	25.84936	14.11916	1.190182	0.194165	
68.14381	25.31358	13.92932	1.184489	0.204278	
61.18251	24.42419	13.54334	1.171267	0.221389	
52.45883	23.15470	12.92382	1.144134	0.244345	
44.00180	22.07100	12.43299	1.123370	0.270271	
35.93219	20.03247	11.72438	1.102069	0.326291	
28.47834	18.11404	11.07032	1.081443	0.388727	
20.66848	15.44914	10.12393	1.046108	0.489824	
14.15138	12.30345	11.43473	1.267754	0.806029	
12.41265	11.39340	11.28133	1.279105	0.894445	
10.53284	9.90451	9.270838	1.069852	0.680183	
8.525375	8.162029	7.853083	0.964924	0.921214	

Page 4

Cyanasid 832A

PSP01349

T _w	8:U/D	Log	Log
dyne/cm ²	(1/s)	T _w	8:U/D
0.914961	83.81147	-0.03859	1.923303
0.438089	57.51767	-0.19511	1.759801
0.418058	59.44069	-0.37876	1.595944

Regression Outputs:
 Constant -2.07273
 Std Err of Y Est 0.010922
 R Squared 0.997942
 No. of Observations 3
 Degrees of Freedom 1

X Coefficient(s) 1.039150
 Std Err of Coef. 0.047185
 K' = 0.009273
 n' = 1.039150

T_w = 3.192290
 Res/fs = 376.9381

Regression Outputs:
 Constant -12.5079
 Std Err of Y Est 0.040061
 R Squared 0.996974
 No. of Observations 6
 Degrees of Freedom 4

X Coefficient(s) 8.699813
 Std Err of Coef. 0.239636

t = 21.1 deg C
 s.d.(t) = ERR deg C

PIP11352 1.0 PS18 Taps 14 1/2/8P 13i50 density viscosity
 g = 0 <C>(ppal)= 10.017 X coeff -0.00025 1.00125 1.001457
 Z = 5.03 [MnCl2]= 0.601014 constant 0.003419 -4.14933

MWD-60 (1/s)	MWD-60 (1/s)	Temp (deg C)	<U> (volts)	<V> (volts)	<U>corr (volts)	Batch (ml)	Vol
0.257	0.258	19.7	2.3815	-0.0345	2.423		
0.234	0.235	19.7	2.011375	-0.0465	2.058375		
0.201	0.202	19.7	1.568272	-0.0475	1.615772		
0.183	0.184	19.7	1.3708	-0.0475	1.4383		
0.157	0.158	19.7	1.032888	-0.0475	1.080388		
0.128	0.129	19.7	0.742875	-0.0475	0.810425		
0.106	0.107	19.7	0.550142	-0.048	0.597892		
0.078	0.079	19.7	0.333875	-0.0475	0.381375		
0.06	0.061	19.7	0.17555	-0.0475	0.227055		
0.039	0.04	19.7	0.073	-0.0475	0.12		
0.035	0.034	19.7	0.058888	-0.0465	0.105388		
0.029	0.03	19.7	0.046777	-0.0465	0.097277		
0.023	0.024	19.7	0.024545	-0.0465	0.070545		
0.016	0.017	19.7	0.005142	-0.0455	0.056142		
0.012	0.013	19.7	-0.007	-0.0445	0.0375		

0	t) ramp (sec)	Re	Tm dyne/cm2	f	Log (ke/f)1/f	Solvent	Tap DL=
0.251933	154.2396	22274.46	35.54230	0.002992	3.085798	11.94319	
0.214021	139.8439	20198.40	30.19372	0.003091	3.050384	11.80153	
0.188001	120.8962	17430.31	23.70131	0.003258	2.997812	11.59124	
0.149548	109.9144	15873.26	21.09801	0.003497	2.972546	11.49018	
0.112334	94.34077	13624.18	15.84792	0.003566	2.910412	11.24164	
0.094285	78.97009	11115.60	11.89083	0.004019	2.848032	10.92212	
0.062166	63.79233	9212.596	8.770322	0.004316	2.781933	10.72773	
0.039453	47.02064	6790.468	5.594282	0.005067	2.684298	10.33719	
0.023608	36.23883	5233.418	3.330614	0.005079	2.571688	9.884753	
0.012477	23.66006	3416.860	1.760246	0.006297	2.433712	9.332851	
0.010957	21.26411	3070.848	1.545920	0.006847	2.405019	9.220078	
0.009074	17.67017	2551.832	1.280233	0.008211	2.346074	9.056396	
0.007335	14.07624	2032.815	1.034811	0.010439	2.317856	8.81426	
0.005213	9.88319	1427.295	0.735531	0.015080	2.243726	8.574906	
0.003899	7.487363	1081.284	0.550076	0.019651	2.180637	8.322551	

122.2234

L	1/f	MHR	1/f	1/f	1/f/PR	1/f/L
76.15137	24.23017	18.28135	1.530492	0.240045		
76.18825	23.55730	17.96591	1.524031	0.256232		
62.16595	24.55843	17.51833	1.511941	0.281768		
58.67144	24.07839	14.90905	1.471407	0.288198		
50.85015	22.89783	14.74551	1.489395	0.329310		
44.04458	21.71241	15.77251	1.434892	0.358087		
37.82804	20.43674	15.22109	1.418654	0.402375		
30.21191	18.50164	14.04757	1.358935	0.464940		
23.31139	14.96287	14.03127	1.419199	0.601936		
16.94699	13.83104	12.60127	1.350204	0.743549		
15.88179	13.29537	12.08478	1.310702	0.740920		
14.45284	12.51740	11.03514	1.218505	0.743526		
12.99381	11.43927	9.777802	1.102147	0.752494		
10.95485	10.23080	8.143654	0.949637	0.743328		
9.473440	9.032118	7.133493	0.857128	0.752981		

P1P11352

Tw	8(U)/D	Log	Log
dynes/cm ²	(1/s)	Tw	8(U)/D
1.740246	129.8256	0.245573	2.113360
1.545920	116.4787	0.189187	2.066991
1.280253	96.95836	0.107295	1.986585
1.034811	77.23802	0.014861	1.887831
0.735531	54.23095	-0.13339	1.734947
0.550076	41.08405	-0.25957	1.613673

Regression Output:
 Constant 1.86264
 Std Err of Y Est 0.005707
 R Squared 0.999402
 No. of Observations 6
 Degrees of Freedom 4

X Coefficient(s) 0.994485
 Std Err of Coef. 0.012158

R² = 0.013720
 n² = 0.994485

Tw = 0.380571
 Res/fg = 126.0793

Regression Output:
 Constant -14.0339
 Std Err of Y Est 0.157977
 R Squared 0.989880
 No. of Observations 8
 Degrees of Freedom 6

X Coefficient(s) 10.49075
 Std Err of Coef. 0.433023

t = 19.7 deg C
 s.d.t = 0.000000 deg C

122-2234

L	MDR	1//6	1//4	1//4	1//4/PR	1//1/L
39.10407	24.13901	22.81405	1.983322	0.385978		
53.28016	23.28302	22.11212	1.752894	0.435018		
49.45002	22.46744	21.38123	1.910207	0.432380		
44.97832	21.88534	20.45408	1.854458	0.454754		
38.90434	20.48964	19.42288	1.828885	0.584343		
31.88350	19.03024	17.47490	1.694468	0.554852		
26.46388	17.50869	15.16797	1.580728	0.573157		
20.89435	15.53961	11.78441	1.236125	0.573612		
18.71924	14.45175	10.73378	1.129202	0.573409		
16.46935	13.48483	9.599281	1.031951	0.574555		
15.00222	12.82523	8.081742	0.886048	0.558702		
13.17406	11.75420	6.909175	0.776693	0.524373		
11.53114	10.45387	5.502405	0.635090	0.477174		

P2P11358

Iw	8(U)/D	Log	Iw	Iw	Log	Iw
dyne/cm2	(1/s)	Tm	8 U /D	8 U /D	8 U /D	8 U /D
2.071101	119.9654	0.316201	2.079056			
1.634685	95.31500	0.213434	1.979161			
1.327244	72.30793	0.122951	1.859185			
1.021470	54.23095	0.092235	1.734247			
0.782349	37.79732	0.10659	1.577461			

Regression Outputs:

Constant -1.38145
 Std Err of Y Est 0.006945
 R Squared 0.998331
 No. of Observations 4
 Degrees of Freedom 2

X Coefficient(s) 0.806261
 Std Err of Coef. 0.023304

K' = 0.041547
 r' = 0.806261

Regression Outputs:

Constant -36.7415
 Std Err of Y Est 0.115000
 R Squared 0.991268
 No. of Observations 4
 Degrees of Freedom 2

X Coefficient(s) 20.04210
 Std Err of Coef. 1.322344

t = 20.47307 deg C
 s.d.) t = 0.077497 deg C

P2P01147 12/29/88 16131

1.0 PSID Tape 19 density viscosity

S = 8 <C>(ppm) = 2.0433 X coeff -0.00025 -0.02281

Z = 5.05 [NaCl] = 0.104675 constant 0.003419 -4.14933

MHD-40	MHD-40	Temp	<U>	<U>	<U>	Batch	Vol
(1/a)	(1/s)	(deg C)	(volts)	(volts)	(volts)	(ml)	(ml)
0.208	0.228	21.3	3.819166	-0.0295	3.850416		
0.184	0.189	21.3	2.894	-0.033	2.927		
0.153	0.144	21.3	2.126733	-0.033	2.140483		
0.139	0.143	21.3	1.7788	-0.0345	1.8133		
0.123	0.125	21.3	1.411	-0.0345	1.4465		
0.105	0.104	21.3	1.061857	-0.0365	1.097857		
0.089	0.09	21.3	0.785875	-0.0355	0.819125		
0.067	0.068	21.3	0.465625	-0.035	0.500875		
0.049	0.051	21.3	0.253571	-0.0355	0.288571		
0.033	0.035	21.3	0.112714	-0.0345	0.147214		
0.026	0.028	21.3	0.062375	-0.0345	0.076875		
0.02	0.022	21.3	0.014	-0.0345	0.04775		
0.013	0.014	21.3	-0.00775	-0.033	0.0255		
0.137	0.158	21.2	2.153555	-0.0355	2.188055		
0.148	0.15	21.2	1.947555	-0.0355	2.003055		
0.136	0.137	21.2	1.672833	-0.0355	1.728333		

ID(cm) = 1.45796 Iap DL =

K(V/psi) = 9.6176 4

XS(cm2) = 1.669479 0.4

t)samp	DP	<U>	Re	Iw	f	Log((Re/f)1/3)	Solvent
(sec)	(paid)	(cm/s)		dyn/cm2			
0.400351	130.5796	19450.91	56.48068	0.006609	3.199039	12.39615	
0.304337	113.2089	16863.40	42.93534	0.006685	3.179497	12.15798	
0.224638	94.93976	14142.06	31.49152	0.007016	3.075561	11.89424	
0.188539	85.65343	12739.08	26.59878	0.007234	3.035520	11.74508	
0.150401	74.87363	11153.04	21.21830	0.007552	2.986945	11.54578	
0.114150	63.49284	9457.783	16.10415	0.007971	2.926558	11.30623	
0.085149	53.90901	8030.193	12.01551	0.008250	2.862961	11.05184	
0.052079	40.73125	6067.257	7.347194	0.008837	2.750150	10.62460	
0.030004	30.54844	4550.443	4.232973	0.00904	2.656412	10.14565	
0.015306	20.94461	3122.853	2.159445	0.009804	2.490260	9.561043	
0.007993	16.77169	2498.282	1.127457	0.007999	2.349178	8.996714	
0.004964	13.17775	1962.936	0.700431	0.008048	2.245772	8.587090	
0.002651	8.385847	1249.141	0.374052	0.010614	2.109256	8.038224	
0.227505	94.44027	14065.68	32.09597	0.007150	3.075329	11.90131	
0.208249	89.84836	13353.49	29.38226	0.007262	3.056147	11.82478	
0.177705	82.06150	12194.19	25.35243	0.007512	3.024114	11.69645	

122.2234

L 1//4	MDR 1//4	1//4	1//4/PK	1//4/L
98.83706	28.38175	12.29985	0.992231	0.124445
86.17421	27.25044	12.23060	1.005972	0.141928
74.03574	25.99746	11.93854	1.003724	0.141253
67.82672	23.27489	11.75706	1.001275	0.173339
66.57943	24.34245	11.50463	0.996609	0.189942
52.77629	23.20461	11.20032	0.990632	0.212222
45.58700	21.99826	11.00943	0.996162	0.241503
35.64763	19.96686	10.43755	1.001218	0.298408
27.05781	17.49184	10.51092	1.034003	0.388461
19.32595	14.91495	10.09928	1.056295	0.522576
13.96556	12.23439	11.18054	1.242736	0.600579
11.00458	10.26968	11.14437	1.298643	1.012700
8.043333	7.681565	9.704339	1.207522	1.206755
74.33784	26.03126	11.82580	0.993655	0.159081
71.12582	25.66679	11.73404	0.992342	0.164975
66.06851	25.05817	11.53744	0.986405	0.174628

P2P01147

1w# = 0.001A14
Res/1# = R.455411

Regression Output:

Constant -0.38124
Std Err of Y Est 0.075275
R Squared 0.979942
No. of Observations 11
Degrees of Freedom 9

X Coefficient(s) 7.979770
Std Err of Coef. 0.189790

t = 21.28125 deg C
s.d.(t) = 0.039031 deg C

P5F01150

12/30/89 16:10

1.0 P81D Taps 14

g = 0 <C> (ppm) = 5.57168 X coeff -0.00025 -0.02281
 Z = 5.05 [NaCl] = 0.164287 constant 0.003419 -0.14933

density viscosity

co)NaCl 1.00417 1.010849

X coeff -0.00025 -0.02281

constant 0.003419 -0.14933

0.003419 -0.14933

MWD-40 0/1 (1/s)	MWD-40 0/h (1/s)	Temp (deg C)	<U> (volts)	<U> (volts)	<U> (volts)	Batch Vol (ml)
0.14	0.214	20.4	2.924428	-0.0355	2.942928	
0.14	0.15	20.4	1.9215	-0.0375	1.96	
0.125	0.131	20.4	1.504777	-0.0395	1.544277	
0.11	0.115	20.4	1.195	-0.0395	1.2345	
0.099	0.102	20.4	0.959777	-0.0395	0.998277	
0.084	0.088	20.4	0.722090	-0.0395	0.741590	
0.073	0.075	20.4	0.5489	-0.0395	0.5804	
0.058	0.06	20.4	0.356777	-0.0395	0.396277	
0.045	0.047	20.4	0.215265	-0.0395	0.254285	
0.031	0.033	20.4	0.09025	-0.0385	0.12875	
0.036	0.039	20.4	0.147102	-0.0385	0.185442	
0.025	0.027	20.45	0.023181	-0.0385	0.045681	
0.015	0.018	20.7	-0.00127	-0.0385	0.034227	
0.01	0.012	20.7	-0.01433	-0.0365	0.022144	
0.11	0.115	20.4	1.205090	-0.0365	1.243090	
0.103	0.104	20.4	1.0553	-0.0395	1.0948	
0.094	0.099	20.4	0.898181	-0.0395	0.927481	
				-0.0395		

ID(cm) = 1.45796	DP (psia)	<U> (cm/s)	Re	Te dyne/cm2	f	Log(Re/f)/f	Tap DL = K(V/psi) = 9.6174 XB(Ce2) = 1.649479	Solvent
0.308073	112.4099	16511.56	43.46236	0.006838	3.135250	12.14100		
0.203793	89.84834	13173.96	28.75049	0.007105	3.045517	11.78207		
0.149567	78.46756	11505.25	22.65257	0.007340	2.993752	11.57500		
0.128358	48.68374	10100.03	18.10853	0.007414	2.943135	11.38054		
0.103794	41.09488	8958.293	14.64345	0.007826	2.897015	11.19406		
0.079187	51.51306	7553.071	11.17156	0.008399	2.849250	10.96100		
0.061179	44.32519	6499.154	8.631074	0.008764	2.78225	10.73690		
0.041203	35.34035	5181.758	5.812887	0.009285	2.698389	10.39355		
0.026439	27.55349	4040.014	3.730045	0.009802	2.602050	10.00820		
0.013386	19.16745	2810.445	1.888597	0.010255	2.454263	9.417052		
0.019302	23.04107	3381.316	2.723143	0.010216	2.533728	9.734914		
0.006421	15.57371	2286.063	0.934130	0.007484	2.301889	8.807539		
0.003746	9.883319	1452.408	0.531407	0.010854	2.179892	8.319370		
0.002304	6.588979	968.2724	0.325156	0.014943	2.073224	7.892899		
0.129251	67.38427	9880.471	18.23455	0.008011	2.946641	11.38656		
0.113832	62.59435	9177.859	16.05931	0.008177	2.919056	11.27422		
0.096456	57.50295	8431.335	13.60790	0.008210	2.883089	11.13235		

122.2234

L	MDR	1//4	1//4	1//4/PR	1//4/L
85.33559	27.16975	12.09294	0.994943	0.141710	
49.40410	25.44403	11.06311	1.006078	0.170925	
41.40732	24.48129	11.47194	1.008374	0.109457	
55.00269	23.55754	11.46608	1.004989	0.208052	
49.53307	22.48129	11.50302	1.009589	0.228199	
43.24438	21.54475	10.91121	0.995457	0.252198	
38.02821	20.50029	10.68144	0.994834	0.280082	
31.20825	18.64959	10.37737	0.998443	0.332520	
24.99945	17.03894	10.10023	1.009197	0.404019	
17.78845	14.23100	9.874424	1.048548	0.555094	
21.34034	15.74004	9.895443	1.016307	0.463178	
12.52477	11.33590	11.40770	1.295217	0.910811	
9.457418	9.017959	9.598342	1.153704	1.014900	
7.597841	6.991274	8.108543	1.036420	1.163777	
55.27402	23.58417	11.17214	0.981149	0.202172	
51.87247	23.04208	11.05819	0.980444	0.213180	
47.74955	22.37849	11.03508	0.991336	0.231120	

PSF01150

Two = 7.711148
Res/16 = 399.9017

Regression Output:
 Constant -0.21894
 Std Err of Y Est 0.171342
 R Squared 0.981117
 No. of Observations 12
 Degrees of Freedom 10
 X Coefficient(s) 3.930414
 Std Err of Coef. 0.249991
 t = 20.61470 deg C
 s.d.t = 0.033275 deg C

PIP11153 1/2/89 17:10 density viscosity
 1.0 PBID Taps 14 8 <C>(ppm)= 10.017 X coeff -0.0025 -0.02281
 B = 5.05 [NaCl]= 0.104987 constant 0.003419 -4.14933
 Z =
 MHD-40 MHD-40 Teop C) <V> <U> <V>corr Batch Vol
 0)l 0)h (l/s) (deg C) (volts) (volts) (volts) (ml)
 0.238 0.241 19.5 3.245425 -0.0435 3.293125
 0.215 0.218 19.4 2.807333 -0.0515 2.859833
 0.188 0.19 19.4 2.2845 -0.0515 2.3355
 0.148 0.17 19.4 1.92725 -0.0505 1.97775
 0.14 0.144 19.4 1.514664 -0.0505 1.543164
 0.108 0.112 19.45 1.013777 -0.0505 1.044277
 0.084 0.088 19.45 0.685142 -0.0505 0.735642
 0.054 0.058 19.5 0.3225 -0.0505 0.372
 0.034 0.041 19.5 0.123375 -0.0485 0.170375
 0.015 0.021 19.5 -0.01154 -0.0475 0.035454
 0.025 0.029 19.5 0.015 -0.0465 0.062
 0.227 0.228 19.5 3.0255 -0.0475 3.073
 -0.0475

ID(cm) = 1.45796 Tap DL =
 K(U/psi) = 9.4174 4
 X8(ca2) = 1.449479 0.4
 Solvent
 0
 (t)amp DP <U> Re Tm f Log(Ke/f)1/f
 (sec) (psid) (cm/s) (dyne/cm2)
 0.342404 143.4578 20518.85 48.30592 0.004681 3.147356 12.18942
 0.297250 129.4811 18504.54 41.93542 0.004973 3.115641 12.06244
 0.242834 113.2089 16155.84 34.25879 0.005331 3.071757 11.88702
 0.205438 101.2291 14446.23 29.01106 0.005666 3.035652 11.74261
 0.162739 85.05444 12139.25 22.95899 0.006329 2.984847 11.59339
 0.110459 65.88879 9413.485 15.61159 0.007172 2.901587 11.20634
 0.076489 51.51304 7359.634 10.79093 0.008110 2.821393 10.88557
 0.038479 34.14237 4883.402 5.456743 0.009336 2.675823 10.29529
 0.017714 23.04107 3298.438 2.499183 0.009372 2.504255 9.617021
 0.003684 10.78180 1542.127 0.520072 0.008923 2.163388 8.253553
 0.004446 16.17270 2313.190 0.909460 0.006935 2.284748 8.738993
 0.319518 136.2700 19490.77 45.07497 0.004841 3.133333 12.12933

Page 3 Cyanamid 832A

122.2234

L	MDR	1//t	1//t	1//t/PM	1//t/L
87.74786	27.39977	14.61492	1.190904	0.164555	
81.37210	26.79757	14.17940	1.175497	0.173829	
75.72880	25.96338	13.89533	1.152124	0.185752	
67.84755	25.27740	13.50765	1.133379	0.196141	
60.35398	24.31210	12.54923	1.089245	0.208248	
49.82729	22.73015	11.86784	1.053656	0.236971	
41.42603	21.20447	11.10357	1.020026	0.269033	
29.49197	18.40265	10.34900	1.003216	0.356909	
19.95884	15.18985	10.32887	1.074020	0.517508	
9.104757	8.704379	10.56599	1.282398	1.162688	
12.04004	11.01021	12.06779	1.374047	0.997320	
84.76944	27.11434	14.37127	1.184836	0.169543	

Page 4

Cyanamid 832A

PIP11153

Tss = 10.11657
Res/1g = 642.4987

Regression Output:

Constant -19.6917
Std Err of Y Est 0.100778
R Squared 0.99461/ B
Mo. of Observations 8
Degrees of Freedom 6
X Coefficient (s) 10.87045
Std Err of Coef. 0.326461
t = 19.45833 deg C
s.d.t = 0.046876 deg C

122.2234

L	MNR	1//t	1//t	1//t/PK	1//t/L
75.67722	26.17861	17.31881	1.451418	0.228851	
69.98954	25.53391	16.72553	1.417825	0.238971	
65.84594	25.03033	15.88455	1.359917	0.241248	
61.67162	25.48990	15.46375	1.330914	0.249835	
54.11477	25.71104	14.59862	1.278438	0.260004	
49.44821	22.66714	13.54784	1.212143	0.274384	
44.13015	21.72825	12.61089	1.146922	0.285745	
34.95649	20.04101	11.54163	1.045499	0.314549	
29.51436	18.40891	10.50900	1.020529	0.314030	
24.17579	16.76251	10.00154	1.005179	0.413760	
20.00240	15.19884	9.753045	1.013764	0.487594	
15.85594	13.28193	10.40911	1.129398	0.456480	
12.18950	11.11201	11.05770	1.262233	0.907149	
10.39347	9.794893	9.273500	1.093114	0.892225	
8.535941	8.172056	7.742917	0.951044	0.907095	

P2P11159

Tw	B(U)/D	Log	Log
dyna/cm2	(1/s)	Tw	B-U /D
2.382496	116.6787	0.377052	2.046991
1.493712	98.60172	0.174267	1.993884
0.882784	80.52474	-0.05414	1.905929
0.640376	57.51767	-0.19356	1.759801
0.431916	39.44069	-0.36459	1.595944

Regression Output:
 Constant 1.96214
 Std Err of Y Est 0.005655
 R Squared 0.999338
 No. of Observations 3
 Degrees of Freedom 1

X Coefficient(s) 1.002366
 Std Err of Coef. 0.025787

K' = 0.010910
 n' = 1.002366

Tw = 7.435025
 Res/fs = 565.3629

Regression Output:
 Constant 44.7502
 Std Err of Y Est 0.111520
 R Squared 0.996354
 No. of Observations 7
 Degrees of Freedom 5

X Coefficient(s) 20.11373
 Std Err of Coef. 0.544102

t = 20.61 deg C
 s.d.(t) = 0.087939 deg C

APPENDIX G

NOMENCLATURE

Latin Symbols

a	Effective backbone chain link length; Mark-Houwink-Kuhn-Surada (MHKS) exponent in equations 2.4-7, 2.4-8, and 2.4-9
A	Dimensionless slope in equations 5.1-1 and 5.2-1; dimensionless constant in equation 2.4-12; dimensionless lin charge density in Appendix A
Å	Angstrom, 10^{-8} cm
b	Polyion effective radius in Appendix A
B	Dimensionless intercept in equations 5.1-1 and 5.2-1; dimensionless constant in equation 2.4-12.
ΔB	Dimensionless upward shift of the mean-velocity profile above Newtonian
C	Constant in equation 3.1-1
c	Polymer concentration in weight parts-per-million (wppm)
c_i	Concentration of species i
C_p	Injected polymer concentration
$\langle C \rangle$	Average concentration in injection experiment assuming total dissolution
C_{uv}	u-v correlation coefficient, $-\langle uv \rangle / (u'v')$
d	Additive diameter
D	Pipe inner diameter
D_h	Hydraulic diameter
DR	Drag reduction
e	Standard error
f	Fanning friction factor, $2T_w / (\rho u_\tau^2)$

Latin Symbols(continued)

f_0	Macromolecular friction coefficient
$1/\sqrt{f}$	Prandtl-Karman ordinate, $\langle \bar{U} \rangle / (\sqrt{2}u_r)$
F	Bursting frequency, $1/T_{bb}$
G	Elastic modulus in equation 2.3-20
g	Acceleration of gravity, 980.6 cm ² /s
$\langle h^2 \rangle$	Root-mean-square end-to-end length
h	Fluid height in manometer
I	Solvent ionic strength, $\frac{1}{2}\sum z_i c_i^2$
K'	MHKS constant, dimensionless; pseudo-power-law coefficient, cm ³ /g(by convention)
k	Boltzman's constant, 1.380667×10^{-23} J/(K · atom)
k'	Huggins constant, 0.35 - 0.40, dimensionless
$k_{s\infty}$	Slope coefficient in equation 2.4-13
L	Length of pipe
L_c	Additive contour length
ℓ	Backbone link distance, C-C
ℓ'	Kuhn statistical segment length, $1/\lambda$
\mathcal{L}	Persistence length
M	Molecular weight, g/mole; maximum drag-reduction(MDR) asymptote
M_v	Viscosity-average molecular weight
M_w	Weight-average molecular weight
m	Average molecular weight per backbone link, g/mole

Latin Symbols(continued)

N	Number of backbone links; turbulent Newtonian PK line; number of convolutions in equation 3.1-1
N_A	Avogadro's number, 6.022×10^{23} mole ⁻¹
n	Number density, cm ⁻³
n'	Pseudo-power-law exponent, dimensionless
P	Pressure in N/m ² or psid; polymeric regime
ΔP	Pressure drop, N/m ² or psid
Q	Flow rate — l/s, cm ³ /s, or gpm; Bjerrum length
q'	Turbulent kinetic energy, $(u'^2 + v'^2 + w'^2)/(2u_r^2)$
R	Pipe inner radius
$\langle R^2 \rangle$	Mean-square radius
R_G	Radius of gyration, $\langle R^2 \rangle^{1/2}$
Re	Reynolds number, $D \langle \bar{U} \rangle / \nu_s$
$Re\sqrt{f}$	Prandtl-Karman abscissa, $\sqrt{2}Du_r/\nu_s$
R_o	Reynolds number in equation 3.1-1
r	Radial position
S'	Apparent slip, $1/\sqrt{f_p} - 1/\sqrt{f_n}$ at same u_r
T	Temperature in K(elvins)
T_{bb}	Time between bursts
t	Temperature, °C
t_p	Polymer relaxation time, s
\bar{U}	Mean velocity

Latin Symbols(continued)

$\langle \bar{U} \rangle$	Average bulk velocity, $4Q/(\pi D^2)$
u	Axial velocity fluctuation
u_r	Friction velocity, $(T_w/\rho)^{1/2}$
$-\rho \langle uv \rangle$	Turbulent Reynolds stress
V	Volume; transducer output voltage; bulk velocity in equation 3.1-1
v	Radial velocity fluctuation
W	Wave number, u_r/ν_s
w	Azimuthal velocity fluctuation
X_v	Additive-pervaded volume fraction
x	Downstream distance
y	Position from wall, $R-r$
z	Azimuthal spacing
z_i	Charge on species i

Greek Symbols

α	Linear expansion factor, $([\eta]/[\eta]_0)^{1/2}$
$\dot{\gamma}$	Shear rate, s^{-1}
δ	Slope increment, $A_p - A_n$, dimensionless
ϵ	Excluded volume exponent
ϵ_0	Vacuum permittivity, $8.8542 \times 10^{-12} C^2/(J \cdot m)$
ϵ_r	Relative permittivity(dielectric constant), dimensionless
η	Viscosity, $g/(cm \cdot s)$
η_r	Relative viscosity, η/η_s , dimensionless

Greek Symbols(continued)

η_{sp}	Specific viscosity, η_r-1 , dimensionless
$[\eta]$	Intrinsic viscosity, cm^3/g
θ	Bond angle between adjacent backbone links
Θ	Theta temperature
κ	Slope modulus; inverse Debye length
λ	Slip modulus; inverse Kuhn statistical length
ξ	Line-charge density ratio, Q/A
ρ	Solvent(solution) density, g/cm^3
σ	Standard deviation
Σ	Intrinsic Slip, $S'/(c/M_w)$
ζ	Bead friction coefficient
T_w	Wall shear stress, $(D/4)(-\Delta P/L)$, dyne/cm^2
Φ	Kirk-Riseman(KR) constant, $\sim 2 \times 10^{23} \text{ mole}^{-1}$
ϕ	Volume fraction, dimensionless
χ	Von-Karman constant; 0.4 and 0.085 for Newtonian and asymptotic maximum drag-reducing flows, respectively
Ω_L	Length-based onset constant, $R_G W^*$
Ω_T	Time-based onset constant, $R_G^3 T_w^*$

Superscripts

+	Normalized by wall units, u_r/ν_s
*	Onset value
#	Retro-onset value
^	Degradation falloff
'	Root-mean-square(RMS) value

Subscripts

e	Elastic (sublayer)
l	Laminar value
M, m	Maximum Drag Reduction(MDR) value
n	Newtonian(turbulence) value
o	Initial conditions, random-flight value
p	Polymer, polymeric
s	Solvent value
v	Viscous (sublayer)

APPENDIX H

REFERENCES

- Achia, B. U.; Thompson, D. W. *J. Fl. Mech.*, **1977**, *81 Part III*, 439-464.
- Ait-Kadi, A.; Carreau, P. J.; Chauveteau, G. *J. Rheol.*, **1987**, *31(7)*, 537-561.
- American Cyanamid Co., New Product Bulletin No. 34, June 1955; American Cyanamid Co., New York.
- Banijamali, S. H.; Merrill, E. W.; Smith, K. A.; Peebles, L. H. *A.I.Ch.E. J.*, **1974**, *20(4)*, 824-826.
- Bartels, P. V. In *I.U.T.A.M. Symposium Essen/Germany: The Influence of Polymer Additives on Velocity and Temperature Fields*; Gampert, B., Ed.; Springer-Verlag: Berlin/Heidelberg, 1984; pp. 279-289.
- Berman, N. S. *Phys. Fl.*, **1977**, *20(10) Part II*, S168-S174.
- Berman, N. S.; Griswold, S. T.; Elihu, S.; Yuen, J. *A.I.Ch.E. J.*, **1978**, *24(1)*, 124-130.
- Bewersdorff, H.-W. *Rheol. Acta*, **1984**, *23(5)*, 522-543.
- Bewersdorff, H.-W.; Berman, N. S. *Rheol. Acta*, **1988**, *27*, 130-136.
- Blackwelder, R. F.; Kaplan, R. E. *J. Fl. Mech.*, **1976**, *76*, 89-112.
- Bobkowicz, A. J.; Gauvin, W. H. *Can. J. Chem. Eng.*, **1965**, *43*, 87-91.
- Bohdanecký, M.; Kovář, J. *Viscosity of Polymer Solutions*. Jenkins, A. D., Ed.; Elsevier Scientific: New York, 1982.
- Brender, C. *J. Chem. Phys.*, **1990**, *7*, 4468-4472.
- Burger, E. D.; Chorn, L. G.; Perkins, T. K. *J. Rheol.*, **1980**, *24(5)*, 603-626.
- Carnie, S. L.; Christos, G. A.; Creamer, T. *J. Chem. Phys.*, **1988**, *10*, 6484-6496.
- Chemical Engineers' Handbook*; Perry, Robert H. (Ed.); McGraw-Hill: New York, 1973; p. 3-71.

REFERENCES(continued)

- CRC Handbook of Chemistry and Physics, 67th Edition*; Weast, Robert C.(Ed.); CRC Press: Boca Raton, Florida, 1986-1987; pp. D-253, F-37.
- Clarke, W. B. Sc.D. Thesis, Massachusetts Institute of Technology, October, 1970.
- Cohen, J.; Priel, Z.; Rabin, Y. *J. Chem. Phys.*, **1988**, *11*, 7111-7116.
- Collinson, E.; Dainton, F. S.; McNaughton, G. S. *Trans. Far. Soc.*, **1956**, *53*, 489-498.
- Debye, P.; Bueche, A. M. *J. Chem. Phys.*, **1948**, *16(6)*, 573-579.
- Del Villar, R.; Carreau, P. J.; Patterson, W. I. *Chem. Eng. Comm.*, **1984**, *25*, 321-331.
- Donohue, G. L.; Tiederman, W. G.; Reischman, M. M. *J. Fl. Mech.*, **1972**, *56 Part III*, 559-575.
- Dunlop, E. H.; Cox, L. R. *Phys. Fl.*, **1977**, *20(10) Part II*, S203-S213.
- Eckelman, L. D.; Fortuna, G.; Hanratty, T. J. *Nature*, **1972**, *236*, 94-96.
- Einvoll, G.; Hemmer, P. C. *J. Chem. Phys.*, **1988**, *1*, 474-484.
- Elson, T. P.; Garside, J. J. *Non-Newt. Fl. Mech.*, **1983**, *12*, 121-133.
- Falco, R. E. *Phys. Fl.*, **1977**, *20(10) Part II*, S124-S132.
- Fanood, M. H. R.; George, M. H. *Polymer*, **1987**, *28*, 2241-2243.
- Farinato, R. S. *Polymer*, **1988**, *29*, 2182-2190.
- Fixman, M. *J. Chem. Phys.*, **1964**, *41*, 937-944.
- Fixman, M. *Macromolecules*, **1981**, *14*, 1710-1717.
- Flory, P. J. *Principles of Polymer Chemistry*; Cornell University: Ithaca, 1953.
- Frings, B. In *I.U.T.A.M. Symposium Essen/Germany: The Influence of Polymer Additives on Velocity and Temperature Fields*; Gampert, B., Ed.; Springer-Verlag: Berlin/Heidelberg, 1984; pp. 209-221.
- Frings, B. *Rheol. Acta*, **1988**, *27*, 92-110.

REFERENCES(continued)

- Fujita, Hiroshi *Macromolecules*, **1988**, *21*, 179-185.
- Fuoss, R. M.; Strauss, U. P. *J. Polym. Sci.*, **1948**, *3*, 245-263.
- Garcia de la Torre, J.; Jimenez, A.; Freire, J. J. *Macromolecules*, **1982**, *15*, 148-154.
- Gramain, Ph.; Borreill, J. *Rheol. Acta*, **1978**, *17*, 303-311.
- Hinze, J. O. *Turbulence*; McGraw-Hill: New York, 1975.
- Hoyt, J. W.; *ASME J. Basic Eng.*, **1972**, *94*, 258-285.
- Hoyt, J. W.; Sellin, R. H. *Rheol. Acta*, **1988**, *27*, 518-522.
- Huggins, M. L. *J. Am. Chem. Soc.*, **1942**, *64*, 2716-2718.
- Inge, C.; Johansson, A. V.; Lindgren, E. R. *Phys. Fl.*, **1979**, *22(5)*, 824-829.
- Interthal, W.; Wilski, H. *Coll. & Polym. Sci.*, **1985**, *263*, 217-229.
- Kagawa, I.; Fuoss, R. M. *J. Polym. Sci.*, **1955**, *18*, 535-542.
- Kale, D.; Metzner, A. B. *A.I.Ch.E. J.*, **1976**, *22(4)*, 669-674.
- Kirkwood, J. G.; Riseman, J. J. *Chem. Phys.*, **1948**, *16(6)*, 565-573.
- Klein, J.; Conrad, K.-D. *Makromol. Chem.*, **1978**, *179*, 1635-1638.
- Klein, J.; Conrad, K.-D. *Makromol. Chem.*, **1980**, *181*, 227-240.
- Kline, J. S.; Reynolds, W. C.; Schraub, F. A.; Runstadler, P. W. *J. Fl. Mech.*, **1967**, *152*, 455-478.
- Kowalik, R. M.; Duvdevani, I.; Peiffer, D. G.; Lundberg, R. D.; Kitano, K.; Schulz, D. N. *J. Non-Newt. Fl. Mech.*, **1987**, *24*, 1-10.
- Kraemer, E. O. *Ind. Eng. Chem.*, **1938**, *30*, 1200-1203.
- Kratky, O.; Porod, G. *Rec. Trav. Chim. Pays.-Bas.*, **1949**, *68*, 1106-1121.
- Kulicke, W.-M.; Kniewske, R.; Klein, J. *Prog. Polym. Sci.*, **1982**, *8*, 373-468.

REFERENCES(continued)

- Kulicke, W.-M.; Kötter, M.; Gräger, H. In *Advances in Polymer Science 89: Polymer Characterization/Polymer Solutions*: Benoit, H., Ed.; Springer-Verlag: Berlin/Heidelberg, 1989; pp. 1-68.
- Kwack, E. Y.; Cho, Y. I.; Harnett, J. P. *J. Non-Newt. Fl. Mech.*, **1981**, *9*, 79-90.
- Laufer, J. *N.A.C.A*, Report No. 1174, 1954, pp. 1-18.
- Lee, P. F. W.; Duffy, G. G. *A.I.Ch.E. J.*, **1976**, *22*, 750-753.
- Lee, W. K.; Vaseleski, R. C.; Metzner, A. B. *A.I.Ch.E. J.*, **1974**, *20*, 301-306.
- Luchik, T. S.; Tiederman, W. G. *J. Fl. Mech.*, **1987**, *174*, 529-552.
- Lumley, J. L. In *Macromolecular Reviews*; Peterlin, A., Ed.; Journal of Polymer Science: Wiley; New York, 1973; Volume 7, pp. 263-290.
- Lyons, S. L.; Nikolaidis, C.; Hanratty, T. J. *A.I.Ch.E. J.*, **1988**, *34(6)*, 938-945.
- Madavan, N. K.; Deutsch, S.; Merkle, C. L. *J. Fl. Mech.*, **1985**, *156*, 237-256.
- Manning, G. S. *J. Chem. Phys.*, **1969**, *31(3)*, 924-933.
- McComb, W. D.; Rabie. *A.I.Ch.E. J.*, **1982a**, *28(4)*, 547-557.
- McComb, W. D.; Rabie. *A.I.Ch.E. J.*, **1982b**, *28(4)*, 558-565.
- McComb, W. D.; Chan, K. T. *J. Nature*, **1981**, *292*, 520-522.
- McComb, W. D.; Chan, K. T. *J. Fl. Mech.*, **1985**, *152*, 455-478.
- McCormick, C. L.; Hester, R. D.; Morgan, S. E.; Safieddine, A. M. *Macromolecules*, **1990a**, *23*, 2124-2131.
- McCormick, C. L.; Hester, R. D.; Morgan, S. E.; Safieddine, A. M. *Macromolecules*, **1990b**, *23*, 2132-2139.
- Merrill, E. W.; Horn A. F. *Polym. Comm.*, **1984**, *25*, 144-146.
- Miyaki, Y.; Fujita, H.; Fukuda, M. *Macromolecules*, **1980**, *13*, 588-592.
- Mizushima, T.; Usui, H. *Phys. Fl.*, **1977**, *20(10) Part II*, S100-S108.

REFERENCES(continued)

- Monin, A. S.; Yaglom, A. M. *Statistical Fluid Mechanics*; M.I.T.: Cambridge, MA, 1971.
- Morawetz, H. *Macromolecules in Solution, 2nd Edition*; Wiley: New York, 1975.
- Morgan, S. E.; McCormick, C. L. *Prog. Polym. Sci.*, **1990**, *15*, 507-549.
- Muller, G.; Laine, J. P.; Fenyó, J. C. *J. Polym. Sci.: Polym. Chem. Ed.*, **1979**, *17*, 659-672.
- Munk, P.; Aminabhavi, T. M.; Williams, P.; Hoffman, D. E.; Chemlir, M. *Macromolecules*, **1980**, *13*, 871-875.
- Noda, I.; Tsuge, T.; Nagasawa, M. *J. Phys. Chem.*, **1970**, *74*, 710-719.
- Odijk, T.; Houwaart, A. C. *J. Polym. Sci.*, **1978**, *16*, 627-639.
- Ogawa, K.; Kuroda, C. *Can. J. Chem. Eng.*, **1986**, *64*, 497-500.
- Ohlendorf, D.; Interthal, W.; Hoffmann, H. *Rheol. Acta*, **1986**, *25*, 468-486.
- Oldaker, D. K.; Tiederman, W. G. *Phys. Fl.*, **1977**, *20(10) Part II*, S133-S144.
- Oliver, D. R.; Bakhtiyarov, S. I. *J. Non-Newt. Fl. Mech*, **1983**, *12*, 113-118.
- Oono, Y.; Kohomoto, M. *J. Chem. Phys.*, **1983**, *78*, 520-528.
- Oosawa, F. *Polyelectrolytes*; Marcel Dekker: New York, 1970.
- Parker, C. A.; Hedley, A. H. *Nature*, **1972**, *236*, 61-62.
- Peterlin, A. J. *J. Chem. Phys.*, **1955**, *23*, 2464-2465.
- Pinho, F. T.; Whitelaw, J. H. *J. Non-Newt. Fl. Mech.*, **1990**, *34*, 129-144.
- Polymers in Solution: Theoretical Considerations and Newer Methods of Characterization*; Forsman, W. C., Ed.; Plenum: New York, 1986.
- Pyun, C. W.; Fixman, M. *J. Chem. Phys.*, **1966**, *44*, 2107-2115.
- Qian, C.; Kholodenko, A. L. *J. Chem. Phys.*, **1988**, *4*, 2301-2311.

REFERENCES(continued)

- Rice, S. A.; Nagasawa, M. *Polyelectrolyte Solutions*; Academic: New York, 1961.
- Rochefort, S.; Middleman, S. In *I.U.T.A.M. Symposium Essen/Germany: The Influence of Polymer Additives on Velocity and Temperature Fields*; Gampert, B., Ed.; Springer-Verlag: Berlin/Heidelberg, 1984; pp. 117-127.
- Schlichting, H. *Boundary Layer Theory, 7th Edition*; McGraw-Hill: New York, 1979.
- Scholtan, W. *Makromol. Chem.*, **1954**, *14*, 169-178.
- Sellin, R. H. J.; Ollis, M. *Ind. Eng. Chem. Prod. Res. & Dev.*, **1983**, *22*, 445-452.
- Sharma, R. S.; Seshradi, V.; Malhotra, R. C. *Chem. Eng. Sci.*, **1979**, *34*, 703-713.
- Stenberg, L.-G.; Lagerstedt, T.; Sehlen, O.; Lindgren, E. R. *Phys. Fl.*, **1977**, *20(5)*, 858-859.
- Takahashi, A.; Nagasawa, M. *J. Am. Chem. Soc.*, **1964**, *86*, 543-548.
- Tam, K. C.; Tiu, C. *Polym. Comm.*, **1989**, *30*, 114-116.
- Tam, K. C.; Tiu, C. *Polym. Comm.*, **1990**, *31*, 102-104.
- Tanford, C. *Physical Chemistry of Macromolecules*; Wiley: New York, 1961.
- Tiederman, W. G.; Luchik, T. S.; Bogard, D. G. *J. Fl. Mech.*, **1985**, *156*, 419-437.
- Ting, R. Y. *Chem. Eng. Comm.*, **1982**, *15*, 331-342.
- Toms, B. A. *Proceedings of the First International Congress on Rheology: Volume II*; North Holland: Amsterdam, 1948; pp. 135-141.
- Usui, H.; Iwata, N.; Sano, Y. In *I.U.T.A.M. Symposium Essen/Germany: The Influence of Polymer Additives on Velocity and Temperature Fields*; Gampert, B., Ed.; Springer-Verlag: Berlin/Heidelberg, 1984; pp. 223-232.
- Usui, H.; Maeguchi, K.; Sano, Y. *Phys. Fl.*, **1988**, *31(9)*, 2518-2523.
- Virk, P. S.; Mickley, H. S.; Smith, K. A. *A.S.M.E. J. Appl. Mech.*, **1970**, *37*, 488-493.
- Virk, P. S. *J. Fl. Mech.*, **1971a**, *45*, 225-246.

REFERENCES(continued)

- Virk, P. S. *J. Fl. Mech.*, **1971b**, *45*, 417-440.
- Virk, P. S. *Nature*, **1975a**, *253*, 109-110.
- Virk, P. S. *A.I.Ch.E. J.*, **1975b**, *21(4)*, 625-656.
- Wells, C. S.; Spangler, J. G. *Phys. Fl.*, **1967**, *10(9)*, 1890-1894.
- White, D. Jr.; Gordon, R. J. *A.I.Ch.E. J.*, **1975**, *21(5)*, 1027-1029.
- Willmarth, W. W.; Wei, T.; Lee, C. O. *Phys. Fl.*, **1987**, *30(40)*, 933-935.
- Wolff, C. *Eur. Polym. J.*, **1977**, *13*, 739-741.
- Yamakawa, H. *Modern Theory of Polymer Solutions*; Harper & Row: New York, 1971.
- Zakin, J. L.; Hunston, D. L. *J. Macromol. Sci.-Phys.*, **1980**, *B18(4)*, 795-814.
- Zimm, B. H. *Macromolecules*, **1980**, *13*, 592-602.

APPENDIX I

BIOGRAPHICAL NOTE

The author was born 7 August 1963 in Baltimore, Maryland and lived in nearby Randallstown for nearly his first five years. His family moved to Palo Alto, California in July 1968, where he attended elementary, middle, and high schools up to mid-1981.

In September 1981, he entered the University of California at Berkeley, starting in the College of Letters and Science with an undeclared major and later pursued chemical engineering, switching to the College of Chemistry. In June 1983, he left UC Berkeley for Gaithersburg, Maryland to do cooperative research at the National Bureau of Standards(now the National Institute for Standards and Technology) in the Center for Fire Research. Returning the following December, he continued the chemical-engineering curriculum. In May 1985, he received a BScE degree with high honors, earned the Mabel Kittredge Wilson Prize from College of Chemistry, being third in the class, and also was elected Phi Beta Kappa.

In September 1985, he entered MIT's department of chemical engineering with a Hertz Graduate Fellowship and a Gilliland Award, the former of which was chosen. After passing the qualifying exams in January 1986, he decided to work with Professor P. S. Virk in turbulent drag reduction. A thesis proposal was submitted in November 1987, and the last of many experiments was done in late December 1990.

During this period, minor degrees were earned in mechanical engineering and political science. Professor P. S. Virk and he coauthored a paper titled "Aspects of Mechanisms in Type B Drag Reduction," which was presented in Zurich, Switzerland at the IUTAM Symposium on the Structure of Turbulence and Drag Reduction in July 1989.

During the writing of this thesis, this author was chosen to be a 1991-1992 AAAS Science, Engineering, and Diplomacy Fellow working for the United States Agency for International Development(USAID) on development problems pertaining to energy and environment in less-developed countries. The position was accepted before the completion of this thesis and the defense thereof. Currently, the author works for the Office of Energy and Infrastructure in USAID's Bureau of Research & Development in Arlington, VA.